CHAPTER 2

SITE CHARACTERISTICS

TABLE OF CONTENTS

TABLE OF CONTENTS (Continued)

TABLE OF CONTENTS (Continued)

TABLE OF CONTENTS (Continued)

TABLE OF CONTENTS (Continued)

TABLE OF CONTENTS (Continued)

TABLE OF CONTENTS (Continued)

TABLE OF CONTENTS (Continued)

TABLE OF CONTENTS (Continued)

TABLE OF CONTENTS (Continued)

TABLE OF CONTENTS (Continued)

TABLE OF CONTENTS (Continued)

TABLE OF CONTENTS (Continued)

LIST OF TABLES

LIST OF TABLES (Continued)

LIST OF TABLES (Continued)

LIST OF TABLES (Continued)

LIST OF TABLES (Continued)

LIST OF TABLES (Continued)

LIST OF TABLES (Continued)

LIST OF TABLES (Continued)

LIST OF TABLES (Continued)

LIST OF TABLES (Continued)

LIST OF TABLES (Continued)

LIST OF TABLES (Continued)

LIST OF TABLES (Continued)

LIST OF FIGURES

LIST OF FIGURES (Continued)

LIST OF FIGURES (Continued)

LIST OF FIGURES (Continued)

LIST OF FIGURES (Continued)

LIST OF FIGURES (Continued)

LIST OF FIGURES (Continued)

LIST OF FIGURES (Continued)

LIST OF FIGURES (Continued)

LIST OF FIGURES (Continued)

LIST OF FIGURES (Continued)

LIST OF FIGURES (Continued)

LIST OF FIGURES (Continued)

LIST OF FIGURES (Continued)

LIST OF FIGURES (Continued)

LIST OF FIGURES (Continued)

LIST OF FIGURES (Continued)

LIST OF FIGURES (Continued)

LIST OF FIGURES (Continued)

CHAPTER 2

SITE CHARACTERISTICS

The introductory information at the beginning of Chapter 2 of the referenced DCD is incorporated by reference with the following departures and/or supplements.

Insert the following subsection at the end of the introductory text of DCD Chapter 2, prior to DCD Section 2.1.

2.0 SITE CHARACTERISTICS

WLS SUP 2.0-1 Chapter 2 describes the characteristics and site-related design parameters of the Lee Nuclear Site (WLS). The site location, characteristics and parameters, as described in the following five sections are provided in sufficient detail to support a safety assessment:

- Geography and Demography (Section 2.1)
- Nearby Industrial, Transportation, and Military Facilities (Section 2.2)
- Meteorology (Section 2.3)
- Hydrology (Section 2.4)
- Geology and Seismology (Section 2.5)

In this chapter, the following definitions and figures are provided to assist the reader in understanding the scope of the discussion:

- Lee Nuclear Station site – the 1,900 acre (ac.) area identified by the site boundary (Figure 2.1-201).
- Lee Nuclear Site vicinity – the area within approximately the 6-mile (mi.) radius around the site (Figure 2.1-202).
- Lee Nuclear Site region – the area within approximately the 50-mi. radius around the site (Figure 2.1-203).

Table 2.0-201 provides a comparison of site-related design parameters for which the AP1000 plant is designed and site characteristics specific to Lee Nuclear Site in support of this safety assessment. The first two columns of Table 2.0-201 are a compilation of the site parameters from DCD Table 2-1 and DCD Tier 1 Table 5.0-1. The third column of Table 2.0-201 is the corresponding site characteristic for the Lee Nuclear Site. The fourth column denotes the place within the Lee Nuclear Site FSAR that this data is presented.

The last column indicates whether or not the site characteristic falls within the AP1000 site parameters. Control room atmospheric dispersion factors (χ/Q) for accident dose analysis are presented in Table 2.0-202. All of the control room χ/Q values fall within the AP1000 parameters.

WLS SUP 2.0-1

TABLE 2.0-201 (Sheet 1 of 8)
COMPARISON OF AP1000 DCD SITE PARAMETERS AND LEE NUCLEAR STATION UNITS 1 & 2 SITE CHARACTERISTICS

	AP 1000 DCD Site Parameters	WLS Site Characteristic	WLS FSAR Reference	WLS Within Site Parameter
Air Temperature				
Maximum Safety	115°F dry bulb / 86.1°F coincident wet bulb[a],[h]	107°F dry bulb / 84°F coincident wet bulb (100-year maximum)	Table 2.3-293	Yes
	86.1°F wet bulb (noncoincident)	85°F (100-year maximum)	Table 2.3-293	Yes
Minimum Safety	-40°F[a]	-5°F (100-year minimum)	Table 2.3-293	Yes
Maximum Normal	101°F dry bulb / 80.1°F coincident wet bulb[b]	91°F dry bulb / 76°F coincident wet bulb (1% exceedance)	Table 2.3-293	Yes
	80.1°F wet bulb (noncoincident)[c]	76°F wet bulb (1% exceedance)	Table 2.3-293	Yes
Minimum Normal	-10°F[b]	24°F (1% exceedance)	Table 2.3-293	Yes
Wind Speed				
Operating Basis	145 mph (3 second gust); importance factor 1.15 (safety), 1.0 (nonsafety); exposure C; topographic factor 1.0	96 mph (3 second gust) (110 mph with 1.15 importance factor); exposure C; topographic factor 1.0	Subsection 2.3.1.2.8	Yes
Tornado	300 mph	230 mph	Subsection 2.3.1.2.2	Yes
	Maximum Pressure Differential of 2.0 lb/in^2	1.2 lb/in^2	Subsection 2.3.1.2.2	Yes

WLS SUP 2.0-1

TABLE 2.0-201 (Sheet 2 of 8)
COMPARISON OF AP1000 DCD SITE PARAMETERS AND LEE NUCLEAR STATION UNITS 1 & 2 SITE CHARACTERISTICS

	AP 1000 DCD Site Parameters	WLS Site Characteristic	WLS FSAR Reference	WLS Within Site Parameter
Seismic				
CSDRS	CSDRS free field peak ground acceleration of 0.30 g with modified Regulatory Guide 1.60 response spectra (See Figures 5.0-1 and 5.0-2). The SSE is now referred to as CSDRS. Seismic input is defined at finished grade, except for sites where the nuclear island is founded on hard rock.(d) The hard rock high frequency (HRHF) envelope response spectra are shown in Figure 5.0-3 and Figure 5.0-4 defined at the foundation level for 5% damping. The HRHF envelope response spectra provide an alternative set of spectra for evaluation of site specific GMRS. A site is acceptable if its site-specific GMRS fall within the AP1000 HRHF envelope response spectra.(e) Evaluation of a site for application of the HRHF envelope response spectra includes consideration of the limitation on shear wave velocity identified for use of the HRHF envelope response spectra. This limitation is defined by a shear wave velocity at the bottom of the basemat equal to or higher than 7,500 fps, while maintaining a shear wave velocity equal to or above 8,000 fps at the lower depths.	GMRS PGA = 0.21g Unit 1 FIRS PGA = 0.22g GMRS and Unit 1 FIRS are below the WEC hard rock high frequency spectrum at all points.	Subsection 2.5.2.6 Subsection 2.5.2.7 Subsection 3.7.1.1.1 Figure 3.7-201 Figure 3.7-202	Yes
Fault Displacement Potential	No potential fault displacement considered beneath the seismic Category I and seismic Category II structures and immediate surrounding area. The immediate surrounding area includes the effective soil supporting media associated with the seismic Category I and seismic Category II structures.	Negligible.	Subsection 2.5.3.8	Yes

WLS SUP 2.0-1

TABLE 2.0-201 (Sheet 3 of 8)
COMPARISON OF AP1000 DCD SITE PARAMETERS AND LEE NUCLEAR STATION UNITS 1 & 2 SITE CHARACTERISTICS

	AP 1000 DCD Site Parameters	WLS Site Characteristic	WLS FSAR Reference	WLS Within Site Parameter
Soil				
Average Allowable Static Bearing Capacity	The allowable bearing capacity, including a factor of safety appropriate for the design load combination, shall be greater than or equal to the average bearing demand of 8,900 lb/ft^2 over the footprint of the nuclear island at its excavation depth.	190,000 to 285,000 lb/ft^2	Subsection 2.5.4.10.1	Yes
Dynamic Bearing Capacity for Normal Plus Safe Shutdown Earthquake (SSE)	The allowable bearing capacity, including a factor of safety appropriate for the design load combination, shall be greater than or equal to the maximum bearing demand of 35,000 lb/ft^2 at the edge of the nuclear island at its excavation depth, or site-specific analyses demonstrate factor of safety appropriate for normal plus safe shutdown earthquake loads.	190,000 to 285,000 lb/ft^2	Subsection 2.5.4.10.1	Yes
Shear Wave Velocity	Greater than or equal to 1,000 ft/sec based on minimum low-strain soil properties over the footprint of the nuclear island at its excavation depth	9000 to 10,000 ft/sec	Subsection 2.5.4.7	Yes

WLS SUP 2.0-1

TABLE 2.0-201 (Sheet 4 of 8)
COMPARISON OF AP1000 DCD SITE PARAMETERS AND LEE NUCLEAR STATION UNITS 1 & 2 SITE CHARACTERISTICS

	AP 1000 DCD Site Parameters	WLS Site Characteristic	WLS FSAR Reference	WLS Within Site Parameter
Lateral Variability	Soils supporting the nuclear island should not have extreme variations in subgrade stiffness. This may be demonstrated by one of the following: 1. Soils supporting the nuclear island are uniform in accordance with Regulatory Guide 1.132 if the geologic and stratigraphic features at depths less than 120 feet below grade can be correlated from one boring or sounding location to the next with relatively smooth variations in thicknesses or properties of the geologic units, or 2. Site-specific assessment of subsurface conditions demonstrates that the bearing pressures below the footprint of the nuclear island do not exceed 120% of those from the generic analyses of the nuclear island at a uniform site, or 3. Site-specific analysis of the nuclear island basemat demonstrates that the site specific demand is within the capacity of the basemat. As an example of sites that are considered uniform, the variation of shear wave velocity in the material below the foundation to a depth of 120 feet below finished grade within the nuclear island footprint and 40 feet beyond the boundaries of the nuclear island footprint meets the criteria in the case outlined below.	Category I structures are founded on hard rock; Case 1 applies	Subsection 2.5.1.2.6	N/A
	Case 1: For a layer with a low strain shear wave velocity greater than or equal to 2500 feet per second, the layer should have approximately uniform thickness, should have a dip not greater than 20 degrees, and should have less than 20 percent variation in the shear wave velocity from the average velocity in any layer.	Case 1 applies. Non-dipping meta-plutonic rock displaying less than 20 percent variation in the shear wave velocity.	Subsection 2.5.4.7.4	Yes

WLS SUP 2.0-1

TABLE 2.0-201 (Sheet 5 of 8)
COMPARISON OF AP1000 DCD SITE PARAMETERS AND LEE NUCLEAR STATION UNITS 1 & 2 SITE CHARACTERISTICS

	AP 1000 DCD Site Parameters	WLS Site Characteristic	WLS FSAR Reference	WLS Within Site Parameter
Minimum Soil Angle of Internal Friction	Minimum soil angle of internal friction is greater than or equal to 35 degrees below the footprint of nuclear island at its excavation depth. If the minimum soil angle of internal friction is below 35 degrees, a site specific analysis shall be performed using the site specific soil properties to demonstrate stability.	Category I structures are founded on hard rock, which satisfies the criterion.	Not applicable	Yes
Liquefaction Potential	No liquefaction considered beneath the seismic Category I and seismic Category II structures and immediate surrounding area. The immediate surrounding area includes the effective soil supporting media associated with the seismic Category I and seismic Category II structures.	None. Category I structures are founded on hard rock. Foundations for adjacent structures have negligible liquefaction potential.	Subsection 2.5.4.8	Yes
Missiles				
Tornado	4000 - lb automobile at 105 mph horizontal, 74 mph vertical	4000 - lb automobile at 105 mph horizontal, 74 mph vertical	Subsection 3.5.1.5(f)	Yes(f)
	275 - lb, 8 in. shell at 105 mph horizontal, 74 mph vertical	275 - lb, 8 in. shell at 105 mph horizontal, 74 mph vertical	Subsection 3.5.1.5(f)	Yes(f)
	1 inch diameter steel ball at 105 mph in the most damaging direction	1 inch diameter steel ball at 105 mph in the most damaging direction	Subsection 3.5.1.5(f)	Yes(f)

WLS SUP 2.0-1

TABLE 2.0-201 (Sheet 6 of 8)
COMPARISON OF AP1000 DCD SITE PARAMETERS AND LEE NUCLEAR STATION UNITS 1 & 2 SITE CHARACTERISTICS

	AP 1000 DCD Site Parameters	WLS Site Characteristic	WLS FSAR Reference	WLS Within Site Parameter
Flood Level	Less than plant elevation 100' (WLS Elevation 590’ msl)	584.8' msl	Subsection 2.4.3.6	Yes
Groundwater Level	Less than plant elevation 98' (WLS Elevation 588’ msl)	Maximum and average groundwater elevation is projected to be around 584 and 579.4 ft. msl, respectively, with AP1000 elevation 100 ft at 590 ft. msl. This allows for approximately 5 to 10 ft. of unsaturated interval below the plant grade elevation 100 ft.	Subsection 2.5.4.1.3	Yes
Plant Grade Elevation	Less than plant elevation 100' (WLS elevation 590’ msl) except for portion at a higher elevation adjacent to the annex building	589.5 ft. msl	Subsection 2.4.1.1.3	Yes
Precipitation				
Rain	20.7 in./hr [1-hr 1-mi^2 PMP]	18.9 in./hr. [1-hr 1-mi^2 PMP]	Table 2.4.2-203	Yes
Snow / Ice	75 pounds per square foot on ground with exposure factor of 1.0 and importance factors of 1.2 (safety) and 1.0 (non-safety)	17.7 pounds per square foot	Subsection 2.3.1.2.7.3	Yes
Atmospheric Dispersion Values $\chi/Q^{(g)}$				
Site Boundary (0-2 hr)	$\leq 5.1 \times 10^{-4}$ sec/m^3	3.46×10^{-4} sec/m^3	Table 2.3-283 Subsection 2.3.4.2	Yes
Site Boundary (Annual Average)	$\leq 2.0 \times 10^{-5}$ sec/m^3	5.8×10^{-6} sec/m^3	Table 2.3-289 (Sheet 1 of 4)	Yes

WLS SUP 2.0-1

TABLE 2.0-201 (Sheet 7 of 8)
COMPARISON OF AP1000 DCD SITE PARAMETERS AND LEE NUCLEAR STATION UNITS 1 & 2 SITE CHARACTERISTICS

	AP 1000 DCD Site Parameters	WLS Site Characteristic	WLS FSAR Reference	WLS Within Site Parameter
Low population zone boundary				
0-8 hr	$\leq 2.2 \times 10^{-4}$ sec/m^3	8.01×10^{-5} sec/m^3	Table 2.3-283	Yes
8-24 hr	$\leq 1.6 \times 10^{-4}$ sec/m^3	5.49×10^{-5} sec/m^3	Table 2.3-283	Yes
24-96 hr	$\leq 1.0 \times 10^{-4}$ sec/m^3	2.42×10^{-5} sec/m^3	Table 2.3-283	Yes
96-720 hr	$\leq 8.0 \times 10^{-5}$ sec/m^3	7.46×10^{-6} sec/m^3	Table 2.3-283	Yes
Control Room	Table 2.0-202	Table 2.0-202	Table 2.0-202	Yes

WLS SUP 2.0-1

TABLE 2.0-201 (Sheet 8 of 8)
COMPARISON OF AP1000 DCD SITE PARAMETERS AND LEE NUCLEAR STATION UNITS 1 & 2 SITE CHARACTERISTICS

	AP 1000 DCD Site Parameters	WLS Site Characteristic	WLS FSAR Reference	WLS Within Site Parameter
Population Distribution				
Exclusion area (site)	0.5 mi	Minimum distance from the Effluent Release Boundary to the Exclusion Area Boundary is 2113 feet. The radius of the effluent release boundary is 550 feet. The total minimum distance from the site center point to the EAB is 2663 feet (0.50 mi).	Subsection 2.1 Figure 2.1-209	Yes

a) Maximum and minimum safety values are based on historical data and exclude peaks of less than 2 hours duration.

b) The maximum normal value is the 1-percent seasonal exceedance temperature. The minimum normal value is the 99-percent seasonal exceedance temperature. The minimum temperature is for the months of December, January, and February in the northern hemisphere. The maximum temperature is for the months of June through September in the northern hemisphere. The 1-percent seasonal exceedance is approximately equivalent to the annual 0.4-percent exceedance. The 99-percent seasonal exceedance is approximately equivalent to the annual 99.6-percent exceedance.

c) The noncoincident wet bulb temperature is applicable to the cooling tower only.

d) With ground response spectra as given in DCD Figure 3.7.1-1 and DCD Figure 3.7.1-2. Seismic input is defined at finished grade except for sites where the nuclear island is founded on hard rock.

e) Sites that fall within the hard rock high frequency envelope response spectra given in DCD Figures 3I.1-1 and 3I.1-2 and satisfy the limitation on shear wave velocity in DCD Subsection 2.5.2.1 are acceptable.

f) Per APP-GW-GLR-020, the kinetic energies of the missiles discussed in DCD Section 3.5 are greater than the kinetic energies of the missiles discussed in Regulatory Guide 1.76 and results in a more conservative design.

g) For AP1000, the term "site boundary" and "exclusion area boundary" are used interchangeably. Thus, the χ/Q specified for the site boundary applies whenever a discussion refers to the exclusion area boundary. At Lee Nuclear Station, the “site boundary” and the “exclusion area boundary” are not interchangeable. See Figure 2.1-209.

h) The containment pressure response analysis is based on a conservative set of dry-bulb and wet-bulb temperatures. These results envelop any conditions where the dry-bulb temperature is 115°F or less and wet-bulb temperature of less than or equal to 86.1°F.

TABLE 2.0-202 (Sheet 1 of 4)
COMPARISON OF CONTROL ROOM ATMOSPHERIC DISPERSION FACTORS FOR ACCIDENT ANALYSIS
FOR AP1000 DCD AND LEE NUCLEAR STATION UNITS 1 & 2 (REFERENCE TABLE 2.3-285)

WLS SUP 2.0-1

	χ/Q (s/m^3) at HVAC Intake for the Identified Release Points[a]			χ/Q (s/m^3) at Annex Building Door for the Identified Release Points[b]		
	Plant Vent or PCS Air Diffuser[c]	Plant Vent	PCS Air Diffuser	Plant Vent or PCS Air Diffuser[c]	Plant Vent	PCS Air Diffuser
	DCD	FSAR	FSAR	DCD	FSAR	FSAR
0 – 2 hours	3.0E-03	2.01E-03	1.78E-03	1.0E-03	4.41E-04	4.83E-04
2 – 8 hours	2.5E-03	1.52E-03	1.45E-03	7.5E-04	3.47E-04	3.69E-04
8 – 24 hours	1.0E-03	5.84E-04	6.36E-04	3.5E-04	1.37E-04	1.61E-04
1 – 4 days	8.0E-04	4.76E-04	5.26E-04	2.8E-04	1.13E-04	1.32E-04
4 – 30 days	6.0E-04	3.56E-04	3.36E-04	2.5E-04	8.22E-05	9.13E-05

	χ/Q (s/m^3) at HVAC Intake for the Identified Release Points[a]				χ/Q (s/m^3) at Annex Building Door for the Identified Release Points[b]			
	Steam Line Break Releases	Steam Line Break Releases	Condenser Air Removal Stack[g]	Condenser Air Removal Stack	Steam Line Break Releases	Steam Line Break Releases	Condenser Air Removal Stack[g]	Condenser Air Removal Stack
	DCD	FSAR	DCD	FSAR	DCD	FSAR	DCD	FSAR
0 – 2 hours	2.4E-02	1.25E-02	6.0E-3	1.59E-03	4.0E-03	8.50E-04	2.0E-2	3.40E-03
2 – 8 hours	2.0E-02	7.22E-03	4.0E-3	1.27E-03	3.2E-03	6.44E-04	1.8E-2	2.91E-03
8 – 24 hours	7.5E-03	2.95E-03	2.0E-3	5.10E-04	1.2E-03	2.84E-04	7.0E-3	1.31E-03
1 – 4 days	5.5E-03	2.40E-03	1.5E-3	3.86E-04	1.0E-03	1.93E-04	5.0E-3	9.21E-04
4 – 30 days	5.0E-03	1.79E-03	1.0E-3	2.82E-04	8.0E-04	1.39E-04	4.5E-3	6.40E-04

TABLE 2.0-202 (Sheet 2 of 4)
COMPARISON OF CONTROL ROOM ATMOSPHERIC DISPERSION FACTORS FOR ACCIDENT ANALYSIS
FOR AP1000 DCD AND LEE NUCLEAR STATION UNITS 1 & 2 (REFERENCE TABLE 2.3-285)

	χ/Q (s/m^3) at HVAC Intake for the Identified Release Points[a]		χ/Q (s/m^3) at Annex Building Door for the Identified Release Points[b]	
	Ground Level Containment Release Points[d]		Ground Level Containment Release Points[d]	
	DCD	FSAR	DCD	FSAR
0 – 2 hours	6.0E-03	2.70E-03	1.0E-03	5.01E-04
2 – 8 hours	3.6E-03	1.79E-03	7.5E-04	3.98E-04
8 – 24 hours	1.4E-03	7.39E-04	3.5E-04	1.59E-04
1 – 4 days	1.8E-03	6.90E-04	2.8E-04	1.36E-04
4 – 30 days	1.5E-03	4.75E-04	2.5E-04	9.76E-05

	χ/Q (s/m^3) at HVAC Intake for the Identified Release Points[a]		χ/Q (s/m^3) at Annex Building Door for the Identified Release Points[b]	
	PORV and Safety Valve Releases[e]		PORV and Safety Valve Releases[e]	
	DCD	FSAR	DCD	FSAR
0 – 2 hours	2.0E-02	1.08E-02	4.0E-03	8.71E-04
2 – 8 hours	1.8E-02	5.62E-03	3.2E-03	6.83E-04
8 – 24 hours	7.0E-03	2.28E-03	1.2E-03	2.96E-04
1 – 4 days	5.0E-03	1.89E-03	1.0E-03	2.05E-04
4 – 30 days	4.5E-03	1.47E-03	8.0E-04	1.46E-04

TABLE 2.0-202 (Sheet 3 of 4)
COMPARISON OF CONTROL ROOM ATMOSPHERIC DISPERSION FACTORS FOR ACCIDENT ANALYSIS FOR AP1000 DCD AND LEE NUCLEAR STATION UNITS 1 & 2 (REFERENCE TABLE 2.3-285)

	χ/Q (s/m^3) at HVAC Intake for the Identified Release Points[a]			χ/Q (s/m^3) at Annex Building Door for the Identified Release Points[b]		
	Fuel Handling Area[f]	Fuel Building Blowout Panel	Radwaste Building Truck Staging Area Door	Fuel Handling Area[f]	Fuel Building Blowout Panel	Radwaste Building Truck Staging Area Door
	DCD	FSAR	FSAR	DCD	FSAR	FSAR
0 – 2 hours	6.0E-03	1.64E-03	1.17E-03	6.0E-03	3.64E-04	3.46E-04
2 – 8 hours	4.0E-03	1.20E-03	8.98E-04	4.0E-03	2.65E-04	2.53E-04
8 – 24 hours	2.0E-03	4.25E-04	3.30E-04	2.0E-03	1.01E-04	9.78E-05
1 – 4 days	1.5E-03	4.09E-04	2.93E-04	1.5E-03	8.87E-05	8.71E-05
4 – 30 days	1.0E-03	3.69E-04	2.59E-04	1.0E-03	7.37E-05	7.57E-05

a) These dispersion factors are to be used 1) for the time period preceding the isolation of the main control room and actuation of the emergency habitability system, 2) for the time after 72 hours when the compressed air supply in the emergency habitability system would be exhausted and outside air would be drawn into the main control room, and 3) for the determination of control room doses when the non-safety ventilation system is assumed to remain operable such that the emergency habitability system is not actuated.

b) These dispersion factors are to be used when the emergency habitability system is in operation and the only path for outside air to enter the main control room is that due to ingress/egress.

c) These dispersion factors are used for analysis of the doses due to a postulated small line break outside of containment. The plant vent and PCS air diffuser are potential release paths for other postulated events (loss-of-coolant accident, rod ejection accident, and fuel handling accident inside the containment); however, the values are bounded by the dispersion factors for ground level releases.

d) The listed values represent modeling the containment shell as a diffuse area source, and are used for evaluating the doses in the main control room for a loss-of-coolant accident, for the containment leakage of activity following a rod ejection accident, and for a fuel handling accident occurring inside the containment.

e) The listed values bound the dispersion factors for releases from the steam line safety and power-operated relief valves. These dispersion factors would be used for evaluating the doses in the main control room for a steam generator tube rupture, a main steam line break, a locked reactor coolant pump rotor, and for the secondary side release from a rod ejection accident.

TABLE 2.0-202 (Sheet 4 of 4)
COMPARISON OF CONTROL ROOM ATMOSPHERIC DISPERSION FACTORS FOR ACCIDENT ANALYSIS
FOR AP1000 DCD AND LEE NUCLEAR STATION UNITS 1 & 2 (REFERENCE TABLE 2.3-285)

f) The listed values bound the dispersion factors for releases from the fuel storage and handling area. The listed values also bound the dispersion factors for releases from the fuel storage area in the event that spent fuel boiling occurs and the fuel building relief panel opens on high temperature. These dispersion factors are used for the fuel handling accident occurring outside containment and for evaluating the impact of releases associated with spent fuel pool boiling.

g) This release point is included for information only as a potential activity release point. None of the design basis accident radiological consequences analyses model release from this point.

2.1 GEOGRAPHY AND DEMOGRAPHY

This section of the referenced DCD is incorporated by reference with the following departures and/or supplements.

WLS COL 2.1-1 This section of the Safety Analysis Report provides information regarding site location and description including the distribution of infrastructure, natural features, and populations in the Lee Nuclear Station area. The discussion below addresses the expectations of NUREG-0800, "Standard Review Plan for the Review of Safety Analysis Reports for Nuclear Power Plants," and Regulatory Guide 1.206, "Combined License Applications for Nuclear Power Plants (LWR Edition)." Radius distances defined by the NUREG-1555 were used for the population analysis rather than the distances described in RG 1.206 as an alternate method. The alternative method was used for correlation of the population data between the SAR and ER. No other exceptions to the regulatory documents noted or alternative methods were applied in development of this section.

Subsection 2.1.1 of the DCD is renumbered as Subsection 2.1.4 and moved to the end of Section 2.1. This is being done to accommodate the incorporation of Regulatory Guide 1.206 numbering conventions for Section 2.1.

STD DEP 1.1-1 ## 2.1.1 SITE LOCATION AND DESCRIPTION

WLS COL 2.1-1 Duke Energy proposes to construct and operate two Westinghouse AP1000 reactors at their Lee Nuclear Station 1,900-acre site, located in rural Cherokee County, South Carolina. The two AP1000 reactors are referred to as Lee Nuclear Station Units 1 and 2. Units 1 and 2 and supporting infrastructure are sited in the area delineated in Figure 2.1-201. Prominent natural and man-made features, including rivers, lakes, state and county lines, and industrial, military, and transportation facilities, are illustrated in Figures 2.1-201, 2.1-202, and 2.1-203. Figure 2.1-202 illustrates the features within the vicinity of the site.

The Lee Nuclear Site lies within the 7.5 minute Blacksburg South and Kings Creek Quadrangles. The Quadrangles that bracket the site area are Blacksburg North, Grover, Kings Mountain, Filbert, Sharon, Hickory Grove, Wilkinsville, Pacolet Mills, Gaffney, and Boiling Springs South. All quadrangles lie completely or partially within South Carolina (References 210 and 212).

The coordinates of the two new reactors are given below:

LONGITUDE AND LATITUDE (degrees/minutes/seconds [NAD83])

UNIT 1:	35° 02’ 12.05” North	81° 30’ 47.38” West
UNIT 2:	35° 02’ 13.84” North	81° 30’ 37.40” West

UNIVERSAL TRANSVERSE MERCATOR NAD83 ZONE 17 (Meters)

	Northing	Easting
UNIT 1:	3877231	453194
UNIT 2:	3877285	453447

2.1.1.1 Specification of Location

Duke Energy owns the property on which the Lee Nuclear Station is located and directs land management activities at the site. Duke Energy is the named applicant and operator for the Lee Nuclear Station. The 1900-ac. site, the area within the site boundary, is bounded by the Broad River to the north and east, by McKowns Mountain Road to the south, and private properties to the south and west (Figure 2.1-202) (References 207 and 208). There are no public transportation routes that cross the Lee Nuclear Station site (Reference 207). Duke Energy owns the mineral rights on the Lee Nuclear Station site. There are no mineral resources, including oil and natural gas, within or adjacent to the site that are being exploited or of any known value (Reference 204).

The location for the Lee Nuclear Station is an industrial site that was evaluated and licensed for the construction of three nuclear units in the 1970s. Approximately 750 ac. of ground were disturbed by this early construction, which began in 1977 and was halted in 1982. These construction activities resulted in extensive alterations of the site. The site was purchased by Earl Owensby Studios in 1986 and used for the production of a movie and commercials. The site sat idle for a number of years and was acquired in 2005 by Cherokee Falls Development Company LLC (a subsidiary of Southern Company). Duke Energy purchased all outstanding ownership shares from Cherokee Falls Development Company in early 2007.

Previous construction activities on the site left in place a large excavated area, partially constructed power unit buildings (one partially completed power block and containment/shield building), and numerous other large and small on-site buildings that were used as warehouses, shops, construction support facilities, and a guard house. Concrete pads and remnant vehicle parking areas are present at various locations on the site. These constructed surface features are linked by a system of paved roads and a related system of unpaved roads that serve peripheral areas of the site. Buried utility pipelines, overhead electric power lines, and communications lines that once served the buildings and construction areas

are still present on the site. The electrical lines are suspended by wooden poles and metal towers. An abandoned railroad spur enters the site at a point on its northern boundary, extends across the north half of the site, and ends in a former construction area. The rails have been removed, so all that remains is the graded bed of the former spur. The site contains three major surface water impoundments that were established by previous construction activities on the site. These are the large Make-Up Pond B (formerly the Standby Nuclear Service Water Pond for the canceled Cherokee Plant) on the west side of the site, Make-Up Pond A on the east side of the site, and Hold-Up Pond A on the north end of the site. The majority of the site is surrounded by chain link fences with gates.

Units 1 and 2 are (upstream) approximately 1 mi. northwest of the Ninety-Nine Islands Hydroelectric Dam. The closest communities to Lee Nuclear Station are the city of Gaffney, South Carolina (8.2 mi. northwest), the city of East Gaffney, South Carolina (7.5 mi. northwest), and the town of Blacksburg, South Carolina (5.8 mi. north) (Reference 202). According to 2005 US Census Bureau population estimates, the city of Gaffney, South Carolina had a population of 12,934 and is the largest community within 10 mi. of the Lee Nuclear Station. The city of Blacksburg, South Carolina, the second largest community within 10 mi. of the Lee Nuclear Station, had a population of 1898 (Reference 206).

The nearest population center (as defined by 10 CFR 100.3) of the Lee Nuclear Station is Gastonia, North Carolina (References 202, 203, 206). Gastonia's urban border, as defined by the US Census Bureau, is situated 16 mi. to the northeast and was estimated in 2005 to have a population of 68,964 (References 203 and 206).

Interstate 85, passing through the northern side of Gaffney, South Carolina and connecting Greenville, South Carolina and Spartanburg, South Carolina with Charlotte, North Carolina, is located approximately 7 mi. north-northwest of the site (Reference 207). There are no military facilities located within the vicinity of the Lee Nuclear Site (Reference 233).

2.1.1.2 Site Area Map

Figure 2.1-203 illustrates the region surrounding the Nuclear Site within a radius of 50 mi. This map includes prominent geophysical and political features in the area. Figure 2.1-202 shows greater detail of the Lee Nuclear Site out to a radius of 6 mi. The Lee Nuclear Station site boundary is boldly outlined. As shown in the figure, there are no industrial and transportation facilities, commercial, institutional, recreational, and residential structures within the site area. Figure 2.1-204 is a USGS topographic map that shows prominent natural and manmade features. Figure 2.1-201 illustrates the site in greater detail. The reactor building, turbine building, and the cooling towers are labeled. The auxiliary buildings are shown in the background. Figure 2.1-209 illustrates the shortest distances from the Effluent Release Boundary to the EAB.

The total area contained by the site boundary is about 1,900 acres of land. There are no industrial, military, transportation facilities, commercial, institutional, recreational, or residential structures within the site area. The EAB generally

follows the site boundary (but extends beyond it on the northern and eastern sides of the site). The Effluent Release Boundary is an assumed 550 ft. radius circle encompassing all site release points. Figure 2.1-209 shows the location of the EAB and the shortest distances from the Effluent Release Boundary. The nearest segment of the EAB to the Effluent Release Boundary is 2113 feet.

2.1.1.2.1 Boundaries for Establishing Effluent Release Limits

There are no residents in the Exclusion Area. No unrestricted areas within the site boundary area are accessible to members of the public. Access within the site boundary is controlled as described in FSAR Section 2.1.2. FSAR Section 2.3 provides details on gaseous release points and their relation to the site boundary. The discussion of normal releases (gaseous and aqueous) are in FSAR Sections 11.2 and 11.3, and accidental releases are discussed in FSAR Chapter 15. All areas outside the exclusion area are unrestricted areas in the context of 10 CFR Part 20. Additionally, the guidelines provided in 10 CFR Part 50 Appendix I, for radiation exposures to meet the criterion "as low as is reasonably achievable" are applied at the Protected Area boundary. For the Lee Nuclear Station, the Restricted Area is the same as the Protected Area. Figure 2.1-201 shows the Protected Area Boundary. For Lee Nuclear Station, the Protected Area is the fenced area surrounding the reactor buildings. It contains all of the buildings required for the operation of the reactor with the exception of the cooling towers (See Figure 2.1-201 for the location of the buildings required for the operation of the reactor).

WLS COL 2.1-1

2.1.2 EXCLUSION AREA AUTHORITY AND CONTROL

The boundary on which limits for the release of radioactive effluents are based is the exclusion area boundary shown in Figure 2.1-209. The site is clearly posted with no trespassing signs that also include actions to be taken in the event of emergency conditions at the plant. The site's physical security plan contains information on actions to be taken by security force personnel in the event of unauthorized persons crossing the EAB during emergency operations.

2.1.2.1 Authority

All of the land inside the Exclusion Area is owned by Duke Energy. Duke Energy controls all activities within the exclusion area boundary including exclusion and removal of personnel from the area during emergency operations. Duke Energy owns the mineral rights on the Lee Nuclear Site. There are no known easements that affect the Lee Nuclear Station.

2.1.2.2 Control of Activities Unrelated to Plant Operation

There are no residences, unauthorized commercial activities, and only limited recreational activities within the Exclusion Area. These recreational activities are limited to the Broad River, which crosses the EAB on the northern and eastern sides of the site. No public highways or active railroads traverse the exclusion area. There are four historical cemeteries within the site boundary. Access to these cemeteries is controlled by security personnel.

2.1.2.3 Arrangements For Traffic Control

Arrangements with Cherokee County for control of traffic in the event of an emergency is not required in that no publicly used transportation modes cross the EAB.

2.1.2.4 Abandonment or Relocation of Roads

There are no public roads presently within the Exclusion Area which, because of their location, have to be abandoned or relocated.

WLS COL 2.1-1

2.1.3 POPULATION DISTRIBUTION

To project total population for the Lee Nuclear Station Region, three Geographical Information System (GIS) mapping processes are used to produce a series of population tables. The first process converts US Census block data to sector data geography, the second process converts county level population projections to sector level data, and the third converts transient population data to sector level data. The data tables produced provide population values that correspond to the geographic area defined by radial distance from the Lee Nuclear Station site center point and 16 compass point directions. These tables correspond directly to the distances and directions displayed in Figure 2.1-205 and Figure 2.1-206.

A sector is defined as an area between two radial distances and two angular lines from a point. In the case of Lee Nuclear Station the radial distances are defined in NUREG-1555, the two angles form a wedge based on each of the 16 compass points and the center point is the designated site center point. Using NUREG-1555 as a guideline, GIS software produced shapefile, called a sector grid, is produced containing sectors in every direction. The population distribution is estimated in nine concentric radial bands at 0 to 2 km (1.24 mi.), 2 to 4 km (2.5 mi.), 4 to 6 km (3.7 mi.), 6 to 8 km (5 mi.), 8 to 10 km (6.2 mi.), 10 to 16 km (10 mi.), 16 to 40 km (25 mi.), 40 to 60 km (37 mi.), and 60 to 80 km (50 mi.) from the designated site center point between the two reactors. These bands are then subdivided into 16 directional sectors centered on the 16 compass points, with each direction consisting of 22.5 degrees as defined in NUREG-1555.

To display all sectors defined by the directions and distances, two maps were produced. Population sectors for 0 to 16 km (10 mi.) are shown in Figure 2.1-206 and 16 to 80 km (50 mi.) in Figure 2.1-205. To convert US Census Block data to sector data, the sector grid shapefile is overlaid onto the census block shapefile, and the shapefiles are integrated. US Census blocks that have been bisected by the sector grid are area weighted. The values falling within each sector are summed. The resulting data has an unrounded population value for each sector for the year 2000. The population distribution surrounding the Lee Nuclear Site, up to an 80-km (50-mi.) radius, is estimated based upon the most recent US Census Bureau decennial census data (Reference 218).

Many states establish official population projections, and county projection information is available from a state's official on-line source. These population projections are used for economic development and planning purposes. Both

North Carolina and South Carolina have population projection data available for specific years for every county in their respective state. North Carolina and South Carolina have projected county populations to 2030. The population projections for both states are derived from county estimates and based on the cohort-component method (References 209 and 232). The data set is reduced to the counties located within, or partially within the region. The plot of this data set illustrates a linear trend for all of the counties in the region. Due to this trend, a least squares linear regression is applied to the counties and an equation is produced for each county. These equations are then used to calculate population estimates for the years not projected by the state. The resulting values from the equations are used in conjunction with the 2000 census data to produce a growth ratio, or index, for each year and each county included in the region. The data is then joined to a county shapefile using GIS. The county indexes are area weighted by sector and summed for each sector, producing a population growth index by sector. For any county with a negative growth rate, a growth ratio of one is used to produce the most conservative results without overestimating. Using a growth ratio of one does not allow the county's population to decline.

The transient population data is collected by location. These locations are converted to points and areas, and using GIS, integrated into the sector polygon. Any area that is bisected by the sector grid is area weighted. The values falling within each sector are summed. The resulting data is the un-rounded transient sector population for the region.

The US Census based sector data (Block 2000) or the transient sector population is multiplied by these indices for each year of interest. Population tables are then generated for each sector and year of interest. Each sector is listed by compass direction and furthest radial distance. Tables 2.1-203 and 2.1-204 correspond to Figures 2.1-205 and 2.1-206 by compass direction and radial distance.

The commercial operation date was initially estimated to be 2016, but has been revised to approximately 2021. The FSAR evaluations are based on 2016; however, Duke Energy has evaluated the change and has determined that it is not significant.

2.1.3.1 Population Within 10 Miles

Figure 2.1-207 shows a portion of the study area within 16 km (10 mi.) of the site center point. The map contains roads, railroads, nearby towns, and counties. Based on the 2000 US Census Bureau estimates the populations of the towns within the 16-km (10-mi.) area are shown in Table 2.1-202.

Table 2.1-203 shows the projected permanent population for each sector and projections for 2007, 2016, 2026, 2036, 2046, and 2056. The distances defining the sectors are 0 to 2 km (1.24 mi.), 2 to 4 km (2.5 mi.), 4 to 6 km (3.7 mi.), 6 to 8 km (5 mi.), 8 to 10 km (6.2 mi.), and 10 to 16 km (10 mi.). These sectors can be seen in Figure 2.1-206. The projections were carried out to 40 years past the initially estimated startup date of 2016. The population in the 16-km (10-mi.) area is shown in the "Cumulative Totals" field of Table 2.1-203 for each projected year.

The percent of the 16-km (10-mi.) permanent population within 8 km (5 mi.) is 12.1 percent for all years of projection.

2.1.3.2 Population Between 10 and 50 Miles

Figure 2.1-205 illustrates a portion of the study area within 80 km (50 mi.) of the site center point. The map contains the sector grid, county boundaries, state boundaries and bodies of water. The distances defining the sectors are 16 km (10 mi.) to 40 km (25 mi.), 40 to 60 km (37 mi.), and 60 to 80 km (50 mi.). Charlotte, North Carolina is the largest city within the 80-km (50-mi.) area. Based on the 2005 US Census Bureau estimates, the population of Charlotte, North Carolina is 610,949. Smaller cities within the 80-km (50-mi.) area include Gastonia, North Carolina; Greenville, South Carolina; Hickory, North Carolina; Rock Hill, South Carolina; and Spartanburg, South Carolina. Based on the 2005 US Census Bureau estimates their populations are 68,964, 56,676, 40,232, 59,554, and 38,379 respectively. Many other small towns, cities, and urban areas with populations less than 25,000 are distributed within the 80-km (50-mi.) area. The cities of Concord, North Carolina and Monroe, North Carolina have very small portions inside the 80-km (50-mi.) area. Both of these cities have population in excess of 25,000 (References 202 and 206).

Table 2.1-204 shows the projected permanent population for each sector and projections for 2007, 2016, 2026, 2036, 2046, and 2056. Again, the projections were carried out 40 years past the initially estimated startup date of 2016 for Unit 1. The number of people in the 16-km (10-mi.) to 80-km (50-mi.) area is shown in the “Cumulative Totals” field of the table for each projected year.

2.1.3.3 Transient Population

Transient population within the region of the Lee Nuclear Station is influenced by several factors. Shopping generates the most transients within 10 mi. of the Lee Nuclear Site. Natural attractions generate most of the remainder of visitors to the 50-mi. region, with the exception of Christmastown USA in McAdenville, North Carolina which gets over 600,000 visitors between December 1st and December 26th annually. McAdenville, North Carolina is approximately 30 mi. from the Lee Nuclear Station.

The city boundaries of Charlotte, North Carolina are enclosed by the Lee Nuclear Site regional boundary. Museums and science attractions make up the bulk of transients in that portion of the region.

Transient data were gathered through personal contact with businesses, companies, and local chambers of commerce within the region. This method for collecting transient data provides a more accurate accounting of people visiting the area and a much more precise location of transient contributors than using county estimates weighted over a sector area. Data out to 15 mi. were collected in accordance with regulation for the EPZ. Major contributors to transient population are listed in Table 2.1-205. Unless otherwise noted, all transient population data are from 2006.

To project the transient information, the transient data per sector were summed. The summed number was multiplied by the sector growth ratio derived from the county growth ratios described above for each year. Because the method for collecting transient data provides point locations, some sectors have a zero value. This is because there are no accountable transient contributors in the zero value sectors. Table 2.1-208 illustrates the projected transient population for each sector and projections for 2007, 2016, 2026, 2036, 2046, and 2056 for the non-zero sectors (References 209, 211, 230, 231, and 232). The projections were carried out to 40 years past the initially estimated startup date of 2016. The sectors that have zero values are not illustrated in this table.

2.1.3.3.1 Transient Population Within 10 Miles

The Prime Outlets at Gaffney, South Carolina is the single largest tourist draw in the area of the Lee Nuclear Site, located approximately 11.7 mi. from the station center point. The Prime Outlets get a average of 7671 shoppers per day or over 2.8 million visitors per year. Forty-six percent of the shoppers are from South Carolina and 54 percent are from out-of-state (Reference 211).

The city of Gaffney, South Carolina is 8 mi. from the Lee Nuclear Site and hosts several events throughout the year (Reference 202). These include the South Carolina Peach Festival and Christmas on Limestone. Each of these events can host between 2,000 and 2,500 people per day during the event. The peach festival can last from five to ten days and the Christmas celebration is a one day event.

2.1.3.3.2 Transient Population Between 10 and 50 Miles

There are three commercial passenger airports within the region: Charlotte-Douglas International Airport (34 mi.) to the northeast, Greenville-Spartanburg International Airport (41 mi.) to the southwest, and Hickory Regional Airport (49 mi.) to the north. (Reference 207). The daily and annual passenger counts for these three airports are shown in Table 2.1-206 (References 213, 214, and 215).

Amtrak has passenger train stations in Spartanburg, South Carolina, Charlotte, North Carolina, and Gastonia, North Carolina. Amtrak also has trackage rights on all rails within the region, meaning that there is a possibility that any rail section can be used to move passengers from one station to another (References 207 and 216).

Charlotte's Thunder Road Marathon occurs every December and includes a marathon, half marathon, marathon relay, and a 5K race. Nearly 4,200 runners entered the 2006 events. This course winds through some of the city's most historic and eclectic neighborhoods before finishing in Uptown Charlotte (Reference 205).

Paramount's Carowinds Theme Park, located in Charlotte, North Carolina, had a 2002 annual attendance of 1.85 million visitors (Reference 234).

The Bank of America Stadium, home to the NFL's Carolina Panthers, has a capacity of 73,248 and a 2006 annual attendance of 587,700 people (Reference 235). The Bobcats Arena, home to the NBA's Charlotte Bobcats, has a capacity of 18,500 and a 2006-2007 season attendance of 637,520 people (Reference 236). Both of these facilities are located in Charlotte, North Carolina.

2.1.3.3.2.1 Recreational Transients

The nearest park to the proposed site is the Kings Mountain State Park, located approximately 8 mi. northeast of the Lee Nuclear Site center point. Other attractions near the Lee Nuclear Site are Cowpens National Battlefield, Kings Mountain National Military Park, and the Prime Outlets of Gaffney, South Carolina. The nearest of these are Cowpens National Battlefield and the Prime Outlets of Gaffney, South Carolina, both located in Gaffney, South Carolina. The Kings Mountain National Military Park immediately adjoins Kings Mountain State Park on its northwest border. A portion of the Francis Marion – Sumter National Forest falls within the region and accounts for an average of almost 3,000 visitors per day (References 211, 217, 219, and 220).

The U.S. National Whitewater Center in Charlotte, North Carolina is home to the world's largest manmade whitewater river and attracts approximately 500,000 visitors a year (Reference 237).

Fishing, hunting, and wildlife watching in the portions of North Carolina and South Carolina included in the region are an important recreational pastime, as shown in Table 2.1-207. The combined wildlife related activities attract approximately 704,901 outdoor enthusiasts per year (References 221 and 222).

2.1.3.3.2.2 Seasonal Populations

Many of the attractions within the vicinity of the Lee Nuclear Site are based around outdoor activities. The peak times for these attractions, with the highest visitor numbers, occur from spring through mid-fall. The lowest levels occur during the winter months.

2.1.3.3.2.3 Transient Workforce

An estimated 4512 workers are required on site at the peak construction phase to complete the facility. In 2000, for the six counties surrounding the site, there was a total of just over 25,607 properties available, including homes for sale and rental properties[a]. (References 223 and 224)

a. The six counties are Cherokee, Union, Spartanburg, and York in South Carolina and Cleveland and Gaston in North Carolina.

2.1.3.3.2.4 Special Facilities (Schools, Hospitals, Nursing Homes, etc.)

There are 33 2-year and 4-year colleges and universities within the region of the Lee Nuclear Site. Total enrollment for these schools is more than 98,145 students (References 225 and 226). The 2-year and 4-year colleges and universities in the region are typically near peak daily capacity for the majority of the year, excluding the summer months (mid-May through mid-August). Even with this educational reduction during the summer months, overall peak levels of transients are thought to still occur over that time period.

There are thirty-two major hospitals and medical centers within 50 mi. of Lee Nuclear Site. These medical facilities have a combined capacity of 5,558 staffed beds and discharge more than 260,810 patients per year. The two closest major medical facilities to the Lee Nuclear Site are Upstate Carolina Medical Center in Gaffney, South Carolina and Kings Mountain Hospital in Kings Mountain, North Carolina. These two facilities account for 125 beds, 4442 annual discharges and 42 beds, 1949 annual discharges, respectively. The largest medical facility within the region is Carolinas Medical Center in Charlotte, North Carolina with 743 beds and more than 41,858 patient discharges annually (References 227 and 228).

The two nearest nursing home facilities to the Lee Nuclear Site are Brookview HealthCare Center and Cherokee County Long Term Care Facility. Brookview HealthCare Center is located in Gaffney, South Carolina and has a 132-bed capacity. Cherokee County Long Term Care Facility, also known as Peachtree Healthcare Center, also located in Gaffney, South Carolina, has a 145-bed capacity. The city of Spartanburg, South Carolina, has several nursing home facilities (Reference 229).

There are no federal prison facilities located within the Lee Nuclear Site Region (References 238 and 239). Eleven state correctional facilities are located within the Lee Nuclear Site region, three in South Carolina and eight in North Carolina (References 201 and 240).

2.1.3.3.3 Total Permanent and Transient Populations

The annual total of the special facilities and the transient populations within the region is approximately 10,316,432 people.The estimated 2007 summed transient population on any given day within the region is calculated to be 71,869[b] (References 211, 219, 230, and 231). The estimated permanent population for 2007 for the region (the sum of entries in Tables 2.1-203 and 2.1-204) is 2,382,474 people (Reference 218). The estimated 2007 total population within the region at any one time is calculated to be approximately 2,454,343 people.

b. The daily total includes numbers from Christmastown USA that runs from December 1st through December 26th only. If this number is averaged out for the whole year the average number of transients per day drops to 41,780.

2.1.3.3.4 Transient Populations Outside the 50-Mile Region

There are two facilities located beyond the 50-mile radius, the Lowe's Motor Speedway and Concord Mills Mall. The Lowe's Motor Speedway is located approximately 51 mi. northeast of Lee Nuclear Site and attracts approximately 1.2 million people a year for events, tours, and driving schools. The peak months are May and October when the NASCAR NEXTEL Cup races occur. Concord Mills Mall is located approximately 51 mi. northeast of the site and reports over 17.6 million visitors a year. Their peak months are June and December.

2.1.3.4 Low-Population Zone

At Lee Nuclear Site, the Low Population Zone (LPZ) is defined as a two mile radius from the site center point. The center point is defined as the midway point between Unit 1 and Unit 2. Using this radius, there are only rural areas and the Lee Nuclear Station within the LPZ (See Figure 2.1-208).

According to the US Census Bureau 2000 data, there are 509 people living within the LPZ, distributed generally to the north and south of the site (see Table 2.1-209). There are no major contributors to the transient population in this area. This area is serviced by McKowns Mountain Road which is routed through the LPZ. No other major transportation features exist in the LPZ. There are no schools, hospitals, prisons, beaches, or parks in the LPZ. There are no facilities within 5 mi. that require special consideration such as hospitals, prisons, jails, or any other (trapped) populations.

The estimated Lee Nuclear Station workforce population is estimated at 957 people, causing the daily permanent population density within the LPZ to go from 41 people per square mile to 117 people per square mile.

At the projected end of Unit 1 reactor operation (2056), the expected permanent population of the LPZ is 880 giving a density value of 70 people per square mile. Combining this number with the estimated Lee Nuclear Station employee number, the total population is 1837 and the LPZ population density becomes 146 people per square mile.

2.1.3.5 Population Center

The nearest population center, as defined by 10 CFR 100.3, is Gastonia, North Carolina. The distance to Gastonia's urban boundary, as defined by US Census Tiger files, is 16 mi. northeast from the center point between the two reactors (Reference 203). By using the county population projection ratios, the population of the city of Shelby, North Carolina may exceed 25,000 in approximately 2045. When this occurs, it is expected to be the nearest population center at a distance of 14.3 mi. north from the center point between the two reactors.

Incorporating transient population into the estimates and projecting the population for both transient and permanent population results in Gaffney, South Carolina having a total population number greater than 25,000 people. Gaffney's closest boundary, defined by the US Census Bureau, is 6 mi. northwest from the center

point between the two reactors. All of these distances are greater than one and one third times the distance from the reactor center point to the boundary of the low population zone as required by NUREG-0800 and complies to the guidance provided by Regulatory Guide 4.7.

2.1.3.6 Population Density

The projected permanent population of the Lee Nuclear Station region was added to the projected transient population producing the total population. These values were plotted as a function of distance from the center point on Graphs 2.1-1, 2.1-2, 2.1-3 in Figure 2.1-210 for the initially estimated first year of operation (2016), about five years after the first year of operation, and the initially estimated projected final year of operation (2056), respectively. These dates used for projecting the population data were obtained from guidance current at the time of analysis. Recently the dates suggested in the guidance have changed. Since negative growth rates were held steady (see Subsection 2.1.3), the reported information is conservative. Plotted on Graph 2.1-1 and 2.1-2 in Figure 2.1-210 is the cumulative population that would result from a uniform population density of 500 people per square mile. Graph 2.1-3 of Figure 2.1-210 contains a similar plot except it contains a plot for a uniform population density of 1,000 people per square mile.

The projected permanent population for 2016 is 2,715,444 and the projected transient population for 2016 is 78,800. Transient population was projected using a ratio generated from transient sector population divided by the US Census Bureau 2000 population. The projected permanent population for years 2016, 2021, and 2056 were multiplied by this ratio to calculate the projected transient population. Thusly, the projected total population within an 80-km (50-mi.) radius for 2016 is 2,794,244 people. The total population density for the startup year is 360 people per square mile.

The projected total population within an 80-km (50-mi.) radius in 2021, about five years after the startup year for the plant, is 2,983,613. This includes the projected permanent population (2,899,824 people) and the projected transient population (83,789 people). The total population density is projected to be 384 people per mile.

The projected total population within an 80-km (50-mi.) radius in 2056, the projected Unit 1 end of licensing year for the plant, is 4,314,056. This includes the projected permanent population (4,195,335 people) and the projected transient population (118,721 people). The total population density in 2056 is projected to be 556 people per square mile.

The population density values in the region are within the values stated in NUREG-0800, Regulatory Guide 1.206, Regulatory Guide 1.70, and Regulatory Guide 4.7.

STD DEP 1.1-1

2.1.4 COMBINED LICENSE INFORMATION FOR GEOGRAPHY AND DEMOGRAPHY

WLS COL 2.1-1 This COL item is addressed in Section 2.1 and Subsections 2.1.1, 2.1.2, and 2.1.3.

2.1.5 REFERENCES

201. North Carolina Department of Correction, North Carolina Prisons Listed by County, Website, http://www.doc.state.nc.us/DOP/list/county.htm, accessed December 12, 2006.

202. USGS Geographic Names Information System (GNIS), Website, http://geonames.usgs.gov/domestic/download_data.htm, accessed on August 8, 2006.

203. US Census Bureau 2000, “TIGER/Line Shapefiles for South Carolina and North Carolina,” ESRI ArcData, Website, http://www.census.gov/geo/www/tiger/, accessed on August 8, 2006.

204. USGS “Active Mines and Mineral Processing Plants in the United States 2003,” Website, http://tin.er.usgs.gov/mineplant/, accessed on August 10, 2006.

205. Thunder Road Marathon, "Race News", website, http://www.runcharlotte.com/racenews.htm, accessed on January 23, 2007.

206. US Census Bureau, “American FactFinder,” Website http://factfinder.US Census.gov/servlet/SAFFPopulation?_submenuId=population_0&_sse=on, accessed on July 26, 2006.

207. US Department of Transportation, “National Transportation Atlas Databases (NTAD) 2005 Shapefile Format,” CD-ROM.

208. National Hydrography Dataset (NHD), “Medium Resolution NHD Dataset,” Website, http://nhdgeo.usgs.gov/viewer.htm, accessed on August 10, 2006.

209. South Carolina State Budget and Control Board, South Carolina Population Projections 2005-2030, Website http://www.ors2.state.sc.us/population/proj2030.asp, accessed June 19, 2006.

210. USGS, USGS Quad Blacksburg South, SC, North American Datum 1927.

211. Grubb & Ellis, The Furman Company, Restaurant & Big Box Retail Pad Sites at Prime Outlets Mall, Website, http://www.furmanco-commercial.com/pdfs/FactoryShopsGaffney%20Site2360.pdf, accessed October 15, 2006.

212. USGS, USGS Quad Kings Creek, SC, North American Datum 1927.

213. Bureau of Transportation Statistics, TranStats, Charlotte, North Carolina – Douglas Municipal, Airport Fact Sheet, Website, http:// www.transtats.bts.gov/ airports.asp?pn=1&Airport=CLT&Airport_Name=Charlotte, accessed October 3, 2006.

214. Bureau of Transportation Statistics, TranStats, Greenville/Spartanburg, South Carolina – Greenville-Spartanburg Airport, Airport Fact Sheet, Website, http://www.transtats.bts.gov/ airports.asp?pn=1&Airport=GSP&Airport_Name=Greenville, accessed October 3, 2006.

215. Bureau of Transportation Statistics, TranStats, Hickory, NORTH CAROLINA – Hickory Municipal Airport, Airport Fact Sheet, Website, http:/ /www.transtats.bts.gov/ airports.asp?pn=1&Airport=HKY&Airport_Name=Hickory, accessed on October 3, 2006.

216. Amtrak, Rail Stations by Region – South, Website, http://www.amtrak.com/ servlet/ContentServer?pagename=Amtrak/Page/ Browse_Stations_Page&c=Page&cid=1081256321449&ssid=78, accessed October 10, 2006.

217. Kings Mountain National Military Park, Website, http://www.nps.gov/kimo/ home.htm, accessed on August 24, 2006.

218. US Census Bureau, Census 2000 SF1 Data, Obtained from: http:// www.census.gov/Press-Release/www/2001/sumfile1.html, accessed on September 15, 2006.

219. Kings Mountain State Park, Camping, Website, http:// www.southcarolinaparks.com/park-finder/state-park/945/camping.aspx, accessed on September 25, 2006.

220. US Department of Agriculture, National Visitor Use Monitoring Results – Francis Marion & Sumter National Forests, USDA Forest Service Region 8.

221. US Fish and Wildlife Service, 2001 National Survey of Fishing, Hunting, and Wildlife-Associated Recreation – North Carolina, March 2003 (Revised).

222. US Fish and Wildlife Service, 2001 National Survey of Fishing, Hunting, and Wildlife-Associated Recreation – South Carolina, March 2003 (Revised).

223. US Census Bureau, 2000 Census of Population and Housing, Summary Population and Housing Characteristics, PHC-1-35, North Carolina, Washington, DC, 2002.

224. US Census Bureau, 2000 Census of Population and Housing, Summary Population and Housing Characteristics, PHC-1-42, South Carolina, Washington, DC, 2002.

225. College Toolkit: Colleges and Universities in North Carolina, Website, http://www.collegetoolkit.com/Colleges/State/37.aspx, accessed October 3, 2006.

226. College Toolkit: Colleges and Universities in South Carolina, Website, http://www.collegetoolkit.com/Colleges/State/45.aspx, accessed October 3, 2006.

227. American Hospital Directory, Individual Hospital Statistics for North Carolina, URL http://www.ahd.com/states/hospital_NC.html, accessed October 3, 2006.

228. American Hospital Directory, Individual Hospital Statistics for South Carolina, URL http://www.ahd.com/states/hospital_SC.html, accessed October 3, 2006.

229. NursinghomeINFO, Results near Gaffney, South Carolina, Website, http://www.nursinghomeinfo.com/nw/temp/nw1010111915.htm, accessed October 10, 2006.

230. North Carolina Department of Commerce, Top Attractions in North Carolina, website, http://www.nccommerce.com/tourism/top/, accessed on October 3, 2006.

231. South Carolina Department of Parks, Recreation and Tourism - State Parks Service, South Carolina Statistical Abstract - State Parks Visitation (Fiscal Year 2004-05, website, http://www.ors2.state.sc.us/abstract/chapter15/recreation8.asp, accessed on November 16, 2006.

232. North Carolina Office of State Budget and Management, Population Overview: 2000-2030, Website http://demog.state.nc.us/demog/pop0030.html, accessed June 20, 2006.

233. US Department of the Interior – National Park Service, “Military Bases in the Continental United States,” Website, http://www.cr.nps.gov/nagpra/DOCUMENTS/BasesMapIndex.htm, accessed on May 19, 2006.

234. Charlotte Business Journal, "Carowinds coasts into new season with regional draw", May 23, 2003.

235. Ballparks.com, Bank of America Stadium, website, http://football.ballparks.com/NFL/CarolinaPanthers/index.htm, accessed September 20, 2007.

236. Ballparks.com, The Charlotte Bobcats Arena, website, http://basketball.ballparks.com/NBA/CharlotteBobcats/index.htm, accessed September 20, 2007.

237. Recreation Management, "Turn on the Tap - U.S. National Whitewater Center in Charlotte, N.C.", website, http://www.recmanagement.com/200702fp01.php, accessed September 20, 2007.

238. Federal Bureau of Prisons, Map of Facilities – Mid-Atlantic Region, Website, http://bop.gov/locations/maps/MXR.jsp, accessed December 12, 2006.

239. Federal Bureau of Prisons, Map of Facilities – Southeast Region, Website, http://bop.gov/locations/maps/SER.jsp, accessed December 12, 2006.

240. South Carolina Department of Corrections, SCDC Institutions, Website, http://www.doc.sc.gov/InstitutionPages/Institutions.htm, accessed December 12, 2006.

TABLE 2.1-201
COUNTIES ENTIRELY OR PARTIALLY LOCATED WITHIN THE
LEE NUCLEAR STATION 50-MI. BUFFER

North Carolina Counties		South Carolina Counties	
Burke	Lincoln	Cherokee	Laurens
Cabarrus	McDowell	Chester	Newberry
Catawba	Mecklenburg	Fairfield	Spartanburg
Cleveland	Polk	Greenville	Union
Gaston	Rutherford	Lancaster	York
Henderson	Union		
Iredell			

Reference 203

TABLE 2.1-202
US CENSUS BUREAU ESTIMATED YEAR 2000 POPULATIONS
WITHIN A 10-MI. RADIUS

Populated Places	Year 2000 Population
Gaffney, South Carolina	12,968
East Gaffney, South Carolina	3,349
Blacksburg, South Carolina	1,880
Smyrna, South Carolina	59
Hickory Grove, South Carolina	337
Grover, North Carolina	698

References 202 and 206

TABLE 2.1-203 (Sheet 1 of 6)
THE PROJECTED PERMANENT POPULATION FOR EACH SECTOR 0- TO 16-KM (0 TO 10–MI.) FOR YEARS 2007, 2016, 2026, 2036, 2046, AND 2056

	Sector						
Direction/Year	0-2 (km)	2-4 (km)	4-6 (km)	6-8 (km)	8-10 (km)	10-16 (km)	0-16 (km)
North							
2007	18	82	183	473	1,976	1,445	4,177
2016	20	90	201	517	2,160	1,569	4,557
2026	22	98	220	566	2,365	1,706	4,977
2036	24	107	239	616	2,570	1,844	5,400
2046	26	115	258	665	2,775	1,981	5,820
2056	28	124	277	714	2,980	2,119	6,242
NNE							
2007	16	67	131	162	247	1,500	2,123
2016	17	74	143	178	270	1,635	2,317
2026	19	81	157	194	295	1,786	2,532
2036	20	88	170	211	321	1,937	2,747
2046	22	95	184	228	346	2,089	2,964
2056	24	102	197	245	372	2,240	3,180
NE							
2007	15	50	67	99	335	466	1,032
2016	17	55	73	108	366	518	1,137
2026	18	60	80	118	401	576	1,253
2036	20	65	87	129	436	635	1,372
2046	21	71	94	139	471	693	1,489
2056	23	76	101	149	505	751	1,605

NOTE:
1. Based on 2000 Census data (Reference 218)

TABLE 2.1-203 (Sheet 2 of 6)
THE PROJECTED PERMANENT POPULATION FOR EACH SECTOR 0- TO 16-KM (0 TO 10–MI.) FOR YEARS 2007, 2016, 2026, 2036, 2046, AND 2056

	Sector						
Direction/Year	0-2 (km)	2-4 (km)	4-6 (km)	6-8 (km)	8-10 (km)	10-16 (km)	0-16 (km)
ENE							
2007	12	21	24	163	299	854	1,373
2016	13	23	26	179	327	979	1,547
2026	14	25	29	196	359	1,119	1,742
2036	15	27	31	213	391	1,259	1,936
2046	17	29	34	230	423	1,399	2,132
2056	18	32	37	247	454	1,539	2,327
EAST							
2007	11	22	16	41	122	583	795
2016	12	25	18	47	140	671	913
2026	13	29	21	54	159	769	1,045
2036	15	32	23	61	179	867	1,177
2046	16	36	26	68	198	965	1,309
2056	17	39	29	74	218	1,063	1,440
ESE							
2007	4	21	37	80	70	464	676
2016	4	24	42	92	81	535	778
2026	4	28	48	105	93	613	891
2036	5	31	54	119	105	691	1,005
2046	5	34	61	132	116	769	1,117
2056	5	38	67	146	128	847	1,231

NOTE:
1. Based on 2000 Census data (Reference 218)

TABLE 2.1-203 (Sheet 3 of 6)
THE PROJECTED PERMANENT POPULATION FOR EACH SECTOR 0- TO 16-KM (0 TO 10–MI.) FOR YEARS 2007, 2016, 2026, 2036, 2046, AND 2056

	Sector						
Direction/Year	0-2 (km)	2-4 (km)	4-6 (km)	6-8 (km)	8-10 (km)	10-16 (km)	0-16 (km)
SE							
2007	1	23	20	38	141	876	1,099
2016	1	26	23	44	163	1,009	1,266
2026	2	29	27	50	187	1,157	1,452
2036	2	32	30	57	210	1,304	1,635
2046	2	35	33	63	234	1,451	1,818
2056	2	37	37	70	258	1,599	2,003
SSE							
2007	7	44	13	18	31	177	290
2016	8	49	14	20	35	202	328
2026	9	53	16	23	40	231	372
2036	9	58	17	25	45	260	414
2046	10	62	18	27	50	288	455
2056	11	67	20	29	55	317	499
SOUTH							
2007	10	57	30	84	44	132	357
2016	11	62	32	91	48	144	388
2026	12	68	35	100	53	158	426
2036	13	74	39	109	58	172	465
2046	14	80	42	117	62	186	501
2056	15	86	45	126	67	200	539

NOTE:
1. Based on 2000 Census data (Reference 218)

TABLE 2.1-203 (Sheet 4 of 6)
THE PROJECTED PERMANENT POPULATION FOR EACH SECTOR 0- TO 16-KM (0 TO 10–MI.) FOR YEARS 2007, 2016, 2026, 2036, 2046, AND 2056

	Sector						
Direction/Year	0-2 (km)	2-4 (km)	4-6 (km)	6-8 (km)	8-10 (km)	10-16 (km)	0-16 (km)
SSW							
2007	7	41	43	47	47	207	392
2016	8	44	47	52	51	226	428
2026	9	49	52	57	56	247	470
2036	10	53	56	62	61	269	511
2046	10	57	61	67	66	290	551
2056	11	61	65	72	71	312	592
SW							
2007	3	57	72	41	102	323	598
2016	3	62	79	44	111	353	652
2026	4	68	87	49	122	386	716
2036	4	74	94	53	132	420	777
2046	4	80	102	57	143	453	839
2056	5	86	109	61	153	487	901
WSW							
2007	0	65	74	89	173	1,583	1,984
2016	0	71	81	97	189	1,731	2,169
2026	0	78	88	107	207	1,895	2,375
2036	0	84	96	116	225	2,059	2,580
2046	0	91	104	125	242	2,224	2,786
2056	0	98	111	134	260	2,388	2,991

NOTE:
1. Based on 2000 Census data (Reference 218)

TABLE 2.1-203 (Sheet 5 of 6)
THE PROJECTED PERMANENT POPULATION FOR EACH SECTOR 0- TO 16-KM (0 TO 10–MI.) FOR YEARS 2007, 2016, 2026, 2036, 2046, AND 2056

	Sector						
Direction/Year	0-2 (km)	2-4 (km)	4-6 (km)	6-8 (km)	8-10 (km)	10-16 (km)	0-16 (km)
WEST							
2007	1	67	169	445	365	4,596	5,643
2016	1	73	185	487	399	5,025	6,170
2026	1	80	202	533	437	5,501	6,754
2036	1	87	220	579	475	5,978	7,340
2046	1	94	237	625	513	6,455	7,925
2056	1	101	255	671	551	6,932	8,511
WNW							
2007	4	64	275	360	664	16,266	17,633
2016	4	70	301	394	726	17,785	19,280
2026	4	76	329	431	795	19,472	21,107
2036	5	83	358	469	864	21,160	22,939
2046	5	89	386	506	933	22,847	24,766
2056	5	96	415	544	1,002	24,535	26,597
NW							
2007	4	43	142	216	293	1,784	2,482
2016	4	47	155	236	321	1,951	2,714
2026	5	52	170	259	351	2,136	2,973
2036	5	56	185	281	381	2,321	3,229
2046	5	61	200	304	412	2,506	3,488
2056	6	65	214	326	442	2,691	3,744

NOTE:
1. Based on 2000 Census data (Reference 218)

TABLE 2.1-203 (Sheet 6 of 6)
THE PROJECTED PERMANENT POPULATION FOR EACH SECTOR 0- TO 16-KM (0 TO 10–MI.) FOR YEARS 2007, 2016, 2026, 2036, 2046, AND 2056

	Sector						
Direction/Year	0-2 (km)	2-4 (km)	4-6 (km)	6-8 (km)	8-10 (km)	10-16 (km)	0-16 (km)
NNW							
2007	8	124	230	372	308	1,436	2,478
2016	9	135	251	407	336	1,568	2,706
2026	10	148	275	446	368	1,715	2,962
2036	11	161	299	484	400	1,863	3,218
2046	12	174	322	523	432	2,010	3,473
2056	13	187	346	561	464	2,157	3,728
Totals							
2007	121	848	1,526	2,728	5,217	32,692	43,132
2016	132	930	1,671	2,993	5,723	35,901	47,350
2026	146	1,022	1,836	3,288	6,288	39,467	52,047
2036	159	1,112	1,998	3,584	6,853	43,039	56,745
2046	170	1,203	2,162	3,876	7,416	46,606	61,433
2056	184	1,295	2,325	4,169	7,980	50,177	66,130

	Sector					
Cumulative Totals	0-2 (km)	0-4 (km)	0-6 (km)	0-8 (km)	0-10 (km)	0-16 (km)
2007	121	969	2,495	5,223	10,440	43,132
2016	132	1,062	2,733	5,726	11,449	47,350
2026	146	1,168	3,004	6,292	12,580	52,047
2036	159	1,271	3,269	6,853	13,706	56,745
2046	170	1,373	3,535	7,411	14,827	61,433
2056	184	1,479	3,804	7,973	15,953	66,130

NOTE:
1. Based on 2000 Census data (Reference 218)

TABLE 2.1-204 (Sheet 1 of 6)
THE PROJECTED PERMANENT POPULATION FOR EACH SECTOR 16-KM (10-MI.) – 80-KM (50-MI.) FOR YEARS 2007, 2016, 2026, 2036, 2046, AND 2056

	Sector			
Direction/Years	16-40 (km)	40-60 (km)	60-80 (km)	16-80 (km)
North				
2007	38,714	16,194	57,871	112,779
2016	40,905	17,691	62,189	120,785
2026	43,339	19,354	66,986	129,679
2036	45,773	21,017	71,784	138,574
2046	48,207	22,680	76,581	147,468
2056	50,641	24,342	81,379	156,362
NNE				
2007	30,164	43,594	71,754	145,512
2016	31,669	49,078	80,489	161,236
2026	33,340	55,171	90,195	178,706
2036	35,011	61,264	99,901	196,176
2046	36,683	67,357	109,606	213,646
2056	38,354	73,450	119,312	231,116
NE				
2007	64,806	63,972	81,956	210,734
2016	68,160	67,825	96,044	232,029
2026	71,887	72,106	111,696	255,689
2036	75,614	76,387	127,349	279,350
2046	79,341	80,668	143,002	303,011
2056	83,068	84,949	158,654	326,671

NOTE:
1. Based on 2000 Census data (Reference 218)

TABLE 2.1-204 (Sheet 2 of 6)
THE PROJECTED PERMANENT POPULATION FOR EACH SECTOR 16-KM (10-MI.) – 80-KM (50-MI.) FOR YEARS 2007, 2016, 2026, 2036, 2046, AND 2056

	Sector			
Direction/Years	16-40 (km)	40-60 (km)	60-80 (km)	16-80 (km)
ENE				
2007	33,928	123,495	444,073	601,496
2016	37,928	141,988	541,141	721,057
2026	42,374	162,536	648,994	853,904
2036	46,819	183,084	756,848	986,751
2046	51,264	203,632	864,701	1,119,597
2056	55,709	224,180	972,554	1,252,443
EAST				
2007	23,554	111,434	237,822	372,810
2016	27,121	129,708	301,029	457,858
2026	31,084	150,012	371,259	552,355
2036	35,047	170,316	441,489	646,852
2046	39,010	190,619	511,719	741,348
2056	42,973	210,923	581,949	835,845
ESE				
2007	17,869	66,163	39,213	123,245
2016	20,575	74,624	44,076	139,275
2026	23,582	84,025	49,480	157,087
2036	26,589	93,426	54,883	174,898
2046	29,595	102,827	60,287	192,709
2056	32,602	112,228	65,690	210,520

NOTE:
1. Based on 2000 Census data (Reference 218)

TABLE 2.1-204 (Sheet 3 of 6)
THE PROJECTED PERMANENT POPULATION FOR EACH SECTOR 16-KM (10-MI.) – 80-KM (50-MI.) FOR YEARS 2007, 2016, 2026, 2036, 2046, AND 2056

	Sector			
Direction/Years	16-40 (km)	40-60 (km)	60-80 (km)	16-80 (km)
SE				
2007	3,922	18,411	9,178	31,511
2016	4,393	19,143	9,594	33,130
2026	4,917	19,956	10,057	34,930
2036	5,440	20,768	10,520	36,728
2046	5,964	21,581	10,983	38,528
2056	6,487	22,394	11,446	40,327
SSE				
2007	2,172	2,690	3,603	8,465
2016	2,338	2,802	3,799	8,939
2026	2,523	2,926	4,017	9,466
2036	2,708	3,050	4,235	9,993
2046	2,892	3,174	4,453	10,519
2056	3,077	3,298	4,671	11,046
SOUTH				
2007	3,691	3,433	6,144	13,268
2016	3,739	3,455	6,487	13,681
2026	3,792	3,480	6,868	14,140
2036	3,844	3,505	7,249	14,598
2046	3,897	3,529	7,630	15,056
2056	3,949	3,554	8,012	15,515

NOTE:
1. Based on 2000 Census data (Reference 218)

TABLE 2.1-204 (Sheet 4 of 6)
THE PROJECTED PERMANENT POPULATION FOR EACH SECTOR 16-KM (10-MI.) – 80-KM (50-MI.) FOR YEARS 2007, 2016, 2026, 2036, 2046, AND 2056

	Sector			
Direction/Years	16-40 (km)	40-60 (km)	60-80 (km)	16-80 (km)
SSW				
2007	17,533	3,002	20,073	40,608
2016	17,675	3,057	21,828	42,560
2026	17,832	3,118	23,778	44,728
2036	17,989	3,179	25,728	46,896
2046	18,147	3,240	27,678	49,065
2056	18,304	3,302	29,628	51,234
SW				
2007	6,257	14,072	31,423	51,752
2016	6,510	15,173	34,451	56,134
2026	6,792	16,396	37,815	61,003
2036	7,074	17,619	41,180	65,873
2046	7,355	18,842	44,544	70,741
2056	7,637	20,065	47,909	75,611
WSW				
2007	44,615	69,520	156,415	270,550
2016	48,564	75,559	171,892	296,015
2026	52,951	82,270	189,088	324,309
2036	57,338	88,981	206,285	352,604
2046	61,725	95,691	223,482	380,898
2056	66,113	102,402	240,679	409,194

NOTE:
1. Based on 2000 Census data (Reference 218)

TABLE 2.1-204 (Sheet 5 of 6)
THE PROJECTED PERMANENT POPULATION FOR EACH SECTOR 16-KM (10-MI.) – 80-KM (50-MI.) FOR YEARS 2007, 2016, 2026, 2036, 2046, AND 2056

	Sector			
Direction/Years	16-40 (km)	40-60 (km)	60-80 (km)	16-80 (km)
WEST				
2007	33,913	68,076	86,269	188,258
2016	36,930	73,990	94,905	205,825
2026	40,282	80,561	104,500	225,343
2036	43,634	87,132	114,095	244,861
2046	46,986	93,703	123,691	264,380
2056	50,338	100,275	133,286	283,899
WNW				
2007	17,054	12,829	21,303	51,186
2016	18,498	14,027	23,784	56,309
2026	20,103	15,358	26,541	62,002
2036	21,707	16,690	29,298	67,695
2046	23,312	18,022	32,055	73,389
2056	24,917	19,353	34,812	79,082
NW				
2007	14,322	38,107	11,067	63,496
2016	15,131	39,630	11,664	66,425
2026	16,029	41,322	12,327	69,678
2036	16,928	43,013	12,991	72,932
2046	17,827	44,705	13,654	76,186
2056	18,725	46,397	14,318	79,440

NOTE:
1. Based on 2000 Census data (Reference 218)

TABLE 2.1-204 (Sheet 6 of 6)
THE PROJECTED PERMANENT POPULATION FOR EACH SECTOR 16-KM (10-MI.) – 80-KM (50-MI.) FOR YEARS 2007, 2016, 2026, 2036, 2046, AND 2056

	Sector			
Direction/Years	16-40 (km)	40-60 (km)	60-80 (km)	16-80 (km)
N-NW				
2007	18,177	7,787	27,708	53,672
2016	19,200	8,145	29,491	56,836
2026	20,337	8,542	31,473	60,352
2036	21,474	8,940	33,455	63,869
2046	22,611	9,338	35,437	67,386
2056	23,747	9,735	37,418	70,900
Totals				
2007	370,691	662,779	1,305,872	2,339,342
2016	399,336	735,895	1,532,863	2,668,094
2026	431,164	817,133	1,785,074	3,033,371
2036	462,989	898,371	2,037,290	3,398,650
2046	494,816	979,608	2,289,503	3,763,927
2056	526,641	1,060,847	2,541,717	4,129,205

	Sector		
Cumulative Totals	16-40 (km)	16-60 (km)	16-80 (km)
2007	370,691	1,033,470	2,339,342
2016	399,336	1,135,231	2,668,094
2026	431,164	1,248,297	3,033,371
2036	462,989	1,361,360	3,398,650
2046	494,816	1,474,424	3,763,927
2056	526,641	1,587,488	4,129,205

NOTE:
1. Based on 2000 Census data (Reference 218)

TABLE 2.1-205
MAJOR CONTRIBUTORS TO TRANSIENT POPULATION WITHIN
80-KM (50-MI.)

Name	Average Daily Transients[a][b]	Peak Daily Transients
Christmastown USA	23,077	
Charlotte Knights Baseball Club		10,000
Prime Outlets at Gaffney	7671	
Sumter National Forest	7,268	
Daniel Stowe Botanical Garden	6,000	
South Carolina Peach Festival		2,500
Christmas on Limestone		2,000
Kings Mountain National Military Park	1,452	
Spartanburg Museum of Art	1,000	
Crowder's Mountain State Park	930	
Mint Museum of Art	750	
Chimney Rock Park	684	
Cowpens National Battlefield	573	
Kings Mountain State Park	548	
South Mountain State Park	527	
Roper Mountain Science Center	515	
Schiele Museum of Natural History	500	
Hollywild Animal Park	411	
Croft State Natural Area	345	
Hatcher Garden and Woodland Preserve	305	
Charlotte Museum of History	113	
Lansford Canal State Park	82	
Chester State Park	64	
Paris Mountain State Park	52	
Charlotte Steeplechase	41	
Gaffney Visitor's Center	35	
Musgrove Mill State Historic Site	28	
Spartanburg County Historical Museum	15	
Rose Hill Plantation State Historic Site	15	

a) Daily transients are peak numbers, when available. Otherwise a daily average derived from the yearly total is used.

b) Additional contributors to transient population are described in Subsection 2.1.3.3.2.

TABLE 2.1-206
DAILY AND ANNUAL PASSENGER COUNTS FOR
COMMERCIAL AIRPORTS IN THE LEE NUCLEAR STATION
REGION

Airport Name	Daily Passenger Count	Annual Passenger Count
Charlotte-Douglas Int'l	72,132	26,328,000
Greenville-Spartanburg Int'l	4,422	1,614,000
Hickory Regional	49	18,000

References 213, 214, and 215

TABLE 2.1-207
FISHING, HUNTING, AND WILDLIFE WATCHING WITHIN THE
LEE NUCLEAR STATION REGION

Activity	SC Total Visitors	Region Visitors
Fishing	812,000	54,729
Hunting	265,000	17,861
Wildlife Watching	1,186,000	79,936
Total	2,263,000	152,526

Activity	NC Total Visitors	Region Visitors
Fishing	1,287,000	189,575
Hunting	295,000	43,454
Wildlife Watching	2,168,000	319,346
Total	3,750,000	552,375

References 221 and 222

TABLE 2.1-208
THE PROJECTED TRANSIENT POPULATION FOR EACH SECTOR 0- TO 80-KM (50-MI.) FOR YEARS 2007, 2016, 2026, 2036, 2046, AND 2056

Distance	Direction	2007	2016	2026	2036	2046	2056
8	N	992	1,084	1,187	1,291	1,394	1,497
16	ENE	38	43	49	55	62	68
16	NE	935	1,040	1,156	1,274	1,391	1,507
16	WNW	4,838	5,290	5,792	6,294	6,795	7,297
40	ENE	200	224	250	277	303	329
40	NE	1,487	1,563	1,649	1,734	1,820	1,905
40	S	146	148	150	152	154	156
40	SSE	77	83	90	96	103	109
40	SW	74	77	81	84	87	91
40	WNW	10,809	11,724	12,741	13,758	14,775	15,792
40	WSW	1,379	1,501	1,637	1,772	1,908	2,044
60	E	11,483	13,366	15,458	17,550	19,642	21,734
60	ENE	32,650	37,539	42,972	48,404	53,837	59,269
60	N	17	19	20	22	24	26
60	NNW	5	5	6	6	6	6
60	S	730	735	740	746	751	756
60	SSE	140	146	153	159	165	172
60	SSW	485	494	503	513	523	533
60	W	441	479	521	564	606	649
60	WSW	327	355	387	418	450	482
80	E	52	65	81	96	111	126
80	ENE	1,026	1,251	1,500	1,749	1,998	2,248
80	ESE	91	102	114	127	139	152
80	N	335	360	387	415	443	471
80	NNW	191	203	217	230	244	258
80	NW	708	746	788	831	873	915
80	S	911	962	1,018	1,075	1,131	1,188
80	SSE	151	159	169	178	187	196
80	SSW	539	587	639	691	744	796
80	W	56	62	68	75	81	87
80	WSW	556	611	672	734	795	856

(References 209, 211, and 230)

TABLE 2.1-209
POPULATION DISTRIBUTION IN THE LOW POPULATION ZONE

	0-1 (mi.)	1-2 (mi.)	0-2 (mi.) TOTAL
N	7	47	54
NNE	5	40	45
NE	5	38	43
ENE	3	27	30
E	2	23	25
ESE	0	17	17
SE	0	17	17
SSE	0	38	38
S	0	46	46
SSW	0	28	28
SW	0	37	37
WSW	0	22	22
W	0	15	15
WNW	1	14	15
NW	1	16	17
NNW	4	56	60
Total	28	481	509

2.2 NEARBY INDUSTRIAL, TRANSPORTATION, AND MILITARY FACILITIES

This section of the referenced DCD is incorporated by reference with the following departures and/or supplements.

WLS COL 2.2-1 The Lee Nuclear Station is located in Cherokee County, South Carolina. Cherokee County is bordered on the west by Spartanburg County, South Carolina, on the north by Rutherford, Cleveland, and Gaston counties, North Carolina, on the east by York County, South Carolina, and on the south by Union County, South Carolina, as seen in Figure 2.1-203.

The Lee Nuclear Station is accessible only by road. Interstate 85 (I-85) connects Gaffney, South Carolina (8.2 miles (mi.) northwest of the site) and Blacksburg, South Carolina (5.8 mi. north of the site) to Spartanburg, South Carolina, and Charlotte, North Carolina (References 201 and 202). Several state and federal highways pass within 5 mi. of the site and are discussed in more detail in Subsections 2.2.2.2.7 and 2.2.2.5. There is also an abandoned rail spur that runs from East Gaffney, South Carolina, to the Lee Nuclear Station (Reference 201).

This section provides information regarding the potential effects on the safe operation of the nuclear facility from industrial, transportation, mining, and military installations in the Lee Nuclear Station area.

STD DEP 1.1-1 Subsection 2.2.1 of the DCD is renumbered as Subsection 2.2.4 and moved to the end of Section 2.2. This is being done to accommodate the incorporation of Regulatory Guide 1.206 numbering conventions for Section 2.2.

2.2.1 LOCATIONS AND ROUTES

WLS COL 2.2-1 Within a 5-mi. radius of the Lee Nuclear Station, there are major industrial facilities, one railroad, four state highways, and one federal highway, all with commercial traffic (Reference 201). The following transportation routes and facilities are shown in Figure 2.2-201:

- Broad River Energy Center
- DSE Systems, LLC
- Herbie Famous Fireworks (South Carolina Distributors)
- Ninety-Nine Islands Hydroelectric Dam
- U.S. Highway 29 (U.S. 29)

Withheld from Public Disclosure Under 10 CFR 2.390(d)(1)
(see COL Application Part 9)

- South Carolina State Highway 5 (South Carolina 5)
- South Carolina State Highway 97 (South Carolina 97)
- South Carolina State Highway 105 (South Carolina 105)
- South Carolina State Highway 329 (South Carolina 329)
- Railroad spur line from Blacksburg to Kings Creek, South Carolina

Environmental Data Resources, Inc. (EDR) provided the results from a database search of storage tanks registered by the state of South Carolina. State regulations for tank registrations were reported to be compliant and consistent with federal regulations. According to the South Carolina Code of Regulations 61-92, an underground storage tank (UST) is defined as any one or combination of tanks (including underground pipes connected thereto) that is used to contain an accumulation of regulated substances, and the volume of which (including the volume of underground pipes connected thereto) is 10 percent or more beneath the surface of the ground. South Carolina requires that all underground storage tanks greater than 110 gal. capacity be registered. The registered tank database includes petroleum storage tanks used for bulk, retail, industrial, private, airport, and government purposes. Farm and residential tanks less than 1100 gal. capacity used for storing motor oil for noncommercial purposes, tanks used for storing heating oil for consumptive use on the premises where stored, and Septic tanks are not classified as USTs and do not fall under these regulations (References 203 and 232).

[

]SRI

In addition to the above storage facility, there are a total of four separate locations within the 5-mi. radius that have registered ASTs or USTs. Table 2.2-201 shows the contents and capacity of all registered storage tanks and Figure 2.2-201 shows the location of all registered storage tanks within 5-mi. radius of the site (Reference 203).

Onsite storage of liquid hydrogen will be in accordance with the approved site plot plan and the AP1000 standard plant design, located in the Bulk Gas Storage Area near the Unit 1 mechanical draft cooling towers,at a safe distance from the nuclear island (Figure 1.1-202). Compressed gas storage will be in the yard adjacent to the Turbine Building. The AP1000 standard plant contains 500 standard cubic feet (scf) bottles of compressed hydrogen gas at 6000 pounds per square inch (psig) and 1500 gallons of liquid hydrogen at 150 psig. Three thousand gallons of liquid nitrogen and 6 tons of liquid carbon dioxide are also located in the Bulk Gas Storage Area to support plant operation. No propane or liquid oxygen is anticipated to be used at the Lee Nuclear Station.

Mining and quarrying operations, drilling operations, and wells are discussed in Subsections 2.2.2.1.5 and 2.2.2.2.4. Oil and gas pipelines are discussed in Subsection 2.2.2.3. Military bases and missile sites are discussed in Subsection 2.2.2.1.6. None of these facilities were found in the 5-mi. radius of the site (military bases and missile sites). Evaluations of explosions postulated to occur on transportation routes near nuclear power plants are addressed in Subsection 2.2.3.

2.2.2 DESCRIPTIONS

The industries within the immediate area of the Lee Nuclear Station are mostly located in Gaffney, East Gaffney, Cherokee Falls, and Blacksburg, South Carolina. All of these industries, with the exception of the Ninety-Nine Islands Hydroelectric Dam, the Broad River Energy Center, and Herbie Famous Fireworks, lie more than 5 mi. from the site. Table 2.2-202 describes the primary function/major products and the number of persons employed at these industrial facilities (References 202, 204, 205, and 206). A brief description of several major industrial facilities is listed below. These industries are some of the largest employers in the area.

2.2.2.1 Description of Facilities

Four major industrial facilities are located within 5 mi. of the Lee Nuclear Site. Descriptions of these facilities are detailed in Subsections 2.2.2.1.1 to 2.2.2.1.3, and 2.2.2.1.7. Subsection 2.2.2.1.4 provides detailed information on electrical generation plants closest to the Lee Nuclear Site. Subsection 2.2.2.1.5 details mining and quarrying activities in the area and Subsection 2.2.2.1.6 details military facilities near the site.

2.2.2.1.1 Ninety-Nine Islands Hydroelectric Dam

The Ninety-Nine Islands Hydroelectric Dam is located on the Broad River adjacent to the Lee Nuclear Site boundary, approximately 1.1 mi. south of the Lee Nuclear Station centerpoint (see Figure 2.1-201).

2.2.2.1.2 Herbie Famous Fireworks

Herbie Famous Fireworks (South Carolina Distributors) is a 1.4G (Class C) consumer fireworks wholesale distribution company. Herbie Famous Fireworks

operates a warehouse facility located approximately 2.7 mi. north to northwest of the site (see Figure 2.2-201) (Reference 202).

2.2.2.1.3 Broad River Energy Center

The Broad River Energy Center is a natural gas-fired peaking electric generation plant located approximately 4.7 mi. northwest of the site (see Figure 2.2-201).

2.2.2.1.4 Electrical Generation Plants

The Mill Creek Combustion Turbine Station is located approximately 9.5 mi. northeast of the site, approximately 1 mi. south of the North Carolina state line. This is a natural gas-fired peaking electric generation plant that opened in 2003. Mill Creek Combustion Turbine Station is an eight-unit facility with a capacity of 640 megawatts. The plant uses natural gas as a primary fuel source and fuel oil as a secondary fuel source (Reference 205).

The Cliffside Steam Station is located approximately 19 mi. northwest of the Lee Nuclear Station. It is a five-unit coal-fired generating facility with a capacity of 760 megawatts. There are plans to expand this facility as early as 2010 by adding a new 800 megawatt, highly efficient, coal-fueled unit (Reference 206).

The Catawba Nuclear Station lies approximately 25 mi. east of the Lee Nuclear Station. The Catawba Nuclear Station, located in Clover, South Carolina on a 391 ac. peninsula, has two Westinghouse PWR reactors producing 1129 megawatts each. A license renewal application was submitted to the NRC on June 14, 2001 and was approved December 5, 2003. These two reactors are the largest in the state (Reference 207).

The McGuire Nuclear Station is located approximately 42 mi. northeast of the Lee Nuclear Station. The McGuire Nuclear Station, located in Cornelius, North Carolina, has two Westinghouse PWR reactors producing 1100 megawatts each. A license renewal application was submitted to the NRC on June 14, 2001 and was approved December 5, 2003 (Reference 208).

2.2.2.1.5 Mining and Quarrying Activities

There are three permitted mines operated by three separate entities located within 5 mi. of the Lee Nuclear Station (Reference 209).

2.2.2.1.6 Military Facilities

There are no military facilities within 5 mi. of the Lee Nuclear Station. The closest military facility is the Charlotte Douglas IAP Air Guard Station. This United States Air Force installation is located approximately 34 mi. to the northeast (Reference 227).

Withheld from Public Disclosure Under 10 CFR 2.390(d)(1)
(see COL Application Part 9)

2.2.2.1.7 DSE Systems, LLC

DSE Systems, LLC has acquired a vacant textile plant near Gaffney, South Carolina. The facility is located 4.6 miles to the northwest of the Lee Nuclear Site boundary on State Highway 329. It is just north of US Highway 29 and on the western bank of the Broad River. The company intends to use the facility for the assembly of ammunition for the US military.

2.2.2.2 Description of Products and Materials

2.2.2.2.1 Ninety-Nine Islands Hydroelectric Dam

The Ninety-Nine Islands Hydroelectric Dam is a six unit facility with an electrical output of 18-megawatts (MW) that was completed in 1909. The dam is about 88 feet (ft.) high (maximum) and 1567 ft. long that creates a reservoir with a surface area of 433 acres (ac.) at 100 percent capacity. There is a 94-ft. high, 197-ft. long concrete intake structure. This facility is currently operated as a peaking facility, primarily in the summer and winter.

2.2.2.2.2 Herbie Famous Fireworks

[

]SRI

2.2.2.2.3 Broad River Energy Center

The facility consists of five combustion turbines with a capacity of 847 megawatts (Reference 204). Information regarding the products stored on the Broad River Energy Center site is summarized in Table 2.2-203. The Occupational Safety and Health Administration (OSHA) permissible exposure limits for the reported toxic materials are in Table 2.2-204 (Reference 233).

2.2.2.2.4 Mining and Quarrying Activities

The closest permitted mine is operated by Thomas Sand Company and is located approximately 1 mi. north of the site. This mine, named Blacksburg Plant, is used to mine sand. Martin Mine, operated by Cunningham Brick Company, is the second closest permitted mine located 3.2 mi. north of the site. This mine is used to mine manganese schist (type of mica). Kings Creek Mine, operated by Industrial Minerals, Inc. is the third permitted mine within 5 mi. of the site. Kings Creek Mine, located approximately 4.9 mi. northeast of the site, is used to mine sericite (type of mica). None of the above mines use explosives (Reference 209).

2.2.2.2.5 Military Facilities

There are no military facilities within 5 mi. of the Lee Nuclear Station. The closest military facility is the Charlotte Douglas IAP Air Guard Station. This United States Air Force installation is located approximately 34 mi. to the northeast (Reference 227).

2.2.2.2.6 Waterways

The Lee Nuclear Station footprint is located approximately 4800 ft. west and approximately 2400 ft. south of the Broad River, and 1.1 mi. upstream (north) of the Ninety-Nine Islands Hydroelectric Dam (See Figure 2.1-201). The Broad River upstream of the Lee Nuclear Station is a shallow, unnavigable river; however, from the Ninety-Nine Islands Hydroelectric Station to the confluence with the Pacolet River, the Broad River is considered navigable waters under Regulation 19-450 of the South Carolina Code of Laws 1976, as amended.

2.2.2.2.7 Highways

The nearest highway with heavy commercial traffic is U.S. 29, passing approximately 4.6 mi. northwest from the site center point at its closest. In addition to U.S. 29, segments of South Carolina 5, 97, 105, and 329 are located within a 5-mi. radius of the site (Reference 201).

Any material registered with the federal government as a hazardous material is allowed to travel along any public road in the state of South Carolina provided it is properly packaged and transported, and the proper credentials are obtained by the carrier. The amount of explosives shipped along the public roads within 5 mi. of the facility is unknown, since no agencies are required by law to keep records of this information.

2.2.2.2.8 Railroads

Norfolk Southern Railroad Company (NSRC) owns and operates a small spur that passes within the 5-mi. radius (Reference 211). This line runs at its closest point approximately 4.7 mi. from the site centerpoint. Any material registered with the federal government as a hazardous material that is legally allowed to be transported via American railroads could potentially be transported at some point along the rails that are situated near the site. Items that may be legally transported on the rails near the site include many types of hazardous materials and other industrial chemicals. The amount of hazardous materials transported along the rails near the site is unknown due to the sensitive nature of this information and confidentiality agreements within NSRC.

2.2.2.2.9 DSE Systems, LLC (Description of Products)

The items intended to be manufactured by DSE Systems, LLC at the Gaffney, South Carolina site include the following:

Withheld from Public Disclosure Under 10 CFR 2.390(d)(1)
(see COL Application Part 9)

- [
-
-
-
-
-

]SRI

2.2.2.3 Description of Pipelines

Nine major pipelines operated by three separate entities are located within 5 mi. of the Lee Nuclear Station. The possibility that any pipeline near the site could carry product other than the one presently carried and whether the pipeline is used for gas storage at higher-than-normal pressure was not released by any pipeline operator in the 5-mi. area due to the sensitive nature of this information.

[

Withheld from Public Disclosure Under 10 CFR 2.390(d)(1)
(see COL Application Part 9)

]SRI

In addition to these major pipelines, there are numerous lines delivering natural gas to residential, commercial, and other industrial units. These lines are operated by Piedmont Natural Gas and vary in size and pressure from 6-inch-diameter 500 psi distribution mains to 1-inch-diameter lines connected to homes and businesses.

2.2.2.4 Description of Waterways

As stated in Subsection 2.2.2.2.6, the Lee Nuclear Station footprint is located approximately 4800 ft. west and approximately 2400 ft. south of the Broad River, and 1.1 mi. upstream (north) of the Ninety-Nine Islands Hydroelectric Dam (See Figure 2.1-201). The Broad River upstream of the Lee Nuclear Station is a shallow, unnavigable river; however, from the Ninety-Nine Islands Hydroelectric Station to the confluence with the Pacolet River, the Broad River is considered navigable waters under Regulation 19-450 of the South Carolina Code of Laws 1976, as amended. In 1991, this entire section was designated a State Scenic River (Reference 214). The Broad River is not classified as a National Wild and Scenic River by the federal government (Reference 215). There are no ports within 50 mi. of the Lee Nuclear Station site (Reference 201).

There are two public access points to the Scenic Corridor of the Broad River. The Ninety-Nine Islands Boat Landing is a public boat access area operated by Duke Energy. This landing is located in Cherokee County, South Carolina at the end of State Secondary Road 43, between the towns of Cherokee Falls in Cherokee County and Hickory Grove in York County, South Carolina. There is a large parking lot, concrete paved double boat ramp, and a wooden wildlife viewing/ fishing dock. The Cherokee Landing is located across the river from the Ninety-Nine Islands Boat Landing at the end of State Secondary Road 13. This landing has a very small paved parking lot and the landing is very steep (Reference 214).

Figure 2.1-201 shows the proposed location of the intake structure in the Broad River for the Lee Nuclear Station. Water from the Broad River will be withdrawn at this location for use as cooling tower makeup, service water cooling system makeup, and other miscellaneous water uses. Figure 2.1-201 shows the proposed location of the release point in the Broad River for the Lee Nuclear Station. Water from the plant is released back into the Broad River at this location when it is no longer needed by the plant.

2.2.2.5 Description of Highways

As stated in Subsection 2.2.2.2.7, the nearest highway with heavy commercial traffic is U.S. 29, passing approximately 4.6 mi. northwest from the site center point at its closest. In addition to U.S. 29, segments of South Carolina 5, 97, 105, and 329 are located within a 5-mi. radius of the site (Reference 201). Interstate 85 could be used as an alternate route of U.S. 29; however it is located outside the 5-mi. radius.

Any material registered with the federal government as a hazardous material is allowed to travel along any public road in the state of South Carolina provided it is properly packaged and transported, and the proper credentials are obtained by the carrier. The amount of explosives shipped along the public roads within 5 mi. of the facility is unknown, since no agencies are required by law to keep records of this information.

Estimated Annual Average Daily Traffic (AADT) counts for 2005 indicate the following:

- 7000 vehicles travel on U.S. 29 between South Carolina 329 and South Carolina 5.
- 5600 vehicles travel on South Carolina 5 between U.S. 29 and South Carolina 55.
- 5000 vehicles also travel along South Carolina 105 between South Carolina 211 and South Carolina 18.
- 1600 vehicles travel on South Carolina 329 between South Carolina 105 and U.S. 29.
- 950 vehicles travel on Cherokee County Highway 13 (McKowns Mountain Road) between South Carolina 105 and the end of the road (near the Broad River).
- 425 vehicles travel on South Carolina 97 between South Carolina 5 and the York County line (Reference 210).

2.2.2.6 Description of Railroads

Norfolk Southern Railroad Company (NSRC) owns and operates a small spur that passes within the 5-mi. radius (Reference 211). This line runs at its closest point approximately 4.7 mi. from the site center point on the northeastern side and has an average of two trains per day (one round trip) on these tracks. The speed limit is 25 mph on the majority of this spur with a speed limit of 10 mph around many of the curves. This spur carries freight only; no passenger trains use this route (Reference 212).

A major rail line owned by NSRC runs at its closest point 5.5 mi. from the site. This line runs from Atlanta, Georgia to Charlotte, North Carolina, eventually on to the

New York City area on the northern end, and to the New Orleans area on the southern end. This line is the main line, or core route, in the northern South Carolina area, running through downtown Gaffney and Blacksburg (Reference 211). This main line averages 22 trains per day and has a speed limit of 50 mph. This line is primarily used for freight service, although one passenger train, the Amtrak Crescent, uses the line (References 211 and 212). The speed limit for passenger trains along this stretch of track is 79 mph, although they are unlikely to reach more than approximately 60 mph between Gaffney, South Carolina and Blacksburg, South Carolina due to curves in the tracks.

As stated in Subsection 2.2.2.2.8, any material registered with the federal government as a hazardous material that is legally allowed to be transported via American railroads could potentially be transported at some point along the rails that are situated near the site. Items that may be legally transported on the rails near the site include many types of hazardous materials and other industrial chemicals.

It is important to note that the proposed Southeast High-Speed Rail Corridor runs through this area. The proposed route is projected to follow the existing tracks that run from Atlanta, Georgia to Charlotte, North Carolina. Trains are expected to travel at a maximum speed of 110 mph along this corridor. The proposed date for implementation of service along this route is 2012 at the earliest and is projected to carry more than 1.6 million passengers annually by the year 2015 (Reference 210).

2.2.2.7 Description of Airports

2.2.2.7.1 Airports

There were no airports found within the Lee Nuclear Station 50- mi. region that meet or exceed the criteria defined in NUREG-0800 Subsection 3.5.1.6 and RG 1.206 Part III Subsections C.I.2.2.2.7 and C.I.3.5.1.6.

There are no airports located within 10 mi. of the Lee Nuclear Station; however, one heliport is located within 10 mi. of the plant (Reference 201). The Milliken & Co. heliport is located approximately 6 mi. to the north of the site and has a 25 ft. square concrete helipad (Reference 216).

York Airport is the closest airport that has reported numbers of operations to the Lee Nuclear Station (14.7 mi. to the east). It has a 2580 ft. turf runway. The airport is exclusively used by single-engine private aircraft with 12 single-engine aircraft based at the field. The average number of operations (landings and takeoffs are counted separately) is approximately 62 per week. General aviation accounts for 69 percent of operations while 31 percent are transient general aviation (Reference 217).

There are two large commercial airports within 50 mi. of the Lee Nuclear Station, Greenville-Spartanburg International Airport (GSP) and Charlotte Douglas International Airport (CLT). GSP is located 41.3 mi. west to southwest of the site and CLT is located 34.4 mi. northeast of the site (Reference 201).

GSP has one 11,001 ft. asphalt runway. Federal Aviation Administration (FAA) information, effective June 7, 2006, indicates that 23 aircraft are based on the field. Five of these are single-engine aircraft, 10 are multi-engine aircraft and eight are jet aircraft. The average number of operations is approximately 182 per day. Air taxi accounts for 69 percent of operations, 17 percent are transient general aviation, 11 percent are commercial, 2 percent are military, and 1 percent is local general aviation (Reference 218).

Fifty-one aviation accidents or incidents have occurred since 1965 in Greenville, South Carolina. Of the 51 accidents, eight have been fatal resulting in 18 deaths (Reference 229). Thirty-eight aviation accidents or incidents have occurred since 1964 in Spartanburg, South Carolina. Of the 38 accidents, four have been fatal resulting in five deaths (Reference 230).

CLT has three runways; the first is a 10,000 ft. concrete runway, the second is an 8674 ft. asphalt/concrete runway, and the third is a 7502 ft. asphalt/concrete runway. FAA information, effective June 7, 2006, indicates that 146 aircraft are based on the field. Twenty-five of these are single-engine aircraft, 22 are multi-engine aircraft, 87 are jet aircraft, 2 are helicopters, and 10 are military aircraft. The average number of operations is approximately 1372 per day. Commercial accounts for 47 percent of operations, 45 percent are air taxi, 7 percent are transient general aviation, and less than 1 percent are military (Reference 219).

One hundred forty-four aviation accidents or incidents have occurred since 1962 in Charlotte, North Carolina. Of the 144 accidents, 21 have been fatal resulting in 162 deaths (Reference 231).

Based on historical flight data recorded from 1963 to 2005 for GSP (Table 2.2-205), projections for air traffic up to fiscal year 2025 are given in Table 2.2-206 for GSP (Reference 220). GSP recently performed a study to determine the projected needs of the airport. They developed a plan to accommodate the projected growth in passenger traffic. Plans are now in place to expand, if needed, the terminal building from the current 13 attached jet gates to as many as 43 attached jet gates and adding a new 8200 ft. runway. This plan is expected to allow them to accommodate the projected 5.3 million passengers the study calculated the airport would see by the year 2023 (References 222 and 223).

Based on historical flight data recorded from 2000 to 2005 for CLT (Table 2.2-207), projections for air traffic up to fiscal year 2025 are given in Table 2.2-208 for CLT (Reference 221). CLT is currently in the middle of a multimillion dollar expansion to meet the needs of future passenger and cargo traffic. Construction has begun on a new 9000 ft. runway and a new 3000 space parking facility has recently been completed. This expansion and renovation is expected to meet the projected demands of the future by expanding many existing airport facilities (Reference 224).

Approach and departure paths at CLT and GSP are not aligned with the Lee Nuclear Station.

2.2.2.7.2 Airways

Two low altitude (below 18,000 ft.) federal air routes are located within 15 mi. of the Lee Nuclear Station - Airway V54 and V415. The centerline of Airway V54 is approximately 4 mi. north of the site and Airway V415 is approximately 10 mi. southwest of the site (Figure 2.2-202) (Reference 225). These routes, also known as Victor air routes, are primarily flown by general aviation aircraft. These routes generally have a width of eight nautical miles and occupy the airspace between 18,000 ft. and the floor of controlled airspace, which is 700 - 1200 ft. There are no Military Training Routes within 10 mi. of the site.

Two high altitude (18,000 ft. above MSL through 45,000 ft. pressure altitude) federal air routes are located within 15 mi. of the Lee Nuclear Station - Airway J208 and J14. The centerline of Airway J208 is located approximately 9 mi. southeast of the site and the centerline of Airway J14 is 12.5 mi. northwest of the site (Figure 2.2-202) (Reference 226). These airways are primarily used by commercial air carriers, the military and high performance general aviation aircraft. These routes also have a width of eight nautical miles and are flown from 18,000 ft. to the top of controlled airspace, 45,000 ft. All flights above 18,000 ft. are required to be IFR flights; hence, all altitudes and routes are assigned by air traffic controllers.

Due to the close proximity of airways to the Lee Nuclear Station, an evaluation of hazards from air traffic along all airways within 10 mi. of the Lee Nuclear Station is presented in Subsection 3.5.1.6.

2.2.2.8 Projections of Industrial Growth

There are no industrial parks within 5 mi. of the Lee Nuclear Station (Reference 228). There are two industrial companies within the 5-mi. radius. The Broad River Energy Center and Herbie Famous Fireworks (South Carolina Distributors) as described in Subsections 2.2.2.1.3 and 2.2.2.1.2, respectively (References 202 and 204). There is no planned industrial growth within the 5 mi. area (Reference 228).

2.2.3 EVALUATION OF POTENTIAL ACCIDENTS

WLS COL 2.2-1 The consideration of a variety of potential accidents, and their effects on the plant or plant operation, is included in this section. Types of accidents considered include explosions, flammable vapor clouds, toxic chemicals, fires, collisions with intake structures, and liquid spills. General Design Criterion 4, “Environmental and Missile Design Basis,” of Appendix A, “General Design Criteria for Nuclear Power Plants,” to 10 CFR Part 50, “Licensing of Production and Utilization Facilities,” requires that nuclear power plant structures, systems, and components important to safety be appropriately protected against dynamic effects resulting from equipment failures that may occur within the nuclear power plant as well as events and conditions that may occur outside the nuclear power plant.

2.2.3.1 Determination of Design Basis Events

Design basis events internal and external to the nuclear power plant are defined as those accidents that have a probability of occurrence on the order of about 10^{-7} per year or greater and potential consequences serious enough to affect the safety of the plant to the extent that the guidelines in 10 CFR Part 100 could be exceeded. The following categories are considered for the determination of design basis events: explosions, flammable vapor clouds with a delayed ignition, toxic chemicals, fires, collision with intake structures, and liquid spills.

2.2.3.1.1 Explosions

2.2.3.1.1.1 Transportation Routes

Accidents were postulated for the nearby highways and railroads. Accidents on the Broad River were not evaluated because this river is considered to be non-navigable. The nearest highway with heavy commercial traffic is US Highway 29, which passes approximately 4.24 miles northwest of the Lee Nuclear Site at its closest point to the site boundary. The accident of concern along US Highway 29 is one that results in the detonation of a highly explosive cargo carried by a truck. It is necessary to demonstrate that such an explosion on the highway does not result in a peak positive incident overpressure that exceeds 1psi at the critical structures on-site. The maximum probable hazardous cargo for a single highway truck is based on Regulatory Guide 1.91, Revision 1, in terms of equivalent trinitrotoluene (TNT). The TNT equivalency is based on (Reference 235):

$W_E = \frac{H^d_{EXP}}{H^d_{TNT}} W_{EXP}$, where W_E is the effective charge weight, H^d_{EXP} is the heat of detonation of the explosive in question, H^d_{TNT} is the heat of detonation of TNT, and W_{EXP} is the weight of the explosive in question.

The methodology presented in Regulatory Guide 1.91, Revision 1, established the safe distance beyond which no damage would be expected (i.e. a peak positive incident overpressure of less than 1 psi at the critical structures on the Lee Nuclear Site) from a truck explosion along U.S. Highway 29 at its closest point. An evaluation performed for materials with a TNT equivalency of 2.24 and using the maximum cargo for two trucks (50,000 lbs. per truck) determined the safe distance to be 0.52 miles, hence, there is considerable margin between the required safe distance and the actual distance. The effects of blast-generated missiles are less than those associated with the blast overpressure levels considered in Regulatory Guide 1.91, Revision 1. Because the overpressure criteria of the guide are not exceeded, the effects of blast-generated missiles are not considered.

The Norfolk Southern Railroad passes approximately 4.18 miles northeast of the site at its closest point. The maximum probable quantity of explosive material shipped by a single railroad boxcar in terms of equivalent pounds of TNT is based on Regulatory Guide 1.91, Revision 1. It is recognized that cargo shipments by

Withheld from Public Disclosure Under 10 CFR 2.390(d)(1)
(see COL Application Part 9)

railroad typically constitute the usage of more than one boxcar. For the purpose of qualifying the explosion hazard involved in this railroad analysis, thirty combined boxcar values for intended explosives are incorporated into the calculation. This corresponds to a TNT equivalency of 8,870,400 lbs (30 boxcars x 132,000 lbs/ boxcar x 2.24). These values may be considered conservatively bounding because it is reasonable to assume the initial explosion would involve only one boxcar associated with initiating the explosion. Should additional boxcars become involved, related explosions would be subsequent in time and neither coincident with, nor additive to, the effects associated with those from the first boxcar explosion. The evaluation determined the required safe distance to be 1.76 miles, which is less than the distance of 4.18 miles from the railroad to the site at its closest point. Therefore the proximity to the railroad does not present an explosion hazard.

2.2.3.1.1.2 Pipelines

If the natural gas pipeline were to rupture resulting in natural gas released into the atmosphere, the vapor plume would not detonate in such a fashion to cause an overpressure event. Instead, it would burn with a relatively slow deflagration rate. A natural gas release would not explode if the release is into an unconfined space, therefore a free vapor cloud explosion of a release is into an unconfined space, and therefore a free vapor cloud explosion of a release from the natural gas pipeline is not credible.

The Colonial Pipeline and Plantation Pipeline contain refined petroleum products and are located 3.24 miles from the Lee Nuclear Site at the closest point. The 40-inch Colonial Pipeline was analyzed because it has the largest diameter of the refined petroleum pipelines. [

]^{SRI} Using Equation 1 from Regulatory Guide 1.91, Revision 1, the safe standoff distance is calculated as 14,948 ft or 2.83 miles.

The result for the unconfined vapor explosion safe standoff distance is less than the distance of the pipeline to the site boundary at its closest point of 3.24 miles. Therefore, the postulated pipeline explosion does not generate an overpressure above 1 psi at the site. Based on several factors, this is a conservative result, e.g., no consideration is taken for depressurization of the pipe, instantaneous evaporation of the leaked gasoline is assumed, and no credit is taken for the fact

Withheld from Public Disclosure Under 10 CFR 2.390(d)(1)
(see COL Application Part 9)

the pipe is buried three to four feet underground. Hence, it is concluded the refined petroleum pipelines are not an explosion hazard for the Lee Nuclear Site.

2.2.3.1.1.3 Nearby Industrial Facilities

Herbie Famous Fireworks is a 1.4G consumer fireworks wholesale distribution company located 2.31 miles from the Lee Nuclear Site boundary. The U.S. Department of Transportation labels Division 1.4G as explosives that present a minor explosion hazard. The explosive effects are largely confined to the package and no blast or projection of appreciable size or range is expected. [

]SRI Using Equation 1 from Regulatory Guide 1.91, Revision 1, the safe standoff distance is calculated as 2,522 ft or 0.48 miles. Since the safe standoff distance is less than the distance to Herbie Famous Fireworks, the postulated explosion at Herbie Famous Fireworks does not generate an overpressure above 1 psi at the site.

As shown in Table 2.2-201, the Broad River Energy Center has the largest capacity of registered storage tanks and has the only above ground tanks listed. The Broad River Energy Center is located 4.34 miles from the site boundary. [

]SRI Using Equation 1 from Regulatory Guide 1.91, Revision 1, the safe standoff distance for a confined vapor explosion is calculated as 7,588 ft (1.44 miles), and the safe standoff distance for an unconfined vapor explosion is calculated as 13,269 ft (2.51 miles). Since the safe standoff distances are less than the distance to the Broad River Energy Center, the postulated confined and unconfined vapor explosions do not generate an overpressure above 1 psi at the site.

[

Withheld from Public Disclosure Under 10 CFR 2.390(d)(1)
(see COL Application Part 9)

]SRI

The other potentially hazardous commodities stored at the DSE Systems location were examined for the potential to generate an overpressure above 1 psi at the site or adversely affect control room environment. Screening criteria based on the toxic release, confined, unconfined, and solid material explosion equations, as defined above in the Broad River Energy Center postulated explosion discussion, were developed to help identify potential explosion or toxic hazard threats. Only materials of NFPA 704 (Reference 238) health hazard, flammability, and reactivity Class 3 and Class 4 were considered for the screening, due to their unstable and volatile physical properties. This evaluation demonstrated that for a given mass, the hazard from a toxic material release would always be limiting when compared to a solid material explosion or confined or unconfined vapor explosion. [

]SRI A DSE Systems facility representative indicated that there are no chemicals stored at the site which would meet the developed screening criterion, and therefore there is no postulated explosion or toxic chemical release hazards to the Lee Nuclear Site from other commodities stored at DSE Systems, LLC.

2.2.3.1.1.4 Onsite Chemicals

WLS COL 2.2-1
WLS COL 6.4-1

As discussed in DCD Section 1.9, the AP1000 uses small amounts of combustible gases for normal plant operation. Most of these gases are used in limited quantities and are associated with plant functions or activities that do not jeopardize any safety-related equipment. These gases are found in areas of the plant that are removed from the nuclear island. The exception to this is the hydrogen supply line to the chemical and volume control system (CVS).

The CVS is the only system on the nuclear island that uses hydrogen gas. Hydrogen is supplied to the AP1000 CVS inside containment from a single hydrogen bottle. The release of the contents of an entire bottle of hydrogen in the most limiting building volumes, both inside containment and in the auxiliary building would not result a volume percent of hydrogen large enough to reach a detonable level.

DCD Subsection 3.5.1.1.2.2 states that the battery compartments are ventilated by a system that is designed to preclude the possibility of hydrogen accumulation. The DCD states further that the storage tank area for plant gases is located sufficiently far from the nuclear island that an explosion would not result in missiles more energetic than the tornado missiles for which the nuclear island is designed.

The plant gas system provides hydrogen, carbon dioxide, and nitrogen gases to the plant systems as required. The effects of the plant gas system on main control room habitability are addressed in DCD Section 6.4 including explosive gases and burn conditions for those gases. For explosions, the plant gas system is designed for conformance with Regulatory Guide 1.91 (DCD Subsection 9.3.2.3).

Table 6.4-202 identifies additional site specific chemicals that are outside the scope of DCD evaluations. These site specific chemicals were screened for solid material explosion, confined and unconfined vapor explosion, flammability, and toxic gas release event hazards. These chemicals are not in solid state and are not flammable; therefore, solid material explosion hazard, confined and unconfined vapor explosion hazard, and flammability hazard evaluations are not required. Based on the screening guidance provided in Regulatory Guide 1.78, none of the site-specific chemicals used were found to be a credible habitability threat to main control room occupants in case of a release.

2.2.3.1.2 Flammable Vapor Clouds (Delayed Ignition)

WLS COL 2.2-1

The potential for detonation in a plume resulting from release of the commodities from a transportation accident is evaluated, as well as a potential release from nearby facilities and pipelines. This evaluation assumes dispersion downwind toward the Lee Nuclear Station, with a delayed ignition. For each commodity of interest, the vapor dispersion is based on a wind speed of 1.8 mph, a Stability Class of D, and a 90°F ambient air temperature. These meteorological conditions are intended to maximize the vaporization rate of the commodity of interest while limiting the downwind dispersion. The ALOHA code (Reference 236) is used to evaluate the dispersion and detonation of the vapor clouds.

Withheld from Public Disclosure Under 10 CFR 2.390(d)(1)
(see COL Application Part 9)

For the evaluation of the potential effects of accidents on US Highway 29, conservatively large tanker truck volumes (9,000 gallons) are assumed along with an assumed 48.4 square feet rupture size. The basis for a 48.4 square feet rupture size is that, for this scenario, this rupture size is the largest permissible by the ALOHA code. ALOHA's constraints do not have an impact on the analysis because all the chemicals from a tanker of this size are capable of being released within the allotted time duration, eliminating the need to postulate a larger rupture. Because almost any commodity can be transported along the highways, various commodities are assumed. Gasoline and propane are analyzed due to the fact that these are commonly transported commodities.

Other less popular commodities are analyzed that have a relatively low flash point and relatively high heats of combustion, hence have a potential to result in a high overpressure if the vapor cloud is ignited. The results are summarized in Table 2.2-210.

Similarly, for the Norfolk Southern Railroad, various commodities are analyzed with the ALOHA code, assuming conservatively large tanker sizes (40,000 gallons) and rupture sizes of 48.4 square feet.The results are summarized in Table 2.2-211.

For the evaluation of the vapor cloud resulting from ruptured pipelines, rupture sizes equivalent to pipe cross-sectional areas are assumed. The pipelines are assumed to leak for a duration of one hour. [

Withheld from Public Disclosure Under 10 CFR 2.390(d)(1)
(see COL Application Part 9)

]SRI

For the postulated accidents on U.S. Highway 29, the Norfolk Southern Railroad, and natural gas pipelines, the overpressure at the Lee Nuclear Station resulting from the delayed ignition of a vapor cloud is negligible. The only postulated accident that results in a slight overpressure at the Lee Nuclear Site is the postulated rupture of the refined petroleum pipeline, where a conservatively large release of gasoline is assumed. Even for this case, the overpressure is less than 1 psi at the Lee Nuclear Site.

In order to demonstrate that the atmospheric conditions assumed were conservative, a sensitivity study was performed for the situation that caused the largest overpressure at the site, which was a pipeline carrying gasoline, which produced a maximum overpressure of 0.459 psi for a release rate of 3,920 ft^3/sec. The wind speed was increased from 1.55 knots (0.8 m/s) to 1 m/s, while at the same time the Stability Class was changed from "D" to "F". For this case the overpressure dropped to 0.455 psi. Increasing the wind speed would allow for the chemical to evaporate more quickly and travel at a quicker rate. However, the higher wind speed would disperse the vapor cloud at a quicker rate causing a less significant overpressure. The Stability Class is a measurement of how turbulent the atmosphere is from solar radiation and other contributing factors. By increasing the Stability Class from "D" to "F" the program is decreasing the amount of solar radiation included in the model, allowing for less dispersion to occur. Decreasing the solar radiation also decreases the amount of evaporation that occurs and therefore causes a decrease in overpressure. These results demonstrate that the assumptions of a wind speed of 1.55 knots and a Stability Class of "D" are conservative for this calculation.

Because the resulting overpressure from the delayed ignition of potential vapor clouds is much less than 1 psi, the Regulatory Guide 1.91, Revision 1, acceptance criteria, it is concluded that the delayed ignition of vapor clouds from nearby transportation routes and pipelines does not pose a hazard to the Lee Nuclear Station.

2.2.3.1.3 Toxic Chemicals

WLS COL 2.2-1
WLS COL 6.4-1

Accidents involving the release of toxic chemicals from on-site storage facilities and nearby mobile and stationary sources are addressed in Section 6.4. For each postulated event, the concentration at the site is determined for use in evaluating the control room habitability.

2.2.3.1.3.1 Background

A control room habitability analysis was performed in accordance with Regulatory Guide 1.78. The Regulatory Guide specifies that mobile and stationary sources of hazardous materials within a five mile radius of the plant be analyzed as a potential threat to plant operations.

Subsections 2.2.1 and 2.2.2 provide sources of potentially airborne hazardous chemicals that may be in the area. These sources are in the form of stationary industrial facilities and transportation pathways in the form of a highway and a rail spur.

The nearby Broad River is not navigable by barges and does not transport commercial traffic, and hence is eliminated from further investigation.

Figure 2.2-201 shows the potential rail, road, and stationary industrial sources within the proximity of Lee Nuclear Station.

The screening criteria for airborne hazardous chemicals is established in Regulatory Guide 1.78 based on the National Institute for Safety and Health (NIOSH) Immediately Dangerous to Life and Health (IDLH) limits for 30 minute exposures. Per Regulatory Guide 1.78, the NIOSH IDLH values were utilized to screen chemicals and to evaluate concentrations of hazardous chemicals to determine their effect on control room habitability.

Regulatory Guide 1.78 specifies the use of HABIT software for evaluating control room habitability. The HABIT software consists of modules that evaluate radiological and toxic chemical transport and exposure. Although HABIT software modules were not used directly, an alternative methodology based on HABIT was utilized to model toxic chemical transport and model chemical exposure to control room personnel using control room design parameters.

2.2.3.1.3.2 Sources of Potentially Dangerous Releases

2.2.3.1.3.2.1 Stationary Sources

There are no site-specific sources of airborne hazardous materials stored on the Lee Nuclear Station site in sufficient quantity to affect control room habitability.

Subsection 2.2.2.1 lists four major industrial facilities within a five mile radius of the site or at greater distances as appropriate based on their significance: Herbie Famous Fireworks, Ninety-Nine Islands Hydroelectric Station, the Broad River Energy Center, and DSE Systems, LLC. Herbie Famous Fireworks has indicated that they do not have potentially dangerous airborne toxic chemicals on site. Although the Broad River Energy Center stores chemicals on site per FSAR Table 2.2-203, there are no stored potentially poisonous gasses such as chlorine or anhydrous ammonia nor other recognizable hazardous chemicals that may affect control room habitability at the site. The exact quantities of the chemicals in Table 2.2-203 are not known. However, an inquiry was sent to Broad River Energy Center to identify chemicals that are stored in quantities greater than 29,000 pounds or that have an Immediately Dangerous to Life or Health rating less than 30 mg/m^3. Further analysis of the chemicals identified by Broad River Energy Center indicates that there are no toxic chemical release threats to the Lee Nuclear Site from the Broad River Energy Center. There are no toxic chemical release threats to the Lee Nuclear Site from DSE Systems, LLC, based on the discussion of chemical screening criteria in Subsection 2.2.3.1.1.3.

2.2.3.1.3.2.2 Mobile Sources

Preliminary statistical analysis evaluated the general risk from mobile sources of hazardous materials. This preliminary risk analysis indicates that although the accident risk is quite low, it is not less than the evaluation limit of 1E-6 per year for mobile sources set in Regulatory Guide 1.78. Therefore, a wholly risk-based approach was not considered.

2.2.3.1.3.2.2.1 Local Highways

As illustrated on Figure 2.2-201, the nearest highway with heavy commercial traffic is U.S. Highway 29, passing approximately 4.5 mi. northwest from the site at its closest point. In addition to U.S. Highway 29, segments of South Carolina State Highways 5, 97, 105, and 329 are located within a 5-mi. radius of the site.

Any material registered with the federal government as a hazardous material is allowed to travel along any public road in the state of South Carolina provided it is properly packaged and transported, and the proper credentials are obtained by the carrier.

Annual Average Daily Traffic (AADT) counts for 2005 indicate a moderate level of traffic on several roads within five miles of the Lee Nuclear Station. This information was used to estimate the total annual vehicle-miles traveled within a 5-mile radius. Calculations to estimate the probability of a hazardous road release were conducted based upon hazardous material risk information from the Federal Motor Carrier Safety Administration. The estimated total annual vehicle-miles were modified using the risk information for the percent of all vehicles that are trucks, percent of trucks that carry hazardous materials, hazardous material truck accident rate, and release rate per hazardous material accident, to ultimately arrive at an annual hazardous release probability for the roads within a 5-mi. radius of Lee Nuclear Station.

The results of a risk study indicate that general hazardous material incidents have a release probability of approximately 1E-2 per year, while DOT Class 2.3 releases have a release probability of approximately 5E-5 per year. Although the results of those calculations indicate that the probability of a road release within a 5-mi. radius of Lee Nuclear Station is very low, the risk of a release is higher than the Regulatory Guide 1.78 evaluation limit of 1E-6 per year for mobile sources, therefore further analysis is required. This further analysis is discussed in Subsection 2.2.3.1.3.3.

2.2.3.1.3.2.2.2 Local Rail Lines

A Norfolk Southern rail line is located approximately 4.5 miles northeast of the site. This rail line is a spur off of the main line running southeast of Blacksburg and terminating in Kings Creek. This rail line carries predominately Iron Ore, and is not expected to carry hazardous materials, and is thus not evaluated for hazardous materials.

2.2.3.1.3.3 Analysis of Hazardous Materials

An analysis of the surrounding area and of the materials that may be in the area reveals that the roadways pose the most significant toxic hazard to control room habitability.

Any chemical sanctioned to be legally transported by state and federal department of transportation guidelines may be transported on the roads, but due to the distance from the site it is determined that only the most toxic gaseous chemicals (DOT class 2.3) could reach the control room intake under ideal calm conditions.

An analysis of a tractor-trailer based chlorine release at the closest point of passage of Route 329 was performed using the methodology of the EXTRAN code contained in the HABIT software package, as specified in Regulatory Guide 1.78 to establish a guideline for further evaluation. Chlorine was deemed to be the worst case release of a toxic gas as it is commonly transported, is highly toxic with an IDLH of 10 PPM, and is heavier than air so it can travel laterally without significant dispersion under calm conditions. The model utilizes AP1000 HVAC parameters, worst-case meteorological conditions, and chemical characteristics of the modeled hazardous materials.

To model the concentration of hazardous chemicals at the control room intake several site specific parameters are gathered. These parameters include release weight, in this case the complete tractor-trailer cargo weight, along with distance to the control room, HVAC intake height, and worst case meteorological conditions.

Meteorological data was analyzed to determine the worst meteorological conditions at the site. In the case of a released gaseous hazardous material cloud, the worst case condition is essentially a calm night. A wind speed of 1 m/s and Class G stability conditions were utilized in the model to represent these worst-case conditions.

Variable parameters utilized in this analysis are provided in Table 2.2-209.

The results of the analysis using the HABIT EXTRAN methodology indicate that under worst case meteorological conditions for the site, a pressurized liquid chlorine tractor-trailer burst type accident would elevate control room HVAC intake concentrations beyond IDLH values, however, the habitability analysis discussed in Section 6.4.4.2 concluded that the concentration in the control room would be less than the chlorine IDLH value.

2.2.3.1.4 Fires

WLS COL 2.2-1
WLS COL 6.4-1

Fires originating from accidents at any of the facilities or transportation routes discussed previously would not endanger the safe operation of the station because of the distances between potential accident locations and the location of the Lee Nuclear Station are at least 2.31 miles away.

The Nuclear Island is situated sufficiently clear of trees and brush. The distance exceeds the minimum fuel modification area requirements of thirty feet per NFPA 1144 (Reference 234). Therefore, there is no threat from brush or forest fires.

Fire and smoke from accidents at nearby homes, industrial facilities, transportation routes, or from area forest or brush fires, does not jeopardize the safe operation of the plant due to the separation distance of potential fires from the plant. The main control room HVAC system continuously monitors the outside air using smoke monitors located at the outside air intake plenum and monitors the return air for smoke upstream of the supply air handling units (DCD Subsection 9.4.1.2.3.1). If a high concentration of smoke is detected in the outside air intake, an alarm is initiated in the main control room and the main control room/ control support area HVAC subsystem is manually realigned to the recirculation mode by closing the outside air and toilet exhaust duct isolation valves. Therefore, any potential heavy smoke problems at the main control room air intakes would not affect the plant operators.

On-site fuel storage facilities are designed in accordance with applicable fire codes, and plant safety is not jeopardized by fires or smoke in these areas. A detailed description of the plant fire protection system is presented in DCD Subsection 9.5.1.

2.2.3.1.5 Collisions with Intake Structure

WLS COL 2.2-1 The raw water intake structure on the Broad River is used to pump raw water into Make-Up Pond A. A makeup intake structure located in Make-Up Pond A is used to pump makeup water to the plant water systems. During low-flow conditions in the Broad River, a makeup intake structure located on Make-Up Pond B is used to pump raw water to Make-Up Pond A to provide makeup water for plant water systems. The portion of the Broad River adjacent to the Lee Nuclear Station is considered to be not navigable, so collisions with the intake structure are not considered to be credible. Likewise, there are no credible events or concerns associated with collisions to intakes on Make-Up Pond A or Make-Up Pond B.

2.2.3.1.6 Liquid Spills

The accidental release of petroleum products or corrosive liquids upstream of the Broad River intake structure would not affect operation of the plant. Normal operation of the water intake structure pumps requires submergence. Liquids with a specific gravity less than unity, such as petroleum products, would float on the surface of the river and consequently are not likely to be drawn into the makeup water system. Liquids with a specific gravity greater than unity could be drawn into the intake pipes. However, such liquids would be diluted by the water in Make-Up Pond A before it its drawn into the makeup intake structure.

The raw water system is not a safety related system and is not designed to function during design basis accidents or following low-probability events such as

seismic, fire, sabotage, passive failures or multiple active failures. Failure of components of the raw water system would not preclude essential functions of safety related systems.

2.2.3.2 Effects of Design Basis Events

Potential design basis events associated with accidents at nearby facilities and transportation routes have been analyzed in Subsection 2.2.3.1. The effects of these events on the safety-related components of the plant are insignificant as discussed in Subsection 2.2.3.1.

STD DEP 1.1-1

2.2.4 COMBINED LICENSE INFORMATION

WLS COL 2.2-1 This COL item is addressed in Subsection 2.2.3.

2.2.5 REFERENCES

201. U.S. Department of Transportation, National Transportation Atlas Databases (NTAD) 2006 Shapefile Format, CD-ROM.

202. U.S. Geological Survey, Geographic Names Information System (GNIS), Website, http://geonames.usgs.gov/domestic/download_data.htm, accessed August 8, 2006.

203. Environmental Data Resources, Inc, *Cherokee – Cherokee, SC*, March 7, 2006.

204. Calpine, Calpine Power Plants – Broad River Energy Center, Website, http://www.calpine.com/power/plant.asp?plant=96, accessed June 26, 2006.

205. Duke Energy, Mill Creek Combustion Turbine Station, Website, http://www.duke-energy.com/about/plants/franchised/combustion/mill_creek/, accessed October 12, 2006.

206. Duke Energy, Cliffside Steam Station, Website, http://www.duke-energy.com/about/plants/franchised/coal/cliffside/, accessed June 26, 2006.

207. Energy Information Administration, Catawba Nuclear Power Plant, South Carolina, Website, http://www.eia.doe.gov/cneaf/nuclear/page/at_a_glance/reactors/catawba.html, accessed June 26, 2006.

208. Energy Information Administration, “U.S. Nuclear Plants – McGuire”, Website, http://www.eia.doe.gov/cneaf/nuclear/page/at_a_glance/reactors/mcguire.html, accessed June 26, 2006.

209. South Carolina Bureau of Land & Waste Management - Division of Mining and Solid Waste, *Search Mining Companies and Solid Waste Disposal Facilities*, Website, http://www.scdhec.gov/lwm/html/min_search.asp, accessed July 13, 2006.

210. South Carolina Department of Transportation, “Average Daily Traffic - June 22, 2006.”

211. Norfolk Southern Corporation, “System Map 2006,” Section N – 15.

212. Amtrak, “Routes serving the South,” Website, http://www.amtrak.com/servlet/ContentServer?pagename=Amtrak/Page/Browse_Routes_Page&c=Page&cid=1081256321428&ssid=136, accessed November 6, 2006.

213. U.S. Department of Transportation Southeast High Speed Rail Corridor, “Southeast High Speed Rail Corridor – from Washington, DC to Charlotte, NC,” Website, http://www.sehsr.org/faq.html, accessed June 16, 2006.

214. Broad Scenic River Advisory Council Report, “Broad Scenic River Management Plan 2003 Update – Report 32.”

215. National Wild and Scenic Rivers System, “Wild and Scenic Rivers by State,” Website, http://www.nps.gov/rivers/wildriverslist.html, accessed August 11, 2006.

216. AirNav.com, “SC84 – Milliken & Company Heliport,” Website, http://www.airnav.com/airport/SC84, accessed June 7, 2006.

217. AirNav.com, “01SC – York Airport,” Website, http://www.airnav.com/airport/01SC, accessed June 7, 2006.

218. AirNav.com, “KGSP – Greenville-Spartanburg International Airport,” Website, http://www.airnav.com/airport/KGSP, accessed June 7, 2006.

219. AirNav.com, “KCLT – Charlotte Douglas International Airport,” Website, http://www.airnav.com/airport/KCLT, accessed June 7, 2006.

220. GSP International Airport, “GSP Passenger Statistics,” Website, http://www.gspairport.com/passenger_stats.shtml, accessed June 8, 2006.

221. Charlotte Douglas International Airport, “Aviation Activity for December 2000 – December 2005.”

222. Greenville-Spartanburg International Airport, “Master Plan Update December 2003 – Section 3: Development Concept.”

223. Greenville-Spartanburg International Airport, “Master Plan Update December 2003 – Section 4: Traffic Projections.”

224. Charlotte Douglas International Airport, “Construction Update,” Website, http://www.charmeck.org/Departments/Airport/About+CLT/Construction+Update.htm, accessed September 11, 2007.

225. U.S. Department of Transportation - Federal Aviation Administration, IFR Enroute Low Altitude – U.S.”, Panel L-20, effective February 16, 2006.

226. U.S. Department of Transportation - Federal Aviation Administration, “IFR Enroute High Altitude – U.S.”, Panel H-9, effective February 16, 2006.

227. U.S. Department of the Interior – National Park Service, “Military Bases in the Continental United States”, Website, http://www.cr.nps.gov/nagpra/DOCUMENTS/BasesMapIndex.htm, accessed May 19, 2006.

228. Cherokee County Chamber of Commerce, “2005-2006 Quality of Life.”

229. U.S. Department of Transportation - Federal Aviation Administration, “Aviation Accident Database and Synopsis – Greenville,” Website, http://www.ntsb.gov/ntsb/query.asp, accessed June 27, 2006.

230. U.S. Department of Transportation - Federal Aviation Administration, “Aviation Accident Database and Synopsis – Spartanburg,” Website, http://www.ntsb.gov/ntsb/query.asp, accessed June 27, 2006.

231. U.S. Department of Transportation - Federal Aviation Administration, “Aviation Accident Database and Synopsis – Charlotte,” Website, http://www.ntsb.gov/ntsb/query.asp, accessed June 27, 2006.

232. South Carolina Legislature, South Carolina Code of Regulations – Regulation 61-92 Underground Storage Tank Control Regulations, Website, http://www.scstatehouse.net/coderegs/c061f.htm#61-92, accessed April 6, 2007.

233. US Department of Labor - Occupational Safety & Health Administration, “Table Z-1,” Website, http://www.osha.gov/pls/oshaweb/owadisp.show_document?p_table=STANDARDS&p, accessed December 22, 2006.

234. Technical Committee on Forest and Rural Fire Protection. “Standard for Protection of Life and Property from Wildfire.” NFPA 1144. National Fire Protection Association, 2002.

235. U.S. Department of the Army, Structures to Resist the Effects of Accidental Explosions, Technical Manual TM 5-1300.

236. U.S. Environmental Protection Agency, ALOHA (Areal Location of Hazardous Atmospheres). Version 5.4 User Manual, February 2006.

237. Department of Defense, Contractor's Safety Manual for Ammunition and Explosives, DoD 4145.26-M, March 13, 2008.

238. National Fire Protection Association. "NFPA 704: Standard System for the Identification of the Hazards of Materials for Emergency Response," 2007.

Withheld from Public Disclosure Under 10 CFR 2.390(d)(1)
(see COL Application Part 9)

WLS COL 2.2-1

TABLE 2.2-201
REGISTERED STORAGE TANKS WITHIN A 5-MI. RADIUS

WLS COL 2.2-1

TABLE 2.2-202
INDUSTRIAL FACILITIES NEAR THE LEE NUCLEAR STATION

Name of Facility	Primary Function / Major Products	Persons Employed
Ninety-Nine Islands Hydroelectric Dam	Hydroelectric peaking electric generation plant	5
Herbie Famous Fireworks (South Carolina Distributors)	1.4G consumer fireworks warehouse facility	40
DSE Systems, LLC	US military ammunitions assembly facility	200
Broad River Energy Center	Natural gas-fired peaking electric generation plant	12
Mill Creek Combustion Turbine Station	Natural gas-fired peaking electric generation plant	5
Cliffside Steam Station	Coal-fired electric generation plant	104

(References 202, 204, 205, 206, and 207)

Withheld from Public Disclosure Under 10 CFR 2.390(d)(1)
(see COL Application Part 9)

WLS COL 2.2-1

TABLE 2.2-203 (Sheet 1 of 11)
PRODUCTS STORED ON SITE AT THE BROAD RIVER ENERGY CENTER

Withheld from Public Disclosure Under 10 CFR 2.390(d)(1)
(see COL Application Part 9)

TABLE 2.2-203 (Sheet 2 of 11)
WLS COL 2.2-1 PRODUCTS STORED ON SITE AT THE BROAD RIVER ENERGY CENTER

Withheld from Public Disclosure Under 10 CFR 2.390(d)(1)
(see COL Application Part 9)

TABLE 2.2-203 (Sheet 3 of 11)
WLS COL 2.2-1 PRODUCTS STORED ON SITE AT THE BROAD RIVER ENERGY CENTER

Withheld from Public Disclosure Under 10 CFR 2.390(d)(1)
(see COL Application Part 9)

TABLE 2.2-203 (Sheet 4 of 11)
WLS COL 2.2-1 PRODUCTS STORED ON SITE AT THE BROAD RIVER ENERGY CENTER

Withheld from Public Disclosure Under 10 CFR 2.390(d)(1)
(see COL Application Part 9)

TABLE 2.2-203 (Sheet 5 of 11)

WLS COL 2.2-1

PRODUCTS STORED ON SITE AT THE BROAD RIVER ENERGY CENTER

Withheld from Public Disclosure Under 10 CFR 2.390(d)(1)
(see COL Application Part 9)

TABLE 2.2-203 (Sheet 6 of 11)
WLS COL 2.2-1 PRODUCTS STORED ON SITE AT THE BROAD RIVER ENERGY CENTER

Withheld from Public Disclosure Under 10 CFR 2.390(d)(1)
(see COL Application Part 9)

TABLE 2.2-203 (Sheet 7 of 11)
WLS COL 2.2-1 PRODUCTS STORED ON SITE AT THE BROAD RIVER ENERGY CENTER

Withheld from Public Disclosure Under 10 CFR 2.390(d)(1)
(see COL Application Part 9)

TABLE 2.2-203 (Sheet 8 of 11)
WLS COL 2.2-1 PRODUCTS STORED ON SITE AT THE BROAD RIVER ENERGY CENTER

Withheld from Public Disclosure Under 10 CFR 2.390(d)(1)
(see COL Application Part 9)

TABLE 2.2-203 (Sheet 9 of 11)

WLS COL 2.2-1

PRODUCTS STORED ON SITE AT THE BROAD RIVER ENERGY CENTER

Withheld from Public Disclosure Under 10 CFR 2.390(d)(1)
(see COL Application Part 9)

WLS COL 2.2-1

TABLE 2.2-203 (Sheet 10 of 11)
PRODUCTS STORED ON SITE AT THE BROAD RIVER ENERGY CENTER

Withheld from Public Disclosure Under 10 CFR 2.390(d)(1)
(see COL Application Part 9)

WLS COL 2.2-1

TABLE 2.2-203 (Sheet 11 of 11)
PRODUCTS STORED ON SITE AT THE BROAD RIVER ENERGY CENTER

Withheld from Public Disclosure Under 10 CFR 2.390(d)(1)
(see COL Application Part 9)

WLS COL 2.2-1

TABLE 2.2-204
BROAD RIVER ENERGY CENTER SITE SPECIFIC OSHA
PERMISSIBLE EXPOSURE LIMITS (PEL) Z-1 TABLE

WLS COL 2.2-1

TABLE 2.2-205 (Sheet 1 of 2)
HISTORICAL AIR TRAFFIC AT GREENVILLE-SPARTANBURG INTERNATIONAL AIRPORT

Year	Total Passengers	Percent Change
1963	158,068	
1964	182,798	15.65
1965	195,893	7.16
1966	195,898	0.00
1967	256,885	31.13
1968	298,221	16.09
1969	332,090	11.36
1970	325,686	-1.93
1971	349,735	7.38
1972	411,683	17.71
1973	462,565	12.36
1974	496,019	7.23
1975	465,058	-6.24
1976	531,695	14.33
1977	569,246	7.06
1978	665,203	16.86
1979	690,904	3.86
1980	666,541	-3.53
1981	582,352	-12.63
1982	513,450	-11.83
1983	620,508	20.85
1984	735,961	18.61
1985	854,092	16.05
1986	937,863	9.81

WLS COL 2.2-1

TABLE 2.2-205 (Sheet 2 of 2)
HISTORICAL AIR TRAFFIC AT GREENVILLE-SPARTANBURG INTERNATIONAL AIRPORT

Year	Total Passengers	Percent Change
1987	1,105,752	17.90
1988	1,139,640	3.06
1989	1,110,314	-2.57
1990	1,184,580	6.69
1991	1,055,823	-10.87
1992	1,097,287	3.93
1993	1,171,826	6.79
1994	1,560,042	33.13
1995	1,322,540	-15.22
1996	1,428,223	7.99
1997	1,450,174	1.54
1998	1,424,669	-1.76
1999	1,518,561	6.59
2000	1,590,786	4.76
2001	1,412,567	-11.20
2002	1,386,828	-1.82
2003	1,350,648	-2.61
2004	1,575,117	16.62
2005	1,792,597	13.81
	AVERAGE	6.53

(Reference 220)

WLS COL 2.2-1

TABLE 2.2-206
PROJECTED AIR TRAFFIC AT GREENVILLE-SPARTANBURG INTERNATIONAL AIRPORT

Year	Total Passengers[a]
2006	1,909,654
2007	2,034,354
2008	2,167,197
2009	2,308,715
2010	2,459,474
2011	2,620,078
2012	2,791,169
2013	2,973,432
2014	3,167,598
2015	3,374,442
2016	3,594,793
2017	3,829,533
2018	4,079,601
2019	4,345,999
2020	4,629,793
2021	4,932,118
2022	5,254,186
2023	5,597,284
2024	5,962,787
2025	6,352,157

a) Projections based upon average of 6.53 percent annual increase in passengers as of 2005 (Reference Table 2.2-205).

(Reference 220)

WLS COL 2.2-1

TABLE 2.2-207
HISTORICAL AIR TRAFFIC AT CHARLOTTE DOUGLAS INTERNATIONAL AIRPORT

Year	Total Passengers	Percent Change
2000	23,088,455	
2001	23,177,555	0.39
2002	23,597,926	1.81
2003	23,062,570	-2.27
2004	25,543,374	10.76
2005	28,206,052	10.42
	AVERAGE	4.22

(Reference 219)

WLS COL 2.2-1

TABLE 2.2-208
PROJECTED AIR TRAFFIC AT CHARLOTTE DOUGLAS INTERNATIONAL AIRPORT

Year	Total Passengers[a]
2006	29,396,347
2007	30,636,873
2008	31,929,749
2009	33,277,185
2010	34,681,482
2011	36,145,040
2012	37,670,361
2013	39,260,050
2014	40,916,825
2015	42,643,515
2016	44,443,071
2017	46,318,568
2018	48,273,212
2019	50,310,342
2020	52,433,438
2021	54,646,129
2022	56,952,196
2023	59,355,578
2024	61,860,384
2025	64,470,892

a) Projections based upon average historical percent change in passengers

WLS COL 2.2-1

TABLE 2.2-209
PARAMETERS USED IN EXTRAN ANALYSIS OF TOXIC CHEMICALS

Parameter	Value	Unit
Initial mass	20000	(kg)
Release height	0	(m)
Storage temperature	25	(Celsius)
Distance to intake	5200	(m)
Intake height	17	(m)
Atmospheric pressure	760	(mm Hg)
Stability class	G	(N/A)
Wind speed	1	m/s

TABLE 2.2-210
LEAKAGE FROM ASSUMED LARGE HOLE (4.5 m^2) FROM A TRUCK ON HIGHWAY 29

Chemical	Truck Capacity (tons)	LEL (ppm)	Pool Diameter (yards)	Flammable Area of Vapor Cloud (yards)	Concentration at site (ppm)	Overpressure at site (psi)
Gasoline (n-heptane)	25.4	10,000	102	113	0.0	0.0
Propane	21.9	20,000	91	0	0.0	0.0
Acetylene	12.3	25,000	(a)	643	0.0	0.0
Ethylacetylene	24.0	16,000	(a)	874	0.0	0.0
Ethylene Oxide	32.2	30,000	(a)	836	0.0	0.0
Propylene Oxide	30.6	19,000	99	412	0.0	0.0
1,3 Propylene Oxide	33.2	28,000	101	252	0.0	0.0

a) Two-phase flow release.

TABLE 2.2-211
LEAKAGE FROM ASSUMED LARGE HOLE (4.5 m^2) FROM A RAILROAD TANKER

Chemical	Tanker Capacity (tons)	LEL (ppm)	Pool Diameter (yards)	Flammable Area of Vapor Cloud (yards)	Concentration at site (ppm)	Overpressure at site (psi)
Gasoline (n-heptane)	113	10,000	214	303	0.0	0.0
Propane	97.3	20,000	191	20	0.0	0.0
Acetylene	54.4	25,000	(a)	902	0.0	0.0
Ethylacetylene	107	16,000	(a)	1,306	0.0	0.0
Ethylene Oxide	143	30,000	(a)	1,220	0.0	0.0
Propylene Oxide	136	19,000	204	846	0.0	0.0
1,3 Propylene Oxide	148	28,000	210	542	0.0	0.0

a) Two-phase flow release.

2.3 METEOROLOGY

This section of the referenced DCD is incorporated by reference with the following departures and/or supplements.

This section discusses regional and local meteorological conditions, the onsite meteorological measurement program, and short-term and long-term diffusion estimates.

2.3.1 REGIONAL CLIMATOLOGY

WLS COL 2.3-1 The description of the general climate of the region is based primarily on climatological records for Greenville/Spartanburg International Airport (GSP), located between Greenville and Spartanburg, South Carolina. This first order station was selected because the terrain and land-use in the surrounding area is similar to the area around the Lee Nuclear Site (i.e., rural). This description uses data from those records, as appropriate, and is augmented by recent data from the Lee Nuclear Station site meteorological tower (Tower 2). Meteorological data for the Lee Nuclear Site collected from 12/1/2005 through 11/30/2006 is presented and used in FSAR Section 2.3. A second year of meteorological data for the Lee Nuclear Site was collected from 12/1/2006 through 11/30/2007. FSAR Appendix 2CC provides an evaluation which concludes that one-year and two-year data sets are consistent and representative of long-term conditions.

Topographical considerations and examination of the records indicate that meteorological conditions at the Greenville/Spartanburg International Airport are representative of the general climate of the region that encompasses the site. Because the Ninety-Nine Islands cooperative observer station (Station No. 386293) in Blacksburg, South Carolina, is the closest National Weather Service (NWS) station (two miles southeast), the tables and figures included are based primarily on data from this location when the period of record and observational procedures are considered adequate. Climate data from the National Oceanic and Atmospheric Administration (NOAA) first order weather station at the Greenville/Spartanburg International Airport (GSP) in Greer, SC approximately 42 miles west are also presented. Data from the National Oceanic and Atmospheric Administration (NOAA) first order weather station in Charlotte, NC (CLT) approximately 35 miles ENE of the site is also used in the cooling tower plume analysis. In cases such as the reoccurrence rate of rare events based on decades of observation (e.g. climatology), the National Weather Service off-site data is preferable, due to the shorter period of meteorological data currently available on site.

2.3.1.1 General Climate

The most important factors controlling the local climate are the state's location in the northern mid-latitudes, its proximity to both the Atlantic Ocean and the

Appalachian Mountains, and local elevation. South Carolina's geographic regions are shown on Figure 2.3-273. The Lee Nuclear Station site is located in the piedmont region of South Carolina. The Lee Nuclear Station is located in Cherokee County which is in South Carolina Climate Division 2. South Carolina's mid-latitude location allows for solar radiation to vary throughout the year, producing four distinct seasons. At the summer solstice, the sun is nearly overhead at solar noon with a maximum zenith angle of approximately 79½º; at winter solstice, the sun is low in the southern horizon at solar noon with a maximum zenith angle of approximately 23½º. This allows for a variance in length of day sufficient to produce ample daytime heating during summer and nighttime cooling during winter (Reference 201).

The state's position on the eastern coast of a continent is important because land and water heat and cool at different rates. This provides for cooling sea breezes during the summer and warms the immediate coast during the winter. Also, it influences the way pressure and wind systems affect the state. During the summer, South Carolina's weather is dominated by a maritime tropical air mass known as the Bermuda High. Airflow passing over the Gulf Stream, as it circulates around the Bermuda High brings warm, moist air inland from the ocean. As the air comes inland, it rises and forms localized thunderstorms, resulting in precipitation maxima (Reference 201).

The Appalachian Mountains also exert a major influence on the state's climate in three ways. First, they tend to block many of the cold air masses arriving from the northwest, thus making the winters somewhat milder. Second, the occurrence of downslope winds, which warm the air by compression, causes the areas leeward of the mountains to experience slightly higher temperatures than the surrounding areas. Hence, the proximity of the mountains to the state results in a more temperate climate than otherwise would be experienced. Lastly, the mountains cause a leeside rain shadow, an area of decreased precipitation across the Midlands and roughly parallel to the fall line where the upland region meets the coastal plain (Reference 201).

The climate of South Carolina is humid and subtropical with a short cold season and a relatively long warm season. Synoptic features during winter cause rather frequent alternation between mild and cool periods with occasional outbreaks of cold air. Such intrusions of cold air, however, are modified in the crossing and descent of the Appalachian Mountains. Summers, noted for their greater persistence in flow pattern, experience fairly constant trajectories from the south and southwest with advection of maritime tropical air. In this area of the Southeast, significant local circulation often results during periods of weak synoptic circulation. These effects, usually induced by the local terrain, are responsible for a redistribution of wind directions and speeds from those expected in the absence of the local terrain (Reference 202). General climatic assessments at the time of Reference 202 remain valid.

The state's annual average temperature, in Fahrenheit, varies from the mid-50's in the Mountains to low 60's along the coast. During the winter, average temperatures range from the mid-30's in the Mountains to low 50's in the Low Country. During summer, average temperatures range from the upper 60's in the

Mountains to the mid-70's in the Low Country (Reference 201). Temperatures in the region indicate warm summers and mild winters.

Precipitation in South Carolina is ample and distributed with two maxima and two minima throughout the year. The maxima occur during March and August; the minima occur during April and November. There is no wet or dry season; only relatively heavy precipitation periods or light precipitation periods. No month averages less than two inches of precipitation anywhere in South Carolina. In northwestern South Carolina, winter precipitation is greater than summer precipitation; the reverse is true for the remainder of the state. During summer and early fall of most years, the state is affected by one or more tropical storms or hurricanes (Reference 201). Average annual precipitation is heaviest in northwestern South Carolina, and annual totals vary directly with elevation, soil type, and vegetation. In the Mountains, 70 to 80 inches of rainfall occur at the highest elevations with the highest annual total at Caesars Head, South Carolina (79.29 inches). Across the Foothills, average annual precipitation ranges from 60 to more than 70 inches. In the eastern and southern portions of the Piedmont, the average annual rainfall ranges from 45 to 50 inches. The driest portion of the state, on average, is the Midlands where annual totals are mostly between 42 and 47 inches (Reference 201).

The annual number of days of precipitation greater than or equal to one inch varies with elevation, varying from more than 24 days in the Upstate to less than 12 days in the Midlands. The annual number of days of precipitation greater than or equal to 0.1 inches varies from 95 in the Upstate to less than 70 in a portion of the Midlands. The annual number of days of precipitation greater than or equal to 0.5 inches varies from 48 in the Upstate to less than 30 in a portion of the Midlands (Reference 201). Yearly average precipitation at Greenville/Spartanburg International Airport based on 30 years of data is about 50 inches (Table 2.3-256).

Snow and sleet may occur separately, together, or mixed with rain during the winter months from November to March, although snow has occurred as late as May in the mountains. Measurable snowfall may occur from one to three times in a winter in all areas except the Low Country where snowfall occurs on average once every three years. Accumulations seldom remain very long on the ground except in the mountains (Reference 201). Typically, snowfall occurs when a mid-latitude cyclone moves northeastward along or just off the coast. Snow usually occurs about 150 to 200 miles inland from the center of the cyclone. The greatest snowfall in a 24-hour period was 24 inches at Rimini, South Carolina, in February 1973. During December 1989, Charleston, South Carolina, experienced its first white Christmas on record, and other coastal locations had more than six inches of snow on the ground for several days following it. The greatest snowfall for Ninety-Nine Islands was 13 inches on January 7, 1988. Figure 2.3-201 shows the annual distribution of snow across the state (Reference 201).

Sleet and freezing rain vary from 3.75 events per year in Chesterfield County to less than 0.75 events per year in the Low Country. The highest frequency by month occurs in January with more than 1.5 events per year in the Charlotte area and Chesterfield County to less than 0.25 events per year in the Low Country. One of the most severe cases of ice accumulation from freezing rain took place

February 1969 in several Piedmont and Midlands counties. Timber losses were tremendous and power and telephone services were seriously disrupted over a large area (Reference 201). Another significant storm was the ice storm of December 2005. This was a damaging winter storm that produced extensive ice damage in a large portion of the Southern United States on December 14 - 16, 2005. It led to enormous and widespread power outages and at least 7 deaths. The ice storm left more than 700,000 people without power in and near the Appalachians, including 30,000 customers in Georgia, 358,000 in South Carolina, 328,000 in North Carolina and 13,000 in Virginia. An ice storm (also called glaze ice) is the accretion of generally clear and smooth ice formed on exposed objects by the freezing of a film of super-cooled water deposited by rain, drizzle, or possibly condensed from super-cooled water vapor. The weight of this ice is often sufficient to greatly damage telephone and electric power lines and poles. Most glaze is the result of freezing rain or drizzle falling on surfaces with temperatures between 25°F and 32°F (Reference 204). The glaze ice belt of the United States includes all of the area east of the Rocky Mountains. However, in the Southeast and Gulf Coast sections of the country, below freezing temperatures seldom last more than a few hours after glaze storms.

Hail occurs infrequently, falling most often during spring thunderstorms from March through May. The incidence of hail varies from 1 to 1.5 hail days per year in the Midlands, Piedmont, and Foothills to 0.5 day per year in the Low Country. Although hail can occur in every month during the year, May has the highest incidence with an average of more than five events per year. Typically, it occurs during the late afternoon and early evening between the hours of 3:00 p.m. and 8:00 p.m. (Reference 201). Severe weather occurs in South Carolina occasionally in the form of violent thunderstorms and tornadoes. Although less frequent than surrounding states, thunderstorms are common in the summer months. The more violent storms generally accompany squall lines and active cold fronts of late-winter or spring. Strong thunderstorms usually bring high winds, hail, considerable lightning, and rarely spawn a tornado (Reference 201).

In the 40-year period from 1950 through 1989, an average of 11 tornadoes occurred per year in South Carolina. Since a tornado is very small and affects a localized area, the probability of a tornado striking a specific point in a given year is low. The majority of tornadoes, 88 percent, occur from February through September. May and August are peak months. The May peak is primarily due to squall lines and cold fronts; the August peak is due to tropical cyclone activity. A secondary maxima, nine percent of all occurrences, happens in November and December (Reference 201). During spring, tornadoes result from active cold fronts, whereas during summer and early fall many are associated with the passage of tropical cyclones. During November and December, it is not uncommon to have active cold fronts and tornadic activity. Tornado frequency is at a minimum in October and January; only 3 percent of the total are experienced during these two months (Reference 201).

Tropical cyclones affect the South Carolina coast on an infrequent basis, but do provide significant influence annually through enhanced rainfall inland during the summer and fall months. Depending on the storm's intensity and proximity to the coast, tropical systems can be disastrous. The major coastal impacts from tropical

cyclones are storm surge, winds, precipitation, and tornadoes. Hurricanes are the most intense warm season coastal storms and are characterized by wind speeds exceeding 64 knots (74 miles per hour) and central pressure usually less than 980 millibars (mb) (28.94 inches of mercury). Less intense, but more frequent, are tropical storms (winds over 34 knots and under 64 knots: greater than 980 mb central pressure) and tropical depressions (winds under 34 knots). (Reference 201) Tracks of tropical cyclones within 75 miles of Greer, South Carolina between 1851 and 2006 are shown on Figure 2.3-272.

Winds are usually the most destructive force associated with tropical cyclones, particularly inland. Strong winds, resulting from the low central pressure and forward movement, also combine to result in significant ocean rise and wave action. This resulting water rise, known as the storm surge, plagues coastal inlands and low-lying inland areas as these storms make landfall. Because of the low central pressure in a hurricane, a 100 mb drop in ocean surface pressure results in about a one meter increase of ocean elevation. (Reference 201).

The Mountains have a strong influence on the prevailing surface wind direction. On a monthly basis, prevailing winds tend to be either from the northeast or southwest. Winds from all directions occur throughout the state during the year, but the prevailing statewide directions by season are as follows: (Reference 201)

Season	Direction	Degrees
Spring	Southwest	210 to 240
Summer	South and Southwest	170 to 250
Autumn	Northeast	20 to 60
Winter	Northeast and Southwest	20 to 60 and 210 to 240

Average surface wind speeds across the state for all months range between six and 10 miles per hour. Winds at more than 1500 meters above msl are usually southwest to northwest in winter and spring, south to southwest in summer, and southwest to west in autumn. The mountains control wind direction during all seasons, but have a more pronounced effect in the winter, summer, and autumn (Reference 201). During winter, most cyclones that affect the state pass to the south of the Mountains. As these systems move around the Mountains, the winds are generally southwest. As the cyclone moves over the Atlantic Ocean, the winds shift to the northeast. During summer, air flows north from the Gulf of Mexico along the western edge of the Bermuda High. Quite often the Mountains form the western extent of the Bermuda High. During autumn, winds are northeast because the mountains form a western barrier to the northeast surface winds wrapping around the predominant continental high pressure centered over New England. This northeast flow wedges in cool air at the surface and moves southward along the eastern seaboard (Reference 201).

The Bermuda High also contributes to air stagnation, especially during the summer. During the period 1936-75, it was shown that the state experienced 20 stagnation days per year in the Coastal Plain, and more than 28 stagnation days per year occurred in the Central Savannah River area. The winds in stagnant air are very light and tend to be rather disorganized in direction (Reference 201).

Relative potential for air pollution can be demonstrated by the seasonal distribution of atmospheric stagnation cases that persist for at least four days. Data for the 50-year period (1948 to 1998), analyzed by Julian X. L. Wang and James K. Angell (Reference 205), show that, in South Carolina, air stagnation conditions exist between 10 and 20 days per year. The meteorological condition which is favorable to an air pollution episode is an air stagnation event. The air stagnation event identifies areas where air may be trapped by poor ventilation due to persistent light or calm winds, and by the presence of inversions. Most air stagnation events happen in an extended summer season from May to October. This is the result of the weaker pressure and temperature gradients, and therefore weaker wind circulation during this period. In the eastern U.S., there is a relative minimum of stagnation in July accompanied by relative maxima in May-June and August-October. This mid-summer decrease of air stagnation is due to the impact of the Bermuda High on the eastern United States. The Bermuda High is strongest in July; and hence, the meridianal wind in the Gulf States is a maximum then due to the increased pressure gradient, resulting in a relative minimum of air stagnation. Therefore, the Bermuda High is an additional and unique controlling factor for air stagnation conditions over the eastern United States, besides the seasonal cycle of minimum wind in summer and maximum wind in winter.

Another unique feature of air stagnation in the eastern U.S. is its early onset in May, compared to the onset in June in the west and central U.S. This results in a prolonged but weaker air stagnation season in the eastern U.S (Reference 205). For the eastern United States, their results show a regionally averaged mean annual cycle of six cases in the spring, 14 cases in the summer, and 11 cases in the fall for the region.

Just to the North of the Lee Nuclear Station site, is the border of North Carolina. The climate in this area is typical of the Piedmont area of North Carolina. The three principal physiographic divisions of the eastern United States are particularly well developed in North Carolina. From east to west, they are the Coastal Plain, the Piedmont, and the Mountains. The fall line is the dividing line between the Coastal Plain and the Piedmont. The Piedmont area, comprising about one-third of the State, rises gently from about 200 feet at the fall line to near 1,500 feet at the base of the Mountains.

The westernmost, or Mountain Division of North Carolina is the smallest of the three, comprising a little more than one-fifth of the total area of the State. Its range of elevation, however, is by far the greatest; it stretches upward from around 1,500 feet along the eastern boundary to 6,684 feet at the summit of Mount Mitchell. Some of the valleys drop to 1,000 feet above sea level while some 125 peaks exceed 5,000 feet and 43 tower above 6,000 feet.

Latitude accounts for some climatic variations, as do soils, plant cover, and inland bodies of water. The Gulf Stream has some direct effect on North Carolina temperatures, especially on the immediate coast. Though the Gulf Stream lies some 50 miles offshore, warm water eddies spin off from it and moderate the winter air temperatures along the Outer Banks. Coastal fronts are common during the winter months, and can push inland, bringing warmer than expected temperatures to coastal areas.

The most important single influence contributing to the variability of North Carolina climate is altitude. In all seasons of the year, the average temperature varies more than 20° Fahrenheit from the lower coast to the highest elevations. The average annual temperature at Southport on the lower coast is nearly as high as that of interior northern Florida, while the average on the summit of Mount Mitchell is lower than that of Buffalo, NY.

In winter, the greater part of North Carolina is partially protected by the mountain ranges from the frequent outbreaks of cold air which move southeastward across the central States. Such outbreaks often move southward all the way to the Gulf of Mexico without attaining sufficient strength and depth to traverse the heights of the Appalachian Range. When cold waves do break across, they are usually modified by the crossing and the descent on the eastern slopes. The temperature drops to 10° or 12° F about once during an average winter over central North Carolina, ranging some 10° F warmer along the coast and 10° F colder in the upper mountains. Temperatures as low as 0° F are rare outside the mountains, but have occurred throughout the western part of the State. The lowest temperature of record is minus 34° F recorded January 21, 1985, at Mount Mitchell. Winter temperatures in the eastern sections are modified by the Atlantic Ocean, which raises the average winter temperature and decreases the average day-to-night range. In spring, the storm systems that bring cold weather southward reach North Carolina less often and less forcefully, and temperatures begin to moderate. The rise in average temperatures is greater in May than in any other month. Occasional invasions of cool dry air from the north continue during the summer, but their effect on temperatures is slight and of short duration.

The increase in sunshine in the spring usually brings temperatures back up quickly. When the dryness of the air is sufficient to keep cloudiness at a minimum for several days, temperatures may occasionally reach 100° F or higher in the interior at elevations below 1,500 feet. Ordinarily, however, summer cloudiness develops to limit the sun's heating while temperatures are still in the 90-degree range. An entire summer sometimes passes without a high of 100° F being recorded in South Carolina. The average daily maximum reading in midsummer is below 90° F for most localities.

Autumn is the season of most rapidly changing temperature, the daily downward trend being greater than the corresponding rise in spring. The drop-off is greatest during October, and continues at a rapid pace in November, so that average daily temperatures by the end of that month are within about five degrees of the lowest point of the year.

While there are no distinct wet and dry seasons in North Carolina, average rainfall does vary around the year. Summer precipitation is normally the greatest, and July is the wettest month. Summer rainfall is also the most variable, occurring mostly in connection with showers and thunderstorms. Daily showers are not uncommon, nor are periods of one to two weeks without rain. Autumn is the driest season, and November the driest month. Precipitation during winter and spring occurs mostly in connection with migratory low pressure storms, which appear with greater regularity and in a more even distribution than summer showers. In southwestern North Carolina, where moist southerly winds are forced upward in passing over the mountain barrier, the annual average rainfall is more than 90 inches. This region is the rainiest in the eastern United States. Less than 50 miles to the north, in the valley of the French Broad River, sheltered by mountain ranges on all sides, is the driest point south of Virginia and east of the Mississippi River. Here the average annual precipitation is only 37 inches. East of the Mountains, average annual rainfall ranges mostly between 40 and 55 inches.

Winter-type precipitation usually occurs with southerly through easterly winds, and is seldom associated with very cold weather. Snow and sleet occur on an average once or twice a year near the coast, and not much more often over the southeastern half of the State. Such occurrences are nearly always connected with northeasterly winds, generated when a high pressure system over the interior, or northeastern United States, causes a southward flow of cold dry air down the coastline, while offshore a low pressure system brings in warmer, moist air from the North Atlantic. Farther inland, over the Mountains and western Piedmont, frozen precipitation sometimes occurs in connection with low pressure storms, and in the extreme west with cold front passages from the northwest. Average winter snowfall over North Carolina ranges from about an inch per year on the outer banks and along the lower coast to about 10 inches in the northern Piedmont and 16 inches in the southern Mountains. Some of the higher mountain peaks and upper slopes receive an average of nearly 50 inches a year.

The average relative humidity does not vary greatly from season to season but is generally the highest in winter and lowest in spring. The lowest relative humidity is found over the southern Piedmont, where the year around average is about 65 percent.

2.3.1.2 Regional Meteorological Conditions for Design and Operating Bases

This section describes severe weather phenomena that may require consideration in design of safety related structures, systems and components. Most recent data is taken from the NCDC storm event database that covers the period from 1950 through 2005 (Reference 207), but even longer data periods are used for some phenomena to try to capture the occurrence of rare events.

Severe synoptic-scale storms are relatively infrequent in the Lee Nuclear Station site area. The effects of such storms are generally restricted to local flooding from heavy rains. Damage from snow, freezing rain, or ice storms in mid-winter are uncommon.

The passive containment cooling system is the ultimate heat sink for the AP1000 and does not rely upon offsite or onsite AC power sources as described in DCD Section 3.1.1. The AP1000 design parameters for the ultimate heat sink are given in DCD Table 2-1. The regional meteorological conditions relevant to the design and operating bases for the Lee Nuclear Station site are discussed below. FSAR Table 2.0-201 gives a comparison of the Lee Nuclear Station site characteristics with the AP1000 DCD design parameters.

General Design Criterion (GDC) 2 in Appendix A to 10 CFR Part 50 requires "consideration of the most severe of the natural phenomena that have been historically reported for the site and surrounding area, with sufficient margin for the limited accuracy, quantity, and period of time in which the historical data have been accumulated."

Extreme weather calculations for Lee Nuclear Station were conducted over the maximum data span available. Certified climatological data obtained from the U.S. National Climatic Data Center (NCDC) was used for the severe weather phenomena evaluations. This data selection supports accurate severe weather phenomena projections for the area in the vicinity of the Lee Nuclear Station site. This extensive historic data record provides the historical climatic trends and severe natural phenomena to be included in the site characterization.

Dry-bulb, coincident wet-bulb, and non-coincident wet-bulb temperatures represent significant site characteristics because this data is used in demonstrating that the AP1000 DCD site parameters are bounding (i.e., more conservative) than the Lee Nuclear Station site characteristics. The Lee Nuclear Station site characteristic temperatures were developed by considering both 100-year return temperatures and 0% exceedance temperatures. These values were calculated using all available hourly data from a 45-year (1963-2007) sequential meteorological data set for Greenville-Spartanburg Airport, Greer, South Carolina, Station No. 03870, National Weather Service (NWS) station. The difference between the Lee Nuclear Station site characteristics and the DCD design parameters, as provided in FSAR Table 2.0-201, provide additional margin to the selected Lee Nuclear Station site characteristic maximum safety temperatures. This margin accounts for any limitations to the accuracy, quantity, and period of time in which the historical data have been accumulated.

General predictions on global or U.S. climatic changes expected during the period of reactor operation are uncertain and are only applicable on a macroclimatic scale. Since the maximum data span available was used in the severe weather analysis, accurate severe weather phenomena have been provided based on best-available historic data. Projections of future severe weather conditions at the Lee Nuclear Station site are speculative at best, based on current understanding and modeling of global climate change.

2.3.1.2.1 Hurricanes

During the period 1899 to 2005 there were 50 documented tropical cyclones that affected either North Carolina (31 cyclones) or South Carolina (19 cyclones) (Reference 209, Reference 210, and Reference 235). See Table 2.3-202. Of

these 50 cyclones, 20 (40 percent) were Category 1, 15 (30 percent) were Category 2, 11 (22 percent) were Category 3, and 4 (8 percent) were Category 4 hurricanes. The storm category cited is the category observed as the cyclone entered either North Carolina or South Carolina. Table 2.3-203 presents a monthly breakdown of the 50 cyclones and provides a definition of the storm categories. Tropical cyclones, including hurricanes, lose strength as they move inland from the coast and the greatest concern for an inland site is possible flooding due to excessive rainfall. The maximum one day rainfall at Ninety-Nine Islands for the years 1949-2005 was 7.16 inches on 8/17/1985 resulting from hurricane Danny which was a tropical depression when it passed through this part of South Carolina (Reference 203).

2.3.1.2.2 Tornadoes

The probability that a tornado will occur at the Lee Nuclear Station site is low. Records show that in a 56-year period (1950-2005) there were 15 tornadoes reported in Cherokee County, the location of the site. The data reported by NOAA's National Environmental Satellite, Data, and Information Service (NESDIS) (Reference 207) is given in Table 2.3-204. From this data, the total tornado area in Cherokee County, ignoring events with a zero path length (i.e., no path length or no path length reported), is approximately 3.6 square miles. Using the principle of geometric probability described by H. C. S. Thom (Reference 211), a mean tornado path area of 0.24 square miles and an average tornado frequency of 0.27 per year was calculated for the area of Cherokee County (392.7 mi^2), the point probability of a tornado striking the Lee Nuclear Station is $1.64x10^{-4}$/year [((total tornado area in Cherokee County)/(area of Cherokee County))*(number of tornadoes per year)]. This corresponds to an estimated recurrence interval of 6108 years.

The tornadoes reported during the years 1950-2005 in the vicinity of Cherokee, Spartanburg, Union, Chester, and York Counties in South Carolina and Cleveland, Gaston, and Mecklenburg Counties in North Carolina are shown in Table 2.3-204. During the period 1950 to 2005, a total of 118 tornadoes touched down in these counties, which have a combined total land area of 5,131.2 square miles (Reference 212). These local tornadoes have a mean path area of 0.46 square miles, excluding tornadoes without a length specified. The site recurrence frequency of tornadoes can be calculated using the point probability method as follows:

Total area of tornado sightings = 5,131.2 sq mi

Average annual frequency = 118 tornadoes/56 years = 2.11 tornadoes/year

Annual frequency of a tornado striking a particular point P = [(0.46 mi^2/tornado) (2.11 tornadoes/year)] / 5,131.2 sq. mi = 0.0002 yr^{-1}

Mean recurrence interval = 1/P = 5000 years.

This result shows that the frequency of a tornado in the immediate vicinity of the site is slightly lower than the frequency in the surrounding counties. Another methodology for determining the tornado strike probability at the Lee Nuclear Station is given in NUREG/CR-4461 (Reference 213). Based on a 2° longitude and latitude box centered on the Lee Nuclear Station site, the number of tornadoes is 221 from data collected from 1950 through August 2003. The corresponding expected maximum tornado wind speed and upper limit (95th percentile) of the expected wind speed is given below with the associated probabilities.

Probability	Expected maximum tornado wind speed mph	Upper limit (95 percent) of the expected tornado wind speed mph
10^{-5}	142	153
10^{-6}	180	190
10^{-7}	215	226

The design basis tornado characteristics are specific to the site location and region of the country in which the site is located. However, rather than conducting site research on tornado characteristics, most sites in past licensing proceedings have relied on NRC-endorsed studies that set conservative values for key design basis tornado characteristics. These characteristics were then used in the design of the subject facility.

Regulatory Guide 1.76, Revision 1, provides design basis tornado characteristics, depending on the proposed site location in the country. Based on these criteria, the best estimated exceedance frequency is 10^{-7} per year. The design basis tornado characteristics defined for Lee Nuclear Station, which is in Region I, are based on the guidance in Regulatory Guide 1.76. The below listed characteristics are associated with a Region I site.

Region I Tornado Characteristics

Maximum wind speed, mph	230
Rotational speed, mph	184
Maximum Translational speed, mph	46
Radius of maximum rotational speed, ft	150
Pressure drop, psi	1.2
Rate of pressure drop, psi/sec	0.5

The above maximum tornado wind speed is bounded by the AP1000 DCD value of 300 mph (see FSAR Table 2.0-201 for a comparison of the Lee Nuclear Station site characteristics with the DCD design parameters). In accordance with Regulatory Guide 1.76, the wind velocities and pressures are not assumed to vary with height. Tornado missiles (including the missile spectrum) are discussed in Section 3.5. Waterspouts are common along the southeast U.S. coast, especially off southern Florida and the Keys and can happen over seas, bays, and lakes worldwide. However, they are not expected to occur at the Lee Nuclear Station site since the only nearby body of water is the Broad River.

2.3.1.2.3 Thunderstorms

Thunderstorms occur an average of approximately 41.6 days a year based on the National Climatic Data Center (NCDC) Local Climatic Data (LCD) when data from Greenville-Spartanburg (Greer), South Carolina (Station ID GSP) (Reference 236) and Charlotte, North Carolina (Station ID CLT) (Reference 239) are combined for the years 1963 through 2007 and 1948 through 2007, respectively. Table 2.3-205 presents the thunderstorm data for Greer and Charlotte for the years 1963 through 2007 and 1948 through 2007, respectively. Approximately 57 percent of the thunderstorms in this area occur during the warm months (June-August), indicating that the majority are warm-air-mass thunderstorms. As shown in Table 2.3-205, the highest occurrence of thunderstorm days is in July with an average of approximately 10 days per year.

2.3.1.2.4 Lightning

Data on lightning strike density is becoming more readily available due to the National Lightning Detection Network (NLDN), which has measured cloud-to-ground (CG) lightning for the contiguous United States since 1989. Prior to the availability of this data, isokeraunic maps of thunderstorm days were used to predict the relative incidence of lightning in a particular region. A general rule, based on a large amount of data from around the world, estimates the earth flash mean density to be 1-2 cloud to ground flashes per 10 thunderstorm days per square kilometer. (Reference 214). The annual mean number of thunderstorm days in the site area is estimated to be 50 based on interpolation from the isokeraunic map (Reference 215); therefore, it is estimated that the annual lightning strike density in the Lee Nuclear Station site area is 26 strikes per square mile per year. Other studies gave a ground flash density (GFD) in strikes/km^2/yr, based on thunderstorm days per year (TSD) as GFD = 0.04 $(TSD)^{1.25}$ = 0.04 $(50)^{1.25}$ = 5.3 strikes/km^2/yr or 14 strikes/mi^2/yr. (Reference 216). Recent studies based on data from the NLDN (Reference 217) indicate that the above strike densities are upper bounds for the Lee Nuclear Station site. Mean annual flash density for 1989-96 is 5 strikes/km^2/yr or 13 strikes/mi^2/yr in northern South Carolina.

2.3.1.2.5 Hail

From January 1, 1995 through May 31, 2006, 432 hailstorms occurred in the region with Cherokee County receiving approximately ten percent, as shown in

Table 2.3-206. For this table, each occurrence of hail was counted as an individual event, even if two counties recorded hail simultaneously. The most probable months of hail occurrence are May and June in Cherokee County. The average number of hailstorms in Cherokee County is approximately 3.5 per year. The maximum hail size reported was 2.75 inch diameter and the average size was slightly more than 1 inch diameter. Property damage occurs infrequently, with no recorded events in Cherokee County, South Carolina in this 12-year period (Reference 207).

2.3.1.2.6 Regional Air Quality

The Clean Air Act, which was last amended in 1990, requires the U.S. Environmental Protection Agency (EPA) to set National Air Quality Standards for pollutants considered harmful to the public health and the environment. The EPA Office of Air Quality Planning and Standards has set National Ambient Air Quality Standards for six principle pollutants, which are called "Criteria" pollutants. Units of measure for the standards are parts per million (ppm), milligrams per cubic meter (mg/m^3), and micrograms per cubic meter of air ($\mu gm/m^3$). Areas are either in attainment of the air quality standards or in non-attainment. Attainment means that the air quality is better than the standard.

The newly promulgated U.S. Environmental Protection Agency (EPA) 8-hour ozone standard (62FR 36, July 18, 1997) is 0.08 ppm in accordance with 40 CFR 50.10. Cherokee is in the Greenville-Spartanburg Intrastate Air Quality Control Region (South Carolina). Cherokee County is in attainment for all criteria pollutants (carbon monoxide, lead, nitrogen dioxide, particulate matter (PM_{10}, particulate matter less than 10 micron), particulate matter ($PM_{2.5}$, particulate matter less than 2.5 micron), ozone, and sulfur oxides. There are six areas in South Carolina that are in non-attainment with the 8-hour ozone standard (Reference 218). Currently designated (as of March 02, 2006) non-attainment areas in South Carolina for the criteria pollutants are as follows:

County	Pollutant	Area Name
Anderson Co	8-Hr Ozone	Greenville-Spartanburg-Anderson, SC
Greenville Co	8-Hr Ozone	Greenville-Spartanburg-Anderson, SC
Lexington Co	8-Hr Ozone	Columbia, SC
Richland Co	8-Hr Ozone	Columbia, SC
Spartanburg Co	8-Hr Ozone	Greenville-Spartanburg-Anderson, SC
York Co	8-Hr Ozone	Charlotte-Gastonia-Rock Hill, NC-SC

The bordering North Carolina counties are Cleveland, Gaston, and Mecklenburg. Both Gaston County and Mecklenburg County are in non-attainment for 8-hr ozone. Cleveland County is in attainment for all criteria pollutants.

The ventilation rate is a significant consideration in the dispersion of pollutants. Higher ventilation rates are better for dispersing pollution than lower ventilation rates. The atmospheric ventilation rate is numerically equal to the product of the mixing height and the wind speed within the mixing layer. A tabulation of daily mixing heights and mixing layer wind speeds for both morning and afternoon was obtained from the EPA's SCRAM Website for 1984-1987 and 1989-1991 at the Greensboro-High Point, North Carolina station (Reference 206). This data was used to generate the morning and afternoon ventilation rates in Table 2.3-207. Morning ventilation is less than 4000 m^2/s throughout the year and is less than 2400 m^2/s from June through October. Afternoon ventilation is higher than 9200 m^2/s from March through June, but lower than 6500 m^2/s from August through January. The highest daily air pollution potentials exist in the morning from June through October when ventilation rates are lower. Lowest air pollution potentials occur from December through March due to the relatively high morning mean ventilation rates.

Other data sources provide independent checks on this conclusion. According to Wang and Angell (Reference 205), the annual average air stagnation cases for South Carolina over a fifty-one year period (1948-1998) was four cases per year with a mean duration of five days. The annual mean days of air stagnation was given as 20 for South Carolina. This report also concluded that the highest number of air stagnation days occurred from July through October with the lowest air stagnation days from November through March. The number of air stagnation days in the South Carolina region exhibited a slightly increasing trend over the 50 years evaluated (see Figure 2.3-202). This almost imperceptible positive trend shown in Figure 2.3-202 in the number of air stagnation days has no impact on the Lee Nuclear Station Site.

2.3.1.2.7 Severe Winter Storm Events

The occurrences and durations of recorded ice storms and heavy snowstorms in the vicinity of the Lee Nuclear Station site for the thirteen-year period 1993-2005 is shown in Table 2.3-208. From these data, the frequency of winter storms is estimated to be 22 events per year in this regional area. For the region, each occurrence of a severe winter storm was counted as an individual event, even if two counties recorded a severe winter event simultaneously. For Cherokee County, the frequency is 3.6 events per year.

The equivalent ice thickness due to freezing rain with concurrent 3-second gust speeds for a 100-year mean recurrence interval is given in "Extreme Ice Thicknesses from Freezing Rain" (Reference 208) as 0.75 inch for the north central South Carolina area.

The 48-hour maximum recorded winter precipitation based on the data for the Greenville-Spartanburg NWS (GSP) at Greer, covering the time period of 1997-2005, is 3.54 inches (Reference 224).

In the Ninety-Nine Islands/Lee Nuclear Station site area, snow melts and/or evaporates quickly, usually within 48 hours and before additional snow is added.

Because the plant site is subjected to a subtropical climate with mild winters, prolonged snowfalls or large accumulations of snow or ice on the ground and structures are not anticipated.

2.3.1.2.7.1 Estimated Weight of the 100-year Return Snowpack

Snowpack, as used in this section, is defined as a layer of snow and/or ice on the ground surface and is usually reported daily in inches by the NWS at all first order weather stations.

The density of the snowpack varies with age and the conditions to which it has been subjected. Thus, the depth of the snowpack is not a true indication of the pressure the snowpack exerts on the surface it covers. Due to the variable density in snowpack, a more useful statistic for estimating the snowpack pressure is the water equivalent (in inches) of the snowpack.

South Carolina is not a heavy snow load region. ANSI/ASCE 7-05, "Minimum Design Loads for Buildings and Other Structures," identifies that the ground snowload for the Greenville-Spartanburg area is 7 lbf/ft^2 based on a 50-yr recurrence. This is converted to a 100-yr recurrence weight of 8.54 lbf/ft^2 (psf) using a factor of 1.22 (1 / 0.82) taken from ANSI/ASCE 7-05 Table C7-3. Local snow measurements support this ANSI/ASCE 7-05 (Reference 220) value.

To estimate the weight of the 100-year snowpack at the Lee Nuclear Station site, the maximum reported snow and/or ice depths at Ninety-Nine Islands, South Carolina, was determined. The current Southeast Regional Climate Office Database (Reference 203) indicates the greatest snow depth in the data period (8/1/1948 to 12/31/2005) occurred on January 7, 1988. The snow depth recorded on this date was 13 inches. The 100-year recurrence snow depth is 15.2 inches based on 57 years of data back to 1948. Based on NCDC Snow Climatology database, the highest observed maximum snowfall amount, maximum snow depth, and 100-year estimate of snowfall for Cherokee County, SC occurred at the Gaffney 6E observation station. The 100-year snowfall for Gaffney 6E, based on data from 1894 through 2006, was 16.3 inches, the maximum snow depth was 17.0 inches, and the observed maximum snowfall was 17.0 inches. The 100-year snow depth of 17.0 inches will be used in determining the snow load (Reference 237).

Freshly fallen snow has a snow density (the ratio of the volume of melted water to the original volume of snow) of 0.07 to 0.15, and glacial ice formed from compacted snow has a maximum density of 0.91 (Reference 221). In the Lee Nuclear Station site area, snow melts and/or evaporates quickly, usually within 48 hours, and before additional snow is added; thus, the water equivalent of the snowpack can be considered equal to the water equivalent of the falling snow as reported hourly during the snowfall. A conservative estimate of the water equivalent of snowpack in the Lee Nuclear Station site area would be 0.20 inches of water per inch of snowpack. Then, the water equivalent of the 100-year return snowpack would be 17.0 inches snowpack x 0.2 inches water equivalent/inch snowpack = 3.4 inches of water.

Because one cubic inch of water is approximately 0.0361 pounds in weight, a one inch water equivalent snowpack would exert a pressure of 5.20 pounds per square foot (0.0361 lb/cu in/in x 144 sq in/sq ft).

For the 100-year return snowpack, the water equivalent would exert a pressure of 17.7 pounds per square foot (5.2 lbm/sq ft/inch x 3.4 inches).

2.3.1.2.7.2 Estimated Weight of the 48-hour Maximum Winter Precipitation

The 48-hour probable maximum winter precipitation (PMWP) based on HMR 53 (Reference 234) is 30.5 inches. The rain load is considered separately from the snow and ice roof load. The roofs of the nuclear island have no lips around the edges, therefore, water and snow melt build up on the roofs of the Nuclear island are negligible. The Shield Building roof is slopped with no lips around the edge of the roof to allow water build up. The PCS tank is flat with no lip; however, there is the central hole that can allow water to drain down in between the Shield wall and the SCV, but not to accumulate on the roof area. The Auxiliary Building. has slopped roofs with three varying elevations (high points given); Area 1&2 155'-6", Area 3&4 163'-0", and Area 5&6 180'-9" (elevations are above plant grade). The south side (directions are relative to called North in the DCD) of the nuclear island wall 1 is above the Radwaste Building roof elevation 136'-4". The east side of the nuclear island, wall 1, is below the Annex Building roof elevation 183'-4.25", but the Auxiliary Building roof is sloped so that areas 3&4 drain on to areas 1&2 roof, which is slopped from east to west. There are no lips on the roof of the Auxiliary Bldg. that could prevent the flow of water. The North side of the nuclear island is also below the Turbine building roof elevation 246'-3", but again Areas 1&2 are slopped such that the run-off will flow off the west side. As a result of the nuclear island roof design there is no loading from the PMWP.

2.3.1.2.7.3 Weight of Snow and Ice on Safety-Related Structures

Based on the evaluations given in "Extreme Ice Thicknesses from Freezing Rain," Reference 208, the probability of freezing rain (glaze ice) with a thickness of 15 mm at the Lee Nuclear site in any year is 0.02. The probability of freezing rain with a thickness of 20 mm at the Lee Nuclear site in any year is 0.01 [Reference 208].

Because the plant site is subjected to a subtropical climate with mild winters, prolonged snowfalls or large accumulations of snow or ice on the ground and structures are not anticipated. The estimated depth of the 100-year return snowpack is 17.0 inches, or 3.4 inches of water equivalent, as discussed above. The safety-related structures at the Lee Nuclear Station would be designed to withstand 17.7 pounds per square foot snow load. No damage from snow or ice loading on structures is expected because the DCD design loading is 75 pounds per square foot (see Table 2.0-201).

2.3.1.2.8 100-Year Return Period Fastest Mile of Wind

The fastest mile of wind speed recorded in 56 years (1950-2006) in the NWS storm events database for Cherokee County is 80.6 mph. A Gumbel-Lieblein

extreme value analysis of this data gives an estimated value of 88 mph for the 100-year return period fastest mile of wind in Cherokee County.

The design basis wind velocity is based on the data from ASCE 7-95 (Reference 222). From Figure 6-1 of ASCE 7-95, the 50-year return 3-second gust wind speed at 33 feet above ground for the Lee Nuclear Station site is 90 mph. This gives a design basis 100-year return wind speed of 96 mph, based on Table C6-5 of ASCE 7-95. The Lee Nuclear Plant site characteristic 3-second gust wind speed of 96 mph is compared to the AP1000 design criteria in Table 2.0-201. The safety and non-safety importance factors, exposure category, and topographic factor are given in Section 3.3.

2.3.1.2.9 Probable Maximum Annual Frequency and Duration of Dust Storms

The occurrence of dust storms (i.e., blowing dust or blowing sand) is a rare phenomenon in the Lee Nuclear Station site area. Although there are categories for dust and sand in the NCDC meteorological database, no hours are identified under this category for Cherokee County in the period from 01/01/1950 to 05/31/2006.

WLS COL 2.3-2

2.3.2 LOCAL METEOROLOGY

This section discusses the local meteorological conditions at the Lee Nuclear Station site. Local site meteorological conditions reflect the synoptic-scale atmospheric processes and are consistent with the regional meteorology. There are two exceptions caused by local effects from the Broad River. First, there is higher humidity directly adjacent to the river. Second, there is a possibility of channeling of low-level winds along the river valley. Channeling of flow from the NW is indicated in the site's wind rose in Figure 2.3-203. This figure shows that the predominant wind direction is from the Northwest, which aligns with the river valley.

The Lee Nuclear Station site is located in a temperate latitude in northern South Carolina about 250 miles northwest of the Atlantic coast and is in a region strongly influenced for much of the year by the Azores-Bermuda anticyclonic circulation (Reference 223). This behavior is shown in Figure 2.3-204 which gives the Atlantic subtropical anticyclone seasonality. In late summer and fall, the position of the subtropical high is such that the region experiences extended periods of fair weather and light wind conditions. In winter and early spring, the frequency of eastward moving migratory highs or low-pressure systems increases, alternately bringing cold and warm air masses into the Lee Nuclear Station site area. Frequent and prolonged incursions of warm moist air from the Atlantic Ocean and the Gulf of Mexico are experienced from late spring through summer.

The general direction of airflow across the region is from the northerly sectors during much of the year, although the prevailing direction may be from one of the southerly sectors during some months. The monthly wind joint frequency distributions for the Greenville/Spartanburg International Airport are shown in Tables 2.3-209 through 2.3-221.

Long-term temperature and precipitation records from Ninety-Nine Islands were compared to records from Greenville/Spartanburg. This comparison indicates that, for these parameters, data from Greenville/Spartanburg reasonably represent meteorological conditions in the vicinity of the site. Presumably, this is indicative of the similarity in controlling synoptic influences throughout the region. Other meteorological parameters are assumed to be subject to the same synoptic controls.

2.3.2.1 Winds

2.3.2.1.1 Greenville/Spartanburg Wind Distribution

Tables 2.3-209 through 2.3-221 provide monthly percent joint frequency distributions for wind directions and speeds, based on a 9-year period of record from 1997 through 2005 for Greenville/Spartanburg. Table 2.3-221 provides an annual summary of the data. On an annual basis, Greenville/Spartanburg wind data collected in the 9 years from 1997 through 2005 show that northeastern wind direction is the most frequent (11 percent). Wind from the ESE was the least likely with a frequency of approximately one percent. At the Greenville/Spartanburg NWS station, winds average 7.1 mph from January through June, and 5.6 mph from July through December. Mean annual wind speed is 6.4 mph (Tables 2.3-209 through 2.3-221).

The Greenville/Spartanburg meteorological station winds are presented graphically in Figures 2.3-205 through 2.3-217. These wind roses cover the period from 1997 through 2005 and represent the frequency of winds from a particular direction by the length of the line in that direction. Greenville/Spartanburg data shows a usual pattern of winds coming from the northeast or southwest. During the fall, winds from the northeast are more common. At Greenville/Spartanburg, winds from the northwest or southeast occur infrequently.

2.3.2.1.2 Lee Nuclear Site Wind Distribution

For the Lee Nuclear site, the annual wind direction frequency is fairly uniform with the NW direction slightly more frequent at approximately 15 percent. Wind from the West was the least frequent at about 3 percent. At the Lee Nuclear site, winds average 5.3 mph from January through June, and 4.5 mph from July through December. Mean annual wind speed is 5.0 mph (Tables 2.3-222 through 2.3-234).

Monthly wind roses for the Lee Nuclear site are given in Figures 2.3-218 through 2.3-229 and seasonal wind roses are given in Figures 2.3-230 through 2.3-233. On a seasonal basis, the prevailing wind direction is from the northwest. This is also shown on the annual wind rose given in Figure 2.3-203. Joint frequency distributions of wind speed and direction by atmospheric stability class are

provided in Tables 2.3-235 through 2.3-241. Stability classes are as defined in Regulatory Guide 1.23 (see Subsection 2.3.4.2).

2.3.2.1.3 Wind Direction Persistence

Hourly weather observation records from the NWS at Greenville/Spartanburg, South Carolina, for the years 1997 through 2005 were examined for wind direction persistence. The longest persistence periods from a single sector (22.5 degrees), three adjoining sectors (67.5 degrees), and five adjoining sectors (112.5 degrees) were determined from each sector during each year. The results are shown in Tables 2.3-242 through 2.3-244. During the period, the single sector maximum persistence was greatest (23 hours) for the NE direction. The average maximum persistence (14.0 hours) was greatest for the NE direction. For the persistence in three adjoining sectors, the NE sector had the longest period of persistence (82 hours). The largest average maximum persistence (57.8 hours) was also for the NE sector, as shown in Table 2.3-243. The longest persistence period (150 hours) from five adjoining sectors occurred in the NE sector (Table 2.3-244). The NE sector also showed the greatest average maximum persistence (91.0 hours).

For the Lee Nuclear Station site, the single sector maximum persistence was greatest (15 hours) for the NW direction. For the persistence in three adjoining sectors, the NW sector had the longest period of persistence (45 hours). The longest persistence period (71 hours) from five adjoining sectors occurred in the NNE sector (Table 2.3-245).

2.3.2.2 Air Temperature

In the Lee Nuclear site area, January average maximum temperatures are between 50 and 55°F with average minimums between 25 and 30°F (see Figures 2.3-234 and 2.3-235). In July, average minimum temperatures are in the vicinity of 65 to 70°F, while the average maximum is between 85 and 90°F, (see Figures 2.3-236 and 2.3-237). The maximum and minimum mean temperatures at the Ninety-Nine Islands weather station in Blacksburg, South Carolina are given in the monthly climate summary Table 2.3-246. The daily maximum, minimum, and average temperatures from the Ninety-Nine Islands weather station, spanning the years 1971 - 2000, are given in Figure 2.3-238.

The annual average maximum monthly temperature at the Ninety-Nine Islands weather station from 8/1/1948 to 12/31/2005 was 71.5°F, and the annual average minimum monthly temperature was 45.6°F. The average maximum monthly temperature was 89.0°F in July, and the average minimum monthly temperature was 26.7°F in January.

Data from the Southeast Regional Climate Center indicates that temperature extremes for Ninety-Nine Islands, South Carolina, for the years 1971 through 2000 have ranged from the highest mean temperature of 94.4°F (July 1993) to the lowest mean minimum temperature of 17.2°F (January 1977) (Reference 203). Table 2.3-246 presents the temperature means and extremes for Ninety-Nine Islands collected over a 30-year period.

The maximum temperature at the Lee Nuclear Station site during the 2005-2006 data collection period was 96°F and the minimum was 20°F which is within the bounds of the historic record for Ninety-Nine Islands, South Carolina (see Figure 2.3-238). The temperature range at the Lee Nuclear Station site is consistent with the temperature ranges for Ninety-Nine Islands and the Greenville/Spartanburg areas. For the Lee Nuclear Station site, the 0% exceedance dry bulb temperature was determined in accordance with the definition provided by Westinghouse AP1000 DCD, Tier 2 Table 2-1 and FSAR Table 2.0-201. The maximum coincident dry bulb/wet bulb temperature limit is based on the maximum dry bulb temperature that has existed for 2 hours or more combined with the maximum wet bulb temperature that exists in that population of dry bulb temperatures. Consequently, the term “coincident wet bulb temperature” is not defined in the same way as used in ASHRAE “Climatic Design Information” (i.e., the Mean Coincident Wet Bulb, MCWB), Reference 238.

The DCD specifies that “[t]he Combined License applicant must provide information to demonstrate that the site parameters are within the limits specified for the standard design.” Consistent with the Westinghouse methodology described above, the highest dry bulb temperature that persists for at least 2 hours has been determined to be 103°F from a 45-year (1963-2007) sequential hourly meteorological data set for the NWS station at Greer Greenville/ Spartanburg Airport, South Carolina (see Table 2.3-293). The highest of the coincident wet bulb temperatures has been determined to be 78°F.

Similar to the approach described above for determining the maximum safety dry bulb temperature, the highest (non-coincident) wet bulb temperature that persists for at least 2 hours has been determined to be 81°F from the 45-year sequential hourly meteorological data set for the Greer Greenville/Spartanburg Airport NWS station. The minimum safety dry bulb temperature persisting for at least 2 hours was also determined, using the approach discussed above, to be -1°F.

1% Exceedance Dry Bulb and Wet Bulb Temperature

The maximum normal limits represent the maximum normal range of operation for power generation systems. The maximum coincident normal temperature limit is based on a 1% exceedance dry bulb temperature that persists for two hours or more in historical meteorological data. The complementary coincident wet bulb temperature is not selected based on a median or a maximum value from the 1% exceedance coincident data set. Since a slightly lower dry bulb temperature with its complementary coincident wet bulb temperature may be more limiting, the 1% exceedance wet bulb value, disregarding any hourly persistence limitation, was selected as the coincident wet bulb temperature. This methodology specified by Westinghouse is considered a conservative approach to the selection of the maximum normal coincident condition. Based on the 45-year sequential hourly meteorological data set for the Greer Greenville/Spartanburg Airport NWS station, the 1% exceedance dry bulb temperature was 91°F and the coincident 1% exceedance wet bulb temperature was 76°F.

The maximum normal non-coincident wet bulb temperature limit is the 1% exceedance wet bulb temperature that has existed at the site for 2 hours or

more based on historical meteorological data. From the 45-year sequential hourly meteorological data set for the Greer Greenville/Spartanburg Airport NWS station, the maximum normal non-coincident wet bulb temperature was determined to be 76°F.

100-Year Return Period Dry Bulb and Wet Bulb Temperature

Because reliable, sequential hourly meteorological data sets do not exist for durations of 100 years, the maximum 100-year return period dry bulb temperature value must be extrapolated. The maximum 100-year return period dry bulb temperature was calculated using the 45-year sequential hourly meteorological data set for the Greer Greenville/Spartanburg Airport NWS station, and was based on methodology provided in ASHRAE Fundamentals Handbook 2001, Chapter 27 – Climatic Design Information (Reference 238). See Equations 1 and 2 below:

$$T_n = M + IFs \qquad \text{Equation 1}$$

where:

T_n = n-year return period value of extreme dry bulb temperature to be estimated, years

M = mean of the annual extreme maximum or minimum dry bulb temperatures, °F

s = standard deviation of the annual extreme maximum or minimum dry bulb temperatures, °F

I = 1, if maximum dry bulb temperatures are being considered

I = -1, if minimum dry bulb temperatures are being considered

$$F = -\frac{\sqrt{6}}{\pi}\left\{0.5772 + \ln\left[\ln\left(\frac{n}{n-1}\right)\right]\right\} \qquad \text{Equation 2}$$

The resultant maximum 100-year return period dry bulb temperature was 107°F.

Since the maximum 100-year return period dry bulb temperature value was extrapolated, there are no occurrences of maximum dry bulb temperatures to pair with concurrent wet bulb temperature values to determine a coincident wet bulb temperature. In order to calculate a 100-year return period coincident wet bulb temperature, the 45-year sequential hourly meteorological data set for the Greer Greenville/Spartanburg Airport NWS station was used to develop a dry bulb to coincident wet bulb correlation curve. The 100-year return period coincident wet-bulb temperature methodology was determined using a dry-bulb to coincident wet-bulb correlation curve reflective of the entire meteorological data set. The resultant 100-year return period coincident wet bulb temperature was 84°F.

Similar to the approach described above for determining the maximum 100-year return period dry bulb temperature, the maximum 100-year return period wet bulb temperature (non-coincident) was calculated to be 85°F using the 45-year sequential hourly meteorological data set for the Greer Greenville/Spartanburg Airport NWS station. Likewise, the minimum 100-year return period dry bulb temperature was calculated to be -5°F.

2.3.2.3 Atmospheric Moisture

All of South Carolina experiences moderately high humidity during much of the year. At Greenville/Spartanburg, during the years 1997-2005, humidities of 50 percent or higher have occurred at any hour of the day. Mean relative humidities for four time periods per day at Greenville/Spartanburg are shown in Table 2.3-255. The highest humidity is most frequent in the early morning hours with an annual average of 81 percent. At times in the summer, a combination of high temperatures and high humidities develops; this usually builds up progressively for several days and becomes oppressive for one or more days. Lower humidities on the order of 50 percent occur on some days each month, usually in the early afternoon hours. (Reference 224).

Relative humidity in Blacksburg, South Carolina, averages near 70 percent for the year (Figure 2.3-239). Climatic records of humidity in Greenville/Spartanburg are shown in Table 2.3-253. These data show that relative humidity in the region is high throughout the year. Nighttime relative humidities are highest in summer and lowest in the winter. Daytime humidities are highest in the summer. Seasonal variations are in the vicinity of 5 to 15 percent. Highest relative humidities occur in the early morning hours (00:00 - 6:00 a.m.), averaging greater than 81 percent during all months. Lowest relative humidities occur during the afternoon with averages below 60 percent for all months. The temperature regime of the region can be described by the data shown in Table 2.3-254.

Similar relative humidity data for the Lee Nuclear Station site is presented in Table 2.3-255. As shown, the site humidity follows the same pattern as the Greenville/Spartanburg data with the highest humidity in the early morning hours with an annual average of 86 percent. The afternoon average relative humidity is 50 percent at the Lee Nuclear Station site.

2.3.2.3.1 Precipitation

Precipitation averages 48.37 inches annually at the Ninety-Nine Islands meteorological station and is generally well distributed throughout the year (Table 2.3-246). The annual precipitation during the fall months (September - November) is slightly less than 12 inches (11.6 inches), and the other seasons have an annual precipitation of more than 12 inches. April is the driest month with an average precipitation of approximately 3 inches (see Table 2.3-246). Precipitation data from the 2005-2006 data period at the Lee Nuclear site is in general agreement with the longer-term data record from Ninety-Nine Islands with a total rainfall of 39.72 inches. This total is below the long-term mean of 47.34 inches for Ninety-Nine Islands but is above the long-term low of 32.27 inches.

For Greenville/Spartanburg, the maximum normal mean monthly precipitation is in March (5.31 inches) based on 30 years of data from the NCDC (Reference 240), and the minimum monthly mean (3.54 inches) occurs in April. Based on 45 years of data from the NCDC (Reference 240), the maximum monthly precipitation in Greenville/Spartanburg is 17.37 inches, which occurred in August 1995 from tropical storm Jerry (Table 2.3-256). Table 2.3-256 provides the monthly frequency distribution of rainfall rates at the Greenville/Spartanburg meteorological station. Table 2.3-201 gives the monthly rainfall intensity frequency distribution for the Greenville/Spartanburg meteorological station.

The maximum short period precipitation frequency for this region is given in Table 2.3-257 (Reference 225). Figure 2.3-240 shows the annual precipitation wind rose for Greenville/Spartanburg, South Carolina, based on data from the years 1997 through 2005 and Figure 2.3-241 gives the annual precipitation wind rose for the Lee Nuclear Station site. Table 2.3-258 provides the monthly precipitation by direction at Greenville/Spartanburg. This data shows that the highest rainfall frequency at Greenville/Spartanburg occurs most often in the months of November through April, and the most common directions are N through ENE. Winds speeds during precipitation average 7.1 mph annually.

Figure 2.3-242 gives the average total monthly precipitation for Ninety-Nine Islands, South Carolina for the period of 1948 through 2005. The daily precipitation average and extreme is given in Figure 2.3-243 for the same time period. Similar data for the Lee Nuclear Station site is provided in Table 2.3-259. This data shows that the highest rainfall frequency is during the months of October through January and the highest frequency directions are N through NE. The Lee Nuclear Station site monthly rainfall frequency distribution is given in Table 2.3-260 and the maximum 24-hour rainfall is given in Table 2.3-261. Monthly precipitation wind roses for Greenville/Spartanburg are given in Figures 2.3-248 through 2.3-259. Similar figures for the Lee Nuclear Site are given in Figures 2.3-260 through 2.3-271.

2.3.2.3.2 Snow

Snowfall is not a rare event in north central South Carolina. During the 59 years from 1947-48 through 2005-06, measurable snow fell on Ninety-Nine Islands in 24 years. As Table 2.3-262 shows, during these 59 years, snow or sleet fell in January in 11 years and February in 12 years (Reference 203). Average winter snowfall at the Ninety-Nine Islands meteorological station is three inches (Table 2.3-262).

Annual average snowfall in the area of the Lee Nuclear Station site is estimated to be approximately 3.0 inches. This estimate is based on 59 years of record (1948-2005) at Ninety-Nine Islands (Reference 203). The monthly and annual snowfall at Ninety-Nine Islands is given in Table 2.3-262. Figure 2.3-244 provides the daily snowfall average and extreme for Ninety-Nine Islands between 1948 and 2005. The maximum monthly snowfall at Ninety-Nine Islands was 14 inches in February 1978-79 (Reference 203).

The Southeast Regional Climate Center snowfall records for Ninety-Nine Islands (8/1/1948 through 12/31/2005) give a maximum 24-hour snowfall of 13.0 inches (Reference 203).

2.3.2.3.3 Fog

Fog is an aggregate of minute water droplets suspended in the atmosphere near the surface of the earth. According to international definition, fog reduces visibility to less than 0.62 miles. Table 2.3-263 indicates that, over the period 1997 to 2005, Greenville/Spartanburg has averaged approximately 38 hours/year of fog with November, December, and January having the greatest frequency of fog.

2.3.2.4 Atmospheric Stability

The frequency and strength of inversion layers are evaluated using seven years of weather balloon data collected at the Greensboro radiosonde station (Reference 226). Weather balloons are released twice daily at 0:00 GMT (7:00 p.m. EST) and 12:00 GMT (7:00 a.m. EST) to obtain vertical profiles of temperature, wind, and dewpoint temperature. The monthly data are provided in Tables 2.3-264 through 2.3-275 in terms of number of mornings and afternoons containing inversions, average inversion layer elevation, and the average strength of the inversions. Table 2.3-276 provides annual average data for the period. An inversion is defined as any three readings on a sounding that show temperatures increasing with elevation (below 3000 meters). The inversion layer height is the point (found by interpolation between readings) at which temperature again starts to decrease with elevation. The maximum inversion strength is the maximum temperature rise divided by elevation difference within the inversion layer.

2.3.2.4.1 Mixing Heights

Mixing heights for Greensboro, North Carolina, are shown in Table 2.3-277. These were obtained from the EPA Support Center for Regulatory Atmospheric Modeling (SCRAM) Mixing Height Data collection for the period 1984-1987 and 1990-1991 (Reference 206). The average mixing heights in the mornings are lowest during the fall, and the average mixing heights in the afternoon are lowest in the winter.

Based on the EPA's SCRAM mixing height data for Greensboro, North Carolina (Reference 206), the mean morning mixing height for the area is approximately 470 meters in the winter, 475 meters in the spring, 470 meters in the summer, 380 meters in the fall, and 450 meters annually. The mean afternoon mixing height for the area is about 860 meters in the winter, 1540 meters in the spring, 1610 meters in the summer, 1140 meters in the fall, and 1290 meters annually (see Table 2.3-277).

The ventilation rate is a measure of the dispersion of pollutants. Higher ventilation rates are better for dispersing pollution than lower ventilation rates. Mean ventilation rates by month for Greensboro, North Carolina, are given in Table 2.3-207. This data was obtained from EPA SCRAM mixing height data (Reference 206) for the years 1984-1987 and 1989-1991.

Morning ventilation is less than 4000 m^2/s throughout the year and is less than 2700 m^2/s from May through October. Afternoon ventilation is higher than 7000 m^2/s from February through July but lower than 6300 m^2/s from August through January. Based on this and the tendency of pollutants to increase in the surface layer during the course of a day, the highest daily air pollution potentials exist during the afternoon from August through January when ventilation rates are lower. Lowest air pollution potentials occur in the spring due to the relatively high mean ventilation rates.

2.3.2.5 Potential Influence of the Plant and Its Facilities on Local Meteorology

The potential for the operation of Units 1 and 2 at the Lee Nuclear site to influence the local climatology is discussed in this section. It is concluded that impacts will be negligible.

The only aspects of the Lee Nuclear Station site that could be categorized as contributing to a unique micro-climate are the presence of the Ninety-Nine Islands Reservoir and the Broad River. The proximity of the river increases the local humidity. There is also a slight tendency for lower level winds to be channeled along the river valley.

New construction at the site is not expected to impact this climatic situation significantly. Although there will be some ground leveling, there are no significant climate-shaping topographic features to be changed. The site is already a relatively flat area with more significant hills to the northwest and southwest that will not be impacted by construction (refer to Figure 2.3-245 for a depiction of topography around the site). There may be some tree removal, but the trees within the construction area are small in number compared to the surrounding forested land. There are no significant changes anticipated or proposed in terms of local hydrologic features. There are no changes to local roadways anticipated in support of the proposed new facility which would impact the local climate. The impacts of more structures, facilities, or activities in this relatively remote, rural area are not expected to be noticeable in terms of local meteorology. The topography of the regional areas within 50-miles and 5-miles of the Lee Nuclear Site are shown in Figure 2.3-245.

Operation of power generation units can affect the local environment in three ways, additional generation of particulates (increased fog or haze), temperature effects on local water sources, and cooling tower plume effects. Since the proposed unit is nuclear, any increase in particulate emissions during operation would be due to a modest increase in automobile traffic and the infrequent operation of diesel generators. Therefore it can be concluded that the net increase in particulates will be negligible and will not cause any noticeable environmental effects.

Lee Nuclear Station Units 1 and 2 utilize cooling towers, so that the vast majority of rejected heat would go to the atmosphere. The amount of heat input to the flow

of the Broad River would be relatively small, with little impact on local meteorology.

The remainder of this section discusses the cooling tower plume effects. From the wind rose of Figure 2.3-203, it can be seen that the prevailing winds are from the northwest. This means that the cooling tower plumes will usually extend out over the Lee Nuclear Station site itself. Therefore, it can be concluded that most of the local climatological effects such as increased moisture and shading will be limited to the Lee Nuclear Station site.

2.3.2.5.1 Cooling Tower Plumes

The following discussion focuses on an evaluation of cooling tower plume effects. An assessment of the contribution of moisture to the ambient environment from cooling tower blowdown waste heat discharge is included. Finally, a qualitative evaluation of the effects of the cooling system on daily variations of several meteorological parameters is presented.

The operation of three circular mechanical draft cooling towers (CMDCTs) for each unit at the site will result in the emission of small water droplets entrained in the tower air flow (i.e., drift). The droplets contain the dissolved solids found in the circulating water (e.g., salts) that may eventually deposit on the ground as well as on structures and vegetation. The drift droplet emissions are controlled by the use of drift eliminators that rely on inertial separation caused by exhaust flow direction changes. State-of-the-art drift eliminators installed in the CMDCTs are capable of reducing the emissions to approximately 0.0005 percent of the circulating water flow. In addition to drift emissions, there is another potential impact of the cooling towers to the environment. The warm saturated air leaving the towers is cooled by the ambient air such that the water vapor condenses into a visible plume that may persist for some distance downwind depending on meteorological conditions (e.g., wind speed, relative humidity). These visible plume occurrences may pose some aesthetic and ground shadowing impacts. Under relatively high wind speeds and humid conditions, the aerodynamic wake turbulence caused by air flowing around the tower housing may result in the visible plume touching down causing ground level fogging and, under freezing conditions, icing.

An analysis of the potential environmental impacts caused by the operation of CMDCTs was conducted using the Electric Power Research Institute (EPRI) sponsored Seasonal/Annual Cooling Tower Impact (SACTI) Program. This model is considered a state-of-the-art cooling tower impact model by EPRI and the nuclear industry. It was developed by Argonne National Laboratory (ANL) using the knowledge obtained from extensive research conducted on cooling tower environmental effects. The SACTI model provides salt drift deposition pattern (i.e., kg/km^2 per month) as a function of distance and direction from the cooling towers as well as the frequency of occurrence of visible plumes, hours of plume shadowing, and ground level fogging and icing occurrences by season resulting from the operation of the cooling towers. The most recent 5-year database (i.e, 2001-2005) from the National Weather Service (NWS) site in Charlotte, North Carolina, was used in the SACTI analysis. Additionally, the seasonal mixing height

values for Greensboro, North Carolina (Reference 219), are used in the SACTI model.

The SACTI results, as presented in Table 2.3-278, indicate that the majority (i.e. >50 percent) of the visible plumes do not reach 1000 meters downwind and 200 meters in height. It also shows that the longest and largest visible plumes occur in the winter with smaller plumes occurring in the spring and fall seasons due to the cold air in winter causing condensation of the moist plumes more readily than in the warmer seasons (i.e., cold air has a much smaller capacity of holding water vapor). The summer visible plumes are noticeably smaller since warmer ambient air results in less condensation of the moist plumes due to its ability to accommodate higher water vapor concentrations. On an annual basis, 40 percent of the plumes reach 400 meters downwind and 170 meters in height. The winter visible plume length frequency as a function of direction is shown on Figure 2.3-274. The winter visible plume radius as a function of distance is shown on Figure 2.3-275.

The largest visible plumes shown in Table 2.3-278 reach a distance of 9900 meters (6.15 miles) downwind of the towers and a height of approximately 1400 meters and occur approximately one percent of the time. It should be noted that the longest plumes occur during conditions of high ambient relative humidity that are conducive to natural fog formation and poor visibility conditions. Under these conditions, the atmosphere is already at, or close to, saturation. Therefore, the largest plumes may not be discernable from the ambient fogging conditions.

Table 2.3-279 provides the downwind distances at which plume shadowing effects are felt for a range of hours of occurrence by season. Consistent with the visible plume frequency results, most shadowing occurs in the winter season with lesser amounts in the spring and fall and the least amounts in the summer. The hours of plume shadowing during the winter season are given in Figure 2.3-276. Annually, plume shadowing effects reach 1100 meters downwind 1 percent of the time with the farthest impact reaching approximately 4600 meters downwind in the winter for 0.5 percent of the time. The SACTI output also shows that there are virtually no occurrences of ground level fogging with only 2 hours of fogging 500 meters south of the tower and only 1 hour of fogging south and southwest of the towers at distances between 400 and 600 meters, mostly in the spring season. The hours of fogging during the spring are shown in Figure 2.3-279. More importantly, no occurrences of ground level icing are predicted.

The salt deposition pattern shown in Table 2.3-280 indicates that there is negligible salt deposition with the highest amount being approximately 1.2 kg/km^2/month occurring 200 meters north of the towers in the summer. The salt deposition rate for the summer is shown in Figure 2.3-277. All other salt deposition amounts are below 1 kg/km^2/month. On an annual basis, the largest amount of deposition is 0.82 kg/m^2/month occurring 200 meters north of the towers. The summer salt deposition rate as a function of downwind sector is shown on Figure 2.3-277. This maximum salt deposition amount can be compared with a value of 400 kg/km^2/month below which damage to vegetation is not expected to occur according to a study of the environmental effects of cooling

towers. In addition, according to NUREG-1555, general guidelines for predicting effects of drift deposition on plants suggest that many species have thresholds for visible leaf damage in the range of 10 to 20 kg/ha/mo of NaCl deposited on leaves during the growing season. This range of deposition corresponds to 1000 to 2000 kg/km^2/month. Therefore, no impacts on vegetation are expected.

While salt deposition from evaporative cooling towers has the potential to build up on bushings of electrical equipment such as transformers, switchyard equipment, and transmission lines, IEEE C57.19.100-1995 “IEEE Guide for Application of Power Apparatus Bushings” (Reference 241), Section 9 and Table 1, indicates that environments of less than 0.03 mg/cm^2 are below the typical measured equivalent salt deposition threshold to be designated the lowest level of contamination.

Assuming the worst case seasonal potential salt deposition rate of 1.2 kg/km^2/month (0.00012 mg/cm^2/month), based on 5 years of CLT meteorological data and no washing/cleaning from rain/wind at the Lee Nuclear Station site for an entire month, the result would be a monthly accumulation of only 0.4 percent (0.4%) of the 0.03 mg/cm^2, or 300 kg/km^2 threshold amount for contamination designation by IEEE C57.19.100-1995. If it was assumed that no washing occurred over an entire year, the annual accumulation rate of 0.000082 mg/cm^2/month would result in only 3.3 percent (3.3%) of the threshold amount. Using the annual salt deposition rate of 0.000082 mg/cm^2/month and no washing/cleaning of electrical equipment and insulators from rain/wind, it would take 365 months (30+ years) before the buildup would equal the minimum buildup level classified as contaminated environment by IEEE C57.19.100-1995.

Due to natural wash off from local precipitation, total deposits are not expected to ever reach a level requiring attention. Therefore, none of the outdoor electrical equipment in the transformer yard or the switchyard requires special consideration for application in the environment at the Lee Nuclear Station site, and cooling tower plume generated salt deposits are not expected to adversely affect any electrical equipment at the Lee Nuclear Station site.

Plant heating, ventilation and air conditioning (HVAC) intakes and equipment are located at distances ranging approximately 200 to 800 meters from the centerline of either group of Unit 1 or Unit 2 cooling towers. Due to the spatially distributed nature of the cooling towers and plant equipment, cooling tower plumes from a wide range of plume directions could potentially impact plant equipment. Plume trajectories moving downwind from Unit 1 cooling towers toward sectors ranging from NE to ESE could potentially result in exposure of HVAC intakes and plant equipment to salt deposition from Unit 1 cooling tower plumes, while plume trajectories from Unit 2 cooling towers toward sectors ranging from WSW to NW could potentially result in salt deposition from Unit 2 cooling tower plumes. FSAR Table 2.3-280 shows that the maximum salt deposition rate anticipated at the distance range and directions where HVAC intakes and equipment are located is less than 0.00005 mg/cm^2/month. Based on guidance provided by IEEE C57.19.100-1995, it would take more than 600 months (50 years) of buildup

without washing/cleaning from rain/wind before the threshold for low level contamination would be reached. Therefore, impacts from cooling tower plume salt deposition on HVAC intakes or equipment are negligible.

The maximum predicted water deposition rate, occurring during the summer season, is 1.7 x 10^3 kg/km^2/month at a downwind distance of 200 meters North of the cooling towers. The water deposition rate during the summer is shown in Figure 2.3-278. This deposition rate is the rainfall equivalent of 0.00007 inch per month based on the density of water (i.e., 1000 kg/m^3), which is a trivial amount. The NWS considers precipitation of less than 0.01 inch as a trace amount.

The drift deposition results are indicative of the performance of the state-of-the-art drift eliminators, minimizing the size of the drift droplets. Small drift droplet sizes tend to evaporate and remain suspended in air. The entrained salt particles would then separate from the vapor and would either deposit out or remain suspended in the air. The trivial drift deposition that does occur is most likely the result of meteorological conditions conducive to reduced plume rise (i.e., stronger wind speeds). The use of fresh water as make-up is also a major contributor to the trivial deposition impacts as this minimizes the total dissolved solids content of the circulating water.

2.3.2.6 Topographical Description of the Surrounding Area

The Lee Nuclear site is located approximately 1000 yards west of the Broad River with mountain ridges of 1000 to 2500 feet above msl to the northwest, north, and northeast. The elevation range over most of the site is approximately 500 to 660 feet above msl.

The terrain surrounding the Lee Nuclear Station site is dominated by Silver Mine Ridge 2.8 miles across the Broad River to the northwest. This ridge runs in a north-east to south-west direction and is 800 feet above mean sea level (MSL) through this area. To the north and west, the terrain is flatter and wooded. The only significant feature in this direction is Draytonville Mountain (see Figure 2.5.1-221), located 4.7 miles west, which has an elevation of approximately 1000 feet above mean sea level. The terrain in the immediate vicinity of the Lee Nuclear Station site can be described as gently rolling hills. The only notable terrain feature in the immediate vicinity of the site is McKowns Mountain to the SSW with an elevation of approximately 800 feet (approximately 200 feet above the site grade elevation). Figure 2.3-246 presents the terrain elevation profiles within 50 miles of the Lee Nuclear Station site. (Reference 227). Topographic maps of the areas within 50 miles and 5 miles of the Lee Nuclear Site are shown on Figure 2.3-245.

2.3.2.7 Current and Projected Site Air Quality Conditions

Attainment areas are areas where the ambient air quality levels are better than the EPA-designated (national) ambient air quality standards. The Lee Nuclear Station site is located within the Greenville-Spartanburg Intrastate Air Quality Control Region (AQCR). This region is designated as being in non-attainment for 8-Hr

Ozone (Reference 228). Currently, Cherokee County is designated as attainment for all criteria pollutants. Criteria pollutants are those for which National Ambient Air Quality Standards (NAAQS) have been established (i.e., sulfur dioxide (SO_2), fine particulate matter (PM_{10}), carbon monoxide (CO), nitrogen dioxide (NO_2), ozone (O_3), and lead (Pb)) (National Ambient Air Quality Standards, 40 CFR Part 50).

South Carolina is also subject to the revised 8-hour O_3 standard and the new standard for $PM_{2.5}$ (fine particulate matter with an aerodynamic diameter of less than or equal to 2.5 microns), both promulgated by the EPA in July 1997 in accordance with 62 CFR Part 38711.

These air quality characteristics are not expected to be a significant factor in the design and operating bases of Units 1 and 2. The new nuclear steam supply system and other related radiological systems are not sources of criteria pollutants or other air toxics. The addition of supporting auxiliary boilers, emergency diesel generators, station blackout generators (and other non-radiological emission sources) are not expected to be significant sources of criteria pollutant emissions because these units operate on an intermittent test and/or emergency basis.

2.3.3 ONSITE METEOROLOGICAL MEASUREMENT PROGRAMS

WLS COL 2.3-3 The meteorological monitoring program is described in this section. This program will provide continuous monitoring from the preapplication through the operational phases. The meteorological monitoring program for the construction and operational phases will entail relocation of the meteorological tower to a permanent site outside the influence of the permanent plant structures.

2.3.3.1 Onsite Meteorological Monitoring Program

The meteorological monitoring for the pre-construction phase utilized the primary meteorological tower (Tower 2), located east of the planned Nuclear Island. Either prior to or during the construction phase, Tower 2 is expected to be terminated. A separate tower is expected to be installed as the primary meteorological tower for the construction and operational phases.

Calculations to determine diffusion estimates for both short- and long-term conditions are provided in Subsection 2.3.4 and 2.3.5 respectively. These analyses were completed using data from the meteorological Tower 2. The short-term χ/Q modeling is based on the 24-month period from December 1, 2005 to November 30, 2007. However, the long-term χ/Q modeling is based on the 12-month period of December 2005 through November 2006. Appendix 2CC evaluates and justifies the use of two years of onsite meteorological data (December 2005 through November 2007) in determining the short-term

atmospheric dispersion of accident releases, and the use of one year of onsite meteorological data (December 2005 through November 2006) in determining the long-term atmospheric dispersion of normal airborne effluent releases. As discussed in Appendix 2CC, direct comparison of the atmospheric dispersion values for the one-year and two-year data sets is not possible because of the large number of source and receptor pairs, with some atmospheric dispersion values decreasing while others increase when using the two different sets of data. Instead, a comparison of the maximum individual and population offsite doses resulting from postulated normal airborne effluent releases using these two sets of data was performed. Comparison of the maximum individual and population doses showed that, although the doses increased slightly when the two-year data set was used, the doses are still only a fraction of the 10 CFR Part 50, Appendix I limits. Therefore, the χ/Q and D/Q values for normal airborne effluent releases based on the one-year of site meteorological data are retained.

The locations of meteorological Towers 1 and 2 relative to other preapplication structures are shown on Figure 2.3-247. The local topography for the Lee Nuclear Site is shown on FSAR Figure 2.3-245. These figures illustrate that the location of meteorological Tower 2 is sufficiently removed from any existing structures or significant topographic features. This ensures that the system provides adequate data to represent onsite meteorological conditions and to describe the local and regional atmospheric transport and diffusion characteristics prior to construction.

The Tower 1 meteorological installation encompassed an original 55-meter (m) tower and a 10-m tower from the original Cherokee Nuclear site. Tower 1 was located at roughly the same elevation (588 ft msl) as the future final grade of the Lee Nuclear Station containment structures. Because of its large size (e.g., transmission style tower), Tower 1 did not meet the structural requirements of Regulatory Guide 1.23, Revision 1, "Meteorological Monitoring Programs for Nuclear Power Plants." Consequently, Tower 1 data was not used for the Lee Nuclear Station COLA analyses and is not discussed further. Tower 1 was decommissioned in May 2011.

Tower 2 is a newly installed 60-m meteorological tower, located farther away from McKowns Mountain and closer to the Broad River. Tower 2 is more representative of both the wider site area and regional weather conditions. The base elevation for Tower 2 is approximately 611 feet (ft.), or approximately 23 ft. above the 588-ft. base elevation of Tower 1. Data collection from the new meteorological tower began on December 1, 2005.

All instrumentation and measurements associated with Tower 2 meet the guidance provided in Regulatory Guide 1.23, Revision 1 (March 2007). The specifications for the meteorological tower instrumentation are provided in Table 2.3-281.

Instrument Description

Meteorological Tower 2 serves as a representative observation station at Lee Nuclear site for the preapplication phase (i.e., meteorological conditions at its location are considered to be representative of the site). Tower 2 is instrumented

at two levels, 10 m and 60 m, and measures temperature, wind speed, wind direction, and vertical temperature gradient. Dewpoint is also measured at the 10 meter level. Station pressure and temperature are measured at the 2-m level in addition to ground-level precipitation. See Table 2.3-281 for a complete listing of the instrumentation provided. A system of lightning and surge protection circuitry with proper grounding is included in the facility design.

Trees and vegetation were cleared around Tower 2 to ensure an open exposure, meeting the "10 obstruction heights" criterion. Instrument booms are oriented in the northwest direction on the tower, with a boom length of 8 ft. A general description of the meteorological sensors for Tower 2 and the future permanent tower is provided below.

SENSOR	HEIGHT (meters)			DESCRIPTION
	Tower 1[(a)]	Tower 2	Future Permanent Tower	
Wind Speed (mph)	10 & 55	10 & 60	10 & 60	Cup anemometer
Wind Direction (degrees from N)	10 & 55	10 & 60	10 & 60	Vane (resolver phase displacement)
Dry-Bulb Temperature (°C)	2, 10, 55	2, 10, 60	10 & 60	Platinum Wire Resistance Detector (RTD) with aspirated radiation shield
Dewpoint (°C)	10	10	10	Chilled Mirror
Station Pressure (mb)	2	2	Optional[(b)]	Static inlet port
Precipitation (inches)	1	1	1	Tipping-bucket rain gauge.
Incoming Solar Radiation (shortwave) (W/m^2)	1	1	Optional[(b)]	Black & White Pyranometer
Outgoing Longwave Radiation (upwelling from ground); (W/m^2)	1	1	Optional[(b)]	Precision Infrared Radiometer

(a) Decommissioned in May 2011.
(b) Not Required by Regulatory Guide 1.23, Revision 1, March 2007.

Replacement sensors, which may be of a different manufacturer or model, satisfy the requirements of Regulatory Guide 1.23, Revision 1.

Data recovery from the Tower 2 instrumentation, based on evaluation of data from December 2005 to November 2006, was 96.5 percent for wind direction, wind speed, and delta temperature after screening the data using flagging criteria based on NUREG-0917 "Nuclear Regulatory Commission Staff Computer Programs for Use with Meteorological Data." Prior to this additional flagging, the data recovery for the Tower 2 meteorological quality-assured data was 99 percent for the same period.

2.3.3.2 Meteorological Data Processing

The data management process for Lee Nuclear Station Site meteorological data involves three basic steps:

- Data acquisition (Subsection 2.3.3.2.1)
- Data processing (Subsection 2.3.3.2.2)
- Data validation (Subsection 2.3.3.2.3)

This subsection includes a summary of the data collection methods and description of the processing and evaluation of the data.

2.3.3.2.1 Data Acquisition

The meteorological data collection system is designed and replacement components are chosen to meet or exceed specifications for accuracy identified in Regulatory Guide 1.23, Revision 1.

All wind speeds are recorded in miles per hour. Wind directions are measured on a 0-540 analog scale and recorded on a digital 0-360 degrees scale. Temperatures are recorded in degrees Celsius (°C). The precipitation measurement is a digital step trace, each step representing 0.01 inches. One-minute data traces can be generated electronically, eliminating the need for stripcharts.

Electronic signals from individual instrument sensors on the tower, or otherwise placed at the meteorological sites, are sent to the signal conditioning equipment in the co-located instrument shelter/building, and from there to the datalogger. The on-site meteorological data are recorded in digital form in the archive. Some additional processing is performed by the datalogger, resulting in the final meteorological measurements.

The measured data are stored by the datalogger and available for remote access. The amount of datalogger storage is affected by the number of parameters and averaging intervals. Typical storage is 4 days or longer. The data are downloaded from the datalogger by a dedicated computer (i.e. "central PC") at the Duke Energy Environmental Center (Huntersville, NC) for validation, reporting, and

archiving. The data are remotely polled and downloaded from the on-site datalogger at each tower, via modem, over data lines installed on-site.

Data quality assurance and archiving of final data occur via the designated, "central PC" located in the Environmental Center. The on-site meteorological data are recorded in digital form.

2.3.3.2.2 Data Processing

The equipment processors and datalogger control data acquisition at each tower location. The output of each meteorological sensor is scanned periodically, scaled, and the data values are stored as 1-minute averages and 1-hour averages, or totals. For precipitation, the total accumulation for the minute and hour is recorded. Digital data compiled as 15-minute averages, as detailed in Regulatory Guide 1.23, is provided for real-time display in the appropriate emergency response facilities (e.g., control room, technical support center, and emergency operations facility).

The Tower 2 datalogger sampling rate is the same for all parameters. Channels are sampled at a minimum of every second. From those data points, 1-minute and 1-hour averages are calculated and recorded. The quality of the samples is reflected in the quality of the averages. The time the average was calculated is recorded with each value. Software data processing routines within the dataloggers accumulate output and perform data calculations to generate the data sampling averages listed below.

1-minute average	Hourly average
wind speed (scalar)	wind speed (scalar)
wind direction (scalar)	wind direction (scalar)
sigma-theta	standard deviation of horizontal wind direction
dry-bulb temperature	dry-bulb temperature
dewpoint temperature	dewpoint temperature
precipitation (total)[a]	precipitation (total)[a]
solar radiation (total)	solar radiation (total)
station pressure	station pressure
longwave radiation (total)[b][c]	longwave radiation (total)[b][c]

a) Total accumulation for the minute and hour.

b) Total sum of upwelling infrared radiation from ground.

c) Total incident for the minute and hour.

The datalogger checks each piece of data to assure it is between the datalogger analog input limits and assigns a quality flag as needed. This quality indication and the time are recorded with each value.

2.3.3.2.3 Data Validation

The Duke Ambient Monitoring Group reviews the daily data, received from the meteorological systems, to detect system problems and perform preliminary data verifications. On-site system checks are performed by the field staff at least monthly to verify proper operation of the systems. After the system checks are completed, site technicians complete a thorough review of all meteorological data collected for the previous month. Data are also reviewed by the ambient monitoring team lead and an in-house meteorologist. Data edits are performed on the central computer database following the data reviews. Both raw (unedited) and QA'd (edited) data files are maintained on the central computer. Backup copies of the data files are maintained.

2.3.3.3 Meteorological Instrumentation Inspection and Maintenance

The meteorological equipment is kept in proper operating condition by staff that are trained and qualified for the necessary tasks. Meteorological instruments are inspected and serviced at a frequency that assures at least a 90 percent data recovery (Regulatory Guide 1.23, Revision 1) and that minimizes extended periods of instrument outage.

Equipment is calibrated or replaced at least after every 6 months of service. The methods for maintaining a calibrated status for the components of the meteorological data collection system (sensors, recorders, electronics, datalogger, etc.) include field checks, field calibration, and/or replacement by a laboratory-calibrated component. More frequent calibration and/or replacement intervals for individual components may be conducted on the basis of the operational history of the component type. Administrative controls such as appropriate maintenance processes procedures, work order/work request documents, etc. are used to calibrate and maintain meteorological and station equipment.

The operational phase of the meteorological program includes those procedures and responsibilities related to activities beginning with the initial fuel loading and continuing through the life of the plant. The meteorological data collection program is continuous without major interruptions during the operational phase. The meteorological program has been developed to be consistent with the guidance given in Regulatory Guide 1.23, Revision 1. The basic objective is to maintain data collection performance to assure at least 90 percent joint recoverability and availability of data needed for assessing the relative concentrations and doses resulting from accidental or routine releases in accordance with Regulatory Guide 1.23, Revision 1.

The restoration of the data collection capability of the meteorological facility in the event of equipment failure or malfunction is accomplished by replacement or repair of affected equipment. A stock of spare parts and equipment is maintained

to minimize and shorten the periods of outages. Equipment malfunctions or outages are detected by personnel during routine or special checks. When an outage of one or more of the critical data items occurs, the appropriate maintenance personnel are notified. Records documenting results of calibrations, major causes of instrument outages or drift from calibration, and corrective action taken are maintained.

2.3.4 SHORT-TERM DIFFUSION ESTIMATES

WLS COL 2.3-4 The consequences of a design basis accident in terms of human exposure is a function of the atmospheric dispersion conditions at the site of the potential release. Atmospheric dispersion consists of two components: 1) atmospheric transport due to organized or mean airflow within the atmosphere and 2) atmospheric diffusion due to disorganized or random air motions. Atmospheric diffusion conditions are represented by relative air concentration (χ/Q) values. This section describes the development of the short-term diffusion estimates for the site boundary, LPZ, and the control room.

2.3.4.1 Calculation Methodology

The efficiency of diffusion is primarily dependent on winds (speed and direction) and atmospheric stability characteristics. Dispersion is rapid during periods of stability classes A through D and much slower during periods of stability classes E through G. (Regulatory Guide 1.145 and NUREG/CR-2858).

Relative concentrations of released gases, χ/Q values, as a function of direction for various time periods at the exclusion area boundary (EAB) and the outer boundary of the low population zone (LPZ), were determined by the use of the computer code PAVAN, NUREG/CR-2858 (Reference 233). This code implements the guidance provided in Regulatory Guide 1.145. The χ/Q calculations are based on the theory that material released to the atmosphere will be normally distributed (Gaussian) about the plume centerline. A straight-line trajectory is assumed between the point of release and all distances for which χ/Q values are calculated in accordance with NUREG/CR-2858 and Regulatory Guide 1.145. NUREG/CR-2858 refers to Regulatory Guide 1.111 for discussion of the effects of spatial and temporal variations in airflow in the region of a site. These effects are not described by the constant mean wind direction model. Consequently, the effects of hill and valley topography on airflow characteristics near the Lee Nuclear Station site were examined to identify any variation of atmospheric transport and diffusion conditions.

As stated in Subsection 2.3.2.6, the terrain in the immediate vicinity of the Lee Nuclear Station site can be described as gently rolling hills. The only notable terrain feature in the immediate vicinity of the site is McKowns Mountain, approximately one mile to the SSW with a peak elevation of approximately 800 feet (approximately 200 feet above the site grade elevation). Given the

distance and minimal elevation rise from Lee Nuclear Station to the peak of McKowns Mountain (see Figures 2.1-204, 2.3-245, and 2.4.2-202), it can be concluded that McKowns Mountain would not have a significant effect on short term diffusion estimates.

The wind characteristics of the site were compared with the same parameters at the Greenville-Spartanburg airport (see Subsection 2.3.2.1). The representativeness of the regional climatology (within 2 miles) was also assessed (see Subsection 2.3.1). Although the Lee Nuclear Station 10 meter meteorological data shows a locally induced NW flow field at low wind speeds within the valley of the Broad River, this trend would not bias short term diffusion estimates. Therefore, no adjustments to represent non-straight line trajectories were applied.

Using joint frequency distributions of wind direction and wind speed by atmospheric stability, PAVAN provides the χ/Q values as functions of direction for various time periods at the EAB and the LPZ. The meteorological data needed for this calculation includes wind speed, wind direction, and atmospheric stability. The meteorological data used for this analysis was obtained from the onsite meteorological Tower 2 data from December 1, 2005 through November 30, 2007. The joint frequency distribution for this period is reported in Tables 2CC-205, 2CC-206, 2CC-209, and 2CC-210. Other plant specific data included tower height at which wind speed was measured (10.0 m) and distances to the EAB and LPZ. The Exclusion Area Boundary (EAB) for Lee Nuclear Station is shown in FSAR Figure 2.1-209. The minimum EAB distances are reported in Table 2.3-282. In this table, the distances are measured from a 550-foot radius effluent release boundary to the EAB. The low population zone (LPZ) is defined as a circle with a 2-mile radius centered on the midpoint between the Unit 1 and 2 containment buildings.

Within the ground release category, two sets of meteorological conditions are treated differently. During neutral (D) or stable (E, F, or G) atmospheric stability conditions when the wind speed at the 10-meter level is less than 6 meters per second (m/s), horizontal plume meander is considered. χ/Q values are determined through the selective use of the following set of equations for ground-level relative concentrations at the plume centerline:

$$\chi/Q = \frac{1}{\bar{U}_{10}(\pi\sigma_y\sigma_z + A/2)} \qquad \text{Equation 1}$$

$$\chi/Q = \frac{1}{\bar{U}_{10}(3\pi\sigma_y\sigma_z)} \qquad \text{Equation 2}$$

$$\chi/Q = \frac{1}{\bar{U}_{10}\pi\Sigma_y\sigma_z} \qquad \text{Equation 3}$$

where:

χ/Q is relative concentration, in sec/m³,

$\bar{U}_{10}$ is wind speed at 10 meters above plant grade, in m/sec

σ_y is lateral plume spread, in meters, a function of atmospheric stability and distance

σ_z is vertical plume spread, in meters, a function of atmospheric stability and distance

Σ_y is lateral plume spread with meander and building wake effects, in meters, a function of atmospheric stability, wind speed, and distance

A is the smallest vertical-plane cross-sectional area of the reactor building, in m²

For wind speeds less than 6 m/sec and neutral or stable stability classes (D through G), PAVAN calculates χ/Q values using Equations 1, 2, and 3. The values from Equations 1 and 2 are compared and the higher value is selected. This value is then compared with the value from Equation 3, and the lower value of these two is selected as the appropriate χ/Q value.

During all other meteorological conditions, unstable (A, B, or C) atmospheric stability and/or 10-meter level wind speeds of 6 m/s or more, plume meander is not considered. The higher value calculated from equation 1 or 2 is used as the appropriate χ/Q value.

From here, PAVAN constructs a cumulative probability distribution of χ/Q values for each of the 16 directional sectors. This distribution is the probability of the given χ/Q values being exceeded in that sector during the total time. The sector χ/Q values and the maximum sector χ/Q value are determined by effectively "plotting" the χ/Q versus probability of being exceeded and selecting the χ/Q value that is exceeded 0.5 percent of the total time. This same method is used to determine the 5 percent overall site χ/Q value.

The χ/Q value for the EAB or LPZ boundary evaluations will be the maximum sector χ/Q or the 5 percent overall site χ/Q, whichever is greater in accordance with Regulatory Guide 1.145. All direction-dependent sector values are also calculated.

2.3.4.2 Calculations and Results

The methodology described in Regulatory Guide 1.145 divides release configurations into two modes, ground release and stack release. A stack or elevated release includes all release points that are effectively greater than two and one-half times the height of the adjacent solid structures. Since the AP1000 release points do not meet this criterion, releases are considered to be ground

level releases. The analysis also assumed a 550 ft radius circle encompassing all release points (sources) when calculating distances to the receptors.

PAVAN requires the meteorological data in the form of joint frequency distributions of wind direction and wind speed by atmospheric stability class. These analyses were completed using data from the Tower 2 meteorological instrumentation during the 24-month period of December 2005 to November 2007.

The stability classes were based on the classification system given in Table 2 of U.S. Nuclear Regulatory Commission Regulatory Guide 1.23, as follows:

Classification of Atmospheric Stability
(Reference, Regulatory Guide 1.23)

Stability Classification	Pasquill Categories	Temperature change with height (ºC/100m)
Extremely unstable	A	$\Delta T \leq -1.9$
Moderately unstable	B	$-1.9 < \Delta T \leq -1.7$
Slightly unstable	C	$-1.7 < \Delta T \leq -1.5$
Neutral	D	$-1.5 < \Delta T \leq -0.5$
Slightly stable	E	$-0.5 < \Delta T \leq 1.5$
Moderately stable	F	$1.5 < \Delta T \leq 4.0$
Extremely stable	G	$\Delta T > 4.0$

Joint frequency distribution tables were developed from the meteorological data with the assumption that if data required as input to the PAVAN program (i.e., lower level wind direction, lower wind speed, and temperature differential) was missing from the hourly data record, all data for that hour was discarded. Also, the data in the joint frequency distribution tables was rounded for input into the PAVAN code.

Building cross-sectional area is defined as the smallest vertical-plane area of the reactor building, in square meters. The area of the reactor building to be used in the determination of building-wake effects will be conservatively estimated as the above grade, cross-sectional area of the shield building. This area was determined to be 2842 m^2. Building height is the height above plant grade of the containment structure used in the building-wake term for the annual-average calculations. The Passive Containment Cooling System (PCCS) tank roof is at Elevation 329 ft. The DCD design grade elevation for the AP1000 is 100 ft; therefore, the height above plant grade of the containment structure or building height is 229 ft.

As described in Regulatory Guide 1.145, a ground release includes all release points that are effectively lower than two and one-half times the height of adjacent solid structures. Therefore, as stated above, a ground release was assumed.

The tower height is the height at which the wind speed was measured. Based on the ground level release assumption, the lower measurement level (i.e., 10-meter level) on the tower height was used.

Table 2.3-283 gives the direction-dependent sector and the direction independent χ/Q values at the EAB and LPZ along with the 5 percent maximum χ/Q values. As shown, the 0.5 percent direction dependent maximum sector relative dispersion exceeds the 5 percent direction independent overall site dispersion at the EAB. Since a higher relative dispersion coefficient is conservative, the 0.5 percent maximum sector (SE at 1339 m) relative dispersion is limiting for the EAB. For the LPZ, the comparison also resulted in the conclusion that the 0.5 percent direction dependent relative dispersion was limiting. A summary of these results is provided below.

Short Term Accident χ/Q VALUES (sec/m^3)
(Based on December 2005-November 2007 Meteorological Data)

	0-2 Hrs	0-8 Hrs	8-24 Hrs	24-96 Hrs	96-720 Hrs
EAB (1339 m, SE sector)	3.46E-04	N/A	N/A	N/A	N/A
LPZ (3219 m, SE sector)	N/A	8.01E-05	5.49E-05	2.42E-05	7.46E-06

The above Lee Nuclear Station site characteristics are compared to the AP1000 design criteria in Table 2.0-201.

2.3.4.3 Short-Term Atmospheric Dispersion Estimates for the Control Room Emergency Air Intake

The atmospheric dispersion estimates for the Lee Nuclear Control Room were calculated based on the guidance provided in Regulatory Guide 1.194. The Control Room χ/Qs were calculated for all probable release points to the Control Room HVAC Intake and the Annex Building Entrance using the ARCON96 computer code (Reference 230) based on the hourly meteorological data. The directions relative to True North from the Control Room HVAC Intake and Annex Building Entrance (receptors) to the assumed release points (sources) are provided in Table 2.3-284. In all cases, the intervening structures between the release points (sources) and the receptors were ignored for calculational simplicity, thereby underestimating the true distance from the release points. This conservatism results in overestimating the Control Room χ/Q values.

Atmospheric stability was determined by the vertical temperature difference (ΔT) measured over the difference in measurement height and the stability classes given in Regulatory Guide 1.23. All releases were assumed to be point sources and ground level releases. For each of the source-to-receptor combinations, the χ/Q value that is not exceeded more than 5.0 percent of the total hours in the meteorological data set (e.g., 95-percentile χ/Q) was determined. The χ/Q values for source-receptor pairs are shown in Table 2.3-285. Atmospheric dispersion used for Control Room habitability is discussed in FSAR Section 6.4.

2.3.4.4 Short-Term Atmospheric Dispersion Estimates for the Technical Support Center

The atmospheric dispersion estimates (χ/Qs) for the Lee Nuclear Technical Support Center (TSC) were calculated based on the guidance provided in Regulatory Guide 1.194. The TSC χ/Qs were calculated for the limiting design basis release point to the nearest point on the maintenance support building using the ARCON96 computer code (Reference 230). The nearest point on the maintenance support building was conservatively selected to bound the distance to the final TSC air intake location. The atmospheric dispersion calculation used hourly meteorological data from December 1, 2005 through November 30, 2007.

Because the limiting TSC radiological consequences are associated with the design basis LOCA and the containment shell is the most probable LOCA release location (see DCD Subsection 15.6.5.3.3, Release Pathways), a release from the containment shell was assumed. Intervening structures between the release point and the surrogate TSC air intake location were ignored for calculational simplicity, thereby underestimating the true distance from the release point to the surrogate TSC air intakes. This conservatism, in addition to using the conservative surrogate TSC air intake location, resulted in overestimating the TSC χ/Q values. A straight-line path from the source to receptor was conservatively assumed to minimize distances. Distances and directions were taken between the release point (center of the containment wall) to the closest point on the maintenance support building for each unit, as listed in Table 2.3-294. The surrogate TSC intake locations were assumed to be 1.5 m above grade.

Atmospheric stability was determined by the vertical temperature difference (ΔT), measured between the 60-meter and 10-meter instrumentation levels, and the stability classes given in Regulatory Guide 1.23. The containment shell was modeled as a diffuse area source with the elevation of the assumed release equal to the vertical center of the projected plane of the containment shell above the Auxiliary Building and below the conical roof (i.e., 35.4 m above grade). The building area used for building wake corrections is the above grade containment shell area which was conservatively calculated to be 2842 m^2. The initial diffusion estimates (i.e., sigma-y and sigma-z) were based on the Regulatory Guide 1.194 methodology, using a source width of 145 ft, and a source height 110.5 ft with the area of the conical roof and PCS air diffuser conservatively neglected. The χ/Q values that are not exceeded more than 5.0 percent of the total hours in the meteorological data set (e.g., 95-percentile χ/Q) were determined. The χ/Q values for Units 1 and 2 LOCA releases to the nearest corner of the Maintenance Support Building are shown in Table 2.3-295.

2.3.5 LONG-TERM DIFFUSION ESTIMATES

WLS COL 2.3-5 For a routine gaseous effluent release, the concentration of radioactive material in the surrounding region depends on the amount of effluent released, the height of the release, the momentum and buoyancy of the emitted plume, the wind speed, atmospheric stability, airflow patterns of the site, and various effluent removal mechanisms. Annual average relative concentration, χ/Q, and annual average relative deposition, D/Q, for gaseous effluent routine releases were calculated.

2.3.5.1 Calculation Methodology and Assumptions

The XOQDOQ Computer Program NUREG/CR-2919 (Reference 231) which implements the assumptions outlined in Regulatory Guide 1.111 was used to generate the annual average relative concentration, χ/Q, and annual average relative deposition, D/Q. Values of χ/Q and D/Q were determined at points of maximum potential concentration outside the site boundary, at points of maximum individual exposure and at points within a radial grid of sixteen 22-1/2° sectors and extending to a distance of 50 miles. Radioactive decay and dry deposition were considered.

Appendix 2CC evaluates the use of two years of onsite meteorological data (December 2005 through November 2007) in determining the atmospheric dispersion of normal airborne effluent releases. As discussed in this appendix, direct comparison of the atmospheric dispersion and deposition values for the one-year and two-year data sets is not meaningful because of the large number of values and the various offsite receptor locations, some of which decrease while others increase. Instead, a comparison of the maximum individual and population doses using these two sets of data was performed. Comparison of the maximum individual and population doses showed that, although the doses increased slightly when the two-year data set was used, the doses are still only a fraction of the 10 CFR Part 50, Appendix I limits. Consequently, the χ/Q and D/Q values for normal releases based on the one-year of site meteorological data are retained. In addition to the gridded receptor locations, receptor locations were determined from the locations obtained from the 2006 land use information. Hourly meteorological data was used in the development of joint frequency distributions, in hours, of wind direction and wind speed by atmospheric stability class. The wind speed categories used were consistent with the Lee Nuclear short-term (accident) diffusion χ/Q calculation discussed above. Calms (wind speeds below the anemometer starting speed of 1 mph) were distributed into the first wind speed class with the same proportion and direction as the direction frequency of the 2nd wind-speed class.

Joint frequency distribution tables were developed from the hourly meteorological data with the assumption that if data required as input to the XOQDOQ program (i.e., lower level wind direction and wind speed, and temperature differential as opposed to upper level wind direction and wind speed) was missing from the hourly data record, all data for that hour would be discarded. This assumption maximizes the data being included in the calculation of the χ/Q and D/Q values

since hourly data is not discarded if only upper data is missing. The joint frequency distribution tables generated using the methodology and data described above are given in Tables 2.3-235 through 2.3-241.

The analysis assumed ground level point source located at the center of the facility midpoint between the Unit 1 and 2 containment buildings. At ground level locations beyond several miles from the plant, the annual average concentration of effluents are essentially independent of release mode; however, for ground level concentrations within a few miles, the release mode is important. Gaseous effluents released from tall stacks generally produce peak ground-level air concentrations near or beyond the site boundary. Near ground level releases usually produce concentrations that decrease from the release point to all locations downwind. Guidance for selection of the release mode is provided in Regulatory Guide 1.111. In general, in order for an elevated release to be assumed, either the release height must be at least twice the height of adjacent buildings or detailed information must be known about the wind speed at the height of the release. For this analysis, the routine releases were conservatively modeled as ground level releases.

The building cross-sectional area and building height are used in calculation of building wake effects. Regulatory Guide 1.111 identifies the tallest adjacent building, in many cases, the reactor building, as appropriate for use. The AP1000 plant arrangement is comprised of five principal building structures; the nuclear island, the turbine building, the annex building, the diesel generator building, and the radwaste building. The nuclear island consists of a free-standing steel containment building, a concrete shield building, and an auxiliary building. As the shield building is the tallest building in the AP1000 arrangement, the shield building cross-sectional area and building height will be used in calculation of building wake effects. The use of the shield building area, as opposed to the area of the nuclear island, is a conservative assumption since use of a smaller area minimizes wake effects resulting in higher calculated relative offsite concentrations.

Consistent with Regulatory Guide 1.111 guidance regarding radiological impact evaluations, radioactive decay and deposition were considered. For conservative estimates of radioactive decay, an overall half-life of 2.26 days is acceptable for short-lived noble gases and a half-life of 8 days for all iodines released to the atmosphere. At sites where there is not a well-defined rainy season associated with a local grazing season such as the region around the Lee Nuclear Site, wet deposition does not have a significant impact. In addition, the dry deposition rate of noble gases is so slow that the depletion is negligible within 50 miles. Therefore, in this analysis only the effects of dry deposition of iodines were considered. The calculation results with and without consideration of dry deposition are identified in the output as "depleted" and "undepleted".

As described in Subsection 2.3.4.1, the gently rolling terrain in the vicinity of the Lee Nuclear Station site would not have a significant effect on atmospheric dispersion estimates. The shallow river valley in which the Lee Nuclear Station site is located does not create a significant topographic barrier to air dispersion. In addition, the wind characteristics of the site are representative of the vicinity.

Therefore, terrain recirculation adjustments as described in Regulatory Guide 1.111 were not applied for the Lee Nuclear Station site.

2.3.5.2 Results

Receptor locations for the long-term atmospheric dispersion at the Lee Nuclear Station site were also evaluated. χ/Q and/or D/Q at points of potential maximum concentration outside the site boundary, at points of maximum individual exposure, and at points within a radial grid of sixteen 22½ degree sectors (centered on true north, north-northeast, northeast, etc.) and extending to a distance of 50 miles from the station were determined. Receptor locations included in the evaluation are given in Table 2.3-286. A set of data points were located within each sector at increments of 0.25 mile to a distance of 1 mile from the plant, at increments of 0.5 mile from a distance of 1 mile to 5 mile, at increments of 2.5 mile from a distance of 5 mile to 10 mile, and at increments of 5 miles thereafter to a distance of 50 miles. Estimates of χ/Q (undecayed and undepleted; depleted for radioiodines) and D/Q radioiodines and particulates is provided at each of these grid points.

The results of the analysis, based on one year of data collected on site, are presented in Tables 2.3-287 through 2.3-292. The limiting atmospheric dispersion factor (χ/Q) at the EAB is in the SE direction at 1339 meters. The limiting atmospheric dispersion at the nearest residence is also in the SE direction at 1607 meters. Atmospheric dispersion factors for other receptors are given in Table 2.3-289. Long term atmospheric dispersion factors are not given in the AP1000 DCD except at the EAB. The DCD site boundary annual average χ/Q is 2.0×10^{-5} sec/m^3. This bounds the Lee Nuclear Station annual average routine release EAB χ/Q value of 5.8×10^{-6} sec/m^3. Table 2.0-201 provided a comparison of the Lee Nuclear Station site characteristics with the DCD design parameters.

2.3.6 COMBINED LICENSE INFORMATION

2.3.6.1 Regional Climatology

WLS COL 2.3-1 This COL item is addressed in Subsection 2.3.1

2.3.6.2 Local Meteorology

WLS COL 2.3-2 This COL item is addressed in Subsection 2.3.2

2.3.6.3 Onsite Meteorological Measurements Program

WLS COL 2.3-3 This COL item is addressed in Subsection 2.3.3

2.3.6.4 Short-Term Diffusion Estimates

WLS COL 2.3-4 This COL item is addressed in Subsection 2.3.4

2.3.6.5 Long-Term Diffusion Estimates

WLS COL 2.3-5 This COL item is addressed in Subsection 2.3.5

2.3.7 REFERENCES

201. South Carolina State Climate Office, South Carolina Department of Natural Resources, Columbia, SC, http://www.dnr.sc.gov/climate/sco/, accessed 8/21/2006.

202. Duke Power Company, Cherokee Nuclear Station - Environmental Report, Amendment 4, October 1975.

203. Southeast Regional Climate Center, South Carolina Department of Natural Resources, Columbia South Carolina, NINETY NINE ISLANDS, SOUTH CAROLINA, Period of Record Daily Climate Summary, Daily Records for station 386293 NINETY NINE ISLANDS. http://cirrus.dnr.state.sc.us/cgi-bin/sercc/cliMAIN.pl?sc6293, accessed 8/15/2006 through 8/31/2006.

204. Ice Storms: Hazardous Beauty, Keith C Heidorn, December 2001, http://www.islandnet.com/~see/weather/elements/icestorm.htm, accessed 6/19/2006.

205. Air Stagnation Climatology for the United States (1948-1998), NOAA/Air Resources Laboratory ATLAS No. 1, Julian X.L. Wang and James K. Angell, April 1999.

206. Environmental Protection Agency (EPA) Research Triangle Park, North Carolina, SCRAM Mixing Height Data for Greensboro, NC for 1984 through 1987, 1990 and 1991. http://www.epa.gov/scram001/mixingheightdata.htm, accessed 4/22/2007.

207. NCDC Storm Event Database, National Climate Data Center (NCDC) Storm Event Data Base, January 1, 1950 through May 31, 2006. http://www4.ncdc.noaa.gov/cgi-win/wwcgi.dll?wwEvent~Storms, accessed 8/31/2006, 9/1/2006.

208. Extreme Ice Thicknesses from Freezing Rain, September 2004, American Lifelines Alliance, Kathleen F. Jones, Project Manager, Neal Lott, and Ronald Thorkildson, http://www.americanlifelinesalliance.org/, accessed 4/22/2007.

209. Atlantic Tropical Storms and Hurricanes Affecting the United States: 1899-1999, NOAA Technical Memorandum NWS SR-206, Donovan Landreneau, National Weather Service Office, Lake Charles, Louisiana.

210. Atlantic Tropical Storms And Hurricanes Affecting The United States: 1899-2002, NOAA Technical Memorandum NWS SR-206, Donovan Landreneau, National Weather Service Office, Lake Charles, Louisiana, (Updated Through 2002).

211. Thom, H. C. S., Tornado Probabilities, Monthly Weather Review, Vol. 91, October-December 1963, pp 730-736.

212. U.S. Census Bureau: State and County QuickFacts, Data derived from Population Estimates, 2000 Census of Population and Housing, http://quickfacts.census.gov/qfd/states, accessed 8/16/2006.

213. NUREG/CR-4461, Rev. 2, Tornado Climatology of the Contiguous United States, Pacific Northwest National Laboratory, February 2007.

214. IAEA Safety Standards Series No. NS-G-3.4, "Meteorological Events in Site Evaluation for Nuclear Power Plants", Vienna: International Atomic Energy Agency, 2003, ISBN 92-0-102103-8.

215. Isokeraunic map contained in Hubbell Power Systems, Lightning: The Most Common Source of Overvoltage, Bulletin EU 1422-H, 2001.

216. A Statistical Analysis of Strike Data From Real Installations Which Demonstrates Effective Protection of Structures Against Lightning, F. D'Alessandro, ERICO Lightning Technologies, Hobart, Australia.

217. American Meteorological Society 1999, "Lightning Ground Flash Density and Thunderstorm Duration in the Continental United States: 1989-96", Gary R. Huffines and Richard E. Orville, Cooperative Institute for Applied Meteorological Studies, Department of Meteorology, Texas A&M University, College Station, Texas.

218. EPA 8-Hour Ozone Non-Attainment State/Area/County Report, 2006.

219. George C. Holzworth, "Mixing Heights, Wind Speeds, and Potential for Urban Air Pollution Throughout the Contiguous United States", Environmental Protection Agency, Office of Air Programs, January 1972.

220. American Society of Civil Engineers, ANSI/ASCE 7-05, Minimum Design Loads for Buildings and Other Structures.

221. Huschke, Ralph E., Ed., Glossary of Meteorology, American Meteorological Society, Boston, Massachusetts, 1959.

222. American Society of Civil Engineers, ASCE 7-95, "Minimum Design Loads for Buildings and Other Structures," June 6, 1996.

223. The North Atlantic Subtropical Anticyclone, Robert E. Davis, Bruce P. Hayden, David A. Gay, William L. Phillips, and Gregory V. Jones, Department of Environmental Sciences, University of Virginia, Charlottesville, Virginia, Journal of Climate: Vol. 10, No. 4, pp. 728-744, August 22, 1996.

224. Local Climatological Data, NCDC Local Climatological Data-Unedited, Online Individual Station, Hourly Surface Data, Greenville/Spartanburg, South Carolina, 1997 to 2005. Quality Controlled online data, Order No. W15119.

225. ""Precipitation-Frequency Atlas of the United States" NOAA Atlas 14, Volume 2, Version 3, G.M. Bonnin, D. Martin, B. Lin, T. Parzybok, M. Yekta, and D. Riley, NOAA, National Weather Service, Silver Spring, Maryland, 2004, Extracted: Thu Aug 24 2006. Location: South Carolina 35.024 N 81.524 W 777 feet. http://hdsc.nws.noaa.gov/hdsc/pfds/orb/sc_pfds.html.

226. Forecast Systems Laboratory (now the Global Systems Division [GSD]) of the Earth System Research Laboratory (ESRL), FSL/NCDC Radiosonde Data Archive, Radiosonde Database Access, http://raob.fsl.noaa.gov/, accessed 6/7-8/2006.

227. DeLorme, Two DeLorme Drive, P.O. Box 298, Yarmouth, ME 04096 USA, Latitude 43°48.491' North, Longitude 70°09.844' West, Topo USA 6.0.

228. EPA - Green Book - Currently Designated Non-Attainment Areas for All Criteria Pollutants, http://www.epa.gov/oar/oaqps/greenbk/ancl.html, assessed 10/2/2006.

229. NUREG-0917, "Nuclear Regulatory Commission Staff Computer Programs for Use with Meteorological Data", July 1982

230. NUREG/CR-6331, Revision 1, May 1997, "Atmospheric Relative Concentrations in Building Wakes".

231. NUREG/CR-2919, XOQDOQ: Computer Program for the Meteorological Evaluation of Routine Effluent Releases at Nuclear Power Stations, September 1982.

232. Blacksburg South Carolina - Climate, Thomson Gale, 2005, http://www.city-data.com/city/Blacksburg-South-Carolina.html, accessed 4/22/2007.

233. PNL-4413, PAVAN: An Atmospheric Dispersion Program for Evaluating Design Basis Accidental Releases of Radioactive Materials from Nuclear Power Stations, November 1982.

234. NUREG/CR-1486, Hydrometeorological Report 53, April 1980, "Seasonal Variation of 10-square-mile Maximum Precipitation Estimates, United States East of the 105th Meridian."

235. National Oceanic and Atmospheric Administration (NOAA) Coastal Service Center, Hurricane data for years 1899 - 2005.

236. National Climatic Data Center (NCDC) Local Climatic Data Annual Summary with Comparative Data for Greenville-Spartanburg (Greer), South Carolina (Station ID GSP), 2007.

237. National Climatic Data Center (NCDC), "Extreme Snowfall Amount Corresponding to 4 Return Periods (plus Observed Extreme)," Gaffney 6 E, South Carolina, last updated 2007.

238. ASHRAE Fundamentals Handbook 2001, Chapter 27 - Climatic Design Information.

239. National Climatic Data Center (NCDC) Local Climatic Data Annual Summary with Comparative Data, for Charlotte, North Carolina (Station ID CLT), 2007.

240. National Climatic Data Center (NCDC) Local Climatic Data (LCD), Data for Greenville-Spartanburg (Greer), South Carolina (Station ID GSP), 2007.

241. IEEE Standard C57.19.100-1995, Guide for Application of Power Apparatus Bushings.

WLS COL 2.3-1

TABLE 2.3-201
RAINFALL FREQUENCY DISTRIBUTION
GREENVILLE/SPARTANBURG, SOUTH CAROLINA
NUMBER OF HOURS PER MONTH, AVERAGE YEAR

Rainfall (inch/hr)	Jan	Feb	Mar	Apr	May	Jun	Jul	Aug	Sep	Oct	Nov	Dec	Average Annual Hours
0.01-0.019	18.2	17.0	19.4	17.1	15.4	14.3	14.2	9.6	12.2	13.6	15.6	17.2	15.3
0.02-.099	33.2	34.0	30.6	26.0	17.9	19.6	14.8	9.2	20.4	17.1	30.2	26.6	23.3
0.10-0.249	8.3	10.8	12.3	9.4	7.3	7.2	5.3	3.6	9.4	5.9	6.9	13.1	8.3
0.25-0.499	1.3	0.6	2.4	2.7	2.0	3.4	3.2	1.3	2.7	2.3	1.4	1.4	2.1
0.50-0.99	0.2	0.1	0.4	0.2	0.9	1.7	1.6	1.6	1.0	0.8	0.4	0.2	0.8
1.00-1.99	0.0	0.0	0.0	0.2	0.0	0.1	0.8	0.3	0.3	0.1	0.0	0.0	0.2
2.0 & over	0.0	0.0	0.0	0.0	0.0	0.0	0.2	0.1	0.0	0.0	0.0	0.0	0.0
Total	61.2	62.5	65.1	55.6	43.5	46.3	40.1	25.7	46.0	39.8	54.5	58.5	49.9

NOTES:

1. Data from NCDC, 1997-2005.

WLS COL 2.3-1

TABLE 2.3-202 (Sheet 1 of 2)
HURRICANES IN NORTH CAROLINA AND SOUTH CAROLINA
1899 – 2005

North Carolina

Year	Month	Name	Category
1899	AUG	-	3
1899	OCT	-	2
1901	JUL	-	1
1904	SEP	-	1
1906	SEP	-	3
1908	JUL	-	1
1913	SEP	-	1
1918	AUG	-	1
1933	AUG	-	2
1933	SEP	-	3
1944	AUG	-	1
1944	SEP	-	3
1953	AUG	Barbara	2
1954	AUG	Carol	2
1954	OCT	Hazel	4
1955	AUG	Connie	3
1955	AUG	Diane	1
1955	SEP	Ione	3
1960	SEP	Donna	3
1964	OCT	Isbell	1
1971	SEP	Ginger	1
1984	SEP	Diana	3
1985	SEP	Gloria	3
1986	AUG	Charley	1
1989	SEP	Hugo	2
1996	JUL	Bertha	2
1996	SEP	Fran	3
1998	AUG	Bonnie	2
1999	SEP	Floyd	2
2003	SEP	Isabel	2
2004	AUG	Charley	1

WLS COL 2.3-1

TABLE 2.3-202 (Sheet 2 of 2)
HURRICANES IN NORTH CAROLINA AND SOUTH CAROLINA
1899 – 2005

South Carolina

Year	Month	Name	Category
1899	OCT	-	2
1904	SEP	-	1
1906	SEP	-	3
1911	AUG	-	2
1913	OCT	-	1
1916	JUL	-	2
1928	SEP	-	1
1940	AUG	-	2
1947	OCT	-	2
1952	AUG	Able	1
1954	OCT	Hazel	4
1959	JUL	Cindy	1
1959	SEP	Gracie	4
1979	SEP	David	2
1985	JUL	Bob	1
1985	NOV	Kate	1
1989	SEP	Hugo	4
2004	AUG	Gaston	1
2004	AUG	Charley	1

NOTES:

1. Data is from "Atlantic Tropical Storms And Hurricanes Affecting The United States:1899-2002," NOAA Technical Memorandum NWS SR-206 (Updated through 2002).

2. Additional data from National Oceanic and Atmospheric Administration (NOAA) Coastal Service Center, years 1899 - 2005.

WLS COL 2.3-1

TABLE 2.3-203 (SHEET 1 OF 2)
FREQUENCY OF TROPICAL CYCLONES (BY MONTH) FOR THE STATES OF SOUTH CAROLINA AND NORTH CAROLINA

	Category of Storm 1899 – 2005 (Saffir-Simpson Scale)							
	1 (No.)	2 (No.)	3 (No.)	4 (No.)	5 (No.)	Monthly Total (No.)	Annual Frequency (yr^{-1})	% of Total
Jun	0	0	0	0	0	0	0.00	0%
Jul	4	2	0	0	0	6	0.06	12%
Aug	8	6	2	0	0	16	0.15	32%
Sep	5	4	9	2	0	20	0.19	40%
Oct	2	3	0	2	0	7	0.07	14%
Nov	1	0	0	0	0	1	0.01	2%
Total	20	15	11	4	0	50	0.47	100%

Note: Storm Category is the category of the storm entering either North Carolina or South Carolina.

TABLE 2.3-203 (SHEET 2 OF 2)
FREQUENCY OF TROPICAL CYCLONES (BY MONTH) FOR THE STATES OF SOUTH CAROLINA AND NORTH CAROLINA

	Number of Hurricanes: 1899 – 2005 Saffir/Simpson Category Number						Annual Frequency (yr^{-1})	Return Period (years)
Area	1	2	3	4	5	Total		
North Carolina (NC)	11	9	10	1	0	31	0.29	3.45
South Carolina (SC)	9	6	1	3	0	19	0.18	5.63

Where the definition of Storm Category is as follows:

Storm Category (Saffir-Simpson Scale)	Wind Speed (mph)	Storm Surge (ft. above normal)
1	74 to 95	4 to 5
2	96 to 110	6 to 8
3	111 to 130	9 to 12
4	131 to 155	13 to 18
5	Greater than 155	Greater than 18

NOTES:

1. Data is from "Atlantic Tropical Storms And Hurricanes Affecting The United States:1899-2002," NOAA Technical Memorandum NWS SR-206 (Updated through 2002), and NOAA Technical Memorandum NWS TPC-4 for data through 2004.
2. Additional data from National Oceanic and Atmospheric Administration (NOAA) Costal Services Center, years 1899 - 2005.

WLS COL 2.3-1

TABLE 2.3-204 (Sheet 1 of 8)
TORNADOES IN CHEROKEE, SPARTANBURG, UNION, CHESTER, AND YORK COUNTIES,
SOUTH CAROLINA AND CLEVELAND, GASTON, AND MECKLENBURG COUNTIES, NORTH CAROLINA

Location or County	Date	Time	Magnitude Fujita Scale	Length (mi.)	Width (yards)	Area (mi^2)
Cherokee County, SC						
1 CHEROKEE	2/16/1954	1902	F1	1	33	0.02
2 CHEROKEE	5/22/1963	1715	F1	1	100	0.06
3 CHEROKEE	7/15/1964	1530	F0	1	100	0.06
4 CHEROKEE	4/18/1969	1430	F2	1	83	0.05
5 CHEROKEE	5/27/1973	1820	F3	20	100	1.14
6 CHEROKEE	12/5/1977	1342	F1	0	17	
7 CHEROKEE	4/4/1989	1645	F1	8	50	0.23
8 CHEROKEE	5/5/1989	1633	F4	3	700	1.19
9 CHEROKEE	2/10/1990	0742	F1	3	50	0.09
10 CHEROKEE	4/28/1990	1655	F1	5	40	0.11
11 Cowpens	8/16/1994	1656	F1	3	75	0.13
12 Blacksburg To	8/16/1994	1736	F2	4	100	0.23
13 Gaffney To	5/1/1995	2025	F0	9	50	0.26
14 Blacksburg	5/29/1996	1610	F0	0	30	
15 Gaffney	9/27/2004	2115	F1	1	50	0.03

WLS COL 2.3-1

TABLE 2.3-204 (Sheet 2 of 8)
TORNADOES IN CHEROKEE, SPARTANBURG, UNION, CHESTER, AND YORK COUNTIES,
SOUTH CAROLINA AND CLEVELAND, GASTON, AND MECKLENBURG COUNTIES, NORTH CAROLINA

Location or County	Date	Time	Magnitude Fujita Scale	Length (mi.)	Width (yards)	Area (mi^2)
Spartanburg County, SC						
1 SPARTANBURG	5/10/1952	1415	F3	16	83	0.75
2 SPARTANBURG	4/7/1964	1208	F1	0	100	
3 SPARTANBURG	4/28/1964	1730	F0	0	0	
4 SPARTANBURG	4/28/1964	1830	F0	0	0	
5 SPARTANBURG	3/22/1968	1730	F1	1	13	0.01
6 SPARTANBURG	5/18/1969	2100	F1	0	50	
7 SPARTANBURG	5/27/1973	1730	F3	11	150	0.94
8 SPARTANBURG	6/19/1976	1630	F1	0	50	
9 SPARTANBURG	9/7/1977	1400	F1	0	77	
10 SPARTANBURG	12/5/1977	1335	F1	0	20	
11 SPARTANBURG	5/23/1980	1910	F2	3	100	0.17
12 SPARTANBURG	8/17/1985	1050	F2	9	100	0.51
13 SPARTANBURG	4/4/1989	1618	F2	2	73	0.08
14 SPARTANBURG	5/5/1989	1620	F4	6	700	2.39
15 SPARTANBURG	2/10/1990	0738	F1	2	50	0.06
16 SPARTANBURG	4/28/1990	1610	F0	2	30	0.03
17 SPARTANBURG	4/28/1990	1620	F1	6	50	0.17

WLS COL 2.3-1

TABLE 2.3-204 (Sheet 3 of 8)
TORNADOES IN CHEROKEE, SPARTANBURG, UNION, CHESTER, AND YORK COUNTIES,
SOUTH CAROLINA AND CLEVELAND, GASTON, AND MECKLENBURG COUNTIES, NORTH CAROLINA

Location or County	Date	Time	Magnitude Fujita Scale	Length (mi.)	Width (yards)	Area (mi^2)
18 Inman	3/27/1994	1655	F2	25	75	1.07
19 Lyman To Blackburg	3/27/1994	1730	F1	33	100	1.88
20 Cross Anchor	10/22/1994	1810	F0	2	75	0.09
21 Walnut Grove	7/26/1996	1555	F1	0	10	
22 Roebuck	2/21/1997	1633	F2	1	75	0.04
23 Pacolet Mills	6/6/1998	1600	F0	1	10	0.01
24 Cherokee Spgs	3/11/2000	1500	F0	0	20	
25 Chesnee	7/7/2005	0951	F0	0	50	
Union County, SC						
1 UNION	4/8/1957	1500	F2	15	100	0.85
2 UNION	8/17/1985	1315	F0	3	30	0.05
3 UNION	6/4/1992	1050	F0	0	40	
4 UNION	6/4/1992	1115	F0	0	23	
5 Southside To	4/15/1993	1626	F2	6	600	2.05
6 Union	7/26/1996	1625	F0	0	10	
7 Carlisle	6/6/1998	1610	F1	2	50	0.06
8 Adamsburg	5/25/2000	1900	F1	1	20	0.01
9 Carlisle	6/9/2001	1415	F0	1	0	

WLS COL 2.3-1

TABLE 2.3-204 (Sheet 4 of 8)
TORNADOES IN CHEROKEE, SPARTANBURG, UNION, CHESTER, AND YORK COUNTIES,
SOUTH CAROLINA AND CLEVELAND, GASTON, AND MECKLENBURG COUNTIES, NORTH CAROLINA

Location or County	Date	Time	Magnitude Fujita Scale	Length (mi.)	Width (yards)	Area (mi^2)
10 Union	9/7/2004	2300	F1	4	225	0.51
11 Santuc	11/24/2004	1425	F0	1	50	0.03
Chester County, SC						
1 CHESTER	4/6/1955	1230	F1	2	100	0.11
2 CHESTER	5/15/1975	1200	F1	0	3	
3 CHESTER	4/19/1981	1845	F1	2	33	0.04
4 Lowrys	4/16/1994	0111	F2	3	75	0.13
5 Chester	8/16/1994	1755	F1	0	75	
6 Chester	5/1/1995	2305	F0	0	20	
7 Richburg	5/29/1996	1700	F1	1	100	0.06
8 Ft Lawn	7/24/1997	1200	F1	0	25	
9 Chester	6/4/1998	1730	F0	0	50	
10 Chester	9/7/2004	1915	F1	1	50	0.03
York County, SC						
1 YORK	7/16/1961	1400	F0	0	7	
2 YORK	6/22/1964	1820	F1	2	53	0.06
3 YORK	5/24/1973	1520	F2	2	67	0.08
4 YORK	5/28/1973	1630	F2	2	100	0.11

WLS COL 2.3-1

TABLE 2.3-204 (Sheet 5 of 8)
TORNADOES IN CHEROKEE, SPARTANBURG, UNION, CHESTER, AND YORK COUNTIES,
SOUTH CAROLINA AND CLEVELAND, GASTON, AND MECKLENBURG COUNTIES, NORTH CAROLINA

Location or County	Date	Time	Magnitude Fujita Scale	Length (mi.)	Width (yards)	Area (mi^2)
5 YORK	3/24/1975	1115	F1	9	100	0.51
6 YORK	12/5/1977	1640	F1	2	100	0.11
7 YORK	5/3/1984	1525	F1	6	10	0.03
8 YORK	8/17/1985	1255	F1	3	30	0.05
9 YORK	8/17/1985	1300	F0	1	30	0.02
10 YORK	3/6/1989	1230	F0	1	10	0.01
11 Clover	3/27/1994	1843	F1	1	30	0.02
12 York	8/16/1994	1650	F0	0	50	
13 YORK	5/1/1995	2103	F0	1	50	0.03
14 Clover	2/21/1997	1720	F0	2	100	0.11
15 Clover	4/19/1998	1430	F0	0	20	
16 Rock Hill	4/19/1998	1508	F0	0	10	
17 Rock Hill	2/22/2003	1005	F0	0	25	
18 Rock Hill	9/7/2004	1043	F1	1	100	0.06
Cleveland County, NC						
1 CLEVELAND	5/27/1973	1900	F3	13	100	0.74
2 CLEVELAND	5/15/1975	1430	F1	0	0	
3 CLEVELAND	6/24/1979	0030	F1	1	300	0.17

WLS COL 2.3-1

TABLE 2.3-204 (Sheet 6 of 8)
TORNADOES IN CHEROKEE, SPARTANBURG, UNION, CHESTER, AND YORK COUNTIES,
SOUTH CAROLINA AND CLEVELAND, GASTON, AND MECKLENBURG COUNTIES, NORTH CAROLINA

Location or County	Date	Time	Magnitude Fujita Scale	Length (mi.)	Width (yards)	Area (mi^2)
4 CLEVELAND	5/5/1989	1654	F4	5	800	2.27
5 CLEVELAND	2/10/1990	0800	F2	0	50	
6 CLEVELAND	4/10/1990	1950	F0	0	30	
7 CLEVELAND	6/4/1992	1602	F0	0	200	
8 CLEVELAND	11/22/1992	2115	F1	5	500	1.42
9 Earl	8/16/1994	1730	F1	2	200	0.23
10 Shelby	9/16/1996	1735	F0	0	180	
11 Polkville	7/12/2003	1925	F1	6	200	0.68
12 Waco	9/17/2004	0505	F0	1	40	0.02
13 Patterson Spgs	9/27/2004	2200	F1	2	30	0.03
Gaston County, NC						
1 GASTON	4/6/1956	1300	F1	56	100	3.18
2 GASTON	5/28/1973	1800	F0	0	0	
3 GASTON	4/2/1974	0153	F1	10	100	0.57
4 GASTON	5/15/1975	1530	F1	0	0	
5 Crowders	2/21/1997	1722	F1	15	200	1.70
6 Cherryville	7/12/2003	2000	F1	18	200	2.05
7 Gastonia	3/8/2005	0715	F0	0	50	

WLS COL 2.3-1

TABLE 2.3-204 (Sheet 7 of 8)
TORNADOES IN CHEROKEE, SPARTANBURG, UNION, CHESTER, AND YORK COUNTIES,
SOUTH CAROLINA AND CLEVELAND, GASTON, AND MECKLENBURG COUNTIES, NORTH CAROLINA

Location or County	Date	Time	Magnitude Fujita Scale	Length (mi.)	Width (yards)	Area (mi^2)
Mecklenburg County, NC						
1 MECKLENBURG	2/18/1960	1245	F1	24	33	0.45
2 MECKLENBURG	4/12/1961	1710	F1	1	200	0.11
3 MECKLENBURG	8/10/1964	1645	F1	0	0	
4 MECKLENBURG	9/12/1965	1930	F2	0	70	
5 MECKLENBURG	6/7/1968	1430	F2	17	200	1.93
6 MECKLENBURG	5/28/1973	0500	F2	10	100	0.57
7 MECKLENBURG	5/28/1973	1700	F1	0	0	
8 MECKLENBURG	10/8/1975	1425	F1	0	50	
9 MECKLENBURG	9/16/1977	1330	F1	0	7	
10 MECKLENBURG	8/14/1978	1145	F0	0	0	
11 MECKLENBURG	5/3/1984	1545	F1	14	100	0.80
12 MECKLENBURG	6/6/1985	1620	F0	1	267	0.15
13 MECKLENBURG	11/28/1990	1940	F1	0	20	
14 MECKLENBURG	3/10/1992	2107	F2	3	180	0.31
15 Mint Hill	3/20/1998	1442	F0	0	25	
16 Cornelius	5/7/1998	1845	F0	6	50	0.17
17 Pineville	8/1/1999	1935	F0	0	10	

WLS COL 2.3-1

TABLE 2.3-204 (Sheet 8 of 8)
TORNADOES IN CHEROKEE, SPARTANBURG, UNION, CHESTER, AND YORK COUNTIES,
SOUTH CAROLINA AND CLEVELAND, GASTON, AND MECKLENBURG COUNTIES, NORTH CAROLINA

Location or County	Date	Time	Magnitude Fujita Scale	Length (mi.)	Width (yards)	Area (mi^2)
18 Charlotte	9/7/2004	1045	F2	2	200	0.23
19 Charlotte	3/8/2005	0740	F1	3	50	0.09

NOTES:

1. Tornado data from all years were used to calculate the annual frequencies given in text.

2. Tornadoes with a zero (or missing) reported area, path length, or width do not represent valid data for statistical purposes.

3. Data recorded in the NOAA's National Environmental Satellite, Data, and Information Service (NEDSIS) - NCDC Storm Event database, 1950-2005, http://www4.ncdc.noaa.gov/cgi-win/wwcgi.dll?wwevent~storms

WLS COL 2.3-1

TABLE 2.3-205
THUNDERSTORMS
GREENVILLE-SPARTANBURG, SC AND CHARLOTTE, NC

Number of Days with Thunderstorms

Station	JAN	FEB	MAR	APR	MAY	JUN	JUL	AUG	SEP	OCT	NOV	DEC	YEAR
GSP(1)	0.8	0.9	2.4	3.2	6.1	7.4	9.8	6.9	3.3	0.8	0.8	0.6	43.0
CLT(2)	0.6	1.0	2.1	3.4	5.3	7.1	9.1	6.9	2.5	1.1	0.7	0.4	40.2
Average	0.7	1.0	2.3	3.3	5.7	7.3	9.5	6.9	2.9	1.0	0.8	0.5	41.6

NOTES:

1. 2007 Local Climatological Data Annual Summary with Comparative Data for Greenville-Spartanburg (Greer), South Carolina (Station ID GSP), data for years 1963 through 2007, National Climatic Data Center (NCDC). (Reference 236)

2. 2007 Local Climatological Data Annual Summary with Comparative Data for Charlotte, North Carolina (Station ID CLT), data for years 1948 through 2007, National Climatic Data Center (NCDC). (Reference 239)

WLS COL 2.3-1

TABLE 2.3-206
HAIL STORM EVENTS
CHEROKEE, SPARTANBURG, UNION, CHESTER, AND YORK COUNTIES, SOUTH CAROLINA AND
CLEVELAND, GASTON, AND MECKLENBURG COUNTIES, NORTH CAROLINA

County	Number of Events	Percentage	Events with Property Damage
Cherokee, SC	42	10%	0
Spartanburg, SC	91	21%	5
Union, SC	42	10%	0
Chester, SC	28	6%	0
York, SC	53	12%	2
Cleveland, NC	55	13%	0
Gaston, NC	49	11%	1
Mecklenburg, NC	72	17%	1
Total	432	100%	9

Number per year = 36

NOTES:

1. Data from NOAA's Satellite & Information System - NCDC Storm Events Database, January 1, 1995 through May 31, 2006, http://www4.ncdc.noaa.gov/cgi-win/wwcgi.dll?wwevent~storms

2. For this table, each occurrence of hail was counted as an individual event, even if two counties recorded hail simultaneously.

WLS COL 2.3-1

TABLE 2.3-207
MEAN VENTILATION RATE BY MONTH
GREENSBORO, NC

	Morning Ventilation Rate (m^2/s)	Afternoon Ventilation Rate (m^2/s)	Mean Ventilation Rate (m^2/s)
Jan	3914	6289	5101
Feb	3937	7379	5658
Mar	3979	9203	6591
Apr	3490	12736	8113
May	2631	9404	6017
Jun	2373	9469	5921
July	2338	7779	5059
Aug	2129	6096	4113
Sep	2172	6228	4200
Oct	2025	6262	4143
Nov	2882	5743	4312
Dec	3719	5904	4811

NOTES:

1. Source of data is EPA SCRAM data for 1984-1987, 1989-1991 for Greensboro, High Point, NC, Station 13723 (Lat 36.083, Long 79.950), http://www.epa.gov/scram001/mixingheightdata.htm

2. Atmospheric ventilation rate is numerically equal to the product of the mixing height and the average wind speed within the mixing layer.

WLS COL 2.3-1

TABLE 2.3-208 (Sheet 1 of 19)
ICE STORMS
CHEROKEE, SPARTANBURG, UNION, CHESTER, AND YORK COUNTIES, SOUTH CAROLINA AND
CLEVELAND, GASTON, AND MECKLENBURG COUNTIES, NORTH CAROLINA

Date	Time	Type	Deaths	Injuries	Property Damage	Crop Damage
Cherokee County, SC						
3/13/1993	0200	Winter Storm	0	0	0	0
12/22/1993	2100	Snow	0	0	0	0
2/10/1994	1800	Freezing Rain/sleet	0	0	0	0
2/11/1994	1110	Ice Storm	0	0	5.0M	0
1/6/1995	1400	Freezing Rain	0	0	100K	0
1/23/1995	1400	Snow	0	0	0	0
2/7/1995	1800	Snow	0	0	0	0
2/10/1995	0500	Snow Freezing Rain	0	0	0	0
1/6/1996	1800	Winter Storm	0	0	50K	0
1/6/1996	0800	Winter Storm	0	0	0	0
1/7/1996	0000	Winter Storm	0	0	50K	0
1/11/1996	2000	Winter Storm	0	0	0	0
2/2/1996	0100	Freezing Rain	0	0	0	0
2/2/1996	1630	Ice Storm	0	0	0	0
2/2/1996	0500	Ice Storm	0	0	0	0

WLS COL 2.3-1

TABLE 2.3-208 (Sheet 2 of 19)
ICE STORMS
CHEROKEE, SPARTANBURG, UNION, CHESTER, AND YORK COUNTIES, SOUTH CAROLINA AND
CLEVELAND, GASTON, AND MECKLENBURG COUNTIES, NORTH CAROLINA

Date	Time	Type	Deaths	Injuries	Property Damage	Crop Damage
2/16/1996	0600	Snow	0	0	0	0
1/9/1997	0000	Ice Storm	0	0	200K	0
2/13/1997	1200	Ice Storm	0	0	0	0
12/29/1997	0530	Snow	0	0	0	0
1/19/1998	0600	Snow	0	0	0	0
12/23/1998	0900	Freezing Rain/sleet	0	0	0	0
12/24/1998	0500	Ice Storm	0	0	0	0
1/2/1999	1800	Ice Storm	0	0	20.0M	0
1/31/1999	1200	Snow And Sleet	0	0	0	0
2/1/1999	0000	Freezing Rain	0	0	0	0
2/19/1999	1200	Snow	0	0	0	0
1/22/2000	1800	Heavy Snow	0	0	0	0
1/24/2000	1000	Heavy Snow	0	0	0	0
1/29/2000	2100	Ice Storm	0	0	0	0
11/19/2000	0600	Snow	0	0	0	0
12/3/2000	0200	Snow	0	0	0	0

WLS COL 2.3-1

TABLE 2.3-208 (Sheet 3 of 19)
ICE STORMS
CHEROKEE, SPARTANBURG, UNION, CHESTER, AND YORK COUNTIES, SOUTH CAROLINA AND
CLEVELAND, GASTON, AND MECKLENBURG COUNTIES, NORTH CAROLINA

Date	Time	Type	Deaths	Injuries	Property Damage	Crop Damage
12/13/2000	1300	Freezing Rain	0	0	0	0
12/19/2000	0200	Snow	0	0	0	0
12/21/2000	1400	Freezing Rain	0	0	0	0
4/17/2001	0700	Snow Showers	0	0	0	0
1/3/2002	0000	Heavy Snow	0	0	0	0
12/4/2002	1500	Ice Storm	0	0	100.0M	0
1/16/2003	1800	Winter Weather/mix	0	0	0	0
1/23/2003	0600	Heavy Snow	0	0	0	0
12/4/2003	0600	Winter Weather/mix	0	0	0	0
1/27/2004	0000	Winter Weather/mix	0	0	0	0
2/26/2004	1000	Heavy Snow	0	0	1.9M	0
1/29/2005	1300	Winter Storm	0	0	0	0
1/29/2005	0400	Winter Weather/mix	0	0	0	0
12/8/2005	1600	Winter Weather	0	0	0	0
12/15/2005	0600	Ice Storm	0	0	900K	0
12/15/2005	0000	Winter Weather	0	0	0	0

WLS COL 2.3-1

TABLE 2.3-208 (Sheet 4 of 19)
ICE STORMS
CHEROKEE, SPARTANBURG, UNION, CHESTER, AND YORK COUNTIES, SOUTH CAROLINA AND
CLEVELAND, GASTON, AND MECKLENBURG COUNTIES, NORTH CAROLINA

Date	Time	Type	Deaths	Injuries	Property Damage	Crop Damage
Spartanburg County, SC						
1/11/1994	0300	Freezing Rain	0	0	0	0
2/10/1994	1800	Freezing Rain/sleet	0	0	0	0
2/11/1994	1110	Ice Storm	0	0	5.0M	0
1/6/1995	1400	Freezing Rain	0	0	100K	0
2/7/1995	1800	Snow	0	0	0	0
2/10/1995	0500	Snow Freezing Rain	0	0	0	0
1/6/1996	1800	Winter Storm	0	0	50K	0
1/6/1996	0800	Winter Storm	0	0	0	0
1/7/1996	0000	Winter Storm	0	0	50K	0
1/11/1996	2000	Winter Storm	0	0	0	0
2/2/1996	0100	Freezing Rain	0	0	0	0
2/2/1996	1630	Ice Storm	0	0	0	0
2/16/1996	0600	Snow	0	0	0	0
12/18/1996	1800	Heavy Snow	0	0	0	0
1/9/1997	0000	Ice Storm	0	0	200K	0

WLS COL 2.3-1

TABLE 2.3-208 (Sheet 5 of 19)
ICE STORMS
CHEROKEE, SPARTANBURG, UNION, CHESTER, AND YORK COUNTIES, SOUTH CAROLINA AND
CLEVELAND, GASTON, AND MECKLENBURG COUNTIES, NORTH CAROLINA

Date	Time	Type	Deaths	Injuries	Property Damage	Crop Damage
2/13/1997	1200	Ice Storm	0	0	0	0
12/29/1997	0530	Heavy Snow	0	0	0	0
1/19/1998	0600	Snow	0	0	0	0
12/23/1998	0900	Freezing Rain/sleet	0	0	0	0
12/24/1998	0500	Ice Storm	0	0	0	0
1/2/1999	1800	Ice Storm	0	0	20.0M	0
1/31/1999	1200	Snow And Sleet	0	0	0	0
2/1/1999	0000	Freezing Rain	0	0	0	0
2/24/1999	0000	Snow	0	0	0	0
3/9/1999	0400	Winter Storm	0	0	0	0
1/22/2000	1800	Heavy Snow	0	0	0	0
1/23/2000	0300	Ice Storm	0	0	0	0
1/24/2000	1000	Heavy Snow	0	0	0	0
1/29/2000	2100	Ice Storm	0	0	0	0
11/19/2000	0600	Snow	0	0	0	0
12/3/2000	0200	Snow	0	0	0	0

WLS COL 2.3-1

TABLE 2.3-208 (Sheet 6 of 19)
ICE STORMS
CHEROKEE, SPARTANBURG, UNION, CHESTER, AND YORK COUNTIES, SOUTH CAROLINA AND
CLEVELAND, GASTON, AND MECKLENBURG COUNTIES, NORTH CAROLINA

Date	Time	Type	Deaths	Injuries	Property Damage	Crop Damage
12/13/2000	1300	Freezing Rain	0	0	0	0
12/19/2000	0200	Snow	0	0	0	0
12/21/2000	1400	Freezing Rain	0	0	0	0
3/20/2001	0700	Heavy Snow	0	0	0	0
4/17/2001	0700	Snow Showers	0	0	0	0
1/3/2002	0000	Heavy Snow	0	0	0	0
12/4/2002	1500	Ice Storm	0	0	100.0M	0
1/16/2003	1800	Winter Weather/mix	0	0	0	0
1/23/2003	0600	Heavy Snow	0	0	0	0
2/16/2003	1400	Winter Storm	0	0	0	0
12/4/2003	0600	Winter Weather/mix	0	0	0	0
1/27/2004	0000	Winter Weather/mix	0	0	0	0
2/2/2004	1800	Winter Weather/mix	0	0	0	0
2/26/2004	1000	Heavy Snow	0	0	1.9M	0
1/29/2005	1300	Winter Storm	0	0	0	0
1/29/2005	0400	Winter Weather/mix	0	0	0	0

WLS COL 2.3-1

TABLE 2.3-208 (Sheet 7 of 19)
ICE STORMS
CHEROKEE, SPARTANBURG, UNION, CHESTER, AND YORK COUNTIES, SOUTH CAROLINA AND
CLEVELAND, GASTON, AND MECKLENBURG COUNTIES, NORTH CAROLINA

Date	Time	Type	Deaths	Injuries	Property Damage	Crop Damage
12/8/2005	1600	Winter Weather	0	0	0	0
12/15/2005	0600	Ice Storm	0	0	900K	0
12/15/2005	0000	Winter Weather	0	0	0	0
Union County, SC						
12/22/1993	2100	Snow	0	0	0	0
2/10/1994	1800	Freezing Rain/sleet	0	0	0	0
2/11/1994	1110	Ice Storm	0	0	5.0M	0
1/6/1995	1400	Freezing Rain	0	0	100K	0
1/7/1996	0300	Winter Storm	0	0	0	0
2/3/1996	0200	Freezing Rain	0	0	0	0
2/16/1996	0600	Snow	0	0	0	0
12/29/1997	0530	Snow	0	0	0	0
1/19/1998	0600	Snow	0	0	0	0
1/2/1999	1800	Ice Storm	0	0	20.0M	0
1/22/2000	1800	Heavy Snow	0	0	0	0
1/23/2000	0300	Ice Storm	0	0	0	0

WLS COL 2.3-1

TABLE 2.3-208 (Sheet 8 of 19)
ICE STORMS
CHEROKEE, SPARTANBURG, UNION, CHESTER, AND YORK COUNTIES, SOUTH CAROLINA AND
CLEVELAND, GASTON, AND MECKLENBURG COUNTIES, NORTH CAROLINA

Date	Time	Type	Deaths	Injuries	Property Damage	Crop Damage
1/24/2000	1000	Heavy Snow	0	0	0	0
1/29/2000	2100	Ice Storm	0	0	0	0
11/19/2000	0600	Snow	0	0	0	0
4/17/2001	0700	Snow Showers	0	0	0	0
1/3/2002	0000	Heavy Snow	0	0	0	0
12/4/2002	1500	Ice Storm	0	0	100.0M	0
1/23/2003	0600	Heavy Snow	0	0	0	0
2/16/2003	1400	Winter Storm	0	0	0	0
1/27/2004	0000	Winter Weather/mix	0	0	0	0
2/26/2004	1000	Heavy Snow	0	0	1.9M	0
1/29/2005	0400	Winter Weather/mix	0	0	0	0
12/15/2005	0700	Ice Storm	0	0	250K	0
12/15/2005	0000	Winter Weather	0	0	0	0
Chester County, SC						
2/10/1994	1800	Freezing Rain/sleet	0	0	0	0
2/11/1994	1110	Ice Storm	0	0	5.0M	0

WLS COL 2.3-1

TABLE 2.3-208 (Sheet 9 of 19)
ICE STORMS
CHEROKEE, SPARTANBURG, UNION, CHESTER, AND YORK COUNTIES, SOUTH CAROLINA AND
CLEVELAND, GASTON, AND MECKLENBURG COUNTIES, NORTH CAROLINA

Date	Time	Type	Deaths	Injuries	Property Damage	Crop Damage
1/6/1996	1200	Ice Storm	0	0	0	0
1/7/1996	0300	Winter Storm	0	0	0	0
1/7/1996	0600	Ice Storm	0	0	0	0
1/11/1996	2200	Ice Storm	0	0	0	0
2/3/1996	0200	Freezing Rain	0	0	0	0
12/29/1997	0530	Snow	0	0	0	0
1/19/1998	0600	Snow	0	0	0	0
1/23/2000	0300	Ice Storm	0	0	0	0
1/24/2000	1000	Heavy Snow	0	0	0	0
1/29/2000	2100	Ice Storm	0	0	0	0
11/19/2000	0600	Snow	0	0	0	0
12/3/2000	0200	Snow	0	0	0	0
1/2/2002	2000	Heavy Snow	0	0	0	0
1/2/2002	2120	Winter Storm	0	0	0	0
12/4/2002	1500	Ice Storm	0	0	100.0M	0
12/4/2002	0755	Ice Storm	0	0	0	0

WLS COL 2.3-1

TABLE 2.3-208 (Sheet 10 of 19)
ICE STORMS
CHEROKEE, SPARTANBURG, UNION, CHESTER, AND YORK COUNTIES, SOUTH CAROLINA AND
CLEVELAND, GASTON, AND MECKLENBURG COUNTIES, NORTH CAROLINA

Date	Time	Type	Deaths	Injuries	Property Damage	Crop Damage
1/23/2003	0600	Heavy Snow	0	0	0	0
1/23/2003	0600	Winter Storm	0	0	0	0
2/16/2003	1400	Winter Storm	0	0	0	0
2/16/2003	2206	Ice Storm	0	22	0	0
1/25/2004	1500	Winter Storm	0	0	0	0
1/27/2004	0000	Winter Weather/mix	0	0	0	0
2/26/2004	0722	Winter Storm	0	0	0	0
2/26/2004	1000	Heavy Snow	0	0	1.9M	0
12/26/2004	0415	Ice Storm	0	0	0	0
12/26/2004	0600	Winter Weather/mix	0	0	0	0
1/29/2005	0400	Winter Weather/mix	0	0	0	0
1/29/2005	1220	Ice Storm	0	0	0	0
12/15/2005	0300	Winter Weather	0	0	0	0
York County, SC						
2/10/1994	1800	Freezing Rain/sleet	0	0	0	0
2/11/1994	1110	Ice Storm	0	0	5.0M	0

WLS COL 2.3-1

TABLE 2.3-208 (Sheet 11 of 19)
ICE STORMS
CHEROKEE, SPARTANBURG, UNION, CHESTER, AND YORK COUNTIES, SOUTH CAROLINA AND
CLEVELAND, GASTON, AND MECKLENBURG COUNTIES, NORTH CAROLINA

Date	Time	Type	Deaths	Injuries	Property Damage	Crop Damage
1/6/1996	1800	Winter Storm	0	0	50K	0
1/6/1996	0800	Winter Storm	0	0	0	0
1/7/1996	0600	Ice Storm	0	0	0	0
1/7/1996	0000	Winter Storm	0	0	50K	0
1/11/1996	2000	Winter Storm	0	0	0	0
2/2/1996	1630	Ice Storm	0	0	0	0
2/16/1996	0600	Snow	0	0	0	0
2/13/1997	1200	Ice Storm	0	0	0	0
12/29/1997	0530	Snow	0	0	0	0
1/19/1998	0600	Snow	0	0	0	0
12/23/1998	0900	Freezing Rain/sleet	0	0	0	0
12/24/1998	0500	Ice Storm	0	0	0	0
2/19/1999	1200	Snow	0	0	0	0
1/22/2000	1800	Snow	0	0	0	0
1/23/2000	0300	Ice Storm	0	0	0	0
1/24/2000	1000	Heavy Snow	0	0	0	0

WLS COL 2.3-1

TABLE 2.3-208 (Sheet 12 of 19)
ICE STORMS
CHEROKEE, SPARTANBURG, UNION, CHESTER, AND YORK COUNTIES, SOUTH CAROLINA AND
CLEVELAND, GASTON, AND MECKLENBURG COUNTIES, NORTH CAROLINA

Date	Time	Type	Deaths	Injuries	Property Damage	Crop Damage
1/29/2000	2100	Ice Storm	0	0	0	0
11/19/2000	0600	Snow	0	0	0	0
12/21/2000	1400	Freezing Rain	0	0	0	0
4/17/2001	0700	Snow Showers	0	0	0	0
1/2/2002	2000	Heavy Snow	0	0	0	0
12/4/2002	1500	Ice Storm	0	0	100.0M	0
1/23/2003	0600	Heavy Snow	0	0	0	0
1/27/2004	0000	Winter Weather/mix	0	0	0	0
2/26/2004	1000	Heavy Snow	0	0	1.9M	0
1/29/2005	1300	Winter Storm	0	0	0	0
1/29/2005	0400	Winter Weather/mix	0	0	0	0
12/15/2005	0300	Winter Weather	0	0	0	0
Cleveland County, NC						
2/10/1994	1000	Ice Storm	0	0	0	0
1/11/1996	1800	Winter Storm	0	0	0	0
2/2/1996	0600	Ice Storm	0	0	10.0M	0

WLS COL 2.3-1

TABLE 2.3-208 (Sheet 13 of 19)
ICE STORMS
CHEROKEE, SPARTANBURG, UNION, CHESTER, AND YORK COUNTIES, SOUTH CAROLINA AND
CLEVELAND, GASTON, AND MECKLENBURG COUNTIES, NORTH CAROLINA

Date	Time	Type	Deaths	Injuries	Property Damage	Crop Damage
2/3/1996	1800	Snow	0	0	0	0
2/16/1996	0200	Snow	0	0	0	0
2/13/1997	1500	Ice Storm	0	0	0	0
2/13/1997	1000	Winter Storm	0	0	0	0
12/29/1997	0530	Snow	0	0	0	0
12/23/1998	0900	Freezing Rain/sleet	0	0	0	0
1/2/1999	1800	Ice Storm	0	0	0	0
2/1/1999	0000	Freezing Rain	0	0	0	0
2/19/1999	1200	Snow	0	0	0	0
3/9/1999	0300	Snow And Sleet	0	0	0	0
1/18/2000	0400	Snow	0	0	0	0
1/22/2000	1500	Heavy Snow	0	0	0	0
1/24/2000	1300	Heavy Snow	0	0	0	0
1/29/2000	2100	Freezing Rain	0	0	0	0
11/19/2000	0600	Snow	0	0	0	0
12/3/2000	0300	Snow	0	0	0	0

WLS COL 2.3-1

TABLE 2.3-208 (Sheet 14 of 19)
ICE STORMS
CHEROKEE, SPARTANBURG, UNION, CHESTER, AND YORK COUNTIES, SOUTH CAROLINA AND
CLEVELAND, GASTON, AND MECKLENBURG COUNTIES, NORTH CAROLINA

Date	Time	Type	Deaths	Injuries	Property Damage	Crop Damage
12/13/2000	1700	Freezing Rain	0	0	0	0
2/22/2001	0300	Snow/sleet	0	0	0	0
3/20/2001	0800	Heavy Snow	0	0	0	0
4/17/2001	0700	Snow Showers	0	0	0	0
1/3/2002	0000	Heavy Snow	0	0	0	0
12/4/2002	1500	Ice Storm	0	0	99.0M	0
1/16/2003	1800	Winter Weather/mix	0	0	0	0
1/23/2003	0400	Heavy Snow	0	0	0	0
2/27/2003	0000	Winter Weather/mix	0	0	0	0
12/4/2003	0600	Winter Weather/mix	0	0	0	0
12/14/2003	0800	Ice Storm	0	0	3K	0
1/27/2004	0000	Winter Weather/mix	0	0	0	0
2/26/2004	1000	Heavy Snow	0	0	3.1M	0
1/29/2005	1300	Winter Storm	0	0	0	0
1/29/2005	0400	Winter Weather/mix	0	0	0	0
3/17/2005	0200	Winter Weather/mix	0	0	0	0

WLS COL 2.3-1

TABLE 2.3-208 (Sheet 15 of 19)
ICE STORMS
CHEROKEE, SPARTANBURG, UNION, CHESTER, AND YORK COUNTIES, SOUTH CAROLINA AND
CLEVELAND, GASTON, AND MECKLENBURG COUNTIES, NORTH CAROLINA

Date	Time	Type	Deaths	Injuries	Property Damage	Crop Damage
12/8/2005	1600	Winter Weather	0	0	0	0
12/15/2005	0600	Ice Storm	0	0	450K	0
12/15/2005	0000	Winter Weather	0	0	0	0
3/20/2006	1200	Winter Weather	0	0	0	0
Gaston County, NC						
2/10/1994	1000	Ice Storm	0	0	0	0
1/6/1996	1800	Winter Storm	0	0	0	0
1/11/1996	1800	Winter Storm	0	0	0	0
2/2/1996	0600	Ice Storm	0	0	10.0M	0
2/3/1996	1800	Snow	0	0	0	0
2/16/1996	0200	Snow	0	0	0	0
2/13/1997	1500	Ice Storm	0	0	0	0
2/13/1997	1000	Winter Storm	0	0	0	0
12/29/1997	0530	Snow	0	0	0	0
1/19/1998	0600	Snow	0	0	0	0
12/23/1998	0900	Freezing Rain/sleet	0	0	0	0

WLS COL 2.3-1

TABLE 2.3-208 (Sheet 16 of 19)
ICE STORMS
CHEROKEE, SPARTANBURG, UNION, CHESTER, AND YORK COUNTIES, SOUTH CAROLINA AND
CLEVELAND, GASTON, AND MECKLENBURG COUNTIES, NORTH CAROLINA

Date	Time	Type	Deaths	Injuries	Property Damage	Crop Damage
12/24/1998	0500	Ice Storm	0	0	0	0
1/2/1999	1800	Ice Storm	0	0	0	0
2/1/1999	0000	Freezing Rain	0	0	0	0
2/19/1999	1200	Snow	0	0	0	0
3/9/1999	0300	Snow And Sleet	0	0	0	0
1/18/2000	0400	Snow	0	0	0	0
1/22/2000	1500	Heavy Snow	0	0	0	0
1/24/2000	1300	Heavy Snow	0	0	0	0
1/29/2000	2100	Ice Storm	0	0	0	0
11/19/2000	0600	Snow	0	0	0	0
4/17/2001	0700	Snow Showers	0	0	0	0
1/3/2002	0000	Heavy Snow	0	0	0	0
12/4/2002	1500	Ice Storm	0	0	99.0M	0
1/16/2003	1800	Winter Weather/mix	0	0	0	0
1/23/2003	0600	Heavy Snow	0	0	0	0
2/27/2003	0000	Winter Weather/mix	0	0	0	0

WLS COL 2.3-1

TABLE 2.3-208 (Sheet 17 of 19)
ICE STORMS
CHEROKEE, SPARTANBURG, UNION, CHESTER, AND YORK COUNTIES, SOUTH CAROLINA AND
CLEVELAND, GASTON, AND MECKLENBURG COUNTIES, NORTH CAROLINA

Date	Time	Type	Deaths	Injuries	Property Damage	Crop Damage
1/27/2004	0000	Winter Weather/mix	0	0	0	0
2/26/2004	1000	Heavy Snow	0	0	3.1M	0
1/29/2005	1300	Winter Storm	0	0	0	0
1/29/2005	0400	Winter Weather/mix	0	0	0	0
12/15/2005	0600	Ice Storm	0	0	450K	0
12/15/2005	0000	Winter Weather	0	0	0	0
Mecklenburg County, NC						
2/10/1994	1000	Ice Storm	0	0	0	0
1/6/1996	1800	Winter Storm	0	0	0	0
1/11/1996	1800	Winter Storm	0	0	0	0
2/2/1996	0600	Ice Storm	0	0	10.0M	0
2/3/1996	1800	Snow	0	0	0	0
2/16/1996	0200	Snow	0	0	0	0
2/13/1997	1500	Ice Storm	0	0	0	0
12/29/1997	0530	Snow	0	0	0	0
1/19/1998	0600	Snow	0	0	0	0

WLS COL 2.3-1

TABLE 2.3-208 (Sheet 18 of 19)
ICE STORMS
CHEROKEE, SPARTANBURG, UNION, CHESTER, AND YORK COUNTIES, SOUTH CAROLINA AND
CLEVELAND, GASTON, AND MECKLENBURG COUNTIES, NORTH CAROLINA

Date	Time	Type	Deaths	Injuries	Property Damage	Crop Damage
12/23/1998	0900	Freezing Rain/sleet	0	0	0	0
12/24/1998	0500	Ice Storm	0	0	0	0
2/19/1999	1200	Snow	0	0	0	0
1/18/2000	0400	Snow	0	0	0	0
1/22/2000	1500	Heavy Snow	0	0	0	0
1/24/2000	1300	Heavy Snow	0	0	0	0
1/29/2000	2100	Ice Storm	0	0	0	0
11/19/2000	0600	Snow	0	0	0	0
1/2/2002	2000	Heavy Snow	0	0	0	0
12/4/2002	1500	Ice Storm	0	0	99.0M	0
1/16/2003	1800	Winter Weather/mix	0	0	0	0
1/23/2003	0600	Heavy Snow	0	0	0	0
2/27/2003	0000	Winter Weather/mix	0	0	0	0
12/4/2003	0600	Winter Weather/mix	0	0	0	0
1/27/2004	0000	Winter Weather/mix	0	0	0	0
2/26/2004	1000	Heavy Snow	0	0	3.1M	0

WLS COL 2.3-1

TABLE 2.3-208 (Sheet 19 of 19)
ICE STORMS
CHEROKEE, SPARTANBURG, UNION, CHESTER, AND YORK COUNTIES, SOUTH CAROLINA AND
CLEVELAND, GASTON, AND MECKLENBURG COUNTIES, NORTH CAROLINA

Date	Time	Type	Deaths	Injuries	Property Damage	Crop Damage
1/29/2005	1300	Winter Storm	0	0	0	0
1/29/2005	0400	Winter Weather/mix	0	0	0	0
12/15/2005	1100	Ice Storm	1	0	300K	0

NOTES:

1. Lee Nuclear Station site is in Cherokee County. The other counties are surrounding Cherokee County.

2. Data recorded in the NOAA Storm Events Database, 01/01/1950 - 12/31/2005 http://www4.ncdc.noaa.gov/cgi-win/wwcgi.dll?wwevent~storms.

WLS COL 2.3-1

TABLE 2.3-209 (Sheet 1 of 2)
PERCENTAGE FREQUENCY OF WIND DIRECTION AND SPEED (MPH)
GREENVILLE/SPARTANBURG, SOUTH CAROLINA
JANUARY, 1997 – 2005

January	Wind Speed (mph)								
	0-3	4-7	8-12	13-17	18-22	23-27	≥28		
Direction From	Frequency of Occurrence (%)							Total (%)	Avg. Speed
N	0.70%	2.36%	3.18%	0.96%	0.33%	0.03%	0.00%	7.56%	9.19
NNE	0.90%	2.76%	2.23%	0.40%	0.15%	0.01%	0.00%	6.45%	7.72
NE	1.00%	3.51%	3.57%	0.90%	0.09%	0.04%	0.00%	9.11%	8.24
ENE	0.55%	2.51%	2.20%	0.64%	0.12%	0.00%	0.00%	6.02%	8.34
E	0.60%	1.43%	1.06%	0.13%	0.04%	0.00%	0.00%	3.27%	7.30
ESE	0.25%	0.63%	0.07%	0.01%	0.00%	0.00%	0.00%	0.97%	5.32
SE	0.27%	0.51%	0.13%	0.00%	0.00%	0.00%	0.00%	0.91%	5.21
SSE	0.33%	0.76%	0.25%	0.00%	0.00%	0.00%	0.00%	1.34%	5.65
S	0.99%	2.24%	0.97%	0.25%	0.00%	0.00%	0.00%	4.45%	6.61
SSW	0.87%	2.17%	2.06%	0.42%	0.04%	0.01%	0.00%	5.57%	7.59
SW	0.76%	2.91%	5.59%	2.24%	0.45%	0.04%	0.01%	12.01%	9.97
WSW	0.42%	2.99%	5.36%	2.26%	0.61%	0.06%	0.00%	11.69%	10.43
W	0.66%	1.99%	2.30%	0.55%	0.09%	0.04%	0.00%	5.63%	8.35

WLS COL 2.3-1

TABLE 2.3-209 (Sheet 2 of 2)
PERCENTAGE FREQUENCY OF WIND DIRECTION AND SPEED (MPH)
GREENVILLE/SPARTANBURG, SOUTH CAROLINA
JANUARY, 1997 – 2005

January	Wind Speed (mph)								
	0-3	4-7	8-12	13-17	18-22	23-27	≥28		
Direction From	Frequency of Occurrence (%)							Total (%)	Avg. Speed
WNW	0.24%	0.75%	0.31%	0.10%	0.01%	0.00%	0.00%	1.42%	6.74
NW	0.25%	0.76%	0.55%	0.12%	0.00%	0.00%	0.00%	1.69%	7.41
NNW	0.37%	1.02%	1.51%	0.51%	0.18%	0.04%	0.00%	3.63%	9.62
CALM	14.22%	0.00%	0.00%	0.00%	0.00%	0.00%	0.00%	14.22%	
MISSING	4.06%							4.06%	
Total	27.43%	29.29%	31.35%	9.50%	2.12%	0.30%	0.01%	100.00%	7.73

NOTES:

1. Calm is classified as a wind speed less than 2.3 mph (anemometer start speed) or a variable wind direction, or no wind direction provided.
2. Missing data is data with missing wind speed, missing wind direction, or denoted as "variable" wind direction.
3. Data from Unedited Local Climatological Data, National Oceanic and Atmospheric Administration, U. S. Department of Commerce, Asheville, NC, Greenville/Spartanburg International Airport, Station No. 03870.
4. Period of Record - 9 years (1997 - 2005).

WLS COL 2.3-1

TABLE 2.3-210 (Sheet 1 of 2)
PERCENTAGE FREQUENCY OF WIND DIRECTION AND SPEED (MPH)
GREENVILLE/SPARTANBURG, SOUTH CAROLINA
FEBRUARY, 1997 – 2005

February	Wind Speed (mph)								
	0-3	4-7	8-12	13-17	18-22	23-27	≥28		
Direction From	Frequency of Occurrence (%)							Total (%)	Avg. Speed
N	0.95%	2.44%	2.40%	0.80%	0.15%	0.00%	0.00%	6.74%	8.28
NNE	0.64%	2.87%	2.82%	0.66%	0.07%	0.02%	0.00%	7.07%	8.02
NE	1.02%	4.18%	5.00%	1.38%	0.51%	0.20%	0.00%	12.29%	9.18
ENE	0.80%	2.46%	2.77%	0.80%	0.33%	0.20%	0.00%	7.37%	9.12
E	0.43%	1.67%	1.35%	0.07%	0.00%	0.02%	0.00%	3.53%	7.17
ESE	0.28%	0.71%	0.23%	0.00%	0.00%	0.00%	0.00%	1.21%	5.71
SE	0.28%	0.74%	0.18%	0.00%	0.00%	0.00%	0.00%	1.20%	5.60
SSE	0.34%	1.28%	0.23%	0.00%	0.00%	0.00%	0.00%	1.85%	5.60
S	0.72%	2.30%	0.95%	0.07%	0.02%	0.00%	0.00%	4.05%	6.41
SSW	0.80%	2.07%	1.62%	0.38%	0.15%	0.05%	0.00%	5.07%	7.96
SW	0.59%	2.72%	3.64%	1.30%	0.43%	0.05%	0.02%	8.74%	9.56
WSW	0.75%	2.23%	3.89%	1.59%	0.43%	0.11%	0.03%	9.04%	10.04
W	0.46%	1.79%	2.13%	0.69%	0.26%	0.05%	0.00%	5.38%	9.25

WLS COL 2.3-1

TABLE 2.3-210 (Sheet 2 of 2)
PERCENTAGE FREQUENCY OF WIND DIRECTION AND SPEED (MPH)
GREENVILLE/SPARTANBURG, SOUTH CAROLINA
FEBRUARY, 1997 – 2005

February	Wind Speed (mph)								
	0-3	4-7	8-12	13-17	18-22	23-27	≥28		
Direction From	Frequency of Occurrence (%)							Total (%)	Avg. Speed
WNW	0.31%	0.59%	0.51%	0.23%	0.08%	0.02%	0.00%	1.74%	8.56
NW	0.33%	0.62%	0.31%	0.20%	0.00%	0.00%	0.00%	1.46%	7.15
NNW	0.25%	0.89%	0.80%	0.34%	0.15%	0.00%	0.00%	2.43%	8.88
CALM	15.76%	0.00%	0.00%	0.00%	0.00%	0.00%	0.00%	15.76%	
MISSING	5.07%							5.07%	
Total	29.79%	29.56%	28.84%	8.50%	2.56%	0.71%	0.05%	100.00%	7.90

NOTES:

1. Calm is classified as a wind speed less than 2.3 mph (anemometer start speed) or a variable wind direction.
2. Missing data is data with missing wind speed, missing wind direction, or denoted as "variable" wind direction.
3. Data from Unedited Local Climatological Data, National Oceanic and Atmospheric Administration, U. S. Department of Commerce, Asheville, NC, Greenville/Spartanburg International Airport, Station No. 03870.
4. Period of Record - 9 years (1997 - 2005).

WLS COL 2.3-1

TABLE 2.3-211 (Sheet 1 of 2)
PERCENTAGE FREQUENCY OF WIND DIRECTION AND SPEED (MPH)
GREENVILLE/SPARTANBURG, SOUTH CAROLINA
MARCH, 1997 – 2005

March	Wind Speed (mph)								
	0-3	4-7	8-12	13-17	18-22	23-27	≥28		
Direction From	Frequency of Occurrence (%)							Total (%)	Avg. Speed
N	0.54%	1.88%	2.70%	1.24%	0.37%	0.00%	0.01%	6.75%	9.66
NNE	0.48%	2.72%	3.24%	0.64%	0.18%	0.00%	0.00%	7.26%	8.60
NE	0.72%	3.23%	5.12%	1.34%	0.30%	0.07%	0.00%	10.78%	9.25
ENE	0.51%	2.33%	3.54%	1.11%	0.09%	0.01%	0.00%	7.59%	8.92
E	0.33%	1.45%	1.52%	0.19%	0.00%	0.00%	0.00%	3.49%	7.57
ESE	0.27%	0.63%	0.28%	0.01%	0.00%	0.00%	0.00%	1.19%	6.07
SE	0.18%	0.75%	0.33%	0.00%	0.00%	0.00%	0.00%	1.25%	6.07
SSE	0.27%	1.31%	0.34%	0.00%	0.00%	0.00%	0.00%	1.93%	6.00
S	0.72%	2.37%	1.57%	0.10%	0.01%	0.00%	0.00%	4.78%	7.03
SSW	0.54%	2.12%	2.27%	0.70%	0.15%	0.01%	0.00%	5.79%	8.69
SW	0.52%	2.09%	3.67%	1.70%	0.51%	0.13%	0.01%	8.65%	10.44
WSW	0.45%	2.08%	3.99%	1.94%	0.76%	0.33%	0.03%	9.57%	11.26
W	0.45%	1.94%	2.42%	1.00%	0.37%	0.16%	0.03%	6.38%	10.03

WLS COL 2.3-1

TABLE 2.3-211 (Sheet 2 of 2)
PERCENTAGE FREQUENCY OF WIND DIRECTION AND SPEED (MPH)
GREENVILLE/SPARTANBURG, SOUTH CAROLINA
MARCH, 1997 – 2005

March	Wind Speed (mph)								
	0-3	4-7	8-12	13-17	18-22	23-27	≥28		
Direction From	Frequency of Occurrence (%)							Total (%)	Avg. Speed
WNW	0.27%	0.66%	0.61%	0.24%	0.06%	0.07%	0.00%	1.91%	9.21
NW	0.16%	0.73%	0.70%	0.12%	0.04%	0.01%	0.00%	1.78%	8.00
NNW	0.30%	0.94%	1.16%	0.51%	0.18%	0.04%	0.00%	3.14%	9.72
CALM	11.66%	0.00%	0.00%	0.00%	0.00%	0.00%	0.00%	11.66%	
MISSING	6.09%							6.09%	
Total	24.45%	27.23%	33.48%	10.86%	3.03%	0.87%	0.09%	100.00%	8.53

NOTES:

1. Calm is classified as a wind speed less than 2.3 mph (anemometer start speed) or a variable wind direction.
2. Missing data is data with missing wind speed, missing wind direction, or denoted as "variable" wind direction.
3. Data from Unedited Local Climatological Data, National Oceanic and Atmospheric Administration, U. S. Department of Commerce, Asheville, NC, Greenville/Spartanburg International Airport, Station No. 03870.
4. Period of Record - 9 years (1997 - 2005).

WLS COL 2.3-1

TABLE 2.3-212 (Sheet 1 of 2)
PERCENTAGE FREQUENCY OF WIND DIRECTION AND SPEED (MPH)
GREENVILLE/SPARTANBURG, SOUTH CAROLINA
APRIL, 1997-2005

April	Wind Speed (mph)								
	0-3	4-7	8-12	13-17	18-22	23-27	≥28		
Direction From	Frequency of Occurrence (%)							Total (%)	Avg. Speed
N	0.82%	1.71%	2.48%	0.76%	0.29%	0.06%	0.00%	6.13%	9.13
NNE	0.56%	1.84%	2.07%	0.68%	0.02%	0.03%	0.02%	5.20%	8.52
NE	0.51%	2.47%	3.43%	1.54%	0.23%	0.03%	0.00%	8.21%	9.62
ENE	0.66%	1.84%	2.05%	0.71%	0.32%	0.00%	0.00%	5.59%	8.85
E	0.42%	1.05%	1.19%	0.11%	0.00%	0.00%	0.00%	2.76%	7.37
ESE	0.03%	0.42%	0.37%	0.02%	0.00%	0.00%	0.00%	0.83%	7.26
SE	0.17%	0.66%	0.46%	0.03%	0.00%	0.00%	0.00%	1.33%	6.74
SSE	0.17%	1.20%	0.80%	0.09%	0.00%	0.00%	0.00%	2.27%	6.86
S	0.82%	2.92%	2.33%	0.40%	0.06%	0.00%	0.00%	6.53%	7.54
SSW	0.62%	2.76%	3.58%	1.02%	0.20%	0.00%	0.00%	8.18%	8.93
SW	0.48%	3.43%	5.54%	2.11%	0.59%	0.11%	0.02%	12.27%	10.11
WSW	0.54%	2.90%	4.20%	2.07%	0.80%	0.29%	0.02%	10.82%	10.46
W	0.43%	2.21%	2.31%	1.02%	0.45%	0.19%	0.06%	6.67%	10.31

WLS COL 2.3-1

TABLE 2.3-212 (Sheet 2 of 2)
PERCENTAGE FREQUENCY OF WIND DIRECTION AND SPEED (MPH)
GREENVILLE/SPARTANBURG, SOUTH CAROLINA
APRIL, 1997-2005

April	Wind Speed (mph)								
	0-3	4-7	8-12	13-17	18-22	23-27	≥28		
Direction From	Frequency of Occurrence (%)							Total (%)	Avg. Speed
WNW	0.17%	0.63%	0.66%	0.25%	0.11%	0.08%	0.00%	1.90%	9.75
NW	0.29%	0.69%	0.54%	0.15%	0.06%	0.00%	0.00%	1.74%	7.89
NNW	0.28%	0.65%	0.97%	0.42%	0.12%	0.00%	0.00%	2.44%	9.25
CALM	11.62%	0.00%	0.00%	0.00%	0.00%	0.00%	0.00%	11.62%	
MISSING	5.52%							5.52%	
Total	24.10%	27.38%	32.99%	11.37%	3.26%	0.79%	0.11%	100.00%	8.66

NOTES:

1. Calm is classified as a wind speed less than 2.3 mph (anemometer start speed) or a variable wind direction.
2. Missing data is data with missing wind speed, missing wind direction, or denoted as "variable" wind direction.
3. Data from Unedited Local Climatological Data, National Oceanic and Atmospheric Administration, U. S. Department of Commerce, Asheville, NC, Greenville/Spartanburg International Airport, Station No. 03870.
4. Period of Record - 9 years (1997 - 2005).

WLS COL 2.3-1

TABLE 2.3-213 (Sheet 1 of 2)
PERCENTAGE FREQUENCY OF WIND DIRECTION AND SPEED (MPH)
GREENVILLE/SPARTANBURG, SOUTH CAROLINA
MAY, 1997-2005

May	Wind Speed (mph)								
	0-3	4-7	8-12	13-17	18-22	23-27	≥28		
Direction From	Frequency of Occurrence (%)							Total (%)	Avg. Speed
N	0.85%	1.96%	1.51%	0.22%	0.06%	0.01%	0.00%	4.61%	7.36
NNE	0.76%	2.99%	2.43%	0.30%	0.03%	0.00%	0.00%	6.51%	7.39
NE	0.55%	2.97%	3.39%	0.90%	0.04%	0.00%	0.00%	7.86%	8.58
ENE	0.45%	1.48%	2.08%	0.48%	0.12%	0.00%	0.00%	4.60%	8.65
E	0.34%	1.14%	1.08%	0.12%	0.03%	0.00%	0.00%	2.70%	7.55
ESE	0.21%	0.49%	0.34%	0.00%	0.00%	0.00%	0.00%	1.05%	6.54
SE	0.21%	0.57%	0.46%	0.00%	0.00%	0.00%	0.00%	1.24%	6.56
SSE	0.27%	1.48%	0.42%	0.01%	0.00%	0.00%	0.00%	2.18%	6.10
S	0.75%	2.70%	1.58%	0.07%	0.00%	0.00%	0.00%	5.11%	6.67
SSW	0.69%	2.39%	2.72%	0.67%	0.12%	0.00%	0.00%	6.59%	8.38
SW	0.57%	3.00%	5.63%	1.87%	0.43%	0.15%	0.01%	11.66%	9.99
WSW	0.55%	3.54%	5.03%	1.85%	0.40%	0.01%	0.00%	11.39%	9.51
W	0.45%	2.49%	2.69%	0.90%	0.21%	0.01%	0.00%	6.75%	8.75

WLS COL 2.3-1

TABLE 2.3-213 (Sheet 2 of 2)
PERCENTAGE FREQUENCY OF WIND DIRECTION AND SPEED (MPH)
GREENVILLE/SPARTANBURG, SOUTH CAROLINA
MAY, 1997-2005

May	Wind Speed (mph)								
	0-3	4-7	8-12	13-17	18-22	23-27	≥28		
Direction From	Frequency of Occurrence (%)							Total (%)	Avg. Speed
WNW	0.16%	0.67%	0.57%	0.19%	0.03%	0.01%	0.00%	1.64%	8.20
NW	0.19%	0.51%	0.36%	0.04%	0.01%	0.00%	0.00%	1.12%	7.32
NNW	0.39%	0.64%	0.39%	0.07%	0.01%	0.00%	0.00%	1.51%	6.70
CALM	16.58%	0.00%	0.00%	0.00%	0.00%	0.00%	0.00%	23.48%	
missing	6.90%							6.90%	
Total	30.87%	29.02%	30.68%	7.71%	1.51%	0.21%	0.01%	100.00%	7.77

NOTES:

1. Calm is classified as a wind speed less than 2.3 mph (anemometer start speed) or a variable wind direction.
2. Missing data is data with missing wind speed, missing wind direction, or denoted as "variable" wind direction.
3. Data from Unedited Local Climatological Data, National Oceanic and Atmospheric Administration, U. S. Department of Commerce, Asheville, NC, Greenville/Spartanburg International Airport, Station No. 03870.
4. Period of Record - 9 years (1997 - 2005).

WLS COL 2.3-1

TABLE 2.3-214 (Sheet 1 of 2)
PERCENTAGE FREQUENCY OF WIND DIRECTION AND SPEED (MPH)
GREENVILLE/SPARTANBURG, SOUTH CAROLINA
JUNE, 1997-2005

June	Wind Speed (mph)								
	0-3	4-7	8-12	13-17	18-22	23-27	≥28		
Direction From	Frequency of Occurrence (%)							Total (%)	Avg. Speed
N	0.82%	2.01%	1.22%	0.23%	0.02%	0.00%	0.00%	4.29%	7.00
NNE	0.88%	3.07%	2.24%	0.35%	0.02%	0.00%	0.00%	6.56%	7.26
NE	0.77%	4.06%	3.33%	0.71%	0.06%	0.00%	0.00%	8.94%	7.89
ENE	0.59%	2.19%	2.58%	0.56%	0.03%	0.00%	0.00%	5.94%	8.19
E	0.62%	1.74%	2.07%	0.34%	0.00%	0.02%	0.00%	4.78%	7.92
ESE	0.26%	0.85%	0.48%	0.02%	0.00%	0.00%	0.00%	1.60%	6.33
SE	0.31%	0.69%	0.45%	0.06%	0.00%	0.00%	0.00%	1.51%	6.54
SSE	0.34%	1.37%	0.74%	0.03%	0.00%	0.00%	0.00%	2.48%	6.34
S	0.88%	2.15%	1.62%	0.26%	0.06%	0.02%	0.00%	4.98%	7.25
SSW	0.43%	1.74%	1.90%	0.23%	0.02%	0.02%	0.00%	4.34%	8.04
SW	0.65%	3.64%	3.83%	0.96%	0.05%	0.00%	0.00%	9.12%	8.28
WSW	0.71%	3.16%	4.65%	0.96%	0.17%	0.05%	0.00%	9.69%	8.80
W	0.62%	2.61%	2.82%	0.42%	0.11%	0.02%	0.00%	6.59%	7.83

WLS COL 2.3-1

TABLE 2.3-214 (Sheet 2 of 2)
PERCENTAGE FREQUENCY OF WIND DIRECTION AND SPEED (MPH)
GREENVILLE/SPARTANBURG, SOUTH CAROLINA
JUNE, 1997-2005

June	Wind Speed (mph)								
	0-3	4-7	8-12	13-17	18-22	23-27	≥28		
Direction From	Frequency of Occurrence (%)							Total (%)	Avg. Speed
WNW	0.39%	1.03%	0.49%	0.08%	0.02%	0.00%	0.00%	2.01%	6.53
NW	0.35%	0.71%	0.26%	0.03%	0.00%	0.00%	0.00%	1.36%	5.99
NNW	0.43%	0.65%	0.45%	0.05%	0.00%	0.00%	0.00%	1.57%	6.33
CALM	17.87%	0.00%	0.00%	0.00%	0.00%	0.00%	0.00%	17.87%	
MISSING	6.36%							6.36%	
Total	33.27%	31.68%	29.12%	5.28%	0.54%	0.11%	0.00%	100.00%	7.28

NOTES:

1. Calm is classified as a wind speed less than 2.3 mph (anemometer start speed) or a variable wind direction.
2. Missing data is data with missing wind speed, missing wind direction, or denoted as "variable" wind direction.
3. Data from Unedited Local Climatological Data, National Oceanic and Atmospheric Administration, U. S. Department of Commerce, Asheville, NC, Greenville/Spartanburg International Airport, Station No. 03870.
4. Period of Record - 9 years (1997 - 2005).

WLS COL 2.3-1

TABLE 2.3-215 (Sheet 1 of 2)
PERCENTAGE FREQUENCY OF WIND DIRECTION AND SPEED (MPH)
GREENVILLE/SPARTANBURG, SOUTH CAROLINA
JULY, 1997-2005

July	Wind Speed (mph)								
	0-3	4-7	8-12	13-17	18-22	23-27	≥28		
Direction From	Frequency of Occurrence (%)							Total (%)	Avg. Speed
N	1.28%	2.42%	0.97%	0.06%	0.00%	0.00%	0.00%	4.73%	5.84
NNE	1.02%	3.70%	1.51%	0.13%	0.01%	0.00%	0.00%	6.38%	6.45
NE	0.97%	3.79%	2.97%	0.54%	0.03%	0.01%	0.00%	8.32%	7.37
ENE	0.43%	1.88%	1.76%	0.12%	0.00%	0.00%	0.00%	4.20%	7.18
E	0.36%	1.84%	1.15%	0.12%	0.00%	0.01%	0.00%	3.48%	7.06
ESE	0.30%	0.81%	0.45%	0.03%	0.00%	0.00%	0.00%	1.58%	6.45
SE	0.46%	1.08%	0.36%	0.06%	0.00%	0.00%	0.00%	1.96%	6.19
SSE	0.39%	1.36%	0.63%	0.04%	0.01%	0.00%	0.00%	2.43%	6.46
S	0.79%	2.06%	1.08%	0.13%	0.03%	0.00%	0.00%	4.09%	6.73
SSW	0.69%	1.85%	1.67%	0.30%	0.06%	0.00%	0.00%	4.57%	7.53
SW	0.73%	3.14%	3.81%	0.64%	0.06%	0.00%	0.00%	8.38%	8.16
WSW	0.84%	3.49%	2.84%	0.42%	0.03%	0.00%	0.00%	7.62%	7.56
W	1.06%	3.21%	2.12%	0.16%	0.01%	0.00%	0.00%	6.57%	6.77

WLS COL 2.3-1

TABLE 2.3-215 (Sheet 2 of 2)
PERCENTAGE FREQUENCY OF WIND DIRECTION AND SPEED (MPH)
GREENVILLE/SPARTANBURG, SOUTH CAROLINA
JULY, 1997-2005

July	Wind Speed (mph)								
	0-3	4-7	8-12	13-17	18-22	23-27	≥28		
Direction From	Frequency of Occurrence (%)							Total (%)	Avg. Speed
WNW	0.63%	1.21%	0.49%	0.04%	0.01%	0.00%	0.00%	2.39%	6.08
NW	0.75%	0.94%	0.43%	0.00%	0.00%	0.00%	0.00%	2.12%	5.65
NNW	0.48%	0.81%	0.49%	0.06%	0.00%	0.00%	0.00%	1.84%	6.15
CALM	21.64%	0.00%	0.00%	0.00%	0.00%	0.00%	0.00%	21.64%	
MISSING	7.71%							7.71%	
Total	40.52%	33.59%	22.73%	2.87%	0.27%	0.03%	0.00%	100.00%	6.73

NOTES:

1. Calm is classified as a wind speed less than 2.3 mph (anemometer start speed) or a variable wind direction.
2. Missing data is data with missing wind speed, missing wind direction, or denoted as "variable" wind direction.
3. Data from Unedited Local Climatological Data, National Oceanic and Atmospheric Administration, U. S. Department of Commerce, Asheville, NC, Greenville/Spartanburg International Airport, Station No. 03870.
4. Period of Record - 9 years (1997 - 2005).

WLS COL 2.3-1

TABLE 2.3-216 (Sheet 1 of 2)
PERCENTAGE FREQUENCY OF WIND DIRECTION AND SPEED (MPH)
GREENVILLE/SPARTANBURG, SOUTH CAROLINA
AUGUST, 1997-2005

August	Wind Speed (mph)								
	0-3	4-7	8-12	13-17	18-22	23-27	≥28		
Direction From	Frequency of Occurrence (%)							Total (%)	Avg. Speed
N	1.45%	2.03%	0.93%	0.09%	0.00%	0.00%	0.00%	4.50%	5.87
NNE	1.43%	4.05%	2.33%	0.18%	0.01%	0.00%	0.00%	8.00%	6.59
NE	1.34%	5.68%	4.21%	0.25%	0.00%	0.00%	0.00%	11.48%	7.06
ENE	0.82%	2.97%	2.30%	0.25%	0.00%	0.00%	0.00%	6.35%	7.11
E	0.64%	1.96%	1.93%	0.19%	0.01%	0.00%	0.00%	4.73%	7.24
ESE	0.24%	0.94%	0.54%	0.01%	0.00%	0.00%	0.00%	1.73%	6.60
SE	0.31%	0.99%	0.42%	0.04%	0.01%	0.00%	0.00%	1.78%	6.39
SSE	0.42%	1.39%	0.61%	0.04%	0.00%	0.00%	0.00%	2.46%	6.26
S	0.76%	2.30%	1.05%	0.06%	0.07%	0.01%	0.00%	4.26%	6.69
SSW	0.51%	2.20%	1.42%	0.15%	0.00%	0.01%	0.00%	4.29%	7.09
SW	0.66%	3.15%	2.43%	0.25%	0.04%	0.00%	0.00%	6.54%	7.40
WSW	0.81%	2.64%	1.94%	0.33%	0.00%	0.00%	0.00%	5.72%	7.12
W	0.75%	1.93%	1.31%	0.07%	0.00%	0.00%	0.00%	4.06%	6.22

WLS COL 2.3-1

TABLE 2.3-216 (Sheet 2 of 2)
PERCENTAGE FREQUENCY OF WIND DIRECTION AND SPEED (MPH)
GREENVILLE/SPARTANBURG, SOUTH CAROLINA
AUGUST, 1997-2005

August	Wind Speed (mph)								
	0-3	4-7	8-12	13-17	18-22	23-27	≥28		
Direction From	Frequency of Occurrence (%)							Total (%)	Avg. Speed
WNW	0.30%	0.60%	0.31%	0.01%	0.00%	0.00%	0.00%	1.22%	5.90
NW	0.27%	0.48%	0.21%	0.00%	0.00%	0.00%	0.00%	0.96%	5.72
NNW	0.33%	0.57%	0.21%	0.03%	0.00%	0.01%	0.00%	1.15%	6.13
CALM	23.72%	0.00%	0.00%	0.00%	0.00%	0.00%	0.00%	23.72%	
MISSING	7.05%							7.05%	
Total	41.80%	33.86%	22.15%	1.99%	0.16%	0.04%	0.00%	100.00%	6.59

NOTES:

1. Calm is classified as a wind speed less than 2.3 mph (anemometer start speed) or a variable wind direction.
2. Missing data is data with missing wind speed, missing wind direction, or denoted as "variable" wind direction.
3. Data from Unedited Local Climatological Data, National Oceanic and Atmospheric Administration, U. S. Department of Commerce, Asheville, NC, Greenville/Spartanburg International Airport, Station No. 03870.
4. Period of Record - 9 years (1997 - 2005).

WLS COL 2.3-1

TABLE 2.3-217 (Sheet 1 of 2)
PERCENTAGE FREQUENCY OF WIND DIRECTION AND SPEED (MPH)
GREENVILLE/SPARTANBURG, SOUTH CAROLINA
SEPTEMBER, 1997-2005

September	Wind Speed (mph)								
	0-3	4-7	8-12	13-17	18-22	23-27	≥28		
Direction From	Frequency of Occurrence (%)							Total (%)	Avg. Speed
N	1.45%	2.61%	1.45%	0.42%	0.02%	0.02%	0.00%	5.96%	6.81
NNE	1.77%	6.76%	4.20%	1.11%	0.12%	0.00%	0.00%	13.97%	7.42
NE	1.65%	5.82%	6.30%	1.73%	0.23%	0.08%	0.00%	15.80%	8.44
ENE	0.76%	2.65%	3.77%	0.76%	0.17%	0.00%	0.00%	8.10%	8.63
E	0.54%	1.94%	1.87%	0.17%	0.09%	0.00%	0.00%	4.61%	7.76
ESE	0.40%	1.03%	0.39%	0.03%	0.03%	0.00%	0.00%	1.88%	6.50
SE	0.31%	1.19%	0.43%	0.06%	0.02%	0.03%	0.00%	2.04%	6.64
SSE	0.32%	1.33%	0.43%	0.03%	0.02%	0.00%	0.00%	2.13%	6.18
S	0.39%	2.08%	1.05%	0.26%	0.02%	0.00%	0.00%	3.80%	7.36
SSW	0.46%	0.94%	0.62%	0.17%	0.03%	0.00%	0.00%	2.22%	7.42
SW	0.28%	1.25%	1.33%	0.15%	0.02%	0.00%	0.00%	3.02%	7.96
WSW	0.42%	1.22%	1.44%	0.19%	0.00%	0.00%	0.00%	3.26%	7.62
W	0.37%	1.22%	1.13%	0.09%	0.02%	0.00%	0.00%	2.82%	7.53

WLS COL 2.3-1

TABLE 2.3-217 (Sheet 2 of 2)
PERCENTAGE FREQUENCY OF WIND DIRECTION AND SPEED (MPH)
GREENVILLE/SPARTANBURG, SOUTH CAROLINA
SEPTEMBER, 1997-2005

September	Wind Speed (mph)								
	0-3	4-7	8-12	13-17	18-22	23-27	≥28		
Direction From	Frequency of Occurrence (%)							Total (%)	Avg. Speed
WNW	0.22%	0.59%	0.32%	0.03%	0.02%	0.00%	0.00%	1.17%	6.97
NW	0.20%	0.39%	0.32%	0.03%	0.02%	0.00%	0.00%	0.96%	7.13
NNW	0.19%	0.51%	0.48%	0.06%	0.05%	0.00%	0.00%	1.28%	7.82
CALM	21.40%	0.00%	0.00%	0.00%	0.00%	0.00%	0.00%	21.40%	
MISSING	5.57%							5.57%	
Total	36.70%	31.53%	25.51%	5.29%	0.85%	0.12%	0.00%	100.00%	7.39

NOTES:

1. Calm is classified as a wind speed less than 2.3 mph (anemometer start speed) or a variable wind direction.
2. Missing data is data with missing wind speed, missing wind direction, or denoted as "variable" wind direction.
3. Data from Unedited Local Climatological Data, National Oceanic and Atmospheric Administration, U. S. Department of Commerce, Asheville, NC, Greenville/Spartanburg International Airport, Station No. 03870.
4. Period of Record - 9 years (1997 - 2005).

WLS COL 2.3-1

TABLE 2.3-218 (Sheet 1 of 2)
PERCENTAGE FREQUENCY OF WIND DIRECTION AND SPEED (MPH)
GREENVILLE/SPARTANBURG, SOUTH CAROLINA
OCTOBER, 1997-2005

October	Wind Speed (mph)								
	0-3	4-7	8-12	13-17	18-22	23-27	≥28		
Direction From	Frequency of Occurrence (%)							Total (%)	Avg. Speed
N	1.19%	1.76%	2.49%	0.46%	0.07%	0.00%	0.00%	5.99%	7.77
NNE	1.16%	4.79%	3.84%	0.40%	0.00%	0.00%	0.00%	10.20%	7.13
NE	1.75%	5.48%	5.70%	0.78%	0.04%	0.00%	0.00%	13.75%	7.68
ENE	0.90%	3.09%	2.84%	0.39%	0.00%	0.00%	0.00%	7.21%	7.52
E	0.60%	1.96%	0.88%	0.07%	0.01%	0.00%	0.00%	3.52%	6.45
ESE	0.16%	0.69%	0.13%	0.00%	0.00%	0.00%	0.00%	0.99%	5.56
SE	0.30%	0.91%	0.15%	0.00%	0.00%	0.00%	0.00%	1.36%	5.43
SSE	0.37%	1.25%	0.30%	0.03%	0.01%	0.00%	0.00%	1.97%	5.82
S	0.72%	2.12%	0.60%	0.03%	0.01%	0.00%	0.00%	3.48%	5.89
SSW	0.67%	1.88%	1.06%	0.15%	0.00%	0.00%	0.00%	3.76%	6.66
SW	0.72%	2.45%	2.31%	0.57%	0.04%	0.00%	0.00%	6.09%	7.90
WSW	0.64%	1.81%	2.05%	0.37%	0.07%	0.00%	0.00%	4.94%	8.01
W	0.49%	1.34%	1.08%	0.19%	0.04%	0.03%	0.00%	3.18%	7.62

WLS COL 2.3-1

TABLE 2.3-218 (Sheet 2 of 2)
PERCENTAGE FREQUENCY OF WIND DIRECTION AND SPEED (MPH)
GREENVILLE/SPARTANBURG, SOUTH CAROLINA
OCTOBER, 1997-2005

October	Wind Speed (mph)								
	0-3	4-7	8-12	13-17	18-22	23-27	≥28		
Direction From	Frequency of Occurrence (%)							Total (%)	Avg. Speed
WNW	0.24%	0.42%	0.12%	0.06%	0.03%	0.00%	0.00%	0.87%	6.50
NW	0.27%	0.61%	0.33%	0.06%	0.00%	0.00%	0.00%	1.27%	6.77
NNW	0.25%	0.64%	0.84%	0.19%	0.01%	0.01%	0.00%	1.96%	8.61
CALM	24.16%	0.00%	0.00%	0.00%	0.00%	0.00%	0.00%	24.16%	
MISSING	5.29%							5.29%	
Total	39.89%	31.21%	24.72%	3.76%	0.37%	0.04%	0.00%	100.00%	6.96

NOTES:

1. Calm is classified as a wind speed less than 2.3 mph (anemometer start speed) or a variable wind direction.
2. Missing data is data with missing wind speed, missing wind direction, or denoted as "variable" wind direction.
3. Data from Unedited Local Climatological Data, National Oceanic and Atmospheric Administration, U. S. Department of Commerce, Asheville, NC, Greenville/Spartanburg International Airport, Station No. 03870.
4. Period of Record - 9 years (1997 - 2005).

WLS COL 2.3-1

TABLE 2.3-219 (Sheet 1 of 2)
PERCENTAGE FREQUENCY OF WIND DIRECTION AND SPEED (MPH)
GREENVILLE/SPARTANBURG, SOUTH CAROLINA
NOVEMBER, 1997-2005

November	Wind Speed (mph)								
	0-3	4-7	8-12	13-17	18-22	23-27	≥28		
Direction From	Frequency of Occurrence (%)							Total (%)	Avg. Speed
N	1.36%	2.58%	1.96%	0.51%	0.14%	0.03%	0.00%	6.57%	7.63
NNE	1.45%	3.56%	1.94%	0.35%	0.03%	0.02%	0.00%	7.36%	6.76
NE	1.42%	4.18%	3.13%	0.57%	0.03%	0.00%	0.00%	9.34%	7.28
ENE	0.57%	2.61%	1.94%	0.22%	0.09%	0.00%	0.00%	5.43%	7.52
E	0.52%	1.28%	0.94%	0.03%	0.00%	0.00%	0.00%	2.78%	6.58
ESE	0.23%	0.59%	0.20%	0.02%	0.00%	0.00%	0.00%	1.03%	5.85
SE	0.28%	0.40%	0.17%	0.02%	0.00%	0.00%	0.00%	0.86%	5.81
SSE	0.31%	0.71%	0.39%	0.06%	0.02%	0.00%	0.00%	1.48%	6.91
S	1.00%	2.08%	1.11%	0.46%	0.09%	0.00%	0.00%	4.75%	7.19
SSW	0.91%	2.41%	2.21%	0.49%	0.19%	0.02%	0.00%	6.22%	7.74
SW	0.83%	3.56%	3.86%	1.19%	0.11%	0.02%	0.00%	9.57%	8.52
WSW	0.66%	2.87%	2.98%	1.13%	0.32%	0.05%	0.00%	8.01%	9.14
W	0.57%	1.71%	1.45%	0.31%	0.02%	0.02%	0.00%	4.07%	8.04

WLS COL 2.3-1

TABLE 2.3-219 (Sheet 2 of 2)
PERCENTAGE FREQUENCY OF WIND DIRECTION AND SPEED (MPH)
GREENVILLE/SPARTANBURG, SOUTH CAROLINA
NOVEMBER, 1997-2005

November	Wind Speed (mph)								
	0-3	4-7	8-12	13-17	18-22	23-27	≥28		
Direction From	Frequency of Occurrence (%)							Total (%)	Avg. Speed
WNW	0.31%	0.79%	0.25%	0.05%	0.00%	0.02%	0.00%	1.40%	6.46
NW	0.25%	0.74%	0.48%	0.09%	0.00%	0.00%	0.00%	1.56%	7.04
NNW	0.32%	0.97%	1.37%	0.25%	0.12%	0.00%	0.00%	3.04%	8.68
CALM	22.82%	0.00%	0.00%	0.00%	0.00%	0.00%	0.00%	22.82%	
MISSING	3.69%							3.69%	
Total	37.52%	31.05%	24.38%	5.74%	1.16%	0.15%	0.00%	100.00%	7.32

NOTES:

1. Calm is classified as a wind speed less than 2.3 mph (anemometer start speed) or a variable wind direction.
2. Missing data is data with missing wind speed, missing wind direction, or denoted as "variable" wind direction.
3. Data from Unedited Local Climatological Data, National Oceanic and Atmospheric Administration, U. S. Department of Commerce, Asheville, NC, Greenville/Spartanburg International Airport, Station No. 03870.
4. Period of Record - 9 years (1997 - 2005).

WLS COL 2.3-1

TABLE 2.3-220 (Sheet 1 of 2)
PERCENTAGE FREQUENCY OF WIND DIRECTION AND SPEED (MPH)
GREENVILLE/SPARTANBURG, SOUTH CAROLINA
DECEMBER, 1997-2005

December	Wind Speed (mph)								
	0-3	4-7	8-12	13-17	18-22	23-27	≥28		
Direction From	Frequency of Occurrence (%)							Total (%)	Avg. Speed
N	1.11%	2.06%	1.91%	0.52%	0.06%	0.00%	0.00%	5.66%	7.86
NNE	0.81%	3.24%	2.06%	0.36%	0.00%	0.00%	0.00%	6.47%	7.22
NE	1.14%	4.08%	5.56%	1.08%	0.01%	0.01%	0.00%	11.87%	8.41
ENE	0.73%	2.76%	2.97%	0.46%	0.03%	0.00%	0.00%	6.96%	7.80
E	0.52%	1.21%	0.78%	0.00%	0.00%	0.00%	0.00%	2.51%	5.98
ESE	0.22%	0.39%	0.07%	0.00%	0.00%	0.00%	0.00%	0.69%	5.28
SE	0.24%	0.42%	0.04%	0.00%	0.00%	0.00%	0.00%	0.70%	4.89
SSE	0.36%	0.79%	0.07%	0.01%	0.00%	0.00%	0.00%	1.24%	5.14
S	0.75%	1.66%	0.66%	0.07%	0.01%	0.01%	0.00%	3.17%	5.91
SSW	0.81%	2.49%	1.57%	0.18%	0.10%	0.00%	0.00%	5.15%	7.03
SW	1.00%	3.30%	4.21%	1.14%	0.30%	0.00%	0.00%	9.95%	8.66
WSW	0.82%	3.12%	4.96%	1.69%	0.43%	0.06%	0.00%	11.08%	9.50
W	0.63%	2.66%	2.37%	0.55%	0.21%	0.01%	0.00%	6.44%	8.34

WLS COL 2.3-1

TABLE 2.3-220 (Sheet 2 of 2)
PERCENTAGE FREQUENCY OF WIND DIRECTION AND SPEED (MPH)
GREENVILLE/SPARTANBURG, SOUTH CAROLINA
DECEMBER, 1997-2005

December	Wind Speed (mph)								
	0-3	4-7	8-12	13-17	18-22	23-27	≥28		
Direction From	Frequency of Occurrence (%)							Total (%)	Avg. Speed
WNW	0.31%	0.67%	0.39%	0.18%	0.01%	0.00%	0.00%	1.57%	7.51
NW	0.28%	0.85%	0.69%	0.13%	0.00%	0.00%	0.00%	1.96%	7.18
NNW	0.43%	0.97%	1.46%	0.19%	0.06%	0.00%	0.00%	3.12%	8.28
CALM	18.32%	0.00%	0.00%	0.00%	0.00%	0.00%	0.00%	18.32%	
MISSING	3.32%							3.32%	
Total	31.63%	30.68%	29.78%	6.57%	1.24%	0.10%	0.00%	100.00%	7.19

NOTES:

1. Calm is classified as a wind speed less than 2.3 mph (anemometer start speed) or a variable wind direction.
2. Missing data is data with missing wind speed, missing wind direction, or denoted as "variable" wind direction.
3. Data from Unedited Local Climatological Data, National Oceanic and Atmospheric Administration, U. S. Department of Commerce, Asheville, NC, Greenville/Spartanburg International Airport, Station No. 03870.
4. Period of Record - 9 years (1997 - 2005).

WLS COL 2.3-1

TABLE 2.3-221 (Sheet 1 of 2)
PERCENTAGE FREQUENCY OF WIND DIRECTION AND SPEED (MPH)
GREENVILLE/SPARTANBURG, SOUTH CAROLINA
ALL MONTHS, 1997-2005

All Months	Wind Speed (mph)								
	0-3	4-7	8-12	13-17	18-22	23-27	≥28		
Direction From	Frequency of Occurrence (%)							Total (%)	Avg. Speed
N	1.04%	2.15%	1.93%	0.52%	0.13%	0.01%	0.00%	5.78%	7.86
NNE	0.99%	3.53%	2.57%	0.46%	0.05%	0.01%	0.00%	7.62%	7.40
NE	1.07%	4.12%	4.31%	0.97%	0.13%	0.04%	0.00%	10.63%	8.25
ENE	0.65%	2.40%	2.56%	0.54%	0.11%	0.02%	0.00%	6.27%	8.21
E	0.49%	1.56%	1.31%	0.13%	0.02%	0.00%	0.00%	3.51%	7.25
ESE	0.24%	0.68%	0.30%	0.01%	0.00%	0.00%	0.00%	1.23%	6.22
SE	0.28%	0.74%	0.30%	0.02%	0.00%	0.00%	0.00%	1.34%	6.13
SSE	0.32%	1.19%	0.43%	0.03%	0.01%	0.00%	0.00%	1.98%	6.19
S	0.77%	2.25%	1.21%	0.18%	0.03%	0.00%	0.00%	4.45%	6.83
SSW	0.67%	2.09%	1.89%	0.40%	0.09%	0.01%	0.00%	5.15%	7.90
SW	0.65%	2.89%	3.82%	1.18%	0.25%	0.04%	0.01%	8.84%	9.14
WSW	0.63%	2.68%	3.61%	1.23%	0.34%	0.08%	0.01%	8.57%	9.44
W	0.58%	2.10%	2.01%	0.50%	0.15%	0.04%	0.01%	5.38%	8.37

WLS COL 2.3-1

TABLE 2.3-221 (Sheet 2 of 2)
PERCENTAGE FREQUENCY OF WIND DIRECTION AND SPEED (MPH)
GREENVILLE/SPARTANBURG, SOUTH CAROLINA
ALL MONTHS, 1997-2005

All Months	Wind Speed (mph)								
	0-3	4-7	8-12	13-17	18-22	23-27	≥28		
Direction From	Frequency of Occurrence (%)							Total (%)	Avg. Speed
WNW	0.30%	0.72%	0.42%	0.12%	0.03%	0.02%	0.00%	1.60%	7.48
NW	0.30%	0.67%	0.43%	0.08%	0.01%	0.00%	0.00%	1.50%	7.01
NNW	0.34%	0.77%	0.85%	0.22%	0.07%	0.01%	0.00%	2.26%	8.38
CALM	18.33%	0.00%	0.00%	0.00%	0.00%	0.00%	0.00%	18.33%	
MISSING	5.56%							5.56%	
Total	30.51%	27.97%	27.97%	6.60%	1.41%	0.29%	0.02%	100.00%	7.63

NOTES:

1. Calm is classified as a wind speed less than 2.3 mph (anemometer start speed) or a variable wind direction.
2. Missing data is data with missing wind speed, missing wind direction, or denoted as "variable" wind direction.
3. Data from Unedited Local Climatological Data, National Oceanic and Atmospheric Administration, U. S. Department of Commerce, Asheville, NC, Greenville/Spartanburg International Airport, Station No. 03870.
4. Period of Record - 9 years (1997 - 2005).

WLS COL 2.3-2

TABLE 2.3-222 (Sheet 1 of 2)
PERCENTAGE FREQUENCY OF WIND DIRECTION AND SPEED (MPH)
LEE NUCLEAR STATION SITE
JANUARY

January	Wind Speed (mph)								
	0-3	4-7	8-12	13-17	18-22	23-27	≥28		
Direction From	Frequency of Occurrence (%)							Total (%)	Avg. Speed
N	2.33%	1.51%	0.55%	0.00%	0.00%	0.00%	0.00%	4.38%	4.52
NNE	2.88%	2.19%	0.41%	0.00%	0.00%	0.00%	0.00%	5.48%	4.32
NE	1.37%	0.82%	0.68%	0.00%	0.00%	0.00%	0.00%	2.88%	4.68
ENE	2.74%	0.27%	0.14%	0.00%	0.00%	0.00%	0.00%	3.15%	2.58
E	2.05%	0.00%	0.00%	0.00%	0.00%	0.00%	0.00%	2.05%	2.02
ESE	4.11%	0.27%	0.00%	0.00%	0.00%	0.00%	0.00%	4.38%	2.44
SE	5.07%	1.37%	0.27%	0.00%	0.00%	0.00%	0.00%	6.71%	3.51
SSE	4.79%	1.78%	0.68%	0.82%	0.27%	0.00%	0.00%	8.36%	5.90
S	2.19%	6.44%	1.51%	0.27%	0.14%	0.00%	0.00%	10.55%	6.28
SSW	0.96%	3.42%	5.48%	0.14%	0.00%	0.00%	0.00%	10.00%	8.00
SW	0.41%	1.78%	4.25%	0.82%	0.27%	0.00%	0.00%	7.53%	9.60
WSW	1.51%	1.10%	0.96%	0.14%	0.00%	0.00%	0.00%	3.70%	5.93
W	1.78%	1.23%	0.14%	0.00%	0.00%	0.00%	0.00%	3.15%	4.30

WLS COL 2.3-2

TABLE 2.3-222 (Sheet 2 of 2)
PERCENTAGE FREQUENCY OF WIND DIRECTION AND SPEED (MPH)
LEE NUCLEAR STATION SITE
JANUARY

January	Wind Speed (mph)								
	0-3	4-7	8-12	13-17	18-22	23-27	≥28		
Direction From	Frequency of Occurrence (%)							Total (%)	Avg. Speed
WNW	3.29%	3.29%	1.37%	1.37%	0.41%	0.00%	0.00%	9.73%	7.00
NW	6.44%	2.47%	0.55%	0.82%	0.14%	0.00%	0.00%	10.41%	4.89
NNW	2.60%	2.05%	0.68%	0.55%	0.55%	0.00%	0.00%	6.44%	6.93
Calm	1.10%	0.00%	0.00%	0.00%	0.00%	0.00%	0.00%	1.10%	0.00
Total	44.52%	30.00%	17.67%	4.93%	1.78%	0.00%	0.00%	100.00%	5.71

NOTES:

1. Calm is classified as a wind speed less than or equal to 1.0 mph.

2. Lee Nuclear Station site Data, 12/1/2005 - 11/30/2006.

WLS COL 2.3-2

TABLE 2.3-223 (Sheet 1 of 2)
PERCENTAGE FREQUENCY OF WIND DIRECTION AND SPEED (MPH)
LEE NUCLEAR STATION SITE
FEBRUARY

February	Wind Speed (mph)								
	0-3	4-7	8-12	13-17	18-22	23-27	≥28		
Direction From	Frequency of Occurrence (%)							Total (%)	Avg. Speed
N	1.49%	2.24%	1.19%	0.60%	0.00%	0.00%	0.00%	5.52%	6.69
NNE	1.64%	2.09%	0.45%	0.00%	0.00%	0.00%	0.00%	4.18%	5.41
NE	0.90%	1.79%	0.00%	0.00%	0.00%	0.00%	0.00%	2.69%	4.77
ENE	2.39%	0.45%	0.00%	0.00%	0.00%	0.00%	0.00%	2.84%	2.98
E	2.54%	0.15%	0.00%	0.00%	0.00%	0.00%	0.00%	2.69%	2.81
ESE	3.88%	0.15%	0.00%	0.00%	0.00%	0.00%	0.00%	4.03%	2.60
SE	2.54%	1.34%	0.00%	0.00%	0.00%	0.00%	0.00%	3.88%	3.22
SSE	2.69%	1.94%	0.15%	0.00%	0.00%	0.00%	0.00%	4.78%	4.18
S	2.39%	4.78%	1.49%	0.15%	0.00%	0.00%	0.00%	8.81%	5.64
SSW	1.49%	5.97%	3.88%	0.15%	0.00%	0.00%	0.00%	11.49%	7.35
SW	1.19%	3.13%	3.43%	0.90%	0.30%	0.00%	0.00%	8.96%	8.72
WSW	1.19%	2.84%	3.28%	0.60%	0.15%	0.00%	0.00%	8.06%	8.01
W	0.75%	2.54%	0.90%	0.30%	0.00%	0.00%	0.00%	4.48%	6.75

WLS COL 2.3-2

TABLE 2.3-223 (Sheet 2 of 2)
PERCENTAGE FREQUENCY OF WIND DIRECTION AND SPEED (MPH)
LEE NUCLEAR STATION SITE
FEBRUARY

February	Wind Speed (mph)								
	0-3	4-7	8-12	13-17	18-22	23-27	≥28		
Direction From	Frequency of Occurrence (%)							Total (%)	Avg. Speed
WNW	3.28%	3.58%	1.64%	0.30%	0.30%	0.00%	0.00%	9.10%	6.00
NW	7.76%	2.99%	1.04%	0.15%	0.00%	0.00%	0.00%	11.94%	4.39
NNW	2.39%	2.24%	0.45%	0.00%	0.00%	0.00%	0.00%	5.07%	4.38
Calm	1.49%	0.00%	0.00%	0.00%	0.00%	0.00%	0.00%	1.49%	0.00
Total	38.51%	38.21%	17.91%	3.13%	0.75%	0.00%	0.00%	100.00%	5.69

NOTES:

1. Calm is classified as a wind speed less than or equal to 1.0 mph.

2. Lee Nuclear Station site Data, 12/1/2005 - 11/30/2006.

WLS COL 2.3-2

TABLE 2.3-224 (Sheet 1 of 2)
PERCENTAGE FREQUENCY OF WIND DIRECTION AND SPEED (MPH)
LEE NUCLEAR STATION SITE
MARCH

March	Wind Speed (mph)								
	0-3	4-7	8-12	13-17	18-22	23-27	≥28		
Direction From	Frequency of Occurrence (%)							Total (%)	Avg. Speed
N	2.44%	2.84%	2.71%	0.14%	0.00%	0.00%	0.00%	8.12%	6.62
NNE	1.35%	2.98%	0.27%	0.00%	0.00%	0.00%	0.00%	4.60%	5.06
NE	1.76%	1.62%	0.27%	0.00%	0.00%	0.00%	0.00%	3.65%	4.83
ENE	2.03%	0.68%	0.00%	0.00%	0.00%	0.00%	0.00%	2.71%	3.32
E	2.98%	0.68%	0.00%	0.00%	0.00%	0.00%	0.00%	3.65%	2.96
ESE	2.03%	0.41%	0.00%	0.00%	0.00%	0.00%	0.00%	2.44%	3.00
SE	3.79%	0.95%	0.00%	0.00%	0.00%	0.00%	0.00%	4.74%	3.35
SSE	1.76%	3.25%	0.27%	0.27%	0.00%	0.00%	0.00%	5.55%	5.43
S	1.08%	5.82%	0.95%	0.41%	0.00%	0.00%	0.00%	8.25%	6.22
SSW	0.41%	4.06%	4.74%	1.49%	0.27%	0.00%	0.00%	10.96%	9.38
SW	0.54%	1.22%	2.71%	2.30%	0.41%	0.00%	0.00%	7.17%	11.40
WSW	0.54%	1.35%	0.41%	0.14%	0.00%	0.00%	0.00%	2.44%	6.51
W	0.54%	0.81%	0.41%	0.00%	0.00%	0.00%	0.00%	1.76%	5.32

WLS COL 2.3-2

TABLE 2.3-224 (Sheet 2 of 2)
PERCENTAGE FREQUENCY OF WIND DIRECTION AND SPEED (MPH)
LEE NUCLEAR STATION SITE
MARCH

March	Wind Speed (mph)								
	0-3	4-7	8-12	13-17	18-22	23-27	≥28		
Direction From	Frequency of Occurrence (%)							Total (%)	Avg. Speed
WNW	2.57%	4.74%	2.44%	1.22%	0.27%	0.00%	0.00%	11.23%	7.36
NW	4.47%	5.28%	2.71%	0.68%	0.41%	0.00%	0.00%	13.53%	6.46
NNW	3.38%	3.79%	1.62%	0.00%	0.00%	0.00%	0.00%	8.80%	5.38
Calm	0.41%	0.00%	0.00%	0.00%	0.00%	0.00%	0.00%	0.41%	0.00
Total	31.66%	40.46%	19.49%	6.63%	1.35%	0.00%	0.00%	100.00%	6.47

NOTES:

1. Calm is classified as a wind speed less than or equal to 1.0 mph.

2. Lee Nuclear Station site Data, 12/1/2005 - 11/30/2006.

WLS COL 2.3-2

TABLE 2.3-225 (Sheet 1 of 2)
PERCENTAGE FREQUENCY OF WIND DIRECTION AND SPEED (MPH)
LEE NUCLEAR STATION SITE
APRIL

April	Wind Speed (mph)								
	0-3	4-7	8-12	13-17	18-22	23-27	≥28		
Direction From	Frequency of Occurrence (%)							Total (%)	Avg. Speed
N	1.39%	2.50%	0.70%	0.00%	0.00%	0.00%	0.00%	4.59%	5.48
NNE	1.53%	1.25%	1.53%	0.00%	0.00%	0.00%	0.00%	4.31%	5.83
NE	2.36%	4.17%	0.42%	0.00%	0.00%	0.00%	0.00%	6.95%	4.87
ENE	1.67%	2.09%	0.83%	0.00%	0.00%	0.00%	0.00%	4.59%	5.13
E	2.92%	1.11%	0.00%	0.00%	0.00%	0.00%	0.00%	4.03%	3.38
ESE	3.06%	0.56%	0.00%	0.00%	0.00%	0.00%	0.00%	3.62%	2.70
SE	4.31%	1.95%	0.00%	0.00%	0.00%	0.00%	0.00%	6.26%	3.48
SSE	2.23%	3.48%	0.00%	0.00%	0.00%	0.00%	0.00%	5.70%	4.29
S	1.25%	4.03%	0.83%	0.14%	0.00%	0.00%	0.00%	6.26%	5.72
SSW	0.56%	2.36%	4.31%	0.83%	0.28%	0.00%	0.00%	8.34%	9.27
SW	0.97%	3.62%	4.87%	1.11%	0.14%	0.00%	0.00%	10.71%	9.01
WSW	1.25%	2.92%	4.31%	0.56%	0.42%	0.00%	0.00%	9.46%	8.63
W	0.70%	0.70%	0.97%	0.14%	0.00%	0.00%	0.00%	2.50%	6.59

WLS COL 2.3-2

TABLE 2.3-225 (Sheet 2 of 2)
PERCENTAGE FREQUENCY OF WIND DIRECTION AND SPEED (MPH)
LEE NUCLEAR STATION SITE
APRIL

April	Wind Speed (mph)								
	0-3	4-7	8-12	13-17	18-22	23-27	≥28		
Direction From	Frequency of Occurrence (%)							Total (%)	Avg. Speed
WNW	3.06%	1.81%	1.39%	0.00%	0.14%	0.00%	0.00%	6.40%	5.55
NW	5.84%	3.06%	0.70%	0.14%	0.14%	0.00%	0.00%	9.87%	4.54
NNW	3.34%	1.11%	0.00%	0.00%	0.00%	0.00%	0.00%	4.45%	3.04
Calm	1.95%	0.00%	0.00%	0.00%	0.00%	0.00%	0.00%	1.95%	0.00
Total	36.44%	36.72%	20.86%	2.92%	1.11%	0.00%	0.00%	100.00%	5.81

NOTES:

1. Calm is classified as a wind speed less than or equal to 1.0 mph.

2. Lee Nuclear Station site Data, 12/1/2005 - 11/30/2006.

WLS COL 2.3-2

TABLE 2.3-226 (Sheet 1 of 2)
PERCENTAGE FREQUENCY OF WIND DIRECTION AND SPEED (MPH)
LEE NUCLEAR STATION SITE
MAY

May	Wind Speed (mph)								
	0-3	4-7	8-12	13-17	18-22	23-27	≥28		
Direction From	Frequency of Occurrence (%)							Total (%)	Avg. Speed
N	2.30%	2.17%	0.27%	0.00%	0.00%	0.00%	0.00%	4.74%	4.59
NNE	1.90%	3.12%	0.00%	0.00%	0.00%	0.00%	0.00%	5.01%	4.76
NE	4.20%	2.71%	0.27%	0.00%	0.00%	0.00%	0.00%	7.18%	4.08
ENE	3.39%	2.44%	0.14%	0.00%	0.00%	0.00%	0.00%	5.96%	3.96
E	2.71%	1.63%	0.00%	0.00%	0.00%	0.00%	0.00%	4.34%	3.43
ESE	3.66%	0.41%	0.00%	0.00%	0.00%	0.00%	0.00%	4.07%	2.64
SE	4.07%	0.68%	0.00%	0.00%	0.00%	0.00%	0.00%	4.74%	3.03
SSE	2.71%	1.63%	0.00%	0.00%	0.00%	0.00%	0.00%	4.34%	3.61
S	1.36%	1.76%	0.00%	0.00%	0.00%	0.00%	0.00%	3.12%	4.77
SSW	1.36%	2.71%	1.90%	0.00%	0.00%	0.00%	0.00%	5.96%	6.66
SW	1.49%	2.17%	5.01%	1.90%	0.14%	0.00%	0.00%	10.70%	9.57
WSW	1.36%	3.25%	1.90%	0.95%	0.14%	0.00%	0.00%	7.59%	8.18
W	1.90%	1.08%	1.22%	0.14%	0.00%	0.00%	0.00%	4.34%	5.71

WLS COL 2.3-2

TABLE 2.3-226 (Sheet 2 of 2)
PERCENTAGE FREQUENCY OF WIND DIRECTION AND SPEED (MPH)
LEE NUCLEAR STATION SITE
MAY

May	Wind Speed (mph)								
	0-3	4-7	8-12	13-17	18-22	23-27	≥28		
Direction From	Frequency of Occurrence (%)							Total (%)	Avg. Speed
WNW	4.47%	2.17%	0.27%	0.14%	0.00%	0.00%	0.00%	7.05%	4.25
NW	9.76%	2.71%	1.08%	0.41%	0.00%	0.00%	0.00%	13.96%	4.44
NNW	5.01%	1.49%	0.14%	0.00%	0.00%	0.00%	0.00%	6.64%	3.32
Calm	0.27%	0.00%	0.00%	0.00%	0.00%	0.00%	0.00%	0.27%	0.00
Total	51.63%	32.11%	12.20%	3.52%	0.27%	0.00%	0.00%	100.00%	5.12

NOTES:

1. Calm is classified as a wind speed less than or equal to 1.0 mph.

2. Lee Nuclear Station site Data, 12/1/2005 - 11/30/2006.

WLS COL 2.3-2

TABLE 2.3-227 (Sheet 1 of 2)
PERCENTAGE FREQUENCY OF WIND DIRECTION AND SPEED (MPH)
LEE NUCLEAR STATION SITE
JUNE

June	Wind Speed (mph)								
	0-3	4-7	8-12	13-17	18-22	23-27	≥28		
Direction From	Frequency of Occurrence (%)							Total (%)	Avg. Speed
N	2.23%	1.25%	2.37%	0.00%	0.00%	0.00%	0.00%	5.85%	6.30
NNE	2.65%	2.65%	1.11%	0.00%	0.00%	0.00%	0.00%	6.41%	5.03
NE	2.23%	2.23%	0.00%	0.00%	0.00%	0.00%	0.00%	4.46%	4.10
ENE	3.06%	1.67%	0.42%	0.00%	0.00%	0.00%	0.00%	5.15%	4.03
E	5.15%	1.39%	0.00%	0.00%	0.00%	0.00%	0.00%	6.55%	3.08
ESE	4.46%	2.09%	0.28%	0.00%	0.00%	0.00%	0.00%	6.82%	3.54
SE	4.74%	3.76%	0.00%	0.00%	0.00%	0.00%	0.00%	8.50%	3.74
SSE	2.51%	4.46%	0.70%	0.00%	0.00%	0.00%	0.00%	7.66%	5.20
S	1.67%	3.62%	0.14%	0.00%	0.00%	0.00%	0.00%	5.43%	5.15
SSW	1.53%	1.53%	0.42%	0.00%	0.00%	0.00%	0.00%	3.48%	4.76
SW	0.70%	3.20%	1.95%	0.14%	0.00%	0.00%	0.00%	5.99%	7.10
WSW	0.97%	2.37%	0.28%	0.00%	0.00%	0.00%	0.00%	3.62%	5.14
W	0.56%	2.37%	0.56%	0.00%	0.00%	0.00%	0.00%	3.48%	6.08

WLS COL 2.3-2

TABLE 2.3-227 (Sheet 2 of 2)
PERCENTAGE FREQUENCY OF WIND DIRECTION AND SPEED (MPH)
LEE NUCLEAR STATION SITE
JUNE

June	Wind Speed (mph)								
	0-3	4-7	8-12	13-17	18-22	23-27	≥28		
Direction From	Frequency of Occurrence (%)							Total (%)	Avg. Speed
WNW	4.74%	1.81%	0.14%	0.00%	0.00%	0.00%	0.00%	6.69%	3.66
NW	9.19%	2.51%	0.56%	0.00%	0.14%	0.00%	0.00%	12.40%	3.88
NNW	4.74%	2.23%	0.56%	0.00%	0.00%	0.00%	0.00%	7.52%	4.12
Calm	0.00%	0.00%	0.00%	0.00%	0.00%	0.00%	0.00%	0.00%	0.00
Total	51.11%	39.14%	9.47%	0.14%	0.14%	0.00%	0.00%	100.00%	4.55

NOTES:

1. Calm is classified as a wind speed less than or equal to 1.0.

2. Lee Nuclear Station site Data, 12/1/2005 - 11/30/2006.

WLS COL 2.3-2

TABLE 2.3-228 (Sheet 1 of 2)
PERCENTAGE FREQUENCY OF WIND DIRECTION AND SPEED (MPH)
LEE NUCLEAR STATION SITE
JULY

July	Wind Speed (mph)								
	0-3	4-7	8-12	13-17	18-22	23-27	≥28		
Direction From	Frequency of Occurrence (%)							Total (%)	Avg. Speed
N	4.17%	0.81%	0.00%	0.00%	0.00%	0.00%	0.00%	4.97%	2.76
NNE	2.28%	1.48%	0.00%	0.00%	0.00%	0.00%	0.00%	3.76%	3.37
NE	4.17%	2.28%	0.27%	0.00%	0.00%	0.00%	0.00%	6.72%	3.79
ENE	4.03%	2.42%	0.13%	0.00%	0.00%	0.00%	0.00%	6.59%	3.81
E	4.57%	0.94%	0.00%	0.00%	0.00%	0.00%	0.00%	5.51%	2.88
ESE	4.30%	1.34%	0.13%	0.00%	0.00%	0.00%	0.00%	5.78%	3.37
SE	4.17%	1.48%	0.00%	0.00%	0.00%	0.00%	0.00%	5.65%	3.12
SSE	4.57%	3.36%	0.27%	0.00%	0.00%	0.00%	0.00%	8.20%	4.11
S	4.17%	4.30%	0.27%	0.13%	0.00%	0.00%	0.00%	8.87%	4.53
SSW	2.69%	5.11%	1.34%	0.00%	0.00%	0.00%	0.00%	9.14%	5.60
SW	0.94%	4.84%	1.88%	0.13%	0.00%	0.00%	0.00%	7.80%	6.69
WSW	1.75%	2.96%	1.08%	0.00%	0.00%	0.00%	0.00%	5.78%	5.56
W	0.67%	1.34%	0.40%	0.00%	0.00%	0.00%	0.00%	2.42%	5.68

WLS COL 2.3-2

TABLE 2.3-228 (Sheet 2 of 2)
PERCENTAGE FREQUENCY OF WIND DIRECTION AND SPEED (MPH)
LEE NUCLEAR STATION SITE
JULY

July	Wind Speed (mph)								
	0-3	4-7	8-12	13-17	18-22	23-27	≥28		
Direction From	Frequency of Occurrence (%)							Total (%)	Avg. Speed
WNW	2.02%	1.21%	0.54%	0.13%	0.00%	0.00%	0.00%	3.90%	4.76
NW	7.66%	1.48%	0.00%	0.00%	0.00%	0.00%	0.00%	9.14%	3.12
NNW	4.84%	0.67%	0.00%	0.00%	0.00%	0.00%	0.00%	5.51%	2.66
Calm	0.27%	0.00%	0.00%	0.00%	0.00%	0.00%	0.00%	0.27%	0.00
Total	56.99%	36.02%	6.32%	0.40%	0.00%	0.00%	0.00%	100.00%	4.15

NOTES:

1. Calm is classified as a wind speed less than or equal to 1.0 mph.

2. Lee Nuclear Station site Data, 12/1/2005 - 11/30/2006.

WLS COL 2.3-2

TABLE 2.3-229 (Sheet 1 of 2)
PERCENTAGE FREQUENCY OF WIND DIRECTION AND SPEED (MPH)
LEE NUCLEAR STATION SITE
AUGUST

August	Wind Speed (mph)								
	0-3	4-7	8-12	13-17	18-22	23-27	≥28		
Direction From	Frequency of Occurrence (%)							Total (%)	Avg. Speed
N	5.53%	0.81%	0.13%	0.00%	0.00%	0.00%	0.00%	6.47%	2.81
NNE	4.72%	2.56%	0.00%	0.00%	0.00%	0.00%	0.00%	7.28%	3.61
NE	4.58%	4.45%	0.94%	0.00%	0.00%	0.00%	0.00%	9.97%	4.78
ENE	4.04%	3.91%	0.54%	0.00%	0.00%	0.00%	0.00%	8.49%	4.68
E	4.72%	2.96%	0.54%	0.00%	0.00%	0.00%	0.00%	8.22%	3.99
ESE	3.77%	1.35%	0.00%	0.00%	0.00%	0.00%	0.00%	5.12%	3.13
SE	4.45%	2.16%	0.00%	0.00%	0.00%	0.00%	0.00%	6.60%	3.52
SSE	4.04%	2.43%	0.00%	0.00%	0.00%	0.00%	0.00%	6.47%	3.84
S	3.10%	2.43%	0.13%	0.00%	0.00%	0.00%	0.00%	5.66%	4.00
SSW	1.75%	2.83%	0.40%	0.00%	0.00%	0.00%	0.00%	4.99%	5.09
SW	1.89%	2.43%	0.40%	0.00%	0.00%	0.00%	0.00%	4.72%	4.89
WSW	1.08%	1.75%	0.00%	0.00%	0.00%	0.00%	0.00%	2.83%	4.78
W	1.21%	0.94%	0.13%	0.00%	0.00%	0.00%	0.00%	2.29%	4.44

WLS COL 2.3-2

TABLE 2.3-229 (Sheet 2 of 2)
PERCENTAGE FREQUENCY OF WIND DIRECTION AND SPEED (MPH)
LEE NUCLEAR STATION SITE
AUGUST

August	Wind Speed (mph)								
	0-3	4-7	8-12	13-17	18-22	23-27	≥28		
Direction From	Frequency of Occurrence (%)							Total (%)	Avg. Speed
WNW	2.29%	2.02%	0.13%	0.00%	0.00%	0.00%	0.00%	4.45%	4.00
NW	6.87%	3.50%	0.00%	0.00%	0.00%	0.00%	0.00%	10.38%	3.49
NNW	4.58%	1.08%	0.00%	0.13%	0.00%	0.00%	0.00%	5.80%	3.22
Calm	0.27%	0.00%	0.00%	0.00%	0.00%	0.00%	0.00%	0.27%	0.00
Total	58.63%	37.60%	3.37%	0.13%	0.00%	0.00%	0.00%	100.00%	3.97

NOTES:

1. Calm is classified as a wind speed less than or equal to 1.0 mph.

2. Lee Nuclear Station site Data, 12/1/2005 - 11/30/2006.

WLS COL 2.3-2

TABLE 2.3-230 (Sheet 1 of 2)
PERCENTAGE FREQUENCY OF WIND DIRECTION AND SPEED (MPH)
LEE NUCLEAR STATION SITE
SEPTEMBER

September	Wind Speed (mph)								
	0-3	4-7	8-12	13-17	18-22	23-27	≥28		
Direction From	Frequency of Occurrence (%)							Total (%)	Avg. Speed
N	5.28%	3.47%	0.42%	0.00%	0.00%	0.00%	0.00%	9.17%	3.94
NNE	4.72%	2.92%	0.14%	0.00%	0.00%	0.00%	0.00%	7.78%	3.78
NE	4.86%	2.36%	0.00%	0.00%	0.00%	0.00%	0.00%	7.22%	3.39
ENE	3.75%	2.36%	0.00%	0.00%	0.00%	0.00%	0.00%	6.11%	3.68
E	3.75%	2.08%	0.14%	0.00%	0.00%	0.00%	0.00%	5.97%	3.61
ESE	3.61%	1.81%	0.00%	0.00%	0.00%	0.00%	0.00%	5.42%	3.45
SE	2.50%	1.11%	0.00%	0.00%	0.00%	0.00%	0.00%	3.61%	3.54
SSE	2.50%	1.39%	0.28%	0.00%	0.00%	0.00%	0.00%	4.17%	4.12
S	2.36%	2.08%	0.00%	0.00%	0.00%	0.00%	0.00%	4.44%	4.19
SSW	0.28%	3.75%	1.67%	0.00%	0.00%	0.00%	0.00%	5.69%	7.14
SW	1.11%	1.67%	2.36%	0.56%	0.00%	0.00%	0.00%	5.69%	8.06
WSW	0.28%	0.83%	0.69%	0.00%	0.00%	0.00%	0.00%	1.81%	7.23
W	0.00%	0.69%	0.00%	0.00%	0.00%	0.00%	0.00%	0.69%	6.12

WLS COL 2.3-2

TABLE 2.3-230 (Sheet 2 of 2)
PERCENTAGE FREQUENCY OF WIND DIRECTION AND SPEED (MPH)
LEE NUCLEAR STATION SITE
SEPTEMBER

September	Wind Speed (mph)								
	0-3	4-7	8-12	13-17	18-22	23-27	≥28		
Direction From	Frequency of Occurrence (%)							Total (%)	Avg. Speed
WNW	2.22%	2.22%	0.00%	0.00%	0.00%	0.00%	0.00%	4.44%	4.17
NW	14.03%	4.58%	0.14%	0.00%	0.00%	0.00%	0.00%	18.75%	3.53
NNW	6.11%	2.64%	0.14%	0.00%	0.00%	0.00%	0.00%	8.89%	3.39
Calm	0.14%	0.00%	0.00%	0.00%	0.00%	0.00%	0.00%	0.14%	0.00
Total	57.36%	35.97%	5.97%	0.56%	0.00%	0.00%	0.00%	100.00%	4.20

NOTES:

1. Calm is classified as a wind speed less than or equal to 1.0 mph.

2. Lee Nuclear Station site Data, 12/1/2005 - 11/30/2006.

WLS COL 2.3-2

TABLE 2.3-231 (Sheet 1 of 2)
PERCENTAGE FREQUENCY OF WIND DIRECTION AND SPEED (MPH)
LEE NUCLEAR STATION SITE
OCTOBER

October	Wind Speed (mph)								
	0-3	4-7	8-12	13-17	18-22	23-27	≥28		
Direction From	Frequency of Occurrence (%)							Total (%)	Avg. Speed
N	3.10%	2.70%	0.27%	0.00%	0.00%	0.00%	0.00%	6.06%	4.12
NNE	2.29%	3.91%	0.94%	0.00%	0.00%	0.00%	0.00%	7.14%	5.73
NE	3.50%	1.89%	2.43%	0.13%	0.00%	0.00%	0.00%	7.95%	5.71
ENE	3.50%	2.02%	0.00%	0.00%	0.00%	0.00%	0.00%	5.53%	3.36
E	4.58%	0.54%	0.13%	0.00%	0.00%	0.00%	0.00%	5.26%	2.61
ESE	2.83%	0.27%	0.00%	0.00%	0.00%	0.00%	0.00%	3.10%	2.75
SE	3.10%	0.27%	0.00%	0.00%	0.00%	0.00%	0.00%	3.37%	2.88
SSE	2.16%	1.08%	0.54%	0.00%	0.00%	0.00%	0.00%	3.77%	4.55
S	1.62%	2.56%	0.13%	0.00%	0.00%	0.00%	0.00%	4.31%	4.66
SSW	0.67%	2.70%	1.08%	0.00%	0.00%	0.00%	0.00%	4.45%	6.32
SW	0.67%	2.02%	1.35%	0.00%	0.00%	0.00%	0.00%	4.04%	6.94
WSW	1.21%	2.02%	1.48%	0.00%	0.00%	0.00%	0.00%	4.72%	6.41
W	1.08%	0.94%	1.08%	0.13%	0.00%	0.00%	0.00%	3.23%	6.02

WLS COL 2.3-2

TABLE 2.3-231 (Sheet 2 of 2)
PERCENTAGE FREQUENCY OF WIND DIRECTION AND SPEED (MPH)
LEE NUCLEAR STATION SITE
OCTOBER

October	Wind Speed (mph)								
	0-3	4-7	8-12	13-17	18-22	23-27	≥28		
Direction From	Frequency of Occurrence (%)							Total (%)	Avg. Speed
WNW	4.31%	2.02%	1.35%	0.67%	0.13%	0.00%	0.00%	8.49%	5.82
NW	12.26%	5.39%	2.29%	0.54%	0.00%	0.00%	0.00%	20.49%	4.78
NNW	5.66%	1.62%	0.67%	0.00%	0.00%	0.00%	0.00%	7.95%	3.79
Calm	0.13%	0.00%	0.00%	0.00%	0.00%	0.00%	0.00%	0.13%	0.00
Total	52.56%	31.94%	13.75%	1.48%	0.13%	0.00%	0.00%	100.00%	4.82

NOTES:

1. Calm is classified as a wind speed less than or equal to 1.0 mph.

2. Lee Nuclear Station site Data, 12/1/2005 - 11/30/2006.

WLS COL 2.3-2

TABLE 2.3-232 (Sheet 1 of 2)
PERCENTAGE FREQUENCY OF WIND DIRECTION AND SPEED (MPH)
LEE NUCLEAR STATION SITE
NOVEMBER

November	Wind Speed (mph)								
	0-3	4-7	8-12	13-17	18-22	23-27	≥28		
Direction From	Frequency of Occurrence (%)							Total (%)	Avg. Speed
N	3.36%	2.24%	1.12%	0.56%	0.00%	0.00%	0.00%	7.28%	5.56
NNE	0.98%	3.50%	4.20%	0.70%	0.00%	0.00%	0.00%	9.38%	8.25
NE	1.54%	1.54%	0.56%	0.28%	0.00%	0.00%	0.00%	3.92%	5.58
ENE	1.96%	1.40%	0.00%	0.00%	0.00%	0.00%	0.00%	3.36%	3.73
E	2.38%	0.56%	0.00%	0.00%	0.00%	0.00%	0.00%	2.94%	2.65
ESE	2.66%	0.14%	0.00%	0.00%	0.00%	0.00%	0.00%	2.80%	2.42
SE	3.78%	1.40%	0.56%	0.00%	0.00%	0.00%	0.00%	5.74%	3.82
SSE	1.68%	0.98%	1.12%	0.00%	0.00%	0.00%	0.00%	3.78%	5.31
S	3.08%	1.54%	0.98%	0.14%	0.00%	0.00%	0.00%	5.74%	5.13
SSW	0.84%	1.12%	0.70%	0.00%	0.00%	0.00%	0.00%	2.66%	6.00
SW	0.56%	1.40%	0.42%	1.12%	0.28%	0.00%	0.00%	3.78%	9.77
WSW	0.84%	0.84%	0.42%	0.28%	0.00%	0.00%	0.00%	2.38%	6.34
W	0.98%	0.98%	0.14%	0.00%	0.00%	0.00%	0.00%	2.10%	4.75

WLS COL 2.3-2

TABLE 2.3-232 (Sheet 2 of 2)
PERCENTAGE FREQUENCY OF WIND DIRECTION AND SPEED (MPH)
LEE NUCLEAR STATION SITE
NOVEMBER

November	Wind Speed (mph)								
	0-3	4-7	8-12	13-17	18-22	23-27	≥28		
Direction From	Frequency of Occurrence (%)							Total (%)	Avg. Speed
WNW	2.52%	2.10%	0.42%	0.00%	0.00%	0.00%	0.00%	5.04%	4.26
NW	9.38%	14.29%	0.98%	0.56%	0.00%	0.00%	0.00%	25.21%	4.69
NNW	4.34%	3.50%	2.80%	0.42%	0.00%	0.00%	0.00%	11.06%	6.18
Calm	2.80%	0.00%	0.00%	0.00%	0.00%	0.00%	0.00%	2.80%	0.00
Total	40.90%	37.54%	14.43%	4.06%	0.28%	0.00%	0.00%	100.00%	5.26

NOTES:

1. Calm is classified as a wind speed less than or equal to 1.0 mph.

2. Lee Nuclear Station site Data, 12/1/2005 - 11/30/2006.

WLS COL 2.3-2

TABLE 2.3-233 (Sheet 1 of 2)
PERCENTAGE FREQUENCY OF WIND DIRECTION AND SPEED (MPH)
LEE NUCLEAR STATION SITE
DECEMBER

December	Wind Speed (mph)								
	0-3	4-7	8-12	13-17	18-22	23-27	≥28		
Direction From	Frequency of Occurrence (%)							Total (%)	Avg. Speed
N	3.35%	1.54%	0.28%	0.00%	0.00%	0.00%	0.00%	5.17%	3.67
NNE	1.68%	2.23%	0.98%	0.00%	0.00%	0.00%	0.00%	4.89%	5.14
NE	1.54%	5.31%	0.28%	0.00%	0.00%	0.00%	0.00%	7.12%	5.36
ENE	3.07%	1.96%	0.42%	0.00%	0.00%	0.00%	0.00%	5.45%	3.83
E	2.09%	0.70%	0.00%	0.00%	0.00%	0.00%	0.00%	2.79%	2.96
ESE	3.63%	0.00%	0.00%	0.00%	0.00%	0.00%	0.00%	3.63%	2.56
SE	4.05%	0.56%	0.00%	0.00%	0.00%	0.00%	0.00%	4.61%	2.66
SSE	3.63%	0.98%	0.00%	0.00%	0.00%	0.00%	0.00%	4.61%	3.28
S	1.54%	3.21%	0.28%	0.00%	0.00%	0.00%	0.00%	5.03%	4.85
SSW	1.12%	3.07%	0.98%	0.00%	0.00%	0.00%	0.00%	5.17%	6.16
SW	1.54%	2.37%	2.65%	0.00%	0.00%	0.00%	0.00%	6.56%	6.83
WSW	1.54%	2.65%	2.09%	0.28%	0.00%	0.00%	0.00%	6.56%	6.77
W	1.26%	1.12%	0.70%	0.14%	0.00%	0.00%	0.00%	3.21%	5.68

WLS COL 2.3-2

TABLE 2.3-233 (Sheet 2 of 2)
PERCENTAGE FREQUENCY OF WIND DIRECTION AND SPEED (MPH)
LEE NUCLEAR STATION SITE
DECEMBER

December	Wind Speed (mph)								
	0-3	4-7	8-12	13-17	18-22	23-27	≥28		
Direction From	Frequency of Occurrence (%)							Total (%)	Avg. Speed
WNW	3.91%	2.79%	1.68%	0.70%	0.00%	0.00%	0.00%	9.08%	5.93
NW	10.34%	6.98%	1.54%	0.14%	0.00%	0.00%	0.00%	18.99%	4.38
NNW	4.33%	0.84%	0.56%	0.00%	0.00%	0.00%	0.00%	5.73%	3.71
Calm	1.40%	0.00%	0.00%	0.00%	0.00%	0.00%	0.00%	1.40%	0.00
Total	48.60%	36.31%	12.43%	1.26%	0.00%	0.00%	0.00%	100.00%	4.70

NOTES:

1. Calm is classified as a wind speed less than or equal to 1.0 mph.

2. Lee Nuclear Station site Data, 12/1/2005 - 11/30/2006.

WLS COL 2.3-2

TABLE 2.3-234 (Sheet 1 of 2)
PERCENTAGE FREQUENCY OF WIND DIRECTION AND SPEED (mph)
LEE NUCLEAR SITE
ALL MONTHS

Direction From	Wind Speed								
	0-3	4-7	8-12	13-17	18-22	23-27	>=28	Total	Avg. Speed
N	3.09%	2.00%	0.83%	0.10%	0.00%	0.00%	0.00%	6.03%	4.78
NNE	2.39%	2.58%	0.83%	0.06%	0.00%	0.00%	0.00%	5.86%	5.15
NE	2.77%	2.60%	0.52%	0.03%	0.00%	0.00%	0.00%	5.92%	4.64
ENE	2.98%	1.82%	0.22%	0.00%	0.00%	0.00%	0.00%	5.02%	3.89
E	3.38%	1.07%	0.07%	0.00%	0.00%	0.00%	0.00%	4.52%	3.17
ESE	3.50%	0.74%	0.03%	0.00%	0.00%	0.00%	0.00%	4.27%	2.97
SE	3.89%	1.42%	0.07%	0.00%	0.00%	0.00%	0.00%	5.37%	3.38
SSE	2.95%	2.23%	0.33%	0.09%	0.02%	0.00%	0.00%	5.63%	4.56
S	2.15%	3.54%	0.55%	0.10%	0.01%	0.00%	0.00%	6.36%	5.24
SSW	1.14%	3.21%	2.23%	0.22%	0.05%	0.00%	0.00%	6.85%	7.21
SW	1.00%	2.49%	2.60%	0.75%	0.13%	0.00%	0.00%	6.96%	8.42
WSW	1.13%	2.07%	1.39%	0.24%	0.06%	0.00%	0.00%	4.89%	6.99
W	0.95%	1.22%	0.55%	0.07%	0.00%	0.00%	0.00%	2.80%	5.67
WNW	3.22%	2.47%	0.94%	0.38%	0.10%	0.00%	0.00%	7.12%	5.55

WLS COL 2.3-2

TABLE 2.3-234 (Sheet 2 of 2)
PERCENTAGE FREQUENCY OF WIND DIRECTION AND SPEED (mph)
LEE NUCLEAR SITE
ALL MONTHS

Direction From	Wind Speed								
	0-3	4-7	8-12	13-17	18-22	23-27	>=28	Total	Avg. Speed
NW	8.66%	4.59%	0.97%	0.29%	0.07%	0.00%	0.00%	14.58%	4.44
NNW	4.29%	1.93%	0.63%	0.09%	0.05%	0.00%	0.00%	6.99%	4.34
Calm	0.84%	0.00%	0.00%	0.00%	0.00%	0.00%	0.00%	0.84%	0.00
Total	47.50%	35.98%	12.77%	2.43%	0.48%	0.00%	0.00%	100.00%	5.03

NOTES:

1. Calm is classified as a wind speed less than or equal to 1.0 mph.

2. Lee Nuclear Site Data, 12/1/2005 - 11/30/2006.

WLS COL 2.3-2

TABLE 2.3-235 (Sheet 1 of 2)
JOINT FREQUENCY DISTRIBUTION OF WIND SPEED AND DIRECTION BY ATMOSPHERIC STABILITY CLASS
STABILITY CLASS A

STABILITY CLASS A HOURS AT EACH WIND SPEED AND DIRECTION

DIR	Wind Speed (m/sec) U≤0.5	0.5<U ≤0.75	0.75<U ≤1.0	1.0<U ≤1.25	1.25<U ≤1.5	1.5<U ≤2.0	2.0<U ≤3.0	3.0<U ≤4.0	4.0<U ≤5.0	5.0<U ≤6.0	6.0<U ≤8.0	U>8	Total	Average Wind Speed (m/sec)
N	0	0	0	0	2	5	10	6	7	2	2	0	35	3.2
NNE	0	0	0	0	0	7	11	16	3	1	2	0	40	3.1
NE	0	0	0	0	0	13	29	16	2	1	0	0	61	2.8
ENE	0	0	0	1	3	8	24	16	3	0	0	0	55	2.7
E	0	0	0	1	1	8	22	3	0	0	0	0	35	2.3
ESE	0	0	0	1	3	15	10	0	0	0	0	0	29	1.9
SE	0	0	0	2	1	13	19	3	0	0	0	0	38	2.1
SSE	0	0	0	1	3	15	30	11	2	0	2	0	64	2.7
S	0	0	0	0	2	13	22	15	3	3	1	0	59	2.8
SSW	0	0	0	0	3	8	24	35	20	16	5	2	113	3.8
SW	0	0	0	0	1	1	16	33	21	25	11	2	110	4.4
WSW	0	0	0	0	2	3	12	26	12	7	2	0	65	3.7
W	0	0	0	1	0	3	6	2	10	1	0	0	24	3.4

WLS COL 2.3-2

TABLE 2.3-235 (Sheet 2 of 2)
JOINT FREQUENCY DISTRIBUTION OF WIND SPEED AND DIRECTION BY ATMOSPHERIC STABILITY CLASS
STABILITY CLASS A

STABILITY CLASS A HOURS AT EACH WIND SPEED AND DIRECTION

	Wind Speed (m/sec)													Average Wind Speed (m/sec)
DIR	U≤0.5	0.5<U ≤0.75	0.75<U ≤1.0	1.0<U ≤1.25	1.25<U ≤1.5	1.5<U ≤2.0	2.0<U ≤3.0	3.0<U ≤4.0	4.0<U ≤5.0	5.0<U ≤6.0	6.0<U ≤8.0	U>8	Total	
WNW	0	0	1	0	4	2	11	8	10	6	10	3	57	4.3
NW	0	0	0	0	1	2	11	6	8	9	9	1	49	4.5
NNW	0	0	0	0	0	4	6	5	2	4	0	0	22	3.4
CALM	0													
TOTAL	0	0	1	7	27	122	264	201	105	76	46	8	857	

NOTES:

1. Data from Lee Nuclear Station site Data, 12/1/2005 - 11/30/2006.
2. Stability class is determined by the upper temperature gradient between 60m and 10m.
3. Wind direction data is from the 10 m level.
4. Calms are wind speeds below 1 mph (0.45 m/sec).
5. Due to listing the joint frequency distribution in hours and rounding the total number of hours may exceed the number of hours in a year.

WLS COL 2.3-2

TABLE 2.3-236 (Sheet 1 of 2)
JOINT FREQUENCY DISTRIBUTION OF WIND SPEED AND DIRECTION BY ATMOSPHERIC STABILITY CLASS
STABILITY CLASS B

STABILITY CLASS B HOURS AT EACH WIND SPEED AND DIRECTION

DIR	Wind Speed (m/sec) U≤0.5	0.5<U ≤0.75	0.75< U≤1.0	1.0<U ≤1.25	1.25< U≤1.5	1.5<U ≤2.0	2.0<U ≤3.0	3.0<U ≤4.0	4.0<U ≤5.0	5.0<U ≤6.0	6.0<U ≤8.0	U>8	Total	Average Wind Speed (m/sec)
N	0	0	0	1	1	4	5	12	10	1	0	0	35	3.3
NNE	0	0	0	0	0	8	13	7	4	3	1	0	37	3.1
NE	0	0	0	0	3	15	10	9	3	1	0	0	41	2.5
ENE	0	0	0	2	7	3	15	5	0	0	0	0	32	2.3
E	0	0	0	2	0	6	11	1	0	0	0	0	21	2.1
ESE	0	0	0	0	2	3	7	1	0	0	0	0	13	2.2
SE	0	0	0	1	0	8	6	0	0	0	0	0	16	2.0
SSE	0	0	0	2	4	7	13	1	0	0	1	0	29	2.2
S	0	0	0	1	4	8	17	6	0	1	0	0	37	2.3
SSW	0	0	0	0	0	3	13	16	15	7	3	2	59	4.0
SW	0	0	0	0	0	4	13	21	23	16	7	1	85	4.2

WLS COL 2.3-2

TABLE 2.3-236 (Sheet 2 of 2)
JOINT FREQUENCY DISTRIBUTION OF WIND SPEED AND DIRECTION BY ATMOSPHERIC STABILITY CLASS
STABILITY CLASS B

STABILITY CLASS B HOURS AT EACH WIND SPEED AND DIRECTION

DIR	Wind Speed (m/sec) U≤0.5	0.5<U ≤0.75	0.75< U≤1.0	1.0<U ≤1.25	1.25< U≤1.5	1.5<U ≤2.0	2.0<U ≤3.0	3.0<U ≤4.0	4.0<U ≤5.0	5.0<U ≤6.0	6.0<U ≤8.0	U>8	Total	Average Wind Speed (m/sec)
WSW	0	0	0	0	0	4	16	19	9	6	5	0	59	3.8
W	0	0	0	0	1	0	7	7	4	5	1	0	26	3.7
WNW	0	0	0	0	0	4	10	8	6	7	5	3	45	4.3
NW	0	0	0	0	1	9	12	5	3	9	3	0	44	3.5
NNW	0	0	1	1	1	0	4	4	5	2	0	1	20	3.6
CALM	0													
TOTAL	0	0	1	10	25	88	175	123	83	59	27	7	599	

NOTES:

1. Data from Lee Nuclear Station site Data, 12/1/2005 - 11/30/2006.

2. Calms are wind speeds below 1 mph (0.45 m/sec).

WLS COL 2.3-2

TABLE 2.3-237 (Sheet 1 of 2)
JOINT FREQUENCY DISTRIBUTION OF WIND SPEED AND DIRECTION BY ATMOSPHERIC STABILITY CLASS
STABILITY CLASS C

STABILITY CLASS C

HOURS AT EACH WIND SPEED AND DIRECTION

DIR	Wind Speed (m/sec) U≤0.5	0.5<U ≤0.75	0.75< U≤1.0	1.0<U ≤1.25	1.25< U≤1.5	1.5<U ≤2.0	2.0<U ≤3.0	3.0<U ≤4.0	4.0<U ≤5.0	5.0<U ≤6.0	6.0<U ≤8.0	U>8	Total	Average Wind Speed (m/sec)
N	0	0	1	1	2	7	10	2	4	1	1	0	30	2.7
NNE	0	0	0	0	3	2	11	10	5	3	0	0	35	3.2
NE	0	0	0	2	3	12	21	7	3	0	0	0	49	2.5
ENE	0	0	0	2	3	6	12	7	1	0	0	0	32	2.4
E	0	0	0	0	1	10	2	2	0	0	0	0	16	2.0
ESE	0	0	0	0	2	8	6	1	0	0	0	0	18	2.0
SE	0	0	0	3	4	16	10	0	0	0	0	0	33	1.8
SSE	0	0	0	0	5	13	18	5	0	1	0	0	42	2.3
S	0	0	1	0	2	5	24	4	2	3	0	0	41	2.7
SSW	0	0	0	0	0	2	21	12	10	5	4	1	56	3.7
SW	0	0	1	0	2	3	18	17	11	4	16	7	79	4.5

WLS COL 2.3-2

TABLE 2.3-237 (Sheet 2 of 2)
JOINT FREQUENCY DISTRIBUTION OF WIND SPEED AND DIRECTION BY ATMOSPHERIC STABILITY CLASS
STABILITY CLASS C

STABILITY CLASS C — HOURS AT EACH WIND SPEED AND DIRECTION

DIR	Wind Speed (m/sec) U≤0.5	0.5<U ≤0.75	0.75< U≤1.0	1.0<U ≤1.25	1.25< U≤1.5	1.5<U ≤2.0	2.0<U ≤3.0	3.0<U ≤4.0	4.0<U ≤5.0	5.0<U ≤6.0	6.0<U ≤8.0	U>8	Total	Average Wind Speed (m/sec)
WSW	0	0	0	1	3	5	24	15	7	4	0	2	61	3.3
W	0	0	0	1	1	2	11	4	2	1	2	0	25	3.1
WNW	0	0	0	3	0	1	10	9	5	3	4	1	37	3.9
NW	0	0	0	0	0	9	16	4	4	6	2	0	41	3.3
NNW	0	0	0	1	0	2	9	5	1	4	0	1	24	3.3
CALM	0													0.0
TOTAL	0	0	3	15	32	106	224	106	57	36	29	12	620	

NOTES:

1. Data from Lee Nuclear Station site Data, 12/1/2005 - 11/30/2006.

2. Calms are wind speeds below 1 mph (0.45 m/sec).

WLS COL 2.3-2

TABLE 2.3-238 (Sheet 1 of 2)
JOINT FREQUENCY DISTRIBUTION OF WIND SPEED AND DIRECTION BY ATMOSPHERIC STABILITY CLASS
STABILITY CLASS D

STABILITY CLASS D

HOURS AT EACH WIND SPEED AND DIRECTION

DIR	Wind Speed (m/sec) U≤0.5	0.5<U ≤0.75	0.75< U≤1.0	1.0<U ≤1.25	1.25< U≤1.5	1.5<U ≤2.0	2.0<U ≤3.0	3.0<U ≤4.0	4.0<U ≤5.0	5.0<U ≤6.0	6.0<U ≤8.0	U>8	Total	Average Wind Speed (m/sec)
N	0	0	6	8	16	25	59	32	17	9	2	0	174	2.7
NNE	0	0	7	8	15	27	78	52	24	6	2	0	219	2.8
NE	0	0	4	7	12	26	65	34	11	5	1	0	167	2.6
ENE	0	1	9	18	12	25	40	20	5	1	0	0	132	2.2
E	0	0	9	7	10	18	22	7	2	0	0	0	76	1.9
ESE	0	1	9	6	15	24	12	2	0	1	0	0	70	1.7
SE	0	0	4	10	26	32	25	2	5	0	0	0	105	1.9
SSE	1	0	6	8	16	36	52	6	8	3	4	3	144	2.5
S	0	0	6	5	21	48	64	25	12	3	5	0	190	2.5
SSW	0	0	5	3	7	23	79	38	34	17	2	0	208	3.1
SW	0	1	3	4	9	17	48	39	27	26	16	1	191	3.6

WLS COL 2.3-2

TABLE 2.3-238 (Sheet 2 of 2)
JOINT FREQUENCY DISTRIBUTION OF WIND SPEED AND DIRECTION BY ATMOSPHERIC STABILITY CLASS
STABILITY CLASS D

STABILITY CLASS D — HOURS AT EACH WIND SPEED AND DIRECTION

DIR	Wind Speed (m/sec) U≤0.5	0.5<U ≤0.75	0.75< U≤1.0	1.0<U ≤1.25	1.25< U≤1.5	1.5<U ≤2.0	2.0<U ≤3.0	3.0<U ≤4.0	4.0<U ≤5.0	5.0<U ≤6.0	6.0<U ≤8.0	U>8	Total	Average Wind Speed (m/sec)
WSW	0	0	3	5	3	17	27	20	16	5	10	3	109	3.5
W	0	0	3	6	3	10	19	12	6	3	1	0	64	2.7
WNW	0	2	4	6	7	9	18	13	13	6	7	3	90	3.3
NW	0	1	6	10	22	26	34	16	15	10	4	5	149	2.8
NNW	0	1	6	10	13	25	31	22	10	9	2	1	132	2.7
CALM	0													
TOTAL	1	7	93	124	207	386	672	341	206	106	57	17	2218	

NOTES:

1. Data from Lee Nuclear Station site Data, 12/1/2005 - 11/30/2006.

2. Calms are wind speeds below 1 mph (0.45 m/sec).

WLS COL 2.3-2

TABLE 2.3-239 (Sheet 1 of 2)
JOINT FREQUENCY DISTRIBUTION OF WIND SPEED AND DIRECTION BY ATMOSPHERIC STABILITY CLASS
STABILITY CLASS E

STABILITY CLASS E

HOURS AT EACH WIND SPEED AND DIRECTION

DIR	Wind Speed (m/sec)													Average Wind Speed (m/sec)
	U≤0.5	0.5<U ≤0.75	0.75< U≤1.0	1.0<U ≤1.25	1.25< U≤1.5	1.5<U ≤2.0	2.0<U ≤3.0	3.0<U ≤4.0	4.0<U ≤5.0	5.0<U ≤6.0	6.0<U ≤8.0	U>8	Total	
N	0	4	22	12	17	27	18	7	2	2	1	0	112	1.8
NNE	0	3	10	12	21	16	11	6	1	0	0	0	81	1.7
NE	0	5	15	20	18	20	16	7	1	0	0	0	100	1.6
ENE	0	6	21	6	15	15	8	0	0	0	0	0	70	1.3
E	0	6	22	23	21	18	3	0	0	0	0	0	92	1.3
ESE	0	3	21	21	18	13	3	1	0	0	0	0	80	1.3
SE	0	0	19	23	27	25	16	0	0	0	0	0	109	1.4
SSE	0	0	7	19	27	32	23	5	1	1	0	0	115	1.8
S	0	0	5	9	15	44	66	25	0	0	0	0	164	2.2
SSW	0	2	3	12	9	12	42	25	21	8	0	0	136	2.8
SW	0	1	6	8	3	16	27	30	27	9	2	0	129	3.1

WLS COL 2.3-2

TABLE 2.3-239 (Sheet 2 of 2)
JOINT FREQUENCY DISTRIBUTION OF WIND SPEED AND DIRECTION BY ATMOSPHERIC STABILITY CLASS
STABILITY CLASS E

STABILITY CLASS E — HOURS AT EACH WIND SPEED AND DIRECTION

DIR	Wind Speed (m/sec) U≤0.5	0.5<U ≤0.75	0.75< U≤1.0	1.0<U ≤1.25	1.25< U≤1.5	1.5<U ≤2.0	2.0<U ≤3.0	3.0<U ≤4.0	4.0<U ≤5.0	5.0<U ≤6.0	6.0<U ≤8.0	U>8	Total	Average Wind Speed (m/sec)
WSW	0	0	5	10	2	19	25	18	10	3	0	0	92	2.6
W	0	2	7	3	2	13	20	11	2	0	0	0	61	2.2
WNW	0	0	9	16	19	28	39	11	7	4	0	0	134	2.2
NW	0	1	9	34	38	41	40	24	6	0	1	0	196	2.0
NNW	0	5	21	18	27	29	32	24	3	0	1	0	160	1.9
CALM	5													
TOTAL	5	39	202	247	277	367	390	195	82	28	5	0	1836	

NOTES:

1. Data from Lee Nuclear Station site Data, 12/1/2005 - 11/30/2006.

2. Calms are wind speeds below 1 mph (0.45 m/sec).

WLS COL 2.3-2

TABLE 2.3-240 (Sheet 1 of 2)
JOINT FREQUENCY DISTRIBUTION OF WIND SPEED AND DIRECTION BY ATMOSPHERIC STABILITY CLASS
STABILITY CLASS F

STABILITY CLASS F

HOURS AT EACH WIND SPEED AND DIRECTION

DIR	Wind Speed (m/sec) U≤0.5	0.5<U ≤0.75	0.75< U≤1.0	1.0<U ≤1.25	1.25< U≤1.5	1.5<U ≤2.0	2.0<U ≤3.0	3.0<U ≤4.0	4.0<U ≤5.0	5.0<U ≤6.0	6.0<U ≤8.0	U>8	Total	Average Wind Speed (m/sec)
N	1	10	20	9	7	3	3	0	0	0	0	0	54	1.0
NNE	1	9	13	5	5	5	1	0	0	0	0	0	40	1.0
NE	1	11	9	8	7	3	0	0	0	0	0	0	40	1.0
ENE	1	10	21	13	5	0	1	0	0	0	0	0	52	1.0
E	0	7	30	15	5	2	0	0	0	0	0	0	59	1.0
ESE	1	10	20	25	6	3	0	0	0	0	0	0	65	1.0
SE	0	1	15	16	18	15	3	0	0	0	0	0	66	1.3
SSE	0	3	6	13	16	12	7	0	1	0	0	0	59	1.5
S	1	1	7	3	6	7	18	2	0	0	0	0	46	1.8
SSW	0	0	5	3	5	3	8	2	0	1	0	0	28	2.0
SW	0	0	2	3	6	6	1	0	0	0	0	0	19	1.5

WLS COL 2.3-2

TABLE 2.3-240 (Sheet 2 of 2)
JOINT FREQUENCY DISTRIBUTION OF WIND SPEED AND DIRECTION BY ATMOSPHERIC STABILITY CLASS
STABILITY CLASS F

STABILITY CLASS F — HOURS AT EACH WIND SPEED AND DIRECTION

DIR	Wind Speed (m/sec) U≤0.5	0.5<U ≤0.75	0.75< U≤1.0	1.0<U ≤1.25	1.25< U≤1.5	1.5<U ≤2.0	2.0<U ≤3.0	3.0<U ≤4.0	4.0<U ≤5.0	5.0<U ≤6.0	6.0<U ≤8.0	U>8	Total	Average Wind Speed (m/sec)
WSW	0	2	7	6	1	6	6	0	0	0	0	0	29	1.4
W	0	3	4	1	3	3	4	1	0	0	0	0	20	1.5
WNW	0	5	22	13	17	26	27	2	1	0	0	0	113	1.6
NW	1	5	28	34	50	48	36	3	0	0	0	0	205	1.5
NNW	0	5	22	20	19	10	8	2	0	0	0	0	86	1.3
CALM	5													
TOTAL	12	85	231	189	176	153	124	12	2	1	0	0	986	

NOTES:

1. Data from Lee Nuclear Station site Data, 12/1/2005 - 11/30/2006.

2. Calms are wind speeds below 1 mph (0.45 m/sec).

WLS COL 2.3-2

TABLE 2.3-241 (Sheet 1 of 2)
JOINT FREQUENCY DISTRIBUTION OF WIND SPEED AND DIRECTION BY ATMOSPHERIC STABILITY CLASS
STABILITY CLASS G

STABILITY CLASS G HOURS AT EACH WIND SPEED AND DIRECTION

DIR	Wind Speed (m/sec) U≤0.5	0.5<U ≤0.75	0.75<U ≤1.0	1.0<U ≤1.25	1.25<U ≤1.5	1.5<U ≤2.0	2.0<U ≤3.0	3.0<U ≤4.0	4.0<U ≤5.0	5.0<U ≤6.0	6.0<U ≤8.0	U>8	Total	Average Wind Speed (m/sec)
N	3	23	37	20	2	1	0	0	0	0	0	0	86	0.9
NNE	2	32	17	8	1	0	0	0	0	0	0	0	60	0.8
NE	2	25	26	5	4	0	1	0	0	0	0	0	63	0.8
ENE	3	25	36	7	1	0	0	0	0	0	0	0	73	0.8
E	4	19	39	18	17	2	0	0	0	0	0	0	98	0.9
ESE	3	12	40	25	13	2	0	0	0	0	0	0	96	1.0
SE	1	21	41	19	12	9	2	0	0	0	0	0	106	1.0
SSE	1	6	17	11	8	4	0	0	0	0	0	0	48	1.0
S	0	7	2	3	2	1	1	0	0	0	0	0	17	1.0
SSW	0	0	2	1	1	2	1	0	0	0	0	0	7	1.4
SW	0	2	2	1	0	1	0	0	0	0	0	0	6	1.0

WLS COL 2.3-2

TABLE 2.3-241 (Sheet 2 of 2)
JOINT FREQUENCY DISTRIBUTION OF WIND SPEED AND DIRECTION BY ATMOSPHERIC STABILITY CLASS
STABILITY CLASS G

STABILITY CLASS G HOURS AT EACH WIND SPEED AND DIRECTION

DIR	Wind Speed (m/sec) U≤0.5	0.5<U ≤0.75	0.75<U ≤1.0	1.0<U ≤1.25	1.25<U ≤1.5	1.5<U ≤2.0	2.0<U ≤3.0	3.0<U ≤4.0	4.0<U ≤5.0	5.0<U ≤6.0	6.0<U ≤8.0	U>8	Total	Average Wind Speed (m/sec)
WSW	0	4	5	2	1	0	0	0	0	0	0	0	12	0.9
W	0	2	8	8	3	1	3	0	0	0	0	0	26	1.2
WNW	2	10	20	21	28	44	27	1	0	0	0	0	152	1.5
NW	4	23	60	83	121	180	90	0	0	0	0	0	561	1.5
NNW	2	26	58	51	23	9	1	0	0	0	0	0	170	1.0
CALM	63													
TOTAL	91	237	411	283	238	257	126	1	0	0	0	0	1645	

NOTES:

1. Data from Lee Nuclear Station site Data, 12/1/2005 - 11/30/2006.

2. Calms are wind speeds below 1 mph (0.45 m/sec).

WLS COL 2.3-1

TABLE 2.3-242 (Sheet 1 of 2)
MAXIMUM NUMBER OF CONSECUTIVE HOURS WITH WIND FROM A SINGLE SECTOR
GREENVILLE/SPARTANBURG, SOUTH CAROLINA

Sector	1997	1998	1999	2000	2001	2002	2003	2004	2005	Maximum	Average
N	8	13	12	10	8	7	10	10	9	13	9.8
NNE	7	5	4	11	13	12	15	10	12	15	9.6
NE	11	13	14	15	13	12	23	11	14	23	14.0
ENE	15	17	13	11	5	6	8	8	6	17	10.4
E	5	9	7	7	7	7	7	8	7	9	7.1
ESE	5	3	5	5	3	6	3	3	3	6	4.1
SE	3	4	4	3	4	7	5	6	5	7	4.5
SSE	4	4	5	4	6	6	5	4	7	6	4.8
S	7	13	6	10	10	10	9	8	12	13	9.1
SSW	5	8	5	8	8	8	9	6	9	9	7.1
SW	5	10	7	10	10	9	12	11	11	12	9.3
WSW	16	19	12	14	9	8	7	11	10	19	12.0
W	8	12	7	8	7	7	6	7	9	12	7.8
WNW	4	4	6	3	4	5	5	3	3	6	4.3

WLS COL 2.3-1

TABLE 2.3-242 (Sheet 2 of 2)
MAXIMUM NUMBER OF CONSECUTIVE HOURS WITH WIND FROM A SINGLE SECTOR
GREENVILLE/SPARTANBURG, SOUTH CAROLINA

Sector	1997	1998	1999	2000	2001	2002	2003	2004	2005	Maximum	Average
NW	3	3	2	6	4	5	4	4	4	6	3.9
NNW	6	6	8	7	7	7	5	5	7	8	6.4

NOTES:

1. Wind values which were either not provided, had a zero speed value, or a VRB wind direction were not included, and assumed to break any consecutive wind direction count.

2. Data from Unedited Local Climatological Data, National Oceanic and Atmospheric Administration, U. S. Department of Commerce, Asheville, NC, Greenville/Spartanburg International Airport, Station No. 03870.

3. Period of Record - 9 years (1997 - 2005).

WLS COL 2.3-1

TABLE 2.3-243 (Sheet 1 of 2)
MAXIMUM NUMBER OF CONSECUTIVE HOURS WITH WIND FROM THREE ADJACENT SECTORS, GREENVILLE/SPARTANBURG, SOUTH CAROLINA

Sector	1997	1998	1999	2000	2001	2002	2003	2004	2005	Maximum	Average
N	17	32	23	28	21	19	25	29	20	32	24.3
NNE	20	17	26	46	24	54	45	32	48	54	33.0
NE	37	60	61	82	32	78	65	47	66	82	57.8
ENE	41	70	66	62	30	16	37	35	23	70	44.6
E	18	22	36	21	11	10	16	19	13	36	19.1
ESE	8	14	9	10	14	10	12	20	13	20	12.1
SE	8	8	9	8	20	12	14	13	14	20	11.5
SSE	8	14	17	11	25	15	11	12	21	25	14.1
S	12	14	16	15	16	27	17	18	26	27	16.9
SSW	16	21	14	18	40	29	21	34	27	40	24.1
SW	24	38	37	26	49	36	49	36	32	49	36.9
WSW	35	53	46	48	43	31	38	45	31	53	42.4
W	33	48	34	28	18	18	25	21	18	48	28.1
WNW	13	16	18	14	18	8	18	10	19	18	14.4
NW	7	7	14	11	16	12	10	8	12	16	10.6

WLS COL 2.3-1

TABLE 2.3-243 (Sheet 2 of 2)
MAXIMUM NUMBER OF CONSECUTIVE HOURS WITH WIND FROM THREE ADJACENT SECTORS, GREENVILLE/SPARTANBURG, SOUTH CAROLINA

Sector	1997	1998	1999	2000	2001	2002	2003	2004	2005	Maximum	Average
NNW	24	27	20	29	41	22	32	19	23	41	26.8

NOTES:

1. Wind values which were either not provided, had a zero speed value, or a VRB wind direction were not included, and assumed to break any consecutive wind direction count.

2. Data from Unedited Local Climatological Data, National Oceanic and Atmospheric Administration, U. S. Department of Commerce, Asheville, NC, Greenville/Spartanburg International Airport, Station No. 03870.

3. Period of Record - 9 years (1997 - 2005).

WLS COL 2.3-1

TABLE 2.3-244 (Sheet 1 of 2)
MAXIMUM NUMBER OF CONSECUTIVE HOURS WITH WIND FROM FIVE ADJACENT SECTORS, GREENVILLE/SPARTANBURG, SOUTH CAROLINA

Sector	1997	1998	1999	2000	2001	2002	2003	2004	2005	Maximum	Average
N	29	44	32	48	43	54	45	41	48	54	42.0
NNE	38	69	64	82	44	96	75	69	114	96	67.1
NE	54	70	107	82	88	150	80	97	146	150	91.0
ENE	61	70	111	82	53	128	66	79	110	128	81.3
E	43	70	76	62	30	18	37	35	38	76	46.4
ESE	18	22	36	24	20	12	17	30	20	36	22.4
SE	10	19	22	13	26	23	18	22	27	26	19.1
SSE	12	14	22	15	26	27	18	22	33	27	19.5
S	16	21	30	18	42	36	24	34	35	42	27.6
SSW	26	49	38	49	54	61	77	65	38	77	52.4
SW	49	114	68	66	81	60	93	76	49	114	75.9
WSW	42	57	67	56	77	70	99	49	83	99	64.6
W	35	55	49	48	43	38	41	45	38	55	44.3
WNW	33	48	45	28	18	19	29	21	24	48	30.1

WLS COL 2.3-1

TABLE 2.3-244 (Sheet 2 of 2)
MAXIMUM NUMBER OF CONSECUTIVE HOURS WITH WIND FROM FIVE ADJACENT SECTORS, GREENVILLE/SPARTANBURG, SOUTH CAROLINA

Sector	1997	1998	1999	2000	2001	2002	2003	2004	2005	Maximum	Average
NW	24	27	20	29	41	22	35	25	34	41	27.9
NNW	28	36	23	47	41	23	33	29	26	47	32.5

NOTES:

1. Wind values which were either not provided, had a zero speed value, or a VRB wind direction were not included, and assumed to break any consecutive wind direction count.

2. Data from Unedited Local Climatological Data, National Oceanic and Atmospheric Administration, U. S. Department of Commerce, Asheville, NC, Greenville/Spartanburg International Airport, Station No. 03870.

3. Period of Record - 9 years (1997 - 2005).

WLS COL 2.3-1

TABLE 2.3-245 (Sheet 1 of 2)
COMPARISON OF MAXIMUM WIND PERSISTENCE
AT LEE NUCLEAR STATION SITE AND GREENVILLE/SPARTANBURG
SOUTH CAROLINA

	Wind Persistence (hrs)								
	Single Sector			Three Adjacent Sectors			Five Adjacent Sectors		
Sector	WLS	GSP[5]	GSP[4]	WLS	GSP[5]	GSP[4]	WLS	GSP[5]	GSP[4]
N	9	15	13	34	32	32	55	76	54
NNE	12	6	15	36	50	54	71	68	96
NE	12	13	23	31	43	82	66	56	150
ENE	6	4	17	20	31	70	34	43	128
E	4	6	9	23	11	36	25	31	76
ESE	5	5	6	19	11	20	26	11	36
SE	6	3	7	15	8	20	26	20	26
SSE	11	5	6	20	19	25	25	19	27
S	7	12	13	22	19	27	40	26	42
SSW	9	7	9	30	23	40	42	70	77
SW	10	11	12	41	33	49	62	88	114
WSW	7	10	19	31	44	53	53	88	99

WLS COL 2.3-1

TABLE 2.3-245 (Sheet 2 of 2)
COMPARISON OF MAXIMUM WIND PERSISTENCE
AT LEE NUCLEAR STATION SITE AND GREENVILLE/SPARTANBURG
SOUTH CAROLINA

	Wind Persistence (hrs)								
	Single Sector			Three Adjacent Sectors			Five Adjacent Sectors		
Sector	WLS	GSP[5]	GSP[4]	WLS	GSP[5]	GSP[4]	WLS	GSP[5]	GSP[4]
W	8	8	12	21	20	48	45	44	55
WNW	6	3	6	30	9	18	48	20	48
NW	15	4	6	45	8	16	47	31	41
NNW	14	8	8	27	31	41	62	36	47
Max	15	15	23	45	50	82	71	88	150
Average	8.8	7.5	11.3	27.8	24.5	39.4	45.4	45.4	69.8

NOTES:

1. Wind values which were either not provided, had a zero speed value, or a VRB wind direction were not included, and assumed to break any consecutive wind direction count.

2. Wind persistence values above are the maximum persistence durations for the period of record.

3. Period of record at Lee Nuclear Station site, 12/1/2005 through 11/30/2006, Tower 2 at 10 meter level.

4. Period of record at Greenville/Spartanburg, 1997 - 2005.

5. Period of record at Greenville/Spartanburg, 12/1/2005 through 11/30/2006.

WLS COL 2.3-1

TABLE 2.3-246 (Sheet 1 of 2)
NINETY-NINE ISLANDS MONTHLY CLIMATE SUMMARY
NCDC 1971-2000 MONTHLY NORMALS

	Jan	Feb	Mar	Apr	May	Jun	Jul	Aug	Sep	Oct	Nov	Dec	Annual
Mean Max. Temperature (°F)	**50.5**	**55.1**	**62.9**	**71.3**	**77.7**	**83.9**	**87.5**	**86**	**80.4**	**71.7**	**62**	**53.2**	**70.2**
Highest Mean Max. Temperature (°F)	59.3	64.3	68.6	76.4	82.9	89.2	94.4	91.8	84.5	77.9	68.4	62.1	94.4
Year Highest Occurred	1974	1976	2000	1986	2000	1986	1993	1999	1973	1984	1999	1984	1993
Lowest Mean Max. Temperature (°F)	39.7	46.1	56.9	66	73.2	77.9	83	81.9	77	66.2	54.4	45.1	39.7
Year Lowest Occurred	1977	1978	1971	1984	1997	1997	1979	1992	1974	1976	1996	2000	1977
Mean Temperature (°F)	**39**	**42.3**	**49.6**	**57.1**	**65.2**	**72.6**	**76.8**	**75.7**	**69.5**	**58.5**	**49**	**41.4**	**58.1**
Highest Mean Temperature (°F)	50	48.6	54.1	61.4	70.3	76.9	81.2	79.4	73.1	65.8	57	49.6	81.2
Year Highest Occurred	1974	1990	2000	1999	1991	1986	1993	1999	1973	1984	1985	1971	1993
Lowest Mean Temperature (°F)	28.5	34	44.1	52.5	60.7	68.2	73.7	72.9	66.8	52.2	42	34.1	28.5
Year Lowest Occurred	1977	1978	1971	1983	1997	1972	1979	1997	1984	1987	1976	2000	1977
Mean Min. Temperature (°F)	**27.4**	**29.5**	**36.2**	**42.9**	**52.7**	**61.3**	**66.1**	**65.3**	**58.5**	**45.2**	**35.9**	**29.5**	**45.9**
Highest Mean Min. Temperature (°F)	40.7	36.4	42.7	49.2	60.6	65.6	69	69.1	62.2	53.9	48	38.8	69.1
Year Highest Occurred	1974	1998	1973	1991	1991	1994	1991	1995	1980	1971	1985	1971	1995
Lowest Mean Min. Temperature (°F)	17.2	21.5	30.5	37.7	47.9	55.5	62.9	61.1	53.5	35.7	28.4	23	17.2
Year Lowest Occurred	1977	1977	1981	1971	1981	1972	1976	1997	1999	1987	1976	2000	1977

WLS COL 2.3-1

TABLE 2.3-246 (Sheet 2 of 2)
NINETY-NINE ISLANDS MONTHLY CLIMATE SUMMARY
NCDC 1971-2000 MONTHLY NORMALS

	Jan	Feb	Mar	Apr	May	Jun	Jul	Aug	Sep	Oct	Nov	Dec	Annual
Mean Precipitation (in.)	**4.53**	**4.07**	**4.93**	**3.05**	**4.15**	**3.76**	**3.78**	**4.83**	**4.08**	**3.85**	**3.67**	**3.67**	**48.37**
Highest Precipitation (in.)	8.25	6.6	9.54	6.65	10.5	10.5	10.9	11.9	9.73	14.9	8.83	8.75	14.93
Year Highest Occurred	1978	1997	1980	1998	1975	1995	1971	1994	1987	1990	1985	1983	1990
Lowest Precipitation (in.)	0.3	0.64	1.15	0.39	1.13	0.17	0.85	0.88	0.59	0	0.88	0.83	0
Year Lowest Occurred	1981	1978	1985	1976	1988	1986	1977	1999	1985	2000	1973	1980	2000
Heating Degree Days (°F)	**807**	**637**	**480**	**243**	**88**	**8**	**0**	**0**	**21**	**236**	**483**	**734**	**3737**
Cooling Degree Days (°F)	0	0	0	7	94	236	366	330	155	33	2	0	1223

NOTES:

1. Ninety-Nine Islands, South Carolina (Station No. 386293), Monthly Climate Summary, Period of Record: 1971 to 2000.
2. Reference: Southeast Regional Climate Center, http://cirrus.dnr.state.sc.us/cgi-bin/sercc/cliMAIN.pl?sc6293

TABLE 2.3-247
DELETED

TABLE 2.3-248
DELETED

TABLE 2.3-249
DELETED

TABLE 2.3-250
DELETED

TABLE 2.3-251
DELETED

TABLE 2.3-252
DELETED

WLS COL 2.3-1

TABLE 2.3-253
RELATIVE HUMIDITY
GREENVILLE/SPARTANBURG, SOUTH CAROLINA
FOR 4 TIME PERIODS PER DAY
1997-2005[a][b]

Time	00:00 - 06:00	06:00-12:00	12:00-18:00	18:00-24:00
Jan	75%	69%	53%	67%
Feb	76%	69%	52%	66%
Mar	73%	65%	49%	63%
Apr	78%	65%	50%	66%
May	84%	68%	53%	71%
Jun	87%	71%	58%	76%
Jul	89%	72%	59%	79%
Aug	87%	72%	56%	77%
Sep	85%	71%	56%	77%
Oct	86%	72%	57%	78%
Nov	81%	71%	56%	74%
Dec	77%	70%	54%	69%
Annual	81%	69%	54%	72%

a) Data from Unedited Local Climatological Data, National Oceanic and Atmospheric Administration, U.S. Department of Commerce, Asheville, NC, Greenville/Spartanburg International Airport, Station No. 03870.

b) Data from Unedited Local Climatological Data, National Oceanic and Atmospheric Administration, U. S. Department of Commerce, Asheville, NC, Greenville/Spartanburg International Airport, Station No. 03870.

TABLE 2.3-254
NINETY-NINE ISLANDS MONTHLY CLIMATE SUMMARY
NINETY-NINE ISLANDS, SOUTH CAROLINA (386293)
PERIOD OF RECORD: 8/1/1948 TO 12/31/2005

	Jan	Feb	Mar	Apr	May	Jun	Jul	Aug	Sep	Oct	Nov	Dec	Annual
Average Max. Temperature (F)	51.5	55.6	63.8	72.6	79.4	85.4	89.0	87.6	82.1	73.2	63.7	54.0	71.5
Average Min. Temperature (F)	26.7	29.1	35.7	43.3	52.7	61.3	65.9	65.1	58.2	45.1	35.6	28.4	45.6
Average Total Precipitation (in.)	4.10	4.06	4.99	3.40	3.94	3.89	4.12	4.69	3.89	3.32	3.30	3.81	47.52
Average Total Snowfall (in.)	1.1	1.1	0.5	0	0	0	0	0	0	0	0	0.4	3.1
Average Snow Depth (in.)	0	0	0	0	0	0	0	0	0	0	0	0	0

Percent of possible observations for period of record.

Max. Temp.: 76.3% Min. Temp.: 76.3% Precipitation: 99.6%: Snowfall: 84.1% Snow Depth: 84.2%.

NOTES:

1. Data from: Southeast Regional Climate Center, http://cirrus.dnr.state.sc.us/cgi-bin/sercc/cliMAIN.pl?sc6293

WLS COL 2.3-2

TABLE 2.3-255
COMPARISON OF RELATIVE HUMIDITY FOR LEE NUCLEAR SITE (2005 – 2006[a]) AND GREENVILLE/SPARTANBURG, SOUTH CAROLINA (1997 – 2005[b]) FOR 4 TIME PERIODS PER DAY

	00:00 - 06:00		06:00 - 12:00		12:00 - 18:00		18:00 - 24:00	
Time	WLS	GSP	WLS	GSP	WLS	GSP	WLS	GSP
Jan	78%	75%	69%	69%	53%	53%	67%	67%
Feb	76%	76%	68%	69%	44%	52%	58%	66%
Mar	73%	73%	63%	65%	41%	49%	54%	63%
Apr	78%	78%	75%	65%	43%	50%	55%	66%
May	88%	84%	77%	68%	50%	53%	67%	71%
Jun	92%	87%	80%	71%	51%	58%	72%	76%
Jul	94%	89%	83%	72%	55%	59%	75%	79%
Aug	94%	87%	86%	72%	60%	56%	78%	77%
Sep	93%	85%	86%	71%	59%	56%	82%	77%
Oct	90%	86%	83%	72%	52%	57%	74%	78%
Nov	85%	81%	74%	71%	46%	56%	74%	74%
Dec	86%	77%	78%	70%	49%	54%	71%	69%
Annual	86%	81%	77%	69%	50%	54%	69%	72%

a) Lee Nuclear Station site Data, 12/1/2005 - 11/30/2006.
b) Data from Unedited Local Climatological Data, National Oceanic and Atmospheric Administration, U.S. Department of Commerce, Ashville, NC, Greenville/Spartanburg International Airport, Station No. 03870.

WLS COL 2.3-1

TABLE 2.3-256
PRECIPITATION DATA (INCHES OF RAIN)
GREENVILLE/SPARTANBURG, SOUTH CAROLINA

GSP Precipitation	Period of Record	Jan	Feb	Mar	Apr	May	Jun	Jul	Aug	Sep	Oct	Nov	Dec	Year
Normal (in)	30	4.41	4.24	5.31	3.54	4.59	3.92	4.65	4.08	3.97	3.88	3.79	3.86	50.24
Maximum Monthly (in)	45	7.19	7.43	11.37	11.30	8.89	10.12	13.57	17.37	11.65	10.24	7.85	8.45	17.37
Year of Occurrence		1993	1971	1980	1964	1972	1994	1984	1995	1975	1964	1992	1983	AUG 1995
Minimum Monthly (in)	45	0.29	0.53	1.13	0.69	1.09	0.17	0.75	0.79	0.16	0.00	0.89	0.37	0.00
Year of Occurrence		1981	1978	1985	1976	1965	1993	1993	1999	2005	2000	2007	1965	OCT 2000
Maximum In 24 Hours (in)	45	3.30	3.57	4.45	3.76	3.79	4.80	4.68	12.32	6.21	4.93	2.83	3.54	12.32
Year of Occurrence		1982	1984	1963	1963	1996	1980	2005	1995	1973	1990	1964	2004	AUG 1995
Normal No. Days With:														
Precipitation >= 0.01	30	11.3	9.3	11.0	8.7	10.6	10.2	11.8	10.2	9.1	7.1	9.4	10.3	119.0
Precipitation >= 1.00	30	1.1	1.1	1.7	1.0	1.4	1.0	1.4	1.0	1.2	1.0	1.2	1.1	14.2

NOTES:

1. National Climatic Data Center (NCDC) Local Climatic Data (LCD), data for Greenville-Spartanburg (Greer), South Carolina (Station ID GSP), 2007. (Reference 240).

WLS COL 2.3-1

TABLE 2.3-257
POINT PRECIPITATION FREQUENCY

	Recurrence Intervals (Years)						
Duration	1	2	5	10	25	50	100
5 minutes	0.4	0.5	0.6	0.6	0.7	0.8	0.8
10 minutes	0.7	0.8	0.9	1.0	1.1	1.2	1.3
15 minutes	0.8	1.0	1.2	1.3	1.4	1.5	1.7
30 minutes	1.1	1.4	1.6	1.9	2.1	2.3	2.5
1 hour	1.4	1.7	2.1	2.4	2.8	3.2	3.5
2 hours	1.6	2.0	2.4	2.8	3.4	3.8	4.2
3 hours	1.7	2.1	2.6	3.0	3.6	4.1	4.7
6 hours	2.1	2.6	3.2	3.7	4.5	5.1	5.8
12 hours	2.6	3.1	3.9	4.5	5.4	6.2	7.1
24 hours	3.1	3.7	4.6	5.4	6.4	7.3	8.1
2 days	3.6	4.4	5.4	6.3	7.5	8.4	9.4
4 days	4.1	4.9	6.0	6.9	8.2	9.2	10.2
7 days	4.7	5.7	6.9	7.9	9.2	10.3	11.5
10 days	5.4	6.4	7.7	8.7	10.1	11.2	12.3

NOTES:

1. From "Precipitation-Frequency Atlas of the United States" NOAA Atlas 14, Volume 2, Version 3, G. M. Bonnin, D. Martin, B. Lin, T. Parzybok, M. Yekta, and D. Riley, NOAA, National Weather Service, Silver Spring, Maryland, 2004, Extracted:Aug 24 2006. Location: South Carolina 35.024 N 81.524 W 777 feet. http://hdsc.nws.noaa.gov/hdsc/pfds/orb/sc_pfds.html

WLS COL 2.3-1

TABLE 2.3-258
PERCENT OF TOTAL OBSERVATIONS (BY MONTH) OF INDICATED WIND DIRECTIONS AND PRECIPITATION
GREENVILLE/SPARTANBURG, SOUTH CAROLINA

Sector	January	February	March	April	May	June	July	August	September	October	November	December	Total
N	1.55	1.39	1.27	1.25	1.25	1.25	1.13	1.09	1.49	0.94	1.35	1.76	15.71
NNE	1.30	0.92	1.60	0.97	0.89	0.73	0.57	0.45	1.00	1.42	1.02	1.20	12.06
NE	2.21	2.57	2.99	2.00	1.03	1.06	1.13	0.65	1.09	1.46	1.25	2.77	20.21
ENE	1.65	1.59	1.78	1.36	0.36	0.43	0.61	0.34	0.59	0.78	0.73	1.42	11.64
E	0.57	0.43	0.39	0.32	0.18	0.41	0.46	0.29	0.31	0.24	0.33	0.39	4.33
ESE	0.15	0.09	0.11	0.13	0.17	0.34	0.20	0.13	0.15	0.04	0.13	0.04	1.68
SE	0.10	0.04	0.05	0.27	0.09	0.17	0.19	0.13	0.17	0.06	0.15	0.03	1.44
SSE	0.10	0.09	0.13	0.29	0.11	0.22	0.29	0.22	0.31	0.11	0.24	0.13	2.24
S	0.69	0.31	0.36	0.65	0.42	0.69	0.29	0.33	0.55	0.20	0.65	0.24	5.37
SSW	0.48	0.38	0.41	0.74	0.50	0.46	0.41	0.15	0.20	0.18	0.66	0.25	4.82
SW	0.93	0.66	0.57	0.60	0.69	0.59	0.60	0.33	0.28	0.28	0.88	0.59	6.98
WSW	0.45	0.65	0.46	0.48	0.62	0.62	0.38	0.43	0.27	0.24	0.59	0.47	5.66
W	0.33	0.37	0.33	0.34	0.39	0.42	0.34	0.22	0.20	0.14	0.31	0.32	3.71
WNW	0.09	0.01	0.11	0.10	0.19	0.24	0.11	0.13	0.06	0.08	0.05	0.04	1.22
NW	0.11	0.08	0.25	0.14	0.15	0.22	0.15	0.06	0.09	0.08	0.10	0.09	1.53
NNW	0.20	0.08	0.13	0.15	0.09	0.14	0.14	0.09	0.06	0.04	0.10	0.18	1.40
Total	10.93	9.64	10.95	9.78	7.12	7.96	7.02	5.04	6.82	6.30	8.52	9.91	100

NOTES:

1. Instances of "trace" precipitation were counted as precipitation.

2. Data from Unedited Local Climatological Data, National Oceanic and Atmospheric Administration, U. S. Department of Commerce, Asheville, NC, Greenville/Spartanburg International Airport, Station No. 03870.

3. Period of Record - 9 years (1997 - 2005).

WLS COL 2.3-2

TABLE 2.3-259 (Sheet 1 of 2)
PERCENT OF TOTAL OBSERVATIONS (BY MONTH) OF PRECIPITATION AND WIND DIRECTION
LEE NUCLEAR SITE

Sector	January	February	March	April	May	June	July	August	September	October	November	December	Total
N	1.38	1.58	0.59	0.40	0.79	0.79	0.20	0.59	0.99	0.59	1.38	1.98	11.26
NNE	1.58	0.59	1.19	0.40	0.59	1.38	0.00	0.79	0.98	0.99	3.56	2.37	14.43
NE	0.00	0.40	0.00	0.79	0.40	0.99	0.00	0.40	1.58	0.99	0.79	2.17	8.50
ENE	0.59	0.40	0.40	0.00	0.40	1.19	0.59	1.38	0.40	0.79	0.40	0.40	6.92
E	0.00	0.00	0.79	0.20	0.20	0.99	0.59	1.78	0.00	0.00	0.00	0.59	5.14
ESE	0.40	0.00	0.00	0.00	0.40	0.99	0.20	0.40	0.00	0.40	0.20	0.40	3.36
SE	1.19	0.20	0.00	0.40	0.20	0.40	0.20	0.00	0.00	0.20	0.99	0.99	4.74
SSE	1.19	0.20	0.00	0.59	0.00	0.40	0.59	0.59	0.00	1.58	0.20	0.20	5.53
S	3.56	1.19	0.20	0.99	0.20	0.20	0.40	0.40	0.20	0.20	0.00	0.40	7.91
SSW	0.79	0.79	0.20	0.99	0.20	0.00	0.40	0.40	0.00	0.20	0.20	0.00	4.15
SW	0.40	0.79	0.40	0.00	0.40	0.40	0.20	0.20	0.00	0.00	0.20	0.99	3.95
WSW	0.00	0.20	0.00	0.40	0.20	0.00	0.59	0.20	0.00	0.20	0.20	0.40	2.37
W	0.40	0.20	0.00	0.20	0.20	0.59	0.59	0.59	0.40	0.00	0.20	0.20	3.56
WNW	0.40	0.00	0.00	0.00	0.59	0.40	0.40	0.40	0.00	1.19	0.20	0.20	3.75
NW	1.19	0.00	0.20	0.59	0.40	0.59	0.59	0.00	0.40	1.98	0.99	0.59	7.51
NNW	0.59	0.79	0.20	0.40	0.00	0.79	0.20	0.59	0.59	0.79	0.99	0.99	6.92

WLS COL 2.3-2

TABLE 2.3-259 (Sheet 2 of 2)
PERCENT OF TOTAL OBSERVATIONS (BY MONTH) OF PRECIPITATION AND WIND DIRECTION
LEE NUCLEAR SITE

Sector	January	February	March	April	May	June	July	August	September	October	November	December	Total
Total	13.64	7.31	4.15	6.32	5.14	10.08	5.73	8.70	5.53	10.08	10.47	12.85	100

NOTES:

1. Instances of "trace" precipitation were counted as precipitation.
2. Data from Lee Nuclear Site Data, 12/1/2005 - 11/30/2006.
3. Hours of missing wind direction or missing precipitation were not included in the frequency calculation.
4. Calm values classified by precipitation occurrences under variable wind direction conditions.

WLS COL 2.3-2

TABLE 2.3-260
RAINFALL FREQUENCY DISTRIBUTION
LEE NUCLEAR STATION SITE
NUMBER OF HOURS PER MONTH

Rainfall (inch/hr)	Jan	Feb	Mar	Apr	May	Jun	Jul	Aug	Sep	Oct	Nov	Dec
0.01-0.019	23	16	8	8	7	15	7	14	8	16	8	10
0.02-.099	37	19	10	15	10	19	13	21	9	22	27	37
0.10-0.249	6	2	4	7	9	13	6	4	7	11	16	19
0.25-0.499	2	0	0	2	3	2	2	3	3	2	1	1
0.50-0.99	1	0	0	0	0	2	0	2	1	0	1	0
1.00-1.99	0	0	0	0	0	0	1	0	0	0	0	0
2.0 & over	0	0	0	0	0	0	0	0	0	0	0	0
Total	69.0	37.0	22.0	32.0	29.0	51.0	29.0	44.0	28.0	51.0	53.0	67.0

NOTES:

1. Lee Nuclear Station site data, 12/1/2005 - 11/30/2006.

WLS COL 2.3-2

TABLE 2.3-261
PRECIPITATION DATA (INCHES OF RAIN)
LEE NUCLEAR STATION SITE

Month	Monthly Hours	Max 24 hour Rain (in)	Number of days with rainfall >0 in
Jan	69	1.35	15
Feb	37	0.29	10
Mar	22	0.97	8
Apr	32	0.92	11
May	29	1.14	9
Jun	51	1.38	13
Jul	29	2.55	9
Aug	44	1.38	11
Sep	28	2.68	10
Oct	51	1.80	13
Nov	53	1.87	7
Dec	67	1.75	8
Annual	512	2.68	124

NOTES:

1. Lee Nuclear Station site data, 12/1/2005 - 11/30/2006.

TABLE 2.3-262 (Sheet 1 of 4)
NINETY-NINE ISLANDS, SOUTH CAROLINA
MONTHLY TOTAL SNOWFALL (INCHES)
1947 - 2006

YEAR(S)	JUL	AUG	SEP	OCT	NOV	DEC	JAN	FEB	MAR	APR	MAY	JUN	Annual
1947-48	0.00z	0.00z	0.00z	0.00z	0.00z	0.00z	0.00z	0.00z	0.00z	0.00z	0.00z	0.00z	0.00
1948-49	0.00z	0.00	0.00	0.00	0.00	0.00	0.00	0.00	0.00	0.00	0.00	0.00	0.00
1949-50	0.00	0.00	0.00	0.00	0.00	0.00	0.00	0.00	0.00	0.00	0.00	0.00	0.00
1950-51	0.00	0.00	0.00	0.00	0.00	0.00z	0.00	0.00	0.00z	0.00z	0.00	0.00	0.00
1951-52	0.00	0.00	0.00	0.00	0.00z	0.00z	0.00	0.00z	0.00z	0.00z	0.00z	0.00z	0.00
1952-53	0.00z	0.00z	0.00z	0.00z	0.00z	0.00z	0.00z	0.00z	0.00z	0.00z	0.00z	0.00z	0.00
1953-54	0.00z	0.00z	0.00z	0.00z	0.00z	0.00z	0.00z	0.00z	0.00z	0.00z	0.00z	0.00z	0.00
1954-55	0.00z	0.00z	0.00z	0.00z	0.00z	0.00z	0.00z	0.00z	0.00z	0.00z	0.00z	0.00z	0.00
1955-56	0.00z	0.00z	0.00z	0.00z	0.00z	0.00z	0.00z	0.00z	0.00z	0.00z	0.00z	0.00z	0.00
1956-57	0.00z	0.00z	0.00z	0.00	0.00z	0.00	0.00z	0.00z	0.00z	0.00z	0.00z	0.00	0.00
1957-58	0.00	0.00z	0.00z	0.00z	0.00z	0.00z	0.00z	0.00z	0.00z	0.00z	0.00z	0.00z	0.00
1958-59	0.00z	0.00	0.00	0.00	0.00	0.00z	0.00	0.00z	0.00z	0.00z	0.00	0.00z	0.00
1959-60	0.00z	0.00	0.00	0.00	0.00	0.00	0.00z	0.00z	0.00z	0.00z	0.00z	0.00z	0.00
1960-61	0.00z	0.00z	0.00z	0.00	0.00	0.00	1.00	0.50	0.00	0.00	0.00	0.00	1.50
1961-62	0.00	0.00	0.00	0.00	0.00	0.00	0.00z	0.00a	1.00	0.00	0.00	0.00	1.00
1962-63	0.00	0.00	0.00	0.00	0.00	0.00	0.00	0.00z	0.00	0.00a	0.00	0.00	0.00
1963-64	0.00	0.00a	0.00	0.00	0.00	2.50	1.50	0.00	0.00	0.00	0.00	0.00	4.00
1964-65	0.00	0.00	0.00	0.00	0.00	0.00z	8.50	2.00	0.00	0.00	0.00	0.00	10.50
1965-66	0.00	0.00	0.00	0.00	0.00	0.00	9.00	1.00	0.00	0.00	0.00	0.00	10.00
1966-67	0.00	0.00	0.00	0.00	0.00	0.00	0.00	2.00	0.00	0.00	0.00	0.00	2.00

TABLE 2.3-262 (Sheet 2 of 4)
NINETY-NINE ISLANDS, SOUTH CAROLINA
MONTHLY TOTAL SNOWFALL (INCHES)
1947 - 2006

YEAR(S)	JUL	AUG	SEP	OCT	NOV	DEC	JAN	FEB	MAR	APR	MAY	JUN	Annual
1967-68	0.00	0.00	0.00	0.00	0.00	0.00	3.00	2.00	0.00	0.00	0.00	0.00	5.00
1968-69	0.00	0.00	0.00	0.00	0.00c	0.00	0.00	12.30	5.00	0.00	0.00z	0.00	17.30
1969-70	0.00	0.00	0.00	0.00	0.00	0.00	1.70	0.00	0.00	0.00	0.00	0.00	1.70
1970-71	0.00	0.00	0.00	0.00	0.00	3.00	0.00	0.00a	6.30	0.00	0.00	0.00	9.30
1971-72	0.00	0.00	0.00	0.00	0.00	12.00	0.00	1.00	2.00	0.00	0.00	0.00	15.00
1972-73	0.00	0.00	0.00	0.00	0.00	0.00	3.80	2.00	0.00	0.00	0.00	0.00	5.80
1973-74	0.00	0.00	0.00	0.00	0.00	0.00a	0.00	0.00	0.00	0.00	0.00	0.00	0.00
1974-75	0.00	0.00	0.00	0.00	0.00	0.00	0.00	0.00	0.00	0.00	0.00	0.00	0.00
1975-76	0.00	0.00	0.00	0.00	0.00	0.00	0.00	0.00	0.00	0.00	0.00	0.00	0.00
1976-77	0.00	0.00	0.00	0.00	0.00	0.00	5.50	0.00	0.00	0.00	0.00	0.00	5.50
1977-78	0.00	0.00	0.00	0.00	0.00	0.00	0.00	0.00	2.50	0.00	0.00	0.00	2.50
1978-79	0.00	0.00	0.00	0.00	0.00	0.00	0.00	14.00	0.00	0.00	0.00	0.00	14.00
1979-80	0.00	0.00	0.00	0.00	0.00	0.00	0.00	0.00b	0.00b	0.00	0.00	0.00	0.00
1980-81	0.00	0.00	0.00	0.00	0.00	0.00	0.00a	0.00	0.00	0.00	0.00	0.00	0.00
1981-82	0.00	0.00	0.00	0.00	0.00	0.00	5.20	0.00a	0.00	0.00	0.00	0.00	5.20
1982-83	0.00	0.00	0.00	0.00	0.00	0.00	0.00a	0.00a	6.00	0.00	0.00	0.00	6.00
1983-84	0.00	0.00	0.00	0.00	0.00	0.00	0.00	4.00	0.00	0.00	0.00	0.00	4.00
1984-85	0.00	0.00	0.00	0.00	0.00	0.00	0.00z	0.00	0.00	0.00	0.00	0.00	0.00
1985-86	0.00	0.00	0.00	0.00	0.00	0.00	0.00	0.00a	0.00	0.00	0.00	0.00	0.00
1986-87	0.00	0.00	0.00	0.00	0.00	0.00	0.00d	0.00	0.00	0.00	0.00	0.00	0.00

TABLE 2.3-262 (Sheet 3 of 4)
NINETY-NINE ISLANDS, SOUTH CAROLINA
MONTHLY TOTAL SNOWFALL (INCHES)
1947 - 2006

YEAR(S)	JUL	AUG	SEP	OCT	NOV	DEC	JAN	FEB	MAR	APR	MAY	JUN	Annual
1987-88	0.00	0.00	0.00	0.00	0.00	0.00	13.00	0.00	0.00	0.00	0.00	0.00	13.00
1988-89	0.00	0.00	0.00	0.00	0.00	0.00	0.00	2.10	0.00	0.00	0.00	0.00	2.10
1989-90	0.00	0.00	0.00	0.00	0.00	0.00	0.00	0.00	0.00	0.00	0.00	0.00	0.00
1990-91	0.00	0.00	0.00	0.00	0.00	0.00	0.00	0.00	0.00	0.00	0.00	0.00	0.00
1991-92	0.00	0.00	0.00	0.00	0.00	0.00	0.00	0.00	0.00	0.00	0.00	0.00	0.00
1992-93	0.00	0.00	0.00	0.00	0.00	0.00	0.00	0.00b	2.00	0.00	0.00	0.00	2.00
1993-94	0.00	0.00	0.00	0.00	0.00	1.00	0.00a	0.00	0.00	0.00	0.00	0.00	1.00
1994-95	0.00	0.00	0.00	0.00	0.00	0.00	0.00	0.00	0.00	0.00	0.00	0.00	0.00
1995-96	0.00	0.00	0.00	0.00	0.00	0.00	0.00a	0.00	0.00	0.00	0.00	0.00	0.00
1996-97	0.00	0.00	0.00	0.00	0.00	0.00	0.00a	0.00a	0.00	0.00	0.00	0.00	0.00
1997-98	0.00	0.00	0.00	0.00	0.00	0.00	0.00	0.00	0.00	0.00	0.00	0.00	0.00
1998-99	0.00	0.00	0.00	0.00	0.00	0.00	0.00	0.00	0.00	0.00	0.00	0.00	0.00
1999-00	0.00	0.00	0.00	0.00	0.00	0.00	0.00	0.00	0.00	0.00	0.00	0.00	0.00
2000-01	0.00	0.00	0.00	0.00	0.00	0.00	0.00	0.00	0.00	0.00	0.00	0.00	0.00
2001-02	0.00	0.00	0.00	0.00	0.00	0.00	2.00	0.00	0.00	0.00	0.00	0.00	2.00
2002-03	0.00	0.00	0.00a	0.00	0.00	0.00	0.00	0.00a	0.00b	0.00a	0.00a	0.00	0.00
2003-04	0.00	0.00	0.00	0.00	0.00	0.00	0.00	8.00a	0.00	0.00	0.00	0.00	8.00
2004-05	0.00	0.00	0.00	0.00	0.00b	0.00	0.00a	0.00	0.00	0.00	0.00	0.00	0.00
2005-06	0.00	0.00	0.00	0.00	0.00	0.00	0.00	0.00	0.00	0.00	0.00	0.00	0.00

TABLE 2.3-262 (Sheet 4 of 4)
NINETY-NINE ISLANDS, SOUTH CAROLINA
MONTHLY TOTAL SNOWFALL (INCHES)
1947 - 2006

YEAR(S)	JUL	AUG	SEP	OCT	NOV	DEC	JAN	FEB	MAR	APR	MAY	JUN	Annual
MEAN	0.00	0.00	0.00	0.00	0.00	0.38	1.11	1.06	0.52	0.00	0.00	0.00	2.88
S.D.	0.00	0.00	0.00	0.00	0.00	1.79	2.71	2.90	1.48	0.00	0.00	0.00	4.22
SKEW	0.00	0.00	0.00	0.00	0.00	5.89	2.86	3.44	3.02	0.00	0.00	0.00	1.53
MAX	0.00	0.00	0.00	0.00	0.00	12.00	13.00	14.00	6.30	0.00	0.00	0.00	15.00
MIN	0.00	0.00	0.00	0.00	0.00	0.00	0.00	0.00	0.00	0.00	0.00	0.00	0.00
NO YRS	49	51	51	53	51	49	49	48	48	48	49	50	41

*** Note *** Provisional Data *** After Year/Month 2006/03

a = 1 day missing, b = 2 days missing, c = 3 days missing, etc.,

z = 26 or more days missing, A = Accumulations present

NOTES:

1. Long-term means based on columns; thus, the monthly row may not sum (or average) to the long-term annual value.

2. Maximum allowable number of missing days: 5

3. Individual months not used for annual or monthly statistics if more than 5 days are missing. Individual years not used for annual statistics if any month in that year has more than 5 days missing.

4. Data from Southeast Regional Climate Center, http://cirrus.dnr.state.sc.us/cgi-bin/sercc/cliMAIN.pl?sc629

WLS COL 2.3-1

TABLE 2.3-263
AVERAGE HOURS OF FOG AND HAZE AT GREENVILLE/SPARTANBURG, SOUTH CAROLINA

	Fog (hours/month)			Haze (hours/month)		
Month	Average	Maximum	Minimum	Average	Maximum	Minimum
Jan	6.8	21.2	0.3	0.3	2.0	0.0
Feb	4.5	10.5	0.0	0.9	2.7	0.0
Mar	2.4	5.3	0.0	0.8	2.8	0.0
Apr	2.5	5.2	0.0	0.4	0.9	0.0
May	0.9	4.9	0.0	2.9	8.0	0.0
Jun	0.9	2.2	0.0	5.8	14.5	1.4
Jul	1.2	2.4	0.1	10.1	20.1	0.9
Aug	1.3	3.7	0.0	7.5	24.4	2.1
Sep	2.1	5.7	0.0	4.2	14.6	0.0
Oct	2.5	6.1	0.0	3.0	13.4	0.0
Nov	6.7	11.6	1.4	1.0	3.9	0.0
Dec	6.3	10.8	2.2	0.1	0.8	0.0
Annual (hours/yr)	38.1	46.5	29.4	37.0	61.6	24.3

NOTES:

1. Data from Unedited Local Climatological Data, National Oceanic and Atmospheric Administration, U. S. Department of Commerce, Asheville, NC, Greenville/Spartanburg International Airport, Station No. 03870.

2. Period of Record - 9 years (1997 - 2005).

WLS COL 2.3-1

TABLE 2.3-264
INVERSION HEIGHTS AND STRENGTHS, GREENSBORO, NORTH CAROLINA
JANUARY, 1999 - 2005

January	Mornings with Inversions[1]	Average Morning Height[2] (m)	Average Morning Strength[3] (0.1ºC/m)	Afternoons with Inversions[1]	Average Afternoon Height[2] (m)	Average Afternoon Strength[3] (0.1ºC/m)
1999	7	632	0.435	9	899	0.301
2000	15	1069	0.181	7	1108	0.334
2001	10	774	0.349	3	938	0.101
2002	12	949	0.256	9	983	0.250
2003	10	961	0.299	4	1131	0.085
2004	12	654	0.443	9	1251	0.263
2005	1	820	0.467	3	1582	0.164
Total	67	864	0.315	44	1092	0.245

NOTES:

1. Inversion is defined as three or more NOAA weather balloon elevation readings showing consecutive increases in temperature with height below 3000 m.

2. Balloons were released each day at 0:00 Greenwich Mean Time (GMT) and 12:00 GMT. Height is defined as elevation in meters where temperature first increases and is averaged only over those days with inversions.

3. Strength is the maximum temperature gradient in tenths of a degree centigrade per meter within the inversion layer.

4. Data from: FSL/NCDC Radiosonde Data Archive, http://raob.fsl.noaa.gov/

WLS COL 2.3-1

TABLE 2.3-265
INVERSION HEIGHTS AND STRENGTHS, GREENSBORO, NORTH CAROLINA
FEBRUARY, 1999 - 2005

February	Mornings with Inversions[1]	Average Morning Height[2] (m)	Average Morning Strength[3] (0.1ºC/m)	Afternoons with Inversions[1]	Average Afternoon Height[2] (m)	Average Afternoon Strength[3] (0.1ºC/m)
1999	9	664	0.704	4	933	0.344
2000	8	955	0.228	7	1217	0.155
2001	7	1107	0.188	6	1787	0.390
2002	7	938	0.523	6	1529	0.225
2003	11	933	0.229	11	874	0.265
2004	14	1035	0.244	13	1146	0.252
2005	0			2	429	0.629
Total	56	941	0.341	49	1174	0.277

NOTES:

1. Inversion is defined as three or more NOAA weather balloon elevation readings showing consecutive increases in temperature with height below 3000 m.

2. Balloons were released each day at 0:00 Greenwich Mean Time (GMT) and 12:00 GMT. Height is defined as elevation in meters where temperature first increases and is averaged only over those days with inversions.

3. Strength is the maximum temperature gradient in tenths of a degree centigrade per meter within the inversion layer.

4. Data from: FSL/NCDC Radiosonde Data Archive, http://raob.fsl.noaa.gov/

WLS COL 2.3-1

TABLE 2.3-266
INVERSION HEIGHTS AND STRENGTHS, GREENSBORO, NORTH CAROLINA
MARCH, 1999 - 2005

March	Mornings with Inversions[1]	Average Morning Height[2] (m)	Average Morning Strength[3] (0.1ºC/m)	Afternoons with Inversions[1]	Average Afternoon Height[2] (m)	Average Afternoon Strength[3] (0.1ºC/m)
1999	5	943	0.290	3	1463	0.277
2000	7	883	0.245	2	1770	0.323
2001	2	1702	0.217	3	2019	0.234
2002	12	842	0.267	6	1281	0.146
2003	3	680	0.338	3	552	0.236
2004	11	1125	0.389	3	2324	0.299
2005	0			1	2891	1.636
Total	40	970	0.303	21	1580	0.300

NOTES:

1. Inversion is defined as three or more NOAA weather balloon elevation readings showing consecutive increases in temperature with height below 3000 m.

2. Balloons were released each day at 0:00 Greenwich Mean Time (GMT) and 12:00 GMT. Height is defined as elevation in meters where temperature first increases and is averaged only over those days with inversions.

3. Strength is the maximum temperature gradient in tenths of a degree centigrade per meter within the inversion layer.

4. Data from: FSL/NCDC Radiosonde Data Archive, http://raob.fsl.noaa.gov/

WLS COL 2.3-1

TABLE 2.3-267
INVERSION HEIGHTS AND STRENGTHS, GREENSBORO, NORTH CAROLINA
APRIL, 1999 - 2005

April	Mornings with Inversions[1]	Average Morning Height[2] (m)	Average Morning Strength[3] (0.1ºC/m)	Afternoons with Inversions[1]	Average Afternoon Height[2] (m)	Average Afternoon Strength[3] (0.1ºC/m)
1999	5	1299	0.321	0		
2000	7	568	0.398	0		
2001	2	1712	0.444	1	2372	0.103
2002	7	956	0.182	0		
2003	8	751	0.294	2	1300	0.302
2004	10	614	0.379	2	647	0.179
2005	1	760	0.162	0		
Total	40	837	0.322	5	1253	0.213

NOTES:

1. Inversion is defined as three or more NOAA weather balloon elevation readings showing consecutive increases in temperature with height below 3000 m.

2. Balloons were released each day at 0:00 Greenwich Mean Time (GMT) and 12:00 GMT. Height is defined as elevation in meters where temperature first increases and is averaged only over those days with inversions.

3. Strength is the maximum temperature gradient in tenths of a degree centigrade per meter within the inversion layer.

4. Data from: FSL/NCDC Radiosonde Data Archive, http://raob.fsl.noaa.gov/

WLS COL 2.3-1

TABLE 2.3-268
INVERSION HEIGHTS AND STRENGTHS, GREENSBORO, NORTH CAROLINA
MAY, 1999 – 2005

May	Mornings with Inversions[1]	Average Morning Height[2] (m)	Average Morning Strength[3] (0.1ºC/m)	Afternoons with Inversions[1]	Average Afternoon Height[2] (m)	Average Afternoon Strength[3] (0.1ºC/m)
1999	5	513	0.401	0		
2000	4	950	0.225	0		
2001	4	1290	0.175	0		
2002	3	627	0.196	2	1187	0.090
2003	1	1576	0.099	2	1248	0.175
2004	1	389	0.104	0		
2005	2	631	0.268	0		
Total	20	832	0.247	4	1217	0.132

1. Inversion is defined as three or more NOAA weather balloon elevation readings showing consecutive increases in temperature with height below 3000 m.

2. Balloons were released each day at 0:00 GTM and 12:00 GMT. Height is defined as elevation in meters where temperature first increases and is averaged only over those days with inversions.

3. Strength is the maximum temperature gradient in tenths of a degree centigrade per meter within the inversion layer.

4. Data from: FSL/NCDC Radiosonde Data Archive, http://raob.fsl.noaa.gov/

WLS COL 2.3-1

TABLE 2.3-269
INVERSION HEIGHTS AND STRENGTHS, GREENSBORO, NORTH CAROLINA
JUNE, 1999 – 2005

June	Mornings with Inversions[1]	Average Morning Height[2] (m)	Average Morning Strength[3] (0.1ºC/m)	Afternoons with Inversions[1]	Average Afternoon Height[2] (m)	Average Afternoon Strength[3] (0.1ºC/m)
1999	4	1479	0.284	0		
2000	1	277	0.667	0		
2001	2	2153	0.255	1	2403	0.667
2002	5	1008	0.456	0		
2003	2	1693	0.436	1	2038	0.211
2004	0			0		
2005	0			1	2548	0.277
Total	14	1352	0.390	3	2330	0.385

1. Inversion is defined as three or more NOAA weather balloon elevation readings showing consecutive increases in temperature with height below 3000 m.

2. Balloons were released each day at 0:00 GMT and 12:00 GMT. Height is defined as elevation in meters where temperature first increases and is averaged only over those days with inversions.

3. Strength is the maximum temperature gradient in tenths of a degree centigrade per meter within the inversion layer.

4. Data from: FSL/NCDC Radiosonde Data Archive, http://raob.fsl.noaa.gov/

WLS COL 2.3-1

TABLE 2.3-270
INVERSION HEIGHTS AND STRENGTHS, GREENSBORO, NORTH CAROLINA
JULY, 1999 - 2005

July	Mornings with Inversions[1]	Average Morning Height[2] (m)	Average Morning Strength[3] (0.1ºC/m)	Afternoons with Inversions[1]	Average Afternoon Height[2] (m)	Average Afternoon Strength[3] (0.1ºC/m)
1999	1	640	0.079	0		
2000	0			0		
2001	1	277	0.101	1	1896	0.238
2002	0			0		
2003	0			0		
2004	0			0		
2005	0			0		
Total	2	459	0.090	1	1896	0.238

1. Inversion is defined as three or more NOAA weather balloon elevation readings showing consecutive increases in temperature with height below 3000 m.

2. Balloons were released each day at 0:00 GMT and 12:00 GMT. Height is defined as elevation in meters where temperature first increases and is averaged only over those days with inversions.

3. Strength is the maximum temperature gradient in tenths of a degree centigrade per meter within the inversion layer.

4. Data from: FSL/NCDC Radiosonde Data Archive, http://raob.fsl.noaa.gov/

WLS COL 2.3-1

TABLE 2.3-271
INVERSION HEIGHTS AND STRENGTHS, GREENSBORO, NORTH CAROLINA
AUGUST, 1999 - 2005

August	Mornings with Inversions[1]	Average Morning Height[2] (m)	Average Morning Strength[3] (0.1ºC/m)	Afternoons with Inversions[1]	Average Afternoon Height[2] (m)	Average Afternoon Strength[3] (0.1ºC/m)
1999	3	661	0.371	0		
2000	3	829	0.461	2	2287	0.306
2001	2	1285	0.515	0		
2002	2	1340	0.188	0		
2003	1	277	0.329	0		
2004	2	1309	0.258	3	2420	0.303
2005	2	1429	0.630	1	1941	0.476
Total	15	1031	0.400	6	2296	0.333

1. Inversion is defined as three or more NOAA weather balloon elevation readings showing consecutive increases in temperature with height below 3000 m.

2. Balloons were released each day at 0:00 GMT and 12:00 GMT. Height is defined as elevation in meters where temperature first increases and is averaged only over those days with inversions.

3. Strength is the maximum temperature gradient in tenths of a degree centigrade per meter within the inversion layer.

4. Data from: FSL/NCDC Radiosonde Data Archive, http://raob.fsl.noaa.gov/

WLS COL 2.3-1

TABLE 2.3-272
INVERSION HEIGHTS AND STRENGTHS, GREENSBORO, NORTH CAROLINA
SEPTEMBER, 1999 - 2005

September	Mornings with Inversions[1]	Average Morning Height[2] (m)	Average Morning Strength[3] (0.1ºC/m)	Afternoons with Inversions[1]	Average Afternoon Height[2] (m)	Average Afternoon Strength[3] (0.1ºC/m)
1999	5	1022	0.427	4	2064	0.232
2000	8	1364	0.233	7	1569	0.279
2001	7	1877	0.318	4	1935	0.425
2002	3	1583	0.223	2	1586	0.105
2003	3	1631	0.217	1	2001	0.118
2004	13	1440	0.248	5	1414	0.272
2005	10	1469	0.387	6	2227	0.331
Total	49	1474	0.299	29	1813	0.285

1. Inversion is defined as three or more NOAA weather balloon elevation readings showing consecutive increases in temperature with height below 3000 m.

2. Balloons were released each day at 0:00 GMT and 12:00 GMT. Height is defined as elevation in meters where temperature first increases and is averaged only over those days with inversions.

3. Strength is the maximum temperature gradient in tenths of a degree centigrade per meter within the inversion layer.

4. Data from: FSL/NCDC Radiosonde Data Archive, http://raob.fsl.noaa.gov/

WLS COL 2.3-1

TABLE 2.3-273
INVERSION HEIGHTS AND STRENGTHS, GREENSBORO, NORTH CAROLINA
OCTOBER, 1999 - 2005

October	Mornings with Inversions[1]	Average Morning Height[2] (m)	Average Morning Strength[3] (0.1ºC/m)	Afternoons with Inversions[1]	Average Afternoon Height[2] (m)	Average Afternoon Strength[3] (0.1ºC/m)
1999	13	1122	0.364	9	1690	0.331
2000	4	596	0.696	1	2089	0.200
2001	9	1890	0.254	3	1925	0.319
2002	7	727	0.291	4	1654	0.215
2003	4	1500	0.338	4	1901	0.365
2004	3	1395	0.263	4	1202	0.311
2005	8	1248	0.358	5	1629	0.360
Total	48	1234	0.351	30	1675	0.317

1. Inversion is defined as three or more NOAA weather balloon elevation readings showing consecutive increases in temperature with height below 3000 m.

2. Balloons were released each day at 0:00 GMT and 12:00 GMT. Height is defined as elevation in meters where temperature first increases and is averaged only over those days with inversions.

3. Strength is the maximum temperature gradient in tenths of a degree centigrade per meter within the inversion layer.

4. Data from: FSL/NCDC Radiosonde Data Archive, http://raob.fsl.noaa.gov/

WLS COL 2.3-1

TABLE 2.3-274
INVERSION HEIGHTS AND STRENGTHS, GREENSBORO, NORTH CAROLINA
NOVEMBER, 1999 – 2005

November	Mornings with Inversions[1]	Average Morning Height[2] (m)	Average Morning Strength[3] (0.1ºC/m)	Afternoons with Inversions[1]	Average Afternoon Height[2] (m)	Average Afternoon Strength[3] (0.1ºC/m)
1999	5	1235	0.464	2	1109	0.177
2000	4	690	0.279	4	1287	0.300
2001	12	941	0.397	5	1987	0.228
2002	9	990	0.525	2	1320	0.198
2003	12	767	0.346	5	1211	0.409
2004	6	907	0.169	3	1185	0.501
2005	14	662	0.593	5	964	0.293
Total	62	856	0.426	26	1322	0.312

1. Inversion is defined as three or more NOAA weather balloon elevation readings showing consecutive increases in temperature with height below 3000 m.

2. Balloons were released each day at 0:00 GMT and 12:00 GMT. Height is defined as elevation in meters where temperature first increases and is averaged only over those days with inversions.

3. Strength is the maximum temperature gradient in tenths of a degree centigrade per meter within the inversion layer.

4. Data from: FSL/NCDC Radiosonde Data Archive, http://raob.fsl.noaa.gov/

WLS COL 2.3-1

TABLE 2.3-275
INVERSION HEIGHTS AND STRENGTHS, GREENSBORO, NORTH CAROLINA
DECEMBER, 1999 – 2005

December	Mornings with Inversions[1]	Average Morning Height[2] (m)	Average Morning Strength[3] (0.1ºC/m)	Afternoons with Inversions[1]	Average Afternoon Height[2] (m)	Average Afternoon Strength[3] (0.1ºC/m)
1999	18	748	0.723	6	1561	0.347
2000	15	873	0.272	14	1026	0.229
2001	11	1398	0.340	7	1035	0.225
2002	18	776	0.333	16	1030	0.273
2003	14	762	0.339	10	1354	0.278
2004	11	840	0.519	9	1566	0.318
2005	12	900	0.294	9	1099	0.233
Total	99	875	0.412	71	1197	0.267

1. Inversion is defined as three or more NOAA weather balloon elevation readings showing consecutive increases in temperature with height below 3000 m.

2. Balloons were released each day at 0:00 GMT and 12:00 GMT. Height is defined as elevation in meters where temperature first increases and is averaged only over those days with inversions.

3. Strength is the maximum temperature gradient in tenths of a degree centigrade per meter within the inversion layer.

4. Data from: FSL/NCDC Radiosonde Data Archive, http://raob.fsl.noaa.gov/

WLS COL 2.3-1

TABLE 2.3-276
INVERSION HEIGHTS AND STRENGTHS, GREENSBORO, NORTH CAROLINA
ANNUAL, 1999 – 2005

Annual	Mornings with Inversions[1]	Average Morning Height[2] (m)	Average Morning Strength[3] (0.1ºC/m)	Afternoons with Inversions[1]	Average Afternoon Height[2] (m)	Average Afternoon Strength[3] (0.1ºC/m)
1999	80	901	0.487	37	1386	0.304
2000	76	915	0.287	44	1295	0.255
2001	69	1325	0.311	34	1675	0.286
2002	85	907	0.328	47	1212	0.223
2003	69	926	0.305	43	1212	0.268
2004	83	981	0.339	51	1396	0.290
2005	50	1009	0.420	33	1491	0.348
Total	512	988	0.352	289	1366	0.279

1. Inversion is defined as three or more NOAA weather balloon elevation readings showing consecutive increases in temperature with height below 3000 m.

2. Balloons were released each day at 0:00 GMT and 12:00 GMT. Height is defined as elevation in meters where temperature first increases and is averaged only over those days with inversions.

3. Strength is the maximum temperature gradient in tenths of a degree centigrade per meter within the inversion layer.

4. Data from: FSL/NCDC Radiosonde Data Archive, http://raob.fsl.noaa.gov/

WLS COL 2.3-1

TABLE 2.3-277
MIXING HEIGHTS AT GREENSBORO, NORTH CAROLINA

Month	Morning (m)	Afternoon (m)
January	480	825
February	477	982
March	502	1310
April	489	1735
May	431	1578
June	445	1764
July	473	1629
August	495	1435
September	394	1384
October	342	1187
November	402	853
December	450	781
Annual	448	1289

NOTES:

1. Data is from the NCDC SCRAM Mixing Height Data collection for the period of 1984-1987 and 1990-1991 http://www.epa.gov/scram001/surfacemetdata.htm#tn

WLS COL 2.3-2

TABLE 2.3-278
VISIBLE PLUME FREQUENCY OF OCCURRENCE BY SEASON
(ALL WIND DIRECTIONS)

	Percent Frequency of Occurrence					
	100	80	60	40	20	1
Winter:						
length (m)	100	200	400	900	5,100	9,900
height (m)	40	120	160	370	1,400	1,400
radius (m)	25	45	60	85	520	1,400
Spring:						
length (m)	100	200	250	300	4,800	9,900
height (m)	40	110	120	160	1,400	1,400
radius (m)	25	35	45	60	470	650
Summer:						
length (m)	100	150	200	250	600	9,800
height (m)	40	110	120	130	330	1,400
radius (m)	25	35	40	45	75	650
Fall:						
length (m)	100	200	250	400	4,700	9,900
height (m)	40	110	125	160	1,400	1,400
radius (m)	25	35	45	60	435	1,400
Annual:						
length (m)	100	200	250	400	4,600	9,900
height (m)	40	110	120	170	1,400	1,400
radius (m)	25	35	40	65	435	1,400

Notes:

1. SACTI results based on: U. S. Department of Commerce, National Oceanic and Atmospheric Administration National Climatic Data Center (NCDC), "Integrated Surface Hourly", 2001-2005, Charlotte, NC.

2. Mixing height from George C. Holzworth, "Mixing Heights, Wind Speeds, and Potential for Urban Air Pollution Throughout the Contiguous United States", Reference 219.

WLS COL 2.3-2

TABLE 2.3-279
FREQUENCY OF PLUME SHADOWING BY SEASON
(AVERAGE FOR ALL WIND DIRECTIONS)

	Percent Frequency of Occurrence				
	10%	5%	2%	1%	0.5%
Winter:					
downwind distance (m)	200	300	600	1,600	4,600
Spring:					
downwind distance (m)	200	300	600	1,200	4,200
Summer:					
downwind distance (m)	100	300	400	600	1,400
Fall:					
downwind distance (m)	200	300	500	1,000	3,200

Notes:

1. SACTI results based on: U. S. Department of Commerce, National Oceanic and Atmospheric Administration National Climatic Data Center (NCDC), "Integrated Surface Hourly", 2001-2005, Charlotte, NC.

2. Mixing height from George C. Holzworth, "Mixing Heights, Wind Speeds, and Potential for Urban Air Pollution Throughout the Contiguous United States", Reference 219.

WLS COL 2.3-2

TABLE 2.3-280 (Sheet 1 of 4)
MAXIMUM SALT DRIFT DEPOSITION RATE (KG/KM^2/MO)

	Summer																
Downwind	Plume Headed																
Distance (m)	S	SSW	SW	WSW	W	WNW	NW	NNW	N	NNE	NE	ENE	E	ESE	SE	SSE	All
100	**0.00**	**0.00**	**0.00**	**0.00**	**0.00**	**0.00**	**0.00**	**0.00**	**0.00**	**0.00**	**0.00**	**0.00**	**0.00**	**0.00**	**0.00**	**0.00**	0.00
200	**0.38**	**0.08**	**0.12**	**0.17**	**0.18**	**0.04**	**0.15**	**0.20**	**1.18**	**0.73**	**0.48**	**0.16**	**0.26**	**0.37**	**0.38**	**0.25**	0.32
300	**0.00**	**0.00**	**0.00**	**0.00**	**0.00**	**0.00**	**0.00**	**0.00**	**0.00**	**0.00**	**0.00**	**0.00**	**0.00**	**0.00**	**0.00**	**0.00**	0.00
400	**0.00**	**0.00**	**0.00**	**0.00**	**0.00**	**0.00**	**0.00**	**0.00**	**0.00**	**0.00**	**0.00**	0.00	0.00	0.00	**0.01**	**0.00**	0.00
500	**0.00**	**0.00**	**0.00**	**0.00**	**0.00**	**0.00**	**0.00**	**0.00**	**0.00**	**0.00**	0.00	0.00	0.00	0.01	**0.01**	**0.00**	0.00
600	**0.00**	**0.00**	**0.00**	**0.00**	**0.00**	**0.00**	**0.00**	**0.00**	0.01	0.00	0.00	0.00	0.00	0.01	**0.01**	**0.00**	0.00
700	**0.00**	**0.00**	**0.00**	**0.00**	**0.00**	**0.00**	**0.00**	0.00	0.01	0.00	0.00	0.00	0.00	0.01	0.01	**0.00**	0.00
800	**0.00**	**0.00**	**0.00**	**0.00**	**0.00**	**0.00**	0.00	0.00	0.01	0.00	0.00	0.00	0.00	0.01	0.01	**0.00**	0.00
900	**0.00**	**0.00**	**0.00**	**0.00**	**0.00**	**0.00**	0.00	0.00	0.01	0.01	0.01	0.00	0.00	0.01	0.01	0.00	0.00
1000	**0.01**	**0.00**	**0.01**	**0.01**	**0.01**	**0.01**	0.01	0.00	0.02	0.02	0.01	0.00	0.00	0.01	0.02	0.00	0.01
1100	**0.01**	**0.00**	**0.01**	**0.01**	**0.01**	**0.01**	0.01	0.01	0.05	0.02	0.01	0.00	0.00	0.02	0.04	0.00	0.01
1200	**0.01**	**0.00**	**0.01**	**0.01**	**0.01**	**0.01**	0.01	0.01	0.05	0.02	0.01	0.00	0.00	0.02	0.04	0.00	0.01
1300	**0.01**	**0.00**	**0.00**	**0.00**	**0.00**	**0.00**	0.00	0.01	0.05	0.01	0.01	0.00	0.00	0.02	0.02	0.00	0.01
1400	**0.01**	**0.00**	**0.00**	**0.00**	**0.00**	**0.00**	0.00	0.01	0.02	0.01	0.01	0.00	0.00	0.02	0.02	0.00	0.01
1500	**0.01**	**0.00**	**0.00**	**0.00**	**0.00**	**0.00**	0.00	0.00	0.02	0.01	0.01	0.00	0.00	0.01	0.02	0.00	0.01
1600	**0.01**	**0.00**	**0.00**	**0.00**	**0.00**	0.00	0.00	0.00	0.02	0.01	0.01	0.00	0.00	0.01	0.02	0.00	0.01
1700	**0.01**	**0.00**	**0.00**	**0.00**	**0.00**	0.00	0.00	0.00	0.02	0.01	0.01	0.00	0.00	0.01	0.02	0.00	0.01
1800	**0.01**	**0.00**	**0.00**	**0.00**	**0.00**	0.00	0.00	0.00	0.02	0.01	0.01	0.00	0.00	0.01	0.02	0.00	0.01
1900	**0.01**	**0.00**	**0.00**	**0.00**	**0.00**	0.00	0.00	0.00	0.02	0.01	0.01	0.00	0.00	0.01	0.02	0.00	0.01
2000	**0.01**	**0.00**	**0.00**	**0.00**	**0.00**	0.00	0.00	0.00	0.02	0.01	0.00	0.00	0.00	0.01	0.01	0.00	0.00

WLS COL 2.3-2

TABLE 2.3-280 (Sheet 2 of 4)
MAXIMUM SALT DRIFT DEPOSITION RATE (kg/km^2/mo)

Fall

Downwind Distance (m)	S	SSW	SW	WSW	W	WNW	NW	NNW	N	NNE	NE	ENE	EW	ESE	SE	SSE	ALL SUM
100	**0.00**	**0.00**	**0.00**	**0.00**	**0.00**	**0.00**	**0.00**	**0.00**	**0.00**	**0.00**	**0.00**	**0.00**	**0.00**	**0.00**	**0.00**	**0.00**	0.00
200	**0.56**	**0.14**	**0.17**	**0.18**	**0.28**	**0.20**	**0.11**	**0.34**	**0.65**	**0.56**	**0.31**	**0.05**	**0.18**	**0.33**	**0.49**	**0.29**	0.30
300	**0.00**	**0.00**	**0.00**	**0.00**	**0.00**	**0.00**	**0.00**	**0.00**	**0.00**	**0.00**	**0.00**	**0.00**	**0.00**	**0.00**	**0.00**	**0.00**	0.00
400	**0.00**	**0.00**	**0.00**	**0.00**	**0.00**	**0.00**	**0.00**	**0.00**	**0.00**	**0.00**	**0.00**	0.00	0.00	0.00	**0.02**	**0.00**	0.00
500	**0.00**	**0.00**	**0.00**	**0.00**	**0.00**	**0.00**	**0.01**	**0.01**	**0.02**	**0.00**	0.00	0.00	0.00	0.02	**0.03**	**0.01**	0.01
600	**0.01**	**0.00**	**0.00**	**0.00**	**0.00**	**0.00**	**0.01**	**0.01**	0.02	0.00	0.00	0.00	0.00	0.02	**0.03**	**0.02**	0.01
700	**0.01**	**0.00**	**0.00**	**0.00**	**0.00**	**0.00**	**0.01**	0.01	0.02	0.00	0.00	0.00	0.00	0.02	0.03	**0.01**	0.01
800	**0.00**	**0.00**	**0.00**	**0.00**	**0.00**	**0.00**	0.01	0.01	0.02	0.00	0.00	0.00	0.00	0.02	0.03	**0.01**	0.01
900	**0.00**	**0.00**	**0.00**	**0.00**	**0.00**	**0.00**	0.01	0.01	0.02	0.01	0.00	0.00	0.00	0.02	0.05	0.01	0.01
1000	**0.01**	**0.00**	**0.00**	**0.00**	**0.01**	**0.01**	0.02	0.02	0.02	0.02	0.00	0.01	0.00	0.02	0.12	0.02	0.02
1100	**0.02**	**0.00**	**0.00**	**0.00**	**0.01**	**0.01**	0.02	0.05	0.06	0.02	0.00	0.01	0.00	0.07	0.12	0.05	0.03
1200	**0.02**	**0.00**	**0.00**	**0.00**	**0.01**	**0.01**	0.02	0.05	0.06	0.02	0.00	0.01	0.00	0.07	0.12	0.05	0.03
1300	**0.02**	**0.00**	**0.00**	**0.00**	**0.00**	**0.00**	0.01	0.05	0.06	0.01	0.00	0.01	0.00	0.07	0.06	0.05	0.02
1400	**0.02**	**0.00**	**0.00**	**0.00**	**0.00**	**0.00**	0.01	0.05	0.05	0.01	0.00	0.00	0.00	0.06	0.05	0.05	0.02
1500	**0.01**	**0.00**	**0.00**	**0.00**	**0.00**	**0.00**	0.01	0.02	0.02	0.01	0.00	0.00	0.00	0.03	0.05	0.02	0.01
1600	**0.01**	**0.00**	**0.00**	**0.00**	**0.00**	0.00	0.01	0.02	0.02	0.01	0.00	0.00	0.00	0.03	0.05	0.02	0.01
1700	**0.01**	**0.00**	**0.00**	**0.00**	**0.00**	0.00	0.01	0.02	0.02	0.01	0.00	0.00	0.00	0.03	0.05	0.02	0.01
1800	**0.01**	**0.00**	**0.00**	**0.00**	**0.00**	0.00	0.01	0.02	0.02	0.01	0.00	0.00	0.00	0.03	0.05	0.02	0.01
1900	**0.01**	**0.00**	**0.00**	**0.00**	**0.00**	0.00	0.01	0.02	0.02	0.01	0.00	0.00	0.00	0.03	0.05	0.02	0.01
2000	**0.01**	**0.00**	**0.00**	**0.00**	**0.00**	0.00	0.01	0.02	0.02	0.01	0.00	0.00	0.00	0.03	0.03	0.02	0.01

WLS COL 2.3-2

TABLE 2.3-280 (Sheet 3 of 4)
MAXIMUM SALT DRIFT DEPOSITION RATE (kg/km^2/mo)

	Winter																
Downwind	Plume Headed																
Distance	S	SSW	SW	WSW	W	WNW	NW	NNW	N	NNE	NE	ENE	E	ESE	SE	SSE	All
100	**0.00**	**0.00**	**0.00**	**0.00**	**0.00**	**0.00**	**0.00**	**0.00**	**0.00**	**0.00**	**0.00**	**0.00**	**0.00**	**0.00**	**0.00**	**0.00**	0.00
200	**0.27**	**0.08**	**0.03**	**0.06**	**0.06**	**0.10**	**0.16**	**0.35**	**0.53**	**0.57**	**0.14**	**0.11**	**0.14**	**0.29**	**0.30**	**0.17**	0.21
300	**0.00**	**0.00**	**0.00**	**0.00**	**0.00**	**0.00**	**0.00**	**0.00**	**0.00**	**0.00**	**0.00**	**0.00**	**0.00**	**0.00**	**0.00**	**0.00**	0.00
400	**0.00**	**0.00**	**0.00**	**0.00**	**0.00**	**0.00**	**0.00**	**0.00**	**0.00**	**0.00**	**0.00**	0.00	0.00	0.00	**0.01**	**0.00**	0.00
500	**0.00**	**0.00**	**0.00**	**0.00**	**0.00**	**0.00**	**0.00**	**0.01**	**0.01**	**0.01**	0.00	0.01	0.01	0.01	**0.01**	**0.01**	0.01
600	**0.00**	**0.00**	**0.00**	**0.00**	**0.00**	**0.00**	**0.00**	**0.01**	0.01	0.01	0.00	0.01	0.01	0.01	**0.01**	**0.01**	0.01
700	**0.00**	**0.00**	**0.00**	**0.00**	**0.00**	**0.00**	**0.00**	0.01	0.01	0.01	0.00	0.01	0.01	0.01	0.01	**0.01**	0.01
800	**0.00**	**0.00**	**0.00**	**0.00**	**0.00**	**0.00**	0.00	0.01	0.01	0.01	0.00	0.01	0.01	0.01	0.01	**0.01**	0.01
900	**0.00**	**0.00**	**0.00**	**0.00**	**0.00**	**0.00**	0.00	0.01	0.01	0.01	0.01	0.01	0.01	0.01	0.02	0.01	0.01
1000	**0.00**	**0.01**	**0.00**	**0.00**	**0.01**	**0.00**	0.00	0.01	0.02	0.03	0.02	0.02	0.01	0.01	0.05	0.01	0.01
1100	**0.01**	**0.01**	**0.00**	**0.00**	**0.01**	**0.00**	0.00	0.02	0.05	0.03	0.02	0.02	0.02	0.03	0.05	0.03	0.02
1200	**0.01**	**0.01**	**0.00**	**0.00**	**0.01**	**0.00**	0.00	0.02	0.05	0.03	0.02	0.02	0.02	0.03	0.05	0.03	0.02
1300	**0.01**	**0.01**	**0.00**	**0.00**	**0.00**	**0.00**	0.00	0.02	0.05	0.02	0.01	0.01	0.02	0.03	0.02	0.03	0.02
1400	**0.01**	**0.00**	**0.00**	**0.00**	**0.00**	**0.00**	0.00	0.02	0.05	0.01	0.01	0.01	0.02	0.03	0.02	0.03	0.01
1500	**0.01**	**0.01**	**0.00**	**0.00**	**0.00**	**0.00**	0.00	0.01	0.02	0.01	0.01	0.01	0.01	0.01	0.02	0.01	0.01
1600	**0.01**	**0.01**	**0.00**	**0.00**	**0.00**	0.00	0.00	0.01	0.02	0.02	0.01	0.01	0.01	0.01	0.02	0.01	0.01
1700	**0.01**	**0.01**	**0.00**	**0.00**	**0.00**	0.00	0.00	0.01	0.02	0.02	0.01	0.01	0.01	0.01	0.02	0.01	0.01
1800	**0.01**	**0.01**	**0.00**	**0.00**	**0.00**	0.00	0.00	0.01	0.02	0.02	0.01	0.01	0.01	0.01	0.02	0.01	0.01
1900	**0.01**	**0.01**	**0.00**	**0.00**	**0.00**	0.00	0.00	0.01	0.02	0.02	0.01	0.01	0.01	0.01	0.02	0.01	0.01
2000	**0.01**	**0.00**	**0.00**	**0.00**	**0.00**	0.00	0.00	0.01	0.02	0.01	0.01	0.01	0.01	0.01	0.01	0.01	0.01

WLS COL 2.3-2

TABLE 2.3-280 (Sheet 4 of 4)
MAXIMUM SALT DRIFT DEPOSITION RATE (kg/km^2/mo)

Downwind Distance (m)	Spring Plume Headed S	SSW	SW	WSW	W	WNW	NW	NNW	N	NNE	NE	ENE	E	ESE	SE	SSE	S
100	**0.00**	**0.00**	**0.00**	**0.00**	**0.00**	**0.00**	**0.00**	**0.00**	**0.00**	**0.00**	**0.00**	**0.00**	**0.00**	**0.00**	**0.00**	**0.00**	0.00
200	**0.18**	**0.08**	**0.08**	**0.07**	**0.12**	**0.06**	**0.08**	**0.27**	**0.92**	**0.60**	**0.17**	**0.07**	**0.13**	**0.33**	**0.16**	**0.20**	0.22
300	**0.00**	**0.00**	**0.00**	**0.00**	**0.00**	**0.00**	**0.00**	**0.00**	**0.00**	**0.00**	**0.00**	**0.00**	**0.00**	**0.00**	**0.00**	**0.00**	0.00
400	**0.00**	**0.00**	**0.00**	**0.00**	**0.00**	**0.00**	**0.00**	**0.00**	**0.00**	**0.00**	**0.00**	0.00	0.00	0.00	**0.00**	**0.00**	0.00
500	**0.01**	**0.00**	**0.00**	**0.00**	**0.00**	**0.00**	**0.00**	**0.00**	**0.01**	**0.00**	0.00	0.00	0.00	0.00	**0.00**	**0.00**	0.00
600	**0.01**	**0.00**	**0.00**	**0.00**	**0.00**	**0.00**	**0.00**	**0.00**	0.01	0.00	0.00	0.00	0.00	0.00	**0.00**	**0.00**	0.00
700	**0.01**	**0.00**	**0.00**	**0.00**	**0.00**	**0.00**	**0.00**	0.00	0.01	0.00	0.00	0.00	0.00	0.01	0.00	**0.00**	0.00
800	**0.01**	**0.00**	**0.00**	**0.00**	**0.00**	**0.00**	0.00	0.00	0.01	0.00	0.00	0.00	0.00	0.00	0.00	**0.00**	0.00
900	**0.01**	**0.00**	**0.01**	**0.00**	**0.00**	**0.00**	0.00	0.00	0.01	0.01	0.00	0.00	0.00	0.00	0.00	0.00	0.00
1000	**0.01**	**0.00**	**0.01**	**0.00**	**0.00**	**0.00**	0.00	0.00	0.01	0.01	0.01	0.00	0.00	0.00	0.01	0.00	0.01
1100	**0.04**	**0.00**	**0.01**	**0.00**	**0.00**	**0.00**	0.00	0.01	0.02	0.01	0.01	0.00	0.00	0.01	0.01	0.01	0.01
1200	**0.04**	**0.00**	**0.01**	**0.01**	**0.00**	**0.00**	0.00	0.01	0.02	0.01	0.01	0.00	0.00	0.02	0.01	0.01	0.01
1300	**0.04**	**0.00**	**0.01**	**0.01**	**0.00**	**0.00**	0.00	0.01	0.02	0.01	0.00	0.00	0.00	0.02	0.01	0.01	0.01
1400	**0.03**	**0.00**	**0.01**	**0.00**	**0.00**	**0.00**	0.00	0.01	0.02	0.01	0.00	0.00	0.00	0.01	0.01	0.01	0.01
1500	**0.01**	**0.00**	**0.01**	**0.00**	**0.00**	**0.00**	0.00	0.00	0.01	0.01	0.00	0.00	0.00	0.01	0.01	0.01	0.00
1600	**0.01**	**0.00**	**0.01**	**0.00**	**0.00**	0.00	0.00	0.00	0.01	0.01	0.00	0.00	0.00	0.01	0.01	0.01	0.00
1700	**0.01**	**0.00**	**0.01**	**0.00**	**0.00**	0.00	0.00	0.00	0.01	0.01	0.00	0.00	0.00	0.01	0.01	0.01	0.00
1800	**0.01**	**0.00**	**0.01**	**0.00**	**0.00**	0.00	0.00	0.00	0.01	0.01	0.00	0.00	0.00	0.01	0.01	0.01	0.00
1900	**0.01**	**0.00**	**0.01**	**0.00**	**0.00**	0.00	0.00	0.00	0.01	0.01	0.00	0.00	0.00	0.01	0.01	0.01	0.00
2000	**0.01**	**0.00**	**0.00**	**0.00**	**0.00**	0.00	0.00	0.00	0.01	0.01	0.00	0.00	0.00	0.01	0.00	0.01	0.00

Notes:
1. Bold Values indicate on-site locations
2. SACTI modeling based on surface meteorological data from CLT, U. S. Department of Commerce, National Oceanic and Atmospheric Administration National Climatic Data Center (NCDC), "Integrated Surface Hourly", 2001-2005, Charlotte, NC.
3. Mixing height from George C. Holzworth, "Mixing Heights, Wind Speeds, and Potential for Urban Air Pollution Throughout the Contiguous United States", Reference 219.

WLS COL 2.3-3

TABLE 2.3-281 (Sheet 1 of 2)
METEOROLOGICAL TOWER INSTRUMENTATION

Tower 2[a]

Meteorological Variable	Range	Units	Accuracy	Resolution	Basis
Wind Speed (10 & 60m)	0 to 60	mph	± 0.5 or 5% of observed wind speed; starting threshold < 1 mph	0.1	NRC Regulatory Guide 1.23
Wind Direction (10 & 60m)	0 to 360	(degrees from True North)	± 5	1	NRC Regulatory Guide 1.23
Temperature[b] (10 & 60m)	-20 to +40	Celsius	± 0.5	0.1	NRC Regulatory Guide 1.23
Delta-T[b] (60m - 10m)	Calculated[c]	Celsius	± 0.1	0.01	NRC Regulatory Guide 1.23
Surface Temperature[d] (2m)	-20 to +40	Celsius	± 0.5	0.1	NRC Regulatory Guide 1.23
Delta-T[d] (10m - 2m)	Calculated[c]	Celsius	± 0.1	0.01	NRC Regulatory Guide 1.23
Dewpoint Temperature (10m)	-50 to +50	Celsius	± 1.5	0.1	NRC Regulatory Guide 1.23
Precipitation	---	Inches	± 10%	0.01	NRC Regulatory Guide 1.23
Station Pressure[d][e]	880 to 1085	millibars	± 3 or 0.25%	0.1	ANSI/ANS 3.11-2005
Incoming Solar Radiation[d][e]	0 to 1400	watts/m^2	± 10 or 5%	1	ANSI/ANS 3.11-2005

WLS COL 2.3-3

TABLE 2.3-281 (Sheet 2 of 2)
METEOROLOGICAL TOWER INSTRUMENTATION

Tower 2[a]

Meteorological Variable	Range	Units	Accuracy	Resolution	Basis
Outgoing Longwave Radiation (upwelling from ground)[d][e]	0 to 700	watts/m^2	± 10 or 5%	1	ANSI/ANS 3.11-2005
Time[f]	0000 to 2359	minutes	± 5	1	NRC Regulatory Guide 1.23
Datalogger Sampling Rate	---	---	At least 5 seconds	---	NRC Regulatory Guide 1.23

a) Tower 2 data has been used for air dispersion modeling and site characterization in the ER and FSAR, as most representative of the site. Equipment operational on December 1, 2005.

b) Delta temperature between the 60m and 10m levels is used in stability class determination.

c) Delta-T is calculated by datalogger from upper and lower temperature sensor output (i.e., $T_{Upper} - T_{Lower}$). Although the range of measureable vertical temperature difference is constrained only by temperature sensor range limitations, a range of -4 to +8 degree Celsius is applied in calibration procedure bases for demonstrating compliance with the ± 0.1 °C accuracy requirement for Delta-T.

d) Optional measurement variable only.

e) There are no accuracies specific in Regulatory Guide 1.23 for these parameters. ANS/ANSI 3.11-2005 accuracy guidance adopted as state-of-the-art specification.

f) The 1-minute readings are averaged into 1-hour averages on Tower 2 during the pre-construction/pre-operational phase. During the operational phase, the 1-minute readings will also be compiled into 15-minute averages and 1-hour averages for real-time display in emergency response facilities. Hourly averaged data is verified and archived.

WLS COL 2.3-4

TABLE 2.3-282
MINIMUM EXCLUSION AREA BOUNDARY (EAB) DISTANCES
[FROM INNER 550 FT (168 M) RADIUS CIRCLE
ENCOMPASSING ALL SITE RELEASE POINTS]

Direction	Distance (ft)	Distance (m)
S	4576	1395
SSW	4576	1395
SW	5075	1547
WSW	5411	1649
W	3964	1208
WNW	3964	1208
NW	3985	1215
NNW	2192	668
N	2113	644
NNE	2113	644
NE	2313	705
ENE	3124	952
E	4207	1282
ESE	5065	1544
SE	4393	1339
SSE	4393	1339

NOTE:

1. Exclusion Area Boundary (EAB) for Lee Nuclear Station is shown in FSAR Figure 2.1-209.

2. In accordance with Regulatory Guide 1.145, the distance to the EAB is the closest distance within a 45-degree section centered on the compass direction of interest.

WLS COL 2.3-4

TABLE 2.3-283
LEE NUCLEAR STATION OFFSITE ATMOSPHERIC DISPERSION
SHORT-TERM DIFFUSION ESTIMATES FOR ACCIDENTAL RELEASES

Exclusion Area Boundary χ/Q Values (sec/m^3)[a]

Time Period	Direction Dependent χ/Q		Direction Independent χ/Q
	0.5% Max Sector χ/Q[b]	Sector/Distance	5% Overall Site Limit
0-2 Hrs	3.46E-04	SE / 1339 m	3.00E-04

Low Population Zone χ/Q Values (sec/m^3)[a]

Time Period	Direction Dependent χ/Q		Direction Independent χ/Q
	0.5% Max χ/Q[b]	Sector	5% Site Limit
0-8 Hrs	8.01E-05	SE	6.26E-05
8-24 Hrs	5.49E-05	SE	4.40E-05
1-4 Days	2.42E-05	SE	2.04E-05
4-30 Days	7.46E-06	SE	6.79E-06

Limiting Relative Dispersion Values[a]
Lee Nuclear 0.5% Maximum χ/Q Values (sec/m^3)

	0 – 2 Hrs	0 – 8 Hrs	8 – 24 Hrs	24 – 96 Hrs	96 – 720 Hrs
EAB (SE, 1339 m)[b]	3.46E-04	N/A	N/A	N/A	N/A
LPZ (SE, 3219 m)[b]	N/A	8.01E-05	5.49E-05	2.42E-05	7.46E-06

a) Based on Lee Nuclear Station meteorological data for December 2005 - November 2007.

b) 0.5% χ/Q values represent the maximum for all sector-dependent values.

WLS COL 2.3-4

TABLE 2.3-284
LEE NUCLEAR STATION CONTROL ROOM χ/Q INPUT DATA

Control Room HVAC Intake (El. 19.9 m) Directions

Release Point	Direction to Source (degrees)
Plant Vent	2
PCS Air Diffuser	33
Fuel Building Blowout Panel	347
Radwaste Building Truck Staging Area Door	337
Steam Line Break Releases	75
PORV/Safety Valves	85
Condenser Air Removal Stack	175
Containment Shell	24

Annex Building Access (El. 1.5 m) Directions

Release Point	Direction to Source (degrees)
Plant Vent	6
PCS Air Diffuser	17
Fuel Building Blowout Panel	358
Radwaste Building Truck Staging Area Door	353
Steam Line Break Releases	21
PORV/Safety Valves	23
Condenser Air Removal Stack	57
Containment Shell	11

Notes:

1. Directions are relative to True North at the Lee Nuclear Station site.

WLS COL 2.3-4

TABLE 2.3-285 (Sheet 1 of 2)
CONTROL ROOM ATMOSPHERIC DISPERSION FACTORS (χ/Q)
FOR ACCIDENT DOSE ANALYSIS (S/M^3)

Control Room χ/Q at HVAC Intake[(a)]

Time Interval	Plant Vent	PCS Air Diffuser	Fuel Bldg. Blowout Panel	Radwaste Bldg. Truck Staging Area Door
0 -2 hours	2.01E-03	1.78E-03	1.64E-03	1.17E-03
2 – 8 hours	1.52E-03	1.45E-03	1.20E-03	8.98E-04
8 – 24 hours	5.84E-04	6.36E-04	4.25E-04	3.30E-04
1 – 4 days	4.76E-04	5.26E-04	4.09E-04	2.93E-04
4 – 30 days	3.56E-04	3.36E-04	3.69E-04	2.59E-04

	Steam Line Break Releases	PORV & Safety Valves	Condenser Air Removal Stack	Containment Shell
0 -2 hours	1.25E-02	1.08E-02	1.59E-03	2.70E-03
2 – 8 hours	7.22E-03	5.62E-03	1.27E-03	1.79E-03
8 – 24 hours	2.95E-03	2.28E-03	5.10E-04	7.39E-04
1 – 4 days	2.40E-03	1.89E-03	3.86E-04	6.90E-04
4 – 30 days	1.79E-03	1.47E-03	2.82E-04	4.75E-04

WLS COL 2.3-4

TABLE 2.3-285 (Sheet 2 of 2)
CONTROL ROOM ATMOSPHERIC DISPERSION FACTORS (χ/Q)
FOR ACCIDENT DOSE ANALYSIS (S/M^3)

Control Room χ/Q at Annex Building Access Door[a]

Time Interval	Plant Vent	PCS Air Diffuser	Fuel Bldg. Blowout Panel	Radwaste Bldg. Truck Staging Area Door
0 -2 hours	4.41E-04	4.83E-04	3.64E-04	3.46E-04
2 – 8 hours	3.47E-04	3.69E-04	2.65E-04	2.53E-04
8 – 24 hours	1.37E-04	1.61E-04	1.01E-04	9.78E-05
1 – 4 days	1.13E-04	1.32E-04	8.87E-05	8.71E-05
4 – 30 days	8.22E-05	9.13E-05	7.37E-05	7.57E-05

	Steam Line Break Releases	PORV & Safety Valves	Condenser Air Removal Stack	Containment Shell
0 -2 hours	8.50E-04	8.71E-04	3.40E-03	5.01E-04
2 – 8 hours	6.44E-04	6.83E-04	2.91E-03	3.98E-04
8 – 24 hours	2.84E-04	2.96E-04	1.31E-03	1.59E-04
1 – 4 days	1.93E-04	2.05E-04	9.21E-04	1.36E-04
4 – 30 days	1.39E-04	1.46E-04	6.40E-04	9.76E-05

a) Based on Lee Nuclear Station meteorological data for December 2005 - November 2007.

WLS COL 2.3-5

TABLE 2.3-286
LEE NUCLEAR SITE OFFSITE RECEPTOR LOCATIONS

Sector	Garden	Milk Cow/Goat	House	Animal for Meat
S			2578	
SSW	2410	1705		1705
SW	1927	2026		2026
WSW	4123	4494	4143	4494
W	3968	3850	2846	3850
WNW	4094	4016		4016
NW	3258	6143	4025	3876
NNW	2431		3245	2360
N	2246	3715		3715
NNE	2203	5449		5449
NE	1794			1792
ENE	1567	1957		1957
E	4469	4926		4469
ESE	4355	5017		5017
SE	6591	7437	1607	2373
SSE	1627	1749	1775	1749

NOTES:

1. Distances, in meters, from the midpoint between Units 1 and 2 to the nearest receptor, of each type, for a given 22.5 degree sector.

2. February 2007 survey results.

WLS COL 2.3-5

TABLE 2.3-287 (Sheet 1 of 3)

ANNUAL AVERAGE χ/Q (SEC/M^3) FOR NORMAL RELEASES NO DECAY, UNDEPLETED
(FOR EACH 22.5° SECTOR AT THE DISTANCES (MILES) SHOWN AT THE TOP)

Sector	0.250	0.500	.750	1.000	1.500	2.000	2.500	3.000	3.500	4.000	4.500
S	1.794E-05	5.298E-06	2.650E-06	1.679E-06	9.275E-07	6.161E-07	4.507E-07	3.581E-07	2.951E-07	2.496E-07	2.153E-07
SSW	1.439E-05	4.283E-06	2.156E-06	1.368E-06	7.541E-07	4.997E-07	3.647E-07	2.888E-07	2.373E-07	2.003E-07	1.724E-07
SW	1.475E-05	4.366E-06	2.195E-06	1.394E-06	7.690E-07	5.100E-07	3.724E-07	2.949E-07	2.423E-07	2.044E-07	1.760E-07
SWS	1.662E-05	4.897E-06	2.439E-06	1.541E-06	8.505E-07	5.650E-07	4.133E-07	3.286E-07	2.708E-07	2.291E-07	1.977E-07
W	1.875E-05	5.487E-06	2.719E-06	1.718E-06	9.491E-07	6.316E-07	4.630E-07	3.695E-07	3.055E-07	2.591E-07	2.241E-07
WNW	1.734E-05	5.082E-06	2.519E-06	1.591E-06	8.818E-07	5.881E-07	4.316E-07	3.442E-07	2.844E-07	2.411E-07	2.084E-07
NW	1.662E-05	4.898E-06	2.450E-06	1.553E-06	8.585E-07	5.706E-07	4.175E-07	3.318E-07	2.734E-07	2.312E-07	1.995E-07
NNW	1.122E-05	3.345E-06	1.706E-06	1.090E-06	6.061E-07	4.029E-07	2.944E-07	2.318E-07	1.895E-07	1.592E-07	1.365E-07
N	8.164E-06	2.487E-06	1.314E-06	8.524E-07	4.779E-07	3.176E-07	2.314E-07	1.799E-07	1.455E-07	1.211E-07	1.030E-07
NNE	5.527E-06	1.693E-06	9.056E-07	5.899E-07	3.296E-07	2.180E-07	1.582E-07	1.220E-07	9.807E-08	8.117E-08	6.872E-08
NE	5.083E-06	1.556E-06	8.276E-07	5.369E-07	2.975E-07	1.958E-07	1.416E-07	1.091E-07	8.763E-08	7.249E-08	6.134E-08
ENE	5.195E-06	1.565E-06	8.105E-07	5.198E-07	2.893E-07	1.917E-07	1.395E-07	1.087E-07	8.801E-08	7.336E-08	6.250E-08
E	4.540E-06	1.357E-06	6.958E-07	4.456E-07	2.475E-07	1.643E-07	1.199E-07	9.425E-08	7.695E-08	6.457E-08	5.534E-08
ESE	1.831E-05	5.358E-06	2.652E-06	1.672E-06	9.285E-07	6.199E-07	4.553E-07	3.631E-07	3.000E-07	2.543E-07	2.199E-07
SE	4.815E-05	1.402E-0	6.850E-06	4.296E-06	2.359E-06	1.567E-06	1.149E-06	9.219E-07	7.657E-07	6.519E-07	5.657E-07
SSE	2.382E-05	6.987E-06	3.469E-06	2.194E-0	1.211E-06	8.049E-07	5.897E-07	4.706E-07	3.891E-07	3.300E-07	2.855E-07

WLS COL 2.3-5

TABLE 2.3-287 (Sheet 2 of 3)
ANNUAL AVERAGE χ/Q (SEC/M^3) FOR NORMAL RELEASES NO DECAY, UNDEPLETED
(FOR EACH 22.5° SECTOR AT THE DISTANCES (MILES) SHOWN AT THE TOP)

SECTOR	5.000	7.500	10.000	15.000	20.000	25.000	30.000	35.000	40.000	45.000	50.000
S	1.888E-07	1.139E-07	7.976E-08	4.841E-08	3.406E-08	2.596E-08	2.081E-08	1.728E-08	1.471E-08	1.276E-08	1.125E-08
SSW	1.509E-07	9.054E-08	6.315E-08	3.815E-08	2.676E-08	2.035E-08	1.629E-08	1.350E-08	1.148E-08	9.955E-09	8.765E-09
SW	1.540E-07	9.243E-08	6.448E-08	3.897E-08	2.735E-08	2.081E-08	1.666E-08	1.382E-08	1.175E-08	1.019E-08	8.973E-09
SWS	1.733E-07	1.047E-07	7.338E-08	4.459E-08	3.140E-08	2.395E-08	1.921E-08	1.595E-08	1.358E-08	1.179E-08	1.040E-08
W	1.969E-07	1.197E-07	8.424E-08	5.146E-08	3.634E-08	2.778E-08	2.232E-08	1.856E-08	1.582E-08	1.375E-08	1.213E-08
WNW	1.830E-07	1.111E-07	7.804E-08	4.758E-08	3.356E-08	2.563E-08	2.057E-08	1.710E-08	1.457E-08	1.265E-08	1.116E-08
NW	1.748E-07	1.055E-07	7.384E-08	4.482E-08	3.154E-08	2.404E-08	1.927E-08	1.600E-08	1.362E-08	1.182E-08	1.042E-08
NNW	1.191E-07	7.058E-08	4.881E-08	2.916E-08	2.031E-08	1.537E-08	1.225E-08	1.011E-08	8.575E-09	7.415E-09	6.513E-09
N	8.919E-08	5.142E-08	3.488E-08	2.029E-08	1.387E-08	1.035E-08	8.153E-09	6.670E-09	5.609E-09	4.816E-09	4.204E-09
NNE	5.925E-08	3.364E-08	2.258E-08	1.294E-08	8.769E-09	6.495E-09	5.089E-09	4.144E-09	3.470E-09	2.969E-09	2.583E-09
NE	5.289E-08	3.006E-08	2.020E-08	1.161E-08	7.892E-09	5.861E-09	4.602E-09	3.755E-09	3.150E-09	2.699E-09	2.352E-09
ENE	5.420E-08	3.149E-08	2.149E-08	1.262E-08	8.700E-09	6.532E-09	5.174E-09	4.252E-09	3.590E-09	3.093E-09	2.708E-09
E	4.823E-08	2.851E-08	1.969E-08	1.173E-08	8.163E-09	6.169E-09	4.913E-09	4.055E-09	3.436E-09	2.970E-09	2.608E-09
ESE	1.931E-07	1.172E-07	8.237E-08	5.023E-08	3.544E-08	2.707E-08	2.173E-08	1.806E-08	1.539E-08	1.336E-08	1.178E-08
SE	4.983E-07	3.061E-07	2.168E-07	1.336E-07	9.490E-08	7.284E-08	5.871E-08	4.895E-08	4.182E-08	3.641E-08	3.218E-08
SSE	2.508E-07	1.525E-07	1.073E-07	6.551E-08	4.626E-08	3.536E-08	2.841E-08	2.362E-08	2.013E-08	1.750E-08	1.543E-08

WLS COL 2.3-5

TABLE 2.3-287 (Sheet 3 of 3)
ANNUAL AVERAGE χ/Q (SEC/M^3) FOR NORMAL RELEASES NO DECAY, UNDEPLETED
(FOR EACH 22.5° SECTOR AT THE DISTANCES (MILES) SHOWN AT THE TOP)

SECTOR	.5-1	1-2	2-3	3-4	4-5	5-10	10-20	20-30	30-40	40-50
S	2.807E-06	9.562E-07	4.578E-07	2.958E-07	2.156E-07	1.154E-07	4.900E-08	2.606E-08	1.731E-08	1.278E-08
SSW	2.278E-06	7.775E-07	3.704E-07	2.379E-07	1.727E-07	9.178E-08	3.864E-08	2.043E-08	1.353E-08	9.966E-09
SW	2.321E-06	7.927E-07	3.781E-07	2.429E-07	1.763E-07	9.370E-08	3.948E-08	2.090E-08	1.384E-08	1.020E-08
WSW	2.586E-06	8.770E-07	4.199E-07	2.714E-07	1.980E-07	1.060E-07	4.513E-08	2.404E-08	1.598E-08	1.181E-08
W	2.889E-06	9.789E-07	4.705E-07	3.061E-07	2.244E-07	1.211E-07	5.202E-08	2.788E-08	1.859E-08	1.376E-08
WNW	2.676E-06	9.087E-07	4.384E-07	2.850E-07	2.087E-07	1.124E-07	4.812E-08	2.572E-08	1.713E-08	1.267E-08
NW	2.595E-06	8.849E-07	4.240E-07	2.740E-07	1.997E-07	1.068E-07	4.536E-08	2.413E-08	1.603E-08	1.183E-08
NNW	1.796E-06	6.233E-07	2.983E-07	1.900E-07	1.368E-07	7.169E-08	2.960E-08	1.544E-08	1.014E-08	7.425E-09
N	1.370E-06	4.899E-07	2.338E-07	1.460E-07	1.033E-07	5.246E-08	2.068E-08	1.041E-08	6.690E-09	4.824E-09
NNE	9.402E-07	3.378E-07	1.597E-07	9.848E-08	6.890E-08	3.441E-08	1.323E-08	6.539E-09	4.157E-09	2.975E-09
NE	8.603E-07	3.055E-07	1.431E-07	8.801E-08	6.151E-08	3.075E-08	1.187E-08	5.899E-09	3.766E-09	2.704E-09
ENE	8.489E-07	2.971E-07	1.411E-07	8.833E-08	6.264E-08	3.209E-08	1.285E-08	6.567E-09	4.263E-09	3.097E-09
E	7.316E-07	2.546E-07	1.215E-07	7.718E-08	5.544E-08	2.897E-08	1.191E-08	6.198E-09	4.064E-09	2.974E-09
ESE	2.818E-06	9.566E-07	4.623E-07	3.006E-07	2.202E-07	1.186E-07	5.080E-08	2.716E-08	1.809E-08	1.338E-08
SE	7.309E-06	2.437E-06	1.170E-06	7.670E-07	5.663E-07	3.092E-07	1.349E-07	7.307E-08	4.902E-08	3.645E-08
SSE	3.684E-06	1.249E-06	5.994E-07	3.899E-07	2.858E-07	1.542E-07	6.624E-08	3.549E-08	2.366E-08	1.751E-08

WLS COL 2.3-5

TABLE 2.3-288 (Sheet 1 of 3)
ANNUAL AVERAGE χ/Q (SEC/M^3) FOR NORMAL RELEASES NO DECAY, DEPLETED
(FOR EACH 22.5° SECTOR AT THE DISTANCES (MILES) SHOWN AT THE TOP)

Sector	0.250	0.500	.750	1.000	1.500	2.000	2.500	3.000	3.500	4.000	4.500
S	1.669E-05	4.819E-06	2.361E-06	1.470E-06	7.877E-07	5.101E-07	3.651E-07	2.845E-07	2.303E-07	1.916E-07	1.628E-07
SSW	1.339E-05	3.896E-06	1.921E-06	1.198E-06	6.404E-07	4.138E-07	2.954E-07	2.294E-07	1.852E-07	1.537E-07	1.304E-07
SW	1.373E-05	3.971E-06	1.956E-06	1.220E-06	6.531E-07	4.223E-07	3.017E-07	2.342E-07	1.891E-07	1.569E-07	1.331E-07
WSW	1.546E-05	4.454E-06	2.173E-06	1.349E-06	7.223E-07	4.678E-07	3.348E-07	2.610E-07	2.113E-07	1.759E-07	1.495E-07
W	1.745E-05	4.991E-06	2.423E-06	1.504E-06	8.060E-07	5.230E-07	3.750E-07	2.935E-07	2.384E-07	1.989E-07	1.694E-07
WNW	1.614E-05	4.622E-06	2.245E-06	1.392E-06	7.489E-07	4.870E-07	3.496E-07	2.734E-07	2.219E-07	1.851E-07	1.576E-07
NW	1.547E-05	4.455E-06	2.183E-06	1.360E-06	7.291E-07	4.725E-07	3.382E-07	2.635E-07	2.133E-07	1.775E-07	1.508E-07
NNW	1.044E-05	3.042E-06	1.520E-06	9.539E-07	5.147E-07	3.336E-07	2.385E-07	1.841E-07	1.479E-07	1.222E-07	1.032E-07
N	7.597E-06	2.262E-06	1.171E-06	7.461E-07	4.059E-07	2.630E-07	1.875E-07	1.429E-07	1.135E-07	9.295E-08	7.788E-08
NNE	5.144E-06	1.540E-06	8.070E-07	5.164E-07	2.799E-07	1.805E-07	1.281E-07	9.694E-08	7.652E-08	6.231E-08	5.195E-08
NE	4.730E-06	1.415E-06	7.375E-07	4.700E-07	2.527E-07	1.621E-07	1.147E-07	8.669E-08	6.838E-08	5.564E-08	4.638E-08
ENE	4.835E-06	1.423E-06	7.222E-07	4.550E-07	2.457E-07	1.587E-07	1.130E-07	8.631E-08	6.867E-08	5.631E-08	4.725E-08
E	4.225E-06	1.235E-06	6.200E-07	3.901E-07	2.102E-07	1.360E-07	9.712E-08	7.486E-08	6.004E-08	4.957E-08	4.184E-08
ESE	1.704E-05	4.874E-06	2.363E-06	1.464E-06	7.885E-07	5.133E-07	3.688E-07	2.884E-07	2.341E-07	1.952E-07	1.662E-07
SE	4.481E-05	1.275E-05	6.104E-06	3.761E-06	2.003E-06	1.298E-06	9.307E-07	7.322E-07	5.975E-07	5.004E-07	4.277E-07
SSE	2.217E-05	6.355E-06	3.091E-06	1.921E-06	1.028E-06	6.665E-07	4.777E-07	3.738E-07	3.036E-07	2.534E-07	2.158E-07

WLS COL 2.3-5

TABLE 2.3-288 (Sheet 2 of 3)
ANNUAL AVERAGE χ/Q (SEC/M^3) FOR NORMAL RELEASES NO DECAY, DEPLETED
(FOR EACH 22.5° SECTOR AT THE DISTANCES (MILES) SHOWN AT THE TOP)

SECTOR	5.000	7.500	10.000	15.000	20.000	25.000	30.000	35.000	40.000	45.000	50.000
S	1.407E-07	8.031E-08	5.359E-08	3.011E-08	1.989E-08	1.437E-08	1.098E-08	8.722E-09	7.132E-09	5.960E-09	5.068E-09
SSW	1.125E-07	6.383E-08	4.243E-08	2.372E-08	1.563E-08	1.126E-08	8.591E-09	6.817E-09	5.568E-09	4.649E-09	3.950E-09
SW	1.148E-07	6.516E-08	4.332E-08	2.423E-08	1.597E-08	1.152E-08	8.788E-09	6.975E-09	5.698E-09	4.759E-09	4.044E-09
WSW	1.292E-07	7.383E-08	4.930E-08	2.773E-08	1.834E-08	1.325E-08	1.013E-08	8.054E-09	6.588E-09	5.507E-09	4.685E-09
W	1.468E-07	8.440E-08	5.660E-08	3.200E-08	2.122E-08	1.537E-08	1.177E-08	9.369E-09	7.672E-09	6.420E-09	5.465E-09
WNW	1.364E-07	7.829E-08	5.243E-08	2.958E-08	1.960E-08	1.418E-08	1.085E-08	8.632E-09	7.064E-09	5.909E-09	5.028E-09
NW	1.303E-07	7.436E-08	4.961E-08	2.787E-08	1.842E-08	1.330E-08	1.017E-08	8.078E-09	6.605E-09	5.520E-09	4.694E-09
NNW	8.878E-08	4.976E-08	3.280E-08	1.813E-08	1.186E-08	8.503E-09	6.459E-09	5.107E-09	4.158E-09	3.463E-09	2.935E-09
N	6.649E-08	3.625E-08	2.343E-08	1.262E-08	8.102E-09	5.726E-09	4.300E-09	3.368E-09	2.720E-09	2.249E-09	1.894E-09
NNE	4.417E-08	2.372E-08	1.517E-08	8.048E-09	5.121E-09	3.594E-09	2.684E-09	2.092E-09	1.683E-09	1.387E-09	1.164E-09
NE	3.943E-08	2.119E-08	1.357E-08	7.219E-09	4.609E-09	3.243E-09	2.427E-09	1.896E-09	1.527E-09	1.260E-09	1.060E-09
ENE	4.040E-08	2.220E-08	1.443E-08	7.845E-09	5.081E-09	3.615E-09	2.729E-09	2.147E-09	1.741E-09	1.444E-09	1.220E-09
E	3.595E-08	2.010E-08	1.323E-08	7.297E-09	4.767E-09	3.414E-09	2.591E-09	2.047E-09	1.666E-09	1.387E-09	1.175E-09
ESE	1.439E-07	8.263E-08	5.534E-08	3.124E-08	2.070E-08	1.498E-08	1.146E-08	9.117E-09	7.462E-09	6.241E-09	5.311E-09
SE	3.715E-07	2.158E-07	1.457E-07	8.308E-08	5.542E-08	4.031E-08	3.097E-08	2.471E-08	2.028E-08	1.701E-08	1.450E-08
SSE	1.869E-07	1.075E-07	7.207E-08	4.074E-08	2.702E-08	1.957E-08	1.498E-08	1.192E-08	9.764E-09	8.171E-09	6.955E-09

WLS COL 2.3-5

TABLE 2.3-288 (Sheet 3 of 3)
ANNUAL AVERAGE χ/Q (SEC/M^3) FOR NORMAL RELEASES NO DECAY, DEPLETED
(FOR EACH 22.5° SECTOR AT THE DISTANCES (MILES) SHOWN AT THE TOP)

SECTOR	.5-1	1-2	2-3	3-4	4-5	5-10	10-20	20-30	30-40	40-50
S	2.511E-06	8.160E-07	3.715E-07	2.310E-07	1.632E-07	8.185E-08	3.078E-08	1.448E-08	8.761E-09	5.977E-09
SSW	2.038E-06	6.635E-07	3.006E-07	1.859E-07	1.307E-07	6.513E-08	2.428E-08	1.136E-08	6.848E-09	4.662E-09
SW	2.077E-06	6.765E-07	3.069E-07	1.897E-07	1.334E-07	6.649E-08	2.480E-08	1.161E-08	7.007E-09	4.772E-09
WSW	2.314E-06	7.484E-07	3.408E-07	2.120E-07	1.498E-07	7.523E-08	2.835E-08	1.336E-08	8.089E-09	5.523E-09
W	2.585E-06	8.354E-07	3.819E-07	2.391E-07	1.698E-07	8.590E-08	3.268E-08	1.549E-08	9.409E-09	6.437E-09
WNW	2.394E-06	7.754E-07	3.557E-07	2.226E-07	1.579E-07	7.971E-08	3.022E-08	1.429E-08	8.669E-09	5.925E-09
NW	2.322E-06	7.552E-07	3.441E-07	2.140E-07	1.511E-07	7.579E-08	2.850E-08	1.341E-08	8.114E-09	5.536E-09
NNW	1.607E-06	5.318E-07	2.421E-07	1.484E-07	1.035E-07	5.089E-08	1.860E-08	8.581E-09	5.132E-09	3.474E-09
N	1.225E-06	4.180E-07	1.898E-07	1.141E-07	7.813E-08	3.727E-08	1.301E-08	5.789E-09	3.388E-09	2.257E-09
NNE	8.406E-07	2.883E-07	1.296E-07	7.694E-08	5.214E-08	2.446E-08	8.329E-09	3.637E-09	2.105E-09	1.392E-09
NE	7.692E-07	2.607E-07	1.161E-07	6.876E-08	4.655E-08	2.186E-08	7.470E-09	3.281E-09	1.907E-09	1.265E-09
ENE	7.592E-07	2.535E-07	1.145E-07	6.900E-08	4.740E-08	2.279E-08	8.081E-09	3.651E-09	2.159E-09	1.449E-09
E	6.544E-07	2.172E-07	9.859E-08	6.029E-08	4.195E-08	2.057E-08	7.490E-09	3.446E-09	2.057E-09	1.391E-09
ESE	2.521E-06	8.163E-07	3.752E-07	2.348E-07	1.666E-07	8.412E-08	3.191E-08	1.510E-08	9.156E-09	6.258E-09
SE	6.540E-06	2.080E-06	9.492E-07	5.990E-07	4.284E-07	2.192E-07	8.470E-08	4.060E-08	2.481E-08	1.705E-08
SSE	3.296E-06	1.066E-06	4.865E-07	3.045E-07	2.162E-07	1.094E-07	4.160E-08	1.972E-08	1.198E-08	8.193E-09

WLS COL 2.3-5

TABLE 2.3-289 (Sheet 1 of 4)
χ/Q AND D/Q VALUES FOR NORMAL RELEASES

Type of Location	Sector	Distance (miles)	Distance (meters)	χ/Q (sec/m^3) No Decay Undepleted	χ/Q (sec/m^3) No Decay Depleted	χ/Q (sec/m^3) 2.26 Day Decay Undepleted	χ/Q (sec/m^3) 8.00 Day Decay Depleted	D/Q (m^{-2})
EAB	S	0.87	1395	2.10E-06	1.90E-06	2.10E-06	1.90E-06	4.80E-09
EAB	SSW	0.87	1395	1.70E-06	1.50E-06	1.70E-06	1.50E-06	4.60E-09
EAB	SW	0.96	1547	1.50E-06	1.30E-06	1.50E-06	1.30E-06	4.00E-09
EAB	WSW	1.02	1649	1.50E-06	1.30E-06	1.50E-06	1.30E-06	3.10E-09
EAB	W	0.75	1208	2.70E-06	2.40E-06	2.70E-06	2.40E-06	4.70E-09
EAB	WNW	0.75	1208	2.50E-06	2.20E-06	2.50E-06	2.20E-06	4.30E-09
EAB	NW	0.75	1215	2.40E-06	2.20E-06	2.40E-06	2.20E-06	5.40E-09
EAB	NNW	0.42	668	4.60E-06	4.20E-06	4.60E-06	4.20E-06	1.50E-08
EAB	N	0.4	644	3.60E-06	3.30E-06	3.60E-06	3.30E-06	1.80E-08
EAB	NNE	0.4	644	2.40E-06	2.20E-06	2.40E-06	2.20E-06	1.90E-08
EAB	NE	0.44	705	1.90E-06	1.80E-06	1.90E-06	1.80E-06	1.70E-08
EAB	ENE	0.59	952	1.20E-06	1.10E-06	1.20E-06	1.10E-06	7.30E-09
EAB	E	0.8	1282	6.30E-07	5.60E-07	6.30E-07	5.60E-07	2.50E-09
EAB	ESE	0.96	1544	1.80E-06	1.60E-06	1.80E-06	1.60E-06	4.80E-09
EAB	SE	0.83	1339	5.80E-06	5.10E-06	5.70E-06	5.10E-06	1.20E-08
EAB	SSE	0.83	1339	2.90E-06	2.60E-06	2.90E-06	2.60E-06	5.90E-09
NEAREST HOUSE	S	1.6	2578	8.40E-07	7.10E-07	8.30E-07	7.10E-07	1.70E-09

WLS COL 2.3-5

TABLE 2.3-289 (Sheet 2 of 4)
χ/Q AND D/Q VALUES FOR NORMAL RELEASES

Type of Location	Sector	Distance (miles)	Distance (meters)	χ/Q (sec/m^3) No Decay Undepleted	χ/Q (sec/m^3) No Decay Depleted	χ/Q (sec/m^3) 2.26 Day Decay Undepleted	χ/Q (sec/m^3) 8.00 Day Decay Depleted	D/Q (m^{-2})
NEAREST HOUSE	WSW	2.57	4143	4.00E-07	3.20E-07	3.90E-07	3.20E-07	6.20E-10
NEAREST HOUSE	W	1.77	2846	7.50E-07	6.30E-07	7.40E-07	6.30E-07	1.10E-09
NEAREST HOUSE	NW	2.5	4025	4.20E-07	3.40E-07	4.10E-07	3.40E-07	6.90E-10
NEAREST HOUSE	NNW	2.02	3245	4.00E-07	3.30E-07	3.90E-07	3.30E-07	1.10E-09
NEAREST HOUSE	SE	1	1607	4.30E-06	3.80E-06	4.30E-06	3.80E-06	8.90E-09
NEAREST HOUSE	SSE	1.1	1775	1.90E-06	1.60E-06	1.90E-06	1.60E-06	3.70E-09
NEAREST GARDEN	SSW	1.5	2410	7.60E-07	6.40E-07	7.50E-07	6.40E-07	1.80E-09
NEAREST GARDEN	SW	1.2	1927	1.10E-06	9.20E-07	1.10E-06	9.20E-07	2.70E-09
NEAREST GARDEN	WSW	2.56	4123	4.00E-07	3.20E-07	3.90E-07	3.20E-07	6.30E-10
NEAREST GARDEN	W	2.47	3968	4.70E-07	3.80E-07	4.60E-07	3.80E-07	6.00E-10
NEAREST GARDEN	WNW	2.54	4094	4.20E-07	3.40E-07	4.10E-07	3.40E-07	5.30E-10
NEAREST GARDEN	NW	2.02	3258	5.60E-07	4.60E-07	5.50E-07	4.60E-07	1.00E-09
NEAREST GARDEN	NNW	1.51	2431	6.00E-07	5.10E-07	5.90E-07	5.10E-07	1.70E-09
NEAREST GARDEN	N	1.4	2246	5.30E-07	4.50E-07	5.30E-07	4.50E-07	2.20E-09
NEAREST GARDEN	NNE	1.37	2203	3.80E-07	3.20E-07	3.70E-07	3.20E-07	2.50E-09
NEAREST GARDEN	NE	1.11	1794	4.60E-07	4.00E-07	4.60E-07	4.00E-07	3.60E-09
NEAREST GARDEN	ENE	0.97	1567	5.40E-07	4.70E-07	5.40E-07	4.70E-07	3.20E-09

WLS COL 2.3-5

TABLE 2.3-289 (Sheet 3 of 4)
χ/Q AND D/Q VALUES FOR NORMAL RELEASES

Type of Location	Sector	Distance (miles)	Distance (meters)	χ/Q (sec/m^3) No Decay Undepleted	χ/Q (sec/m^3) No Decay Depleted	χ/Q (sec/m^3) 2.26 Day Decay Undepleted	χ/Q (sec/m^3) 8.00 Day Decay Depleted	D/Q (m^{-2})
NEAREST GARDEN	E	2.78	4469	1.00E-07	8.40E-08	1.00E-07	8.30E-08	2.90E-10
NEAREST GARDEN	ESE	2.71	4355	4.10E-07	3.30E-07	4.10E-07	3.30E-07	7.90E-10
NEAREST GARDEN	SE	4.1	6591	6.30E-07	4.80E-07	6.20E-07	4.80E-07	7.50E-10
NEAREST GARDEN	SSE	1.01	1627	2.20E-06	1.90E-06	2.10E-06	1.90E-06	4.30E-09
MILK COW/GOAT	SSW	1.06	1705	1.30E-06	1.10E-06	1.20E-06	1.10E-06	3.30E-09
MILK COW/GOAT	SW	1.26	2026	9.90E-07	8.50E-07	9.80E-07	8.50E-07	2.50E-09
MILK COW/GOAT	WSW	2.79	4494	3.60E-07	2.90E-07	3.50E-07	2.90E-07	5.40E-10
MILK COW/GOAT	W	2.39	3850	4.90E-07	4.00E-07	4.80E-07	4.00E-07	6.30E-10
MILK COW/GOAT	WNW	2.5	4016	4.30E-07	3.50E-07	4.20E-07	3.50E-07	5.50E-10
MILK COW/GOAT	NW	3.82	6143	2.50E-07	1.90E-07	2.40E-07	1.90E-07	3.30E-10
MILK COW/GOAT	N	2.31	3715	2.60E-07	2.10E-07	2.60E-07	2.10E-07	9.20E-10
MILK COW/GOAT	NNE	3.39	5449	1.00E-07	8.10E-08	1.00E-07	8.00E-08	5.10E-10
MILK COW/GOAT	ENE	1.22	1957	3.90E-07	3.40E-07	3.90E-07	3.40E-07	2.20E-09
MILK COW/GOAT	E	3.06	4926	9.20E-08	7.30E-08	9.00E-08	7.20E-08	2.40E-10
MILK COW/GOAT	ESE	3.12	5017	3.50E-07	2.70E-07	3.40E-07	2.70E-07	6.10E-10
MILK COW/GOAT	SE	4.62	7437	5.50E-07	4.10E-07	5.30E-07	4.10E-07	6.10E-10
MILK COW/GOAT	SSE	1.09	1749	1.90E-06	1.70E-06	1.90E-06	1.70E-06	3.80E-09

WLS COL 2.3-5

TABLE 2.3-289 (Sheet 4 of 4)
χ/Q AND D/Q VALUES FOR NORMAL RELEASES

Type of Location	Sector	Distance (miles)	Distance (meters)	χ/Q (sec/m^3) No Decay Undepleted	χ/Q (sec/m^3) No Decay Depleted	χ/Q (sec/m^3) 2.26 Day Decay Undepleted	χ/Q (sec/m^3) 8.00 Day Decay Depleted	D/Q (m^{-2})
ANIMAL FOR MEAT	SSW	1.06	1705	1.30E-06	1.10E-06	1.20E-06	1.10E-06	3.30E-09
ANIMAL FOR MEAT	SW	1.26	2026	9.90E-07	8.50E-07	9.80E-07	8.50E-07	2.50E-09
ANIMAL FOR MEAT	WSW	2.79	4494	3.60E-07	2.90E-07	3.50E-07	2.90E-07	5.40E-10
ANIMAL FOR MEAT	W	2.39	3850	4.90E-07	4.00E-07	4.80E-07	4.00E-07	6.30E-10
ANIMAL FOR MEAT	WNW	2.5	4016	4.30E-07	3.50E-07	4.20E-07	3.50E-07	5.50E-10
ANIMAL FOR MEAT	NW	2.41	3876	4.40E-07	3.60E-07	4.30E-07	3.60E-07	7.40E-10
ANIMAL FOR MEAT	NNW	1.47	2360	6.30E-07	5.30E-07	6.20E-07	5.30E-07	1.80E-09
ANIMAL FOR MEAT	N	2.31	3715	2.60E-07	2.10E-07	2.60E-07	2.10E-07	9.20E-10
ANIMAL FOR MEAT	NNE	3.39	5449	1.00E-07	8.10E-08	1.00E-07	8.00E-08	5.10E-10
ANIMAL FOR MEAT	NE	1.11	1792	4.60E-07	4.00E-07	4.60E-07	4.00E-07	3.60E-09
ANIMAL FOR MEAT	ENE	1.22	1957	3.90E-07	3.40E-07	3.90E-07	3.40E-07	2.20E-09
ANIMAL FOR MEAT	E	2.78	4469	1.00E-07	8.40E-08	1.00E-07	8.30E-08	2.90E-10
ANIMAL FOR MEAT	ESE	3.12	5017	3.50E-07	2.70E-07	3.40E-07	2.70E-07	6.10E-10
ANIMAL FOR MEAT	SE	1.47	2373	2.40E-06	2.10E-06	2.40E-06	2.10E-06	4.50E-09
ANIMAL FOR MEAT	SSE	1.09	1749	1.90E-06	1.70E-06	1.90E-06	1.70E-06	3.80E-09

WLS COL 2.3-5

TABLE 2.3-290 (Sheet 1 of 3)
ANNUAL AVERAGE χ/Q (SEC/M^3) FOR NORMAL RELEASES
2.26 DAY DECAY, UNDEPLETED
(FOR EACH 22.5° SECTOR AT THE DISTANCES (MILES) SHOWN AT THE TOP)

SECTOR	0.25	0.5	0.75	1	1.5	2	2.5	3	3.5	4	4.5
S	1.79E-05	5.27E-06	2.63E-06	1.67E-06	9.16E-07	6.06E-07	4.41E-07	3.49E-07	2.86E-07	2.41E-07	2.07E-07
SSW	1.44E-05	4.27E-06	2.14E-06	1.36E-06	7.45E-07	4.92E-07	3.57E-07	2.82E-07	2.30E-07	1.94E-07	1.66E-07
SW	1.47E-05	4.35E-06	2.18E-06	1.38E-06	7.60E-07	5.02E-07	3.65E-07	2.88E-07	2.35E-07	1.98E-07	1.69E-07
WSW	1.66E-05	4.87E-06	2.42E-06	1.53E-06	8.39E-07	5.55E-07	4.04E-07	3.20E-07	2.62E-07	2.21E-07	1.90E-07
W	1.87E-05	5.46E-06	2.70E-06	1.70E-06	9.36E-07	6.20E-07	4.53E-07	3.59E-07	2.96E-07	2.50E-07	2.15E-07
WNW	1.73E-05	5.06E-06	2.50E-06	1.58E-06	8.70E-07	5.78E-07	4.22E-07	3.35E-07	2.76E-07	2.33E-07	2.00E-07
NW	1.66E-05	4.88E-06	2.44E-06	1.54E-06	8.50E-07	5.63E-07	4.11E-07	3.25E-07	2.67E-07	2.25E-07	1.94E-07
NNW	1.12E-05	3.33E-06	1.70E-06	1.08E-06	6.01E-07	3.98E-07	2.90E-07	2.28E-07	1.85E-07	1.55E-07	1.33E-07
N	8.15E-06	2.48E-06	1.31E-06	8.49E-07	4.75E-07	3.15E-07	2.29E-07	1.78E-07	1.43E-07	1.19E-07	1.01E-07
NNE	5.52E-06	1.69E-06	9.03E-07	5.88E-07	3.28E-07	2.17E-07	1.57E-07	1.21E-07	9.69E-08	8.01E-08	6.77E-08
NE	5.08E-06	1.55E-06	8.26E-07	5.35E-07	2.96E-07	1.94E-07	1.40E-07	1.08E-07	8.65E-08	7.15E-08	6.04E-08
ENE	5.19E-06	1.56E-06	8.08E-07	5.18E-07	2.87E-07	1.90E-07	1.38E-07	1.07E-07	8.66E-08	7.20E-08	6.12E-08
E	4.53E-06	1.35E-06	6.93E-07	4.44E-07	2.46E-07	1.63E-07	1.18E-07	9.29E-08	7.56E-08	6.33E-08	5.41E-08
ESE	1.83E-05	5.34E-06	2.64E-06	1.66E-06	9.20E-07	6.12E-07	4.48E-07	3.56E-07	2.93E-07	2.48E-07	2.14E-07
SE	4.81E-05	1.40E-05	6.82E-06	4.27E-06	2.34E-06	1.55E-06	1.13E-06	9.05E-07	7.50E-07	6.36E-07	5.50E-07
SSE	2.38E-05	6.96E-06	3.45E-06	2.18E-06	1.20E-06	7.94E-07	5.80E-07	4.61E-07	3.80E-07	3.21E-07	2.77E-07

WLS COL 2.3-5

TABLE 2.3-290 (Sheet 2 of 3)
ANNUAL AVERAGE χ/Q (SEC/M^3) FOR NORMAL RELEASES
2.26 DAY DECAY, UNDEPLETED
(FOR EACH 22.5° SECTOR AT THE DISTANCES (MILES) SHOWN AT THE TOP)

SECTOR	5	7.5	10	15	20	25	30	35	40	45	50
S	1.81E-07	1.07E-07	7.29E-08	4.23E-08	2.85E-08	2.08E-08	1.60E-08	1.27E-08	1.04E-08	8.63E-09	7.31E-09
SSW	1.45E-07	8.48E-08	5.78E-08	3.34E-08	2.24E-08	1.63E-08	1.25E-08	9.91E-09	8.08E-09	6.72E-09	5.67E-09
SW	1.48E-07	8.66E-08	5.91E-08	3.42E-08	2.30E-08	1.67E-08	1.29E-08	1.02E-08	8.34E-09	6.95E-09	5.88E-09
WSW	1.65E-07	9.75E-08	6.67E-08	3.86E-08	2.59E-08	1.89E-08	1.45E-08	1.15E-08	9.35E-09	7.77E-09	6.56E-09
W	1.88E-07	1.12E-07	7.66E-08	4.47E-08	3.01E-08	2.20E-08	1.69E-08	1.35E-08	1.10E-08	9.15E-09	7.75E-09
WNW	1.75E-07	1.04E-07	7.14E-08	4.16E-08	2.81E-08	2.06E-08	1.58E-08	1.26E-08	1.03E-08	8.63E-09	7.32E-09
NW	1.69E-07	1.00E-07	6.90E-08	4.05E-08	2.76E-08	2.03E-08	1.58E-08	1.27E-08	1.04E-08	8.76E-09	7.48E-09
NNW	1.15E-07	6.73E-08	4.58E-08	2.64E-08	1.78E-08	1.31E-08	1.01E-08	8.07E-09	6.63E-09	5.56E-09	4.74E-09
N	8.71E-08	4.96E-08	3.32E-08	1.89E-08	1.26E-08	9.16E-09	7.04E-09	5.62E-09	4.61E-09	3.87E-09	3.30E-09
NNE	5.82E-08	3.28E-08	2.18E-08	1.23E-08	8.17E-09	5.95E-09	4.58E-09	3.66E-09	3.01E-09	2.53E-09	2.17E-09
NE	5.19E-08	2.92E-08	1.95E-08	1.10E-08	7.32E-09	5.33E-09	4.11E-09	3.29E-09	2.71E-09	2.28E-09	1.95E-09
ENE	5.30E-08	3.04E-08	2.05E-08	1.17E-08	7.90E-09	5.78E-09	4.47E-09	3.58E-09	2.95E-09	2.48E-09	2.12E-09
E	4.70E-08	2.74E-08	1.87E-08	1.09E-08	7.36E-09	5.42E-09	4.20E-09	3.38E-09	2.79E-09	2.35E-09	2.01E-09
ESE	1.87E-07	1.12E-07	7.72E-08	4.55E-08	3.11E-08	2.30E-08	1.79E-08	1.45E-08	1.20E-08	1.01E-08	8.65E-09
SE	4.83E-07	2.93E-07	2.04E-07	1.22E-07	8.42E-08	6.28E-08	4.92E-08	3.99E-08	3.32E-08	2.81E-08	2.42E-08
SSE	2.42E-07	1.45E-07	9.99E-08	5.89E-08	4.02E-08	2.96E-08	2.30E-08	1.85E-08	1.52E-08	1.28E-08	1.09E-08

WLS COL 2.3-5

TABLE 2.3-290 (Sheet 3 of 3)
ANNUAL AVERAGE χ/Q (SEC/M^3) FOR NORMAL RELEASES
2.26 DAY DECAY, UNDEPLETED
(FOR EACH 22.5° SECTOR AT THE DISTANCES (MILES) SHOWN AT THE TOP)

SECTOR	.5-1	1-2	2-3	3-4	4-5	5-10	10-20	20-30	30-40	40-50
S	2.79E-06	9.44E-07	4.48E-07	2.87E-07	2.07E-07	1.08E-07	4.30E-08	2.09E-08	1.27E-08	8.65E-09
SSW	2.27E-06	7.68E-07	3.63E-07	2.31E-07	1.66E-07	8.61E-08	3.39E-08	1.64E-08	9.95E-09	6.73E-09
SW	2.31E-06	7.83E-07	3.71E-07	2.36E-07	1.70E-07	8.80E-08	3.47E-08	1.68E-08	1.03E-08	6.96E-09
WSW	2.57E-06	8.65E-07	4.10E-07	2.63E-07	1.90E-07	9.89E-08	3.92E-08	1.90E-08	1.15E-08	7.79E-09
W	2.87E-06	9.66E-07	4.60E-07	2.96E-07	2.15E-07	1.13E-07	4.53E-08	2.21E-08	1.35E-08	9.17E-09
WNW	2.66E-06	8.97E-07	4.29E-07	2.76E-07	2.01E-07	1.05E-07	4.22E-08	2.07E-08	1.27E-08	8.65E-09
NW	2.58E-06	8.77E-07	4.17E-07	2.68E-07	1.94E-07	1.02E-07	4.11E-08	2.04E-08	1.27E-08	8.78E-09
NNW	1.79E-06	6.18E-07	2.94E-07	1.86E-07	1.33E-07	6.84E-08	2.69E-08	1.31E-08	8.09E-09	5.57E-09
N	1.37E-06	4.87E-07	2.31E-07	1.44E-07	1.01E-07	5.07E-08	1.93E-08	9.22E-09	5.64E-09	3.88E-09
NNE	9.38E-07	3.36E-07	1.58E-07	9.73E-08	6.79E-08	3.36E-08	1.26E-08	5.99E-09	3.68E-09	2.54E-09
NE	8.58E-07	3.04E-07	1.42E-07	8.69E-08	6.05E-08	2.99E-08	1.12E-08	5.37E-09	3.30E-09	2.28E-09
ENE	8.46E-07	2.95E-07	1.40E-07	8.69E-08	6.14E-08	3.10E-08	1.20E-08	5.82E-09	3.60E-09	2.49E-09
E	7.29E-07	2.53E-07	1.20E-07	7.58E-08	5.42E-08	2.79E-08	1.10E-08	5.45E-09	3.39E-09	2.36E-09
ESE	2.81E-06	9.48E-07	4.55E-07	2.94E-07	2.14E-07	1.13E-07	4.62E-08	2.32E-08	1.45E-08	1.01E-08
SE	7.28E-06	2.42E-06	1.15E-06	7.51E-07	5.51E-07	2.96E-07	1.23E-07	6.31E-08	4.00E-08	2.82E-08
SSE	3.67E-06	1.24E-06	5.89E-07	3.81E-07	2.77E-07	1.46E-07	5.97E-08	2.98E-08	1.85E-08	1.28E-08

WLS COL 2.3-5

TABLE 2.3-291 (Sheet 1 of 3)

ANNUAL AVERAGE χ/Q (SEC/M^3) FOR NORMAL RELEASES 8.00 DAY DECAY, DEPLETED
(FOR EACH 22.5° SECTOR AT THE DISTANCES (MILES) SHOWN AT THE TOP)

SECTOR	0.25	0.5	0.75	1	1.5	2	2.5	3	3.5	4	4.5
S	1.67E-05	4.81E-06	2.36E-06	1.47E-06	7.85E-07	5.08E-07	3.63E-07	2.82E-07	2.28E-07	1.90E-07	1.61E-07
SSW	1.34E-05	3.89E-06	1.92E-06	1.20E-06	6.38E-07	4.12E-07	2.94E-07	2.28E-07	1.84E-07	1.52E-07	1.29E-07
SW	1.37E-05	3.97E-06	1.95E-06	1.22E-06	6.51E-07	4.20E-07	3.00E-07	2.33E-07	1.88E-07	1.55E-07	1.32E-07
WSW	1.55E-05	4.45E-06	2.17E-06	1.35E-06	7.20E-07	4.65E-07	3.33E-07	2.59E-07	2.09E-07	1.74E-07	1.48E-07
W	1.74E-05	4.98E-06	2.42E-06	1.50E-06	8.03E-07	5.20E-07	3.73E-07	2.91E-07	2.36E-07	1.97E-07	1.67E-07
WNW	1.61E-05	4.62E-06	2.24E-06	1.39E-06	7.46E-07	4.85E-07	3.48E-07	2.71E-07	2.20E-07	1.83E-07	1.56E-07
NW	1.55E-05	4.45E-06	2.18E-06	1.36E-06	7.27E-07	4.71E-07	3.37E-07	2.62E-07	2.12E-07	1.76E-07	1.50E-07
NNW	1.04E-05	3.04E-06	1.52E-06	9.52E-07	5.13E-07	3.33E-07	2.38E-07	1.83E-07	1.47E-07	1.21E-07	1.02E-07
N	7.60E-06	2.26E-06	1.17E-06	7.45E-07	4.05E-07	2.62E-07	1.87E-07	1.42E-07	1.13E-07	9.25E-08	7.74E-08
NNE	5.14E-06	1.54E-06	8.06E-07	5.16E-07	2.80E-07	1.80E-07	1.28E-07	9.67E-08	7.63E-08	6.21E-08	5.17E-08
NE	4.73E-06	1.42E-06	7.37E-07	4.70E-07	2.52E-07	1.62E-07	1.14E-07	8.64E-08	6.81E-08	5.54E-08	4.62E-08
ENE	4.83E-06	1.42E-06	7.22E-07	4.54E-07	2.45E-07	1.58E-07	1.13E-07	8.60E-08	6.84E-08	5.60E-08	4.70E-08
E	4.22E-06	1.23E-06	6.19E-07	3.90E-07	2.10E-07	1.36E-07	9.68E-08	7.45E-08	5.98E-08	4.93E-08	4.16E-08
ESE	1.70E-05	4.87E-06	2.36E-06	1.46E-06	7.86E-07	5.12E-07	3.67E-07	2.87E-07	2.33E-07	1.94E-07	1.65E-07
SE	4.48E-05	1.27E-05	6.10E-06	3.75E-06	2.00E-06	1.29E-06	9.27E-07	7.29E-07	5.94E-07	4.97E-07	4.24E-07
SSE	2.22E-05	6.35E-06	3.09E-06	1.92E-06	1.03E-06	6.64E-07	4.75E-07	3.72E-07	3.02E-07	2.51E-07	2.14E-07

WLS COL 2.3-5

TABLE 2.3-291 (Sheet 2 of 3)
ANNUAL AVERAGE χ/Q (SEC/M^3) FOR NORMAL RELEASES 8.00 DAY DECAY, DEPLETED
(FOR EACH 22.5° SECTOR AT THE DISTANCES (MILES) SHOWN AT THE TOP)

SECTOR	5	7.5	10	15	20	25	30	35	40	45	50
S	1.39E-07	7.88E-08	5.22E-08	2.90E-08	1.89E-08	1.35E-08	1.01E-08	7.95E-09	6.42E-09	5.29E-09	4.44E-09
SSW	1.11E-07	6.26E-08	4.14E-08	2.28E-08	1.48E-08	1.06E-08	7.94E-09	6.22E-09	5.01E-09	4.13E-09	3.46E-09
SW	1.13E-07	6.40E-08	4.23E-08	2.33E-08	1.52E-08	1.08E-08	8.14E-09	6.38E-09	5.14E-09	4.24E-09	3.56E-09
WSW	1.28E-07	7.23E-08	4.80E-08	2.66E-08	1.73E-08	1.24E-08	9.31E-09	7.30E-09	5.89E-09	4.85E-09	4.07E-09
W	1.45E-07	8.27E-08	5.51E-08	3.07E-08	2.01E-08	1.43E-08	1.08E-08	8.50E-09	6.87E-09	5.67E-09	4.76E-09
WNW	1.35E-07	7.68E-08	5.11E-08	2.85E-08	1.86E-08	1.33E-08	1.00E-08	7.88E-09	6.37E-09	5.26E-09	4.42E-09
NW	1.29E-07	7.33E-08	4.87E-08	2.71E-08	1.77E-08	1.27E-08	9.59E-09	7.54E-09	6.11E-09	5.05E-09	4.26E-09
NNW	8.80E-08	4.91E-08	3.22E-08	1.76E-08	1.14E-08	8.11E-09	6.10E-09	4.77E-09	3.85E-09	3.17E-09	2.67E-09
N	6.60E-08	3.59E-08	2.31E-08	1.24E-08	7.88E-09	5.53E-09	4.12E-09	3.20E-09	2.57E-09	2.11E-09	1.76E-09
NNE	4.40E-08	2.35E-08	1.50E-08	7.93E-09	5.02E-09	3.51E-09	2.60E-09	2.02E-09	1.62E-09	1.33E-09	1.11E-09
NE	3.92E-08	2.10E-08	1.34E-08	7.10E-09	4.51E-09	3.16E-09	2.35E-09	1.83E-09	1.46E-09	1.20E-09	1.00E-09
ENE	4.01E-08	2.20E-08	1.42E-08	7.69E-09	4.94E-09	3.49E-09	2.62E-09	2.04E-09	1.65E-09	1.36E-09	1.14E-09
E	3.57E-08	1.99E-08	1.30E-08	7.14E-09	4.63E-09	3.29E-09	2.48E-09	1.94E-09	1.57E-09	1.30E-09	1.09E-09
ESE	1.43E-07	8.15E-08	5.43E-08	3.04E-08	1.99E-08	1.43E-08	1.08E-08	8.53E-09	6.92E-09	5.73E-09	4.83E-09
SE	3.68E-07	2.13E-07	1.43E-07	8.09E-08	5.35E-08	3.86E-08	2.94E-08	2.33E-08	1.89E-08	1.57E-08	1.33E-08
SSE	1.85E-07	1.06E-07	7.06E-08	3.95E-08	2.59E-08	1.86E-08	1.41E-08	1.11E-08	8.99E-09	7.45E-09	6.28E-09

WLS COL 2.3-5

TABLE 2.3-291 (Sheet 3 of 3)
ANNUAL AVERAGE χ/Q (SEC/M^3) FOR NORMAL RELEASES 8.00 DAY DECAY, DEPLETED
(FOR EACH 22.5° SECTOR AT THE DISTANCES (MILES) SHOWN AT THE TOP)

SECTOR	.5-1	1-2	2-3	3-4	4-5	5-10	10-20	20-30	30-40	40-50
S	2.51E-06	8.13E-07	3.69E-07	2.29E-07	1.61E-07	8.04E-08	2.96E-08	1.36E-08	7.99E-09	5.31E-09
SSW	2.04E-06	6.61E-07	2.99E-07	1.84E-07	1.29E-07	6.40E-08	2.34E-08	1.07E-08	6.25E-09	4.14E-09
SW	2.07E-06	6.74E-07	3.05E-07	1.88E-07	1.32E-07	6.53E-08	2.39E-08	1.09E-08	6.41E-09	4.25E-09
WSW	2.31E-06	7.46E-07	3.39E-07	2.10E-07	1.48E-07	7.38E-08	2.72E-08	1.25E-08	7.34E-09	4.87E-09
W	2.58E-06	8.32E-07	3.79E-07	2.37E-07	1.68E-07	8.42E-08	3.14E-08	1.45E-08	8.55E-09	5.69E-09
WNW	2.39E-06	7.73E-07	3.54E-07	2.21E-07	1.56E-07	7.82E-08	2.91E-08	1.34E-08	7.92E-09	5.28E-09
NW	2.32E-06	7.53E-07	3.43E-07	2.13E-07	1.50E-07	7.48E-08	2.77E-08	1.28E-08	7.58E-09	5.07E-09
NNW	1.61E-06	5.31E-07	2.41E-07	1.48E-07	1.03E-07	5.02E-08	1.81E-08	8.19E-09	4.80E-09	3.19E-09
N	1.22E-06	4.17E-07	1.89E-07	1.14E-07	7.77E-08	3.69E-08	1.28E-08	5.59E-09	3.22E-09	2.12E-09
NNE	8.40E-07	2.88E-07	1.29E-07	7.67E-08	5.19E-08	2.43E-08	8.21E-09	3.55E-09	2.03E-09	1.33E-09
NE	7.69E-07	2.60E-07	1.16E-07	6.85E-08	4.63E-08	2.17E-08	7.36E-09	3.20E-09	1.84E-09	1.21E-09
ENE	7.59E-07	2.53E-07	1.14E-07	6.87E-08	4.71E-08	2.26E-08	7.92E-09	3.53E-09	2.06E-09	1.36E-09
E	6.54E-07	2.17E-07	9.83E-08	6.00E-08	4.17E-08	2.04E-08	7.33E-09	3.32E-09	1.95E-09	1.30E-09
ESE	2.52E-06	8.14E-07	3.74E-07	2.33E-07	1.65E-07	8.30E-08	3.10E-08	1.44E-08	8.57E-09	5.75E-09
SE	6.53E-06	2.08E-06	9.45E-07	5.95E-07	4.25E-07	2.17E-07	8.26E-08	3.89E-08	2.34E-08	1.58E-08
SSE	3.29E-06	1.06E-06	4.84E-07	3.02E-07	2.14E-07	1.08E-07	4.04E-08	1.87E-08	1.12E-08	7.47E-09

WLS COL 2.3-5

TABLE 2.3-292 (Sheet 1 of 3)
D/Q (M^{-2}) AT EACH 22.5° SECTOR FOR NORMAL RELEASES
(FOR EACH DISTANCE (MILES) SHOWN AT THE TOP)

SECTOR	0.25	0.5	0.75	1	1.5	2	2.5	3	3.5	4	4.5
S	3.52E-08	1.19E-08	6.12E-09	3.76E-09	1.87E-09	1.14E-09	7.68E-10	5.57E-10	4.23E-10	3.33E-10	2.70E-10
SSW	3.42E-08	1.16E-08	5.93E-09	3.64E-09	1.82E-09	1.10E-09	7.44E-10	5.39E-10	4.10E-10	3.23E-10	2.62E-10
SW	3.49E-08	1.18E-08	6.06E-09	3.72E-09	1.85E-09	1.12E-09	7.60E-10	5.51E-10	4.19E-10	3.30E-10	2.67E-10
WSW	3.00E-08	1.01E-08	5.21E-09	3.20E-09	1.59E-09	9.66E-10	6.53E-10	4.74E-10	3.60E-10	2.84E-10	2.30E-10
W	2.70E-08	9.12E-09	4.68E-09	2.87E-09	1.43E-09	8.69E-10	5.88E-10	4.26E-10	3.24E-10	2.55E-10	2.07E-10
WNW	2.51E-08	8.47E-09	4.35E-09	2.67E-09	1.33E-09	8.08E-10	5.46E-10	3.96E-10	3.01E-10	2.37E-10	1.92E-10
NW	3.16E-08	1.07E-08	5.49E-09	3.37E-09	1.68E-09	1.02E-09	6.89E-10	4.99E-10	3.80E-10	2.99E-10	2.42E-10
NNW	3.32E-08	1.12E-08	5.77E-09	3.54E-09	1.77E-09	1.07E-09	7.24E-10	5.25E-10	3.99E-10	3.14E-10	2.54E-10
N	3.67E-08	1.24E-08	6.37E-09	3.91E-09	1.95E-09	1.18E-09	8.00E-10	5.80E-10	4.41E-10	3.47E-10	2.81E-10
NNE	4.01E-08	1.36E-08	6.96E-09	4.28E-09	2.13E-09	1.29E-09	8.74E-10	6.34E-10	4.82E-10	3.80E-10	3.07E-10
NE	4.11E-08	1.39E-08	7.14E-09	4.38E-09	2.19E-09	1.33E-09	8.96E-10	6.49E-10	4.94E-10	3.89E-10	3.15E-10
ENE	2.83E-08	9.56E-09	4.91E-09	3.01E-09	1.50E-09	9.11E-10	6.16E-10	4.47E-10	3.40E-10	2.68E-10	2.17E-10
E	1.59E-08	5.38E-09	2.76E-09	1.70E-09	8.45E-10	5.13E-10	3.47E-10	2.51E-10	1.91E-10	1.50E-10	1.22E-10
ESE	4.16E-08	1.41E-08	7.23E-09	4.44E-09	2.21E-09	1.34E-09	9.07E-10	6.57E-10	5.00E-10	3.94E-10	3.19E-10
SE	8.31E-08	2.81E-08	1.44E-08	8.86E-09	4.42E-09	2.68E-09	1.81E-09	1.31E-09	9.98E-10	7.86E-10	6.36E-10
SSE	4.08E-08	1.38E-08	7.09E-09	4.35E-09	2.17E-09	1.32E-09	8.90E-10	6.45E-10	4.90E-10	3.86E-10	3.13E-10

WLS COL 2.3-5

TABLE 2.3-292 (Sheet 2 of 3)
D/Q (M^{-2}) AT EACH 22.5° SECTOR FOR NORMAL RELEASES
(FOR EACH DISTANCE (MILES) SHOWN AT THE TOP)

SECTOR	5	7.5	10	15	20	25	30	35	40	45	50
S	2.23E-10	1.09E-10	6.86E-11	3.47E-11	2.10E-11	1.41E-11	1.01E-11	7.58E-12	5.89E-12	4.71E-12	3.84E-12
SSW	2.16E-10	1.06E-10	6.65E-11	3.36E-11	2.04E-11	1.37E-11	9.78E-12	7.34E-12	5.71E-12	4.56E-12	3.72E-12
SW	2.21E-10	1.08E-10	6.80E-11	3.44E-11	2.08E-11	1.39E-11	9.99E-12	7.50E-12	5.83E-12	4.66E-12	3.80E-12
WSW	1.90E-10	9.31E-11	5.84E-11	2.95E-11	1.79E-11	1.20E-11	8.58E-12	6.45E-12	5.01E-12	4.00E-12	3.27E-12
W	1.71E-10	8.37E-11	5.25E-11	2.66E-11	1.61E-11	1.08E-11	7.72E-12	5.80E-12	4.51E-12	3.60E-12	2.94E-12
WNW	1.59E-10	7.78E-11	4.88E-11	2.47E-11	1.49E-11	1.00E-11	7.18E-12	5.39E-12	4.19E-12	3.35E-12	2.73E-12
NW	2.00E-10	9.82E-11	6.16E-11	3.11E-11	1.88E-11	1.26E-11	9.05E-12	6.80E-12	5.29E-12	4.22E-12	3.45E-12
NNW	2.10E-10	1.03E-10	6.47E-11	3.27E-11	1.98E-11	1.33E-11	9.51E-12	7.14E-12	5.55E-12	4.44E-12	3.62E-12
N	2.33E-10	1.14E-10	7.15E-11	3.61E-11	2.19E-11	1.47E-11	1.05E-11	7.89E-12	6.14E-12	4.90E-12	4.00E-12
NNE	2.54E-10	1.25E-10	7.81E-11	3.95E-11	2.39E-11	1.60E-11	1.15E-11	8.62E-12	6.71E-12	5.36E-12	4.37E-12
NE	2.60E-10	1.28E-10	8.01E-11	4.05E-11	2.45E-11	1.64E-11	1.18E-11	8.84E-12	6.87E-12	5.49E-12	4.48E-12
ENE	1.79E-10	8.78E-11	5.51E-11	2.78E-11	1.69E-11	1.13E-11	8.09E-12	6.08E-12	4.73E-12	3.78E-12	3.08E-12
E	1.01E-10	4.94E-11	3.10E-11	1.57E-11	9.47E-12	6.35E-12	4.55E-12	3.42E-12	2.66E-12	2.12E-12	1.73E-12
ESE	2.64E-10	1.29E-10	8.11E-11	4.10E-11	2.48E-11	1.66E-11	1.19E-11	8.95E-12	6.96E-12	5.56E-12	4.54E-12
SE	5.26E-10	2.58E-10	1.62E-10	8.18E-11	4.95E-11	3.32E-11	2.38E-11	1.79E-11	1.39E-11	1.11E-11	9.06E-12
SSE	2.59E-10	1.27E-10	7.95E-11	4.02E-11	2.43E-11	1.63E-11	1.17E-11	8.78E-12	6.82E-12	5.45E-12	4.45E-12

WLS COL 2.3-5

TABLE 2.3-292 (Sheet 3 of 3)
D/Q (M^{-2}) AT EACH 22.5° SECTOR FOR NORMAL RELEASES
(FOR EACH DISTANCE (MILES) SHOWN AT THE TOP)

SECTOR	.5-1	1-2	2-3	3-4	4-5	5-10	10-20	20-30	30-40	40-50
S	6.36E-09	1.96E-09	7.81E-10	4.27E-10	2.71E-10	1.17E-10	3.62E-11	1.43E-11	7.65E-12	4.74E-12
SSW	6.16E-09	1.90E-09	7.57E-10	4.14E-10	2.63E-10	1.13E-10	3.50E-11	1.39E-11	7.42E-12	4.59E-12
SW	6.29E-09	1.94E-09	7.74E-10	4.23E-10	2.69E-10	1.15E-10	3.58E-11	1.42E-11	7.57E-12	4.69E-12
WSW	5.41E-09	1.67E-09	6.65E-10	3.63E-10	2.31E-10	9.92E-11	3.08E-11	1.22E-11	6.51E-12	4.03E-12
W	4.86E-09	1.50E-09	5.98E-10	3.27E-10	2.08E-10	8.92E-11	2.77E-11	1.10E-11	5.86E-12	3.62E-12
WNW	4.52E-09	1.40E-09	5.56E-10	3.04E-10	1.93E-10	8.29E-11	2.57E-11	1.02E-11	5.44E-12	3.37E-12
NW	5.70E-09	1.76E-09	7.01E-10	3.83E-10	2.44E-10	1.05E-10	3.24E-11	1.29E-11	6.87E-12	4.25E-12
NNW	5.99E-09	1.85E-09	7.37E-10	4.03E-10	2.56E-10	1.10E-10	3.41E-11	1.35E-11	7.21E-12	4.46E-12
N	6.62E-09	2.05E-09	8.14E-10	4.45E-10	2.83E-10	1.21E-10	3.77E-11	1.49E-11	7.97E-12	4.93E-12
NNE	7.24E-09	2.24E-09	8.90E-10	4.86E-10	3.09E-10	1.33E-10	4.12E-11	1.63E-11	8.71E-12	5.39E-12
NE	7.42E-09	2.29E-09	9.12E-10	4.98E-10	3.17E-10	1.36E-10	4.22E-11	1.67E-11	8.93E-12	5.53E-12
ENE	5.10E-09	1.58E-09	6.27E-10	3.43E-10	2.18E-10	9.35E-11	2.90E-11	1.15E-11	6.14E-12	3.80E-12
E	2.87E-09	8.86E-10	3.53E-10	1.93E-10	1.23E-10	5.26E-11	1.63E-11	6.47E-12	3.45E-12	2.14E-12
ESE	7.51E-09	2.32E-09	9.23E-10	5.04E-10	3.21E-10	1.38E-10	4.27E-11	1.69E-11	9.04E-12	5.59E-12
SE	1.50E-08	4.63E-09	1.84E-09	1.01E-09	6.40E-10	2.75E-10	8.52E-11	3.38E-11	1.80E-11	1.12E-11
SSE	7.36E-09	2.28E-09	9.05E-10	4.95E-10	3.14E-10	1.35E-10	4.19E-11	1.66E-11	8.86E-12	5.49E-12

TABLE 2.3-293
LEE NUCLEAR STATION DESIGN TEMPERATURES

	Frequency of Occurrence		
	0%	100-year	1 %
Cooling dry-bulb temperature, °F	103	107	91
Coincident wet-bulb temperature, °F	78	84	76
Evaporation wet-bulb (noncoincident), °F	81	85	76

	Dry Bulb Temperature °F	
	Maximum	Minimum
1 percent exceedance	91	24
0 percent exceedance	103	-1
100-year return	107	-5

Notes:

1. Based on 45 years (1963-2007) of meteorological data measured at the NWS station at Greenville-Spartanburg Airport (GSP).

TABLE 2.3-294
LEE NUCLEAR STATION TSC HVAC DISTANCES AND DIRECTIONS

WLS COL 2.3-4

Release Point	Distance (m)	Direction to Source from receptor (°)
Unit 1 Containment Shell	196	330
Unit 2 Containment Shell	213	16

Notes:

1. Distances and directions based on the nearest point on the Maintenance Support Building from each unit's containment shell.

2. Directions are relative to true North.

TABLE 2.3-295
TSC ATMOSPHERIC DISPERSION FACTORS (χ/Q) FOR
ACCIDENT DOSE ANALYSIS (S/M^3)

WLS COL 2.3-4

Time Interval	Unit 1 Containment Shell Release	Unit 2 Containment Shell Release
0 – 2 hours	1.51E-04	1.34E-04
2 – 8 hours	1.03E-04	1.13E-04
8 – 24 hours	3.93E-05	4.71E-05
1 – 4 days	2.90E-05	3.90E-05
4 – 30 days	2.15E-05	2.71E-05

2.4 HYDROLOGIC ENGINEERING

This section of the referenced DCD is incorporated by reference with the following departures and/or supplements

---

Section 2.4 describes the hydrological characteristics of the Lee Nuclear Site. The site location and description are provided in Section 2.1 of this report in sufficient detail to support the safety analysis. This section discusses characteristics and natural phenomena that have the potential to affect the design basis for the Westinghouse AP1000 reactor (AP1000) units. The section is divided into the following 14 subsections:

- 2.4.1 Hydrologic Description.
- 2.4.2 Floods.
- 2.4.3 Probable Maximum Flood on Streams and Rivers.
- 2.4.4 Potential Dam Failures.
- 2.4.5 Probable Maximum Surge and Seiche Flooding.
- 2.4.6 Probable Maximum Tsunami Flooding.
- 2.4.7 Ice Effects.
- 2.4.8 Cooling Water Canals and Reservoirs.
- 2.4.9 Channel Diversions.
- 2.4.10 Flood Protection Requirements.
- 2.4.11 Low Water Considerations.
- 2.4.12 Groundwater.
- 2.4.13 Accidental Releases of Liquid Effluents in Ground and Surface Waters.
- 2.4.14 Technical Specifications and Emergency Operation Requirements.

Subsection 2.4.1 of the DCD is renumbered as Subsection 2.4.15. This is being done to accommodate the incorporation of Regulatory Guide 1.206 numbering conventions for Section 2.4.

WLS COL 2.4-1
STD DEP 1.1-1

2.4.1 HYDROLOGIC DESCRIPTION

Information provided in this subsection includes descriptions of the site and its features, hydrosphere, hydrologic characteristics, drainage, dams and reservoirs, water management changes, and surface water uses.

2.4.1.1 Site and Facilities

The 1900-acre (ac.) Lee Nuclear Site is located south and west of the Broad River in eastern Cherokee County, South Carolina (Figure 2.2-201). The nuclear island for the Lee Nuclear Station is located south and west of the Ninety-Nine Islands Reservoir portion of the Broad River, approximately 1 mile (mi.) due northwest of the Ninety-Nine Islands Dam. In addition to the Broad River and several tributaries, the Ninety-Nine Islands Reservoir, Make-Up Pond B, Make-Up Pond A, and Hold-Up Pond A (Figure 2.4.1-201) make up the majority of the surface water features in the vicinity of the site. Make-Up Pond C is an off-site facility, located on a tributary of the Broad River, west of the Lee Nuclear Station (Figure 2.4.1-213).

2.4.1.1.1 Previous Construction Activities

The Lee Nuclear Site, formerly known as Cherokee Nuclear Station, was evaluated for and received a construction permit from the U.S. Nuclear Regulatory Commission to construct three Combustion Engineering System 80+ nuclear units. Approximately 750 ac. of ground were disturbed during the 1977-1982 construction activities, which resulted in extensive alteration of the site. This alteration included vegetation clearing; establishment of on-site construction roads; establishment of a railroad spur to the site; extensive excavation and grading with heavy equipment; building of on-site warehouses, shops, and construction support facilities; and construction of power unit buildings (portion of one power block building and about half of its associated cylindrical reactor containment/shield building). About 25 ac. were excavated into underlying bedrock for construction of the reactor units.

The site currently consists of open, partially-developed industrial land with low groundcover vegetation and scattered areas of sparse tree growth. However, the terrestrial environment surrounding the site consists primarily of deciduous hardwood forest and farms. The aquatic environs are dominated by the Broad River and the Ninety-Nine Islands Reservoir.

The Lee Nuclear Station is planned within the large, open, contiguous area of land that was cleared for previous construction activities on the site. The partially built reactor containment building is to be razed prior to new construction. The base mat slab and several warehouses will be kept. Construction of the intake structure

is planned on the Broad River, and the blowdown discharge sparger is planned on upstream side of Ninety-Nine Islands Dam.

2.4.1.1.2 Plant Design

Duke Energy selected the AP1000 certified plant design for the Lee Nuclear Station combined operating license application. The AP1000 units (Units 1 and 2) are planned to be in the vicinity of the previously proposed Cherokee Units 1 and 3. The AP1000 is rated at 3400 megawatts thermal (MWt) with a minimum electrical output of 1000 megawatts electrical (MWe). Each unit uses three mechanical draft towers for circulating water system cooling with the intake system providing all raw water requirements. During normal flow conditions raw water is pumped from Broad River raw water intake structure to Make-Up Pond A through the raw water discharge structure. During low-flow conditions raw water from Make-Up Pond B is pumped from the Make-Up Pond B intake structure to Make-Up Pond A through the raw water discharge structure. If Make-Up Pond B usable storage is not sufficient to meet plant needs, Make-Up Pond C is then used to supply supplemental water. Water is pumped from the Make-Up Pond C intake structure to a discharge structure in Make-Up Pond B and then is pumped from Make-Up Pond B to Make-Up Pond A, as previously described. The ultimate heat sink for the Lee Nuclear Station is the atmosphere.

2.4.1.1.3 Safety-Related Structures

The plant arrangement is comprised of five principal structures (as described in DCD Section 1.2.1.6): nuclear island, turbine building, annex building, diesel generator building, and radioactive waste building. Of the five principal structures, only the nuclear island is designed to Category I seismic requirements, and it contains all safety-related equipment for accident mitigation. The nuclear island consists of a free-standing steel containment building, a concrete shield building, and an auxiliary building. The foundation for the nuclear island is an integral basemat that supports these buildings.

The DCD reference floor elevation of 100 ft. corresponds to the nuclear island finished floor elevation set at 590 ft. above msl. Therefore, the nuclear island basemat elevation is 550.5 ft. above msl. Yard grade elevation is 589.5 ft. above msl, which keeps water from pooling in areas of safety related structures (Subsection 2.4.2.3). An extensive site stormwater drainage system is planned and is slated for implementation before the construction commences on Units 1 and 2. The elevations of safety-related components are presented on Table 2.4.1-201.

2.4.1.1.4 Plant Water Systems

Plant water consumption and water treatment for the Lee Nuclear Station are determined from the AP1000 Design Control Document, site characteristics, and engineering evaluations. The raw water system supplies water to Make-Up Pond A for plant use, including make-up to the circulating water system (CWS) cooling towers, to makeup for water consumed as a result of evaporation, drift and blowdown. The raw water intake structure is located on the west bank of the

Broad River, north-northeast of Unit 2 (Figure 2.4.1-201). The raw water discharge structure is located at the north end of Make-Up Pond A near the Unit 2 cooling towers. Water withdrawn from the Broad River is pumped into Make-Up Pond A and from there enters the make-up water intake structure. Raw water is also processed through the clarifier and used in plant water systems including the service water system, the demineralized water treatment system and the fire protection system. Effluent from the Lee Nuclear Station is to be diffused into the river at the upstream face of the Ninety-Nine Islands Dam near the intakes for the hydroelectric station (Reference 256), avoiding recirculation of the plant effluent to the intake structure located approximately 1.25 river miles upstream (Figure 2.4.1-201).

Intake System

The intake system provides all raw water requirements for the plant. During normal flow conditions, raw water is pumped from the Broad River raw water intake structure to Make-Up Pond A through the raw water discharge structure. During low flow conditions, raw water from Make-Up Pond B is pumped from the Make-Up Pond B intake structure to Make-Up Pond A through the raw water discharge structure. If Make-Up Pond B usable storage is not sufficient to meet plant needs, Make-Up Pond C is then used to supply supplemental water. Water is pumped from the Make-Up Pond C intake structure to a discharge structure in Make-Up Pond B and then is pumped from Make-Up Pond B to Make-Up Pond A, as previously described.

After low flow conditions have ceased, Make-Up Pond B is replenished using water from the Broad River which is pumped into Make-Up Pond A and subsequently into Make-Up Pond B. Raw water is pumped from the Make-Up Pond A intake structure to Make-Up Pond B using the same piping to supply Make-Up Pond A with water from Make-Up Pond B. Water is discharged into Make-Up Pond B using the Make-Up Pond B intake structure. An alternative refill path is to use the refill pumps on the river intake structure that pump directly to Make-Up Pond B.

Make-Up Pond C is normally refilled directly from the river using the same refill pumps on the river intake structure that pump directly to Make-Up Pond B. The section of pipe between Make-Up Pond B and Make-Up Pond C is used to both supply Make-Up Pond B from Make-Up Pond C and to refill Make-Up Pond C from the river. Water is discharged into Make-Up Pond C using the Make-Up Pond C intake structure. An alternative refill path for Make-Up Pond C is to pump from the Broad River into Make-Up Pond A, then pump from Make-Up Pond A to Make-Up Pond B, and then pump from Make-Up Pond B to Make-Up Pond C using a dedicated line only for refilling Make-Up Pond C. The intake, discharge, and pump structures for Make-Up Ponds A and B are shown in Figure 2.4.1-201. Make-Up Pond C is an off-site facility, located west of the Lee Nuclear Station, as shown in Figure 2.4.1-213.

The river intake structure serves as a platform to support trash racks, traveling screens, pumps, motors, and other equipment. Intake water taken from the Broad River passes through bar screens and traveling screens designed to minimize

uptake of aquatic biota and debris. Each traveling screen has fish collection and return capability. Return of impinged fish is to a location downstream of the intake. Debris collected by the trash racks and traveling screens is collected and disposed of as solid waste (Reference 256).

The raw water requirements vary depending on the operating mode, therefore the flow rates and intake velocities also vary. During the first four modes of operation, which include power operation, startup, hot standby, and safe shutdown, both the CWS and the service water system (SWS) require makeup water. The raw water system (RWS) supplies an average of 35,030 gallons per minute (gpm) (60,001 gpm maximum) raw water flow as makeup to the CWS, the SWS, and the demineralized treatment system (DTS) for the two units. Flow to the fire protection system (FPS) and the waste water system (WWS) is intermittent. The screens are sized so that the average through-screen velocity is in accordance with the Section 316 (b) of the Clean Water Act. The intake velocity is less than 0.5 fps. For the remaining two modes of operation, cold shutdown and refueling, the flow rate and the intake velocity is less as only the SWS requires makeup water from the raw water intake. For these final two modes of operation, the flow rate is 650 gpm per unit and the intake velocity is negligible.

Discharge System

The primary purpose of the discharge system is to disperse cooling tower blowdown into the Broad River along with other wastewater streams to limit the concentration of dissolved solids in the heat rejection system. Any additives in the discharge are as approved by the U.S. Environmental Protection Agency (EPA) as safe for humans and the environment. The volume and concentration of the constituents discharged to the environment will meet the requirements established in the South Carolina Department of Health and Environmental Control (SCDHEC) administered National Pollution Discharge Elimination System (NPDES) permit.

Effluent from the Lee Nuclear Station is to be diffused into the river at the upstream face of the Ninety-Nine Islands Dam near the intakes for the hydroelectric generating units. This discharge includes non-radioactive process waste (including cooling tower blowdown) and low level liquid radioactive waste (at an average rate of 4 gpm within regulatory limits).

The discharge structure consists of a submerged pipe that is perforated for the last portion of its length, diffusing the effluent into the hydroelectric station intakes. The effluent discharge rate to the Broad River during normal operations is approximately 8216 gpm with a maximum plant water discharge rate of 28,778 gpm (for two units).

2.4.1.2 Hydrosphere

The location of the Lee Nuclear Station, as described in Subsection 2.4.1.1, falls within the Broad River basin. The Broad River and Ninety-Nine Islands Reservoir are the main hydrologic features that may affect or be affected by construction activities in the immediate vicinity of the Lee Nuclear Site. Ninety-Nine Islands

Reservoir is the nearest major body of surface water to the Lee Nuclear Site. This reservoir is an impoundment of the Broad River by Ninety-Nine Islands Dam. The Lee Nuclear Site is located adjacent to the reservoir, which surrounds the site to the north and east. Land along the south boundary of the site is private property. Current surface water features at the site include Make-Up Pond B, Make-Up Pond A, and Hold-Up Pond A. Make-Up Pond C is an off-site facility, located on a tributary of the Broad River, west of the Lee Nuclear Station. A brief description of local groundwater conditions is also provided in this subsection.

2.4.1.2.1 Physiography and Topography

The Lee Nuclear Site is located within the Piedmont physiographic province, a southwest to northeast-oriented province of the Appalachian Mountain System (Figure 2.4.1-203). The Piedmont province is 80 – 120 mi. wide, and it is situated between the Blue Ridge province, a mountainous region to the northwest, and the Atlantic Coastal Plain province to the southeast. The province is a seaward-sloping plateau, dominated by a monotonous topography of low rounded ridges with gentle slopes and ravines largely underlain by saprolite developed on crystalline rock.

The principal drainageway in the region of the Lee Nuclear Site is the Broad River. Near the larger streams, tributaries cut through deep and steep valleys that (when traced headward) become wide, shallow, and of gentle gradient. The regional southeastward drainage of the Broad River basin is reflected in the trend of the Broad River (Reference 220). The Piedmont region of the Broad River basin is a plateau of forested, rolling hills with tight, dissected river valleys that generally contain small floodplains. The tributaries of the Broad River generally follow a dendritic pattern before draining to the Broad River and eventually the Atlantic Ocean.

Construction activities at the former Cherokee Nuclear Site altered local topography to cut and fill the site to a yard-grade elevation of 588 ft. above msl. Following excavation in the power block area, site topography changed from hills and valleys to a relatively flat upland setting punctuated by a massive excavation to competent rock, which over time filled with water from both groundwater seepage and precipitation. Subsection 2.4.12.2.3 describes the dewatering of this excavation in support of exploration activities for the Lee Nuclear Station. Numerous springs and seeps identified during the 1973 investigation (Reference 214) were disturbed during the 1975 – 1982 construction activities for the Cherokee Nuclear Station. Those springs and seeps were located within valley draws and natural drainage ways. Surface conditions around these springs appear to have been altered so that no flow-through discharge occurs. The undisturbed topography remaining at the Lee Nuclear Site is generally characterized by rounded hilltops and narrow valleys with elevations ranging from 511 ft. at the Broad River to around 810 ft. along the ridgeline of McKowns Mountain, located west of the power block area and south of Make-Up Pond B.

2.4.1.2.2 Upper Broad River Watershed

The Broad River basin region, the Broad River, and the majority of its tributaries originate in the Blue Ridge Mountains of North Carolina and extend toward the foothills before entering the Piedmont ecoregion, all within the larger Santee River basin, U.S. Geological Survey (USGS) (six-digit Hydrological Unit Code [HUC] 030501) (Figure 2.4.1-204) (Reference 290).

The USGS divides the Broad River basin into the Upper Broad (HUC 03050105) and Lower Broad (HUC 03050106) River basins with the Lee Nuclear Site positioned within the Upper Broad River basin (Figure 2.4.1-204). The Upper Broad River basin is located in both North and South Carolina. The Broad River drainage basin above Ninety-Nine Islands Dam is located within the Upper Broad River basin and includes the Green River, First Broad River, Second Broad River, and Buffalo Creek as major tributaries (Figure 2.4.1-205) (Reference 231). The drainage area of the Upper Broad River basin is approximately 2500 sq. mi. (Table 2.4.1-202) and is situated over the North Carolina-South Carolina state border. The drainage area of the Upper Broad River basin to Ninety-Nine Islands Dam (one-half river mile downstream from the site) is approximately 1550 sq. mi. (Reference 216).

Watershed elevations range from about 1200 ft. above msl at the headwaters of the First Broad River in the mountains of North Carolina to 620 ft. above msl when the Broad River crosses the North Carolina/South Carolina border. Watershed elevations along the Broad River continue to decrease southward to 511 ft. above msl upstream of Ninety-Nine Islands Dam, and 440 ft. below Ninety-Nine Islands Dam. At the confluence of the Broad River with the Saluda River in Columbia, South Carolina the elevation is 140 ft. above msl. The slope percentage of the Broad River is 0.55, and it has a gradient of 28.9 ft/mi (Reference 290).

The Broad River starts in Buncombe County, flows through Henderson, Rutherford and Cleveland counties in North Carolina and then into Cherokee County, South Carolina. In North Carolina, the basin encompasses most of Cleveland, Polk, and Rutherford counties and small portions of Buncombe, Henderson, Lincoln, Gaston, Burke and McDowell counties (Figure 2.4.1-206). Larger municipalities within the basin include the towns of Forest City, Kings Mountain, Lake Lure, Rutherfordton, Shelby, and Spindale. Approximately one-half of the basin is covered in forest; however, agriculture is still widespread (Reference 231).

2.4.1.2.2.1 Local Watersheds

The Broad River accepts drainage from Ross Creek (Sarratt Creek), Mikes Creek, Bowens River (Wylies Creek), the Buffalo Creek watershed, and the Cherokee watershed (Figure 2.4.1-207). Further downstream, Peoples Creek (Furnace Creek, Toms Branch) drains into the Broad River near the city of Gaffney. Doolittle Creek enters the river near the town of Blacksburg, followed by London Creek (which feeds Lake Cherokee and Make-Up Pond C, and has the Little London Creek as a tributary), Bear Creek, McKowns Creek (which feeds Make-Up Pond B at the site), Dry Branch, the Kings watershed, and Quinton Branch. Mud Creek

enters the Broad River next, downstream from Mud Islands, followed by Guyonmbore Creek, Mountain Branch, Abington Creek (Wolf Branch, Service Branch, and Jenkins Branch), the Thicketty Creek watershed, Beaverdam Creek (McDaniel Branch), the Bullock Creek watershed, and Dry Creek (Nelson Creek). There are numerous ponds and lakes located off-site (totaling 246 ac., not including the approximately 620 ac. Make-Up Pond C) in this watershed (03050105-090) and all 133 stream mi. are classified as fresh water (Reference 268).

The Lee Nuclear Site is located in USGS Hydrologic Unit 03050105-090 of Cherokee and York counties, South Carolina, and this unit consists primarily of the Broad River and its tributaries from the North Carolina border to the Pacolet River (Figure 2.4.1-205). Land use/land cover in the watershed includes: 67.8 percent forested, 18.8 percent agriculture land, 5 percent scrub/shrub land, 4.5 percent urban land, 2.8 percent water, and 1.1 percent barren (Reference 268).

2.4.1.2.2.2 Broad River Description

The Broad River has a length of about 185 river mi. The drainage area of the Upper Broad River basin is approximately 2500 sq. mi. (North Carolina and South Carolina). The drainage area of the Upper Broad River basin to Ninety-Nine Islands Dam, one-half river mile downstream from the site, is approximately 1550 sq. mi. The Broad River drainage basin above Ninety-Nine Islands Dam includes these major tributaries: Green River, First Broad River, Second Broad River, and Buffalo Creek (Reference 232).

The Broad River originates upstream of Lake Lure. Lake Lure Dam is located on the east side of Lake Lure, and the majority of the lake water is provided by the Broad River (also known as the Rocky Broad River).

The middle and lower portions of the Broad River in North Carolina cover about 40 river mi. from Lake Lure to the confluence of the Second Broad River near the Cleveland-Rutherford county line. Major tributaries in this section include the Green and Second Broad Rivers. The headwaters of these tributaries begin in the Mountains and then flow into the Piedmont ecoregion. Smaller tributary catchments of the Broad River include Mountain and Cleghorn creeks (Reference 232). The headwater reaches of the Green River are located in Henderson County, North Carolina.

Discharge Characteristics

The nature of flow in the Broad River was characterized by USGS gauging stations described in Table 2.4.1-203. The 2005 annual mean flows are also provided in Table 2.4.1-203 to illustrate the Broad River's gaining stream characteristics. USGS gauging stations are shown on Figure 2.4.1-205.

Broad River discharge recorded at the USGS Station No. 02153551 located just below Ninety-Nine Islands Dam ranged from 138 cubic feet per second (cfs) on September 14, 2002, to over 60,000 cfs in September 2004. Additionally, the

Gaffney USGS Station (No. 02133500) located approximately 8 mi. north of the Lee Nuclear Site and having about 60 sq. mi. less drainage area than Ninety-Nine Islands Reservoir, detected the highest recorded flow on record of 119,100 cfs, recorded on August 14, 1940 (Reference 214).

Based on an 83-year period of record (1926 – 2008) for the Broad River at the Gaffney Station, an average annual flow of the Broad River was determined to be approximately 2500 cfs. The 83-year period of record was derived using three USGS stream gauges located on the Broad River. The Broad River gauge near Gaffney, SC (USGS 02153500) is located just upstream of the Lee Nuclear Site and has available data from 1938-1971 and 1986-1990. The Gaffney gauge data was used without correction for drainage area size and applied to the site.

The Broad River gauge near Blacksburg, SC (USGS 02153200) is located upstream from the Gaffney gauge and has available data from 1997-2008. The Blacksburg gauge data was corrected by a ratio of drainage areas for the Gaffney gauge to the Blacksburg gauge and then applied to the site. The Broad River gauge near Boiling Springs, NC (USGS 02151500) is located upstream from the Blacksburg gauge and has available data from 1926-2008. Only data from the absent years of the Gaffney and Blacksburg gauges were corrected by a ratio of drainage areas for the Gaffney gauge to the Boiling Springs gauge and then applied to the site. The overlapping data from the Boiling Springs gauge were not utilized.

Low-flow conditions on the Broad River are a function of natural flow in the rivers and streams, available storage capacity of upstream reservoirs, and regulated discharge flow from upstream dams. Low-flow conditions are generally defined as the lowest consecutive 7-day stream flow that is likely to occur every 10 years (7Q10). The 7Q10 was calculated with the same database described above to be 439 cfs using Log-Pearson Type III distribution (Subsection 2.4.11.5).

The South Carolina climate is subject to periodic droughts. Since 1900, severe droughts have occurred statewide in 1925, 1933, 1954, 1977, 1983, 1986, 1990, 1993, 1998, 2002, 2007, and 2008. The drought that officially began in June 1998 abated in the late summer of 2002 with the onset of the hurricane season. The effects of these droughts are reflected in the Broad River discharge characteristics. Low-flow conditions are further discussed in Subsection 2.4.11.

In September 2006, during a bathymetry study (Reference 298), water velocities were characterized in the vicinity of the intake structure. Station No. 02153551 (located below the Ninety-Nine Islands Dam) measured Broad River discharge ranging from 1960–3090 cfs at the time of this assessment. Bathymetry at the intake structure shows a narrow linear feature (i.e., scour hole) aligned along the direction of flow and appears to be approximately 30-ft. deep (elevation 480 ft. msl). This linear feature is located in a section of the Broad River channel that is approximately 240 ft. across. Water velocities were measured at seven stations along a transect crossing the Broad River perpendicular to the intake at channel depths of 1, 5, 10, and 15 ft. Water velocity around the intake structure had an average flow rate of 0.32 feet per second (fps) with a standard deviation of 0.04 fps. No water velocity measurements were obtained near the dam and the proposed

plant discharge location due to access restrictions and safety considerations related to hydroelectric operations.

To supplement characterization of the Broad River as a heat sink for the discharge of cooling water blowdown, temperature data from USGS Station No. 02156500 (located near Carlisle, South Carolina, in Union County) were compiled and are presented in Table 2.4.1-204. For the period 1996 to 2006, the monthly water temperatures ranged from 40.8°F to 85.3°F (4.9°C to 29.6°C).

Generally, the Broad River flow conditions and discharge characteristics are consistent with those observed in the 1970's. As such, the bedforms and sediment transport observations presented in the Cherokee Nuclear Station Construction Permit Environmental Report (ER) are relevant today and are discussed below.

Bedforms

The bottom of the Broad River is influenced by the formation of bedforms. Bedforms are likely to be (1) scoured in bedrock, (2) formed from sand resulting in migrating dunes, (3) created from alluvial bed material of mixed sizes forming pools and riffles, or (4) produced by a combination of the above. Pools and riffles are the most common bedforms. At low flow, riffles are essentially flow-resistant dams forming each upstream pool. Water velocity over the riffles at low flow is considerably greater than that in adjacent pools. Therefore, fine sediment such as sand or silt is found on riffles.

At high flow, the stepped water surface characteristic of pools and riffles at low flow tends to disappear, and bedform conditions may be greatly altered from that found at low flow. At high flow, pools become areas of greater scour and thus may have similar water velocity as that found in the adjacent riffle areas. Although pools are quiet environments similar to impoundments during low flow, they generally have a high water velocity at the center of the river and the outside bends of the river. During high river flows the riparian vegetation and inside bends of the river provide the low velocity regions typically provided by the pools at low flow. The boundary between a pool and the adjacent riffles is primarily a function of discharge. The basic morphology of these forms does not change through exposure to a variety of flow levels. The most distinct break is between a riffle and an upstream pool; the deepest part of the pool is likely to be fairly close to the adjacent downstream riffle (Reference 214).

Bedform surveys for areas on the Broad River upstream and downstream of the Lee Nuclear Station were conducted in the 1970s. Between the Gaston Shoals impoundment and U.S. Highway 29 (U.S. 29), the Broad River channel was characterized by pools and riffles. The riffles were bedrock ridges cut into felsic schist. The bed material in pools and moving through riffles was entirely composed of uniform sand. Between U.S. 29 and Cherokee Falls, a resistant outcrop of felsic gneiss formed a long, continuous area of shallow riffles in which no pools had developed. From Cherokee Falls to Ninety-Nine Islands Reservoir, the stream was again characterized by bedrock highs (riffles) formed from schist, alternating with deeper pools in which the substrate material was nearly all sand. Below the reservoir another resistant gneiss bedrock outcrop created a long,

continuous shallow riffle area that gave way downstream to more pools and riffles. Below the Irene Bridge, the pools became larger and much longer while the riffles became smaller and less conspicuous. This dominance of pools was accompanied by steeper river banks, a diminution of sand beds, and the introduction of silt and mud substrates in the pools (Reference 214).

In summary, alternating pools and riffles cut in bedrock are the dominant bedforms of the Broad River above and below the Lee Nuclear Station. Where bands of resistant gneiss cross the course of the river, they create anomalous shallow riffles. The bedload is mostly coarse sand, making scoured rock outcrops and sand beds the two common substrate types (Reference 214).

Sediment Transport

The Broad River is generally wide and fairly shallow (Figure 2.4.1-208), and it normally carries a high bedload composed mainly of sands with some coarse gravels and cobbles. Water samples were collected in the early 1970s to estimate the suspended sediment load in the river for the Cherokee Nuclear Station Construction Permit Environmental Report (ER). Samples were collected from October 1973 through September 1974.

Sample results from Station 8, located just above the proposed site (Figure 2.4.1-206), ranged from 20 to 282 mg/L and an average sediment concentration of 73.9 mg/L, with a standard deviation of 63.3 mg/L (Reference 214). In a study conducted in 1989 – 1990 for the Ninety-Nine Islands Dam license renewal, the Broad River exhibited a mean TSS of 41 mg/L, ranging from 6 to 243 mg/L (Reference 216). Suspended solids concentrations can vary widely as a function of stream flow.

Analytical results from samples collected quarterly in 2006 show a mean TSS concentration of 11.5 mg/L. TSS concentrations ranged from 1 to 62 mg/L with a standard deviation of 12.4 mg/L. The waters within the main channel of the Broad River near the intake structure exhibited a mean TSS concentration of 10.2 mg/L. Additional sampling of the Ninety-Nine Islands Reservoir, conducted in 2007, reported a TSS range of less than 4 to 204 mg/L. Particle size analyses of suspended solids revealed a range from 0.00035 (clay) to 0.35355 millimeters (mm) (medium grade sand). From the five water samples collected and analyzed, the average of their median particle sizes was 0.0171 mm (medium silt) with a settling velocity calculated to be 0.0001 feet per second (fps).

The values used for the design basis are an average TSS concentration of 75 mg/L and a maximum TSS concentration of 300 mg/L, based on current Broad River data from Duke's surrounding power plants.

Modeling studies conducted for the water intake structure of the former Cherokee Nuclear Station demonstrated that local flows near the intake are expected to deter significant sediment accumulation in the local scour hole near the intake structure. However, this same study noted some bedload sediment deposits in the intake structure as a result of pump operations and high-flow events, which will require

annual maintenance dredging. Dredging would usually be limited to approximately 150 cubic yards (cu. yd.) annually.

2.4.1.2.2.3 Major Tributaries

The four major tributaries of the Broad River above the Lee Nuclear Site include the First Broad River, Second Broad River, Green River, and Buffalo Creek (Figure 2.4.1-206) (Reference 233).

First Broad River

The First Broad River originates in Rutherford County and flows into the Broad River in Cleveland County, North Carolina, just above the South Carolina border (Figure 2.4.1-205). The entire First Broad River and its tributaries are located in USGS Hydrologic Subbasin 030804. Tributaries of the First Broad River include Brier Creek and North Fork First Broad Creek, Brushy, Hinton, Knob, and Wards creeks (Reference 231, Figure 2.4.1-206).

Approximately two-thirds of the 426 sq mi. (Table 2.4.1-202) of the First Broad River subbasin are forested and one-third is in pasture. The largest urbanized areas in this subbasin are the towns of Shelby and Boiling Springs. These municipalities are restricted to the southern third of the subbasin and are concentrated along the U.S. 74 corridor. There are 11 permitted dischargers in the subbasin, including the towns of Shelby and Boiling Springs, wastewater treatment plants, and PPG Industries (Reference 232). The First Broad River has a slope of 0.33 percent and a gradient of 17.4 ft./mi., based on analysis of a USGS topographic map (Reference 290).

Second Broad River

The Second Broad River originates in McDowell County and flows into the Broad River near the Rutherford and Cleveland counties border (Figures 2.4.1-205 and 2.4.1-206). The Second Broad River and its tributaries lie within USGS Hydrologic Subbasin 030802; it has a drainage area of approximately 513 sq mi. (Table 2.4.1-202). Tributaries of the Second Broad River include Catheys, Hollands, and Roberson creeks (Figure 2.4.1-206). The largest urbanized areas are the towns of Spindale and Forest City. There are three permitted dischargers in this subbasin that release greater than 0.5 million gallons per day (Mgd) of effluent to the Second Broad River watershed. These are the wastewater plants for the towns of Spindale, Forest City, and Cone Denim LLC (Reference 232). The Second Broad River has a slope of 0.37 percent and a gradient of 19.7 ft./mi. (Reference 289).

Green River

The Green River has been impounded at two locations to form Lake Summit and Lake Adger (Figure 2.4.1-205). Both reservoirs are used to produce hydroelectric power. The Green River and its tributaries lie within USGS Hydrologic Subbasins 030802 and 030803 (Figures 2.4.1-205 and 2.4.1-206) and comprise a drainage area of approximately 137 sq. mi. (Table 2.4.1-202). This drainage area

is mostly undeveloped with more than 90 percent of the surface area forested. Tributaries of the Green River include the Hungry River and Brights Creek (Figure 2.4.1-206). R.J.G. Inc.'s Six Oaks Complex has the only permit to discharge on the Green River (above Summit Dam). The Bright's Creek Golf Club development has a temporary construction discharge permit; however, once the facility is operational, it is expected to have a nondischarge permit (Reference 232). The Green River has a slope of 0.69 percent and a gradient of 36.5 ft./mi. (Reference 289).

Buffalo Creek

Buffalo Creek drains eastern Cleveland, southwestern Lincoln, and northwestern Gaston counties in North Carolina (Figure 2.4.1-206), and this creek and its tributaries flow south through USGS Hydrologic Subbasins 030805 and 100 (Figure 2.4.1-206). The Buffalo Creek drainage area is approximately 181 sq. mi. (Table 2.4.1-202) in North Carolina and 16 sq. mi. in South Carolina. Approximately 40 percent of the surface area is pasture land, and almost 50 percent continues to be forested. Tributaries of Buffalo Creek include Muddy Fork and Beason Creek (Figure 2.4.1-206). Buffalo Creek is impounded approximately 16 river mi. northeast of the Lee Nuclear Site to form Kings Mountain Reservoir in North Carolina. The creek discharges into the Broad River approximately 7 river mi. north of Ninety-Nine Islands Dam (Reference 232). Buffalo Creek has a slope percentage of 0.29 and a gradient of 15.1 ft/mi (Reference 289).

2.4.1.2.2.4 Local Tributaries

In addition to the Broad River and its major tributaries, there are several smaller streams in the vicinity of the Lee Nuclear Site (above Ninety-Nine Islands Dam), including Cherokee Creek, Doolittle Creek, London Creek, and McKowns Creek. In addition, an intermittent stream flows into Make-Up Pond A (Figure 2.4.1-206).

The most significant of these features is McKowns Creek, which is dammed at the Lee Nuclear Site to form Make-Up Pond B (see Subsection 2.4.1.2.2.6). McKowns Creek's drainage area is estimated to be 1633 ac., including a small impoundment feeding the creek. The small impoundment has a drainage area of approximately 181 ac. (Reference 254). The intermittent stream mentioned in the previous paragraph features a drainage area of approximately 385 ac.

There are a number of other creeks and impoundments within a 6-mi. radius of the Lee Nuclear Site. Most of these features are hydraulically insignificant (i.e., small storage, low hazard structures, or outside drainage) with the exception of Make-Up Pond C. The largest of these features within this radius is Make-Up Pond C located on London Creek, as shown in Figure 2.4.1-213, which has a maximum storage of approximately 22,000 acre-feet (ac.-ft.). Details of Make-Up Pond C are provided in Subsection 2.4.1.2.3.1. Lake Cherokee (also known as Wildlife Dam and Reservoir) is located on London Creek just upstream of Make-Up Pond C. Lake Cherokee has a maximum storage of 720 ac.-ft. and is hydraulically insignificant.

2.4.1.2.2.5 Ninety-Nine Islands Reservoir

Ninety-Nine Islands Dam is located on the Broad River approximately 1 linear mi. southeast of the Lee Nuclear Station. The reservoir backs up to Cherokee Falls Dam, approximately 3 mi. to the north. The Ninety-Nine Islands Dam and associated hydroelectric plant were constructed in 1910, and the dam structure is a concrete gravity dam 62 ft. in height and 1568 ft. in length (References 216 and 217).

The Federal Energy Regulatory Commission (FERC) operating license for Ninety-Nine Islands Hydroelectric Station limits reservoir drawdown to 1 ft. below full pond (511 ft. above msl) from March through May and 2 ft. below full pond elevation from June through February. In addition, the minimum flows to be maintained below the dam are: 966 cfs January through April; 725 cfs May, June, and December; and 483 cfs July through November (Reference 216). When river flow drops below 483 CFS and the elevations drop to the maximum drawdown limit, the Ninety-Nine Islands Hydroelectric Station must discharge accumulated inflow on an hourly basis.

Reservoir Characteristics

Ninety-Nine Islands Dam impounds a 433-ac. mainstem “run-of-the-river” reservoir[a] with a normal water level at 511 ft. above msl and a shoreline of approximately 14 mi. (Reference 216). Flow through Ninety-Nine Islands Reservoir is dominated by the flow of the river channel, which divides the reservoir into two backwater regions. The two backwater regions exhibit very little circulation during nonflood periods. Therefore, the average transit time through the reservoir is conservatively estimated from the volume of the reservoir along the main channel excluding the backwater areas. Based on a storage volume of 570 ac-ft along the main channel to a point about 0.7 river mi. upstream from the dam and an average annual flow of the Broad River of approximately 2500 cfs, the average transit time for water flow through the reservoir is approximately 3 hours. During low flow conditions the transit time slows to around 14 hours (Subsection 2.4.11).

From October 1998 to 2006, the USGS recorded a minimum pool elevation in the Ninety-Nine Islands Reservoir of 508.20 ft. on February 14, 2005 (Reference 293). Duke Power data from 1964 to 1973 indicate that the minimum pool elevation was 505.6 ft. during May 1965 (Reference 214). Low water considerations are discussed in Subsection 2.4.11. The Broad River design basis flood elevation is 549.77 ft above msl (Subsections 2.4.2 and 2.4.3). Based on the flood frequency curve generated from analysis of the USGS Gaffney gauge, the projected 100-yr flow is 97,900 cfs and the projected 500-year flow is 127,000 cfs.

a. The mainstem refers to the main channel of the river in a river basin, as opposed to the streams and smaller rivers that feed into it. A “run-of-the-river” dam is a dam without a large reservoir and, therefore, with only a limited capacity for water storage.

The corresponding elevations based on interpolation of the rating curve for Ninety-Nine Islands Dam and assuming flashboard failure are 520.95 ft. and 522.63 ft. for the 100-year and 500-year events, respectively.

Because the Ninety-Nine Islands Reservoir is a “run-of-the-river” reservoir, evaporation and seepage have little effect on the water budget of the reservoir. The aspects of annual yield and dependability as they relate to the construction or operation of Lee Nuclear Station are discussed above in terms of discharge and low-flow characteristics of the Broad River.

Morphology

Ninety-Nine Islands Reservoir is characterized by three hydrographic areas, the main river channel and two backwater areas, that have developed because of sedimentation patterns since impoundment of the reservoir. The reservoir is a dynamic system that is constantly changing, due to the effects of floods, low flow, sedimentation, and scouring. In its present state the reservoir is a combination of two large backwater areas separated by the river channel and its associated sediment bars, spits, banks, and coves. A bathymetry study of the reservoir was conducted in the fall of 1973 by Duke Power Company (Reference 214). In the fall of 2006, additional bathymetry of the reservoir and the Broad River was conducted. This impoundment exhibited a maximum depth of 35.2 ft. (Figure 2.4.1-209, Sheet 1) and a mean depth of 9.2 ft. The impoundment is relatively shallow and relatively minor fluctuations in reservoir levels can result in significant changes in surface area. The estimated volume of storage is 1691 ac.-ft. based on the limited 233-ac. survey area. The U.S. Army Corps of Engineers (USACE) National Inventory of Dams (NID) reports the storage volume as 2300 ac.-ft. Deltaic sedimentation associated with creeks was evident in the backwater areas and limited the aerial extent of the survey.

The backwater areas can be divided into two hydrographic sections: one paralleling the river-influenced channel areas (being separated from them by an area of sediment deposition) and the other located at the lower end of each backwater area perpendicular to the main stream flow. Shallow backwater sections parallel to the main channel areas contain large deposits of river-borne sediments deposited during flooding conditions. The areas of backwater perpendicular to the river flow are less influenced by the main channel sediment transport. These sections exhibit relatively deeper waters with shoreline and bathymetric profiles more reflective of local topography and original reservoir characteristics (Reference 214).

The main channel area is characterized by a shallow sand and gravel bed extending through the center of the reservoir area and between the two major backwater areas. Unlike the previously described backwater areas, the main channel portion of the reservoir has a strong current when the hydroelectric station is operating and has relatively homogeneous physiochemical characteristics.

River-borne sedimentation has greatly altered the reservoir from its original condition. Dredging in the dam area has been performed periodically to ensure

efficient hydroelectric generating operations. Dredging activities include keeping the hydroelectric intakes clear of sediment, which is a routine maintenance issue for most hydroelectric projects in this area. Large areas of the stream bed in the original reservoir have been filled completely and stabilized by heavy vegetation growth. During the 1973 study, backwater areas that were not already completely filled, exhibited changes in some water depths in the first 6-month sampling period, thus illustrating the influence of heavy sedimentation (Reference 214).

Circulation and Mixing

Ninety-Nine Islands Reservoir circulation and mixing characteristics are influenced primarily by discharge. The central channel is almost completely dominated by river discharge and accounts for the primary circulation pattern of the reservoir during nonflood periods. Currents through the Ninety-Nine Islands Reservoir are much stronger than expected for an impoundment, although less than currents in the upstream and downstream river. Based on data from the 1975 Cherokee Nuclear Station Construction Permit ER, temperature and chemical constituents were homogeneous at all depths due to thorough turbulent mixing. Sampling performed in 2006 confirms the thorough mixing (Reference 214).

Backwater areas exhibit a very different flow regime because of the lack of circulation in these waters, especially during nonflood periods. Stagnation is common during low-flow periods. The backwater areas are influenced by temperature and tend to slightly stratify during periods of warm weather.

Wind apparently has little effect upon circulation in these backwater areas because they are protected by topographic relief and heavy vegetation, especially in the limited floodplain areas. Lower than normal dissolved oxygen (DO) concentrations result from decomposition of organic materials and poor circulation.

Flooding conditions greatly alter the normal hydrologic setting. Washover from the river channel portion of the reservoir during high flow tends to flush waters from the upper backwaters toward the lower portion of the reservoir. During these periods, extremely turbid conditions prevail throughout the impoundment due to the import of river-borne sediments and the resuspension of lake sediments (Reference 214).

2.4.1.2.2.6 Surface Water Impoundments

The Lee Nuclear Site has three manmade impoundments: (1) Make-Up Pond B, (2) Make-Up Pond A, and (3) Hold-Up Pond A. These features, along with the constructed earthen dams and site structures, are shown in Figure 2.4.1-201. New retention ponds are constructed or existing ponds are used, if necessary, to accommodate surface water runoff and allow sediment-laden water from dewatering activities to pass through the impoundments prior to discharge at a NPDES permitted outfall. Make-Up Pond C is an off-site facility, located on a tributary of the Broad River, west of the Lee Nuclear Station. Details of Make-Up Pond C are provided in Subsection 2.4.1.2.3.1.

Make-Up Pond B

Make-Up Pond B was formed by constructing an earthen dam that impounds McKowns Creek west of Lee Nuclear Station. This reservoir was constructed in the 1970s in the initial construction phase of the Cherokee Nuclear Station. A cofferdam within Make-Up Pond B was utilized to support the original construction of the Make-Up Pond B dam. Upon filling of the pond, the cofferdam was submerged creating a bathymetric division of the pond. Very little to no sediment accumulation is observed within this impoundment.

The cofferdam is apparent on the bathymetric map, Figure 2.4.1-209 (Sheet 2 of 4), as two approximately parallel 540 ft. contours midway between McKowns Mountain and the Make-Up Pond B dam. This cofferdam will be breached to allow full communication between the two bathymetric divisions within Make-Up Pond B.

Make-Up Pond B dam crest elevation is 590 ft. with a low elevation west of the spillway bridge at about 588 ft. above msl. Make-Up Pond B has a normal full pond elevation of 570 ft. above msl (spillway elevation) and occupies approximately 11 percent of the total drainage area of McKowns Creek. Bathymetry exhibited a maximum depth of 59.3 ft., a mean depth of 31.4 ft., total storage capacity of approximately 4000 ac.-ft. and the surface area at full pond is approximately 150 ac. (Figure 2.4.1-209, Sheet 2). The useable storage is approximately 3200 ac.-ft.

During 2006 – 2007, water levels in Make-Up Pond B varied 0.49 ft., representing approximately 73 ac-ft or approximately 1.8 percent of the total storage volume. It should be noted that Make-Up Pond B was receiving waters from dewatering activities, thus affecting the water balance. These activities were conducted to remove water from the original excavation for Cherokee Nuclear Station which was full of water prior to site characterization activities in 2006. All of this water was pumped to Make-Up Pond B. Inflow from rainfall and runoff contribute approximately 1271 gpm to the impoundment. Site observations and aerial photographs indicate that Make-Up Pond B retains water to near full pond level under natural conditions.

A shoreline management program is established along the banks of Make-Up Pond B. The shoreline management program consists of removing all the trees from the water's edge at elevation 570 ft. msl to 50 ft. beyond the contour elevation 585 ft. msl around the perimeter of Make-Up Pond B. This area is paved, grassed, or other suitable alternative where appropriate, and is maintained in this manner throughout the operational life of the plant.

The maximum flood level at the Lee Nuclear Station is elevation 584.8 ft. msl. This elevation would result from a Probable Maximum Flood (PMF) event on Make-Up Pond B watershed with the added effects of coincident wind wave activity as described in Subsection 2.4.3. The Lee Nuclear Station safety-related structures have a grade elevation of 590 ft. msl.

Make-Up Pond A

Make-Up Pond A was also constructed in the 1970s during the initial construction phase of the Cherokee Nuclear Station. The basin is situated east of the proposed Lee Nuclear Station reactor locations and was formed by constructing an earthen dam across a backwater arm of Ninety-Nine Islands Reservoir. Very little to no sediment accumulation is observed within this impoundment.

Make-Up Pond A crest elevation varies from 557.5 ft. to a low point of 555 ft. above msl (Reference 254). At the time of the survey, the impoundment elevation was approximately 546.1 ft. above msl with full pond elevation at 547 ft. This is a relatively small surface water impoundment with a full pond surface area of approximately 62 ac. Bathymetry exhibited a maximum depth of 59.6 ft., a mean depth of 26.1 ft., and an estimated volume storage of 1425 ac.-ft. (Figure 2.4.1-209, Sheet 3). The useable storage is approximately 1200 ac.-ft.

During 2006 – 2007, water levels in Make-Up Pond A varied 0.89 ft., representing approximately 53 ac-ft or 3.7 percent of the total storage volume. Rainfall and runoff contribute on average 396 gpm to the impoundment. Based on site observations and review of available historical aerial photographs, Make-Up Pond A retains water to near full pond level under natural conditions.

Hold-Up Pond A

Hold-Up Pond A is a small impoundment located north of the proposed reactor locations (Figure 2.4.1-209, Sheet 4). Two dams were built in the 1970s to form this impoundment. The crest elevation of the dam is approximately 539.7 ft. above msl, and it has a current normal pond elevation of approximately 536 ft. above msl (Reference 254). Very little to no sediment accumulation was observed in this impoundment. The surface area at full pond is 4.4 ac. and the total storage volume at full pond is 56.4 ac-ft. Rainfall and runoff contribute on average 18 gpm to the pond. Based on site observation and review of available historical aerial photographs, Hold-Up Pond A retains water to near full pond level under natural conditions.

2.4.1.2.2.7 Local Wetlands

Wetlands are areas that are inundated or saturated by surface water or groundwater at a frequency and duration sufficient to support, and that under normal circumstances do support, a prevalence of vegetation typically adapted for life in saturated soil conditions. At the Lee Nuclear Site, wetlands occupy a total of 46.4 ac. or 2.4 percent of the site. They are currently represented by Alluvial Wetlands, Non-alluvial Wetlands, and Non-jurisdictional Wetlands that total 3.2 ac. (0.2 percent), 10.8 ac. (0.6 percent), and 32.4 ac. (1.7 percent) of the total site area, respectively. No appreciable seasonal variations of wetland settings were documented during 2006.

2.4.1.2.3 Dams and Reservoirs

There have been dams in the Upper Broad River drainage basin since the construction of Cherokee Falls Dam in 1826. The primary functions of the larger storage reservoirs are water supply and hydroelectric power. Table 2.4.1-205 presents information for the six major reservoirs in the Upper Broad River Basin including drainage areas, elevation-storage relationships, and short term (maximum storage) and long term (normal storage) storage allocations. Ninety-Nine Islands Dam, Cherokee Falls Dam, and Gaston Shoals Dam are in the vicinity of the Lee Nuclear Site, and all are used for hydroelectric power. Most of the dams within the Upper Broad River basin were not constructed for flood control.

There are approximately 132 dams (five recreational dams are listed as breached) upstream from the Lee Nuclear Site (Reference 276). Six large dams (see Subsection 2.4.1.2.3.1 below) are upstream from the site and represent approximately 88 percent of the total storage capacity for the Broad River basin. There are two additional smaller dams (Cherokee Falls and Gaston Shoals) immediately upstream of the site on the Broad River; however, they possess less than 2 percent of the total storage capacity for the basin. Both of these dams are essentially run-of-river structures used for hydroelectric power and not flood control. Currently, Cherokee Falls Dam is not operating and is a low-head structure without much volume/storage.

In addition, according to the *Federal Register* (Reference 224), USACE and the Cleveland County Sanitary District are proposing to construct an upstream dam and reservoir on the First Broad River (a tributary of the Broad River) approximately 1 mi. north of Lawndale, North Carolina (about 22 mi. north of the Lee Nuclear Site). Additional information on this dam is presented in Subsection 2.4.1.2.3.3.

2.4.1.2.3.1 Upstream Dams and Reservoirs

Make-Up Pond C, shown in Figure 2.4.1-213, is located approximately 2 mi. west of the Lee Nuclear Station on London Creek in Cherokee County, South Carolina. Make-Up Pond C is formed by construction of an earthen dam and saddle dikes that impound London Creek just upstream of the confluence with Little London Creek. The Make-Up Pond C dam crest elevation is 660 ft. above msl. A labyrinth spillway sets the normal pool elevation at 650 ft. above msl. Make-Up Pond C has a drainage area of 2479 ac. At normal pool elevation, bathymetry exhibits a maximum depth of 116 ft., a total storage capacity of approximately 22,000 ac.-ft., and a surface area of approximately 620 ac. Make-Up Pond C water is used to supplement the Lee Nuclear Station during low flow conditions. The useable storage is approximately 17,500 ac.-ft.

Lake Whelchel is located approximately 8 mi. northwest of the Lee Nuclear Site on Cherokee Creek in Cherokee County, South Carolina. This Lake Whelchel dam is an earthen design that was constructed in 1964 and modified in 1989. The dam height is 61 ft. and the length is 2100 ft. The dam creates a reservoir that is owned by and used as a water supply source for Gaffney, South Carolina. The

dam and associated reservoir are owned and operated by the city of Gaffney. The normal pool elevation of the reservoir is 670 ft. above msl (Table 2.4.1-205). The reservoir has a surface area of approximately 177 ac. and a normal storage of approximately 2438 ac.-ft. The maximum storage of Lake Whelchel at the dam crest elevation of 685 ft. is approximately 5698 ac.-ft. No hydroelectric power plant is associated with this dam.

Kings Mountain Reservoir (Moss Lake Dam) is located in Cleveland County, North Carolina, approximately 16 mi. northeast of the Lee Nuclear Site. Discharge waters from this dam are released to Buffalo Creek. The dam was constructed in 1973 and created Kings Mountain Reservoir, which is owned by the city of Kings Mountain and used as a water supply source for the city of Shelby, North Carolina, as well as several smaller communities. In addition, the reservoir is used for recreational activities such as boating and fishing. Moss Lake Dam is an earthen structure that is 840 ft. long and 99 ft. in height. The normal pool elevation of Kings Mountain Reservoir is 736 ft. above msl (Table 2.4.1-205). The reservoir has a surface area of approximately 1329 ac. and a normal storage of 44,400 ac.-ft. and a maximum storage capacity of 53,280 ac.-ft. No hydroelectric power plant is associated with this dam.

Lake Adger (also Turner Shoals) is located on the Green River approximately 44 mi. northwest of the Lee Nuclear Site in Polk County, North Carolina. The Lake Adger dam and associated hydroelectric plant were constructed in 1925 and are owned and operated by Hydro LLC. In addition, the reservoir (Lake Adger) is used for recreational activities such as boating and fishing. Lake Adger Dam is a concrete multiple-arch design that is 689 ft. in length and 90 ft. in height. The normal pool elevation of Lake Adger is 912 ft. above msl (Table 2.4.1-205). The lake has a surface area of approximately 460 ac. and an estimated normal storage of 11,700 ac.-ft. The maximum storage is 16,760 ac.-ft.

Lake Lure is located on the Broad River in Rutherford County, North Carolina, approximately 46 mi. northwest of the Lee Nuclear Site. The Lake Lure dam and associated hydroelectric plant were constructed in 1927 and are owned and operated by the town of Lake Lure. In addition, the reservoir is used for recreational activities such as boating and fishing. Lake Lure Dam is a concrete multiple-arch design that is 480 ft. in length and 124 ft. in height. The normal pool elevation of Lake Lure is 991 ft. above msl (Table 2.4.1-205). The lake has a surface area of approximately 740 ac., a normal storage of 32,295 ac.-ft. and a maximum capacity of 44,914 ac.-ft.

Lake Summit Dam is located on the Green River in Henderson County, North Carolina, approximately 52 mi. northwest of the Lee Nuclear Site. The dam and associated hydroelectric plant were constructed in 1920 and are owned and operated by Duke Energy. In addition, the reservoir is used for recreational activities such as boating and fishing. Lake Summit Dam is a single-concrete-arch design with a concrete buttress structure that is 254 ft. in length and 130 ft. in height. The normal pool elevation of Lake Summit is 2012.6 ft. above msl (Table 2.4.1-205). The lake has a surface area of approximately 276 ac. and a normal storage of 9300 ac.-ft. and maximum storage of 15,840 ac.-ft. The maximum drawdown is 20 ft., yielding a useable storage of 4134 ac-ft.

2.4.1.2.3.2 Downstream Dams and Reservoirs

There are two significant reservoirs located downstream from the Lee Nuclear Site: Ninety-Nine Islands Reservoir and the Lockhart Reservoir. Similar to the Cherokee Falls and Gaston Shoals dams, Ninety-Nine Islands and Lockhart dams are run-of-river structures and are not used for flood control. Dams located further downstream include Neal Shoals Dam (approximately 50 mi.) and Parr Shoals Dam (approximately 52 mi.).

As shown on Figure 2.4.1-205, Lockhart Dam is located in Union County, South Carolina, on the Broad River, 3 mi. south of the confluence with the Pacolet River and approximately 19 mi. south to southeast of the Lee Nuclear Site. The normal pool elevation of the Lockhart Reservoir is around 395 ft. above msl with a surface area of approximately 300 ac. and a normal storage of 2400 ac-ft. The Lockhart Dam and its associated hydroelectric power plant were constructed in 1921 and are currently owned and operated by Lockhart Power Company of Lockhart, South Carolina.

Completed in 1905, the Neal Shoals Dam is located in Chester and Union Counties. The normal pool elevation of Neal Shoals reservoir is around 325 ft. above msl. with a surface area of approximately 550 ac. and a normal storage of 1350 ac-ft.

2.4.1.2.3.3 Water Management Changes

As mentioned in Subsection 2.4.1.2.3, USACE and the Cleveland County Sanitary District (CCSD) are proposing to construct a dam on the First Broad River (upstream and hydraulically connected to the Broad River) approximately 1 mi. north of Lawndale, North Carolina. This is about 26 mi. north of the Lee Nuclear Site. The USACE permit application (Section 404 of the Clean Water Act) states that the dam affects approximately 24 mi. of river and stream habitat and approximately 1 ac. of wetlands. Initial feasibility estimates state that an earth-filled dam across the First Broad River may be approximately 83 ft. high and 1245 ft. wide at the base. The associated emergency spillway, located south of the dam, is approximately 1000 ft. wide. The dam creates a reservoir with a surface area of approximately 2245 ac., impounding those areas below 860 ft. above msl. A 100-ft. buffer zone would likely surround the reservoir (Reference 224).

The CCSD is proposing this dam to increase the water supply for the region. Based on current rates of growth, CCSD projects that water needs for its customers would double by 2050 (Reference 224). The reservoir is also projected to lessen the occurrence of water shortages during drought conditions.

2.4.1.2.4 Regional Hydrogeology

The Piedmont aquifer system is basically a two-layered slope-aquifer system. The shallow water table aquifer is comprised of the saprolite and residual soil, which is typically low-yielding. The underlying bedrock aquifer consists of weathered and unweathered crystalline igneous and metamorphic rocks that store and transmit

water through fractures. The shallow aquifer is unconfined, meaning that the upper surface of the saturated zone is not effectively separated from the ground surface by a low-permeability clay layer. The bedrock fracture system is a network of discontinuities that increases in prevalence upward through the crystalline rock as it transitions into saprolite (Figure 2.4.1-210). Because of the permeability of the transition zone, the bedrock aquifer is also considered unconfined and not effectively isolated. Thus, the saprolite and bedrock zones function as one interconnected aquifer system (Reference 266).

Groundwater occurs almost everywhere throughout the Piedmont region; however, it is not in a single, widespread aquifer. It occurs in various local aquifer systems and compartments that have similar characteristics and are hydraulically connected. Groundwater recharge in this area is derived entirely from infiltration by local precipitation. Groundwater flow within this combined system can be complex. The fractures, relic rock textures, and directional differences in permeability or ease of groundwater movement may significantly affect the local groundwater flow direction. Recharging of the groundwater in the Piedmont occurs by the addition of rainwater, first to the shallow saprolite aquifer and then to the uppermost fracture zone. Recharge occurs mostly on upland topographic highs or at least above the slopes of stream valleys.

The average annual rainfall in the region is about 50 inches. The annual pan evaporation rate is 51.8 inches for the region. Pan evaporation rates are higher than actual lake evaporation due to radiation and heat exchange effects. The pan coefficients range from 0.64 and 0.81, with an average of 0.7 used for the United States. Therefore, the annual evaporation rate is 36.26 inches. Groundwater is contained in the pores that occur in the weathered material (residual soil, saprolite) above the relatively unweathered rock and within the fractures in the igneous and metamorphic rock. The depth to the water table depends on climate, topography, rock type, and rock weathering. The water table varies from ground surface elevation in valleys to more than 100 ft. below the surface on sharply rising hills. Although the precipitation in the Piedmont is relatively evenly distributed throughout the year, the water table fluctuates noticeably, typically declining during the late spring and summer due to evapotranspiration and rising in the late fall and winter when the evaporation potential is reduced (Reference 297).

A detailed discussion of regional and local groundwater characteristics is presented in Subsection 2.4.12. A detailed discussion of regional and local geology and soil properties is presented in Section 2.5.

2.4.1.2.5 Water Use

This subsection describes surface water and groundwater in the vicinity of the Lee Nuclear Site that could affect or be affected by the construction and operation of two AP1000 units. The information provided in this subsection includes descriptions of surface water and groundwater uses that could affect or be affected by construction or operation of the Lee Nuclear Station, including transmission corridors and off-site facilities. In addition, a detailed assessment of water use within the vicinity of the facility, types of consumptive and

nonconsumptive water uses, identification of their locations, and qualification of water withdrawals and returns are discussed in this subsection.

2.4.1.2.5.1 Surface Water Use

The Lee Nuclear Site is located on the west bank of the Broad River approximately 3 mi. south-southeast (downstream) of Cherokee Falls and 1 mi. north-northwest (upstream) of the Ninety-Nine Islands Dam and Hydroelectric Station. Surface water in the vicinity of the Lee Nuclear Site consists of the Broad River, three on-site man-made impoundments, and one off-site man-made impoundment. These features are discussed in detail in Subsections 2.4.1.2.2.6 and 2.4.1.2.3.1.

According to available SCDHEC information on water use for 2005 (Reference 267), total water usage in Cherokee County was 8.4 Mgd. This information is presented in Table 2.4.1-206. Total 2005 water withdrawals from Cherokee, Chester, Greenville, Spartanburg, Union, and York counties, South Carolina, are presented in Table 2.4.1-207 (Reference 267).

No surface water usage in Cherokee County was reported for domestic self-supplied systems, aquaculture, golf courses, irrigation, livestock, mining, or thermoelectric power uses. According to SCDHEC, water use for hydroelectric power was 1116 Mgd in 2005 for Cherokee County (Reference 267). The USGS 2000 data did not reference hydroelectric power water use; however, these data were included in the 1995 data set. According to the U.S. Army Corps of Engineers National Inventory of Dams, there have been no hydroelectric dams constructed in the watershed since 1995. Therefore, the USGS 1995 data remains unchanged. According to the USGS, there were 2037.1 Mgd of instream water use for hydroelectric power in 1995 for Cherokee County. Surface water-use details for the Broad River watershed within 60 mi. of the Lee Nuclear Site are presented in Tables 2.4.1-207 and 2.4.1-208.

Nineteen permitted surface water intakes at sixteen separate facilities are located in the Upper Broad River basin upstream from the Lee Nuclear Site (Table 2.4.1-209, Figure 2.4.1-211). The closest surface water intake is the Gaffney Board of Public Works intake about 8 mi. upstream on the Broad River. In addition to the existing intakes, Duke Energy anticipates modernizing and expanding the Cliffside Steam Station (located 19 mi. upstream from the site in Cleveland County, North Carolina), which will use the existing surface water intake from the Broad River. Cliffside Steam Station expansion is discussed in Subsections 2.2.2.1.4 and 2.4.11.4.

Three permitted surface water intakes for public water supply are located downstream from the Lee Nuclear Site (Figure 2.4.1-211). The closest of these is the city of Union, which withdraws water from the Broad River about 21 mi. downstream from the site and has a maximum withdrawal rate of 23.8 Mgd. The second and third are the Carlisle Cone Mills (approximately 30 miles downstream; maximum capacity 8.1 Mgd) and the V.C. Summer Nuclear Station (approximately 52 miles downstream; maximum capacity 3.1 Mgd) (Table 2.4.1-209). Two additional AP1000 units are planned for the V.C. Summer Nuclear Station. Details

Withheld from Public Disclosure Under 10 CFR 2.390(a)(9)
(see COL Application Part 9)

are not currently available. Additional surface water uses not included in the table are located within 20 – 50 mi. of the site. These additional intakes are relatively insignificant because they are located outside the watershed or on tributaries that join the Broad River downstream from the site.

The plant water use is discussed in Subsection 2.4.1.1.4. Table 2.4.1-210 and Table 2.4.1-211 present raw water use and effluent discharge as a percentage of Broad River flow rates. The maximum consumption rate of Broad River water, predominantly resulting from evaporation during plant operations, is expected to be 63 cfs, approximately 3 percent of the average annual mean discharge of the Broad River (approximately 2500 cfs).

2.4.1.2.5.2 Groundwater Use

Groundwater produced for water supply in counties located in the Piedmont aquifer system is reported to be approximately 79 Mgd (122.5 cfs). This can be compared to some Upper Coastal Plain counties that withdraw up to several thousand Mgd of groundwater (Reference 293).

A reported 1.02 million gal. of groundwater were used for thermoelectric power generation in Cherokee County (Reference 267). No groundwater usage in Cherokee County for domestic self-supplied systems, aquaculture, golf courses, irrigation, livestock, mining, or thermoelectric power was reported in the 2005 SCDHEC data (Reference 267). According to a private well report from SCDHEC, based on data from January 1985 to June 2006, the number of reported private wells in Cherokee County was 1076 (Reference 261). The USGS and state water-use data were reviewed, and groundwater withdrawals are presented in Tables 2.4.1-207 and 2.4.1-208. Groundwater withdrawals for Cherokee and surrounding counties in South Carolina (Table 2.4.1-207) only account for 4.7 Mgd, and the majority (85 percent) of that volume is pumped from Spartanburg County, approximately 25 mi. west of the Lee Nuclear Site.

[

Withheld from Public Disclosure Under 10 CFR 2.390(a)(9)
(see COL Application Part 9)

]SRI

The Lee Nuclear Site is not expected to use groundwater as a source of water for any purpose. Water for temporary fire protection, concrete batching, and other construction uses will be obtained from the Draytonville Water District. Groundwater is not used as a safety-related source of water or as a primary water supply resource for any purpose. Further discussion regarding groundwater characteristics and use is provided in Subsection 2.4.12.

WLS COL 2.4-2

2.4.2 FLOODS

2.4.2.1 Flood History

Floods on the Broad River occur primarily as a result of precipitation runoff over the watershed. There have been dams in the Upper Broad River drainage basin since the construction of Cherokee Falls Dam in 1826. However, the majority are not flood control dams. The primary function of the larger storage reservoirs are water supply and hydroelectric power. Ninety-Nine Islands Dam, Cherokee Falls Dam, and Gaston Shoals Dam, in the vicinity of the Lee Units 1 and 2, are all used for hydroelectric power (Reference 276). The hydroelectric facility at Cherokee Falls Dam is not currently operating. Although these structures affect the low flow conditions of the Broad River, peak flow conditions at Lee Units 1 and 2 are generally not affected by regulation. The limited flood control dams in the basin are small storage structures and would have limited effect on peak flows.

The Gaffney stream gauge station (USGS No. 02153500) is located about 5 river miles upstream of Lee Units 1 and 2 between Gaston Shoals Dam and Cherokee Falls Dam. Figure 2.4.2-201 shows the location of area gauges. The Gaffney gauge has a drainage area of 1490 sq. mi., about 96 percent of the drainage area at the site. The drainage area of the Broad River at the Lee Nuclear Station is about 1550 sq. mi. Table 2.4.2-201 summarizes peak flow for the broken period of record from 1939 to 1990 (Reference 290). The flood of record for the Gaffney gauge, 119,000 cfs on August 14, 1940, corresponds to a Ninety-Nine Islands reservoir elevation of about 522.5 ft. at Lee Nuclear Station.

The Ninety-Nine Islands reservoir elevation is maintained by Duke Energy and recorded on a daily basis from 1999 to 2005 by USGS gauge No. 02153550. The USGS gauge record high is 107.29 ft. on September 8, 2004 for a reservoir elevation of 518.75 ft. (Reference 208). The gauge datum is 411.46 ft. above the National Geodetic Vertical Datum of 1929 (NGVD 1929). Earlier reservoir records from 1964 to 1973 indicate that the highest elevation was about 513.6 ft. during May 1972.

The stream gauge station below Ninety-Nine Islands Dam (USGS No. 02153551, listed in Table 2.4.1-203 as Broad River below Cherokee Falls, SC) is located in the tailrace and has a drainage area of 1550 sq. mi. Peak flow records are limited for this station and the gauge is not calibrated for large flows. Table 2.4.2-202 summarizes peak flow and gauge height for the period of record from 1999 to 2005 (Reference 290).

No historical data exists regarding flooding due to surges, seiches, tsunamis, dam failures, or landslides. Surge and seiches are discussed in Subsection 2.4.5. Tsunamis are discussed in Subsection 2.4.6. Dam failures are discussed in Subsection 2.4.4. Channel diversions are discussed in Subsection 2.4.9. Historical information related to icing and ice jams is provided in Subsection 2.4.7.

2.4.2.2 Flood Design Considerations

The Lee Nuclear Station conforms to Regulatory Position 1 of Regulatory Guide 1.59. There are no safety-related structures that could be affected by floods and flood waves.

The type of events evaluated to determine the worst potential flood include (1) probable maximum precipitation (PMP) on the total watershed and critical sub-watersheds including seasonal variations and potential consequent dam failures, as discussed in Subsection 2.4.3, (2) dam failures, as discussed in Subsection 2.4.4, including in a postulated safe shutdown earthquake with a coincident 25-year flood or operating basis earthquake with a coincident one-half probable maximum flood (PMF), (3) local intense precipitation, and (4) two year coincident wind waves as discussed in Subsection 2.4.3. Local intense precipitation is discussed below. Both static and dynamic assumed hypothetical conditions to determine the design flood protection level are evaluated in Subsections 2.4.3 and 2.4.4.

Specific analysis of Broad River flood levels resulting from ocean front surges, seiches, and tsunamis is not required because of the inland location and elevation characteristics of the Lee Nuclear Station. Additional details are provided in Subsection 2.4.5 and Subsection 2.4.6. Snowmelt and ice effect considerations are unnecessary because of the temperate zone location of the Lee Nuclear Station. Additional details are provided in Subsection 2.4.7. Flood waves from landslides into upstream reservoirs required no specific analysis, in part because of the absence of major elevation relief. In addition, elevation characteristics of the vicinity relative to the Broad River, combined with the limited storage volume availability of nearby upstream reservoirs, prohibit significant landslide induced flood waves. Additional details are provided in Subsection 2.4.9.

The maximum flood level at the Lee Nuclear Station is elevation 584.8 ft. msl. This elevation would result from a PMF event on Make-Up Pond B watershed with the added effects of coincident wind wave activity as described in Subsection 2.4.3. The Lee Nuclear Station safety-related plant elevation is 590 ft. msl. The maximum flood level is identified as a site characteristic in Table 2.0-201.

2.4.2.3 Effects of Local Intense Precipitation

The Lee Nuclear Station drainage system was evaluated for a storm producing the PMP on the local area. The site is relatively flat; however, the site is graded such that overall runoff will drain away from safety-related structures to Make-Up Pond B, Make-Up Pond A, or directly to the Broad River. The PMP flood analysis assumes that all discharge structures are non-functioning. Computed water surface elevations in the vicinity of safety-related structures are below plant elevation of 590 ft. The site grading and drainage plan is shown in Figure 2.4.2-202.

The site is graded to drain runoff away from the power blocks. The finished floor elevation is 590 ft. The areas immediately surrounding the power blocks are elevation 589.5 ft. The immediate surrounding area is flat and generally is bounded by the roadway surrounding the power blocks also at elevation 589.5 ft. The power block area bounded by the roadway is either paved or gravel surface. Further from the power blocks the site gently slopes away from the roadway to a general elevation of 588 ft. Areas beyond the roadway are generally maintained grass surfaces.

To analyze the effects of local intense precipitation, the site was divided into four drainage areas (northwest, northeast, southwest, southeast) based on the contours of the grading and drainage plan. Each area was modeled using the U.S. Army Corps of Engineers HEC-RAS version 3.1.3 (Reference 273) (standard-step, backwater analysis) computer software. Cross sections for each of the four areas were determined based on the grading and drainage plan and flows were modeled under steady state conditions. Buildings were modeled to obstruct flow and were not assumed to provide any storage. Tailwater elevations for the Broad River, Make-Up Pond B, and Make-Up Pond A correspond with the higher of the peak PMF water surface elevation provided in Subsection 2.4.3 or the peak dam failure water surface elevation provided in Subsection 2.4.4. A Manning's roughness coefficient, n = 0.025, was used for the paved or gravel surfaces. A Manning's roughness coefficient, n = 0.050 was used for the grass surfaces.

In the northwest drainage area, a wide, shallow, flat sloped swale directs runoff west to Make-Up Pond B. In the northeast drainage area, a wide shallow swale directs runoff east to the back waters of the Broad River. The swales are bounded by the roadway surrounding the power blocks and the embedded railway track to the north. The at-grade railroad tracks were not considered to provide any type of obstruction. Beyond the railway tracks are several warehouse structures and open areas with a yard elevation of 588 ft. The yard elevation then slopes steeply into Hold-Up Pond A or the backwaters of the Broad River. Because the yard elevation area is graded flat, approximately half of these areas are assumed to contribute runoff to the modeled areas and are also available for storage. The remaining half of the area is assumed to runoff toward the steeper slopes.

The division for the northern swales begins at the road running between the power blocks to the warehouses. The northeast swale drains runoff to backwaters of the Broad River. The swale width narrows as it passes the elevated cooling tower pad for Unit 2 then widens as it approaches the steeper slopes into the

backwaters of the Broad River. The narrowing location is used as the critical cross section for determining the time of concentration in the drainage calculations.

The northwest swale drains runoff to Make-Up Pond B. The swale width narrows as it passes the elevated cooling tower pad for Unit 1 then empties into a wider area adjacent to Make-Up Pond B. The narrowing location is used as the critical cross section for determining the time of concentration in the drainage calculations.

In the southwest drainage area, a narrow, shallow, flat sloped swale directs runoff west to Make-Up Pond B and in the southeast drainage area, a wide, shallow, flat sloped swale directs runoff east to Make-Up Pond A. The swales are bounded by the roadway surrounding the power blocks and further to the south by steeply rising elevation up to a hill feature and the transmission yard.

The division for the southern swales begins at the series of structures identified as the maintenance support building, and administration building. The southwest swale narrows as it passes through a cut area between the elevated cooling tower pad for Unit 1 and a hill feature. The narrowing location is used as the critical cross section for determining the time of concentration in the drainage calculations. Beyond the narrowest point the cut swale widens and steepens before it drops into Make-Up Pond B.

The southeast swale maintains a relatively constant width as it passes between the elevated cooling tower pad for Unit 2 and the elevated transmission yard. This location is used as the critical cross section for determining the time of concentration in the drainage calculations. Beyond the critical cross section, the swale widens and the slope gradually increases as the elevation drops into Make-Up Pond A.

The local intense PMP is defined by Hydrometeorological Report (HMR) Nos. 51 and 52. PMP values for durations from 6-hr. to 72-hr. are determined using the procedures as described in HMR No. 51 for areas of 10-sq. mi. (Reference 255). Using the Lee Nuclear Station location, the rainfall depth is read from the HMR No. 51 PMP charts for each duration.

The 1-sq. mi. PMP values for durations of 1-hour and less are determined using the procedures as described in HMR No. 52 (Reference 225). Using the Lee Nuclear Station location, the rainfall depth is read from the HMR No. 52 PMP charts for each duration. A smooth curve is fitted to the points. The derived PMP curve is detailed in Table 2.4.2-203. The corresponding PMP depth duration curve is shown in Figure 2.4.2-203.

HMR 52 guidance indicates that PMP rates for 10-sq. mi. areas are the same as point rainfall. Also indicated in HMR 52, the 1-sq. mi. PMP rates may also be considered the point rainfall for areas less than 1-sq. mi. Therefore, intensities for any drainage areas with durations longer than 1-hr. are derived from the PMP rates for 10-sq. mi. areas. Intensities for drainage areas with durations equal to or less than 1-hr. are derived from the PMP rates for 1-sq. mi. areas.

The AP1000 plant design is based on a PMP of 20.7 in/hr. As shown in Figure 2.4.2-203, the site is within the plant design limits for PMP. The PMP is identified as a precipitation site characteristic in Table 2.0-201. Roofs are sloped to preclude ponding of water.

The rational method (Reference 201) was used to determine peak runoff rates for the areas between each cross section of the four HEC-RAS models. The rational method is given by the equation:

$$Q = k * C * i * A$$

where: Q = runoff (cfs)

k = constant (1 for English units)

C = unitless coefficient of runoff

i = intensity (in/hr)

A = drainage area (ac.)

No runoff losses were assumed. Therefore the runoff coefficient was assumed equal to one. Rainfall durations are assumed equal to or greater than the time of concentrations for each site drainage area.

The intensity component of the rational method was determined for each of the four HEC-RAS models using the corresponding time of concentration for the drainage area and the depth duration curve for the local intense PMP provided in Table 2.4.2-203 and Figure 2.4.2-203. Because the site is so flat, with slopes less than one-half percent, an iterative process was used to determine the time of concentration.

For each HEC-RAS model an assumed time of concentration was used for the first trial. The time of concentration was converted to an intensity using the depth duration curve. The rational method was used to determine the flow at each cross section up to the critical cross section using the total drainage area at each cross section. The flow at the critical cross section was carried over to each successive downstream cross section. The calculated flows were inputted into the HEC-RAS models.

The resulting flow velocities from the HEC-RAS model at each cross section were averaged between successive cross sections and a travel time was determined based on the distance between successive cross sections. The total travel time to the critical cross section was then used as a new time of concentration. The process was repeated until the total travel time converged with the time of concentration.

The resulting water surface elevations at the safety-related structures are identified in Table 2.4.2-204. All Lee Nuclear Station safety-related structures are located above the effects of local intense precipitation at plant elevation 590 ft. For

each of the four areas modeled, the table also identifies: the total drainage area, the converged time of concentration for the drainage area, the corresponding PMP depth from the depth duration curve, the converted intensity used in the rational method formula, and the resulting flow rate at the critical cross section.

Due to the temperate climate and relatively light snowfall, significant icing is not expected. Based on the site layout and grading, any potential ice accumulation on site facilities is not expected to affect flooding conditions or damage safety-related facilities. Ice effects are discussed in Subsection 2.4.7.

2.4.3 PROBABLE MAXIMUM FLOOD ON STREAMS AND RIVERS

WLS COL 2.4-2 The guidance in Appendix A of U.S. Nuclear Regulatory Commission (NRC) Regulatory Guide 1.59 was followed in determining the Probable Maximum Flood (PMF) by applying the guidance of ANSI/ANS-2.8-1992 (Reference 202). ANSI/ANS-2.8-1992 was issued to supersede ANSI N170-1976, which is referred to by Regulatory Guide 1.59. Although ANSI/ANS-2.8-1992 has been withdrawn, there has been no replacement standard issued. The NRC NUREG-0800 retains both Regulatory Guide 1.59 and ANSI/ANS-2.8-1992 as historical technical references.

Broad River

The PMF for the Broad River above the Lee Nuclear Station is determined from the probable maximum precipitation (PMP) for the watershed of Ninety-Nine Islands Dam. Lee Nuclear Station is located about 1 mi. upstream from the dam and adjacent to the Broad River. The 1550-sq. mi. Broad River drainage basin at Ninety-Nine Islands Dam is shown in Figure 2.4.1-205.

McKowns Creek/Make-Up Pond B

The PMF for McKowns Creek and Make-Up Pond B is determined from the PMP for the 2.55-sq. mi. drainage basin of Make-Up Pond B. Make-Up Pond B drainage basin is shown in Figure 2.4.3-201.

Intermittent Stream/Make-Up Pond A

The PMF for the intermittent stream and Make-Up Pond A are determined from the PMP for the 0.60-sq. mi. drainage basin of Make-Up Pond A. Make-Up Pond A drainage basin is shown in Figure 2.4.3-201.

London Creek/Make-Up Pond C

The Make-Up Pond C reservoir is located on a tributary of the Broad River, west of the Lee Nuclear Station, as shown in Figure 2.4.1-213, but is not adjacent to the Lee Nuclear Station. However, the PMF for London Creek and Make-Up Pond C is

determined for combination with dam failure permutations as discussed in Subsection 2.4.4.1. The PMF is determined from the PMP for the 3.87-sq. mi. drainage basin of Make-Up Pond C. The Make-Up Pond C drainage basin is shown in Figure 2.4.3-239.

2.4.3.1 Probable Maximum Precipitation

Broad River

The PMP for the watershed above the Lee Nuclear Station is defined by Hydrometeorological Report (HMR) Nos. 51 and 52 (References 255 and 225). The PMP is based on an existing study for Ninety-Nine Islands Dam (Reference 217) and modified to include antecedent storm conditions, as specified by Appendix A of Regulatory Guide 1.59.

Using the location of the drainage basin, HMR-51 PMP charts are used to determine generalized estimates of the all-season PMP for drainage areas from 10 to 20,000 sq. mi. for durations from 6 to 72 hrs. The resulting depth-area-duration (DAD) values are shown in Table 2.4.3-201.

HMR-52 is used to determine spatial and temporal distribution of PMP estimates derived from HMR-51. The recommended elliptical isohyetal pattern from HMR-52, shown in Figure 2.4.3-202, is used for the watershed. The watershed model contains 20 subbasins and is shown in Figure 2.4.3-203. The Lake Whelchel and Make-Up Pond C subbasins were not included in the existing study for Ninety-Nine Islands Dam. Both the Lake Whelchel and Make-Up Pond C watersheds are contained within the original subbasin labeled BR-15. Therefore, appropriate modifications were made to subbasin BR-15 to accommodate subbasins for Lake Whelchel and Make-Up Pond C.

HMR-52 computer software (Reference 271), developed by the U.S. Army Corps of Engineers (USACE), is used to determine the optimum storm size and orientation to produce the greatest PMP over the entire basin using the HMR-51 derived DAD table. The HMR-52 recommended temporal distribution is also used and provided by the HMR-52 computer software. Several storm centers were examined and the critical storm center was found to be near the centroid of the watershed for Gaston Shoals Dam, located upstream of Ninety-Nine Islands Dam based on the runoff model discussed in Subsection 2.4.3.3. The critical storm area was found to be 1000 sq. mi., corresponding to isohyet I in Figure 2.4.3-202. The critical storm orientation was found to be 270 degrees. Refer to Figure 2.4.1-205 for structure locations and watershed.

The critical 72-hr. storm PMP rainfall total is 25.48 in. for the entire watershed. The corresponding temporal arrangement of 6-hr. precipitation increments is provided in Table 2.4.3-202. The hourly temporal distribution of the 72-hr. PMP rainfall of each of the 20 subbasins is provided in Table 2.4.3-203.

In accordance with Appendix A of NRC Regulatory Guide 1.59, the 72-hr. PMP storm is combined with an antecedent storm equal to 40 percent of the PMP. Therefore, the complete sequential storm considered includes a 3-day, 40 percent

PMP event followed by a 3-day dry period, which is followed by the 3-day full PMP event.

The PMP estimates are associated with the summer months. HMR 53 (Reference 260) provides estimates for maximum seasonal precipitation. Although HMR 53 applies to 10 sq. mi. drainage areas, it is used as a basis for the larger Broad River watershed. HMR 53 winter precipitation estimates for December through February are less than 57 percent of the all-season PMP estimates identified in Table 2.4.3-201 for the 10 sq. mi. drainage area. The 57 percent ratio is applied to the all-season PMP for the Broad River watershed identified in Table 2.4.3-202 to determine the maximum winter precipitation estimates.

According to guidance (Reference 202) the winter precipitation is evaluated coincident with the 100-yr. snowpack. The water equivalent of the 100-yr. snowpack identified in Subsection 2.3.1.2.7.1 is approximately13 percent of the 72-hr. PMP for the Broad River watershed identified in Table 2.4.3-202. It is assumed that the 100-yr. snowpack is distributed across the entire watershed and completely melts during a winter precipitation event. The combined result of winter precipitation and 100-yr. snowpack is approximately 70 percent of the PMP. Therefore, snowmelt is not considered to be a factor in modeling the PMF event.

McKowns Creek /Make-Up Pond B

The PMP for McKowns Creek and Make-Up Pond B is defined in Subsection 2.4.2.3. Two storms were modeled on the basis of the PMP curve detailed in Table 2.4.2-203 and Figure 2.4.2-203. The total PMP depth of the 72-hr. duration storm is 46.8 in. A 6-hr. storm with a 5-min. precipitation interval was examined to capture the effect of the short-term, high intensity on the peak flow. In addition, a 72-hr. storm with a 1-hr. precipitation interval was examined to identify the total runoff volume of a PMP event.

Several time distributions were examined for both modeled events. For the 72-hr. storm, an end peaking storm event was found to provide the greatest runoff. For the 6-hr. storm, a two-thirds peaking storm event was found to provide the greatest runoff. However, an end peaking storm event was found to provide the controlling water surface elevation as discussed in Subsection 2.4.3.5. Hyetographs are provided in Figure 2.4.3-204 and Figure 2.4.3-205 for the two-thirds peaking storm events. Hyetographs are provided in Figure 2.4.3-235 and Figure 2.4.3-236 for the end peaking storm events.

Intermittent Stream/Make-Up Pond A

The PMP for the intermittent stream and Make-Up Pond A is defined in Subsection 2.4.2.3. Two storms were modeled on the basis of the PMP curve detailed in Table 2.4.2-203 and Figure 2.4.2-203. The total PMP depth of the 72-hr. duration storm is 46.8 in. A 6-hr. storm with a 5-min. precipitation interval was examined to capture the effect of the short-term, high intensity on the peak flow. In addition, a 72-hr. storm with a 1-hr. precipitation interval was examined to identify the total runoff volume of a PMP event.

Several time distributions were examined for both modeled events. For each storm, a two-thirds peaking storm event was found to provide the greatest runoff. Hyetographs are provided in Figures 2.4.3-204 and 2.4.3-205.

London Creek/Make-Up Pond C

The PMP for London Creek and Make-Up Pond C is defined in Subsection 2.4.2.3. The storm is modeled on the basis of the 72-hr. PMP curve detailed in Table 2.4.2-203 and Figure 2.4.2-203. The total PMP depth of the 72-hr. duration storm is 46.8 in.

The 72-hr. PMP storm is combined with an antecedent storm equal to 40 percent of the PMP. Therefore, the complete sequential storm considered includes a 3-day, 40 percent PMP event followed by a 3-day dry period, which is followed by the 3-day full PMP event.

Several time distributions were examined for the PMP event using a 1-hr. precipitation interval. An end peaking storm event was found to provide the greatest discharge and water surface elevation at Make-Up Pond C. The hyetograph is provided in Figure 2.4.3-240.

2.4.3.2 Precipitation Losses

Broad River

Precipitation losses are based on an existing study (Reference 217) using the U.S. Department of Agriculture (USDA), Soil Conservation Service (SCS) (now the Natural Resources Conservation Service [NRCS]) curve number method. The initial study used geographic information systems (GIS) and the NRCS state soil geographic database (STATSGO) to determine hydrologic soil group values. The GIS and U.S. Geological Survey (USGS) information were also used to determine land-use and impervious cover. An average antecedent moisture condition (AMC II) was then used to compute a weighted curve number for each subbasin.

The SCS Curve Number method was also used to determine precipitation losses for the Lake Whelchel subbasin and the Make-Up Pond C subbasin. The NRCS Web Soil Survey (Reference 300 and Reference 301) was used to determine hydrologic soil group values. Aerials and USGS information were used to determine land-use and impervious cover. An average antecedent moisture condition (AMC II) was also used to compute a weighted curve number for the subbasin.

Precipitation losses are incorporated into the USACE HEC-HMS model discussed in Subsection 2.4.3.3. Initial losses of the SCS Curve Number loss model are developed using the initial abstraction formula.

$I_a = 0.2 * S$

where I_a = initial abstraction (in.)

S = maximum potential storage of the watershed (in.)

where S = 1000 / CN – 10 and CN = average curve number for the watershed

Initial losses for each subbasin are provided in Table 2.4.3-204.

The SCS Curve Number loss model collectively includes interception, infiltration, storage, evaporation, and transpiration. Precipitation losses are derived from the equation for precipitation excess.

$P_e = (P - I_a)^2 / (P - I_a + S)$

where P_e = accumulated precipitation excess at time t (in.)

P = accumulated rainfall depth at time t (in.)

I_a = initial abstraction (in.)

S = maximum potential storage of the watershed (in.)

where S = 1000 / CN – 10 and CN = average curve number for the watershed

The precipitation loss rate is variable and decreases as cumulative rainfall increases during the storm. The total precipitation depth, losses, and excess for each subbasin are provided in Table 2.4.3-204. Antecedent precipitation is 40 percent of the PMP, preceding the main storm for 3 days, with a 3 day dry period between. During the antecedent storm, precipitation losses account for between 37 and 74 percent of the total rainfall with an average of 53 percent. During the main storm, precipitation losses only account for between 3 to 22 percent with an average of 9 percent.

As discussed in Subsection 2.4.3.3, the existing study used three significant storm events occurring in October 1964, June 1972, and October 1976 to verify the subbasin unit hydrographs. As part of the verification process, loss rates were verified by comparison with back calculated curve numbers from the three historical extreme storm events.

McKowns Creek/Make-Up Pond B

No precipitation losses were assumed for evaluation of Make-Up Pond B watershed. All rainfall was assumed to be transformed to runoff.

Intermittent Stream/Make-Up Pond A

No precipitation losses were assumed for evaluation of Make-Up Pond A watershed. All rainfall was assumed to be transformed to runoff.

London Creek/Make-Up Pond C

Precipitation losses are incorporated into the USACE HEC-HMS model, as discussed in Subsection 2.4.3.3, using the SCS Curve Number method as previously described for the Broad River. The NRCS Web Soil Survey (Reference 300) was used to determine hydrologic soil group values. Aerials and USGS information were used to determine land-use and impervious cover. An average antecedent moisture condition (AMC II) was then used to compute a weighted curve number for the watershed.

The SCS Curve Number loss model collectively includes interception, infiltration, storage, evaporation, and transpiration. Initial losses and precipitation losses are derived as previously described for the Broad River. The precipitation loss rate is variable and decreases as cumulative rainfall increases during the storm. Most losses occur during the antecedent precipitation as identified in the hyetograph, Figure 2.4.3-240. The total precipitation depth is 65.52 in., including the antecedent storm. Precipitation losses account for 4.57 in. resulting in 60.95 in. of precipitation converted to runoff.

2.4.3.3 Runoff and Stream Course Models

Broad River

The Broad River runoff and stream course model is based on an existing HEC-1 study (Reference 217) and modified to include the antecedent rainfall conditions. The watershed in Figure 2.4.1-205 was divided into 20 subbasins as shown in Figure 2.4.3-203. The watershed is predominately identified as Piedmont, as discussed in Subsection 2.4.1.2.1. Referencing Figure 2.4.3-203, subbasins labeled LS-1, LA-2, LL-4, CC-16, 2BR-19, and USS-18A correspond to mountainous areas and foothills of the Blue Ridge Mountains. Topographic characteristics of the Broad River watershed are also discussed in Subsection 2.4.1.2.2. The USACE HEC-HMS, Version 3.0.1 (Reference 272), modeling software was used for rainfall runoff and routing calculations. Figure 2.4.3-206 shows the HEC-HMS model watershed routing layout.

Unit hydrographs for all subbasins except Make-Up Pond C were derived from the techniques described in the regional unit hydrograph study for South Carolina, which was performed by the USGS (Reference 203). The USGS study uses a multiple regression analysis to describe regional unit hydrographs with an adjusted lag time, based on each region of the study. For the HEC-1 study, the unit hydrographs were subsequently converted to 1-hr. durations.

Methods adopted to account for nonlinear basin response at high rainfall rates include increasing the peak of each unit hydrograph by 20 percent and reducing the time to peak by approximately 33 percent. The remaining ordinates of the modified unit hydrographs were adjusted to maintain smooth unit hydrographs with the standard characteristic of 1 in. of runoff. To accommodate the Lake Whelchel subbasin and the Make-Up Pond C subbasin, the BR-15 subbasin unit hydrograph was also modified based on the decrease in drainage area. The resulting unit hydrographs for 19 of the subbasins except Make-Up Pond C are

presented in Figure 2.4.3-207, Figure 2.4.3-208, and Figure 2.4.3-209 and tabulated in Table 2.4.3-205.

For the Make-Up Pond C subbasin, the SCS unit hydrograph method was used as a basis for a modified unit hydrograph to transform rainfall to runoff and account for nonlinear basin response. An equivalent SCS unit hydrograph was first determined using the equations and ratios of the SCS dimensionless unit hydrograph. The equivalent SCS unit hydrograph was then modified by increasing the peak of the unit hydrograph by 20 percent and reducing the time to peak by approximately 33 percent. The remaining ordinates of the modified unit hydrograph were adjusted to maintain a smooth unit hydrograph with the standard characteristic of 1 in. of runoff.

The best calibration of the modified SCS unit hydrograph with the initial SCS unit hydrograph was found using a 10-min. computational time step in the HEC-HMS modeling software. Therefore, the time step used to define the ordinates of the modified SCS unit hydrograph is also 10 min. The Make-Up Pond C subbasin has a lag time of 77 min. The initial SCS unit hydrograph and modified unit hydrograph to account for the effects of nonlinear basin response are provided in Figure 2.4.3-241. The modified SCS unit hydrograph is tabulated in Table 2.4.3-207.

The Muskingum-Cunge 8-point cross section method was used for the river routing reaches, except for the Green River reach between Lake Summit and Lake Adger. Because of the Lake Adger backwater effects on the reach, the Modified Puls storage routing method was used. Channel slope, length, and cross section data were developed using USGS quadrangles. Cross sections were field-verified as part of the existing study and modified as necessary. Manning's roughness coefficients were estimated on the basis of accepted published tables by Chow (Reference 206).

The existing study (Reference 217) contained discharge rating curves for the Tuxedo, Turner Shoals, Gaston Shoals and Ninety-Nine Islands dams. These curves were developed from Duke Power Company project file data. The rating curves for Lake Lure, Kings Mountain Reservoir, Cherokee Falls, and Lockhart dams were estimated in the existing study by using drawings obtained from the dam owners and the North Carolina State Dam Safety Engineer's office. Reservoirs were modeled using full-pond starting elevations and no turbine discharges were assumed. The flashboards at Gaston Shoals and Ninety-Nine Islands dams were assumed to fail due to overtopping and were incorporated into the rating curves. Additionally, the gates at Lake Lure were assumed to be closed. Reservoir rating curves are presented in Figure 2.4.3-210, Figure 2.4.3-211, Figure 2.4.3-212, Figure 2.4.3-213, Figure 2.4.3-214, Figure 2.4.3-215, Figure 2.4.3-216, and Figure 2.4.3-217.

The Lake Whelchel discharge rating curve is based on a riser with outlet pipe and spillway configuration. The riser maintains the normal pool elevation of 670 ft. The outlet pipe through the dam is a 48 in. concrete pipe. The spillway elevation varies from 680 ft. to 683 ft. The Lake Whelchel rating curve is presented in

Figure 2.4.3-238. Lake Whelchel was modeled using a full-pond starting elevation.

The Make-Up Pond C discharge rating curve is based on the designed 4-cycle labyrinth spillway rating curve. Each cycle has a lateral width of 20 ft. The spillway crest elevation is 650 ft. Sensitivity analyses were performed based on a 10 percent increase and decrease of the designed labyrinth spillway rating curve. The Make-Up Pond C rating curve is presented in Figure 2.4.3-242. Make-Up Pond C was modeled using a full-pond starting elevation.

The entire watershed and individual subbasin unit hydrographs of the existing HEC-1 study were verified using three significant storm events occurring in October 1964, June 1972, and October 1976. Base-flow separation was estimated by evaluating semilog plots of each storm event and confirmed with historical daily mean flows at USGS gauging locations. Several USGS gauges are located throughout the watershed. Subbasin input parameters, including the modified BR-15 subbasin, Lake Whelchel subbasin, and Make-Up Pond C subbasin, are listed in Table 2.4.3-206. The exponential recession method is used to model baseflow. The Lake Whelchel subbasin and the Make-Up Pond C subbasin use the same baseflow characteristics as the BR-15 subbasin with an adjusted recession threshold based on the ratio of drainage areas for the two subbasins. Snowmelt is not considered to be a factor in modeling the PMF event, as described in Subsection 2.4.3.1.

To assure HEC-HMS model calibration with the existing study, the HEC-HMS model was first examined using the existing HEC-1 model inputs without antecedent conditions or the modifications for the addition of the Lake Whelchel subbasin and the Make-Up Pond C subbasin. The results were satisfactorily comparable. The HEC-HMS model was then examined using the modifications for the addition of the Lake Whelchel subbasin and the Make-Up Pond C subbasin and the PMP with antecedent rainfall conditions.

Because of large magnitude flows and backwater effects at Gaston Shoals, Cherokee Falls, and Ninety-Nine Islands dams, a standard step method, unsteady-flow hydraulic analysis was performed to more accurately determine the water surface elevation at the Lee Nuclear Station. The USACE HEC-RAS, Version 3.1.3 (Reference 273), modeling software was used to route hydrographs from above Gaston Shoals Dam to Lockhart Dam.

Cross sections were estimated using the existing study, USGS quadrangles, and the USACE NID database. Cross section interpolations were done as necessary to provide a stabilized HEC-RAS model. Manning's roughness coefficients range from 0.03 to 0.08. Contraction and expansion coefficients are based on gradual transitions. Reservoir cross sections were created to approximate the volumes associated with each reservoir. Rating curves were approximated using modeled inline structures. The HEC-RAS model uses a 5-min. computation interval.

The HEC-RAS model is based on the existing study's NWS DAMBRK model. To assure HEC-RAS model calibration, the HEC-RAS model was examined using the DAMBRK input and without antecedent conditions. The results were

satisfactorily comparable. Hydrographs from the HEC-HMS analysis, including antecedent rainfall and accounting for nonlinear basin response, were then used as inflow to the HEC-RAS model. Lateral inflows representing local flow between Gaston Shoals Dam and Ninety-Nine Islands Dam were also included in the model. Input hydrographs are shown in Figure 2.4.3-218, Figure 2.4.3-219, Figure 2.4.3-220, Figure 2.4.3-221, Figure 2.4.3-243, and Figure 2.4.3-245.

McKowns Creek/Make-Up Pond B

For McKowns Creek and Make-Up Pond B, HEC-HMS modeling software was used for rainfall runoff and storage routing calculations. The watershed is shown in Figure 2.4.3-201. Methods adopted to account for nonlinear basin response at high rainfall rates include increasing the peak of the unit hydrograph by 20 percent and reducing the time to peak by approximately 33 percent. Topographic characteristics of the site and watershed are described in Subsection 2.4.1.2.1.

The Soil Conservation Service (SCS) unit hydrograph method was used as a basis for a modified unit hydrograph to transform rainfall to runoff. An equivalent SCS unit hydrograph was first determined using the equations and ratios of the SCS dimensionless unit hydrograph. The equivalent SCS unit hydrograph was then modified by increasing the peak of the unit hydrograph by 20 percent and reducing the time to peak by approximately 33 percent. The remaining ordinates of the modified unit hydrograph were adjusted to maintain a smooth unit hydrograph with the standard characteristic of 1 in. of runoff.

The best calibration of the modified SCS unit hydrograph with the initial SCS unit hydrograph was found using a 10-min. computational time step in the HEC-HMS modeling software. Therefore, the time step used to define the ordinates of the modified SCS unit hydrograph is also 10 min. The Make-Up Pond B subbasin has a lag time of 77 min. The initial SCS unit hydrograph and modified unit hydrograph to account for the effects of nonlinear basin response are provided in Figure 2.4.3-237. The modified SCS unit hydrograph is tabulated in Table 2.4.3-208.

The drainage area, length of watercourse, and average slope of the watershed were determined from aerial topography created for the area. The lag time was determined using the standard SCS curve number regression equation:

$$T_{lag} = (L^{0.8} * (S+1)^{0.7}) / (1900 * Y^{0.5})$$

where

T_{lag}	=	lag time (hr.)
L	=	hydraulic length of the watershed (ft.)
S	=	maximum potential storage of the watershed (in.); where S = 1000/CN -10 and CN = average curve number for the watershed
Y	=	average watershed land slope (percent)

The resulting characteristic parameters for the watershed are as follows:

Drainage Area (sq. mi.)	L (ft.)	CN	S (in.)	Y (%)	T_{lag} (hr.)
2.55	10,320	87	1.49	1.60	1.28

The curve number is used to determine the lag time only. During rainfall routing, the model does not use the curve number loss method, under the conservative assumption that precipitation losses do not occur. The curve number was developed using the NRCS Web Soil Survey (Reference 278) to determine the soil types in the watershed. About 95 percent of the soil belongs to Hydrologic Soil Group B, and the remaining 5 percent to Hydrologic Soil Group C. The land use is predominately wooded. Make-Up Pond B is modeled as impervious cover. Wet antecedent moisture conditions (AMC III) were also assumed.

Base flow was determined using the minimum average monthly flow of the Gaffney and Ninety-Nine Island gauges (USGS No. 02153500 and 02153551). The flow was then corrected on the basis of a ratio of drainage basin areas. Base flow was estimated to be 2.07 cfs and applied to the model as a constant rate.

Make-Up Pond B outflow structure rating curve was developed using standard weir and orifice flow equations with coefficients of 3.5 and 0.8 respectively. The structure is a 35 ft. wide concrete ogee spillway with a crest elevation of 570 ft. The road along Make-Up Pond B crest restricts the opening of the structure to a height of 13.5 ft. The outlet empties into backwaters of the Broad River. The rating curve is provided in Figure 2.4.3-222. Available storage was determined based on aerial topography. Figure 2.4.3-223 provides the storage capacity curve. Full pond elevation of 570 ft. was assumed for antecedent conditions.

Intermittent Stream/Make-Up Pond A

For the intermittent stream and Make-Up Pond A, HEC-HMS modeling software was used for rainfall runoff calculations. The watershed is shown in Figure 2.4.3-201. The following analysis for Make-Up Pond A does not account for nonlinear basin response at high rainfall rates. During severe flooding events, Make-Up Pond A is inundated by backwaters of the Broad River. Broad River flooding coincident with dam failures, as discussed in Subsection 2.4.4, exceeds the maximum flooding elevation for Make-Up Pond A. Therefore, coincident wind wave activity for Make-Up Pond A is based on flooding from the Broad River. By incorporating the Broad River analysis to determine the maximum water surface elevation, the Make-Up Pond A coincident wind wave evaluation accounts for nonlinear basin response at high rainfall rates as discussed above. Topographic characteristics of the site and watershed are described in Subsection 2.4.1.2.1.

The SCS unit hydrograph method was used to transform rainfall to runoff. The drainage area, length of watercourse, and average slope of the watershed were determined from aerial topography created for the area. The lag time was determined using the standard SCS curve number regression equation:

$T_{lag} = (L^{0.8} * (S+1)^{0.7}) / (1900 * Y^{0.5})$

where

T_{lag} = lag time (hr.)

L = hydraulic length of the watershed (ft.)

S = maximum potential storage of the watershed (in.);

where S = 1000/CN -10 and CN = average curve number for the watershed

Y = average watershed land slope (percent)

The resulting characteristic parameters for the watershed are as follows:

Drainage Area (sq. mi.)	L (ft.)	CN	S (in.)	Y (%)	T_{lag} (hr.)
0.60	3340	92	0.87	3.48	0.29

The curve number is used to determine the lag time only. During rainfall routing, the model does not use the curve number loss method, under the conservative assumption that precipitation losses do not occur. The curve number was developed using the NRCS Web Soil Survey (Reference 278) to determine the soil types in the watershed. About 95 percent of the soil belongs to Hydrologic Soil Group B, and the remaining 5 percent to Hydrologic Soil Group C. The land use is predominately industrial. Make-Up Pond A is modeled as impervious cover. Wet antecedent moisture conditions (AMC III) were also assumed.

Base flow was determined using the minimum average monthly flow of the Gaffney and Ninety-Nine Island gauges (USGS No. 02153500 and 02153551). The flow was then corrected on the basis of a ratio of drainage basin areas. Base flow was estimated to be 0.49 cfs and applied to the model as a constant rate.

Although the full pond elevation is 547 ft., the crest elevation low point of 555.1 ft. was assumed for water surface elevation antecedent conditions. Make-Up Pond A overtopping flows empty into backwaters of the Broad River. The outflow rating curve was developed using the standard weir flow equation with a 2.6 discharge coefficient. The embankment crest is approximately 1500 ft. long and has an irregular shape. The rating curve is provided in Figure 2.4.3-224. Available storage was determined based on aerial topography. Figure 2.4.3-225 provides the storage capacity curve.

London Creek/Make-Up Pond C

For London Creek and Make-Up Pond C, HEC-HMS modeling software was used for rainfall runoff calculations. The watershed is shown in Figure 2.4.3-239. The SCS unit hydrograph method was used as a basis for a modified unit hydrograph to transform rainfall to runoff and account for nonlinear basin response. As

discussed above for the Make-Up Pond C subbasin in the Broad River watershed, an equivalent SCS unit hydrograph was first determined using the equations and ratios of the SCS dimensionless unit hydrograph. The equivalent SCS unit hydrograph was then modified by increasing the peak of the unit hydrograph by 20 percent and reducing the time to peak by approximately 33 percent. The remaining ordinates of the modified unit hydrograph were adjusted to maintain a smooth unit hydrograph with the standard characteristic of 1 in. of runoff.

The best calibration of the modified SCS unit hydrograph with the initial SCS unit hydrograph was found using a 10-min. computational time step in the HEC-HMS modeling software. Therefore, the time step used to define the ordinates of the modified SCS unit hydrograph is also 10 min. The initial SCS unit hydrograph and modified unit hydrograph to account for the effects of nonlinear basin response are provided in Figure 2.4.3-241. The modified SCS unit hydrograph is tabulated in Table 2.4.3-207.

The drainage area, length of watercourse, and average slope of the watershed were determined from aerial topography created for the area. The lag time was determined using the standard SCS curve number regression equation:

$$T_{lag} = (L^{0.8} * (S+1)^{0.7}) / (1900 * Y^{0.5})$$

Where:

T_{lag}	=	lag time (hr.)
L	=	hydraulic length of the watershed (ft.)
S	=	maximum potential storage of the watershed (in.); where S = 1000/CN -10 and CN = average curve number for the watershed
Y	=	average watershed land slope (percent)

The resulting characteristic parameters for the watershed are as follows:

Drainage Area (sq. mi.)	L (ft.)	CN	S (in.)	Y (%)	T_{lag} (min.)
3.87	5393	63.9	5.65	2.23	77

The curve number was developed using the NRCS Web Soil Survey (Reference 300) to determine the soil types in the watershed. About 87.4 percent of the soil belongs to Hydrologic Soil Group B, 10.4 percent belonging to Hydrologic Soil Group C, and the remaining 2.2 percent to Hydrologic Soil Group C/D and D. The land use is predominately wooded, grassland, and large lot residential. The watershed contains approximately 27.8 percent impervious cover, including Make-Up Pond C and Lake Cherokee. Average antecedent moisture conditions (AMC II) were used, along with the 40 percent PMP antecedent rainfall.

Base flow was determined based on the Broad River watershed BR-15 subbasin. The recession baseflow method was used with an initial discharge per area of 1.63 cfs/sq. mi. and a recession constant of 0.4919. The recession threshold was calculated to be 23 cfs based on a ratio of the Make-Up Pond C and BR-15 subbasin drainage areas.

The Make-Up Pond C discharge rating curve is based on the designed 4-cycle labyrinth spillway rating curve. Each cycle has a lateral width of 20 ft. The spillway crest elevation is 650 ft. Sensitivity analyses were performed based on a 10 percent increase and decrease of the designed labyrinth spillway rating curve. The Make-Up Pond C rating curve is presented in Figure 2.4.3-242. Available storage was determined based on aerial topography. Figure 2.4.3-244 provides the storage capacity curve. A full pond elevation of 650 ft. msl was assumed for antecedent conditions.

2.4.3.4 Probable Maximum Flood Flow

Broad River

Applying the precipitation, described in Subsection 2.4.3.1, and the precipitation losses, described in Subsection 2.4.3.2, to the runoff model, described in Subsection 2.4.3.3, the peak PMF discharge at the Lee Nuclear Station was determined to be 823,212 cfs resulting from the 1000-sq. mi. storm centered near the centroid of the Gaston Shoals Dam drainage basin. The resulting flow hydrograph at the Lee Nuclear Station is shown in Figure 2.4.3-226. Temporal distribution of the PMP and storm location is discussed in Subsection 2.4.3.1. Inclusion of upstream and downstream river structures is discussed in Subsection 2.4.3.3. Dam failures are discussed in Subsection 2.4.4. No credit is taken for the lowering of flood levels at the site due to downstream dam failure.

McKowns Creek/Make-Up Pond B

Applying the precipitation, described in Subsection 2.4.3.1, with no precipitation losses, described in Subsection 2.4.3.2, to the runoff model, described in Subsection 2.4.3.3, the McKowns Creek and Make-Up Pond B peak PMF runoff was determined to be 20,784 cfs resulting from the 6-hr. two-thirds peaking storm event. The routed peak discharge is 7457 cfs. However, the 72-hr. end peaking storm event resulting in a peak PMF runoff of 19,376 cfs and a routed discharge of 8430 cfs provided the controlling water surface elevation. The resulting flow hydrograph for the 72-hr. end peaking storm event is shown in Figure 2.4.3-227. Temporal distribution of the PMP is discussed in Subsection 2.4.3.1. Because the watershed is small, the position of the PMP is considered point rainfall affecting the entire watershed equally. There are no upstream structures. No credit is taken for the lowering of flood levels at the site due to downstream dam failure.

Intermittent Stream/Make-Up Pond A

Applying the precipitation, described in Subsection 2.4.3.1, with no precipitation losses, described in Subsection 2.4.3.2, to the runoff model, described in Subsection 2.4.3.3, the intermittent stream and Make-Up Pond A peak PMF runoff was determined to be 10,703 cfs resulting from the 6-hr. storm event. The routed peak discharge is 9079 cfs. The resulting flow hydrograph is shown in Figure 2.4.3-228. Temporal distribution of the PMP is discussed in Subsection 2.4.3.1. Because the watershed is small, the position of the PMP is considered point rainfall affecting the entire watershed equally. There are no upstream structures. No credit is taken for the lowering of flood levels at the site due to downstream dam failure.

London Creek/Make-Up Pond C

Applying the precipitation, described in Subsection 2.4.3.1, and the precipitation losses, described in Subsection 2.4.3.2, to the runoff model, described in Subsection 2.4.3.3, the London Creek and Make-Up Pond C peak PMF runoff providing the highest water surface elevation from the 72-hr. end peaking storm event was determined to be 29,167 cfs. The routed peak discharge is 10,577 cfs. Temporal distribution of the PMP is discussed in Subsection 2.4.3.1. Because the watershed is small, the position of the PMP is considered point rainfall affecting the entire watershed equally. The upstream Lake Cherokee watershed was incorporated into the Make-Up Pond C watershed. Therefore, Lake Cherokee was assumed to pass runoff flow without any detention. No credit is taken for the lowering of flood levels at the Lee Nuclear Station due to downstream dam failure.

2.4.3.5 Water Level Determinations

Broad River

Subsection 2.4.4.3 addresses coincident wind wave activity for the Broad River. The maximum Lee Nuclear Station flood elevation is 551.49 ft. resulting from the 1000-sq. mi. storm centered near the centroid of the Gaston Shoals Dam drainage basin. Subsection 2.4.3.3 describes the models used to translate the PMP discharge to the elevation hydrograph. The resulting elevation hydrograph at the Lee Nuclear Station is shown in Figure 2.4.3-229. The maximum flood elevation is well below the station's safety-related plant elevation of 590 ft.

McKowns Creek/Make-Up Pond B

Subsection 2.4.3.6 addresses coincident wind wave activity for Make-Up Pond B. The maximum water surface elevation of Make-Up Pond B, resulting from the 6-hr. two-thirds peaking storm event modeled with a 5-min. time step, was found to be 583.70 ft. The elevation hydrograph is provided in Figure 2.4.3-230. The maximum water surface elevation of Make-Up Pond B resulting from the 72-hr. end peaking storm event modeled with a 10-min. time step was found to be 584.48 ft. The elevation hydrograph is provided in Figure 2.4.3-231. Subsection 2.4.3.3 describes the models used to translate the PMP discharge to the elevation hydrographs.

Make-Up Pond B includes an adequately sized outlet structure and is not located on a sizeable river or stream. Therefore, the potential for significant debris to be picked up by a rise in the water level and then transported to the outlet structure where it could collect as an obstruction is minimal. Blockage of the outlet structure was not considered in the analysis. In addition, Duke Energy's shoreline management program includes removal of trees from the water's edge at elevation 570 ft. msl to 50 ft. beyond contour elevation 585 ft. msl around the perimeter of Make-Up Pond B. This area is paved, grassed, or other suitable alternative where appropriate, and is maintained in this manner throughout the operational life of the plant. Therefore, debris blockage of the outlet structure is not considered to be a credible event.

Intermittent Stream/Make-Up Pond A

Subsection 2.4.4.3 addresses coincident wind wave activity for Make-Up Pond A. The maximum water surface elevation of Make-Up Pond A, resulting from the 6-hr. storm modeled with a 5-min. time step, was found to be 558.06 ft. The elevation hydrograph is provided in Figure 2.4.3-233. Subsection 2.4.3.3 describes the models used to translate the PMP discharge to elevation.

London Creek/Make-Up Pond C

The Make-Up Pond C reservoir is located on a tributary of the Broad River, west of the Lee Nuclear Station, as shown in Figure 2.4.1-213, but is not adjacent to the Lee Nuclear Station. However, the PMF for London Creek and Make-Up Pond C is determined for the purpose of combination with dam failure permutations as discussed in Subsection 2.4.4.1. Because the PMF discharge flow from Make-Up Pond C is bounded by the Broad River watershed PMF, spillover from Make-Up Pond C during a PMF event is not a limiting event for flooding at the Lee Nuclear Station when taken as an isolated event. For reference to the dam failure permutations, the maximum water surface elevation of Make-Up Pond C, resulting from the 72-hr storm modeled with a 10 min. time step, was found to be 656.68 ft. Subsection 2.4.3.3 describes the models used to translate the PMP discharge to elevation.

2.4.3.6 Coincident Wind Wave Activity

Coincident wind wave activity is evaluated for the Broad River, Make-Up Pond A and Make-Up Pond B. Fetch lengths are determined using the longest straight line fetch based on U.S. Geological Survey quadrangles and the site grading and drainage plan. Wave height, setup, and runup are estimated using U.S. Army Corps of Engineers guidance (Reference 295). A coincident 2-year annual extreme mile wind speed of 50 mph is estimated based on ANSI/ANS-2.8-1992 (Reference 202). Wind setup is estimated using additional U.S. Army Corps of Engineers guidance (Reference 269).

Broad River

Coincident wind wave activity for the Broad River is addressed in Subsection 2.4.4.3.

Intermittent Stream/Make-Up Pond A

Coincident wind wave activity for Make-Up Pond A is addressed in Subsection 2.4.4.3.

McKowns Creek/Make-Up Pond B

Wind wave activity on Make-Up Pond B is evaluated coincident with the maximum water surface elevation of the PMF as discussed in Subsection 2.4.3.5. The determined critical fetch length of 1.48 mi. is shown in Figure 2.4.3-234. The 2-year annual extreme mile wind speed is adjusted based on the factors of fetch length, level overland or over water, critical duration, and stability. The critical duration is approximately 36 min. The adjusted wind speed is 50.22 mph.

Significant wave height (average height of the maximum one-third of waves) is estimated to be 2.07 ft., crest to trough. The maximum wave height (average height of the maximum 1 percent of waves) is estimated to be 3.44 ft., crest to trough. The corresponding wave period is 2.2 sec.

The 0.66 percent slopes along the banks of Make-Up Pond B adjacent to the site are used to determine the wave setup and runup. The maximum runup, including wave setup, is estimated to be 0.26 ft. The maximum wind setup is estimated to be 0.08 ft. Therefore, the total wind wave activity is estimated to be 0.34 ft. The PMF and the coincident wind wave activity results in a flood elevation of 584.8 ft. msl. The Lee Nuclear Station safety-related plant elevation is 590 ft. msl and is unaffected by flood conditions and coincident wind wave activity.

London Creek/Make-Up Pond C

The Make-Up Pond C reservoir is located on a tributary of the Broad River, west of the Lee Nuclear Station, as shown in Figure 2.4.1-213, such that wind wave activity has no consequence to the Lee Nuclear Station. However, a postulated failure of the Make-Up Pond C dam would release water to the Broad River prior to reaching the Lee Nuclear Station. A failure of the Make-Up Pond C dam coincident with the PMF is discussed in Subsection 2.4.4.1, and flooding effects as a result of wind wave activity are bounded by that discussion.

2.4.4 POTENTIAL DAM FAILURES

WLS COL 2.4-2 The guidance in Appendix A of NRC Regulatory Guide 1.59, Rev. 2, *Design Basis Floods for Nuclear Power Plants*, was followed in evaluating potential dam failures, by applying the guidance of American National Standards Institute/American Nuclear Society-2.8-1992, *Determining Design Basis Flooding at Power Reactor Sites* (Reference 202).

The Upper Broad River drainage basin above Ninety-Nine Islands Dam derives water from several tributaries that contain a considerable number of dams. According to the U.S. Army Corps of Engineers (USACE), National Inventory of Dams, there are approximately 131 upstream dams, not including Make-Up Pond C, and five of those have been breached (Reference 276). Most of the dams in the drainage basin have small to insignificant storage capacity. The six largest reservoirs in the basin represent about 88 percent of the total storage capacity for the basin. Two additional dams, Cherokee Falls and Gaston Shoals, located immediately upstream from the Lee Nuclear Station, possess less than 2 percent of the total storage capacity for the basin.

Make-Up Pond B and Make-Up Pond A are located at elevations much lower than the Lee Nuclear Station's safety-related facilities. Failure of these water features would result in a discharge to smaller ponds and then directly to the Broad River. The respective volumes are small compared to the available capacity of the Broad River and the freeboard available at the site. Failure of the on-site reservoirs would not affect the safety-related facilities.

Make-Up Pond C is located on a tributary of the Broad River, west of the Lee Nuclear Station. As described below, the critical dam failure evaluation coincident with the PMF for the Broad River watershed includes the assumed overtopping failure of Make-Up Pond C. Assumed overtopping dam failure coincident with the PMF for the Make-Up Pond C watershed has also been evaluated, but does not exceed the maximum flood elevation associated with the Broad River critical dam failure event and, thus, is bounded by the critical dam failure event. Therefore, there are no safety-related structures that could be affected by flooding due to a Make-Up Pond C dam failure.

The described studies have been made solely to ensure the safety-related facilities of the Lee Nuclear Station are protected against floods caused by the assumed failure of dams. The postulated dam failure events do not infer or concede that the dams are unsafe.

The critical dam failure event is the assumed overtopping failures of Lake Lure Dam, Tuxedo Dam, Turner Shoals Dam, Lake Whelchel Dam, Kings Mountain Reservoir Dam, and Make-Up Pond C Dam, including the dam at Lake Cherokee, coincident with the probable maximum flood (PMF). The resulting flow rate and water surface elevation at the station is provided in the discussion below. There are no safety-related structures that could be affected by flooding due to dam failure. All elevations provided in this subsection are above mean sea level.

2.4.4.1 Dam Failure Permutations

According to guidance (Reference 202), seismic dam failure is to be examined using the safe shutdown earthquake coincident with the peak of the 25-year flood and operating basis earthquake coincident with the peak of one-half PMF or the 500-year flood. Dam failure permutations were first examined assuming hydrologic failure of dams coincident with the PMF. Many of the upstream structures are designed to withstand overtopping. However, structural analysis of each structure has not been performed. The PMF is a more extreme event than

the listed hydrologic events coincident with seismic dam failure. Seismic dam failure coincident with lesser flooding would result in lower flood elevations and has not been examined. Therefore, the evaluations described below comply with Regulatory Guide 1.59.

The considered upstream structures are described below. Reservoirs were modeled using normal water surface elevations with no turbine discharges. Additionally, the gates at Lake Lure were assumed to be closed. Antecedent conditions are discussed in Subsection 2.4.3.

Failure of the downstream structure, Ninety-Nine Islands Dam, would result in lowering the water surface elevation at the Lee Nuclear Station to some degree. Conservatively, Ninety-Nine Islands Dam has not been considered to fail during any of the dam failure scenarios. However, failure of the flashboards has been incorporated into the rating curve.

Cherokee Falls and Gaston Shoals

Cherokee Falls Dam is approximately 4.5 river mi. upstream of Ninety-Nine Islands Dam on the Broad River in Cherokee County, South Carolina. The dam, built in 1826, is a concrete gravity structure approximately 1700 ft. long and 16 ft. high. It has an ogee spillway elevation of 531.5 ft. with 4-ft. flashboards raising the operating pond level to 535.5 ft. The impounded reservoir has an estimated storage capacity of 200 ac.-ft. at normal water surface elevation. Flashboard failure is incorporated into the discharge rating curve used for the structure.

Gaston Shoals Dam is approximately 11.5 river mi. upstream of Ninety-Nine Islands Dam on the Broad River in Cherokee County, South Carolina. The dam, built in 1908, is a series of three gravity structures. The upper masonry gravity spillway is about 707 ft. long with an overflow spillway crest elevation of 599.40 ft. and 6-ft. flashboards that raise the operating pond level to 605.4 ft. The middle concrete gravity section was built in 1917 and is about 381 ft. long. The overflow spillway crest elevation is 601.2 ft. with 4-ft. flashboards up to 605.2 ft. The masonry gravity bulkhead section is about 472 ft. long with a crest elevation of 613.4 ft. The impounded reservoir has an estimated storage capacity of 2500 ac.-ft. at normal water surface elevation. Flashboard failure is incorporated into the discharge rating curve used for the structure.

Both dams are significantly overtopped for a lengthy duration during PMF conditions. Dam failure has been conservatively assumed to occur coincident with the PMF peak flood wave in order to maximize water surface elevations. The breach characteristics for Cherokee Falls assume complete failure of the full height and length of the structure to occur in 0.5 hours (hr.). The breach characteristics for Gaston Shoals assume failure of the full height and length of the middle spillway structure to occur in 0.5 hr., along with failure of the embankment abutments separating the three structures.

An overtopping breach of Gaston Shoals, coincident with the PMF, results in a flow of 824,000 cfs and a water surface elevation of 551.52 ft. at the Lee Nuclear Station. Overtopping breaches of both Gaston Shoals and Cherokee Falls,

coincident with the PMF, result in the same flow and water surface elevation. Because of the small reservoir volumes and large PMF discharge, the dam failures have little effect on the resulting flow and water surface elevations.

Major Upstream Structures

Lake Lure is about 47 mi. northwest of the Lee Nuclear Station on the Broad River in Rutherford County, North Carolina. The dam, built in 1927, is a concrete, multiple-arch structure approximately 480 ft. long and 124 ft. high, with a full pond elevation at 991 ft. There are gated spillways and the arches are set at various elevations, providing additional discharge capacity. The discharge rating curve, used for modeling purposes, conservatively assumes the gates are in the closed position. The impounded reservoir has an estimated storage capacity of about 32,295 ac.-ft. at normal water surface elevation.

Tuxedo Dam, impounding Lake Summit, is about 52 mi. northwest of the Lee Nuclear Station on the Green River in Henderson County, North Carolina. The dam, built in 1920, is a concrete-arch structure approximately 254 ft. long and 130 ft. high, with a full pond elevation at 2012.6 ft. The impounded reservoir has an estimated storage capacity of about 9300 ac.-ft. at normal water surface elevation.

Turner Shoals Dam, impounding Lake Adger, is about 43 mi. northwest of the Lee Nuclear Station, downstream of Tuxedo Dam on the Green River in Polk County, North Carolina. The dam, built in 1925, is a concrete, multiple-arch structure approximately 689 ft. long and 90 ft. high, with a full pond elevation at 911.6 ft. The impounded reservoir has an estimated storage capacity of about 11,700 ac.-ft. at normal water surface elevation.

Kings Mountain Reservoir Dam, also referred to as Moss Lake Dam, is about 17 mi. northeast of the Lee Nuclear Station on Buffalo Creek in Cleveland County, North Carolina. The dam, built in 1973, is a compacted earth-fill structure approximately 840 ft. long and 99 ft. high. The top of the dam is at an elevation of 750 ft. The spillway is located at the right abutment and consists of a 350 ft. long concrete ogee section with a crest elevation of 736 ft. The impounded reservoir has an estimated storage capacity of 44,400 ac.-ft. at normal water surface elevation.

Lake Whelchel is located approximately 8 mi. northwest of the Lee Nuclear Station on Cherokee Creek in Cherokee County, South Carolina. The dam at Lake Whelchel, built in 1964, is a compacted earth-fill structure approximately 2100 ft. long and 61 ft. high. The dam crest elevation is 685 ft. A riser and 48 in. concrete pipe outlet works sets the normal pool elevation at 670 ft. The spillway is 565 ft. long and varies in elevation from 680 ft. to 683 ft. Lake Whelchel has an estimated storage capacity of approximately 2438 ac.-ft. at normal water surface elevation.

Make-Up Pond C is located approximately 2 mi. west of the Lee Nuclear Station on London Creek in Cherokee County, South Carolina. Make-Up Pond C is formed by construction of an earthen dam and saddle dikes that impound London Creek just upstream of the confluence with Little London Creek. The Make-Up

Pond C dam crest elevation is 660 ft. A labyrinth spillway sets the normal pool elevation at 650 ft. The designed 4-cycle labyrinth spillway has a lateral width of 20 ft. per cycle. The dam is 132 ft. high. The impounded reservoir has an estimated storage capacity of approximately 22,000 ac.-ft. at normal water surface elevation.

Lake Lure Dam, Tuxedo Dam, and Turner Shoals Dam are designed to withstand overtopping. However, the structural integrity of the dams and foundations has not been examined. The degree and duration of overtopping each dam is capable of withstanding is not considered in this evaluation. Therefore, overtopping dam failure has been calibrated to occur coincident with the PMF peak flood wave in order to maximize water surface elevations for Lake Lure Dam and Tuxedo Dam. Lake Summit and Lake Adger are located in series on the Green River. Overtopping failure of the Turner Shoals Dam was calibrated to coincide with the resulting peak flood wave of the Tuxedo Dam failure. Breach parameters assume failure of the complete structures to occur in 0.1 hr.

Kings Mountain Reservoir Dam, the Lake Whelchel Dam, and the Make-Up Pond C Dam are not expected to be overtopped based on the PMF analysis with antecedent storm conditions. However, overtopping failure is postulated for this analysis, and dam failures have been calibrated to occur coincident with the PMF peak flood wave in order to maximize water surface elevations.

Lake Cherokee is located just upstream of Make-Up Pond C on a tributary of London Creek in Cherokee County, South Carolina. The dam is a compacted earth-fill structure approximately 940 ft. long, 40 ft. high and has an estimated maximum storage capacity of 720 ac.-ft. The dam at Lake Cherokee is assumed to fail by overtopping based on the full height of the structure. The peak failure flow is derived using the HEC-HMS dam failure equation identified below. No tailwater elevation was assumed, maximizing the head difference and breach outflow. The peak outflow is added to the PMF peak flood wave for the Make-Up Pond C watershed to maximize the Make-Up Pond C dam failure.

$$Q_{max} = 1.7 * W_b * h^{1.5} + 1.35 * S * h^{2.5}$$

Where:

Q_{max}	=	peak outflow (cfs)
W_b	=	width of breach (ft.)
h	=	smaller of the head difference between the reservoir interior water surface elevation and the tailwater surface elevation, or head difference between the reservoir interior water surface elevation and the breach bottom invert elevation (ft.)
S	=	side slope of the breach

Embankment breach characteristics are based on the USACE RD-13 (Reference 250). Failure development time for embankment sections is estimated to occur from 0.5 to 4 hr. Breach width for embankment sections is estimated to be

from 0.5 to 3 times the dam height. Side slopes for an embankment breach are estimated to be from 0:1 to 1:1 (horizontal:vertical). To maximize the peak outflow, a breach width of 3 times the dam height was used along with 1:1 side slopes and the shortest failure development time of 0.5 hr.

Sensitivity was also performed based on the time of failure for the various structures. Additionally, several failure times were examined based on the peak outflow time at Ninety-Nine Islands Dam. Using the same breach parameters as discussed above, all structures were assumed to fail simultaneously, rather than individually based on the peak flood wave at each dam. It was determined that the critical dam failure scenario occurred when all dams failed simultaneously with a failure time near to the peak PMF outflow at Ninety-Nine Islands Dam.

The multiple failures due to overtopping, coincident with the PMF, result in a peak flow of approximately 1,720,000 cfs. The peak flow is determined using the HEC-HMS model discussed in Subsection 2.4.4.2.

Make-Up Pond C Dam

Assumed overtopping dam failure of the Make-Up Pond C Dam has also been evaluated coincident with a more intense PMF confined to the smaller Make-Up Pond C watershed as described in Subsection 2.4.3. As previously discussed, failure of the dam at Lake Cherokee was also included to maximize the peak dam failure outflow from Make-Up Pond C.

The Make-Up Pond C peak dam failure outflow was combined with the maximum historical flow recorded on the Broad River at Gaffney, identified in Table 2.4.2-201, to account for any coincidental flow in the Broad River. However, the resulting combined peak outflow of 1,307,000 cfs does not exceed the critical dam failure event for the Broad River watershed previously described. Therefore, even if routed to the Lee Nuclear Station without attenuation, the resulting water surface elevation would not exceed the elevation determined from the critical multiple dam failure scenario coincident with the Broad River watershed PMF.

Cleveland County Sanitary District

According to the Federal Register (Reference 226), a notice of intent was filed on July 11, 2006, for a Draft Environmental Impact Statement (DEIS) to be prepared for a proposed reservoir on the First Broad River in Cleveland County, North Carolina. The Cleveland County Sanitary District applied for a permit to construct a water supply reservoir about 1 mi. north of Lawndale, North Carolina. The DEIS is currently in preparation. Lawndale is about 26 mi. northeast of the Lee Nuclear Station.

The proposed embankment dam may be about 83 ft. high and 1245 ft. long, impounding a surface area of 2245 ac. and inundating areas lower than 860 ft. Using USGS quadrangle contours, volume calculations estimate the storage to be about 47,500 ac.-ft. The embankment is approximately the same size as Kings Mountain Reservoir. The reservoir contains approximately the same storage with twice the surface area of the Kings Mountain Reservoir. It is assumed that the

dam is designed to prevent failure during a PMF event. Based on the distance from the Lee Nuclear Station and available freeboard, it is also assumed that any failure effects due to seismic activity coincident with lesser flood events would be no worse than those estimated for the Kings Mountain Reservoir. The above evaluation includes failure of the Kings Mountain Reservoir Dam during the PMF. Therefore, any failure effects from the proposed embankment dam would be less than those provided.

Other Considerations

There are no safety-related facilities that could be affected by loss of water supply due to dam failure. This is addressed further in Subsection 2.4.11. Additionally, there are no safety-related facilities that could be affected by water supply blockages due to sediment deposition or erosion during dam failure induced flooding. There are no onsite water control or storage structures located above site grade that may induce flooding. As discussed in Subsection 2.4.4.3, the Lee Nuclear Station's safety-related facilities are located above the resulting water surface elevation. Therefore, no safety-related structures could be affected by waterborne missiles.

2.4.4.2 Unsteady-Flow Analysis of Potential Dam Failures

The failures for the dams immediately upstream of the Lee Nuclear Station, Cherokee Falls and Gaston Shoals, were examined using the same HEC-RAS unsteady flow model from the PMF calculation described in Subsection 2.4.3. The model was modified by including the HEC-RAS breach feature and adjusting the computation interval to 30 sec. Unsteady state flow is computer solved using the principles of the continuity and momentum equations.

The failures of the additional dams upstream of the Lee Nuclear Station, were first examined using the same HEC-HMS quasi-unsteady flow model from the PMF calculation described in Subsection 2.4.3. The dam breach feature in the HEC-HMS model was used to determine the resulting flow of the Broad River at Ninety-Nine Islands Dam. HEC-HMS employs finite difference methods approximating the continuity and momentum equations.

The HEC-HMS peak flow determined at Ninety-Nine Islands Dam was then used as input to the HEC-RAS model from the PMF calculation described in Subsection 2.4.3. Steady state analysis was performed to determine the water surface elevation at the Lee Nuclear Station. Steady state flow is computer solved using the principles of the continuity and energy equations.

Verification of the models is discussed in Subsection 2.4.3. However, verifying the models with actual data approaching the magnitude of the PMF is not possible. The resulting extreme flows determined using HEC-HMS, HEC-RAS unsteady state flow, and HEC-RAS steady state flow are discussed below. The comparative results indicate the models are appropriate for artificially large floods.

The HEC-RAS models are used to route the flood flow through downstream Ninety-Nine Islands Dam and Lockhart Dam. Coefficients, antecedent conditions,

and coincident flow are discussed above and in Subsection 2.4.3. Domino-type failure is discussed above. As discussed in Subsection 2.4.4.3, the Lee Nuclear Station's safety-related facilities are located above the resulting water surface elevation. Therefore, no safety-related structures could be affected by flood waves.

2.4.4.3 Water Level at the Plant Site

The methods and models used to determine the resulting water surface elevation are described above and in Subsection 2.4.3. Model verification and reliability is also discussed above and in Subsection 2.4.3. The HEC-RAS model, as described above, was used to model a resulting steady state flow of 1,720,000 cfs to determine the water surface elevation at the station.

The resulting water surface elevation at the Lee Nuclear Station is 573.26 ft. The maximum flood elevation is well below the station's safety-related plant elevation of 590 ft. The resulting water surface elevation of the dam failure analysis using HEC-HMS and HEC-RAS was compared with the resulting water surface elevations of the PMF analysis using HEC-HMS and HEC-RAS. The comparison is provided in Table 2.4.4-201. Given the significant freeboard remaining at the site, a full unsteady-flow analysis to determine dam breach flows and resulting water surface elevations with greater precision was determined to be unnecessary.

Coincident Wind Wave Activity

Coincident wind wave activity is evaluated for the Broad River, Make-Up Pond A and Make-Up Pond B. Fetch lengths are estimated using the longest straight line fetch based on U.S. Geological Survey quadrangles and the site grading and drainage plan. Wave height, setup, and runup are estimated using U.S. Army Corps of Engineers guidance (Reference 295). A coincident 2-year annual extreme mile wind speed of 50 mph is estimated based on ANSI/ANS-2.8-1992 (Reference 202). Wind setup is estimated using additional U.S. Army Corps of Engineers guidance (Reference 269).

Broad River

Wind wave activity on the Broad River is evaluated coincident with the maximum water surface elevation of the PMF including the effects of dam failures as discussed above. The determined fetch length of 2.77 mi., shown in Figure 2.4.4-201, has a runup slope of 46 percent. The PMF including effects of dam failures and the coincident wind wave activity results in a flood elevation of 582.35 ft. msl. The Lee Nuclear Station safety-related plant elevation is 590 ft. msl and is unaffected by flood conditions and coincident wind wave activity. A more critical wind wave activity result was determined considering a fetch length through Make-Up Pond A, which becomes inundated by backwaters of the Broad River during severe flooding events. Therefore, the critical wind wave activity for the Broad River is equal to the wind wave activity for Make-Up Pond A, as discussed below.

Intermittent Stream/Make-Up Pond A

During severe flooding events, Make-Up Pond A is inundated by backwaters of flooding of the Broad River. Therefore, wind wave activity on Make-Up Pond A is evaluated coincident with the maximum water surface elevation of the PMF on the Broad River including the effects of dam failures as discussed above. The determined critical fetch length of 2.69 mi. is shown in Figure 2.4.4-202. The 2-year annual extreme mile wind speed is adjusted based on the factors of fetch length, level overland or over water, critical duration, and stability. The critical duration is approximately 53 min. The adjusted wind speed is 49.9 mph.

Significant wave height (average height of the maximum 33-1/3 percent of waves) is estimated to be 2.76 ft., crest to trough. The maximum wave height (average height of the maximum 1 percent of waves) is estimated to be 4.59 ft., crest to trough. The corresponding wave period is 2.6 sec.

The 53 percent slopes along the banks of Make-Up Pond A adjacent to the site are used to determine the wave setup and runup. The maximum runup, including wave setup, is estimated to be 9.45 ft. The maximum wind setup is estimated to be 0.08 ft. Therefore, the total wind wave activity is estimated to be 9.53 ft. The PMF including effects of dam failures and the coincident wind wave activity results in a flood elevation of 582.79 ft. msl for Make-Up Pond A and the Broad River. The Lee Nuclear Station safety-related plant elevation is 590 ft. msl and is unaffected by flood conditions and coincident wind wave activity.

McKowns Creek/Make-Up Pond B

Coincident wind wave activity for Make-Up Pond B is addressed in Subsection 2.4.3.6.

London Creek/Make-Up Pond C

The Make-Up Pond C reservoir is located on a tributary of the Broad River, west of the Lee Nuclear Station, as shown in Figure 2.4.1-213, such that a postulated failure of the Make-Up Pond C dam would release water to the Broad River prior to reaching the Lee Nuclear Station. Failure of the Make-Up Pond C dam coincident with the PMF for the Make-Up Pond C watershed is discussed in Subsection 2.4.4.1. Flooding effects as a result of dam failure due to wind wave activity are bounded by that discussion.

Other Smaller Upstream Dams

Numerous other ponds and small lakes with dam structures are located in the Ninety-Nine Islands watershed. However, these numerous features have negligible storage capacity. A breach would have no measurable effect on the water surface elevations determined by the PMF analysis.

2.4.5 PROBABLE MAXIMUM SURGE AND SEICHE FLOODING

WLS COL 2.4-2

Regulatory guidance prescribed by Regulatory Guide 1.59 describes the probable maximum surge and seiche flooding based on a probable maximum hurricane (PMH), probable maximum windstorm (PMWS), or moving squall line. The region of occurrence for a PMH is along U.S. coastline areas (Reference 202). The PMWS region of occurrence is along coastline areas and large bodies of water such as the Great Lakes. A moving squall line is considered for the Great Lakes region.

The U.S. Army Corps of Engineers guideline procedures for geologic hazard evaluations consider seiche waves greater than 7 ft. to be rare (Reference 281). According to U.S. Army Corps of Engineers guidance, the seiche hazard can be screened out for sites located more than 7 ft. above the adjacent water body.

Regulatory guidance prescribed by Regulatory Guide 1.59 indicates consideration of a PMH for areas within 200 miles of coastal areas. The Lee Nuclear Station is located approximately 175 miles inland from the Atlantic Coast. The safety-related plant elevation is 590 ft. The normal maximum water surface elevation of the Broad River is 511.1 ft., the spillway flashboard elevation at Ninety-Nine Islands Dam (Reference 217).

The Broad River is a tributary of the Santee River which flows to the Atlantic Ocean. The mouth of the Santee River is about 45 mi. northeast of Charleston, South Carolina. The Santee River is also diverted by a series of lakes, Lake Marion and Lake Moultrie, to the Cooper River. The Cooper River flows into the Atlantic Ocean at Charleston, South Carolina.

According to Regulatory Guide 1.59, the probable maximum surge estimate for Folly Island, located at Charleston, South Carolina, is 28.2 ft. above mean low water. The surge estimate includes wind setup of 17.15 ft., pressure setup of 3.23 ft., initial water level of 1.0 ft., and 10 percent exceedance high tide of 6.80 ft. Mean sea level is 2.7 ft. higher than mean low water at Charleston, South. Carolina (Reference 202). The maximum surge estimate is 25.5 ft. above mean sea level. A sea level anomaly of 1.0 ft. has been known to occur for the predicted astronomical tides at Charleston, South Carolina (Reference 202). Therefore, the probable maximum surge estimate is 26.5 ft. above mean sea level.

Regulatory Guide 1.59 only contains surge data up to 1975. The maximum storm surge along the Atlantic Coast after 1975 occurred as a result of hurricane Hugo. Storm surge from hurricane Hugo inundated the South Carolina coast from Charleston to Myrtle Beach in 1989. Maximum storm tides of 20 ft. were observed. Although the site is within 200 miles of the coastline, surge due to a PMH event would not cause flooding at the site. Transposition of the probable maximum surge, without any type of reduction for distance or instream structures, is nearly three times less than the 78.9-ft. difference in elevation between the station and the adjacent river.

There are no known documented surge or seiche occurrences on the Broad River. Based on data provided above, and site location and elevation characteristics, the station's safety-related facilities are not considered at risk from surge and seiche flooding. Resonance wave phenomena including oscillations of waves at natural periodicity, lake reflection, and harbor resonance are traditionally characteristics of harbors, estuaries, and large lakes and not associated with river settings. Any effects on the Broad River produced by similar phenomena would not affect the Lee Nuclear site. Coincident wind-generated wave activity is discussed in Subsection 2.4.3.6. Additionally, there are no safety-related facilities that could be affected by water supply blockages due to sediment deposition or erosion during storm surge or seiching.

Surge flooding is evaluated for Make-Up Pond A and Make-Up Pond B using the maximum wind speed identified in Subsection 2.3.1.2.8. This is consistent with the maximum wind speeds identified in U.S. Army Corps of Engineers guidance (Reference 295). Fetch lengths are estimated using the longest straight line fetch directed toward the site for each water body. Wave height, setup, and runup are estimated using U.S. Army Corps of Engineers guidance (Reference 295). Wind setup is estimated using additional U.S. Army Corps of Engineers guidance (Reference 269).

Estimates for surge flooding are made coincident with 100-yr. flood levels of Make-Up Pond A and Make-Up Pond B. Resulting 100-yr. runoff rates for the watersheds are determined using USGS regression equations for small watersheds in South Carolina (Reference 296). The overflow rating curves for the respective ponds, discussed in Subsection 2.4.3.3, are used to determine the resulting coincident water surface elevations.

Make-Up Pond A

Make-Up Pond A surge flooding is evaluated coincident with the 100-yr. water surface elevation of 556.07 ft. The critical fetch length is 0.37 mi. as shown in Figure 2.4.5-201. The wind speed is adjusted based on the factors of fetch length, level overland or over water, critical duration, and stability using U.S. Army Corps of Engineers guidance (Reference 295). The critical duration is 10 min. The adjusted wind speed is 97.4 mph.

Significant wave height (average height of the maximum 33-1/3 percent of waves) is estimated to be 2.36 ft., crest to trough. The maximum wave height (average height of the maximum 1 percent of waves) is estimated to be 3.94 ft., crest to trough. The corresponding wave period is 1.8 sec.

The slopes along the banks of Make-Up Pond A adjacent to the site area are approximately 52 percent at most and are used to determine the wave setup and runup. The maximum runup, including wave setup, is estimated to be 6.40 ft. The maximum wind setup is estimated to be 0.08 ft. Therefore, the total water surface elevation increase due to high speed wind wave activity is estimated to be 6.48 ft. The resulting flood elevation is 562.55 ft. The Lee Nuclear Station safety-related plant elevation is 590 ft. and is unaffected by high speed wind wave activity flooding conditions.

Make-Up Pond B

Make-Up Pond B surge flooding is evaluated coincident with the 100-yr. water surface elevation of 576.22 ft. The critical fetch length is 1.21 mi. as shown in Figure 2.4.5-202. The wind speed is adjusted based on the factors of fetch length, level overland or over water, critical duration, and stability using U.S. Army Corps of Engineers guidance (Reference 295). The critical duration is 21 min. The adjusted wind speed is 90.6 mph.

Significant wave height (average height of the maximum 33-1/3 percent of waves) is estimated to be 3.87 ft., crest to trough. The maximum wave height (average height of the maximum 1 percent of waves) is estimated to be 6.46 ft., crest to trough. The corresponding wave period is 2.6 sec.

The slopes along the banks of Make-Up Pond B adjacent to the site area are approximately 9 percent and are used to determine the wave setup and runup. The maximum runup, including wave setup, is estimated to be 3.28 ft. The maximum wind setup is estimated to be 0.21 ft. Therefore, the total water surface elevation increase due to high speed wind wave activity is estimated to be 3.49 ft. The resulting flood elevation is 579.71 ft. The Lee Nuclear Station safety-related plant elevation is 590 ft. and is unaffected by high speed wind wave flooding conditions.

Seiche evaluation is based on the natural fundamental period for Make-Up Pond A and Make-Up Pond B. The natural fundamental period of both water bodies is determined using Merian's formula (Reference 295).

$$T = 2 * L / (g * h)^{0.5}$$

where;

T = natural oscillation period at the fundamental mode (sec.)

L = fetch length (ft.)

g = gravitational acceleration (ft/sec2)

h = depth of water (ft.)

Based on bathymetry mapping, an average depth of 29.81 ft. is determined for Make-Up Pond A and used as the depth of water. The resulting natural fundamental period is 2.1 min. The Make-Up Pond B average depth is 33.05 ft. The resulting natural fundamental period is 6.5 min. The wave periods determined above (1.8 sec. and 2.6 sec.) are much shorter than the natural fundamental period for both water bodies (2.1 min. and 6.5 min.). Furthermore, natural fundamental periods are significantly shorter than meteorologically induced wave periods (e.g., synoptic storm pattern frequency and dramatic reversals in steady wind direction necessary for wind setup). Since the natural periods of Make-Up Pond A and Make-Up Pond B are significantly different than the period of the

excitations, they are not susceptible to meteorologically induced seiche waves. Seismically induced waves are discussed in Subsection 2.4.6.

Make-Up Pond C

The Make-Up Pond C reservoir is located on a tributary of the Broad River, west of the Lee Nuclear Station, as shown in Figure 2.4.1-213, such that a postulated failure of the Make-Up Pond C dam would release water to the Broad River prior to reaching the Lee Nuclear Station. Failure of the Make-Up Pond C dam coincident with the PMF for the Make-Up Pond C watershed is discussed in Subsection 2.4.4.1. Flooding effects as a result of dam failure due to surge and seiche are bounded by that discussion.

WLS COL 2.4-2

2.4.6 PROBABLE MAXIMUM TSUNAMI

Tsunamis affecting the Atlantic Coast have not been extensively studied due to the lack of significant trigger mechanisms. No specific tsunami hazard maps are available for the East Coast of the United States. The U.S. Army Corps of Engineers has developed a general tsunami risk map (Figure 2.4.6-201) (Reference 281). The East Coast is located in Zone 1, which corresponds to a wave height of 5 ft.

According to the National Oceanic & Atmospheric Administration (NOAA) tsunami database (Reference 228), the maximum recorded tsunami wave height along the East Coast is about 20 ft. This was recorded at Daytona Beach, Florida, on July 3, 1992. The database notes that the wave was probably meteorologically induced.

The Lee Nuclear Station is located approximately 175 mi. inland from the Atlantic Coast. The safety-related plant elevation is 590 ft. Based on data provided above, and site location and elevation characteristics, the station’s safety-related facilities are not considered at risk from tsunami flooding.

Significant landslide generated waves triggered by hill slope failure are not plausible for the on-site Ponds A and B. No irregular weathering conditions or natural landslide hazards are noted in field investigations, as discussed in Subsection 2.5.1.1. There is no documented evidence that landslides of sufficient magnitude (e.g., size and velocity) at the site or adjacent to the ponds would occur. Potential slope failures that could occur would be of limited size and characterized as shallow soil or fill 'popouts'. Landslides of this type are considered minor, contain an insufficient volume of material, and are of low velocity so that potential landslide-induced waves would be insignificant.

Slopes surrounding Make-up Ponds A and B are either natural slopes that have existed for a long period of time (through most or all of the Holocene; natural slopes), or cut and fill slopes developed as part of the Cherokee Nuclear Station construction in the early 1980's. These slopes exhibit acceptable stability without visual evidence of groundwater seepage, past failure, incipient movement, or major creep, as discussed in Subsection 2.5.5.1.

Seismic induced waves resulting from surface fault rupture are also not plausible. As discussed in Subsection 2.5.3, there are no capable tectonic sources within the Lee Nuclear Site vicinity (25 mi. radius), and there is negligible potential for tectonic fault rupture at the site and within the site vicinity. Any seismic event that could occur would generate potential waves that would be insignificant compared to the available freeboard of the on-site make-up ponds.

As shown in Figure 2.4.1-209, Make-Up Pond A and Make-Up Pond B have normal pool elevations of 547 ft. msl and 570 ft. msl, respectively. Safety-related facilities are located at an elevation of 590 ft. Therefore, Make-Up Pond A has an available freeboard of 43 ft. and Make-Up Pond B has an available freeboard 20 ft. The geology and seismology and geotechnical engineering characteristics of the Lee Nuclear Station are presented in Section 2.5.

Make-Up Pond C

The Make-Up Pond C reservoir is located on a tributary of the Broad River, west of the Lee Nuclear Station, as shown in Figure 2.4.1-213, such that a postulated failure of the Make-Up Pond C dam would release water to the Broad River prior to reaching the Lee Nuclear Station. Failure of the Make-Up Pond C dam coincident with the PMF for the Make-Up Pond C watershed is discussed in Subsection 2.4.4.1. Flooding effects as a result of dam failure due to seismic- or landslide-induced waves are bounded by that discussion.

2.4.7 ICE EFFECTS

WLS COL 2.4-2 There are 10 U.S. Geological Survey (USGS) gauging stations, located upstream of the Lee Nuclear Site on the Broad River and its tributaries, that recorded water temperatures for different periods between 1962 and 1981 (Reference 290). Figure 2.4.2-201 identifies the location of area gauges. The lowest recorded water temperatures during winter periods range from 32°F to 48.2°F. The lowest was recorded on the Broad River near Earl, North Carolina (USGS No. 02152622), located about 14 river mi. upstream of the site. The lowest was also recorded on Buffalo Creek near Grover, North Carolina (USGS No. 02153456), located about 14 river mi. upstream of the site.

The USGS gauging station on the Broad River east of Gaffney (USGS No. 02153500), located about 5 river mi. upstream of the site at the U.S. Highway 29 bridge crossing, is most representative of water temperatures near the site. The gauge recorded water temperatures from 1969 to 1973. The lowest recorded water temperature was 41.9°F. The recordings are summarized in Table 2.4.7-201. The longest record from a gauge near the site is located about 40 river mi. downstream of the site on the Broad River near Carlisle, South Carolina (USGS No. 02156500). The gauge recorded water temperatures from 1962 to 1975. The lowest recorded water temperature near Carlisle was 38.3°F.

According to the EPA STORET database (Reference 284), four stations located on the Broad River near the site recorded water temperatures between 1959 and

2004. The lowest water temperature recorded was 35.6°F near Gaffney, South Carolina (Station B-042). This gauge is located about 8 river mi. upstream of the site. A second station also recorded a water temperature of 35.6°F (Station B-044). This station is located about 9 river mi. downstream from the site.

The North Carolina Department of Environmental and Natural Resources collected temperature data from 1995 to 2000 at nine gauging stations in North Carolina on the Broad River and its tributaries (Reference 231). Minimum temperatures vary from 33.8°F to 39.2°F. The nine gauging stations are in the vicinity of 10 USGS gauging stations discussed above. The resulting minimum temperatures are also within the range measured by USGS gauges. Historical and more recent measurements consistently indicate that Broad River water temperatures remain above freezing.

According to the U.S. Army Corps of Engineers (Reference 275), ice jams occur in 36 states, primarily in the northern tier of the United States (Figure 2.4.7-201). Neither South Carolina nor North Carolina is included in this coverage. The U.S. Army Corps of Engineers Cold Regions Research and Engineering Laboratory historical ice jam database was consulted for the Broad River (Reference 274). There are no recorded ice jams for the Broad River. A query for ice jams in South Carolina also yielded no historical occurrence of an ice jam. However, one ice jam was recorded in North Carolina on the Neuse River at Kinston from January 26 to January 29, 1940. The maximum stage of the Neuse River resulting from the ice jam was well below flood stage. Kinston is located about 220 mi. east of the site. There are no known documented ice sheet or ice ridge occurrences on the Broad River.

The Lee Nuclear Station's safety-related plant elevation is 590 ft. The normal maximum water surface elevation for the Broad River adjacent to the Lee Nuclear Station is 511.1 ft., due to operation of the Ninety-Nine Islands Dam and hydropower plant (Reference 217). The maximum water surface elevation during a probable maximum flood event is more than 40 ft. below the site (Subsection 2.4.3). The possibility of inundating the site due to an ice jam is remote.

According to the U.S. Army Corps of Engineers, frazil ice forms in supercooled, turbulent water in rivers and lakes (Reference 275). Anchor ice is defined as frazil ice attached to the river bottom, irrespective of the nature of its formation. Although the potential for freezing (i.e., frazil or anchor ice) and subsequent ice jams on the Broad River is remote, the numerous pond and lake features adjacent to the site may be susceptible to some degree of freezing. However, there are no safety-related water storage bodies. Additionally, sustained periods of subfreezing water temperatures are not characteristic of the region. The climate and operation of Ninety-Nine Islands Reservoir prevent any significant icing on the Broad River. There are no safety-related facilities that could be affected by ice-induced low flow of the Broad River or reduction in capacity of water storage facilities.

2.4.8 COOLING WATER CANALS AND RESERVOIRS

WLS COL 2.4-3 There are no current or proposed safety-related cooling water canals or reservoirs required for the Lee Nuclear Station. The atmosphere provides the ultimate heat sink (UHS) with the containment vessel and passive containment cooling system (PCS) providing the heat transfer mechanism. Additional details are provided in Subsection 2.4.11.

2.4.9 CHANNEL DIVERSIONS

WLS COL 2.4-3 There is no evidence to suggest historical diversions or realignments of the Broad River. Several shoals are located in the Broad River near the Lee Nuclear Site. However, these features are confined within the natural banks of the river. The topography does not suggest potential diversions or landslides. The streams and rivers in the region are characterized by traditional shaped valleys with no steep, unstable side slopes that could contribute to landslide cutoffs or diversions. There is no evidence of ice-induced channel diversion.

Several instream dams are located upstream and downstream of the Lee Nuclear Station (References 217 and 276). Cherokee Falls Dam was completed in 1826. Gaston Shoals Dam was completed in 1908. Both are located immediately upstream of the site and are run-of-river hydroelectric power plants. Ninety-Nine Islands Dam, completed in 1910, is located immediately downstream and is also a run-of-river hydroelectric power plant.

The greatest potential for geothermal energy exists in areas of above average heat flow, generally the result of recent volcanic activity or active tectonics. The eastern United States has below average to average geothermal heat flow and is characterized as low temperature (Reference 251). The eastern United States is relatively tectonically stable (Reference 252). No thermal anomalies in the eastern United States are attributed to young-to-contemporary volcanic or other igneous activity (Reference 291). Therefore, channel diversion because of geothermal activity is not expected.

The atmosphere provides the UHS with the containment vessel and PCS providing the heat transfer mechanism. The UHS does not directly rely on the Broad River intake. Therefore, channel diversion cannot adversely affect safety-related structures or systems. Additional details are provided in Subsection 2.4.11. Geologic and seismic characteristics of the region are discussed in Section 2.5.

2.4.10 FLOODING PROTECTION REQUIREMENTS

All safety-related facilities are located at an elevation above the maximum flood levels resulting from all types of flooding as described in Subsection 2.4.2. The
WLS COL 2.4-2 critical flooding event is identified in Subsection 2.4.2 and discussed in detail in Subsection 2.4.3. Based on the design information provided above, flood

protection measures and emergency procedures to address flood protection are not required.

2.4.11 LOW WATER CONSIDERATIONS

2.4.11.1 Low Flow in Rivers and Streams

WLS SUP 2.4.11-1 The headwaters of the Broad River and its major tributaries originate in the higher elevations of the Appalachian Mountains of North Carolina before descending into the foothills and Piedmont region of North Carolina (Reference 231). The Broad River continues its course though the gently rolling hills and narrow stream valleys of the Piedmont region in South Carolina (Reference 259). The Lee Nuclear Station is located on this section of the river, just upstream of Ninety-Nine Islands Dam.

The Upper Broad River drainage basin above the Ninety-Nine Islands Dam derives water from several smaller tributaries that contain a considerable number of dams. According to the U.S. Army Corps of Engineers National Inventory of Dams, there are approximately 132 upstream dams of which five dams have been breached (Reference 276). Therefore, the water volume available during low-flow conditions on the Broad River is a function of natural flow in contributing rivers and streams, available storage capacity of upstream reservoirs, and regulated discharge flow from upstream dams.

Dam failure could affect normal operation during low-flow conditions. Failure of Ninety-Nine Islands Dam would drain the associated reservoir. In this portion of the Broad River, flow would resemble a function of natural flow. However, there are no safety-related facilities that could be affected by low-flow or drought conditions, since the passive cooling system does not rely on the Broad River as a source of water. If necessary, the make-up ponds can be used to supplement natural flow to support continued operations for additional periods of time. Non-safety related water supply during drought is addressed in Subsection 2.4.11.5.

2.4.11.2 Low Water Resulting from Surges, Seiches, or Tsunami

There are no safety-related facilities that could be affected by low water. The site is not at risk to low water resulting from surge, seiche, or tsunami effects, due to the inland location on a run-of-river reservoir with limited storage capacity. See Subsection 2.4.5 and 2.4.6 for additional details.

Flooding due to ice jams has not been recorded at the site. It is unlikely that an ice jam would occur based on the historical water temperatures of the Broad River. Therefore, low flow due to or exaggerated by ice effects is not expected to occur at the site. See Subsection 2.4.7 for additional details.

2.4.11.3 Historical Low Water

Low-flow conditions at the site were analyzed based on stream flow records at USGS gauging stations on the Broad River (Reference 290). Low-flow conditions typically exist during the months of July through November. The six largest reservoirs in the basin, Lake Lure, Lake Summit, Lake Adger, Kings Mountain Reservoir, Lake Whelchel, and Make-Up Pond C represent about 88 percent of the total storage capacity for the basin. Two additional dams, Cherokee Falls and Gaston Shoals, immediately upstream from the Lee Nuclear Site, possess less than 2 percent of the total storage capacity for the basin.

The Gaston Shoals Dam has affected the drainage basin upstream of the site since 1908. Ninety-Nine Islands Dam downstream of the site was completed in 1910. Cherokee Falls Dam, located upstream of the site between Gaston Shoals Dam and Ninety-Nine Islands Dam, was completed in 1826.

Gaston Shoals Dam is part of a hydropower facility owned and operated by Duke Energy. The facility is regulated by the Federal Energy Regulatory Commission (FERC). During the months of July through November, license requirements maintain a release of at least 434 cfs or the natural flow in the Broad River, whichever is less. Should natural flow in the Broad River become less than 434 cfs, the FERC license provides measures for flow to be stored and released on an hourly basis (Reference 222).

Cherokee Falls Dam is part of a hydropower facility owned and operated by the Broad River Electric Cooperative. However, the hydroelectric facility at Cherokee Falls Dam is not currently operating. The dam is essentially a run-of-river facility with spillway flow at high-flow conditions and low-level outlets to provide constant flow under low-flow conditions (Reference 204).

The Ninety-Nine Islands Dam is part of a hydropower facility owned and operated by Duke Energy. The facility is regulated by the FERC. During the months of July through November, license requirements maintain a release of at least 483 cfs or the natural flow in the Broad River, whichever is less. Should natural flow in the Broad River become less than 483 cfs, the FERC license provides measures for the reservoir to be drawn down, at most 2 ft. below the full pool elevation of 511.1 ft., depending on the time of year. Release of accumulated flow is then made on an hourly basis (Reference 223).

There is a USGS gauging station (USGS No. 02153551) located about 2 river mi. downstream from the site in the tailrace below Ninety-Nine Islands Dam. The drainage area associated with this gauge is 1550 sq. mi. This is essentially the same drainage basin for the Broad River adjacent to the site. The annual minimum daily flows for the period of record (1998 to 2006) are presented in Table 2.4.11-201. The minimum flow observed during the period of record is 138 cfs on September 14, 2002. While these data are insufficient to determine the frequency of low-flow occurrences or to determine the lowest recorded flow, they are instructive in that this flow occurred during a period of severe drought. The flow gauge is located downstream of the Ninety-Nine Islands dam and does not

measure the flow passing in front of the plant intake, although it is representative of river conditions.

The USGS gauging station (USGS No. 02153500), located about 5 river mi. upstream from the site on the Broad River near Gaffney, South Carolina, has a drainage area of 1490 sq. mi. This gauge is located downstream from Gaston Shoals Dam and upstream from Cherokee Falls Dam. The annual minimum daily flows for the period of record (1938 to 1990) are presented in Table 2.4.11-202. The gauge was discontinued in 1990 by the USGS. The minimum flow observed during the period of record is 224 cfs on October 24, 1954.

Low-flow frequency analysis was performed in accordance with USGS Bulletin 17B using the Log-Pearson Type III distribution method (Reference 253, Reference 270, and Reference 287). Due to the importance of the more recent drought years, not included in the period of record for the Gaffney gauge, the Ninety-Nine Islands gauge data were combined with the Gaffney gauge data to determine low-flow frequencies. The results provide more conservative flow estimates than if only the Gaffney gauge had been used in the analysis.

Table 2.4.11-203 provides 100-yr. drought flow rates at different durations. The 30-day 100-yr. drought flow rate is 346 cfs. A 100-yr. return period is defined as a 1 percent chance the event will occur during any one year. Therefore, the 30-day 100-yr. drought flow rate has a 1 percent chance each year that the flow rate or less will occur for at least 30 consecutive days.

Historical flow data at Gaffney, South Carolina (USGS No. 02153500) indicate that 30-day 100-yr. drought flow rates or less have been achieved on 12 days from 1938 to 1990. Historical flow data from the gauging station just below Ninety-Nine Islands Dam (USGS No. 02153551) indicate that 30-day 100-yr. drought flow rates or less have been achieved 79 days from 1998 to 2002. During this time, there were 26 consecutive days with less than 30-day 100-yr. drought flow rates. Additionally, there were 54 days of 30-day 100-yr. drought flows concentrated over a 61-day period.

Since 1900, according to the South Carolina Department of Health and Environmental Control, severe droughts have occurred statewide in 1925, 1933, 1954, 1977, 1983, 1986, 1990, 1993, and 1998 (Reference 267). USGS reports indicate more recent droughts occurred from 1998 to 2002 in areas of North Carolina belonging to the headwaters of the Broad River and in South Carolina (Reference 294). Most of the drainage area for the Broad River adjacent to the site is in North Carolina. The Gaffney gauge period of record includes the 1954, 1977, 1983, 1986 and 1990 drought years, while the gauge at Ninety-Nine Islands Dam includes the more recent years. Mid-to-late 2007 weather pattens indicate a potential for Broad River flows to drop to levels characteristic of drought conditions. While 2007 data are continuing to be collected, an analysis of these data was not available in time to be included with the application. An analysis will be conducted upon termination of current drought conditions and provided to the NRC.

The normal full pool elevation of the Ninety-Nine Islands reservoir is 511.1 ft. (Reference 217). Provisions are made to draw the reservoir down by at most 2 ft. below normal full pool during periods of low flow. Due to maintenance operations, the pool has dropped below the 2 ft. drawdown limit for short periods. The following historical lows were due to maintenance. According to USGS water year reports, the historical minimum pool elevation was 508.2 ft. on February 14, 2005 (Reference 208). The water year reports have a period of record from October 1998 to the present. Additional historical data from 1964 to 1973 indicate the minimum pool elevation was about 505.7 ft. during May 1965.

The U.S. Army Corps of Engineers historical database of ice jams on the Broad River was reviewed (Reference 274). See Subsection 2.4.7 for additional discussion. Ice effects are not a concern for low water considerations, due to the climate and reservoir operations.

2.4.11.4 Future Controls

The majority of the Broad River drainage basin upstream of the site is in North Carolina. According to the North Carolina State Water Supply Plan, public supply water use in the Broad River watershed is projected to increase by about 56 percent from 2000 to 2020 (Reference 233). This includes both surface water and groundwater use. Available supply is noted as the withdrawal capacity in Table 2.4.1-209.

According to the North Carolina Local Water Supply Plans, none of the upstream surface water public supply systems require more than 80 percent of their maximum use rate before 2030. Of the five surface water public supply systems, only the Cleveland County Sanitary District indicated exceeding 80 percent of their maximum use rate before 2050. Demand is expected to increase 238 percent by 2050, for a total demand of 28.6 million gpd.

According to the Federal Register, a Notice of Intent was filed on July 11, 2006 for a Draft Environmental Impact Statement (DEIS) to be prepared for a proposed reservoir on the First Broad River in Cleveland County, North Carolina (Reference 226). The Cleveland County Sanitary District applied for a permit to construct a water supply reservoir with a surface area of approximately 2245 ac., about 1 mi. north of Lawndale, North Carolina. The DEIS is currently in preparation. Lawndale is about 26 miles north of the Lee Nuclear site.

The USGS maintained a gauge (USGS No. 02152500) about 2.5 mi. southeast of Lawndale on the First Broad River from 1940 to 1971. During this period, the average monthly flow at Lawndale represented about 11 percent of the flow in the Broad River at Gaffney. The drainage area at the Lawndale gauge is 200 sq. mi., or roughly 13 percent of the drainage area at the USGS gauge near Gaffney.

Duke Energy is planning to expand the Cliffside Steam Station by as early as 2010. The incremental additional consumptive use withdrawal from the Broad River upstream from the station is estimated to be 17 cfs. However, four of the five existing units at Cliffside will be retired. Additional intake sources not represented by the USGS stream gauges include an expansion of the Shelby, North Carolina,

water system. Shelby has constructed an intake on the Broad River, and it may withdraw up to 10 million gpd on a temporary emergency basis (Reference 207).

The North Carolina General Statutes require registration for interbasin transfers of 100,000 gpd or more (Reference 249). The North Carolina Division of Water Resources does not require a transfer certificate unless the transfer is 2 million gpd or more. Total known interbasin transfers include about 1.47 million gpd out of the basin and about 0.15 million gpd into the basin (Reference 230). North Carolina also requires registration of withdrawals of 100,000 gpd or more.

State regulations for South Carolina currently require registration of withdrawals of surface water in excess of 3,000,000 gallons per month (Reference 258). This is essentially 100,000 gpd. The construction of the embayment and intake structure requires coordination with the U.S. Army Corps of Engineers. The design and placement of the embayment and intake structure are done in accordance with the appropriate federal and state regulations. There are no safety-related facilities that could be adversely affected by any increase in water use or drought conditions.

2.4.11.5 Plant Requirements

WLS COL 2.4-3

Raw water needs, including makeup to the normal heat sink cooling towers, are supplied by the intake as described in Subsection 2.4.1.1.4. The intake structure includes necessary intake screens, pumps, etc. to convey the river water to Make-Up Pond A. Use of raw water from Make-Up Pond A is described in Subsection 2.4.1.1.4. Intake screen locations consider the Broad River minimum level. There are no safety-related plant requirements provided by the Broad River.

WLS SUP 2.4.11-2

The normal river intake flow rate for the station is approximately 35,000 gpm. The maximum expected river intake flow is approximately 60,000 gpm. Institutional restraints on water use are imposed by Federal and State agencies as discussed. Title 40 Code of Federal Regulations Part 125 Section 84 requires that for cooling water intake structures located in a freshwater river or stream, the total design intake flow must be no greater than five percent of the source water annual mean flow. Water use and annual mean flow are discussed in Subsection 2.4.1.2.5.1 and Subsection 2.4.1.2.2.2. The South Carolina Code of Laws Title 49 Chapter 23 Part 40 identifies that during a drought declaration, the use of water from a managed watershed impoundment shall not be restricted as long as minimum streamflow or flow equal to the 7Q10 is maintained, whichever is less. Make-Up Pond B and Make-Up Pond C are expected to be used to supplement flow during periods of low flow.

The 7Q10 for the Gaffney gauge was determined to be 439 cfs using the USGS recommended Log-Pearson Type III distribution. However, because the 7Q10 is less than the Ninety-Nine Islands Dam FERC license minimum flow requirement of 483 cfs for July through November (Subsection 2.4.11.3), the FERC license

minimum flow was used as a constraint in evaluating operation during low flow conditions. Furthermore, FERC license minimum flow requirements are more restrictive than the 100-year drought flow rates described in Subsection 2.4.11.3 and Table 2.4.11-203. Therefore, the following low flow analysis applies to the discussion of nonsafety related water supply during a 100-year drought.

A low flow analysis was performed based on the FERC licensed 483 cfs minimum flow requirements at Ninety-Nine Islands Dam and the Lee Nuclear Station consumptive use requirements. Consumptive use is estimated to be approximately 55 cfs. When flows in the Broad River drop below 538 cfs, combined FERC licensed 483 cfs minimum flow plus 55 cfs consumptive use, makeup water to the station is supplemented by on-site water storage, Make-Up Pond B and off-site Make-Up Pond C. When flows in the Broad River drop below 483 cfs, the station relies only on Make-Up Pond B and Make-Up Pond C storage for consumptive uses of the station.

Detailed bathymetry mapping of the on-site Make-Up Pond B (Figure 2.4.1-209 Sheet 2) and Make-Up Pond A (Figure 2.4.1-209 Sheet 3) was performed in September 2006. Make-Up Pond A is designed for a normal full pond elevation of 547 ft. Based on current topography Make-Up Pond A retains a volume of 1425 ac.-ft. The usable storage is approximately 1200 ac.-ft.

Make-Up Pond B is designed for a normal full pond elevation of 570 ft. Based on current topography, Make-Up Pond B retains a volume of approximately 4000 ac.-ft. The usable storage is approximately 3200 ac.-ft.

Make-Up Pond C is designed for a normal full pond elevation of 650 ft. Based on the bathymetry shown in Figure 2.4.1-213, Make-Up Pond C retains a volume of approximately 22,000 ac.-ft. The usable off-site storage capacity is approximately 17,500 ac.-ft. The total usable storage capacity of Make-Up Pond B and Make-Up Pond C is approximately 20,700 ac.-ft. Make-Up Pond C has sufficient capacity to support full power operation for approximately 160 days. Make-Up Pond B has sufficient capacity to support full power operations for approximately 30 days.

There are no safety-related water requirements for normal plant shutdown associated with the AP1000. Make-Up Pond A nominally provides for approximately 1200 ac.-ft. of usable water storage. Make-Up Pond A has sufficient capacity to conduct a normal plant shutdown and to maintain shutdown conditions for both units. Make-Up Pond A can be replenished with water from the Broad River, from Make-Up Pond B, and from Make-Up Pond C via Make-Up Pond B.

The circulating water system for the station is a closed-cycle type system coupled with mechanical draft, wet cooling towers. For each unit the circulating water system flow rate is estimated at 560,050 gpm (Subsection 10.4.5). Figure 10.4-201 presents the circulating water system. Make-Up Ponds A and B are used to supplement flow during periods of low flow. Emergency cooling is discussed in Subsection 2.4.11.6.

Effluent from the new facility discharges into the river at the upstream face of the Ninety-Nine Islands Dam near the intakes for the hydroelectric generating units. This configuration ensures no recirculation to the embayment area and intake screens of the new facility.

2.4.11.6 Heat Sink Dependability Requirements

The atmosphere is the ultimate heat sink (UHS). A continuous natural circulation flow of air removes heat from the containment vessel. The steel containment vessel and passive containment cooling system (PCS) provides the heat transfer mechanism, as described in Section 6.2. A separate gravity-drained, passive containment cooling water storage tank provides containment wetting. The PCS is not reliant on the source of water from the river intake. Makeup to the passive containment cooling water storage tank is provided by demineralized water from the passive containment cooling ancillary water storage tank. Therefore, no warning of impending low flow from the river water makeup system is required. Low river water conditions would not affect the ability of the emergency cooling water systems and the UHS to provide the required cooling for emergency conditions.

The passive containment cooling water storage tank has a volume capacity for 72 hours of containment wetting. The passive containment cooling ancillary water storage tank has a volume capacity to maintain containment wetting for an additional 4 days. Makeup for long-term containment wetting can be supplied to the PCS by Make-Up Pond A or alternate external resources, through multiple system paths. Site-related events and natural phenomena would not affect the atmosphere functioning as the UHS. As described in Subsection 2.4.3, the station is capable of withstanding the PMF. Seismic design is addressed in Section 3.7.

2.4.12 GROUNDWATER

WLS COL 2.4-4

2.4.12.1 Description and On-Site Use

2.4.12.1.1 Regional Aquifers, Formations, Sources, and Sinks

The Lee Nuclear Site is located within the Piedmont physiographic province, a southwest-northeast-oriented province of the Appalachian Mountain System (Figure 2.4.1-203). The Piedmont province is 80 – 120 mile (mi.) wide and situated between the Blue Ridge province, a mountainous region to the northwest, and the Atlantic Coastal Plain province to the southeast. The majority of rocks in the Piedmont are medium-to high-grade metamorphic rocks. These rocks are generally stratified and compositionally layered with distinct foliation. In addition, lineaments and fault systems are common in the region, and several major thrust sheets are present in the basin. Numerous granitic plutons and stocks have intruded older metamorphic rocks, and are often marked by areas of higher topography; a result of the massive, resistant nature of these intrusive rocks. The Lee Nuclear Site is located within the Kings Mountain Belt of the Piedmont province, which contains a complex series of deformed rocks consisting of felsic

and mafic schists and gneisses, quartzites, conglomerates, and marble, generally considered to be of Precambrian and early Paleozoic age (Subsection 2.5.1).

Throughout the Piedmont region, bedrock is overlain by a mantle of unconsolidated material known as regolith. The regolith includes, where present, the soil zone, a zone of weathered and decomposed bedrock known as saprolite, and alluvium. Saprolite, the product of chemical and mechanical weathering of underlying bedrock, is typically composed of clay and coarser granular material that may reflect the texture of the rock from which it was formed. Typically, the formation of soils is attributed to the in-place weathering of the underlying rock and the deposition of material transported by water and laid down as clay, silt, sand, or large rock fragments (Reference 285). Crystalline rocks are commonly weathered in the Piedmont region because of the warm, humid conditions. Iron oxide-stained kaolinite and other aluminosilicate clay minerals are the dominant constituents of upland soils in many areas. Modern fluvial sediments generally occupy only the active beds and small floodplains of local streams and rivers.

The Piedmont aquifer system is basically a two layered slope-aquifer system (Figure 2.4.1-210). The shallow water table aquifer is composed of the saprolite and residual soil, which is typically low yielding. The shallow water table aquifer is unconfined, meaning that the upper surface of the saturated zone is not effectively separated from the ground surface by a low-permeability clay layer. The underlying bedrock aquifer consists of weathered and unweathered crystalline igneous and metamorphic rocks that store and transmit water through fractures. The fracture system in the bedrock is a network of discontinuities that increase in prevalence upward through the crystalline rock as it transitions into saprolite. Because of the permeability of the transition zone, the bedrock aquifer is also considered unconfined and not effectively isolated. Thus, the saprolite and bedrock zones function as one interconnected aquifer system (Reference 266). While confined settings can occur in fracture bedrock, none were indicated in this study. The rocks typically yield small amounts of water to domestic users, small cities, and low-water-demanding industries.

Groundwater occurs almost everywhere throughout the Piedmont province; however, it is not a single, widespread aquifer. Groundwater occurs in various local aquifer systems and compartments that have similar characteristics and are hydraulically connected. Groundwater recharge in this area is derived from infiltration by local precipitation or infiltration from nearby surface water. Additionally, with the construction of the on-site impoundments, recharge also occurs from these surface waters.

The on-site impoundments consist of Make-Up Pond B, Make-Up Pond A, and Hold-Up Pond A. Details of these impoundments are discussed in Subsection 2.4.1.2.2.6. Surface water in these impoundments is in direct communication with groundwater and the water levels represent the water table.

The water table varies from ground surface elevation in valleys to more than 100 ft. below the surface on sharply rising hills. The groundwater levels in the Piedmont typically decline during the late spring and summer due to

evapotranspiration and rise in the late fall and winter when the evaporation potential is reduced (Reference 297).

The fractures, relic rock textures, and directional differences in permeability or ease of groundwater movement may significantly affect the direction of local groundwater flow. Recharging of the groundwater in the Piedmont is by the addition of precipitation water, first to the shallow soil/saprolite aquifer (referred to as the water table aquifer in the regional discussion) and then to the uppermost fracture zone (transition zone). Recharge mostly occurs on upland topographic highs or at least above the slopes of stream valleys. Water does not generally move to great depths, but it is directed almost laterally by reduced permeabilities of crystalline rock with lower fracture density.

Cross-sections of the Lee Nuclear Site are presented in Figure 2.4.12-205, Sheets 1 to 4, and depict the relationship between groundwater beneath the site and the surface water bodies surrounding the site.

2.4.12.1.2 Local Aquifers, Formations, Sources, and Sinks

The Lee Nuclear Site overlies rocks of the Battleground Formation with the exception of later diabase dikes (Figures 2.5.1-218a, 2.5.1-219a, and 2.5.1-220). The Battleground Formation comprises rocks primarily felsic to intermediate in composition (dacite to andesite protoliths), volcaniclastic sequences with intrusions of similar composition (meta granodiorite to metatonalite, metadiorite, and meta gabbro), and interfingered, marine-influenced metasedimentary sequences. Petrographic examination of thin sections obtained from the Lee Nuclear Station site revealed the following rock types: Mica Schist, Meta Quartz Diorite, Meta Dacite Porphyry, and Meta Basalt (Section 2.5). Geologic maps show the distribution of rock types, which tend to have locally erratic outcrop and subsurface distribution patterns, but regionally trend northeast to southwest.

Subsurface investigations performed at the Lee Nuclear Site in 1973 for the former Cherokee Nuclear Station and in March 2006 reveal that geologic and hydrologic conditions at the Lee Nuclear Site are similar to the regional conditions described above in Subsection 2.4.12.1.1. The first occurrence of groundwater beneath the Lee Nuclear Site is within the surficial hydrogeologic unit. The groundwater flows under unconfined conditions in the surficial hydrogeologic unit, which is generally composed of three different media beneath the site: (1) fill material placed in valley lows during site grading using on-site borrow materials, (2) the soil and saprolite zone that overlies the bedrock, and (3) partially weathered rock. The shallow groundwater beneath the site is mostly affected by the excavated area and the current dewatering activities (effects of the dewatering are discussed in Subsection 2.4.12.2).

WLS COL 2.4-4

2.4.12.2 Sources

The AP1000 reactor design has no safety-related heat sink that relies on groundwater supplies. The Lee Nuclear Site is not expected to use groundwater as a source of water for any purpose. Additional information related to local and on-site groundwater use is presented in Subsection 2.4.1.2.5.2.

2.4.12.2.1 Regional and Local Groundwater Uses

Groundwater supplies in the Piedmont physiographic province of South Carolina occur in three types of hydrogeologic environments. These are the unweathered and fractured crystalline rocks, overlying saprolite and residuum, and to a lesser extent, alluvial valley-fill deposits. Most public water supply wells are completed in fractured igneous and metamorphic rocks, often referred to as “crystalline bedrock,” while some private wells are simply dug or bored into the overlying saprolite. Yields of 4 – 170 gpm have been recorded from 30 South Carolina ambient groundwater quality network wells in the Piedmont bedrock (Reference 257). Regional groundwater studies consulted during the Cherokee Nuclear Station site investigation indicated that most domestic wells are not drilled to develop maximum yield, are generally less than 150 ft. deep, and have flow rates ranging from 3 to 150 gpm with a median flow rate of 7 gpm (Reference 214).

According to South Carolina Department of Health and Environmental Control (SCDHEC) water-use data for 2005, 1.02 million gallons (gal.) of groundwater were used for thermoelectric power generation in Cherokee County. No groundwater use in Cherokee County for domestic self-supplied systems, aquaculture, golf courses, industry, irrigation, livestock, mining, or hydroelectric power was reported in the 2005 SCDHEC data (Reference 267). According to a private well report from SCDHEC, based on data from January 1985 to June 2006, the number of domestic wells completed in Cherokee County was 1076 (Reference 261). The USGS and state water-use data were reviewed, and groundwater withdrawals for counties located in the Upper Broad River watershed are presented in Table 2.4.1-208. Groundwater withdrawals for Cherokee and surrounding counties in South Carolina (Table 2.4.1-207) account for only 4.7 million gal. per day (Mgd), and the majority (85 percent) of that volume is pumped from Spartanburg County, outside the watershed for the Lee Nuclear Site.

Local groundwater use in the vicinity of Lee Nuclear Station is predominantly from domestic wells, and is described in Subsection 2.4.1.2.5.2.

2.4.12.2.2 Historical On-Site Conditions

Site hydrologic data were gathered prior to construction activities (through the early 1970s) and during the construction activities (late 1970s to the early 1980s). Surface and groundwater conditions at the Lee Nuclear Site have changed because of the excavation and site grading conducted as part of the construction activities for the former Cherokee Nuclear Station. No significant changes to the Lee Nuclear site have occurred since those construction activities.

Prior to the construction activities for the Cherokee Nuclear Station, a subsurface investigation was conducted, and water level measurements were obtained to develop an understanding of the groundwater setting. A groundwater table elevation map was developed to represent site conditions at that time and is presented in Figure 2.4.12-201. Initial potentiometric surface data collected from July, August, and September 1973 indicated site-specific groundwater flow

Withheld from Public Disclosure Under 10 CFR 2.390(a)(9)
(see COL Application Part 9)

directions were primarily toward the north and east from the reactor area, which generally mimicked the preconstruction site topography. A north-south-trending groundwater divide was apparent west of the reactor area and east of the Nuclear Service Water Reservoir, now known as Make-Up Pond B.

According to the former Cherokee Nuclear site groundwater investigation, measured depths to groundwater beneath ridges ranged from about 40 to 80 ft. below ground surface. The groundwater table was reportedly at or near the surface in valleys and draws, as was evidenced by observed springs. Near the proposed locations of the reactor buildings, the groundwater table varied between depths of 10 – 60 ft. below ground surface with potentiometric surface elevations ranging from 570 to around 605 ft. above msl (Reference 220).

Construction activities for the Cherokee Nuclear Station began in the late 1970s, resulting in significant alterations to on-site topography. Because of the relationship between topography and depth to water, changes to the potentiometric surface were monitored with a network of observation wells across the site. A review of historical data identified groundwater levels in observation wells prior to and during the construction. Based on water level data, construction dewatering from the site excavation was indicated around January 1977. Between November 1977 and March 1978, approximately 5.74 million gal. of water were reportedly pumped from the water table aquifer through dewatering wells over the 5-month period. These wells were pumped at average rates ranging from 38 to 65 gpm with well depths from 200 to 280 ft. below ground surface. The effect of construction dewatering was assessed on the basis of historical groundwater measurements collected across the site and in the nearest residential well during construction dewatering activities. The apparent drawdown in the observation wells, caused by the cumulative dewatering activities, is shown on Figure 2.4.12-202. The dewatering activities did not affect observation wells outside the area shown. In addition, the nearest residential well, the [ ]^{SRI} well, was not affected by construction dewatering activities (References 215 and 218). The [ ]^{SRI} well is completed in the Piedmont Aquifer and is located approximately 5000 ft. south of the center of the excavation on the north side of McKowns Mountain Road. Several wells located adjacent to the excavation, around the site, and at a nearby residence (the [ ]^{SRI} well) were gauged on a monthly basis between 1976 and 1985, providing limited-term historical water level data. Only observation wells nearest the excavation, as shown in Figure 2.4.12-202, appeared to be affected by the Cherokee site dewatering activities.

2.4.12.2.3 Current On-Site Conditions

In March 2006, the current groundwater investigation was initiated as part of the subsurface study to evaluate hydrogeologic conditions for the Lee Nuclear Site. The dewatering of the existing excavation preceded the subsurface investigation, thus returning the site to hydrogeologic conditions similar to those of the previous construction phase. Approximately 740 million gal. of water were removed from

the excavation from December 19, 2005, through September 7, 2006. Following the initial dewatering, an apparent 5-foot thick interval of staining was observed on the existing Cherokee concrete structures, the top of which was surveyed at an elevation of 578.72 ft. msl. Given the range of apparent water table fluctuations as indicated by the concrete staining (574 – 579 ft. msl), the hydrostatic equilibrium elevation for the excavation area was estimated to be the midpoint of the range (576.5 ft. msl). A comparison of the apparent water levels in this impoundment, as shown on the February 1994 and February 2005 aerial photographs, with the topographic survey conducted in 2006 indicated a similar range of water levels in the excavation area (574 ft. msl in 1994 to 579 ft. msl in 2005). Precipitation data for the period preceding these observations indicated near normal conditions, confirming the aerial images captured typical impoundment water levels. Ongoing maintenance dewatering activities are expected to end following construction activities.

As part of the 2006-2007 groundwater investigation, fifteen borings were drilled into the crystalline bedrock, and monitoring wells were installed in partially weathered rock intervals. In July 2006, nine additional monitoring wells were installed to evaluate shallow groundwater conditions across the site. Details regarding well construction are presented in Table 2.4.12-201.

WLS COL 2.4-5 Following well development, water levels were measured monthly from April 2006 to April 2007 (Table 2.4.12-202) to characterize seasonal trends in groundwater levels and to identify flow pathways surrounding the Lee Nuclear Site. The hydrograph for this groundwater data is presented on Figure 2.4.12-203. Surface waters at four locations were also gauged as part of the monitoring program. These locations included Make-Up Pond B, a water retention impoundment below Make-Up Pond B, Make-Up Pond A, and Hold-Up Pond A. Based on this year of study, groundwater levels were observed to fluctuate, with the highest groundwater elevations observed between January and April 2007 and the lowest groundwater elevations between September and November 2006. This trend correlates with both the river flow and rainfall patterns and confirms that both groundwater levels and river flow are governed by local precipitation (Section 2.3).

Potentiometric surface maps developed from water level data showed that during the recent construction dewatering and site investigation, groundwater surrounding the excavation is drawn toward the excavation (Figure 2.4.12-204, Sheets 1 - 7). During the dewatering activities, continuous decline of water levels in areas downgradient of the excavation was observed, as recharge entering the power block area from the south was intercepted by the excavation and discharged to Make-Up Pond B. Following the completion of construction dewatering, the potentiometric surface beneath the reactor buildings is expected to rebound to equilibrium conditions.

Under natural conditions the topography of the water table within the Piedmont mimics the topography of the land surface, but has less relief. Cross-sections of the Lee Nuclear Site are presented in Figure 2.4.12-205, Sheets 1 - 4. These figures depict the relationship between groundwater beneath the site and the surface water bodies surrounding the site. Groundwater flow in the Piedmont

province is typically restricted to the topographic area underlying the slope that extends from a divide to an adjacent stream.

Both regionally and locally, surface topography plays a dominant role in groundwater occurrence. Post-construction topography was observed to affect groundwater conditions such that cuts in topography induce a lowered water table and fill induces a raised water table. Field evidence for this is based on comparison between the Cherokee water table map (Figure 2.4.12-201) and the maps developed from the Lee Nuclear Site investigation (Figure 2.4.12-204, Sheet 1-7). For example, MW-1204, located on the Unit 2 Cooling Tower Pad, is where construction fill was placed during Cherokee construction, resulting in a significantly higher land surface elevation (approximately 610 ft. msl compared to its pre-grading elevation of around 560 ft. msl). Consequently, the water table elevation is higher in MW-1204: groundwater elevation of approximately 570 ft. msl compared with the former groundwater elevation of less than 550 ft. msl. Another example includes MW-1200, located west-northwest of Unit 1, where construction cuts resulted in a significantly lower land surface elevation (approximately 590 ft. msl compared to its pre-grading elevation of approximately 670 ft. msl). Consequently, the water table elevation has lowered (groundwater elevation of 565 ft. msl compared with the former groundwater elevation of more than 585 ft. msl).

Upon returning to post-dewatering conditions, the post-construction water table is expected to mimic land surface, consistent with slope-aquifer conditions of the Piedmont physiographic province. The potentiometric surface beneath Lee Units 1 and 2 is expected to rebound to an elevation near the apparent hydrostatic equilibrium (576.5 ft. msl). This apparent hydrostatic equilibrium is considered conservative since it represents the directly exposed water table in the post-Cherokee open excavation, allowing for recharge of all local precipitation less evaporation. In contrast, post-construction groundwater recharge would be significantly reduced due to impervious and semi-impervious areas (buildings, pavement, compacted road base material, and hardscape), site grading to effect drainage away from the nuclear islands, and installation of stormwater controls and roof drainage systems to further limit infiltration near Lee Units 1 and 2. Placement of impervious/semi-impervious surfaces is also expected to overlie the granular fill surrounding Units 1 and 2 such that infiltration in this area will be limited. Granular fill placement and characteristics are described in Subsection 2.5.4.5.

Seasonal water table fluctuations, as observed at the site, do not exceed 5 to 10 ft. Review of regional groundwater levels indicates that groundwater levels at Lee Nuclear Site are unlikely to fluctuate more than 15 ft. total. Using the more conservative regional seasonal water level fluctuation (±7.5 ft.) as a bounding condition to fluctuate around the apparent hydrostatic equilibrium (576.5 ft. msl), a conservative estimate of the post-construction maximum groundwater elevation in the area of the excavation was established at 584 ft. msl.

The projected post-dewatering water table conditions are illustrated in Figure 2.4.12-204, Sheet 8. The potentiometric conditions shown in Figure 2.4.12-204, Sheet 8 affect the directions of groundwater flow surrounding

the Lee Nuclear Station. Each of the ponds serves as a constant head flow boundary. The crests of the water table indicate groundwater divides within the slope-aquifer system. These features indicate distinct compartments of groundwater flow at the site, with the nuclear site area flowing to the north toward the Broad River, the area west of the north divide flowing toward Make-Up Pond B, and the area east of the south divide flowing toward Make-Up Pond A. Surface water bodies located within the same hydrologic compartment as the Lee Nuclear Station are topographically downgradient such that surface runoff will drain away from the power block area and any interaction between groundwater and surface water would be well below the Lee Nuclear Station plant grade elevation. Ultimately, all groundwater flow discharges to the Broad River, the groundwater sink for the site and the surrounding area.

Based on site observations, a network of storm drains and buried piping was partially installed during the Cherokee project to manage surface water runoff. While no as-built drawings for the existing storm drain system for the former Cherokee Nuclear Station exist, a review of stormwater plans was conducted to assess the drain system's potential effect on groundwater movement. Storm drains located more than 500 ft. upgradient (south) of the power block could potentially intercept the water table and allow shallow groundwater movement towards Make-Up Pond A; these drains do not affect groundwater movement in the power block area. Other storm drains appear to be above the water table and would not affect the movement of groundwater. One exception is a storm drain originally designed to transfer stormwater from the Cherokee power block area to Hold-Up Pond A. The depth of this storm drain pipe appears to be below the projected water table. Therefore, if left in place, this conduit could potentially cause a preferential groundwater pathway from the power block area downgradient to Hold-Up Pond A once groundwater recovers from the construction dewatering activities. The existing storm drain and bedding materials will be removed by overexcavation. The remaining void will then be plugged with low-permeability backfill material, and compacted to density sufficient to assure no short-circuiting can occur.

Stormwater controls at the Lee Nuclear Station include a combination of surface grading to facilitate surface water flow, construction of a stormwater drainage system (DRS), and construction of a roof drain and collection system. The Lee Nuclear Station DRS is designed to facilitate and control the runoff of precipitation along surface water flow paths, diverting surface runoff away from the power block area and reducing the potential for flooding. The site grading and drainage plan is shown in Figure 2.4.2-202. The site is relatively flat; however, the site is graded such that overall runoff will drain away from safety-related structures to Make-Up Pond B, Make-Up Pond A, or directly to the Broad River. Precipitation falling on buildings is captured by a roof drain and collection system, channeled through drainage downspouts, and directed to the DRS. The DRS is not expected to directly affect groundwater flow system of the limiting groundwater flow pathway.

WLS COL 2.4-5

2.4.12.2.4 Aquifer Characteristics

2.4.12.2.4.1 Porosity

Site-specific subsurface materials in the area surrounding the power block include fill, residual soil, saprolite, and partially weathered rock (PWR). Based on the results of the geotechnical investigation, representative engineering properties of the soils were determined according to methods described in Subsection 2.5.4.2. Characterization of porosity and effective porosity were made using the data provided in Table 2.5.4-211.

Fill materials are located in former drainageways, which were built up to existing elevations during Cherokee construction. Based on the specific gravity (particle density, 2.71 grams per cubic centimeter, g/cc) and dry unit weight (101 pounds per cubic foot, pcf) provided for fill material, a mean total porosity of 40 percent was determined. The effective porosity is assumed to be equivalent to specific yield, and was estimated using grain size distribution described within Water Supply Paper 1662-D (Reference 299). This technique indicates effective porosity was estimated to be 9 percent. Fill materials have been cut from other areas of the site, and they are typically comprised of undifferentiated materials (residual soils, saprolite, and/or PWR) similar to native materials.

The residual soils have undergone relatively complete weathering and lack the relict features found in the saprolite zone. Saprolite is the isovolumetrically weathered zone which does not reflect the characteristics of surficial soil development processes, but does reflect some of the physical properties of the underlying parent rock from which it was formed. According to the U.S. Department of Agriculture (USDA) Natural Resources Conservation Service (NRCS), surficial soils in the vicinity of the power block area consisted predominantly of Tatum silty clay loam and Tatum very fine sandy loam with variable slope and erosion (Figure 2.4.12-206). Tatum soils are well-drained (not seasonally saturated) and are typically derived from sericite schist, phyllite, and/or other related metamorphic rocks of the Piedmont. Tatum soils are typically composed of a surficial 0 - 8 in. silty clay loam or very fine sandy loam (CL, CL-ML, ML). These soil horizons grade subsoils of clay, silty clay, and/or silty clay loam (CH, MH). Clay content in the subsoil stratum of Tatum soils ranges from 12 to 60 percent. Tatum soils transition at depths of 45-60 inches to saprolite materials reflecting the characteristics of the underlying parent rock. The saturated hydraulic conductivity of Tatum soils is reported by the NRCS to be moderately permeable: 4 to 14 micrometers per second (μm/s) (4 to 14 x 10^{-4} centimeters per second [cm/s]). Tatum soils are not prone to flooding and exhibit erosion factors (Kf) that range from 0.32 to 0.43. The soils are highly corrosive to both concrete and steel (Reference 278). Based on geotechnical analyses of both the residual soil and saprolite, a mean total porosity of 45 percent was estimated for these materials. The effective porosity was estimated to be approximately 20 percent. The native soils in the immediate area of the power block were essentially completely removed or mixed with deeper saprolite materials to become site fill materials during Cherokee-era activities. Regardless, knowledge of the natural properties of these surface soil materials is

useful in understanding characteristics of site soils, and conditions in the undisturbed portions of the site.

PWR is a transitional weathering zone between the saprolite and the hard, competent, underlying bedrock. The PWR materials are similar to the overlying saprolite zone, but include more fragments of less weathered and less porous rock. PWR was conservatively estimated to have an effective porosity of 8 percent. This value is based on the free drainage (specific yield) represented by the difference between saturated unit weight (140 pcf) and the wet unit weight (135 pcf). The total porosity of PWR, based on saturated unit weight, is estimated to be 27 percent.

2.4.12.2.4.2 Permeability

The permeability of a material is a measure of its ability to transmit water. Generally within the Piedmont region, the soil/saprolite zone has a low permeability. Also, fractures within the competent bedrock become sparse and poorly connected at increasing depths, thus limiting crystalline bedrock permeability. Fracture permeability consistently occurs in the transition zone, including the uppermost part of bedrock; therefore, this zone often exhibits the highest consistent permeability.

During the Cherokee investigation in the 1970's, 135 field and laboratory tests were conducted to characterize soil and rock permeability. Fifty-five packer tests were conducted in soil and rock intervals in 17 soil borings across the site. An additional 42 field and 38 laboratory tests were performed to evaluate soil permeability. The recent investigation supplements the above investigation with the performance of an additional 11 packer tests in bedrock materials, 16 slug-out tests across the site, and one multi-well aquifer pump test performed within the limiting groundwater flow path (i.e., the flow path with the shortest time-of-travel) from the nuclear island area toward the Broad River to the north.

Based on results from the Cherokee investigation, packer tests, multiwell pumping tests, geotechnical laboratory analyses, and field tests (combined with the results of the 2006 slug tests, packer tests, and multiwell pumping tests), the following conclusions are made regarding aquifer permeability at the Lee Nuclear Site, noting that maintenance dewatering is ongoing and may have affected the recent aquifer test results:

- Reported vertical soil hydraulic conductivities (Kv) of soil and saprolite ranges from 2.45×10^{-8} cm/s to a maximum value of 2.55×10^{-4} cm/s with a median of 2.10×10^{-6} cm/s. For samples exceeding the median hydraulic conductivity of the data set, the geometric mean (4.4×10^{-5} cm/s) represents a conservative vertical hydraulic conductivity value for the residuum. For the purpose of permeability analysis, a conservative value is one that increases the rate of water movement. Vertical hydraulic conductivity generally increases with depth.

- Reported horizontal hydraulic conductivities (Kh) of soil and saprolite ranges from 9.67 x 10^{-7} cm/s (i.e., the lower limit of the test range) to a maximum value of 2.26 x 10^{-3} cm/s with a median of 1.14 x 10^{-4} cm/s. For samples exceeding the median hydraulic conductivity of the data set, the geometric mean (4.5 x 10^{-4} cm/s) represents a conservative hydraulic conductivity value for the residuum.

- Reported hydraulic conductivities measured in the partially weathered rock (PWR), or transition zone, range from approximately 9.67 x 10^{-7} cm/s to a maximum value of 9.89 x 10^{-3} cm/s with a median of 1.53 x 10^{-4} cm/s. For samples exceeding the median hydraulic conductivity of the data set, the geometric mean (1.0 x 10^{-3} cm/s) represents a conservative hydraulic conductivity value for the PWR transition zone across the site. Based on its thorough review of the properties of the PWR zone, Duke asserts that a value of 1.4 x 10^{-3} cm/s is a scientifically-sound, conservative, and representative hydraulic conductivity value for PWR materials at the Lee site. This is the value obtained from an aquifer test in 2006 for an area believed to best represent the limiting groundwater flow path, and is used as the representative value of hydraulic conductivity for PWR. Figure 2.4.12-207 includes three PWR samples that were subsequently excavated in the area of the reactors.

- Values of hydraulic conductivity reported in the Cherokee-era studies represent the upper 100 ft. of the saturated interval. This undifferentiated aquifer zone is comprised of residual soil, saprolite, and partially weathered rock. The resultant hydraulic conductivity values range from 2.21 x 10^{-4} cm/s to 3.90 x 10^{-3} cm/s. These results are consistent with and support the recent findings of the Lee-era site investigation. These more recent studies determined the hydraulic conductivity of PWR, the most hydraulically conductive aquifer material, to be 1.4 x 10^{-3} cm/s.

- Fill materials placed in former valleys during site grading are currently groundwater aquifer materials in some areas. Slug tests conducted in 2006 and 2007 characterized these materials to have hydraulic conductivities ranging from 1.81 x 10^{-5} cm/s to 7.44 x 10^{-5} cm/s. The median hydraulic conductivity for the fill material is 5.39 x 10^{-5} cm/s. For samples equal to and greater than the median hydraulic conductivity of the data set, the geometric mean (7.0 x 10^{-5} cm/s) represents a conservative hydraulic conductivity value for the fill materials.

A summary of the various test results is presented in Table 2.4.12-204. Figure 2.4.12-207 depicts the distribution of hydraulic conductivities with depth. This figure shows the wide variability of hydraulic conductivities observed across the site during both the Cherokee and Lee site investigations. Hydraulic conductivities generally decrease with depth as partially weathered rock transitions to continuous rock. Figure 2.4.12-207 includes the results for partially

weathered rock samples that were subsequently removed during excavation for the Cherokee Nuclear Station reactor buildings.

WLS COL 2.4-5

2.4.12.3 Groundwater Movement

2.4.12.3.1 Groundwater Pathways

The nature and depth of groundwater circulation in the Piedmont is predictably variable. This variability is a function of the singular aquifer system being comprised of weathered saprolite, partially weathered rock, and fractured bedrock, and the degree of interconnection of pores and fractures between these materials. Typical of the Piedmont, groundwater flow is from topographic positions (recharge areas) to the regional drainage features (discharge areas). Groundwater flow at this site likewise generally mirrors the surface topography, with strong gradients and flow paths from the power block area, northward to the Broad River.

The projected groundwater movement in the vicinity of the Lee Nuclear Station power block was assessed to evaluate contaminant migration for the postulated release scenario (Subsection 2.4.13). For the release scenario, radwaste contaminant sources include the Units 1 and 2 radwaste storage tanks, located 33.5 ft. below plant grade (elevation 556.5 ft. above msl). For the assessment of alternative pathways, five locations were assumed to be plausible points of exposure (i.e., locations at which groundwater would be discharged to the surface to allow human contact or to facilitate transport). The pathways evaluated are:

- Pathway 1: Unit 2 to Hold-Up Pond A
- Pathway 2: Unit 2 to the Broad River
- Pathway 3: Unit 2 to Make-Up Pond A
- Pathway 4: Unit 1 to the non-jurisdictional wetland located northwest of Unit 1
- Pathway 5: Unit 1 to Make-Up Pond B

The impacts of construction and operation of Make-Pond Up C within the London Creek watershed were evaluated and determined not to affect groundwater conditions beyond Little London Creek drainage way. Consequently, Make-Up Pond C does not affect the groundwater flow regime at the Lee Nuclear Station, including the evaluation of hydrostatic loading (Subsection 2.4.12.5) or analyses of accidental releases of radioactive liquid effluents (Subsection 2.4.13).

2.4.12.3.2 Groundwater Velocity

The rate of flow (i.e., the velocity) of groundwater depends on (1) the permeability and effective porosity of the medium through which it is moving and (2) the

hydraulic gradient. Average interstitial groundwater flow velocity within the water table aquifer was determined using a form of the Darcy equation as follows:

$$V = K (dh/dl)/n_e$$

Where: V = average groundwater velocity (ft/yr)

K = hydraulic conductivity (cm/s converted to ft/yr)

dh/dl = groundwater gradient (ft/ft)

n_e = effective porosity (%)

After construction dewatering and the return to static conditions, the potentiometric surface in the area of the reactor buildings is expected to rebound to a maximum elevation of approximately 584 ft. msl. These conditions reflect the maximum anticipated groundwater level during operations.

Travel distances for contaminants from postulated release points at the reactors to downgradient receptors were estimated from site information for each of five possible flow paths. Although the aquifer is comprised principally of saprolite and PWR, the more conservative PWR values for hydraulic conductivity and effective porosity were used in the analysis of groundwater velocities. Estimated travel times for the five groundwater flow paths are as follows:

- Pathway 1: Groundwater travels from Unit 2 to Hold-Up Pond A in approximately 1.5 years.
- Pathway 2: From Unit 2 to the Broad River in approximately 2.5 years.
- Pathway 3: From Unit 2 to Make-Up Pond A in approximately 4.2 years.
- Pathway 4: From Unit 1 to the non-jurisdictional wetland area in approximately 4.7 years.
- Pathway 5: From Unit 1 to Make-Up Pond B in approximately 5.5 years.

These flow paths are represented on Figure 2.4.12-208. This analysis indicates the limiting flow path for the evaluated postulated release to be from the Unit 2 radwaste storage tank to Hold-Up Pond A (Pathway 1, Figure 2.4.12-205, Sheet 3).

Soil distribution characteristics for radiological isotopes (i.e., Co-60, Cs-137, Fe-55, I-129, Ni-63, Pu-242, Tc-99, U-235) were determined from soil and water samples collected along the preferred groundwater flow path. This data is presented in Subsection 2.4.13 to assist in the development of calculations for fate and transport analyses in the event of accidental releases of effluents to groundwater.

2.4.12.3.3 Effects of Local Area Pumping

While the groundwater is not intended to be used at the Lee Nuclear Site, consideration is given to the movement of groundwater beneath the site in response to potential pumping associated with dewatering or domestic well use. Based on permeability characteristics beneath the site and an understanding of typical wells in the vicinity, a radius of influence can be estimated. For unconfined aquifers, such as those encountered in the Piedmont province, the radius of influence can be determined using the following equation provided by the Departments of the Army, the Navy, and the Air Force in Publication TM5-818-5:

$$R = 3\Delta H (K \times 10^4)^{1/2}$$

Where: R = the radius of influence of a pumping well (ft.)

ΔH = the drawdown within the well (ft.)

K = the hydraulic conductivity of the aquifer (cm/s)

Most domestic wells in the vicinity of the Lee Nuclear Site are completed as either shallow bored wells, or deeper drilled wells. Shallow bored wells are usually completed in the saprolite zone, typically no deeper than 75 ft. Deeper drilled wells are installed in the PWR and fractured bedrock zones. Both types of wells generally have yields of 5-10 gpm, or less. Using these conditions provides a conservative estimate of the potential reach of a typical domestic well producing at full capacity. Assuming the hydraulic conductivities are consistent with partially weathered rock, as listed in Table 2.4.12-204, the radius of influence is approximately 1700 ft. (0.32 mi.) from these wells. The lateral area of influence of the dewatered excavation is approximately 500 ft. (0.095 mi.).

Based on site reconnaissance of the area, the closest domestic water supply well is located approximately 5000 ft. (0.95 mi.) south of the nuclear island. The influence of the surrounding impoundments (i.e., Make-Up Pond B and Make-Up Pond A) would further buffer the potential draw created from off-site pumping or on-site pumping, if needed. No off-site wells are considered capable of reversing groundwater flow beneath the site, or vice versa, based on the geographic positions of these wells (i.e., the distance of the domestic wells) and the character of these wells (i.e., the typical low-flow rates and the relatively shallow completion depths).

The Cherokee Nuclear Station Construction Permit ER identified 50 domestic water wells and provided construction details for these wells, including well diameter, well depth, and depth to water (see Table 2.4.1-212 and Figure 2.4.1-212). Only three of these 50 wells have total depths of 150 ft. or greater. Since 1985, 19 wells have been installed within a 1-mi. radius of the Lee Nuclear Site property boundary and to a depth greater than 150 ft. (Reference 261). However, according to information provided by the Draytonville Water District, public water supply lines were installed in the late 1990s and continue to be added in the area surrounding the Lee Nuclear Site. As of 2007,

since public water supply lines were installed in the area, approximately 55 percent of residents within a 2-mi. radius of the reactor buildings have converted from self-supplied groundwater systems to public water supplies. Furthermore, with the addition of water-supply lines planned for completion in 2009, the public water is expected to be available to approximately 83 percent of those residents within the 2-mi. radius of the plant. The projected use of self-supplied groundwater systems is expected to continue to decline as public water supply lines are built into rural areas and residents increase their dependence on the public water supply.

2.4.12.4 Monitoring or Safeguard Requirements

WLS COL 2.4-5 There are two potential sources for radiological impacts to groundwater: (1) leaks from radioactive waste tanks and (2) leaks from the spent fuel pool. To minimize the potential for contact of radioactive material with groundwater, the Lee Nuclear Site is equipped with a water barrier around the building foundation up to 1 ft. above grade. The water barrier is installed to prevent water from seeping into the auxiliary building that holds the liquid radioactive waste (LRW) tanks. In addition, groundwater monitoring will be conducted at the Lee Nuclear Site. The groundwater monitoring program will be consistent with the guidance in "Generic FSAR Template Guidance for Life Cycle Minimization of Contamination" (NEI 08-08). The groundwater monitoring program will include a network of wells for early detection (near-field wells) and for verification of no off-site migration (far-field wells). Wells will be installed in proximity to plant systems that may be a source of radiological releases, and/or in nearby plausible down-gradient flow direction from such sources. Both shallow and deep wells will be utilized as needed to monitor the location closest to the potential release area. The laboratory analyses of groundwater samples will include gamma isotopes and tritium.

The groundwater monitoring program is described in Subsection 12AA.5.4.14. Accident effects are discussed in Subsection 2.4.13. Additionally, analysis of the relationship of the Lee Nuclear Site groundwater to seismicity and the potential for related soil liquefaction and the potential for undermining of safety-related structures is discussed in Section 2.5.

2.4.12.5 Site Characteristics for Subsurface Hydrostatic Loading

WLS COL 2.4-4 According to the AP1000 Design Control Document (DCD), the design maximum groundwater elevation is 2 ft. below plant elevation. The Lee Nuclear Station plant elevation is 590.0 ft. above msl and the yard grade is 589.5 ft. above msl; therefore, the design maximum groundwater elevation is 588.0 ft. above msl. The maximum static groundwater level anticipated in the vicinity of Units 1 and 2 power blocks during operations is expected to be a maximum of 584 ft. msl (Figure 2.4.12-204, Sheet 8). The hydrostatic loading is not expected to exceed design criteria. An unsaturated zone of at least 5 ft. below grade level will be

maintained during operations. The installation and operation of a permanent dewatering system is not a facility design requirement.

2.4.13 ACCIDENTAL RELEASES OF RADIOACTIVE LIQUID EFFLUENTS IN GROUND AND SURFACE WATERS

WLS COL 2.4-5
WLS COL 15.7-1

2.4.13.1 Groundwater

This section provides a conservative analysis of a postulated accidental liquid effluent release to the environment at the Lee Nuclear Site. The following sections describe the scenario and conceptual model used to evaluate the transport pathways to the nearest potable water supply in an unrestricted area. RESRAD-OFFSITE Version 2.0 is used to model the transport and provide resulting radionuclide concentration values in the potable water receptor body.

Acceptable results are those that are less than the effluent concentrations listed in 10 CFR 20 Appendix B, Table 2, Column 2. Individual radionuclide concentration results and the sum of fractions value are compared against these limits. The sum of fractions (i.e., unity value) is a comparison of the ratio of known radionuclides to their limit. This unity value may not exceed "1". As applied through Branch Technical Position 11-6, these criteria apply to the nearest potable water supply in an unrestricted area.

Historical and projected groundwater flow paths were evaluated in Subsection 2.4.12 to characterize groundwater movement from the nuclear island area to a point of exposure. Groundwater at the Lee Site exists as a single, undifferentiated aquifer, comprised of soil, saprolite, partially weathered rock (PWR), competent bedrock, and, to a limited extent, fill soils. Although the projected groundwater flow paths travel through zones with saprolite, fill, and PWR, the more conservative hydrogeologic characteristics of PWR were used in both the determination of the limiting groundwater flow path and as inputs, where appropriate, into the RESRAD-OFFSITE model. Using the PWR characteristics for hydraulic conductivity, bulk density, and effective porosity, the flow path from the Unit 2 effluent hold-up tank to Hold-Up Pond A is assumed to be the limiting pathway of radionuclide migration, with the shortest (i.e., most rapid) travel time to a surface water body. For purposes of this analysis, because the spillway and dam of Hold-Up Pond A are proximal to the Broad River, entry concentrations at Hold-Up Pond A are assumed to be entry concentrations at the Broad River. This direct conveyance to the Broad River thus provides for no additional retardation, hold-up, or restrictions to transport between Hold-Up Pond A and the Broad River. Figures 2.4.12-204, Sheet 8 and 2.4.12-205, Sheet 3 depict subsurface conditions that control the movement of groundwater beneath the Lee Nuclear Station.

While groundwater functions as the transport media for fugitive radionuclides, interaction of individual radionuclides with the soil matrix can potentially delay

their movement. The solid/liquid distribution coefficient, K_d, is, by definition, an equilibrium constant that describes the process wherein a species (e.g., a radionuclide) is partitioned between a solid phase (soil, by adsorption or precipitation) and a liquid phase (groundwater, by dissolution). Soil properties affecting the distribution coefficient include the texture of soils (sand, loam, clay, or organic soils), the organic matter content of the soils, pH values, the soil solution ratio, the solution or pore water concentration, and the presence of competing cations and complexing agents. Because of its dependence on many soil properties, the value of the distribution coefficient for a specific radionuclide in soils can range over several orders of magnitude under different conditions. The measurement of distribution coefficients of radionuclides within the limiting groundwater pathway allows further characterization of the rate of movement of fugitive radionuclides in groundwater.

Soil and groundwater samples were collected from Monitoring Wells MW-1208 and MW-1210 located on the north and south sides of the nuclear island (Figure 2.4.12-205, Sheet 1). Three soil samples were collected from the saturated zone at depths ranging from 45 to 73 ft. below ground level. The samples were submitted for laboratory analysis of soil distribution characteristics for specific radiological isotopes (Co-60, Cs-137, Fe-55, I-129, Ni-63, Pu-242, Sr-90, Tc-99, U-235). Results of these analyses are presented in Table 2.4.13-201, along with default K_d values found in literature, for comparison. For conservatism, those radionuclides which had been evaluated for site-specific distribution coefficients used the lowest measured K_d values in the evaluation, regardless of the media from which the samples were collected. The values are adjusted to the low limit of their reporting range (e.g., for a reported Cs-137 value of 1156±163 cm^3/g, a value of 993 cm^3/g was used in the analysis). All other radionuclides use the most conservative K_d value of 0.

2.4.13.2 Accident Scenario

The limiting postulated failure of a Unit 2 effluent holdup tank, located in the Unit 2 auxiliary building, is analyzed to estimate the resulting concentration of radioactive contaminants entering Hold-Up Pond A via groundwater flow. Contaminant concentrations at this point are then assumed to represent entry concentrations to the surface water receptor, the Broad River, which is located proximal to Hold-Up Pond A.

The event is defined as an unexpected and uncontrolled release of radioactive water produced by plant operations from a tank rupture. The AP1000 tanks which normally contain radioactive liquid are listed in Table 2.4.13-202. The contents from the effluent holdup tank are conservatively assumed to enter the environment instantaneously, allowing radionuclides to be transported in the direction of groundwater flow. The flow path from Unit 2 to Hold-Up Pond A is determined to be the limiting pathway based on travel time.

It is noted that no outdoor tanks contain radioactivity. In particular, the AP1000 does not require boron changes for load follow and so does not recycle boric acid or water; therefore, the boric acid tank is not radioactive.

The spent resin tanks are excluded from consideration, because most of their activity is bound to the spent resins; they have minimal free water that would be capable of migrating from the tank in the event of a tank failure. Tanks inside the containment building were not considered because the containment building, a seismic Category I structure, is a freestanding cylindrical steel containment vessel (DCD Subsection 1.2.4.1). Credit is taken for the steel liner to mitigate the effect of a postulated tank failure.

The Liquid Radwaste System (WLS) monitor tanks located in the radwaste building extension are considered because of their location in a non-seismic building. These tanks have a maximum capacity of 15,000 gallons each. They receive fluid that has been processed and must be monitored prior to discharge. The radwaste building has a well sealed, contiguous basemat with integral curbing that can hold the maximum liquid inventory of any tank. Floor drains in the area lead to the liquid radwaste system. The foundation for the entire building is a reinforced concrete mat on grade. Liquid spilled due to failure of any one of these tanks would be contained within the building, and would involve low activity liquids being held for discharge. Any release to the environment would be leakage through cracks in the concrete. The radiological consequences of such leakage are bounded by the analysis for the effluent holdup tanks. Therefore, these monitor tanks are not the limiting fault.

The remaining four tank applications were considered - the effluent holdup tanks, waste holdup tanks, monitor tanks (located in the auxiliary building), and chemical waste tanks. Of these tanks, the effluent holdup tanks have both the highest potential radioactive isotope inventory and the largest volume. The other tanks need not be considered further because they have lower isotopic inventory and, with the exception of one of the monitor tanks, because the rooms in which they are located are not on the lowest level of the auxiliary building (and thus intervening interior floors would mitigate the uncontrolled release of a ruptured tank). Therefore, an effluent holdup tank is limiting for the purpose of calculating the effects of the failure of a radioactive liquid-containing tank.

The effluent holdup tanks are located in an unlined room on the lowest level of the auxiliary building. This level is 33 feet 6 inches below the existing surface grade elevation of the plant. Each unit has two effluent holdup tanks, one of which is postulated to fail.

The analysis considers the tank liquid level, decay of the tank contents, potential paths of spilled liquid to the environment, and other pertinent factors.

The total volume of each effluent holdup tank is 28,000 gallons. Since credit can not be taken for liquid retention by unlined building foundations; a conservative analysis assumes that the tank content (80 percent of capacity, or 22,400 gallons) is immediately released through cracks in the auxiliary building walls and floor into the surrounding sub-surface soil. These assumptions follow the position in Branch Technical Position 11-6, March 2007.

2.4.13.3 Source Term

The radioactive source term is:

- Tritium source term concentration is 1.0 microcuries per gram taken from DCD Table 11.1-8;
- Corrosion product source terms Cr-51, Mn-54, Mn-56, Fe-55, Fe-59, Co-58, and Co-60 taken from DCD Table 11.1-2;Other isotope source terms taken from DCD Table 11.1-2 multiplied by 0.12/0.25 to adjust the radionuclide concentrations to the required 0.12 percent failed fuel fraction outlined in Branch Technical Position 11-6, March, 2007; and
- Gaseous state nuclides and nuclides with short half-lives not included in the RESRAD default library are removed from consideration as they have no impact on the evaluation. These radionuclides include:

Ba-137m	Br-83	Br-85	I-131
I-133	Kr-83m	Kr-85	Kr-85m
Kr-87	Kr-88	Kr-89	Rh-106
Te-131	Te-131m	Xe-131m	Xe-133
Xe-133m	Xe-135	Xe-137	Xe-138

WLS COL 2.4-5 Analysis of failure of the effluent holdup tank of Unit 2 rather than Unit 1 is conservative in that the pathway from the Unit 2 effluent holdup tank to Hold-Up Pond A has the shortest (i.e., most rapid) travel duration, assuming conservative PWR characteristics along the entire flow path.

The impacts of construction and operation of Make-Up Pond C within the London Creek watershed were evaluated and determined not to affect groundwater conditions beyond Little London Creek drainage way. Consequently, Make-Up Pond C does not affect the groundwater flow regime at the Lee Nuclear Station and therefore has no impact on the transport paths and accidental release analyses discussed in this subsection.

As discussed in Subsection 2.4.12, dewatering activities are currently occurring at the site. After construction is complete, dewatering activities will end.

The conceptual model of radionuclide transport through groundwater, from Unit 2 to Hold-Up Pond A, is shown in Figure 2.4.12-205 (Sheet 3). As stated in Subsection 2.4.13.1, a direct conveyance between Hold-Up Pond A and the Broad River is assumed. With the failure of the effluent holdup tank and subsequent liquid release to the environment, radionuclides enter the subgrade soils at an elevation of 33 feet 6 inches below the surrounding grade. The contaminated zone is, therefore, a volume of contaminated soil for which the effective porosity is saturated with contaminated water released from the liquid effluent holdup tank. The contaminated zone soil is assumed to exhibit PWR characteristics. Because RESRAD-OFFSITE considers soil at the source of the

contamination, the liquid initial source term concentrations were converted to an equivalent concentration on a soil mass basis.

Currently, the overburden soils continually receive the average annual onsite precipitation. In general, the precipitation that does not run off or is not lost to evapotranspiration infiltrates the overlying unsaturated zone and contributes to groundwater as recharge. However, as an additional conservative measure in the model, runoff was assumed to be zero, and precipitation not lost to evapotranspiration was treated by RESRAD-OFFSITE as recharge.

2.4.13.4 Conceptual Model

The conceptual model assumes that one of the liquid effluent tanks, located at the lowest level of the auxiliary building, ruptures while containing 80 percent of its total capacity. The liquid is assumed to be released in accordance with Branch Technical Position 11-6 of NUREG-0800. The liquid from the ruptured tank would flood the tank room and proceed to the auxiliary building radiologically controlled area sump by way of the floor drains. The sump pumps are assumed to be inoperable to create a bounding case. The liquid then enters the environment outside the auxiliary building. The consequence is a release of 22,400 gallons of contaminated liquid into the soil. The liquid is transported via groundwater flow to the surface water receptor, the Broad River. Because Hold-Up Pond A is the surface water body with the shortest (i.e., most rapid) groundwater transport time, assuming PWR characteristics, the model calculates radionuclide concentrations in a hypothetical well at the edge of this pond. The dam and spillway of Hold-Up Pond A are proximal to the Broad River. This model then assumes that concentrations in Hold-Up Pond A are immediately conveyed to the Broad River, without any additional intermediate retardation, hold up, or transport restrictions between Hold-Up Pond A and the Broad River. The conceptual model then assumes the liquid is diluted in the Broad River reservoir upstream of the Ninety-Nine Islands Dam. This is conservative because the nearest potable water supply using the Broad River surface water is located approximately 21 miles downstream from the postulated release point, at the City of Union public water supply. Concentrations are modeled for an evaluation period of 1,000 years.

The conceptual model is conservative because it provides for the shortest (i.e., most rapid) travel time to a surface water body, even though that surface water body is not the receptor body, and it also includes faulting the limiting tank. The analysis uses conservative estimates for parameters that are not developed from site-specific data. In addition, site-specific inputs to the model are also conservative, including the use of the lowest K_d values and the assumption that all groundwater pathways traveled through geo-media with the porosity and conductivity properties of PWR. Values used as inputs in the model are shown in Table 2.4.13-203. The straight-line flow path is used, which is also conservative as actual groundwater pathways are more tortuous, have longer transport times, and lower hydraulic conductivities for the fractures and joints.

Radionuclide concentrations in the hypothetical well at the edge of Hold-Up Pond A and in the Broad River at the Ninety-Nine Islands Dam are modeled using

RESRAD-OFFSITE (Reference 212). The model considers the effects of different transport rates for radionuclides and progeny nuclides, while allowing radioactive decay during the transport process. The concentration of each radionuclide transmitted to the Broad River is determined by the transport through the groundwater system, dilution by groundwater and infiltrating surface water from the overburden soils, adsorption, and radioactive decay.

Radionuclide decay during transport by groundwater occurs and is considered in the analysis. Radionuclide transport by groundwater is assumed to be affected by adsorption by the surrounding soils. As discussed in Subsection 2.4.12, the soils surrounding the auxiliary building at the elevation of the liquid release are modeled as having the porosity and hydraulic conductivity characteristics of PWR.

The saturated zone dispersion values are set to mimic infusion, rather than injection, of the contaminated liquid into the groundwater flow by assigning a value to the longitudinal dispersivity equal to one-tenth the length of the contaminated zone. Horizontal lateral and vertical lateral dispersivity values are set at one-tenth the longitudinal dispersivity. These settings allow the contamination to move with the natural groundwater flow rather than be pushed through the groundwater and arrive over a longer time frame in a more dilute state.

2.4.13.5 Sensitive Parameters

Sensitivity analyses were performed on a number of input parameters to evaluate the sensitivity of the RESRAD-OFFSITE model to a range of values for specific input factors. A parameter is considered sensitive if the resulting effect on the evaluated radionuclide concentration varied by more than 10 percent. Input parameters evaluated in the sensitivity analyses include:

- Hydraulic gradient of the saturated zone (varied by a factor of 1.5);
- Well pump intake depth (varied by a factor of 2);
- Volume of the surface water receptor (varied by a factor of 2); and
- K_d values in the saturated zone for site-specific (non-zero) radionuclides (varied by a factor of 10).

Overall, the sensitivity analyses indicate that variations in the single parameters analyzed have no significant impact on the resulting concentrations; in no case do the resulting concentrations exceed 10 CFR 20 Appendix B, Table 2, Column 2 limits or a sum of fractions calculation. Of particular note:

- When the surface water volume is reduced by a factor of 2, concentrations doubled, but the sum of fractions remained in the E-05 range. This expected outcome confirmed that even with a significant reduction in available volume, the sum of fractions remained below the unity value of one.

- Even with a relatively high hydraulic gradient (0.06 ft/ft considered not plausible for this site), increases in radionuclide concentrations varied by less than 10 percent, and the sum of fractions remained below 10 CFR 20 Appendix B, Table 2, Column 2 limits and unity standard.

2.4.13.6 Regulatory Compliance

WLS COL 2.4-5 10 CFR 20 Appendix B states, "The columns in Table 2 of this appendix captioned "Effluents," "Air," and "Water," are applicable to the assessment and control of dose to the public, particularly in the implementation of the provisions of §20.1302. The concentration values given in Columns 1 and 2 of Table 2 are equivalent to the radionuclide concentrations which, if inhaled or ingested continuously over the course of a year, would produce a total effective dose equivalent of 0.05 rem (50 millirem or 0.5 millisieverts)." Thus, meeting the concentration limits of 10 CFR 20 Appendix B, Table 2 Column 2 results in a dose of less than 0.05 rem and therefore demonstrates that the requirements of 10 CFR 20.1301 and 10 CFR 20.1302 are met.

The radiological consequence of a postulated failure of the Unit 2 effluent holdup tank as the limiting fault is evaluated and determined not to exceed 10 CFR 20 Appendix B, Table 2, Column 2 limits at the nearest waters adjoining the Lee site (Broad River). The analysis demonstrates that radionuclide concentrations in both the hypothetical well located at the edge of Hold-Up Pond A and in the Broad River at the Ninety-Nine Islands Dam are below 10 CFR 20 Appendix B, Table 2, Column 2 limits. Further, the nearest potable water supply located in an unrestricted area using the Broad River surface water is the City of Union public water supply located approximately 21 miles downstream of the Ninety-Nine Islands Dam.

The maximum radionuclide concentration for each isotope sum of fractions of 10 CFR 20 Appendix B, Table 2, Column 2 limits calculated for both the hypothetical well at the edge of Hold-Up Pond A and in the receptor body, the Broad River, during the 1,000-year period, is below a value of 1. Table 2.4.13-204 provides the fraction of effluent concentration for the significant radionuclide.

2.4.14 TECHNICAL SPECIFICATIONS AND EMERGENCY OPERATION REQUIREMENTS

WLS COL 2.4-6 The maximum flood level at the Lee Nuclear Station is elevation 584.8 ft. msl. This elevation would result from a Probable Maximum Flood (PMF) event on the Make-Up Pond B watershed with the added effects of coincident wind wave activity as described in Subsection 2.4.3.6. The Lee Nuclear Station safety-related structures have a plant elevation of 590 ft. msl. Also, Subsection 2.4.12.5

describes plant elevation relative to the maximum anticipated groundwater level. The hydrostatic loading is not expected to exceed design criteria.

There are no safety-related facilities that could be affected by low-flow or drought conditions of the Broad River. At low flow conditions, water is drawn from Make-Up Ponds B and C (Subsection 2.4.11.5). Full power plant operations could be sustained for approximately 190 days with water from Make-Up Ponds B and C, with sufficient water remaining in Make-Up Pond A to shutdown the plant and maintain safe shutdown conditions.

Based on site-specific conditions of the Lee Nuclear Station, there are no emergency protective measures designed to minimize the impact of adverse hydrology-related events on safety-related facilities.

STD DEP 1.1-1

2.4.15 COMBINED LICENSE INFORMATION

2.4.15.1 Hydrological Description

WLS COL 2.4-1 This COL item is addressed in Subsection 2.4.1.

2.4.15.2 Floods

WLS COL 2.4-2 This COL item is addressed in Subsections 2.4.2, 2.4.3, 2.4.4, 2.4.5, 2.4.6, 2.4.7, and 2.4.10.

2.4.15.3 Cooling Water Supply

WLS COL 2.4-3 This COL item is addressed in Subsections 2.4.8, 2.4.9, and 2.4.11.5.

2.4.15.4 Groundwater

WLS COL 2.4-4 This COL item is addressed in Subsections 2.4.12.1, 2.4.12.2, 2.4.12.3, and 2.4.12.5.

2.4.15.5 Accidental Release of Liquid Effluents into Ground and Surface Water

WLS COL 2.4-5 This COL item is addressed in Subsections 2.4.12.2.3, 2.4.12.2.4, 2.4.12.3, 2.4.12.4, and 2.4.13.

2.4.15.6 Emergency Operation Requirement

WLS COL 2.4-6 This COL item is addressed in Subsection 2.4.14.

2.4.16 REFERENCES

201. American Iron and Steel Institute, “Modern Sewer Design,” AISC, Washington, D.C., Fourth Edition 1999.

202. American Nuclear Society, “American National Standard for Determining Design Basis Flooding at Power Reactor Sites,” ANSI/ANS-2.8-1992, American Nuclear Society, La Grange Park, Illinois, July 28, 1992.

203. Bohman, L.R., “Determination of Flood Hydrographs for Streams in South Carolina: Volume 1. Simulation of Flood Hydrographs for Rural Watersheds in South Carolina” U.S. Geological Survey, Water-Resources Investigations Report 89-4087, Columbia, South Carolina, 1990.

204. Broad River Electric Cooperative, Inc., Written Communication from Douglas E. Wilson to Gerald Gotzmer regarding the Cherokee Falls Hydro Minimum Flow, July 15, 2002.

205. Calpine, Website, Website, www.calpine.com/power/plant.asp?plant=96, accessed April 3, 2007.

206. Chow, V.T., “Open Channel Hydraulics,” McGraw-Hill, New York, 1959.

207. City of Shelby, "2003 Annual Water Quality Report," Website, http://www.cityofshelby.com/econdev/water.htm, accessed March 2006.

208. Cooney, T.W, P.A Drewes, S.W. Ellisor, T.H. Lanier, and F. Melendez, “Water Resources Data, South Carolina, Water Year 2005,” U.S. Geological Survey Water-Data Report SC-05-1, 2006.

209. C. Yu, C. Loureiro, J.-J. Cheng, L.G. Jones, Y.Y. Wang, Y.P. Chia, and E. Faillace, Environmental Assessment and Information Sciences Division, Argonne National Laboratory, *Data Collection Handbook to Support Modeling Impacts of Radioactive Material in Soil*, 1993.

210. C. Yu, A.J. Zielen, J.-J. Cheng, D.J., LePoire, E. Gnanapragasam, S. Kamboj, J. Arnish, A. Wallo III,* W.A. Williams,* and H. Peterson*, Environmental Assessment Division, Argonne National Laboratory, *User's Manual for RESRAD Version 6*, Appendix E, pg. E9-E13, 2001.

211. Devine, Tarbell & Associates Inc, Cherokee Hydrology Summary Report, 2005.

212. U.S. Department of Energy, “User’s Manual for RESRAD-Offsite Version 2,” ANL/EVS/TM/07-1, DOE/HS-0005, NUREG/CR-6937, Argonne National Laboratory, Environmental Science Division, Argonne, Illinois, June 2007.

213. Removed

214. Duke Power Company, Cherokee Nuclear Station – Environmental Report, Sections 2.2, 2.4 and 2.5, revised 1975.

215. Duke Power Company, Groundwater Levels Notebook, Site Groundwater Monitoring Field Observations 1976 -1985, Project 81 Cherokee Nuclear Station, Cherokee County, SC.

216. Duke Power Company, Ninety-Nine Islands Dam Project License Renewal, Environmental Report, 1996.

217. Duke Power Company, “Ninety-Nine Islands Hydro Project, FERC Project No. 2331, Determination of the Probable Maximum Flood,” Duke Engineering Services, Charlotte, North Carolina, November 7, 1997.

218. Duke Power Company, Powerhouse Groundwater Control, 1977-1978, Cherokee Nuclear Project Manual, Cherokee Nuclear Station.

219. Duke Energy, "Preliminary Application for Certificate of Public Convenience and Necessity Cleveland County & Rutherford County Cliffside Project," May 11, 2005.

220. Duke Power Company, *Preliminary Safety Analysis Report, Project 81 – Cherokee Nuclear Station, Cherokee County, SC,* 1974.

221. Environmental Data Resources, Environmental Database and Geocheck® search, date extracted March 2006.

222. Federal Energy Regulatory Commission, "Order Issuing New License to Duke Power Company, Project No. P-2332-003," June 12, 1996.

223. Federal Energy Regulatory Commission, "Order Issuing New License to Duke Power Company, Project No. P-2331-002," June 17, 1996.

224. Federal Register Vol. 71, No. 133, Pages 39308-39309 (July 12, 2006).

225. Hansen, E.M., L.C. Schreiner, and J.F. Miller, “Application of Probable Maximum Precipitation Estimates - United States East of the 105th Meridian,” Hydrometeorological Report No. 52, U.S. Department of Commerce, National Oceanic and Atmospheric Administration, National Weather Service, Washington, D.C., August 1982.

226. National Archives and Records Administration, Federal Register Document 06-6139, Vol. 71, No. 133, July 12, 2006.

227. Removed

228. National Oceanic & Atmospheric Administration, National Geophysical Data Center Tsunami Database, Website, http://www.ngdc.noaa.gov/seg/hazard/tsu_db.shtml, accessed July 2006.

229. National Weather Services Greenville-Spartanburg Station historical records, Website, www.erh.noaa.gov/gsg/climate/climatology/climatology.htm, April 10, 2007.

230. North Carolina Department of Environment and Natural Resources, “Broad River Basinwide Water Quality Plan,” March 2003.

231. North Carolina Department of Environmental and Natural Resources, Division of Water Quality, "Basinwide Assessment Report, Broad River Basin,” December, 2001.

232. North Carolina Department of Environmental and Natural Resources, Basinwide Assessment Report, Broad River Basin, 2006.

233. North Carolina Department of Environment and Natural Resources, "North Carolina State Water Supply Plan," January 2001.

234. North Carolina Division of Water Resources, 2002 Local Water Supply Plan for Broad River Water Authority, Website, http://www.ncwater.org/Water_Supply_Planning/Local_Water_Supply_Plan/, accessed March 2007.

235. North Carolina Division of Water Resources, 2002 Local Water Supply Plan for Cleveland County Sanitary District, Website, http://www.ncwater.org/Water_Supply_Planning/Local_Water_Supply_Plan/, accessed March 2007.

236. North Carolina Division of Water Resources, 2002 Local Water Supply Plan for Forest City, Website, http://www.ncwater.org/Water_Supply_Planning/Local_Water_Supply_Plan/, accessed March 2007.

237. North Carolina Division of Water Resources, 2002 Local Water Supply Plan for Kings Mountain, Website, http://www.ncwater.org/Water_Supply_Planning/Local_Water_Supply_Plan/, accessed March 2007.

238. North Carolina Division of Water Resources, 2002 Local Water Supply Plan for Shelby, Website, http://www.ncwater.org/Water_Supply_Planning/Local_Water_Supply_Plan/, accessed March 2007.

239. North Carolina Division of Water Resources, 1999 Water Withdrawal Registration 0028-0002 J.C. Cowan Plant, Website, http://dwr.ehnr.state.nc.us/cgi-bin/foxweb.exe/c:/foxweb/reg99a, accessed June 2006.

240. North Carolina Division of Water Resources, 1999 Water Withdrawal Registration 0057-0002 Cliffside Steam Station, Website, http://dwr.ehnr.state.nc.us/cgi-bin/foxweb.exe/c:/foxweb/reg99a, accessed June 2006.

241. North Carolina Division of Water Resources, 1999 Water Withdrawal Registration 0057-0007 Tuxedo Hydro-Electric Facility, Website, http://dwr.ehnr.state.nc.us/cgi-bin/foxweb.exe/c:/foxweb/reg99a, accessed June 2006.

242. North Carolina Division of Water Resources, 1999 Water Withdrawal Registration 0219-0028 Kings Mountain Quarry, Website, http://dwr.ehnr.state.nc.us/cgi-bin/foxweb.exe/c:/foxweb/reg99a, accessed June 2006.

243. North Carolina Division of Water Resources, 1999 Water Withdrawal Registration 0351-0001 Kenmure Golf Course, Website, http://dwr.ehnr.state.nc.us/cgi-bin/foxweb.exe/c:/foxweb/reg99a, accessed June 2006.

244. North Carolina Division of Water Resources, 1999 Water Withdrawal Registration 0354-0001 Cleveland Country Club Golf Course, Website, http://dwr.ehnr.state.nc.us/cgi-bin/foxweb.exe/c:/foxweb/reg99a, accessed June 2006.

245. North Carolina Division of Water Resources, 1999 Water Withdrawal Registration 0359-0001 Ticona-Shelby Facility, Website, http://dwr.ehnr.state.nc.us/cgi-bin/foxweb.exe/c:/foxweb/reg99a, accessed June 2006.

246. North Carolina Division of Water Resources, 1999 Water Withdrawal Registration 0360-0001 Cleveland-Caroknit, Website, http://dwr.ehnr.state.nc.us/cgi-bin/foxweb.exe/c:/foxweb/reg99a, accessed June 2006.

247. North Carolina Division of Water Resources, 1999 Water Withdrawal Registration 0361-0002 Turner Shoals Hydroelectric Plant, Website, http://dwr.ehnr.state.nc.us/cgi-bin/foxweb.exe/c:/foxweb/reg99a, accessed June 2006.

248. North Carolina Division of Water Resources, 1999 Water Withdrawal Registration 0361-0003 Stice Shoals Hydroelectric Plant (mislabeled as Spencer Mountain Hydroelectric Project), Website, http://dwr.ehnr.state.nc.us/cgi-bin/foxweb.exe/c:/foxweb/reg99a, accessed June 2006.

249. North Carolina General Statutes, Chapter 143-215.22H, 2005.

250. Owen, J.H., “Flood Emergency Plans, Guidelines for Corps Dams,” U.S. Army Corps of Engineers, RD-13, June 1980.

251. Reed, M.J., "Assessment of Low-Temperature Geothermal Resources of the United States - 1982," U.S. Geological Survey Circular 892, 1982.

252. Renner, J.L. and T.L. Vaught, "Geothermal Resources of the Eastern United States," U.S. Department of Energy DOE/ET/28373-T2, Gruy Federal Inc., Arlington, Virginia, December 1979.

253. Riggs, H.C., "Techniques of Water-Resources Investigations of the United States Geological Survey," Book 4, Chapter B1, “Low-Flow Investigations,” United States Government Printing Office, Washington, D.C., 1972.

254. Sanborn LLC, Ground Control Surveying Report of Duke-Cherokee County, South Carolina Site, 2006.

255. Schreiner, L.C., and J.T., Riedel, “Probable Maximum Precipitation Estimates, United States East of the 105th Meridian,” Hydrometeorological Report No. 51, U.S. Department of Commerce, National Oceanic and Atmospheric Administration, National Weather Service, Washington, D.C., June 1978.

256. Shaw Stone & Webster Inc., WS. Lee Units 1 and 2 COLA Conceptual Design Package (CDP) for the Raw Water System (RWS), August 2007.

257. South Carolina Ambient Groundwater Quality Monitoring Network Annual Report, Summary, revised 2004, Website, http://www.scdhec.gov/water/pubs/amb2004.pdf#search=22Technical20Report3A22Technical 20Report3A20005-0620South20Carolina20Ambient20South20 Carolina20Ambient22, accessed April 9, 2007.

258. South Carolina Code of Laws, Title 49, Chapter 4, Section 49-4-20, 2005.

259. South Carolina Department of Health and Environmental Control, "Broad River Water Quality Assessment," 2001.

260. Ho, F.P., and J.T. Riedel, "Seasonal Variation of 10-Square Mile Probable Maximum Precipitation Estimates, United States East of the 105th Meridian," Hydrometeorological Report No. 53, U.S. Department of Commerce, National Oceanic and Atmospheric Administration, National Weather Service, Washington D.C., April 1980.

261. South Carolina Department of Health and Environmental Control, "LASTREP2 - Private Well Report for Cherokee County for dates 01/01/1985 to 06/22/2006" (text file), revised 2006.

262. South Carolina Department of Health and Environmental Control, "Source Water Assessment Carlisle Cone Mills System No 4430003," April 29, 2003.

263. South Carolina Department of Health and Environmental Control, "Source Water Assessment City of Union System No 4410001," April 29, 2003.

264. South Carolina Department of Health and Environmental Control, "Source Water Assessment Gaffney BPW System No 1110001," April 29, 2003.

265. South Carolina Department of Health and Environmental Control, "Source Water Assessment VC Summer Nuclear Station System No 2030004," April 29, 2003.

266. South Carolina Department of Health and Environmental Control, South Carolina Source Water Assessment and Protection Program, revised 1999, Website, http://www.scdhec.net/water/pubs/swpplan.pdf, accessed April 9, 2007.

267. South Carolina Department of Health and Environmental Control, South Carolina Water Use Report 2005 Summary, Technical Document Number: 006-06, 2006.

268. South Carolina Department of Health and Environmental Control, Watershed Water Quality Assessment – Broad River Basin, Technical Report No. 001-01, 2001.

269. U.S. Army Corps of Engineers, “Engineering and Design Hydrologic Engineering Requirements for Reservoirs.” EM 1110-2-1420, October 31, 1997.

270. U.S. Army Corps of Engineers, "Engineering and Design Hydrologic Frequency Analysis," EM 1110-2-1415, March 5, 1993.

271. U.S. Army Corps of Engineers, Hydrologic Engineering Center, Generalized Computer Program, HMR52, Probable Maximum Storm, Revised April 1991.

272. U.S. Army Corps of Engineers, Hydrologic Engineering Center, Hydrologic Modeling System, HEC-HMS computer software, version 3.0.1.

273. U.S. Army Corps of Engineers, Hydrologic Engineering Center, River Analysis System, HEC-RAS computer software, version 3.1.3.

274. U.S. Army Corps of Engineers, Ice Jam Database, Website, http://www.crrel.usace.army.mil/ierd/ijdb/, data extracted April, 2006.

275. U.S. Army Corps of Engineers, “Ice Jam Flooding: Causes and Possible Solutions,” EP 1110-2-11, November 30, 1994.

276. U.S. Army Corps of Engineers, National Inventory of Dams, Website, http://crunch.tec.army.mil/nid/webpages/nid.cfm, accessed June 2006.

277. Removed

278. U.S. Department of Agriculture, Natural Resources Conservation Service, Web Soil Survey, Website, http://websoilsurvey.nrcs.usda.gov/app/, accessed January 2007.

279. Removed

280. United States Department of Agriculture, Soil Conservation, Cherokee County, South Carolina Soil Survey, 1977.

281. U.S. Department of Defense, “Unified Facilities Criteria, Design: Seismic Design for Buildings,” UFC 3-310-03A, March 1, 2005.

282. Removed

283. Removed

284. U.S. Environmental Protection Agency, STORET, Website, http://www.epa.gov/storet/, accessed May 2006.

285. LeGrand, Harry E. Sr., A Master Conceptual Model for Hydrogeological Site Characterization in the Piedmont and Mountain Region of North Carolina, Website, http://h2o.enr.state.nc.us/aps/gpu/documents/legrand_04.pdf#search=%22A%20Master%20Conceptual%20Model%20for%20Hydrogeological%20Site%20Characterization%20in%20the%20Piedmont%20and%20Mountain%20%22A%20Master%20Conceptual%20Model%20for%20Hydrogeological%20Site%20Characterization%20in%20the%20Piedmont%20and%20Mountain%20%22, November 11, 2006.

286. U.S. Geological Survey, “Estimated Use of Water in the United States, County-Level Data for 2000,” Website, http://water.usgs.gov/watuse/data/2000/index.html, accessed April 11, 2007.

287. U.S. Geological Survey, “Guidelines for Determining Flood Flow Frequency, Bulletin #17B of the Hydrology Subcommittee,” March 1982.

288. U.S. Geological Survey, Horton, Jr., Wright and Dicken, C., “Preliminary Digital Geologic Map of the Appalachian Piedmont and Blue Ridge, South Carolina Segment,” U.S. Geological Survey Open-File Report 01-298, revised 2004, Website, http://pubs.usgs.gov/of/2001/of01-298/, accessed on November 5,2006.

289. U.S. Geological Survey, Igage Mapping Corp., USGS topographic map using All Topo Maps V7, The Carolina’s, 2004.

290. U.S. Geological Survey, National Water Information System: Web Interface, USGS Surface-Water Data for the Nation, Website, http://waterdata.usgs.gov/usa/nwis/sw, accessed July 2006.

291. U.S. Geological Survey, "Potential of Hot-Dry-Rock Geothermal Energy in the Eastern United States," Open-File Report 93-377, November 1993.

292. Removed

293. U.S. Geological Survey, Water Resources Data, South Carolina Water Year 2005, 2006.

294. Weaver, J.C., "The Drought of 1998 - 2002 in North Carolina, Precipitation and Hydrologic Conditions," U.S. Geological Survey Scientific Investigations Report 2005-5053, Reston, Virginia, 2005.

295. U.S. Army Corps of Engineers, "Engineering and Design, Coastal Engineering Manual," EM 1110-2-1100, Change 2: June 1, 2006.

296. U.S. Geological Survey, Estimating the Magnitude of Peak Discharges for Selected Flood Frequencies on Small Streams in South Carolina [1975], Open File Report 82-337, 1975.

297. LeGrand, Harry E. Sr., *A Master Conceptual Model for Hydrogeological Site Characterization in the Piedmont and Mountain Region of North Carolina,* North Carolina Department of Environment and Natural Resources, Division of Water Quality, Groundwater Section, 2004.

298. Enercon Services, Inc., *Summary Report for Bathymetry Study*, September 2006.

299. U.S. Department of Interior, Johnson, A.I., “Specific Yield – Compilation of Specific Yields for Various Materials,” Geological Survey Water Supply Paper 1662-D, prepared in accordance with California Department of Water Resources, 1967, Table 1.

300. U.S. Department of Agriculture, Natural Resources Conservation Service, Web Soil Survey, Website, http://websoilsurvey.nrcs.usda.gov/app/HomePage.htm, accessed November 2008.

301. U.S. Department of Agriculture, Natural Resources Conservation Service, Web Soil Survey, Website, http://websoilsurvey.nrcs.usda.gov/app/HomePage.htm, accessed August 2009.

WLS COL 2.4-1

TABLE 2.4.1-201 (Sheet 1 of 2)
SITE FEATURES AND ELEVATIONS

Site Feature	Elevation (ft. msl)
Nuclear Island	590
Railcar Bay/Filter Storage Area door	590
Bottom of Basemat (Units 1 and 2)	550.5
Annex Building	590
Temporary Electric Power Supply Room door	590
Door to SO3 Stairs	590
Door to SO4 Stairs	590
Men's Change Room door	590
Corridor 40321 door	590
Corridor door 40311	590
Access Area 40300 doors	590
Containment Access Corridor Hatch and Door	597.1
Diesel Generator Building	590
Diesel Generator Room A doors	590
Diesel Generator Room B doors	590
Combustion Air Cleaner Area A plenum	590
Combustion Air Cleaner Area B plenum	590
Radwaste Building	590
Mobile Systems Facility doors	590
HVAC Equipment Room door	590
Electrical/Mechanical Equipment Room door	590
Turbine Building	590
Mobile Systems Facility doors	590
Door to SO2 Stairs	590
Aux Boiler Room door	590
Motor Driven Fire Pump Room door	590
Door to SO1 Stairs	590
Turbine Building Grade Deck Room 20300	590

Source: Westinghouse AP1000 DCD Rev 19; Tier 2, Chapter 1.2.

WLS COL 2.4-1

TABLE 2.4.1-201 (Sheet 2 of 2)
SITE FEATURES AND ELEVATIONS

Site Feature	Elevation (ft. msl)
Other Features	
Heavy Haul Road	588
Raw Water Intake Pumping Station (base)	497.3
Raw Water Intake Pumping Station (entry)	508
Lampson Crane	589
LLW Storage Area	588
Wastewater Treatment Area	588
Ninety-Nine Islands Dam Crest	511
Broad River above Ninety-Nine Islands Dam	511
Broad River below Ninety-Nine Islands Dam	440
Make-Up Pond A	547
Make-Up Pond B	570
Hold-Up Pond A	536
Make-Up Pond C	650
Cooling Tower Pad	610

ft. - feet

msl - mean sea level

WLS COL 2.4-1

TABLE 2.4.1-202 (Sheet 1 of 2)
DESCRIPTION OF UPPER BROAD RIVER WATERSHEDS

Watershed Name	Basin	Subbasin	Drainage Area (sq. mi.)	Drainage Area Above Ninety-Nine Islands Dam (sq. mi.)
Upper Broad River Basin (03050105) of North Carolina				
Upper Broad River and Lake Lure	03050105	030801	184	184
Second Broad River and tributaries	03050105	030802	513	513
Green River	03050105	030803	137	137
First Broad River	03050105	030804	426	426
Buffalo Creek	03050105	030805	181	163
North Palocet	03050105	030806	73	0
Upper Broad River Basin (03050105) of South Carolina				
Broad River	03050105	050	26	26
Broad River	03050105	090	129	65
Buffalo Creek	03050105	100	16	16
Cherokee Creek	03050105	110	23	23
Kings Creek	03050105	120	52	0
Thicketty Creek	03050105	130	157	0
Bullock Creek	03050105	140	118	0
North Pacolet River	03050105	150	49	0

WLS COL 2.4-1

TABLE 2.4.1-202 (Sheet 2 of 2)
DESCRIPTION OF UPPER BROAD RIVER WATERSHEDS

Watershed Name	Basin	Subbasin	Drainage Area (sq. mi.)	Drainage Area Above Ninety-Nine Islands Dam (sq. mi.)
South Pacolet River	03050105	160	91	0
Pacolet River	03050105	170	115	0
Lawsons Fork Creek	03050105	180	85	0
Pacolet River	03050105	190	102	0
Totals			2477	1553

Source (SC): Reference 268

Source (NC): Reference 230

sq. mi. - square miles

WLS COL 2.4-1

TABLE 2.4.1-203 (Sheet 1 of 2)
USGS GAUGING STATIONS ON THE BROAD RIVER

Station Name	Station Number	Location	Drainage Area (sq. mi.)	2005 Water Year Annual Mean Flow (cfs)
Broad River near Boiling Springs, NC	02151500	Lat. 35°12’39”, Long. 81°41’51”, on right bank half mi. upstream from Sandy Creek, 3 mi. downstream from Second Broad River, and 3½ mi. SW of Boiling Springs, Cleveland County.	864	NIA
Broad River near Blacksburg, SC	02153200	Lat 35°07'26", Long 81°35'17", at upstream side of bridge on SC Highway 18, 1.2 mi upstream of Buffalo Creek, 1.2 mi downstream of Gaston Shoals Reservoir, 3.2 mi west of Blacksburg, and at mile 275.2.	1290	1802
Broad River near Gaffney, SC	02153500	Water-stage recorder, Lat. 35°05’20”, Long. 81°34’20”, at a bridge on US Hwy. 29, 0.3 mi. upstream from Cherokee Creek, 4.4 mi. downstream from Gaston Shoals Dam, and 4.5 mi. ENE of Gaffney, Cherokee County.	1490	NIA
Broad River below Cherokee Falls, SC	02153551	Water-stage recorder, Lat. 35°01’52”, Long. 81°29’34”, at left bank of tailrace below Ninety-Nine Islands Reservoir, 3.1 mi. downstream of Cherokee Falls, and 0.3 mi. upstream of Kings Creek.	1550	2532

WLS COL 2.4-1

TABLE 2.4.1-203 (Sheet 2 of 2)
USGS GAUGING STATIONS ON THE BROAD RIVER

Station Name	Station Number	Location	Drainage Area (sq. mi.)	2005 Water Year Annual Mean Flow (cfs)
Broad River near Carlisle, SC	02156500	Water-stage recorder, Lat. 34°35'46", Long. 81°25'20", on right bank at downstream side of bridge on State Highway 72, 1.3 mi upstream from Sandy River, 2.0 mi downstream from Seaboard Coast Line Railroad bridge, 2.5 mi east of Carlisle, 5.0 mi downstream from Neal Shoals Dam, and at mile 226.0., Union County.	2790	3892

Source: References 214, 290, and 293.

See Figure 2.4.1-205

NIA = No Information Available

mi. - miles

sq. mi. - square miles

WLS COL 2.4-1

TABLE 2.4.1-204 (Sheet 1 of 2)
BROAD RIVER MONTHLY DISCHARGE AND TEMPERATURE VARIABILITY

DISCHARGE VARIABILITY

	Monthly Mean Stream Flow Recorded in Cubic Feet Per Second (cfs)											
Year	Jan	Feb	Mar	Apr	May	Jun	Jul	Aug	Sep	Oct	Nov	Dec
1998											1098	1253
1999	2021	2040	1812	1851	1422	964	796	517	538	925	1137	1338
2000	1619	1840	2142	1997	1301	713	591	518	678	669	1129	890
2001	865	985	1727	1318	793	801	1020	589	764	574	630	843
2002	1336	1139	1473	1104	835	560	377	242	505	865	1592	3312
2003	1441	2747	6686	8733	7433	5608	5051	4983	1838	1619	2094	2727
2004	1744	3100	1637	2104	1439	2626	1503	1219	8764	2219	3541	4710
2005	2615	2229	3930	3162	1926	2489	5418	1998	1356	2658	997	2031
2006	2659	1773	1516	1382	1100	1394	982	1254	2054	1245	1828	2143
Mean of Monthly Discharge	1852	2102	2779	2935	2202	2085	2194	1583	2285	1493	1655	2323
Max:	2659	3100	6686	8733	7433	5608	5418	4983	8764	2658	3541	4710
Min:	865	985	1473	1104	793	560	377	242	393	574	630	843

Notes:

Average annual flow: Approximately 2500 cfs (1926-2008)
Maximum monthly flow: 8764 cfs (1926-2006)
Minimum monthly flow: 242 cfs (1998-2006)
cfs - cubic feet per second
Source:
USGS 02153551 Broad River Below Ninety Nine Islands Reservoir, SC (1998 to 2006)

Cherokee County, South Carolina
Hydrologic Unit Code 03050105
Latitude 35°01'52", Longitude 81°29'34" NAD27
Drainage area 1550 square miles
Gauge datum 412.20 feet above sea level NGVD29
Missing data - No information available from USGS

Maximum and Minimum Monthly Average Flows
1998 - 2006

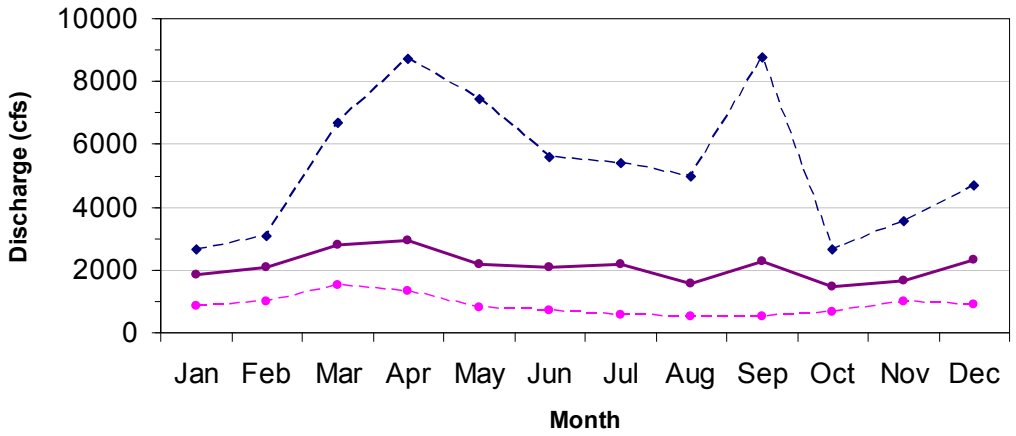

TABLE 2.4.1-204 (Sheet 2 of 2)
BROAD RIVER MONTHLY DISCHARGE AND TEMPERATURE VARIABILITY

TEMPERATURE VARIABILITY

	Monthly Mean Water Temperature (deg. C)											
YEAR	Jan	Feb	Mar	Apr	May	Jun	Jul	Aug	Sep	Oct	Nov	Dec
1996										16.9	11.3	7.55
1997	7.89	9.30	14.2	15.8	19.5	22.5	27.2	26.6	23.6	18.0	9.77	6.60
1998	7.40	8.77	11.3					27.2	25.4	19.1	13.4	9.81
1999	7.29	9.38	11.1	18.6	21.3	25.3	28.3	29.1	24.3	18.1	13.3	8.42
2000	6.87	8.33	14.0	16.5	23.7			27.9	23.6	18.4	11.9	
2001	4.92	9.86	11.7	18.3	23.3	26.4	27.0	28.3	23.6	17.3	12.7	10.6
2002	6.07	9.57	12.8	20.9	22.8	28.1	29.6	28.3	25.5	20.0		
2003		8.02	13.1	15.5	19.6	23.5	25.9	25.5		18.1	14.8	7.37
2004	6.83	6.83	13.4	17.5	24.4	26.0		26.4			14.0	7.54
2005	8.05	8.33	11.1	16.6	21.0				25.7	19.6	12.4	6.67
2006	8.42	8.51	13.0	19.8	22.2			28.5	24.3			
Mean of Monthly Temp.	7.10	8.70	12.6	17.7	22.0	25.4	27.7	27.5	24.5	18.4	12.6	8.10
Max:	8.4	9.9	14.2	20.9	24.4	28.1	29.6	29.1	25.7	20.0	14.8	10.6
Min:	4.9	6.8	11.1	15.5	19.5	22.5	25.9	25.5	23.6	16.9	9.8	6.6

Notes:

Average monthly temperature: 17.7°C
Average monthly maximum temperature: 19.6°C
Average monthly minimum temperature: 15.7°C
Maximum monthly temperature: 29.6°C
Minimum monthly temperature: 4.9°C
Degree Celsius - °C
Source:
USGS 02156500 Broad River Near Carlisle, SC (1996 to 2006)
No incomplete Data is used for Statistical Calculation

Union County, South Carolina
Hydrologic Unit Code 03050106
Latitude 34°35'46", Longitude 81°25'20" NAD27
Drainage area 2790 square miles
Gauge datum 290.79 feet above sea level NGVD29
Missing data - No information available

Maximum and Minimum Monthly Temperatures
1996 - 2006

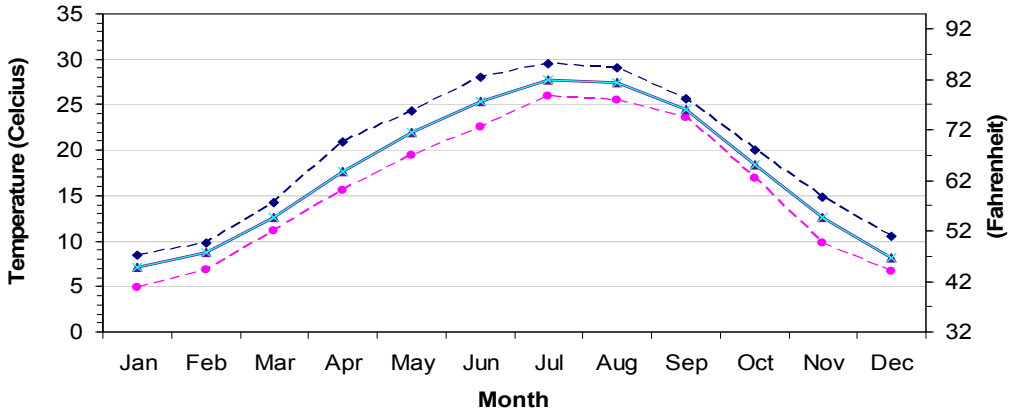

WLS COL 2.4-1

TABLE 2.4.1-205
MAJOR RESERVOIRS LOCATED IN THE UPPER BROAD RIVER BASIN

Name	In Service Date	Owner	Type	Drainage Area (sq. mi.)	Water Surface Area (ac.)	Dam Height (ft.)	Dam Length (ft.)	Spillway Width (ft.)	Normal Storage (ac.-ft.)	Flood Storage[a] (ac.-ft.)	Normal Pool Elevation (ft. msl)
Ninety-Nine Islands	1910	DPC	CNPG	1550	433	62	1568	891[2]	2300	2300	511[2]
King Mountain Reservoir (Moss Lake)	1973	City of King Mtn.	RE	68[1]	1329	99	840	(b)	44,400	53,280	736[2]
Lake Lure	1927	Town of Lake Lure	CNVA	95	740	124	480	(b)	32,295	44,914	991[2]
Lake Adger (Turner Shoals)	1925	Hydro, LLC	CNVA	138[1]	460[1]	90	689	(b)	11,700[1]	16,760	912[2]
Lake Summit	1920[2]	Duke Energy	CNSA	43[1]	276	130[2]	254[2]	(b)	9300	15,840	2012.6[2]
Lake Whelchel	1964	City of Gaffney	RE	14.7	177	61	2100	565	2438	5698	670[4]
Make-Up Pond C	(c)	Duke Energy	RE	3.87	620	132	2370	80	22,000	28,764	650

ac. - acre

ac.-ft. - acre-foot

sq. mi. - square miles

ft. - feet

msl - mean sea level

DPC - Duke Power Company

RE – earth filled

CN – concrete

CNPG – concrete gravity arch

CNVA - Concrete mult-arch

CNSA - Concrete single-arch

a) Dams and reservoirs on the Broad River and its major tributaries are utilized for thermoelectric power, water supply, and recreation and not for significant flood control.
b) No seismic design or spillway design criteria available for review.
c) Under development.

Sources:

1) Reference 230; North Carolina Department of Environmental and Natural Resources, "Broad River Basinwide Water Quality Plan", March 2003.

2) Reference 217; Duke Power Company, "Ninety-Nine Islands Hydro Project, FERC Project No. 2331, Determination of Probable Maximum Flood", Duke Engineering Services, Charlotte, North Carolina, November 7, 1997."

3) Reference 276; U.S. Army Corps of Engineers, "National Inventory of Dams, Website, http:/crunch/tec.army.mil/nid/webpages/nid.cfm, accessed June 2006

4) USGS Quadrangle, Blacksburg South, South Carolina

WLS COL 2.4-1

TABLE 2.4.1-206
SCDHEC 2005 WATER USAGE FOR CHEROKEE COUNTY, SOUTH CAROLINA

Usage	Quantity		
	Million Gallons	Mgd(1)	cfs
Public Supply	2561.1	7.02	10.9
Industrial	504.13	1.38	2.14
TOTAL	3065.23	8.4	13.02

Source: Reference 267

Mgd - Million gallons per day

cfs - cubic feet per second

SCDHEC - South Carolina Department of Health and Environmental Control

(1) Quantity reported by SCDHEC in Million Gallons. Mgd was estimated by dividing SCDHEC's reported 2005 water use by 365 days.

WLS COL 2.4-1

TABLE 2.4.1-207
SCDHEC 2005 WATER USAGE FOR CHEROKEE, CHESTER,
GREENVILLE, SPARTANBURG, UNION, AND YORK COUNTIES, SOUTH CAROLINA

County Name	Total Withdrawals					
	Groundwater		Surface Water		Total	
	Mgd	cfs	Mgd	cfs	Mgd	cfs
Cherokee, SC	0.003	0.005	8.39	13.0	8.40	13.0
Chester, SC	0.07	0.11	3.55	5.50	3.62	5.61
Greenville, SC	0.34	0.53	66.6	103	67.0	104
Spartanburg, SC	4.01	6.22	41.6	64.5	45.6	70.7
Union, SC	0.008	0.012	4.88	7.56	4.89	7.58
York, SC	0.27	0.42	93.1	144	93.4	145

Note: Withdrawal totals excluded hydroelectric power usage

Source: Reference 267

Mgd - Million gallons per day

cfs - cubic feet per second

WLS SUP 2.4-1

TABLE 2.4.1-208
2000 WATER USE TOTALS BY COUNTY IN THE UPPER BROAD RIVER WATERSHED

	Total Withdrawals					
	Groundwater		Surface Water		Total	
County Name	Mgd	cfs	Mgd	cfs	Mgd	cfs
Cherokee, SC	0.44	0.68	15.4	23.9	15.9	24.6
Chester, SC	1.80	2.79	4.6	7.1	6.4	9.9
Greenville, SC	3.03	4.70	53.3	82.6	56.3	87.1
Spartanburg, SC	4.01	6.22	57.0	88.3	61.0	94.4
Union, SC	0.25	0.39	8.2	12.7	8.5	13.2
York, SC	8.52	13.2	209	324	217	335.7
Buncombe, NC	8.77	13.6	33.7	52.3	42.5	65.8
Burke, NC	3.09	4.79	21.0	32.5	24.1	37.3
Catawba, NC	6.18	9.58	1182	1832	1188	1838
Cleveland, NC	2.51	3.89	189	293	192	297
Gaston, NC	7.67	11.9	965	1495	972	1504
Henderson, NC	3.7	5.74	13.4	20.8	17.1	26.5
Lincoln, NC	3.77	5.84	6.15	9.53	9.9	15.3
McDowell, NC	4.39	6.80	4.09	6.34	8.5	13.2
Polk, NC	1.24	1.92	1.48	2.29	2.7	4.2
Transylvania, NC	1.88	2.91	22.1	34.2	23.9	36.9

NOTES:

1. Greenville, Union, and York Counties within the Broad River Watershed are not part of the drainage basin for the Broad River adjacent to the site.

2. Cherokee, Cleveland, Polk, and Rutherford Counties compose the majority of the area in the Broad River Watershed above the site.

3. Total withdrawals for aquaculture and mining were 0 Mgd for all counties.

4. Hydroelectric water use not included.

Mgd - Million gallons per day

cfs - cubic feet per day

Source: Reference 286

WLS COL 2.4-1

TABLE 2.4.1-209 (Sheet 1 of 3)
AREA SURFACE WATER INTAKES IN AND DOWNSTREAM FROM THE UPPER BROAD RIVER WATERSHED

Facility	County, State	Distance		Source	Withdrawal Capacity		Consumptive Use(f)		Use Type
		mi.[a]	Direction		Mgd	cfs	Mgd	cfs	
Gaffney BPW	Cherokee, SC	8	Upstream	Lake Whelchel	12	18.6	NIA	NIA	Public Supply
Gaffney BPW	Cherokee, SC	9	Upstream	Broad River	(b)	(b)	NIA	NIA	Public Supply
CNA Holdings, Inc. – Ticona-Shelby	Cleveland, NC	12	Upstream	Buffalo Creek	1.15	1.78	0.290	0.45	Industrial
Shelby	Cleveland, NC	13	Upstream	Broad River	10 [c]	15.5	0	0	Public Supply
Northbrook Carolina Hydro, LLC – Stice Shoals Plant	Cleveland, NC	14	Upstream	First Broad River	(e)	(e)	(e)	(e)	Instream Hydro
Martin Marietta Materials, Inc (Kings Mountain Quarry)	Cleveland, NC	16	Upstream	Storm Water Quarry	0.23	0.36	0	0	Industrial
Kings Mountain	Cleveland, NC	17	Upstream	Moss Lake	37.6	58.3	1.611	2.50	Public Supply
Cleveland County Country Club	Cleveland, NC	18	Upstream	Lake/Pond	1.15	1.79	0.047	0.07	Golf Course
Shelby	Cleveland, NC	19	Upstream	First Broad River	18	28	2.424	4	Public Supply
Duke Energy Corp. – Cliffside Steam Station	Cleveland, NC	19	Upstream	Broad River	288	446	75	116	Industrial
Duke Energy Corp. – Cliffside Steam Station (planned)[d]	Cleveland, NC	19	Upstream	Broad River	32	50	20.645	32	Industrial
Cleveland-Caroknit	Cleveland, NC	25	Upstream	First Broad River	1	1.55	0.017	0.03	Industrial

WLS COL 2.4-1

TABLE 2.4.1-209 (Sheet 2 of 3)
AREA SURFACE WATER INTAKES IN AND DOWNSTREAM FROM THE UPPER BROAD RIVER WATERSHED

Facility	County, State	Distance		Source	Withdrawal Capacity		Consumptive Use(f)		Use Type
		mi.[(a)]	Direction		Mgd	cfs	Mgd	cfs	
Mako Marine International (formerly ITG/Burlington Industries – J.C. Cowan Plant)	Rutherford, NC	26	Upstream	Second Broad River	3	4.65	0.07	0.11	Industrial
Cleveland County Sanitary District	Cleveland, NC	27	Upstream	First Broad River	6	9.3	3.364	5.21	Public Supply
Cleveland County Sanitary District (planned)	Cleveland, NC	27	Upstream	Knob Creek	6	9.3	3.445	5.3	Public Supply
Forest City	Rutherford, NC	31	Upstream	Second Broad River	12	18.60	1.483	2.30	Public Supply
Broad River Water Authority (formerly Rutherfordton-Spindale)	Rutherford, NC	33	Upstream	Broad River	13	20.15	4.733	7.34	Public Supply
Northbrook Carolina Hydro, LLC – Turner Shoals Plant	Polk, NC	43	Upstream	Green River	(e)	(e)	(e)	(e)	Instream Hydro
Duke Energy Corp. – Tuxedo Hydro	Henderson, NC	52	Upstream	Lake Summit	(e)	(e)	(e)	(e)	Instream Hydro
Kenmure Country Club	Henderson, NC	54	Upstream	King Creek	0.82	1.26	0.97	1.50	Golf Course
City of Union	Union, SC	21	Downstream	Broad River	23.80	36.89	NIA	NIA	Public Supply
Carlisle Cone Mills	Union, SC	30	Downstream	Broad River	8.10	12.56	NIA	NIA	Public Supply
V.C. Summer Nuclear Station	Fairfield, SC	52	Downstream	Lake Monticello	3.1	4.81	NIA	NIA	Industrial

WLS COL 2.4-1

TABLE 2.4.1-209 (Sheet 3 of 3)
AREA SURFACE WATER INTAKES IN AND DOWNSTREAM FROM THE UPPER BROAD RIVER WATERSHED

Facility	County, State	Distance		Source	Withdrawal Capacity		Consumptive Use(f)		Use Type
		mi.[(a)]	Direction		Mgd	cfs	Mgd	cfs	
V.C. Summer Nuclear Station (planned)	Fairfield, SC	52	Downstream	Lake Monticello	NIA	NIA	NIA	NIA	Industrial

Notes:

a) Distance provided is a linear distance and not river miles.

b) The Gaffney BPW (Board of Public Works) system is authorized 18 Mgd and uses Lake Whelchel for storage.

c) The Shelby Broad River intake is used as a temporary emergency supply intake.

d) Additional Cliffside Steam Plant use rate is based on anticipated expansion of 1 unit. “Planned” figures include the consumption of the existing Cliffside Unit 5 (15 cfs), and the planned expansion unit (17 cfs)

e) Instream hydro facilities maximum use rate not reported. Instream water use indicates water is returned directly to source. Additional hydro facilities are present within watershed, but no withdrawal permits exist.

f) Consumptive Use based on reported withdrawals and returns from 1999 registration and 2002 LWSP reports.

Source: Reference 268, References 234 - 248, References 262 - 265.

See Figure 2.4.1-211

NIA - No Information Available

Mgd - Million gallons per day

cfs - cubic feet per second

WLS COL 2.4-1

TABLE 2.4.1-210
ESTIMATED SURFACE WATER WITHDRAWAL AND CONSUMPTION FOR LEE NUCLEAR STATION OPERATIONS

Broad River Flow Rates[a]		Average Withdrawal		Maximum Withdrawal	
cfs	gpm	gpm	cfs	gpm	cfs
Mean Annual Flow Approximately 2500 cfs (1926-2008)	1,122,000	35,030	78	60,001	134
Regulatory Low Flow[b] (FERC) 483 cfs	216,867	35,030	78	NA	NA

Broad River Flow Rates[a]		Average Consumption		Maximum Consumption	
cfs	gpm	gpm	cfs	gpm	cfs
Mean Annual Flow Approximately 2500 cfs (1926-2008)	1,122,000	24,813	55	28,274	63
Regulatory Low Flow[b] (FERC) 483 cfs	216,867	24,813	55	NA	NA

gpm - gallons per minute

cfs - cubic feet per second

NA - not applicable

Notes:

a) Broad River flow rates were compiled from USGS measurements recorded at the Gaffney Gauge (USGS Gauge #02153500), the Blacksburg Gauge (#02153200) and Boiling Springs Gauge (#02151500) for average annual flow.

b) The 7Q10 for the Gaffney gauge was determined to be 439 cfs using the USGS recommended Log-Pearson Type III distribution. However, because the 7Q10 is less than the Ninety-Nine Islands Dam FERC license minimum flow requirement of 483 cfs for July through November, the FERC license minimum flow was used as a constraint in evaluating operation during low flow conditions.

WLS COL 2.4-1

TABLE 2.4.1-211
ESTIMATED DISCHARGE VOLUME FROM STATION OPERATIONS

Broad River Flow Rates[a]		Average Discharge		Maximum Discharge	
cfs	gpm	gpm	cfs	gpm	cfs
Mean Annual Flow Approximately 2500 cfs (1926-2008)	1,122,000	8,216	18	28,778	64
Regulatory Low Flow[b] (FERC) 483 cfs	216,867	8,216	18	28,778	64

Notes:

a) Broad River flow rates were compiled from USGS measurements recorded at the Gaffney Gauge (USGS Gauge #02153500), the Blacksburg Gauge (#02153200) and Boiling Springs Gauge (#02151500) for average annual flow.

b) The 7Q10 for the Gaffney gauge was determined to be 439 cfs using the USGS recommended Log-Pearson Type III distribution. However, because the 7Q10 is less than the Ninety-Nine Islands Dam FERC license minimum flow requirement of 483 cfs for July through November, the FERC license minimum flow was used as a constraint in evaluating operation during low flow conditions.

Withheld from Public Disclosure Under 10 CFR 2.390(a)(6) & (a)(9)
(see COL Application Part 9)

TABLE 2.4.1-212 (Sheet 1 of 3)

WLS COL 2.4-4

HISTORICAL DOMESTIC WELLS IN VICINITY OF SITE

Withheld from Public Disclosure Under 10 CFR 2.390(a)(6) & (a)(9)
(see COL Application Part 9)

TABLE 2.4.1-212 (Sheet 2 of 3)

WLS COL 2.4-4

HISTORICAL DOMESTIC WELLS IN VICINITY OF SITE

Withheld from Public Disclosure Under 10 CFR 2.390(a)(6) & (a)(9)
(see COL Application Part 9)

TABLE 2.4.1-212 (Sheet 3 of 3)

WLS COL 2.4-4

HISTORICAL DOMESTIC WELLS IN VICINITY OF SITE

TABLE 2.4.2-201 (Sheet 1 of 2)
PEAK STREAMFLOW OF THE BROAD RIVER NEAR
GAFFNEY, SOUTH CAROLINA
WLS COL 2.4-2 (USGS STATION 02153500) 1939-1990

Water Year[(a)]	Date	Discharge (cfs)
1939	8/18/1939	21,000
1940	8/14/1940	119,000
1941	7/17/1941	26,000
1942	2/17/1942	21,800
1943	1/28/1943	38,400
1944	3/20/1944	21,700
1945	9/18/1945	61,600
1946	1/7/1946	43,400
1947	6/15/1947	27,800
1948	8/4/1948	25,600
1949	11/29/1948	35,700
1950	10/7/1949	31,000
1951	12/8/1950	23,900
1952	3/4/1952	44,200
1953	2/21/1953	21,900
1954	1/23/1954	41,000
1955	2/7/1955	14,700
1956	4/16/1956	22,400
1957	4/6/1957	23,400
1958	4/28/1958	37,900
1959	9/30/1959	38,600
1960	2/6/1960	37,200
1961	6/22/1961	26,600
1962	12/13/1961	28,400
1963	3/13/1963	41,800
1964	4/8/1964	31,100
1965	10/6/1964	67,100
1966	3/4/1966	32,600

TABLE 2.4.2-201 (Sheet 2 of 2)
PEAK STREAMFLOW OF THE BROAD RIVER NEAR
GAFFNEY, SOUTH CAROLINA
WLS COL 2.4-2 (USGS STATION 02153500) 1939-1990

Water Year[a]	Date	Discharge (cfs)
1967	8/24/1967	33,800
1968	3/13/1968	25,900
1969	4/19/1969	25,400
1970	8/10/1970	47,500
1971	10/31/1970	14,300
1972	10/16/1971	46,900
1973	3/17/1973	42,900
1974	4/5/1974	34,400
1975	3/15/1975	55,300
1976	10/18/1975	32,100
1977	10/10/1976	84,900
1978	11/7/1977	38,100
1980	7/21/1980	37,600
1981	10/1/1980	10,500
1982	1/4/1982	33,900
1983	2/3/1983	21,900
1984	2/14/1984	39,900
1985	8/18/1985	26,600
1986	8/18/1986	10,900
1987	3/1/1987	65,800
1988	1/20/1988	8,700
1989	2/28/1989	12,500
1990	10/2/1989	38,800

a) Water Year = October 1 to September 30

Note: Peak streamflow for water year 1979 not available.

(Reference 290)

TABLE 2.4.2-202
PEAK GAUGE HEIGHT OF THE BROAD RIVER BELOW
NINETY-NINE ISLANDS RESERVOIR, SOUTH CAROLINA
(USGS STATION 02153551) 1999-2005

WLS COL 2.4-2

Water Year[a]	Date	Gauge Height[b] (feet)	Discharge (cfs)
1999	4/2/1999	30.77	4,350
2000	3/21/2000	32.91	[c]
2001	3/30/2001	31.37	[c]
2002	1/24/2002	30.01	4,490
2003	3/20/2003	38.22	[c]
2004	9/9/2004	40.43	[c]
2005	12/10/2004	35.19	[c]

a) Water Year = October 1 to September 30

b) Datum = 412.2 feet above NGVD29

c) not recorded

(Reference 290)

TABLE 2.4.2-203
LOCAL INTENSE PROBABLE MAXIMUM PRECIPITATION FOR
THE LEE NUCLEAR SITE

WLS COL 2.4-2

	Duration								
	5-min.	15-min.	30-min.	1-hr.	6-hr.	12-hr.	24-hr.	48-hr.	72-hr.
PMP(in.)	6.2	9.7	14	18.9	29.9	35.5	40.4	44.3	46.8

Note: Durations from 5-min. to 1-hr. derived from HMR No. 52, 1-sq. mi. point rainfall. Durations from 6-hr. to 72-hr. derived from HMR No. 51, 10-sq. mi. point rainfall.

TABLE 2.4.2-204
SITE DRAINAGE AREAS DETAILS

WLS COL 2.4-2

Drainage Area	Area (ac.)	Time of Concentration (min.)	PMP Depth (in.)	Intensity (in/hr)	Flow Rate (cfs)	Water Surface Elevation[a] (ft.)
NW	50.26	54	18.2	20.2	1015	589.08
NE	38.49	122	22.6	11.1	427	588.88
SW	50.90	420	31.5	4.5	229	589.57
SE	33.50	55	18.4	20.1	673	588.81

a) Resulting water surface elevation at safety-related structures using HEC-RAS steady state flow analyses.

TABLE 2.4.3-201
BROAD RIVER WATERSHED PMP (IN.)
DEPTH-AREA-DURATION RELATIONSHIP

WLS COL 2.4-2

Area (sq. mi.)	Duration (hr.) 6	12	24	48	72
10	29.7	35.3	40	43.5	46
200	21.5	25.8	30.1	33.5	36
1000	15.9	20.7	24.8	28.2	30.1
5000	9.3	13.1	16.9	20.9	23
10,000	7.1	10.4	13.9	17.7	19.7
20,000	5.1	8.4	11.2	14.8	16.8

Note: Values derived from the all-season PMP charts published in HMR-51 (Reference 255).

TABLE 2.4.3-202
BROAD RIVER WATERSHED 6-HR.
INCREMENTAL PMP ESTIMATES

WLS COL 2.4-2

Duration (hr.)	Incremental PMP (in.)
6	0.38
12	0.46
18	0.59
24	0.83
30	1.38
36	4.30
42	12.80
48	2.09
54	1.03
60	0.69
66	0.52
72	0.41
Total	25.48

Note: Values derived from HMR-51 (Reference 255), HMR-52 (Reference 225) and the use of the USACE HMR-52 computer software (Reference 271). Critical storm was determined to be 1000 sq. mi. with a 270 degree orientation centered near the centroid of the watershed for Gaston Shoals Dam.

TABLE 2.4.3-203 (Sheet 1 of 7)

WLS COL 2.4-2

BROAD RIVER WATERSHED SUBBASIN HOURLY INCREMENTAL PMP ESTIMATES

	Subbasin Hourly Incremental PMP (in.)									
Time (hr.)	LS-1	LA-2	GD-3	LL-4	BR-5	BD3-6	2BR-7	BD2-8	SS-09	WLCHL
Day 1 0100	0.045	0.067	0.069	0.064	0.069	0.066	0.069	0.064	0.067	0.039
0200	0.045	0.067	0.069	0.064	0.069	0.066	0.069	0.064	0.067	0.039
0300	0.045	0.067	0.069	0.064	0.069	0.066	0.069	0.064	0.067	0.039
0400	0.045	0.067	0.069	0.064	0.069	0.066	0.069	0.064	0.067	0.039
0500	0.045	0.067	0.069	0.064	0.069	0.066	0.069	0.064	0.067	0.039
0600	0.045	0.067	0.069	0.064	0.069	0.066	0.069	0.064	0.067	0.039
0700	0.055	0.082	0.084	0.078	0.084	0.080	0.084	0.078	0.082	0.047
0800	0.055	0.082	0.084	0.078	0.084	0.080	0.084	0.078	0.082	0.047
0900	0.055	0.082	0.084	0.078	0.084	0.080	0.084	0.078	0.082	0.047
1000	0.055	0.082	0.084	0.078	0.084	0.080	0.084	0.078	0.082	0.047
1100	0.055	0.082	0.084	0.078	0.084	0.080	0.084	0.078	0.082	0.047
1200	0.055	0.082	0.084	0.078	0.084	0.080	0.084	0.078	0.082	0.047
1300	0.070	0.106	0.108	0.100	0.108	0.103	0.108	0.101	0.105	0.061
1400	0.070	0.106	0.108	0.100	0.108	0.103	0.108	0.101	0.105	0.061
1500	0.070	0.106	0.108	0.100	0.108	0.103	0.108	0.101	0.105	0.061
1600	0.070	0.106	0.108	0.100	0.108	0.103	0.108	0.101	0.105	0.061
1700	0.070	0.106	0.108	0.100	0.108	0.103	0.108	0.101	0.105	0.061
1800	0.070	0.106	0.108	0.100	0.108	0.103	0.108	0.101	0.105	0.061
1900	0.098	0.148	0.151	0.140	0.151	0.144	0.151	0.141	0.147	0.085
2000	0.098	0.148	0.151	0.140	0.151	0.144	0.151	0.141	0.147	0.085
2100	0.098	0.148	0.151	0.140	0.151	0.144	0.151	0.141	0.147	0.085
2200	0.098	0.148	0.151	0.140	0.151	0.144	0.151	0.141	0.147	0.085
2300	0.098	0.148	0.151	0.140	0.151	0.144	0.151	0.141	0.147	0.085
2400	0.098	0.148	0.151	0.140	0.151	0.144	0.151	0.141	0.147	0.085

TABLE 2.4.3-203 (Sheet 2 of 7)

WLS COL 2.4-2

BROAD RIVER WATERSHED SUBBASIN HOURLY INCREMENTAL PMP ESTIMATES

	Subbasin Hourly Incremental PMP (in.)									
Time (hr.)	LS-1	LA-2	GD-3	LL-4	BR-5	BD3-6	2BR-7	BD2-8	SS-09	WLCHL
Day 2 0100	0.143	0.215	0.220	0.204	0.220	0.210	0.220	0.205	0.215	0.124
0200	0.149	0.225	0.230	0.213	0.229	0.219	0.229	0.214	0.224	0.129
0300	0.157	0.237	0.242	0.224	0.242	0.231	0.242	0.225	0.236	0.136
0400	0.167	0.251	0.257	0.238	0.256	0.244	0.256	0.239	0.250	0.144
0500	0.178	0.267	0.274	0.253	0.274	0.261	0.274	0.255	0.266	0.154
0600	0.190	0.286	0.293	0.271	0.294	0.279	0.294	0.273	0.285	0.165
0700	0.357	0.542	0.563	0.511	0.576	0.530	0.574	0.520	0.541	0.311
0800	0.411	0.628	0.655	0.591	0.674	0.614	0.670	0.602	0.628	0.361
0900	0.465	0.715	0.750	0.672	0.778	0.700	0.773	0.687	0.715	0.407
1000	0.517	0.803	0.849	0.753	0.889	0.788	0.881	0.775	0.804	0.450
1100	0.567	0.891	0.950	0.834	1.007	0.878	0.995	0.865	0.894	0.489
1200	0.616	0.980	1.054	0.916	1.131	0.971	1.115	0.958	0.985	0.526
1300	0.774	1.272	1.415	1.185	1.594	1.281	1.551	1.275	1.288	0.641
1400	1.040	1.804	2.067	1.667	2.418	1.837	2.332	1.839	1.836	0.838
1500	1.261	2.429	2.821	2.211	3.324	2.462	3.202	2.459	2.473	1.002
1600	1.309	3.994	4.838	3.430	5.757	3.954	5.539	3.908	4.069	1.040
1700	1.182	2.167	2.512	1.987	2.970	2.208	2.858	2.210	2.209	0.942
1800	0.964	1.637	1.865	1.518	2.170	1.665	2.095	1.666	1.665	0.782
1900	0.311	0.471	0.487	0.445	0.497	0.461	0.495	0.452	0.470	0.269
2000	0.279	0.419	0.432	0.397	0.439	0.410	0.438	0.402	0.418	0.242
2100	0.252	0.377	0.387	0.357	0.391	0.368	0.391	0.361	0.376	0.218
2200	0.230	0.343	0.351	0.325	0.354	0.335	0.354	0.328	0.342	0.199
2300	0.213	0.318	0.325	0.302	0.327	0.311	0.327	0.304	0.317	0.185
2400	0.201	0.302	0.309	0.286	0.310	0.295	0.310	0.288	0.301	0.174

TABLE 2.4.3-203 (Sheet 3 of 7)

WLS COL 2.4-2

BROAD RIVER WATERSHED SUBBASIN HOURLY INCREMENTAL PMP ESTIMATES

	Subbasin Hourly Incremental PMP (in.)									
Time (hr.)	LS-1	LA-2	GD-3	LL-4	BR-5	BD3-6	2BR-7	BD2-8	SS-09	WLCHL
Day 3 0100	0.123	0.185	0.189	0.175	0.189	0.180	0.189	0.176	0.184	0.106
0200	0.123	0.185	0.189	0.175	0.189	0.180	0.189	0.176	0.184	0.106
0300	0.123	0.185	0.189	0.175	0.189	0.180	0.189	0.176	0.184	0.106
0400	0.123	0.185	0.189	0.175	0.189	0.180	0.189	0.176	0.184	0.106
0500	0.123	0.185	0.189	0.175	0.189	0.180	0.189	0.176	0.184	0.106
0600	0.123	0.185	0.189	0.175	0.189	0.180	0.189	0.176	0.184	0.106
0700	0.082	0.123	0.126	0.117	0.126	0.120	0.126	0.117	0.123	0.071
0800	0.082	0.123	0.126	0.117	0.126	0.120	0.126	0.117	0.123	0.071
0900	0.082	0.123	0.126	0.117	0.126	0.120	0.126	0.117	0.123	0.071
1000	0.082	0.123	0.126	0.117	0.126	0.120	0.126	0.117	0.123	0.071
1100	0.082	0.123	0.126	0.117	0.126	0.120	0.126	0.117	0.123	0.071
1200	0.082	0.123	0.126	0.117	0.126	0.120	0.126	0.117	0.123	0.071
1300	0.061	0.092	0.095	0.088	0.095	0.090	0.095	0.088	0.092	0.053
1400	0.061	0.092	0.095	0.088	0.095	0.090	0.095	0.088	0.092	0.053
1500	0.061	0.092	0.095	0.088	0.095	0.090	0.095	0.088	0.092	0.053
1600	0.061	0.092	0.095	0.088	0.095	0.090	0.095	0.088	0.092	0.053
1700	0.061	0.092	0.095	0.088	0.095	0.090	0.095	0.088	0.092	0.053
1800	0.061	0.092	0.095	0.088	0.095	0.090	0.095	0.088	0.092	0.053
1900	0.049	0.074	0.076	0.070	0.076	0.072	0.076	0.071	0.074	0.043
2000	0.049	0.074	0.076	0.070	0.076	0.072	0.076	0.071	0.074	0.043
2100	0.049	0.074	0.076	0.070	0.076	0.072	0.076	0.071	0.074	0.043
2200	0.049	0.074	0.076	0.070	0.076	0.072	0.076	0.071	0.074	0.043
2300	0.049	0.074	0.076	0.070	0.076	0.072	0.076	0.071	0.074	0.043
2400	0.049	0.074	0.076	0.070	0.076	0.072	0.076	0.071	0.074	0.043
Total	15.44	26.84	29.54	24.79	32.51	26.64	31.81	26.33	27.05	12.96

TABLE 2.4.3-203 (Sheet 4 of 7)

WLS COL 2.4-2

BROAD RIVER WATERSHED SUBBASIN HOURLY INCREMENTAL PMP ESTIMATES

	Subbasin Hourly Incremental PMP (in.)									
Time (hr.)	FB-10	GS-11	BD1-12	KMR-13	BC-14	BR-15	CC-16	USS-18A	2BR-19	MUPC
Day 1 0100	0.064	0.046	0.045	0.065	0.052	0.031	0.064	0.064	0.065	0.024
0200	0.064	0.046	0.045	0.065	0.052	0.031	0.064	0.064	0.065	0.024
0300	0.064	0.046	0.045	0.065	0.052	0.031	0.064	0.064	0.065	0.024
0400	0.064	0.046	0.045	0.065	0.052	0.031	0.064	0.064	0.065	0.024
0500	0.064	0.046	0.045	0.065	0.052	0.031	0.064	0.064	0.065	0.024
0600	0.064	0.046	0.045	0.065	0.052	0.031	0.064	0.064	0.065	0.024
0700	0.078	0.057	0.055	0.079	0.063	0.038	0.078	0.078	0.080	0.029
0800	0.078	0.057	0.055	0.079	0.063	0.038	0.078	0.078	0.080	0.029
0900	0.078	0.057	0.055	0.079	0.063	0.038	0.078	0.078	0.080	0.029
1000	0.078	0.057	0.055	0.079	0.063	0.038	0.078	0.078	0.080	0.029
1100	0.078	0.057	0.055	0.079	0.063	0.038	0.078	0.078	0.080	0.029
1200	0.078	0.057	0.055	0.079	0.063	0.038	0.078	0.078	0.080	0.029
1300	0.100	0.073	0.070	0.102	0.081	0.049	0.101	0.100	0.102	0.038
1400	0.100	0.073	0.070	0.102	0.081	0.049	0.101	0.100	0.102	0.038
1500	0.100	0.073	0.070	0.102	0.081	0.049	0.101	0.100	0.102	0.038
1600	0.100	0.073	0.070	0.102	0.081	0.049	0.101	0.100	0.102	0.038
1700	0.100	0.073	0.070	0.102	0.081	0.049	0.101	0.100	0.102	0.038
1800	0.100	0.073	0.070	0.102	0.081	0.049	0.101	0.100	0.102	0.038
1900	0.140	0.102	0.098	0.142	0.114	0.069	0.141	0.140	0.143	0.053
2000	0.140	0.102	0.098	0.142	0.114	0.069	0.141	0.140	0.143	0.053
2100	0.140	0.102	0.098	0.142	0.114	0.069	0.141	0.140	0.143	0.053
2200	0.140	0.102	0.098	0.142	0.114	0.069	0.141	0.140	0.143	0.053
2300	0.140	0.102	0.098	0.142	0.114	0.069	0.141	0.140	0.143	0.053
2400	0.140	0.102	0.098	0.142	0.114	0.069	0.141	0.140	0.143	0.053

TABLE 2.4.3-203 (Sheet 5 of 7)

WLS COL 2.4-2

BROAD RIVER WATERSHED SUBBASIN HOURLY INCREMENTAL PMP ESTIMATES

	Subbasin Hourly Incremental PMP (in.)									
Time (hr.)	FB-10	GS-11	BD1-12	KMR-13	BC-14	BR-15	CC-16	USS-18A	2BR-19	MUPC
Day 2 0100	0.204	0.148	0.143	0.207	0.165	0.100	0.206	0.204	0.208	0.077
0200	0.213	0.155	0.149	0.216	0.173	0.105	0.215	0.213	0.217	0.080
0300	0.224	0.163	0.157	0.228	0.182	0.110	0.226	0.224	0.229	0.085
0400	0.238	0.173	0.166	0.241	0.193	0.117	0.239	0.238	0.243	0.090
0500	0.254	0.184	0.178	0.257	0.205	0.124	0.255	0.253	0.259	0.096
0600	0.271	0.198	0.190	0.276	0.220	0.133	0.273	0.271	0.277	0.103
0700	0.511	0.370	0.357	0.516	0.410	0.247	0.514	0.510	0.527	0.181
0800	0.590	0.426	0.411	0.596	0.471	0.285	0.595	0.590	0.611	0.205
0900	0.670	0.481	0.465	0.676	0.533	0.319	0.675	0.670	0.697	0.225
1000	0.750	0.536	0.517	0.756	0.594	0.349	0.757	0.750	0.785	0.243
1100	0.831	0.589	0.567	0.835	0.656	0.376	0.839	0.832	0.876	0.258
1200	0.913	0.641	0.616	0.914	0.718	0.398	0.923	0.913	0.968	0.271
1300	1.180	0.811	0.774	1.171	0.918	0.468	1.196	1.182	1.282	0.309
1400	1.657	1.097	1.040	1.632	1.261	0.589	1.686	1.663	1.843	0.373
1500	2.191	1.335	1.261	2.159	1.572	0.690	2.233	2.198	2.470	0.429
1600	3.354	1.386	1.309	3.310	1.829	0.717	3.439	3.358	3.967	0.445
1700	1.972	1.251	1.182	1.939	1.456	0.652	2.009	1.979	2.216	0.407
1800	1.510	1.017	0.964	1.488	1.162	0.554	1.534	1.515	1.670	0.355
1900	0.445	0.323	0.311	0.450	0.359	0.216	0.448	0.445	0.458	0.162
2000	0.397	0.289	0.279	0.402	0.322	0.195	0.400	0.397	0.408	0.149
2100	0.357	0.261	0.252	0.363	0.291	0.177	0.360	0.357	0.366	0.137
2200	0.326	0.238	0.230	0.331	0.266	0.162	0.328	0.326	0.333	0.126
2300	0.302	0.221	0.213	0.307	0.246	0.150	0.304	0.302	0.308	0.117
2400	0.286	0.209	0.201	0.291	0.233	0.142	0.288	0.286	0.293	0.110

TABLE 2.4.3-203 (Sheet 6 of 7)

WLS COL 2.4-2

BROAD RIVER WATERSHED SUBBASIN HOURLY INCREMENTAL PMP ESTIMATES

	Subbasin Hourly Incremental PMP (in.)									
Time (hr.)	FB-10	GS-11	BD1-12	KMR-13	BC-14	BR-15	CC-16	USS-18A	2BR-19	MUPC
Day 3 0100	0.175	0.127	0.123	0.178	0.142	0.086	0.176	0.175	0.179	0.066
0200	0.175	0.127	0.123	0.178	0.142	0.086	0.176	0.175	0.179	0.066
0300	0.175	0.127	0.123	0.178	0.142	0.086	0.176	0.175	0.179	0.066
0400	0.175	0.127	0.123	0.178	0.142	0.086	0.176	0.175	0.179	0.066
0500	0.175	0.127	0.123	0.178	0.142	0.086	0.176	0.175	0.179	0.066
0600	0.175	0.127	0.123	0.178	0.142	0.086	0.176	0.175	0.179	0.066
0700	0.117	0.085	0.082	0.119	0.095	0.057	0.118	0.117	0.119	0.044
0800	0.117	0.085	0.082	0.119	0.095	0.057	0.118	0.117	0.119	0.044
0900	0.117	0.085	0.082	0.119	0.095	0.057	0.118	0.117	0.119	0.044
1000	0.117	0.085	0.082	0.119	0.095	0.057	0.118	0.117	0.119	0.044
1100	0.117	0.085	0.082	0.119	0.095	0.057	0.118	0.117	0.119	0.044
1200	0.117	0.085	0.082	0.119	0.095	0.057	0.118	0.117	0.119	0.044
1300	0.088	0.064	0.061	0.089	0.071	0.043	0.088	0.088	0.089	0.033
1400	0.088	0.064	0.061	0.089	0.071	0.043	0.088	0.088	0.089	0.033
1500	0.088	0.064	0.061	0.089	0.071	0.043	0.088	0.088	0.089	0.033
1600	0.088	0.064	0.061	0.089	0.071	0.043	0.088	0.088	0.089	0.033
1700	0.088	0.064	0.061	0.089	0.071	0.043	0.088	0.088	0.089	0.033
1800	0.088	0.064	0.061	0.089	0.071	0.043	0.088	0.088	0.089	0.033
1900	0.070	0.051	0.049	0.071	0.057	0.034	0.071	0.070	0.072	0.026
2000	0.070	0.051	0.049	0.071	0.057	0.034	0.071	0.070	0.072	0.026
2100	0.070	0.051	0.049	0.071	0.057	0.034	0.071	0.070	0.072	0.026
2200	0.070	0.051	0.049	0.071	0.057	0.034	0.071	0.070	0.072	0.026
2300	0.070	0.051	0.049	0.071	0.057	0.034	0.071	0.070	0.072	0.026
2400	0.070	0.051	0.049	0.071	0.057	0.034	0.071	0.070	0.072	0.026
Total	24.64	16.14	15.44	24.63	18.48	9.82	24.96	24.67	26.60	6.91

TABLE 2.4.3-203 (Sheet 7 of 7)

WLS COL 2.4-2

BROAD RIVER WATERSHED SUBBASIN HOURLY INCREMENTAL PMP ESTIMATES

	Subbasin Hourly Incremental PMP (in.)

Notes:

Reference Figure 2.4.3-203 for subbasin locations
LS-1, Lake Summit/Tuxedo Hydro
LA-2, Lake Adger/Turner Shoals
GD-3, Green River (Turner Shoals to Broad R.)
LL-4, Lake Lure/hydro
BR-5, Broad River (Lake Lure to Green R.)
BD3-6, Broad River (Green R. to Second Broad R.)
2BR-7, Second Broad River
BD2-8, Broad River (Second Broad R. to First Broad R.)
SS-09, Stice Shoals
FB-10, First Broad River (Stice Shoals to Broad R.)
GS-11, Broad River (First Broad to Gaston Shoals)
BD1-12, Broad River (Gaston Shoals to Buffalo Creek)
KMR-13, Kings Mountain Reservoir (Buffalo Cr.)
BC-14, Buffalo Creek (Kings Mountain Reservoir to Broad R.)
BR-15, Broad River (Buffalo Cr. to Ninety-Nine Islands)
CC-16, Cove Creek (Broad R. near Lake Lure)
USS-18A, Upper First Broad River
2BR-19, Upper Second Broad River
MUPC, Make-Up Pond C
WLCHL, Lake Whelchel

TABLE 2.4.3-204 (Sheet 1 of 2)
BROAD RIVER WATERSHED SUBBASIN PRECIPITATION LOSSES

WLS COL 2.4-2

		Initial	Antecedent Precipitation			PMP Precipitation		
Subbasin	CN	Losses (in.)	Depth (in.)	Losses (in.)	Excess (in.)	Depth (in.)	Losses (in.)	Excess (in.)
LS-1	55	1.64	6.18	4.51	1.66	15.44	2.86	12.57
LA-2	56	1.57	10.73	5.76	4.97	26.84	2.21	24.63
GD-3	60	1.33	11.81	5.41	6.40	29.54	1.64	27.89
LL-4	56	1.57	9.92	5.55	4.37	24.79	2.28	22.50
BR-5	58	1.45	13.01	5.90	7.11	32.51	1.77	30.74
BD3-6	64	1.13	10.66	4.67	5.99	16.64	1.33	25.31
2BR-7	60	1.33	12.72	5.54	7.18	31.81	1.57	30.23
BD2-8	66	1.03	10.53	4.35	6.17	26.33	1.16	25.16
SS-09	68	0.94	10.82	4.13	6.69	27.05	0.99	26.06
FB-10	71	0.82	9.86	3.63	6.23	24.64	0.83	23.81
GS-11	65	1.08	6.46	3.70	2.76	16.14	1.58	14.54
BD1-12	67	0.99	6.18	3.45	2.73	15.44	1.42	14.01
KMR-13	68	0.94	9.85	3.95	5.90	24.63	1.03	23.60
BC-14	67	0.99	7.39	3.70	3.69	18.48	1.30	17.18
BR-15	65	1.08	3.93	2.89	1.03	9.82	1.88	7.93
CC-16	56	1.57	9.99	5.63	4.35	24.96	2.30	22.67
USS-18A	56	1.57	9.87	5.61	4.26	24.67	2.31	22.36
2BR-19	56	1.57	10.64	5.78	4.86	26.60	2.23	24.37
MUPC	63.9	1.13	2.76	1.74	1.03	6.91	1.54	5.37
WLCHL	63.7	1.14	5.18	3.42	1.77	12.96	1.86	11.10

TABLE 2.4.3-204 (Sheet 2 of 2)
BROAD RIVER WATERSHED SUBBASIN PRECIPITATION LOSSES

Notes:

Reference Figure 2.4.3-203 for subbasin locations
LS-1, Lake Summit/Tuxedo Hydro
LA-2, Lake Adger/Turner Shoals
GD-3, Green River (Turner Shoals to Broad R.)
LL-4, Lake Lure/hydro
BR-5, Broad River (Lake Lure to Green R.)
BD3-6, Broad River (Green R. to Second Broad R.)
2BR-7, Second Broad River
BD2-8, Broad River (Second Broad R. to First Broad R.)
SS-09, Stice Shoals
FB-10, First Broad River (Stice Shoals to Broad R.)
GS-11, Broad River (First Broad to Gaston Shoals)
BD1-12, Broad River (Gaston Shoals to Buffalo Creek)
KMR-13, Kings Mountain Reservoir (Buffalo Cr.)
BC-14, Buffalo Creek (Kings Mountain Reservoir to Broad R.)
BR-15, Broad River (Buffalo Cr. to Ninety-Nine Islands)
CC-16, Cove Creek (Broad R. near Lake Lure)
USS-18A, Upper First Broad River
2BR-19, Upper Second Broad River
MUPC, Make-Up Pond C
WLCHL, Lake Whelchel

TABLE 2.4.3-205 (Sheet 1 of 7)

WLS COL 2.4-2

BROAD RIVER WATERSHED SUBBASIN UNIT HYDROGRAPHS

Time (hr.)	Subbasin Unit Hydrograph Discharge (cfs)								
	LS-1	LA-2	GD-3	LL-4	BR-5	BD3-6	2BR-7	BD2-8	SS-09
1	389	377	2	402	2	1	1	1	1
2	1597	2058	33	2055	33	22	24	32	12
3	2660	3601	144	3596	144	134	108	140	56
4	2883	4806	353	4799	352	380	270	364	156
5	2700	5306	660	5296	660	768	581	719	329
6	2400	4940	1051	5000	1050	1217	943	1140	589
7	2126	4490	1501	4500	1500	1729	1374	1712	941
8	1881	4138	1982	4086	1981	2272	1852	2254	1304
9	1652	3795	2470	3745	2469	2818	2354	2800	1705
10	1453	3437	2940	3390	2939	3163	2860	3147	2130
11	1271	3092	3276	3084	3275	3295	3350	3314	2565
12	1096	2805	3364	2798	3366	3200	3598	3250	3000
13	934	2515	3300	2508	3300	3080	3693	3110	3422
14	788	2232	3200	2225	3200	2950	3610	2950	3822
15	659	1964	3080	1958	3080	2800	3500	2825	4193
16	547	1715	2930	1709	2930	2670	3350	2700	4282
17	451	1488	2780	1483	2780	2560	3200	2600	4200
18	370	1283	2640	1279	2650	2439	3050	2457	4090
19	302	1101	2504	1097	2506	2327	2920	2349	3960
20	245	941	2379	937	2353	2197	2800	2220	3830
21	198	800	2238	797	2213	2079	2693	2105	3700
22	159	678	2087	675	2089	1976	2567	2003	3560
23	128	573	1954	570	1981	1864	2455	1893	3440
24	102	482	1816	480	1866	1747	2332	1777	3330
25	82	405	1700	403	1747	1627	2201	1657	3196
26	65	339	1603	337	1626	1507	2091	1537	3093
27	52	283	1504	282	1506	1389	1977	1438	2976
28	41	236	1404	235	1407	1291	1884	1338	2849
29	32	196	1306	195	1308	1194	1788	1240	2747
30	26	163	1209	162	1211	1101	1690	1145	2638
31	20	135	1116	134	1118	1011	1591	1053	2523

TABLE 2.4.3-205 (Sheet 2 of 7)

WLS COL 2.4-2 BROAD RIVER WATERSHED SUBBASIN UNIT HYDROGRAPHS

Time (hr.)	Subbasin Unit Hydrograph Discharge (cfs)								
	LS-1	LA-2	GD-3	LL-4	BR-5	BD3-6	2BR-7	BD2-8	SS-09
32	16	112	1026	111	1028	925	1493	965	2404
33	12	92	940	92	942	843	1396	881	2312
34	10	76	859	76	860	766	1301	802	2217
35	8	63	782	62	784	695	1209	728	2119
36	6	52	710	51	712	628	1121	659	2020
37	5	42	643	42	645	566	1036	595	1921
38	4	35	581	35	575	509	956	536	1822
39	3	28	524	28	519	457	880	482	1724
40	2	23	472	23	467	409	807	432	1627
41	2	19	423	19	419	365	740	387	1533
42	1	16	379	15	375	326	676	345	1442
43	1	13	339	13	336	290	617	308	1353
44	1	10	303	10	300	258	562	274	1268
45	1	8	270	8	267	228	511	243	1185
46	0	7	240	7	238	202	464	216	1107
47	0	6	213	6	211	179	421	191	1032
48	0	5	189	5	187	158	381	169	960
49	0	4	167	4	166	139	344	149	892
50	0	3	148	3	147	122	311	131	828
51	0	2	131	2	130	108	280	116	768
52	0	2	115	2	114	94	252	102	711
53	0	2	102	2	101	83	227	89	657
54	0	1	89	1	89	72	203	78	607
55	0	1	79	1	78	63	182	68	560
56	0	1	69	1	68	55	163	60	516
57	0	1	60	1	60	48	146	52	475
58	0	1	53	1	53	42	131	46	436
59	0	0	46	0	46	37	117	40	401
60	0	0	41	0	40	32	104	35	368
61	0	0	35	0	35	28	93	30	337
62	0	0	31	0	31	24	83	26	309

TABLE 2.4.3-205 (Sheet 3 of 7)

WLS COL 2.4-2 BROAD RIVER WATERSHED SUBBASIN UNIT HYDROGRAPHS

Time (hr.)	Subbasin Unit Hydrograph Discharge (cfs)								
	LS-1	LA-2	GD-3	LL-4	BR-5	BD3-6	2BR-7	BD2-8	SS-09
63	0	0	27	0	27	21	74	23	283
64	0	0	23	0	23	18	65	20	258
65	0	0	20	0	20	16	58	17	236
66	0	0	18	0	18	14	52	15	216
67	0	0	15	0	15	12	46	13	197
68	0	0	13	0	13	10	41	11	179
69	0	0	12	0	12	9	36	10	163
70	0	0	10	0	10	8	32	8	149
71	0	0	9	0	9	7	28	7	135
72	0	0	8	0	8	6	25	6	123
73	0	0	7	0	7	5	22	5	112
74	0	0	6	0	6	4	19	5	101
75	0	0	5	0	5	4	17	4	92
76	0	0	4	0	4	3	15	3	83
77	0	0	4	0	4	3	13	3	76
78	0	0	3	0	3	2	12	3	68
79	0	0	3	0	3	2	10	2	62
80	0	0	2	0	2	2	9	2	56
81	0	0	2	0	2	1	8	2	51
82	0	0	2	0	2	1	7	1	46
83	0	0	2	0	1	1	6	1	41
84	0	0	1	0	1	1	5	1	37
85	0	0	1	0	1	1	5	1	34
86	0	0	1	0	1	1	4	1	30
87	0	0	1	0	1	1	4	1	27
88	0	0	1	0	1	1	3	1	25
89	0	0	1	0	1	0	3	0	22
90	0	0	0	0	0	0	0	0	0

TABLE 2.4.3-205 (Sheet 4 of 7)

WLS COL 2.4-2 BROAD RIVER WATERSHED SUBBASIN UNIT HYDROGRAPHS

	Subbasin Unit Hydrograph Discharge (cfs)									
Time (hr.)	FB-10	GS-11	BD1-12	KMR-13	BC-14	BR-15	CC-16	USS-18A	2BR-19	WLCHL
1	5	12	18	2	2	7	339	392	358	55
2	103	154	224	45	34	94	1754	1862	1723	566
3	366	521	701	203	142	346	3273	3826	3509	1125
4	772	1041	1290	536	347	800	4323	5139	4670	1366
5	1243	1679	1481	1008	651	1409	4625	5785	5112	1230
6	1814	1823	1400	1606	1037	2104	4360	5530	4840	1050
7	2070	1695	1220	2175	1483	2270	3950	5080	4430	886
8	1970	1540	1039	2581	2021	2170	3568	4684	4059	736
9	1810	1390	852	2747	2522	2020	3203	4237	3715	606
10	1640	1248	698	2710	3008	1870	2870	3865	3321	482
11	1496	1108	549	2580	3301	1730	2554	3500	2979	376
12	1366	965	430	2420	3392	1595	2292	3159	2634	284
13	1245	829	338	2260	3320	1489	2034	2851	2354	213
14	1123	707	261	2110	3180	1359	1786	2547	2084	156
15	996	600	197	1974	3020	1249	1555	2255	1828	112
16	879	501	147	1838	2870	1129	1344	1982	1592	80
17	766	412	108	1705	2730	1007	1153	1731	1377	56
18	660	336	78	1581	2580	899	984	1503	1185	38
19	562	270	56	1469	2444	794	836	1298	1014	26
20	474	215	40	1351	2324	695	707	1116	863	18
21	396	170	28	1232	2214	603	595	956	732	12
22	329	134	20	1129	2092	519	499	815	619	8
23	271	104	14	1028	1987	443	417	693	521	5
24	222	80	9	930	1875	376	347	587	438	3
25	181	62	6	836	1781	318	288	496	366	2
26	146	47	4	747	1682	267	239	418	306	1
27	118	36	3	665	1581	223	198	352	255	1
28	94	27	2	589	1479	185	163	295	212	1
29	75	21	1	519	1378	153	134	247	176	0
30	60	15	1	456	1278	126	110	206	145	0
31	47	12	1	399	1181	104	90	172	120	0

TABLE 2.4.3-205 (Sheet 5 of 7)

WLS COL 2.4-2 BROAD RIVER WATERSHED SUBBASIN UNIT HYDROGRAPHS

Time (hr.)	Subbasin Unit Hydrograph Discharge (cfs)									
	FB-10	GS-11	BD1-12	KMR-13	BC-14	BR-15	CC-16	USS-18A	2BR-19	WLCHL
32	37	9	0	347	1088	85	74	143	99	0
33	29	6	0	302	999	69	60	119	82	0
34	23	5	0	261	914	56	49	99	67	0
35	18	4	0	226	834	46	40	82	55	0
36	14	3	0	194	759	37	33	68	45	0
37	11	2	0	167	689	30	27	56	37	0
38	8	1	0	143	623	24	22	46	30	0
39	7	1	0	122	563	19	17	38	25	0
40	5	1	0	104	507	15	14	31	20	0
41	4	1	0	89	456	12	11	26	16	0
42	3	0	0	75	410	10	9	21	13	0
43	2	0	0	64	367	8	7	18	11	0
44	2	0	0	54	328	6	6	14	9	0
45	1	0	0	46	293	5	5	12	7	0
46	1	0	0	39	261	4	4	10	6	0
47	1	0	0	33	232	3	3	8	5	0
48	1	0	0	27	206	2	3	6	4	0
49	0	0	0	23	183	2	2	5	3	0
50	0	0	0	19	162	2	2	4	3	0
51	0	0	0	16	143	1	1	4	2	0
52	0	0	0	13	127	1	1	3	2	0
53	0	0	0	11	112	1	1	2	1	0
54	0	0	0	9	99	1	1	2	1	0
55	0	0	0	8	87	0	1	2	1	0
56	0	0	0	7	76	0	0	1	1	0
57	0	0	0	5	67	0	0	1	1	0
58	0	0	0	4	59	0	0	1	0	0
59	0	0	0	4	52	0	0	1	0	0
60	0	0	0	3	45	0	0	1	0	0
61	0	0	0	3	40	0	0	0	0	0
62	0	0	0	2	35	0	0	0	0	0

TABLE 2.4.3-205 (Sheet 6 of 7)

WLS COL 2.4-2 BROAD RIVER WATERSHED SUBBASIN UNIT HYDROGRAPHS

	Subbasin Unit Hydrograph Discharge (cfs)									
Time (hr.)	FB-10	GS-11	BD1-12	KMR-13	BC-14	BR-15	CC-16	USS-18A	2BR-19	WLCHL
63	0	0	0	2	30	0	0	0	0	0
64	0	0	0	1	26	0	0	0	0	0
65	0	0	0	1	23	0	0	0	0	0
66	0	0	0	1	20	0	0	0	0	0
67	0	0	0	1	17	0	0	0	0	0
68	0	0	0	1	15	0	0	0	0	0
69	0	0	0	1	13	0	0	0	0	0
70	0	0	0	0	11	0	0	0	0	0
71	0	0	0	0	10	0	0	0	0	0
72	0	0	0	0	9	0	0	0	0	0
73	0	0	0	0	7	0	0	0	0	0
74	0	0	0	0	6	0	0	0	0	0
75	0	0	0	0	6	0	0	0	0	0
76	0	0	0	0	5	0	0	0	0	0
77	0	0	0	0	4	0	0	0	0	0
78	0	0	0	0	4	0	0	0	0	0
79	0	0	0	0	3	0	0	0	0	0
80	0	0	0	0	3	0	0	0	0	0
81	0	0	0	0	2	0	0	0	0	0
82	0	e	0	0	2	0	0	0	0	0
83	0	0	0	0	2	0	0	0	0	0
84	0	0	0	0	2	0	0	0	0	0
85	0	0	0	0	1	0	0	0	0	0
86	0	0	0	0	1	0	0	0	0	0
87	0	0	0	0	1	0	0	0	e	0
88	0	0	0	0	1	0	0	0	0	0
89	0	0	0	0	1	0	0	0	0	0
90	0	0	0	0	0	0	0	0	0	0

TABLE 2.4.3-205 (Sheet 7 of 7)

WLS COL 2.4-2

BROAD RIVER WATERSHED SUBBASIN UNIT HYDROGRAPHS

Notes:

Reference Figure 2.4.3-203 for subbasin locations
LS-1, Lake Summit/Tuxedo Hydro
LA-2, Lake Adger/Turner Shoals
GD-3, Green River (Turner Shoals to Broad R.)
LL-4, Lake Lure/hydro
BR-5, Broad River (Lake Lure to Green R.)
BD3-6, Broad River (Green R. to Second Broad R.)
2BR-7, Second Broad River
BD2-8, Broad River (Second Broad R. to First Broad R.)
SS-09, Stice Shoals
FB-10, First Broad River (Stice Shoals to Broad R.)
GS-11, Broad River (First Broad to Gaston Shoals)
BD1-12, Broad River (Gaston Shoals to Buffalo Creek)
KMR-13, Kings Mountain Reservoir (Buffalo Cr.)
BC-14, Buffalo Creek (Kings Mountain Reservoir to Broad R.)
BR-15, Broad River (Buffalo Cr. to Ninety-Nine Islands)
CC-16, Cove Creek (Broad R. near Lake Lure)
USS-18A, Upper First Broad River
2BR-19, Upper Second Broad River
WLCHL, Lake Whelchel

TABLE 2.4.3-206 (Sheet 1 of 2)
BROAD RIVER WATERSHED SUBBASIN INPUT PARAMETERS

			Base Flow (Recession Method), Recession Constant, k = 0.4919		Loss Rates (SCS Method)	
	Subbasin	Area (sq. mi.)	Initial Discharge per Area (cfs / sq. mi.)	Recession Threshold (cfs)	Curve Number CN	% Impervious Area
WLS COL 2.4-2	LS-1	42.4	1.62	254	55	0.91
	LA-2	94.5	1.64	567	56	0.63
	GD-3	106.6	1.64	640	60	0.01
	LL-4	94.3	1.64	566	56	1.18
	BR-5	106.7	1.64	640	58	0
	BD3-6	101.8	1.64	611	64	0
	2BR-7	131	1.65	786	60	0
	BD2-8	103.3	1.64	620	66	0.45
	SS-09	182	1.66	1092	68	0
	FB-10	36.4	1.61	218	71	0
	GS-11	27.6	1.61	166	65	1.7
	BD1-12	17.38	1.59	102	67	1.7
	KMR-13	67.97	1.63	408	68	1.7
	BC-14	108.44	1.64	648	67	1.7
	BR-15	44.61	1.63	378	65	1.7
	CC-16	79	1.64	474	56	0
	USS-18A	106	1.64	636	56	0
	2BR-19	90	1.64	540	56	0
	MUPC	3.87	1.63	23	63.9	27.8
	WLCHL	14.71	1.63	88	63.7	2.5

TABLE 2.4.3-206 (Sheet 2 of 2)
BROAD RIVER WATERSHED SUBBASIN INPUT PARAMETERS

Notes:

Reference Figure 2.4.3-203 for subbasin locations
LS-1, Lake Summit/Tuxedo Hydro
LA-2, Lake Adger/Turner Shoals
GD-3, Green River (Turner Shoals to Broad R.)
LL-4, Lake Lure/hydro
BR-5, Broad River (Lake Lure to Green R.)
BD3-6, Broad River (Green R. to Second Broad R.)
2BR-7, Second Broad River
BD2-8, Broad River (Second Broad R. to First Broad R.)
SS-09, Stice Shoals
FB-10, First Broad River (Stice Shoals to Broad R.)
GS-11, Broad River (First Broad to Gaston Shoals)
BD1-12, Broad River (Gaston Shoals to Buffalo Creek)
KMR-13, Kings Mountain Reservoir (Buffalo Cr.)
BC-14, Buffalo Creek (Kings Mountain Reservoir to Broad R.)
BR-15, Broad River (Buffalo Cr. to Ninety-Nine Islands)
CC-16, Cove Creek (Broad R. near Lake Lure)
USS-18A, Upper First Broad River
2BR-19, Upper Second Broad River
MUPC, Make-Up Pond C
WLCHL, Lake Whelchel

TABLE 2.4.3-207
MAKE-UP POND C SUBBASIN UNIT HYDROGRAPH

Time (min.)	Discharge (cfs)	Time (min.)	Discharge (cfs)	Time (min.)	Discharge (cfs)
10	124	150	333	290	21
20	380	160	273	300	17
30	843	170	227	310	14
40	1472	180	187	320	12
50	1641	190	154	330	10
60	1590	200	125	340	8
70	1410	210	103	350	7
80	1240	220	85	360	6
90	1083	230	69	370	4
100	942	240	57	380	3
110	794	250	46	390	2
120	660	260	38	400	1
130	533	270	31	410	0
140	419	280	26	420	0

Notes:
Reference Figure 2.4.3-203 for subbasin locations
MUPC, Make-Up Pond C

TABLE 2.4.3-208
MAKE-UP POND B SUBBASIN UNIT HYDROGRAPH

Time (min.)	Discharge (cfs)	Time (min.)	Discharge (cfs)	Time (min.)	Discharge (cfs)
10	81	150	220	290	14
20	251	160	180	300	11
30	556	170	150	310	9
40	971	180	123	320	8
50	1082	190	102	330	6
60	1050	200	82	340	5
70	930	210	68	350	5
80	820	220	56	360	4
90	714	230	45	370	3
100	621	240	37	380	2
110	523	250	30	390	2
120	435	260	25	400	1
130	352	270	21	410	0
140	277	280	17	420	0

TABLE 2.4.4-201
PEAK FLOWS AND RESULTING WATER SURFACE ELEVATIONS

WLS COL 2.4-2

Event	Model	Peak Flow (cfs)	Lee Nuclear Station Water Surface Elevation (ft.)	Ninety-Nine Islands Dam Elevation (ft.)
PMF (no breach)	HEC-HMS	802,000	(a)	542.78
PMF (no breach)	HEC-RAS (unsteady state)	823,000	551.49	546.06
PMF (no breach)	HEC-RAS (steady state)	823,000	552.61	546.06
Gaston Shoals Dam failure coincident with the PMF	HEC-RAS (unsteady state)	824,000	551.52	546.09
Gaston Shoals Dam and Cherokee Falls Dam failures coincident with the PMF	HEC-RAS (unsteady state)	824,000	551.52	546.09
Major upstream structures failures coincident with the PMF(b)	HEC-HMS	1,720,000	(a)	559.76
Major upstream structures failures coincident with the PMF(b)	HEC-RAS (steady state)	1,720,000	573.26	561.70

a) Not calculated. Resulting hydrographs or peak flow used as input to the HEC-RAS model to determine the water surface elevations at the Lee Nuclear Station.

b) Upstream failures include overtopping failure of Lake Lure Dam, Tuxedo Dam, Turner Shoals Dam, Kings Mountain Reservoir Dam, Lake Whelchel, Lake Cherokee, and Make-Up Pond C. All failures occur simultaneously with a failure time near to the peak PMF outflow at Ninety-Nine Islands Dam.

WLS SUP 2.4.7-1

TABLE 2.4.7-201 (SHEET 1 OF 2)
WATER TEMPERATURE DATA FOR THE BROAD RIVER NEAR GAFFNEY, SOUTH CAROLINA
(USGS STATION 02153500)

SAMPLE DATE	°F
8/26/1969	75.0
9/24/1969	68.7
10/22/1969	65.8
11/17/1969	44.6
12/15/1969	44.1
1/11/1970	43.7
1/20/1970	42.6
2/19/1970	52.2
3/20/1970	53.4
4/27/1970	65.1
5/21/1970	76.1
6/16/1970	77.4
7/7/1970	83.1
8/18/1970	78.4
9/15/1970	80.6
10/15/1970	73.0
11/20/1970	52.7
12/21/1970	48.2
1/11/1971	43.7
2/22/1971	54.5
3/23/1971	53.6
4/19/1971	66.2
5/10/1971	69.8
6/14/1971	77.9
7/8/1971	76.1
8/24/1971	78.8
9/13/1971	76.1
10/4/1971	75.2

WLS SUP 2.4.7-1

TABLE 2.4.7-201 (SHEET 2 OF 2)
WATER TEMPERATURE DATA FOR THE BROAD RIVER NEAR GAFFNEY, SOUTH CAROLINA
(USGS STATION 02153500)

SAMPLE DATE	°F
11/22/1971	45.5
12/9/1971	49.1
1/19/1972	42.8
2/9/1972	41.9
3/24/1972	50
4/20/1972	68.9
5/22/1972	67.1
6/13/1972	72.5
7/25/1972	83.3
8/24/1972	79.7
10/2/1972	64.4
10/25/1972	62.6
11/16/1972	51.8
12/29/1972	46.4
1/23/1973	50.9
2/8/1973	48.2
3/20/1973	53.6
4/25/1973	64.4
5/30/1973	69.8
6/21/1973	71.6
Min T, 2/9/1972	41.9
Max T, 7/25/1972	83.3

(Reference 290)

WLS SUP 2.4.11-1

TABLE 2.4.11-201
MINIMUM DAILY STREAMFLOW OBSERVED ON THE BROAD RIVER BELOW NINETY-NINE ISLANDS DAM, SOUTH CAROLINA, (USGS STATION 02153551)
1998-2006

Climatic Year[a]	Date	Minimum Flow, cfs
1998[b]	11/2/1998	805
1999	9/18/1999	233
2000	9/16/2000	342
2001	9/14/2001	224
2002	9/14/2002	138
2003	9/21/2003	1,230
2004	8/18/2004	605
2005	11/7/2005	851
2006[b]	7/12/2006	534

a) Climatic Year – April 1 to March 31

b) Year 1998 incomplete, available data 10/30/1998 – 3/31/1999
Year 2006 incomplete, available data 4/1/2006 – 9/30/2006

(Reference 290)

WLS SUP 2.4.11-1

TABLE 2.4.11-202 (SHEET 1 OF 2)
MINIMUM DAILY STREAMFLOW OBSERVED ON THE BROAD RIVER NEAR GAFFNEY, SOUTH CAROLINA, (USGS STATION 02153500) 1938-1990

Climatic Year[a]	Date	Minimum Flow, cfs
1938[b]	12/24/1938	985
1939	10/22/1939	586
1940	7/2/1940	443
1941	10/14/1941	466
1942	7/21/1942	659
1943	9/27/1943	699
1944	9/10/1944	730
1945	9/3/1945	743
1946	10/7/1946	811
1947	9/22/1947	657
1948	7/6/1948	845
1949	7/5/1949	1,260
1950	10/16/1950	991
1951	10/21/1951	598
1952	7/29/1952	746
1953	8/30/1953	466
1954	10/24/1954	224
1955	9/20/1955	444
1956	9/3/1956	300
1957	9/8/1957	381
1958	12/7/1958	867
1959	8/24/1959	986
1960	9/26/1960	1,050
1961	10/10/1961	908
1962	9/3/1962	947
1963	8/19/1963	651
1964	9/28/1964	942
1965	9/19/1965	916

WLS SUP 2.4.11-1

TABLE 2.4.11-202 (SHEET 2 OF 2)
MINIMUM DAILY STREAMFLOW OBSERVED ON THE BROAD RIVER NEAR GAFFNEY, SOUTH CAROLINA, (USGS STATION 02153500) 1938-1990

Climatic Year[a]	Date	Minimum Flow, cfs
1966	9/11/1966	682
1967	8/20/1967	874
1968	9/4/1968	468
1969	7/21/1969	1,140
1970	7/21/1970	836
1971[b]	7/19/1971 & 9/16/1971	1,270
1986[b]	7/15/1986	261
1987	10/11/1987	560
1988	7/29/1988	300
1989	8/11/1989	656
1990[b]	9/28/1990	1,030

a) Climatic Year – April 1 to March 31

b) Year 1938 incomplete, available data 12/1/1938 - 3/31/1939

Year 1971 incomplete, available data 4/1/1971 - 9/30/1971

No data available from 9/30/1971 - 6/9/1986

Year 1986 incomplete, available data 6/9/1986 - 3/31/1987

Year 1990 incomplete, available data 4/1/1990 - 9/30/1990

(Reference 290)

TABLE 2.4.11-203
100-YR. RETURN PERIOD LOW FLOW RATES[a]

		Duration, days		
		1	7	30
WLS SUP 2.4.11-1	Flow Rate, cfs	172	269	346

a) Low flow based on statistical analysis of combined data for USGS gauges on the Broad River near Gaffney, South Carolina (USGS No. 02153500 climatic years from 1938 to 1990) and below Ninety-Nine Islands Dam (USGS No. 02153551 climatic years from 1998 to 2002).

WLS COL 2.4-4

TABLE 2.4.12-201 (Sheet 1 of 4)
WELL CONSTRUCTION AND WATER TABLE ELEVATIONS (FT ABOVE MSL)

	Reference Elevations		Well Construction Depths							Additional Info	
Well I.D.	GL Elev	TOC Elev	Boring Depth	TD from TOC	B/Screen	T/Screen	T/Sand	T/Seal	Material	DTW WD	Date Plugged
MW-1200	591.93	593.99	41	41.93	40	25	23	20	2-inch PVC Sch40	23.0	NA
MW-1201	589.91	592.12	102.5	103.81	101.5	86.5	84.5	82.5	2-inch PVC Sch40	37.0	NA
MW-1201A	590.07	592.11	48	49.78	47	37	36	34	2-inch PVC Sch40	37.0	NA
MW-1202	587.47	589.68	78.5	79.82	77.5	62.5	58	55	2-inch PVC Sch40	20.6	NA
MW-1203	589.51	591.87	77	77.67	75	60	58	55	2-inch PVC Sch40	22.5	NA
MW-1204	609.92	612.42	115	116.59	114	99	97	95	2-inch PVC Sch40	37.1	NA
MW-1204A	609.93	612.42	50	51.82	49	39	37	35	2-inch PVC Sch40	37.1	NA
MW-1205	609.99	612.59	124	125.33	123	108	106	104	2-inch PVC Sch40	43.9	NA
MW-1206	589.66	591.51	68.5	69.89	67.5	52.5	50	47.5	2-inch PVC Sch40	31.7	NA
MW-1206A	589.75	591.43	43	44.09	42	32	31	29	2-inch PVC Sch40	31.7	NA
MW-1207	589.03	591.39	108	110.02	107	92	90	88	2-inch PVC Sch40	29.2	NA
MW-1207A	588.91	591.05	43	44.68	42	32	31	29	2-inch PVC Sch40	29.2	NA
MW-1208	587.77	590.00	79	78.92	76.5	61.5	59	56	2-inch PVC Sch40	47.0	NA
MW-1209	586.91	588.91	106	106.28	104	89	87	84.6	2-inch PVC Sch40	16.3	NA
MW-1209A	586.93	589.03	28	29.45	27	17	16	14	2-inch PVC Sch40	16.3	NA
MW-1210	589.78	592.27	101.5	103.10	101.5	86.5	84.5	82.5	2-inch PVC Sch40	16.5	NA
MW-1210A	589.42	591.66	30	32.06	29	19	18	16	2-inch PVC Sch40	16.5	NA
MW-1211	589.88	591.63	39	39.94	37.5	22.5	20.5	18	2-inch PVC Sch40	21.5	NA
MW-1212	610.24	612.29	47.5	48.88	46.5	31.5	29.5	26.5	2-inch PVC Sch40	31.0	NA
MW-1213	NA	NA	78.30	NA	NA	NA	NA	NA	NA	18.0	4/11/06
MW-1214	605.00	606.51	44.5	44.74	43	28	26	23	2-inch PVC Sch40	14.0	NA

WLS COL 2.4-4

TABLE 2.4.12-201 (Sheet 2 of 4)
WELL CONSTRUCTION AND WATER TABLE ELEVATIONS (FT ABOVE MSL)

	Reference Elevations		Well Construction Depths							Additional Info	
Well I.D.	GL Elev	TOC Elev	Boring Depth	TD from TOC	B/Screen	T/Screen	T/Sand	T/Seal	Material	DTW WD	Date Plugged
MW-1215	590.22	592.13	101.5	101.20	100	40	38	35.5	6-inch PVC	35.0	NA
MW-1216	588.01	590.69	29.0	31.31	28.0	18	17	15	2-inch PVC Sch40	18.0	NA
MW-1217	587.64	590.10	24.0	24.85	22.3	12	11	9	2-inch PVC Sch40	10.5	NA
MW-1218	588.12	590.18	16.0	18.31	15.0	5	4	2	2-inch PVC Sch40	17.5	NA
DW2	588.94	589.67	NIA	~150	NIA	NIA	NIA	NIA	6-inch Metal	NIA	NA
DW3	590.56	591.34	NIA	~107.5	NIA	NIA	NIA	NIA	6-inch PVC	NIA	NA
DW4	591.22	591.51	NIA	~130	NIA	NIA	NIA	NIA	6-inch PVC	NIA	NA
DW5	587.73	589.20	NIA	>201	NIA	NIA	NIA	NIA	6-inch Metal	NIA	NA

WLS COL 2.4-4

TABLE 2.4.12-201 (Sheet 3 of 4)
WELL CONSTRUCTION AND WATER TABLE ELEVATIONS (FT ABOVE MSL)

	Location Information				Reference Elevations		Well Construction Elevations				
Well I.D.	Latitude	Longitude	Northing	Easting	GL Elev	TOC Elev	T/Sand Elev.	T/Screen Elev.	B/Screen Elev.	Boring Depth Elev.	Date Completed
MW-1200	35.03776	-81.51582	1166348.442	1845571.069	591.93	593.99	568.93	566.93	551.93	550.93	4/10/06
MW-1201	35.03872	-81.51247	1166689.304	1846578.824	589.91	592.12	505.41	503.41	488.41	487.41	4/14/06
MW-1201A	NM	NM	1166693.529	1846576.539	590.07	592.11	554.07	553.07	543.07	542.07	7/18/06
MW-1202	35.03962	-81.50948	1167018.978	1847472.030	587.47	589.68	529.47	524.97	509.97	508.97	4/14/06
MW-1203	35.03874	-81.50824	1166702.120	1847838.422	589.51	591.87	531.51	529.51	514.51	512.51	4/11/06
MW-1204	35.03719	-81.50761	1166141.154	1848033.400	609.92	612.42	512.92	510.92	495.92	494.92	4/14/06
MW-1204A	NM	NM	1166133.724	1848034.258	609.93	612.42	572.93	570.93	560.93	559.93	7/17/06
MW-1205	35.03582	-81.50665	1165631.431	1848304.849	609.99	612.59	503.99	501.99	486.99	485.99	4/15/06
MW-1206	35.03862	-81.50948	1166655.908	1846689.086	589.66	591.51	539.66	537.16	522.16	521.16	4/18/06
MW-1206A	NM	-81.50948	1166656.288	1846693.299	589.75	591.43	558.75	557.75	547.75	546.75	7/17/06
MW-1207	35.03912	-81.51216	1166849.173	1846668.764	589.03	591.39	499.03	497.03	482.03	481.03	4/24/06
MW-1207A	NM	NM	1166846.232	1846673.410	588.91	591.05	557.91	556.91	546.91	545.91	7/18/06
MW-1208	35.04006	-81.51243	1167188.532	1846583.513	587.77	590.00	528.77	526.27	511.27	508.77	4/13/06
MW-1209	35.03431	-81.50742	1165084.761	1848071.547	586.91	588.91	499.91	497.91	482.91	480.91	4/18/06
MW-1209A	NM	NM	1165076.658	1848072.885	586.93	589.03	570.93	569.93	559.93	558.93	7/17/06
MW-1210	35.03496	-81.50956	1165321.305	1847439.208	589.78	592.27	505.28	503.28	488.28	488.28	4/16/06
MW-1210A	NM	NM	1165312.832	1847436.803	589.42	591.66	571.42	570.42	560.42	559.42	7/17/06
MW-1211	35.03460	-81.51307	1165197.583	1846406.261	589.88	591.63	569.38	567.38	552.38	550.88	4/11/06
MW-1212	35.03508	-81.51621	1165365.927	1845452.195	610.24	612.29	580.74	578.74	563.74	562.74	4/10/06
MW-1213	35.03876	-81.51229	NM	NM	NA	NA	NA	NA	NA	NA	NA
MW-1214	35.03181	-81.51050	1164177.882	1847153.830	605.00	606.51	579.00	577.00	562.00	560.50	4/11/06

WLS COL 2.4-4

TABLE 2.4.12-201 (Sheet 4 of 4)
WELL CONSTRUCTION AND WATER TABLE ELEVATIONS (FT ABOVE MSL)

	Location Information				Reference Elevations		Well Construction Elevations				
Well I.D.	Latitude	Longitude	Northing	Easting	GL Elev	TOC Elev	T/Sand Elev.	T/Screen Elev.	B/Screen Elev.	Boring Depth Elev.	Date Completed
MW-1215	35.03876	-81.51230	1166710.545	1846624.819	590.22	592.13	552.22	550.22	490.22	488.72	4/17/06
MW-1216	35.03452	-81.51129	1165171.882	1846927.273	588.01	590.69	571.01	570.01	560.01	559.01	7/19/06
MW-1217	35.03419	-81.51109	1165042.463	1846983.878	587.64	590.10	574.64	573.64	563.64	563.64	7/19/06
MW-1218	35.03368	-81.51059	1164859.672	1847139.635	588.12	590.18	584.12	583.12	573.12	572.12	7/18/06
DW2	35.03489	-81.51162	1165319.974	1846821.466	588.94	589.67	NIA	NIA	NIA	NIA	~1977
DW3	35.03521	-81.51028	1165408.943	1847234.503	590.56	591.34	NIA	NIA	NIA	NIA	~1977
DW4	35.03412	-81.51358	1165035.485	1846277.086	591.22	591.51	NIA	NIA	NIA	NIA	~1977
DW5	NM	NM	1167933.393	1847896.940	587.73	589.20	NIA	NIA	NIA	NIA	~1977

TOC Elev. = top of casing elevations obtained from professional surveyors (McKim & Creed)

GL Elev. = ground level elevations obtained from professional surveyors (McKim & Creed)

Latitude, Longitude: Obtained using hand-held Garmin Rino 120 GPS unit

Northing/Easting: Obtained from professional surveyors (McKim & Creed)

Wells designated "A" wells are the shallow cluster wells located around 5 feet from the cluster twin well.

Location 1213 was completed as a boring only. MW-1215 is the aquifer test pumping well.

Units are ft.

DTW WD = Depth to water while drillng

NIA = No Information Available

NA = Not Applicable

NM = Not Measured

DW Wells completed during Cherokee activities, records not available, possibly used for dewatering

WLS COL 2.4-4

TABLE 2.4.12-202 (Sheet 1 of 8)
WATER TABLE ELEVATIONS

	Reference Elev.		4/18/2006		5/14/2006		5/23/2006		5/29/2006		6/6/2006	
Location	TOC	GL	DTW	WT Elev	DTW	WT Elev	DTW	WT Elev	DTW	WT Elev	DTW	WT Elev
MW-1200	593.99	591.93	31.80	562.19	32.51	561.48	32.77	561.2	32.90	561.1	33.13	560.9
MW-1201	592.12	589.91			34.69	557.43	35.17	557.0	35.35	556.8	35.60	556.5
MW-1201A	592.11	590.07										
MW-1202	589.68	587.47	23.90	565.78	24.49	565.19	24.76	564.9	24.86	564.8	24.99	564.7
MW-1203	591.87	589.51	20.60	571.27	21.05	570.82	21.40	570.5	21.51	570.4	21.65	570.2
MW-1204	612.42	609.92	39.80	572.62	39.87	572.55	40.25	572.2	40.33	572.1	40.36	572.1
MW-1204A	612.42	609.93										
MW-1205	612.59	609.99	46.90	565.69	46.89	565.70	47.28	565.3	47.33	565.3	47.20	565.4
MW-1206	591.51	589.66			32.98	558.53	33.43	558.1	33.63	557.9	33.89	557.6
MW-1206A	591.43	589.75										
MW-1207	591.39	589.03			33.31	558.08	33.74	557.6	33.93	557.5	34.17	557.2
MW-1207A	591.05	588.91										
MW-1208	590.00	587.77	41.30	548.70	41.84	548.16	42.25	547.8	42.37	547.6	42.46	547.5
MW-1209	588.91	586.91			19.21	569.70	19.55	569.4	19.62	569.3	19.57	569.3
MW-1209A	589.03	586.93										
MW-1210	592.27	589.78	19.50	572.77	20.08	572.19	20.17	572.1	20.51	571.8	20.64	571.6
MW-1210A	591.66	589.42										
MW-1211	591.63	589.88	27.50	564.13	27.93	563.70	27.99	563.6	28.11	563.5	28.21	563.4
MW-1212	612.29	610.24	35.45	576.84	36.26	576.03	36.62	575.7	36.81	575.5	37.17	575.1
MW-1214	606.51	605.00	16.80	589.71	17.60	588.91	18.01	588.5	18.25	588.3	18.61	587.9
MW-1215	592.13	590.22			34.65	557.48	35.14	557.0	35.34	556.8	35.56	556.6
MW-1216	590.69	588.01										

WLS COL 2.4-4

TABLE 2.4.12-202 (Sheet 2 of 8)
WATER TABLE ELEVATIONS

	Reference Elev.		4/18/2006		5/14/2006		5/23/2006		5/29/2006		6/6/2006	
Location	TOC	GL	DTW	WT Elev	DTW	WT Elev	DTW	WT Elev	DTW	WT Elev	DTW	WT Elev
MW-1217	590.10	587.64										
MW-1218	590.18	588.12										
DW2	589.67	588.94	33.80	555.87	37.11	552.56	37.11	552.56	37.56	552.11	37.75	551.92
DW3	591.34	590.56	22.50	568.84	23.59	567.75	23.59	567.75	24.65	566.69	24.63	566.71
DW4	591.51	591.22										
DW5	589.20	587.73										
SG-1		568.23			0.98	569.21						
SG-2		547.81			1.40	546.41						
SG-3		536.09			2.40	533.69						
SG-4		525.64			1.40	524.24						

WLS COL 2.4-4

TABLE 2.4.12-202 (Sheet 3 of 8)
WATER TABLE ELEVATIONS

	Reference Elev.		6/12/2006		7/15/2006		7/21/2006		8/15/2006		9/11/2006	
Location	TOC	GL	DTW	WT Elev	DTW	WT Elev	DTW	WT Elev	DTW	WT Elev	DTW	WT Elev
MW-1200	593.99	591.93	33.29	560.7	34.13	559.9	34.31	559.68	34.95	559.0	36.64	557.3
MW-1201	592.12	589.91	35.80	556.3	36.80	555.3	36.97	555.15	37.55	554.6	38.19	553.9
MW-1201A	592.11	590.07					38.60	553.51	36.69	555.4	37.10	555.0
MW-1202	589.68	587.47	25.10	564.6	25.73	563.9	25.82	563.86	26.28	563.4	26.81	562.9
MW-1203	591.87	589.51	21.78	570.1	22.51	569.4	22.65	569.22	23.14	568.7	24.70	567.2
MW-1204	612.42	609.92	40.45	572.0	41.06	571.4	41.17	571.25	41.58	570.8	42.14	570.3
MW-1204A	612.42	609.93					33.54	578.88	33.06	579.4	33.44	579.0
MW-1205	612.59	609.99	47.25	565.3	47.66	564.9	47.75	564.84	47.98	564.6	48.50	564.1
MW-1206	591.51	589.66	34.10	557.4	35.10	556.4	35.29	556.22	35.89	555.6	36.51	555.0
MW-1206A	591.43	589.75					35.31	556.12	35.92	555.5	36.54	554.9
MW-1207	591.39	589.03	34.39	557.0	35.39	556.0	35.54	555.85	36.21	555.2	36.84	554.5
MW-1207A	591.05	588.91					34.77	556.28	35.39	555.7	36.03	555.0
MW-1208	590.00	587.77	42.62	547.4	43.18	546.8	43.38	546.62	43.69	546.3	44.20	545.8
MW-1209	588.91	586.91	19.62	569.3	20.10	568.8	20.20	568.71	20.51	568.4		
MW-1209A	589.03	586.93					17.72	571.31	17.78	571.3	18.27	570.8
MW-1210	592.27	589.78	20.95	571.3	21.67	570.6	21.91	570.36	22.26	570.0	22.61	569.7
MW-1210A	591.66	589.42					20.42	571.24	20.81	570.8	21.25	570.4
MW-1211	591.63	589.88	28.33	563.3	28.62	563.0	28.80	562.83	28.85	562.8	28.73	562.9
MW-1212	612.29	610.24	37.42	574.9	38.69	573.6	38.90	573.39	39.62	572.7	40.14	572.2
MW-1214	606.51	605.00	18.91	587.6	20.31	586.2	20.62	585.89	21.38	585.1	22.04	584.5
MW-1215	592.13	590.22	35.75	556.4	36.73	555.4	36.91	555.22	37.50	554.6	38.15	554.0
MW-1216	590.69	588.01					25.00	565.69	25.96	564.7	26.92	563.8
MW-1217	590.10	587.64					22.19	567.91	23.33	566.8	24.41	565.7

WLS COL 2.4-4

TABLE 2.4.12-202 (Sheet 4 of 8)
WATER TABLE ELEVATIONS

	Reference Elev.		6/12/2006		7/15/2006		7/21/2006		8/15/2006		9/11/2006	
Location	TOC	GL	DTW	WT Elev	DTW	WT Elev	DTW	WT Elev	DTW	WT Elev	DTW	WT Elev
MW-1218	590.18	588.12					16.63	573.55	17.22	573.0	17.77	572.4
DW2	589.67	588.94	37.73	551.94	38.90	550.77	39.41	550.26	40.03	549.64	40.42	549.25
DW3	591.34	590.56	25.24	566.10	26.24	565.10	26.88	564.46	26.90	564.44	27.33	564.01
DW4	591.51	591.22			23.82	567.69	23.91	567.60	23.94	567.57		
DW5	589.20	587.73							58.35	530.85	58.72	
SG-1		568.23			0.84	569.07					1.02	569.25
SG-2		547.81			1.70	546.11					1.6	546.21
SG-3		536.09			2.48	533.61					1.7	534.39
SG-4		525.64			1.20	524.44					1.38	524.26

WLS COL 2.4-4

TABLE 2.4.12-202 (Sheet 5 of 8)
WATER TABLE ELEVATIONS

	Reference Elev.		9/14/2006		10/10/2006		11/14/2006		12/20/2006		1/17/2006	
Location	TOC	GL	DTW	WT Elev	DTW	WT Elev	DTW	WT Elev	DTW	WT Elev	DTW	WT Elev
MW-1200	593.99	591.93	35.67	558.3	35.99	558.00	36.44	557.55	35.03	558.96	32.20	561.79
MW-1201	592.12	589.91			38.88	553.24	39.44	552.68	40.35	551.77	40.74	551.38
MW-1201A	592.11	590.07			38.12	553.99	37.90	554.21	39.04	553.07	39.64	552.47
MW-1202	589.68	587.47	26.82	562.9	27.19	562.49	27.67	562.01	28.02	561.66	28.06	561.62
MW-1203	591.87	589.51	23.64	568.2	23.93	567.94	24.17	567.70	23.97	567.90	23.59	568.28
MW-1204	612.42	609.92	41.95	570.5	42.37	570.05	42.68	569.74	42.95	569.47	42.81	569.61
MW-1204A	612.42	609.93	33.17	579.2	33.58	578.84	33.71	578.71	34.75	577.67	35.16	577.26
MW-1205	612.59	609.99	48.23	564.4	48.61	563.98	48.76	563.83	49.20	563.39	49.22	563.37
MW-1206	591.51	589.66			37.27	554.24	37.83	553.68	38.60	552.91	38.96	552.55
MW-1206A	591.43	589.75			37.31	554.12	37.85	553.58	38.62	552.81	38.98	552.45
MW-1207	591.39	589.03			36.88	554.51	38.16	553.23	38.90	552.49	39.25	552.14
MW-1207A	591.05	588.91			37.64	553.41	37.38	553.67	38.10	552.95	38.44	552.61
MW-1208	590.00	587.77			44.73	545.27	45.02	544.98	45.73	544.27	45.89	544.11
MW-1209	588.91	586.91	20.85	568.1	21.22	567.69	21.44	567.47	21.75	567.16	21.67	567.24
MW-1209A	589.03	586.93	18.01	571.0	18.46	570.57	18.80	570.23	20.02	569.01	20.21	568.82
MW-1210	592.27	589.78	22.18	570.1	23.06	569.21	22.54	569.73	22.67	569.60	21.66	570.61
MW-1210A	591.66	589.42	21.11	570.5	21.64	570.02	21.49	570.17	21.55	570.11	20.74	570.92
MW-1211	591.63	589.88	28.12	563.5	28.70	562.93	28.21	563.42	27.86	563.77	26.83	564.80
MW-1212	612.29	610.24	40.15	572.1	40.25	572.04	40.03	572.26	37.78	574.51	33.44	578.85
MW-1214	606.51	605.00	22.02	584.5	22.40	584.11	22.35	584.16	21.05	585.46	20.01	586.50
MW-1215	592.13	590.22			38.89	553.24	39.43	552.70	40.28	551.85	40.65	551.48
MW-1216	590.69	588.01	26.91	563.8	27.49	563.20	27.89	562.80	26.92	563.77	25.75	564.94
MW-1217	590.10	587.64	24.33	565.8	24.47	565.63	24.49	565.61	24.14	565.96	22.47	567.63

WLS COL 2.4-4

TABLE 2.4.12-202 (Sheet 6 of 8)
WATER TABLE ELEVATIONS

	Reference Elev.		9/14/2006		10/10/2006		11/14/2006		12/20/2006		1/17/2006	
Location	TOC	GL	DTW	WT Elev	DTW	WT Elev	DTW	WT Elev	DTW	WT Elev	DTW	WT Elev
MW-1218	590.18	588.12	8.60	581.6	17.88	572.30	17.77	572.41	16.63	573.55	15.10	575.08
DW2	589.67	588.94	40.12	549.55	40.64	549.03	40.44	549.23	40.11	549.56	38.99	550.68
DW3	591.34	590.56	25.92	565.42	27.88	563.46	26.50	564.84	26.54	564.80	24.57	566.77
DW4	591.51	591.22	23.32	568.19	23.88	567.63	23.51	568.00	23.05	568.46	21.93	569.58
DW5	589.20	587.73	58.62	530.58	58.84	530.36	58.92	530.28	59.12	530.08	59.08	530.12
SG-1		568.23			0.68	568.91	0.97	569.20	0.95	569.18	1.00	569.23
SG-2		547.81			1.95	545.86	1.87	545.94	1.47	546.34	1.25	546.56
SG-3		536.09			2.34	533.75	1.74	534.35	1.37	534.73	1.78	534.31
SG-4		525.64			1.47	524.17	1.38	524.26	0.00	525.64	1.38	524.27

WLS COL 2.4-4

TABLE 2.4.12-202 (Sheet 7 of 8)
WATER TABLE ELEVATIONS

	Reference Elev.		2/19/07		3/13/07		4/19/07	
Location	TOC	GL	DTW	WT Elev	DTW	WT Elev	DTW	WT Elev
MW-1200	593.99	591.93	32.00	561.99	28.88	565.11	31.26	562.73
MW-1201	592.12	589.91	40.91	551.21	41.14	550.98	41.46	550.66
MW-1201A	592.11	590.07	39.69	552.42	40.04	552.07	40.36	551.75
MW-1202	589.68	587.47	27.82	561.86	27.80	561.88	28.00	561.68
MW-1203	591.87	589.51	23.00	568.87	22.79	569.08	23.20	568.67
MW-1204	612.42	609.92	42.14	570.28	41.85	570.57	41.96	570.46
MW-1204A	612.42	609.93	34.71	577.71	35.06	577.36	35.00	577.42
MW-1205	612.59	609.99	48.59	564.00	48.56	564.03	48.39	564.20
MW-1206	591.51	589.66	39.22	552.29	39.46	552.05	39.82	551.69
MW-1206A	591.43	589.75	39.25	552.18	39.50	551.93	39.85	551.58
MW-1207	591.39	589.03	39.50	551.89	39.72	551.67	40.08	551.31
MW-1207A	591.05	588.91	38.71	552.34	38.92	552.13	39.29	551.76
MW-1208	590.00	587.77	45.77	544.23	45.89	544.11	45.92	544.08
MW-1209	588.91	586.91	20.92	567.99	20.79	568.12	20.61	568.30
MW-1209A	589.03	586.93	18.72	570.31	18.70	570.33	18.15	570.88
MW-1210	592.27	589.78	21.33	570.94	20.85	571.42	20.94	571.33
MW-1210A	591.66	589.42	20.24	571.42	19.83	571.83	19.93	571.73
MW-1211	591.63	589.88	27.06	564.57	26.53	565.10	26.83	564.80
MW-1212	612.29	610.24	34.08	578.21	31.21	581.08	33.91	578.38
MW-1214	606.51	605.00	18.68	587.83	17.72	588.79	17.32	589.19
MW-1215	592.13	590.22	40.84	551.29	41.06	551.07	41.40	550.73
MW-1216	590.69	588.01	24.66	566.03	23.91	566.78	24.24	566.45
MW-1217	590.10	587.64	21.46	568.64	20.33	569.77	20.97	569.13
MW-1218	590.18	588.12	14.76	575.42	13.69	576.49	14.19	575.99

WLS COL 2.4-4

TABLE 2.4.12-202 (Sheet 8 of 8)
WATER TABLE ELEVATIONS

	Reference Elev.		2/19/07		3/13/07		4/19/07	
Location	TOC	GL	DTW	WT Elev	DTW	WT Elev	DTW	WT Elev
DW2	589.67	588.94	38.94	550.73	37.62	552.05	38.17	551.50
DW3	591.34	590.56	24.77	566.57	23.14	568.20	23.26	568.08
DW4	591.51	591.22	22.66	568.85	21.72	569.79	18.19	573.32
DW5	589.20	587.73	58.95	530.25	58.65	530.55	58.49	530.71
SG-1		568.23	0.98	569.21	1.00	569.23	1.17	569.40
SG-2		547.81	1.23	546.58	1.23	546.58	1.06	546.75
SG-3		536.09	1.86	534.23	1.81	534.28	1.70	534.39
SG-4		525.64	1.38	524.27	1.50	524.14	1.34	524.30

TOC = top of casing elevation
GL = ground level elevation
SG-1 = DTW value is height above reference elevation
All values expressed as feet above msl, except DTW, expressed in feet.

DTW = depth to water
WT Elev = water table elevation
BLANK - no data

TABLE 2.4.12-203
DELETED

WLS COL 2.4-4

TABLE 2.4.12-204
AQUIFER CHARACTERISTICS

Material	Hydraulic Conductivity (K) Minimum	Median	Conservative Estimate	Maximum	Source
Saprolite/Soil K_v	2.45×10^{-8}	2.10×10^{-6}	4.4×10^{-5}	2.55×10^{-4}	1973 investigation laboratory analyses.
Saprolite/Soil K_h	9.67×10^{-7}	1.14×10^{-4}	4.5×10^{-4}	2.26×10^{-3}	1973 investigation field tests and 2006 slug tests.
Bedrock - PWR K_h	9.67×10^{-7}	1.53×10^{-4}	1.4×10^{-3}	9.89×10^{-3}	1973 investigation packer tests and 2006 slug, aquifer pumping, and packer tests.
Undifferentiated Material	2.21×10^{-4}	4.10×10^{-4}	1.5×10^{-3}	3.90×10^{-3}	1977 aquifer pumping tests.
Fill Material	1.81×10^{-5}	5.39×10^{-5}	7.0×10^{-5}	7.44×10^{-5}	2006 slug tests.

Units are in centimeters per second (cm/sec).
PWR - Partially weathered rock.
K_v - Vertical hydraulic conductivity.
K_h - Horizontal hydraulic conductivity.

Conservative Estimate - The geometric mean of samples exceeding the median (applicable to Saprolite/Soil K_v, K_h and Fill Material).
Conservative Estimate for Bedrock K_h was obtained from results of 2006 pumping test and was used to calculate the groundwater velocity. The Bedrock K_h of 1.4E-03 cm/s bounded the geometric mean of samples exceeding the median (i.e., 1E-03 cm/s).
Undifferentiated Material -Identification used for 1977 data where well screens bracketed the entire saturated zone, and did not differentiate between the fill material, soil, saprolite, or partially weathered rock. Conservative estimate of Undifferentiated Material K_h is presented for comparison purposes only and is based on an average of results from 1977 pumping tests.

WLS COL 2.4-5

TABLE 2.4.13-201 (Sheet 1 of 2)
DISTRIBUTION COEFFICIENTS (K_d)

	K_d Analytical Results per Argonne National Laboratory			Default K_d Values Used by RESRAD and Values From Other Sources[a]			
Sample Loc.	MW-1208	MW-1208	MW-1210	Sheppard & Thibault	IAEA	NUREG/ CR-5512 Kennedy & Strenge (1992)	RESRAD (v. 5.62 & later)
Sample Depth ft bgs[b]	45-46	58.5-59	69-73				
Sample Zone	Soil/Saprolite	Soil/Saprolite	Soil/Saprolite				
Soil Sample Texture	Sand, silty (SM)	Sand, silty (SM)	Silt, sandy (ML)	Loam	Loam	Sand	NIA[c]
Element	cm^3/g	cm^3/g	cm^3/g	cm^3/g	cm^3/g	cm^3/g	cm^3/g
Co	1103 ± 118	1971 ± 214	>7714	1300	1300	60	1000
Cs	3704 ± 524	2117 ± 299	1156 ± 163	4600	4400	270	1000
Fe	1689 ± 239	5478 ± 775	3628 ± 513	800	810	160	1000
I	1.4 ± 0.2	0.07 ± 0.01	2.5 ± 0.4	5	5	1	0.1
Ni	269 ± 38	167 ± 24	152 ± 22	300	300	400	1000

WLS COL 2.4-5

TABLE 2.4.13-201 (Sheet 2 of 2)
DISTRIBUTION COEFFICIENTS (K_d)

	K_d Analytical Results per Argonne National Laboratory			Default K_d Values Used by RESRAD and Values From Other Sources[a]			
Pu-242	89 ± 13	>1921	987 ± 140	1200	1200	550	2000
Sr	739 ± 82	262 ± 33	73 ± 9	20	810	-	30
Tc-99	0.28 ± 0.04	0.04 ± 0.01	0.42 ± 0.06	0.1	-	0.1	0
U-235	>3159	1702 ± 241	>3636	15	-	15	50

a) References 209 and 210

b) Below ground surface

c) No information available

WLS COL 2.4-5

TABLE 2.4.13-202 (Sheet 1 of 2)
AP1000 TANKS CONTAINING RADIOACTIVE LIQUID

Tank	Location[(a)]	Nominal Tank Volume	Radioisotope Contents	Considerations/Features to Mitigate Release
PXS Tanks (IRWST and CMT's)	Inside Containment	NA	NA	Inside Containment; release need not be considered.
Spent Fuel Pool	Auxiliary Building	NA	NA	Not a tank, per se. Fully lined and safety related. Located entirely inside Auxiliary Building; does not have any potential for foundation cracks to allow leakage directly to environment. Leakage would be to another room of Auxiliary Building.
WLS Reactor coolant drain tank	Inside Containment	NA	NA	Inside containment; release need not be considered.
WLS Containment sump	Inside Containment	NA	NA	Inside containment; release need not be Considered.
WLS Effluent Holdup Tanks	Auxiliary building El. 66'-6"	28,000 gal	Essentially reactor coolant	Located in unlined room at lowest portion of Auxiliary Building
WLS Waste Holdup Tanks	Auxiliary Building El. 66'-6"	15,000 gal	Less than reactor coolant	Located in unlined room at lowest portion of Auxiliary Building
WLS Monitor Tanks A, B, C	Auxiliary Building El. 66'-6", 92'-6" and 107'- 2"	15,000 gal	Effluent prepared for environmental discharge - much less than reactor coolant	Located in unlined room at lowest portion of Auxiliary Building

WLS COL 2.4-5

TABLE 2.4.13-202 (Sheet 2 of 2)
AP1000 TANKS CONTAINING RADIOACTIVE LIQUID

Tank	Location[(a)]	Nominal Tank Volume	Radioisotope Contents	Considerations/Features to Mitigate Release
WLS Monitor Tanks D, E, F	Radwaste Building	15,000 gal	Effluent prepared for environmental discharge - much less than reactor coolant	Located in unlined room at grade level in curbed, non-seismic building
WLS Chemical Waste Tank	Auxiliary Building El. 66'-6"	8,900 gal	Less than reactor coolant	Located in unlined room at lowest portion of Auxiliary Building
WSS Spent Resin Storage Tanks	Auxiliary Building El. 100'[(a)]	300 ft^3 (liquid volume will be much less)	Approx. reactor coolant	Located entirely inside Auxiliary Building; does not have any potential for foundation cracks to allow leakage directly to environment. Leakage would be to another room of aux. building.

a) Floor elevations are based on design plant grade of 100 ft. as provided in the DCD.

WLS COL 2.4-5

TABLE 2.4.13-203 (Sheet 1 of 6)
LISTING OF LEE NUCLEAR STATION DATA AND MODELING PARAMETERS SUPPORTING THE EFFLUENT HOLDUP TANK FAILURE

Soil Parameter	Parameter Description	Parameter Value [a] [b]	Parameter Justification
Silver Transport K_d Coefficient (cm^3/g)[b]	Radionuclide-specific retardation coefficient	0	A value of 0 assumes no retardation.
Barium Transport K_d Coefficient (cm^3/g)	Radionuclide-specific retardation coefficient	0	A value of 0 assumes no retardation.
Bromine Transport K_d Coefficient (cm^3/g)	Radionuclide-specific retardation coefficient	0	A value of 0 assumes no retardation.
Cerium Transport K_d Coefficient (cm^3/g)	Radionuclide-specific retardation coefficient	0	A value of 0 assumes no retardation.
Cobalt Transport K_d Coefficient (cm^3/g)	Radionuclide-specific retardation coefficient	985	Radionuclide-specific K_d values are measured by Argonne National Laboratory using Lee soil. Lowest value of the laboratory reporting range is used.
Chromium Transport K_d Coefficient (cm^3/g)	Radionuclide-specific retardation coefficient	0	A value of 0 assumes no retardation.
Cesium Transport K_d Coefficient (cm^3/g)	Radionuclide-specific retardation coefficient	993	Radionuclide-specific K_d values are measured by Argonne National Laboratory using Lee soil. Lowest value of the laboratory reporting range is used.
Iron Transport K_d Coefficient (cm^3/g)	Radionuclide-specific retardation coefficient	1,450	Radionuclide-specific K_d values are measured by Argonne National Laboratory using Lee soil. Lowest value of the laboratory reporting range is used.
Tritium Transport K_d Coefficient (cm^3/g)	Radionuclide-specific retardation coefficient	0	A value of 0 assumes no retardation.
Iodine Transport K_d Coefficient (cm^3/g)	Radionuclide-specific retardation coefficient	0.06	Radionuclide-specific K_d values are measured by Argonne National Laboratory using Lee soil. Lowest value of the laboratory reporting range is used.
Lanthanum Transport K_d Coefficient (cm^3/g)	Radionuclide-specific retardation coefficient	0	A value of 0 assumes no retardation.

WLS COL 2.4-5

TABLE 2.4.13-203 (Sheet 2 of 6)
LISTING OF LEE NUCLEAR STATION DATA AND MODELING PARAMETERS SUPPORTING THE EFFLUENT HOLDUP TANK FAILURE

Soil Parameter	Parameter Description	Parameter Value [a] [b]	Parameter Justification
Manganese Transport K_d Coefficient (cm^3/g)	Radionuclide-specific retardation coefficient	0	A value of 0 assumes no retardation.
Molybdenum Transport K_d Coefficient (cm^3/g)	Radionuclide-specific retardation coefficient	0	A value of 0 assumes no retardation.
Niobium Transport K_d Coefficient (cm^3/g)	Radionuclide-specific retardation coefficient	0	A value of 0 assumes no retardation.
Promethium Transport K_d Coefficient (cm^3/g)	Radionuclide-specific retardation coefficient	0	A value of 0 assumes no retardation.
Rubidium Transport K_d Coefficient (cm^3/g)	Radionuclide-specific retardation coefficient	0	A value of 0 assumes no retardation.
Rhodium Transport K_d Coefficient (cm^3/g)	Radionuclide-specific retardation coefficient	0	A value of 0 assumes no retardation.
Ruthenium Transport K_d Coefficient (cm^3/g)	Radionuclide-specific retardation coefficient	0	A value of 0 assumes no retardation.
Strontium Transport K_d Coefficient (cm^3/g)	Radionuclide-specific retardation coefficient	64	Radionuclide-specific K_d values are measured by Argonne National Laboratory using Lee soil. Lowest value of the laboratory reporting range is used.
Technetium Transport K_d Coefficient (cm^3/g)	Radionuclide-specific retardation coefficient	0.03	Radionuclide-specific K_d values are measured by Argonne National Laboratory using Lee soil. Lowest value of the laboratory reporting range is used.
Tellurium Transport K_d Coefficient (cm^3/g)	Radionuclide-specific retardation coefficient	0	A value of 0 assumes no retardation.
Yttrium Transport K_d Coefficient (cm^3/g)	Radionuclide-specific retardation coefficient	0	A value of 0 assumes no retardation.

WLS COL 2.4-5

TABLE 2.4.13-203 (Sheet 3 of 6)
LISTING OF LEE NUCLEAR STATION DATA AND MODELING PARAMETERS SUPPORTING THE EFFLUENT HOLDUP TANK FAILURE

Soil Parameter	Parameter Description	Parameter Value [a] [b]	Parameter Justification
Zirconium Transport K_d Coefficient (cm^3/g)	Radionuclide-specific retardation coefficient	0	A value of 0 assumes no retardation.
Precipitation (meters per year)	Average quantity of precipitation annually	1.27	Based on the 50 inches per year typical annual precipitation for Cherokee County.
Area of contaminated zone (square meters)	Area containing liquids released by the tank failure	~104	This is the area of a cube required to contain 80% of the effluent tank total capacity, distributed into that portion of the soil voids represented by the effective porosity (for PWR).
Thickness of contaminated zone (meters)	Describes the thickness of the area considered to be the contaminated zone	~10.2	The volume is assumed to be a cube. The area required to contain a volume with 80% of the liquid effluent tank (22,400 gallons), accounting for effective porosity of the contaminated zone.
Length of Primary Contamination in X direction (meters)	Describes the X-axis length of the primary contamination	~10.2	The width of the area of soil saturated with water from the effluent tank failure. The shape is assumed to be a cube.
Length of Primary Contamination in Y direction (meters)	Describes the Y-axis length of the primary contamination	~10.2	The length of the area of soil saturated with water from the effluent tank failure. The shape is assumed to be a cube.
Evapotranspiration coefficient	Describes the fraction of precipitation and irrigation water penetrating the topsoil that is lost to evaporation and by transpiration by vegetation	0.64	This is a parameter used by RESRAD-OFFSITE to determine the amount of available water obtained from either precipitation or irrigation that infiltrates to the saturated zone. The value, when used in conjunction with precipitation and runoff, creates a recharge rate of ~18 inches/yr. This value is suggested by a study of regional data and is conservative when considering conditions likely present following construction.
Runoff coefficient (unitless)	Coefficient (fraction) of precipitation that runs off the surface and does not infiltrate into the soil	0	This is a parameter used by RESRAD-OFFSITE to determine the amount of available water obtained from either precipitation or irrigation that infiltrates to the saturated zone. The value, when used in conjunction with precipitation and evapotranspiration, creates a recharge rate of ~18 inches/yr. This value is suggested by a study of regional data and is conservative when considering conditions likely present following construction.

WLS COL 2.4-5

TABLE 2.4.13-203 (Sheet 4 of 6)
LISTING OF LEE NUCLEAR STATION DATA AND MODELING PARAMETERS SUPPORTING THE EFFLUENT HOLDUP TANK FAILURE

Soil Parameter	Parameter Description	Parameter Value [(a) (b)]	Parameter Justification
Contaminated zone total porosity (unitless)	Total porosity of the contaminated sample, which is the ratio of the soil pore volume to the total volume	2.7E-01	On-site data collected at Lee. A value representative of partially weathered rock is used for conservatism.
Density of contaminated zone (g/cm^3)	Density of the contaminated soil impacted by the liquid tank failure	1.8E+00	On-site data collected at Lee. A value representative of partially weathered rock is used for conservatism.
Contaminated zone hydraulic conductivity (meters per year)	Flow velocity of groundwater through the contaminated zone under a hydraulic gradient	~4.42E+02	The hydraulic conductivity was calculated from on-site data collected at Lee. Based on a value representative of 1.40E-03 cm/s for partially weathered rock is used for conservatism, converted to m/y.
Density of saturated zone (g/cm^3)	Density of the saturated zone soil that transmits groundwater	1.98E+00	On-site data was collected at Lee. A value representative of partially weathered rock is used for conservatism.
Saturated zone total porosity (unitless)	Total porosity of the saturated zone soil, which is the ratio of the pore volume to the total volume	2.7E-01	On-site data was collected at Lee. A value representative of partially weathered rock is used for conservatism.
Saturated zone effective porosity (unitless)	Ratio of the part of the pore volume where water can circulate to the total volume of a representative sample	8.0E-02	On-site data was collected at Lee. A value representative of partially weathered rock is used for conservatism.
Saturated zone hydraulic gradient to surface water body (unitless)	Change in groundwater elevation per unit of distance in the direction of groundwater flow to a surface water body	4.0E-02	The site-specific hydraulic gradient, representative of partially weathered rock, for the pathway having shortest (i.e., most rapid) travel time to the nearest off-site surface water body. Assumed to be nearest on-site surface water body (Hold-Up Pond A) for conservatism.

WLS COL 2.4-5

TABLE 2.4.13-203 (Sheet 5 of 6)
LISTING OF LEE NUCLEAR STATION DATA AND MODELING PARAMETERS SUPPORTING THE EFFLUENT HOLDUP TANK FAILURE

Soil Parameter	Parameter Description	Parameter Value [a] [b]	Parameter Justification
Longitudinal dispersivity to surface water body (meters)	Describes the ratio between the longitudinal dispersion coefficient and the pore water velocity, The parameter depends on the length of the saturated zone	3.71E+00	Follows recommendations in the RESRAD-OFFSITE User Manual.
Lateral (horizontal) dispersivity to surface water body (meters)	Describes the ratio between the horizontal lateral dispersion coefficient and the pore water velocity	3.71E-01	Follows recommendations in the RESRAD-OFFSITE User Manual.
Lateral (vertical) dispersivity to the surface water body (meters)	Describes the vertical dispersion. The user may either model (a) vertical dispersion in the saturated zone and ignore the effects of clean infiltration along the length of the saturated zone or (b) ignore vertical dispersion in the saturated and model the effects of clean infiltration along the length of the saturated zone.	3.71E-02	Follows recommendations in the RESRAD-OFFSITE User Manual.
Distance to the nearest surface water body (meters)	Distance to the nearest off-site surface water body that contributes to a potable drinking water source	370.8	Site-specific value corresponding to the distance from the Unit 2 auxiliary building to the “hypothetical” well location, i.e., the nearest edge of Hold-Up Pond A minus the length of the contaminated zone.
Volume of the surface water body (m^3)	Describes the size of the surface water body	856,036	Site-specific value corresponding to the volume of the Broad River reservoir from the postulated release point downstream to the Ninety-Nine Islands Dam.

WLS COL 2.4-5

TABLE 2.4.13-203 (Sheet 6 of 6)
LISTING OF LEE NUCLEAR STATION DATA AND MODELING PARAMETERS SUPPORTING THE EFFLUENT HOLDUP TANK FAILURE

Soil Parameter	Parameter Description	Parameter Value [(a) (b)]	Parameter Justification
Residence time (yrs)	The average time that water spends in the surface water body	0.00397	Site-specific value obtained by dividing the volume of the surface water body by the volume of water that is extracted annually from it.

a) Parameter values are provided in metric units as used with RESRAD-OFFSITE.

b) K_d values reported in the laboratory analysis for nickel, plutonium, and uranium are not included in the liquid effluent source term and, therefore, are not listed in this RESRAD-OFFSITE input table.

WLS COL 2.4-5

TABLE 2.4.13-204
RADIONUCLIDE CONCENTRATION AT NEAREST DRINKING WATER SOURCE IN AN UNRESTRICTED AREA DUE TO EFFLUENT HOLDUP TANK FAILURE

Detected Radionuclide	Radionuclide Concentration microcuries/ml	10 CFR 20 Appendix B Table 2 Column 2 microcuries/ml	Sum of Fractions Contribution[a]
H-3	3.35E-08	1.00E-03	3.35E-05
			Sum of Fractions[b] 3.38E-05

a) Those radionuclides with Sum of Fractions Contribution less than 1.0E-5 are negligible and not included in the table.

b) Total for all detected radionuclides.

2.5 GEOLOGY, SEISMOLOGY, AND GEOTECHNICAL ENGINEERING

This section of the referenced DCD is incorporated by reference with the following departures and/or supplements:

STD DEP 1.1-1 Section 2.5 is renumbered to follow Regulatory Guide 1.206. The COL information items in DCD Subsections 2.5.1 through 2.5.6 and addressed in Subsection 2.5.6.

WLS COL 2.5-2 This section presents information on the geological, seismological, and geotechnical engineering properties of the Lee Nuclear Station and complies with Regulatory Guide (RG) 1.206. Subsection 2.5.1 describes basic geological and seismologic data. Subsection 2.5.2 describes the vibratory ground motion at the site, including an updated seismicity catalog, description of seismic sources, and development of the Ground Motion Response Spectra (GMRS) and Foundation Input Response Spectra (FIRS) for the Lee Nuclear Site. Subsection 2.5.3 describes the potential for surface faulting in the site area. Subsection 2.5.4, describes the stability of subsurface materials and foundations. Lastly, Subsection 2.5.5 describes the stability of slopes.

RG 1.208 provides guidance for the level of investigation recommended at different distances from a proposed site for a nuclear facility.

The following four terms for site map areas are designated by RG 1.208:

- Site region - area within 200 mi (320 km) of the site location.
- Site vicinity - area within 25 mi (40 km) of the site location.
- Site area - area within 5 mi (8 km) of the site location.
- Site - area within 0.6 mi (1 km) of the proposed Lee Nuclear Station Unit 1 and 2 locations.

These terms are used in Subsections 2.5.1 through 2.5.5 to describe these specific areas of investigation. These terms are not applicable to other sections of this COL application.

Extensive field investigations and research of relevant geologic literature indicate that no geologic hazards have the potential to affect the Lee Nuclear Site with exception of vibratory ground motion. Seismic hazard at the Lee Nuclear Station is discussed in greater technical detail in Subsection 2.5.2.

2.5.1 BASIC GEOLOGIC AND SEISMIC INFORMATION

WLS COL 2.5-1 Subsection 2.5.1 presents information on the geological and seismological characteristics of the Lee Nuclear Site region and site area. The information is divided in two parts. Subsection 2.5.1.1 describes the geologic and tectonic setting of the site region (200 mi.), and Subsection 2.5.1.2 describes the geology and structural geology of the site vicinity (25 mi.), site area (5 mi.), and site (0.6 mi.). The geological and seismological information was developed in accordance with the guidance presented in RG 1.206 and RG 1.208 and satisfies the requirements of 10 CFR 100.23(c). The geological and seismological information presented in this section is used as a basis for evaluating the detailed geologic, seismic, and man-made hazards at the site.

Subsection 2.5.2 describes the methodology used to develop the ground motion GMRS and FIRS for the Lee Nuclear Site. RG 1.208 further requires that the geological, seismological, and geophysical database is updated and any new data are evaluated to determine whether revisions to the 1986 Electric Power Research Institute (EPRI) seismic source model are required (Subsections 2.5.2.1 through 2.5.2.4 describe the EPRI model in detail). This section, therefore, provides an update of the geological, seismological, and geophysical database for the Lee Nuclear Site, focusing on whether any data published since 1986 indicates a significant change to the 1986 EPRI seismic source model.

Subsection 2.5.1 presents geological and seismological information developed from a review of previous reports prepared for the Lee Nuclear Site, published geologic literature, interviews with experts in the geology and seismotectonics of the site region, and geologic field work performed as part of this study (including new boreholes drilled at the site of the Lee Nuclear Station Units, and geologic field reconnaissance). A review of published geologic literature supplements and updates the previous geological and seismological information.

2.5.1.1 Regional Geology

Subsection 2.5.1.1 describes the regional geology within a 200 mi. radius of the Lee Nuclear Site. The regional physiography, geomorphology, stratigraphy, and tectonic setting are discussed below. The information provided is a brief summary of the region, with an extensive and current bibliography. This regional information provides the basis for evaluating the geologic and seismologic hazards discussed in the succeeding sections.

Rocks within the site area are igneous and metamorphic crystalline rocks that are neither susceptible to karst-type dissolution collapse nor to subsidence due to fluid withdrawal. No irregular weathering conditions or natural landslide hazards are noted in field investigations. The stability of natural and manmade slopes for which failure could adversely impact safety-related structures is discussed in Subsection 2.5.5.

According to the 1997 Mineral Resource Map of South Carolina (Reference 402) there are neither areas of significant subsurface mineral extraction nor hydrocarbon extraction within the site area. This map shows one area of sand dredging within the site area. Additionally, this map shows one area of common clay extraction about five miles northwest of the site and one area of sericite schist extraction about five miles east-northeast of the site. This map shows no other areas of mineral extraction within the site area.

2.5.1.1.1 Regional Physiography, Geomorphology, and Stratigraphy

The Lee Nuclear Site is located in the Piedmont physiographic province (Figure 2.5.1-201). From northwest to southeast, the Lee Nuclear Site region includes portions of five physiographic provinces: the Appalachian Plateau (the "Cumberland Plateau" at the latitude of the site region), Valley and Ridge, Blue Ridge, Piedmont, and Coastal Plain. Portions of major lithotectonic divisions of the Appalachian orogen (mountain belt) are found within a 200 mi. radius of the site. The structures and stratigraphic sequences within these divisions represent a complex geologic evolution that ends in the modern day passive margin of the Atlantic continental margin.

Each of these five physiographic provinces is described below, from northwest to southeast, in terms of their physiography, geomorphology, and stratigraphy. A more detailed discussion is provided for the Piedmont Physiographic Province, the province in which the Lee Nuclear Site is located. Although they do not technically constitute a physiographic province, Mesozoic rift basins are also discussed in this section because they contain a distinct assemblage of non-metamorphosed sedimentary rocks and are distributed across both the Piedmont and Coastal Plain provinces.

Depending on the focus of a given study, the Appalachian orogenic belt has been subdivided in a variety of ways by various researchers. These subdivisions, in the past, included provinces, belts, and terranes. More recent syntheses have been organized around lithotectonic associations based on common tectonic or depositional origins, mainly relative to the lapetus ocean and it marginal continental masses, Laurentia and Gondwana (Hibbard et al. (2002) (Reference 204); Hibbard et al. (2006) (Reference 260); Hibbard et al. (2007) (Reference 428); Hatcher et al. (2007) (Reference 404)). Physiographic provinces are defined based on both physiography (landforms) and geology. However, with the modern emphasis on lithotectonic association, the influence of physiography has become subordinate and the "belt" concept has been abandoned. Figure 2.5.1-235 diagrams how the modern lithotectonic classification schemata of Hibbard et al. (2006) (Reference 260) and Hibbard et al. (2007) (Reference 428) relate and compare to Hatcher et al. (2007) (Reference 404) and to the nomenclature for the physiographic provinces. Note for instance that the Tugaloo terrane of Hatcher et al. (2007) (Reference 404) falls on both sides of the Brevard Fault Zone, which roughly coincides with the boundary of the Blue Ridge and Piedmont Physiographic provinces. Similarly, this same fundamental physiographic boundary also transects the Hibbard et al. (2006) (Reference 260) Piedmont Domain. Also, note that the Piedmont physiographic province, in the schema of Hibbard et al. (2006) (Reference 260), is divided by the Central

Piedmont shear zone into the Piedmont Domain to the west and Carolinia (i.e., the "Carolina Zone" in Hibbard et al. (2002) (Reference 204)) to the east. These examples serve to illustrate the decreased role of physiography in modern lithotectonic classifications.

2.5.1.1.1.1 The Appalachian Plateau Physiographic Province

The Appalachian Plateau physiographic province includes the western part of the Appalachian Mountains, stretching from New York State to Alabama. The Appalachian Plateau is bounded on the west by the Interior Low Plateaus and on the east by the Valley and Ridge Province. The Appalachian Plateau surface slopes gently to the northwest and merges imperceptibly into the Interior Low Plateaus.

The Appalachian Plateau physiographic province overlies unmetamorphosed sedimentary rocks of Permian to Cambrian age. These strata are generally subhorizontal to gently folded and exhibit relatively little deformation.

2.5.1.1.1.2 The Valley and Ridge Physiographic Province

The Valley and Ridge physiographic province extends from the Hudson Valley in New York State through Pennsylvania, Maryland, and Virginia, and is about 50 mi. wide from southern Virginia southward to Alabama. The Valley and Ridge Province is bounded on the west by the Appalachian Plateau and on the east by the Blue Ridge. A topographic escarpment known as the Alleghany front in Pennsylvania and the Cumberland escarpment in Tennessee and Virginia marks the northwestern boundary of the Valley and Ridge Province. This physiographic province is underlain by a folded and faulted sequence of Paleozoic sedimentary rocks. The characteristic linear valleys and ridges of this province are the result of differential weathering and erosion of different rock types.

The eastern boundary of the Valley and Ridge province marks a change from folded, lesser-deformed Paleozoic sedimentary rocks to more penetratively deformed Precambrian rocks in the Blue Ridge.

2.5.1.1.1.3 The Blue Ridge Physiographic Province

The Blue Ridge physiographic province is located west of and adjacent to the Piedmont province. The Blue Ridge province extends from Pennsylvania to northern Georgia and varies from about 30 to 75 mi. wide. Elevations are highest in North Carolina and Georgia, with several peaks in North Carolina exceeding 5,900 ft. above mean sea level (msl), including Mount Mitchell, North Carolina, the highest point (6,684 ft. msl) in the Appalachian Mountains. The east-facing Blue Ridge escarpment, which is about 300 mi. in length and averages 1000 to 1650 ft. msl elevation, separates the highlands of the Blue Ridge from the lower relief Piedmont province in the southern Appalachians (Reference 205).

The Blue Ridge province is bounded on the northwest by the Valley and Ridge physiographic province and to the southeast by the Piedmont physiographic province delineated by the Brevard fault zone (References 206 and 207)

(Figures 2.5.1-201 and 202b). The province is a complexly folded, faulted, penetratively deformed, and intruded metamorphosed basement/cover sequence. These rocks record multiple, late Proterozoic to late Paleozoic deformation events (extension and compression) associated with the formation of the Iapetus Ocean and the Appalachian orogen (References 206, 208, 209, 210, and 211). The Blue Ridge province consists of a series of westward-vergent thrust sheets, each with different tectonic histories and lithologies, including gneisses, plutons, and metavolcanic and metasedimentary rift sequences, as well as continental and platform deposits (see References 203 and 206 for an expanded bibliography). The Blue Ridge–Piedmont fault system thrusts the entire Blue Ridge province northwest over Paleozoic sedimentary rock of the Valley and Ridge province during the Alleghanian orogeny (References 212, 213, 214, and 215). The Blue Ridge province reaches its greatest width in the southern Appalachians.

The Blue Ridge is divided into western and eastern portions. The western Blue Ridge consists of an assemblage of Middle Proterozoic crystalline continental (Grenville) basement rock nonconformably overlain by Late Proterozoic to Early Paleozoic rift-facies sedimentary rock (Reference 203). The basement consists of various types of gneisses, amphibolite, gabbroic and volcanic rock, and metasedimentary rock. Grenville basement rock is metamorphosed to granulite or uppermost amphibolite facies (Reference 203). The calculated radiometric ages of these rocks generally range from 1,000 to 1,200 million years old (Ma) (e.g., References 216, 217, and 218). The rifting event during the Late Proterozoic through Early Paleozoic that formed the Iapetus Ocean is recorded in the terrigenous, clastic, rift-drift sedimentary sequence of the Ocoee Supergroup and Chillhowie Group (e.g., References 219, 220, 221, 222, 223). Taconic and possibly Acadian deformation and metamorphism later affected these rocks, along with the basement and sedimentary cover. The entire composite thrust sheet was transported west as an intact package during the Alleghanian collision event on the Blue Ridge–Piedmont thrust.

The eastern Blue Ridge comprises metasedimentary rocks originally deposited on a continental slope and rise and ocean floor metasedimentary rocks in association with oceanic or transitional to oceanic crust (for expanded bibliography see References 203 and 224). This is in contrast to the western Blue Ridge that contains metasedimentary rocks, thereby suggesting continental rift-drift facies of a paleomargin setting. The eastern Blue Ridge is structurally complex, with several major thrust faults, multiple fold generations, and two high-grade metamorphic episodes (Reference 203). Metamorphism occurred during the Taconic and possibly Acadian orogenies. The stratigraphy within the eastern Blue Ridge includes rare Grenville (Precambrian) gneisses, metasedimentary rocks of the Tallulah Falls Formation and the Coweeta Group, metamorphosed Paleozoic granitoids, and mafic and ultramafic complexes and rocks of the Dahlonega Gold Belt. The Paleozoic granitoids are part of a suite of similar granites found in the western Inner Piedmont, suggesting a common intrusive history. Metasedimentary rock sequences in the eastern Blue Ridge are correlated along strike as well as across some thrust fault boundaries, also suggesting a commonality in the original depositional history. Based on geochemical data, the mafic and ultramafic complexes found in particular thrust sheets in the eastern Blue Ridge have oceanic as well as continental affinities. However, their exact tectonic origin is not

clear because the contacts with the host metasedimentary rock are obscure. The Brevard fault zone forms the southeastern boundary of the Blue Ridge with the Inner Piedmont.

2.5.1.1.1.4 The Piedmont Physiographic Province

The Lee Nuclear Site is located in the Piedmont physiographic province. The Piedmont physiographic province extends southwest from New York State to Alabama and lies west of and adjacent to the Atlantic section of the Coastal Plain. It is the easternmost physiographic province of the Appalachian Mountains. The Piedmont is a seaward-sloping plateau varying in width from about 10 mi. in southeastern New York State to almost 125 mi. in South Carolina; it is the least rugged of the Appalachian provinces. Elevation of the inland boundary ranges from about 200 ft. msl in New Jersey to over 1,800 ft. msl in South Carolina.

Within the Lee Nuclear Site region, the area of the Piedmont physiographic province is also divided on the basis of its geologic history and lithology into different lithotectonic associations, which include the Carolina Zone and the Piedmont Zone.

The Carolina Zone is also referred to in more recent literature as "Carolinia" (Hibbard et al. (2006 and 2007) (References 260 and 428)) or as the "Carolina Superterrane" (Hatcher et al. (2007) (Reference 404)). The terranes that compose the Carolina Zone are all considered to be of peri-Gondwanan association and are representative of volcanic arcs resulting from subduction in the Gondwanan realm of Iapetus (Hibbard et al. (2006) (Reference 260): Hibbard et al. (2007) (Reference 428); Hatcher et al. (2007) (Reference 404)). In detail, there is disagreement in the assignment of some terranes into this division. For instance, Hibbard et al. (2002) (Reference 204) consider the Gaffney terrane (i.e., the Kings Mountain terrane of Hatcher et al. (2007) (Reference 404)) to be exclusively of peri-Gondwanan association. However, Hatcher et al. (2007) (Reference 404) consider the Kings Mountain terrane to have both Laurentian and peri-Gondwanan associations.

These two lithotectonic elements, the Piedmont and Carolina zones, are separated by a series of faults collectively referred to as the Central Piedmont Shear Zone.

West of the Central Piedmont Shear Zone, the Piedmont Zone contains the Inner Piedmont block, the Smith River allochthon of Virginia and North Carolina, and the Sauratown Mountains anticlinorium in north central North Carolina (Reference 226) (Figure 2.5.1-202a). The province is a composite stack of thrust sheets containing a variety of gneisses, schists, amphibolite, sparse ultramafic bodies, and intrusive granitoids (References 227 and 228). The protoliths are immature quartzo-feldspathic sandstone, pelitic sediments, and mafic lavas.

The Inner Piedmont block is a fault-bounded, composite thrust sheet with metamorphic complexes of different tectonic affinities (Reference 226). Rocks within the Inner Piedmont block include gneisses, schists, amphibolites, sparse ultramafic bodies, and intrusive granitoids (References 227 and 228). There is

some continental basement within the block (Reference 228) and scattered mafic and ultramafic bodies and complexes (Reference 229), suggesting the presence of oceanic crustal material (Reference 226). The remainder of the block contains a coherent, though poorly understood, sequence of metasedimentary rock, metavolcanic gneisses, and schists (Reference 226).

The Smith River allochthon is a completely fault-bounded terrane that contains two predominantly metasedimentary units and a suite of plutonic rocks (Figure 2.5.1-202b). The Sauratown Mountains anticlinorium is a complex structural window of four stacked thrust sheets exposed in eroded structural domes (Figure 2.5.1-202b). Each sheet contains Precambrian basement with an overlying sequence of younger Precambrian to Cambrian metasedimentary and metaigneous rocks (Reference 226).

The stratigraphic and structural geologic data in the Western Piedmont reflect complex tectonic history from the Precambrian Grenville through Late Paleozoic Alleghanian orogenies. Metamorphism affected the basement rocks of the Sauratown Mountains anticlinorium at least twice: during the Precambrian Grenville orogen and later during the Paleozoic. A metamorphic event in the Paleozoic affected the metasedimentary cover sequence, the Smith River allochthon, and the Inner Piedmont block (Reference 226). The Alleghanian continental collision is reflected in the thrust and dextral strike slip fault systems such as the Brevard and Bowens Creek fault zones. A few late Paleozoic granites were emplaced in the Inner Piedmont block; however, the majority lies further east in the Carolina Zone. Early Mesozoic extension resulted in the formation of rift basins (Dan River and Davie County basins).

The Central Piedmont shear zone (Reference 225) (Figure 2.5.1-202a) includes the Ocmulgee, Middleton-Lowndesville, Cross Anchor, Kings Mountain, Eufola, and Hyco fault zones (Hibbard et al. (2006) (Reference 260) and Hatcher et al. (2007) (Reference 404)). Since the Central Piedmont Shear Zone marks the boundary between rocks on both sides of Iapetus, it is associated with a "suture," (Hatcher et al. (2007) (Reference 404)) although the polarity and timing of the subduction and suturing event are under debate, (Hibbard et al. (2007) (Reference 428); (Hatcher et al. (2007) (Reference 404)). The detailed relationship of the Central Piedmont Shear Zone to the original structure associated with the suture is obscured by the fact that the original structure has been tectonically modified and overprinted by the final orogenic effects of the interactions of the Gondwanan and Laurentian continents during the Carboniferous (late Alleghanian orogeny). Hibbard et al. (2002) (Reference 204) and Hibbard et al. (2007) (Reference 428) consider the Central Piedmont Shear Zone to be a Late Alleghanian thrust that cut the original suture off in the subsurface and that the portion of the hanging wall containing the cut off suture has been eroded away (Hibbard et al. (1998) (Reference 417)). Hatcher et al. (1989) (Reference 429) also consider that the Central Piedmont Shear Zone has been tectonically modified in the late Alleghanian orogeny, in large part by folding. This allows infolding of rocks with Laurentian affinities and rocks of peri-Gondwanan affinities to explain terranes considered to have mixed associations such as the Kings Mountain Terrane (Hatcher et al. (2007) (Reference 404)).

The Lee Nuclear Site is located east of the Central Piedmont shear zone in the Carolina Zone (Hibbard et al. (2007) (Reference 428); (Carolina Superterrane of Hatcher et al. (2007) (Reference 404)). The Carolina Zone represents an amalgamation of metaigneous-dominated terranes along the eastern flank of the southern Appalachians. The Carolina Zone and the terranes within the zone are intended to replace the archaic 'belt' terminology of the southern Appalachians (Reference 204). The Carolina terrane extends for more than 300 mi. from central Virginia to eastern Georgia and is characterized by generally low-grade metaigneous and metasedimentary rocks. The original definition of the Carolina terrane (Secor et al. 1983) (Reference 231) includes higher-grade metamorphic rocks along its western margin, but more recent classification (Reference 204) includes these rocks in the Charlotte terrane to the west.

The Lee Nuclear Site lies within the Charlotte terrane, the westernmost terrane of the Carolina Zone (Figure 2.5.1-202a). Neoproterozoic to Early Paleozoic plutonic rocks that intrude a suite of mainly metaigneous rocks dominate the Charlotte terrane (Reference 204). The rocks of the Carolina Zone are unconformably overlain by sediments of the Carolina Coastal Plain southeast of the Fall Line (Figure 2.5.1-202a).

The Carolina Zone is part of a late Precambrian–Cambrian composite arc terrane, exotic to North America (References 231 and 238), and accreted either during the Ordovician to Silurian (Hibbard et al. (2002) (Reference 204)) or during the Middle Devonian to Early Mississippian (Hatcher et al. (2007) (Reference 404)) sometime during the Ordovician to Devonian Period (Reference 239); (Reference 240)). It comprises felsic to mafic metaigneous and metasedimentary rock. Middle Cambrian fossil fauna indicate a European or African affinity for the Carolina Zone (Reference 231).

Hibbard et al. (2002) (Reference 204) propose updated nomenclature for the Carolina Zone ("Carolinia" in Hibbard et al. (2006)) Reference 260) based on the tectonothermal overprint of units. Suprastructural terranes (i.e., the upper structural layer in an orogenic belt subjected to relatively shallow or near-surface processes) comprise rocks of lower-grade metamorphism where original rock fabric is preserved. Infrastructural terranes (produced at relatively deep crustal levels at elevated temperature and pressure, located beneath suprastructural terranes) comprise higher-grade metamorphic units where original rock fabric has been completely destroyed.

The western part of the Carolina Zone in central Georgia, South Carolina, and North Carolina consists of the infrastructural Charlotte terrane and, to a lesser extent, the Savannah River terrane. The easternmost portion of the Carolina Zone in South Carolina and portions in North Carolina contains the Suprastructural Albemarle and South Carolina Sequence (Figure 2.5.1-202a). Metamorphic grade increases to the northwest from lower greenschist facies to upper amphibolite facies. Rocks include amphibolite, biotite gneiss, hornblende gneiss, and schist, and likely derived from volcanic, volcanoclastic, or sedimentary protoliths. Structures of Pre-Alleghanian age are predominantly northeast-trending, regional-scale folds with steeply dipping axial surfaces. The country rock of the Charlotte terrane was penetratively deformed during the Late Proterozoic to Early Cambrian

(Hibbard et al. (2002) (Reference 204), thereby producing axial plane cleavage and foliation (Reference 203). The Charlotte terrane also contains numerous granitic and gabbroic intrusions dating to about 300 Ma.

2.5.1.1.1.5 The Atlantic Coastal Plain Physiographic Province

The Atlantic section of the Coastal Plain physiographic province extends southeastward from the Fall Line to the coastline, and southwestward from Cape Cod, Massachusetts to south-central Georgia where it merges with the Gulf section of the Coastal Plain. The Atlantic section of the Coastal Plain is a low-lying, gently rolling terrain developed on a seaward-dipping section of Cretaceous and younger semi-consolidated sedimentary rocks. Coastal Plain sediments generally thicken coastward. Sediment thickness at the New Jersey coastline is about 4,000 ft., increasing southward to as much as 8,000 ft. along the coast of Maryland and about 10,000 ft. along the coast of North Carolina. At the latitude of the Lee Nuclear Site, sediment thickness increases from zero at the Fall Line to about 4,000 ft. at the South Carolina coastline. Topographic relief is generally less than a few hundred feet, and the topographic gradient is usually less than about 5 ft/mi.

2.5.1.1.1.6 Mesozoic Rift Basins

Mesozoic-age rift basins are found along the entire eastern continental margin of North America from Nova Scotia to the Gulf Coast. The basins formed in response to the continental rifting that broke up the supercontinent Pangea and led to the formation of the Atlantic Ocean basin. Rift basins are locally exposed in the Piedmont province, generally buried beneath Coastal Plain sediments, and some basins are located offshore. Structurally, the basins are grabens or half-grabens generally elongated in a northeast direction and bounded by normal faults on one or both sides (Reference 242). Some basins are localized along reactivated Paleozoic fault zones (References 243, 244, 245, 246, and 247).

The basins are located in extended or rifted continental crust. The western boundary of this zone of extended crust is defined by the western-most edge of Triassic–Jurassic onshore rift basins or the boundaries of the structural blocks in which they occur (References 248 and 249). The eastern boundary of the zone of extended crust is the continental shelf (Reference 250).

The rift basins generally are filled with sedimentary and igneous rocks. Sedimentary strata consist mainly of non-marine sandstone, conglomerate, siltstone, and shale. Carbonate rocks and coal are found locally in several basins. Igneous rocks of basaltic composition occur as flows, sills, and stocks within the basins and as extensive dike swarms within and outside the basins (Reference 251). Basin fill strata are named the Newark Supergroup and can be divided into three sections (References 252 and 253):

- The lowest section is characteristically fluvial (References 254 and 255) and contains reddish-brown, arkosic, coarse-grained sandstone and conglomerate.

- The middle section mainly includes sediments of lacustrine origin (Reference 254). These sediments include gray-black, fossiliferous siltstone, carbonaceous shale, and thin coal beds (Reference 253).

- The uppermost section is a complex of deltaic, fluvial, and lacustrine sediments (References 256 and 257). These sediments include red-brown siltstone, arkosic sandstone, pebble sandstone, red and gray mudstone, and conglomerate (Reference 253).

A number of Mesozoic rift basins are located within the Lee Nuclear Site region. These include the Florence, Dunbarton, South Georgia, Riddleville, Jedburg, Deep River, Dan River, and Crowburg basins, as well as additional unnamed basins.

2.5.1.1.2 Regional Tectonic Setting

The regional tectonic setting of the Lee Nuclear Site is presented below. This section includes discussions of regional tectonic stresses, regional gravity and magnetic data, geophysical anomalies and lineaments, principal regional tectonic structures, and regional seismicity.

2.5.1.1.2.1 Regional Geologic History

Numerous researchers have mapped the geology of the Lee Nuclear Site region. Figures 2.5.1-203a and 203b present geologic mapping by King and Beikman (1974) (Reference 258) [as digitized by Schruben et al. (1994) (Reference 259)]. A more recent compilation of Appalachian lithotectonic mapping compiled by Hibbard et al. (2006) (Reference 260) covers much of the Lee Nuclear Site region (Figures 2.5.1-204a and 204b).

The Lee Nuclear Site lies within the southern part of the northeast-southwest-trending Appalachian orogenic belt, which extends nearly the entire length of the eastern United States from southern New York State to Alabama. The Appalachian orogenic belt formed during the Paleozoic Era and records multiple orogenic events related to the opening and closing of the proto-Atlantic along the eastern margin of ancestral North America.

Prior to the Appalachian orogenies, the continental mass ancestral to North America (i.e., Laurentia) was locally deformed and metamorphosed. This deformational event is called Grenville orogeny and occurred about 1.1 billion years ago. Portions of Grenvillian crust are exposed as external massifs in crystalline thrust sheets of the Blue Ridge geologic province and also as an internal massif in the Sauratown Mountains window (Reference 261). Beginning about 750 to 700 Ma, continental rifting of Laurentia led to the opening of the Iapetus Ocean, which formed a new eastern margin of ancestral North America.

Subsequent closing of the Iapetus and other proto-Atlantic ocean basins resulted in the accretion of exotic terranes to the eastern margin of Laurentia. These accreted terranes were of different sizes and represented fragments of oceanic crust, volcanic island arcs, and other continental masses, each with its own

geologic history. This long period of ocean closing and continental accretion during the Paleozoic was punctuated by four episodes of compression (collision) and associated metamorphism and magmatism (Reference 261). These four episodes occurred in the Late Cambrian to Early Ordovician (Penobscottian orogeny), Ordovician (Taconic orogeny), Devonian (Acadian orogeny), and Pennsylvanian to Permian (Alleghanian orogeny).

The Grenville Front is the leading edge of a northeast-southwest-trending Precambrian collisional orogen that involved rocks of the pre-Appalachian basement of Laurentia. The following discussion is summarized from White et al. (2000) (Reference 264). Like the younger Appalachian orogen, the Grenville orogen may have formed in part from exotic terranes that were assembled prior to 1,160 Ma, then deformed and thrust westward over the pre-Grenville Laurentian margin between 1,120 and 980 Ma. The Grenville orogen and Grenville front are exposed primarily in southeastern Canada, and can be traced in outcrop southwest to the latitude of Lake Ontario. Grenville-age rocks and structures continue on trend to the southeast into the United States, but are depositionally and structurally overlain by younger rocks, including terranes of the Appalachian orogen (References 262 and 263). Seismic reflection profiles indicate that the Grenville front and other prominent reflectors generally dip toward the east and extend to lower crustal depths (Reference 264). Bollinger and Wheeler (1988) (Reference 265) note that Iapetan normal faults that formed as a result of Iapetan extension likely decrease in size, abundance, and slip northwestward from the Grenville front.

The Penobscottian event is the earliest major orogeny recognized in the Appalachian belt and primarily is expressed in the northern Appalachians. Horton et al. (1989) (Reference 201) states that evidence for the Penobscottian orogeny has not been observed south of Virginia, where the orogeny is bracketed in age between Late Cambrian metavolcanic rocks and an Early Ordovician pluton.

The earliest Paleozoic deformation along or adjacent to the ancestral North American margin at the latitude of the Lee Nuclear Site region occurred in the Middle Ordovician and is known as the Taconian event or orogeny. The onset of the Taconian event is marked regionally throughout much of the Appalachian belt by an unconformity in the passive-margin sequence and deposition of clastic sediments derived from an uplifted source area or areas to the east. Horton et al. (1989) (Reference 201) and Hatcher et al. (1994) (Reference 203) interpret the Taconic event at the latitude of the Lee Nuclear Site region as the result of the collision of one or more terranes with North America. Rocks of the eastern Blue Ridge and Inner Piedmont are interpreted to have originated east of the Laurentian passive margin in Middle Ordovician time and, thus, are candidates for Taconic collision(s).

Horton et al. (1989) (Reference 201) includes the eastern Blue Ridge at the latitude of the site in the Jefferson terrane, a large body of sandstones, shales, basalt, and ultramafic rocks interpreted to be a metamorphosed accretionary wedge that accumulated above a subduction zone. Hatcher et al. (1994) (Reference 203) suggests that the Hayesville thrust, which forms the western structural boundary of the eastern Blue Ridge and dips eastward beneath it, may

be the “up-dip leading edge of an early Paleozoic subduction zone.” If this interpretation is correct, then the Hayesville thrust fault may be a Taconic suture. Horton et al. (1989) (Reference 201) and Hatcher et al. (1994) (Reference 203) interpret the Carolina-Avalon terrane as accreted during the Taconic orogeny. If this is correct, then the Towaliga fault between the Inner Piedmont and Carolina-Avalon terranes may be a Taconic structure.

According to Horton et al. (1989) (Reference 201), evidence for the middle Paleozoic Acadian orogeny is “neither pervasive nor widespread” south of New England. The Acadian event primarily is expressed at the latitude of the study region by unconformities in foreland stratigraphic succession, plutonism, and activity of several major faults (Hatcher et al. 1994) (Reference 203), and possibly ductile folding elsewhere in the southern Appalachians (Reference 201). To date, there is no compelling evidence for a major accretion event at the latitude of the Lee Nuclear Site region during the Acadian orogeny (References 201 and 203).

The final and most significant collisional event in the formation of the Appalachian belt is the late Paleozoic Alleghanian orogeny, during which Gondwana collided with Laurentia, closing the intervening Paleozoic ocean basin. At the latitude of the Lee Nuclear Site region, the Alleghanian collision telescoped the previously accreted Taconic terranes and drove them westward up and across the Laurentian basement, folding the passive margin sequence before them and creating the Valley and Ridge fold-and-thrust belt. The collisional process also thrust a fragment from the underlying Laurentian basement eastward over the passive margin sequence, forming the western Blue Ridge. Significant strike-slip faulting and lateral transport of terranes are interpreted to have occurred during the Alleghanian orogeny (Reference 203). According to Horton and Zullo (1991) (Reference 261), the evident effects of the Alleghanian orogeny in the Carolinas include:

- Numerous granitoid plutons southeast of the Brevard fault zone.
- Amphibolite-facies regional metamorphism and deformation in the Kiokee and Raleigh metamorphic belts of the eastern Piedmont.
- Strike-slip movement, along major faults from the Brevard fault zone southeastward to the eastern Piedmont fault system.
- Westward transport of a composite stack of crystalline thrust sheets which now constitutes the western Piedmont and Blue Ridge.
- Imbricate thrusting and folding in the Valley and Ridge province occurred during this orogeny.

Despite uncertainties regarding the precise origin, emplacement, and boundaries of belts and terranes, there is good agreement among tectonic models regarding first-order structural features of the southern Appalachian orogenic belt. At the latitude of the Lee Nuclear Site region, the ancestral North American basement of the Paleozoic passive margin underlies the Valley and Ridge, Blue Ridge, and Inner Piedmont provinces at depths of less than 6 to 9 mi., and possibly as

shallow 3 mi. or less beneath the Valley and Ridge. A basal decollement along the top of the North American basement is the root zone for Paleozoic thrust faults in the Valley and Ridge, Blue Ridge, and Inner Piedmont provinces. Although potential seismogenic sources may be present within the North American basement below the decollement (References 265 and 267), the locations, dimensions, and geometries of these deeper potential sources are not necessarily expressed in the exposed fold-thrust structures above the detachment.

The modern continental margin includes Mesozoic rift basins that record the beginning of extension and continental rifting during the early to middle Mesozoic leading to the formation of the current Atlantic Ocean. During the later stage of rifting (early Jurassic), the focus of extension shifted eastward to the major marginal, proto-Atlantic ocean basins. Eventually, rifting of continental crust ceased as sea floor spreading began in the Atlantic spreading center sometime around 175 Ma (Reference 248). The oldest ocean crust in contact with the eastern continental margin is late middle Jurassic (Reference 266). The significance of the age of transition from rifting to sea floor spreading is that the tectonic regime of rifting is no longer acting on the continental crust along the Eastern Atlantic margin.

Wheeler (1995) (Reference 267) suggests that many earthquakes in the eastern part of the Piedmont province and beneath the Coastal Plain province may be associated spatially with buried normal faults related to rifting that occurred during the Mesozoic Era. Normal faults in this region that bound Triassic basins may be listric into the Paleozoic detachment faults (Reference 268) or may penetrate through the crust as high-angle faults. However, no definitive correlation of seismicity with Mesozoic normal faults has been conclusively demonstrated.

After the continental extension and rifting ended, a prograding shelf-slope began to form over the passive continental margin. The offshore Jurassic–Cretaceous clastic-carbonate bank sequence covered by younger Cretaceous and Tertiary marine sediments, and onshore Cenozoic sediments, represents a prograding shelf-slope and the final evolution to a passive margin (Reference 203). Cretaceous and Cenozoic sediments thicken from near zero at the Fall Line to about 4,000 ft. at the South Carolina coast. The fluvial-to-marine sedimentary wedge consists of alternating sand and clay with tidal and shelf carbonates common in the downdip Tertiary section.

2.5.1.1.2.2 Tectonic Stress in the Mid-Continent Region

Earth science teams (ESTs) that participated in the EPRI (1986) (Reference 269) evaluation of intra-plate stress found that tectonic stress in the Central and Eastern United States (CEUS) region is primarily characterized by northeast-southwest-directed horizontal compression. In general, the ESTs conclude that the likely source of tectonic stress in the mid-continent region is ridge-push force associated with the Mid-Atlantic ridge, transmitted to the interior of the North American plate by the elastic strength of the lithosphere. The ESTs judge other potential forces acting on the North American plate to be less significant in contributing to the magnitude and orientation of the maximum compressive principal stress. Some of the ESTs note that the regional northeast-southwest

trend of principal stress may vary in places along the east coast of North America and in the New Madrid region. They assess the quality of stress indicator data and discuss various hypotheses to account for what are interpreted as variations in the regional stress trajectories.

Since 1986, an international effort to collate and evaluate stress indicator data culminated in publication of a new World Stress Map (References 270 and 271). Data for this map are ranked in terms of quality. Plate-scale trends in the orientations of principal stresses are assessed qualitatively based on analysis of high-quality data (Reference 272). Subsequent statistical analyses of stress indicators confirmed that the trajectory of the maximum compressive principal stress is uniform across broad continental regions at a high level of statistical confidence. In particular, the northeast-southwest orientation of principal stress in the CEUS inferred by the EPRI ESTs is statistically robust and is consistent with the theoretical trend of compressive forces acting on the North American plate from the mid-Atlantic ridge (Reference 272).

The more recent assessments of lithospheric stress do not support inferences by some EPRI ESTs that the orientation of the principal stress may be locally perturbed in the New England area, along the east coast of the United States, or in the New Madrid region (References 270, 271, and 272). Zoback and Zoback (1989) (Reference 270) summarize a variety of data, including well-bore breakouts, results of hydraulic fracturing studies, and newly calculated focal mechanisms, which indicate that the New England and eastern seaboard regions of the U.S. are characterized by uniform horizontal northeast-southwest to east-west compression. Similar trends are present in the expanded set of stress indicators for the New Madrid region. Zoback and Zoback (1989) (Reference 271) group all of these regions, along with a large area of eastern Canada, with the CEUS in an expanded "Mid-Plate" stress province characterized by northeast-southwest-directed horizontal compression.

In addition to better documenting the orientation of stress, research conducted since 1986 addresses quantitatively the relative contributions of various forces that may be acting on the North American plate to the total stress within the plate. Richardson and Reding (1991) (Reference 273) describe the results of numerical modeling of stress in the continental U.S. interior and consider the contribution to total tectonic stress to be from three classes of forces:

- Horizontal stresses that arise from gravitational body forces acting on lateral variations in lithospheric density. These forces commonly are called buoyancy forces. Richardson and Reding (1991) (Reference 273) emphasize that what is commonly called ridge-push force is an example of this class of force. Rather than a line-force that acts outwardly from the axis of a spreading ridge, ridge-push arises from the pressure exerted by positively buoyant, young oceanic lithosphere near the ridge against older, cooler, denser, less buoyant lithosphere in the deeper ocean basins (Reference 274). The force is an integrated effect over oceanic lithosphere ranging in age from about 0 to 100 Ma (Reference 275). The ridge-push force transmits as stress to the interior of continents by the elastic strength of the lithosphere.

- Shear and compressive stresses transmit across major plate boundaries (strike-slip faults and subduction zones).

- Shear tractions acting on the base of the lithosphere from relative flow of the underlying asthenospheric mantle.

Richardson and Reding (1991) (Reference 273) concludes that the observed northeast-southwest trend of principal stress in the CEUS dominantly reflects ridge-push forces. They estimate the magnitude of these forces to be about 2 to 3 x 10^{12} Newtons per meter (i.e., the total vertically integrated force acting on a column of lithosphere 3.28 ft [1 m] wide), which corresponds to average equivalent stresses of about 40 to 60 megapascals (MPa) distributed across a 30-mi.-thick elastic plate. Richardson and Reding (1991) (Reference 273) find that the fit of the model stress trajectories to data is improved by adding compressive stress (about 5 to 10 MPa) acting on the San Andreas fault and Caribbean plate boundary structures. The fit of the model stresses to data further indicates that shear stresses acting on these plate boundary structures must also be in the range of 5 to 10 MPa.

Richardson and Reding (1991) (Reference 273) note that numerical models that assume horizontal shear tractions acting on the base of the North American plate reproduce the general northeast-southwest orientation of principal stress in the CEUS. Richardson and Reding (1991) (Reference 273) do not favor this as a significant contributor to total stress in the mid-continent region because their model would require an order-of-magnitude increase in the horizontal compressive stress from the eastern seaboard to the Great Plains.

To summarize, analyses of regional tectonic stress in the CEUS since EPRI (1986) (Reference 269) do not significantly alter the characterization of the northeast-southwest orientation of the maximum compressive principal stress. The orientation of a planar tectonic structure relative to the principal stress direction determines the magnitude of shear stress resolved onto the structure. Given that the current interpretation of the orientation of principal stress is similar to that adopted in EPRI (1986) (Reference 269), a new evaluation of the seismic potential of tectonic features based on a favorable or unfavorable orientation to the stress field would yield similar results. Thus, there is no significant change in the understanding of the static stress in the CEUS since the publication of the EPRI source models in 1986, and there are no significant implications for existing characterizations of potential activity of tectonic structures.

2.5.1.1.2.3 Gravity and Magnetic Data of the Site Region and Site Vicinity

In 1987, the Geological Society of America published regional maps of the gravity and magnetic fields in North America as part of the Society's Decade of North American Geology (DNAG) project. These maps include the Committee for the Gravity Anomaly Map of North America (Reference 276) and the Committee for the Magnetic Anomaly Map of North America (Reference 277). The maps present the potential field data at 1:5,000,000-scale and are useful for identifying and assessing regional gravity and magnetic anomalies with wavelengths on the order

of about 6 mi. or greater. Published maps of the gravity and aeromagnetic fields for the state of South Carolina (Reference 278) and the digital data from these maps are the basis of the gravity and magnetic maps in Figures 2.5.1-205 and 2.5.1-206, respectively. Gravity and magnetic data were incorporated in the DNAG E-4 crustal transect, which traverses the Appalachian orogen to the northeast of the Lee Nuclear Site (Figure 2.5.1-207). The DNAG E-4 transect extends from central Kentucky to the Carolina trough in the offshore Atlantic basin, just north of the South Carolina-North Carolina state line (Reference 282) and passes a few miles to the northeast of the Lee Nuclear Site. Figure 2.5.1-207 presents geologic and potential field data from the DNAG E-4 transect.

2.5.1.1.2.3.1 Gravity Data of the Site Region and Site Vicinity

The 1987 DNAG gravity map (Reference 276), and the gravity profile along the DNAG E-4 crustal transect (Figure 2.5.1-207), document a long-wavelength anomaly east of the Brevard fault zone. The Brevard fault zone marks the tectonic boundary between the Blue Ridge province to the west and the Piedmont province to the east (Figure 2.5.1-201). Bouguer gravity values increase by about 80 to 120 milliGals (mGal) across an approximately 125 to 155 mi. reach of the Piedmont east of the Blue Ridge (Figure 2.5.1-207). As documented by the DNAG gravity map, this gradient is present across the Piedmont physiographic province along much of the length of the Appalachian belt.

Previous workers refer to this long-wavelength feature in the gravity field as the “Piedmont gradient” (References 279 and 280). At the latitude of Virginia, north of the Lee Nuclear Site region, Harris et al. (1982) (Reference 279) interpret the Piedmont gradient to reflect the eastward thinning of the North American continental crust and associate positive relief on the Moho with proximity to the Atlantic margin. Gravity models by Iverson and Smithson (1983) (Reference 281) along the southern Appalachian COCORP (Consortium for Continental Reflection Profiling) seismic reflection profile, and by Dainty and Frazier (1984) (Reference 280) in northeastern Georgia, suggest that the gradient likely arises from both eastward thinning of continental crust and the obduction of the Inner Piedmont and Carolina-Avalon terranes. These terranes have higher average densities than the underlying Precambrian basement of North America. The Lee Nuclear Site is located just northwest of the location where the gradient starts to flatten out as it passes into the Carolina – Avalon terrane to the east (Figure 2.5.1-207).

Superimposed on the long-wavelength Piedmont gradient are numerous high and low gravity anomalies that have wavelengths of about 6 to 12 mi., and are elliptical to irregular in plan view. These anomalies are especially well expressed in the Carolina-Avalon terrane (per Reference 203) to the south of the Lee Nuclear Site between the Central Piedmont shear zone and the Modoc shear zone (Figure 2.5.1-205). Based on comparison of the gravity maps with geologic maps, many of these anomalies are spatially associated with Paleozoic igneous intrusions and plutons. The basement of the Carolina-Avalon terrane at this latitude is interpreted as the crust of an oceanic island arc terrane or terranes that was accreted to the Appalachian orogen during the Taconic orogeny (References 201 and 203). The composition of this crust generally is intermediate

between felsic and mafic (Reference 282). The intrusions and plutons in the Carolina-Avalon terrane with associated gravity anomalies fall more toward the extremes in felsic and mafic compositional ranges for igneous rocks. This gives rise to density contrasts with the country rock they intrude. In general, gravity highs are associated with mafic intrusions and mafic basement rocks, and gravity lows are associated with granitic plutons. Detailed gravity modeling by Cumbest et al. (1992) (Reference 283) in the vicinity of the Savannah River Site supports the general association of 6- to 12-mi.-high and -low anomalies in the Piedmont gravity field with mafic and felsic intrusions, respectively.

The origin of the high and low gravity anomalies beneath the Coastal Plain southeast of the Lee Nuclear Site (Figure 2.5.1-205) is uncertain due to lack of data on basement rock composition. Several high gravity anomalies appear to be associated with Triassic basin structures approximately 60 to 90 mi. southeast of the Lee Nuclear Site. A possible analogue for interpreting these anomalies is the well-studied Triassic Dunbarton basin beneath the Savannah River Site south of the Lee Nuclear Site. As shown on Figure 2.5.1-205, there is a pronounced gravity high along the southern margin of the Dunbarton basin. From a synthesis of borehole data and gravity modeling, Cumbest et al. (1992) (Reference 283) demonstrate that the extremes in the local gravity field at the Savannah River Site are highs associated with Triassic-Jurassic mafic intrusive complexes southeast of the Dunbarton basin, and lows associated with granitic plutons mapped to the north-northeast and east-northeast of the basin. Cumbest et al. (1992) (Reference 283) show that the predicted anomaly associated with the Mesozoic Dunbarton basin fill is a subordinate feature of the gravity field compared to the anomalies associated with the plutons and mafic intrusions. If similar geologic relations apply for the Triassic basins southeast of the Lee Nuclear Site, then it is likely that the high gravity anomalies are associated with Triassic mafic intrusions. Gravity lows associated with the basin fill strata may be obscured by the relatively high amplitude of the anomalies associated with the mafic rocks.

Gravity data for the Lee Nuclear Site vicinity are coarse (spacing approximately 4 mi.), with consequent low-resolution information available for the gravity field (Figure 2.5.1-208). The site is located on a long wavelength gravity gradient of about 2 mGal/mi. that marks the transition from the relative gravity lows of the Inner Piedmont to the high field elliptical anomalies that represent the denser crustal components contained in the Carolina Zone. Across the site area the regional field ranges from about -42 mGal in the west to -30 mGal in the east (Figure 2.5.1-208). The regional gravity field is marked by approximately 25 mi. wavelength undulations, of about 5-mGal amplitude, as the regional gradient flattens and steepens slightly. The site occurs in the trough of one of these features. Correlation of the detailed response of the gravity field to specific features in the site area is unresolved due to the poor data density.

To summarize, gravity data published since the mid-1980s document that long-wavelength anomalies in the vicinity of the Lee Nuclear Site are characteristic of large parts of the Appalachian belt. (Reference 276) Furthermore, these data reflect first-order features of the various provinces and accreted Paleozoic terranes, as well as west-to-east thinning of the ancestral North American continental crust. The dominant short-wavelength characteristics of the gravity

field in the vicinity of the Lee Nuclear Site are gravity highs and lows associated with mafic and granitic intrusions, respectively.

In general, there is better spatial correlation in the Lee Nuclear Site study region among gravity anomalies and igneous intrusions than faults. The exceptions are the Paleozoic Modoc shear zone and the Brevard zone. The Modoc shear zone appears to separate higher density rocks to the northwest from lower density rocks to the southeast. The Brevard zone marks the western boundary of the Piedmont gravity gradient. The juxtaposition of basement terranes with varying densities across these faults occurred during the Paleozoic Alleghanian orogeny (Reference 203), and therefore does not reflect Cenozoic activity. The mapped trace of the southern segment of the East Coast fault system (ECFS) is not expressed in the gravity field and cuts across anomalies with wavelengths on the order of tens of miles without noticeable perturbation. This implies that the southern segment of the ECFS, if present, has not accumulated sufficient displacement to systematically juxtapose rocks of differing density, and thus produce an observable gravity anomaly at the scale of Figure 2.5.1-205.

2.5.1.1.2.3.2 Magnetic Data of the Site Region and Site Vicinity

Data compiled for the DNAG magnetic map reveal numerous regional northeast-southwest-trending magnetic anomalies that are generally parallel to the structural grain of the Paleozoic Appalachian orogenic belt (Reference 270). In contrast to the gravity data, the magnetic field does not exhibit a long-wavelength anomaly east of the Brevard fault zone coincident with the accreted Taconic terranes of the Piedmont. As shown on the magnetic profile for the DNAG E-4 transect (Figure 2.5.1-207), the magnetic field across the Piedmont generally is characterized by high and low anomalies with wavelengths on the order of about 3 to 6 mi. Key features of the regional magnetic field include the following:

- The western Piedmont between the Brevard fault zone and Central Piedmont shear zone is characterized by a relatively uniform to smoothly varying magnetic field about a background value of approximately –500 nanotesla (nT) (Figures 2.5.1-206 and 2.5.1-207).

- The Carolina-Avalon terrane east of the Central Piedmont shear zone is characterized by numerous circular, elliptical, and irregular anomalies with plan dimensions on the order of about 3 to 12 mi. The change in character between the magnetic field of the Inner Piedmont and Carolina-Avalon terrane is very distinct across the Central Piedmont shear zone. Comparison of the magnetic data to geologic mapping indicates that the majority of these anomalies are associated with mafic and felsic intrusions or with zones of hydrothermal alteration resulting in magnetite mineralization associated with stratiform ores.

- The Modoc shear zone is clearly associated with elongate, east-northeast trending high and low magnetic anomalies. This is also characteristic of several other nearby Paleozoic faults that can be clearly traced under the Coastal Plain cover (i.e., faults of the Eastern Piedmont fault system.) The

very short wavelengths and linear trends of the anomalies are characteristic of those produced by a susceptibility contrast across a dipping structural contact (Reference 283).

- Regionally extensive magnetic anomalies occur beneath the Coastal Plain east of the Modoc shear zone. The magnetic anomalies are relatively high, indicating the presence of rocks with higher magnetic susceptibility at depth, and they are paired with high gravity anomalies (Figures 2.5.1-205 and 2.5.1-206), indicating that the rocks are also relatively dense. Detailed modeling of magnetic data from the Savannah River Site on the South Carolina-Georgia border south of the Lee Nuclear Site indicates that these anomalies may be associated with mafic intrusions (Reference 283). Felsic plutons in this region are inferred to exist from borehole data and gravity modeling. These felsic plutons have modest susceptibility contrasts with the country rock they intrude and thus do not generate high-amplitude magnetic anomalies (Reference 283). Similarly, Mesozoic basin sediments are inferred to have relatively low susceptibility contrasts with the pre-intrusive basement rock. Modeling by Cumbest et al. (1992) (Reference 283) suggests that the anomaly associated with the sediments and margins of the Dunbarton basin is a second-order feature of the magnetic field relative to the amplitudes of the anomalies produced by the intrusive mafic rocks.

Several of the characteristics of the regional magnetic field and its relation to geology are illustrated in the magnetic field for the site vicinity (Figure 2.5.1-233) and on a northwest-southeast-trending profile that passes through the Lee Nuclear Site (Figure 2.5.1-208). The magnetic field for the site vicinity is modeled on a 1,312 ft. (400 m) grid that is based on flight lines spaced one mile apart, flown at 500 ft. above the ground surface, in an east-west orientation. The magnetic intensities northwest of the Central Piedmont Shear Zone are relatively low compared to the magnetic field characterized by intense northeast trending magnetic highs and lows to the southeast. This expression in the magnetic field results from the exposures of mafic to intermediate composition metavolcanic basement rocks of the Charlotte terrane to the southeast and the relative lack of intense magnetic sources in the Inner Piedmont terrane to the northwest. In the site vicinity, the difference in the response of the magnetic field does not occur abruptly at the boundary between the Charlotte terrane and the Inner Piedmont (Central Piedmont Shear Zone), but is transitional over about a mile east of the Central Piedmont Shear Zone. This behavior has been attributed to a Central Piedmont Shear Zone that dips relatively shallowly to the east so that the rocks of the Charlotte terrane form a thin, easterly thickening upper plate over the Inner Piedmont (Milton (1981) (Reference 408); (Hatcher et al. (2007) (Reference 404)).

In the Charlotte terrane, southeast of the Central Piedmont Shear Zone, the northeast-trending fabric in the magnetic field defined by the intense magnetic highs and lows is interrupted by several elliptical shaped areas defined by a subdued magnetic response. Based on comparison with geologic maps, these subdued areas in the magnetic field correspond to late Paleozoic intrusions such as the Bald Rock, York and Clover plutons, and several related smaller intrusive bodies, which are felsic in composition and relatively nonmagnetic. In addition,

other plutonic masses such as the Lowery's Pluton and the Greensboro Plutonic suite also correspond with subdued magnetic field response. Lowery's Pluton is part of the Silurian Concord suite (McSween et al. (1991) (Reference 409)). Although the Concord suite consists of mafic lithologies, Lowery's Pluton does not give rise to the intense magnetization present in the surrounding metavolcanic country rock. The faults within the Charlotte terrane such as the Tinsley Bridge fault and the Boogertown shear zone parallel the regional northeasterly trending magnetic fabric, and their magnetic signature and effects on the magnetic field are not readily apparent.

In a discussion of the Central Piedmont Suture, Hatcher et al. (2007) (Reference 404) noted a gravity and magnetic linear anomaly that they identified as possibly representing the trace of the subsurface northeastern extension of the Central Piedmont suture. This feature passed through the southeastern portions of the site vicinity approximately 12 miles southeast of the site (Figure 2.5.1-233).

The data within the site area reveal several elongate to elliptical dipole anomalies that are characterized by magnetic highs of various amplitudes, with associated magnetic lows to the northwest. The elongation direction and alignment of the magnetic highs form prominent northeast to north-northeasterly striking linear features throughout the site area (Figure 2.5.1-206). One of the most prominent linear anomalies trends northeast–southwest and is formed by several individual, elongate magnetic highs in the northern portion of the site area. The most salient anomaly of this group (Shown as A on Figure 2.5.1-234) that comprises this feature has amplitude of about 300 nT and is located about 3.5 mi. northwest of the site (near the town of Cherokee Falls, South Carolina). This anomaly is accompanied to the northeast by two anomalous highs (about 180 nT) and to the southwest by a 50 nT high. The linear alignment generally follows the regional geologic trend and the southeastern flank of the Cherokee Falls synform (discussed in Subsection 2.5.1.2.4.1). This coincides with the location of stratiform iron deposits of massive and disseminated magnetite and other metallic sulphides (References 284 and 285).

Adjacent to and just southeast of the anomaly that marks the northeastern termination of the linear feature discussed above, an elongate magnetic high of about 230 nT (Shown as B on Figure 2.5.1-234) is oriented in a more northerly direction at a relatively high angle to the regional geologic trend. This location is closely associated with a zone of alteration as shown by Howard (2004) (Reference 286). The anomaly is parallel to a reentrant of the zone of alteration into the crystal metatuff unit to the south. Several small outcrops of diabase also occur in this area. The relatively high amplitude of the anomaly and the presence of the alteration zone suggest that concentrations of magnetite due to hydrothermal alteration are present and account for a significant amount of the magnetic response. However, the alignment of diabase outcrops in this area may exert some control on the orientation of this feature.

A 70 nT circular magnetic high is located about 3 mi. northeast of the site (Shown as C on Figure 2.5.1-234). This feature is accompanied by a more elongate north-northeasterly trending magnetic high to the south that shows amplitude of approximately 60 nT. These locations both correspond to diabase outcrops and

are likely the magnetic response of these mafic lithologies. In contrast, the metagabbro unit just southwest of these anomalies only produces a slight bending of the magnetic contours. This is a consistent magnetic response compared to that of the mafic units of Lowery's Pluton, as discuss above. However, the association of the metagabbro with the Concord Suite is not demonstrated.

An elongate magnetic high (amplitude about 120 nT) is located about 2.5 mi. south of the site (Shown as D on Figure 2.5.1-234). This anomaly trends northeasterly, concordant with the regional geologic trend, and coincident with quartzite outcrops. The magnetic signature of this feature is likely the result of magnetite and other metallic sulphides associated with hydrothermal alteration.

To summarize, magnetic data published since the mid-1980s provide additional characterization of the magnetic field in the Lee Nuclear Site region (Reference 277). The first-order magnetic anomalies are associated primarily with northeast-southwest-trending Paleozoic terranes of the Paleozoic Appalachian orogen. Superimposed on this regional magnetic field are anomalies with wavelengths on the order of 3 to 12 mi. that are associated with intrusive bodies or stratiform ore bodies resulting from hydrothermal alteration. The anomalous response of concentrations of magnetite associated with stratiform metallogenic deposits typically produce anomaly amplitudes of 100 to 300 nT, and are typically aligned with the regional geologic trend. Diabase dikes and other small outcrops produce secondary anomalous effects with amplitudes of about 50 nT. The metagabbro unit located about one mile east of the Lee Nuclear Site produces minimal effects on the magnetic field, and this response is consistent with the magnetic signature of Lowery's Pluton further to the southeast in the site vicinity.

The magnetic data generally are not of sufficient resolution to identify or map discrete faults such as border faults along the Triassic basins. In particular, the southern segment of the ECFS has no expression in the magnetic field and cuts across anomalies with wavelengths on the order of tens of miles without noticeably perturbing or affecting them. If the ECFS exists as mapped, then it has not accumulated sufficient displacement to juxtapose rocks of varying magnetic susceptibility, and thus does not produce an observable magnetic anomaly at the scale of Figure 2.5.1-206.

2.5.1.1.2.4 Principal Regional Tectonic Structures

Principal tectonic structures and features in the southeastern U.S. and within the 200 mi. Lee Nuclear Site region can be divided into four categories based on their age of formation or reactivation as shown in Figures 2.5.1-209 and 210. These categories include structures that were most active during Paleozoic, Mesozoic, Cenozoic, or Quaternary time. Most of the Paleozoic and Mesozoic structures are regional in scale, and are geologically and geophysically recognizable. The Mesozoic rift basins and bounding faults show a high degree of parallelism with the structural grain of the Paleozoic Appalachian orogenic belt, which generally reflects reactivation of pre-existing Paleozoic structures. Tertiary and Quaternary structures are generally more localized and may be related to reactivation of portions of older bedrock structures.

2.5.1.1.2.4.1 Regional Geophysical Anomalies and Lineaments

A number of regional geophysical anomalies are located within 200 mi. of the Lee Nuclear Site (Figures 2.5.1-209, 210 and 211). From southeast to northwest these include the East Coast Magnetic Anomaly, the southeast boundary of Iapetan normal faulting, Clingman lineament, Ocoee lineament, New York-Alabama lineaments, the Appalachian gravity gradient, the northwest boundary of Iapetan normal faulting, Appalachian thrust front, and the Grenville Front. These features are described below, with more detail provided for those features within the 200-mi site region.

East Coast Magnetic Anomaly. The East Coast Magnetic Anomaly (ECMA) is a broad, 200 to 300 nT magnetic high that is located approximately 30 to 120 mi. off the coast of North America, and is continuously expressed for about 1,200 mi. from the latitude of Georgia to Nova Scotia (References 248 and 289) (Figure 2.5.1-211). The ECMA is subparallel to the Atlantic coastline, and is spatially associated with the eastern limit of North American continental crust (Reference 248). The ECMA has been variously interpreted to be a discrete, relatively magnetic body such as a dike or ridge, or an “edge effect” due to the juxtaposition of continental crust on the west with oceanic crust (higher magnetic susceptibility) on the east (in Reference 287). In the vicinity of the ECMA, deep seismic reflection profiling in the Atlantic basin has imaged packages of east-dipping reflectors that underlie the sequence of Mesozoic-Tertiary passive-margin marine strata (Reference 288). The rocks associated with the east-dipping reflectors are interpreted to be an eastward-thickening wedge of volcanic and volcaniclastic rocks that were deposited during the transition between rifting of the continental crust and opening of the Atlantic basin during the Mesozoic (Reference 289). Models of the magnetic data show that the presence of this volcanic “wedge” can account for the wavelength and amplitude of the ECMA (Reference 248).

To summarize, the ECMA is a relict of the Mesozoic opening of the Atlantic basin, and likely arises from the presence of a west-tapering wedge of relatively magnetic volcanic rocks deposited along the eastern margin of the continental crust as the Atlantic basin was opening, rather than juxtaposition of rocks with differing magnetic susceptibilities across a fault. The ECMA is not directly associated with a fault or tectonic feature, and thus is not a potential seismic source.

Appalachian Gravity Gradient. This regional gravity gradient extends the length of the Appalachian orogen (Figure 2.5.1-209) and exhibits a southeastward rise in Bouguer gravity values as much as 50 to 80 mGal (References 265 and 295). The Appalachian gravity gradient represents the southeastern thinning of relatively intact Precambrian continental crust, and the early opening of the Iapetan Ocean (Reference 265).

Southeast and Northwest Boundaries of Iapetan Normal Faults. The southeast and northwest boundaries of Iapetan normal faults shown in Figure 2.5.1-209 define the extent of the Iapetan margin of the craton containing normal faults that accommodated extension during the late Proterozoic to early Paleozoic rifting that

formed the Iapetan Ocean basin. Wheeler (1996) (Reference 295) defines the southeast boundary as the southeastern limit of the intact Iapetan margin, which is nearly coincident with the Appalachian gravity gradient in the southeastern United States. The Iapetan normal faults are concealed beneath Appalachian thrust sheets that overrode the margin of the craton during the Paleozoic. A few of these Iapetan faults are thought to be reactivated and responsible for producing earthquakes in areas such as eastern Tennessee; Giles County, Virginia; and Charlevoix, Quebec (References 265 and 295).

The southeast margin of the Iapetan normal faults shown on Figure 2.5.1-209 does not represent a potential seismic source since it does not represent a discrete crustal discontinuity or tectonic structure. The linear feature shown in the figure represents the southeastern extent of the intact Iapetan margin (with a location uncertainty of about 20 mi.), and therefore, the southeastern limit of potentially seismogenic Iapetan faults (Reference 295).

The New York-Alabama, Clingman, and Ocoee Lineaments. King and Zietz (1978) (Reference 290) identify a 1,000-mi.-long lineament in aeromagnetic maps of the eastern U.S. that they name the “New York-Alabama lineament” (NYAL) (Figure 2.5.1-209). The NYAL primarily is defined by a series of northeast-southwest-trending linear magnetic gradients in the Valley and Ridge province of the Appalachian fold belt that systematically intersect and truncate other magnetic anomalies. The NYAL also is present as complementary but less-well-defined lineament on regional gravity maps (Reference 290).

The Clingman lineament is an approximately 750-mi.-long, northeast-trending aeromagnetic lineament that passes through parts of the Blue Ridge and eastern Valley and Ridge provinces from Alabama to Pennsylvania (Reference 291). The Ocoee lineament splays southwest from the Clingman lineament at about latitude 36°N (Reference 292). The Clingman-Ocoee lineaments are sub-parallel to and located about 30 to 60 mi. east of the NYAL.

King and Zietz (1978) (Reference 290) interpret the NYAL to be a major strike-slip fault in the Precambrian basement beneath the thin-skinned fold-and-thrust structures of the Valley and Ridge, and suggest that it may separate rocks on the northwest that acted as a mechanical buttress from the intensely deformed Appalachian fold belt to the southeast. Shumaker (2000) (Reference 293) interpret the NYAL to be a right-lateral strike-slip fault that formed during an initial phase of late Proterozoic continental rifting that eventually led to the opening of the Iapetan Ocean. The Clingman lineament also is interpreted to arise from a source or sources in the Precambrian basement beneath the accreted and transported Appalachian terranes (Reference 291).

Johnston et al. (1985) (Reference 292) observe that the “preponderance of southern Appalachian seismicity” occurs within the “Ocoee block”, a Precambrian basement block bounded by the NYAL and Clingman-Ocoee lineaments [the Ocoee block was previously defined by Johnston and Reinbold 1985 (Reference 294)]. Based on the orientations of nodal planes from focal mechanisms of small earthquakes, Johnston et al. (1985) (Reference 292) note that most events within the Ocoee block occurred by strike-slip displacement on

north-south and east-west striking faults, and thus these researchers do not favor the interpretation of seismicity occurring on a single, through-going northeast-southwest-trending structure parallel to the Ocoee block boundaries.

The Ocoee block lies within a zone that Wheeler (1995 [Reference 267], 1996 [Reference 295]) defines as the cratonward limit of normal faulting along the ancestral rifted margin of North America that occurred during the opening of the Iapetan ocean in late Precambrian to Cambrian time. Synthesizing geologic and geophysical data, Wheeler (1995, 1996) (References 267 and 295) maps the northwest extent of the Iapetan faults in the subsurface below the Appalachian detachment, and proposes that earthquakes within the Ocoee block may be the result of reactivation of Iapetan normal faults as reverse or strike-slip faults in the modern tectonic setting.

Appalachian Thrust Front. The northwestern limit of allochthonous crystalline Appalachian crust was termed the Appalachian thrust front by Seeber and Armbruster (1988) (Reference 399) (Figure 2.5.1-209). This front is a sharply defined boundary interpreted as a major splay of the master Appalachian detachment.

Grenville Front. The Grenville front (Figure 2.5.1-209) is defined by geophysical, seismic reflection, and scattered drill hole data in the southeastern U.S. This feature lies within the continental basement and is interpreted to separate the relatively undeformed eastern granite-rhyolite province on the northwest from the more highly deformed rocks of the Grenville province on the southeast (Reference 400).

2.5.1.1.2.4.2 Regional Paleozoic Tectonic Structures

The Lee Nuclear Site region encompasses portions of the Coastal Plain, Piedmont, Blue Ridge, Valley and Ridge, and Appalachian Plateau physiographic provinces (Figure 2.5.1-201). Rocks and structures within these provinces are often associated with thrust sheets that formed during convergent Appalachian orogenic events of the Paleozoic Era. Tectonic structures of this affinity also exist beneath the sedimentary cover of the Coastal Plain province. These types of structures are shown on Figure 2.5.1-209 and Figure 2.5.1-210, and include the following:

- Sutures juxtaposing allochthonous (tectonically transported) rocks with autocthonous (non-transported North American crust) rocks.
- Regionally extensive Appalachian thrust faults and oblique-slip shear zones.
- Numerous smaller structures that accommodated Paleozoic deformation within individual belts or terranes.

The majority of these structures dip eastward, initially at a steep angle that becomes shallower as they approach the basal Appalachian decollement (Figure 2.5.1-207). The Appalachian orogenic crust is relatively thin across the

Valley and Ridge province, Blue Ridge province, and western part of the Piedmont province, and thickens eastward beneath the eastern part of the Piedmont province and the Coastal Plain province. Below the decollement are rocks that form the North American basement complex. These basement rocks contain northeast-striking, Late Precambrian to Cambrian normal faults that formed during the Iapetan rifting that preceded the deposition of Paleozoic sediments.

Researchers observe that much of the sparse seismicity in eastern North America occurs within the North American basement below the basal decollement. Therefore, seismicity within the Appalachians may be unrelated to the abundant, shallow thrust sheets mapped at the surface (Reference 267). For example, seismicity in the Giles County seismic zone, located in the Valley and Ridge province, is occurring at depths ranging from 3 to 16 mi. (see Subsection 2.5.1.1.3.2.3) (References 265 and 371), which is generally below the Appalachian thrust sheets and basal decollement (Reference 265).

Paleozoic faults within 200 mi. of the Lee Nuclear Site are shown on Figure 2.5.1-209 and those within 25 mi. and 50 mi. are shown on Figure 2.5.1-210. The faults that are considered most important, either because of their regional tectonic significance or their proximity to the site, are discussed below. Not every fault depicted in Figures 2.5.1-209 and 2.5.1-210 is discussed explicitly.

Kings Mountain Shear Zone (Central Piedmont Shear Zone). The northeast-striking Kings Mountain shear zone is a zone of mylonitic deformation that separates the Inner Piedmont terrane from the Carolina terrane, and is considered part of the larger Central Piedmont shear zone (References 236, 296, and 297). The Kings Mountain shear zone comprises smaller, localized shear zones, including the Blacksburg and Kings Creek shear zones. At its nearest point, the Kings Mountain shear zone is located 5 mi. north of the Lee Nuclear Site (Figure 2.5.1-210). The sense of motion on the Kings Mountain shear zone is unclear, but structural data suggest that the zone is a steeply northwest-dipping reverse fault (Reference 236). Mylonitic deformation in the Kings Mountain shear zone is overprinted by semi-brittle cleavage. Pegmatitic dikes in North Carolina intruded parallel to the semi-brittle cleavage and some have been ductiley deformed. Hence, the dikes are interpreted as syn- to post-kinematic and their Rb/Sr whole rock isochron age of 340 ± 5 Ma indicates that the late-stage semi-brittle deformation occurred in the Mississippian (Horton (1981) (Reference 421)).

Cross Anchor Fault. The greater than 60-mi.-long Cross Anchor fault is mapped by Hibbard et al. (2006) (Reference 260) as a thrust fault of variable strike. At its nearest point, the Cross Anchor fault is located approximately 10 mi. west of the Lee Nuclear Site (Figure 2.5.1-210). West (1998) (Reference 297) interprets the Cross Anchor fault as the Carolina-Inner Piedmont terrane boundary. Dennis and Wright (1995) (Reference 422) interpreted an unnamed granite, dated at 326 ± 3 Ma, to cut and post-date the Central Piedmont shear zone. However, West (1998) (Reference 297) interpreted the same pluton as syn- to pre-kinematic to deformation on the fault and interpreted movement on the fault to be approximately 325 Ma.

Hyco Shear Zone. In northern North Carolina and southern Virginia, the Hyco shear zone dips shallow to steeply to the southeast and juxtaposes the Carolina terrane rocks over the Milton terrane, rocks correlated with the Inner Piedmont or Piedmont zone (Hibbard et al. (1998) (Reference 417)) (FSAR Figure 209). Hence, it is interpreted as part of the Central Piedmont shear zone (Hibbard et al. (2002) (Reference 204)). Ages on granitoids interpreted as syn-kinematic to deformation on this structure range from about 320 Ma to about 335 Ma, and indicate a Mississippian age for deformation (Wortman et al. (1998) (Reference 418)).

Brindle Creek Thrust Fault. The Brindle Creek thrust was recognized in North Carolina as a low-angle fault with an extensive mylonite zone, but authors have indicated that the mapping of this structure in South Carolina is speculative (Bream (2002), Reference 403). According to Hatcher et al., 2007 (Reference 404), the following lines of evidence are used to map the Brindle Creek fault:

- The fault separates areas with different stratigraphy,
- The fault separates areas with different detrital zircon age distributions,
- The fault separates areas with different mafic and ultramafic rocks, and
- The fault separates areas with different age and character of plutons.

The fault is interpreted as an early Paleozoic unconformity that was activated as a mylonitic fault in the late Paleozoic during the Alleghanian orogeny (Dennis, 2007; Reference 405) or as a Neoacadian (early Mississippian) thrust (Hatcher et al., 2007; Reference 404). In North Carolina, a granite exposed only in the hanging-wall of the Brindle Creek fault has zircons with a weighted $^{206}Pb/^{238}U$ ion microprobe age of 366 ± 3 Ma (Giorgis et al. (2002) (Reference 415)). This field relationship was interpreted to indicate that the Brindle Creek fault was active after the intrusion of the granite, or is Devonian or younger in age. Also in North Carolina, migmatitic, high-temperature deformation is spatially associated with the Brindle Creek fault (Giorgis et al. (2002) (Reference 415)). Metamorphic rims in migmatitic rocks in the immediate footwall of the Brindle Creek fault yield ion-microprobe U-Pb ages of ca. 350 Ma, probably correlative with emplacement of the Brindle Creek hanging-wall (Merschat and Kalbas (2002) (Reference 416)).

Tinsley Bridge Fault. The Tinsley Bridge fault is a less than 20-mi.-long zone of retrograde mylonite with apparent down-to-the-northwest sense of slip (Dennis (1995) (Reference 298)). At its nearest point, the Tinsley Bridge fault is located 5 mi. southwest of the Lee Nuclear Site (Figure 2.5.1-210). Based on the observations that mylonitic deformation occurred after peak metamorphic conditions (early Cambrian) and that the fault is cut by the undeformed Pacolet granite (whole-rock Rb/Sr age of 383 ± 5 Ma) the fault was active in the early Paleozoic (Reference 298).

Southwest Extension of the Boogertown Shear Zone. The northeast-striking Boogertown shear zone marks the boundary between the Kings Mountain belt and the Charlotte belt (Reference 236). At its nearest point, this shear zone is located 8 mi. east of the Lee Nuclear Site (Figure 2.5.1-210). The northeastern end of the Boogertown shear zone is truncated by an unsheared granitic pluton (Milton (1981) (Reference 408)). This pluton is undated, but the youngest plutons within the Carolina Zone are 300-265 Ma (Hatcher et al. (2007) (Reference 404)).

Reedy River Thrust Fault. The Reedy River thrust fault is a northeast-striking structure in the Inner Piedmont (References 260, 299, and 300). At its nearest point, the Reedy River thrust fault is located 18 mi. west-northwest of the Lee Nuclear Site (Figure 2.5.1-210).

Gold Hill-Silver Hill Shear Zone. The Gold Hill-Silver Hill shear zone is a dextral strike-slip shear zone located approximately 30 mi. south of the Lee Nuclear Site (Figure 2.5.1-210). Based upon cross-cutting relationships with intrusive igneous bodies and the Cross Anchor fault, West (1998) (Reference 297) constrains motion on this shear zone to between approximately 400 and 325 Ma. Work along the Gold Hill-Silver Hill shear zone to the northeast has variably indicated deformation events of earliest Cambrian dextral-reverse faulting (Allen et al. (2007) (Reference 427)), Late Ordovician sinistral deformation (Hibbard et al. (2007) (Reference 425)), and Devonian to Mississippian remobilization (Hibbard et al (2007 (Reference 425); Hibbard et al. (2008) (Reference 426)). The best evidence for the latest movement on the GHSZ, however, is based on its cross-cutting relationship with the Cross Anchor fault that indicates latest motion was sometime prior to 325 Ma (West (1998) (Reference 297)).

Middleton-Lowndesville Shear Zone. The Lowndesville shear zone is located approximately 40 mi. south of the Lee Nuclear Site (Figure 2.5.1-210), and is a zone of predominantly mylonitic gneisses, along with local muscovite phyllonites and silicified breccias, with a subvertical, N65°E-striking foliation, bearing subhorizontal stretching lineations (West (1998) (Reference 297)). It coincides with the sharply defined southeastern boundary of the Piedmont zone (or Inner Piedmont terrane), characterized by amphibolites-facies to migmatitic rocks (Griffin (1981) (Reference 423)), and is interpreted as part of the Central Piedmont shear zone (West (1998) (Reference 297)). Where it extends south into Georgia, it is described as a cataclastic zone, striking northeast, where it is mapped in geophysical data (Rozen (1981) (Reference 235)). The ductile and brittle deformation features associated with this structure all occurred at a minimum of greenschist-facies conditions and the brittle features are interpreted to have formed near the brittle-ductile transition (Nelson (1981) (Reference 424)). In South Carolina the Lowndesville shear zone is mapped as being truncated by the Cross Anchor fault, and hence was active older than approximately 325 Ma (West (1998) (Reference 297)).

Beaver Creek Shear Zone. The Beaver Creek shear zone is a 4 km wide zone of mylonitic paragneiss, amphibolites and paragneiss (West (1998) (Reference 297)). The N80°E, subvertically dipping fabric bears dextral shear sense indicators and is cut by the Newberry granite, which is 415 ± 9 Ma in age

(West (1998) (Reference 297)). The shear zone is also truncated by the Cross Anchor fault (West (1998) (Reference 297).

Modoc Shear Zone. The Modoc shear zone is a region of high ductile strain separating the Carolina terrane (Carolina Slate and Charlotte belts) from amphibolite facies migmatitic and gneissic rocks (Reference 301). The northeast-trending Modoc zone dips steeply to the northwest and is traced through the Piedmont from central Georgia to central South Carolina based on geological and geophysical data. The Modoc shear zone appears to continue northeastward to North Carolina beneath the Coastal Plain, as demonstrated by geologic mapping and aeromagnetic data (Figure 2.5.1-206). At its nearest point, the Modoc shear zone is about 75 mi. south of the Lee Nuclear Site. The Modoc shear zone contains fabrics characterized by brittle and ductile deformation produced by ductile shear during an early phase of the Alleghanian orogeny (References 302, 303, 304, and 305). Geochronologic data from Dallmeyer et al. (1986) (Reference 410) indicate movement occurred between 315 and 290 Ma. Howard et al. (2005) (Reference 411) and McCarney et al. (2005) (Reference 412) describe the Modoc fault zone as exposed by construction of Saluda Dam on Lake Murray, west of Columbia, South Carolina. They interpret brittle features in the Saluda Dam spillway as the result of readjustment from different loading and unloading, as well as tectonic movement associated with latest Alleghanian deformation and initial Triassic rifting.

Hatcher et al. (1977) (Reference 306) suggest that the Modoc shear zone, the Irmo shear zone, and the Augusta fault are part of the proposed Eastern Piedmont fault system, an extensive series of faults and splays extending from Alabama to Virginia. Aeromagnetic, gravity, and seismic reflection data indicate that the Augusta fault zone continues northeastward in the crystalline basement beneath the Coastal Plain province sediments.

Brevard Fault Zone. The northeast-trending Brevard fault zone extends for over 400 mi. from Alabama to Virginia (References 260 and 307). At its nearest point, the Brevard fault zone is located approximately 55 mi. northwest of the Lee Nuclear Site (Figure 2.5.1-210). The Brevard fault zone separates the Blue Ridge province to the west from the Piedmont province to the east. Diabase dikes preclude post Jurassic slip on the Brevard fault and cooling age histories indicate that no slip has occurred on the Brevard fault since the late Paleozoic (Reference 226).

Chappells Shear Zone. Horton and Dicken (2001) (Reference 308) and Hibbard et al. (2006) (Reference 260) map the 60-mi.-long Chappells shear zone as an approximately northeasterly-trending, 2-mi.-wide zone of ductile deformation. At its nearest point, the Chappells shear zone is located approximately 57 mi. south of the Lee Nuclear Site (Figure 2.5.1-210). Post-Paleozoic slip on the Chappells shear zone is precluded by cross-cutting relationships with the late Paleozoic (309 Ma; Reference 309) Winnsboro pluton.

Other Paleozoic Faults. Other Paleozoic faults are present in the site region, most are located northwest of the site and are oriented parallel to the regional structural grain (Figure 2.5.1-209). These include, but are not limited to, the Eufola and

Tumblebug Creek faults shown on FSAR Figure 2.5.1-210, and the Pine Mountain, Bowens Creek, and Fries faults shown on Figure 2.5.1-209. While definitive timing evidence does not exist for many of the faults within the site region, any combination of many factors may have prompted workers to assess them as Paleozoic including:

- Mapping that indicates that these faults only deform rocks of Paleozoic or older age,
- Geometries and kinematics similar to other faults with established Paleozoic ages (e.g., west-directed thrusts), and/or
- Textural fabrics or mineral assemblages consistent with deformation at ductile high-temperature metamorphic conditions, the latest of which generally occurred during the late Paleozoic collision with Gondwana (e.g., Hatcher et al. (2007) (Reference 404)). For example, the Tumblebug Creek fault was active during upper amphibolites, sillimanite-grade metamorphism (Davis (1993) (Reference 419)).

Furthermore, no seismicity is attributed to the Paleozoic faults in the site region, and published literature does not indicate that any of these faults offset late Cenozoic deposits or exhibit a geomorphic expression indicative of Quaternary deformation. In addition, Crone and Wheeler (2000) (Reference 310) and Wheeler (2005) (Reference 311) do not show any of these faults to be potentially active Quaternary faults. Therefore, these Paleozoic structures in the site region are not considered to be capable tectonic sources. No new information has been published since 1986 on any Paleozoic fault in the site region that would cause a significant change in the EPRI seismic source model.

2.5.1.1.2.4.3 Regional Mesozoic Tectonic Structures

Tectonic features in the site region of known or postulated Mesozoic age include faults and extensional rift basins. These features, which are described below, are shown and labeled on Figure 2.5.1-210. The features also are shown on Figure 2.5.1-209, but not all features are labeled due to the scale limitations of the figure.

Wateree Creek fault. Secor et al. (1982) (Reference 312) map the greater than 8-mi.-long Wateree Creek fault as an approximately north-striking, unsilicified fault zone. At its nearest point, the Wateree Creek fault is located approximately 55 mi. south of the Lee Nuclear Site. Based upon cross-cutting relationships with Triassic or Jurassic diabase dikes, Secor et al. (1982) (Reference 312) estimate a minimum age of Triassic for the Wateree Creek fault. More recent maps of the site area by Maher et al. (1991) (Reference 314) reinterpret the northernmost portion of the fault as striking northeast. The central and southern portion of the fault is well located due to roadcut and trench exposures (Reference 313). Detailed magnetometer surveys and trench studies of the central and southern portions of the Wateree Creek fault demonstrate the continuity of an unfaulted diabase dike of probable Triassic age across the fault, thereby constraining most-recent activity

on the Wateree Creek fault to the Mesozoic or pre-Mesozoic (References 312 and 313).

Summers Branch fault. The approximately 8-mi.-long Summers Branch fault is mapped by Secor et al. (1982) (Reference 312) as an approximately north-striking, unsilicified fault zone. At its nearest point, the Summers Branch fault is located approximately 55 mi. south of the Lee Nuclear Site. By association with the Wateree Creek fault, Secor et al. (1982) (Reference 312) estimate a minimum age of Triassic for the Summers Branch fault. More recent maps of the site area have omitted the speculative Summers Branch fault (Reference 314). Despite questions regarding its existence, the Summers Branch fault is shown on Figures 2.5.1-209 and 2.5.1-210.

Ridgeway Fault. Secor et al. (1998) (Reference 315) map the greater than 9-mi.-long Ridgeway fault as an approximately north-striking, unsilicified fault zone located approximately 60 mi. southeast of the Lee Nuclear Site. By association with both the Wateree Creek and Summers Branch faults, Secor et al. (1998) (Reference 315) estimate a minimum age of Triassic for the Ridgeway fault.

Longtown Fault. The Longtown fault strikes west-northwest in the Ridgeway-Camden area, about 60 mi. southeast of the Lee Nuclear Site. As mapped by Secor et al. (1998) (Reference 315), the Longtown fault terminates eastward against the Camden fault. The Longtown fault is associated with fracturing and brecciation of crystalline rocks, and fragments of silicified breccia are found along its trace (Reference 315). Total slip on the Longtown fault is uncertain, although Secor et al. (1998) (Reference 315) suggest total displacement on the order of hundreds to thousands of feet is likely in order to explain the apparent disruption of crystalline rocks across the fault. Secor et al. (1998) (Reference 315) suggest possible Cenozoic (pre-Oligocene) slip on the Longtown fault. However, more recent mapping by Barker and Secor (2005) (Reference 316) shows four diabase dikes of probable Triassic age that cross, but are not offset by, the Longtown fault. Based on these cross-cutting relationships, a minimum age of Triassic is established for the Longtown fault.

Mulberry Creek Fault. The Mulberry Creek fault is located approximately 55 mi. southwest of the Lee Nuclear Site. This subvertical fault contains silicified breccia, microbreccia, and cataclasite (Reference 297). Evidence for the timing of slip on the Mulberry Creek fault is indirect. By association with other similar silicified breccias in North and South Carolina, West (1998) (Reference 297) suggests a Late Triassic to Early Jurassic age for the Mulberry Creek fault.

Mesozoic Rift Basins. A broad zone of fault-bounded, elongate, depositional basins associated with crustal extension and rifting formed during the opening of the Atlantic Ocean in early Mesozoic time. These rift basins are common features along the eastern coast of North America from Florida to Newfoundland (Figures 2.5.1-201 and 210). Wheeler (1995) (Reference 267) suggests that many earthquakes in the eastern part of the Piedmont province and beneath the Coastal Plain province may be associated spatially with buried normal faults related to rifting that occurred during the Mesozoic Era. However, definitive correlation of seismicity with Mesozoic normal faults is not conclusively demonstrated.

Figure 2.5.1-210 shows the lack of spatial correlation between Mesozoic basins and seismicity within 50 miles of the site. As of March 2009, there was no positive correlation between earthquakes in the site region and Mesozoic basins. Normal faults in this region that bound Triassic basins may be listric into the Paleozoic detachment faults (Reference 268) or may penetrate through the crust as high-angle faults. Within regions of stable continental cratons, areas of extended crust potentially contain the largest earthquakes (Reference 317) (Figure 2.5.1-212). Mesozoic basins have long been considered potential sources for earthquakes along the eastern seaboard (Reference 318) and were considered by most EPRI teams in their definition of seismic sources (Reference 269).

No seismicity is attributed to these Mesozoic features, and published literature does not indicate that any of these faults offset late Cenozoic deposits or exhibit a geomorphic expression indicative of Quaternary deformation. In addition, Crone and Wheeler (2000) (Reference 310) and Wheeler (2005) (Reference 311) do not show any of these faults to be potentially active Quaternary faults. Therefore, these Mesozoic structures in the site region are not considered to be capable tectonic sources.

2.5.1.1.2.4.4 Regional Cenozoic Tectonic Structures

Within 200 mi. of the Lee Nuclear Site, only a few tectonic features, including faults, arches, domes, and embayments, demonstrate Cenozoic activity. These features are shown on Figures 2.5.1-209 and 2.5.1-210, and are described below.

Camden Fault. The northeast-striking Camden fault is located in the eastern part of the Ridgeway-Camden area, about 70 mi. southeast of the Lee Nuclear Site. Along much of its length, the Camden fault juxtaposes crystalline rocks of the Carolina terrane on the northwest against crystalline rocks interpreted to be part of the Alleghanian Modoc shear zone on the southeast (Reference 315). Total slip on the Camden fault is uncertain, although Secor et al. (1998) (Reference 315) suggest total displacement on the order of miles is likely in order to explain the apparent disruption of crystalline rocks across the fault.

Up-to-the-north vertical separation of the basal Late Cretaceous unconformity of about 50 to 80 ft. suggests Late Mesozoic and possibly Cenozoic (pre-Oligocene) reactivation of the Camden fault (References 315 and 319). Map relationships in the northeastern Rabon Crossroads Quadrangle suggest a northwest-side up vertical separation of the unconformity at the base of the sand unit of about 82 ft., and map relationships at the southeastern corner of the Longtown Quadrangle suggest a northwest-side-up vertical separation of the unconformity of about 55 ft. (Reference 315).

Knapp et al. (2001) (Reference 320) describe seismic reflection and gravity data they interpret as suggesting an 80 to 100 ft. offset of the base of the Coastal Plain section. Knapp et al. (2001) (Reference 320) suggest that deposits of the Tertiary Upland formation cover the Camden fault, providing a potential upper age limit on the Cenozoic movement of the fault.

Prowell (1983) Faults. As part of the U.S. Geological Survey's Reactor Hazards Program, Prowell (1983) (Reference 321) compiled and mapped information regarding possible Cretaceous and younger faults in the eastern U.S. Three of these postulated faults are located within 50 mi. of the Lee Nuclear Site. Prowell's (1983) (Reference 321) faults numbered 63, 64, and 65 are located about 50 mi. northwest of the Lee Nuclear Site near Saluda, North Carolina (Figure 2.5.1-210). As noted by Prowell (1983) (Reference 321), faults numbered 63 and 64 are spatially associated with a slump block, and fault numbered 65 is a probable gravity slide plane. These features are likely the result of gravity-induced mass wasting processes and not the result of tectonic processes.

Arches and Embayments. The basement surface on which Coastal Plain sediments were deposited is not a simple planar platform. Instead, it is characterized by broad structural upwarps (arches) that separate depositional basins (embayments) (Horton and Zullo (1991) (Reference 261)). The hinge lines of these upwarps are aligned roughly perpendicular to the coastline. Two of these upwarps, the Cape Fear and Yamacraw arches, are located within the site region. The Cape Fear Arch is located near the South Carolina-North Carolina border and the Yamacraw Arch is located near the South Carolina-Georgia border (Figure 2.5.1-209).

Evidence constraining the timing of most-recent movement on the Cape Fear and Yamacraw arches is limited. Gohn (1998) (Reference 413) indicates that the Cape Fear Arch has affected the thickness and distribution of Late Cretaceous to late Tertiary strata. Prowell and Obermeier (1991) (Reference 414) suggest that upwarping on the Cape Fear Arch may have continued through the Pleistocene Epoch. Data constraining the timing of most-recent movement on the Yamacraw Arch are unavailable. However, since the tectonic history of the Yamacraw Arch likely is analogous to that of the Cape Fear Arch, the timing of most-recent movement on these two arches is assessed to be similar. Crone and Wheeler (2000) (Reference 310) classify the Cape Fear Arch as a Class C feature based on lack of evidence for Quaternary faulting and do not include the Yamacraw Arch in their assessment.

2.5.1.1.2.4.5 Regional Quaternary Tectonic Structures

In an effort to provide a comprehensive database of Quaternary tectonic features, Crone and Wheeler (2000) (Reference 310) and Wheeler (2005) (Reference 311) compiled geological information on Quaternary faults, liquefaction features, and possible tectonic features in the CEUS. They evaluate and classified these features into one of four categories (Classes A, B, C, and D; see Table 2.5.1-201 for definitions) based on strength of evidence for Quaternary activity. Charleston area liquefaction features are the only features identified by Crone and Wheeler (2000) (Reference 310) and Wheeler (2005) (Reference 311) with demonstrated Quaternary deformation (Class A) within the site region.

Within a 200 mi. radius of the Lee Nuclear Site, Crone and Wheeler (2000) (Reference 310) and Wheeler (2005) (Reference 311) identify 15 potential Quaternary features (Table 2.5.1-201 and Figure 2.5.1-213). These include:

- Fall Lines of Weems (1998) (Reference 322) (Class C).
- Belair fault (Class C).
- Pen Branch fault (Class C).
- Cooke fault (Charleston feature, Class C).
- East Coast fault system (Charleston feature, Class C).
- Charleston liquefaction features (Charleston feature, Class A).
- Bluffton liquefaction features (Charleston feature, Class A).
- Georgetown liquefaction features (Charleston feature, Class A).
- Giles County seismic zone (Class C).
- Eastern Tennessee seismic zone (Class C).
- Cape Fear arch (Class C).
- Hares Crossroads fault (Class C).
- Lindside fault zone (Class C).
- Stanleytown-Villa Heights faults (Class C).
- Pembroke faults (Class B).

Each of these 15 potential features is discussed in detail. The Charleston features (including the East Coast fault system; the Cooke fault; and the Charleston, Georgetown, and Bluffton paleoliquefaction features) are discussed in Subsection 2.5.1.1.3.2.1. The Eastern Tennessee and Giles County seismic zones are discussed in Subsections 2.5.1.1.3.2.2 and 2.5.1.1.3.2.3. The remaining eight potential Quaternary features (namely, the Fall Lines of Weems (1998), the Belair fault zone, the Pen Branch fault, the Cape Fear arch, the Hares Crossroads fault, the Lindside fault zone, the Stanleytown-Villa Heights faults, and the Pembroke faults) are discussed in detail below:

Fall Lines of Weems (1998). The Fall Lines of Weems (1998) (Reference 322) are alignments of rapids or anomalously steep sections of rivers draining the Piedmont and Blue Ridge Provinces of North Carolina and Virginia. The Weems (1998) (Reference 322) delineation of these fall zones is crude, but, as presented in his Figure 8, the Western Piedmont Fall Line appears to be located as close as 5 mi. from the Lee Nuclear Site at its nearest point (Figure 2.5.1-213). Wheeler (2005) (Reference 311) classifies the Fall Lines of Weems (1998) (Reference 322) as a Class C feature (Table 2.5.1-201) because: (1) identification of the fall zones is subjective and the criteria for recognizing them are not stated clearly enough to make the results reproducible; and (2) a tectonic faulting origin has not yet been

demonstrated for the fall zones. Based on review of published literature, field reconnaissance, and work performed as part of the North Anna ESP application (Reference 398), the Fall Lines of Weems (1998) (Reference 322) are interpreted to be erosional features related to contrasting erosional resistances of adjacent rock types, and are not tectonic in origin.

Belair Fault zone. The Belair fault zone is mapped for at least 15 mi. as a series of northeast-striking, southeast-dipping, oblique-slip faults located 125 mi. south of the Lee Nuclear Site near Augusta, Georgia (Figure 2.5.1-213). The Belair fault juxtaposes Paleozoic phyllite over Late Cretaceous sands of the Coastal Plain province (References 323 and 324). Mapping and structural analysis by Bramlett et al. (1982) (Reference 301) indicate that the Belair fault likely is a tear fault or lateral ramp associated with the Augusta fault when displacement on these faults initiated during the Paleozoic Alleghanian orogeny. While simultaneous post-Paleozoic reactivation of the Belair and Augusta faults cannot be precluded by available data, it is not well established that these two faults share a common slip history and sense of displacement. Prowell et al. (Reference 324) and Prowell and O'Connor (Reference 323) document Cenozoic brittle reverse slip on the Belair fault. The latest well-constrained movement on the Augusta fault, as demonstrated by brittle overprinting of ductile fabrics, exhibits a normal sense-of-slip. Brittle slip occurred late in the Alleghanian during the transition from ductile to brittle conditions (References 320 and 321), with possible minor localized reactivation under Mesozoic hydrothermal conditions (Reference 320). No geomorphic expression of the fault has been reported (Reference 310).

Shallow trenches excavated across the Belair fault near Fort Gordon in Augusta, Georgia, were initially interpreted as revealing evidence for Holocene movement (Reference 324). However, the apparent youthfulness of movement is postulated as the result of contaminated radiocarbon samples. Prowell and O'Connor (1978) (Reference 323) demonstrate that the Belair fault cuts beds of Late Cretaceous and Eocene age. Overlying, undeformed strata provide a minimum constraint on the last episode of faulting, which is constrained to sometime between post-late Eocene and pre-26,000 years ago.

There is no evidence of historic or recent seismicity associated with the Belair fault. Crone and Wheeler (2000) (Reference 310) classify the Belair fault zone as a Class C feature because the most recent faulting is not demonstrably of Quaternary age. Quaternary slip on the Belair fault zone is permitted, but not demonstrated, by the available data.

Pen Branch fault. The more than 20-mi.-long Pen Branch fault is located about 150 mi. south of the Lee Nuclear Site. The northeast-striking Pen Branch fault bounds the northwest side of the Mesozoic Dunbarton Basin. The Pen Branch fault traverses the central portion of the Savannah River Site, and strikes southwestward into Georgia (References 325 and 326). The Pen Branch fault is not exposed or expressed at the surface (References 326, 327, and 328). Borehole and seismic reflection data collected from the Savannah River Site show no evidence for post-Eocene slip on the Pen Branch fault (Reference 328). Savannah River Site studies and work performed as part of the Vogtle ESP application specifically designed to assess the youngest deformed strata overlying

the fault through shallow, high-resolution reflection profiles, drilling of boreholes, and geomorphic analyses consistently concludes that the youngest strata deformed are late Eocene in age. Crone and Wheeler (2000) (Reference 310) classify the Pen Branch fault zone as a Class C feature based on lack of evidence for Quaternary faulting.

Cape Fear Arch. The Cape Fear Arch is discussed previously in Subsection 2.5.1.1.2.4.4. Crone and Wheeler (2000) (Reference 310) classify the Cape Fear Arch as a Class C feature based on lack of evidence for Quaternary faulting.

Hares Crossroads fault. The postulated Hares Crossroads fault (identified by Prowell [1983] (Reference 321) as fault numbered 46) in east-central North Carolina is a single reverse fault that offsets the base of the Coastal Plain section, approximately 200 mi. east-northeast of the Lee Nuclear Site. This fault is recognized in a roadcut exposure. The fault is not recognized beyond this exposure, and geomorphic expression is negligible. This fault is likely the result of landsliding and is therefore likely non-tectonic in origin. Crone and Wheeler (2000) (Reference 310) classify the Hares Crossroads fault as a class C feature based on lack of evidence for Quaternary faulting.

Lindside fault zone. The northeast-striking, normal-slip Lindside fault is located in southern West Virginia, about 170 mi. north of the Lee Nuclear Site (Reference 310). The Lindside fault is mapped for a length of greater than 30 mi., with variable width up to about 1 mi. Dennison and Stewart (1998) (Reference 329) suggest that the Lindside fault zone accommodated latest Paleozoic gravitational collapse of Appalachian crust. The Lindside fault zone is poorly oriented for reactivation in the current stress field, and no evidence of Quaternary slip is reported for the zone. Crone and Wheeler (2000) (Reference 310) classify the Lindside fault zone as a class C feature based on lack of evidence for Quaternary faulting.

Stanleytown-Villa Heights faults. The postulated Stanleytown-Villa Heights faults are located in the Piedmont of southern Virginia, approximately 150 mi. northeast of the Lee Nuclear Site. These approximately 655-ft.-long faults juxtapose Quaternary alluvium against rocks of Cambrian age. The Stanleytown-Villa Heights faults are both short in mapped length, drop their east sides down in the downhill direction, and no other faults are mapped nearby (Reference 310). Evidence suggests these faults are likely the result of landsliding and are therefore likely non-tectonic in origin. Crone and Wheeler (2000) (Reference 310) classify the Stanleytown-Villa Heights faults as a Class C feature based on lack of evidence for Quaternary faulting.

Pembroke faults. The postulated Pembroke faults of western Virginia are located within alluvial deposits of probable Quaternary age (Reference 310), approximately 150 mi. north of the Lee Nuclear Site. The Pembroke faults are identified by geologic mapping, seismic profiles, gravity and magnetics, and ground-penetrating radar. The Pembroke faults are not expressed geomorphically, and it is unclear if these faults are of tectonic origin or the result of dissolution

collapse. Crone and Wheeler (2000) (Reference 310) classify the Pembroke faults as a Class B feature based on evidence suggesting possible Quaternary faulting.

Crone and Wheeler (2000) (Reference 310) and Wheeler (2005) (Reference 311) identify potential Quaternary tectonic features in the CEUS. Work performed as part of this study, including literature review, interviews with experts, and geologic reconnaissance, did not identify any additional potential Quaternary tectonic features within the Lee Nuclear Site region.

2.5.1.1.3 Regional Seismicity and Paleoseismology

Subsection 2.5.1.1.3 includes descriptions of instrumental and historic earthquake activity in the Lee Nuclear Site region and beyond. Special emphasis is placed on the Charleston seismic zone because it one of the largest earthquakes in eastern U.S. history.

2.5.1.1.3.1 Central and Eastern U.S. Seismicity

Seismicity in the CEUS is in general broadly distributed, but areas of concentrated earthquake activity are shown in Figure 2.5.1-214. Areas of concentrated seismicity are described in this section.

2.5.1.1.3.2 Seismic Sources Defined by Regional Seismicity

Within 200 mi. of the Lee Nuclear Site, there are five principal areas of concentrated seismicity (Figure 2.5.1-214). Three of these (the Middleton-Place Summerville, Bowman, and Adams Run seismic zones) are located within 50 mi. of Charleston, South Carolina. Subsection 2.5.1.1.3.2.1 presents discussion of these three areas of concentrated seismicity near Charleston. The Eastern Tennessee and Giles County seismic zones are discussed in Subsections 2.5.1.1.3.2.2 and 2.5.1.1.3.2.3, respectively. Two additional areas of concentrated seismicity beyond the site region (i.e., the New Madrid and Central Virginia seismic zones) are discussed in Subsection 2.5.1.1.3.2.4.

2.5.1.1.3.2.1 Charleston Tectonic Features

The August 31, 1886, Charleston, South Carolina, earthquake is the largest historical earthquake in the eastern United States. The event produced Modified Mercalli Intensity (MMI) X shaking in the epicentral area and was felt strongly as far away as Chicago (Reference 330). As a result of this earthquake and the relatively high risk in the Charleston area, government agencies funded numerous investigations to identify the source of the earthquake and recurrence history of large magnitude events in the region. In spite of this effort, the source of the 1886 earthquake is not definitively attributed to any particular fault shown in Figure 2.5.1-215.

The 1886 Charleston earthquake produced no identifiable primary tectonic surface deformation; therefore, the source of the earthquake is inferred based on the geology, geomorphology, and instrumental seismicity of the region (Figures 2.5.1-215, 2.5.1-216, and 2.5.1-217). Talwani (1982) (Reference 331)

suggests that the inferred north-northeast-striking Woodstock fault produced the 1886 earthquake near its intersection with the northwest-striking Ashley River fault. Both the postulated Woodstock and Ashley River faults are inferred on the basis of seismicity (Reference 331). More recently, Marple and Talwani (1993, 2000) (References 337 and 338) suggest that a northeast-trending zone of river anomalies, referred to as the ECFS, represents the causative fault for the 1886 Charleston event. The southern segment of the ECFS coincides with a linear zone of micro-seismicity that defines the northeast-trending Woodstock fault of Talwani (1982) (Reference 331) and the isoseismal zone from the 1886 earthquake.

Johnston (1996) (Reference 330) estimates a moment magnitude (**M**) 7.3±0.26 for the 1886 Charleston event. More recently, Bakun and Hopper (2004) (Reference 333) estimate a smaller magnitude of **M** 6.9 with a 95 percent confidence level corresponding to a range of **M** 6.4 to 7.1. Both of these more recent estimates of maximum magnitude (M_{max}) are similar to the upper-bound maximum range of M_{max} values used in EPRI (1986) (using body wave magnitudes [m_b] 6.8 to 7.5) (Reference 269). However, significant new information regarding the source geometry and earthquake recurrence of the Charleston seismic source warrants an update of the EPRI (1986) (Reference 269) source models in the PSHA. The updated Charleston seismic source parameters are presented in Subsection 2.5.2.2.2.3.

Potential Charleston Source Faults. Since development of the EPRI (1986) (Reference 269) source models, a number of faults have been identified or described in the literature as possible sources related to the 1886 Charleston earthquake. These include paleoliquefaction features and numerous faults localized in the Charleston meizoseismal area.

There is evidence, in the form of paleoliquefaction features in the South Carolina Coastal Plain, that the source of the 1886 Charleston earthquake has repeatedly generated vibratory ground motion. Paleoliquefaction evidence is lacking for prehistoric earthquakes elsewhere along much of the eastern seaboard (e.g., References 334, 335, and 336). While the 1886 Charleston earthquake was likely produced by a capable tectonic source, the causative tectonic structure has yet to be identified. Various studies propose potential candidate faults for the 1886 event; however, a positive linkage between a discrete structure and the Charleston earthquake has yet to be determined.

These potential causative features are shown in Figures 2.5.1-215 and 2.5.1-216, and are described below:

- *East Coast Fault System*. The inferred ECFS, the southern section of which is also known as the “zone of river anomalies” or ZRA based on the alignment of river bends, is a northeast-trending, approximately 370-mi-long fault system extending from west of Charleston, South Carolina, to southeastern Virginia (Reference 338). The ECFS comprises three approximately 125-mi.-long, right-stepping sections (southern, central, and northern). Evidence for the southern section is strongest, with evidence becoming successively weaker northward (Reference 311). Marple and

Talwani (1993) (Reference 337) identify a series of geomorphic anomalies (i.e., ZRA) located along and northeast of the Woodstock fault and attribute these to a buried fault much longer than the Woodstock fault. Marple and Talwani (References 337 and 338) suggest that this structure, the ECFS, may have been the source of the 1886 Charleston earthquake. Marple and Talwani (2000) (Reference 338) provide additional evidence for the existence of the southern section of the ECFS, including seismic reflection data, linear aeromagnetic anomalies, exposed Plio-Pleistocene faults, local breccias, and upwarped strata. Because most of the geomorphic anomalies associated with the southern section of the ECFS are in late Pleistocene sediments, Marple and Talwani (2000) speculate that the fault has been active in the past 130 to 10 ka, and perhaps remains active. Wildermuth and Talwani (2001) (Reference 339) use gravity and topographic data to postulate the existence of a pull-apart basin between the southern and central sections of the ECFS, implying a component of right-lateral slip on the fault. Wheeler (2005) (Reference 311) classifies the ECFS as a Class C feature based on the lack of demonstrable evidence that the ECFS has or can generate strong ground motion and the lack of any demonstrable evidence for any sudden uplift anywhere along the proposed fault.

- *Adams Run Fault*. Weems and Lewis (2002) (Reference 340) postulate the existence of the Adams Run fault on the basis of microseismicity and borehole data. Their interpretation of borehole data suggests the presence of areas of uplift and subsidence separated by the inferred fault. However, review of these data shows that the pattern of uplift and subsidence does not appear to persist through time (i.e., successive stratigraphic layers) in the same locations and that the intervening structural lows between the proposed uplifts are highly suggestive of erosion along ancient river channels. In addition, there is no geomorphic evidence for the existence of the Adams Run fault, and analysis of microseismicity in the vicinity of the proposed Adams Run fault does not clearly define a discrete structure (Figure 2.5.1-217).

- *Ashley River Fault*. Talwani (1982) (Reference 331) identifies the Ashley River fault on the basis of a northwest-oriented, linear zone of seismicity located about 6 mi. west of Woodstock, South Carolina, in the meizoseismal area of the 1886 Charleston earthquake. The postulated Ashley River fault, a southwest-side-up reverse fault, is thought to offset the north-northeast-striking Woodstock fault about 3 to 4 mi. to the northwest near Summerville (References 331, 332, and 340).

- *Charleston Fault*. Lennon (1986) (Reference 341) proposes the Charleston fault on the basis of geologic map relations and subsurface borehole data. Weems and Lewis (2002) (Reference 340) suggest that the Charleston fault is a major, high-angle reverse fault that has been active at least intermittently in Holocene to modern times. The Charleston fault has no clear geomorphic expression, nor is it clearly defined by microseismicity (Figure 2.5.1-217).

- *Cooke Fault*. Behrendt et al. (1981) (Reference 342) and Hamilton et al. (1983) (Reference 343) identify the Cooke fault based on seismic reflection profiles in the meizoseismal area of the 1886 Charleston earthquake. This east-northeast-striking, steeply northwest-dipping fault has a total length of about 6 mi. (References 342 and 343). Marple and Talwani (References 337and 338) reinterpret these data to suggest that the Cooke fault may be part of a longer, more northerly striking fault (i.e., the ZRA of Marple and Talwani [1993] [Reference 337] and the ECFS of Marple and Talwani [2000] [Reference 338]). Crone and Wheeler (2000) (Reference 310) classify the Cooke fault as a Class C feature based on lack of evidence for faulting younger than Eocene.

- *Helena Banks Fault Zone*. Seismic reflection lines offshore of South Carolina clearly image the Helena Banks fault zone (References 344 and 345). The six EPRI ESTs were aware of the Helena Banks fault at the time of EPRI (1986) (Reference 269) as a possible Cenozoic-active fault zone. Some ESTs recognized the offshore fault zone as a candidate tectonic feature for producing the 1886 event and include it in their Charleston seismic source zones. However, since 1986, three additional sources of information have become available:

  - In 2002, two magnitude m_b3.5 earthquakes (m_b 3.5 and 4.4) occurred offshore of South Carolina in the vicinity of the Helena Banks fault zone in an area previously devoid of seismicity.

  - Bakun and Hopper (2004) (Reference 333) reinterpret intensity data from the 1886 Charleston earthquake and show that the calculated intensity center is located about 100 mi. offshore from Charleston (although they ultimately conclude that the epicentral location most likely lies onshore in the cluster of seismicity in the Middleton Place–Summerville area).

  - Crone and Wheeler (2000) (Reference 310) describe the Helena Banks fault zone as a potential Quaternary tectonic feature (although it is classified as a Class C feature that lacks sufficient evidence to demonstrate Quaternary activity). The occurrence of the 2002 earthquakes and the location of the Bakun and Hopper (2004) (Reference 333) intensity center offshore suggest, at a low probability, that the fault zone could be considered a potentially active fault. If the Helena Banks fault zone is an active source, its length and orientation may explain the distribution of paleoliquefaction features along the South Carolina coast.

- *Sawmill Branch Fault*. Talwani and Katuna (2004) (Reference 346) postulate the existence of the Sawmill Branch fault on the basis of microseismicity and further speculate that this feature experienced surface rupture in the 1886 earthquake. According to Talwani and Katuna (2004) (Reference 346), this approximately 3-mi.-long, northwest-trending fault, a segment of the larger Ashley River fault, offsets the Woodstock fault in a

left-lateral sense. Talwani and Katuna (2004) (Reference 346) use earthquake damage to infer that surface rupture occurred in 1886. Field review of these localities, however, indicates that they are unlikely the direct result of earthquake surface rupture. Features along the banks of the Ashley River (small, discontinuous cracks in a tomb that dates to 1671 AD and displacements [less than 4 in] in the walls of colonial Fort Dorchester) are almost certainly the product of shaking effects as opposed to fault rupture. Moreover, assessment of microseismicity in the vicinity of the proposed Sawmill Branch fault does not clearly define a discrete structure distinct or separate from the larger Ashley River fault (Figure 2.5.1-217).

- *Summerville Fault*. Weems et al. (1997) (Reference 347) postulate the existence of the Summerville fault near Summerville, South Carolina, on the basis of previously located microseismicity. However, there is no geomorphic or borehole evidence for the existence of the Summerville fault. Analysis of microseismicity in the vicinity of the proposed Summerville fault does not clearly define a discrete structure (Figure 2.5.1-217).

- *Woodstock Fault*. Talwani (1982) (Reference 331) identifies the Woodstock fault, a postulated north-northeast-trending, dextral strike-slip fault, on the basis of a linear zone of seismicity located approximately 6 mi. west of Woodstock, South Carolina, in the meizoseismal area of the 1886 Charleston earthquake. Madabhushi and Talwani (References 348 and 349) use a revised velocity model to relocate Middleton Place–Summerville seismic zone earthquakes. The results of this analysis are used to further refine the location of the postulated Woodstock fault. Talwani (References 332 and 350) subdivides the Woodstock fault into two segments that are offset in a left-lateral sense across the northwest-trending Ashley River fault. Marple and Talwani include the Woodstock fault as part of their larger ZRA (Reference 337) and ECFS (Reference 338).

Charleston Area Seismic Zones. Three zones of increased seismic activity have been identified in the greater Charleston area. These include the Middleton Place–Summerville, Bowman, and Adams Run seismic zones. Each of these features is described in detail below, and the specifics of the seismicity catalog are discussed in Subsection 2.5.2.1.2.

- *Middleton Place–Summerville Seismic Zone*. The Middleton Place–Summerville seismic zone is an area of elevated microseismic activity located about 12 mi. northwest of Charleston (References 346, 349, 351, and 352) (Figure 2.5.1-216). Between 1980 and 1991, 58 events with Md 0.8 to 3.3 were recorded in a 7- by 9-mi. area, with hypocentral depths ranging from about 1 to 7 mi. (Reference 349). The elevated seismic activity of the Middleton Place–Summerville seismic zone has been attributed to stress concentrations associated with the intersection of the Ashley River and Woodstock faults (References 331, 346, 349, and 353). Persistent foreshock activity was reported in the Middleton

Place–Summerville seismic zone area (Reference 355), and it is speculated that the 1886 Charleston earthquake occurred within this zone (e.g., References 331, 333, and 351).

- *Bowman Seismic Zone*. The Bowman seismic zone is located about 50 mi. northwest of Charleston, South Carolina, outside of the meizoseismal area of the 1886 Charleston earthquake (Figure 2.5.1-216). The Bowman seismic zone is identified on the basis of a series of local Magnitude (M_L) $3<M_L<4$ earthquakes that occurred between 1971 and 1974 (References 352 and 354).

- *Adams Run Seismic Zone*. The Adams Run seismic zone, located within the meizoseismal area of the 1886 Charleston earthquake, is identified on the basis of four M < 2.5 earthquakes, three of which occurred in a 2-day period in December 1977 (Reference 351). Bollinger et al. (1991) (Reference 352) downplay the significance of the Adams Run seismic zone, noting that, in spite of increased instrumentation, no additional events were detected after October 1979.

Charleston Area Seismically Induced Liquefaction Features. The presence of liquefaction features in the geologic record may be indicative of past earthquake activity in a region. Liquefaction features are recognized throughout coastal South Carolina and are attributed to both the 1886 Charleston and earlier moderate to large earthquakes in the region.

- *1886 Charleston Earthquake Liquefaction Features.* Liquefaction features produced by the 1886 Charleston earthquake are most heavily concentrated in the meizoseismal area (References 334, 355, and 356), but are reported as far away as Columbia, Allendale, Georgetown (Reference 356) and Bluffton, South Carolina (Reference 357) (Figures 2.5.1-215 and 2.5.1-216).

- *Paleoliquefaction Features in Coastal South Carolina.* Liquefaction features predating the 1886 Charleston earthquake are found throughout coastal South Carolina (Figures 2.5.1-215 and 2.5.1-216). The spatial distribution and ages of paleoliquefaction features in coastal South Carolina constrain possible locations and recurrence rates for large earthquakes (References 334, 335, 336, 358, and 359). Talwani and Schaeffer (2001) (Reference 357) combine previously published data with their own studies of liquefaction features in the South Carolina coastal region to derive possible earthquake recurrence histories for the region. Talwani and Schaeffer's (2001) (Reference 357) Scenario 1 allows for the possibility that some events in the paleoliquefaction record are smaller in magnitude (approximately **M** 6+), and that these more moderate events occurred to the northeast (Georgetown) and southwest (Bluffton) of Charleston. In Talwani and Schaeffer's (2001) (Reference 357) Scenario 2, the earthquakes in the record are large events (approximately **M** 7+) located near Charleston. Talwani and Schaeffer (2001)

(Reference 357) estimate recurrence intervals of about 550 years and approximately 900 to 1,000 years from their two scenarios.

Because there is no surface expression of faults within the Charleston seismic zone, earthquake recurrence estimates are based largely on dates of paleoliquefaction events. The most recent summary of paleoliquefaction data (Reference 357) suggests a mean recurrence time of 550 years for Charleston. The 2002 U.S. Geological Survey (USGS) model incorporates this 550-year estimate (Reference 360). This recurrence interval is less than the 650-year recurrence interval used in the earlier USGS hazard model (Reference 361) and is roughly an order of magnitude less than the seismicity-based recurrence estimates used in EPRI (1986). Refinements of the estimate of Charleston area earthquake recurrence are presented in detail in Subsection 2.5.2.2.2.3.

2.5.1.1.3.2.2 Eastern Tennessee Seismic Zone

The Eastern Tennessee Seismic Zone (ETSZ) is one of the most active seismic zones in eastern North America. The ETSZ is located in the Valley and Ridge province of eastern Tennessee, approximately 150 mi. west-northwest of the Lee Nuclear Site (Figure 2.5.1-214). The ETSZ is about 185 mi. long and 30 mi. wide and has not produced a damaging earthquake in historical time (Reference 362). Despite its high rate of activity, the largest known earthquake is magnitude 4.6 (magnitude scale not specified) (Reference 375).

Earthquakes in the ETSZ are occurring at depths from 3 to 16 mi. within Precambrian crystalline basement rocks buried beneath the exposed thrust sheets of Paleozoic rocks. The mean focal depth within the seismic zone is 9 mi., well below the Appalachian basal decollement's maximum depth of 3 mi. (Reference 362). The lack of seismicity in the shallow Appalachian thrust sheets implies that the seismogenic structures in the ETSZ are unrelated to the surface geology of the Appalachian orogen (Reference 292). The majority of earthquake focal mechanisms show right-lateral slip on northerly-striking planes or left-lateral slip on easterly-striking planes (Reference 364). A smaller number of focal plane solutions show right-lateral motion on northeasterly trending planes that parallel the overall trend of seismicity (Reference 363). Statistical analyses of focal mechanisms and epicenter locations suggest that seismicity is occurring on a series of northeast-striking en-echelon basement faults intersected by several east-west-striking faults (Reference 364). Potential structures most likely responsible for the seismicity in Eastern Tennessee are reactivated Cambrian or Precambrian normal faults formed during the rifting that formed the Iapetan Ocean and presently located beneath the Appalachian thrust sheets (Reference 267).

Earthquakes within the ETSZ cannot be attributed to known surface faults (Reference 362), and no capable tectonic sources are identified within the seismic zone. However, the seismicity is spatially associated with major geophysical lineaments. The western margin of the ETSZ is sharply defined and is coincident with the prominent gradient in the magnetic field defined by the New York-Alabama magnetic lineament (Reference 363).

The EPRI SOG source model (Reference 269) includes various source geometries and parameters to represent the seismicity of the ETSZ. Each of the EPRI ESTs model source zones captures this area of seismicity and some ESTs include multiple source zones (see detailed discussion in Subsection 2.5.2.2.1). A wide range of maximum magnitude (M_{max}) values and associated probabilities were assigned to these sources to reflect the uncertainty of multiple experts from each EST. The EPRI M_{max} distributions for these sources range from m_b 5.2 to 7.2.

Subsequent hazard studies use M_{max} values almost entirely within the range of maximum magnitudes used by the six EPRI models. Collectively, upper-bound maximum values of M_{max} used by the EPRI teams range from **M** 6.3 to 7.5 [conversion from m_b to **M** by arithmetic mean of three equally weighted relations: Atkinson and Boore 1995 (Reference 365), Frankel et al. 1996 (Reference 361), and EPRI (Reference 367).] Subsection 2.5.2.2.2.5 describes M_{max} values used for the ETSZ in hazard studies subsequent to the EPRI models.

In spite of the observations of small to moderate earthquakes in the ETSZ, no geological evidence, such as paleoliquefaction, demonstrates the occurrence of prehistoric earthquakes larger than any historical shocks within the seismic zone (References 311 and 363). As a result, Wheeler (2005) (Reference 311) classifies the ETSZ as a Class C feature for lack of geological evidence of large earthquakes. While the lack of large earthquakes in the relatively short historical record cannot preclude the future occurrence of large events, there is a much higher degree of uncertainty associated with the assignment of M_{max} for the ETSZ than other CEUS seismic source zones, such as New Madrid and Charleston, where large historical earthquakes have occurred. In conclusion, no new information has been developed since 1986 that requires a revision to the magnitude distribution of EPRI representations of the ETSZ.

A recent evaluation of the Tennessee Valley Authority Bellefonte site (Reference 368) also concludes that the EPRI representations of the ETSZ, in terms of geometry, recurrence and M_{max}, are appropriate and encompass the range of values used in more recent characterizations of the ETSZ such as the Trial Implementation Project (TIP study) (Reference 369) and USGS source model (Reference 360). The Bellefonte site lies either within or adjacent to each of the EPRI source zones representing the ETSZ. A comparison of seismicity rates from the EPRI SOG study and new rates developed from an updated seismicity catalog for the region demonstrate no significant change in the rate of earthquake recurrence for the ETSZ (Reference 368).

2.5.1.1.3.2.3 Giles County Seismic Zone

The Giles County seismic zone is located in Giles County, southwestern Virginia, near the border with West Virginia, approximately 160 mi. from the Lee Nuclear Site (Figure 2.5.1-214). The largest known earthquake to occur in Virginia and the second largest earthquake in the entire southeastern United States is the 1897

M 5.9 (Reference 370) Giles County event. This event likely produced MMI VIII shaking intensities in the epicentral area.

Earthquakes in the Giles County seismic zone occur within Precambrian crystalline basement rocks beneath the Appalachian thrust sheets at depths from 3 to 16 mi. (Reference 265). Earthquake foci define a 25-mi.-long, northeasterly striking, tabular zone that dips steeply to the southeast beneath the Valley and Ridge thrust sheets (References 265 and 371). The lack of seismicity in the shallow Appalachian thrust sheets, estimated to be about 2 to 3.5 mi. thick, implies that the seismogenic structures in the Giles County seismic zone, similar to those inferred for the ETSZ, are unrelated to the surface geology of the Appalachian orogen (Reference 265). The spatial distribution of earthquake hypocenters, together with considerations of the regional tectonic evolution of eastern North America, suggest that the earthquake activity is related to contractional reactivation of late Precambrian or Cambrian normal faults that initially formed during rifting associated with opening of the Iapetan Ocean (References 265 and 352).

No capable tectonic sources are identified within the Giles County seismic zone, nor does the seismic zone have recognizable geomorphic expression (Reference 311). Thus, in spite of the occurrence of small to moderate earthquakes, no geological evidence demonstrates the occurrence of prehistoric earthquakes larger than any historical shocks within the zone (Reference 311). As a result, Wheeler (2005) (Reference 311) classifies the Giles County seismic zone as a Class C feature for lack of geological evidence of large earthquakes.

Crone and Wheeler (2000) (Reference 310) identify a zone of small, Late Pleistocene faults within the Giles County seismic zone near Pembroke, Virginia. The Pembroke faults are a set of extensional faults exposed in terrace deposits overlying limestone bedrock along the New River. Crone and Wheeler (2000) (Reference 310) rate these faults as Class B features because it has not yet been determined whether these faults are tectonic or the result of solution collapse in underlying limestone units. The shallow Pembroke faults do not appear to be related to the Giles County seismic zone. Seismicity in the Giles County seismic zone is located at depth beneath the Appalachian basal decollement in the North American basement.

The EPRI source model includes various source geometries and parameters to represent the seismicity of the Giles County seismic zone (Reference 269). Subsequent hazard studies use M_{max} values that are within the range of maximum magnitudes used by the six EPRI models (e.g., References 265 and 384). Collectively, upper-bound maximum values of M_{max} used by the EPRI teams ranged from m_b 6.6 to 7.2 (discussed in Subsection 2.5.2.2.1). More recently, Bollinger (1992) (Reference 366) estimates an M_{max} of m_b 6.3 for the Giles County seismic source using three different methods. Chapman and Krimgold (1994) (Reference 371) use an M_{max} of m_b 7.25 for the Giles County zone and most other sources in their seismic hazard analysis of Virginia. Both of these more recent estimates of M_{max} are similar to the range of M_{max} values used in EPRI

(1986) (Reference 269). Therefore, no new information has been developed since 1986 that would require a significant revision to the EPRI seismic source model.

2.5.1.1.3.2.4 Selected Seismogenic and Capable Tectonic Sources Beyond the Site Region

In addition to the areas of concentrated seismicity within the site region, Subsection 2.5.1.1.3.2.4 describes two additional areas of concentrated seismicity beyond the site region (i.e., the New Madrid and Central Virginia seismic zones):

New Madrid Seismic Zone. The New Madrid seismic zone extends from southeastern Missouri to southwestern Tennessee and is located more than 450 mi. west of the Lee Nuclear Site (Figure 2.5.1-214). The New Madrid seismic zone lies within the Reelfoot rift and is defined by post-Eocene to Quaternary faulting and historical seismicity.

The New Madrid seismic zone is approximately 125 mi. long and 25 mi. wide. Research conducted since 1986 identifies three distinct fault segments embedded within the seismic zone. These three fault segments include a southern northeast-trending dextral slip fault, a middle northwest-trending reverse fault, and a northern northeast-trending dextral strike-slip fault (Reference 373). In the current east-northeast to west-southwest directed CEUS regional stress field, Precambrian and Late Cretaceous age extensional structures of the Reelfoot rift appear to be reactivated as right-lateral strike-slip and reverse faults.

The New Madrid seismic zone produced three historical, large-magnitude earthquakes between December 1811 and February 1812 (Reference 374). The December 16, 1811, earthquake is associated with strike-slip faulting along the southern portion of the New Madrid seismic zone. Johnston (1996) (Reference 330) estimates a magnitude of **M** 8.1±0.31 for the December 16, 1811, event. However, Hough et al. (2000) (Reference 374) re-evaluate the isoseismal data for the region and concluded that the December 16 event had a magnitude of **M** 7.2 to 7.3. Bakun and Hopper (2004) (Reference 333) similarly conclude this event had a magnitude of **M** 7.2.

The February 7, 1812, New Madrid earthquake is associated with reverse fault displacement along the middle part of the New Madrid seismic zone (Reference 375). This earthquake most likely occurred along the northwest-trending Reelfoot fault that extends approximately 43 mi. from northwestern Tennessee to southeastern Missouri. The Reelfoot fault is a northwest-striking, southwest-vergent reverse fault. The Reelfoot fault forms a topographic scarp developed as a result of fault-propagation folding (References 376, 377, and 378). Johnston (1996) (Reference 330) estimates a magnitude of **M** 8.0±0.33 for the February 7, 1812, event. However, Hough et al. (2000) (Reference 374) re-evaluate the isoseismal data for the region and conclude that the February 7, 1812 event had a magnitude of **M** 7.4 to 7.5. More recently, Bakun and Hopper (2004) (Reference 333) estimate a similar magnitude of **M** 7.4.

The January 23, 1812, earthquake is associated with strike-slip fault displacement on the East Prairie fault along the northern portion of the New Madrid seismic zone. Johnston (1996) (Reference 330) estimates a magnitude of **M** 7.8±0.33 for the January 23, 1812, event. Hough et al. (2000) (Reference 374), however, re-evaluate the isoseismal data for the region and conclude that the January 23, 1812 event had a magnitude of **M** 7.1. More recently, Bakun and Hopper (2004) (Reference 333) estimate a similar magnitude of **M** 7.1.

Because there is very little surface expression of faults within the New Madrid seismic zone, earthquake recurrence estimates are based largely on dates of paleoliquefaction and offset geological features. The most recent summaries of paleoseismologic data (References 379, 380, and 381) suggest a mean recurrence time of 500 years, which was used in the 2002 USGS model (Reference 360). This recurrence interval is half of the 1,000-year recurrence interval used in the 1996 USGS hazard model (Frankel et al. 1996) (Reference 361), and an order of magnitude less than the seismicity-based recurrence estimates used in EPRI (1986) (Reference 269).

The upper-bound maximum values of M_{max} used in EPRI (1986) (Reference 269) range from m_b 7.2 to 7.9. Since the EPRI study, estimates of M_{max} have generally been within the range of maximum magnitudes used by the six EPRI models. The most significant update of source parameters in the New Madrid seismic zone since the 1986 EPRI study is the reduction of the recurrence interval to 500 years.

Central Virginia Seismic Zone. The Central Virginia seismic zone is an area of persistent, low-level seismicity in the Piedmont province, located more than 250 mi. from the Lee Nuclear Site (Figure 2.5.1-214). The zone extends about 75 mi. in a north-south direction and about 90 mi. in an east-west direction from Richmond to Lynchburg, Virginia (Reference 382). The largest historical earthquake that has occurred in the Central Virginia seismic zone is the body-wave magnitude (m_b) 5.0 Goochland County event on December 23, 1875 (Reference 382). The maximum intensity estimated for this event is MMI VII in the epicentral region.

Seismicity in the Central Virginia seismic zone ranges in depth from about 2 to 8 mi. (Reference 383). Coruh et al. (1988) (Reference 384) suggest that seismicity in the central and western parts of the zone may be associated with west-dipping reflectors that form the roof of a detached antiform, while seismicity in the eastern part of the zone near Richmond may be related to a near-vertical diabase dike swarm of Mesozoic age. However, given the depth distribution of 2 to 8 mi. (Reference 383) and broad spatial distribution, it is difficult to uniquely attribute the seismicity to any known geologic structure, and it appears that the seismicity extends both above and below the Appalachian detachment.

No capable tectonic sources are identified within the Central Virginia seismic zone, but two paleoliquefaction sites are identified within the seismic zone (References 310 and 385). The paleoliquefaction sites reflect prehistoric occurrences of seismicity within the Central Virginia seismic zone and do not indicate the presence of a capable tectonic source.

The 1986 EPRI source model includes various source geometries and parameters to capture the seismicity of the Central Virginia seismic zone (Reference 269). Subsequent hazard studies use M_{max} values that are within the range of maximum magnitudes used by the six EPRI models. Collectively, upper-bound maximum values of M_{max} used by the EPRI ESTs range from m_b 6.6 to 7.2 (discussed in Subsection 2.5.2.2.1). More recently, Bollinger (1992) (Reference 366) estimates M_{max} of m_b 6.4 for the Central Virginia seismic source. Chapman and Krimgold (1994) (Reference 371) use M_{max} of m_b 7.25 for the Central Virginia seismic source and most other sources in their seismic hazard analysis of Virginia. This more recent estimate of M_{max} is similar to the M_{max} values used in EPRI (1986) (Reference 269). Similarly, the distribution and rate of seismicity in the Central Virginia seismic source have not changed since the 1986 EPRI study (discussed in Subsection 2.5.2.3). Thus, there is no change to the source geometry or rate of seismicity. Therefore, the conclusion is that no new information has been developed since 1986 that requires a significant revision to the EPRI seismic source model of the Central Virginia seismic zone.

2.5.1.2 Site Geology

Subsection 2.5.1.2 presents descriptions of the geologic conditions present in the Lee Nuclear Site vicinity (25 mi. radius), Lee Nuclear Site area (5 mi. radius) and at the Lee Nuclear Site (0.6 mi. radius). Subsections detailing the physiography and geomorphology, geologic history, stratigraphy, structural geology, engineering geology, seismicity and paleoseismology, and groundwater of the site area are included.

The geology of the site and surrounding area is extensively studied (Figures 2.5.1-218a, 218b, 219a, 219b, and 220), and typical of the region. The Duke Power Co. Project 81 Preliminary Safety Analysis Report presents previous investigations of the Lee Nuclear Site (Reference 401). More recently-published literature and mapping, as well as field reconnaissance and detailed studies conducted in 2006 and 2007 as part of this project, supplement these data.

2.5.1.2.1 Site Area Physiography and Geomorphology

The site is located within the Piedmont physiographic province of central South Carolina (Figure 2.5.1-201). The Piedmont Physiographic Province is bounded on the southeast and northwest by the Coastal Plain and Blue Ridge physiographic provinces, respectively. The site lies approximately 8.5 mi. southeast of Gaffney, South Carolina on the western bank of the Broad River (Figure 2.5.1-218a and 218b). The site topography is characteristic of the region, with gently to moderately rolling hills and generally well-drained mature valleys. Within the 5 mi. site area, topography ranges from about 400 to 1,000 ft. msl (Figure 2.5.1-221). Elevations at the Lee Nuclear Site range from about 500 to 700 ft. msl (Figure 2.5.1-222).

The primary drainage in the site area is the Broad River. Typical of most first order Piedmont streams, the Broad River flows southeast normal to trend of most geologic contacts and structures. The streambed is at about 500 ft. msl and has

incised into the Piedmont surface about 200 ft. below the drainage divides. The Broad River lacks a well-developed flood plain in the Lee Nuclear Site area.

The local tributaries drain into the Broad River. The local drainage pattern is generally dendritic, the result of lithologic control and rock jointing. In the vicinity of the Broad River, these tributaries occupy steep valleys that shallow headward. Drainage divides generally range in elevation from 630 to 750 ft. msl.

Surficial geologic materials consist predominantly of residual soils and saprolite that mantle igneous and metamorphic bedrock. Relatively few natural bedrock outcrops are present within the site area, characteristic of the long weathering history of the Piedmont. The long history of weathering and erosion has created a relatively flat, rolling plain with local relief generally the result of variations in the weathering resistance of bedrock and/or stream incision. In the site area, the most erosion-resistant rock types contain large amounts of quartz (typically metaconglomerate or chert deposits), and often support linear ridges (Figures 2.5.1-219a, 219b and 2.5.1-220). The highest point in the Lee Nuclear Site area is Draytonville Mountain at about 1,010 ft. msl. Draytonville Mountain is an elongated, east-west-trending ridge located 4 mi. west-northwest of the site and underlain by quartzite pebble-cobble metaconglomerate (References 386 and 387). Other ridges in the site area include McKowns Mountain, Silver Mine Ridge, and unnamed ridges near Cherokee Falls, South Carolina. The site area ridges are associated with erosion-resistant quartzite rocks.

The Preliminary Safety Analysis Report (PSAR) Project 81 prepared for the former Duke Cherokee nuclear site identifies five lineaments within the site vicinity based on 1:500,000- and 1:250,000-scale aerial photographs (Reference 401). These lineaments are interpreted to be the result of drainage patterns, variations in bedrock resistance to weathering, and/or land use. These lineaments are not attributed to differential surface movement from capable tectonic features. Field reconnaissance and review of aerial photography and digital topography of the site vicinity performed as part of this project confirm the findings of the earlier lineament study.

One of the lineaments identified by PSAR Project 81 (Lineament No. 1) (Figures 2.5.1-219a and 2.5.1-221) is of particular interest for two reasons: (1) its orientation parallel to the predominant regional structural grain, and (2) its proximity to the site (Reference 401). This 4- to 5-mi.-long linear feature is located approximately 2 mi. northwest of the Lee Nuclear Site, and strikes approximately N55°E, and is a relatively steep northwest-facing slope. London Creek flows northeastward along much of the length of the northwestern base of the slope, before joining with the Broad River near the southernmost tip of Ninety-Nine Islands. The lineament, most easily recognizable on the 1:40,000-scale USGS photography, terminates northeastward at the Broad River and is not expressed in the topography northeast of the river. Field reconnaissance performed for this project and geologic mapping by Nystrom (2004) (Reference 391) reveal that resistant, northeast-striking quartzite layers outcrop along the top of the slope. The linear topographic expression of this slope or ridge is the result of erosion by London Creek (and the erosion resistance of the quartzite layers) and is assessed to be non-tectonic in origin.

In summary, Lee Nuclear Site area topography records no expression of differential surface movement but is strongly controlled by variations in bedrock resistance to weathering. The most resistant rock types in the site area are mainly quartz-rich rocks such as metaconglomerate and chert.

2.5.1.2.2 Site Area Geologic Setting and History

The site area is underlain by a complexly deformed and metamorphosed plutonic–volcanic sequence and associated sediments. Under the “older” belt nomenclature these rocks are considered part of the “Kings Mountain Belt” (Reference 207). More recent classification of Hibbard et al. (2002) (Reference 204) associates these rocks with other Neoproterozoic – Early Paleozoic metaigneous terranes that were formed in volcanic arc systems. The subduction associated with these systems occurred distant from Laurentia, and based on fossil evidence was in the Gondwana realm. This schema groups these diverse terranes into the Carolina Zone, which in more recent publications is called “Carolinia” (References 425 and 428) and is given “Domain” status. Carolinia forms the exposed eastern margin of the Appalachian system.

Hatcher et al. (2007) (Reference 404) use "Carolina Superterrane" to describe the amalgamated peri-Gondwanan volcanic arcs, but they consider the Kings Mountain Belt to have both Laurentian and peri-Gondwanan components. They consider the volcanic arc protoliths of the Battleground Formation to be of peri-Gondwanan origin, but consider the sedimentary protoliths of the Blacksburg Formation to have Laurentian affinities. However, they place the surface expression of the Carolina terrane suture to the west of the Battleground Formation.

Hibbard et al. (2002) (Reference 204) assign both the metasediments of the Blacksburg Formation and the metavolcanic rocks of the Battleground Formation to the Charlotte terrane of Carolinia. Their rationale for this association is the occurrence of similar rock types in both units, including protolithic felsic volcanics, quartzites that probably represent siliceous exhalatives related to hydrothermal activity associated with felsic volcanism, and similar styles of gold mineralization. Hibbard et al. (2002) (Reference 204) consider the metasediments of the Blacksburg Formation to represent the late stage clastic and carbonate sedimentary cap to the volcanic arc comprising the Battleground Formation, and therefore assign all the formations of the Kings Mountain Belt to have peri-Gondwanan associations.The following geologic scenarios and discussion are based on the detailed discussion of the characteristics of the Charlotte terrane in Hibbard et al. (2002) (Reference 204).

The site area is located in the western portion of the Charlotte terrane. This terrane represents an “infrastructural” element of the Carolina Zone, characterized by lack of primary features due to regionally penetrative tectonothermal processes in Hibbard et al. (2002) (Reference 204). The Charlotte terrane contains elements from a long and complex geologic history (Figures 2.5.1-202a and 202b) that began with arc related magmatic activity in the Neoproterozoic, and extends through the rift related Triassic extension and magmatism associated with the opening of the modern Atlantic Ocean basin. Figure 2.5.1-223 is based on PSAR

(1974) (FSAR Reference 401), Schaeffer (1981) (Reference 392), Hibbard et al. (2002) (Reference 204), and Hatcher et al. (2007) (Reference 404), and summarizes the geologic history of the site area.

The protoliths for the lithologies in the western portion of the Charlotte terrane are the result of magmatic activity (Stage II of Hibbard et al. (2002)) associated with subduction and arc rifting that straddled the Neoproterozoic–Cambrian boundary. An early stage of magmatism and deposition at about 570 Ma resulted in both felsic and mafic volcanism and shallow intrusion of tonalite and granodiorite plutonic bodies into the volcanic accumulation itself. Deposition of volcanic material was accompanied in later stages with deposition of both clastic and carbonate sediments that produced a volcaniclastic sequence with interfingered marine sediments. Locally, intense hydrothermal activity from the interaction of seawater with hot volcanic centers has significantly modified the bulk chemistry of these units. This modification occurred by severe leaching, transport, and redeposition of certain chemical components.

Subsequently, in the 549 to 535 Ma interval, the volcanic pile and its sedimentary units were intensely deformed and metamorphosed to upper greenschist to amphibolite facies, probably resulting from the complex thermal and tectonic interactions occurring in the subduction-magmatic environment (i.e., the Virgilina Event) (Reference 204). This event is associated with at least two deformational episodes (D1 and D2) and produced most of the more noticeable foliation, structures, and map patterns of geologic units in the site area. The ages of structures and fabrics associated with D1 and D2 are constrained to pre-535 Ma by crosscutting relationships with post-tectonic and post-metamorphic diorite in Hibbard et al. (2002) (Reference 204). At least three scenarios are proposed in the literature for the cause(s) of this tectonothermal activity. These three scenarios include: (1) back arc rifting and closure, (2) subduction of a block of isotopically different material into the subduction zone, and (3) assembly of the composite Charlotte and Carolina terranes. Other locations of the Charlotte terrane contain rock types resulting from a later stage of magmatism that occurred around 540 to 530 Ma (Stage III; Figure 2.5.1-223) resulting in intrusion of large mafic–ultramafic complexes and granitic material. In the site area, these do not appear to occur (Reference 204) unless they are possibly represented by late gabbro intrusions (Figures 2.5.1-219a and 219b).

The Charlotte terrane also shows tectonic and thermal evidence from later events in the Silurian, Devonian, and Carboniferous-Permian (i.e., the Alleghanian event; Subsection 2.5.1.1.2.1). However, the record for pre-Carboniferous tectonic activity is obscure in the Charlotte terrane in Hibbard et al. (2002) (Reference 204) probably due to thermal and structural overprinting by Alleghanian tectonic processes (Hatcher et al. 2007) (Reference 404). Hibbard et al. (2002) (Reference 204) and subsequent publications (References 428 and 430) argue for Late Ordovician - Silurian subduction of Carolinia and consequently the Charlotte terrane beneath Laurentia based on evidence from other portions of Carolinia and the Silurian thermal activity in the Charlotte terrane.

Amphibole $^{40}Ar/^{39}Ar$ cooling ages (425 - 430 Ma) in North Carolina record the time when the thermal environment in that location cooled through the

temperature at which radiogenic argon would be lost from the amphibole (about 500 ± 50°C; Reference 388). Hibbard et al. (2002) (Reference 204) interpret this to indicate cooling following the elevated thermal conditions associated with the subduction of Carolinia beneath Laurentia.

Based on detrital zircon ages in the Cat Square Terrane of the Inner Piedmont, Hatcher et al. (2007) (Reference 404) argue against Late Ordovician - Silurian subduction of Carolinia beneath Laurentia and for Neoacadian to early Alleghanian (post ~405 Ma) subduction of Laurentia beneath the Carolina Subterrane. Hatcher et al. (2007) (Reference 404) also cite the existence of the Concord suite, which represents Devonian mafic plutonism that resulted from this subduction event. In any case, in addition to the Concord suite plutons, the record for Devonian tectonothermal activity in the Charlotte terrane is confined to the Gold Hill–Silver Hill Shear zone. This indicates that Devonian effects may have been highly localized (Reference 204).

Alleghanian (Carboniferous-Permian) tectonothermal activity is heterogeneously distributed in the Charlotte terrane (Reference 204). Deformation occurs mainly in discrete shear zones within the terrane and at the Central Piedmont shear zone, which in the site vicinity comprises the Cross Anchor fault and the Kings Mountain shear zone. Metamorphism associated with Alleghanian orogenesis ranges from greenschist to amphibolite facies in the Charlotte terrane. Late Alleghanian tectonic activity is attributed to the thrusting of the Charlotte terrane onto the Inner Piedmont terrane in the site vicinity (References 204 and 404). However, proposed accretion of Carolinia to Laurentia in either the Late Ordovician - Silurian (Reference 204) or in the Neoacadian - Early Alleghanian (Reference 404) means that the suture between Carolinia and Laurentia is an older structure and the Alleghanian activity on the Central Piedmont shear zone must represent a later event. One explanation for this relationship is that the present surface expression of the Central Piedmont shear zone represents the head of the suture that was decapitated in the subsurface during the late Alleghanian collision of Laurentia and Gondwana (References 204 and 404). Hatcher et al. (2007) (Reference 404) map the surface trace of the subsurface suture throughout the Carolina Superterrane based on geophysical evidence.

Although the Charlotte terrane experienced accretion either during the Late Ordovician - Silurian or during the Neoacadian - early Alleghanian, the thermal and structural record is limited or obscure as discussed above. This has no doubt contributed to the controversy surrounding the timing and nature of the event. One K-Ar age for the site yields an age of 290 ± 7 Ma for hornblende (Table 2.5.1-202), and therefore it is uncertain if the site and site area experienced pre-late Alleghanian thermal elevation and therefore the extent of Late Ordovician or Neoacadian - early Alleghanian tectonogenesis.

The fact that both Rubidium-Strontium ages (Rb–Sr; 291 ± 10 Ma; sample B-51, 76 ft.) and Potassium-Argon (K–Ar; 296 ± 7 Ma; sample BP-7, 59 ft.) for undeformed biotite (closure to argon loss at about 300°C and undeformed hornblende K–Ar (290 ± 9; sample B-28, 106 ft.) (closure to Ar loss at about 500°C) are the same within analytical uncertainty indicates rapid cooling at the site following Alleghanian tectonic activity, presumably from rapid unroofing

following emplacement of the Charlotte terrane upon the Inner Piedmont (at about 335 to 320 Ma) (Reference 404). Undeformed potassium feldspar from the site gives a K–Ar age of 219 ± 1 Ma (closure to argon loss at about 250°C) shows that the rate of cooling decreased and that the site area and site passed below about 250°C around 219 Ma. These data suggest that the site has not experienced thermal conditions that could be associated with greenschist grade metamorphism since at least 219 Ma, and likely since around 300 Ma.

Based on the relatively limited record in the Charlotte terrane for Late Ordovician - Silurian and Devonian tectonics, the activity associated with Alleghanian tectonics is likely the cause of the last three deformational phases (D3 - Q5) at the site and site area. However, any or all of these structures could have resulted from earlier accretion events and could have been overprinted by the thermal elevation associated with the late Alleghanian interaction of Gondwana with Laurentia.

Mesozoic extensional tectonics associated with opening of the Atlantic Ocean almost certainly affected the area, at least to a limited extent, with the development of joints and fractures with associated quartz and zeolite mineralization. Mesozoic extension-related fracturing and brittle faulting associated with development of cataclasites, silicification, and zeolite mineralization are widespread features throughout the Piedmont in the site region and site vicinity (Reference 420). These features also are associated with late kinematic open to healed fractures lined with crystalline quartz and syntaxial extension veins filled with anhedral quartz. Garahan et al. (1993) (Reference 420) report brittle faulting associated with Mesozoic reactivation of the Kings Mountain shear zone, northwest of the site. Murphy and Butler (1981) (Reference 389) report limited displacement (less than 10 cm), small scale brittle faulting in the site area. Schaeffer (1981) (Reference 392) reports laumontite - calcite mineralization associated with S5 kink planes. Undeformed Triassic diabase dikes are the only documented evidence of Mesozoic activity in the site area. Subsequent to this rifting, broad flexure occurred as a result of erosional unloading and the onset of drift margin sedimentation.

In summary, the majority of rock types, metamorphism, and deformation in the site area can be attributed to Neoproterozoic–Early Cambrian subduction zone-related magmatic and tectonic activity. However, the site area may have experienced thermal environments and stresses associated with Silurian and/or Devonian orogenic events. Based on regional considerations, any effects resulting from these events are to be limited in the site area. In contrast, Alleghanian tectonic activity likely produced folding and shearing localized in discrete zones under greenschist to amphibolite grade conditions as recorded in the mineral cooling ages. Alleghanian emplacement of the Charlotte terrane upon the Inner Piedmont was followed by rapid cooling that resulted from rapid unroofing and cooling. Extensional tectonics associated with the opening of the modern Atlantic Ocean probably caused some jointing and fracturing in the Lee Nuclear Site area. In addition, magmatism associated with this extension is evident in the site area as a set of undeformed diabase dikes.

2.5.1.2.3 Site Area Stratigraphy and Lithology

Rock units in the site area generally belong to the Battleground Formation (References 308, 391, 286, and 260). There is disagreement, however, as to whether the rock mass mapped at the site (map unit "Zto" on Figures 2.5.1-218 through 2.5.1-220) belongs to the Battleground Formation. Murphy and Butler (1981) (Reference 389) suggest that these rocks belong to the Battleground Formation, whereas more recent publications by Horton and Dicken (2001) (Reference 308) and Nystrom (2004) (Reference 391) indicate that rock mass Zto comprises plutonic rocks that intruded into the Battleground Formation. For the purposes of this COL application, rock mass Zto is assessed to be separate from, and younger than (or possibly coeval with), the Battleground Formation. Other rocks in the site area include Mesozoic diabase dikes (References 236 and 389) and Quaternary alluvial deposits (References 286 and 391).

Subsection 2.5.1.2.3.1 describes the Battleground Formation. Subsection 2.5.1.2.3.2 describes intrusive rock mass Zto. Subsection 2.5.1.2.3.3 describes the Mesozoic diabase dikes and Quaternary alluvial deposits within the site area.

Figure 2.5.1-219a presents geologic mapping of the site area performed at two different scales by three different researchers (References 308, 286, and 391). As such, unit contacts do not match perfectly across adjacent source map boundaries.

2.5.1.2.3.1 Battleground Formation

The Battleground Formation primarily comprises metavolcanic and metasedimentary rocks of Neoproterozoic age (Reference 308) (Figures 2.5.1-219a and 219b). The occurrence of metasedimentary carbonate rocks is indicative of a marine depositional environment. The Battleground Formation includes felsic metavolcanic rocks, intermediate to mafic metavolcanic rocks, and quartz-rich metasedimentary rocks. Major units within the Battleground Formation are described below, with additional detail provided in Figures 2.5.1-219a and 219b.

Mafic to intermediate metavolcanic rocks (map unit Zbvm). Nystrom (2004) (Reference 391) maps mafic to intermediate metavolcanic rocks west and south of the site. These rocks are described as medium gray, dark gray, and green hornblende phyllite, hornblende gneiss, and amphibolite. Nystrom (2004) (Reference 391) maps the contact separating Zbvm from the western edge of plutonic rock mass Zto as nearly linear (Figure 2.5.1-219a). Subsection 2.5.3.1.3 describes evidence indicating the irregular and intrusive nature of this contact, as shown in Figures 2.5.1-220 and 2.5.1-229.

Felsic metavolcanic rocks (map unit Zbvf). Nystrom (2004) (Reference 391) maps assorted felsic metavolcanic rocks in the southeast corner of the Blacksburg South quadrangle. These rocks are described as medium gray, dark gray, and green in color.

Interlayered mafic and felsic gneiss (map unit Ztrs). Howard (2004) (Reference 286) maps interlayered mafic and felsic gneiss in the southwest corner of the Kings Creek quadrangle. Based on general unit descriptions and mapped location, units Ztrs and Zbvf are assessed to be roughly equivalent across the quadrangle boundary. However, Nystrom (2004) (Reference 391) indicates that Zbvf is part of the Battleground Formation, whereas Howard (2004) (Reference 286) suggests that Ztrs is not part of the Battleground Formation. For the purposes of this COL application, rock masses Zbvf and Ztrs are assessed to be equivalent and part of the Battleground Formation.

Plagioclase crystal metatuff (map unit Zbct). Nystrom (2004) (Reference 391) describes unit Zbct as gray, generally well foliated, assorted metavolcanics of mainly felsic to intermediate composition with crystal and less abundant lithic metatuffs. This unit is assessed to be the equivalent of Howard's (2004) (Reference 286) crystal metatuff (Zbct).

Phyllitic metatuff (map unit Zbmp). Nystrom (2004) (Reference 391) describes unit Zbmp as gray to dark gray varied metavolcanics including crystal and lithic metatuffs. This unit is assessed to be equivalent to Howard's (2004) (Reference 286) mottled phyllite (lapilli metatuff) (map unit Zbmp). Howard (2004) (Reference 286) maps a siliceous alteration zone within unit Zbmp (shown as Zbmp-a on Figure 2.5.1-219a) that does not appear on Nystrom's (2004) (Reference 391) map.

Quartzite and metaconglomerate (map units Zbq, Zbkq, Zbdc, Zbc). Nystrom (2004) (Reference 391) maps various north- and northeast-striking quartzite and quartz metaconglomerate units within the site area. These long and thin "stringers" are described as white to gray, fine- to medium-grained quartzite and medium- to coarse-grained, schistose metaconglomerate. As described in Subsection 2.5.1.2.1, some of these quartzite and metaconglomerate units are mapped atop ridges in the site area, including McKowns Mountain.

Due to intense deformation, few primary features survive with which to determine stratigraphic order within the Battleground Formation. However, inferred relationships (References 236, 389, and 390) suggest the proposed northeast-striking South Fork antiform forms a homocline such that units within the Battleground decrease in age to the northwest (Reference 236) (Figure 2.5.1-219a). If these inferred relationships are correct, then the oldest rocks would occur in the antiform’s core and rocks farther from the core to the northwest would be younger. This inference is supported by the occurrence of the metasedimentary component primarily to the northwest, the expected stratigraphic relationships for deposition of marine-dominated clastic and chemical precipitate rocks at the later stages of the volcanic pile accumulation (Reference 308). Figure 2.5.1-224 schematically shows the stratigraphic relationships of the various units in the site area.

2.5.1.2.3.2 Site Pluton (Rock Mass Zto)

The site is underlain by a metamorphosed plutonic rock mass, shown on Figures 2.5.1-218 through 2.5.1-220, 2.5.1-224, and 2.5.1-229 as rock mass Zto.

Goldsmith et al. (1988) (Reference 228) report a discordant $^{207}Pb/^{206}Pb$ age of approximately 590 Ma for rock mass Zto. This rock mass has been mapped at various scales by various geologists and, consequently, has been described differently, as indicated below.

Murphy and Butler (1981) (Reference 389) note the similarity between the compositions of volcaniclastic units of the Battleground Formation and the plutonic units that intrude them (Zto). Based on this observation, they suggest that these metavolcanics were intruded by their own parent magmas, and assign both to the Battleground Formation. However, more recent mapping separates these plutonic rocks (Zto) from the Battleground Formation host units. For the purposes of this COL application, rock mass Zto not considered to be part of the Battleground Formation. This distinction largely is semantic, however, since the Battleground Formation and rock mass Zto likely formed at approximately the same time in the Neoproterozoic (Reference 389).

Horton and Dicken's (2001) (Reference 308) 1:500,000-scale mapping describes rock mass Zto at the site as Neoproterozoic metatonalite (Figures 2.5.1-218a and 218b), comprising metamorphosed biotite tonalite and lesser amounts of hornblende tonalite, trondhjemite, and granodiorite. Rock mass Zto locally contains angular xenoliths of Battleground Formation metavolcanic and metasedimentary rocks (Reference 308).

Nystrom's (2004) (Reference 391) 1:24,000-scale mapping of the Blacksburg South quadrangle describes rock mass Zto at the site as metatonalite (Figures 2.5.1-219a and 219b). This metatonalite is described as light to medium gray, coarse-grained, with large potassium feldspar and quartz grains (Reference 391).

Howard's (2004) (Reference 286) 1:24,000-scale mapping of the adjacent Kings Creek quadrangle describes rock mass Zto as metatonalite and volcaniclastic rocks (Figures 2.5.1-219a and 219b). These felsic rocks are of mixed origin, comprising intrusive tonalite, dacitic flows, and epiclastic byproducts of both (Reference 286). Howard (2004) (Reference 286) maps Zto approximately 3 miles east of the site (Figure 2.5.1-219a).

Whereas rock mass Zto generally is metatonalite, its composition varies spatially (Reference 286). Subsection 2.5.3.1 indicates that meta-granodiorite is the most abundant rock type present within map unit Zto exposed by the excavation at the site, based on petrographic analyses (Reference 401). As such, Figure 2.5.1-229 and discussions throughout Subsection 2.5.3, describe rock mass Zto within the site excavation as meta-granodiorite.

2.5.1.2.3.3 Other Lithologic and Stratigraphic Units within the Site Area

In addition to the rocks described above, Mesozoic diabase dikes and Quaternary alluvial deposits are mapped within the site area. The diabase dikes primarily are of plagioclase, pyroxene, and olivine composition. These dikes crosscut, and therefore post-date, the units described above. These diabase dikes are

undeformed and unmetamorphosed rocks of Jurassic-Triassic age (References 236 and 389).

Quaternary alluvial deposits are mapped in active river and stream channels in the site area. These deposits primarily are modern channel deposits and bars that are actively transported by the Broad River and its tributaries comprising gravels, sands, and silts.

2.5.1.2.4 Site Area Structural Geology

Previous geologic investigations include specific studies conducted for the Lee Nuclear Site and geologic mapping of the surrounding area. Schaeffer (1981) (Reference 392), Butler (1981) (Reference 285), and Murphy and Butler (1981) (Reference 389) present structural analyses for the site area. Schaeffer (1981) (Reference 392) incorporates much of the structural data obtained as part of the PSAR Project 81 (Reference 401). According to Schaeffer (1981) (Reference 392), the site area has experienced five deformational episodes (D_1 through D_5), which are expressed as associated cleavage development (S_1 through S_5), folding (F_1 through F_5), and lineations (L_1 through L_5) (Table 2.5.1-203). In addition to these penetrative fabrics, discrete zones of both ductile and brittle deformation are present, mainly concentrated in sheared-out fold limbs (Table 2.5.1-203). The map pattern of surface geology is mainly controlled by the planar S_1 and S_2 foliations, and by the axial surfaces of F_2 folds. Because the S_2 foliation is the best developed, these features are the most commonly seen. Both the D_1 and D_2 deformations are closely related and formed during the same greenschist- to amphibolite-grade metamorphic event. This metamorphism and deformation has been shown to have occurred near the Neoproterozoic-Cambrian boundary (549 to 535 Ma) in Hibbard et al. (2002) (Reference 204). In addition to the structures described above, Schaeffer (1981) (Reference 392) also notes probable effects resulting from Mesozoic extension.

The D_1 deformation phase resulted in a foliation (S_1) axial planar to small scale (0.4 to 1.2 in. wavelength) isoclinal upright folds (F_1). Schaefer (1981) (Reference 392) reports that S_1 is probably parallel to S_0 (where S_0 is the primary bedding expressed as compositional layering). In some locations, the early foliation (S_1) can only be found in the hinge areas of the larger scale F_2 folds. In most locations, the limbs of F_1 folds are sheared out. Schaeffer (1981) (Reference 392) demonstrates that, in the hinge area of the Cherokee Falls synform, F_1 fold axes were rotated into the plane defined by S_2 (Figure 2.5.1-225). The D_1 deformation event formed an intersection lineation of S_0 and S_1. The rotation of the F_1 fold axes and the sub-parallel orientation of S_1 and S_2 indicate the transposition of D_1 structures during the D_2 event.

D_2 deformation caused isoclinal to closed upright folding (F_2) associated with a well-developed axial planar cleavage (S_2). The nature of the F_2 folding shows some lithologic control with isoclinal folding developing in more tightly foliated rocks (schist and phyllite) and close to tight folding in more massive units

(quartzite, metaconglomerate, and gneiss). This resulted in a lineation defined by the intersection of S_1 and S_2. In addition, the alignment of stretched bodies of biotite schist and quartzite form a lineation perpendicular to the F_2 axes. Rheologically less competent material (marble) shows stretching both parallel and perpendicular to F_2 fold axes to form pillow like structures.

The D_3 deformation event folded the S_2 foliation into asymmetric, flexural-slip folds with longer limbs to the southeast. These F_3 fold axes plunge at moderate angles to the northeast, with axial planes that dip steeply to the northwest, and display a well-developed axial planar cleavage (Figure 2.5.1-225). In places F_3 folds are observed to fold F_2 folds. An intersection lineation associated with D_3 is defined by the intersection of S_2 and S_3. The D_3 phase also caused reactivation of D_2 shear zones with a later brittle overprint. Both the ductile and cataclastic fabrics record post kinematic overgrowths and veins with a lower greenschist assemblage consisting of quartz, epidote, muscovite, biotite, chlorite and potassium feldspar.

A fourth deformational event (D_4) produced open to tight flexural slip folds with poorly developed axial planar cleavage with axes that plunge gently to the northeast (Figure 2.5.1-225). The axial planar cleavage (S_4) is almost horizontal and dips gently both northeast and northwest. The intersection of S_4 and S_2 define the L_4 lineation.

The final deformation episode recognized in the site area resulted in kink folding and gentle to open warping of S_2. The plunge of the fold axes is variable but primarily confined to the southeastern quadrant. Some of the kink folds occur in conjugate sets with sub-vertical axial and kink planes that strike northeast and northwest. The intersection lineation of S_5 and S_2 plunges steeply down dip on S_2.

Based on the limited amount of evidence for Silurian and Devonian fabric development, D_3, D_4, and D_5 structures are likely Carboniferous (Alleghanian) in age. The youngest possible age of D_3, D_4, and D_5 structures is constrained by the post-kinematic greenschist overgrowth (pre-296 Ma), based on radiometric dating discussed in Subsection 2.5.1.2.2.

2.5.1.2.4.1 Structures Within the Site Area

Subsection 2.5.1.2.4.1 describes relevant geologic structures located within 5 mi. of the Lee Nuclear Site.

Cherokee Falls Synform. Mapping by Murphy and Butler (1981) (Reference 389) shows the axial trace of the Cherokee Falls synform about 4.5 mi. northwest of the Lee Nuclear Site (Figures 2.5.1-219a and 219b). Murphy and Butler (1981) (Reference 389) interpret this structure as an overturned synform, with a shallowly northeast-plunging fold axis and an axial surface that dips steeply to the southeast, characteristic of F_2 structures. The core of the synform contains

metatrondhjemite complex lithologies while mafic schist and sericite schist wrap around the nose and form the outer limbs of the synform. This structural relationship is modified by subsidiary folding that results in protrusions of mafic schist into the core parallel to the fold axis. The northwest limb is apparently sheared off as the map units are truncated. As noted previously, F_1 fold axes are rotated into the surface defined by the axial planar cleavage (S_2). Also, folding of S_1 is observed in the hinge area. This is an F_2 structure resulting from the D_2 phase of deformation. More recent mapping by Nystrom (2004) (Reference 391) does not include the Cherokee Falls synform.

Draytonville Synform. The Draytonville synform is located about 4.5 mi. northwest of the Lee Nuclear Site where a prominent metaconglomerate (the Draytonville metaconglomerate) is folded into an overturned syncline (Reference 389) (Figures 2.5.1-219a and 219b). The fold axis plunges shallowly to the northeast and the axial surface dips steeply southeast. Based on the fact that only compositional layering and one other surface is observed to be folded (Reference 389) and the similarity in fold geometry to the Cherokee Falls synform, the Draytonville synform is also considered an F_2 generation fold (Reference 387). More recent mapping by Nystrom (2004) (Reference 391) does not include the Draytonville synform.

Minor Striated Surfaces. Field reconnaissance for PSAR Project 81 (Reference 401) identifies several surfaces with mineralization and slickenside development within the Lee Nuclear Site area. These are not traceable beyond a single exposure, thereby indicating that they are small-displacement features and are not associated with any through-going fault. These features are characteristic of the Piedmont regionally, and are described below:

- PSAR Project 81 (Reference 401) maps a series of en echelon, epidote-covered slickensided surfaces at Cherokee Falls, South Carolina, about 3 mi. northwest of the site. These surfaces dip 45° east, with west-stepping en echelon geometry. These features are not traceable beyond Cherokee Falls. Detailed examination reveals that epidote crystals grew across the surfaces in addition to defining the slickenside lineation (Reference 401). This demonstrates that some epidote formed after movement on the surfaces had ceased. The stability field for epidote therefore precludes movement on these surfaces in a near-surface regime.

- PSAR Project 81 (Reference 401) maps another set of slickensides in a schistose zone in the Draytonville, South Carolina area about 4 mi. west of the site. This zone has a moderate southeasterly dip. These slickensides could not be traced beyond this single exposure.

- PSAR Project 81 (Reference 401) maps a minor offset with vertical dip and northwest strike about 4 mi. north of the site. Murphy and Butler (1981) (Reference 389) note a small amount of lateral offset, no measurable offset could be obtained.

- PSAR Project 81 (Reference 401) maps two offsets about 6 mi. northwest of the sites; however, the poor condition of the exposure prevented resolution of the fault orientation. One of the offsets indicated normal movement while the other indicates reverse movement.

The PSAR (Reference 401) does not describe precise locations of these minor features, and fieldwork performed for this project did not locate the minor features described above. As described in the PSAR, these minor features were not traced beyond a single exposure, and are not expressed geomorphically. These minor, localized features are similar to those found throughout the Piedmont, and are not evidence for recent movement.

2.5.1.2.5 Site Geology

Subsection 2.5.1.2.5 presents a detailed description of the site (0.6 mile radius) geology.

2.5.1.2.5.1 Site Physiography and Geomorphology

The physiographic and geomorphologic characteristics of the site are typical of those described for the site area. Elevations at the site range from 510 to 820 ft. msl (Figure 2.5.1-222). Site relief is largely the result of tributary drainage incision. McKowns Mountain, the linear, north-trending ridge west of the site, is the result of erosion-resistant quartzite.

The variation in bedrock resistance to weathering locally control drainage directions, and is also discussed in Subsection 2.5.1.2.1. Topography controlled by differential erosion is particularly evident in the orientations of McKowns Creek and a smaller creek that occurs between McKowns Mountain and a smaller quartzite ridge to the east. The smaller creek is essentially sub-parallel to the quartzite ridges and McKowns Creek and the confluence of the smaller creek can be seen to bend around the nose of McKowns Mountain.

2.5.1.2.5.2 Site Geologic Setting and History

The site geologic history is congruent with the scenario outlined above for the site area. However, whereas five deformational events are documented within the site area (Reference 392), at least two are recognized in rocks at the site. The reasons why all five events are not recorded in site rocks are: (1) the emplacement of the site plutonic rocks in Neoproterozoic time (FSAR Reference 308) post-dates some of the older deformational events recorded in site vicinity country rocks; and (2) the contrasting rheological properties between the site plutonic rocks and the surrounding metavolcanic country rocks makes correlation of deformational events problematic. These contrasting rheological properties make correlation of deformational events recorded in the pluton and the country rocks difficult because the plutonic mass probably developed different structures in response to stress relative to the surrounding country rock. The site is underlain by a pluton of granodiorite to tonalite composition that has intruded into mafic to felsic volcaniclastic country rock. Lee Nuclear Site rocks have undergone at least two deformational events and metamorphism to upper

greenschist to amphibolite facies. These deformation events produced two foliations, and the second deformation event produced tight to isoclinal folding. These deformation events occurred in Neoproterozoic and Early Cambrian time in association with island arc subduction, probably located proximal to Gondwana (Reference 204).

2.5.1.2.5.3 Site Stratigraphy and Lithology

The eastern portion of the site, including the area for the facility foundations, is underlain by a meta-granodiorite to meta-diorite intrusive body (Figure 2.5.1-220). Western portions of the site are underlain by mafic to intermediate metavolcanic rocks that consist primarily of hornblende phyllite, hornblende gneiss, and amphibolite. The metavolcanic rocks locally contain quartzite bodies that form geomorphically prominent linear ridges.

Deep weathering has produced a mantle of saprolite at the site up to 100 ft. thick (typically 40 to 80 ft. thick). This weathering profile grades downward to partially weathered and unweathered rock. The saprolite varies from micaceous sandy silt to silty sand, and preserves relict rock textures and structure. The upper 2 to 8 ft. of saprolite has weathered to form a soil B-horizon consisting of clayey silty sand with no relict texture or structure.

Quaternary alluvial deposits are mapped in active stream channels at the site and include gravels, sands, and silts (Figure 2.5.1-220). These deposits primarily are modern channel deposits and bars that are actively transported by the Broad River and its tributaries.

2.5.1.2.5.4 Site Area Structure

As in the site area, the major control on geologic trends in the country rock and map patterns are foliations and folding due to the D_2 deformation. However, the intrusive metagranodiorite-diorite pluton is massive in nature and locally contains discrete zones expressed as joints, fractures and shear/breccia zones. These features are discussed in detail below.

The relatively massive nature of the pluton compared to the surrounding country rock which is composed of volcaniclastic protoliths, probably indicates that there has been a significant difference in rheological properties between these two lithologies, both in strength and anisotropy. That this is the case, is indicated by the fact that the volcaniclastic country rock carries a well developed, penetrative foliation compared to the pluton in which strain is expressed in more discrete zones. This rheological difference makes correlation of deformational events between the pluton and country rock problematic in that the strain from a single deformational event may be expressed as different structures in the country rock verses the pluton (i.e., folding in the foliated country rock verses discrete shearing in the pluton). For this reason the deformational events associated with the structures in the pluton will be annotated with lower case (i.e., d_1) as opposed to the deformational events in the site area (i.e., country rock) which are expressed as upper case (i.e., D_1) (Table 2.5.1-204).

McKowns Creek Antiform. Mapping by Butler (1981) (Reference 285) indicates that the metagranodiorite - diorite body that serves as the foundation for the Lee Nuclear Site structures is located in the nose of McKowns Creek antiform. This antiform is shown at the map scale by metatonalite-dacite-complex lithologies that are folded about a core of metaandesite (Figures 2.5.1-219a and 219b). Two prominent north-south oriented quartzite ridges are located in the western portion of the site on the eastern flank of the structure (Figures 2.5.1-219a and 219b). The dominant axial planar foliation is S_2, which occurs at an angle to the lithologic contacts and an earlier foliation (S_1), is folded in the nose of the structure, Schaeffer (1981) (Reference 392). Based on these observations and the orientation of the fold axes and axial surface, Schaeffer (1981) (Reference 392) assigns this structure to F_2. Therefore, this structure results from D_2 deformation and is Neoproterozoic to Early Cambrian in age. More recent mapping by Nystrom (2004) (Reference 391) does not include the McKowns Creek antiform.

Shear and Breccia Zones. Several “shear-breccia” zones were investigated during field studies performed for the Project 81 PSAR (Reference 401) and in subsequent foundation excavation mapping. These zones were mapped and studied in great detail including borings and detailed petrographic descriptions of the structural fabric.

Detailed mapping shows that these zones comprise smaller-scale anastomozing zones that are preferentially developed in the smaller dikes or along the margins of the larger dikes of the more mafic lithologies. The structural fabric in these zones contains an early ductile (foliated) component (d_1) with a late-stage brittle overprint (d_2). The orientation data for these zones are shown plotted on a stereonet in Figure 2.5.1-231. The most well developed zones strike a few degrees east of north and dip steeply east. A second, less well-developed set strikes northwest and dips moderately southwest.

The early ductile fabric is composed primarily of elongated “polygonalized” polycrystalline quartz aggregates indicative of dynamic recrystallization and annealing recovery mechanisms. These quartz aggregates occur in a foliated matrix of white mica and sometimes biotite. Potassium feldspar and plagioclase porphyroclasts are reported and this fabric is described as mylonitic. The feldspars fraction is highly altered to white mica and epidote. Iron staining of the shear planes is ubiquitous. Biotite in the protolith is reported to be “olive green” in color. In contrast, biotite reported in association with the shear zones is almost always reported to be “brown.”

A brittle fabric that contains fractured and broken plagioclase, quartz and quartz aggregates in a finer grained matrix of smaller clasts and fine-grained material overprints the early ductile fabric. This fine-grained matrix is overgrown by undeformed white mica. This white mica occasionally stitches the boundary between larger clasts and the fine-grained matrix. In addition, the matrix contains randomly oriented chlorite plates and masses, along with epidote, calcite and pyrite.

Veins containing quartz, calcite, epidote, white mica, chlorite, pyrite and what is reported to be a low birefringent material (likely albite) cut the ductile and brittle fabrics. Veins also occur that contain various mixtures of these minerals and potassium feldspar. These veins are in various states of deformation ranging from undeformed, to slightly deformed, to folded and bent. In addition, stringers of the vein material are reported sub-parallel to the dominant foliation, and ground up in the brittle matrix. This indicates that these veins are both syn- and post-kinematic with respect to both the ductile and brittle phases of deformation.

The relationships described above indicate that fluid-dominated metamorphic processes accompanied the ductile and brittle strain. This metamorphism resulted in a granodiorite to tonalite mineralogy consisting mainly of plagioclase (andesine–oligoclase), quartz, potassium feldspar, biotite, and amphibole transformed into more hydrous and carbon-rich phases. The presence of calcite and potassium feldspar in the metamorphic assemblage indicates that the fluid contained significant amounts of CO_2, and water. In addition to hydration of the mineralogy, this metamorphism is characterized by the release of significant amounts of calcium from the plagioclase due to removal of the anorthic component as the stable phase becomes albite in the presence of both H_20 and CO_2 (Reference 393):

$$4CaAl_2Si_2O_8 + KAlSi_3O_8 + H_2O \rightarrow KAl_3O_{10}(OH)_2 + 2Ca_2Al_3Si_3O_{12}(OH) + 2SiO_2$$

anorthite + Kspar + water → muscovite + epidote + quartz

in the presence of water and potassium feldspar (Reference 394), or:

$$2CaAl_2Si_2O_8 + CO_2 + H_2O \rightarrow CaAl_4Si_2O_{10}(OH)_2 + CaCO_3 + 2SiO_2$$

anorthite + CO_2 + water → margarite + calcite + quartz

These reactions are characteristic of greenschist-grade metamorphism (Reference 394). Additional potassium would be added to this system as a result of the breakdown of biotite and amphibole to chlorite.

The kinematic history of the shear-breccia zones began with a ductile event (d_1). The dynamic recrystallization and recovery features recorded in quartz indicate that this occurred at mid- to upper-greenschist facies conditions in the presence of a fluid with an aqueous component. During this initial stage, in association with mechanical processing of the other mineralogy, protolith plagioclase and potassium feldspar were metamorphosed to produce a foliated assemblage of dynamically recrystallized quartz, albite, white mica and possibly biotite. Subsequently, either due to reduced temperature, increased strain rate, or both, brittle deformation produced a cataclastic fabric (d_2) that contains clasts of the earlier fabric and probably protolith material. The metamorphic reactions discussed above and the breakdown of biotite and amphibole to chlorite produced white mica, calcite, quartz, epidote and chlorite.

Coeval with the ductile and brittle shearing, extensional fractures were generated and filled with metamorphic fluids that resulted in the crystallization of reaction products in the fracture void. Fractures initially formed parallel to the maximum compression direction (Figure 2.5.1-230), which occurred at some angle to the shear zone boundaries. As the shear strain increased, fractures rotated into the field of compression and were folded. Further shear continued to rotate the fractures out of the field of compression into the field of extension. The extensional strain deformed fractures and strung out into the structural fabric.

The persistence of elevated thermal conditions after the brittle deformation is indicated by the occurrence of extensional fractures with infilling of the metamorphic products that are undeformed and that crosscut the foliation that defines the structural fabric. This also resulted in the overgrowth of undeformed metamorphic products on the matrix material.

The K-Ar radiometric data reported for potassium feldspar from an undeformed vein in a dilatational feature that cross cuts one of the shear zones is an important constraint on the minimum age possible for the shear-breccia zones. This sample gives a mineral age of 219 $\pm$ 1 Ma (sample GTP-7). This result is significant in two respects: (1) because the feldspar is undeformed and cross-cuts the shear zone, and the feldspar is older than 219 Ma, the timing of deformation related to shear zone formation is constrained to some time before 219 Ma; (2) the temperature for closure to argon loss for potassium feldspar is about 250°C (Reference 388). These data indicate that the thermal environment at the site has not been sufficient to produce greenschist facies metamorphic effects since at least 219 Ma.

Although feldspar geochronology constrains the formation of the shear-breccia zones to be pre-219 Ma, the K-Ar biotite mineral age indicates cooling from greenschist grade thermal conditions at 296 $\pm$ 7 Ma. This cooling was probably associated with unroofing following thrusting of the Charlotte terrane over the Inner Piedmont along the nearby Kings Mountain shear zone. Schaeffer (1981) (Reference 392) assigns the development of ductile fabric in these zones to D_2 and the later brittle overprint to D_3 similar to features seen in sheared out F_2 fold limbs in the site area. The D_2 event is associated with upper greenschist to amphibolite grade metamorphism which would be consistent with the features observed in the ductile fabric elements. If this association is correct, then the ductile fabric in the shear - breccia zones would be Late Proterozoic to Early Cambrian in age. However, because of the probability that the pluton may have seen elevated thermal conditions and stresses in the Late Ordovician - Silurian, Hibbard et al. (2002) (Reference 204), or Devonian to late Mississippian, Hatcher et al. (2007) (Reference 404) or late Alleghanian, Hibbard et al. (2002) (Reference 204), Hatcher et al. (2007) (Reference 404) the ductile fabric (d_1) and subsequent cataclasis (d_2) in the shear-breccia zones could have resulted from, or been reactivated by stresses associated with any of these events. The only constraints are that the ductile fabric (d_1) is older than the cataclasis (d_2) and that the cataclasis is older than approximately 300 Ma based on the radiometric ages of the post-kinematic greenschist facies assemblage. It should be noted that ductile fabrics with brittle overprint are commonly reported with late stage

Alleghanian tectonism. Therefore it is also possible that these shear breccia zones are related to, or have been reactivated by localized deformation of the pluton in response to stresses associated with this thrusting event and may be Alleghanian in age.

Dilation Fractures. Dilation fractures (d_3) less than or equal to 4 in. thick and partially filled with undeformed quartz, potassium feldspar and minor amounts of calcite, pyrite and fluorite cut across the shear-breccia zones with no apparent effect except for the dilatational separation. The open spaces have euhedral crystals indicating growth from a hydrothermal fluid. These are straight breaks similar to joints and in locations where they change direction they become wider.

Based on the occurrence of similar mineralogy in the fracture filling, these dilational features were probably produced during the metamorphic event described above for the shear - breccia zones. In any event, the potassium feldspar that constrains the age of the shear-breccia zones cross cuts one of these features and places the same constraints on the age.

Joints. Joints are common at the site and in the surrounding area (Figure 2.5.1-225). Most of these features are steeply dipping (60° to 90°) and exhibit a range of strike directions, including slightly east of north, northeast, and east-west. The joint spacing ranges from one inch to several feet. Comparison of the orientations of the joint surfaces with Mesozoic structures in the site vicinity, Garahan et al. (1993) (Reference 420), indicates that at least one population of the joint sets may be related to Mesozoic extension (d_5).

Slickensides on Joint Surfaces. In some cases slickensides are mapped on joint surfaces and contacts between rock types. Study of these features in the geologic test pits indicate that they may extend from 2 to 20 ft. These surfaces cut across both the shear-breccia zones and the dilation fractures. These striated surfaces show various stages of development ranging from poorly developed with incipient chlorite films and striations to chlorite-calcite films up to 0.04 in. thick with well-developed striations. Chlorite is the most common phase on these surfaces but traces of calcite are commonly found. Microscopic study of these features shows that most of the movement has occurred in the chlorite, and that calcite is rarely deformed.

The displacement on the slickensided surfaces ranges from 0 to 1 in. in unweathered rock. One example in partially weathered rock measured 4 in., and a similar feature in saprolite recorded a 2 ft. displacement. These features apparently post-date both the dilatational fractures and the shear breccia zones, but the close association of chlorite with the movement on these surfaces indicates that they were also associated with the pre-219 Ma greenschist facies event (d_4).

Slickensides in Weathered Rock and Saprolite. Partially weathered rock and saprolite show slickensides (d_6) on surfaces coated with white clay and a black secondary material. The black material consists of gelatinous iron and

manganese hydroxides of varying proportions. This material also contains clay (7 angstrom), which results from weathering of biotite and has a high iron content.

2.5.1.2.5.5 Site Geologic Mapping

Geologic mapping of the site in 2006 consisted of mapping available outcrops and exposures (Figure 2.5.1-220), including open exposures in the former Duke Cherokee nuclear site Units 2 and 3 excavations (Figures 2.5.1-228 and 2.5.1-229). Previous excavation mapping completed as part of the construction of the Cherokee Nuclear Station was used to provide geologic information beneath the former Duke Cherokee nuclear site Unit 1 foundation.

Principal objectives of the excavation mapping program include the following:

- Confirm previous mapping accomplished as part of the construction activities (see discussion on Previous Rock Mapping).
- Document the age and structural relationship between rock masses.
- Investigate and document any evidence of tectonic movement or ground deformation.
- Identify and delineate the western pluton boundary.
- Delineate the thickness and character of the weathering profile as exposed around the perimeter of the excavation.
- Identify areas of groundwater seepage within the excavation.

The following discussion of previous rock mapping, its confirmation, and synthesis with local mapping data summarizes the results of previous and current mapping and the suitability of foundation bedrock (Subsection 2.5.1.2.6)

Previous Rock Mapping Program

An extensive mapping program was conducted during the initial construction phase at the former Duke Cherokee nuclear site. The program included mapping excavations opened during construction. Two primary maps for each of the 3 units were developed. First, a top-of-rock map was produced after overburden was stripped, and completed prior to blasting operations. After blasting operations were completed and the rock debris removed, top-of-foundation maps were produced. By the time mapping was started, blasting operations were underway for the former Duke Cherokee nuclear site Unit 1, and top-of-rock mapping was completed for the former Duke Cherokee nuclear site Units 2 and 3 locations. Top-of-foundation mapping was subsequently completed for the former Duke Cherokee nuclear site Unit 1 while only a portion of former Duke Cherokee nuclear site Unit 2 was completed before construction activities were halted. As a result, a small area in the northern excavation for former Duke Cherokee nuclear site Unit 2 was available to confirm the geologic mapping previously completed for the Top-of-foundation. This was important to confirm the geologic mapping

completed for the Top of Foundation beneath the former Duke Cherokee nuclear site Unit 1.

Confirmation of Previous Mapping

Maps produced for both top-of-rock and top-of-foundation were acquired from the Duke archives as part of this project. Confirmation testing of the archived scanned records as well as original mapping technique was evaluated by visually comparing the exposed rock within the excavation directly to these areas on the scaled archived maps. Also, major features and contacts that were noted in the field as well as on the maps were marked and surveyed. The survey control could then be used to plot against the archive maps to compare the alignment of actual points on the map. Because construction activities had resulted in covering most of the area for the top-of-foundation maps produced for the former Duke Cherokee nuclear site Unit 1, confirmation was concentrated on the area within the former Duke Cherokee nuclear site Unit 2 area where top-of-foundation mapping was completed and remained exposed.

Top-of-foundation mapping was completed for the former Duke Cherokee nuclear site Unit 2 in the northern area of the excavation. Two large metadiorite dikes cross-cut the area and provide several contacts in a east-west and north-south orientation. Points were established by WLA geologists and were surveyed in multiple locations. These coordinates were then compared to the digitized maps.

Synthesis of Local Mapping Data. Subsection 2.5.4.2 presents a detailed discussion of the boring, test pit, and trenching program. Boring data, test pits, trenches, existing exposures, and outcrops were used to map the distribution and geometry of the granitoid pluton within the site area (Figure 2.5.1-226). Top-of-rock maps and final foundation maps developed during construction of the Cherokee Nuclear Station and exposures in the existing excavation show the top of the rock generally dips to the northeast resulting in a thicker section of residuum and saprolite (Figure 2.5.1-227).

The western margin of the pluton was mapped using lithologic descriptions from borings, limited outcrops and test pits. As shown on Figure 2.5.1-226, borings located along the western edge of the site were used to constrain the alignment of the pluton. Test pits were used to confirm the contact zone between the granodiorite and metavolcanic country rock.

2.5.1.2.6 Site Area Engineering Geology

From an engineering geology perspective, the Lee Nuclear Site provides favorable geologic conditions for the construction of Lee Nuclear Station Units 1 and 2. The site and surrounding area is underlain by hard, crystalline rock of the Battleground Formation. In situ measurements of shear wave velocities (V_s) demonstrate that the unweathered or fresh rock underlying the site exhibits average V_s values in excess of 9,200 ft/sec, which classifies the site as a hard rock site, for the purposes of computing the GMRS.

Subsection 2.5.4 presents detailed description of V_s and other static and dynamic properties of foundation materials. Subsection 2.5.4 also presents a discussion of engineering soil properties, including index properties, static and dynamic strength, and compressibility. Variability and distribution of properties for the foundation-bearing layer will be evaluated and mapped as the excavation is completed. Settlement monitoring for the Lee Nuclear Station Units 1 and 2 nuclear island is not required because settlement is calculated to be 1/15 of an inch or less (Subsection 2.5.4.10.2).

The foundation-bearing unit is a felsic and mafic granitoid complex. Some minor zones of weathering along contacts between the felsic and mafic units are mapped. The widths of these weathering zones, however, do not exceed one foot, and vertical exposures along these contacts indicate that weathering is limited to the near surface. No evidence of weathered contact zones between rock units is noted in the rock core collected as part of the foundation investigation. Excavation will likely expose desiccation features, weathered zones, joints, and fractures. Removal and treatment of weathered rock is described in Subsection 2.5.4.12.

No deformational zones related to post plutonic activity are noted. The excavation mapping procedures used for verification and quality control of the nuclear island foundation materials are described in Subsection 2.5.4.5.3.

No mining operations (other than aggregate mines), excessive extraction or injection of groundwater, or impoundment of water are located within the site area that could affect geologic conditions. The crystalline and metamorphic bedrock at the site is not susceptible to subsidence due to groundwater withdrawal.

2.5.1.2.7 Site Area Seismicity and Paleoseismology

Neither the EPRI seismicity catalog nor the updated EPRI earthquake catalog (discussed in Subsection 2.5.2.1.2) includes any earthquakes of $m_b \geq 3.0$ in the Lee Nuclear Site vicinity (25 mi. radius). The largest earthquake within 25 mi. of the Lee Nuclear Site included in the updated EPRI seismicity catalog is an m_b 2.7 event that occurred in 1986.

The highest recorded shaking intensities estimated for the Lee Nuclear Site resulted from earthquakes located outside of the site area. The August 31, 1886, Charleston, South Carolina, earthquake is one of the largest historical earthquakes in the eastern United States. The event produced Modified Mercalli Intensity (MMI) X shaking in the epicentral area (Reference 395). Maximum MMI shaking intensity at the Lee Nuclear Site is estimated at approximately VI (Figure 2.5.1-215). The Charleston earthquake is discussed in greater detail in Subsections 2.5.1.1.3.2.1 and 2.5.2.2.2.3.

The January 1, 1913 m_b 4.8 Union County, South Carolina earthquake (Reference 269) was felt over an area of approximately 43,000 square mi., with an estimated Rossi-Forel shaking intensity VIII (Reference 396, as reported in Reference 397). Rossi-Forel shaking intensity at the Lee Nuclear Site is estimated at approximately VI (Reference 396, as reported in Reference 397)

(Figure 2.5.1-232). The epicenter of the Union County earthquake is poorly located and the fault on which this earthquake occurred has not been identified.

There are no published reports of paleoseismologic studies within the site area. Extensive studies of outcrops performed as part of this project have not indicated any evidence for post-Miocene earthquake activity within the site area.

The potential for reservoir-induced seismicity (RIS) is considered low and it is unlikely the induced magnitudes would exceed **M** > 4, a value well below the short-period controlling earthquake as described in Subsection 2.5.2.1.3.

2.5.1.2.8 Site Groundwater Conditions

Subsection 2.4.12 provides a detailed discussion of groundwater conditions.

2.5.1.3 References

201. Horton, J.W., Drake, A.A., and Rankin, D.W., *Tectonostratigraphic Terranes and Their Paleozoic Boundaries in the Central and Southern Appalachians,* Geological Society of America, Special Paper 230:213-245, 1989.

202. Horton, J.W., Drake, A.A., Rankin, D.W., and Dallmeyer, R.D., *Preliminary Tectonostratigraphic Terrane Map of the Central and Southern Appalachians*, U.S. Geological Survey, Miscellaneous Investigations Series Map I-2163, 1991.

203. Hatcher R.D. Jr., Colquhoun, D.J., Secor D.T. Jr., Cook, F.A., Dillon, W.P., Klitgord, K., Popenoe, P., Merschat, C.E., Wiener, L.E., Milici, R.C., Nelson, A.E., Sheridan, R.E., and Snoke, A.W., *Continent-Ocean Transect E5- Cumberland Plateau (North American Craton) to Blake Plateau Basin*, Geological Society of America, 2 plates, with 55p. accompanying text, 1994.

204. Hibbard, J.P., Stoddard, E.F., Secor, D.T., and Dennis, A.J., "The Carolina Zone: Overview of Neoproterozoic to Early Paleozoic Peri-Gondwanan Terranes Along the Eastern Flank of the Southern Appalachians," *Earth Science Reviews* (57):299-339, 2002.

205. Spotila, J.A., Bank, G.C., Reiners, P.W., Naeser, C.W., Naeser, N.D., and Henika, B.S., "Origin of the Blue Ridge Escarpment Along the Passive Margin of Eastern North America," *Basin Research* (16):41-63, 2004.

206. Hatcher, R.D. Jr. and Goldberg, S.A., "The Blue Ridge Geologic Province," in *The Geology of the Carolinas – Carolina Geological Society 50th Anniversary Volume*, University of Tennessee Press, 1991.

207. King, P.B., “A Geologic Cross Section Across the Southern Appalachians, An Outline of the Geology in the Segment in Tennessee, North Carolina, and South Carolina,” in *Guides to Southeastern Geology*, Geological Society of America Annual Meeting, 1955.

208. Hopson, J.L., Hatcher, R.D. Jr., and Stieve, A.L., “Geology of The Eastern Blue Ridge of Northeast Georgia and the Adjacent Carolinas,” in *Georgia Geological Society Guidebook* (9):1-38, 1989.

209. Hatcher, R.D. Jr., Costello, J.O., Edelman, S.H., “The Smokies Foothills Duplex and Possible Significance of the Guess Creek Fault: A Corollary to the Mapping of King and Neuman,” *Geological Society of America Abstracts with Programs* (18):226, 1986.

210. Nelson, K.D., Arrow, J.A., McBride, J.H., Willemin, J.H., Huang, J., Zheng, L., Oliver, J.E., Brown, L.D., and Kaufman, S., “New COCORP Profiling in the Southeastern United States. Part I: Late Paleozoic Suture and Mesozoic Rift Basin,” *Geology* (13):714-718, 1985.

211. Hatcher, R.D. Jr., “Tectonics of the Western Piedmont and Blue Ridge, Southern Appalachians: Review and Speculation,” *American Journal of Science* (278):276-304, 1978.

212. Hatcher, R.D. Jr., “Stratigraphic, Petrologic, and Structural Evidence Favoring a Thrust Solution to the Brevard Problem,” *American Journal of Science* 270 (9):177-202, 1971.

213. Hatcher, R.D. Jr., “Developmental Model for the Southern Appalachians,” *Geological Society of America Bulletin* 83 (9):2,735-2,760, 1972.

214. Cook, F.A., Albaugh, D.S., Brown, L.D., Kaufman, S., Oliver, J.A., and Hatcher R.D. Jr., “Thin-Skinned Tectonics in the Crystalline Southern Appalachians; COCORP Seismic-Reflection Profiling of the Blue Ridge and Piedmont,” *Geology* 7 (12): 563-567, 1979.

215. Coruh, C., Costain, J.K., Hatcher, R.D. Jr., Pratt, T.L., Williams, R.T., Phinney R.A., “Results from Regional Vibroseis Profiling: Appalachian Ultradeep Core Hole Site Study,” *Geophysical Journal of the Royal Astronomical Society* 89 (1): 147-156, 1987.

216. Fullagar, P.D., Hatcher, R.D. Jr., and Merschat, C.E., “1,200-m.y.-old gneisses in the Blue Ridge Province of North and South Carolina,” *Southeastern Geology* (20):69-78, 1979.

217. Fullagar, P.D. and Bartholomew, M.J., “Rubidium-Strontium Ages of the Watauga River, Cranberry, and Crossing Knob Gneisses, Northwestern North Carolina,” in *Geological Investigations in the Blue Ridge of Northwestern North Carolina - 1983 Guidebook for the Carolina Geological Society*, North Carolina Division of Land Resources, 1983.

218. Fullagar, P.D. and Odom, A.L., “Geochronology of Precambrian Gneisses in the Blue Ridge Province of Northwestern North Carolina and Adjacent Parts of Virginia and Tennessee,” *Geological Society of America Bulletin* 84 (9):3,065-3,080, 1973.

219. Wehr, F. and Glover, L. III, “Stratigraphy and Tectonics of the Virginia-North Carolina Blue Ridge - Evolution of a Late Proterozoic-Early Paleozoic Hinge Zone,” *Geological Society of America Bulletin* (96):285-295, 1985.

220. Rast, N. and Kohles, K.M., “The Origin of the Ocoee Supergroup,” *American Journal of Science* (286):593-616, 1986.

221. King, P.B., Neuman, R.B., and Hadley, J.B., *Geology of the Great Smoky Mountains National Park, Tennessee and North Carolina*, U.S. Geological Survey Professional Paper 587, 1968.

222. Neuman, R.B. and Nelson, W.H., *Geology of the Western Great Smoky Mountains, Tennessee*, U.S. Geological Survey Professional Paper 349-D, 1:62,500-scale, 1965.

223. King, P.B., *Geology of the Central Great Smoky Mountains, Tennessee*, U.S. Geological Survey Professional Paper 340-C, 1964.

224. Hopson, J.L., “Structure, Stratigraphy, and Petrogenesis of the Lake Burton Mafic-Ultramafic Complex,” *Georgia Geological Society Guidebook* (9):93-100, 1989.

225. Hatcher, R.D. Jr., “Tectonics of the Southern and Central Appalachian Internides,” *Annual Review of Earth and Planetary Sciences* (15):337-362, 1987.

226. Horton, J.W. Jr., and McConnell, K.I., “The Western Piedmont,” in *The Geology of the Carolinas - Carolina Geological Society 50th Anniversary Volume*, ed. J.W. Horton, Jr. and V.A. Zullo, University of Tennessee Press, 1991.

227. Nelson, A.E., Horton, J.W. Jr., and Clarke, J.W., *Generalized Tectonic Map of the Greenville 1° x 2° Quadrangle, Georgia, South Carolina, and North Carolina*, U.S. Geological Survey Miscellaneous Field Studies Map MF-1898, scale 1:25,000, 1987.

228. Goldsmith, R., Milton, D.J. and Horton, J.W. Jr., *Geologic Map of the Charlotte 1° x 2° Quadrangle, North Carolina and South Carolina*, U.S. Geological Survey Miscellaneous Investigations Series Map I-1251-E, 1:250,000 scale, 1988.

229. Mittwede, S.K., Odegard, M., and Sharp, W.E., “Major Chemical Characteristics of the Hammett Grove Meta-Igneous Suite, Northwestern South Carolina,” *Southeastern Geology* 28 (1):49-63, 1987.

230. Hatcher, R.D. Jr., Hopson, J.L., Edelman, S.H., Liu, A., McClellan, E.A., Stieve, A.L., “Detailed Geologic Map of the Appalachian Ultradeep Core Hole (ADCOH) Region: New Constraints on the Structure of the Southern Appalachian Internides,” *Geological Society of America Abstracts with Programs* (18):631, 1986.

231. Secor, D.T. Jr., Samson, S.L., Snoke, A.W., and Palmer, A.R., “Confirmation of Carolina Slate Belt as an Exotic Terrane,” *Science* (221):649-651, 1983.

232. Hatcher R.D. Jr., Odom, A.L., Engelder, T., Dunn, D.E., Wise, D.U., Geiser, P.A., Schamel, S., and Kish, S.A., “Characterization of Appalachian faults,” *Geology* (16):178-181, 1988.

233. Hooper, R.J. and Hatcher, R.D. Jr., “Pine Mountain Terrane, a Complex Window in the Georgia and Alabama Piedmont; Evidence from the Eastern Termination,” *Geology* (16):307-310, 1988.

234. Steltenpohl, M.G., “Kinematics of the Towaliga, Bartletts Ferry, and Goat Rock Fault Zones, Alabama: The Late Paleozoic Dextral Shear System in the Southernmost Appalachians,” *Geology* (16):852-855, 1988.

235. Rozen, R.W., “The Middleton-Lowdensville Cataclastic Zone in the Elberton East Quadrangle, Georgia,” in *Geological Investigations of the Kings Mountain Belt and Adjacent Areas in the Carolinas*, Carolina Geological Society Guidebook, 1981.

236. Horton, J.W. Jr., “Geologic Map of the Kings Mountain Belt Between Gaffney, South Carolina and Lincolnton, North Carolina,” in *Geological Investigations of the Kings Mountain Belt and Adjacent Areas in the Carolinas*, Carolina Geological Society Field Trip Guidebook, 1981.

237. McConnell, K.I., “Geology of the Sauratown Mountains Anticlinorium: Vienna and Pinnacle 7.5-Minute Quadrangles,” in *Structure of the Sauratown Mountains Window, North Carolina*, Carolina Geological Society Guidebook, 1988.

238. Samson, S., Palmer, A.R., Robinson, R.A., and Secor, D.T. Jr., “Biogeographical Significance of Cambrian Trilobites from the Carolina Slate Belts,” *Geological Society of America Bulletin* 102 (11):1,459-1,470, 1990.

239. Vick, H.K., Channell, J.E.T., and Opdyke, N.D., “Ordovician Docking of the Carolina Slate Belt - Paleomagnetic Data,” *Tectonics* (6):573-583, 1987.

240. Noel, J.R., Spariosu, D.J., and Dallmeyer, R.D., “Paleomagnetism and 40Ar/39Ar Ages from the Carolina Slate Belt, Albemarle, North Carolina - Implications for Terrane Amalgamation,” *Geology* (16):64-68, 1988.

241. Butler, J.R., “The Carolina Slate Belt in North Carolina and Northeastern South Carolina - a Review,” *Geological Society of America Abstracts with Programs* (11):172, 1979.

242. Manspeizer, W., Puffer, J.H., and Cousminer, H.L., “Separation of Morocco and Eastern North America: a Triassic-Liassic Stratigraphic Record,” *Geological Society of America Bulletin* 89 (6):901-920, 1978.

243. Petersen, T.A., Brown, L.D., Cook, F.A., Kaufman, S., and Oliver, J.E., “Structure of the Riddleville Basin from COCORP Seismic Data and Implications for Reactivation Tectonics,” *Journal of Geology*, 1984.

244. Hutchinson, D.R. and Klitgord, K.D., “Evolution of Rift Basins on the Continental Margin off Southern New England, in *Triassic-Jurassic Rifting; Continental Breakup and the Origin of the Atlantic Ocean and Passive Margins - Developments in Geophysics* 22 (AB):81-98, 1988.

245. Ratcliffe, N.M., “The Ramapo Fault System in New York and Adjacent Northern New Jersey: A Case of Tectonic Heredity,” *Geological Society of America Bulletin* 82 (1):125-142, 1971.

246. Lindholm, R.C., “Triassic-Jurassic Faulting in Eastern North America - a Model Based on pre-Triassic Structures*,” Geology* 6 (6):365-368, 1978.

247. Glover, L., III, Poland, F.B., Tucker, R.D. and Bourland, W.C., “Diachronous Paleozoic Mylonites and Structural Heredity of Triassic-Jurassic Basins in Virginia,” *Geological Society of America Abstracts with Programs* 12, 1980.

248. Klitgord, K.D., Hutchinson, D.R., Schouten, H., “U.S. Atlantic Continental Margin: Structural and Tectonic Framework,” in *The Geology of North America, The Atlantic Continental Margin: U.S.*, Decade of North American Geology Publication I-2, Geological Society of America, 1988.

249. Kanter, L.R., “Tectonic Interpretation of Stable Continental Crust,” in *The Earthquakes of Stable Continental Regions*, prepared for Electric Power Research Institute, 1994.

250. Grow, J.A., Klitgord, K.D., and Schlee, J.S., “Structure and Evolution of Baltimore Canyon Trough,*”* in *The Atlantic Continental Margin: U.S.*, Decade of North American Geology Publication I-2, Geological Society of America, 1988.

251. King, P.B., *Systematic Pattern of Triassic Dikes in the Appalachian Region - Second report*, U.S. Geological Survey Professional Paper 750-D, 1971.

252. Froelich, A.J. and Olsen, P.E*., Newark Supergroup, a Revision of the Newark Group in Eastern North America*, U.S. Geological Survey Bulletin 1537A, 1984.

253. Olsen, P.E., Froelich, A.J., Daniels, D.L., Smoot, J.P., and Gore, P.J.W., "Rift Basins of Early Mesozoic Age," in *The Geology of the Carolinas*, ed. J.W. Horton, Jr. and V.A. Zullo, University of Tennessee Press, 1991.

254. Smoot, J.P., "The Closed-Basin Hypothesis and its Use in Facies Analysis of the Newark Supergroup," in *Proceedings of the second U.S. Geological Survey Workshop on the Early Mesozoic Basins of the Eastern U.S.*, U.S. Geological Survey Circular 946, 1985.

255. Gore, P.J.W., "Depositional Framework of a Triassic Rift Basin - the Durham and Sanford Sub-Basins of the Deep River Basin, North Carolina," in *Society of Economic Paleontologists and Mineralogists Field Guidebook*, 1986.

256. Olsen, P.E. and Schlische, R.W., *"*Unraveling the Rules of Rift Basins,*" Geological Society of America Abstracts with Programs* 20:A123, 1988.

257. Schlische, R.W. and Olsen, P.E., "Quantitative Filling Model for Continental Extensional Basins with Application to the Early Mesozoic Rifts of Eastern North America*," Journal of Geology* 98:135-155, 1990.

258. King, P.B. and Beikman H.M., *Geologic Map of the United States (Exclusive of Alaska and Hawaii),* U.S. Geological Survey, 3 sheets, 1:250,000 scale, 1974.

259. Schruben, P.G., Arndt, R.E., Bawiec, W.J., King, P.B., and Beikman, H.M., *Geology of the Conterminous United States at 1:2,500,000 Scale - a Digital Representation of the 1974 P.B. King and H.M. Beikman Map*, U.S. Geological Survey Digital Data Series DDS-11, 1994.

260. Hibbard, J.P., van Staal, C.R., Rankin, D.W., Williams, H., *Lithotectonic Map of the Appalachian Orogen, Canada - United States of America*, Geological Society of Canada, map 2096A, 1:1,500,000 scale, 2006.

261. Horton, J.W. Jr. and Zullo, V.A., eds., *The Geology of the Carolinas - Carolina Geological Survey 50th Anniversary Volume*, University of Tennessee Press, 1991.

262. Bickford, M.E., Van Schmus, W.R., and Zietz, I., "Proterozoic History of the Midcontinent Region of North America," *Geology* 14 (6):492-496, 1896.

263. Hauser, E.C., "Grenville Foreland Thrust Belt Hidden Beneath the Eastern U.S. Mid-Continent," *Geology* 21(1):61-64, 1993.

264. White, T.S., Witzke, B.J., and Ludvingson, G.A., "Evidence for an Albian Hudson Arm Connection Between the Cretaceous Western Interior Seaway of North American and the Labrador Sea," *Bulletin of the Geological Society of America* 112 (9):1,342-1,355, 2000.

265. Bollinger, G.A. and Wheeler, R.L., *The Giles County, Virginia, Seismic Zone- Seismological Results and Geological Interpretations*, U.S. Geological Survey Professional Paper 1355, 1988.

266. Klitgord, K.D., Hutchinson, D.R., and Schouten, H.S. *Atlantic Continental Margin; Structural and Tectonic Framework*, in *The Geology of North America, v. I-2: The Atlantic Continental Margin: U.S.*, Decade of North American Geology Publication, Geological Society of America, 1988.

267. Wheeler, R.L., "Earthquakes and the Cratonward Limit of Iapetan Faulting in Eastern North America," *Geology* 23:105-108, 1995.

268. Dennis, A.J., Shervais, J.W., Mauldin, J., Maher, H.D., Jr., and Wright, J.E., "Petrology and Geochemistry of Neoproterozoic Volcanic Arc Terranes Beneath the Atlantic Coastal Plain, Savannah River Site, South Carolina," *Geological Society of America Bulletin* 116 (5-6):572-593, 2004.

269. Electric Power Research Institute (EPRI), *Seismic Hazard Methodology for the Central and Eastern United States, Tectonic Interpretations*, EPRI NP-4726, volumes 5-10, July 1986.

270. Zoback, M.L. and Zoback, M.D., "Tectonic Stress Field of the Continental United States," in *Geophysical Framework of the Continental United States*, Geological Society of America Memoir 172:523-539, 1989.

271. Zoback, M.L., Zoback, M.D., Adams, J., Assumpcao, M., Bell, S., Bergman, E.A., Bluemling, P., Brereton, N.R., Denham, D., Ding, J., Fuchs, K., Gay, N., Gregersen, S., Gupta, H.K., Gvishiani, A., Jacob, K., Klein, R., Knoll, P., Magee, M., Mercier, J.L., Mueller, B.C., Paquin, C., Rajendran, K., Stephansson, O., Suarez, G., Suter, M., Udias, A., Xu, Z.H., and Zhizin, M., "Global Patterns of Tectonic Stress," *Nature* 341 (6240):291-298, 1989.

272. Zoback, M.L., "Stress Field Constraints on Intraplate Seismicity in Eastern North America," *Journal of Geophysical Research* 97 (B8):11,761-11,782, 1992.

273. Richardson, R.M., and Reding, L.M., "North American Plate Dynamics," *Journal of Geophysical Research* 96 (B7):12,201-212,223, 1991.

274. Turcotte, D.L. and Schubert, G., *Geodynamics*, Cambridge University Press, 2002.

275. Dahlen, F.A., "Isostasy and the Ambient State of Stress in the Oceanic Lithosphere," *Journal of Geophysical Research* 86 (B9):7,801-7,807, 1981.

276. Committee for the Gravity Anomaly Map of North America, *Gravity Anomaly Map of North America,* Geological Society of America, Continent-Scale Map-002, scale 1:5,000,000, 1987.

277. Committee for the Magnetic Anomaly Map of North America, *Magnetic Anomaly Map of North America*, Geological Society of America, Continent-Scale Map-003, scale 1:5,000,000, 1987.

278. Daniels, D.L., South Carolina Aeromagnetic and Gravity Maps and Data: a Website for Distribution of Data, U.S. Geological Survey Open-File Report 2005-1022, Website, http://pubs.usgs.gov/of/2005/1022/, accessed August 17, 2006.

279. Harris, L.D., de Witt, W. Jr., and Bayer, K.C., *Interpretive Seismic Profile Along Interstate I-64 from the Valley and Ridge to the Coastal Plain in Central Virginia*, U.S. Geological Survey, Oil and Gas Investigations Chart OC-123, 1982.

280. Dainty, A.M. and Frazier, J.E., "Bouguer Gravity in Northeastern Georgia - a Buried Suture, a Surface Suture, and Granites," *Geological Society of America Bulletin* 95:1,168-1,175, 1984.

281. Iverson, W.P. and Smithson, S.B., "Reprocessing and Reinterpretation of COCORP Southern Appalachian Profiles," *Earth and Planetary Science Letters* 62:75-90, 1983.

282. Rankin, D.W., Dillon, W.P., Black, D.F., Boyer, S.E., Daniels, D.L., Goldsmith, R., Grow, J.A., Horton, J.W., Jr., Hutchinson, D.R., Klitgord, K.D., McDowell, R.C., Milton, D.J., Owens, J.P., and Phillips, J.D., "Continent-Ocean Transect E-4, Central Kentucky to Carolina Trough," in *Publication of Decade of North American Geology*, Geological Society of America, 1991.

283. Cumbest, R.J., Price, V. and Anderson, E.E., "Gravity and Magnetic Modeling of the Dunbarton Triassic Basin, South Carolina," *Southeastern Geology* 33 (1):37-51, 1992.

284. Posey, H.H., "A Model for the Origin of Metallic Mineral Deposits in the Kings Mountain Belt," in *Geological Investigations of the Kings Mountain Belt and Adjacent Areas in the Carolinas*, Carolina Geological Society Field Trip Guidebook, 1981.

285. Butler, J.R., "Geology of the Blacksburg South Quadrangle, South Carolina," in *Geological Investigations of the Kings Mountain Belt and Adjacent Areas in the Carolinas*, Carolina Geological Society Field Trip Guidebook, 1981.

286. Howard S., *Geologic Map of the Kings Creek 7.5-Minute Quadrangle, Cherokee County, South Carolina*, South Carolina Department of Natural Resources Geological Survey, 1:24,000-scale, 2004.

287. Austin, J.A., Stoffa, P.L., Phillips, J.D., Oh, J., Sawyer, D.S., Purdy, G.M., Reiter, E., and Makris, J., "Crustal Structure of the Southeast Georgia Embayment-Carolina Trough: Preliminary Results of a Composite Seismic Image of a Continental Suture (?) and a Volcanic Passive Margin," *Geology* 18:1,023-1,027, 1990.

288. Sheridan, R.E., Musser, D.L., Glover III, L., Talwani, M., Ewing, J.L., Holbrook, W.S., Purdy, G.M., Hawman, R., and Smithson, S., "Deep Seismic Reflection Data of EDGE U.S. Mid-Atlantic Continental-Margin Experiment – Implications for Appalachian Sutures and Mesozoic Rifting and Magmatic Underplating," *Geology* 21: 563-567, 1993.

289. Withjack, M.O., Schlische, R.W., and Olsen, P.E., "Diachronous Rifting, Drifting, and Inversion on the Passive Margin of Central Eastern North America: An Analog for Other Passive Margins," *American Association of Petroleum Geologists Bulletin* 82 (5A):817-835, 1998.

290. King, E.R. and Zietz, I., "The New York-Alabama Lineament: Geophysical Evidence for a Major Crustal Break in the Basement Beneath the Appalachian Basin," *Geology* 6:312-318, 1978.

291. Nelson, A.E. and Zietz, I, "The Clingman Lineament: Aeromagnetic Evidence for a Major Discontinuity in the North American Basement," *Geological Society of America Abstracts with Programs* 13(1):31, 1981.

292. Johnston, A.C., Reinbold, D.J., and Brewer, S.I., "Seismotectonics of the Southern Appalachians," *Bulletin of the Seismological Society of America* 75(1): 291-312, 1985.

293. Shumaker, R.C., "The New York-Alabama Lineament; An Early Iapetan Wrench Fault?," *American Association of Petroleum Geologists Bulletin* 84 (9): 1393, September 2000.

294. Johnston, A.C. and Reinbold, D.J., "A Basement Block Model for Southern Appalachian Seismicity," *Geological Society of America Abstracts with Programs* 17 (2):97, 1985.

295. Wheeler, R.L., "Earthquakes and the Southeastern Boundary of the Intact Iapetan Margin in Eastern North America," *Seismological Research Letters* 67:77-83, 1996.

296. Dennis, A.J., 1991, "Is the Central Piedmont Suture a Low-Angle Normal Fault?," *Geology* 19:1,081–1,084, 1991

297. West Jr., T.E., "Structural Analysis of the Carolina-Inner Piedmont Terrane Boundary: Implications for the Age and Kinematics of the Central Piedmont Suture, a Terrane Boundary that Records Paleozoic Laurentia-Gondwana Interactions," *Tectonics* 17 (3):379-394, 1998.

298. Dennis, A.J., *Rocks of the Carolina Terrane in the Spartanburg 30- x 60-degree Quadrangle*, prepared for the 1995 Carolina Geological Survey annual meeting, 1:100,000 scale, 1995.

299. Nystrom, P.G. Jr., "Structure and Stratigraphy Across the Reedy River Thrust Fault, Inner Piedmont of South Carolina," *Geological Society of America Abstracts with Programs*, Southeastern 50th annual meeting, 2001.

300. Maybin, A.H. and Nystrom, P.G., *Geology of the Reedy River Thrust in the Vicinity of Southwest Spartanburg, South Carolina*, South Carolina Geological Survey Open-File Report 143, 2002.

301. Bramlett, K.W., Secor, D.T., and Prowell, D.C., "The Belair Fault: A Cenozoic Reactivation Structure in the Eastern Piedmon*t," Geological Society of America Bulletin* 93:1,109-1,117, 1982.

302. Maher, H.D., Dallmeyer, R.D., Secor Jr., D.T., and Sacks, P.E., "40-Ar/39-Ar Constraints on Chronology of Augusta Fault Zone Movement and Late Alleghanian Extension, Southern Appalachian Piedmont, South Carolina and Georgia,*" American Journal of Science* 294:428-448, 1994.

303. Secor, D.T. Jr., Snoke, A.W., Bramlett, K.W., Costello, O.P., and Kimbrell, O.P., "Character of the Alleghanian Orogeny in the Southern Appalachians Part I. – Alleghanian Deformation in the Eastern Piedmont of South Carolina," *Geological Society of America Bulletin* 97:1,319-1,328, 1986.

304. Secor Jr., D.T., Snoke, A.W., and Dallmeyer, R.D*., "*Character of the Alleghanian Orogeny in the Southern Appalachians: Part III Regional Tectonic Relations," *Geological Society of America Bulletin* 97:1,345-1,353, 1986.

305. Sacks, P.E., and Dennis, A.J., "The Modoc Zone-D2 (Early Alleghanian in the Eastern Appalachian Piedmont, South Carolina and Georgia: Anatomy of the Alleghanian Orogeny as Seen from the Piedmont of South Carolina and Georgia," in *South Carolina Geological Survey/Carolina Geological Society Field Trip Guidebook*, 1987.

306. Hatcher, R.D., Jr., Howell, D.E., and Talwani, P., "Eastern Piedmont Fault System: Speculations on its Extent," *Geology* 5:36-640, 1977.

307. Vauchez, A., "Brevard Fault Zone, Southern Appalachians a Medium-Angle, Dextral, Alleghanian Shear Zone," *Geology* 15:669-672, 1987.

308. Horton, J.W. Jr. and Dicken, C.L., *Preliminary Digital Geologic Map of the Appalachian Piedmont and Blue Ridge, South Carolina Segment,* U.S. Geological Survey Open-File Report 01-298, 1:500,000 scale, 2001.

309. Halpin, M.A. and Barker, C A., “Geological Investigation of the Carolina Terrane and Charlotte Terrane Boundary in North-Central South Carolina,” *Geological Society of America Abstracts with Programs*, South-Central Section 38th annual meeting, 2004.

310. Crone, A.J. and Wheeler, R.L., *Data for Quaternary Faults, Liquefaction Features, and Possible Tectonic Features in the Central and Eastern United States, East of the Rocky Mountain Front*, U.S. Geological Survey Open-File Report 00-260, 2000.

311. Wheeler, R.L., *Known or Suggested Quaternary Tectonic Faulting, Central and Eastern United States - New and Updated Assessments for 2005*, U.S. Geological Survey Open-File Report 2005-1336, 2005.

312. Secor, D.T. Jr., Peck, L.S., Pitcher, D.M., Prowell, D.C., Simpson, D.H., Smith, W.A., and Snoke, A.W., “Geology of the Area of Induced Seismic Activity at Monticello Reservoir, South Carolina,” *Journal of Geophysical Research* 87 (B8):6,945-6,957, 1982.

313. Simpson, D.H*., The Wateree Creek Fault Zone*, unpublished M.S. thesis, University of South Carolina, 1981.

314. Maher Jr., H.D., Sacks, P.E., and Secor Jr., D. T., “The Eastern Piedmont of South Carolina,” in *The Geology of the Carolinas – Carolina Geological Society 50th Anniversary Volume*, ed. J.W. Horton, Jr. and V.A. Zullo, University of Tennessee Press, 1991.

315. Secor, D.T. Jr., Barker, C.A., Gillon, K.A., Mitchell, T.L., Bartholomew, M.H., Hatcher, R.D., and Balinsky, M.G*., A Field Guide to the Geology of the Ridgeway-Camden Area, South Carolina Piedmont*, Carolina Geological Society Field Trip Guidebook, 1998.

316. Barker, C.A. and Secor Jr. D.T., *Geologic Map of the Longtown and Ridgeway 7.5-minute Quadrangles, Fairfield, Kershaw, and Richland Counties, South Carolina*, South Carolina Department of Natural Resources, GQM-32, 1:24,000-scale, 2005.

317. Johnston, A.C., Coppersmith, K.J., Kanter, L.R., and Cornell, C.A., *The Earthquakes of Stable Continental Regions, Volume I: Assessment of Large Earthquake Potential*, Final Report TR-102261-V1, prepared for Electric Power Research Institute, 1994.

318. Wentworth, C.M., and Mergner-Keefer, M., “Regenerate Faults of Small Cenozoic Offset – Probable Earthquake Sources in the Southeastern United States,” in *Studies Related to the Charleston, South Carolina Earthquake of 1886 Tectonics and Seismicity*, U.S. Geological Survey Professional Paper 1313:S1-S20, 1983.

319. Balinsky, M.G*., Field Evidence for Late Mesozoic and/or Cenozoic Reactivation Faulting Along the Fall Line Near Camden, South Carolina,* unpublished M.S. thesis, University of South Carolina, 1994.

320. Knapp, J.H., Domoracki, W.J., Secor, D.T., Waddell, M.G., Diaconescu, C.C., Peavy, S.T., Ackerman, S., Baldwin, W., Gangopadhyay, A., Kastner, T., Kepple, K., Luc, M., Morrison, K., Shehane, G., and Varga, M., "Shallow Seismic Profiling of the Camden Fault, South Carolina Coastal Plain," *Geological Society of America Abstracts with Programs*, Southeastern Section 50th annual meeting, 2001.

321. *Prowell, D.C., Index of Faults of Cretaceous and Cenozoic Age in the Eastern United States*, U.S. Geological Survey miscellaneous field studies map MF-1269, 2 sheets, 1:2,500,000 scale, 1983.

322. Weems, R.E., *Newly Recognized En Echelon Fall Lines in the Piedmont and Blue Ridge Provinces of North Carolina and Virginia, With a Discussion of Their Possible Ages and Origins*, U.S. Geological Survey Open-File Report 98-0374, 1998.

323. Prowell, D.C. and O'Connor, B.J., "Belair Fault Zone: Evidence of Tertiary Fault Displacement in Eastern Georgia," *Geology* 6:681-684, 1978.

324. Prowell, D.C., O'Connor, B.J., and Rubin, M., *Preliminary Evidence for Holocene Movement Along the Belair Fault Zone Near Augusta, Georgia*, U.S. Geological Survey Open-File Report 75-680, 15p., 1975.

325. Snipes, D.S., Fallaw, W.C., and Price Jr., V*., The Pen Branch Fault: Documentation of Late Cretaceous and Tertiary Faulting in the Coastal Plain of South Carolina (DRAFT)*, Westinghouse Savannah River Company draft report, January 8, 1989.

326. Snipes, D.S., W.C. Fallaw, V. Price, Jr., and R.J. Cumbest, "The Pen Branch Fault: Documentation of Late Cretaceous-Tertiary Faulting in the Coastal Plain of South Carolina," *Southeastern Geology* 33 (4):195-218, 1993.

327. Stieve, A. and Stephenson, D.E., "Geophysical Evidence for Post Late Cretaceous Reactivation of Basement Structures in the Central Savannah River Area," *Southeastern Geology* 35(1):1-20, 1995.

328. Cumbest, R.J., Wyatt, D.E., Stephenson, D.E., and Maryak, M., *Comparison of Cenozoic Faulting at the Savannah River Site to Fault Characteristics of the Atlantic Coast Fault Province: Implications for Fault Capability*, Westinghouse Savannah River Company, Technical Report 2000-00310, 2000.

329. Dennison, J.M. and Stewart, K.G., *Geologic Field Guide to Extensional Structures Along the Alleghany Front in Virginia and West Virginia Near the Giles County Seismic Zone*, Geological Society of America Southeastern Section Fieldtrip Guidebook, 1998.

330. Johnston, A.C., "Seismic Moment Assessment of Earthquake in Stable Continental Regions - III. New Madrid 1811-1812, Charleston 1886 and Lisbon 1755," *Geophysical Journal International* 126:314-344, 1996.

331. Talwani, P., "An Internally Consistent Pattern of Seismicity Near Charleston, South Carolina," *Geology* 10(12):654-658, 1982.

332. Talwani, P., "The Charleston Earthquake Cycle," *Seismological Research Letters* 71 (1):121, 2000.

333. Bakun, W.H. and Hopper, M.G., "Magnitudes and Locations of the 1811-1812 New Madrid, Missouri and the 1886 Charleston, South Carolina Earthquakes," *Bulletin of the Seismological Society of America* 94(1):64-75, 2004.

334. Amick, D.C., "A Reinterpretation of the Meizoseismal Area of the 1886 Charleston Earthquake," *Eos, Transactions of the American Geophysical Union* 61 (17): 289, 1980.

335. Amick, D., Gelinas, R., Maurath, G., Cannon, R., Moore, D., Billington, E., and Kemppinen, H., *Paleoliquefaction Features Along the Atlantic Seaboard,* U.S. Nuclear Regulatory Commission Report, NUREG/CR-5613, 1990.

336. Amick, D., Maurath, G., and Gelinas, R., "Characteristics of Seismically Induced Liquefaction Sites and Features Located in the Vicinity of the 1886 Charleston, South Carolina Earthquake," *Seismological Research Letters* 61 (2):117-130, 1990.

337. Marple, R.T. and Talwani, P., "Evidence for possible tectonic upwarping along the South Carolina coastal plain from an examination of river morphology and elevation data," *Geology* 21:651-654, 1993.

338. Marple, R.T. and Talwani, P., "Evidence for a Buried Fault System in the Coastal Plain of the Carolinas and Virginia - Implications for Neotectonics in the Southeastern United States," *Geological Society of America Bulletin* 112 (2):200-220, 2000.

339. Wildermuth, E. and Talwani, P., "A Detailed Gravity Survey of a Pull-Apart Basin in Northeast South Carolina," *Geological Society of America Abstracts with Programs* 33 (6):240, 2001.

340. Weems, R.E. and Lewis, W.C., "Structural and Tectonic Setting of the Charleston, South Carolina, Region: Evidence From the Tertiary Stratigraphic Record," *Geological Society of America Bulletin* 114 (1):24-42, 2002.

341. Lennon, G., *Identification of a Northwest Trending Seismogenic Graben Near Charleston, South Carolina*, U.S. Nuclear Regulatory Commission Report, NUREG/CR-4075, 1986.

342. Behrendt, J.C., Hamilton, R.M., Ackermann, H.D., and Henry, V.J., "Cenozoic Faulting in the Vicinity of the Charleston, South Carolina, 1886 Earthquake," *Geology* 9 (3):117-122, 1981.

343. Hamilton, R.H., Behrendt, J.C., and Ackermann, H.D., "Land Multichannel Seismic-Reflection Evidence for Tectonic Features Near Charleston, South Carolina," in *Studies Related to the Charleston, South Carolina Earthquake of 1886 - Tectonics and Seismicity,* U.S. Geological Survey Professional Paper 1313-I:I1-I18, 1983.

344. Behrendt, J.C., Hamilton, R.M., Ackermann, H.D., Henry, V.H., and Bayer, K.C., "Marine Multichannel Seismic-Reflection Evidence for Cenozoic Faulting and Deep Crustal Structure Near Charleston, South Carolina," in *Studies Related to the Charleston, South Carolina, Earthquake of 1886 - Tectonics and Seismicity*, U.S. Geological Survey Professional Paper 1313-J:J1-J29, 1983.

345. Behrendt, J.C. and Yuan, A., "The Helena Banks Strike-Slip (?) Fault Zone in the Charleston, South Carolina Earthquake Area: Results from a Marine, High-Resolution, Multichannel, Seismic-Reflection survey," *Geological Society of America Bulletin* 98:591-601, 1987.

346. Talwani, P. and Katuna, M., *Macroseismic effects of the 1886 Charleston earthquake*, Carolina Geological Society Field Trip Guidebook, 2004.

347. Weems, R.E., Lemon, E.M. Jr., and Nelson, M.S., *Geology of the Pringletown, Ridgeville, Summerville, and Summerville Northwest 7.5-Minute Quadrangles, Berkeley, Charleston, and Dorchester Counties, South Carolina*, U.S. Geological Survey Miscellaneous Investigations Map 2502, 1:24,000 scale, 1997.

348. Madabhushi, S. and Talwani, P., "Composite Fault Plane Solutions of Recent Charleston, South Carolina, Earthquakes," *Seismological Research Letters* 61 (3-4):156, 1990.

349. Madabhushi, S. and Talwani, P., "Fault Plane Solutions and Relocations of Recent Earthquakes in Middleton Place-Summerville Seismic Zone Near Charleston, South Carolina," *Bulletin of the Seismological Society of America* 83 (5):1,442-1,466, 1993.

350. Talwani, P., “Fault Geometry and Earthquakes in Continental Interiors,” *Tectonophysics* 305:371-379, 1999.

351. Tarr, A.C. and Rhea, B.S., “Seismicity Near Charleston, South Carolina, March 1973 to December 1979,” in *Studies Related to the Charleston, South Carolina Earthquake of 1886 Tectonics and Seismicity*, U.S. Geological Survey Professional Paper 1313:R1-R17, 1983.

352. Bollinger, G.A., Johnston, A.C., Talwani, P., Long, L.T., Shedlock, K.M., Sibol, M.S., and Chapman, M.C., “Seismicity of the Southeastern United States; 1698-1986,” in *Neotectonics of North America: Decade map volume to accompany the neotectonic maps*, Geological Society of America, Boulder, CO, 1991.

353. Gangopadhyay, A. and Talwani, P*.,* “Fault Intersections and Intraplate Seismicity in Charleston, South Carolina: Insights from a 2-D Numerical Model,” *Current Science* 88 (10), 2005.

354. Tarr, A.C., Talwani, P., Rhea, B.S., Carver, D., and Amick, D., “Results of Recent South Carolina Seismological Studies,” *Bulletin of the Seismological Society of America* 71 (6):1,883-1,902, 1981.

355. Dutton, C.E., *The Charleston Earthquake of August 31, 1886*, U.S. Geological Survey ninth annual report 1887-88, 1889.

356. Seeber, L. and Armbruster, J.G., “The 1886 Charleston, South Carolina Earthquake and the Appalachian Detachment,” *American Geophysical Research* 86 (B9):7,874-7,894, 1981.

357. Talwani, P. and Schaeffer, W.T., “Recurrence Rates of Large Earthquakes in the South Carolina Coastal Plain Based on Paleoliquefaction Data,” *Journal of Geophysical Research* 106 (B4):6,621-6,642, 2001.

358. Obermeier, S.F., Gohn, G.S., Weems, R.E., Gelinas, R.L., and Rubin, M., “Geologic Evidence for Recurrent Moderate to Large Earthquakes Near Charleston, South Carolina,” *Science* 227 (4685):408-411, 1985.

359. Obermeier, S.F., Jacobson, R.B., Smoot, J.P., Weems, R.E., Gohn, G.S., Monroe, J.E., and Powars, D.S*., Earthquake-Induced Liquefaction Features in the Coastal Setting of South Carolina and in the Fluvial Setting of the New Madrid Seismic Zone*, U.S. Geological Survey professional paper 1504, 1990.

360. Frankel, A.D., Petersen, M.D., Mueller, C.S., Haller, K.M., Wheeler, R.L., Leyendecker, E.V., Wesson, R.L., Harmsen, S.C., Cramer, C.H., Perkins, D.M., and Rukstales, K.S., *Documentation for the 2002 Update of the National Seismic Hazard Maps*, U.S. Geological Survey Open-File Report 02-420, 2002.

361. Frankel, A.D., Barnhard, T., Perkins, D.M., Leyendecker, E.V., Hanson, K.L., and Hopper, M.G., *National Seismic-Hazard Maps: Documentation*, U.S. Geological Survey Open-File Report 96-532, 1996.

362. Powell, C.A., Bollinger, G.A., Chapman, M.C., Sibol, M.S., and Johnston, A.R., "A Seismotectonic Model for the 300-Kilometer-Long Eastern Tennessee Seismic Zone," *Science* 264:686-688, 1994.

363. Chapman, M.C., Munsey, J.W., Powell, C.A., Whisner, S.C., and Whisner, J., "The Eastern Tennessee Seismic Zone: Summary After 20 Years of Network Monitoring," *Seismological Research Letters* 73 (2):245, 2002.

364. Chapman, M.C., Powell, C.A., Vlahovic, G., and Sibol, M.S., "A Statistical Analysis of Earthquake Focal Mechanisms and Epicenter Locations in the Eastern Tennessee Seismic Zone," *Bulletin of the Seismological Society of America* 87 (6):1,522-1,536, 1997.

365. Atkinson, G.M. and Boore, D.M., "Ground-Motion Relations for Eastern North America," *Bulletin of the Seismological Society of America* 85 (1):17-30, 1995.

366. Bollinger, G.A., "Specification of Source Zones, Recurrence Rates, Focal Depths, and Maximum Magnitudes for Earthquakes Affecting the Savannah River Site in South Carolina," *U.S. Geological Survey Bulletin* 2017, 1992.

367. Electric Power Research Institute (EPRI), *Guidelines for determining design basis ground motions – volume 5 – Quantification of seismic source effects*, EPRI TR-102293, Project 3302, Final Report, November 1993.

368. CH2MHill and Geomatrix Consultants Inc., *Geotechnical, Geological, and Seismological (GG&S) Evaluation for the Bellefonte Site, North Alabama, Revision 1, Volume 1 of 2*, prepared for TVA-Bellefonte, March 2006.

369. Savy, J.B., Foxall, W., Abrahamson, N., and Bernreuter, D., *Guidance for Performing Probabilistic Seismic Hazard Analysis for a Nuclear Power Plant Site: Example Application to the Southeastern United States*, U.S. Nuclear Regulatory Commission NUREG/CR-6607, 2002.

370. Johnston, A.C., Coppersmith, K.J., Kanter, L.R., and Cornell, C.A., *The Earthquakes of Stable Continental Regions, Volume I: Assessment of Large Earthquake Potential - Final Report TR-102261-V1*, prepared for Electric Power Research Institute, 1994.

371. Chapman, M.C. and Krimgold, F., *Seismic Hazard Assessment for Virginia,* Virginia Tech Seismological Observatory report, Virginia Tech Department of Geological Sciences, 1994.

372. Removed

373. Wheeler, R.L. and Crone, A.J., "Known and Suggested Quaternary Faulting in the Mid-Continent United States," *Engineering Geology* 62:51-78, 2001.

374. Hough, S.E., Armbruster J.G., Seeber, L., and Hough, J.F., "On the Modified Mercalli Intensities and Magnitudes of the 1811-1812 New Madrid Earthquakes," *Journal of Geophysical Research* 105 (B10):23,839-23,864, 2000.

375. Johnston, A.C. and Schweig, G.D., "The Enigma of the New Madrid Earthquakes of 1811-1812," *Annual Review of Earth and Planetary Sciences* 24:339-384, 1996.

376. Van Arsdale, R.B., Kelson, K.I., and Lurnsden, C.H., "Northern Extension of the Tennessee Reelfoot Scarp into Kentucky and Missouri," *Seismological Research Letters* 66 (5):57-62, 1995.

377. Kelson, K.I., Simpson, G.D., Van Arsdale, R.B., Harden, C.C., and Lettis, W.R., "Multiple Late Holocene Earthquakes Along the Reelfoot Fault, Central New Madrid Seismic Zone," *Journal of Geophysical Research* 101 (B3):6,151-6,170, 1996.

378. Van Arsdale, R.B., "Displacement History and Slip Rate on the Reelfoot Fault of the New Madrid Seismic Zone," *Engineering Geology* 55:219-226, 2000.

379. Tuttle, M.P., Schweig, E.G., Sims, J.D., Lafferty, R.H., Wolf, L.W., and Haynes, M.L., "The Earthquake Potential of the New Madrid Seismic Zone," *Bulletin of the Seismological Society of America* 92 (6):2,080-2,089, 2002.

380. Tuttle, M.P., Schweig, E.S., Campbell, J., Thomas, P.M., Sims, J.D., and Lafferty, R.H., *Evidence for New Madrid Earthquakes in A.D. 300 and 2350 B.C.*, Seismological Research Letters 76 (4):489-501, 2005.

381. Guccione, M.J., "Late Pleistocene and Holocene Paleoseismology of an Intraplate Seismic Zone in a Large Alluvial Valley, The New Madrid Seismic Zone, Central USA," *Tectonophysics* 408:237-264, 2005.

382. Bollinger, G.A. and Sibol, M.S., "Seismicity, Seismic Reflection Studies, Gravity and Geology of the Central Virginia Seismic Zone: Part I – Seismicity," *Geological Society of America Bulletin* 96:49-57, 1985.

383. Wheeler, R.L., and Johnston, A.C., "Geologic Implications of Earthquake Source Parameters in Central and Eastern North America," *Seismological Research Letters* 63 (4):491-505, 1992.

384. Coruh, C., Costain, J.K., Glover, L., III, Pratt, T., and Brennan, J., *Seismicity, Seismic Reflection, Gravity and Geology of the Central Virginia Seismic Zone: Part I, Reflection Seismology*, U.S. Nuclear Regulatory Commission Report NUREG/CR-5123, 1988.

385. Obermeier, S.F. and McNulty, W.E., "Paleoliquefaction Evidence for Seismic Quiescence in Central Virginia During the Late and Middle Holocene Time," *Eos Transactions of the American Geophysical Union* 79 (17):S342, 1998.

386. France, N.A. and Brown, H.S.*, "*A Petrographic Study of Kings Mountain Belt Metaconglomerates," in *Geological Investigations of the Kings Mountain Belt and Adjacent Areas in the Carolinas*, Carolina Geological Society Field Trip Guidebook, 1981.

387. Hatcher, R.D., Jr. and Morgan, B.K.*, "*Finite Strain and Regional Implications of the Deformed Draytonville Metaconglomerate Near Gaffney, South Carolina," in *Geological Investigations of the Kings Mountain Belt and adjacent areas in the Carolinas*," Carolina Geological Society Field Trip Guidebook, 1981.

388. McDougall, I. and Harrison, T.M., *Geochronology and Thermochronology by the $^{40}Ar/^{39}Ar$ method*, 2nd edition, Oxford University Press, New York, 1999.

389. Murphy, C.F. and Butler, J.R., "Geology of the Northern Half of the Kings Creek Quadrangle, South Carolina," in *Geological Investigations of the Kings Mountain Belt and Adjacent Areas in the Carolinas*, Carolina Geological Society Field Trip Guidebook, 1981.

390. Horton, J.W., Jr. and Butler, J.R., "Geology and Mining History of the Kings Mountain Belt in the Carolinas; a Summary and Status Report," in *Geological investigations of the Kings Mountain Belt and Adjacent Areas in the Carolinas*, Carolina Geological Society Field Trip Guidebook, 1981.

391. Nystrom Jr., P.G, *Geologic Map of the Blacksburg South 7.5 - Minute Quadrangle, Cherokee County, South Carolina [preliminary draft]*, South Carolina Department of Natural Resources Geological Survey, 1:24,000 scale, 1 sheet, 2004.

392. Schaffer, M.F., "Polyphase Folding in a Portion of the Kings Mountain Belt, North-Central South Carolina," in *Geological Investigations of the Kings Mountain Belt and Adjacent Areas in the Carolinas*, Carolina Geological Society Field Trip Guidebook, 1981.

393. Guidotti, C.V., "Micas in Metamorphic Rocks," in *Reviews in Mineralogy Volume 13*, ed. S.W. Bailey, Mineralogical Society of America, 1984.

394. Ramberg, H., “The Facies Classification of Rocks, a Clue to the Origin of Quartzo-Feldspathic Massifs and Veins,” *Journal of Geology* 57 (1):18-54, 1949.

395. Bollinger, G.A., “Reinterpretation of the Intensity Data for the 1886 Charleston, South Carolina, Earthquake*,”* in *Studies Related to the Charleston, South Carolina, Earthquake of 1886 - A Preliminary Report*, U.S. Geological Survey Professional Paper 1028:17-32, 1977.

396. Taber, S., “The South Carolina Earthquake of January 1, 1913,” *Bulletin of the Seismological Society of America* 3:6-13, 1913.

397. Visvanathan, T.R*., “*Earthquakes in South Carolina, 1698-1975*,” South Carolina Geological Survey Bulletin* 40, 1980.

398. U.S. Nuclear Regulatory Commission, *Safety Evaluation Report for an Early Site Permit (ESP) at the North Anna ESP Site*, U.S. Nuclear Regulatory Commission Report, NUREG-1835, September 2005.

399. Seeber, L., and Armbruster, J.G., "Seismicity Along the Atlantic Seaboard of the U.S.; Intraplate Neotectonics and Earthquake Hazard," in The Atlantic Continental Margin: U.S., The Geology of North America, vol. I-2, ed. R.E. Sheridan and J.A. Grow, Geological Society of America, Boulder, CO, 1988.

400. Van Schmus, W.R., Bickford, M.E., and Turek, A., "Proterozoic Geology of the East-Central Midcontinent Basin," in Basement and Basins of Eastern North America, ed. B.A. van der Plujm and P. A. Catacosinos, Geological Society of America Special Paper 308, Boulder, CO, 1996.

401. Cherokee Nuclear Station Preliminary Safety Analysis Report (PSAR), prepared by Law Engineering Testing Company for Duke Power Company, Project 81, 1974.

402. Maybin, A.H., Mineral Resources Map of South Carolina, South Carolina Geological Survey, GGMS-3, 1:500,000-Scale, 1997.

403. Bream, B.R., 2002, The Southern Appalachian Inner Piedmont: New Perspectives Based on Recent Detailed Geologic Mapping, Nd Isotopic Evidence, and Zircon Geochronology, in Hatcher, R.D., Jr., and Bream, B.R., eds., Inner Piedmont Geology in the South Mountains-Blue Ridge Foothills and the Southwestern Brushy Mountains, Central-Western North Carolina: North Carolina Geological Survey, Carolina Geological Society Annual Field Trip Guidebook, p. 45-63.

404. Hatcher, R. D., Bream, B. R., and Merschat, A. J., 2007, Tectonic Map of the Southern and Central Appalachians: A Tale of Three Orogens and a Complete Wilson Cycle, in Hatcher, R. D., Carlson, M. P., McBride, J. H., and Martinez Catalan, J. R., eds., 4-D Framework of Continental Crust: Geological Society of America Memoir 200, p. 595-632.

405. Dennis, A. J., 2007, Cat Square Basin, Catskill Clastic Wedge: Silurian-Devonian Orogenic Events in the Central Appalachians and the Crystalline Southern Appalachians: Geological Society of America Special Paper 433, p. 313-329.

406. Goldsmith, R, Milton, D. J., Horton, J. W., 1988, Geologic Map of the Charlotte 1x2 Degrees Quadrangle, North Carolina and South Carolina: USGS Miscellaneous Investigations Series Map I-1251-E; 1:250,000. Website http://pubs.er.usgs.gov/usgspubs/i/i1251E accessed February 6, 2009.

407. North Carolina Geological Survey (NCGS), Geology of North Carolina vector digital data onemap_prod.SDEADMIN.geo, Website http://www.nconemap.com/Default.aspx?tabid=286, accessed June 12, 2007, publication date 1998.

408. Milton, D. J., The northern termination of the Kings Mountain belt. In Geological investigations of the Kings Mountain belt and adjacent areas in the Carolinas, Carolina Geological Society Field Trip Guidebook 1982, p. 1-5, 1981.

409. McSween, H. Y. Jr., Speer, J. A., Fullagar, P. D., 1991, Chapter 7. Plutonic Rocks. *In*, The Geology of the Carolinas. Horton, J. W. Jr., Zullo, V. A. eds., University of Tennessee Press, p. 109-126.

410. Dallmeyer, R.D., Wright, J.E., Secor, D.T., Jr., and Snoke, A.W., Character of the Alleghanian Orogeny in the Southern Appalachians: Part II-Geochronological constraints on the tectonothermal evolutions of the Eastern Piedmont in South Carolina: Geological Society of America Bulletin. v. 97, p. 1,329-1,344, 1986.

411. Howard, C.S., Charleton, J.E., and McCarney, K.J., New geologic synthesis of the Dreher Shoals and Carolina Terranes, Lake Murray and Saluda Dam, Columbia, SC: Geological Society of America Abstracts with Programs, v. 37, no. 2, p. 36, 2005.

412. McCarney, K.J., Charleton, J.E., and Howard C.S., Brittle features mapped along a shear zone at Saluda Dam, central South Carolina: Geological Society of America Abstracts with Programs. v. 37. no. 2, p. 5. 2005.

413. Gohn, G.S., 1988, "Late Mesozoic and early Cenozoic geology of the Atlantic Coastal Plain: North Carolina to Florida," in *The Geology of North America vol. 1-2, The Atlantic Continental Margin*, The Geological Society of America.

414. Prowell, D.C. and Obermeier, S.F., 1991, "Evidence of Cenozoic Tectonism," in *The Geology of the Carolinas - Carolina Geological Society 50th Anniversary Volume*, University of Tennessee Press.

415. Giorgis, S. D., Mapes, R. W., Bream, B. R., The Walker Top Granite: Acadian granitoid or eastern Inner Piedmont basement, in Hatcher, R. D. and Bream, B. R., eds., Inner Piedmont geology in the South Mountains-Blue Ridge foothills and the southwestern Brushy Mountains, central-western North Carolina: North Carolina Geological Survey, Carolina Geological Society annual fieldtrip guidebook, p. 33-43, 2002.

416. Merschat, A. J., Kalbas, J. L., Geology of the southwestern Brushy Mountains, North Carolina Inner Piedmont: A summary and synthesis of recent studies, in Hatcher, R. D. and Bream, B. R., eds., Inner Piedmont geology in the South Mountains-Blue Ridge foothills and the southwestern Brushy Mountains, central-western North Carolina: North Carolina Geological Survey, Carolina Geological Society annual fieldtrip guidebook, p. 101-126, 2002.

417. Hibbard, J. P., Shell, G. S., Bradley, P. J., Samson, S. D., Wortman, G. L., 1998, The Hyco shear zone in North Carolina and southern Virginia: implications for the piedmont zone-Carolina zone boundary in the southern Appalachians: American Journal of Science, v. 298, p. 85-107.

418. Wortman, G. L., Samson, S. D., Hibbard, J. P., Precise timing constraints on the kinematic development of the Hyco shear zone: implications for the Central Piedmont shear zone, southern Appalachian orogen: American Journal of Science, v. 298, p. 108-130, 1998.

419. Davis, T. L., Geology of the Columbus promontory, western Piedmont, North Carolina, southern Appalachians, in Hatcher, R. D. and Davis, T. L., Studies of Inner Piedmont geology with a focus on the Columbus promontory: Carolina Geological Society Fieldtrip Guidebook, p. 17-39, 1993.

420. Garahan, J. M., Preddy, M. S., Ranson, W. A. (1993) Summary of Mid-Mesozoic Brittle Faulting in the Inner Piedmont and Nearby Charlotte Belt of the Carolinas. In Studies of Inner Piedmont Geology with a focus on the Columbus Promontory. Carolina Geological Society Field Trip Guidebook. p. 55-65.

421. Horton, J. W., Shear zone between the Inner Piedmont and Kings Mountain belts in the Carolinas: Geology, v. 9, p. 28-33, 1981.

422. Dennis, A. J., Wright, J. E., Mississippian (ca. 326-323 Ma) U-Pb crystallization for two granitoids in Spartanburg and union counties, South Carolina: Carolina Geological Society Guidebook, p. 43-47. 1995.

423. Griffin, V. S., The Lowndesville belt north of the South Carolina-Georgia border, in Horton, J. W., Butler, J. R., and Milton, D. J., eds. Geological investigations in the Kings Mountain belt and adjacent areas, Carolina Geological Society Fieldtrip Guidebook, p. 166-173, 1981.

424. Nelson, A. E., Polydeformed rocks of the Lowndesville shear zone in the Greenville 2 degree quadrangle, South Carolina and Georgia, in Horton, J. W., Butler, J. R., and Milton, D. J., eds. Geological investigations in the Kings Mountain belt and adjacent areas, Carolina Geological Society Fieldtrip Guidebook, p. 181-193, 1981.

425. Hibbard, J., Miller, B., Hames, W., Allen, J., and Standard, I., Carolinia; definition and recent finding in central North Carolina: Geological Society of America, Southeastern Section Abstracts with Programs, v. 39, p. 11-12, 2007.

426. Hibbard, J., Pollock, J., Allen, J., and Brennan, M., The heart of Carolinia: Stratigraphic and tectonic studies in the Carolina terrane of central North Carolina, Geological Society of America Southeast Section Fieldtrip Guidebook. 54 p., 2008.

427. Allen, J.S., Miller, B., Hibbard, J., and Boland, I., Significance of intrusive rocks along the Charlotte-Carolina terrane boundary: evidence for the timing of deformation in the Gold Hill fault zone near Waxhaw, NC: Geological Society of America Southeast Section Abstracts with Programs, v. 39, p. 12, 2007.

428. Hibbard, J. P., van Staal, C., Rankin, D. W., Comparative analysis of pre-Silurian crustal building blocks of the northern and the southern Appalachian orogen: American Journal of Science, v.307, p.23-45, 2007.

429. Hatcher, R. D. Jr., Tectonic synthesis of the U. S. Appalachians; in The Geology of North America, The Appalachian-Ouachita Orogen in the United States, Volume F-2, The Geological Society of America, p.511-535, 1989.

430. Hibbard, J. P., van Staal, C. R., Miller, B. V., Links among Carolinia, Avalonia, and Ganderia in the Appalachian peri-Gondwanan realm, Geological Society of America Special Paper 433, p.291-311, 2007,

431. Nystrom, P.G. Jr., Late Cretaceous-Cenozoic Brittle Faulting Beneath the Western South Carolina Coastal Plain: Reactivation of the Eastern Piedmont Fault System, Geological Society of America Abstracts with Programs, Southeastern Section 55th annual meeting, 2006.

2.5.2 VIBRATORY GROUND MOTION

WLS COL 2.5-2 This section provides a detailed description of vibratory ground motion assessments, specifically the criteria and methodology for establishing the Ground Motion Response Spectra (GMRS) and Foundation Input Response Spectra (FIRS) for the Lee Nuclear Station Units 1 and 2. The section begins with a review of the approach in Regulatory Guide (RG) 1.208, *A Performance-Based Approach to Define The Site-Specific Earthquake Ground Motion*, which satisfies the requirements set forth in Section 100.23, "Geologic and Seismic Siting Criteria," of Title 10, Part 100, of the Code of Federal Regulations (10 CFR 100),

"Reactor Site Criteria." The GMRS for the Lee Nuclear Station Site was developed by adopting methodology consistent with the approach recommended in RG 1.208.

Following this introductory section, the remainder of the Subsection is presented as follows:

- Seismicity (Subsection 2.5.2.1)
- Geologic and Tectonic Characteristics of the Site and Region (Subsection 2.5.2.2)
- Correlation of Earthquake Activity with Seismic Sources (Subsection 2.5.2.3)
- Probabilistic Seismic Hazard Analysis (PSHA) and Controlling Earthquake (Subsection 2.5.2.4)
- Seismic Wave Transmission Characteristics of the Site (Subsection 2.5.2.5)
- Ground Motion Response Spectrum (GMRS) developed for Lee Nuclear Station Unit 2 (Subsection 2.5.2.6)
- Foundation Input Response Spectra (FIRS) developed for Lee Nuclear Station Unit 1 (Subsection 2.5.2.7)

RG 1.208 provides guidance on methods acceptable to the U. S. Nuclear Regulatory Commission (NRC) to satisfy the requirements of the seismic and geologic regulation, 10 CFR 100.23, for assessing the appropriate Safe Shutdown Earthquake (SSE) ground motion levels for new nuclear power plants. RG 1.208 states that an acceptable starting point for this assessment at sites in the Central and Eastern United States (CEUS) is the PSHA conducted by the EPRI-SOG in the 1980s (References 201, 203, and 207). The EPRI-SOG evaluation involved a comprehensive compilation of geological, geophysical, and seismological data, evaluations of the scientific knowledge concerning earthquake sources, maximum earthquakes, and earthquake rates in the CEUS by six multi-disciplinary teams of experts in geology, seismology, geophysics, and, separately, development of state of knowledge earthquake ground motion modeling, including epistemic and aleatory uncertainties. The uncertainty in characterizing the frequency and maximum magnitude of potential future earthquakes associated with these sources and the ground motion that they may produce was assessed and explicitly incorporated in the seismic hazard model. RG 1.208 further specifies that the adequacy of the EPRI-SOG hazard results must be evaluated in light of more recent data and evolving knowledge pertaining to seismic hazard evaluation in the CEUS.

The GMRS and FIRS are developed using the graded, performance-based, risk-consistent method described in RG 1.208. The methodology for developing the GMRS is based on ASCE/SEI Standard 43-05, *Seismic Design Criteria for*

Structures, Systems, and Components in Nuclear Facilities (Reference 295). The method specifies the level of conservatism and rigor in the seismic design process such that the performance of structures, systems, and components of the plant achieve a uniform seismic safety performance consistent with the NRC's safety goal policy statement (51 FR 28044 and 51 FR 30028, 10 CFR Part 50). The ASCE/SEI Standard 43-05 approach is designed to achieve a quantitative safety performance goal (PF). The method is based on the use of site-specific mean seismic hazard and assumes that the seismic design criteria (SDC) and procedures contained in NUREG-0800 are applied in seismic source characterization (SSC) design.

The ASCE/SEI Standard 43-05 (Reference 295) approach aims conservatively to assure a seismic safety target, or performance goal of mean 10^{-5} per year for SDC-5 SSCs. ANSI/ANS Standard 2.26-2004 *Categorization of Nuclear Facility Structures, Systems, and Components for Seismic Design* (Reference 296) provides the criteria for selecting SDC and Limit State that establishes the Seismic Design Basis (SDB) for each SSC at a nuclear facility. The target mean annual performance goal for nuclear plants is achieved by coupling site-specific design response spectrum (DRS) with the deterministic SDC and procedures specified by NUREG-0800. The ASCE/SEI Standard 43-05 criteria for deriving a site-specific DRS are based on the conservative assumption that the SDC specified by NUREG-0800 achieve less than a 1 percent chance of failure for a given DRS. The conservatism of this assumption is demonstrated by analyses described in McGuire et al. (Reference 274) that show plant level risk reduction factors ranging from about 20 to about 40 are attained by the NRC's SDC. The method is based on the use of mean hazard results consistent with the recommendation contained in McGuire et al. (Reference 274) and with the NRC's general policy on the use of seismic hazard in risk-informed regulation.

Subsections 2.5.2.1 through 2.5.2.4 document the review and update of the available EPRI seismicity, seismic source, and ground motion models. Subsection 2.5.2.5 summarizes information about the seismic wave transmission characteristics of the Lee Nuclear Site with reference to more detailed discussion of all engineering aspects of the subsurface in Subsection 2.5.4. Subsection 2.5.2.6 describes the development of the site-specific GMRS for the Lee Nuclear Site. Regulatory Guide 1.208 provides guidance for development of the GMRS. Subsection 2.5.2.7 describes the development of the foundation input response spectra (FIRS) for Unit 1, to evaluate potential site response effects attributed to existing fill concrete and structural concrete materials placed during construction of the existing Cherokee Nuclear Station as well as new fill concrete for Lee Nuclear Station placed above the existing Cherokee Nuclear Station concrete materials. For Unit 2, sound, continuous rock meeting the hard rock definitions is located at the foundation level. Therefore, the calculated GMRS defines the input motion at Unit 2.

2.5.2.1 Seismicity

The seismic hazard analysis conducted in 1989 by EPRI NP-6395-D (Reference 203) relies in part on an analysis of historical seismicity in the Central

and Eastern United States (CEUS) to estimate seismicity parameters (rates of activity and Richter b-values) for individual seismic sources. The historical earthquake catalog used in the EPRI analysis is complete through 1984. Earthquake data for the site region since 1984 are reviewed and used to update the EPRI catalog through 2005.

The 1989 EPRI NP-6395-D study (Reference 203) is a broad regional study of nuclear sites in the eastern U.S. (east of the Rocky Mountains). The goal of this EPRI study is to develop seismic hazard curves for these sites based on regional PSHA information. For the seismic-source component of the analysis, the EPRI study utilizes a large number of geoscientists grouped into six Earth Science Teams (ESTs), whose interpretations of geologic, geophysical, and seismic information were elicited, team-by-team, using a formal expert elicitation process. The results of the EST analyses are presented in the 1986 EPRI NP-4726 volumes 5 through 10 (Reference 201) and summarized in the 1989 EPRI NP-6452-D EQHAZARD Primer (Reference 207). The ground-motion component of the analysis comprises a weighted combination of models developed by the ESTs. The PSHA results are based on a combination of the seismic source and ground motion information.

As described in Subsection 2.5.4.8, there is no potential for earthquake-induced liquefaction at the site. The stability of natural and manmade slopes where failure could adversely impact safety-related structures is discussed in Subsection 2.5.5.

2.5.2.1.1 Regional Seismicity Catalog Used for 1989 EPRI Seismic Hazard Analysis Study

In the CEUS, multiple regional seismic networks record earthquakes. A large effort was made during the EPRI seismic hazard analysis study to combine available data on historical earthquakes and to develop a homogenous earthquake catalog containing all recorded earthquakes for the region. “Homogenous” means that the estimates of body-wave magnitude (m_b) for all earthquakes are consistent, that duplicate earthquakes have been eliminated, that non-earthquakes (e.g., mine blasts and sonic booms) have been eliminated, and that significant events in the historical records have not been missed. Thus, the EPRI catalog (Reference 204) forms a strong basis on which to estimate seismicity parameters used in the 1989 EPRI PSHA (Reference 203).

2.5.2.1.2 Updated Seismicity Data

The EPRI earthquake catalog, which covers CEUS seismicity for the period ending in 1984, is updated to include seismicity that has occurred within the site region from 1985 to 2005. In updating the EPRI catalog, a rectangular region is defined with a latitude interval of 30° to 38° N and a longitude interval of 77° to 87° W. This rectangular region encompasses the 200-mile radius site region and is judged to include seismic sources contributing significantly to Lee Nuclear Site earthquake hazard, including the Charleston seismic source. Figure 2.5.2-201 shows the Lee Nuclear Site and its associated circular site region, along with the rectangular area for which the EPRI earthquake catalog was updated.

Figures 2.5.2-202, 203, 204, 205, 206, 207 and 208 also show the EPRI earthquake catalog and updated seismicity to illustrate the spatial distribution of earthquakes with respect to regional geologic structures and EPRI seismic source zones significant to the Lee Nuclear Site. The updated earthquake catalog is examined to evaluate the possible correlation of seismicity to geologic structures, possible changes to the EPRI source geometry or seismicity parameters (a- and b-values), and any possible new or previously unrecognized seismic source.

The updated seismicity data for the 1985 to 2005 period is compiled primarily from the Southeastern U.S. Seismic Network (SEUSSN) and the Advanced National Seismic System (ANSS). The SEUSSN covers the entire site region and is the primary catalog used to compile the national ANSS seismicity catalog. While the SEUSSN catalog is taken as the preferred catalog for this region of the CEUS, some additional events listed only in the ANSS catalog are also included in the update. The National Earthquake Information Center (NEIC) catalog is used to obtain magnitudes for five events from the ANSS catalog.

The SEUSSN catalog is available from the Virginia Tech Seismological Observatory (VTSO) website (Reference 205) and was downloaded on August 26, 2006. As acquired, the SEUSSN catalog contained 12,787 events for the period from 1568 through 2004. The catalog is filtered to exclude events that either occurred prior to January 1985 or beyond the rectangular project region defined with a latitude interval of 30° to 38° N and a longitude interval of 77° to 87° W. The resulting list includes 1,579 events from 1985 through 2004.

The ANSS catalog (Reference 206) was searched on August 29, 2006, for all records within the rectangular site region, resulting in 2,056 records from 1928 through 2005. Of these, 1,659 events occurred in 1985 or later. Combining the SEUSSN and ANSS listings and eliminating duplicate records results in a composite catalog of 1,670 earthquakes within the rectangular site region for the period of 1985 through 2005.

To achieve consistency with the EPRI seismicity catalog, the magnitudes given in both SEUSSN and ANSS catalogs are converted to best or expected estimate of m_b magnitude ($E[m_b]$, also called Emb), using the conversion factors given as Equation 4-1 and Table 4-1 in EPRI NP-4726-A (Reference 204):

$$Emb = 0.253 + 0.907 \cdot Md \qquad \text{(Equation 2.5.2-1)}$$

$$Emb = 0.655 + 0.812 \cdot ML \qquad \text{(Equation 2.5.2-2)}$$

where Md is duration or coda magnitude and ML is “local” magnitude.

Equation 4-2 of EPRI NP-4726-A (Reference 204) indicates that the equation from which m_b^* or Rmb is estimated from the best estimate of magnitude $E[m_b]$ or Emb and the variance of m_b, σ^2_{mb}, or Smb^2 is:

$$m_b^* = E[m_b] + (1/2) \cdot ln(10) \cdot b \cdot \sigma^2_{mb} \qquad \text{(Equation 2.5.2-3)}$$

where b = 1.0.

Values for σ^2_{mb} or Smb^2 are estimated for the two catalogs, and m_b [Rmb] is assigned to each event added to the updated catalog.

The result of the above process is a post-1984 catalog of 89 earthquakes with Emb magnitude 3.0 or greater that updates the EPRI NP-4726-A (Reference 204) seismicity catalog recommended for the site region. Table 2.5.2-201 provides a listing of these 89 earthquakes that occurred within the rectangular region defined by a latitude-longitude window of 30° to 38° N, 77° to 87° W for the period 1985 through 2005. For the purpose of recurrence analysis, these earthquakes are considered independent events.

2.5.2.1.3 Evaluation of the Potential for Reservoir-Induced Seismicity

This subsection presents information on the potential for RIS at the Lee Nuclear Station associated with the construction and operation of Make-Up Pond C (Figure 1.1-202). No documented RIS is associated with the impoundment of Make-Up Pond B, which was constructed as part of the former Cherokee Nuclear Station.

Evaluations to assess the potential for RIS associated with the Make-Up Pond C impoundment indicate a low potential for RIS and negligible risk to safe operations for Lee Nuclear Station Units 1 and 2. RIS has sometimes been observed at comparable-sized reservoirs and is usually confined to earthquake magnitudes of **M** < 4 for this depth of reservoir. Factors controlling the presence or absence of RIS are strongly dependent on local geologic properties, including reservoir rock type, fault and fracture characteristics, local and regional tectonics, and reservoir operation characteristics.

These evaluations consider RIS potential associated with the configuration and operating parameters for Make-Up Pond C and include an extensive review of RIS literature and scientific understanding of the potential for RIS based on crustal (e.g., underlying geologic and tectonic) properties and reservoir operations. The evaluations also include a review of past worldwide cases of RIS associated with reservoirs with similar or greater hydraulic heights to Make-Up Pond C, an analysis of seismicity associated with reservoirs operated in the Carolina Piedmont, and an analysis of U.S. Bureau of Reclamation dams and reservoirs located in metamorphic terranes with historic hydraulic height and operating configurations comparable to or exceeding Make-Up Pond C hydraulic height or hydraulic height variation operating parameters.

NUREG/CR-5503 (Reference 300) notes that almost all the largest magnitude RIS has occurred in areas where there is active Quaternary faulting. NUREG/CR-5503 makes several important distinctions. First, NUREG/CR-5503 distinguishes between a seismogenic fault, defined as being capable of producing a moderate to large earthquake (**M** > 5), and a nonseismogenic fault that is not

capable of producing a moderate to large earthquake. Second, NUREG/CR-5503 defines a tectonic fault as produced by deep-seated crustal-scale processes acting at or below seismogenic depths and a nontectonic feature as a feature produced by shallow crustal or surficial processes acting above seismogenic depth (note seismogenic in this context refers to **M** > 5 earthquakes). These distinctions are important because they directly correspond to distinctions made between the most common form of RIS (nontectonic nonseismogenic shallow earthquakes with **M** ≤ 5) and **M** > 5 triggered seismicity that occurs on tectonic seismogenic faults. The operation of Make-Up Pond C represents a surficial process. Based on NUREG/CR-5503, the lack of identified active seismogenic faults in the Make-Up Pond C reservoir area indicates that **M** > 5 triggered seismicity is unlikely.

The analysis considers reservoirs from regions of ongoing tectonic activity, such as California, as well as regions with low rates of tectonic deformation, such as the Carolina Piedmont.

Following NUREG/CR-5503, it is important to make a distinction between triggered seismicity in regions of active faulting that are characterized by **M** > 5 tectonic seismogenic earthquakes in the historical record, such as the region west of the Rocky Mountains, and RIS in regions that are not associated with ongoing seismic activity and generally lack **M** > 4 historical seismicity. Triggered seismicity implies that a tectonic seismogenic earthquake that was likely to occur at a later date is triggered and occurs earlier as a result of perturbations of elastic stresses and/or pore pressures associated with reservoir operations. The most significant example of triggered seismicity appears to be the 2008 **M** 7.9 Wenchuan, China earthquake (Klose (2008) (Reference 301)). This earthquake occurred in a tectonically active region of China on a large pre-existing active fault with a recurrence interval of large-magnitude (**M** ~ 8) surface-rupturing earthquakes in the late Holocene of ~1000-1200 yr (Lin et al. (2009) (Reference 302)). The reservoir did not influence the maximum size or the long-term likelihood that the earthquake would occur; it may have caused the earthquake to occur earlier than if the reservoir had not been impounded (Reference 301). The 2008 **M** 7.9 Wenchuan, China earthquake was inevitable in the geologic timeframe of seismic source characterization (Reference 302) and is the type of tectonic seismogenic source that would be accounted for in a probabilistic seismic hazard analysis and related ground motion analyses.

Analysis of documented cases of RIS for reservoirs located in metamorphic terranes, including reservoirs in the Carolina Piedmont, suggests that for low seismicity rate regions, maximum RIS magnitudes for reservoirs with hydraulic heights < 60 m are less than **M** 4. Considering all U.S. Bureau of Reclamation reservoirs located in metamorphic terranes and all earthquakes located within 30 km of the reservoirs, post-impoundment maximum magnitudes have been less than **M** 4 for reservoirs located in regions of low historical seismicity and have been less than or equal to **M** 5 for reservoirs located in regions where historical pre-impoundment maximum magnitudes were ≥ **M** 5.5.

Consequently, available information indicates that any RIS that might be associated with Make-Up Pond C operating parameters would likely have a

maximum RIS magnitude of **M** < 4 and is unlikely to have a maximum magnitude of **M** ≥ 5. The current short-period design is controlled by a local **M** 5-5.5 as described in Subsection 2.5.2.4.5. There is no observed precedent for **M** > 5 RIS associated with reservoirs located in low seismicity rate metamorphic terranes.

In metamorphic terranes comparable to the Make-Up Pond C site, if through-going fault(s) and/or fractures that intersect the reservoir exist, increasing fluid pore pressure is likely to be the dominant mechanism that would induce earthquakes (Talwani et al. (2007) (Reference 303)). Talwani et al. (2007) shows that earthquakes are only induced over a specific range of fault and fracture hydraulic diffusivities. Outside the range of hydraulic diffusivity of 0.1 to 10 m^2/s, induced seismicity rarely occurs and is mostly associated with injection-induced seismicity (Reference 303). The largest observed Carolina Piedmont RIS magnitude of **M** 4.3 occurred as a delayed response at Clark Hill (Strom Thurmond) Reservoir (Talwani (1976) (Reference 304) and Secor (1987) (Reference 305)). Assuming the Talwani et al. (2007) evaluation of hydraulic diffusivities is correct (Reference 303), it follows that steeply dipping faults and/or fractures with hydraulic diffusivity of 0.1 to 10 m^2/s exist at Clark Hill (Strom Thurmond) Reservoir to produce the observed delayed RIS. The nearly universal observation of metamorphic RIS maximum magnitudes being less than **M** 4 documented in the Carolina Piedmont, the western United States, and the Brazilian craton strongly suggests that metamorphic terranes rarely contain steep faults and/or fractures with sufficient hydraulic diffusivities to allow pore pressure perturbations to propagate to sufficient depths to create enough fault area for maximum RIS magnitudes to exceed **M** > 4. Thus, metamorphic site RIS is typically caused by nontectonic nonseismogenic processes (NUREG/CR-5503) associated with initial elastic/pore pressure responses at shallow depths, such as observed at Monticello Reservoir (Chen and Talwani (2001a and 2001b) (References 306 and 307) and Secor et al. (1982) (Reference 310)), relatively tight faults/fractures that confine RIS to relatively shallow depths, or where more permeable faults/fractures exist, as observed at Jocassee Reservoir (Rajendran (1995) (Reference 308)), Keowee Reservoir (Schaeffer (1991) (Reference 309)), and Clark Hill (Strom Thurmond) Reservoir (References 304 and 305).

By analogy, there is no documented RIS associated with Make-Up Pond B, located approximately 2.5 miles to the southeast and constructed over 30 years ago as part of the former Cherokee Nuclear Station project. It is likely that no significant steeply dipping faults or fractures exist beneath the Make-Up Pond C location that are oriented nearly orthogonal to the local direction of minimum compressive stress. Therefore, it would appear unlikely that RIS with maximum magnitudes exceeding **M** > 4 are probable at Make-Up Pond C, if at all. This is because of (1) the likely confinement of RIS responses to the top several km of the crust by low-effective hydraulic diffusivity and (2) the limited maximum magnitudes associated with coupled elastic/pore pressure initial loading and shallow confinement of fault/fracture-related RIS responses (Reference 307), and the nearly instantaneous poroelastic response (Reference 303).

Based on the review of the Carolina Reservoirs, it appears that five conditions are needed for RIS to occur:

(1) Rock stressed close to failure conditions (a situation more likely to occur in felsic-crystalline rock rather than felsic to intermediate metavolcanic and metasedimentary crystalline rock underlying Make-Up Pond C),

(2) Through-going fractures favorably oriented relative to the maximum horizontal stress direction,

(3) Hydraulic diffusivity in the range of 0.1 to 10 m^2/s as determined by Talwani et al. (2007) (Reference 303),

(4) A maximum reservoir depth greater than 140 feet, and

(5) A site dominated by medium to coarse grained felsic rocks.

RIS has been shown to not occur when one of these conditions does not exist. As an example, Bad Creek is a deep reservoir with primarily felsic rocks (condition 5), but the lack of RIS at Bad Creek shows that RIS does not occur when one of the first three conditions (condition 3 for Bad Creek) does not exist (References 309, 311, 312, and 313). The lack of RIS at most of the deepest Carolina Piedmont reservoirs is consistent with condition (5). The two deepest Carolina Piedmont Reservoirs lacking RIS with maximum depths > 200 ft (Murray and Badin Lake) share similarities with the Make-Up Pond C metavolcanic site geology, with Murray having metasedimentary rocks with locally interbedded intermediate to felsic fragmental metavolcanic rocks, and felsic to intermediate crystal-lapilli tuff with lenticular lenses of metasedimentary rocks, and Badin Lake having crystal and lithic tuffs of rhyolitic to rhyodacitic composition with minor ash flow tuffs and tuff breccias and siltstone and siltstone/mudstone; siltstone and argilite with minor tuff beds; graywacke, sandstone and minor siltstone; and mafic and intermediated metavolcanic rocks, primarily tuffs and flows with hypabyssal intrusives (References 317, 318, and 319). The three other non-RIS Carolina Piedmont reservoirs with maximum depths greater than the Lake Keowee maximum depth are Hartwell, Richard Russell, and W. Scott Kerr, which also are comprised of more intermediate metamorphic rocks than the four felsic rock Carolina reservoirs with RIS (References 320, 321, and 322). Thus, while condition 5 is empirical, the occurrence of RIS at a dominantly fine-grained felsic metavolcanic site like Make-Up Pond C would be without precedent.

There is a NE-striking joint set at the William States Lee site that is optimally oriented to maximize seismic diffusivity. At Make-Up Pond B the dominant shears are oriented about 30° oblique to S_{Hmax}, with the dominant shear set at existing Make-Up Pond B striking N19°E and dipping 61° SE. Despite this, there have been no documented cases of RIS at Make-Up Pond B since it was impounded.

Geologic mapping demonstrates a more easterly structural orientation in the impoundment area of Make-Up Pond C. Dominant schistosity at Make-Up Pond C strikes N47°E and dips 55° SE (Reference 323). This mean orientation is subparallel to S_{Hmax}. Detailed shear orientation measurements have not been made in the vicinity of Make-Up Pond C but it is reasonable to expect that shears

would be parallel the overall structural fabric (which is best indicated by the schistosity data). Thus, condition (2) is not met at Make-Up Pond C.

At Make-Up Pond B and possibly Make-Up Pond C, there are a small number of northwest-striking shears that dip 48°-62° NE that are reasonably oriented to accommodate shallow reverse-faulting consistent with condition (2). However, these dips are relatively steep in relation to the more optimally oriented shallow dipping shears observed at Monticello Reservoir (Reference 324). Thus, if RIS were to occur at Make-Up Pond C, it is most likely to be associated with **M** < 3 shallow reverse-faulting similar to that observed at Monticello Reservoir.

Review of the Lee Nuclear Station site conditions indicates that the Make-Up Pond C site properties are not conducive to satisfying conditions (1), (2), (3), (4) and (5). Thus **M** > 3 RIS is not expected to be associated with the Make-Up Pond C impoundment. Specifically, it is concluded that condition (1) is not met for depths greater than 0.5 km based on Carolina Piedmont in situ stress measurements (Reference 325), and that condition (2) is only partially satisfied at depths greater than 0.5-1.0 km because a 60° shear-plane dip is not optimal for predominant strike-slip faulting due to the rotation of the maximum principal stress toward vertical with increasing depth observed by Moos and Zoback (Reference 325). The conclusion that **M** > 3 RIS is not expected to be associated with the Make-Up Pond C impoundment is further supported by the fact that no known recorded RIS is associated with the Lee Nuclear Station Make-Up Pond B impoundment. Furthermore, there are no documented instances of RIS for reservoirs of similar maximum depth in rocks of similar lithologies (e.g., primarily felsic to intermediate mostly fine-grained metavolcanic and metasedimentary rock types).

In the event that RIS associated with Make-Up Pond C occurs, it is unlikely the induced magnitudes would exceed **M** > 4, a value well below the short-period controlling earthquake. Ground motions associated with RIS events (**M** < 4) typically display high frequency and modest peak ground accelerations with low energy. The potential for RIS associated with the Make-Up Pond C impoundment is considered low with a negligible risk to safe operations for Lee Nuclear Station Units 1 and 2.

2.5.2.2 Geologic and Tectonic Characterizations of the Site and Region

As described in Subsection 2.5.1, a comprehensive review of available geological, seismological, and geophysical data has been performed for the Lee Nuclear Site region and adjoining areas. Subsection 2.5.1.1.1 describes regional physiography, geomorphology, and stratigraphy. Subsection 2.5.1.1.2 describes regional tectonic setting, including stress regimes and tectonic structures. The following subsections summarize seismic source interpretations from the 1989 EPRI PSHA study (Reference 203) and from relevant post-EPRI seismic source characterization studies and the updated interpretations of new and existing sources based on more recent data.

Since publication of the EPRI seismic source model, significant new information has been developed for assessing the earthquake source that produced the

1886 Charleston earthquake and the New Madrid seismic zone. This new information shows that the Charleston and New Madrid seismic sources should be updated according to RG 1.208. Results from the 1989 EPRI study show that the Charleston seismic source is the most significant contributor to seismic hazard at the Lee Nuclear Site (Reference 203). Thus, an update of the Charleston and New Madrid seismic sources has been developed in support of Subsection 2.5.2. Subsection 2.5.2.2.2.4 presents details of the Updated Charleston Seismic Source (UCSS). Subsection 2.5.2.4.3.2 presents details of the New Madrid seismic source update.

Sensitivity studies evaluating the potential significance of the UCSS model to seismic hazard at the Lee Nuclear Station show that the Charleston seismic source as characterized by the UCSS still dominates the seismic hazard at the Lee Nuclear Site. These new interpretations of the possible locations, sizes, and recurrence intervals of large earthquakes in the Charleston area form a strong basis with which to calculate the seismic ground motion hazard for the site.

2.5.2.2.1 Summary of EPRI Seismic Sources

This subsection summarizes the seismic sources and parameters used in the 1986 EPRI project (Reference 201). The description of seismic sources is limited to those sources within the Lee Nuclear Site region and those beyond the site region that may affect the seismic hazard at the Lee Nuclear Station.

In the 1986 EPRI project, six independent ESTs evaluate geological, geophysical, and seismological data to develop a model of seismic sources in the CEUS. These sources are used to model the occurrence of future earthquakes and evaluate earthquake hazards at nuclear power plant sites across the CEUS.

The six ESTs involved in the 1986 EPRI project are Bechtel Group, Dames & Moore, Law Engineering, Rondout Associates, Weston Geophysical Corporation, and Woodward-Clyde Consultants. Each team produced a report (volumes 5 through 10 of EPRI NP-4726, Reference 201) providing detailed descriptions of how they identify and define seismic sources. The results were implemented into a PSHA study (Reference 203). For the computation of hazard in the 1989 study, a few seismic source parameters are modified or simplified from the original parameters determined by the six ESTs. EPRI NP-6452-D (Reference 207) summarizes the parameters used in the final PSHA calculations, and this reference is the primary source for the seismicity parameters used in Subsection 2.5.2. Each EST provides more detailed descriptions of the rationale and methodology used in evaluating tectonic features and establishing the seismic sources (Reference 201).

The most significant seismic sources developed by each EST are shown in Figures 2.5.2-203 through 2.5.2-208. For the 1989 EPRI seismic hazard calculations, a screening criterion identifies those sources whose combined hazard exceeds 99 percent of the total hazard from all sources, for two ground motions measures. These sources are identified in the descriptions below as “primary” seismic sources. Other sources, which together contribute less than one percent of the total hazard from all sources for the two ground motion measures,

are identified in the descriptions below as “additional” seismic sources. Figures 2.5.2-203 through 2.5.2-208 also show earthquakes with body-wave magnitude $m_b \geq 3.0$ to illustrate the spatial relationships between seismicity and seismic sources. Earthquake epicenters include events from the EPRI earthquake catalog and for the period between 1985 and 2005 as described in Subsection 2.5.2.1.2.

The maximum magnitude (M_{max}), interdependencies, and probability of activity for each EPRI EST’s seismic sources are presented in Tables 2.5.2-202 through 2.5.2-207. These tables present the parameters assigned to each source, including primary and additional seismic sources as defined above. The tables also indicate whether new information has been identified that would lead to a revision of the source’s geometry, M_{max}, or recurrence parameters. The seismicity recurrence parameters (a- and b-values) used in the seismic hazard studies are computed for each 1° latitude and longitude cell that intersects any portion of a seismic source.

The nomenclature used by each EST to describe the various seismic sources in the CEUS varies from team to team. In other words, different EPRI teams used a number of different names to describe the same or similar tectonic features or sources, or one team may describe seismic sources that another team does not. For example, the Charleston seismic source is modeled by each team but is called the “Charleston Area” and “Charleston Faults” by the Bechtel Group team; the “Charleston Seismic Zone” by the Dames & Moore, Law, and Weston teams; and “Charleston” by the Rondout and Woodward-Clyde teams. Each team’s source names, data, and rationale are included in its team-specific documentation (Reference 201).

The EPRI PSHA study expresses maximum magnitude values in terms of body-wave magnitude (m_b), whereas most modern seismic hazard analyses describe M_{max} in terms of moment magnitude (**M**). To provide a consistent comparison between magnitude scales, this section relates body-wave magnitude to moment magnitude using the arithmetic average of three equations, or their inversions, presented in Atkinson and Boore (1995) (Reference 208), Frankel et al. (1996) (Reference 209), and EPRI TR-102293 (Reference 273). Table 2.5.2-208 lists m_b and **M** equivalences developed from these relations over the range of interest for this study. Throughout this subsection, the largest assigned values of M_{max} distributions assigned by the ESTs to seismic sources are presented for both magnitude scales (m_b and **M**) to give perspective on the maximum earthquakes that were considered possible in each seismic source. For example, EPRI m_b values of M_{max} are followed by the equivalent **M** values.

The following subsections describe the most significant EPRI sources (both primary and additional seismic sources) for each EST with respect to the Lee Nuclear Site. Assessment of these and other EPRI sources within the site region shows that the EPRI source parameters (M_{max}, geometry, and recurrence) are sufficient to capture the current understanding of the seismic hazard in the site region.

Except for the Charleston and New Madrid seismic sources, no new geological, geophysical, or seismological information in the literature published since the EPRI NP-6395-D (Reference 203) source model suggests that these sources should be modified. Each EST's characterization of the Charleston seismic source is replaced by four alternative source geometries. For each geometry, large earthquake occurrences (**M** 6.7 to 7.5) are modeled with a range of mean recurrence rates, and smaller earthquakes (m_b 5 to 6.7) are modeled with an exponential magnitude distribution, with rates and b-values determined from historical seismicity. Also, all surrounding sources for each team are redrawn so that the new Charleston source geometries are accurately represented as a "hole" in the surrounding source, and seismic activity rates and b-values are recalculated for the modified surrounding sources, based on historical seismicity. Subsection 2.5.2.2.2.4. presents additional discussion of the updated Charleston seismic source model.

The Dames & Moore team is the only EST for which the New Madrid seismic source contributes, albeit at a low level, to the hazard at the Lee Nuclear Site. Subsection 2.5.2.4.3.2 presents additional discussion of the updated New Madrid seismic source model.

2.5.2.2.1.1 Sources Used for EPRI PSHA – Bechtel Group

Bechtel Group identifies and characterizes seven primary seismic sources. All seven of these primary seismic sources are located within the site region. These sources are:

- Charleston Area (H)
- Charleston Faults (N3)
- Atlantic Coastal Region (BZ4)
- S Appalachians (BZ5)
- SE Appalachians (F)
- NW South Carolina (G)
- Combination Source H-N3 (C07)

In addition to these primary sources, the Bechtel Group characterizes six additional seismic sources. These additional seismic sources are:

- Eastern Mesozoic Basins (13)
- Rosman Fault (15)
- Belair Fault (16)

- Bristol Trends (24)
- New York-Alabama Lineament (25)
- New York-Alabama Lineament – alternative configuration (25A)

Table 2.5.2-202 lists primary and additional seismic sources characterized by the Bechtel Group team. Figure 2.5.2-203 shows locations and geometries of the Bechtel primary seismic sources. Following is a brief discussion of each of the primary seismic sources characterized by the Bechtel Group team.

Charleston Area (H). The Charleston Area source (H) is located about 110 mi. from the Lee Nuclear Site. This oblong combination source area is defined based on the historic earthquake pattern (including the Middleton Place-Summerville and Bowman seismic zones), is elongated northwest-southeast, and encompasses all of source zone N3 (described below). Sources H and N3 are interdependent; if N3 is active, it is unlikely that H is active, and vice versa. The Bechtel Group assigns a maximum M_{max} value of m_b 7.4 (**M** 7.9) to this zone, reflecting its assumption that Charleston-type earthquakes are produced within this source.

Charleston Faults (N3). The Charleston Faults (N3) source zone is a small area set within the Charleston Area (H) source zone and encompassing a number of identified and postulated faults in the Charleston, South Carolina, area, including the Ashley River, Charleston, and Woodstock faults. Source N3 is located approximately 150 mi. from the Lee Nuclear Site. Sources H and N3 are interdependent; if N3 is active, it is unlikely that H is active, and vice versa. According to EPRI NP-4726, this combination was created for computational simplicity. The Bechtel Group assigns a maximum M_{max} value of m_b 7.4 (**M** 7.9) to this zone, reflecting its assumption that Charleston-type earthquakes are produced within this source.

Atlantic Coastal Region (BZ4). The Atlantic Coastal Region background (BZ4) source zone is located about 100 mi. from the Lee Nuclear Site. Source BZ4 is a large background zone that extends from offshore New England to Alabama and encompasses portions of the Coastal Plain from Georgia to southern Virginia. The Bechtel Group assigns a maximum M_{max} value of m_b 7.4 (**M** 7.9) to this source, reflecting its assumption that there is a small probability that a Charleston-type earthquake could occur within this region.

S Appalachians (BZ5). The Lee Nuclear Site is located within the Southern Appalachians background source (BZ5). This source is a large background region that extends from New York to Alabama, including portions of the Southern Appalachians, Piedmont, and Coastal Plain. The Bechtel Group assigns a maximum M_{max} value of m_b 6.6 (**M** 6.5) to this source.

SE Appalachians (F). The Lee Nuclear Site is located within the Southeastern Appalachians source (F), a combination source zone that includes parts of Georgia and the Carolinas and flanks the southwest and northeast borders of Zone G (described below). Source Zone F is mutually exclusive with Zone G; if F

is active, G is inactive, and vice versa. The Bechtel Group assigns a maximum M_{max} value of m_b 6.6 (**M** 6.5) to this source.

NW South Carolina (G). The Lee Nuclear Site is located within the Northwestern South Carolina combination source (G). Source Zone G is mutually exclusive with Zone F; if G is active, F is inactive, and vice versa. The Bechtel Group assigns a maximum M_{max} value of m_b 6.6 (**M** 6.5) to this source.

Combination Zone (C07). Combination Zone (C07) includes both the Charleston Area (H) and the Charleston Faults (N3) sources. The Bechtel Group assigns a maximum M_{max} value of m_b 7.4 (**M** 7.9) to this combination zone, reflecting its assumption that Charleston-type earthquakes are produced within this source.

2.5.2.2.1.2 Sources Used for EPRI PSHA – Dames & Moore

Dames & Moore identifies and characterizes eight primary seismic sources. These eight sources are:

- Appalachian Fold Belt (04)
- Kink in Fold Belts (4A)
- Kink in Fold Belts (4B)
- New Madrid (21)
- S Cratonic Margin (Default Zone) (41)
- S Appalachian Mobile Belt (Default Zone) (53)
- Charleston Seismic Zone (54)
- Combination Zone [4-4A-4B-4C-4D] (C01)

In addition to these primary sources, Dames & Moore identifies six additional seismic sources. These additional seismic sources are:

- Dan River Basin (46)
- Jonesboro Basin (49)
- Buried Triassic Basins (50)
- Florence Basin (51)
- Charleston Mesozoic Rift (52)
- Dunbarton Triassic Basin (65)

Table 2.5.2-203 lists primary and additional seismic sources characterized by the Dames & Moore team. Figure 2.5.2-204 shows locations and geometries of the Dames & Moore primary seismic sources. Following is a brief discussion of these primary seismic sources.

Appalachian Fold Belt (04). The Appalachian Fold Belt (04) source is located about 80 mi. northwest of the Lee Nuclear Site. This source is mutually exclusive with Kink in Fold Belts sources 4A and 4B. Dames & Moore assigns a maximum M_{max} value of m_b 7.2 (**M** 7.5) to this source.

Kink in Fold Belts (4A). The Kink in Fold Belts (4A) source is located about 120 mi. northwest of the Lee Nuclear Site. Source 4A is contained within, and is mutually exclusive with, source 04 (Appalachian Fold Belt). Dames & Moore assigns a maximum M_{max} value of m_b 7.2 (**M** 7.5) to this source.

Kink in Fold Belts (4B). The Kink in Fold Belts (4B) source is located about 110 mi. north of the Lee Nuclear Site and includes the both the Giles County seismic zone and the failed arm of an ancient rift. Source 4B is contained within, and is mutually exclusive with, source 04 (Appalachian Fold Belt). Dames & Moore assigns a maximum M_{max} value of m_b 7.2 (**M** 7.5) to this source.

New Madrid (21). The New Madrid (21) source is located about 440 mi. west of the Lee Nuclear Site, and includes a linear zone of microseismicity within the Reelfoot Rift as well as the sequence of large earthquakes that occurred in 1811 and 1812. Dames & Moore assigns a maximum M_{max} value of m_b 7.5 (**M** 8.0) to this source.

S Cratonic Margin (Default Zone) (41). The Lee Nuclear Site is located within the Southern Cratonic Margin (Default Zone) source. This large default zone is located between the Appalachian Fold Belt (4) and the Southern Appalachian Mobile Belt (53) sources and includes the region of continental margin deformed during Mesozoic rifting. Numerous Triassic basins and border faults are located within this default zone. Dames & Moore assigns a maximum M_{max} value of m_b 7.2 (**M** 7.5) to this source.

S Appalachian Mobile Belt (Default Zone) (53). The Lee Nuclear Site is located about 25 mi. northwest of the Southern Appalachian Mobile Belt (Default Zone) source (53). This default zone comprises crustal rocks that have undergone several periods of divergence and convergence. The East Coast magnetic anomaly bounds source 53 on the east, and the westernmost boundary of the Appalachian gravity gradient bounds source 53 on the west. Dames & Moore assigns a maximum M_{max} value of m_b 7.2 (**M** 7.5) to this source.

Charleston Seismic Zone (54). The Charleston Seismic Zone (54) is a northwest-southeast oriented polygon located about 110 mi. from the Lee Nuclear Site. This source includes the Ashley River, Woodstock, Helena Banks, and Cooke faults, as well as the Bowman and Middleton Place-Summerville seismic

zones and is designed to capture the occurrence of Charleston-type earthquakes. Dames & Moore assigns a maximum M_{max} value of m_b 7.2 (**M** 7.5) to this source.

Combination Zone [4-4A-4B-4C-4D] (C01). Combination source C01 comprises five source zones (Appalachian Fold Belt (04), Kink in Fold Belts (4A), Kink in Fold Belts (4B), Kink in Fold Belt (4C), and Kink in Fold Belt (4D)). This large combination source zone is located about 80 mi. from the Lee Nuclear Site. Dames & Moore assigns a maximum M_{max} value of m_b 7.2 (**M** 7.5) to this source.

2.5.2.2.1.3 Sources Used for EPRI PSHA – Law Engineering

Law Engineering identifies and characterizes sixteen primary seismic sources all within the site region. These sources are:

- Eastern Basement (17)
- Reactivated E Seaboard Normal (22)
- Charleston Seismic Zone (35)
- Eastern Piedmont (107)
- Brunswick, NC Background (108)
- 22 – 35 (C11)
- 22 – 24 (C12)
- 22 – 24 – 25 (C13)
- Eight mafic pluton sources (M31 through M37, and M39)

In addition to these primary sources, Law Engineering characterizes three additional seismic sources. These additional seismic sources are:

- Mesozoic Basins (8-bridged) (C09)
- 8 – 35 (C10)
- One mafic pluton source (M38)

Table 2.5.2-204 lists primary and additional seismic sources characterized by the Law Engineering team. Figure 2.5.2-205 shows locations and geometries of the Law Engineering primary seismic sources. Following is a brief discussion of Law's primary seismic sources.

Eastern Basement (17). The Lee Nuclear Site is located about 10 mi. from the Eastern Basement (17) source. This source is defined as an area containing pre-Cambrian and Cambrian normal faults, developed during the opening of the

proto-Atlantic Ocean, in the basement rocks beneath the Appalachian decollement. This source includes both the Giles County and Eastern Tennessee seismic zones. Law Engineering assigns a maximum M_{max} value of m_b 6.8 (**M** 6.8) to this source.

Reactivated E Seaboard Normal (22). The Reactivated Eastern Seaboard Normal (22) source is characterized as a region along the eastern seaboard in which Mesozoic normal faults are reactivated as high-angle reverse faults. Law Engineering assigns a single M_{max} of m_b 6.8 (**M** 6.8) to this source.

Charleston Seismic Zone (35). The Charleston Seismic Zone source (35) is a northeast-southwest elongated polygon that includes the Charleston, Ashley River, and Woodstock faults, as well as parts of the offshore Helena Banks fault and most of the more recently discovered liquefaction features identified by Amick (1990) and others. This source is designed to capture the occurrence of Charleston-type earthquakes. This source is located about 100 mi. from the Lee Nuclear Site and overlaps with the Reactivated E Seaboard Normal (22; described above) and Buried Mesozoic Basins (additional source) sources. Law Engineering assigns a maximum M_{max} value of m_b 6.8 (**M** 6.8) to this source.

Eastern Piedmont (107). The Lee Nuclear Site is located within the Eastern Piedmont (107) source zone. This source zone is characterized as a region believed to represent a crustal block overlying mafic transitional or mafic crust located east of the relict North American continental margin and possibly underlain by a regional detachment. Law Engineering assigns a maximum M_{max} value of m_b 5.7 (**M** 5.3) to this source.

Brunswick, NC Background (108). The Lee Nuclear Site is located 100 mi. from the Brunswick, NC Background source zone (108). Despite its name, Law Engineering source 108 does not include any portion of North Carolina. However, Law Engineering source 108 does include Brunswick, Georgia. This discrepancy is potentially misleading, and apparently is the result of a minor naming error in EPRI NP-6452-D (Reference 207). To be consistent with EPRI NP-6452-D (Reference 207), the source name “Brunswick, NC Background” is reported herein. This source represents a zone defined by a low-amplitude, long-wavelength magnetic anomaly pattern. The Law Engineering team interprets this pattern as possibly indicating a zone of Mesozoic extended crust. Law Engineering assigns a maximum M_{max} value of m_b 6.8 (**M** 6.8) to this source.

22 – 35 (C11). The Lee Nuclear Site is located within the 22 – 35 combination source (C11). Law Engineering assigns a maximum M_{max} value of m_b 6.8 (**M** 6.8) to this source.

22 – 24 (C12). The Lee Nuclear Site is located 60 mi. from the 22 – 24 combination source (C12). Law Engineering assigns a maximum M_{max} value of m_b 6.8 (**M** 6.8) to this source.

22 – 24 – 35 (C13). The Lee Nuclear Site is located 60 mi. from the 22 – 24 – 35 combination source (C13). Law Engineering assigns a maximum M_{max} value of m_b 6.8 (**M** 6.8) to this source.

Eight Mafic Pluton Sources (M31 through M37, and M39). The Law Engineering team identifies a number of mafic pluton sources located within the Lee Nuclear Site region. The Law Engineering team considers pre- and post-metamorphic plutons in the Appalachians to be stress concentrators and, thus, potential earthquake sources. Law Engineering assigns a single M_{max} of m_b 6.8 (**M** 6.8) to all mafic pluton sources.

2.5.2.2.1.4 Sources Used for EPRI PSHA – Rondout Associates

Rondout Associates identifies and characterizes five primary seismic sources within the site region. These sources are:

- Charleston (24)
- Southern Appalachians (25)
- South Carolina (26)
- Tennessee-Virginia Border Zone (27)
- Giles County (28)

In addition to these primary sources, Rondout Associates identifies five additional seismic sources within the site region. These additional seismic sources are:

- Background 49 (C01)
- Background 50 (C02)
- 50 (02) + 12 (C07)
- 49 + 32 (C09)
- Grenville Province (50)

Table 2.5.2-205 lists primary and additional seismic sources characterized by the Rondout Associates team. Figure 2.5.2-206 shows locations and geometries of the Rondout Associates primary seismic sources. Following is a brief discussion of both of these primary seismic sources.

Charleston (24). The Charleston source is a northwest-southeast-oriented area set within the larger South Carolina (26) source and located about 100 mi. from the Lee Nuclear Site. Source 24 includes the Helena Banks, Charleston, Ashley River, and Woodstock faults, as well as the Bowman and Middleton Place-Summerville seismic zones, and is designed to capture the occurrence of

Charleston-type earthquakes. The Rondout Associates team assigns a maximum M_{max} of m_b 7.0 (**M** 7.2) to this source.

Southern Appalachians (25). The Lee Nuclear Site is located about 90 mi. southeast of the Southern Appalachians (25) source. Source 25 includes portions of the New York-Alabama and Clingman lineaments, and deep-seated seismicity. The Rondout Associates team assigns a maximum M_{max} of m_b 7.0 (**M** 7.2) to this source.

South Carolina (26). The Lee Nuclear Site is located within the South Carolina source (26). The South Carolina source (26) is a northwest-southeast elongated area that surrounds, but does not include, Source 24 (described above). Source 26 includes most of South Carolina except the Charleston area. The Rondout Associates team assigns a maximum M_{max} of m_b 6.8 (**M** 6.8) to this source.

Tennessee-Virginia Border Zone (27). The Lee Nuclear Site is located about 75 mi. south-southeast of the Tennessee-Virginia border zone (27) source. Source 27 includes portions of the New York-Alabama and Clingman lineaments, and lies between the more active East Tennessee and Giles County areas. The Rondout Associates team assigns a maximum M_{max} of m_b 6.5 (**M** 6.3) to this source.

Giles County (28). The Lee Nuclear Site is located about 110 mi. south-southwest of the Giles County Seismic Zone (28) source. Source 28 includes an area of elevated historical seismicity, potentially associated with the possible reactivation of Paleozoic normal faults inferred from aeromagnetic data. The Rondout Associates team assigns a maximum M_{max} of m_b 7.0 (**M** 7.2) to this source.

2.5.2.2.1.5 Sources Used for EPRI PSHA – Weston Geophysical

Weston Geophysical identifies and characterizes nine primary seismic sources within the site region. These sources are:

- Giles County (23)
- New York-Alabama-Clingman (24)
- Charleston Seismic Zone (25)
- South Carolina (26)
- S Appalachian (103)
- 103 – 23 (C17)
- 103 – 24 (C18)

- 103 – 23 – 24 (C19)
- 26 – 25 (C33)

In addition to these primary sources, Weston Geophysical characterizes thirteen additional seismic sources. These additional seismic sources are:

- S Coastal Plain (104)
- 28A through E (C01)
- 104 – 22 (C20)
- 104 – 25 (C21)
- 104 – 26 (C22)
- 104 – 22 – 26 (C23)
- 104 – 22 – 25 (C24)
- 104 – 28BCDE (C25)
- 104 – 28BCDE – 22 (C26)
- 104 – 28BCDE – 22 – 25 (C27)
- 104 – 28BCDE – 22 – 26 (C28)
- 104 – 28BE – 26 (C34)
- 104 – 28BE – 25 (C35)

Table 2.5.2-206 lists primary and additional seismic sources characterized by the Weston Geophysical team. Figure 2.5.2-207 shows locations and geometries of the Weston Geophysical primary seismic sources. Following is a brief discussion of each of the Weston Geophysical team's primary seismic sources.

Giles County (23). A discrete cluster of seismicity in Giles County, Virginia defines the Giles County source (23). Source 23 is about 120 mi. north of the Lee Nuclear Site and is contained within the S. Appalachians source (103, described below). Weston Geophysical assigns a maximum M_{max} of m_b 6.6 (**M** 6.5) to this source.

New York-Alabama-Clingman (24). Source 24 represents the crustal block bounded by the New York-Alabama and Clingman lineaments. Source 24 is about 90 mi. from the Lee Nuclear Site and is contained within the S. Appalachians source (103, described below)**.** Weston Geophysical assigns a maximum M_{max} of m_b 6.6 (**M** 6.5) to this source.

Charleston Seismic Zone (25). The Charleston Seismic Zone source is an irregularly shaped hexagon centered just northeast of Charleston, South Carolina, and located about 80 mi. from the Lee Nuclear Site. This source includes the Helena Banks, Charleston, Ashley River, and Woodstock faults, but does not include the Bowman seismic zone. This source is designed to capture the occurrence of Charleston-type earthquakes. Weston Geophysical assigns a maximum M_{max} of m_b 7.2 (**M** 7.5) to this source.

South Carolina (26). The South Carolina source (26) is a large area covering most of South Carolina and the Lee Nuclear Site. Weston Geophysical assigns a maximum M_{max} of m_b 7.2 (**M** 7.5) to this source.

S Appalachian (103). The S Appalachian source (103) is a large area covering much of the Appalachian Mountains from Pennsylvania to Alabama. Weston Geophysical assigns a maximum M_{max} of m_b 6.6 (**M** 6.5) to this source.

Four Combination Zones (103 – 23 (C17); 103 – 24 (C18); 103 – 23 – 24 (C19); and 26 – 25 (C33)). Weston Geophysical specifies a number of combination seismic source zones, four of which are primary sources for the Lee Nuclear Site. Weston Geophysical assigns a maximum M_{max} of m_b 6.6 (**M** 6.5) to sources C17 through C19, and m_b 7.2 (**M** 7.5) to source C33.

2.5.2.2.1.6 Sources Used for EPRI PSHA – Woodward-Clyde Consultants

Woodward-Clyde Consultants identifies and characterizes seven primary seismic sources within the site region. These sources are:

- S Carolina Gravity Saddle (Extended) (29)
- SC Gravity Saddle No. 2 (Combo C3) (29A)
- SC Gravity Saddle No. 3 (NW Portion) (29B)
- Charleston (includes “none of the above,” NOTA) (30)
- Blue Ridge Combination (31)
- Blue Ridge Combination – Alternate Configuration (31A)
- Lee Nuclear Station Background

Woodward-Clyde Consultants does not identify any additional seismic sources.

Table 2.5.2-207 lists primary and additional seismic sources characterized by the Woodward-Clyde team. Figure 2.5.2-208 shows the locations and geometries of the Woodward-Clyde primary seismic sources. Following is a brief discussion of each of the primary seismic sources identified by the Woodward-Clyde team.

S Carolina Gravity Saddle (Extended) (29). The South Carolina Gravity Saddle (Extended) source (29) covers most of South Carolina and parts of Georgia, including the Lee Nuclear Site. The South Carolina Gravity Saddle source (29) is mutually exclusive with Sources 29A, 29B, and 30; if 29 is active, the other three are inactive, and vice versa. The Woodward-Clyde Consultants team assigns a maximum M_{max} value of m_b 7.4 (**M** 7.9) to this zone, reflecting the assumption that Charleston-type earthquakes can occur in this zone.

SC Gravity Saddle No. 2 (Combo C3) (29A). The South Carolina Gravity Saddle No. 2 source (29A) is an irregularly shaped polygon set within the larger area of Source 29 that includes the Lee Nuclear Site. The SC Gravity Saddle No. 2 source (29A) is mutually exclusive with Sources 29, 29B, and 30; if 29A is active, the other three are inactive, and vice versa. The Woodward-Clyde Consultants team assigns a maximum M_{max} value of m_b 7.4 (**M** 7.9) to this zone, reflecting the assumption that Charleston-type earthquakes can occur in this zone.

SC Gravity Saddle No. 3 (NW Portion) (29B). The South Carolina Gravity Saddle No. 3 source (29B) is a polygon set within the larger area of Source 29 and includes the Lee Nuclear Site. The SC Gravity Saddle No. 3 source (29B) is mutually exclusive with Sources 29, 29A, and 30; if 29B is active, the other three are inactive, and vice versa. The Woodward-Clyde Consultants team assigns a maximum M_{max} value of m_b 7.0 (**M** 7.2) to this zone.

Charleston (includes NOTA) (30). The Charleston seismic source (30) is a northeast-southwest-oriented rectangle that includes most of the Charleston earthquake MMI IX and X area and the Charleston, Ashley River, and Woodstock faults. Source 30 is located about 150 mi. from the Lee Nuclear Site and is designed to capture the occurrence of Charleston-type earthquakes. The Charleston source (30) is mutually exclusive with Sources 29, 29A, and 29B; if 30 is active, the other three are inactive, and vice versa. The Woodward-Clyde Consultants team assigns a maximum M_{max} value of m_b 7.5 (**M** 8.0) to this zone, reflecting the assumption that Charleston-type earthquakes can occur in this zone.

Blue Ridge Combination (31). The Blue Ridge Combination source (31) includes an isostatic gravity low that extends from eastern Tennessee and western North Carolina to the Virginia-Maryland border. Source 31 is located about 40 mi. from the Lee Nuclear Site, and is mutually exclusive with source 31A. The Woodward-Clyde Consultants team assigns a maximum M_{max} value of m_b 7.0 (**M** 7.2) to this zone.

Blue Ridge Combination – Alternate Configuration (31A). The Blue Ridge Combination - Alternate Configuration source (31A) represents an alternative interpretation of source 31, and is located about 40 mi. from the Lee Nuclear Site. Source 31A is mutually exclusive with source 31. The Woodward-Clyde Consultants team assigns a maximum M_{max} value of m_b 7.0 (**M** 7.2) to this zone.

Lee Nuclear Station Background. The Lee Nuclear Station Background source is represented as a large box containing the Lee Nuclear Site and covering most

of South Carolina and Georgia as well as parts of adjoining states and extending offshore. This source is a background zone defined as a rectangular area surrounding the Lee Nuclear Site and is not based on any geological, geophysical, or seismological features. The Woodward-Clyde Consultants team assigns a maximum M_{max} value of m_b 6.6 (**M** 6.5) to this zone.

2.5.2.2.2 Post-EPRI Seismic Source Characterization Studies

Since the EPRI seismic hazard project (References 201, 203, and 204), three recent studies characterize seismic sources within the Lee Nuclear Site region for PSHAs. These studies include the U.S. Geological Survey's (USGS) National Seismic Hazard Mapping Project (References 209 and 210), the South Carolina Department of Transportation's (SCDOT) seismic hazard mapping project (Reference 211), and the U.S. Nuclear Regulatory Commission's (NRC) Trial Implementation Project (TIP) study (Reference 212). These three studies are described below in Subsections 2.5.2.2.2.1 through 2.5.2.2.2.3. Review of recent studies highlights the need for an update of the Charleston and New Madrid seismic source models described by the EPRI (References 201, 203, and 204) seismic hazard project. Subsection 2.5.2.2.2.4 presents a discussion regarding the update to the Charleston seismic source model. Subsection 2.5.2.4.3.2 presents a discussion regarding the update to the New Madrid seismic source model. In addition, within the Lee Nuclear Site region is what is now identified as the Eastern Tennessee Seismic Zone (ETSZ). Subsection 2.5.2.2.2.5 presents a discussion regarding the significance of the ETSZ on the Lee Nuclear Station seismic hazard.

2.5.2.2.2.1 U.S. Geological Survey Model (Frankel et al. 2002)

In 2002, the USGS produced updated seismic hazard maps for the conterminous United States based on new seismological, geophysical, and geological information (Reference 210). The 2002 maps reflect changes to the source model used to construct the previous version of the national seismic hazard maps (Reference 209). The most significant modifications to the CEUS portion of the source model include changes in the recurrence, M_{max}, and geometry of the Charleston and New Madrid seismic sources.

Unlike the EPRI models that incorporate many local sources, the USGS source model in the CEUS includes only five sources: the Extended Margin background, Stable Craton background, Charleston, Eastern Tennessee, and New Madrid (Table 2.5.2-209). Except for the Charleston and New Madrid zones, where earthquake recurrence is modeled by paleoliquefaction data, the hazard for the large background or "maximum magnitude" zones is largely based on historical seismicity and the variation of that seismicity. The USGS source model defines the M_{max} distribution for the Extended Margin background source zone as a single magnitude of **M** 7.5 with a weight of 1.0. The EPRI model, however, includes multiple source zones for each of the six ESTs for this region containing the eastern seaboard and the Appalachians. The EPRI M_{max} distributions for these sources capture a wide range of magnitudes and weights, reflecting considerable uncertainty in the assessment of M_{max} for the CEUS. An **M** 7.5 M_{max} is captured

in most of the EPRI source zones, although at a lower weight than assigned by the USGS model.

As part of the 2002 update of the National Seismic Hazard Maps, the USGS developed a model of the Charleston source that incorporates available data regarding recurrence, M_{max}, and geometry of the source zone. The USGS model uses two equally weighted source geometries, one an areal source enveloping most of the tectonic features and liquefaction data in the greater Charleston area, and the second a north-northeast-trending elongated areal source enveloping the southern half of the southern segment of the East Coast fault system (ECFS) (Figure 2.5.2-209). The Frankel et al. (2002) (Reference 210) report does not specify why the entire southern segment of the ECFS is not contained in the source geometry. For M_{max}, the study defines a distribution of magnitudes and weights of **M** 6.8 [0.20], 7.1 [0.20], 7.3 [0.45], and 7.5 [0.15]. For recurrence, Frankel et al. (2002) (Reference 210) adopt a mean paleoliquefaction-based recurrence interval of 550 years and represent the uncertainty with a continuous lognormal distribution.

2.5.2.2.2.2 South Carolina Department of Transportation Model (Chapman and Talwani 2002)

Chapman and Talwani (2002) (Reference 211) present probabilistic seismic hazard maps created for the South Carolina Department of Transportation. In the SCDOT model, treatment of the 1886 Charleston, South Carolina, earthquake and similar events dominates estimates of seismic hazard statewide.

The SCDOT model employs a combination of line and area sources to characterize Charleston-type earthquakes using three separate geometries and a slightly different M_{max} range (**M** 7.1 to 7.5) than the USGS 2002 model (Table 2.5.2-210 and Figure 2.5.2-209). Three equally weighted source zones defined for this study include (1) a source capturing the intersection of the Woodstock and Ashley River faults, (2) a larger Coastal South Carolina zone that includes most of the paleoliquefaction sites, and (3) a southern ECFS source zone. The respective magnitude distributions and weights used for M_{max} are **M** 7.1 [0.20], 7.3 [0.60], and 7.5 [0.20]. The mean recurrence interval used in the SCDOT study is 550 years, based on the paleoliquefaction record.

2.5.2.2.2.3 The Trial Implementation Project Study

The purpose of the Lawrence Livermore National Laboratory Trial Implementation Project (TIP) study is to “test and implement the guidelines developed by the Senior Seismic Hazard Analysis Committee (SSHAC) developed under FIN L2503 (NRC 1997)” (Reference 212) (p. 1). To test the SSHAC PSHA methodology, the TIP study focuses on seismic zonation and earthquake recurrence models for the Watts Bar site in Tennessee and the Vogtle site in Georgia. The TIP study uses an expert elicitation process to characterize the Charleston seismic source, considering published data through 1996. The TIP study identifies multiple alternative zones for the Charleston source and for the South Carolina–Georgia seismic zone, as well as alternative background

seismicity zones for the Charleston region. However, the TIP study focuses primarily on implementing the SSHAC PSHA methodology (Reference 213) and was designed to be as much of a test of the methodology as a real estimate of seismic hazard. As a result, its findings are not included explicitly in the Lee Nuclear Station source model. However, Subsection 2.5.2.2.2.5 describes the TIP study in connection with the Eastern Tennessee Seismic Zone.

2.5.2.2.2.4 Updated Charleston Seismic Source (UCSS) Model

It has been more than 20 years since the six EPRI ESTs evaluated hypotheses for earthquake causes and tectonic features and assessed seismic sources in the CEUS (Reference 201). Figure 2.5.2-209 and Table 2.5.2-211 summarize the EPRI Charleston source zones developed by each EST. Several studies that post-date the 1986 EPRI EST assessments demonstrate that the source parameters for geometry, M_{max}, and recurrence of M_{max} in the Charleston seismic source need to be updated to capture a more current understanding for both the 1886 Charleston earthquake and the seismic source that produced this earthquake. In addition, recent PSHA studies of the South Carolina region (References 211 and 212) and the southeastern United States (Reference 210) describe models of the Charleston seismic source that differ significantly from the earlier EPRI characterizations. Therefore, Subsection 2.5.2 presents an update of the Charleston seismic source model, as developed for the Vogtle Electric Generating Plant's Early Site Permit (ESP) application.

The UCSS model is summarized below, in Figures 2.5.2-209 and 2.5.2-210, and presented in detail in Bechtel (2006) (Reference 214). Methods used to update the Charleston seismic source follow guidelines provided in RGs 1.165 and 1.208. A SSHAC Level 2 study was performed to incorporate current literature and data and the understanding of experts into an update of the Charleston seismic source model. This level of effort is outlined in the SSHAC report (Reference 213), which provides guidance on incorporating uncertainty and the use of experts in PSHA studies.

The UCSS model incorporates new information to re-characterize geometry, M_{max}, and recurrence for the Charleston seismic source. The following subsections present discussions of these source parameters. Paleoliquefaction data imply that the Charleston earthquake process is defined by repeated, relatively frequent, large earthquakes located in the vicinity of Charleston, indicating that the Charleston source is different from the rest of the eastern seaboard.

2.5.2.2.2.4.1 UCSS Geometry

The UCSS model includes four mutually exclusive source zone geometries (A, B, B', and C; Figures 2.5.2-209 and 2.5.2-210). Table 2.5.2-212 presents the latitude and longitude coordinates that define these four source zones. The four geometries of the UCSS model are defined based on current understanding of geologic and tectonic features in the 1886 Charleston earthquake epicentral region; the 1886 Charleston earthquake shaking intensity; distribution of

seismicity; and geographic distribution, age, and density of liquefaction features associated with both the 1886 and prehistoric earthquakes. These features strongly suggest that the majority of evidence for the Charleston source is concentrated in the Charleston area and is not widely distributed throughout South Carolina (Figures 2.5.2-211 and 2.5.1-215 through 2.5.1-217). Table 2.5.2-213 provides a subset of the Charleston tectonic features differentiated by pre- and post-EPRI information. In addition, Figures 2.5.1-215 through 2.5.1-217 show pre- and post-1986 instrumental seismicity ($m_b \geq 3$). Seismicity continues to be concentrated in the Charleston region in the Middleton Place–Summerville seismic zone (MPSSZ), which has been used to define the intersection of the Woodstock and Ashley River faults (References 215 and 216). Notably, two earthquakes in 2002 (m_b 3.5 and 4.4) are located offshore of South Carolina along the Helena Banks fault zone in an area previously devoid of seismicity of $m_b \geq 3$. Figure 2.5.2-209 presents a compilation of the EPRI EST Charleston source zones, the USGS model Charleston seismic source zones, the SCDOT Charleston seismic source zones, and the UCSS model geometries.

Geometry A - Charleston. Geometry A is an approximately 100 x 50 km, northeast-oriented area centered on the 1886 Charleston meizoseismal area (Figure 2.5.2-209). Geometry A is intended to represent a localized source area that generally confines the Charleston source to the 1886 meizoseismal area (i.e., a stationary source in time and space). Geometry A completely incorporates the 1886 earthquake MMI X isoseismal (Reference 217), the majority of identified Charleston-area tectonic features and inferred fault intersections, and the majority of reported 1886 liquefaction features. Geometry A excludes the northern extension of the southern segment of the East Coast fault system because this system extends well north of the meizoseismal zone and is included in its own source geometry (Geometry C). Geometry A also excludes outlying liquefaction features, because liquefaction occurs as a result of strong ground shaking that may extend well beyond the areal extent of the tectonic source. Geometry A also envelops instrumentally located earthquakes spatially associated with the MPSSZ (References 215, 216, and 218).

The preponderance of evidence strongly supports the conclusion that the seismic source for the 1886 Charleston earthquake is located in a relatively restricted area defined by Geometry A. Geometry A envelops (1) the meizoseismal area of the 1886 earthquake, (2) the area containing the majority of local tectonic features (although many have large uncertainties associated with their existence and activity, as described earlier), (3) the area of ongoing concentrated seismicity, and (4) the area of greatest density of 1886 liquefaction and prehistoric liquefaction. These observations show that future earthquakes having magnitudes comparable to the Charleston earthquake of 1886 most likely will occur within the area defined by Geometry A. The UCSS model assigns a weight of 0.70 to Geometry A (Figure 2.5.2-210). To confine the rupture dimension to within the source area and to maintain a preferred northeast fault orientation, Geometry A is represented in the model by a series of closely spaced, northeast-trending faults parallel to the long axis of the zone.

Geometries B, B', and C. Whereas the preponderance of evidence supports the assessment that the 1886 Charleston meizoseismal area and Geometry A define the area where future events will most likely be centered, it is possible that the tectonic feature responsible for the 1886 earthquake either extends beyond or lies outside Geometry A. Therefore, the remaining three geometries (B, B', and C) are assessed to capture the uncertainty that future events may not be restricted to Geometry A. The distribution of liquefaction features along the entire coast of South Carolina and observations from the paleoliquefaction record that a few events were localized (moderate earthquakes to the northeast and southwest of Charleston), suggest that the Charleston source could extend well beyond Charleston proper. Geometries B and B' represent a larger source zone, while Geometry C represents the southern segment of the East Coast fault system as a possible source zone. The UCSS model assigns a weight of 0.20 to the combined geometries of B and B', and a weight of 0.10 to Geometry C. Geometry B' a subset of B, formally defines the onshore coastal area as a source (similar to the SCDOT coastal source zone) that restricts earthquakes to the onshore region. Geometry B, which includes the onshore and offshore regions, and Geometry B' are mutually exclusive. The UCSS model assigns equal weights of 0.10 to Geometries B and B'.

Geometry B - Coastal and Offshore Zone. Geometry B is a coast-parallel, approximately 260 x 100 km source area that (1) incorporates all of Geometry A, (2) is elongated to the northeast and southwest to capture other, more distant liquefaction features in coastal South Carolina (References 219, 220, 221, and 222), and (3) extends to the southeast to include the offshore Helena Banks fault zone (Reference 223) (Figure 2.5.2-209). The elongation and orientation of Geometry B is roughly parallel to the regional structural grain as well as roughly parallel to the elongation of 1886 isoseismals. The mapped extent of paleoliquefaction features (References 219, 220, 221, and 222) defines the northeastern and southwestern extents of Geometry B.

The location and timing of paleoliquefaction features in the Georgetown and Bluffton areas to the northeast and southwest of Charleston suggest to some researchers that the earthquake source may not be restricted to the Charleston area (References 220, 222, 224, and 225). Geometry B accounts for the possibility that there may be an elongated source or multiple sources along the South Carolina coast. Paleoliquefaction features in the Georgetown and Bluffton areas may be explained by an earthquake source both northeast and southwest of Charleston, as well as possibly offshore.

Geometry B extends southeast to include an offshore area and the Helena Banks fault zone. The Helena Banks fault zone is clearly shown by multiple seismic reflection profiles and has demonstrable late Miocene offset (Reference 223). Offshore earthquakes in 2002 (m_b 3.5 and 4.4) suggest a possible spatial association of seismicity with the mapped trace of the Helena Banks fault system (Figure 2.5.2-209). Whereas these two events in the vicinity of the Helena Banks fault system do not provide a positive correlation with seismicity or demonstrate recent fault activity, these small earthquakes are new data that post-date the EPRI studies. The EPRI earthquake catalog (Reference 204) is devoid of any events

($m_b \geq 3.0$) offshore from Charleston. The recent offshore seismicity also post-dates the development of the USGS and SCDOT source models that exclude any offshore Charleston source geometries.

The UCSS model assigns a low weight of 0.10 to Geometry B (Figure 2.5.2-210), because the preponderance of evidence indicates that the seismic source that produced the 1886 earthquake lies onshore in the Charleston meizoseismal area and not in the offshore region. To confine the rupture dimension to within the source area and to maintain a preferred northeast fault orientation, the UCSS model represents Geometry B as a series of closely spaced, northeast-trending faults parallel to the long axis of the zone.

Geometry B' - Coastal Zone. Geometry B' is a coast-parallel, approximately 260 x 50 km source area that incorporates all of Geometry A, as well as the majority of reported paleoliquefaction features (References 219, 220, 221, and 222). Unlike Geometry B, however, Geometry B' does not include the offshore Helena Banks fault zone (Figure 2.5.2-209).

The Helena Banks fault system is excluded from Geometry B' because the preponderance of data and evaluations support the assessment that the fault system is not active and because evidence strongly suggests that the 1886 Charleston earthquake occurred onshore in the 1886 meizoseismal area and not on an offshore fault. Whereas there is little uncertainty regarding the existence of the Helena Banks fault, there is a lack of evidence that this feature is still active. Isoseismal maps documenting shaking intensity in 1886 indicate an onshore meizoseismal area (the closed bull's eye centered onshore north of downtown Charleston, Figures 2.5.1-215 and 2.5.1-216). An onshore source for the 1886 earthquake and prehistoric events is supported by the instrumentally recorded seismicity in the MPSSZ and the corresponding high-density cluster of 1886 and prehistoric liquefaction features.

Similar to Geometry B above, the UCSS model assigns a weight of 0.10 to Geometry B', reflecting the assessment that Geometry B' has a much lower probability of being the source zone for Charleston-type earthquakes than Geometry A (Figure 2.5.2-210). To confine the rupture dimension to within the source area and to maintain a preferred northeast fault orientation, the UCSS model represents Geometry B' as a series of closely spaced, northeast-trending faults parallel to the long axis of the zone.

Geometry C - East Coast Fault System - South (ECFS-s). Geometry C is an approximately 200 x 30 km, north-northeast-oriented source area (Figure 2.5.2-209) enveloping the southern segment of the proposed East Coast fault system (ECFS-s) shown in Figure 3 of Marple and Talwani (2000) (Reference 226). The USGS hazard model (Reference 210) (Figure 2.5.2-209) incorporates the ECFS-s as a distinct source geometry (also known as the zone of river anomalies [ZRA]); however, as described earlier, the USGS model truncates the northeastern extent of the proposed fault segment. The South Carolina Department of Transportation hazard model (Reference 211) also incorporates the ECFS-s as a distinct source geometry; however, this model extends the

southern segment of the proposed East Coast fault system farther to the south than originally postulated by Marple and Talwani (2000) (Reference 226) to include, in part, the distribution of liquefaction in southeastern South Carolina (Figure 2.5.2-211).

The area of Geometry C is restricted to envelop the original depiction of the ECFS-s by Marple and Talwani (2000) (Reference 226). Rationale for the truncation of the zone to the northeast as shown by the 2002 USGS model is not well documented (Figure 2.5.2-209). The presence of liquefaction in southeastern South Carolina is best captured in Geometries B and B', rather than extending the Marple and Talwani (2000) (Reference 226) depiction of the ECFS-s farther to the south.

The UCSS model assigns a low weight of 0.10 to Geometry C to reflect the assessment that Geometries B, B', and C all have equal, but relatively low, likelihoods of producing Charleston-type earthquakes (Figure 2.5.2-210). As with the other UCSS geometries, the UCSS model represents Geometry C as a series of parallel, vertical faults oriented northeast-southwest and parallel to the long axis of the narrow rectangular zone. The faults and extent of earthquake ruptures are confined within the rectangle depicting Geometry C.

UCSS Model Parameters. Based on studies by Bollinger et al. (1985, 1991) (References 227 and 228) and Bollinger (1992) (Reference 229), the UCSS model assumes a 20-km-thick seismogenic crust. To model the occurrence of earthquakes in the characteristic part of the Charleston distribution (**M** > 6.7), the model uses a series of closely-spaced, vertical faults parallel to the long axis of each of the four source zones (A, B, B', and C). Faults and earthquake ruptures are limited to within each respective source zone and are not allowed to extend beyond the zone boundaries, and ruptures are constrained to occur within the depth range of 0 to 20 km. The UCSS model assumes fault rupture areas have a width-to-length aspect ratio of 0.5, conditional on the assumed maximum fault width of 20 km. To obtain M_{max} earthquake rupture lengths from magnitude, the UCSS model uses the Wells and Coppersmith (1994) (Reference 230) empirical relationship between surface rupture length and **M** for earthquakes of all slip types.

To maintain as much similarity as possible with the original EPRI model, the UCSS model treats earthquakes in the exponential part of the distribution (**M** < 6.7) as point sources uniformly distributed within the source area (full smoothing), with a constant depth fixed at 10 km.

2.5.2.2.2.4.2 UCSS Maximum Magnitude

The six EPRI ESTs developed a distribution of weighted M_{max} values and weights to characterize the largest earthquakes that could occur on Charleston seismic sources. On the low end, the Law Engineering team assesses a single M_{max} of m_b 6.8 to seismic sources it considers capable of producing earthquakes comparable in magnitude to the 1886 Charleston earthquake. On the high end, four teams defined M_{max} upper bounds ranging between m_b 7.2 and 7.5. The

m_b magnitude values have been converted to moment magnitude (**M**) as described previously. The m_b value and converted moment magnitude value for each team are shown below. The range in **M** for the six ESTs is 6.5 to 8.0.

Team	Charleston M_{max} range
Bechtel Group	m_b 6.8 to 7.4 (**M** 6.8 to 7.9)
Dames & Moore	m_b 6.6 to 7.2 (**M** 6.5 to 7.5)
Law Engineering	m_b 6.8 (**M** 6.8)
Rondout	m_b 6.6 to 7.0 (**M** 6.5 to 7.2)
Weston Geophysical	m_b 6.6 to 7.2 (**M** 6.5 to 7.5)
Woodward-Clyde Consultants	m_b 6.7 to 7.5 (**M** 6.7 to 8.0)

The **M** equivalents of EPRI m_b estimates for Charleston M_{max} earthquakes show that the upper bound values are similar to, and in two cases exceed, the largest modern estimate of **M** 7.3 $\pm$ 0.26 (Johnston 1996, Reference 231) for the 1886 earthquake. The upper bound values for five of the six ESTs also exceed the preferred estimate of **M** 6.9 by Bakun and Hopper (2004) (Reference 232) for the Charleston event. The EPRI M_{max} estimates are more heavily weighted toward the lower magnitudes, with relatively low weights given to the upper bound magnitudes by several ESTs (Tables 2.5.2-202 through 2.5.2-207). Therefore, updating the M_{max} range and weights to reflect the current range of technical interpretations is warranted for the UCSS.

Based on assessment of the currently available data and interpretations regarding the range of modern M_{max} estimates (Table 2.5.2-214), the UCSS model modifies the USGS magnitude distribution (Reference 210) to include a total of five discrete magnitude values, each separated by 0.2 **M** units (Figure 2.5.2-210). The UCSS M_{max} distribution includes a discrete value of **M** 6.9 to represent the Bakun and Hopper (2004) (Reference 232) best estimate of the 1886 Charleston earthquake magnitude, as well as a lower value of **M** 6.7 to capture a low probability that the 1886 earthquake was smaller than the Bakun and Hopper (2004) (Reference 232) mean estimate of **M** 6.9. Bakun and Hopper (2004) (Reference 232) do not explicitly report a 1-sigma range in magnitude estimate of the 1886 earthquake, but do provide a 2-sigma range of **M** 6.4 to **M** 7.2.

The UCSS magnitudes and weights are as follows:

M	Weight	
6.7	0.10	
6.9	0.25	Bakun and Hopper (2004) mean (Reference 232)
7.1	0.30	
7.3	0.25	Johnston (1996) mean (Reference 231)
7.5	0.10	

This results in a weighted M_{max} mean magnitude of **M** 7.1 for the UCSS, which is slightly lower than the mean magnitude of **M** 7.2 in the USGS model (Reference 210).

2.5.2.2.2.4.3 UCSS Recurrence Model

In the 1989 EPRI study (Reference 203), the six EPRI ESTs use an exponential magnitude distribution to represent earthquake sizes for their Charleston sources. Parameters of the exponential magnitude distribution are estimated from historical seismicity in the respective source areas. This results in recurrence intervals for M_{max} earthquakes (at the upper end of the exponential distribution) of several thousand years.

The UCSS model for earthquake recurrence is a composite model consisting of two distributions. The first is an exponential magnitude distribution used to estimate recurrence between the lower-bound magnitude used for hazard calculations and m_b 6.7. The parameters of this distribution are estimated from the earthquake catalog, as they were for the 1989 EPRI study. This is the standard procedure for smaller magnitudes and is the model used, for example, by the USGS 2002 national hazard maps (Reference 210). The second distribution treats M_{max} earthquakes (**M** $\geq$ 6.7) according to a characteristic model, with discrete magnitudes and mean recurrence intervals estimated through analysis of geologic data, including paleoliquefaction studies. Subsection 2.5.2 uses M_{max} to describe the range of largest earthquakes in both the characteristic portion of the UCSS recurrence model and the EPRI exponential recurrence model.

This composite model achieves consistency between the occurrence of earthquakes with **M** < 6.7 and the earthquake catalog and between the occurrence of large earthquakes (**M** $\geq$ 6.7) with paleoliquefaction evidence. It is a type of “characteristic earthquake” model, in which the recurrence rate of large events is higher than what would be estimated from an exponential distribution inferred from the historical seismic record.

M_{max} Recurrence. This subsection describes how the UCSS model determines mean recurrence intervals for M_{max} earthquakes. The UCSS model incorporates geologic data to characterize the recurrence intervals for M_{max} earthquakes. As described earlier, identifying and dating paleoliquefaction features provides a basis for estimating the recurrence of large Charleston area earthquakes. Most of the available geologic data pertaining to the recurrence of large earthquakes in the Charleston area were published after 1990 and therefore were not available to the six EPRI ESTs. In the absence of geologic data, the six EPRI EST estimates of recurrence for large, Charleston-type earthquakes are based on a truncated exponential model using historical seismicity (References 201 and 203). The truncated exponential model also provides the relative frequency of all earthquakes greater than m_b 5.0 up to M_{max} in the EPRI PSHA. The recurrence of M_{max} earthquakes in the EPRI models is on the order of several thousand years, which is significantly greater than more recently published estimates of about 500 to 600 years, based on paleoliquefaction data (Reference 222).

Paleoliquefaction Data. Strong ground shaking during the 1886 Charleston earthquake produced extensive liquefaction, and liquefaction features from the 1886 event are preserved in geologic deposits at numerous locations in the South Carolina coastal region. Documentation of older liquefaction-related features in geologic deposits provides evidence for prior strong ground motions during prehistoric large earthquakes. Estimates of the recurrence of large earthquakes in the UCSS are based on dating paleoliquefaction features. Many potential sources of ambiguity and/or error are associated with dating and interpreting paleoliquefaction features. This assessment does not reevaluate field interpretations and data; rather, it reevaluates criteria used to define individual paleoearthquakes in the published literature. In particular, the UCSS reevaluates the paleoearthquake record interpreted by Talwani and Schaeffer (2001) (Reference 222) based on that study's compilation of sites with paleoliquefaction features.

Talwani and Schaeffer (2001) (Reference 222) compile radiocarbon ages from paleoliquefaction features along the coast of South Carolina. These data include ages that provide contemporary, minimum, and maximum limiting ages for liquefaction events. Radiocarbon ages are corrected for past variability in atmospheric ^{14}C using well established calibration curves and converted to "calibrated" (approximately calendric) ages. From their compilation of calibrated radiocarbon ages from various geographic locations, Talwani and Schaeffer (2001) (Reference 222) correlate individual earthquake episodes. They identify an individual earthquake episode based on samples with a "contemporary" age constraint that have overlapping calibrated radiocarbon ages at approximately 1-sigma confidence interval. The estimated age of each earthquake is "calculated from the weighted averages of overlapping contemporary ages" (Reference 222) (p. 6,632). They define as many as eight events (named 1886, A, B, C, D, E, F, and G in order of increasing age) from the paleoliquefaction record, and offer two scenarios to explain the distribution and timing of paleoliquefaction features (Table 2.5.2-215).

The two scenario paleoearthquake records proposed by Talwani and Schaeffer (2001) (Reference 222) have different interpretations for the size and location of prehistoric events (Table 2.5.2-215). In their Scenario 1, the four prehistoric events that produced widespread liquefaction features similar to the large 1886 Charleston earthquake (A, B, E, and G) are interpreted to be large, 1886 Charleston-type events. Three events, C, D, and F, are defined by paleoliquefaction features that are more limited in geographic extent than other events and are interpreted to be smaller, moderate-magnitude events (approximately **M** 6). Events C and F are defined by features found north of Charleston in the Georgetown region, and Event D is defined by sites south of Charleston in the Bluffton area. In their Scenario 2, all events are interpreted as large, 1886 Charleston-type events. Furthermore, Events C and D are combined into a large Event C'. Talwani and Schaeffer (2001) (Reference 222) justify the grouping of the two events based on the observation that the calibrated radiocarbon ages that constrain the timing of Events C and D are indistinguishable at the 95 percent (2-sigma) confidence interval.

The length and completeness of the paleoearthquake record based on paleoliquefaction features is a source of epistemic uncertainty in the UCSS model (epistemic uncertainty is the result of inaccurate or incomplete information and can be reduced or eliminated given better models or additional observations, as opposed to aleatory uncertainty that results from randomness and cannot be reduced with more or better observations). The paleoliquefaction record along the South Carolina coast extends from 1886 to the mid-Holocene (Reference 222). The consensus of the scientists who have evaluated these data (Reference 222) is that the paleoliquefaction record of earthquakes is complete only for the most-recent about 2,000 years and that it is possible that liquefaction events are missing from the older portions of the record. The suggested incompleteness of the paleoseismic record is based on the argument that past fluctuations in sea level have produced time intervals of low water table conditions (and thus low liquefaction susceptibility), during which large earthquake events may not have been recorded in the paleoliquefaction record (Reference 222). While this assertion may be true, it is possible that the paleoliquefaction record may be complete back to the mid-Holocene.

2-Sigma Analysis of Event Ages. The Talwani and Schaeffer (2001) (Reference 222) data compilation of liquefaction is the basis for analysis of the coastal South Carolina paleoliquefaction record performed in support of Subsection 2.5.2. As described above, Talwani and Schaeffer (2001) use calibrated radiocarbon ages with 1-sigma error bands to define the timing of past liquefaction episodes in coastal South Carolina. The standard in paleoseismology, however, is to use calibrated ages with 2-sigma (95.4 percent confidence interval) error bands (Reference 233). Likewise, in paleoliquefaction studies, to more accurately reflect the uncertainties in radiocarbon dating, Tuttle (2001) (Reference 234) advises the use of calibrated radiocarbon dates with 2-sigma error bands (as opposed to narrower 1-sigma error bands). Talwani and Schaeffer's (2001) (Reference 222) use of 1-sigma error bands may lead to over-interpretation of the paleoliquefaction record such that more episodes are interpreted than actually occurred. In recognition of this possibility, the conventional radiocarbon ages presented in Talwani and Schaeffer (2001) are recalibrated and reported with 2-sigma error bands. The recalibration of individual radiocarbon samples and estimation of age ranges for paleoliquefaction events show broader age ranges with 2-sigma error bands that are used to obtain broader age ranges for paleoliquefaction events in the Charleston area.

Event ages based on overlapping 2-sigma ages of paleoliquefaction features are presented in Table 2.5.2-215. Paleoearthquakes are distinguished based on grouping paleoliquefaction features that have contemporary radiocarbon samples with overlapping calibrated ages. Event ages are defined by selecting the age range common to each of the samples. For example, an event defined by overlapping 2-sigma sample ages of 100 to 200 cal yr BP and 50 to 150 cal yr BP has an event age of 100 to 150 cal yr BP. The UCSS model considers these "trimmed" ages to represent the approximately 95 percent confidence interval, with a "best estimate" event age as the midpoint of the approximately 95 percent age range.

The UCSS model 2-sigma analysis identifies six distinct paleoearthquakes in the data presented by Talwani and Schaeffer (2001) (Reference 222). As noted by that study, Events C and D are indistinguishable at the 95 percent confidence interval, and in the UCSS, those samples define Event C' (Table 2.5.2-215). Additionally, the UCSS 2-sigma analysis suggests that Talwani and Schaeffer (2001) Events F and G are a single, large event, defined in the UCSS as F'. One important difference between the UCSS result and that of Talwani and Schaeffer (2001) is that the three Events C, D, and F in their Scenario 1, which are inferred to be smaller, moderate-magnitude events, are grouped into more regionally extensive Events C' and F' (Table 2.5.2-215). Therefore, in the UCSS, all earthquakes in the 2-sigma analysis are interpreted to represent large, Charleston-type events. The incorporation of large Events C' and F' into the UCSS model is, in effect, a conservative approach. In the effort to estimate the recurrence of M_{max} events (**M** 6.7 to 7.5), moderate-magnitude (about **M** 6) earthquakes C and D would be eliminated from the record of large (M_{max}) earthquakes in the UCSS model, thereby increasing the calculated M_{max} recurrence interval and lowering the hazard without sufficient justification. For these reasons the UCSS model uses a single, large Event C' (instead of separate, smaller Events C and D) and a single, large Event F' (instead of separate, smaller Events F and G). Analysis suggests that there have been four large earthquakes in the most-recent, about 2,000-year portion of the record (1886 and Events A, B, and C'). In the entire 5,000-year paleoliquefaction record, there is evidence for six large, Charleston-type earthquakes (1886, A, B, C', E, F'; Table 2.5.2-215). Figure 2.5.2-211 shows the geographic distribution of liquefaction features associated with each event in the UCSS model. The distributions of paleoliquefaction sites for Events A, B, C', E, and F' are all very similar to the coastal extent of the liquefaction features from the 1886 earthquake.

Recurrence intervals developed from the earthquakes recorded by paleoliquefaction features assume that these features were produced by large M_{max} events and that both the 2,000-year and 5,000-year records are complete. However, the UCSS model highlights at least two concerns regarding the use of the paleoliquefaction record to characterize the recurrence of past M_{max} events. First, it is possible that multiple, moderate-sized earthquakes closely spaced in time produced the paleoliquefaction features associated with one or more of the pre-1886 events. If this is the case, then the calculated recurrence interval would yield artificially short recurrence for M_{max}, since it is calculated using repeat times of both large (M_{max}) events and smaller earthquakes. Limitations of radiocarbon dating and limitations in the stratigraphic record often preclude identifying individual events in the paleoseismologic record that are closely spaced in time (i.e., separated by only a few years to a few decades). Several seismic sources have demonstrated tightly clustered earthquake activity in space and time that are indistinguishable in the radiocarbon and paleoseismic record:

- New Madrid (December 1811, January 1812, February 1812)
- North Anatolian Fault (August 1999 and November 1999)
- San Andreas Fault (1812 and 1857)

Therefore the UCSS acknowledges the distinct possibility that M_{max} occurs less frequently than what is calculated from the paleoliquefaction record.

A second concern is that the recurrence behavior of the M_{max} event may be highly variable through time. For example, the UCSS considers it unlikely that **M** 6.7 to **M** 7.5 events have occurred on a Charleston source at an average repeat time of about 500 to 600 years (Reference 222) throughout the Holocene Epoch. Such a moment release rate would likely produce tectonic landforms with clear geomorphic expression, such as are present in regions of the world with comparably high rates of moderate to large earthquakes (for example, faults in the Eastern California shear zone with sub-millimeter per year slip rates and recurrence intervals on the order of about 5,000 years have clear geomorphic expression [Reference 235]). Perhaps it is more likely that the Charleston source has a recurrence behavior that is highly variable through time, such that a sequence of events spaced about 500 years apart is followed by quiescent intervals of thousands of years or longer. This sort of variability in inter-event time may be represented by the entire mid-Holocene record, in which both short inter-event times (e.g., about 400 years between Events A and B) are included in a record with long inter-event times (e.g., about 1,900 years between Events C' and E).

Recurrence Rates. The UCSS model calculates two average recurrence intervals covering two different time intervals. The UCSS model represents these two recurrence intervals as separate branches on the logic tree (Figure 2.5.2-210). The first average recurrence interval is based on the four events that occurred within the past about 2,000 years. This time period is considered to represent a complete portion of the paleoseismic record (Reference 222). These events include 1886, A, B, and C' (Table 2.5.2-215). The average recurrence interval calculated for the most recent portion of the paleoliquefaction record (four events over the past about 2,000 years) is given 0.80 weight on the logic tree (Figure 2.5.2-210).

The second average recurrence interval is based on events that occurred within the past about 5,000 years. This time period represents the entire paleoseismic record based on paleoliquefaction data (Reference 222). These events include 1886, A, B, C', E, and F' as listed in Table 2.5.2-215. Published literature and researchers questioned suggest that the older part of the record (older than about 2,000 years ago) may be incomplete. Whereas this assertion may be true, it is also possible that the older record, which exhibits longer inter-event times, is complete. The UCSS model assigns a weight of 0.20 to the average recurrence interval calculated for the 5,000-year record (six events) (Figure 2.5.2-210). The 0.80 and 0.20 weighting of the 2,000-year and 5,000-year paleoliquefaction

records, respectively, reflects incomplete knowledge of both the short- and long-term recurrence behavior of the Charleston source.

The mean recurrence intervals for the most-recent 2,000-year and 5,000-year records represent the average time interval between earthquakes attributed to the Charleston seismic source. The mean recurrence intervals and their parametric uncertainties are calculated according to the methods outlined by Savage (1991) (Reference 236) and Cramer (2001) (Reference 237). The methods provide a description of mean recurrence interval, with a best estimate mean T_{ave} and an uncertainty described as a lognormal distribution with median $T_{0.5}$ and parametric lognormal shape factor $\sigma_{0.5}$.

The lognormal distribution is one of several distributions, including the Weibull, Double Exponential, and Gaussian, among others, used to characterize earthquake recurrence (Reference 238). Ellsworth et al. (1999) (Reference 238) and Matthews et al. (2002) (Reference 239) propose a Brownian-passage time model to represent earthquake recurrence, arguing that it more closely simulates the physical process of strain build-up and release. This Brownian-passage time model is currently used to calculate earthquake probabilities in the greater San Francisco Bay region (Reference 240). Analyses show that the lognormal distribution is very similar to the Brownian-passage time model of earthquake recurrence for cases where the time elapsed since the most recent earthquake is less than the mean recurrence interval (References 238 and 246). This is the case for Charleston, where 120 years have elapsed since the 1886 earthquake and the mean recurrence interval determined over the past 2,000 years is about 548 years. The UCSS model calculates average recurrence intervals using a lognormal distribution because its statistics are well known (Reference 242) and numerous other studies use this method (References 236, 237, and 241).

The average interval between earthquakes is expressed as two continuous lognormal distributions. The average recurrence interval for the 2,000-year record, based on the three most recent inter-event times (1886-A, A-B, B-C'), has a best estimate mean value of 548 years and an uncertainty distribution described by a median value of 531 years and a lognormal shape factor of 0.25. The average recurrence interval for the 5,000-year record, based on five inter-event times (1886-A, A-B, B-C', C'-E, E-F'), has a best estimate mean value of 958 years and an uncertainty distribution described by a median value of 841 years and a lognormal shape factor of 0.51. At one standard deviation, the average recurrence interval for the 2,000-year record is between 409 and 690 years; for the 5,000-year record, it is between 452 and 1,564 years. Combining these mean values of 548 and 958 years with their respective logic tree weights of 0.8 and 0.2 results in a weighted mean of 630 years for Charleston M_{max} recurrence.

The UCSS model uses mean recurrence values that are similar to those determined by earlier studies. Talwani and Schaeffer (2001) (Reference 222) consider two possible scenarios to explain the distribution in time and space of paleoliquefaction features. In their Scenario 1, large earthquakes have occurred with an average recurrence of 454 ±21 years over about the past 2,000 years; in their Scenario 2, large earthquakes have occurred with an average recurrence of

523 ±100 years over the past 2,000 years. Talwani and Schaeffer (2001) state that, “In anticipation of additional data we suggest a recurrence rate [*sic*] between 500 and 600 years for **M** 7+ earthquakes at Charleston.” For the 2,000-year record, the 1-standard-deviation range of 409 to 690 years completely encompasses the range of average recurrence interval reported by Talwani and Schaeffer (2001). The best-estimate mean recurrence interval value of 548 years is comparable to the midpoint of the Talwani and Schaeffer (2001) best-estimate range of 500 to 600 years. The best estimate mean recurrence interval value from the 5,000-year paleoseismic record of 958 years is outside the age ranges reported by Talwani and Schaeffer (2001), although they did not determine an average recurrence interval based on the longer record.

The USGS updated seismic hazard maps for the conterminous United States use a mean recurrence value of 550 years for characteristic earthquakes in the Charleston region (Reference 210). This value is based on the above-quoted 500 to 600 year estimate from Talwani and Schaeffer (2001) (Reference 222). The USGS updated seismic hazard maps for the conterminous United States do not incorporate uncertainty in mean recurrence interval in their calculations.

For computation of seismic hazard, discrete values of activity rate (inverse of recurrence interval) are required as input to the PSHA code (Reference 243). To evaluate PSHA based on mean hazard, the mean recurrence interval and its uncertainty distribution should be converted to mean activity rate with associated uncertainty. The final discretized activity rates used to model the UCSS in the PSHA reflect a mean recurrence of 548 years and 958 years for the 2,000-year and 5,000-year branches of the logic tree, respectively. Lognormal uncertainty distributions in activity rate are obtained by the following steps: (1) invert the mean recurrence intervals to get mean activity rates; (2) calculate median activity rates using the mean rates and lognormal shape factors of 0.25 and 0.51 established for the 2,000-year and 5,000-year records, respectively; and (3) determine the lognormal distributions based on the calculated median rate and shape factors. The lognormal distributions of activity rate can then be discretized to obtain individual activity rates with corresponding weights.

2.5.2.2.2.5 Eastern Tennessee Seismic Zone

The Eastern Tennessee Seismic Zone (ETSZ) is one of the most active seismic zones in Eastern North America. This region of seismicity in the southern Appalachians is described in detail in Subsection 2.5.1.1.3.2.2. Despite its high rate of activity, the largest known earthquake in the ETSZ is magnitude 4.6 (magnitude scale unspecified) (Reference 244). There is no evidence (such as paleoliquefaction features) for larger prehistoric earthquakes (References 244 and 245). While the lack of large earthquakes in the relatively short historical record cannot preclude the future occurrence of large events, there is a much higher degree of uncertainty associated with the assignment of M_{max} for the ETSZ than other CEUS seismic source zones, such as New Madrid and Charleston, where large historical earthquakes are known to have occurred.

The EPRI source model (References 201 and 207) includes various source geometries and parameters to represent the seismicity of the ETSZ. All but one of the EPRI Earth Science Teams (ESTs) models local source zones to capture this area of seismicity and some ESTs include more than one zone. The Law Engineering team does not include a specific, local source for the ETSZ, however the ETSZ and Giles County seismic zones are included in a larger seismic source zone called the Eastern Basement (17). A wide range of M_{max} values and associated probabilities are assigned to these sources to reflect the uncertainty of multiple experts from each EST. The **M** equivalents of m_b assessments of M_{max} values assigned by the ESTs range from **M** 4.8 to 7.5. The Dames & Moore sources for the ETSZ included the largest upper-bound M_{max} value of **M** 7.5. Sources from the Woodward-Clyde and Rondout teams are assigned large upper-bound M_{max} values of **M** 7.2.

Subsequent hazard studies use M_{max} values within the range of maximum magnitudes used by the six EPRI models. Collectively, upper-bound maximum values of M_{max} used by the EPRI teams range from **M** 6.3 to 7.5. Using three different methods specific to the Eastern Tennessee seismic source, Bollinger (1992) (Reference 229) estimates an M_{max} of **M** 6.3. The Bollinger (1992) model includes the possibility that the ETSZ is capable of generating a larger magnitude event and includes an **M** 7.8 (m_b 7.37) with a low probability of 5% in the M_{max} distribution. The 5% weighted **M** 7.8 by Bollinger (1992) slightly exceeds the ERPI range, but the **M** 6.3 value is given nearly the entire weight (95%) in his characterization of the ETSZ. This smaller magnitude is much closer to the mean magnitude (approximately **M** 6.2) of the EPRI study. The Trial Implementation Project (TIP) (Reference 212) also provides a broad M_{max} distribution for the ETSZ. This study develops magnitude distributions for all ETSZ source zone representations that range from as low as **M** 4.5 to as high as about **M** 7.5, with a mode of about **M** 6.5 for almost each distribution (Reference 212, pages F-12 to F-19 of Appendix F). The broad distribution of the TIP study magnitude distribution for the ETSZ source zones is similar to the EPRI distribution of **M** 4.8 to **M** 7.5. The USGS source model assigns a single M_{max} value of **M** 7.5 for the ETSZ (Reference 210). The most recent characterizations of the ETSZ M_{max} by the USGS and TIP study consider **M** 7.5 as the largest magnitude in the distribution and this magnitude is captured by the range of M_{max} values used in EPRI NP-6452-D (Reference 207). Therefore, it is concluded that no new information has been developed since 1986 that would require a significant revision to the EPRI seismic source model.

The ground motion hazard at the Lee Nuclear Site is dominated by the Charleston seismic source, and the inclusion of new recurrence values for Charleston based on paleoliquefaction serves to increase the relative contribution of Charleston with respect to any distant source, such as the ETSZ. No modifications to the EPRI parameters for ETSZ source zones were made.

2.5.2.3 Correlation of Earthquake Activity with Seismic Sources

The final part of the review and update of the 1989 EPRI seismic source model is a correlation of updated seismicity with the 1989 model source. The EPRI seismicity catalog covers earthquakes in the CEUS through 1984, as described in Subsection 2.5.2.1. Figures 2.5.2-203 through 2.5.2-208 show the distribution of earthquake epicenters from both the EPRI (pre-1985) and updated (post-1984 through August 2006) earthquake catalogs in comparison to the seismic sources identified by each of the EPRI ESTs.

Comparison of the additional events of the updated earthquake catalog to the EPRI earthquake catalog shows:

- There are no new earthquakes within the site region that can be associated with a known geologic structure.
- There are no unique clusters of seismicity that suggest a new seismic source not captured by the EPRI seismic source model.
- The updated catalog does not show a pattern of seismicity that would require significant revision to the geometry of any of the EPRI seismic sources.
- The updated catalog neither shows nor suggests any increase in M_{max} for any of the EPRI seismic sources.

The updated catalog does not imply a significant change in seismicity parameters (rate of activity, b-value) for any of the EPRI seismic sources (see also Subsection 2.5.2.4.2).

2.5.2.4 Probabilistic Seismic Hazard Analysis and Controlling Earthquake

The 1989 EPRI study (Reference 203) is the starting point for probabilistic seismic hazard calculations. This follows the recommendation of RG 1.208. An underlying principle of this study is that expert opinion on alternative, competing models of earthquake occurrence (size, location, and rates of occurrence) and of ground motion amplitude and its variability should be used to weight alternative hypotheses. The result is a family of weighted seismic hazard curves from which mean and fractile seismic hazard can be derived.

The first task is to calculate seismic hazard using the assumptions on seismic sources and ground motion equations developed in the 1989 EPRI study to ensure that seismic sources are modeled correctly and that the software being used (Risk Engineering, Inc.'s FRISK88 software) accurately reproduces the 1989 study results. The 1989 EPRI study did not calculate seismic hazard at the Lee site, so verification of the seismic sources, ground motion equations, and software is made by comparing seismic hazard results calculated for the Lee site to 1989 EPRI results calculated for other sites in the generally vicinity.

Table 2.5.2-216 compares the mean annual frequencies of exceedance calculated for the Lee site to published annual frequencies of exceedance from the 1989 EPRI site for three other sites (Catawba, McGuire, and Oconee). All results are for hard rock conditions. The "% difference" row shows the percent difference of hazard calculated for the Lee site compared to each of the other three sites. For all three comparisons the current results are higher than those published from the 1989 EPRI study. The smallest difference is seen in the comparisons with the Oconee site, because the Lee site and the Oconee site lie in many of the same seismic sources designated by the 1989 EPRI teams. The largest difference is seen with the McGuire site because this site lies to the northeast in North Carolina and is outside many of the seismic sources drawn by the EPRI teams to represent seismicity in South Carolina.

The comparisons shown in Table 2.5.2-216 are considered acceptable agreement, given that the comparisons are made with other sites in the vicinity of Lee using independent software. Comparisons were made using mean annual frequencies of exceedance because these are the most important results used to derive seismic design spectra.

2.5.2.4.1 Effects of Updated Earthquake Catalog

An important consideration in updating seismic hazard calculations is to determine if additional seismicity that has occurred since the 1989 EPRI study leads to increased estimates of earthquake occurrence rates. Seismicity rates in the 1989 EPRI study were based on an earthquake catalog that extended through 1984. This sensitivity study used an updated catalog extended through 2005 and calculated rates of earthquake occurrence in regions surrounding the Lee site.

Figure 2.5.2-212 shows historical seismicity in the region of the site, with three test sources that were used to examine the effects of the additional earthquakes that occurred from 1985 to 2005. These test sources consist of a polygonal area encompassing seismicity in central South Carolina, a rectangular area encompassing seismicity in the southern Appalachian region, and a square area around Charleston, South Carolina. These test sources are chosen because many of the 1989 EPRI teams drew a seismic source to encompass seismicity in central South Carolina, and because the southern Appalachian-eastern Tennessee region and the Charleston region are areas where seismicity is studied.

To examine the effect of the seismicity that has occurred from 1985 to 2005, the EPRI software EQPARAM is used, first with the original EPRI earthquake catalog (through 1984) and then with the updated catalog (through 2005). The EQPARAM software calculates seismicity rates (a- and b-values) from which annual rates of earthquake occurrences can be derived. For these calculations, earthquake occurrences in each source are assumed to be spatially homogeneous.

Figures 2.5.2-213, 214, and 215 show comparisons of annual frequencies of occurrence of earthquakes with magnitudes (on the m_b scale) greater than specified values. The solid lines indicate rates derived from the 1989 EPRI

catalog, the dashed lines indicate rates derived from the updated catalog with 21 years of additional seismicity, 1985 through 2005. For all three areas, recent seismicity indicates a slightly lower rate of earthquake occurrence than what was used for the 1989 EPRI study.

These comparisons indicate that the original seismicity rates calculated for the 1989 EPRI project are adequate. These seismicity rates are calculated using specific assumptions on spatial smoothing and estimates of b-values for the exponential magnitude distribution, as specified by the EPRI teams, and these rates do not need to be updated to reflect the additional 21 years of seismicity data.

2.5.2.4.2 New Maximum Magnitude Information

As discussed in earlier subsections, no new scientific information has been published that would lead to a change in the EPRI seismic source characterization or parameters, including the assessment of M_{max}. The only exception is for the Charleston, South Carolina region, which is addressed in the next subsection. As a result, the maximum magnitude distributions assigned to the 1989 EPRI sources are not modified for the calculation of seismic hazard.

2.5.2.4.3 New Seismic Source Characterizations

Two new seismic source characterizations are included to reflect updated information regarding the Charleston and New Madrid seismic sources. Subsections 2.5.2.2.2.4 and 2.5.2.4.3.1 describe the new Charleston source characterization, and Subsection 2.5.2.4.3.2 describes the New Madrid seismic source characterization.

2.5.2.4.3.1 Charleston Seismic Source Characterization

The new Charleston source model (the Updated Charleston Seismic Source, or UCSS) reflects updated estimates of the possible geometries of seismic sources in the Charleston region. Subsection 2.5.2.2.2.4 presents discussion of the UCSS. The UCSS model also updates the characteristic earthquake magnitudes that might occur and the possible mean recurrence rates associated with those characteristic magnitudes. The following four geometries and weights are used:

Geometry A, weight 0.7

Geometry B, weight 0.1

Geometry B', weight 0.1

Geometry C, weight 0.1

Subsection 2.5.2.2.2.4.2 describes the distribution of characteristic magnitudes for the UCSS model. This distribution is represented with five discrete values and associated weights: **M**=6.7 (0.1), 6.9 (0.25), 7.1 (0.3), 7.3 (0.25), and 7.5 (0.1).

The distribution of the mean recurrence interval is described in Subsection 2.5.2.2.2.4.3 and is based on two data periods for paleoliquefaction events. For each data period, a separate mean recurrence interval and uncertainty is estimated, and a five-point discrete distribution (with weights) is used to quantify each distribution. This results in a total of 10 estimates of mean recurrence interval, each with an associated weight.

The four geometries described above are shown in Figure 2.5.2-216. For seismic hazard calculations these geometries are represented with parallel faults spaced 6 mi. (10 km) apart, and the activity rate estimated for the Charleston source is distributed equally among the parallel faults. A general rupture length equation (Reference 230) is used to model a finite rupture length for each earthquake. The distance between the Lee site and the Charleston sources, and the general northeast-southwest trend of the UCSS geometries (resulting in the fault ruptures being generally perpendicular to a line drawn between the site and the Charleston faults) means that the seismic hazard at Lee is not very sensitive to the details of the faults or rupture length equation.

In addition to the UCSS fault model, four area sources for the Charleston region are included in the seismic hazard calculation, in order to represent small magnitude, exponentially distributed earthquakes. Because large-magnitude earthquakes are modeled with the UCSS, the exponential distribution Charleston sources are modeled with magnitude distributions up to m_b 6.5. The rates of occurrence and b-values for these four area sources are calculated with the EPRI EQPARAM software using the EPRI earthquake catalog through 1984.

The EPRI ESTs modeled seismicity in the Charleston area. In order not to double-count seismicity and seismic hazard, the EPRI team Charleston sources are removed from the seismic hazard analysis. Other EPRI team sources surrounding the Charleston area are modified in order to have sources that fully surrounded the UCSS geometries, without any areas that would leave a gap in seismicity. As an example, Figures 2.5.2-217, 218, 219, and 220 show Rondout source 26 with UCSS geometries A, B, B', and C as holes, so that there are no gaps in seismicity. The seismicity parameters for these modified EPRI team sources are recalculated using the EPRI EQPARAM software and using the same seismicity parameter assumptions specified by each team for that source, for the 1989 EPRI study. For consistency, the EPRI earthquake catalog (through 1984) is used for these calculations. Other assumptions about these sources (specifically the maximum magnitude distributions) are not modified.

The source logic of the EPRI teams is also modified to reflect the new source logic of the UCSS and to reflect the weights (given above) of the UCSS geometries. The probabilities of activity of other EPRI team sources in the eastern US are not modified.

2.5.2.4.3.2 New Madrid Seismic Source Characterization

A screening study defines the primary seismic sources that contribute to 99 percent of the Lee Nuclear Site seismic hazard. The original EPRI study

screened for these sources before calculating the final hazard for each of the participating plant sites in the CEUS. Because the Lee Nuclear Site is not part of the original EPRI study, these sources are defined in the screening study for the Lee Nuclear Site in order to be consistent with EPRI methodology.

The screening study reveals that one EPRI EST New Madrid source (Dames & Moore source 21) is considered a primary source that contributes to 99 percent of the total seismic hazard. The contribution of Dames & Moore source 21 is minimal in that it contributes zero percent and 0.8 percent of hazard at PGA and 1 Hz, respectively.

Given the inclusion of the Dames & Moore New Madrid source, it is necessary to develop an update of New Madrid parameters for the Lee Nuclear Station seismic source model. Because the New Madrid source is only a minor contributor to the Lee Nuclear Site hazard, a simple model is used to account for post-EPRI characterizations of the New Madrid source.

Subsection 2.5.1.1.3.2.4 presents a detailed discussion of the New Madrid seismic zone. The New Madrid seismic zone produced a series of historical, large-magnitude earthquakes between December 1811 and February 1812 (Reference 247). Several studies that post-date the 1986 EPRI EST assessments demonstrate that the source parameters for geometry, M_{max}, and recurrence of M_{max} in the New Madrid region need to be updated to capture a more current understanding of this seismic source (References 210, 231, 232, 237, and 248).

The updated New Madrid seismic source model described in Exelon (2006) (Reference 293) forms the basis for determining the potential contribution from the New Madrid seismic zone to seismic hazard at the Lee Nuclear Site (Figures 2.5.2-221 and 222). This model accounts for new information on recurrence intervals for large earthquakes in the New Madrid area, for recent estimates of possible earthquake sizes on each of the active faults, and for the possibility of multiple earthquake occurrences within a short period of time (earthquake clusters).

Three sources are identified in the New Madrid seismic zone, each with two alternative fault geometries, as follows:

Seismic Source	Fault Geometry
Southern New Madrid	Blytheville Arch/Bootheel Lineament Blytheville Arch/ Blytheville Fault Zone
Northern New Madrid	New Madrid North, New Madrid North Plus Extension
Reelfoot Fault	Reelfoot Central Section, Reelfoot Full Length

Earthquakes are treated as characteristic events in terms of magnitudes, with the following sets of magnitudes modeled for each seismic source (Reference 293):

Southern	Reelfoot	Northern	Weight
7.3	7.5	7.0	0.1667
7.2	7.4	7.0	0.1667
7.2	7.4	7.2	0.0833
7.6	7.8	7.5	0.25
7.9	7.8	7.6	0.1667
7.8	7.7	7.5	0.1667

The above magnitudes represent the centers of characteristic magnitude ranges that extend ±0.25 magnitude units above and below the indicated magnitude.

Seismic hazard is calculated considering the possibility of clustered earthquake occurrences. In the New Madrid model, all three sources rupture during each "event," and hazard is computed using this simplified model. This simplified model results in slightly higher ground motion hazard than if the possibility of two source ruptures is considered, or if a smaller-magnitude earthquake is considered for one of the three ruptures. The occurrence rate of earthquake clusters is developed using two models, a Poisson model and a lognormal renewal model with a range of coefficients of variation (Reference 293). Consistent with (Exelon 2006) (Reference 293), all faults are assumed to be vertical and to extend from the surface to 12 mi. (20 km) depth. A finite rupture model is used to represent an extended rupture on all sources. Because of the large distance between the New Madrid seismic zone and the Lee Nuclear Site, the details of the geometrical representation of each fault are not critical to the seismic hazard calculations.

2.5.2.4.4 New Ground Motion Models

Since the 1989 EPRI study (Reference 203), ground motion models for the CEUS have evolved. An EPRI project was conducted to summarize knowledge about CEUS ground motions, and results were published in EPRI (2004) (Reference 202). These updated equations estimate median spectral acceleration and its uncertainty as a function of earthquake magnitude and distance. Epistemic uncertainty is modeled using multiple ground motion equations with weights, and multiple estimates of aleatory uncertainty, also with weights. Different sets of sources are recommended for seismic sources that represent rifted versus non-rifted regions of the earth's crust. Equations are available for spectral frequencies at hard rock sites of 100 Hz (which is equivalent to peak ground acceleration, PGA), 25 Hz, 10 Hz, 5 Hz, 2.5 Hz, 1 Hz, and 0.5 Hz.

The aleatory uncertainties published in the EPRI 1009684 (2004) (Reference 202) model are re-examined by Abrahamson and Bommer (2006) (Reference 249), because it was thought that the EPRI 2004 aleatory uncertainties were probably

too large, resulting in over-estimates of seismic hazard. The Abrahamson and Bommer (2006) (Reference 249) study recommends a revised set of aleatory uncertainties and weights that can be used to replace the original EPRI 2004 aleatory uncertainties.

To correctly model the damageability of small magnitude earthquakes to engineered facilities, the Cumulative Absolute Velocity (CAV) model of Hardy et al. (2006) (Reference 250) is used. The CAV model in effect filters out the fraction of small magnitude earthquakes that will not cause damage, and leaves in the hazard calculations only those ground motions with CAV values greater than 0.15 g-sec. The filter that is used is based on empirical ground motion records and depends on ground motion amplitude, duration of motion (which depends on earthquake magnitude), and on shear-wave velocity in the top 100 ft. (30 m) at the site. The ground motions for frequencies other than 100 Hz are assumed to be partially correlated with the ground motions at 100 Hz, so that the filtering is consistent from frequency to frequency.

In summary, the ground motion model used in the seismic hazard calculations consists of the median equations from EPRI 1009684 (2004) (Reference 202) combined with the updated aleatory uncertainties of the Abrahamson and Bommer (2006) (Reference 249) study. The CAV filter is applied to account for the damageability of small magnitude earthquake ground motions.

2.5.2.4.5 Updated Probabilistic Seismic Hazard Analysis and Deaggregation

The seismic hazard at the Lee site is recalculated with the previously described changes to the Charleston source model, with the changes to the surrounding EPRI team sources, with the addition of the New Madrid faults, and with the updated ground motion model for the CEUS. This calculation is for hard rock conditions, which is consistent with the updated ground motion model.

A PSHA consists of calculating annual frequencies of exceeding various ground motion amplitudes for all possible earthquakes that are hypothesized in a region. The seismic sources specify the rates of occurrence of earthquakes as a function of magnitude and location, and the ground motion prediction model estimates the distribution of ground motions at the site for each event. Multiple weighted hypotheses on seismic sources, earthquake rates of occurrence, and ground motions (characterized by the median ground motion amplitude and its uncertainty) result in multiple, weighted seismic hazard curves, and from these the mean and fractile seismic hazard can be determined. The calculation is made separately for each of the seismic source characterizations from the six EPRI teams, and the seismic hazard distribution for the teams is combined, weighting each team equally. This combination gives the overall mean and distribution of seismic hazard at the site.

Figures 2.5.2-223, 224, 225, 226, 227, 228, and 229 show mean and fractile (15^{th}, median, and 85^{th}) seismic hazard curves from this calculation for the 7 spectral frequencies that are available from the EPRI 2004 ground motion model. Figure 2.5.2-230 shows mean and median UHRS for 10^{-4} and 10^{-5} annual

frequencies of exceedance. The mean UHRS values are also documented in Table 2.5.2-217 for annual frequencies of exceedance of 10^{-4}, 10^{-5}, and 10^{-6}.

The seismic hazard is deaggregated following the guidelines of RG 1.208. Specifically, the mean contributions to seismic hazard for 1 Hz and 2.5 Hz are deaggregated by magnitude and distance for the mean 10^{-4} ground motions at 1 Hz and 2.5 Hz, and these deaggregations are combined. Figure 2.5.2-231 shows this combined deaggregation. Similar deaggregations of the mean hazard are performed for 5 and 10 Hz spectral accelerations (Figure 2.5.2-232). Figures 2.5.2-233 and 234 show deaggregations of the mean hazard for 10^{-5} ground motions, and Figures 2.5.2-235 and 236 show deaggregations of the mean hazard for 10^{-6} ground motions. RG 1.206 recommends deaggregation of the mean seismic hazard. Table 2.5.2-218 summarizes the mean magnitude and distance resulting from these deaggregations, for the mean 10^{-4}, 10^{-5}, and 10^{-6} ground motion amplitudes for all contributions to hazard and for contributions with distances exceeding 62 miles (100 km).

The deaggregation plots in Figures 2.5.2-231, 232, 233, 234, 235, and 236 indicate that the Charleston and New Madrid seismic sources contribute to seismic hazard at the Lee site. For 10^{-4} annual frequency of exceedance, these sources are the largest contributor to seismic hazard for both 1 and 2.5 Hz (Figure 2.5.2-231) and 5 and 10 Hz (Figure 2.5.2-232). For annual frequencies of 10^{-5} and 10^{-6}, the contribution is smaller, particularly for 5 and 10 Hz (Figures 2.5.2-234 and 2.5.2-236). The local sources representing seismicity in central South Carolina dominate for these annual frequencies and for 5 and 10 Hz.

Smooth UHRS are developed from the UHRS amplitudes in Table 2.5.2-217, using the hard rock spectral shapes for CEUS earthquake ground motions recommended in NUREG/CR-6728 (Reference 251). Separate spectral shapes are developed for high frequencies (HF) and low frequencies (LF). In order to reflect accurately the UHRS values calculated by the PSHA as shown in Table 2.5.2-217, the HF spectral shape is anchored to the UHRS values from Table 2.5.2-217 at 100 Hz, 25 Hz, 10 Hz, and 5 Hz. In between these frequencies, the spectrum is interpolated using shapes anchored to the next higher and lower frequency and using weights on the two shapes equal to the inverse logarithmic difference between the intermediate frequency and the next higher or lower frequency. Below 5 Hz, the HF shape is extrapolated from 5 Hz. For the LF spectral shape, a similar procedure is used except that the LF spectral shape is anchored to the UHRS values at 2.5 Hz, 1 Hz, and 0.5 Hz. Above 2.5 Hz, the LF shape was extrapolated from those frequencies. Below 0.5 Hz the HF and LF spectra are extrapolated by assuming that spectral amplitudes are proportional to f (where f is spectral frequency) down to f=0.125 Hz, and proportional to f^2 between f=0.125 Hz and f=0.1 Hz. This is the low frequency spectral shape recommended by Building Seismic Safety Council for seismic design (Reference 294).

Figures 2.5.2-237 and 2.5.2-238 show the horizontal HF and LF spectra calculated in this way for 10^{-4} and 10^{-5} annual frequencies of exceedance, respectively. As mentioned previously, these spectra accurately reflect the UHRS amplitudes in Table 2.5.2-217 that are calculated for the seven spectral frequencies at which PSHA calculations are performed.

2.5.2.5 Seismic Wave Transmission Characteristics of the Site

The Lee Nuclear Site is a hard rock site located on igneous and metamorphic rocks of Paleozoic age. Subsection 2.5.1.2 describes the geology of the site area. Subsection 2.5.4 presents a detailed discussion of dynamic and static properties of the site foundation materials. The majority of shear wave velocity measurements at the site exceed 9,200 ft/sec, the hard rock definition used by CEUS attenuation relations (2.83 km/s, 9,282 ft/sec) (Reference 202). Some near-surface shear wave velocity measurements fall below 9,200 ft/sec. Variation in shear wave velocity measurements of several hundred ft/sec centered at the hard rock condition result in a negligible variation in site response calculations.

In summary, the Lee Nuclear Site is a hard rock site with a shear-wave velocity exceeding 9,200 ft/sec. Therefore the EPRI 1009684 (2004) (Reference 202) ground motion equations are used directly, without calculation of site response. The recommended uniform hazard response spectrum reflects this hard rock condition.

2.5.2.6 Ground Motion Response Spectra (GMRS)

This subsection presents the performance goal-based approach used to develop the ground motion response spectrum GMRS for the Lee Nuclear Site, based on the PSHA methodology and results described in Subsection 2.5.2.4. Specifically, the envelope of the horizontal HF and LF spectra shown in Figures 2.5.2-237 and 238 are used to represent the 10^{-4} and 10^{-5} UHRS, and the horizontal GMRS is determined from the following equations:

$$A_R = SA(10^{-5})/SA(10^{-4}) \qquad \text{Equation 2.5.2-4}$$

$$DF = 0.6\ A_R^{0.8} \qquad \text{Equation 2.5.2-5}$$

$$GMRS = \max([SA(10^{-4}) \times \max(1, DF)], 0.45\ SA(10^{-5})) \qquad \text{Equation 2.5.2-6}$$

where A_R is the ground motion slope ratio, DF is the design factor, and $SA(10^{-4})$ and $SA(10^{-5})$ are the horizontal envelope spectral amplitudes corresponding to UHRS annual frequencies of 10^{-4} and 10^{-5}, respectively.

Figure 2.5.2-239 shows the horizontal Lee Nuclear Station GMRS calculated at the top of hard rock. Table 2.5.2-219 documents the horizontal 10^{-4} UHRS, the resulting A_R values (Equation 2.5.2-4), DF values (Equation 2.5.2-5), and the horizontal GMRS (Equation 2.5.2-6).

For the vertical GMRS (Table 2.5.2-220), a fully probabilistic approach is used to develop the vertical hazard curves along with UHRS and GMRS to maintain exceedance probabilities consistent with the horizontal UHRS (Subsection 2.5.2.7.1.1). The method employed, Approach 3 (Subsection 2.5.2.7.1), integrates the horizontal hazard curves with distributions of V/H ratios resulting in vertical hazard curves, which are intended to maintain the same exceedance probability as the horizontal hazard. For the V/H ratios, the stochastic point source model is used to compute both horizontal (normally incident SH-waves) and vertical (incident inclined P-SV waves) motions (References 280 and 281) using the hard rock crustal model (Table 2.5.2-221). For the hard rock profile, because the shear-wave velocities are high, a linear analysis is performed for the horizontal as well as vertical motions (References 273 and 286) (Subsection 2.5.2.7.1.1). Table 2.5.2-221 lists the source distances and depths intended to cover the range in expected hard rock horizontal peak acceleration values at exceedance probabilities ranging from 10^{-2} to 10^{-7} yr^{-1}. Because V/H ratios typically vary with source distance (Reference 292), the range is also intended to cover the distance deaggregation. While the hard rock V/H ratios are largely independent of **M** (Reference 251), **M** 5.1 is selected as small magnitudes dominate the contribution at close distances and at high frequency (Figures 2.5.2-231, 232, and 233), where the V/H ratios typically reach maximum values (References 251, 286, and 292). The median estimates of the computed V/H ratios are shown in Figure 2.5.2-240. Only a subset of the computed ratios are shown in Figure 2.5.2-240, as there is little change at distances beyond about 6 to 9 mi. (10 to 15 km), with an abrupt jump in the ratios within about 6 mi. (10 km). The ratios are largely independent of frequency with a peak near 60 Hz and range in amplitude from about 0.5 to about 1 as distance decreases. These values, at low frequency, are lower than empirical hard rock central and eastern North America (CENA) V/H ratios, which average about 0.8, decreasing from about 0.9 at 1 Hz to about 0.7 at 10 Hz (References 297 and 298). While these empirical V/H ratios are for Fourier amplitude spectra and not 5% damped response spectra and are dominated by small **M** earthquakes ($\leq$ about 4) and large distances ($D \geq$ about 125 mi.), the results illustrate the large uncertainty in vertical hard rock hazard for CENA and suggest large distant ratios may be greater than model predictions at low frequency. To accommodate the large uncertainty, a minimum V/H ratio of 0.7, the average of the empirical and simulations, is adopted. To accommodate the change in source distance with both annual exceedance probability and structural frequency shown in the deaggregation plots (Figures 2.5.2-231, 232, 233, 234, 235, and 236), V/H ratios computed at a suite of distances are given relative weights (Table 2.5.2-223). The distances selected are 17 mi. (28 km), 4 mi. (7 km), and 0 mi. (0 km) to cover ratios reflecting distant, intermediate, and near source contributions. Table 2.5.2-220 lists the resulting vertical 10^{-4} yr^{-1} and 10^{-5} yr^{-1} UHRS and GMRS, and Figure 2.5.2-239 shows the horizontal and vertical GMRS.

2.5.2.7 Development of FIRS for Unit 1

This subsection presents the location-specific Lee Nuclear Station Unit 1 FIRS. As previously stated, the Lee Nuclear Station Unit 1 foundation is supported on new

and previously placed concrete materials positioned directly over continuous hard rock with shear wave velocity dominantly over 9,200 ft/sec. To address this configuration, location-specific FIRS analyses are conducted for the Unit 1 nuclear island, referred to as Unit 1 FIRS. Subsection 2.5.4.7 describes the material dynamic properties and Figure 2.5.4-252 shows the dynamic profile Base Case A1 that represents the Unit 1 FIRS configuration. Unit 1 FIRS defines the Unit 1 nuclear island centerline foundation input motion and is based on the Lee Nuclear Station GMRS developed at the top of a hypothetical outcrop (continuous rock) transferred up through previously placed Cherokee Nuclear Station concrete materials and newly placed Lee Nuclear Station concrete materials to the basemat foundation level at 550.5 ft (NAVD). Unit 1 FIRS as described in this subsection is calculated using the mean and fractiles hazard curves described in Subsection 2.5.2.4.5.

2.5.2.7.1 Site Response Analysis

In calculating the probabilistic ground motions at the Lee Nuclear Site, the Unit 1 FIRS must be hazard consistent (i.e., the annual exceedance probability of the uniform hazard spectrum (UHRS) from which the Unit 1 FIRS is derived should be the same as the hard rock UHRS, referred to herein as the hypothetical rock outcrop UHRS). NUREG/CR-6728 (Reference 251), recommends several site response approaches to produce soil or rock motions consistent with the hypothetical outcrop UHRS. These approaches incorporate site-specific aleatory variabilities into the motions. NUREG/CR-6728 (Reference 251) identifies four basic approaches for determining the site response at the site, referred to as Approaches 1 through 4. The approaches range from performing a PSHA using ground motion attenuation relations developed for the specific site (profile) of interest (Approach 4) to scaling the hypothetical UHRS on the basis of a site response analysis using a broadband input (control, UHRS) motion (Approach 1). The probabilistic method, Approach 3, described in NUREG/CR-6728 is used to compute the location-specific foundation ground motion shaking hazard (FIRS) at the Lee Nuclear Station Unit 1.

The analysis methodology presented in this subsection is described in a supplemental technical report (Reference 299). The report describes, in detail, the analysis methodology used to develop horizontal and vertical site-specific FIRS that are hazard-consistent and incorporate both aleatory and epistemic variabilities in dynamic material properties at the Lee Nuclear Station Unit 1. The report addresses, in detail, the Random Vibration Theory (RVT) approach to equivalent-linear site response, as well as the fully probabilistic method used to incorporate the effects of site-specific dynamic material properties and their variabilities into the hard rock UHRS.

Using Approach 3, the location-specific amplification is characterized by suites of frequency-dependent amplification factors. Approach 3 involves approximations to the hazard integration using suites of transfer functions that result in complete hazard curves at the foundation level for specific ground motion parameters (e.g., spectral accelerations) and a range of structural frequencies.

There are two ways to implement Approach 3: (1) by the integration method, or (2) by simply modifying the attenuation relation ground motion value during the hazard analysis with a suite (distribution) of transfer functions (Reference 275). Both approaches tend to double count site aleatory variability, once in the suite of transfer function realizations and again in the aleatory variability about each median attenuation relation. The full integration method tends to lessen any potential impacts of the large total site aleatory variability (Reference 278).

Potential conservatism introduced by double counting site aleatory variability may be reduced by removing the site-specific aleatory variability (sigma of the transfer functions) from the resulting hazard curves. This is accomplished using the analytical Approach 3 approximation given in References 278 and 202 and setting the slope of the transfer function to zero. The equation for amplitude becomes:

$$A_C = A_e^{\frac{-k\sigma^2}{2}}$$ Equation 2.5.2-7

where A_C is the corrected amplitude at a given annual probability of exceedance (APE), *k* is the slope (log) of the hazard curve, and sigma is the standard deviation of the transfer function. For hazard curve slopes of about 3 and sigma in the 0.2 to 0.3 range, the correction (reduction) is about 10%. This correction can be applied to either implementations of Approach 3. Alternatively, in the implementation of Approach 3 wherein attenuation relations are modified, one can simply use the median transfer function rather than the full distribution, or remove the transfer function sigma from the attenuation relation aleatory variability and use the full distribution. Any of these corrections will approximately remove potential double counting of site aleatory variability.

A distinct advantage of Approach 3 is the proper incorporation of site epistemic variability. Using Approach 3, multiple hazard curves may be developed reflecting multiple site profiles (e.g., velocity profiles, G/G_{max}, and hysteretic damping curves) that are then averaged over probability to develop mean, median, and fractile estimates. Additionally, vertical hazard curves may be developed that are consistent with the horizontal hazard by integrating distributions of V/H ratios (transfer functions) with the resulting site-specific horizontal hazard curves.

2.5.2.7.1.1 Implementation of Approach 3

The Lee Nuclear Station Unit 1 FIRS site response analysis utilizes Approach 3 with the following main steps:

- Randomization of the base case site-dynamic velocity profile (A1) to produce a suite of velocity profiles that incorporates site-specific randomness.

- Transfer functions (amplification for horizontal motions and V/H ratios for vertical motions) as characterized by distributions developed using the RVT based equivalent-linear site response method.

- Based on the deaggregation (Subsection 2.5.2.4.5 describes deaggregation procedure), transfer functions are computed for **M** 5.1 using the omega-square source model and CEUS parameters (Table 2.5.2-221). Because the site-specific condition is quite stiff (concrete), linear site response analyses are used requiring a single (large or small **M**) earthquake.

- Full integration of the generic hard rock and location-specific mean hazard curves with transfer functions to arrive at a distribution of location-specific horizontal and vertical hazard curves reflecting location-specific site aleatory and epistemic variabilities.

- Computation of location-specific UHRS and FIRS.

2.5.2.7.1.1.1 Development of Transfer Functions

Transfer functions are spectral ratios (5% damping) of horizontal top of concrete foundation (firm rock) motions to hard rock (Table 2.5.2-221) as well as vertical-to-horizontal ratios (5% damping) computed for the location-specific profile Unit 1 FIRS. Horizontal amplification factors reflect motions (5% damping response spectra) computed at the top of profile Unit 1 FIRS (concrete) divided by motions computed for a hypothetical (hard) rock outcrop (9,300 ft/sec, Table 2.5.2-221). Due to the profile stiffness, 7,500 ft/sec for concrete, linear analyses are performed.

For vertical motions, site-specific V/H ratios are developed using the point-source model to compute both horizontal (normally incident SH-waves) and vertical (incident inclined P- SV waves) (References 280 and 281) over a range in source distances and depths (Table 2.5.2-221).

Empirical western North America (WNA) V/H ratios are included in the development of vertical motions in addition to site-specific point-source simulations. The use of WNA empirical V/H ratios implicitly assumes similarity in shear- and compression-wave profiles and nonlinear dynamic material properties between site conditions in WNA and location-specific soft rock columns (Figure 2.5.4-252). Whereas this may not be the case for the average WNA rock site profile (Reference 281), the range in site conditions sampled by the WNA empirical generic rock relations likely accommodates site-specific conditions. The relative weights listed in Table 2.5.2-223 reflect the assumed appropriateness of WNA soft rock empirical V/H ratios for Unit 1. Additionally, because the model for vertical motions is not as thoroughly validated as the model for horizontal motions (References 277, 280, and 281), inclusion of empirical models is warranted. The additional epistemic variability introduced by inclusion of both analytical and empirical models also appropriately reflects the difficulty and lack of consensus regarding the modeling of site-specific vertical motions (Reference 282). In the implementation of Approach 3 to develop vertical hazard curves, the epistemic variability is properly accommodated in the vertical mean UHRS, reflecting a weighted average over multiple vertical hazard curves computed for the Unit 1 FIRS (Base Case Profile A1, Figure 2.5.4-252) model (empirical and numerical).

The vertical FIRS (and UHRSs) then maintain the desired risk and hazard levels, consistent with the horizontal design response spectra (GMRS) and UHRSs.

2.5.2.7.1.1.1.1 Horizontal Amplification Factors

Horizontal amplification factors are developed using hard rock spectral shapes as control motions (Reference 251). Base Case Profile A1 is placed on top of the regional hard rock crustal model (Table 2.5.2-221, Reference 273). A hard rock kappa value of 0.006 sec (Table 2.5.2-221) is used, consistent with that incorporated in the hard rock attenuation relations (Reference 273). With a hysteretic damping in concrete between 0.5% and 1.0% any additional damping in the shallow concrete profile is neglected as its impacts will be beyond the fundamental shallow column resonance, well above 50 Hz.

While the site response analyses are linear and therefore strictly independent of control motion spectral shape for Fourier amplitude spectral ratios, at high frequency, 5% damped response spectral ratios may not be strictly independent of control motion spectral shape. This can occur because the width of the simple harmonic oscillator transfer function is constant in log frequency and increases directly with frequency, averaging over a wider range in frequencies as oscillator frequency increases. At very large distances, where crustal damping has depleted high frequencies (spectral shapes shift to lower frequencies, Reference 251) and the site resonance is not highly excited, response spectral ratios may depart from those computed using control motions relatively rich in high frequency energy (close distances). To accommodate the possibility of distance dependent transfer functions in a linear analysis, a suite of spectral shapes is used as control motions at distances of 0.6, 12, 62,125, 250 mi (1, 20, 100, 200, and 400 km). Results are shown in Figure 2.5.2-241 and reveal the shallow site resonance, median amplification of about 10% near 60 Hz to 70Hz, with a very slight difference only at 250 mi (400 km). The width of the resonance is broadened by the profile randomization with shear-wave velocities varying ±10% about the Unit 1 FIRS value of 7,500 ft/sec along with depth to hard rock at 20 ft, randomly varied ± 3 ft.

2.5.2.7.1.1.1.2 Site Aleatory Variability

For the Lee Nuclear Station, the concrete profile is randomized between depths of 17 to 23 ft, the range in depths to hard rock conditions [shear-wave velocity exceeding, on average, 9,300 ft/sec (2.83 km/sec)] (Reference 273). A uniform distribution is assumed for the depth randomization. For the shear-wave velocity randomization, a soft rock correlation model was used (References 277 and 280). Because concrete velocities show much less variability than firm rock, being a uniform and controlled emplacement material, variations in velocity were constrained to ±10% about the base case value of 7,500 ft/sec with a COV of 0.1.

To accommodate random fluctuations in compression-wave velocity when modeling vertical motions, Poisson ratio is held constant at the base-case values, and random compression-wave velocities are then generated based on shear-wave velocity realizations and base-case Poisson ratios. In reality, Poisson ratio will vary but is likely correlated with shear-wave velocity. As a result, varying Poisson ratio, when properly correlated with shear-wave velocity, will likely not

result in a greater variation in compression-wave velocity than assumed here. Additionally, variation in compression-wave velocity has a much smaller effect on motions than shear-wave velocity as the wavelengths typically are 2 to 5 times greater.

2.5.2.7.2 Development of V/H Ratios

To model vertical motions, incident inclined P-SV waves are modeled from the source to the site using the plane-wave propagators of Silva et al. (1996) (Reference 288) assuming a shear-wave point-source spectrum (References 277, 280, and 281). The point source model is used to accommodate the effects of distance and source depth on V/H ratios (Table 2.5.2-221). For consistency, both the horizontal and vertical motions are modeled using the same parameters (Table 2.5.2-221). The horizontal motions are modeled as vertically propagating shear-waves. For the vertical motions, the angles of incidence are computed by two-point ray tracing through the crust and site-specific profile. To model site response, the near-surface V_P and V_S profiles (Figure 2.5.4-252) are placed on top of the crustal structure (Table 2.5.2-221), the incident P-SV wavefield is propagated to the surface, and the vertical motions are computed.

In the implementation of the equivalent-linear approach to estimate V/H response spectral ratios for the Lee Nuclear Station Unit 1 FIRS, the horizontal component analyses are performed for vertically propagating shear waves. To compute the vertical motions, a linear analysis is performed for incident inclined P-SV waves using low-strain VP and VS derived from the profile Unit 1 FIRS (Subsection 2.5.4.7). The P-wave damping is set equal to the low strain S-wave damping (Reference 289). The horizontal component and vertical component analyses are performed independently.

The approximations of linear analysis for the vertical component and uncoupled vertical and horizontal components are validated in two ways. Fully nonlinear modeling using a 3-D soil model shows that the assumption of largely independent horizontal and vertical motions for loading levels up to about 0.5g (soil surface, horizontal component) for moderately stiff profiles is appropriate (Reference 280). Additionally, validation exercises with recorded motions have been conducted at over 50 sites that recorded the 1989 **M** 6.9 Loma Prieta, California earthquake (Reference 273). These validations show the overall bias and variability is low but is higher than that for horizontal motions. The vertical model does not perform as well as the model for horizontal motions (References 280 and 281). An indirect validation is also performed by comparing V/H ratios from WNA empirical attenuation relations with model predictions (Reference 281) over a wide range in loading conditions (Reference 281). The results show a favorable comparison with the model exceeding the empirical V/H ratios at high frequency, particularly at high loading levels. In the V/H comparisons with empirical relations, the model also shows a small under prediction at low frequency ($\leq$ 1 Hz) and at large distance ($\geq$ 12 mi.).

For the vertical analyses, a hard rock kappa value of 0.003 sec, half that of the horizontal, is used. This factor of 50% is based on observations of kappa at strong

motion sites (Reference 290), validation exercises (Reference 280), and the observation that the peak in the vertical spectral acceleration (5% damped) for WNA rock and soil sites is generally near 10 to 12 Hz compared to the horizontal motion peak that occurs at about 5 Hz, conditional on **M** 6.5 at a distance of about 6 to 20 mi. This difference of about 2 in peak frequency is directly attributable to differences in kappa of about 2. Similar trends are seen in CEUS hard rock spectra with the vertical component peaking at higher frequencies than the horizontal component (Reference 251).

For Lee Nuclear Station Unit 1 FIRS the site-specific V/H ratios, Figure 2.5.2-240 shows median estimates computed with the stochastic model for **M** 5.1. For **M** 5.1, the distances range from 50 to 0 mi. (80 to 0 km) (Table 2.5.2-221) with expected horizontal hard rock peak accelerations ranging from 0.01 to 0.50g. Figure 2.5.2-240 shows that the V/H for the shallow concrete profile Unit 1 FIRS are nearly constant with frequency and increase rapidly as distance decreases, within about a 9 mi. source distance. For distances beyond 6 to 9 mi., the V/H ratio is about 0.5 and increases rapidly to about 0.9. The peak near 60 Hz is likely due to the peak in the horizontal amplification factors (Figure 2.5.2-241). In Figure 2.5.2-240, the multiple peaks beginning near 1 Hz reflect deep crustal resonances (structure below 0.5 mi., Table 2.5.2-221) that would be smoothed if the crustal model were randomized and discrete layers replaced with steep velocity gradients to reflect lateral variability and a more realistic crustal structure. The **M** 5.1 distance ranges more than adequately accommodate the hazard deaggregation (Subsection 2.5.2.4.5).

As previously discussed (Subsection 2.5.2.7.1.1.1), the model predictions of V/H ratios at low frequency may be slightly unconservative and at high frequency they may be conservative. While it is important to include site-specific effects on the vertical hazard, potential model deficiencies can be compensated with inclusion of empirical V/H ratios computed from WNA generic rock and soil site attenuation relations. Additionally, empirical V/H ratios of Fourier amplitude spectra based on CENA recordings at hard rock sites have median values near about 0.8 and vary slowly with frequency. As with the development of the hard rock V/H ratios (Subsection 2.5.2.6), to adequately accommodate potential model deficiencies as well as the large uncertainty in hard and firm rock V/H ratios for CENA, a minimum value of 0.7 is adopted.

For the empirical V/H ratios, both Abrahamson and Silva (Reference 290) and Campbell and Bozorgnia (Reference 292) soft rock WNA relations are used with equal weights (Table 2.5.2-222). As an example, Figure 2.5.2-242 shows the Campbell and Bozorgnia V/H ratios computed for **M** 5.1. Distance bins differ between the empirical and analytical V/H ratios because the empirical ratios use a generic suite of distances used on many projects while the analytical V/H ratios are region specific. For distances beyond 35 mi. (57 km), the empirical V/H ratios are nearly constant with increasing distance. Additionally, for the smaller **M** (**M** < 5.5), there are few strong motion data available at larger distances (Reference 292). Because the ratios vary slowly with distance, the differences in distances are not significant. The empirical WNA soft rock ratios show more distance (loading level) dependence than the firm rock analytical ratios (Figure 2.5.2-242), perhaps due to nonlinearity in the horizontal soft rock motion

(Reference 286). Figure 2.5.2-243 shows the empirical soft rock V/H ratios computed for **M** 8.0. Similar trends are seen with the **M** 5.1 V/H ratios, suggesting a **M** (loading level) sensitivity for soft rock that is much less than that for soil (Reference 286). These trends, with the **M** independence of V/H ratios, are expected for firm rock conditions. That is, as the profile becomes stiffer, nonlinearity decreases, and for distances within about 6 to 9 mi., distance becomes the dominant controlling factor in V/H ratios (Reference 274).

It is important to note the site-specific and generic V/H ratios peak at very different frequencies, about 60 Hz and about 10 to 20 Hz, respectively, with the site-specific having generally higher V/H ratios, particularly at close distances. Use of an empirical V/H ratio alone may underestimate the vertical hazard at high frequency, provided the model predictions are reasonably accurate.

In assigning the V/H ratios in the Approach 3 analysis, the source **M** and ***D*** change significantly with structural frequency as probability changes. To accommodate the deaggregation in (contributing sources) integrating the horizontal hazard with the distributions of V/H ratios, the **M** and ***D*** distribution used is listed in Table 2.5.2-223. The magnitudes selected are intended to capture the dominant sources: **M** 5.1 for close-in sources and **M** 7.0 and **M** 8.0 for the Charleston, South Carolina, and New Madrid, Missouri sources, respectively, both at distances well beyond 60 mi. (100 km) (Subsection 2.5.2.4.3.2). The distances used for the V/H ratios (Table 2.5.2-223) reflect the distance sensitivity, or lack of sensitivity beyond about 6 to 9 mi. (10 to 15 km) for the site-specific ratios and beyond about 30 mi. (50 km) for the empirical ratios, considering the contributing source distances (Subsection 2.5.2.4.3.2). The weights listed in Table 2.5.2-223 are intended to approximate the relative contributions of the three sources across structural frequency and exceedance probability. Because the V/H ratios vary slowly with distance, only a smooth approximation to the hazard deaggregation is necessary. To adequately capture the change in **M** and ***D*** with AEP, only a few distance bins are required: 3 and 35 mi. (5 and 57 km) for the empirical and 0, 4, and 17 mi. (0, 7, and 28 km) for the analytical (Table 2.5.2-223).

2.5.2.7.3 UHRS Interpolation and Extrapolation

Because the hard rock hazard is computed at only seven frequencies, namely 0.5, 1.0, 2.5, 5.0, 10.0, 25.0, and 100.0 Hz (taken as peak acceleration), the site-specific hazard has been both extrapolated to 0.1 Hz and interpolated to 100 points per decade from 0.1 to 100.0 Hz (about 300 points). At high frequency, hard rock hazard curves are interpolated at 34 and 50 Hz, as these are the critical frequencies to define the Unit 1 FIRS and UHRS shapes beyond 25 Hz. This interpolation is performed by using the deterministic shapes (Reference 251) for the appropriate **M** to interpolate the hard rock UHRS at AEP of 10^{-4}, 10^{-5}, and 10^{-6} yr^{-1}, resulting in three points on 34 and 50 Hz hazard curves. The adjacent hazard curves at 25 and 100 Hz are then used as shapes to extrapolate to lower and higher exceedance probabilities, resulting in approximate hard rock hazard curves. Approach 3 is then applied to develop site-specific horizontal and vertical UHRS at the same exceedance probability as the 25 and 100 Hz hard rock hazard. For the vertical component, because the site specific V/H ratios peak at

very high frequency (beyond 50 Hz), it is important to maintain the appropriate hazard levels between 25 and 50 Hz. Below 0.5 Hz, the extrapolation is performed in a similar way using the 0.5 Hz hazard curve as a shape taken through estimates of the 10^{-4}, 10^{-5}, and 10^{-6} yr^{-1} hazard at frequencies below 0.5 Hz. Because the aleatory variability in attenuation relations increases with period (References 202, 290, 291, and 292), use of a median spectral shape (Reference 274) to extrapolate at low frequency may be inappropriate and result in potentially unconservative hazard or higher probability than desired. To address this uncertainty, a conservative approach is adopted by extrapolating the 0.5 Hz 10^{-4}, 10^{-5}, and 10^{-6} hard rock UHRSs, assuming a constant slope in spectral velocity (+1 slope in pseudo-absolute spectral acceleration) (Reference 294). The extrapolation is extended at low frequency to the earthquake source corner frequency, where the slope is increased to a constant spectral displacement. Since the source corner frequency, or transition from approximately constant spectral velocity to spectral displacement, depends on magnitude, an average representative magnitude of **M** 7.2, based on the deaggregations, is assumed to apply for frequencies below 0.5 Hz, based on the low-frequency deaggregation (Subsection 2.5.2.4.5). Application of the empirical relation

$$\text{Log } T = -1.25 + 0.3\mathbf{M} \qquad \text{Equation 2.5.2-8}$$

(Reference 294) results in a corner period (T) of approximately 8 sec (0.125 Hz). To accommodate this expected change in slope, the extrapolations are performed at 0.125 and 0.1 Hz, assuming constant spectral velocity from 0.5 to 0.125 Hz and constant spectral displacement for frequencies below 0.125 Hz.

2.5.2.7.4 Design Basis Response Spectra

Table 2.5.2-224 and Figures 2.5.2-244 and 245 show horizontal and vertical Unit 1 FIRS developed compared to the horizontal and vertical GMRS developed for Unit 2. Figure 2.5.2-246 shows both the horizontal and vertical FIRS. Figure 2.5.2-247 shows the horizontal and vertical UHRS at exceedance levels of 10^{-4}, 10^{-5}, and 10^{-6} yr^{-1}. Through Approach 3, both the horizontal and vertical UHRS and Unit 1 FIRS are hazard- and performance-based consistent across structural frequency from 0.5 to 100 Hz, the frequency range over which the hard rock hazard is computed (Reference 273). For frequencies below 0.5 to 0.1 Hz, the extrapolation employed is intended to reflect conservatism, likely resulting in motions of lower probability. Table 2.5.2-224 lists discrete FIRS and UHRS horizontal and vertical spectral acceleration values for Unit 1. Section 3.7 compares the site-specific ground motions to the AP-1000 design ground motions.

2.5.2.8 References

201. Electric Power Research Institute (EPRI), *Seismic Hazard Methodology for the Central and Eastern United States, Tectonic Interpretations*, EPRI Report NP-4726, volumes 5-10, July 1986.

202. Electric Power Research Institute (EPRI), *CEUS Ground Motion Project Final Report*, EPRI Technical Report 1009684, December 2004.

203. Electric Power Research Institute (EPRI), *Probabilistic Seismic Hazard Evaluation at Nuclear Plant Sites in the Central and Eastern United States, Resolution of the Charleston Earthquake Issue*, EPRI Report 6395-D, April 1989.

204. Electric Power Research Institute (EPRI), *Seismic Hazard Methodology for the Central and Eastern United States, Volume 1, Part 2: Methodology (Revision 1)*, EPRI NP-4726-A, November 1988.

205. South Eastern United States Seismic Network (SEUSSN) catalog, Virginia Tech Seismic Observatory, Website, http://www.geol.vt.edu/outreach/vtso/anonftp/catalog/susn2004cat.txt, accessed August 26, 2006.

206. Advanced National Seismic System (ANSS), Website, http://quake.geo.berkeley.edu/ anss/catalog-search.html, accessed August 29, 2006.

207. Electric Power Research Institute (EPRI), *EQHAZARD Primer*, EPRI Special Report NP-6452-D, Prepared by Risk Engineering for Seismicity Owners Group and EPRI, June 1989.

208. Atkinson, G. M. and D. M. Boore, "Ground-Motion Relations for Eastern North America," *Bulletin of the Seismological Society of America* 85 (1):17-30, 1995.

209. Frankel, A., Barnhard, T., Perkins, D., Leyendecker, E.V., Dickman, N., Hanson, S., and Hopper, M., *National Seismic-Hazard Maps: Documentation*, U.S. Geological Survey Open-File Report 96-532, 1996.

210. Frankel, A.D., Petersen, M.D., Mueller, C.S., Haller, K.M., Wheeler, R.L., Leyendecker, E.V., Wesson, R.L., Harmsen, S.C., Cramer, C.H., Perkins, D.M., and Rukstales, K.S., *Documentation for the 2002 Update of the National Seismic Hazard Maps*, U.S. Geological Survey Open-File Report 02-420, 2002.

211. Chapman, M.C. and Talwani, P., *Seismic Hazard Mapping for Bridge and Highway Design in South Carolina*, South Carolina Department of Transportation (SCDOT) Report, 2002.

212. Savy, J.B., Foxall, W., Abrahamson, N., and Bernreuter, D., *Guidance for Performing Probabilistic Seismic Hazard Analysis for a Nuclear Plant Site: Example Application to the Southeastern United States*, U.S. Nuclear Regulatory Commission Report, NUREG/CR-6607, 2002.

213. Senior Seismic Hazard Analysis Committee (SSHAC), *Recommendations for Probabilistic Seismic Hazard Analysis: Guidance on Uncertainty and Use of Experts*, U.S. Nuclear Regulatory Commission Report, NUREG/CR-6372, 1997.

214. Bechtel Corp., *Update of Charleston Seismic Source and Integration with EPRI Source Models*, Engineering Study Report 25144-006-V14-CY06-00006, revision 002, 2006.

215. Tarr, A. C., Talwani, P., Rhea, S., Carver, D., and Amick, D., "Results of Recent South Carolina Seismological Studies," *Bulletin of the Seismological Society of America* 71 (6):1,883-1,902, 1981.

216. Madabhushi, S. and Talwani, P., "Fault Plane Solutions and Relocations of Recent Earthquakes in Middleton Place-Summerville Seismic Zone near Charleston, South Carolina," *Bulletin of the Seismological Society of America* 83 (5):1,442-1,466, 1993.

217. Bollinger, G.A., "Reinterpretation of the Intensity Data for the 1886 Charleston, South Carolina, Earthquake," in *Studies Related to the Charleston, South Carolina, Earthquake of 1886 - A Preliminary Report*, U.S. Geological Survey Professional Paper 1028:17-32, 1977.

218. Tarr, A.C., and Rhea, B.S., "Seismicity Near Charleston, South Carolina, March 1973 to December 1979," in *Studies Related to the Charleston, South Carolina Earthquake of 1886 Tectonics and Seismicity*, U.S. Geological Survey Professional Paper 1313:R1-R17, 1983.

219. Amick, D., *Paleoliquefaction Investigations Along the Atlantic Seaboard With Emphasis on the Prehistoric Earthquake Chronology of Coastal South Carolina*, unpub. Ph.D. dissertation, University of South Carolina, 1990.

220. Amick, D., Gelinas, R., Maurath, G., Cannon, R., Moore, D., Billington, E., and Kemppinen, H., *Paleoliquefaction Features along the Atlantic Seaboard*, U.S. Nuclear Regulatory Commission Report, NUREG/CR-5613, 1990.

221. Amick, D., Maurath, G., and Gelinas, R., "Characteristics of Seismically Induced Liquefaction Sites and Features Located in the Vicinity of the 1886 Charleston, South Carolina Earthquake," *Seismological Research Letters* 61 (2):117-130, 1990.

222. Talwani, P. and Schaeffer, W.T., "Recurrence Rates of Large Earthquakes in the South Carolina Coastal Plain Based on Paleoliquefaction Data," *Journal of Geophysical Research* 106 (B4):6,621-6,642, 2001.

223. Behrendt, J.C. and Yuan, A., "The Helena Banks Strike-Slip (?) Fault Zone in the Charleston, South Carolina Earthquake Area: Results from a Marine, High-Resolution, Multichannel, Seismic-Reflection Survey," *Geological Society of America Bulletin* 98:591-601, 1987.

224. Obermeier, S.F., Weems, R.E., Jacobson, R.B., and Gohn, G.S., "Liquefaction Evidence for Repeated Holocene Earthquakes in the Coastal Region of South Carolina," in “Earthquake Hazards and the Design of Constructed Facilities in the Eastern United States,” *Annals of the New York Academy of Sciences* 558:183-195, 1989.

225. Obermeier, S., "Liquefaction-Induced Features," in *Paleoseismology*, ed. J. McCalpin, Academic Press, San Diego, 1996.

226. Marple, R.T. and Talwani, P., "Evidence for a Buried Fault System in the Coastal Plain of the Carolinas and Virginia - Implications for Neotectonics in the Southeastern United Sates," *Geological Society of America Bulletin* 112 (2):200-220, 2000.

227. Bollinger, G.A., Chapman, M.C., Sibol, M.S., and Costain, J.K., "An Analysis of Earthquake Focal Depths in the Southeastern U.S.," *Geophysical Research Letters* 12 (11):785-788, 1985.

228. Bollinger, G. A., Johnston, A. C., Talwani, P., Long, L. T., Shedlock, K. M., Sibol, M. S., and Chapman, M. C., "Seismicity of the Southeastern United States; 1698-1986," in *Neotectonics of North America, Decade Map Volume to Accompany the Neotectonic Maps,* ed. D.B. Slemmons, E.R. Engdahl, M.D. Zoback, and D.B. Blackwell, Geological Society of America, 1991.

229. Bollinger, G.A. Specification of Source Zones, *Recurrence Rates, Focal Depths, and Maximum Magnitudes for Earthquakes Affecting the Savannah River Site in South Carolina*, U.S. Geological Survey Bulletin 2017, 1992.

230. Wells D.L. and K.J. Coppersmith, "New Empirical Relationships Among Magnitude, Rupture Length, Rupture Width, Rupture Area, and Surface Displacement," *Bulletin Seismological Society of America* 84 (4):974-1002, 1994.

231. Johnston, A.C., "Seismic Moment Assessment of Earthquakes in Stable Continental Regions - III. New Madrid 1811-1812, Charleston 1886 and Lisbon 1755," *Geophysical Journal International* 126:314-344, 1996.

232. Bakun, W.H. and Hopper, M.G., "Magnitudes and Locations of the 1811-1812 New Madrid, Missouri, and the 1886 Charleston, South Carolina, Earthquakes," *Bulletin of the Seismological Society of America* 94 (1):64-75, 2004.

233. Grant, L.B. and Sieh, K., "Paleoseismic Evidence of Clustered Earthquakes on the San Andreas Fault in the Carrizo Plain, California," *Journal of Geophysical Research* 99 (B4):6819-6841, 1994.

234. Tuttle, M.P., "The Use of Liquefaction Features in Paleoseismology: Lessons Learned in the New Madrid Seismic Zone, Central United States," *Journal of Seismology* 5:361-380, 2001.

235. Rockwell, T.K., Lindvall, S., Herzberg, M., Murbach, D., Dawson, T., and Berger, G., "Paleoseismology of the Johnson Valley, Kickapoo, and Homestead Valley Faults: Clustering of Earthquakes in the Eastern California Shear Zone," *Bulletin of the Seismological Society of America* 90 (5):1,200-1,236, 2000.

236. Savage, J. C., "Criticism of Some Forecasts of the National Earthquake Evaluation Council," *Bulletin of the Seismological Society of America* 81 (3):862-881, 1991.

237. Cramer, C.H., "A Seismic Hazard Uncertainty Analysis for the New Madrid Seismic Zone," *Engineering Geology* 62:251-266, 2001.

238. Ellsworth, W.L., Matthews, M.V., Nadeau, R.M., Nishenko, S.P., Reasenberg, P.A., and Simpson, R.W., *A Physically-Based Earthquake Recurrence Model for Estimation of Long-Term Earthquake Probabilities*, U.S. Geological Survey Open-File Report 99-522, 1999.

239. Matthews, M.V., Ellsworth, W.L., and Reasenberg, P.A., "A Brownian Model for Recurrent Earthquakes," *Bulletin of the Seismological Society of America* 92:2,233-2,250, 2002.

240. Working Group on California Earthquake Probabilities (WGCEP), *Earthquake Probabilities in the San Francisco Bay Region: 2002-2031*, U.S. Geological Survey Open-File Report 03-2134, 2003.

241. Working Group on California Earthquake Probabilities (WGCEP), "Seismic Hazards in Southern California: Probable Earthquakes, 1994 to 2024," *Bulletin of the Seismological Society of America* 85:379-439, 1995.

242. NIST/SEMATECH, e-Handbook of Statistical Methods, Website, http://www.itl.nist.gov/div898/handbook/, accessed January 11, 2006.

243. Cornell, C.A., "Engineering Seismic Risk Analysis," *Bulletin of the Seismological Society of America* 58 (5):1,583-1,606, 1968.

244. Chapman, M.C., Munsey, J.W., Powell, C.A., Whisner, S.C., and Whisner J., "The Eastern Tennessee Seismic Zone - Summary after 20 Years of Network Monitoring," *Seismological Research Letters* 73 (2):245, 2002.

245. Wheeler, R.L., *Known or Suggested Quaternary Tectonic Faulting, Central and Eastern United States- New and Updated Assessments for 2005*, U.S. Geological Survey Open-File Report 2005-1336, 2005.

246. Cornell, C.A. and Winterstein, S.R., "Temporal and Magnitude Dependence in Earthquake Recurrence Models," *Bulletin of the Seismological Society of America* 79:1,522-1,537, 1988.

247. Hough, S.E., Armbruster J.G., Seeber, L., and Hough, J.F., "On the Modified Mercalli Intensities and Magnitudes of the 1811-1812 New Madrid Earthquakes," *Journal of Geophysical Research* 105 (B10):23,839-23,864, 2000.

248. Tuttle, M.P., Schweig, E.G., Sims, J.D., Lafferty, R.H., Wolf, L.W., and Haynes, M.L., "The Earthquake Potential of the New Madrid Seismic Zone," *Bulletin of the Seismological Society of America* 92 (6):2,080-2,089, 2002.

249. Abrahamson, N.A., and Bommer, J., *Program on Technology Innovation: Truncation of the Lognormal Distribution and Value of the Standard Deviation for Ground Motion Models in the Central and Eastern United States*, Electric Power Research Institute (EPRI) Technical Report 1014381, August 2006.

250. Hardy, G., Merz, K., Abrahamson, N.A., and Watson-Lamprey, J. *Program on Technology Innovation: Use of Cumulative Absolute Velocity (CAV) in Determining Effects of Small Magnitude Earthquakes on Seismic Hazard Analyses*, Electric Power Research Institute (EPRI) Report 1014099, August 2006.

251. McGuire, R.K., Silva, W.J., and Constantino, C.J. *Technical Basis for Revision of Regulatory Guidance on Design Ground Motions: Hazard and Risk-Consistent Ground Motions Spectra Guidelines*, U.S. Nuclear Regulatory Commission Report Prepared for Division of Engineering Technology, Washington, D.C., NUREG/CR-6728, 2001.

252. Weems, R.E., and Lewis, W.C., "Structural and Tectonic Setting of the Charleston, South Carolina, Region; Evidence from the Tertiary Stratigraphic Record," *Geological Society of America Bulletin* 114 (1):24-42, 2002.

253. Talwani, P., "An Internally Consistent Pattern of Seismicity Near Charleston, South Carolina," *Geology* 10:655-658, 1982.

254. Talwani, P., *Macroscopic Effects of the 1886 Charleston Earthquake, A Compendium of Field Trips of South Carolina Geology*, South Carolina Geological Survey Guidebook, 2000.

255. Cook, F.A., Albaugh, D.S., Brown, L.D., Kaufman, S., Oliver, J. E., Hatcher, R.D. Jr., "Thin-skinned Tectonics in the Crystalline Southern Appalachians: COCORP Seismic Reflection Profiling of the Blue Ridge and Piedmont," *Geology* 7:563-567, 1979.

256. Cook, F.A., Brown, L.D., Kaufman, S., Oliver, J.E. and Petersen, T.A., "COCORP Seismic Profiling of the Appalachian Orogen Beneath the Coastal Plain of Georgia," *Geological Society of America Bulletin* 92 (10):738-748, 1981.

257. Behrendt, J.C., Hamilton, R.M., Ackermann, H.D., and Henry, V.J., "Cenozoic Faulting in the Vicinity of the Charleston, South Carolina, 1886 Earthquake," *Geology* 9 (3):117-122, 1981.

258. Behrendt, J.C., Hamilton, R.M., Ackermann, H.D., Henry, V.J., and Bayer, K.C., *Marine Multichannel Seismic-reflection Evidence for Cenozoic Faulting and Deep Crustal Structure Near Charleston, South Carolina*, U.S. Geological Survey Professional Paper 1313-J, 1983.

259. Seeber, L., and Armbruster, J.G., "The 1886 Charleston, South Carolina Earthquake and the Appalachian Detachment," *Journal of Geophysical Research* 86 (B9):7,874-7,894, 1981.

260. Smith, W.A., and Talwani, P., "Preliminary Interpretation of a Detailed Gravity Survey in the Bowman and Charleston, S.C. Seismogenic Zones," *Abstracts with Programs - Geological Society of America Southeastern Section* 17 (2):137, 1985.

261. Lennon, G., *Identification of a Northwest Trending Seismogenic Graben Near Charleston, South Carolina*, U.S. Nuclear Regulatory Commission Report, NUREG/CR-4075, 1986.

262. Hamilton, R.M., Behrendt, J.C., and Ackermann, H.D., "Land Multichannel Seismic-Reflection Evidence for Tectonic Features Near Charleston, South Carolina," in *Studies Related to the Charleston, South Carolina, Earthquake of 1886- Tectonics and Seismicity*, ed. G.S. Gohn, U.S. Geologic Survey Professional Paper 1313-I, 1983.

263. Wentworth, C.M., and Mergner-Keefer, M., "Regenerate Faults of the Southeastern United States," in *Studies Related to the Charleston, South Carolina, Earthquake of 1886- Tectonics and Seismicity*, ed. G.S. Gohn, U.S. Geological Survey Professional Paper 1313-S, 1983.

264. Marple, R.T. and Talwani, P., "Evidence for Possible Tectonic Upwarping Along the South Carolina Coastal Plain from an Examination of River Morphology and Elevation Data," *Geology* 21:651-654, 1993.

265. Marple, R.T. and Talwani, P., "Proposed Shenandoah Fault and East Coast-Stafford Fault System and Their Implications for Eastern U.S. Tectonics," *Southeastern Geology* 43 (2):57-80, 2004.

266. Talwani, P. and Katuna M., *Macroseismic Effects of the 1886 Charleston Earthquake*, Carolina Geological Society Field Trip Guidebook, 2004.

267. Weems, R.E., Lemon, E.M., Jr., and Nelson, M. S., *Geology of the Pringletown, Ridgeville, Summerville, and Summerville Northwest 7.5-minute Quadrangles, Berkeley, Charleston, and Dorchester Counties, South Carolina*, U.S. Geological Survey Miscellaneous Investigations Series Map, 1997.

268. Talwani, P., "Fault Geometry and Earthquakes in Continental Interiors," *Tectonophysics* 305:371-379, 1999.

269. Johnston, A.C., Coppersmith, K.J., Kanter, L.R., and Cornell, C.A., *The Earthquakes of Stable Continental Regions, Volume I: Assessment of Large Earthquake Potential*, EPRI Final Report TR-102261-V1, 1994.

270. Martin, J.R. and Clough, G.W., "Seismic Parameters from Liquefaction Evidence," *Journal of Geotechnical Engineering* 120 (8):1,345-1,361, 1994.

271. Bronk Ramsey, C., "Radiocarbon Calibration and Analysis of Stratigraphy: the OxCal program," *Radiocarbon* 37 (2):425-430, 1995.

272. Bronk Ramsey, C., "Development of the Radiocarbon Calibration Program," *Radiocarbon* 43 (2A):355-363, 2001.

273. Electric Power Research Institute (EPRI), *Guidelines for Determining Design Basis Ground Motions, Volume 5- Quantification of Seismic Source Effects*, EPRI Report TR-102293, Project 3302, Final Report, November 1993.

274. McGuire, R.K., Silva, W.J., and Costantino, C.J., *Technical Basis for Revision of Regulatory Guidance on Design Ground Motions*: Development of Hazard- and Risk-consistent Seismic Spectra for Two Sites, U.S. Nuclear Regulatory Commission Report, NUREG/CR-6769, 2002.

275. Bazzurro, P. and Cornell, C.A., "Nonlinear Soil-Site Effects in Probabilistic Seismic-Hazard Analysis," *Bulletin of the Seismological Society of America* 94:2,110-2,123, 2004.

276. Lee, R., Silva, W.J., and Cornell, C.A., "Alternatives in Evaluating Soil- and Rock-Site Seismic Hazard," *Seismological Research Letters* 69:81, 1998.

277. Lee, R., Maryak, M.E., and Kimball, J., "A Methodology to Estimate Site-Specific Seismic Hazard for Critical Facilities on Soil or Soft-Rock Sites," *Seismological Research Letters* 70:230, 1999.

278. Anderson, J.G. and Hough, S.E., "A Model for the Shape of the Fourier Amplitude Spectrum of Acceleration at High Frequencies," *Bulletin of the Seismological Society of America* 74 (5):1,969-1,993, 1984.

279. Deleted.

280. Electric Power Research Institute (EPRI), *Proceedings: Engineering Characterization of Small-Magnitude Earthquakes*, EPRI Project 2556-25 Final Report NP-6389, Section 1-6, 1989.

281. Silva, W.J., "Body Waves in a Layered Anelastic Solid," *Bulletin of the Seismological Society of America* 66:1,539-1,554, 1976.

282. Silva, W.J., Li, S., Darragh, B., and Gregor, N., "Surface Geology Based Strong Motion Amplification Factors for the San Francisco Bay and Los Angeles Areas," in *A PEARL Report to PG&E/CEC/Caltrans*, Award No. SA2120-59652, 1999.

283. Bakun, W.H. and Wentworth, C.M., "Estimating Earthquake Location and Magnitude from Seismic Intensity Data," *Bulletin of the Seismological Society of America* 87:1,502-1,521, 1997.

284. Toro, G.R., Abrahamson, N.A., and Schneider, J.F., "Model of Strong Ground Motions from Earthquakes in Central and Eastern North America: Best Estimates and Uncertainties," *Seismological Research Letters* 68(1):41-57, 1997.

285. Silva, W.J., Darragh, R., Gregor, N., Martin, G., Kircher, C., and Abrahamson, N., *A Reassessment of Site Coefficients and Near-Fault Factors for Building Code Provisions*, U.S. Geological Survey Grant Award #98-HQ-GR-1010 Final Report, 2000.

286. Silva, W.J., "Characteristics of Vertical Strong Ground Motions for Applications to Engineering Design," in *Proceedings of the FHWA/NCEER Workshop on the National Representation of Seismic Ground Motion for New and Existing Highway Facilities*, ed. I.M. Friedland, M.S Power and R. L. Mayes, Technical Report NCEER-97-0010, 1997.

287. Atkinson, G.M., "Source Spectra for Earthquakes in Eastern North America," *Bulletin of the Seismological Society America* 83 (6):1,778 1,798, 1993.

288. Silva, W.J., Abrahamson, N., Toro, G., and Costantino, C., *Description and Validation of the Stochastic Ground Motion Model*, unpub. report prepared by Pacific Engineering and Analysis for Brookhaven National Laboratory, 1996.

289. Johnson, L.R. and Silva W.J., "The Effects of Unconsolidated Sediments Upon the Ground Motion During Local Earthquakes," *Bulletin of the Seismological Society of America* 71:127-142, 1981.

290. Abrahamson, N.A. and Silva, W.J, "Empirical Response Spectral Attenuation Relations for Shallow Crustal Earthquakes," *Seismological Research Letters* 68 (1):94-127, 1997.

291. Campbell, K.W., “Empirical Near Source Attenuation Relationships for Horizontal and Vertical Components of Peak Ground Acceleration, Peak Ground Velocity, and Pseudo Absolute Acceleration Response Spectra,” *Seismological Research Letters* 68 (1):154-176, 1997.

292. Campbell, K.W. and Bozorgnia, Y., "Updated Near-Source Ground Motion (Attenuation) Relations for the Horizontal and Vertical Components of Peak Ground Acceleration and Acceleration Response Spectra," *Bulletin of the Seismological Society of America* 93 (1):314-331, 2003.

293. Exelon Generation Company, LLC, Site Safety Analysis Report for the Clinton ESP site, Rev. 4, April 2006.

294. Building Seismic Safety Council (BSSC), *National Earthquake Hazards Reduction Program (NEHRP)*, *Recommended Provisions for Seismic Regulations for New Buildings and Other Structures (FEMA 450)*, Report prepared for the Federal Emergency Management Agency (FEMA), 2004.

295. American Society of Civil Engineers (ASCE)/Structural Engineering Institute (SEI), *Seismic Design Criteria for Structures, Systems, and Components in Nuclear Facilities*, ASCE/SEI 43-05, 2005.

296. American National Standards Institute (ANSI)/American Nuclear Society (ANS), Categorization of Nuclear Facility Structures, Systems, and Components for Seismic Design, ANSI/ANS-2.26-2004, 2004.

297. Atkinson, G.M., “Empirical Attenuation of Ground Motion Spectral Amplitudes in Southeastern Canada and the Northeastern United States,” Bulletin of the Seismological Society of America 94 (3): 1079-1095, 2004

298. Atkinson, G.M., “Notes on Ground Motion Parameters for Eastern North America: Duration and H/V Ratio,” Bulletin of the Seismological Society of America 83 (2): 587-596, 1993.

299. Bryan J. Dolan to Document Control Desk, U.S. Nuclear Regulatory Commission, Development of Horizontal and Vertical Site-Specific Hazard Consistent Uniform Hazard Response Spectra at the Lee Nuclear Station Unit 1, dated April 30, 2008 (ML081230546).

300. NUREG/CR-5503, Techniques for Identifying Faults and Determining their Origins, authored by K. L. Hansen, K. I. Kelson, M. A. Angell, and W. R. Lettis, Office of Nuclear Regulatory Research, U.S. Nuclear Regulatory Commission, Washington, DC, 1999.

301. Klose, C.D., The 2008 M7.9 Wenchuan Earthquake - Result of Local and Abnormal Mass Imbalances?, Eos Transactions. AGU, 89(53), Fall Meeting Supplement, Abstract U21C-08, 2008.

302. Lin, A., Ren, Z., Jia, D., and X. Wu, Co-Seismic Thrusting Rupture and Slip Distribution Produced by the 2008 Mw 7.9 Wenchuan Earthquake, China, Tectonophysics, Vol. 471, p. 203–215., 2009.

303. Talwani, P., L. Chen, and K. Gahalaut, Seismogenic Permeability, ks, Journal of Geophysical Research, v. 112, B07309, doi:10.1029/2006JB004665, 2007.

304. Talwani, P., Earthquakes Associated with the Clark Hill Reservoir, South Carolina—A Case of Induced Seismicity, Engineering. Geology., 10, 239-253, 1976.

305. Secor, D.T., Jr., Regional Overview, p. 1-18, in, Secor, D.T, Jr., ed., Anatomy of the Alleghanian Orogeny as seen from the Piedmont of South Carolina and Georgia: Carolina Geological Society Field Trip Guidebook, November 14-15, 1987, 97p, 1987.

306. Chen, L., and P. Talwani, Renewed Seismicity near Monticello Reservoir, South Carolina, 1996–1999, Bulletin of the Seismological Society of America, 91, 94-101, 2001a.

307. Chen, L., and P. Talwani, Mechanism of Initial Seismicity Following Impoundment of the Monticello Reservoir, South Carolina, Bulletin of the Seismological Society of America, 91, 1582–1594., 2001b.

308. Rajendran, K., Sensitivity of a Seismically Active Reservoir to Low-Amplitude Fluctuations: Observations from Lake Jocassee, S. Carolina, Pure and Applied Geophysics, v. 145, 87-95, 1995.

309. Schaeffer, M.F., A Relationship between Joint Intensity and Induced Seismicity at Lake Keowee, Northwestern South Carolina, Bulletin of the Association of Engineering Geologists, v. 28, no. 1, p. 7-30, 1991.

310. Secor, D.T., Jr., L.S. Peck, D.M. Pitcher, D.C. Prowell, D.H. Simpson, W.A. Smith, and A.W. Snoke, Geology of the Area of Induced Seismicity Activity at Monticello Reservoir, South Carolina: Journal of Geophysical Research, vol. 87, no. B8, p. 6945-6957, 1982.

311. Talwani, P., A Onwby, K. Rajendran, and M. F. Schaeffer, A Field Study of Reservoir Induced Seismicity at Bad Creek, South Carolina; the Preimpoundment Phase, Seismological Research Letters, v. 61, No. 3-4, p. 162, 1990a.

312. Talwani, P., A Onwby, K. Rajendran, and M. F. Schaeffer, Bad Creek Project: A Progress Report, EOS, Transactions, American Geophysical Union, v. 71, No. 43, p. 1453, 1990b.

313. Widdowson, M.A., Meadows, M.E., Dickerson, J.R., Talwani, P., Schaffer, M., Orne, W.H., Hydrologic Impact of Reservoir Filling on a Fractured Crystalline Rock Aquifer, Proc. of the 1991 National Conf. on Irrigation and Drainage Engineering, Ed. Ritter, W.F., American Society of Civil Engineers, New York, pp.161-167, 1991.

314. Deleted.

315. Deleted.

316. Deleted.

317. Secor, D.T., Jr., and Snoke, A.W., Stratigraphy, structure and plutonism in the central South Carolina Piedmont, p. 65-123, in, Snoke, A.W., ed., Geological investigations of the eastern Piedmont, southern Appalachians (with a field trip guide on the bedrock geology of central South Carolina): Carolina Geological Society Field Trip Guidebook, 123 p., October 7-8, 1978.

318. Secor, D.T., Jr., Geology of the eastern Piedmont in South Carolina, p. 204-225, in, Secor, D.T., Jr., ed., Southeastern Geological Excursions – Guidebook for Geological Excursions: Geological Society of America Southeastern Section Annual Meeting, Columbia, South Carolina, 350 p. April 4-10, 1988.

319. Goldsmith, R., Milton, D.J. and Horton, J.W., Jr., Geologic map of the Charlotte 1° x 2° Quadrangle, North Carolina and South Carolina: United States Geological Survey, Miscellaneous Investigations Series, Map I-2175, 1:250,000, 1988.

320. Nelson, A.E., Horton, J.W., Jr., and Clarke, J.W., Geologic map of the Greenville 1° x 2° Quadrangle, Georgia, South Carolina, and North Carolina and South Carolina: United States Geological Survey, Miscellaneous Investigations Series, Map I-1251-E, 1:250,000, 1998.

321. Bryant, B. and Reed, J.C., Jr., Geology of the Grandfather Mountain Window and vicinity, North Carolina and Tennessee: United States Geological Survey Professional Paper 615, 190 p., 1:62,500, 1970.

322. North Carolina Geological Survey, Geologic map of North Carolina: Department of Natural Resources and Community Development, Division of Land Resources, North Carolina Geological Survey, 1:500,000, 1985.

323. Nystrom, P., Jr., 2008, Geologic map of the Blacksburg South quadrangle, Cherokee County, South Carolina (draft): South Carolina Department of Natural Resources, S.C. Geological Survey, Map GQM-XX.

324. Zoback, M.D., and Hickman, S., In situ study of the physical mechanisms controlling induced seismicity at Monticello Reservoir, South Carolina, Journal of Geophysical Research, vol. 87, p. 6959-6974, 1982.

325. Moos, D., and Zoback M.D., Near surface, "Thin Skin" reverse faulting stresses in the Southeastern United States, International Journal of Rock Mechanics and Mining Science & Geomechanics Abstracts, vol.30, No.7, p. 965-971, 1993.

2.5.3 SURFACE FAULTING

WLS COL 2.5-4 NRC Regulatory Guide 1.208 defines a capable tectonic source as a tectonic structure that can generate both vibratory ground motion and tectonic surface deformation, such as faulting or folding at or near the earth's surface, in the present seismotectonic regime. This section evaluates the potential for tectonic surface deformation and non-tectonic surface deformation at the William States Lee III Nuclear Station Site (Lee Nuclear Site). Information contained in Subsection 2.5.3 was developed in accordance with Regulatory Guide (RG) 1.208 and is intended to satisfy 10 CFR 100.23, *Geologic and Seismic Siting Criteria*.

There are no capable tectonic sources within the Lee Nuclear Site vicinity (25 mi. radius), and there is negligible potential for tectonic fault rupture at the site and within the site vicinity. There is also negligible potential for non-tectonic surface deformation at the site and within the site area (5 mi. radius). The following subsections provide the data, observations, and references to support these conclusions.

2.5.3.1 Geological, Seismological, and Geophysical Investigations

The following investigations were performed to assess the potential for tectonic and non-tectonic deformation within the Lee Nuclear Site vicinity and area:

- Compilation and review of existing data and literature.
- Interpretation of aerial photography and satellite imagery.
- Field and aerial reconnaissance.
- Review of historical and recorded seismicity.
- Discussions with current researchers in the area.

An extensive body of information is available for the Lee Nuclear Site. This information is contained in four main sources:

- Previous investigations performed for the former Duke Cherokee nuclear site, presented in the Preliminary Safety Analysis Report (PSAR) and supporting basis documents (References 201, 202, and 203).

- Geologic mapping published by the U.S. Geological Survey (USGS), the South Carolina Department of Natural Resources, and other researchers.

- Articles published in peer-reviewed journals by various researchers and field trip guidebooks published primarily by the Carolina Geological Society.

- Seismicity data compiled and analyzed in published journal articles, EPRI (Reference 204), and the updated EPRI catalog, performed as part of this license application.

This existing information is supplemented by aerial and field reconnaissance performed within and beyond the site vicinity, and by interpretation of aerial photography and satellite imagery within and beyond the site area.

2.5.3.1.1 Previous Lee Nuclear Site Investigations

The results of previous site investigations are presented in the PSAR (References 201, 202, and 203). This previous work does not identify the existence of tectonic faulting within the site area.

Detailed geologic mapping and inspection of excavations during construction for Units 1, 2, and 3 of the former Duke Cherokee nuclear site reveal no evidence of active or geologically recent faulting within the site area (Subsection 2.5.1.2.5.4 provides detailed discussion of site area geology and recorded deformation events). These excavations did expose minor bedrock shears that are related to mafic intrusions (e.g., meta-diorite and amphibolite rock units) in the meta-granodiorite pluton (e.g., meta-granodiorite to meta-quartz diorite rock units). Most of this minor deformation is associated with the contact between the mafic intrusions and the meta-granodiorite pluton (Figure 2.5.1-229). A more detailed discussion of the minor bedrock features is provided in Subsections 2.5.1.2 and 2.5.4.1.

2.5.3.1.2 Published Geologic Mapping

This subsection describes the geologic mapping completed, at a variety of scales, by the USGS, South Carolina Geological Survey, and other researchers in the site vicinity. This mapping suggests no evidence of geologically recent or active faulting within the site area.

Regional geologic mapping compilations assembled by experts in the geology of the Carolinas that cover the Lee Nuclear Site are incorporated into geologic maps of the site region, vicinity, and area (Figures 2.5.1-203a, 203b, 204a, 204b, 218a, 218b, 219a, and 219b). Hibbard et al.'s (2006, Reference 210) 1:1,500,000-scale lithotectonic map of the Appalachian Orogen is a compilation of geologic and structural mapping that spans eastern North America from Alabama to Lake Ontario. This map presents integrated data and interpretations from a variety of pre-existing sources (see references in Hibbard et al. 2006) (Figure 2.5.1-204a). Horton and Dicken (2001, Reference 209) compile geologic mapping of the Piedmont and Blue Ridge of South Carolina at 1:500,000-scale. This map

presents integrated data and interpretations from a variety of pre-existing sources (see references in Horton and Dicken 2001). Horton and Dicken's (Reference 209) geologic mapping supplements those areas not covered by more-detailed, 1:24,000-scale mapping (Figures 2.5.1-218a, 218b, 219a and 219b).

The South Carolina Geological Survey's 1:24,000-scale maps present the most-detailed published geologic mapping in the site area. Nystrom's (2004, Reference 205) geologic map of the Blacksburg South 7.5-minute quadrangle covers the Lee Nuclear Site (Figures 2.5.1-219a and 219b). Howard (2004, Reference 206) and Nystrom (2003, Reference 207) presents geologic mapping of the two adjacent 7.5-minute quadrangles to the east (Kings Creek and Filbert). Portions of the Kings Creek quadrangle provide 1:24,000-scale mapping within the Lee Nuclear Site area (Figure 2.5.1-218a and 218b).

The USGS has also published 1:24,000-scale geologic maps that cover portions of the site vicinity. The coverage area of Horton's (2006, Reference 208) geologic mapping of the Kings Mountain and Grover 7.5-minute quadrangles, South Carolina and North Carolina is beyond the site area, but entirely within the site vicinity (Figures 2.5.1-218a and 218b).

The most detailed mapping of the Duke Lee Nuclear Site is the unpublished mapping developed by Duke Power geologists performed as part of the Cherokee nuclear site construction. This detailed mapping at both the 1:24,000 scale for the site area and more detailed mapping of the top of rock and foundation grade exposures at 1:120 and 1:240 scales was performed for investigations of the former Duke Cherokee nuclear site. The 1:24,000-scale mapping of the Blacksburg South quadrangle, which includes the Duke Lee Nuclear Site, is nearly identical to the 2004 preliminary geologic map of the same quadrangle by Nystrom (Reference 205).

In addition to the geologic mapping discussed above, the USGS has published a compilation of all known or suggested Quaternary faults, liquefaction features, and possible tectonic features in the central and eastern United States (Reference 211, updated in Reference 212) (Figure 2.5.1-213). Only one such feature identified by these authors is potentially located within the Lee Nuclear Site area radius. The Fall Lines of Weems (1998, Reference 213) are alignments of rapids or anomalously steep sections of rivers draining the Piedmont and Blue Ridge Provinces of North Carolina and Virginia. Weems's (1998, Reference 213) delineation of these fall zones is crude, but, as presented in his Figure 8, the Western Piedmont Fall Line appears to be located within or close to the Lee Nuclear Site area at its nearest point (Figure 2.5.1-213). Wheeler (2005, Reference 212) classifies the Fall Lines of Weems (1998, Reference 213) as a Class C feature (Table 2.5.1-201) because: (1) identification of the fall zones is subjective and the criteria for recognizing them are not stated clearly enough to make the results reproducible, and (2) a tectonic faulting origin is not demonstrated for the fall zones (Subsection 2.5.1.1.2.4.5 presents a more detailed discussion of the Fall Lines). Based on review of published literature, field reconnaissance, and work performed as part of the North Anna ESP application (Reference 214), the Fall Lines of Weems (1998, Reference 213) are interpreted

as erosional features related to contrasting erosional resistances of adjacent rock types, and are not tectonic in origin.

No other Crone and Wheeler (Reference 211) or Wheeler (Reference 212) suspected Quaternary features are located within the Lee Nuclear Site vicinity. In addition, reviews of literature and consultations with experts for this project found no additional tectonic features.

2.5.3.1.3 Current Geologic Mapping

The existing geologic maps discussed in the preceding Subsection 2.5.3.1.2 form the basis for the geologic maps presented in Subsection 2.5.1. Field reconnaissance of the site (0.6 mile radius), site area (5 mile radius), and site vicinity (25 mile radius) included field checks of existing mapping and, where necessary, refinement of previous geologic maps.

A very linear geologic contact at the Lee Nuclear Site was investigated in detail to preclude the presence of a fault. Nystrom (2004, Reference 205) maps at 1:24,000-scale the western margin of a meta-granodiorite pluton at the Lee Nuclear Site as a linear, north-northwest-trending contact (Figures 2.5.1-219a, 2.5.1-219b, and 2.5.1-226). The nature of this contact between the meta-granodiorite pluton and metavolcanic country rock was investigated by means of detailed geologic mapping, compilation and review of borehole information, and geologic logging of six test pits. The results of this investigation demonstrate that this contact is more irregular than mapped by Nystrom (2004, Reference 205), and confirm the intrusive nature of the contact. The more irregular map pattern (Figures 2.5.1-220 and 2.5.1-226) and the intrusive nature of the contact preclude a fault interpretation for the western margin of the pluton.

Refinements were made to existing geologic maps at the site vicinity, site area and site scale as well as at the scale of the existing excavation to develop the geologic maps as described in Subsection 2.5.1.2.5.5 and presented in Figures 2.5.1-218a, 2.5.1-218b, 2.5.1-219a, 2.5.1-219b, 2.5.1-220, 2.5.1-226 and 2.5.1-229. These modifications reflect new geologic mapping performed as part of this project, as well as efforts to reconcile previous geologic and structural mapping from various sources conducted at varying scales.

The geologic map of the site vicinity (Figures 2.5.1-218a and 2.5.1-218b) comprises 1:500,000-scale mapping of South Carolina by Horton and Dicken (2001, Reference 209) and 1:500,000-scale mapping of North Carolina by the North Carolina Geological Survey (1998, Reference 243). Geologic contacts and descriptions from these two sources are presented in Figures 2.5.1-218a and 2.5.1-218b without modification, but unit colors have been altered for consistency across the South Carolina-North Carolina state border. Fault locations shown on Figure 2.5.1-218a are slightly modified after 1:1,500,000-scale mapping by Hibbard et al. (2006, Reference 210), such that the faults "snap" to geologic contacts.

The site area geologic maps (Figures 2.5.1-219a and 2.5.1-219b) are modified after 1:24,000-scale geologic mapping by Nystrom (2004, Reference 205) and

Howard (2004, Reference 206), as well as 1:500,000-scale mapping by Horton and Dicken (2001, Reference 209). This geologic mapping is supplemented on Figure 2.5.1-219a with fold axes from Butler (1981, Reference 235) and fault locations slightly modified after 1:1,500,000-scale mapping by Hibbard et al. (2006, Reference 210), such that the faults "snap" to geologic contacts.

The site geologic map (Figure 2.5.1-220) is modified after 1:24,000-scale geologic mapping by Nystrom (2004, Reference 205) and Howard (2004, Reference 206), and represents the only geologic map that incorporates significant revisions to previously published data. As described above, Nystrom (2004, Reference 205) maps a metatonalite (herein referred to as meta-granodiorite) pluton that underlies much of the site. Nystrom (2004, Reference 205) maps a relatively straight western boundary of this pluton (Figure 2.5.1-219a). The nature of this western pluton boundary was investigated in detail and remapped as part of this project. Figure 2.5.1-226 and Subsection 2.5.4.2 present the details of this remapping, and the refined mapping of the western pluton boundary is incorporated into the site geologic map (Figure 2.5.1-220).

Of particular interest at the site scale is the western boundary of the pluton (Nystrom 2004, Reference 205), which is the foundation bearing unit as shown on Figure 2.5.1-219a. Nystrom (2004, Reference 205) maps the western margin of the pluton (noted as Zto) as a pronounced linear feature. Field reconnaissance indicated that this boundary is not constrained by actual observation or data although it is shown as a solid line contact on Nystrom (2004, Reference 205).

To improve the control on the western margin of the pluton, borings from the Cherokee Nuclear Station as well as this investigation were evaluated. Previous mapping performed during the original site construction for a cooling water corridor had previously exposed the contact between the pluton and country rock outside of the north western corner of the excavation for Unit 1 as shown on Figure 2.5.1-226. A series of geologic trenches were located along the western margin to confirm this contact.

As shown on Figure 2.5.1-226, existing boring and test pits were evaluated to refine the western pluton contact with the metavolcanic country rock. Also, two geologic trenches were excavated to investigate the margin location and nature of the rock lithologies to correlate with the boring log descriptions. The exposed rock in the first trench indicated saprolitic and partially weathered rock indicative of plutonic rock and a second trench was opened about 300 feet to the west. The second trench indicated that the western saprolite lithology was not typical of saprolites of plutonic origin and that the fabric was foliated thus suggesting a metamorphic lithology more representative of the metavolcanic country rocks of the region. The borings, geologic trenches, and field reconnaissance as shown on Figure 2.5.1-226 were thus used to refine the geologic map presented as Figure 2.5.1-220.

At the scale of the excavation, because extensive mapping during the original construction had been performed but was not completed or verified, mapping of the existing exposure was completed. Specifically, the noted rock lithologies were cataloged for correlation with more general nomenclature established during

Cherokee Nuclear Station evaluations. The exposed limits of the excavation were mapped to document the spatial relationship of major lithologic units and structural features observed in the excavation area. Figure 2.5.1-229 shows the major lithologic units and structural features within the former Cherokee Nuclear Station Unit 2 and 3 areas and limited areas bordering the former Cherokee Nuclear Station Unit 1 area. Also shown on this map are the limits of available exposure for mapping.

2.5.3.1.4 Previous Seismicity Data

The highest recorded ground shaking intensities at the Lee Nuclear Site are the result of earthquakes located beyond the site vicinity. The EPRI seismicity catalog (1986) does not include any earthquakes of $m_b \geq 3.0$ within the site vicinity (25-mile radius), and includes only three earthquakes with $m_b \geq 3.0$ within 30 miles of the Lee Nuclear Site (Figure 2.5.2-202). The largest of these is the January 1, 1913 m_b 4.8 Union County, South Carolina earthquake, located approximately 25 mi. southwest of the Lee Nuclear Station (Reference 204).

The Union County earthquake was felt over an area of approximately 43,000 square miles, with an estimated Rossi-Forel shaking intensity VIII (Reference 215, as reported in Reference 216) (Figure 2.5.1-232). Rossi-Forel shaking intensity at the Lee Nuclear Site is estimated at VI (Reference 215, as reported in Reference 216). The epicenter of the Union County earthquake is poorly located and there is no known causative fault for this event.

The 1886 Charleston earthquake was likely located more than 150 mi. from the Lee Nuclear Site, and produced shaking intensity of about MMI VI at the site (Reference 217) (Figure 2.5.1-217). The fault on which this earthquake occurred remains unknown.

2.5.3.1.5 Current Seismicity Data

As described in Subsection 2.5.2.1, the EPRI earthquake catalog of the central and eastern United States is updated to incorporate earthquakes that occurred between 1984 and 2005 within the site region. The updated earthquake catalog contains no earthquakes with $m_b \geq 3.0$ within the Lee Nuclear Site vicinity.

In 2006, after the EPRI seismicity catalog was updated through 2005, four minor earthquakes occurred in northeast South Carolina. Two of these events that occurred in January were less than m_b 3.0, and two events that occurred in September were larger than m_b 3.0. In an unpublished online report, Talwani (2006a, Reference 218) describes the two January earthquakes located near Jonesville, South Carolina, approximately 20 mi. southwest of the Lee Nuclear Site. Talwani (2006a, Reference 218) suggests that the January 24, 2006 magnitude 2.5 and January 25, 2006 magnitude 1.5 (magnitude scale unspecified) earthquakes are associated with the western margin of the Baldrock granitic pluton. Talwani (2006a, Reference 218) does not provide estimates of location uncertainty for these two micro-earthquakes, but the epicentral locations are likely inaccurate due to the small magnitudes of these events.

Two additional, minor earthquakes occurred in northeast South Carolina near the town of Bennettsville in September 2006. In unpublished online reports, the USGS National Earthquake Information Center describes the September 22, 2006 m_b 3.5 and the September 25, 2006 m_b 3.7 earthquakes (References 219 and 220). The epicenters of these two earthquakes are not precisely located, but are more than 75 mi. east-southeast of the Lee Nuclear Site. Estimates of location uncertainty for the September 22, 2006 event are: ±4.5 mi. horizontal, ±7.9 mi. depth (±7.3 km horizontal, ±12.8 km depth) (Reference 219). Estimates of location uncertainty for the September 25, 2006 event are: ±6.8 mi. horizontal, with depth fixed at 3.1 mi. by the location program (±10.9 km horizontal, depth fixed at 5 km) (Reference 220). Due to the lack of nearby seismograph stations, focal mechanisms are not determined for these events. The September 2006 earthquakes are spatially associated with a small Mesozoic extensional basin mapped beneath the Coastal Plain by Benson (1992, Reference 221) (Figure 2.5.2-202). In an unpublished online report, Talwani (2006b, Reference 222) suggests that these two earthquakes may be spatially related to the Eastern Piedmont fault system, a broad zone of faults interpreted by Hatcher et al. (1977, Reference 223) as a regional fault zone (Figure 2.5.1-209). At the latitude of the two September 2006 earthquakes, the Eastern Piedmont fault system is up to 40 mi. wide. Given the uncertainty associated with the locations of the two September 2006 earthquakes and the broad regional extent of the Eastern Piedmont fault system, these two minor events cannot be positively correlated with this fault system.

2.5.3.1.6 Current Aerial and Field Reconnaissance

Aerial photography, satellite imagery, and topographic maps of varying scales and vintages reveal no evidence of geomorphic features indicative of the potential for tectonic surface deformation (e.g., faulting or warping) within the site area. Imagery reviewed as part of this license application includes:

- 1:20,000-scale, black and white, stereo aerial photographs from the U.S. Department of Agriculture (1959) covering the entire site area and beyond.
- 1:40,000-scale, color-infrared, stereo aerial photographs from the USGS (1994) covering the majority of the site area.
- Landsat satellite imagery of varying color bands covering the site vicinity and beyond.
- Shaded relief topographic imagery with 100-foot (30-m) grid spacing covering the site vicinity and beyond.

Review of aerial photography reveals a linear topographic feature within the Lee Nuclear Site area that, because of its orientation parallel to the predominant regional structural grain and its proximity to the site, was investigated in detail to assess its origin. This approximately 4.5-mi.-long, linear feature is located approximately 2 mi. northwest of the site, and strikes approximately N55°E with a steeper slope facing to the northwest (shown as “Lineament No. 1” on

Figure 2.5.1-221). London Creek flows northeastward along much of the length of the northwestern base of the ridge, before joining with the Broad River near the southernmost tip of Ninety-Nine Islands. The lineament, which is most easily recognized on the 1:40,000-scale USGS photography, terminates northeastward at the Broad River and is not expressed in the topography northeast of the river. Field reconnaissance and previous geologic mapping by Nystrom (2004, Reference 205) reveal that resistant, northeast-striking quartzite layers core this linear ridge. The linear topographic expression of this ridge is the result of erosion by London Creek (and the erosion resistance of the quartzite layers) and is assessed to be non-tectonic in origin.

Field and aerial reconnaissance inspections reveal no evidence for surface rupture, surface warping, or the offset of geomorphic features indicative of active faulting within the site area.

2.5.3.2 Geological Evidence, or Absence of Evidence, for Surface Deformation

As shown in Figures 2.5.1-218a and 218b and discussed in Subsection 2.5.1.1.2.4, six bedrock faults of Paleozoic age are mapped within the site vicinity. These six faults are:

- Kings Mountain shear zone, including the Blacksburg shear zone and the Kings Creek shear zone.
- Tinsley Bridge fault.
- Southwestern extension of the Boogertown shear zone.
- Brindle Creek thrust fault.
- Reedy River thrust fault.
- Unnamed fault north of Gaffney.

No deformation or geomorphic features suggestive of potential Quaternary activity are reported in the literature for these six faults. Aerial and field reconnaissance and interpretation of aerial photographs and satellite imagery show that no geomorphic features indicative of Quaternary activity exist along any of the mapped fault traces. These six features are discussed in Subsection 2.5.1.1.2.4.2, summarized in Table 2.5.3-201 and described below.

- Kings Mountain shear zone. The northeast-striking Kings Mountain shear zone (Figure 2.5.1-210) in the Lee Nuclear Site vicinity is a zone of mylonitic deformation (References 224, 225, 226, 227, and 228) and considered part of the Central Piedmont shear zone separating the Carolina and Piedmont Zones (Figure 2.5.1-218a) (Reference 224). The sense of motion on the Kings Mountain shear zone is uncertain, but structural data suggest that the zone is a steeply northwest-dipping reverse fault (Reference 224). Deformation of this mylonitic shear zone is

overprinted by semi brittle cleavage. Pegmatitic dikes in North Carolina intruded parallel to the semi-brittle cleavage and some have been ductile deformed. Hence, the dikes are interpreted as syn- to post-kinematic and their Rb-Sr whole rock isochron age of 352 ± 10 Ma indicates that the late-stage semi-brittle deformation occurred in the Late Devonian (Reference 224). Furthermore, an unnamed granite with a 326 ± 3 Ma U-Pb upper-intercept age cuts and is undeformed by the central Piedmont shear zone in South Carolina south of the intersection of the Kings Mountain shear zone and the Tinsley Bridge faults (Reference 236).

- Tinsley Bridge fault. The Tinsley Bridge fault (Figure 2.5.1-210) is a zone of retrograde mylonite with apparent down-to-the-northwest sense of slip and is less than 20 mi. in length (Reference 229). Mineral assemblages in the mylonite indicate that deformation on the Tinsley Bridge fault occurred after peak metamorphic conditions (Reference 229). The fault is cut by the undeformed Pacolet granite with a whole rock Rb/Sr age of 383 ± 5Ma (Reference 229).

- Southwest extension of the Boogertown shear zone. The northeast-striking Boogertown shear zone (Figure 2.5.1-210) is sometimes interpreted as a terrane boundary (References 225 and 230). The northeastern end of the Boogertown shear zone is mapped terminating into an unsheared granitic pluton (References 237 and 210). This pluton is undated, but the youngest plutons within the Carolina Zone are generally 300–265 Ma (Reference 238). There is no evidence to suggest post-Paleozoic motion on the southwest extension of the Boogertown shear zone.

- Brindle Creek thrust fault. The Brindle Creek thrust was recognized in North Carolina as a low-angle fault with an extensive mylonite zone, but authors have indicated that the mapping of this structure in South Carolina is speculative (Reference 239). In North Carolina, a granite found only in the hanging-wall of the Brindle Creek fault (and hence older than movement on the structure) has zircons with a weighted $^{206}Pb/^{238}U$ ion microprobe age of 366 ± 3 Ma (Reference 240). These field relations were interpreted to indicate that the Brindle Creek fault was active after the intrusion of the granite, or is Devonian or younger in age. In North Carolina, migmatitic, high-temperature deformation is spatially associated with the Brindle Creek fault (Reference 240). Metamorphic rims on migmatitic rocks in the immediate footwall of the Brindle Creek fault yield ion-microprobe U-Pb ages of ~350 Ma, probably correlative with emplacement of the Brindle Creek hanging-wall (Reference 241).

- Reedy River thrust fault. The Reedy River thrust fault is a northeast-striking structure in the Inner Piedmont (References 208, 231, 232, and 233) (Figure 2.5.1-210). There is no evidence to suggest post-Paleozoic motion on the Reedy River thrust fault.

- Unnamed fault north of Gaffney. In their tectonostratigraphic compilation map of the Appalachians, Hibbard et al. (2006, Reference 210) suggest that this approximately 20-mi.-long, northerly striking fault records up-to-the-east displacement and Goldsmith et al. (1988, Reference 242) indicate it is a northwest-vergent thrust fault. Horton and Dicken (2001, Reference 209) do not include this fault in their compilation of South Carolina Piedmont and Blue Ridge geology. There is no evidence to suggest post-Paleozoic motion on the unnamed fault North of Gaffney.

There is direct geologic evidence to preclude the presence of northeast- or east-striking faults projecting through the Lee Nuclear Site. The predominant structural grain of the site area, vicinity, and region is oriented northeast. As mapped by Nystrom (2004, Reference 205) and confirmed by reconnaissance mapping, two elongated, north-striking quartzite bodies are located in the western portion of the site area (Figures 2.5.1-219a, 219b and 2.5.1-220). These unfaulted, continuous quartzite beds, oriented at a high angle to the regional structural grain, demonstrate the absence of any northeasterly or easterly striking fault through the Lee Nuclear Site. In addition, the northerly striking western margin of the pluton provides an additional strain marker that precludes the presence of any northeasterly or easterly striking faults through the Lee Nuclear Site. The timing of emplacement of this pluton is uncertain, but according to Butler (1981, Reference 235), it is likely early Paleozoic or older in age.

2.5.3.3 Correlation of Earthquakes With Capable Tectonic Sources

Seismicity with the Lee Nuclear Site vicinity is shown in Figure 2.5.2-202. As shown on this figure, there is no spatial correlation of earthquake epicenters with known or postulated faults or other tectonic features. No faults or geomorphic features within the site vicinity can be correlated with earthquakes. Based on review of existing literature, no reported historical earthquake epicenters have been associated with bedrock faults within the Lee Nuclear Site vicinity (Figure 2.5.2-202). None of these faults within the Lee Nuclear Site vicinity are classified as capable tectonic sources.

The EPRI seismicity catalog (1986) does not include any earthquakes of $m_b \geq 3.0$ within the site vicinity (25-mi. radius), and includes only three earthquakes with $m_b \geq 3.0$ within 30 mi. of the Lee Nuclear Site (Figure 2.5.2-202). The largest of these is the January 1, 1913 m_b 4.8 Union County, South Carolina earthquake, located approximately 25 mi. southwest of the Lee Nuclear Station (Reference 204). The fault on which this earthquake occurred has not been identified. The updated EPRI seismicity catalog does not include any earthquakes of $m_b > 3.0$ within the site radius. However, several small events ($m_b < 3.0$) have occurred within the site vicinity.

2.5.3.4 Ages of Most Recent Deformations

The six faults mapped in the Lee Nuclear Site vicinity (i.e., the Kings Mountain shear zone, the Tinsley Bridge fault, the southwest extension of the Boogertown shear zone, the Brindle Creek thrust, the Reedy River thrust fault, and the

unnamed fault north of Gaffney) have not been active since Paleozoic time (References 224 and 229), although Garihan et al. (1993, Reference 231) suggest the possibility that the Kings Mountain shear zone may have experienced localized Mesozoic reactivation.

2.5.3.5 Relationships of Tectonic Structures in the Site Area to Regional Tectonic Structures

Of the five faults identified within the site area (i.e., the Kings Mountain shear zone, the Tinsley Bridge fault, the southwest extension of the Boogertown shear zone, the Reedy River thrust fault, and the unnamed fault north of Gaffney), at least four are considered part of a larger regional shear zone known as the Central Piedmont shear zone (the relationship between the unnamed fault and the Central Piedmont suture is unclear). The Central Piedmont shear zone extends northeastward from Georgia, through the Carolinas, and into Virginia. At the latitude of the Lee Nuclear Site, the Central Piedmont shear zone separates the Piedmont zone from the Charlotte terrane (Reference 234) (Figure 2.5.1-202a).

As described in Subsection 2.5.3.6, none of the potential faults within the site area is considered a capable tectonic feature.

2.5.3.6 Characterization of Capable Tectonic Sources

Based on reviews of updated geologic, seismic, and geophysical data from published literature, interviews with expert earth scientists, and the COL investigations, no evidence for capable tectonic sources is identified within the Lee Nuclear Site vicinity. These data are presented in detail throughout Subsection 2.5.1, and are summarized in Subsection 2.5.3.2. This interpretation is consistent with investigations performed for the former Cherokee nuclear site. The Tinsley Bridge fault and the Kings Mountain shear zone are the nearest mapped faults to Lee Nuclear Site (located approximately 5 mi. away at their nearest points), and have not been active since Paleozoic time (References 224 and 229), although Garihan et al. (1993, Reference 231) suggest the possibility that the Kings Mountain shear zone may have experienced localized Mesozoic reactivation.

2.5.3.7 Designation of Zones of Quaternary Deformation in the Site Region

Based on reviews of updated geologic, seismic, and geophysical data from published literature, interviews with expert earth scientists, and the COL investigations, no evidence of Quaternary deformation is identified. These data are presented in detail throughout Subsection 2.5.1. Based on this finding, no investigation is required.

2.5.3.8 Potential for Surface Tectonic Deformation at the Site

The potential for tectonic deformation at the site is negligible. Detailed geologic mapping and inspection of excavations during construction of the former Duke Cherokee nuclear site reveal no evidence of geologically recent or active faulting (References 201, 202, and 203). Based on reviews of updated geologic, seismic,

and geophysical data from published literature, interviews with expert earth scientists, and the COL investigations, there are no Quaternary faults or capable tectonic sources within the site vicinity. The potential for non-tectonic surface deformation, including RIS, within the site area is negligible. There is no information suggesting the potential for non-tectonic surface deformation within the site area. Rocks within the site area are igneous and metamorphic crystalline rocks (References 205 and 206) that are neither susceptible to karst-type dissolution collapse nor to subsidence due to fluid withdrawal. Evaluations related to the potential of RIS associated with Make-Up Pond C are described in Subsection 2.5.2.1.3.

2.5.3.9 References

201. Cherokee Nuclear Station Preliminary Safety Analysis Report (PSAR), vol. 4, Appendix 2C - Seismology, Attachment V - Seismic Refraction Data, prepared by Law Engineering Testing Company for Duke Power Company Project 81, June 1974a.

202. Cherokee Nuclear Station Preliminary Safety Analysis Report (PSAR), vol. 4, Appendix 2C - Geology, prepared by Law Engineering Testing Company for Duke Power Company Project 81, July 1974b.

203. Cherokee Nuclear Station Preliminary Safety Analysis Report (PSAR), vol. 4, Appendix 2E - Seismology, prepared by Law Engineering Testing Company for Duke Power Company Project 81, January 1974c.

204. Electric Power Research Institute, *Seismic Hazard Methodology for the Central and Eastern United States, Tectonic Interpretations*, EPRI NP-4726, Volumes 5-10, July 1986.

205. Nystrom, P.G., *Geologic Map of the Blacksburg South 7.5-Minute Quadrangle, Cherokee and York Counties, South Carolina (Preliminary Draft)*, South Carolina Geological Survey, GQM-X, 1:24,000-scale, 2004.

206. Howard, C.S., *Geologic Map of the Kings Creek 7.5-Minute Quadrangle, York County, South Carolina*, South Carolina Geological Survey, GQM-6, 1:24,000-scale, 2004.

207. Nystrom, P.G., *Geologic Map of the Filbert 7.5-Minute Quadrangle, Cherokee and York Counties, South Carolina*, South Carolina Geological Survey, GQM-25, 1:24,000-scale, 2003.

208. Horton J.W. Jr., *Geologic map of the Kings Mountain and Grover Quadrangles, Cleveland and Gaston Counties, North Carolina, and Cherokee and York Counties, South Carolina*, U.S. Geological Survey Open-File Report 2006-1238, 2006.

209. Horton, J.W. Jr. and Dicken, C.L., *Preliminary Digital Geologic Map of the Appalachian Piedmont and Blue Ridge, South Carolina Segment*, U.S. Geological Survey Open-File Report 01-298, 1:500,000 scale, 2001.

210. Hibbard, J.P., van Staal, C.R., Rankin, D.W., Williams, H., *Lithotectonic Map of the Appalachian Orogen, Canada - United States of America*, Geological Society of Canada, map 2096A, 1:1,500,000 scale, 2006.

211. Crone, A.J. and Wheeler, R.L., *Data for Quaternary Faults, Liquefaction Features, and Possible Tectonic Features in the Central and Eastern United States, East of the Rocky Mountain Front*, U.S. Geological Survey Open-File Report 00-260, 2000.

212. Wheeler, R.L., *Known or Suggested Quaternary Tectonic Faulting, Central and Eastern United States- New and Updated Assessments for 2005*, U.S. Geological Survey Open-File Report 2005-1336, 37 pp., 2005.

213. Weems, R.E., *Newly Recognized En Echelon Fall Lines in the Piedmont and Blue Ridge Provinces of North Carolina and Virginia, With a Discussion of their Possible Ages and Origins*, U.S. Geological Survey Open-File Report 98-0374, 1998.

214. U.S. Nuclear Regulatory Commission, *Safety Evaluation Report for an Early Site Permit (ESP) at the North Anna ESP Site*, U.S. Nuclear Regulatory Commission Report, NUREG-1835, September 2005.

215. Taber, S., "The South Carolina Earthquake of January 1, 1913," *Bulletin of the Seismological Society of America* 3:6-13, 1913.

216. Visvanathan, T.R., "Earthquakes in South Carolina, 1698-1975," *South Carolina Geological Survey Bulletin* 40, 1980.

217. Bollinger, G.A., "Reinterpretation of the Intensity Data for the 1886 Charleston, South Carolina, Earthquake," in *Studies Related to the Charleston, South Carolina, Earthquake of 1886- A Preliminary Report*, ed. D.W. Rankin, U.S. Geological Survey Professional Paper 1028, 1977.

218. South Carolina Seismic Network, Website, Talwani, P., "The Jonesville Earthquake," http://scsn.seis.sc.edu/images/jonesville.pdf, accessed October 16, 2006a.

219. U.S. Geological Survey National Earthquake Information Center, Website, "Magnitude 3.7 Earthquake, South Carolina, Monday September 25, 2006 at 05:44:23 UTC," http://earthquake.usgs.gov/eqcenter/recenteqsus/Quakes/ustbaj.php, accessed September 25, 2006.

220. U.S. Geological Survey National Earthquake Information Center, Website, "Magnitude 3.5 Earthquake, South Carolina, Friday September 22, 2006 at 11:22:01 UTC," http://earthquake.usgs.gov/eqcenter/recenteqsus/Quakes/semc0922a.php accessed on September 25, 2006.

221. Benson, R.N., *Map of Exposed and Buried Early Mesozoic Rift Basins/ Synrift Rocks of the U.S. Middle Atlantic Continental Margin*, Delaware Geological Survey Miscellaneous map series no. 5, 1:1,000,000 scale, 1992.

222. South Carolina Seismic Network, Website, Talwani, P., "Two Felt Earthquakes Hit Northeast South Carolina," http://scsn.seis.sc.edu/ images/Sept2006earthquakes.pdf accessed October 16, 2006b.

223. Hatcher R.D. Jr., Howell, D.E., and Talwani, P., "Eastern Piedmont Fault System - Speculations on its Extent," *Geology* 5:636-640, 1977.

224. Horton Jr., J.W., "Shear Zone Between the Inner Piedmont and Kings Mountain Belts in the Carolinas," *Geology* 9:28-33, 1981a.

225. Horton, J.W. Jr., "Geologic Map of the Kings Mountain Belt Between Gaffney, South Carolina and Lincolnton, North Carolina," in *Geological Investigations of the Kings Mountain Belt and Adjacent Areas in the Carolinas*, Carolina Geological Society Field Trip Guidebook, 1981b.

226. Dennis, A.J., "Is the Central Piedmont Suture a Low-Angle Normal Fault?" *Geology* 19:1081-1084, 1991.

227. Wilkins, J.K., Shell, G.S., and Hibbard, J.P., "Geologic Contrasts Across the Central Piedmont Suture in North-Central, North Carolina," in *Carolina Geological Society Guidebook for 1995 Annual Meeting*, South Carolina Geology 38:25-32, 1995.

228. West, T.E. Jr., "Structural Analysis of the Carolina-Inner Piedmont Terrane Boundary: Implications for the Age and Kinematics of the Central Piedmont Suture, a Terrane Boundary that Records Paleozoic Laurentia-Gondwana Interactions," *Tectonics* 17 (3):379-394, 1998.

229. Dennis, A.J., Rocks of the Carolina Terrane in the Spartanburg 30- x 60-Degree Quadrangle, prepared for the 1995 Carolina Geological Survey annual meeting, 1:100,000 scale, 1995.

230. Maybin, A.H. and Nystrom, P.G., *Geologic Map of South Carolina*, South Carolina Geological Survey GGMS-1, 1:1,00,000-scale, 1997.

231. Garihan, J.M., Preddy, M.S., and Ranson, W.A., "Summary of Mid-Mesozoic Brittle Faulting in the Inner Piedmont and Nearby Charlotte Belt of the Carolinas," in *Carolina Geological Society Field Trip Guidebook - Studies of Inner Piedmont Geology with a Focus on the Columbus Promontory*, Carolina Geological Society Field Trip Guidebook, 1993.

232. Nystrom, P.G., "Structure and Stratigraphy Across the Reedy River Thrust Fault, Inner Piedmont of South Carolina," *Geological Society of America Abstracts with Programs*, Southeastern Section 50th annual meeting, 2001.

233. Maybin, A.H. and Nystrom, P.G., *Geology of the Reedy River Thrust in the Vicinity of Southwest Spartanburg, South Carolina*, South Carolina Geological Survey Open-File Report 143, 2002.

234. Hibbard, J.P., Stoddard, E.F., Secor, D.T., and Dennis, A.J., "The Carolina Zone: Overview of Neoproterozoic to Early Paleozoic Peri-Gondwanan Terranes Along the Eastern Flank of the Southern Appalachians," *Earth Science Reviews* 57:299-339, 2002.

235. Butler, J.R., Geology of the Blacksburg South Quadrangle, South Carolina, in *Geological investigations of the Kings Mountain Belt and Adjacent Areas in the Carolinas*, Carolina Geological Society Field Trip Guidebook, 1981.

236. Dennis, A. J., Wright, J. E., 1995, Mississippian (ca. 326-323 Ma) U-Pb crystallization for two granitoids in Spartanburg and Union counties, South Carolina, in Dennis et al., eds., Geology of the western part of the Carolina terrane in northwestern South Carolina, CGS Fieldtrip Guidebook v. 37, p. 43-47.

237. Milton, D. J., 1981, The northern termination of the Kings Mountain belt, in Horton, J. W., Butler, J. R., Milton, D. M., eds., Geological investigations of the Kings Mountain belt and adjacent areas in the Carolinas: Carolina Geological Society Field Trip Guidebook, p. 1-5.

238. Hatcher, R. D., Bream, B. R., and Merschat, A. J., 2007, Tectonic map of the southern and central Appalachians: A tale of three orogens and a complete Wilson cycle, *in* Hatcher, R. D., Carlson, M. P., McBride, J. H., and Martinez Catalan, J. R., eds., 4-D Framework of Continental Crust: Geological Society of America Memoir 200, p. 595-632.

239. Bream, B.R., 2002, The southern Appalachian Inner Piedmont: New perspectives based on recent detailed geologic mapping, Nd isotopic evidence, and zircon geochronology, *in* Hatcher, R.D., Jr., and Bream, B.R., eds., Inner Piedmont geology in the South Mountains-Blue Ridge Foothills and the southwestern Brushy Mountains, central-western North Carolina: North Carolina Geological Survey, Carolina Geological Society annual field trip guidebook, p. 45-63.

240. Giorgis, S. D., Mapes, R. W., Bream, B. R., 2002, The Walker Top Granite: Acadian granitoid or eastern Inner Piedmont basement? *in* Hatcher, R. D. and Bream, B. R., eds., Inner Piedmont geology in the South Mountains-Blue Ridge foothills and the southwestern Brushy Mountains, central-western North Carolina: North Carolina Geological Survey, Carolina Geological Society annual fieldtrip guidebook, p. 33-43.

241. Merschat, A. J., Kalbas, J. L., 2002, Geology of the southwestern Brushy Mountains, North Carolina Inner Piedmont: A summary and synthesis of recent studies, *in* Hatcher, R. D. and Bream, B. R., eds., Inner Piedmont geology in the South Mountains-Blue Ridge foothills and the southwestern

Brushy Mountains, central-western North Carolina: North Carolina Geological Survey, Carolina Geological Society annual fieldtrip guidebook, p. 101-126.

242. Goldsmith, R, Milton, D. J., Horton, J. W., 1988, Geologic map of the Charlotte 1x2 degrees quadrangle, North Carolina and South Carolina: USGS Miscellaneous Investigations Series Map I-1251-E; 1:250,000. Website http://pubs.er,usgs.gov/usgspubs/i/i/25/E, accessed February 6, 2009.

243. North Carolina Geological Survey (NCGS), Geology of North Carolina vector digital data onemap_prod.SDEADMIN.geo, Website http://www.nconemap.com/Default.aspx?tabid=286, accessed June 12, 2007, publication date 1998.

2.5.4 STABILITY OF SUBSURFACE MATERIALS AND FOUNDATIONS

This Section presents information on the properties and stability of soils and rock that may affect the nuclear power plant facilities, under both static and dynamic conditions, including vibratory ground motions associated with the Ground Motion Response Spectrum (GMRS) and Foundation Input Response Spectra (FIRS) for seismic Category I structures at the Lee Nuclear Station Site. The discussion focuses on the stability of subsurface materials and foundations as they influence the safety of seismic Category I facilities and presents a comparison of the site conditions and geologic features to the DCD design criteria.

As specified in Regulatory Guide 1.206, pages C.III.1-44 to C.III.1-47, this Subsection is organized into the following Subsections. These include:

- Geologic Features (2.5.4.1)
- Properties of Subsurface Materials (2.5.4.2)
- Foundation Interfaces (2.5.4.3)
- Geophysical Surveys (2.5.4.4)
- Excavations and Backfill (2.5.4.5)
- Groundwater Conditions (2.5.4.6)
- Response of Soil, Granular Fill, and Rock to Dynamic Loading (2.5.4.7)
- Liquefaction Potential (2.5.4.8)
- Earthquake Site Characteristics (2.5.4.9)
- Static Stability (2.5.4.10)

- Design Criteria (2.5.4.11)
- Techniques to Improve Subsurface Conditions (2.5.4.12).

The information presented in this Subsection was developed on the basis of evaluations of historic field explorations performed for the Cherokee Nuclear Station (CNS) and field investigations for Lee Nuclear Station, Units 1 and 2 completed between early 2006 and mid-2007. Further information was gathered using geophysical investigations and laboratory tests conducted on soil and rock samples obtained during the field exploration program for Lee Nuclear Station. Results from historic site investigations for Cherokee Nuclear Station are presented in the Preliminary Safety Analysis Report (PSAR) (Reference 201) and Final Safety Evaluation Report (Reference 202).

2.5.4.1 Geologic Features

WLS COL 2.5-1
WLS COL 2.5-5

This Subsection evaluates non-tectonic processes and features that may cause permanent ground deformation or foundation instability at the Lee Nuclear Station Site. Processes and features evaluated include areas of actual or potential surface or subsurface subsidence, solution activity, uplift or collapse, and causes of these conditions. This subsection also addresses zones of alteration, irregular weathering profiles, zones of structural weakness, the geologic history and unrelieved residual stresses in bedrock at the site, and of rocks or soils that may be unstable due to physical or chemical properties.

All of the data collected serve as the basis for evaluating excavation and backfill issues, construction excavation and dewatering, earth fill and granular fill requirements, groundwater, response of soil, granular fill, and rock to dynamic loading, liquefaction potential, static stability, techniques to improve subsurface conditions, and issues related to construction. The results of these evaluations, along with methods and results of field and laboratory programs, are summarized in the following Subsections.

- Subsection 2.5.4.1.1, Geologic History and Stress Conditions, reviews aspects of geologic history that are relevant to the potential for uplift and residual stresses in the bedrock or soil. There is no evidence for uplift occurring at the present time, and there are no geologic or human-induced processes that are expected to lead to uplift at the site.
- Subsection 2.5.4.1.2, Stratigraphy, Lithology, and Soil and Rock Characteristics, presents information on the physical and chemical properties of the rock and soil, and an evaluation of erosion, zones of alteration, and zones of potential weakness. There are no rocks which may be unstable because of their erosive potential, mineralogy, lack of consolidation, water content, or potentially undesirable response to seismic or other events.

- Subsection 2.5.4.1.3, Groundwater, discusses groundwater conditions at the site and how they may affect weathering and stability of the rock and soil.

- Subsection 2.5.4.1.4, Effects of Human Activities, evaluates the effects of human activities such as mineral, or, water, oil, and gas extraction on the potential for subsidence and collapse at the Lee Nuclear Station Site. These activities are found to have not affected the site. The potential for RIS associated with Make-Up Pond C is also evaluated. This activity is not expected to affect the site.

- Subsection 2.5.4.1.5, Summary of Geologic Hazards, summarizes the conclusions of the preceding four Subsections regarding the potential for non-tectonic deformation beneath the Units 1 and 2 nuclear islands.

As background for this subsection, descriptions, maps, and profiles of regional and site geology are described in detail in Subsections 2.5.1 and 2.5.2. Detailed descriptions of site and geotechnical conditions encountered during the field investigations at the Lee Nuclear Station Site are presented in Subsections 2.5.4.2, 2.5.4.3 and 2.5.4.4.

The Lee Nuclear Station Units 1 and 2 power block excavation area is defined by a rectangular boundary with an approximate dimension of 2000 feet by 1200 feet. Exploration was focused within the power block excavation and adjacent area, with an appropriately focused exploration effort to characterize the surrounding site area. Figure 2.5.4-201 shows site features at the Lee Nuclear Station Site. Relative topographic site change between the pre-Cherokee Nuclear Station and Lee Nuclear Station ground elevations is shown on Figure 2.5.4-202.

2.5.4.1.1 Geologic History and Stress Conditions

This Subsection describes aspects of geologic history that are relevant to the potential for uplift and unrelieved residual stresses in the bedrock. Information on the site geologic history is summarized from Subsection 2.5.1.2.

The Lee Nuclear Station Site lies within the northeast-southwest trending Appalachian orogenic belt. This orogenic belt formed during the Paleozoic Era and has undergone multiple orogenic events related to the opening and closing of the proto-Atlantic along the eastern margin of ancestral North America.

The most recent and significant major tectonic event to affect the Appalachian orogenic belt was the late Paleozoic Alleghanian orogeny. At the latitude of the Lee Nuclear Station Site region, the Alleghanian collision telescoped and drove previously accreted Taconic terranes westward up and across the Laurentian basement, folding the passive margin sequence before them and creating the Valley and Ridge fold-and-thrust belt. The collisional process also thrust a fragment from the underlying Laurentian basement eastward over the passive margin sequence, forming the western Blue Ridge. Significant strike-slip faulting and lateral transport of terranes are interpreted to have occurred during the Alleghanian orogeny (Reference 203).

Earth science teams (ESTs) that participated in the EPRI (1986) (Reference 204) evaluation of intra-plate stress found that tectonic stress in the Central and Eastern United States (CEUS) region is primarily characterized by northeast-southwest-directed horizontal compression. In general, the ESTs concluded that the most likely source of tectonic stress in the mid-continent region was ridge-push force associated with the Mid-Atlantic ridge, transmitted to the interior of the North American plate by the elastic strength of the lithosphere. Some of the ESTs noted that the regional northeast-southwest trend of principal stress may vary in places along the east coast of North America and in the New Madrid region. Further analyses of regional tectonic stress in the CEUS conducted since EPRI (1986) (Reference 204) have not significantly altered the characterization of the northeast-southwest orientation of the maximum compressive principal stress.

Unrelieved stress in bedrock could potentially result from thermally induced stresses, unloading due to removal of overburden by erosion or excavation, and tectonic stresses imposed during past deformation. Thermally induced stresses result from differences of cooling-related contraction along adjacent mineral grains of different composition. Residual stresses are typically small and tend to be relieved as the rocks are exposed by erosion or excavation. The relief of such residual stresses is time dependent and depends on the rate at which the ambient stress conditions of the rock change.

Thermally induced stresses are unlikely to be present. At a shallow depth of burial, the bedrock has equilibrated to surficial temperatures and any intergranular stress has had considerable time to be relieved. Likewise, stresses resulting from the removal of overburden are likely to be largely relieved due to the long period of the time when the rocks were near the surface with relatively low over-burden pressures. Relief of those residual stresses and CNS blasting and excavation methods account for the relatively increased frequency of subhorizontal fractures observed at shallow depths in borehole televiewer logs, refer to Subsection 2.5.4.3. The long-term residence of the bedrock near the surface provided ample time for the relief of residual stresses due to the release of overburden pressure.

Intragranular stresses may be preserved from deformation dating from Precambrian and Paleozoic tectonic events. However, thermal annealing of strained minerals coincident with late Paleozoic metamorphism and Mesozoic intrusions of mafic igneous rocks may have relieved much if not all of the elastic strain energy stored in older, strained mineral grains. Additionally, long residence near the surface and the presence of multiple fractures provides ample means to relieve any residual stresses and the likelihood that residual stresses from past tectonic events are preserved at the magnitude that result in creep or rebound is unlikely.

2.5.4.1.2 Stratigraphy, Lithology, and Soil and Rock Characteristics

This Subsection summarizes bedrock and stratigraphic information collected from previous studies and the Lee Nuclear Site exploration program. Following this, information relating to the characteristics of soil and rock at the Lee Nuclear Station Site, the physical and chemical properties of the rock and soil, and an

evaluation of zones of alteration and zones of potential weakness are presented. This data is primarily derived from the compilation and analysis of borehole and other site-specific information presented in Cherokee Nuclear Station PSAR (Reference 205), Cherokee Nuclear Station construction documents and the Lee Nuclear Site investigation collected during the 2006 - 2007 field exploration.

2.5.4.1.2.1 Site Area Stratigraphy and Lithology

Locally, the Lee Nuclear Station Site is underlain by a complexly deformed and metamorphosed plutonic-volcanic sequence that is mantled in most places by thick residual soils and saprolites. These soils and saprolites are evidence of a long weathering history. The relatively flat rolling plains and limited outcrop exposure are also evidence of the prolonged period of weathering. Local relief is caused by differences in the weathering resistance of bedrock and stream incision.

Rock units in the site area belong to the Battleground Formation, with the exception of later Mesozoic diabase dikes (References 206 and 207). The Battleground Formation is comprised primarily of felsic metavolcanic rocks, intermediate to mafic metavolcanic rocks, and quartz-rich metasedimentary rocks of Neoproterozoic age (Reference 226). Based on textures and the similarity of composition of the plutonic and volcaniclastic units, the entire sequence is considered to be a volcaniclastic pile that has been intruded by its own parent magmas (Reference 206). The occurrence of carbonate in the metasedimentary component is indicative of a marine environment, and reworking of the pile has resulted in both clastic and chemical deposition. Locally the composition of the volcaniclastics has been altered to various degrees by hydrothermal leaching due to large-scale circulation of seawater interacting with hot volcanic rocks.

The Lee Nuclear Station site itself is underlain by a metamorphosed pluton variously ascribed to intrusion of the Battleground Formation by the parent magmas of the Battleground volcaniclastics (Reference 207), intrusive metatonalite containing angular xenoliths of the Battleground Formation (Reference 226), and intrusive metatonalite and volcaniclastic rocks (Reference 227). This plutonic unit is generally composed of metatonalite that exhibits spatially variable composition. Within the plutonic unit exposed by excavation at the site, meta-granodiorite is the most abundant rock type based on petrographic analyses (Reference 205). This pluton is assessed to be separate from, and younger than (or possibly coeval with), the Battleground Formation (Reference 207).

Due to intense deformation, few primary features survive with which to determine stratigraphic order. Tentative inferences (References 206, 207, and 208) consider the South Fork antiform to be an upright feature and the Battleground Formation to be a homocline that “youngs” to the northwest (Reference 206). This inference is supported by the occurrence of the metasedimentary component primarily to the northwest, the expected stratigraphic relationships for deposition of marine-dominated clastic and chemical precipitate rocks at the later stages of the volcanic pile accumulation. Stratigraphic relationships of the various units are shown schematically in Figure 2.5.1-224.

2.5.4.1.2.2 Soil and Rock Characteristics

Borehole data show that the bedrock at the Lee Nuclear Station Site is overlain by residual soil comprised of silt and fine sand, 0 to greater than 100 feet, typically 40 to 80, feet thick, derived from in situ weathering of intact rock material. In some areas, this saprolite has developed a 'B' soil horizon. In many places the silts and sands preserve relict bedrock structures such as rock fabric and mineral foliation. The transition from saprolite to intact rock material can be gradual or abrupt.

Rock core and hand specimen samples collected from the Cherokee Nuclear Station and Lee Nuclear Station Sites have been logged using various classification systems. Historically, bedrock units at Cherokee Nuclear Station were described and grouped as either felsic (light color) gneiss or mafic (dark color) gneiss. Rocks described during the Lee Nuclear Station exploration program, were systematically classified into the following primary groups based on estimated mineral composition and texture: meta-diorite, meta-granodiorite, and meta-quartz diorite. Representative rock samples recovered core Lee Nuclear Station borings were sent for petrologic analysis to more precisely identify the mineralogy and rock types. Table 2.5.4-201 presents the petrographic analysis results. For purposes of consistency, rock descriptions described in Section 2.5 use the rock classification system developed for the Lee Nuclear Station Site unless indicated otherwise.

Petrologic examination of thin sections obtained from the site revealed the following rock types: mica schist, meta-quartz diorite, meta-dacite porphyry, and meta-basalt. These rock types are generally consistent with the rock types categorized as Felsic Gneiss and Mafic Gneiss rock groups described for the Cherokee Nuclear Station site (Reference 205, PSAR, Appendix 2C, Table 2C-2). The mineralogical characterizations of these rock types including description of rock name, estimated modal mineralogy, primary and secondary textures and structures, and alteration and metamorphism features are described in the following paragraphs.

Meta-quartz diorite at the site probably formed by hydrothermal alteration and regional dynamo-thermal metamorphism of quartz diorite intrusions. This rock type composes the bulk of the bedrock at the Lee Nuclear Station Site. Samples examined contain 38% to 55% plagioclase, 18% and 26% quartz, 5% to 20% biotite, 5% to 18% sericite, up to 9% actinolite, 3% to 10% ferroan calcite, and traces of chlorite, clinozoisite, apatite, FeOH, zircon, and opaques. Texturally, the meta-quartz diorite is phaneritic, holocrystalline, equigranular, fine to medium grained with a non- to weakly directed fabric. Figure 2.5.4-203 shows a representative hand sample photograph and photomicrograph of typical meta-quartz diorite.

Mica schist found on the site probably formed by hydrothermal alteration and regional dynamo-thermal metamorphism of fine grained siliciclastic or feldspathic sedimentary protoliths. These samples are composed of 25% to 68% quartz, 8% to 40% biotite, 10% to 35% sericite, up to 10% plagioclase, 3% to 10% ferroan calcite and traces of chlorite, clinozoisite, and opaques. Texturally the mica schist is phaneritic, holocrystalline, porphyroblastic to granoblastic, fine grained, and has

a non-directed to moderately directed fabric. Figure 2.5.4-204 shows a representative hand sample photograph and photomicrograph of typical mica schist.

Meta-dacite porphyry rock on the site probably formed by hydrothermal alteration of dacite porphyry shallow intrusions. These samples are composed of 45% to 65% plagioclase, 18% to 25% biotite, 8% to 15% quartz, up to 18% actinolite and traces of ferroan calcite, chlorite, apatite, garnet, and opaques. Texturally these samples are phaneritic, holocrystalline, porphyritic, fine to coarse grained and have a non-directed fabric. Figure 2.5.4-205 shows a representative hand sample photograph and photomicrograph of typical meta-dacite.

Meta-basalt at the site probably formed by hydrothermal alteration of an aphanitic basalt protolith. These samples are composed of 36% to 41% plagioclase, 25% to 30% actinolite, up to 10% quartz, 5% to 10% clinozoisite / epidote, up to 9% biotite, 3% to 7% ferroan calcite and traces of K-feldspar, and opaques. Texturally these samples are phaneritic, holocrystalline, aphyric, equigranular, fine grained and have non-directed to moderately directed fabrics. Figure 2.5.4-206 shows a representative hand sample photograph and photomicrograph of typical meta-basalt.

Numerous alteration features were noted in the examination of the thin-sections. Many of the samples had fine intrusive veins containing some or all of: quartz, ferroan calcite, sericite, biotite, and K-feldspar. Cataclastic and ductile metamorphism features were also noted. Some biotite has altered to chlorite and opaque minerals. Some plagioclase has weakly to moderately altered to sericite, ferroan calcite, chlorite, clinozoisite, and/or K-feldspar. Some actinolite has weakly altered to ferroan calcite.

Foliation joints, typically at high angles, are the most common type of discontinuities found within the partially weathered and slightly weathered bedrock. Foliation features were observed in both outcrop exposures, hand sample sized specimens and in petrologic examination of thin sections. Foliation planes represent zones of weakness within the rock and when additional stresses act on the rock (e.g., diamond coring), it is these zones that preferentially fracture. It is important to note that the more highly fractured rock, classified as partially weathered rock, was excavated and removed during construction of the Cherokee Nuclear Station Unit 1, excavated and removed on Unit 2 and partially excavated on Unit 3. The exposed slightly weathered bedrock has very few discontinuities, and these do not represent significant zones of weakness.

Rock at the Lee Nuclear Station Site is not soluble in groundwater. While some are composed of up to 10% ferroan calcite, this mineral is broadly distributed within the rock mass. If it were to completely weather out, which is highly unlikely, it would not leave voids of large size to endanger safety-related structures, or sufficiently interconnected to serve as a significant groundwater flow path.

2.5.4.1.3 Groundwater

The primary drainage in the site area is the Broad River and associated tributary drainages. Typical of most first order Piedmont streams, the Broad River flows southeast directly across the regional trend of most geologic contacts and structure. The streambed is at about 500 ft msl and has incised into the Piedmont surface about 200 ft below the drainage divides. The Broad River lacks a well-developed flood plain in the Lee Nuclear Station Site area.

The high historic groundwater level in the plant area is at Elevation 579 feet mean sea level (msl). This elevation value is based on the existing well delineated high water mark along the exterior of the Cherokee Nuclear Station (CNS) Unit 1 reactor building. The existing excavations flooded naturally after cessation of dewatering operations when the plant construction was halted in the early 1980's. The water level in the excavations rose to, or near, the typical (static) groundwater table and remained in this state for over 20 years prior to dewatering for the Lee Nuclear Station project. Long-term standing water in the vacated CNS excavation left a high water mark on the partially constructed CNS Unit 1 reactor building structure that was surveyed at an elevation of 579 feet msl. The design groundwater level for Lee Nuclear Station is Elevation 579±5 feet msl, allowing for a 5-foot seasonal variation over the high water mark level (see Table 2.0-201).

2.5.4.1.4 Effects of Human Activities

Human activities such as mining or groundwater withdrawal have the potential to cause surface deformation. There are no mining operations with the potential to impact the Lee Nuclear Station Site. There is no excessive extraction or injection of groundwater, or impoundment of water occurring within the site area that can affect geologic conditions. One active sand mine, hydraulic dredge and wash operation, is located along the Broad River approximately one mile north of the Site. This mining operation does not present a potential hazard to the Lee Nuclear Station Site.

RIS associated with the filling and operation of Make-Up Pond C is considered negligible, and it is unlikely the induced magnitudes would exceed **M** > 4, a value well below the short-period controlling earthquake. Evaluations related to the potential of RIS associated with Make-Up Pond C are described in Subsection 2.5.2.1.3.

2.5.4.1.5 Summary of Geologic Hazards

The Lee Nuclear Station Site investigation did not encounter adverse geologic conditions in the safety-related explorations that pose a stability or surface hazard. Major safety related structures can be founded on fresh, hard bedrock or on engineered fill placed over fresh, hard bedrock.

There are no significant unrelieved stresses in the bedrock that could cause creep or rebound. Erosion rates are slow. These conditions are not conducive to "locked-in" residual stresses.

No zones of alteration or structural weakness are present. Bedrock contains foliation joints and foliated zones, which do not significantly reduce rock strength.

There are no human activities, such as mining or groundwater extraction, which could cause subsidence or collapse.

As noted in Subsection 2.5.3, earthquake activity with its resulting ground motion effects is judged to be the primary geologic hazard to the Lee Nuclear Station Site. The potential for tectonic surface deformation within the site area is judged to be negligible. The potential for non-tectonic surface deformation within the site area, including surface deformation associated with potential Make-Up Pond C RIS, is negligible. A detailed discussion of vibratory ground motion and potential for surface faulting at the Lee Nuclear Station Site is presented in Subsections 2.5.2 and 2.5.3, respectively.

2.5.4.2 Properties of Subsurface Materials

WLS COL 2.5-6 This subsection presents a summary of the field investigation and subsurface material properties at the Lee Nuclear Station Site. The laboratory testing and sample control procedures are discussed as well. Refer to Subsection 2.5.4.3 for drawings showing the boring and other field investigation locations and for sections of the subsurface conditions. Soil, granular fill, and rock dynamic material properties are presented in Subsection 2.5.4.7.

The procedures used to perform field investigations for determining the engineering properties of soil and rock materials conform to Regulatory Guide 1.132, "Site Investigations for Foundations of Nuclear Power Plants." The field exploration and laboratory testing program conform with this regulatory standard.

Information from literature, regional and local maps, and historical information from exploration activities completed for the Cherokee Nuclear Station were all used as additional guidance for planning the field exploration program. The exploration program included multiple methods of exploration and utilized both traditional and state-of-the-practice methods of subsurface exploration and in situ testing. Soil and rock sampling was planned to meet the requirements for spacing, depth, and sample frequency provided in the regulatory guide. Borings in the nuclear island foundation areas were generally extended at least 20 feet into sound rock materials in accordance with the guidance from Regulatory Guide 1.132. Geophysical testing was included in the exploration program and included both surface and borehole geophysical methods. Samples of site materials obtained during the exploration work were documented and logged by geologists and engineers and preserved in the field for further analysis and laboratory testing. Further details regarding the field exploration program are provided in Subsections 2.5.4.2.1 and 2.5.4.2.2. The field exploration and laboratory testing plan provide detailed coverage of the safety-related structures and other site areas. This information was integrated with available historic site

data and published information to develop a comprehensive characterization and evaluation of the subsurface materials.

The laboratory testing program was planned and conducted using the guidance provided by Regulatory Guide 1.138. Information from the historic field exploration program, literature, and information from the historic laboratory testing completed for the Cherokee Nuclear Station were all used as additional guidance for planning the laboratory testing program for Lee Nuclear Station. The laboratory testing program for soil included samples obtained using disturbed and undisturbed sampling methods. The testing program included a variety of tests on the significant soil and rock materials encountered during the field exploration program. Static and dynamic laboratory test methods were performed. Further details regarding the laboratory testing program are provided in Subsections 2.5.4.2.3 and 2.5.4.2.4. Liquefaction potential of the foundation materials is discussed in Subsection 2.5.4.8.

2.5.4.2.1 Site Explorations

WLS COL 2.5-6 Site subsurface exploration described in this subsection includes soil and rock borings, installation of groundwater monitoring wells and performing packer tests, surface geophysical surveys, cone penetration testing (standard and seismic), geotechnical test pit and geologic trench excavations, and borehole and geophysical in situ testing methods. These explorations (referred to as exploration points) were performed specifically for the Lee Nuclear Station Unit 1 and Unit 2. Geophysical explorations are described in Subsection 2.5.4.4. The number and type of explorations performed for the Lee Nuclear Station investigations are summarized in the following tables.

- Table 2.5.4-202 Summary of Lee Nuclear Station Geotechnical Exploration
- Table 2.5.4-203 Summary of Completed Exploration Borings and Field Tests
- Table 2.5.4-204 Summary of Geotechnical Borings for Completed Monitoring Wells
- Table 2.5.4-205 Summary of Completed Cone Penetrometer Test Soundings
- Table 2.5.4-206 Summary of Completed Geotechnical Test Pit and Geologic Trench Locations
- Table 2.5.4-207 Summary of Completed Surface Geophysical Test Locations

The exploration map explanation is provided in Figure 2.5.4-207. The site exploration points for the complete site geotechnical exploration are shown on Figure 2.5.4-208. The exploration points for the Lee Nuclear Station power blocks and adjacent areas are shown on Figure 2.5.4-209.

The as-built site explorations were recorded by horizontal and vertical survey of the locations. Horizontal and vertical surveys were completed to third order accuracy standards. The surveyed horizontal and vertical coordinate values are provided on the individual test results (logs, records, etc.) for surface exploration points.

Site explorations were also performed at this site location prior to construction of the Cherokee Nuclear Station. The historic exploration results from the Cherokee Nuclear Station work are published in the Cherokee Nuclear Station Preliminary Safety Analysis Report (Reference 201) and additionally, more historic explorations were conducted during construction of the Cherokee Nuclear Station. These historic explorations from the Cherokee Nuclear Station were used to guide the planning of additional explorations made during the Lee Nuclear Station exploration. Portions of the historic Cherokee Nuclear Station exploratory work are used to supplement the information obtained specifically for Lee Nuclear Station. These Cherokee Nuclear Station results, where mentioned in the following text, are identified as historic results.

2.5.4.2.1.1 Soil, Rock, and Concrete Borings

Subsurface explorations were performed using geotechnical drill rigs mounted on trucks or tracked vehicles. Specific equipment used at each borehole is recorded on the boring logs. Field boring logs and other field records were maintained by a rig geologist (geologist or geotechnical engineer). A rig geologist was assigned to each drill rig and was responsible for maintaining the field records associated with activities conducted at a specific exploration point.

Borings for geotechnical purposes were advanced in soil using solid or hollow stem auger (HSA) and/or mud rotary (wash) drilling techniques until refusal (defined as the physical inability to advance the hole using soil drilling procedures) was encountered. In geotechnical borings the drilling method for depths greater than 15 ft was generally mud rotary (wash) drilling. Standard Penetration Test (SPT) samples were typically obtained on 5-foot intervals, beginning 3.5 ft. below ground surface, in soil materials. Additional details concerning sampling are provided in Subsection 2.5.4.2.2.1.

The Cherokee Nuclear Station Unit 1 structure had to be penetrated with geotechnical borings to explore the underlying materials for the Lee Nuclear Station geotechnical investigation.

Structural concrete from the Cherokee Nuclear Station Unit 1 structure was pre-cored using a thin-walled concrete coring machine. The 6-inch diameter thin-walled bit was advanced through the upper and lower level rebar within the structural slab. Coring continued to depths of approximately 4 to 6 ft. or approximately 6 to 12 inches beyond the lower level rebar. The concrete plug was

removed and geotechnical core drills were used to continue coring to the final depth.

Once refusal was encountered, and if rock coring was required, a steel or PVC casing was set if soil was present. The holes were advanced using wire-line rock coring equipment and procedures, ASTM D 2113-99. A five-foot or ten-foot long NQ or HQ size core barrel was used for all rock coring. Additional details concerning coring are provided in Subsection 2.5.4.2.2.2.

Permanent PVC casing was installed and grouted in place extending a short distance above the soil or rock surface in several locations where downhole geophysics was assigned. PVC casing for this purpose was 4-inch diameter riser pipe grouted in place using a cement bentonite grout mix to provide a consistent seal between the casing and the surrounding soil and rock.

The boreholes, including the grouted-in PVC casings for geophysical tests, were filled using a cement-bentonite grout prior to demobilizing from the site. The grout was placed by pumping through a tremie pipe.

Copies of Lee Nuclear Station exploration records including boring logs and monitoring well construction diagrams, SPT energy measurements, geotechnical test pit and geologic trench logs, and packer test results are provided in Appendix 2AA. This appendix is comprised of five attachments as described below.

- Appendix 2AA, Attachment 1, Lee Nuclear Station Geotechnical Borings Logs and Groundwater Monitoring Well Construction Logs
- Appendix 2AA, Attachment 2, Lee Nuclear Station SPT Energy Measurements
- Appendix 2AA, Attachment 3, Lee Nuclear Station Geotechnical Test Pit and Geologic Trench Logs
- Appendix 2AA, Attachment 4, Lee Nuclear Station Packer Test Results
- Appendix 2AA, Attachment 5, Lee Nuclear Station Cone Penetration Testing Logs.

Copies of Cherokee Nuclear Station historic geotechnical boring logs are provided in Appendix 2BB. These borings logs represent historic records that were developed during various stages of field exploration for the Cherokee Nuclear Station.

2.5.4.2.1.2 Groundwater Monitoring Wells

Geotechnical exploratory borings for Monitoring Well (MW) locations were generally drilled using hollow stem augers through which a Central Mine Equipment Company (CME) type continuous soil sampler was used. In some instances, a geoprobe continuous sampler was used. Continuous samples were

obtained in 5-foot segments beginning 3.5 feet below the initial ground surface. The CME sampling continued to refusal after which NQ rock coring was utilized to reach the required borehole depth. Occasionally refusal of the CME sampler was reached prior to reaching material suitable for rock coring. When this occurred, rotary drilling using wash water without bentonite was used to advance the borehole combined with Standard Penetration Test sampling to obtain samples until material suitable for NQ coring was reached.

Observation wells were installed in hollow stem auger or air rotary drilled holes of appropriate diameter (at least 6 inches). The wells consist of 2-inch diameter PVC screen and riser pipe, sand filter pack, bentonite chips or pellets, and cement bentonite grout. Protective steel well covers and concrete pads were placed at the surface. One 6-inch diameter well of similar construction was installed to use as a pumping well for permeability testing. The location of groundwater monitoring wells constructed as part of the Lee Nuclear Station exploration is shown on Figure 2.5.4-210.

WLS SUP 2.5-2
WLS SUP 2.5-3
The exploratory boreholes for monitoring well locations were backfilled as described above. PVC monitoring well locations were not grouted, but were left open for continued monitoring.

Additional information regarding the groundwater monitoring wells is included in Subsection 2.4.12.

2.5.4.2.1.3 Surface Geophysical Testing

Surface geophysical testing was performed using the Spectral Analysis of Surface Waves (SASW) technique. Fifteen SASW surveys were performed during site investigation activities at the Lee Nuclear Station Site. Survey depths ranged from tens of feet up to approximately 150 feet below ground surface, depending on material attenuation conditions and length of survey lines. Figure 2.5.4-211 shows the locations of SASW survey lines at the Lee Nuclear Station Site. Discussion of SASW survey testing methodology and results is located in Subsection 2.5.4.4.1.

2.5.4.2.1.4 Cone Penetration Testing

Cone Penetration Testing (CPT) was performed at twenty-nine locations using a 20 ton self-contained rig mounted on a tracked all-terrain vehicle. CPT locations were advanced to an assigned depth or to the depth of refusal of the CPT probe. The CPT testing was performed using an electronic cone system. CPT measurements were performed using procedures described in ASTM D 5778-95.

Seismic Cone Penetration Testing (SCPT) was completed in ten of the CPT locations at intervals of one meter. Of these tests, nine provided useful data. Pore pressure dissipation tests were performed in twelve of the CPT locations at depths selected during performance of the CPT.

Figure 2.5.4-212 shows the CPT and SCPT test locations performed as part of the Lee Nuclear Station exploration. Discussion of the SCPT testing methodology and results is described in Subsection 2.5.4.4.2.

2.5.4.2.1.5 Geotechnical Test Pits and Geologic Trenches

Both geotechnical test pits and geologic trenches were excavated during Lee Nuclear Station Site investigations. Geotechnical test pits were designed to collect bulk samples for laboratory testing, and the geologic trenches were designed to examine large-scale subsurface geologic features.

Geotechnical test pits and geologic trenches were excavated at fourteen locations, to depths ranging from approximately 4 feet up to 20 feet. A track-mounted backhoe was used to excavate and then later to backfill the test pits. A rig geologist selected the materials to be sampled and collected the bulk samples. At each test pit, portions of soil from the upper 3 feet were collected and combined to form a single representative bulk sample of surface material at that particular location. Sampling of geotechnical test pits is described in Subsection 2.5.4.2.2.4.

The four corners of the geotechnical test pit or geologic trench were marked and are documented in the survey record. The survey coordinates for the northernmost corner of the geotechnical test pits and geologic trenches are summarized in Table 2.5.4-206. The locations of test pits and trenches excavated as part of the Lee Nuclear Station exploration is shown on Figure 2.5.4-213.

2.5.4.2.1.6 In Situ Testing

In situ testing was performed to estimate elastic compressibility properties of rock materials using the Goodman Jack and borehole pressuremeter. In situ testing was also performed in rock materials using downhole geophysical techniques including optical televiewer, acoustic televiewer, P-S suspension logging, and downhole velocity logging. Some P-S suspension logging was also performed in soil materials. In situ testing to estimate the permeability of rock materials was performed using the borehole packer test.

2.5.4.2.1.6.1 Goodman Jack Testing

Fourteen Goodman Jack tests were performed in two boreholes at multiple depth intervals to measure elastic modulus in situ using procedures described in ASTM D 4971-02. The Goodman Jack is a borehole probe used for the measurement of wall deformation as a function of applied load. Data obtained from the load-deformation measurements gives the elastic modulus of rock directly. Hydraulic pressure is transmitted to the rock through the movable plates.

2.5.4.2.1.6.2 Borehole Pressuremeter Testing

Twenty-four pressuremeter tests were performed in two boreholes at multiple depth intervals to measure elastic modulus in situ using procedures described in ASTM D 4719-00. Of these tests, twenty-two provided useful data. The pressuremeter test is an in situ stress-strain test performed on the wall of a borehole using a cylindrical probe that is expanded radially.

The Goodman Jack and borehole pressuremeter test locations performed as part of the Lee Nuclear Station exploration are shown on Figure 2.5.4-214. Tables 2.5.4-208 and 2.5.4-209 present the results of Goodman Jack and borehole pressuremeter tests, respectively.

2.5.4.2.1.6.3 Borehole Geophysical Testing

Geophysical testing using multiple test methods was performed in fifteen borings. Geophysical logging performed included P-S suspension logging in thirteen borings with comparative downhole velocity profiles in four selected borings, and borehole televiewer logging in thirteen borings using optical and/or acoustic methods. Test procedures and results of the downhole geophysical testing are presented in Subsection 2.5.4.4. The borehole geophysical test locations performed as part of the Lee Nuclear Station exploration are shown on Figure 2.5.4-215.

2.5.4.2.1.6.4 Packer Testing

Field permeability testing by the packer method was conducted in selected borings using test procedures described in ASTM D 4630-96 (2002), modified to use a manually-read flow meter rather than a digitally recorded one. The packer testing method involved establishing and maintaining a constant pressure in the packer test interval or test length, measured by a gauge at the surface, and determining the rate of inflow associated with maintaining the pressure. The test method is thus known as the “constant head injection test.” Three or more pressure values were generally used in each assigned test interval. The purpose of the packer testing was to establish the coefficient of permeability (also called hydraulic conductivity) of the rock within the packer test length. The packer test locations performed as part of the Lee Nuclear Station exploration are shown on Figure 2.5.4-210.

2.5.4.2.1.7 Petrographic Testing

Petrographic testing was performed on fifteen rock core samples collected from nine borings. Selected rock core samples were prepared into standard 27 x 46 mm covered thin sections stained for K-feldspar and calcite/ferroan carbonate. Petrographic analyses and photomicrography of thin sections was performed using a petrographic microscope at magnifications ranging from 25X to 500X. The petrographic test locations performed as part of the Lee Nuclear Station exploration are shown on Figure 2.5.4-216.

2.5.4.2.2 Soil and Rock Sampling

2.5.4.2.2.1 Standard Penetration Test Sampling

Soil sampling in the geotechnical borings using the SPT was generally conducted at intervals of 5 feet using equipment and methods described in ASTM D 1586-99. Sampling generally started at 3.5 feet below the ground surface. Automatic hammers were used to perform the SPT tests. The sampler was typically driven 18 inches in soil with blows recorded for each six-inch interval of penetration. In

very hard soils and weathered rock, driving was terminated at 50 blows and the actual penetration recorded for the penetrated interval (e.g., 50 blows / 3 inches).

Fill soils in place at the site at the time of the Lee Nuclear Station explorations in 2006 and 2007 were explored in detail to assist in characterizing the backfill that was initially planned to be used around the Lee Nuclear Station Unit 1 and Unit 2 nuclear island areas. These fill soils were in-place at the time of the Lee Nuclear Station exploration in 2006 and 2007 and had been placed and compacted during site preparation work for the Cherokee Nuclear Station. These areas where fill materials were explored were designated ”test fill” areas. In several borings drilled in the “test fill” areas, SPT sampling was conducted at intervals of 2 feet. For these locations a 30-inch sampler was used and was driven 24 inches with blows recorded for each six-inch interval of penetration. Sampling at these “test fill” locations started at the ground surface. Subsequent to the exploration of the “test fill” areas, a decision was made that granular fill materials instead of fill soils will be used as backfill around the Lee Nuclear Station Unit 1 and Unit 2 nuclear island areas. Therefore, the “test fill” areas have no special significance subsequent to the decision to use granular fill.

In the geotechnical borings for the Lee Nuclear Station exploration in 2006 and 2007, the split tube sampler was opened at the drill site and the recovered materials were visually described and classified by the rig geologist. A selected portion of the sample was placed in a glass sample jar with a moisture-proof lid. Sample jars were labeled, placed in cardboard boxes, and transported to the on-site storage area.

Energy measurements were made on the drill rigs that performed SPT testing for the Lee Nuclear Station exploration. Energy measurements were recorded during sampling at several different depth intervals. The energy measurement work was done in general accordance with ASTM D 4633-05. The ratio of the average measured energy to the theoretical potential energy of the SPT system (140-pound weight with the specified 30-inch fall) is the energy transfer ratio (ETR).

The ETR range of the automatic hammers used at the Lee Nuclear Station Site is 76.8% to 82.8% of the theoretical potential energy. These ETR values are within the range of typical values for automatic hammers.

2.5.4.2.2.2 Coring

For the borings of the Lee Nuclear Station exploration in 2006 and 2007, rock coring was performed, when assigned, for those materials that could not be penetrated with soil drilling methods. For purposes of determining the depth at which to begin rock coring procedures, refusal to soil drilling was defined as the physical inability to advance the hole using soil drilling procedures. Rock coring was performed in accordance with ASTM D 2113-99. Rock recovered by the coring process was carefully removed from the inner barrel and placed in wooden core boxes with wooden blocks used to mark ends of runs. Wood spacers were placed in the core box when needed to stabilize the core laterally. Filled core

boxes were taken to the on-site sample storage facility. Photographs of the cores were taken in the field.

The rig geologist visually described the rock core and noted the presence of joints and fractures, distinguishing mechanical breaks from natural breaks where possible. The rig geologist also calculated percent recovery and Rock Quality Designation (RQD) prior to moving the core from the drill site. Field boring logs and photographs were used to document the drilling operations and recovered materials. The construction of casing for completion of drilling was recorded on a casing installation field log. In borings to be geophysically logged, PVC casing was grouted in place in lieu of the temporary casing. The grouting process was recorded on grouting field logs.

2.5.4.2.2.3 Undisturbed Sampling

For the Lee Nuclear Station exploration in 2006 and 2007, undisturbed samples were taken in separately drilled boreholes located adjacent to geotechnical boring locations. Undisturbed soil samples were taken using a 3-inch diameter thin-walled tube sampler in accordance with ASTM D 1587-00. Depth intervals for undisturbed samples were assigned based on a review of the field log from the geotechnical boring.

When subsurface material was too dense or hard to allow satisfactory samples to be recovered by pressing the tube sampler into the material, a Pitcher sampler was used. The Pitcher is a rotary sampler which drills the 3-inch tube into the subsurface material. Pitcher samplers were generally used when SPT blow counts from the adjacent borehole were greater than 30 blows per foot at the desired sample depth. Undisturbed samples were sealed at the top and bottom against moisture loss, labeled, kept in an upright condition, and transported to the climate-controlled on-site storage area in accordance with ASTM D 4220-95 (2000).

2.5.4.2.2.4 Bulk Sampling (Test Pits)

For the Lee Nuclear Station exploration in 2006 and 2007, a track mounted backhoe was used to excavate and backfill the test pits for soil sampling purposes. Bulk samples were obtained from the materials excavated from the test pit. A rig geologist selected the materials to be sampled and collected the bulk samples. Bulk samples were placed in new 5-gallon plastic buckets with lids and handles for carrying. Glass jar samples were obtained and sealed for moisture retention. The buckets and jar samples were labeled and transported to the on-site storage area. The rig geologist prepared a Geotechnical Test Pit Log based on visual description of the excavated materials according to ASTM D 2488-00. The backhoe was used to backfill the test pit excavation using the excavated materials. The backfilled materials were tamped in-place using the backhoe bucket.

The bulk sampling of the geotechnical test pits was for testing to characterize soils for use in constructing Group I fill. Group I fill is a term specific to the former Cherokee Nuclear Station construction documents. Group I fill is a conventional

quality fill of selected soil types compacted to 95 percent of the standard Proctor (ASTM D 698-00) maximum dry density. Group I fill performs no safety function for the Lee Nuclear Station because select granular fill materials surround the nuclear islands and support the structures adjacent to the nuclear islands. No further reference to the Group I fill testing or results is contained herein. Group I fill is illustrated on selected figures to convey the backfill relationship of select granular fill and Group I fill within the existing excavation.

2.5.4.2.2.5 Sample Control and Preservation

An on-site sample storage facility was established for the Lee Nuclear Station exploration in 2006 and 2007 in a warehouse building that remained on-site from Cherokee Nuclear Station Site construction activities. Electrical power, overhead lighting, and a ventilation fan were installed in the warehouse building. A travel trailer was brought to the site to serve as the field office during site exploration. The field office trailer was located inside the sample storage facility and housed the on-site temporary file storage system and provided office space for the field geologists and engineers. The warehouse building was not climate controlled; however, the field office trailer was capable of providing a climate controlled environment when necessary, such as for storage of undisturbed samples. The warehouse building served as the sample storage facility, supply storage building, sample examination area, and field exploration project headquarters.

Soil samples were obtained from split spoon sampler or undisturbed tube samples as part of the geotechnical exploration process for the Lee Nuclear Station exploration in 2006 and 2007. Split spoon samples were placed in glass jars and sealed with a moisture-tight lid. Undisturbed tube samples were sealed on both ends in the field using beeswax, covered with plastic caps, and sealed with duct tape. All samples were labeled with identifying information and transferred to the on-site lockable temporary storage area.

Samples were transported daily from the field to the sample storage warehouse by the rig geologists. SPT samples were transported as Group B samples in their compartmentalized cardboard boxes, each labeled to show the contents. The CME soil core samples and rock cores were transported in wooden core boxes, kept horizontal, and labeled to show the contents. The undisturbed tube samples were transported according to ASTM D 4220-95 (2000), Group C samples. Undisturbed samples were stored inside the field office trailer which provided a climate-controlled environment until the samples could be transported to the laboratory. Rock and concrete cores were transported according to ASTM D 5079-02 (2006).

A portion of the warehouse was designated as the sample storage area. Rock core boxes were placed on wooden pallets located within the sample storage area of the warehouse and were grouped by boring. SPT sample boxes were placed with the core boxes for borings having both SPT sampling and coring. For borings with SPT sampling only, SPT samples were placed on wood tables inside the sample storage area of the warehouse. Test pit sample buckets were also placed within the sample storage area.

Boring field records were reviewed and samples were identified for possible laboratory testing. Work instructions were issued listing samples to be removed from the site storage and shipped to the laboratories. Following the work instructions, samples were removed from the site storage area and prepared for shipping.

Soil samples were handled and transported or shipped to the appropriate laboratory in accordance with ASTM D 4220. Samples for index testing were handled as Group B samples, while undisturbed tube samples were handled as Group C samples. The undisturbed samples were transported by MACTEC or WLA personnel in personal, company, or rented passenger vehicles. All samples were shipped under chain of custody, and the receiving laboratory signed for them upon receipt. At the laboratory, prior to testing, the undisturbed samples were stored in the controlled laboratory environment in a secure location. Work instructions were prepared by MACTEC engineers and provided to the laboratories.

For soil samples which were selected for chemical testing, a portion of the total sample received was prepared by MACTEC laboratory personnel, as directed in a work instruction, and placed in jars with moisture-tight lids before being shipped under chain of custody to the chemical testing laboratory.

Representative portions of jar and undisturbed tube samples were taken to complete the assigned tests. In many cases, the entire sample was used for testing. Some unused portions of the jar or undisturbed tube sample were returned to the sample storage facility if the portion was of reasonable size.

2.5.4.2.3 Laboratory Testing

For the Lee Nuclear Station exploration in 2006 and 2007, laboratory testing was performed on disturbed, undisturbed, and bulk soil samples, and on rock cores obtained during the subsurface investigation. Testing was performed in accordance with ASTM standards or other standards where applicable. Other standards used for laboratory testing included Environmental Protection Agency methods for chemical analysis of soils.

The quantity of each test completed on each sample type is identified in Table 2.5.4-210. Test standards used for laboratory testing are listed in this subsection. Laboratory testing was in accordance with the standard method or procedure. Additional descriptions for selected test methods are provided in Subsections 2.5.4.2.3.1 through 2.5.4.2.3.12.

- Moisture content, ASTM D 2216-05
- Atterberg limits, ASTM D 4318-05
- Grain size testing (sieve + hydrometer and sieve), ASTM D 422-63 (2002) and ASTM D 6913-04
- Specific gravity, ASTM D 854-06

- Chemical analysis,
  - pH, ASTM G 51-95 (2005)
  - Resistivity, ASTM G 57-95a (2001)
  - Chloride, EPA SW-846 9056/300.0,
  - Sulfate, EPA SW-846 8056/300.0
- Unit weight of soil, ASTM D 5084-03 (Sections 5.7 – 5.9. 8.1, 11.3.2)
- Consolidated-undrained triaxial shear, ASTM D 4767-04
- Specimen preparation – rock cores, ASTM D 4543-04
- Compressive strength and elastic moduli – rock cores, ASTM D 7012-04
- Consolidation tests, ASTM D 2435-04

Petrographic analysis of selected rock samples was also performed. The descriptions and results of petrographic analyses are provided in Subsection 2.5.4.1 and Table 2.5.4-201.

2.5.4.2.3.1 Particle Size Analysis, ASTM D 422-63 (2002) and ASTM D 6913-04

Sieve Analysis – The dried soil sample is separated into a series of fractions using a standard set of nested sieves. The sieving operation is conducted by means of a lateral and vertical motion of the nest of sieves, accompanied by jarring action to keep the sample moving continuously over the surface of the sieves. The weights retained on each of the set of nested sieves are used to calculate the percent of the sample passing each sieve size.

Hydrometer Analysis – The portion of the soil sample passing the No. 200 (75 micrometers) sieve is soaked in water and dispersed using a dispersing agent. The solution is placed in a cylinder and stirred, and the density of the solution is monitored over time with a hydrometer to observe the settling out of suspended soil particles. Diameters corresponding to the readings of the hydrometer are then calculated using Stoke's law.

At the time of laboratory testing ASTM D 6913-04 was the current specification for grain size analysis, but it did not include hydrometer testing. Where hydrometer testing was required, Section 1.4 of the specification allows that ASTM D 422 – 63 (2002) be used.

Section 5.1.1 of ASTM D 422 – 63 (2002) and Table 1 of ASTM D 6913 – 04 give minimum sample mass requirements (the minimum depends on the maximum particle size present) for each test. In cases where there was not enough sample to meet the appropriate recommended mass, the test was completed using the

available sample and it was noted in the Remarks section of the Particle Size Distribution Report.

2.5.4.2.3.2 Chemical Analysis (pH, Resistivity), ASTM G 51-95 (2005), ASTM G 57-95a (2001)

For purposes of corrosion testing, soil pH measurements in the laboratory are made within 24 hours from the time of sampling. Measurements are made at the soil's natural moisture content using a pH-sensitive electrode system, and reported to the nearest 0.1 pH units. Soil resistivity measurements indicate the ability of soil to resist electrical currents, and are the reciprocal of electrical conductivity. Resistivity was reported in units of Ohm-cm at the natural ("as received") moisture content and saturated.

2.5.4.2.3.3 Chemical Analysis (Chloride, Sulfate), EPA SW-846 9056/ 300.0, EPA SW-846 8056/300.0

A small quantity of soil was split from the original sample, placed in a separate clean jar, and sent to the laboratory for analysis of chloride ion and sulfate ion concentration. The concentrations are measured using an ion chromatograph with results reported in units of milligrams per kilogram. In many cases the measured concentrations were below the reporting limit of the test equipment, and were noted as estimated results less than the reporting limit in the report.

2.5.4.2.3.4 Unit Weight of Soil, ASTM D 5084-03 (Sections 5.7 – 5.9. 8.1, 11.3.2)

Sections of the undisturbed samples were extruded from the sampling tubes and trimmed to remove any surface irregularities. Dimensions of the sample were measured and recorded and the weight is determined. Unit weight is calculated by dividing the sample weight by volume. If the moisture content is known, dry unit weight can be calculated by dividing the wet sample unit weight by the quantity (1 + moisture content, in decimal format).

2.5.4.2.3.5 Deleted

2.5.4.2.3.6 Deleted

2.5.4.2.3.7 Consolidated – Undrained Triaxial Shear Testing, ASTM D 4767-04

Consolidated – undrained (CU) testing was performed on undisturbed test specimens. Undisturbed specimens were extruded from sampling tubes and trimmed to appropriate dimensions. The specimens, encased in the rubber membranes, were then saturated by back-pressure prior to shearing. Drainage was allowed from the specimen during the consolidation phase, thus allowing equilibrium under the confining stress, but no drainage was allowed during the loading phase. For undisturbed specimens failure was defined at the point of maximum pore pressure. The maximum pore pressure failure criterion was investigated to compare with historic triaxial tests performed for construction of

the former Cherokee Nuclear Station. Information contained in Brandon, et al. (2006) confirms the conclusion that peak pore pressure is a conservative method for assigning the failure criterion for the CU triaxial tests (Reference 210).

Vertical load, vertical displacement, chamber pressure, and pore pressures generated during the loading phase were measured. The test is termed consolidated-undrained and total stresses result if no pore pressure corrections are included. When the pore pressures generated during the loading phase are subtracted from the total stresses, effective stresses result.

Section 8.2.3.1 of the ASTM standard describes how to determine when the specimen is saturated. Specifically, it states that a sample is considered saturated if the B-parameter is equal to 0.95 or greater, or if B remains unchanged with additional increments of back-pressure.

2.5.4.2.3.8 Deleted

2.5.4.2.3.9 Deleted

2.5.4.2.3.10 Specimen Preparation – Rock Cores, ASTM D 4543-04

This procedure specifies the methods for laboratory specimen preparation and determination of the length and diameter of rock core specimens and the conformance of the dimensions with established standards. Because the dimensional, shape, and surface tolerances of rock core specimens are important for determining rock properties of intact specimens, great care must be exercised when preparing core samples for strength testing. The prepared cores are measured to determine the straightness of elements on the cylindrical surface, flatness of the specimen ends, parallelism of the specimen ends, and perpendicularity of end surfaces to the specimen axis.

Possible deviations to core preparation include side straightness, end flatness, parallelism, and perpendicularity. Deviations to the specimen preparation criteria were unavoidable for several cores. Where deviations occurred they were reported on the individual test reports.

2.5.4.2.3.11 Compressive Strength and Elastic Moduli – Rock Cores, ASTM D 7012-04

This procedure specifies the manner in which to determine the strength of rock, in this case the uniaxial or unconfined compressive strength. This method also specifies the apparatus, instrumentation, and procedures for determining the stress-axial strain and the stress-lateral strain curves, as well as Young's modulus and Poisson's ratio.

The prepared specimen is placed in a loading frame and axial load is increased continuously on the specimen until peak load or failure of the specimen is obtained. To determine the elastic moduli, the specimen is instrumented with four strain gauges (two mounted axially, two mounted laterally) prior to placement in the loading frame. Axial strain gauges were 2 inches in length and lateral strain

gauges were 1 inch in length. Axial load and deformation (axial and lateral) readings are obtained as the load is applied to the specimen. Unconfined compressive strength is determined based on the cross-sectional area and the maximum recorded load applied to the specimen. Young's modulus (the slope of the stress-axial strain curve) and Poisson's ratio (ratio of lateral strain to axial strain) are calculated using the strain gauge data from a portion of the data range generally between 40 and 60% of maximum strain. The specific data range for each core was individually selected based on review of the data. The selection utilized the average slope method over a range where both the axial and lateral stress-strain curves appeared most linear.

Two-inch axial strain gauges were used for all cores. Two-inch gauges were used to comply with the minimum axial strain gauge length of 10 mineral grain diameters specified in the test standard.

2.5.4.2.3.12 Consolidation Tests, ASTM D 2435-04

Sections of the undisturbed samples were extruded from the sampling tube for consolidation testing. The specimen was then trimmed into a disc 2.5 inches in diameter and 1-inch thick. The disc was confined in a stainless steel ring and sandwiched between porous plates. No saturation of the samples was performed, but the samples were carefully covered to prevent loss of moisture to evaporation during the test. The specimen was then subjected to incrementally increasing vertical loads and the resulting changes in specimen height with respect to time were measured with a linear variable differential transformer (LVDT). The load increments were typically doubled with each loading phase, and deformation (consolidation) under each load increment was considered complete when the deformations versus time plot was analyzed using the log-time method.

The vertical load on the sample and number of loading increments varied slightly among the samples.

2.5.4.2.3.13 Deleted

2.5.4.2.3.14 Deleted

2.5.4.2.4 Material Properties

2.5.4.2.4.1 Geotechnical Model

A geotechnical model of the site was developed in the Cherokee Nuclear Station Preliminary Safety Analysis Report document prepared in the early to mid-1970s. This model has been adopted for use at the Lee Nuclear Station Site to maintain consistency with the work completed during Cherokee Nuclear Station construction activities. The conditions at the site are amenable to being classified into a geotechnical model that consists of existing engineered fill soils, alluvial soils, residual soils, saprolite, partially weathered rock (PWR), existing concrete, and rock. Also added to the model is the granular backfill material placed around the nuclear islands.

2.5.4.2.4.1.1 Pre-existing Engineered Fill Soils

The pre-existing site fill soils at the time of the Lee Nuclear Station geotechnical exploration in 2006-2007 were placed during the site grading activities for the Cherokee Nuclear Station project beginning in the mid 1970's and continuing until abandonment of the Cherokee Nuclear Station project in 1983. The fill soils characterized in this Subsection were constructed as Group 1 or Group 2 fills as defined in the Cherokee Nuclear Station Preliminary Safety Analysis Report. These fill soils were derived from the materials excavated from cut areas, and therefore their composition is made of the same soil types (predominantly ML and SM and relatively minor amounts of MH and CL) as the residual soil, saprolite, and partially weathered rock zones. None of these engineered fill soils will be adjacent to the walls of the nuclear islands or beneath the structures adjacent to the nuclear islands.

2.5.4.2.4.1.2 Alluvial Soils

In drainage channels and along the Broad River, residual soils washed from higher ground have settled to form alluvial deposits. During the Cherokee Nuclear Station construction, these alluvial soils were removed from beneath former safety-related man-made fills and structures such as the dam that now serves as the Lee Nuclear Station Make-Up Pond B Dam. Significant amounts of alluvial soil are not expected to remain anywhere within the areas explored for Lee Nuclear Station. Minor amounts of alluvial soil were encountered in borings B-1028, B-1052, MW-1205, and MW-1209 of the Lee Nuclear Station Site exploration.

2.5.4.2.4.1.3 Residual Soils

The residual soils are the near-surface zone of the pre-construction undisturbed profile. The residual soils have undergone relatively complete weathering, and lack the relict features found in the saprolite zone. These are called the "B-horizon" soils in the Cherokee Nuclear Station Preliminary Safety Analysis Report. Most of the "B-horizon" soils at the site were utilized in the central core area of the former Cherokee Nuclear Station Nuclear Service Water Dam, now known as Lee Nuclear Station Make-Up Pond B Dam, so relatively minor amounts were encountered in the borings for the Lee Nuclear Station.

2.5.4.2.4.1.4 Saprolite Soils

Saprolite soils are the natural soils of the undisturbed weathering profile that retain relict features from the parent bedrock from which they were formed. The borings for Lee Nuclear Station found soil types consistent with data in the Cherokee Nuclear Station Preliminary Safety Analysis Report which indicates these saprolitic soils are comprised of about 2/3 of the samples being ML (silt of low plasticity), and about 1/3 being SM (silty sand).

2.5.4.2.4.1.5 Partially Weathered Rock (PWR)

Partially Weathered Rock, termed PWR, is a transitional weathering zone between the saprolite and the less weathered bedrock. Texturally, the partially

weathered rock materials are similar to the SM and ML soils in the overlying saprolite zone, but include more pieces of less weathered rock. As a practical matter and consistent with the Cherokee Nuclear Station Preliminary Safety Analysis Report, the PWR zone is usually associated with SPT values of 100 blows per foot or higher.

2.5.4.2.4.1.6 Pre-existing Concrete

Pre-existing reinforced concrete mat foundations and unreinforced fill concrete are present from the Cherokee Nuclear Station construction. The fill concrete was used to extend from the bottom of the Cherokee Nuclear Station foundation mats down to the rock foundation support. At the time of the Lee Nuclear Station exploration program in 2006 and 2007, the pre-existing concrete was encountered in the Cherokee Nuclear Station Unit 1 construction area. The Cherokee Nuclear Station concrete remains under portions of the Lee Nuclear Station Unit 1 structure, as described in Subsection 2.5.4.5.

2.5.4.2.4.1.7 Rock

The parent bedrock materials underlie the residual soil, saprolite, and partially weathered rock throughout the site. The Cherokee Nuclear Station Preliminary Safety Analysis Report describes the rock as felsic and mafic gneiss, a metamorphic crystalline rock that is often closely banded and jointed. The Lee Nuclear Station Site exploration identifies rock as being made up of predominant rock types as described in Subsection 2.5.4.1.2.2. The rock is fine to medium grained. Moderately dipping joints are healed with quartz and very thinly healed joints with calcite and epidote. The rock surface is uneven due to differential a depth to which weathering has advanced into the mass. The rock forms the foundation support for the Unit 1 and Unit 2 nuclear islands at the Lee Nuclear Station.

2.5.4.2.4.1.8 Granular Backfill

No safety-related structures will be placed on granular fill. Granular fill composed of select materials from a quarry rock crushing product will be placed and compacted around the walls of the nuclear islands and extending outward to form the support for the structures adjacent to the nuclear islands. These select granular materials will be compacted to a minimum relative compaction of 96 percent of the modified Proctor (ASTM D 1557-02) maximum dry density.

2.5.4.2.4.2 Static Properties of Geotechnical Materials

Static geotechnical properties were compiled for the materials which comprise the Geotechnical Model, as described in Subsection 2.5.4.2.4.1. Material properties for alluvial soils are not included due to the limited presence of these materials at the site.

Static geotechnical properties for the soil materials described in the Geotechnical Model are provided in Table 2.5.4-211. Table 2.5.4-211 lists soil properties used to support non-safety related structures as no safety related structures are

supported on soil. No table values are listed for remolded fill soil samples as these materials are not used in the vicinity of the nuclear islands or beneath the structures adjacent to the nuclear islands. Only granular backfill materials are placed around the nuclear islands. The properties of the granular materials are used as input for calculation of the static and dynamic lateral earth pressure against the nuclear island walls. Corrosion test results (pH, resistivity, chlorides, and sulfates) for soil fill are provided in Table 2.5.4-212. Static geotechnical properties for the granular backfill materials are provided in Table 2.5.4-211. Table values listed for granular backfill materials are for typical granular materials and will be verified by laboratory testing when the source of and specific materials to be used are known, as outlined in Table 2.5.4-222. Static geotechnical properties for the rock materials described in the Geotechnical Model are provided in Table 2.5.4-213. The properties reported in these tables are average properties based on the laboratory results from samples obtained during the Lee Nuclear Station Site exploration in 2006 and 2007. Standard deviations are reported when the amount of data was sufficient to allow calculation of this value. Data from the Cherokee Nuclear Station Preliminary Safety Analysis Report was used, only where indicated in the table, to supplement the information obtained during the Lee Nuclear Station Site exploration for soils where limited data was available, such as the partially weathered rock.

Portions of the Cherokee Nuclear Station concrete that will remain under Lee Nuclear Station Unit 1 are described in Subsection 2.5.4.5. The existing Cherokee Nuclear Station concrete meets the strength requirements for concrete in DCD Subsection 2.5.4.1.3.

Dynamic geotechnical properties for the soil, granular fill, and rock materials described in the Geotechnical Model are described in Subsection 2.5.4.7.

2.5.4.3 Foundation Interfaces

WLS COL 2.5-1 This Subsection provides graphically the relationship between site exploration, subsurface materials, and the foundations of seismic Category I facilities. The information was developed on the basis of field explorations performed at the Lee Nuclear Station Units 1 and 2 and on laboratory tests performed on soil and rock samples obtained during the field exploration program which took place in 2006-2007. Field investigations performed at the Cherokee Nuclear Station in the late 1970s and early 1980s (Reference 201), shown on Figure 2.5.4-209, were also considered in this assessment, as these historic exploration points are co-located within the Lee Nuclear Station facility footprints.

The Lee Nuclear Station Site investigation program was conducted in 2006 and 2007. Geotechnical data collected during the field and laboratory exploration program were analyzed and evaluated. The analysis included preparing tables and figures that represent interpretations of the subsurface geotechnical conditions beneath and adjacent to safety-related structures.

2.5.4.3.1 Power Block Exploration

A comprehensive exploration program of surface geophysics, in situ testing, and subsurface drilling and sampling was conducted in 2006-2007 as shown in a site view on Figure 2.5.4-208 and Power Block and Adjacent Areas on Figure 2.5.4-209. These figures show the principal and secondary exploration borings and other field explorations performed. The historic boring locations on this figure are identified to distinguish them from the 2006-2007 boring and test locations. The locations of groundwater monitoring wells constructed and packer test performed as part of the Lee Nuclear Station exploration are shown on Figure 2.5.4-210. Figure 2.5.4-211 shows the location of SASW survey lines at the Lee Nuclear Station Site. The location of CPT tests performed as part of the Lee Nuclear Station exploration is shown on Figure 2.5.4-212. The location of test pits and trenches excavated as part of the Lee Nuclear Station exploration is shown on Figure 2.5.4-213. The Goodman Jack and borehole pressuremeter test locations performed as part of the Lee Nuclear Station exploration are shown on Figure 2.5.4-214. The borehole geophysical test locations performed as part of the Lee Nuclear Station exploration are shown on Figure 2.5.4-215. The petrographic test locations performed as part of the Lee Nuclear Station exploration are shown on Figure 2.5.4-216.

2.5.4.3.2 Surrounding and Adjacent Structures Exploration

Exploration of facilities beyond the power block was conducted to support an understanding of the distribution of geological features (e.g. rock, soil, extent of weathering, etc.) at the site and to characterize site condition and material properties of non-safety related site features such as cooling towers, switchyard, pipelines, and general facilities. These explorations included profile borings for characterization and siting of monitoring wells, cooling towers, switchyard, pipelines, and general facilities, and confirm previous explorations. Several test pits and trenches were also excavated. The exploration locations are shown on Figure 2.5.4-208.

2.5.4.3.3 Geotechnical Data Logs and Records

WLS COL 2.5-2
WLS COL 2.5-3

Contemporary and historic geotechnical data sets were used to compile the geotechnical figures contained in this Subsection. The Lee Nuclear Station field exploration records are presented in Appendix 2AA. The Cherokee Nuclear Station field exploration records are presented in Appendix 2BB.

WLS COL 2.5-1

As-built survey data and topographic surveys were used to prepare maps of the final geotechnical data exploration program as presented in Figures 2.5.4-208 and 2.5.4-209. The locations of exploratory borings, monitoring wells, test pits, and surface geophysical lines were recorded in digital format. These data were

uploaded into a geographic information system (GIS). The GIS was used to prepare plan view maps and profile drawings that were used to develop geologic interpretations.

Geotechnical borings, surface geophysical testing, CPT soundings, borehole in situ testing, including Goodman Jack and pressuremeter testing, and borehole geophysical testing, including P-S Suspension logging, downhole velocity, televiewer surveys were integrated to interpret the geologic and geotechnical properties presented in the geotechnical profiles, as discussed below in Subsection 2.5.4.3.5.

In addition, in situ and laboratory test results of rock strength and petrographic test locations are provided on the borehole summary sheets described below.

2.5.4.3.4 Borehole Summaries

The compilation of the geologic and geotechnical data collected from the field program is essential to interpret the subsurface conditions. Data including lithology, laboratory strength, borehole and surface geophysical results, in situ test results, Standard Penetration Test (SPT), Rock Quality Designation (RQD), and percent recovery were used to compile borehole summaries of power block and other important borings. An explanatory figure showing these data sources is included as Figure 2.5.4-218, followed by 14 Borehole Summaries, Figures 2.5.4-219 through Figure 2.5.4-232. These summaries convey the integrated field, laboratory, and geologic framework essential for creating profiles across the nuclear islands as discussed in Subsection 2.5.4.3.5.

2.5.4.3.5 Geotechnical Profiles

WLS COL 2.5-1
WLS COL 2.5-5

The borehole summaries are evaluated in the geologic context described in more detail in Subsections 2.5.1 and 2.5.4.1 to construct geotechnical profiles. Eight geologic cross sections intersecting the Lee Nuclear Station Unit 1 and 2 nuclear islands and adjacent areas are presented; the locations of these cross sections are shown on Figure 2.5.4-208. Cross Sections A-A', B-B', C-C', E-E', F-F', R-R', U-U', and V-V' are shown on Figures 2.5.4-233 through 2.5.4-240.

Key cross sections in this evaluation include the following:

- Figure 2.5.4-234, Cross Section B-B', west-east profile through Unit 1 and Unit 2 centerline
- Figure 2.5.4-239, Cross Section U-U', west-east profile through the north end of the Unit 1 nuclear island
- Figure 2.5.4-240, Cross Section V-V', north-south profile along the west wall of the Unit 1 nuclear island

- Figure 2.5.4-236, Cross Section E-E', north-south profile through the Unit 1 centerline
- Figure 2.5.4-237, Cross Section F-F', north-south profile through the Unit 2 centerline

These profiles depict former and existing ground surface, plant and yard grade representations including nuclear island foundation and other important power block foundation features and relevant boring and geophysical test data.

A detailed description of the site geology is presented in Subsections 2.5.1 and 2.5.4.1. Material properties are discussed in Subsection 2.5.4.2. Groundwater is discussed in Subsection 2.5.4.6. Continuous rock is discussed in Subsection 2.5.4.7.3.

2.5.4.3.6 Extent of Granular Fill

WLS COL 2.5-6
WLS COL 2.5-7

To indicate the extent of the granular fill to be placed around the nuclear islands and extending out to form the supporting materials for the adjacent buildings (radwaste, annex, and turbine buildings), eight geologic cross sections intersecting the Lee Nuclear Station Unit 1 and 2 nuclear islands and adjacent areas are presented. The locations of these cross sections are shown on Figure 2.5.4-208. Cross Sections B-B', C-C', E-E', F-F', U-U', V-V', Y-Y', and Z-Z' are shown on Figures 2.5.4-245, 2.5.4-246, and 2.5.4-260 through 2.5.4-265. Six of these eight geologic cross sections correspond to the geotechnical profiles presented in Subsection 2.5.4.3.5.

Geologic cross sections depicting the granular fill are the following:

- Figure 2.5.4-260, Planned Excavation Profile, Cross Section B-B', west-east profile through Unit 1 and Unit 2 centerline
- Figure 2.5.4-261, Planned Excavation Profile, Cross Section C-C', west-east profile through the south end of Units 1 and 2 turbine building
- Figure 2.5.4-245, Planned Excavation Profile, Cross Section U-U', west-east profile through the north end of the Unit 1 nuclear island
- Figure 2.5.4-246, Planned Excavation Profile, Cross Section V-V', north-south profile along the west wall of the Unit 1 nuclear island
- Figure 2.5.4-262, Planned Excavation Profile, Cross Section E-E', north-south profile through the Unit 1 centerline
- Figure 2.5.4-263, Planned Excavation Profile, Cross Section F-F', north-south profile through the Unit 2 centerline

- Figure 2.5.4-264, Planned Excavation Profile, Cross Section Y-Y', west-east profile through the north end of the Unit 1 nuclear island
- Figure 2.5.4-265, Planned Excavation Profile, Cross Section Z-Z', west-east profile through the south end of the Unit 1 nuclear island

These profiles depict the original and existing ground surface, extent of granular fill, plant and yard grade representations, nuclear island foundation and other important power block foundation features, and the location of borings and geophysical tests in the vicinity of each profile. The granular fill depicted on these cross sections extends horizontally outward from the walls of the nuclear island a distance of 100 feet or 6 feet beyond the edge of the adjacent buildings (radwaste, annex, and turbine buildings), whichever is the greater distance.

2.5.4.4 Geophysical Surveys

WLS COL 2.5-6 Surface and borehole geophysical surveys were conducted on the Lee Nuclear Station Site in 2006-2007 to characterize the subsurface conditions of the soil and bedrock including dynamic properties and geologic features. Information obtained from these surveys was utilized in the analysis of and discussions pertaining to the site geology in Subsection 2.5.1.2, surface faulting potential presented in Subsection 2.5.3, and characterization of geologic features as presented in Subsection 2.5.4.1.

The investigations were conducted using methods described in Subsection 4.4, Geophysical Investigations, of Regulatory Guide 1.132. Planning and exploration layout and data collection was coordinated by project engineering geologists and geotechnical engineers. All geophysical survey activities were performed in accordance with approved procedures.

Four geophysical survey methods were performed in 2006-2007 at the Lee Nuclear Station Site:

- Spectral Analysis of Surface Waves (SASW) performed by the University of Texas – Austin;
- Seismic cone wave velocity measurements in overburden soils by Gregg In Situ Inc.;
- Suspension and downhole velocity logging tests by GEOVision; and
- Televiewer (acoustic and optical) boring wall logging by GEOVision.

2.5.4.4.1 Spectral Analysis of Surface Waves (SASW) Surveys

SASW surveys were conducted at 15 locations on the Lee Nuclear Station Site, as discussed in Subsection 2.5.4.2.1.3. The goal of conducting these tests was to characterize the shear wave velocity of native soil, undisturbed existing fill, and rock underlying the Lee Nuclear Station Site. The SASW surveys of the Lee Nuclear Station Site were conducted by Dr. K.H. Stokoe II of the Geotechnical Engineering Center at the University of Texas at Austin under the supervision of project personnel. Survey depths ranged from tens of feet to approximately 100 feet below ground surface, depending on site survey conditions, material attenuation properties, and the length of survey line. Collection and processing of SASW survey data was performed pursuant to a proprietary protocol authored by Dr. Stokoe.

2.5.4.4.1.1 Survey Method

The SASW surveys determined shear wave (Vs) by measuring dispersion of surface seismic waves as they propagated through subsurface materials. Rayleigh-type surface waves were generated using truck-mounted vibroseis equipment and motions perpendicular to the ground surface were measured at points arranged on a single radial path from the source. Each array consisted of a source and three receivers with variable spacing dependent on a particular survey goal and location. Testing was conducted using Mark Products Model L-4C vertical velocity transducers with natural frequencies of 1 Hz. Data were recorded using a four-channel Agilent 35670A Dynamic Signal Analyzer. Field data were transferred to a desktop computer for analysis using WinSASW software. Data were converted into composite dispersion curves and iterative forward modeling was used to create layer stiffness models with synthetic dispersion curves that most closely matched the experimental curves. The SASW survey locations conducted at Lee Nuclear Station Site are shown on Figure 2.5.4-211. The SASW results are tabulated in Table 2.5.4-214.

2.5.4.4.1.2 Survey Results

Taking into account that the SASW technique yields average Vs values from across the length of each survey line, results of the SASW surveys compare very favorably when compared to adjacent borehole P-S suspension and downhole velocity logs. The results of SASW and borehole Vs measurements are presented on the Boring Summary Sheets, Figures 2.5.4-219 to 2.5.4-232.

2.5.4.4.2 Seismic Cone Penetration Tests (SCPT)

CPT seismic shear wave velocity tests were performed at nine CPT locations, as discussed in Subsection 2.5.4.2.1.4. The SCPT test locations are shown on Figure 2.5.4-212. Each of the CPT seismic shear wave velocity tests was performed in residuum, saprolite, or pre-existing fill soils above bedrock.

2.5.4.4.2.1 Seismic CPT Methods

A modified CPT cone containing a built-in seismometer was used to measure compression and shear wave velocities in addition to the standard piezocone parameters. Seismic tests were usually performed at 3-foot (1-meter) intervals. Shear waves (S-waves) were generated by a sledgehammer striking a traction beam coupled to the ground surface by a hydraulic cylinder under the CPT rig. The sledgehammer used also acted as a trigger, initiating the recording of the seismic wave trace. Before measurements were taken, the rods were decoupled from the CPT rig to prevent energy transmission down the rods.

Geophones in the body of the piezocone measured the arriving waves generated at the ground surface. Any waves received by the geophones on the cone penetrometer were transmitted via a cable back up to the truck to be displayed on an oscilloscope and stored on a computer. On site software then used wave amplitude versus time to calculate the point wave velocity. At least two waves were recorded for each test depth so the operator could check consistency of the waveforms.

The shear wave velocity provides information about small-strain stiffness. From point shear wave velocity and the mass density of a soil layer, the dynamic shear modulus of the soil was calculated at the specific point location. The dynamic shear modulus is a key parameter for the analysis of soil behavior in response to dynamic loading such as from earthquakes.

The CPT seismic test results summarized in Table 2.5.4-215 indicate that the shear wave velocity of the overburden soils at the Lee Nuclear Station Site ranges from 616 to 2990 feet per second (fps).

2.5.4.4.3 Suspension and Downhole Velocity Logging

A total of 13 borehole velocity surveys were performed at the Lee Nuclear Station site. The borehole velocity surveys consisted of 13 P-S suspension logging tests with four companion downhole velocity tests. The surveys were performed within uncased and cased boreholes. Downhole surveys were performed in four boreholes with P-S suspension surveys as a means to compare and validate P-S suspension results. Comparison of downhole velocity measurements to the companion P-S suspension measurements indicated good correlation of velocity values. Table 2.5.4-216 provides a summary of the borehole geophysical testing performed. Figure 2.5.4-215 shows the locations of the borehole surveys. The objective of the suspension and downhole logging tests was to obtain shear wave (Vs) and compressional wave (Vp) velocity measurements as a function of depth within each borehole. The Vs velocity values were used to determine whether the unweathered rock met the hard rock requirements for the site response analyses and development of the GMRS as discussed in Subsection 2.5.2. The seismic hazard model defines hard rock as having a minimum Vs of 9200 fps.

2.5.4.4.3.1 P-S Velocity Logging Methods

The suspension logging tests were performed using an OYO Model 170 Suspension Logging Recorder and Probe. In this OYO downhole configuration, the seismic source is mounted near the base of the probe, and a pair of receivers is mounted approximately 3 feet (0.91 meters) apart from one another, centered approximately 12 feet (3.7 meters) above the source. The source generates a Vp wave in the pore fluid near the base of the probe, which was converted to a Vs wave and separate Vp wave at the borehole wall. The shear wave travels up along the wall, and the resulting wave is measured by the receiver pair. The S-wave and P-wave velocities for the interval between the receivers were calculated based on the difference in wave arrival times.

2.5.4.4.3.2 Downhole Velocity Logging Methods

The downhole velocity measurements were performed using a Geostuff BHG-3, 3-component geophone ("probe"). The probe consists of a horizontal and vertical geophone mounted on a rotatable structure with a fluxgate compass sensor. This probe was lowered down the hole with the orientation of the geophone components held parallel to the axis of excitation at the surface. Seismic energy was produced by hitting a steel capped traction plank or a welded steel box bolted to the rock surface using a 20-pound sledgehammer. For Vs energy, the side of the steel plate was hit; for Vp wave energy, the top of the steel plate was hit.

The probe was lowered down the holes in 3.28-foot intervals and locked in place using an inflatable air bladder before each test was conducted. Multiple blows were used to stack the data and improve the signal-to-noise ratio. Signals from the probe were recorded using a Geometrics Strataview seismograph. The Vs and Vp wave velocity for the interval between the receivers was then calculated based on the difference in wave arrival times.

2.5.4.4.3.3 Velocity Logging Results

The travel-time data from the P-S suspension logging and the downhole tests were used to create velocity layer models. The resultant velocity layers are presented on the Lee Nuclear Station boring summary sheets Figures 2.5.4-218 to 2.5.4-232. The interpreted P-S Suspension and Downhole velocity layer models are presented in Tables 2.5.4-217 and 2.5.4-218, respectively.

2.5.4.4.4 Acoustic and Optical Televiewer Logging

Acoustic televiewer logging was conducted in thirteen boreholes and optical televiewer logging was conducted in nine boreholes on the Lee Nuclear Station Site. The goals of these tests included: (1) correction of soil, rock and geophysical log depths to true depths where needed, (2) acoustic imaging of the boring wall to identify fractures, and determine the dip and azimuth of these features, and (3) perform borehole deviation surveys. The fracture orientation data was used to estimate the Rock Mass Rating for the various layers and to evaluate observed discontinuity characteristics.

The acoustic and optic televiewer logging was collected using a High Resolution Acoustic Televiewer (HiRAT) manufactured by Robertson Geologging, Inc. that was lowered down the borings via connection to an armored conductor cable that also acted as a conduit for the data to travel to the Robertson Micrologger II at the surface. The probe is 7.58 feet long, 1.9 inches in diameter and is fitted with upper and lower four-band centralizers. The acoustic sensors produce images of the boring wall based on the amplitude and travel time of an ultrasonic beam reflected from the formation wall. The borings are kept filled with water during this testing because the contact between clear water and the rock formation provide a high contrast. The data were stored on hard disk for later processing.

2.5.4.5 Excavations and Backfill

WLS COL 2.5-5 The Lee Nuclear Station utilizes a combination of excavation slopes and temporary retaining structures to facilitate construction of below grade portions of the nuclear island. The excavation remaining from Cherokee Nuclear Station construction activities is utilized and enlarged or reconfigured, as needed, to support Lee Nuclear Station construction. Backfill is placed within the excavation against the below grade nuclear island walls to create the ground surface surrounding the nuclear island structure. The ground surface surrounding the nuclear island is at Elevation 589.5 feet which is 0.5 feet below the building floor slab elevation.

The seismic Category I structures consist of the Unit 1 and Unit 2 nuclear islands. Other structures within the power block are not seismic Category I structures and are not safety related. The location of the nuclear island structures is shown on Figures 2.5.4-201 and 2.5.4-208. The Lee Nuclear Station nuclear island is constructed with a building floor slab elevation of approximately 590 feet. Below grade portions of the nuclear island extend approximately 39.5 feet below building slab elevation, to Elevation 550.5 feet. Foundation materials, consisting of continuous rock or concrete, are located at this elevation or below for support of the nuclear island. Fill concrete is used in areas where continuous rock or Cherokee Nuclear Station concrete is below Elevation 550.5 feet to bring that surface up to the Lee Nuclear Station base of foundation elevation.

2.5.4.5.1 Sources and Quantities

WLS COL 2.5-6
WLS COL 2.5-7 The Lee Nuclear Station Site requires granular backfill material described in Subsection 2.5.4.5.3.5 to fill the area around the below-grade nuclear island walls out to the extents shown on Figures 2.5.4-245 and 2.5.4-246, and 2.5.4-260 through 2.5.4-265. This backfill also forms the yard elevation and supporting materials for the power block structures outside but adjacent to the nuclear island.

The source for the granular fill is not identified. At a rock quarry, material is crushed to form granular product consisting of a mixture of gravel, sand, and some fines. The granular fill material will likely be obtained from an off-site source such as an operating rock quarry. Imported granular fill intended to be placed adjacent to seismic Category I structures or beneath other important adjacent facilities will be verified as compatible with Lee Nuclear Station site response calculations.

2.5.4.5.2 Extent of Excavation

WLS COL 2.5-6
WLS COL 2.5-7

A large excavation was constructed during site preparation work for Cherokee Nuclear Station construction. This excavation is utilized as the initial excavation for the Lee Nuclear Station. Additional excavation for Lee Nuclear Station extends about 10 feet laterally into the fill and natural soil materials comprising the Cherokee Nuclear Station construction slope and removes softened, sloughed, or other loose soil and rock materials. This excavation extends sufficient distance into the slope to reach materials that are relatively undisturbed by erosion or shallow sloughing during the time the excavation remained open following Cherokee Nuclear Station construction.

In addition to the 10-foot slope trimming described above, additional excavation of the soil and partially weathered rock slope that formed the Cherokee Nuclear Station excavation limits is necessary to provide relatively uniform thickness of fill for support conditions beneath the Lee Nuclear Station power block structures adjacent to the nuclear island. Excavation to a reasonably uniform subgrade elevation is performed within the limits of the adjacent non safety-related power block structures and outside the structure limits to a point defined by a line extended at 0.5 horizontal to 1 vertical or flatter from the base edge of the structure foundations. For the nuclear island foundation, the 0.5 horizontal to 1 vertical or flatter line begins at a point located 6 feet or more horizontally from the perimeter of the nuclear island foundation limits. This geometry defines the foundation support zone for the nuclear island. These nuclear island area excavation limits, as estimated prior to construction of Lee Nuclear Station, are shown on Figure 2.5.4-243. Excavation to a uniform subgrade elevation for adjacent non-safety structures exposes fill concrete, rock, partially weathered rock, or saprolite.

Outside the Unit 1 and Unit 2 foundation subgrade excavation limits the construction excavation slope or backfill slope is constructed up to the ground surface elevation. The limit of this slope projected to the ground surface, as estimated prior to construction of Lee Nuclear Station, is shown on Figure 2.5.4-243. The construction excavation slope exists until backfill is placed to gain access to the nuclear island structure with construction cranes operating from yard level.

Soil excavation slopes for Lee Nuclear Station are constructed with a maximum slope of 1.5 horizontal to 1.0 vertical or flatter and a maximum height of 40 feet. Soil excavation slopes requiring heights greater than 40 feet are constructed using benches to maintain adequate safety factors for stability. Excavations

slopes are backfilled to yard grade during placement of fill materials around the below-grade nuclear island structures.

2.5.4.5.2.1 Unit 1 Excavation Conditions

Excavation to a uniform foundation subgrade elevation of approximately 540 to 545 feet was required for Lee Nuclear Station due to the depth of the pre-existing Cherokee Nuclear Station excavation and the elevation of the Cherokee Nuclear Station structural elements that remained beneath the Lee Nuclear Station foundations. Excavation within the foundation support zone of the nuclear island extends to pre-existing concrete, pre-existing fill concrete, or to continuous rock where no pre-existing concrete exists. Fill concrete is utilized to bring the subgrade elevation up to the nuclear island foundation elevation within the foundation support zone of the nuclear island for the Lee Nuclear Station.

Excavation to the foundation subgrade elevation includes removal of the Cherokee Nuclear Station reactor building superstructure and Cherokee Nuclear Station auxiliary building mat foundations within the nuclear island foundation support zone. The Cherokee Nuclear Station reactor building foundation mat is left in place. To avoid damage to the reactor building mat, 3 to 6 inches of the vertical walls may remain above the mat surface after the walls are removed. In areas where the Cherokee auxiliary building basemat is removed, the isolation joint surrounding the Cherokee Nuclear Station reactor building mat is also removed to reduce the discontinuity between reactor building basemat and new fill concrete. Removal of the Cherokee Nuclear Station foundation mats exposes underlying fill concrete or continuous rock. Additional excavation is performed beyond the Cherokee Nuclear Station concrete edges as needed to reach the continuous rock subgrade.

Construction procedures for Cherokee Nuclear Station required removal of soil and weathered rock materials prior to placement of foundation concrete and fill concrete. Cherokee Nuclear Station foundation concrete was placed on material described as continuous rock, or on fill concrete that was used as a leveling pad above continuous rock. This same procedure is followed for the Lee Nuclear Station. Therefore concrete placed during Cherokee Nuclear Station construction and Lee Nuclear Station construction are supported on the same quality rock materials.

The Cherokee Nuclear Station foundation mat for the reactor building and auxiliary building was underlain by a groundwater drainage system. When this drainage system is exposed by excavation for the Lee Nuclear Station nuclear island foundation it is sealed with fill concrete material as illustrated by Figures 2.5.4-244a through 2.5.4-244d. Exposure of this drainage system is most likely to occur at the perimeter of the Cherokee Nuclear Station reactor building mat and at the perimeter of the Lee Nuclear Station nuclear island foundation.

One area where Cherokee Nuclear Station concrete does not underlie the Lee Nuclear Station nuclear island foundation is at the northwest corner of the Lee Nuclear Station Unit 1 nuclear island. At this location the Lee Nuclear Station nuclear island structure extends beyond the limits of the Cherokee Nuclear Station

structure. Because this area is outside the limits of the Cherokee Nuclear Station structure, the area was not excavated down to continuous rock during Cherokee Nuclear Station construction. This area therefore remained underlain by naturally existing soil and weathered rock. Geotechnical borings drilled in 2006 and 2007 in this area, but west of the nuclear island footprint, revealed a deep weathered rock profile with low Rock Quality Designation values extending to as deep as approximately Elevation 448 feet. Under the limits of the nuclear island area the geotechnical borings encountered continuous rock at Elevation 529.5 feet or higher.

Excavation of soil and weathered rock materials is required to reach suitable foundation quality continuous rock material in this northwest corner area of Lee Nuclear Station Unit 1. A concept of the excavation required at the northwest corner of the Unit 1 nuclear island is shown on Figures 2.5.4-245, 2.4.5-246, and 2.5.4-264. The excavation at this location requires sloped excavation in the upper soil and partially weathered rock materials and a near vertical excavation in the weathered rock materials. Excavation support for the weathered rock in the form of rock bolts, or similar reinforcement, is used as needed to provide support for this material during construction. Excavation support also maintains the strength and density of the weathered rock material where it underlies power block structures adjacent to the Lee Nuclear Station Unit 1 nuclear island. Soil or other materials that may have been deposited on top of continuous rock or concrete materials in the time following the excavation and foundation preparation activities for Cherokee Nuclear Station Unit 1 are also removed.

2.5.4.5.2.2 Unit 2 Excavation Conditions

Excavation to a uniform foundation subgrade elevation of approximately 549.5 feet is possible for Lee Nuclear Station because the Cherokee Nuclear Station excavation in this area generally remained above this elevation.

During the site exploration for Lee Nuclear Station in 2006 and 2007, the base of the Cherokee Nuclear Station excavation generally consisted of exposed rock beneath the location of the Lee Nuclear Station Unit 2 nuclear island. In much of the Lee Nuclear Station Unit 2 nuclear island foundation area the elevation of the rock was higher than the Lee Nuclear Station foundation elevation. Excavation into soil, partially weathered rock, weathered or loose rock, and continuous rock is required to reach the Lee Nuclear Station Unit 2 nuclear island foundation elevation. These materials are excavated and removed down below the Unit 2 nuclear island foundation elevation. Below this elevation soil, partially weathered rock, and weathered or loose rock materials are excavated until continuous rock is reached.

Backfill material is required where the rock surface elevation is below the Lee Nuclear Station foundation elevation or where additional rock removal is required to reach continuous rock due to localized weathering conditions. One area where the rock surface was already below the Lee Nuclear Station Unit 2 nuclear island foundation elevation is the east side of the nuclear island near the boring location B-1014. Fill concrete is used in this and any other area to bring the bearing surface back up to the Unit 2 nuclear island foundation elevation.

2.5.4.5.3 Specifications and Control

2.5.4.5.3.1 Nuclear Island Foundation Materials

WLS COL 2.5-6
WLS COL 2.5-7

Properties of the nuclear island foundation materials are discussed in Subsection 2.5.4.2. This Subsection describes methods and procedures used for verification and quality control of the nuclear island foundation materials.

Quality control will verify foundation quality materials are reached prior to placement of fill materials. This applies to continuous rock as well as to fill concrete or structural concrete within the Lee Nuclear Station nuclear island foundation limits that remains from Cherokee Nuclear Station construction. The foundation quality rock and fill concrete provide very high safety margins against bearing capacity failure under both static and seismic loading of the nuclear island, and only nominal settlements occur. Quality Control testing requirements for continuous rock and remaining Cherokee Nuclear Station concrete foundation material is provided in Table 2.5.4-219. The procedure for verification of foundation conditions consists of geologic mapping of the final exposed excavation surface prior to placement of foundation concrete or fill concrete materials.

Geologic mapping of the final exposed excavation rock surface beneath both of the nuclear islands, and any required extension due to depth of suitable continuous rock material, is performed at a scale of 1 inch equals 10 feet. Geologic mapping is performed at a scale of 1 inch equals 5 feet for local areas where further detail is needed to document significant features. The geologic mapping program includes photographic documentation of the exposed surface and laboratory testing and documentation for significant features.

2.5.4.5.3.2 Fill Concrete beneath the Nuclear Island Foundation Limits

Quality control of backfill materials will be conducted during fill concrete placement below the nuclear island foundation areas of Lee Nuclear Station. Fill concrete mix designs are in accordance with ACI 318-02 (DCD Chapter 2 Reference 1). Field observation is provided to verify that the approved mixes are used and to obtain test specimens that are used to verify required compressive strengths. Test specimens are also prepared to verify that the average design shear wave velocity of 7500 ft/sec are obtained for compatibility with Lee Nuclear Station site response calculations. Quality control sampling and testing requirements for these materials are provided in Table 2.5.4-220.

Fill concrete to build up the nuclear island foundation support area is required in varying thicknesses beneath the nuclear island. This fill concrete is placed in layers, and lower layers are hardened by curing before the succeeding layers are placed. At Unit 1, fill concrete is placed on top of the Cherokee Nuclear Station Unit 1 reactor building basemat, or on Cherokee Nuclear Station fill concrete exposed by removal of the Cherokee Nuclear Station auxiliary building basemat.

The former reactor building for Cherokee Nuclear Station Unit 1 is completely removed down to the top of the basemat as described in Subsection 2.5.4.5.2.1.

The pits in the Cherokee Nuclear Station Unit 1 basemat, such as the pipe chases and sump pits, are backfilled with fill concrete level with the top of the basemat during Lee Nuclear Station Construction. The top of the reactor building basemat for Cherokee Nuclear Station Unit 1 is nominally level at an approximate elevation of 545 feet after removal of the structural components and filling the pits in the Cherokee Nuclear Station basemat. The resulting surface is then intentionally roughened approximately one-quarter inch using the guidance in ACI 349, Part 4 – Construction Requirements, Section 11.7.9 (Reference 209), which reads "when concrete is placed against previously hardened concrete, the interface for shear transfer shall be clean and free of laitance. If μ is assumed equal to 1.0, interface shall be roughened to a full amplitude approximately ¼ inch."

The roughening criterion described above is also applied to other hardened concrete layers on which additional fill concrete is placed. This includes the top layer of fill concrete against which the waterproofing membrane layer or the structural mat concrete is placed. Use of wet sandblasting, chipping hammers, or other similar methods are acceptable procedures for roughening the surface. The top of the concrete mass is considered roughened when about one-quarter inch of the surface had been removed to expose the aggregate in the concrete.

2.5.4.5.3.3 Foundation Materials Outside the Nuclear Island

Outside the limits of the nuclear island support zone, steps are used to determine the presence of suitable foundation materials prior to placement of granular backfill materials beneath the non safety-related structures. This applies to continuous rock, existing concrete remaining from Cherokee Nuclear Station construction, weathered rock, partially weathered rock, or saprolite that remains in place below the non safety-related power block structures adjacent to the nuclear island. Steps for verification of proper foundation conditions consist of:

- Removing loose soil, rock, and any organic materials.
- Determine if the base of excavation consists of saprolite having N_{60} values, equal to or greater than 15 blows per foot, measured at a depth of 3 feet below the base of the excavation. Partially weathered rock, weathered rock, or rock would also be suitable in these areas provided it meets or exceeds the minimum criteria stated for saprolite and any loose material or soft zones are removed.
- Fill any depressions or cavities in the surface of the foundation soil or rock with fill concrete or properly compacted granular fill materials. This forms a uniform surface grade for the placement of additional granular fill.
- Continue placing granular fill materials in layers according to the procedures described in Subsection 2.5.4.5.3.5.

2.5.4.5.3.4 Fill Concrete Outside the Nuclear Island Foundation Limits

Fill concrete mix design is approved in advance. Field observation verifies that the approved mixes are used and obtains test specimens that verify the required design parameters are reached. A quality control sampling and testing program is developed that verifies the fill concrete material properties are consistent with the design parameters.

2.5.4.5.3.5 Granular Backfill Outside the Nuclear Island

Outside the below grade nuclear island walls (Units 1 and 2), a granular backfill will be placed up to approximately the yard elevation or to the underside of the adjacent buildings. The backfill adjacent to the nuclear island walls and extending outward to form the foundation support of the adjacent buildings (radwaste, annex, and turbine buildings) will be an engineered granular backfill. Outside the limits of the granular fill, soil backfill will be used. This subsection describes the specifications and controls of granular fill materials. The soil backfill placed beyond the granular fill limits is non safety-related and the placement specifications will be developed as part of construction.

Static properties of typical granular backfill materials are discussed in Subsection 2.5.4.2. Dynamic properties of typical granular backfill materials are discussed in Subsection 2.5.4.7.

Quality control for granular backfill includes verification that the material was obtained from an approved source (e.g., an approved quarry). The maximum dry density and optimum moisture content are determined according to the modified Proctor (ASTM D 1557) method. For gradation and moisture content testing, the test samples are obtained after placing the material but before compaction. Measurement of in-place dry density of each lift after compaction is performed using the sand cone (ASTM D 1556) or rubber balloon (ASTM D 2167) method. The nuclear gauge (ASTM D 6938) method is used to augment (but not completely replace) the other methods.

A quality control sampling and testing program for the granular backfill inclusive of the items provided by Table 2.5.4-222 is implemented during construction of the granular backfill. This quality control sampling and testing program verifies that the granular backfill is constructed in accordance with the parameters described in this subsection. To ensure that the engineering properties of the backfill meet the values used to calculate the static and dynamic lateral earth pressures, and the values used to establish seismic requirements for the Category II structures (annex building and turbine building Bay 1), the backfill will be tested in the laboratory. Testing to be performed on granular backfill before construction begins is also provided by Table 2.5.4-222. Prior to constructing the backfill around the nuclear island structures, a “test fill” pad will be constructed on-site using the equipment and granular fill materials to be used in the backfill. Before the production backfill commences, an engineering report will exist that concludes that the equipment and methods used to construct the “test fill” are capable of producing acceptable and consistent results.

The non safety-related structures adjacent to the nuclear island (radwaste, annex, and turbine buildings) will be supported on the granular fill. The following criteria are required for granular backfill placed adjacent to the nuclear island walls and extending outward to form the supporting material for the adjacent structures:

- The granular fill is obtained from a quarry and will conform to SCDOT gradation limits (Reference 224, SCDOT, 2007).

- The material is from an approved source (e.g., a quarry) and meets the assigned gradation requirements after the material is hauled and placed (before compaction).

- The coarse particles (materials retained on and above the No. 4 sieve) have an abrasion loss no more than 40 percent when subjected to the Los Angeles Abrasion Test (ASTM C 131) and has an apparent specific gravity (ASTM C 127) that is greater than or equal to approximately 2.65.

- The material has a defined moisture-density relationship to allow a maximum dry density to be determined in accordance with ASTM D 1557 (modified Proctor) for compaction control.

- Care is taken to prevent segregation of the materials during handling and placement.

- To achieve the required degree of compaction, the moisture content is maintained at or near the optimum moisture content as determined by the modified Proctor (ASTM D 1557) laboratory compaction test.

- The lift thickness is appropriate for the type of compaction equipment, but generally does not exceed about 8 inches (compacted thickness) for mechanized equipment nor about 4 inches for hand-guided compactors. Lift thicknesses may vary from the above values depending on the capability of the equipment being used.

- Steel wheel tandem drum rollers weighing on the order of 10 tons are generally effective for compacting granular fill materials.

- Within confined areas, or within 5 feet of the nuclear island walls, hand-guided compactors are used to prevent excessive lateral pressures against the walls from the residual soil stress caused by heavy compactors. The compactors have sufficient weight and striking power to produce the same degree of compaction that is obtained on the other portions of the fill by the rolling equipment, as specified.

- The granular fill is compacted to a minimum of 96 percent of the maximum dry density determined in accordance with the modified Proctor test method (ASTM D 1557) with a moisture content that is not more than 2 percentage points above the optimum moisture content, nor less than the optimum. This relative compaction is selected to produce a granular fill

equivalent to a relative density of 80 percent (Reference 225), and thus highly resistant to liquefaction.

Lateral pressures applied against the below grade nuclear island walls are evaluated and discussed in Subsection 2.5.4.10.3. Evaluation and discussion of liquefaction issues related to the backfill materials is provided in Subsection 2.5.4.8.

2.5.4.5.4 Groundwater Control

WLS COL 2.5-8 Dewatering of the nuclear island areas was successfully performed on several occasions in the history of the site. Dewatering during Cherokee Nuclear Station construction was performed using a dewatering well system outside the excavated area combined with local sump areas and pumps within the excavated area. Dewatering of the nuclear island area during Lee Nuclear Station Site exploration activities in 2006-2007 was performed using a sump pit and pump system within the excavation. Existing low areas of the site acted as the sump pits and a series of pump systems were maintained to periodically pump accumulated water from these pits to the nearby Make-Up Pond B.

Dewatering during Lee Nuclear Station construction is performed using a series of dewatering wells located outside the existing excavation limits. Localized sump and pump systems are utilized to supplement the dewatering wells in areas of the site where water accumulates. This is the same combination of dewatering methods used for the Cherokee Nuclear Station construction.

The construction dewatering system maintains the groundwater elevation below the elevation of construction activities during foundation construction and during placement and compaction of engineered backfill materials outside the nuclear island. Following completion of engineered backfill placement and compaction activities, the groundwater is allowed to return to static levels.

Additional discussion of groundwater and site dewatering activities is provided in Subsection 2.5.4.6.

2.5.4.6 Groundwater Conditions

The nuclear island structure extends below grade to Elevation 550.5 feet. This elevation is below the long term static groundwater elevation. Construction dewatering is required during construction of the below grade nuclear island walls and placement of backfill materials. Dewatering beyond construction is not required as the foundation basemat and below grade walls are waterproofed during construction and designed for hydrostatic pressure.

2.5.4.6.1 Groundwater Occurrence

Groundwater at the location of the nuclear island is present as a result of infiltration of precipitation upgradient of the nuclear island. Groundwater flow occurs primarily in the fractured portions of the bedrock and in the relict fracturing in the weathered rock and saprolite material above the bedrock. Additional discussion regarding the occurrence and movement of groundwater at the Lee Nuclear Station Site is provided in Subsection 2.4.12.1.

Immediately following construction the groundwater elevation remains artificially depressed as a result of dewatering activities required to support construction. After construction of the nuclear island and the backfill surrounding the nuclear island is placed, dewatering activities cease and the groundwater is allowed to return to static levels. The long term groundwater elevation at the Unit 1 and Unit 2 nuclear island structures is expected to fluctuate over time between Elevation 584 feet and 574 feet. The upper end of this groundwater elevation range is below the design groundwater elevation of 588 feet (standard plant Elevation 98 feet) used in the DCD Table 2-1. Additional discussion of groundwater elevations and fluctuations at the site is provided in Subsection 2.4.12.

2.5.4.6.2 Permeability Testing

Field and laboratory permeability testing was initially performed at the site during the Cherokee Nuclear Plant Site exploration. Additional testing including in situ permeability from packer tests and slug tests and laboratory hydraulic conductivity is performed during the Lee Nuclear Station Site exploration. Results of in situ permeability testing performed at the site are presented in Subsection 2.4.12.2.4. Results of laboratory permeability testing performed on remolded samples obtained from Lee Nuclear Station borrow areas are discussed in Subsection 2.5.4.2.

2.5.4.6.3 Construction Dewatering

Dewatering during construction is accomplished by a combination of pumping from sumps within the construction excavation and groundwater pumping wells located outside the construction excavation limits. Experience during Cherokee Nuclear Station construction and Lee Nuclear Station Site exploration indicated the foundation excavation area could be dewatered using internal sumps only. However, construction experience during Cherokee Nuclear Station suggested that a combination of external dewatering wells and internal sumps was more practical for construction activities.

Open pumping locations inside the excavation are established where needed based on observed conditions. The open pumping locations are operated while the backfill is being placed by incrementally extending suitable diameter casing pipe vertically above the pumping location to provide for the pump and discharge lines. A granular filter is placed on the excavation floor around the casing pipe to prevent erosion of the backfill into the open pumping location. After the backfill is completed, the pumping from the wells and open pumping locations ceases.

The location of casing for the open pumping locations is selected to avoid creating a “hard spot” affecting foundation support for the structures supported on the backfill adjacent to the nuclear islands.

The casing for the open pumping locations are left in place and backfilled with concrete or cement grout having a compressive strength of at least 2,500 psi. Following the completion of construction activities, the pumping wells to be abandoned are grouted as required by South Carolina Department of Health & Environmental Control (SCDHEC) regulations.

2.5.4.6.4 Groundwater Impacts on Foundation Stability

WLS COL 2.5-8 A history of groundwater elevation measurements at the Lee Nuclear Station Site is provided in Subsection 2.4.12. Groundwater measurements prior to construction of Lee Nuclear Station were influenced by site dewatering activities. Monitoring of groundwater elevations following cessation of site dewatering to confirm long term site groundwater elevations is not needed because the design groundwater level per the DCD (elevation 588-feet) exceeds the upper bound of the expected groundwater elevation range (elevation 584-feet) (see Table 2.0-201).

The Lee Nuclear Station Unit 1 and Unit 2 nuclear island foundations are supported on continuous crystalline rock or on fill concrete supported on the continuous rock. Rock materials are described in Subsections 2.5.1.2 and 2.5.4.1. The continuous crystalline rock and concrete materials below the nuclear island foundation are not susceptible to softening or solution due to long term groundwater movements at the site. These materials are also not susceptible to piping or disturbance from groundwater movement.

Groundwater conditions required to facilitate placement and compaction of soil backfill adjacent to the nuclear island structures are discussed in Subsections 2.5.4.5.4 and 2.5.4.6.3. The effects of groundwater related to lateral pressures on the below grade nuclear island walls are discussed in Subsection 2.5.4.10.3.

2.5.4.7 Response of Soil, Granular Fill, and Rock to Dynamic Loading

WLS COL 2.5-6 This subsection provides a description of the response of soil, granular fill, and rock to dynamic loading including the following:

- Investigations of the effects of historic earthquakes on soil and rock such as paleoliquefaction (Subsection 2.5.4.7.1).

- Compressional and shear (P and S) wave velocity profiles from surface or borehole geophysical surveys, including data and interpretation (Subsection 2.5.4.7.2).

- Foundation conditions and uniformity (Subsection 2.5.4.7.4).

- Presentation of dynamic profiles (Subsection 2.5.4.7.5).

The dynamic properties for the site (seismic wave velocity, shear modulus, and damping) were developed from extensive field measurements of rock. These data are compiled and statistically analyzed to develop a suite of dynamic velocity profiles to evaluate epistemic variability (uncertainty in the mean) in rock properties for general classification of the site (e.g., hard rock, DCD Subsection 2.5.4.5), develop the site GMRS (Subsection 2.5.2.6) and the Lee Nuclear Station Unit 1 FIRS (Subsection 2.5.2.7), and for comparison to the Certified Seismic Design Response Spectra (CSDRS) as presented in DCD Subsection 2.5.2.1. The GMRS and Unit 1 FIRS analysis, and comparison to the CSDRS are described in Subsections 2.5.2.6 and 2.5.2.7, and Section 3.7, respectively.

Granular backfill material obtained from an off-site source will be placed adjacent to the nuclear islands and beneath adjacent structures. Samples of this granular backfill material will be laboratory tested to determine its dynamic properties once the off-site source has been identified. Dynamic properties, modulus, Poisson's ratio, Vp and Vs wave velocities developed for granular fill are estimates based on Menq (2003) (Reference 223). The lower range and upper range of the shear modulus values (Gmax x 1.5 and Gmax / 1.5) are considered for analysis (ASCE 4-98) (Reference 220).

2.5.4.7.1 Prior Earthquake Effects and Geologic Stability

As discussed in Subsections 2.5.1 and 2.5.3, no active or potentially active faults or seismic deformation zones occur at the Lee Nuclear Station. Geologic mapping and subsurface explorations discussed in Subsection 2.5.4.1, and presented in the Cherokee Nuclear Station PSAR (Reference 201), confirm that rock and soil materials at Lee Nuclear Station Units 1 and 2 nuclear island structures have not experienced seismically-induced ground failure (e.g., slope failure, liquefaction, lurching, subsidence) from historic or paleoearthquakes. The Lee Nuclear Station site investigation included geologic mapping of exposed rock surfaces within the existing Cherokee Nuclear Station excavation, and review of detailed historic construction records that include foundation level excavation mapping and rock structure zone report assessments developed during construction of the Cherokee Nuclear Station.

As described in Subsection 2.5.4.1, bedrock underlying the Lee Nuclear Station Units 1 and 2 nuclear island structures is Middle Proterozoic to Permian (1,100 to 265 Ma) meta-granodiorite to meta-quartz diorite intruded by mafic dikes. These dense rock units are competent and not vulnerable to liquefaction or earthquake-induced ground failure. Continuity of bedrock below, between, and adjacent to the Lee Nuclear Station Units 1 and 2 nuclear islands is confirmed in the subsurface

by a dense network of continuously-logged vertical and inclined rock core borings (to a maximum depth of 255 feet) as shown in Figures 2.5.4-233 to 2.5.4-240.

Surficial geologic materials consist predominantly of medium dense to dense silty sand (SM) residual soils and saprolite developed over the igneous and metamorphic bedrock, and typically ranging in thickness between about 15 to 50 feet beyond the perimeter of the existing Cherokee Nuclear Station excavation. During construction of the Cherokee Nuclear Station unconsolidated materials were stripped off the bedrock in the former Units 1 and 2 and portions of Unit 3 excavations. Exposed non-weathered bedrock surfaces within the Cherokee Nuclear Station Units 2 and 3 excavations were evaluated during the Lee Nuclear Station investigation.

The maximum groundwater elevation is estimated to be at 579±5 ft msl and is described in Subsection 2.5.4.6.

2.5.4.7.2 Field Dynamic Measurements

The following techniques were used to measure field dynamic properties in 2006-2007:

- Borehole P-S seismic velocity suspension logging surveys in 13 borings ranging in depth between about 95 to 255 feet and including rock and soil;
- Borehole downhole seismic velocity surveys in four borings (boring B-1000, B-1011, B-1024, and B-1037A) ranging in depth between about 84 to 215 feet that also were surveyed with P-S suspension logging for independent comparison of velocities measured in rock and soil;
- SASW surveys consisting of 15 linear arrays ranging in length from about 30 to 300 feet and including measurements in rock and soil;
- Seismic CPT seismic velocity surveys made in ten soundings ranging in depth between 32 to 84 feet and include measurements in soil.

Borehole P-S suspension log seismic velocity surveys were performed in the nuclear island footprint areas for both Lee Nuclear Station Unit 1 and 2, at the northwest corner of Unit 1, and between the two plant footprints, as shown on Figure 2.5.4-215. The distribution of velocity measurements allowed confirmation of uniform seismic response under the Lee Nuclear Station nuclear island structures, evaluation of the local lower velocities at the Lee Nuclear Station Unit 1 northwest corner, and also within selected existing engineered fills. Each individual borehole velocity profile was evaluated and compared against the stratigraphic logging and laboratory test data of borehole samples to correlate velocities with rock type and structure (e.g., comparison of host and dike rock velocity) by elevation and corresponding depth below ground surface. After each individual borehole velocity data set was evaluated, borehole profiles were grouped based on site-specific location and were compiled using a common reference point (elevation or depth below ground surface).

Four downhole seismic surveys were completed in boreholes that also were surveyed using P-S Suspension logging methods to provide an independent verification of rock velocity. The two methods produced velocity profiles that are very similar, as shown in Figure 2.5.4-219, Figure 2.5.4-222, Figure 2.5.4-226, and Figure 2.5.4-227. Data from both borehole survey techniques were integrated for development of the site velocity profiles. The comparative P-S suspension and downhole methods show quite consistent Vs values in the continuous rock throughout the 255 foot maximum velocity survey depth range with most borehole-average shear wave velocities generally centered at about 9,500 to 10,000 feet per second indicating uniform hard rock conditions. The P-S and downhole surveys show a good match, providing an independent check of the accuracy of measured velocities. The P-S velocity profiles show discrete velocity "spikes" or zones that range from about 1-foot to several tens of feet thick that are not observed by the "averaging" method inherent in the downhole surveys. These velocity differences are attributed to differing sample measurement intervals and methods between P-S suspension and downhole techniques. Additionally, the P-S velocity spikes may also correlate to variations in rock type, structure (e.g., jointing intensity), and intrusional dikes, but in other cases appear to represent limited randomness in velocity or possible survey-induced fluctuations, as measurement intervals using the P-S method are more closely spaced (3.3-foot intervals) than the downhole method (10-foot intervals). Even though the profiles are jagged with these localized vertical variations, the ranges in velocity fall within a tight range for the composite of all surveys.

A third geophysical method, Spectral Analysis of Surface Waves (SASW) described in Subsection 2.5.4.4 was performed in the Lee Nuclear Station Unit 2 footprint area in the floor of the excavation and in existing fill materials located in both Unit 1 and Unit 2 Cooling Tower Pads. The SASW is a surface method, and penetration into the hard bedrock exposed in the Cherokee Nuclear Station excavation floor was limited using the attempted wave generation sources. Therefore, a complete velocity profile for comparison against the borehole surveys was not possible. However, the shear wave velocities measured at the rock surface in the excavation floor by the SASW technique generally agree with the borehole survey measurements as shown on Figure 2.5.4-224 and Figure 2.5.4-225.

A fourth geophysical method, Seismic Cone Penetrometer Test (SCPT) surveys, was performed in soil.

2.5.4.7.3 Deleted

2.5.4.7.4 Foundation Conditions and Uniformity

Figure 2.5.4-241 shows the Lee Nuclear Station Units 1 and 2 footprints superimposed on a contour map showing the surface of continuous rock (rock defined with a minimum RQD of 65 percent). The contours illustrated on this figure represent the top of rock surface, defined as continuous rock with a minimum RQD of 65 percent, developed using borehole data. Figure 2.5.4-241 also shows the extent of the partially constructed Cherokee Nuclear Station Unit 1 structures

and the position of the Lee Nuclear Station Units 1 and 2 power block structures relative to the Cherokee Nuclear Station excavation.

2.5.4.7.4.1 Lee Nuclear Station, Unit 1 Nuclear Island

The foundation rock consists primarily of slightly weathered to fresh meta-granodiorite and meta-quartz diorite that exhibits high average seismic wave velocity (e.g., typical shear wave velocity range of about 9,000 to 10,000 feet per second). Northeast-trending meta-diorite dikes are present in the meta-granodiorite and meta-quartz diorite host rock. Rock in these dikes is similar in strength to the host rock, and contact margins typically are tight or minor local narrow altered/weathered zones. Borehole P-S and downhole seismic velocities measured in the intrusive dikes are similar to the host rock, and the dikes do not form significant zones of varied velocity. Therefore these intrusive bodies do not significantly influence the dynamic response of the rock mass. Relative variability in rock properties between the host rocks and dikes/intrusions are not deemed significant as their high strength and moduli are well above requirements for foundation bearing capacity, settlement, etc. and therefore do not represent a potential for differential site velocity or foundation performance.

Within the influence zone of the nuclear island foundation, the Lee Nuclear Station Unit 1 nuclear island footprint is mainly (approximately 90 percent) underlain by sound concrete that was placed over continuous rock during construction of the Cherokee Nuclear Station Unit 1 as shown on Figure 2.5.4-241. The Cherokee Nuclear Station concrete was placed over a prepared rock surface of sound, continuous rock that met the DCD Subsection 2.5.4.5 Subsurface Uniformity criteria. In some places, new fill concrete is placed over a sound prepared rock surface, or a cleaned and roughened Cherokee Nuclear Station concrete surface, to develop the level basemat grade as part of the Lee Nuclear Station Unit 1 foundation construction. The thicknesses of the composite concrete, defined as Lee Nuclear Station and Cherokee Nuclear Station Unit 1 fill and structural concretes, under Lee Nuclear Station Unit 1 nuclear island basemat generally ranges between several feet to about 25 feet thick. For development of the Lee Nuclear Station dynamic velocity model, the Unit 1 concrete materials are assumed to be of similar composition, strength, quality, and dynamic properties. Assumed dynamic properties for Cherokee Nuclear Station fill and structural concrete materials are estimated using static and dynamic field and laboratory correlations developed by Boone (2005) (Reference 211). The composite sound rock and fill concrete underlying the Lee Nuclear Station Unit 1 nuclear island basemat comply with the subsurface uniformity criteria as described in DCD Subsection 2.5.4.5.

Rock conditions change beneath the northwest corner of the Lee Nuclear Station Unit 1 nuclear island. In this area, the Lee Nuclear Station Unit 1 nuclear island overlies a localized zone of weathered and fractured rock, extending approximately 15 to 25 feet deep, below the Unit 1 basemat footprint Elevation 550.5 feet, as shown in Figures 2.5.4-239 and 2.5.4-240. This minor localized weathered zone of rock, exhibits lower Vs velocities, ranging from approximately 4500 to 6000 fps, than the underlying and adjacent sound rock with average Vs of approximately 9500 fps, and represents a different velocity profile

condition. Excavation of this isolated lower velocity material to continuous rock at northwest corner of Lee Nuclear Station Unit 1 nuclear island to a depth of 15 to 25 feet below basemat subgrade removes a significant portion of the lower velocity weathered rock, and extends the excavation deeper within the support zone beyond the Lee Nuclear Station Unit 1 nuclear island footprint shown in Figures 2.5.4-245, 2.5.4-246, 2.5.4-264, and 2.5.4-265, as described in Subsection 2.5.4.10. The remaining continuous rock with Vs below 9200 fps represents less than 2 percent of the total rock volume beneath the Unit 1 nuclear island with an average Vs of 7300 fps and does not represent a potential for differential site amplification or foundation performance. The rock conditions described for the Lee Nuclear Station Unit 1 nuclear island northwest corner have no practical significance on differential shear wave velocity, site amplification or foundation performance and comply with the subsurface uniformity criteria as described in DCD Subsection 2.5.4.5. The excavation backfill condition for the Lee Nuclear Station Unit 1 northwest corner is described in Subsection 2.5.4.5. The nuclear island foundation rock is characterized as sound, massive meta-granodioritic to meta-quartz dioritic rock, no dipping layers exist and the rock supporting the nuclear island foundation meet DCD case 1 criteria.

2.5.4.7.4.2 Lee Nuclear Station, Unit 2 Nuclear Island

The Lee Nuclear Station Unit 2 nuclear island basemat at subgrade elevation is underlain by sound, massive meta-granodiorite and meta-quartz diorite bedrock with meta-diorite dikes. Rock in these intrusions is strong and similar in strength to the host rock, and contact margins are tight with minor local narrow altered/ weathered zones. The rock underlying the Lee Nuclear Station Unit 2 nuclear island complies with the subsurface uniformity criteria as described in DCD Subsection 2.5.4.5. Minor localized areas of rock excavation or infilling with fill concrete is required under portions of the Lee Nuclear Station Unit 2 nuclear island footprint to develop a level bearing surface. Low areas will be backfilled with fill concrete to achieve basemat subgrade of similar composition and quality as that described above for Lee Nuclear Station Unit 1 nuclear island concrete fill to provide a dense, coupled interface with sound rock. The maximum thickness of fill concrete is about 16 feet beneath the east portion of the nuclear island, but generally will be less than about 1 to 2 feet. The excavation backfill condition for the Lee Nuclear Station Unit 1 northwest corner is described in Subsection 2.5.4.5. The nuclear island foundation rock is characterized as sound, massive meta-granodioritic to meta-quartz dioritic rock, no dipping layers exist and the rock supporting the nuclear island foundation meet DCD case 1 criteria.

2.5.4.7.5 Dynamic Profiles

This subsection presents the methodology and approach to develop site-specific dynamic velocity profiles at the Lee Nuclear Station site. Dynamic velocity profiles were compiled and applied at three locations for evaluation of site ground motion characteristics of Class I safety-related plant facilities with a fourth profile developed to evaluate generic engineered granular fill properties. These profiles are defined below.

- Smoothed Dynamic Profile A, Unit 1 nuclear island centerline
- Smoothed Dynamic Profile B, Unit 1, nuclear island northwest corner
- Smoothed Dynamic Profile C, Unit 2 nuclear island centerline
- Best Estimate Layer Velocity Profile G, Generic engineered granular fill

Figure 2.5.4-247 shows the locations of the dynamic profiles (Profiles A through C) developed for the Duke Lee Nuclear Station. Smoothed dynamic profiles, Dynamic Profiles A through C, are shown on Figures 2.5.4-248 through 2.5.4-250, respectively. The site GMRS, discussed below and in Subsection 2.5.2, is represented by Profile A. Dynamic Profile B is applied for sensitivity site response analysis to evaluate possible ground motion variability between Profile A, Unit 1 centerline, and the Unit 1 northwest corner. Dynamic Profile C is used to evaluate possible differences in site response between Lee Nuclear Station Units 1 (Profile A) and 2 (Profile C) as a result of the spatial separation and possible lateral variability in the rock properties.

A fourth, artificial generic engineered granular fill profile, identified as Best Estimate Layer Velocity Profile G, was developed to represent engineered granular fill placed over the bedrock and around the plant nuclear islands to develop the plant grade. It represents a reasonable range of granular engineered fill materials, well-graded gravel (GW) (Figure 2.5.4-251a), poorly-graded gravel (GP) (Figure 2.5.4-251b), and well graded sand (SW) (Figure 2.5.4-251c) that may be placed adjacent to the AP1000 nuclear islands. These generic engineered granular fill seismic velocity profiles were constructed by estimating the maximum shear wave velocities, the elastic modulus values and the corresponding Poisson's ratio, and compression wave velocities for granular fill materials, well-graded gravel (GW) (Table 2.5.4-224a), poorly-graded gravel (GP) (Table 2.5.4-224b), and well graded sand (SW) (Table 2.5.4-224c) that may be typical of that to be placed at the site. The modulus ratio and damping ratio at various values of shear strain for generic granular fill materials, well-graded gravel (GW), poorly-graded gravel (GP), and well-graded sand (SW) are summarized in Tables 2.5.4-224d, 2.5.4-224e, and 2.5.4-224f. Shear modulus and damping ratio plots of these data are illustrated in Figures 2.5.4-253a, 2.5.4-253b, and 2.5.4-253c. Generic granular fill Profile G extends to a depth that envelops the greatest estimated depth of granular fill to be placed in the vicinity of the northwest corner of Lee Nuclear Station Unit 1. The generic granular fill is described in Subsection 2.5.4.5.3.5.

Following the development of the dynamic profiles, one base case dynamic velocity profile was developed for the Lee Nuclear Station Unit 1 centerline. This base case models the Lee Unit 1 nuclear island configuration and is described below.

- Base Case A1, Unit 1 Nuclear Island Centerline
  - Defines the GMRS and the typical relationship of the Lee Nuclear Station fill concrete (5.5 feet) overlying Cherokee Nuclear Station

structural and fill concrete (composite 15 feet) above continuous rock.

The model representing Dynamic Profile Base Case A1, Unit 1 Centerline is shown on Figure 2.5.4-252. Base Case A1 defined for the Lee Nuclear Station considers variability of site conditions such as material thickness and lateral variability within foundation rock, including Cherokee and Lee Nuclear Station concrete materials based on an average shear wave velocity of 7500 ft/sec. Assumed typical index properties for Cherokee Nuclear Station and Lee Nuclear Station concrete materials are summarized in Table 2.5.4-223. The site GMRS and Unit 1 FIRS (Base case profile A1) analysis are described in Subsections 2.5.2.6 and 2.5.2.7, respectively.

2.5.4.8 Liquefaction Potential

WLS COL 2.5-1
WLS COL 2.5-9

In meeting the requirements of 10 CFR Parts 50 and 100, if the foundation materials at the site adjacent to and under Category I structures and facilities are saturated soils and the water table is above bedrock, then an analysis of the liquefaction potential at the site is required. The need for a detailed analysis is determined by a study on a case-by-case basis of the site stratigraphy, critical soil parameters, and the location of safety-related foundations.

All seismic Category I safety-related plant foundations for Lee Nuclear Station Units 1 and 2 will bear on rock, or fill concrete over rock. Neither fill concrete nor rock are susceptible to liquefaction. Plan maps, cross sections, and summary boring logs presented in Subsection 2.5.4.3 show the locations and rock foundation conditions of the Category I nuclear island structures that have a design subgrade elevation of 550.5 feet. The design basemat subgrade places the foundation for the Lee Nuclear Station Unit 1 nuclear island on existing concrete that was placed over a sound and cleaned rock surface remaining from the Cherokee Nuclear Station Unit 1, and directly on a newly-excavated and cleaned sound rock surface for Lee Nuclear Station Unit 2. Therefore, a liquefaction hazard does not exist that could affect the Category I plant structures and facilities.

Outside the nuclear islands, compacted engineered granular fill is placed adjacent to seismic Category I structures over the exposed rock/fill concrete surfaces to the extent shown on Figures 2.5.4-245, 2.5.4-246, and 2.5.4-260 through 2.5.4-265. This granular backfill forms the supporting materials for the power block structures outside but adjacent to the nuclear islands. The typical thickness of granular fill is about 30 to 40 feet with a maximum thickness of about 80 feet. Beyond the perimeter of the granular fill as shown on the above-referenced figures, Group I engineered soil fill is placed as necessary to completely backfill the Cherokee Nuclear Station excavation, encompassing the granular backfill around the Lee Nuclear Station nuclear island structures up to yard grade Elevation 589.5 feet. As discussed in Subsection 2.5.4.6, groundwater will rise above the bedrock surface

within the engineered granular fill to elevations between about 574 feet to 584 feet msl.

Shallow foundations for non-Category I plant facilities adjacent to the nuclear island (i.e., seismic Category II part of the annex building, non-seismic radwaste building, and seismic Category II part of the turbine building) are completely founded on or over compacted engineered granular fill over partially weathered rock/continuous rock, or compacted engineered granular fill over fill concrete and partially weathered rock/continuous rock. The non-seismic part of the annex building and non-seismic part of the turbine building are founded on or over compacted engineered granular fill over partially weathered rock/continuous rock, compacted engineered granular fill over fill concrete and partially weathered rock/continuous rock, or compacted engineered granular fill over saprolite soils overlying partially weathered rock/continuous rock.

Subsection 2.5.4.5.1 describes the sources and extents of granular fill. The granular fill will likely have Unified Soil Classification System (USCS) classification symbol GW to GP (well-graded gravel to poorly-graded gravel) or SW (well-graded sand). Subsection 2.5.4.5 describes material specifications and compaction for engineered granular fill. Granular fill will be compacted to 96 percent modified Proctor (ASTM D 1557) maximum dry density. Using an empirical relationship from Reference 225 (Lee and Singh, 1971), the relative density of the granular fill compacted to 96 percent of the modified Proctor maximum dry density is 80 percent. According to an empirical correlation from Reference 232 (Rollins, et al., 1998), gravel having 80 percent relative density would have a corresponding $(N_1)_{60}$ blow count of 45 blows per foot. According to Reference 230 (Idriss and Boulanger, 2008), sand having 80 percent relative density would have a corresponding $(N_1)_{60}$ blow count of 29-30 blows per foot. These $(N_1)_{60}$ values may be considered as $(N_1)_{60cs}$ values owing to the low fines contents of the typical granular fill materials. Granular soils having $(N_1)_{60cs}$ blow counts of 29-30 or higher are classified as non-liquefiable according to Figure 2 of Reference 231 (Youd, et al., 2001). Therefore the granular fill compacted to 96 percent modified Proctor relative compaction is not subject to liquefaction. Additionally, the floor of the excavation is relatively flat, and potential sloping basal surfaces do not exist adjacent to or below the granular fill that could present a potential lateral spread condition.

Subsection 2.5.4.5.3.3 describes the criteria and steps for verification of proper foundation support conditions below the base of the granular fill. Figures 2.5.4-245, 2.5.4-246, and 2.5.4-260 through 2.5.4-265 depict the conditions below the base of the granular fill. No saprolite underlies the granular fill supporting the seismic Category II parts of the annex and turbine buildings for Unit 1 and Unit 2 or the non-seismic radwaste buildings for Unit 1 and Unit 2. The same is true for the northern portions of the non-seismic part of the annex buildings for Unit 1 and Unit 2, the non-seismic part of the turbine building for Unit 1, and the northern portion of the non-seismic part of the turbine building for Unit 2. Some saprolite may underlie the granular fill supporting the southernmost areas of the non-seismic part of the annex buildings for Unit 1 and Unit 2 and for the southern area of the non-seismic part of the turbine building for Unit 2.

Saprolite to support the granular fill has N_{60} values greater than or equal to 15 blows per foot, measured at a depth of 3 feet below the base of the open excavation. Table 2.5.4-211 indicates the saprolite soils have mean fines content of 46 percent with a standard deviation of 15 percent. The mean minus one standard deviation fines content is thus 31 percent. For a fines content conservatively assumed as on the order of 15 percent, saprolite with N_{60} equal to 15 blows per foot at a depth of 3 feet below the base of the open excavation has $(N_1)_{60cs}$ values equal to 26-27 blows per foot, and thus may be considered as highly resistant to liquefaction per Figure 2 of Reference 231 (Youd, et al., 2001).

The preceding analysis determines that no liquefaction hazard exists to seismic Category I safety-related plant structures and facilities, supported on sound rock or concrete over rock. As described above, neither fill concrete nor rock are susceptible to liquefaction. The analysis also determines that no liquefaction hazard exists for adjacent seismic Category II structures and facilities supported on compacted engineered granular fill over partially weathered rock/continuous rock, or compacted engineered granular fill over fill concrete and partially weathered rock/continuous rock. The compacted engineered granular fill and partially weathered rock will exhibit neither potential for liquefaction and related deformation, nor potential for adverse effects attributed to cyclic strain-softening or pore pressure build-up. Thus, any structure that could affect the Lee Nuclear Station Unit 1 and Unit 2 nuclear islands (including the seismic Category II portions of both the annex building and the turbine building, the non-seismic radwaste building, the entire non-seismic turbine building for Unit 1, and the northern area of the non-seismic parts of the turbine building for Unit 2) is on compacted engineered granular fill over partially weathered rock/continuous rock or compacted engineered granular fill over fill concrete over partially weathered rock/continuous rock, and is not subject to liquefaction.

The southern ends of the non-seismic portions of the annex buildings for Unit 1 and Unit 2 and the southern end of the non-seismic portion of the turbine building for Unit 2 may be founded on granular fill over saprolite. These areas will be highly resistant to liquefaction per Figure 2 of Reference 231, and will exhibit low to nil potential for liquefaction and related deformation, and low potential for adverse effects attributed to cyclic strain-softening or pore pressure build-up. These locations are also remote from the nuclear islands and thus have no potential for affecting the nuclear islands.

2.5.4.9 Earthquake Site Characteristics

WLS COL 2.5-6 A performance-based site-specific GMRS and FIRS was developed in accordance with the methodology provided in Regulatory Guide 1.208. This methodology and the development of the Unit 2 location-specific GMRS and Unit 1 location-specific FIRS are described in Subsections 2.5.2.6 and 2.5.2.7, respectively. The GMRS and FIRS satisfies the requirements of 10 CFR 100.23

for development of a site-specific Safe Shutdown Earthquake (SSE) ground motion.

As recommended in RG 1.208, the following general steps were undertaken:

- Review and update the EPRI (1986) (Reference 204) seismic source model for the site region (200-mile radius).
- Update the EPRI (1989) (Reference 212) ground motion attenuation model using the EPRI (2004) (Reference 219) ground motion attenuation model.
- Perform sensitivity studies and an updated Probabilistic Seismic Hazard Analysis (PSHA) to develop rock hazard spectra and define the controlling earthquakes.
- Derive performance-based GMRS for Unit 2 and FIRS for Unit 1 from the updated PSHA at a free field hypothetical outcrop of the top of competent material beneath the proposed nuclear island.

The dynamic properties of soil, granular fill, concrete, and rock at the site were determined through a program of field exploration, laboratory testing, and analysis as described in Subsections 2.5.4.2, 2.5.4.4, and 2.5.4.7. The Lee Nuclear Station site is considered a hard rock site with rock having a shear wave velocity generally greater than 8000 fps. Results of site response analysis are described in Subsection 2.5.2, and a comparison to DCD design parameters is presented in Table 2.0-201.

2.5.4.10 Static Stability

WLS COL 2.5-6 The static stability of the Lee Nuclear Station nuclear island is evaluated for foundation bearing capacity, foundation settlement, and lateral pressures against below-grade walls. Evaluation of static stability includes the safety-related nuclear island facilities and the non-safety related structures adjacent to the nuclear island facilities. A discussion of bearing capacity, settlement, and lateral pressure evaluations is provided in Subsections 2.5.4.10.1 through 2.5.4.10.3. Foundation materials at the location of Lee Nuclear Station Unit 1 and Unit 2 nuclear islands consist of continuous rock and fill concrete placed on top of continuous rock. The fill concrete is used where the elevation of continuous rock is below the elevation of the nuclear island foundation.

Shallow foundations for non-Category I plant facilities adjacent to the nuclear island (i.e., seismic Category II part of the annex building, non-seismic radwaste building, and seismic Category II part of the turbine building) are completely founded on or over compacted engineered granular fill over partially weathered rock/continuous rock, or compacted engineered granular fill over fill concrete and partially weathered rock/continuous rock. The non-seismic part of the annex building and non-seismic part of the turbine building are founded on or over

compacted engineered granular fill over partially weathered rock/continuous rock, compacted engineered granular fill over fill concrete and partially weathered rock/ continuous rock, or compacted engineered granular fill over saprolite soils overlying partially weathered rock/continuous rock.

WLS COL 2.5-13 The Unit 1 and Unit 2 nuclear island foundations are supported directly on continuous rock or fill concrete placed on top of continuous rock. Bearing capacity and settlement estimates of foundations supported on these materials are well within the limits provided in the DCD Subsections 2.5.4.2 and 2.5.4.3 as discussed in Subsections 2.5.4.10.1 and 2.5.4.10.2. Subsurface improvement of foundation materials is performed when necessary as described in Subsection 2.5.4.12. Cleaning and preparation of the continuous rock and fill concrete surfaces is also completed as described in Subsection 2.5.4.12 prior to placement of nuclear island foundation concrete. Instrumentation to monitor performance of the nuclear island foundations supported on the properly prepared continuous rock and on fill concrete materials supported on continuous rock is not necessary. As discussed in Subsection 2.5.4.6.1, the design groundwater elevation is 588 feet per the DCD. The basemat and below-grade walls are waterproofed to accommodate hydrostatic pressure due to groundwater. Groundwater loads are depicted in Figures 2.5.4-255a, 2.5.4-255b, and 2.5.4-255c.

2.5.4.10.1 Bearing Capacity

2.5.4.10.1.1 Bearing Capacity of Nuclear Islands

WLS COL 2.5-10 The bearing capacity of the Unit 1 and Unit 2 nuclear island foundation is evaluated separately for each unit. Two independent methods are used to determine the bearing capacity of the foundation materials. These methods are:

- Peck, Hanson and Thornburn (Reference 213) for allowable bearing pressure based on RQD of the rock as recorded at individual boring locations, and

- Ultimate Bearing Capacity based on the strength of the rock mass.

The Peck, Hanson, and Thornburn method utilizes an empirical relationship between allowable bearing pressure and average Rock Quality Designation. The allowable bearing pressure determined from this empirical relationship is compared to the required allowable bearing capacity provided in the DCD Subsection 2.5.4.2. Calculations using this method estimate a minimum allowable bearing pressure of 190,000 lb/ft^2 at Unit 1 and 285,000 lb/ft^2 at Unit 2. These allowable bearing pressures exceed the bearing requirements of 8,900 lb/ft^2 static and 35,000 lb/ft^2 combined (static plus seismic) loading provided in the DCD Subsection 2.5.4.2 and DCD Table 2-1.

The Ultimate Bearing Capacity method utilizes Hoek-Brown parameters of the rock mass to establish the Mohr-Coulomb parameters of friction angle and cohesion for the rock. The bearing capacity factors, as developed in EM 1110-1-2908 (Reference 214) and in Sowers (Reference 215), are determined based on the established Mohr-Coulomb parameters. Shape, size, and eccentricity correction factors are applied to the foundation conditions based on the size and shape of the nuclear island. The ultimate bearing capacity is then calculated using these parameters and factors. Bearing capacity calculations using these methods estimate an ultimate bearing capacity of at least 3,725,000 lb/ft^2 under static conditions and 3,590,000 lb/ft^2 under combined (static plus seismic) loading conditions.

The ultimate static bearing capacity of the foundation materials at the Lee Nuclear Station Site exceeds the DCD Subsection 2.5.4.2 and DCD Table 2-1 average static bearing reaction requirement of 8,900 lb/ft^2 by a factor of safety of at least 3.0. The ultimate bearing capacity of the foundation materials also exceeds the DCD Subsection 2.5.4.2 and DCD Table 2-1 required amount of 35,000 lb/ft^2 under all combined loads by a factor of safety of at least 1.5.

2.5.4.10.1.2 Bearing Capacity of Adjacent Structures

The bearing capacity of the non-safety related structures adjacent to the nuclear islands [radwaste buildings, annex buildings (both non-seismic and Category II portions), and turbine buildings] is evaluated and the results are applicable to each unit. The methods used are:

- Peck, Hanson and Thornburn (Reference 213) for allowable bearing pressure on the granular backfill to limit settlement, and
- Ultimate Bearing Capacity based on the strength of the granular fill divided by a factor of safety equal to 3 to determine the safe bearing capacity.

The method of Peck, Hanson and Thornburn (Reference 213) is used to estimate the allowable bearing pressure to limit settlement based on SPT blow count of the granular fill. The Peck, Hanson and Thornburn (Reference 213) method determines the allowable foundation loading which, if not exceeded, will result in settlements not to exceed 1 inch for smaller footings and not to exceed 2 inches for larger foundation areas (e.g., mat foundations). However, Peck, Hanson and Thornburn (Reference 213) recommend that the ultimate bearing capacity also be calculated to verify that foundations that would appear not to undergo the limiting settlement also have an acceptable margin of safety against a bearing capacity failure.

The $(N_1)_{60cs}$ values for the granular fill mentioned in Subsection 2.5.4.8 are used as the SPT $(N_1)_{60}$ blow counts of the potential granular fill.

Peck, Hanson and Thornburn (Reference 213) published a convenient chart for proportioning shallow foundations bearing on granular soil, shown on their Figure 19.3. In the Peck, Hanson and Thornburn (Reference 213) Figure 19.3, the

allowable bearing pressure is plotted on the y-axis and foundation width is plotted on the x-axis. For a given N value, the allowable bearing pressure increases as the foundation width increases until a maximum value is reached at a particular foundation width; beyond this point, allowable bearing pressure is constant, independent of foundation width. The sloping lines rising up from the origin as the width of footing increases represent the region where the safe bearing capacity governs. The horizontal lines for various N values represent the region where the allowable settlement governs.

Peck, Hanson and Thornburn (Reference 213) state that footing foundations proportioned in accordance with the chart on their Figure 19.3 will, on the basis of experience, not settle more than 1 inch total, and the differential settlements between individual foundations will not exceed tolerable limits.

For large mat foundations (such as those that support the project structures), Peck, Hanson, and Thornburn (Reference 213) indicate that, based on geotechnical experience, if total foundation settlement is limited to 2 inches, differential settlement will be limited to 0.75 inch, and the performance of the structure should not be impacted.

Peck, Hanson, and Thornburn (Reference 213) thus determines the allowable foundation loading which, if not exceeded, will result in settlements not to exceed 1 inch for smaller footings and not to exceed 2 inches for larger foundation areas (e.g., mat foundations). If the safety factor against exceeding the ultimate bearing capacity as calculated earlier herein is adequate, the maximum applied bearing pressure to cause settlement not to exceed 1 or 2 inches according to Peck, Hanson, and Thornburn (Reference 213) is:

$$q_{allowable\_1\ inch} = 0.11\ (N_1)_{60} \times C_w\ (tsf), \text{ and}$$

$$q_{allowable\_2\ inches} = 0.22\ (N_1)60 \times C_w\ (tsf)$$

where C_w is the effect of the water table, as discussed below.

The chart on Peck, Hanson, and Thornburn (Reference 213) Figure 19.3 is for the conditions where the supporting granular material remains above the water table. If the depth of the groundwater table (D_w) will be less than the sum of the foundation depth (D_f) and the width (B), then the allowable bearing pressure to limit total settlement is adjusted for water table depth using the water table correction factor (C_w):

$$C_w = 0.5 + \frac{0.5D_w}{D_f + B}$$

where:

D_w = depth to groundwater measured from the ground surface surrounding the foundation; and

C_w = adjustment factor for depth of the groundwater table (D_w) if less than the sum of the foundation depth below the ground surface (D_f) and smallest foundation dimension (B); the minimum value is 0.5; the maximum value is 1.0.

Note: If $D_w \leq D_f$, $C_w = 0.5$.

The future water table may be as high as an elevation of 584 ft, which would be about 5.5 ft below the yard surface at the perimeter of the buildings. For a depth to the bottom of the mat equal to 1.5 ft, this would place the future water table at a depth of 4 ft below the bottom of the perimeter foundation for computing C_w. This depth of water table, about 4 ft below the bottom of the foundation, is reasonable to apply to the foundations for the radwaste and annex buildings. The foundation bearing levels in the turbine building are at generally lower elevations than those of the radwaste and annex buildings, and D_f is appropriately assigned.

The ultimate bearing capacity calculation utilizes the unit weight and shear strength parameters of the potential granular fill materials found in Table 2.5.4-211 in conjunction with the bearing capacity equations by Hanson as found in Bowles (5th ed., Reference 216).

The radwaste buildings, annex buildings (Category II portion), and turbine buildings have mat foundations that occupy the entire building area. Therefore, the case for limiting settlement equal to 2 inches is applicable for these buildings. The annex building (non-Category II portion) may have individual spread footing foundations.

Building dimensions in Table 2.5.4-230 are based on Reference 235; the best estimates of loading of the building foundations in Table 2.5.4-230 are based on Reference 236. The calculated allowable bearing pressures (with a factor of safety of 3 against the ultimate bearing capacity) on the granular fill are shown in Table 2.5.4-228. The calculated allowable bearing pressures for settlements not to exceed 2 inches for mats are shown in Table 2.5.4-229. The results show the maximum safe bearing pressures based on the factor of safety are significantly greater than the applied pressures (Table 2.5.4-230). The allowable pressures to limit settlement are also greater than the applied pressures.

The bearing capacity calculations indicate the mat foundations of the radwaste buildings, annex buildings (Category II portion), and turbine buildings will perform as intended. This is consistent with the expected performance of foundations supported on dense granular fill. The calculations demonstrate that the allowable safe bearing pressure with a factor of safety of 3 against exceeding the ultimate bearing capacity will not govern foundation performance for the mat foundations. The allowable bearing pressure for settlements not to exceed 2 inches for mat foundations will exceed the applied pressures on the foundations. The granular fill will provide acceptable support for the buildings to be placed on it (radwaste,

annex (Category II portion), and turbine buildings) and anticipated settlement of these foundations are less than the published limit of 2 inches.

2.5.4.10.2 Settlement

WLS COL 2.5-12

2.5.4.10.2.1 Settlement of Nuclear Islands

Estimates of post-construction settlement are calculated separately for Unit 1 and Unit 2 based on the theory of elasticity. Three settlement methods (equations) are employed for estimation of settlement beneath the nuclear island using this approach. The three methods used are:

- The Steinbrenner equation (Reference 216).
- The Corps of Engineers equation (Reference 214).
- The Boussinesq equation (Reference 217).

The calculations estimate settlement resulting from static loading of the nuclear island foundation bearing directly on rock or bearing on a depth of fill concrete in turn resting on rock. An equivalent area approach is used to model the nuclear island as one or more rectangular areas for purposes of estimating settlement.

The theory of elasticity based on the elastic modulus (Young's modulus) and Poisson's ratio is used to develop a subsurface model of the fill concrete and rock layers below the foundation. Poisson's ratio measurements from P-S suspension logging (as described in Subsection 2.5.4.2) are used along with Young's modulus values measured from laboratory tests on intact cores and from P-S suspension logging measurements. Young's modulus values based on laboratory core measurements are reduced to account for Rock Quality Designation based on a relationship by Zhang and Einstein (Reference 218) to develop a representative in situ rock mass modulus. Young's modulus values based on P-S suspension logging measurements were reduced by 50 percent to develop a representation of in situ rock mass modulus independent of the Rock Quality Designation.

Young's modulus values for continuous rock are used even where rock of lesser Rock Quality Designation is removed and replaced with fill concrete. This is because modulus values of the in situ foundation quality rock are lower than that of the fill concrete. This results in additional conservatism for the settlement estimate because the rock modulus values are used in place of fill concrete modulus values.

An estimate of settlement is also performed using the results of the empirical approach described by Peck, Hanson, and Thornburn (Reference 213) which is based on the Rock Quality Designation of the rock below the foundation. The allowable bearing pressure determined using this method assumes that the

foundation settlement is limited to one-half inch. The settlement is assumed to be proportional to the ratio of allowable bearing pressure (as described in Subsection 2.5.4.10.1) versus the required allowable average bearing pressure (as developed in DCD Table 2-1).

Lee Nuclear Station nuclear island structures are founded on rock and fill concrete which does not incur sufficient settlement to disrupt the operation of the structure. Settlement of Lee Nuclear Station Unit 1 and Unit 2 nuclear island structures founded on rock or fill concrete is calculated to be 1/15 of an inch or less. The maximum estimated settlement is 0.055 inches beneath Unit 1 and 0.048 inches beneath Unit 2 using the elastic modulus methods. The maximum estimated settlement is 0.023 inches beneath Unit 1 and 0.015 inches beneath Unit 2 using the empirical Rock Quality Designation based method. Differential settlement, even if equivalent to the estimated maximum total settlement, is within the limits allowed by DCD Subsection 2.5.4.3 (0.5 inch in 50 ft allowable).

The settlement calculations assumed the foundation load is applied while the water table is maintained at the bottom elevation of the nuclear island. Some of the settlement is recovered as heave (also called rebound) when the water table is allowed to rise and thus apply buoyant unloading to the nuclear island. This is of no practical significance because the settlements calculated are small and therefore the portion of settlement recovered as heave (rebound) is small and insignificant.

2.5.4.10.2.2 Settlement of Adjacent Structures

Settlement of the structures adjacent to the nuclear islands is discussed in Subsection 2.5.4.10.1.2 as part of the evaluation of bearing capacity of the granular fill. These results indicate the mat foundations of the radwaste buildings, annex buildings (Category II portion), and turbine buildings will settle less than 2 inches. The foundation performance of these buildings supported on the granular fill will meet the DCD Subsection 2.5.4.3 criterion of 3-inch differential settlement relative to the settlement of the nuclear islands.

2.5.4.10.3 Lateral Pressures

WLS COL 2.5-11 Lateral pressures are developed against the below-grade nuclear island wall resulting from the placement and compaction of granular backfill materials. Earth pressure envelopes are calculated for active, at-rest, and passive pressure conditions as developed in Figures 2.5.4-255a, 2.5.4-255b, and 2.5.4-255c. Lateral earth pressure values based on the maximum groundwater elevation are provided in Tables 2.5.4-225a, 2.5.4-225b, and 2.5.4-225c. Potential compaction-induced earth pressures are presented in Figure 2.5.4-256a. Numerical values of compaction-induced earth pressure are given in Table 2.5.4-226. Assumptions or references used to develop the active, at-rest, passive, and compaction-induced earth pressure envelopes are described in the following list.

Earth Pressure Assumptions:

- The granular fill used to backfill around the nuclear islands will likely come from an off-site borrow source such as an operating quarry, as described in Subsection 2.5.4.5. The granular fill will likely be USCS group symbol GW to GP (well-graded gravel to poorly-graded gravel) or SW (well-graded sand) and have material properties as described in Subsection 2.5.4.2.

- Granular backfill is compacted to 96 percent of the maximum dry density determined from the modified Proctor laboratory test performed in accordance with ASTM D 1557.

- To achieve the required degree of compaction, the moisture content should be maintained at or near the optimum moisture content as determined by the ASTM D 1557 laboratory compaction test.

- Light hand-guided compaction equipment is used to compact the granular fill within 5 feet of the nuclear island walls. Heavier compaction equipment may be used at distances greater than 5 feet from the walls. The use of light, hand-guided compaction equipment near the wall avoids excessive compaction-induced stresses against the wall.

- The potential compaction-induced earth pressures area computed using the method in Peck and Mesri, 1987 (Reference 229).

- The groundwater table elevation may vary over time between elevations 584 and 574 feet. The design water table elevation from the Design Control Document is up to elevation 588.

- The nuclear island walls do not yield due to the lateral earth pressure applied to them. The at-rest pressure is the appropriate earth pressure to assume for design of the walls.

The Rankine earth pressure theory is used to compute the active and passive (ultimate) earth pressure.

The dynamic lateral earth pressure in Table 2.5.4-227 and plotted on Figure 2.5.4-256b is calculated in accordance with Reference 220 - ASCE 4-98, Section 3.5.3, Figure 3.5-1, "Variation of Normal Dynamic Soil Pressures for the Elastic Solution." Backfill properties for granular fill adjacent to the vertical surface of the nuclear island exterior walls and basemat for dynamic earth pressure calculation are as follows:

- Saturated unit weight of backfill (γ) = 150 lb/ft^3 (GW)
  = 142 lb/ft^3 (GP)
  = 136 lb/ft^3 (SW)
  (from Table 2.5.4-211)

- Poisson's ratio (ν) = 0.5 (see discussion below)

The Poisson's ratio, ν = 0.5, is used because the granular fill is predominantly below the design groundwater table.

The seismic acceleration used, (a) = 0.30g, is applied as a uniform seismic acceleration to the granular backfill along the height of the nuclear island wall.

2.5.4.11 Design Criteria

Table 2.0-201 compares the DCD site parameter criteria and the site characteristics, including the following items:

- Average Allowable Static Bearing Capacity
- Maximum Allowable Dynamic Bearing Capacity for Normal Plus SSE
- Shear Wave Velocity
- Site and Structures Conditions and Geologic Features
- Properties of the Underlying and Adjacent Subsurface Materials and Geologic Features
- Lateral Variability of Foundation Bearing Material Stiffness
- Liquefaction Potential

Design of safety-related foundations is based on the nuclear island foundation mat being supported by continuous rock or by fill concrete supported on continuous rock. Continuous rock is defined, for this purpose, as rock that is fresh to moderately weathered and has a Rock Quality Designation of at least 65%, based on the boring logs. Soil and rock not meeting this definition of continuous rock is removed down to the level of continuous rock. Where the elevation of continuous rock is below the elevation of the base of the foundation mat, fill concrete is placed between the continuous rock and the foundation mat. Fill concrete material meets the requirements for structural plain concrete as defined in Section 2.1 of ACI 318-02 (Reference 233).

Discussions of design criteria, assumptions, and conservatism used in analysis of soil and rock response to dynamic loading are included in Subsection 2.5.4.7.

Discussions of design criteria, assumptions, and conservatism in liquefaction analysis are included in Subsection 2.5.4.8.

The design criteria used for static stability analyses are identified in Subsection 2.5.4.10. Factors of safety estimates are applicable to the calculation of bearing capacity only and are discussed in Subsection 2.5.4.10.1. Discussion of assumptions and conservatism in static stability analyses are included in Subsection 2.5.4.10.

2.5.4.12 Techniques to Improve Subsurface Conditions

For Unit 1 and Unit 2, the nuclear island foundation mat is supported by continuous rock, or by fill concrete that is supported on continuous rock. Soil, rock, and concrete material above the design foundation subgrade elevation in the nuclear island area is removed by mechanical excavators or by controlled blasting. Poor quality rock, if present, is excavated and removed down to continuous rock. Continuous rock is based on criteria of fresh to moderate weathering and Rock Quality Designation (RQD) greater than 65%, based on the boring logs. Relatively minor zones of lower RQD rock are allowed to remain. The verification program to monitor the effectiveness of this foundation improvement is described as follows. The final excavation surface is observed and geologically mapped to document the presence of suitable materials prior to placement of fill concrete or foundation concrete. Mapping of the final excavation surface is completed as described in Subsection 2.5.4.5 prior to foundation treatment or placement of any fill materials.

When suitable continuous rock or concrete at or below the foundation elevation is reached, the rock or concrete surface is cleaned and prepared to receive fill concrete or foundation concrete. Cleaning and preparation of foundation materials consists of the following:

- Removing loose soil, rock, or other materials from the foundation surface.
- Removing protrusions and overhangs within the rock or concrete.
- Washing the exposed rock or concrete surface with air and/or water.
- Treating isolated depressions or cracks in the rock or concrete surface with fill concrete.
- Roughening exposed concrete surfaces as described in Subsection 2.5.4.5.3.2.

The cleaning and preparation of the rock foundation surface, to support the nuclear islands and fill concrete, extends to expose continuous rock for a distance of at least 6 feet beyond the nuclear island foundation limits. Beyond the 6-foot distance, the excavations extend to expose continuous rock for supporting fill concrete within the 0.5 horizontal to 1 vertical distance needed for lateral extension due to depth of suitable materials below the fill concrete surface.

Beneath the nuclear island footprints and within the 6-foot zone around the nuclear island foundation footprint, or beneath the slope of fill concrete associated with the nuclear island, isolated weathered rock or joints in the rock surface that were filled with soil-like material are excavated and treated with fill concrete. This generally applies to relatively steeply dipping linear features less than five feet in horizontal width as shown in Figure 2.5.4-257. Steeply dipping linear features less than three feet in horizontal width remain as their presence does not adversely affect the stresses in the thick, heavily reinforced structural basemat of the nuclear island. The soil or weathered rock material filling the joint is excavated to a depth equal to at least twice the width of the joint and the excavated area replaced with fill concrete. If a feature is found to be more shallowly dipping, it is similarly treated to remove the soil, facilitate cleaning, and allow placement of fill concrete as shown in Figure 2.5.4-258. The presence of other intersecting joints and fractures within the rock surface, if present, requires the removal of overhanging rock surfaces as shown in Figure 2.5.4-259.

The Cherokee Nuclear Station Unit 1 circular reactor building and the structures adjacent to it were designed for the dewatered condition and were constructed with an under slab drainage system. This drainage system consists of a network of channels located below the Cherokee Nuclear Station foundation slabs. The under slab drainage network is contained within the footprint of the Cherokee Nuclear Station structures and was sealed at the Cherokee foundation perimeter. Removal of the structures surrounding the Cherokee Nuclear Station circular reactor building exposes portions of this existing drainage network. Where the Cherokee Nuclear Station drainage system is exposed by Lee Nuclear Station construction it is sealed off to keep the Lee Nuclear Station fill materials from eroding into the Cherokee Nuclear Station drainage channels. The sealing of these drainage channels applies to portions of the Cherokee Nuclear Station structures left in place below the Lee Nuclear Station foundations as well as any portions of the Cherokee Nuclear Station structures that are left in place outside the limits of the Lee Nuclear Station structure areas. The Cherokee Nuclear Station foundation basemat drainage system and an outline of the Lee Nuclear Station nuclear island foundation limits are shown on Figures 2.5.4-244a through 2.5.4-244d.

2.5.4.13 References

201. Duke Power Company, Project 81, Cherokee Nuclear Station Preliminary Safety Analysis Report, 1974.

202. NUREG-0189, “Final Safety Evaluation Report, Cherokee Nuclear Station, Units 1, 2, and 3, Duke Power Company,” Office of Nuclear Reactor Regulation, Docket Nos. STN 50-491, 50-492, and 50-493, pp 2-20-2-25.

203. Horton, J.W., Drake, A.A., and Rankin, D.W., “Tectonstratigraphic terranes and their Paleozoic boundaries in the central and southern Appalachians,” Geological Society of America, Special Paper 230, p. 213-245, 1989.

204. Electric Power Research Institute (EPRI), "Seismic Hazard Methodology for the Central and Eastern United States, Tectonic Interpretations," EPRI NP-4726, v.10, 1986.

205. Duke Power Company, Project 81, "Preliminary Safety Analysis Report (PSAR), vol. 4, Appendix 2C – Geology," Prepared by Law Engineering Testing Company – Cherokee Nuclear Station, 270p., July 1974.

206. Horton, J.W. Jr., "Geologic Map of the Kings Mountain Belt Between Gaffney, South Carolina and Lincolnton, North Carolina," in *Geological Investigations of the Kings Mountain Belt and Adjacent Areas in the Carolinas*, Carolina Geological Society field trip guidebook, 1981.

207. Murphy, C.F. and Butler, J.R., "Geology of the Northern Half of the Kings Creek Quadrangle, South Carolina," in *Geological Investigations of the Kings Mountain Belt and Adjacent Areas in the Carolinas*," Carolina Geological Society field trip guidebook, 1981.

208. Horton, J.W., Jr. and Butler, J.R., "Geology and Mining History of the Kings Mountain Belt in the Carolinas; a Summary and Status Report," in *Geological Investigations of the Kings Mountain Belt and Adjacent Areas in the Carolinas*, Carolina Geological Society field trip guidebook, 1981.

209. American Concrete Institute (ACI), "Code Requirements for Nuclear Safety Related Concrete Structures," ACI 349-02, Chapter 11.7.

210. Brandon, Thomas M., Rose, Andrew T., and Duncan, J. Michael, (2006), "Drained and Undrained Strength Interpretations for Low-Plasticity Silts," Journal of Geotechnical and Geoenvironmental Engineering, ASCE Volume 132, No. 2, February, 2006, pages 250-257.

211. Boone, S.D., 2005, "A Comparison Between the Compressive Strength and the Dynamic Properties of Concrete as a Function of Time" MS Thesis, University of Tennessee, Knoxville, May 2005.

212. Electric Power Research Institute (EPRI), "Probabilistic Seismic Hazard Evaluation at Nuclear Plant Sites in the Central and Eastern United States, Resolution of the Charleston Earthquake Issue," EPRI Report 6395-D, Palo Alto, CA, April 1989.

213. Peck, Ralph B., Hanson, Walter E., and Thornburn, Thomas H., Foundation Engineering, 2nd Edition, John Wiley and Sons, NY, pp. 362, 1974.

214. US Army Corps of Engineers, 1994, "EM 1110-1-2908, Engineering and Design – Rock Foundations," Chapter 6.

215. Sowers, George F., "Introductory Soil Mechanics and Foundations: Geotechnical Engineering," 4th Edition, McMillian, NY, Chapter 10, 1979.

216. Bowles, Joseph E., "Foundation Analysis and Design," 5th Edition pp. 303-310, 4th Edition pp. 256-261, 443-447, McGraw-Hill, Inc., 1996, 1988.

217. Li, K. S. (1995). "Discussion of Foundation Uniform Pressure and Soil-structure Interaction," ASCE Journal of Geotechnical Engineering, December 1995, page 912.

218. Zhang, Lianyang and Einstein, H.H., 2004, "Using RQD to estimate the deformation modulus of rock masses," Intl. Journal of Rock Mechanics & Mining Sciences 41, pp. 337-341.

219. Electric Power Research Institute (EPRI), *CEUS Ground Motion Project Final Report,* EPRI Technical Report 1009684, December 2004.

220. ASCE Standard 4-98, *Seismic Analysis of Safety-Related Nuclear Structures and Commentary,* American Society of Civil Engineers, 2000.

221. Not used.

222. Deleted.

223. Menq, F.Y. 2003. Dynamic Properties of Sandy and Gravelly Soils, Ph.D. Dissertation, University of Texas at Austin, 364 pages.

224. South Carolina Department of Transportation (SCDOT), 2007. Standard Specifications for Highway Construction, Subsection 305.2.5.5 (Macadam Base Course) and Subsection 408.2.2 (Washed Screenings).

225. Lee, K.L., and Singh, A., 1971. Relative Density and Relative Compaction, Journal of the Soil Mechanics and Foundation Division, Proc. of the American Society of Civil Engineers, Vol. 97, No. SM7, July, pp. 1049 – 1052.

226. Horton, J.W. Jr., and Dicken, C.L., Preliminary Digital Geologic Map of the Appalachian Piedmont and Blue Ridge, South Carolina Segment, U.S. Geological Survey Open-File Report 01-298, 1:500,000 scale, 2001.

227. Nystrom Jr., P.G. Geologic Map of the Blacksburg South 7.5 Minute Quadrangle, Cherokee County, South Carolina [preliminary draft], South Carolina Department of Natural Resources Geological Survey, 1:24,000 scale, 1 sheet, 2004.

228. NAVFAC, 1986. Soil Mechanics, Design Manuals 7.01 and 7.02, Naval Facilities Engineering Command, Alexandria, VA.

229. Peck, R. B., and Mesri, G., 1987. "Discussion of Compaction - Induced Earth Pressure under K_0 Conditions," Journal of Geotechnical Engineering, ASCE, 113 (11), pp. 1406-1408.

230. Idriss, I. M., and Boulanger, R. W., 2008. Soil Liquefaction during Earthquakes, Monograph MNO 12, Earthquake Engineering Research Institute, Oakland, CA, Equation (37), page 87.

231. Youd, T. L., Idriss, I. M., Andrus, R. D., Arango, I., Castro, G., Christian, J. T., Dobry, R., Finn, W. D., Harder Jr., L. F., Hynes, M. E., Ishihara, K., Koester, J. P., Liao, S. C., Marcuson III, W. F., Martin, G. R., Mitchell, J. K., Moriwaki, Y., Power, M. S., Robertson, P. K., Seed, R. B., and K. H. Stokoe II, 2001. Liquefaction Resistance of Soils: Summary Report from the 1996 NCEER and 1998 NCEER/NSF Workshops on Evaluation of Liquefaction Resistance of Soils, Journal of Geotechnical and Geoenvironmental Engineering, Vol. 127, No. 10, American Society of Civil Engineers, October, 2001, pages 817 to 833. Also, see Errata in Closure to “Liquefaction Resistance of Soils: Summary Report from the 1996 NCEER and 1998 NCEER/NSF Workshops on Evaluation of Liquefaction Resistance of Soils”, Journal of Geotechnical and Geoenvironmental Engineering, Vol. 129, No. 3, American Society of Civil Engineers, March, 2003, pages 284 to 286.

232. Rollins, K. M., Evans, M., Diehl, N. and Daily, W., 1998. "Shear Modulus and Damping Relationships for Gravels," Journal of Geotechnical and Geoenvironmental Engineering, ASCE, Vol. 124, No. 5, pp. 396 – 405, Equation (7), page 397.

233. American Concrete Institute (ACI), “Building Code Requirements for Structural Concrete,” ACI 318-02, Chapter 2.1, 2002.

234. Not used.

235. Westinghouse Electric Company LLC. AP1000 Plant Grid Coordinates and Column Line Identification Plan, Drawing APP-0030-X4-001, Revision C.

236. Westinghouse Electric Company LLC, 2009. APC/WLG0068, Letter to Mr. John McConaghy, Duke Energy, Subject: “RAI No. 2098: Interface Information for Differential Settlement Evaluations”, dated April 8.

2.5.5 STABILITY OF SLOPES

WLS COL 2.5-14 This section provides an evaluation of the stability of earth and rock slopes, both natural and manmade, failure of which could adversely affect the safety of the seismic Category I plant components. The plant design for Lee Nuclear Station Units 1 and 2 does not require external safety cooling, ultimate heat sink, or related embankments. No safety related retaining walls, bulkheads, or jetties are constructed at the site.

WLS COL 2.5-15 No manmade earth or rock dams are present on the site that could adversely affect the safety of the nuclear power plant facilities. Potential dam failure is addressed in Subsection 2.4.4.

WLS COL 2.5-14 The plants are centrally sited within a backfilled excavation forming a broad, relatively level yard grade at approximate elevation 589.5 feet, for a distance of approximately 300 feet from the perimeter of the excavation. No natural or manmade slopes exist in proximity to the safety related nuclear island structures that pose a potential slope stability hazard to the safe operation of the plant. Additionally, no natural descending slopes, such as river banks or ridge slopes, exist around the perimeter of the Lee Nuclear Station plant yard area that pose a potential encroachment or undermining hazard. Site investigations, subsurface geotechnical characterizations, and excavation and backfill profiles used for the slope stability evaluation are presented in Subsections 2.5.4.1, 2.5.4.2, 2.5.4.3, and 2.5.4.5.

2.5.5.1 Slope Characteristics

2.5.5.1.1 General Discussion

Permanent slopes within a one-quarter mile distance of the Lee Nuclear Station Units 1 and 2 nuclear island structures were evaluated to determine the potential hazard to the safety-related structures. The locations of permanent slopes within this search area are identified on Figure 2.5.5-201 and include both natural slopes and cut slopes in native soil and rock materials, and engineered fill slopes. The permanent slope conditions, including features such as slope number, constructed condition, slope height and inclination, and approximate distances from the Units 1 and 2 nuclear islands, are summarized in Table 2.5.5-201. Additional descriptions for several of these slopes nearest to the nuclear island structures are provided below.

The permanent slopes are either natural slopes that have existed for a long period of time (through most or all of the Holocene; natural slopes), or cut and fill slopes developed as part of the Cherokee Nuclear Station construction in the early 1980's. These slopes exhibit acceptable stability without visual evidence of groundwater seepage, past failure, incipient movement, or major creep.

Liquefaction potential, as discussed in Subsection 2.5.4.8, indicates that the native soils and engineered fill are not prone to liquefaction. Therefore, a potential liquefaction-induced slope stability hazard does not exist under static or dynamic conditions that could adversely affect the seismic Category I plant components.

The nearest permanent slopes to the Lee Nuclear Station nuclear island areas are the cooling tower pad for Unit 1 to the west (Slope 1) and the cooling tower pad for Unit 2 to the east (Slope 2). These slopes are at least 500 feet away from the nearest safety related structure. These cooling tower pads were constructed using natural soil and engineered earthen (Group I) fill during site preparation for Cherokee Nuclear Station. The pads are constructed to an elevation of

approximately 610 feet, which is approximately 20 feet above the yard elevation of 589.5 feet. The cooling tower pads are constructed at a slope of approximately 2 horizontal to 1 vertical or shallower. The closest distance to the toe of the slope is approximately 25 times the height of the slope. No credible mechanism of slope failure would predict movement of the slope failure material over such a large distance. On the basis of engineering judgment and past performance, these Cooling Tower slopes (slopes 1 and 2) do not pose a hazard to the Lee Nuclear Station safety related structures due to their limited height, significant distance to the nuclear island, and the existing slope angle.

The highest slope within the one-quarter mile search area is a natural hill slope located southwest of the Unit 1 (Slope 5). This hill rises approximately 100 feet above the yard elevation. This hill was identified as a borrow source for engineered backfill to surround the Lee Nuclear Station Units and is identified as borrow area 6A, refer to Subsection 2.5.4.5. The hill has a slope of approximately 2.5 horizontal to 1 vertical and is located greater than 900 feet from the Unit 1 nuclear island. The closest distance to the toe of the slope is approximately 9 times the height of the slope. No credible mechanism of slope failure would predict movement of the slope failure material over such a large distance. Based on the past stable history, slope height and inclination, and the distance from the nuclear island, this hill does not pose a hazard to safety related structures. Excavation of this hill for borrow source material will likely reduce the slope height, and the toe of slope will likely be relocated in a southerly direction away from the plant area, further reducing the already negligible potential hazard.

Another large slope is a natural hill slope located northwest of the Unit 1 (Slope 4). This hill rises approximately 70 feet above the yard elevation. This hill has a slope of approximately 2 horizontal to 1 vertical and is located greater than 800 feet from the Unit 1 nuclear island. As part of the site development, this hill is designated for removal during construction for Lee Nuclear Station. The closest distance to the toe of the slope is approximately 11 times the height of the slope. No credible mechanism of slope failure would predict movement of the slope failure material over such a large distance. This hill does not pose a hazard to the safety related structures due to its distance from the nuclear island and slope inclination.

The nearest permanent slope that descends below the plant yard grade and the nuclear island area is an engineered slope located north of Unit 2 (Slope 7). The top of this slope is greater than 1100 feet from the nuclear island. This slope descends 55 feet below the plant yard to the surface of a pond adjacent to the Broad River. The slope is inclined approximately 2 horizontal to 1 vertical. There is no credible mechanism whereby failure of a descending slope 55 feet high and 800 feet away could affect the nuclear island. Based on the distance, height, and inclination of this slope from the nuclear island, it does not pose a hazard to the safety related structures.

2.5.5.1.2 Exploration Program

Site investigations and subsurface geotechnical characterization used for the slope stability evaluation are presented in Subsections 2.5.4.1, 2.5.4.2, and

2.5.4.3. The geological interpretation and geotechnical material properties presented in these sections were considered in this stability assessment of permanent slopes. The site exploration and testing data provide information regarding the stratigraphy, and engineering properties of rock, soil, and engineered fill that form the permanent slopes.

2.5.5.1.3 Groundwater and Seepage

A detailed discussion of groundwater conditions and characterization, including water levels and in situ rock mass and soil hydraulic conductivity, is provided in Subsections 2.4.12 and 2.5.4.6. Groundwater characterization included installation of monitoring wells and pump test wells adjacent to the Lee Nuclear Station Units 1 and 2 power block excavation area, and an evaluation of existing information from the Duke Power Company Project 81 Preliminary Safety Analysis Report Amendment 31 (Reference 201). As discussed in Subsection 2.5.4.6, the maximum groundwater elevation is estimated to be at 579±5 feet mean sea level. This 579 foot elevation value was based on the water mark along the exterior of the Cherokee Nuclear Station Unit 1 reactor building. At the time of this measurement in 2006, the Cherokee Nuclear Station excavation was being dewatered using a series of automated pumps that conveyed discharge water to the nearby Make-Up Pond B.

Groundwater seepage in natural and manmade slopes is not considered a hazard as no natural or manmade slopes exist in close proximity to the safety-related structures.

2.5.5.1.4 Slope Materials and Properties

Permanent slopes include slopes comprised of existing engineered fill and native residual and saprolitic soil and the material properties are described in Subsection 2.5.4.2. Geologic maps and cross sections presented in Subsection 2.5.4.3 show the distribution of geologic materials with respect to the locations of permanent slopes. Permanent slopes will not affect seismic Category I structures, the selection of material properties is not necessary.

The stability assessment consisted of an evaluation of the slope locations, geometries, inclinations, past stability, distance from the Units 1 and 2 nuclear island structures, and observed long-term slope performance. Slope materials and properties were used in a general sense to help guide engineering judgment regarding set back distances between the slopes and safety-related structures, including consideration of reasonable angle of friction values for various site slope materials in the event of a large slope failure.

Existing permanent slope inclinations are inclined at about 2 horizontal to 1 vertical (about 26.5 degrees) or less. Angles of friction for materials comprising the slopes are higher than this angle of slope inclination. Because the permanent slope inclinations are less than the material angles of friction, the evaluated slopes are determined to be inherently stable even when ignoring the cohesive component of the shear strength of the material. Consideration of the cohesive component considerably increases the perceived inherent stability of the slopes.

In the unlikely event of slope failure induced by groundwater rise, seepage, or dynamic loading, any mobilized materials will not travel significantly from the toe of slope. In a similar sense, potential headscarp inclinations related to failure of descending slopes likely would be steeply inclined due to the cohesive strength component of the slope materials. In any event, the long-term static stability of permanent slopes located within the one-quarter mile evaluation distance do not pose a hazard to the safety related structures.

As discussed in Subsection 2.5.4.1, no continuous, adversely-oriented weak clay or mylotinized zones, or planes of past slope failure were observed, or are expected, in the bedrock underlying the Lee Nuclear Station Units 1 and 2 power block area that could affect stability of the plant. As described in Subsection 2.5.4.8, the native residual soils, and engineered fill composed of native residual soils are not prone to liquefaction. Therefore, a potential slope stability hazard does not exist under static or dynamic conditions that could adversely affect the seismic Category I plant components.

2.5.5.2 Design Criteria and Analyses

Analyses of permanent slope conditions were limited to a review of permanent slopes within a one-quarter mile distance from the Units 1 and 2 nuclear island structures. This conservative evaluation is based on past performance, height, slope angle, and distance from the safety related structures. The nearest permanent slopes are 500 feet or more away from the Units 1 and 2 nuclear island structures. These permanent slopes do not require further analysis, including quantitative pseudostatic analysis, to calculate a safety factor because there is no failure mechanism that would create a hazard to the safety related structures.

No permanent slopes were identified in which failure would pose a hazard to the Lee Nuclear Station Units 1 and 2 safety-related structures.

2.5.5.3 Logs of Borings

No borings, test pits, or trenches were used for stability analyses of permanent slope conditions surrounding the Lee Nuclear Station Units 1 and 2 safety-related nuclear island structures. Boring logs for general site conditions are discussed in Subsection 2.5.4.3.

2.5.5.3.1 Soil Borings

No logs of soil borings were used for stability analyses of permanent slope conditions because there were no slopes determined to be a hazard to safety related structures.

2.5.5.3.2 Rock Borings

No logs of rock borings were used for stability analyses of permanent slope conditions because there were no slopes determined to be a hazard to safety related structures.

2.5.5.3.3 Test Pits and Trenches

No logs of test pits or trenches were used for stability analyses of permanent slope conditions because there were no slopes determined to be a hazard to safety related structures.

2.5.5.4 Compacted Fill

There are no safety-related permanent dams, dikes, or embankments constructed at the Lee Nuclear Station site. Therefore, design/performance criteria for compacted fills are not described.

2.5.5.5 References

201. Duke Power Company, Project 81, *Preliminary Safety Analysis Report, Amendment 31*.

STD DEP 1.1-1 2.5.6 COMBINED LICENSE INFORMATION

2.5.6.1 Basic Geologic and Seismic Information

WLS COL 2.5-1 This COL item is addressed in Subsections 2.5.1, 2.5.4.1, 2.5.4.3, 2.5.4.3.3, 2.5.4.3.5, 2.5.4.8, Appendix 2AA, and Appendix 2BB.

2.5.6.2 Site Seismic and Tectonic Characteristics Information

WLS COL 2.5-2 This COL item is addressed in Section 2.5 and Subsections 2.5.2 and 2.5.4.3.3.

2.5.6.3 Geoscience Parameters

WLS COL 2.5-3 This COL item is addressed in Subsection 2.5.4.3.3.

2.5.6.4 Surface Faulting

WLS COL 2.5-4 This COL item is addressed in Subsection 2.5.3.

2.5.6.5 Site and Structures

WLS COL 2.5-5 This COL item is addressed in Subsections 2.5.4.1, 2.5.4.3.5, and 2.5.4.5.

2.5.6.6 Properties of Underlying Materials

WLS COL 2.5-6 This COL item is addressed in Subsections 2.5.4.2, 2.5.4.2.1, 2.5.4.3.6, 2.5.4.4, 2.5.4.5.1, 2.5.4.5.2, 2.5.4.5.3, 2.5.4.7, 2.5.4.9, and 2.5.4.10.

2.5.6.7 Excavation and Backfill

WLS COL 2.5-7 This COL item is addressed in Subsections 2.5.4.3.6, 2.5.4.5.1, 2.5.4.5.2, and 2.5.4.5.3.

2.5.6.8 Groundwater Conditions

WLS COL 2.5-8 This COL item is addressed in Subsections 2.5.4.5.4 and 2.5.4.6.4.

2.5.6.9 Liquefaction Potential

WLS COL 2.5-9 This COL item is addressed in Subsection 2.5.4.8.

2.5.6.10 Bearing Capacity

WLS COL 2.5-10 This COL item is addressed in Subsection 2.5.4.10.1.

2.5.6.11 Earth Pressures

WLS COL 2.5-11 This COL item is addressed in Subsection 2.5.4.10.3.

2.5.6.12 Static and Dynamic Stability of Facilities

WLS COL 2.5-12 This COL item is addressed in Subsection 2.5.4.10.2.

2.5.6.13 Subsurface Instrumentation

WLS COL 2.5-13 This COL item is addressed in Subsection 2.5.4.10.

2.5.6.14 Stability of Slopes

WLS COL 2.5-14 This COL item is addressed in Subsection 2.5.5.

2.5.6.15 Embankments and Dams

WLS COL 2.5-15 This COL item is addressed in Subsection 2.5.5.

2.5.6.16 Settlement of Nuclear Island

WLS COL 2.5-16 This COL item is not addressed because it relates only to soil sites. Lee Nuclear Station is a rock site.

2.5.6.17 Waterproofing Systems

WLS COL 2.5-17 This COL item is addressed in Subsection 14.3.3.1.

TABLE 2.5.1-201
DEFINITIONS OF CLASSES USED IN THE COMPILATION OF QUATERNARY FAULTS, LIQUEFACTION FEATURES, AND DEFORMATION IN THE CENTRAL AND EASTERN UNITED STATES

	Class Category	Definition
WLS COL 2.5-1	Class A	Geologic evidence demonstrates the existence of a Quaternary fault of tectonic origin, whether the fault is exposed for mapping or inferred from liquefaction to other deformational features.
	Class B	Geologic evidence demonstrates the existence of a fault or suggests Quaternary deformation, but either (1) the fault might not extend deeply enough to be a potential source of significant earthquakes, or (2) the currently available geologic evidence is too strong to confidently assign the feature to Class C but not strong enough to assign it to Class A.
	Class C	Geologic evidence is insufficient to demonstrate (1) the existence of tectonic fault, or (2) Quaternary slip or deformation associated with the feature.
	Class D	Geologic evidence demonstrates that the feature is not a tectonic fault or feature; this category includes features such as demonstrated joints or joint zones, landslides, erosional or fluvial scarps, or landforms resembling fault scarps, but of demonstrable non-tectonic origin.

Source: Crone and Wheeler (2000) (Reference 310); Wheeler (2005) (Reference 311)

TABLE 2.5.1-202
RADIOMETRIC AGE DETERMINATIONS FROM UNDISTURBED SITE ROCKS

Rubidium-Strontium Analyses

Sample ID	Sample Material	Rb (ppm)	Sr (ppm)	Rb/Sr	Rb^{87}/Sr^{86}	Apparent Age (millions of yrs.)
B-51, 76 ft	Biotite from undisturbed felsic gneiss behind slickenside	247.6	43.68	5.669	16.52	291 ± 10
B-64, 120 ft	Biotite from felsic gneiss	184.4	40.92	4.516	13.14	277 ± 10

Potassium-Argon Analyses

Sample ID	Sample Material	K (weight %)	Sample weight (g)	% radiogenic Ar	Apparent Age (millions of yrs.)
BP-7, 59 ft	Biotite from undisturbed felsic gneiss behind slickenside	6.74	0.0433	95.4	296 ± 7
B-28, 106 ft	Hornblende from undisturbed mafic gneiss behind slickenside	0.248	0.4345	84.8	290 ± 9
B-37, 70.5 ft	Whole rock very fine-grained felsic gneiss (metagraywacke?)	1.054	0.8759	88.2	322 ± 2
B-53, 69 ft	Whole rock felsic gneiss	1.371	0.2697	35.5	362 ± 7
B-58, 33 ft	Whole rock felsic gneiss	0.931	1.0103	87.9	288 ± 1
B-236, 72 ft	Whole rock felsic gneiss	4.975	0.5395	92.6	234 ± 1
GTP-7, Sta. 18	Potassium feldspar and quartz from undisturbed pegmatitic quartz vein crossing a shear zone	8.946	0.1984	87.8	219 ± 1

Source: Duke PSAR Table 2C-3B (Reference 401).

TABLE 2.5.1-203 (Sheet 1 of 2)
DEFORMATION PHASES AND STRUCTURAL ELEMENTS IN THE STUDY AREA

Deformation Phase	D_1	D_2	D_3	D_4	D_5
Folds	F_1, isoclinal, upright	F_2, isoclinal to tight, upright	F_3 open, upright (crenulations)	F_4, close to tight	F_5, gentle to open warp, kink folds
Surface Folded	S_o, bedding and/or compositional layering	S_0 and S_1 foliation	S_0, S_1, S_2	S_0, S_1, S_2, S_3	S_0, S_1, S_2, S_3, S_4
Planar Structures	S_1, generally present only in hinge area of F_2 folds, transposed by later D_2 deformation, axial planar to F_1	S_2, dominant metamorphic schistosity, axial planar to F_2	S_3, crenulation cleavage, axial planar to F_3	S_4, crenulation (weak)	S_5, kink planes
Linear Structures	L_1, locally intersection of S_o with S_1	L_2, intersection of S_1 and S_2, boudinage of thin biotite schist layers and quartz veins, mineral elongation lineation	L_3, crenulation axes, intersection S_3 with S_2	L4, crenulation axes (?), intersection S_4 with S_2	L_5, axes of kink folds, intersection of S_5 with S_2
Attitude	F_1 -NE to SE axes rotated in plane of S_2, S_1 dips to SE	F_2 -N to NE axes, S to SW axes, S_2 predominantly dips steeply SE, in areas dips NW	F_3 -NE axes, S_3 strikes NE, dips steeply NW	F_4 -NE axes, plunge at low angles, axial planar S_4 cleavage subhorizontal	F_5 -NE and SE axes, axial planes and kink planes sub-vertical, strike NE and NW, intersection of S_5 and S_2 plunges steeply down dip on S_2
Shearing and Faulting	Ductile, N to NE strike, parallel to limbs of F_2 folds, possibly due to the attenuation of limbs during F_2 fold event		Brittle, brecciation, NE and NW strikes reactivation of earlier ductile shear zones		

WLS COL 2.5-1

TABLE 2.5.1-203 (Sheet 2 of 2)
DEFORMATION PHASES AND STRUCTURAL ELEMENTS IN THE STUDY AREA

Deformation Phase	D_1	D_2	D_3	D_4	D_5
Metamorphism	M_1, progressive regional metamorphism to amphibolite grade, central portion of belt to upper greenschist grade, M_1, D_1, and D_2 closely related in time, thermal peak of regional metamorphism after major D_1 deformation and during or after D_2 deformation		Lower greenschist conditions present, shear and breccia zones healed by quartz, epidote, mica, and K-feldspar, near end M_1		M_2, hydrothermal zeolite event, probably occurs after D_5

Source: Schaeffer (1981) (Reference 392)

TABLE 2.5.1-204
DEFORMATION EVENTS RECORDED AT THE SITE LOCATION

WLS COL 2.5-1

Site Deformation Event	Structural Expression	Correlation to Site Area Deformational Events	Age Constraint
d_1	Ductile fabric in shear - breccia zones	Possibly D_2 but may be D_3 or D_4	Pre-300 Ma greenschist facies overprint
d_2	Brittle overprint of ductile fabric in shear - breccia zones	Possibly D_3 but may be D_4 or D_5	Pre-300 Ma greenschist facies overprint
d_3	Dialation fractures	Possibly D_3 but may be D_4 or D_5	Pre-300 Ma greenschist facies overprint
d_4	Joints and joints with slickensides on surfaces associated with calcite and chlorite	Possibly D_3 but may be D_4 or D_5	Pre-300 Ma greenschist facies overprint
d_5	Joints and joints with slickensides	Mesozoic extension	Mesozoic
d_6	Slickensides in saprolite	weathering	soil development

TABLE 2.5.2-201 (Sheet 1 of 5)
1985–2005 UPDATE TO THE EARTHQUAKE CATALOG FOR EVENTS ≥ EMB 3.0

WLS COL 2.5-2

Year	Mon	Day	Hr	Min	Sec	Latitude	Longitude	Z (km)	MMI	Emb	Smb	Rmb	CAT
1985	6	10	12	22	38.30	37.2480	-80.4850	11.10	4	3.30	0.10	3.31	SEUSSN
1985	12	22	0	56	5.00	35.7010	-83.7200	13.40		3.25	0.30	3.35	SEUSSN
1986	1	7	1	26	43.30	35.6100	-84.7610	23.10		3.06	0.30	3.17	SEUSSN
1986	2	13	11	35	45.55	34.7550	-82.9430	5.00		3.50	0.10	3.51	ANSS
1986	3	13	2	29	31.40	33.2290	-83.2260	5.00	4	3.30	0.25	3.37	SEUSSN
1986	3	26	16	36	23.90	37.2450	-80.4940	11.90	4	3.30	0.25	3.37	SEUSSN
1986	7	11	14	26	14.80	34.9370	-84.9870	13.00	6	3.80	0.10	3.81	SEUSSN
1986	9	17	9	33	49.50	32.9310	-80.1590	6.70	4	3.30	0.25	3.37	SEUSSN
1986	12	3	9	44	21.20	37.5800	-77.4580	1.60	4	3.30	0.25	3.37	SEUSSN
1986	12	10	11	30	6.10	37.5850	-77.4680	1.20	5	3.50	0.10	3.51	SEUSSN
1986	12	24	17	58	38.30	37.5830	-77.4580	1.00	4	3.30	0.25	3.37	SEUSSN
1987	1	13	14	50	40.90	37.5840	-77.4650	2.50	4	3.30	0.25	3.37	SEUSSN
1987	3	16	13	9	26.80	34.5600	-80.9480	3.00		3.06	0.30	3.17	SEUSSN
1987	3	27	7	29	30.50	35.5650	-84.2300	18.50	6	4.20	0.10	4.21	SEUSSN
1987	6	4	17	19	23.40	37.9390	-85.8000	7.60		3.06	0.30	3.17	SEUSSN
1987	7	11	0	4	29.50	36.1050	-83.8160	25.10	5	3.79	0.10	3.80	SEUSSN
1987	7	11	2	48	5.90	36.1030	-83.8190	23.80	4	3.43	0.10	3.44	SEUSSN
1987	9	1	23	2	49.40	35.5150	-84.3960	21.10		3.06	0.30	3.17	SEUSSN
1987	9	22	17	23	50.10	35.6230	-84.3120	19.40	5	3.50	0.10	3.51	SEUSSN
1987	11	27	18	58	29.30	36.8520	-83.1100	26.80	5	3.50	0.10	3.51	SEUSSN

TABLE 2.5.2-201 (Sheet 2 of 5)
1985–2005 UPDATE TO THE EARTHQUAKE CATALOG FOR EVENTS ≥ EMB 3.0

Year	Mon	Day	Hr	Min	Sec	Latitude	Longitude	Z (km)	MMI	Emb	Smb	Rmb	CAT
1987	12	12	3	53	28.79	34.2440	-82.6280	5.00		3.00	0.10	3.01	ANSS
1988	1	9	1	7	40.60	35.2790	-84.1990	12.20	4	3.30	0.25	3.37	SEUSSN
1988	1	23	1	57	16.40	32.9350	-80.1570	7.40	5	3.50	0.25	3.57	SEUSSN
1988	2	16	15	26	54.80	36.5950	-82.2740	4.00	4	3.30	0.10	3.31	SEUSSN
1988	2	18	0	37	45.40	35.3460	-83.8370	2.40	4	3.50	0.10	3.51	SEUSSN
1988	4	14	23	37	31.10	37.2380	-81.9870	0.00		4.10	0.10	4.11	ANSS
1988	8	27	16	52	29.50	37.7180	-77.7750	14.30	4	3.30	0.25	3.37	SEUSSN
1989	4	10	18	12	16.00	37.1360	-82.0680	0.00		4.30	0.10	4.31	ANSS
1989	6	2	5	4	34.00	32.9340	-80.1660	5.80	4	3.30	0.25	3.37	SEUSSN
1990	8	17	21	1	15.90	36.9340	-83.3840	0.60	5	4.00	0.10	4.01	SEUSSN
1990	11	8	10	8	25.40	37.1080	-83.0310	0.40		3.16	0.30	3.26	SEUSSN
1990	11	13	15	22	13.00	32.9470	-80.1360	3.40	5	3.50	0.10	3.51	SEUSSN
1991	3	15	6	54	8.30	37.7460	-77.9090	15.50	5	3.80	0.10	3.81	SEUSSN
1991	4	22	1	1	20.20	37.9420	-80.2050	14.80	4	3.50	0.10	3.51	SEUSSN
1991	6	2	6	5	34.90	32.9800	-80.2140	5.00	5	3.50	0.25	3.57	SEUSSN
1991	9	24	7	21	7.00	35.7010	-84.1170	13.30	4	3.30	0.10	3.31	SEUSSN
1991	10	30	14	54	12.60	34.9040	-84.7130	8.10		3.06	0.30	3.17	SEUSSN
1992	1	3	4	21	23.90	33.9810	-82.4210	3.30	5	3.50	0.25	3.57	SEUSSN
1992	8	21	16	31	56.10	32.9850	-80.1630	6.50	6	4.10	0.10	4.11	SEUSSN
1993	1	15	2	2	50.90	35.0390	-85.0250	8.10	4	3.30	0.10	3.31	SEUSSN

TABLE 2.5.2-201 (Sheet 3 of 5)
1985–2005 UPDATE TO THE EARTHQUAKE CATALOG FOR EVENTS ≥ EMB 3.0

Year	Mon	Day	Hr	Min	Sec	Latitude	Longitude	Z (km)	MMI	Emb	Smb	Rmb	CAT
1993	7	12	4	48	20.80	36.0350	-79.8230	5.00	4	3.30	0.10	3.31	SEUSSN
1993	8	8	9	24	32.40	33.5970	-81.5910	8.50	5	3.50	0.10	3.51	SEUSSN
1994	2	12	2	40	24.50	36.8000	-82.0000	5.00		3.42	0.41	3.61	ANSS
1994	4	5	22	22	0.40	34.9690	-85.4910	24.30	5	3.50	0.10	3.51	SEUSSN
1994	4	16	20	10	12.20	35.7520	-83.9680	1.80	5	3.50	0.25	3.57	SEUSSN
1995	3	11	8	15	52.32	36.9590	-83.1330	1.00		3.80	0.10	3.81	ANSS
1995	3	11	9	50	4.44	36.9900	-83.1800	1.00		3.30	0.10	3.31	ANSS
1995	3	18	22	6	20.80	35.4220	-84.9410	26.00		3.25	0.30	3.35	SEUSSN
1995	4	17	13	46	0.00	32.9970	-80.1710	8.40	6	3.90	0.10	3.91	SEUSSN
1995	6	26	0	36	17.10	36.7520	-81.4810	1.80	5	3.40	0.10	3.41	SEUSSN
1995	7	5	14	16	44.70	35.3340	-84.1630	10.00	4	3.70	0.10	3.71	SEUSSN
1995	7	7	21	1	3.00	36.4930	-81.8330	10.00	4	3.06	0.10	3.08	SEUSSN
1995	10	26	0	37	28.96	37.0530	-83.1210	1.00		3.90	0.41	4.10	ANSS
1996	4	19	8	50	14.01	36.9810	-83.0180	0.00		3.90	0.10	3.91	ANSS
1996	6	29	19	30	42.67	37.1870	-81.9500	1.00		4.10	0.10	4.11	ANSS
1997	5	19	19	45	35.80	34.6220	-85.3530	2.70	4	3.06	0.10	3.08	SEUSSN
1997	7	19	17	6	34.40	34.9530	-84.8110	2.80	4	3.61	0.10	3.62	SEUSSN
1997	7	30	12	29	25.30	36.5120	-83.5470	23.00	5	3.80	0.10	3.81	SEUSSN
1997	10	28	10	36	46.56	37.1620	-82.0250	1.00		3.42	0.41	3.61	ANSS
1998	4	13	9	56	15.60	34.4710	-80.6030	6.60	5	3.90	0.10	3.91	SEUSSN

TABLE 2.5.2-201 (Sheet 4 of 5)
1985–2005 UPDATE TO THE EARTHQUAKE CATALOG FOR EVENTS ≥ EMB 3.0

Year	Mon	Day	Hr	Min	Sec	Latitude	Longitude	Z (km)	MMI	Emb	Smb	Rmb	CAT
1998	6	5	2	31	3.90	35.5540	-80.7850	9.40		3.34	0.10	3.35	SEUSSN
1998	6	17	8	0	23.90	35.9440	-84.3920	11.30	5	3.60	0.10	3.61	SEUSSN
1998	10	21	5	56	46.90	37.4220	-78.4390	12.60	3	3.80	0.10	3.81	SEUSSN
1999	1	17	18	38	5.10	36.8930	-83.7990	1.00	3	3.06	0.27	3.15	SEUSSN
2000	1	18	22	19	32.20	32.9200	-83.4650	19.20	5	3.50	0.10	3.51	SEUSSN
2001	3	7	17	12	23.80	35.5520	-84.8500	6.80	3	3.20	0.10	3.21	SEUSSN
2001	3	21	23	35	34.90	34.8470	-85.4380	0.00	3	3.16	0.27	3.24	SEUSSN
2001	6	11	18	27	54.25	30.2260	-79.8850	10.00		3.33	0.41	3.53	ANSS
2001	7	26	5	26	46.00	35.9710	-83.5520	14.30	3	3.25	0.10	3.26	SEUSSN
2001	12	4	21	15	13.90	37.7260	-80.7520	8.50		3.10	0.10	3.11	SEUSSN
2001	12	8	1	8	22.40	34.7100	-86.2310	0.00	5	3.90	0.10	3.91	SEUSSN
2002	11	8	13	29	3.19	32.4220	-79.9500	3.90		3.50	0.41	3.69	ANSS
2002	11	11	23	39	29.72	32.4040	-79.9360	2.40		4.23	0.41	4.42	ANSS
2003	3	18	6	4	24.21	33.6890	-82.8880	5.00		3.50	0.41	3.69	ANSS
2003	4	29	8	59	38.10	34.4450	-85.6200	9.10	6	4.70	0.10	4.71	SEUSSN
2003	4	29	9	45	45.00	34.4400	-85.6400	3.10		3.01	0.41	3.20	ANSS
2003	5	2	10	48	44.00	34.4900	-85.6100	14.50		3.17	0.41	3.37	ANSS
2003	5	5	10	53	49.90	33.0550	-80.1900	11.40		3.06	0.30	3.17	SEUSSN
2003	5	5	16	32	33.90	37.6550	-78.0550	2.80	5	3.90	0.10	3.91	SEUSSN
2003	7	13	20	15	16.96	32.3350	-82.1440	5.00		3.58	0.41	3.77	ANSS

TABLE 2.5.2-201 (Sheet 5 of 5)
1985–2005 UPDATE TO THE EARTHQUAKE CATALOG FOR EVENTS ≥ EMB 3.0

Year	Mon	Day	Hr	Min	Sec	Latitude	Longitude	Z (km)	MMI	Emb	Smb	Rmb	CAT
2003	12	9	20	59	18.70	37.7740	-78.1000	10.00	6	4.50	0.10	4.51	SEUSSN
2004	5	9	8	56	10.40	33.2310	-86.9600	5.00	3	3.30	0.10	3.31	SEUSSN
2004	7	20	9	13	14.40	32.9720	-80.2480	10.30		3.06	0.30	3.17	SEUSSN
2004	8	19	23	51	49.40	33.2030	-86.9680	5.00	3	3.50	0.10	3.51	SEUSSN
2004	9	17	15	21	43.60	36.9330	-84.0040	1.30	5	3.70	0.10	3.71	SEUSSN
2005	2	18	14	21	54.00	34.0500	-81.1100	5.00		3.17	0.41	3.37	ANSS
2005	4	5	20	37	43.00	36.1500	-83.6900	10.00		3.01	0.41	3.20	ANSS
2005	8	25	3	9	42.00	35.8800	-82.8000	7.90		3.66	0.41	3.85	ANSS
2005	10	12	6	27	30.00	35.5100	-84.5400	8.20		3.58	0.41	3.77	ANSS

Notes:

Z = hypocentral depth

MMI = Modified Mercalli Index intensity

Emb = estimated body wave magnitude (see Equations 2.5.2-1 and 2.5.2-2)

Smb = estimate of variance for Emb

Rmb = best estimate of body wave magnitude from the largest calculated value of Emb and the variance

CAT = source catalog; SEUSSN = Southeastern United States Seismic Network; ANSS = Advanced National Seismic System

TABLE 2.5.2-202 (Sheet 1 of 3)
SUMMARY OF EPRI SEISMIC SOURCES - BECHTEL

WLS COL 2.5-2

Source	Description	Pa[a]	Mmax (m_b) and Weights[b]	Smoothing Options and Weights[c]	Inter-dependencies[d]	Geom.[e]	Mmax[f]	RI[g]
Primary sources that contribute to 99% of hazard								
F	S.E. Appalachians	0.35	5.4 [0.10] 5.7 [0.40] 6.0 [0.40] 6.6 [0.10]	1 [0.33] 2 [0.34] 4 [0.33]	ME with G, 13, 15, 16, 17	No	No	No
G	NW South Carolina	0.35	5.4 [0.10] 5.7 [0.40] 6.0 [0.40] 6.6 [0.10]	1 [0.33] 2 [0.34] 4 [0.33]	ME with F, 13, 15, 16, 17	No	No	No
H	**Charleston Area**	0.50	6.8 [0.20] 7.1 [0.40] 7.4 [0.20]	1 [0.33] 2 [0.34] 4 [0.33]	P(H|N3)=0.15	**Yes**[h]	**Yes**[h]	**Yes**[h]
N3	**Charleston Faults**	0.53	6.8 [0.20] 7.1 [0.40] 7.4 [0.20]	1 [0.33] 2 [0.34] 4 [0.33]	P(N3|H)=0.15	**Yes**[h]	**Yes**[h]	**Yes**[h]
BZ4	Atlantic Coastal Region	1.00	6.6 [0.10] 6.8 [0.40] 7.1 [0.40] 7.4 [0.10]	1 [0.33] 2 [0.34] 3 [0.33]	Background; P_B=1.00	No	No	No

TABLE 2.5.2-202 (Sheet 2 of 3)
SUMMARY OF EPRI SEISMIC SOURCES - BECHTEL

WLS COL 2.5-2

Source	Description	Pa[a]	Mmax (m_b) and Weights[b]	Smoothing Options and Weights[c]	Inter-dependencies[d]	Geom.[e]	Mmax[f]	RI[g]
BZ5	S. Appalachians	1.00	5.7 [0.10] 6.0 [0.40] 6.3 [0.40] 6.6 [0.10]	1 [0.33] 2 [0.34] 3 [0.33]	Background; P_B=1.00	No	No	No
C07	H-N3	NA	6.8 [0.20] 7.1 [0.40] 7.4 [0.20]	1 [0.33] 2 [0.34] 4 [0.33]	NA	No	No	No
Additional sources that do not contribute to 99% of hazard								
13	Eastern Mesozoic Basins	0.10	5.4 [0.10] 5.7 [0.40] 6.0 [0.40] 6.6 [0.10]	1 [0.33] 2 [0.34] 4 [0.33]	No overlap with H or N3; ME with all sources in BZ5	No	No	No
15	Rosman Fault	0.05	5.4 [0.10] 5.7 [0.40] 6.0 [0.40] 6.6 [0.10]	1 [0.33] 2 [0.34] 4 [0.33]	ME with all other sources	No	No	No
16	Belair Fault	0.05	5.4 [0.10] 5.7 [0.40] 6.0 [0.40] 6.6 [0.10]	1 [0.33] 2 [0.34] 4 [0.33]	ME with all other sources	No	No	No
24	Bristol Trends	0.25	5.7 [0.10] 6.0 [0.40] 6.3 [0.40] 6.6 [0.10]	1 [0.33] 2 [0.34] 4 [0.33]	ME with 19, 25, 25A	No	No	No

TABLE 2.5.2-202 (Sheet 3 of 3)
SUMMARY OF EPRI SEISMIC SOURCES - BECHTEL

WLS COL 2.5-2

Source	Description	Pa[a]	Mmax (m_b) and Weights[b]	Smoothing Options and Weights[c]	Inter-dependencies[d]	Geom.[e]	Mmax[f]	RI[g]
25	New York-Alabama Lineament	0.30	5.4 [0.10] 5.7 [0.40] 6.0 [0.40] 6.6 [0.10]	1 [0.33] 2 [0.34] 4 [0.33]	ME with 24, 25A	No	No	No
25A	NY-AL Lineament- alt. config.	0.45	5.4 [0.10] 5.7 [0.40] 6.0 [0.40] 6.6 [0.10]	1 [0.33] 2 [0.34] 4 [0.33]	ME with 24, 25	No	No	No

a) Pa = probability of activity (from EPRI NP-6452-D 1989) (Reference 207)

b) Maximum Magnitude (Mmax) and weights (from EPRI NP-6452-D 1989)

c) Smoothing options are defined as follows (from EPRI NP-6452-D 1989):
1 = constant a, constant b (no prior b);
2 = low smoothing on a, high smoothing on b (no prior b);
3 = low smoothing on a, low smoothing on b (no prior b);
4 = low smoothing on a, low smoothing on b (weak prior of 1.05).
Weights on magnitude intervals are [1.0, 1.0, 1.0, 1.0, 1.0, 1.0, 1.0].

d) ME = mutually exclusive; PD = perfectly dependent

e) No, unless (1) new geometry proposed in literature or (2) new seismicity pattern

f) No, unless (1) new data suggests Mmax exceeds or differs significantly from the EPRI Mmax distribution or (2) exceeded by historical seismicity.

g) RI = recurrence interval; assumed no change if no new paleoseismic data or rate of seismicity has not significantly changed

h) Replace this source with the Updated Charleston Seismic Source (UCSS) Model - original Charleston sources shown in bold.

TABLE 2.5.2-203 (Sheet 1 of 2)
SUMMARY OF EPRI SEISMIC SOURCES - DAMES & MOORE

WLS COL 2.5-2

Source	Description	Pa[a]	Mmax (m_b) and Weights[b]	Smoothing Options and Weights[c]	Inter-dependencies[d]	Geom.[e]	Mmax[f]	RI[g]
Primary sources that contribute to 99% of hazard								
04	Appalachian Fold Belt	0.35	6.0 [0.80] 7.2 [0.20]	1 [0.75] 2 [0.25]	ME with 4A, 4B, 4C, 4D	No	No	No
4A	Kink in Fold Belts	0.35	6.8 [0.75] 7.2 [0.25]	3 [0.75] 4 [0.25]	ME with 4	No	No	No
4B	Kink in Fold Belts	0.65	6.2 [0.75] 7.2 [0.25]	3 [0.75] 4 [0.25]	ME with 4	No	No	No
21	New Madrid	1.00	7.2 [0.25] 7.5 [0.75]	3 [0.75] 4 [0.25]	none	Yes[h]	Yes[h]	Yes[h]
41	S. Cratonic Margin (default Zone)	0.12	6.1 [0.80] 7.2 [0.20]	1 [0.75] 2 [0.25]	Default for 42, 43, 46	No	No	No
53	So. Appal. Mobile Belt (default zone)	0.26	5.6 [0.80] 7.2 [0.20]	1 [0.75] 2 [0.25]	Default for 47 thru 52, 65	No	No	No
54	**Charleston Seismic Zone**	1.00	6.6 [0.75] 7.2 [0.25]	1 [0.22] 2 [0.08] 3 [0.52] 4 [0.18]	none	**Yes**[i]	**Yes**[i]	**Yes**[i]
C01	4-4A-4B-4C-4D	NA	6.0 [0.80] 7.2 [0.20]	1 [0.75] 2 [0.25]	NA	No	No	No
Additional sources that do not contribute to 99% of hazard								
46	Dan R. Basin	0.28	6.0 [0.75] 7.2 [0.25]	3 [0.75] 4 [0.25]	ME with 42, 43	No	No	No

TABLE 2.5.2-203 (Sheet 2 of 2)
SUMMARY OF EPRI SEISMIC SOURCES - DAMES & MOORE

WLS COL 2.5-2

Source	Description	Pa[a]	Mmax (m_b) and Weights[b]	Smoothing Options and Weights[c]	Inter-dependencies[d]	Geom.[e]	Mmax[f]	RI[g]
49	Jonesboro B.	0.28	6.0 [0.75] 7.2 [0.25]	3 [0.75] 4 [0.25]	PD with 47, 48, 50, 51, 65; ME with 52	No	No	No
50	Buried Tr. B		6.0 [0.75] 7.2 [0.25]	3 [0.75] 4 [0.25]	PD with 47, 48, 49, 51, 65; ME with 52	No	No	No
51	Florence B.	0.28	6.0 [0.75] 7.2 [0.25]	3 [0.75] 4 [0.25]	PD with 47 thru 50, 65; ME with 52	No	No	No
52	Charleston Mes. Rift	0.46	4.7 [0.75] 7.2 [0.25]	3 [0.75] 4 [0.25]	ME with 47 thru 51, 65	No	No	No
65	Dunbarton Tr. Basin	0.28	5.9 [0.75] 7.2 [0.25]	3 [0.75] 4 [0.25]	PD with 47 thru 51; ME with 52	No	No	No

a) Pa = probability of activity (from EPRI NP-6452-D 1989) (Reference 207)

b) Maximum Magnitude (Mmax) and weights (from EPRI NP-6452-D 1989)

c) Smoothing options are defined as follows (from EPRI NP-6452-D 1989):
1 = No smoothing on a, no smoothing on b (strong prior of 1.04);
2 = No smoothing on a, no smoothing on b (weak prior of 1.04);
3 = Constant a, constant b (strong prior of 1.04);
4 = Constant a, constant b (weak prior of 1.04).
Weights on magnitude intervals are [0.1, 0.2, 0.4, 1.0, 1.0, 1.0, 1.0]

d) ME = mutually exclusive; PD = perfectly dependent

e) No, unless (1) new geometry proposed in literature or (2) new seismicity pattern

f) No, unless (1) new data suggests Mmax exceeds or differs significantly from the EPRI Mmax distribution or (2) exceeded by historical seismicity.

g) RI = recurrence interval; assumed no change if no new paleoseismic data or rate of seismicity has not significantly changed

h) Source updated using to Clinton ESP New Madrid seismic source model.

i) Replace this source with the Updated Charleston Seismic Source (UCSS) Model - original Charleston sources shown in bold

TABLE 2.5.2-204 (Sheet 1 of 2)
SUMMARY OF EPRI SEISMIC SOURCES - LAW ENGINEERING

WLS COL 2.5-2

Source	Description	Pa[a]	Mmax (m_b) and Weights[b]	Smoothing Options and Weights[c]	Inter-dependencies[d]	Geom.[e]	Mmax[f]	RI[g]
Primary sources that contribute to 99% of hazard								
17	Eastern Basement	0.62	5.7 [0.20] 6.8 [0.80]	1b [1.00]	none	No	No	No
22	Reactivated E. Seaboard	0.27	6.8 [1.00]	2a [1.00]	ME with 8, 21; overlaps 24, 35, 39	No	No	No
35	**Charleston Seismic Zone**	0.45	6.8 [1.00]	2a [1.00]	Overlaps 8 and 22	**Yes**[h]	**Yes**[h]	**Yes**[h]
107	Eastern Piedmont	1.00	4.9 [0.30] 5.5 [0.40] 5.7 [0.30]	1a [1.00]	Background; P_B=0.42	No	No	No
108	Brunswick, NC Background	1.00	4.9 [0.50] 5.5 [0.30] 6.8 [0.20]	2a [1.00]	Background; P_B=0.42	No	No	No
C11	22 - 35	NA	6.8 [1.00]	2a [1.00]	NA	No	No	No
C12	22 – 24	NA	6.8 [1.00]	2a [1.00]	none	No	No	No
C13	22 – 24 - 25	NA	6.8 [1.00]	2a [1.00]	none	No	No	No
M31	Mafic Pluton	0.43	6.8 [1.00]	5 [1.00]	none	No	No	No
M32	Mafic Pluton	0.43	6.8 [1.00]	5 [1.00]	none	No	No	No
M33	Mafic Pluton	0.43	6.8 [1.00]	5 [1.00]	none	No	No	No
M34	Mafic Pluton	0.43	6.8 [1.00]	5 [1.00]	none	No	No	No
M35	Mafic Pluton	0.43	6.8 [1.00]	5 [1.00]	none	No	No	No
M36	Mafic Pluton	0.43	6.8 [1.00]	5 [1.00]	none	No	No	No
M37	Mafic Pluton	0.43	6.8 [1.00]	5 [1.00]	none	No	No	No
M39	Mafic Pluton	0.43	6.8 [1.00]	5 [1.00]	none	No	No	No

TABLE 2.5.2-204 (Sheet 2 of 2)
SUMMARY OF EPRI SEISMIC SOURCES - LAW ENGINEERING

WLS COL 2.5-2

Source	Description	Pa[a]	Mmax (m_b) and Weights[b]	Smoothing Options and Weights[c]	Inter-dependencies[d]	Geom.[e]	Mmax[f]	RI[g]
Additional sources that do not contribute to 99% of hazard								
M38	Mafic Pluton	0.43	6.8 [1.00]	5 [1.00]	none	No	No	No
C09	Mesozoic Basins (8 - Bridged)	NA	6.8 [1.00]	2a [1.00]	NA	No	No	No
C10	8 - 35	NA	6.8 [1.00]	2a [1.00]	NA	No	No	No

a) Pa = probability of activity (from EPRI NP-6452-D 1989) (Reference 207)

b) Maximum Magnitude (Mmax) and weights (from EPRI NP-6452-D 1989)

c) Smoothing options are defined as follows (from EPRI NP-6452-D 1989):
1a = High smoothing on a, constant b (strong prior of 1.05);
1b = High smoothing on b, constant b (strong prior of 1.00);
1c = High smoothing on a, constant b (strong prior of 0.95);
1d = High smoothing on a, constant b (strong prior of 0.90);
1e = High smoothing on a, constant b (strong prior of 0.70);
2a = Constant a, constant b (strong prior of 1.05);
2c = Constant a, constant b (strong prior of 0.95);
2d = Constant a, constant b (strong prior of 0.90).
Weights on magnitude intervals are all 1.0 for above options.
3a = High smoothing on a, constant b (strong prior of 1.05).
Weights on magnitude intervals are [0.0, 1.0, 1.0, 1.0, 1.0, 1.0, 1.0] for option 3a.

d) ME = mutually exclusive; PD = perfectly dependent

e) No, unless (1) new geometry proposed in literature or (2) new seismicity pattern

f) No, unless (1) new data suggests Mmax exceeds or differs significantly from the EPRI Mmax distribution or (2) exceeded by historical seismicity.

g) RI = recurrence interval; assumed no change if no new paleoseismic data or rate of seismicity has not significantly changed

h) Replace this source with the Updated Charleston Seismic Source (UCSS) Model - original Charleston sources shown in bold.

TABLE 2.5.2-205 (Sheet 1 of 2)
SUMMARY OF EPRI SEISMIC SOURCES - RONDOUT ASSOCIATES

WLS COL 2.5-2

Source	Description	Pa[a]	Mmax (m_b) and Weights[b]	Smoothing Options and Weights[c]	Inter-dependencies[d]	Geom.[e]	Mmax[f]	RI[g]
Primary sources that contribute to 99% of hazard								
24	**Charleston**	1.00	6.6 [0.20] 6.8 [0.60] 7.0 [0.20]	1 [1.00] (a=-0.710, b=1.020)	none	**Yes**[h]	**Yes**[h]	**Yes**[h]
25	Southern Appalachians		6.6 [0.30] 6.8 [0.60] 7.0 [0.10]	1 [1.00] (a=-0.630, b=1.150)	none	No	No	No
26	South Carolina	1.00	5.8 [0.15] 6.5 [0.60] 6.8 [0.35]	1 [1.00] (a=-1.390, b=0.970)	none	No	No	No
27	TN-VA Border Zone	0.99	5.2 [0.30] 6.3 [0.55] 6.5 [0.15]	1 [1.00] (a=-1.120, b=0.930)	none	No	No	No
28	Giles County	1.00	6.6 [0.30] 6.8 [0.60] 7.0 [0.10]	1 [1.00] (a=-1.130, b=0.900)	none	No	No	No
Additional sources that do not contribute to 99% of hazard								
C01	Background 49	NA	4.8 [0.20] 5.5 [0.60] 5.8 [0.20]	3 [1.00]	none	No	No	No
C02	Background 50	NA	4.8 [0.20] 5.5 [0.60] 5.8 [0.20]	3 [1.00]	none	No	No	No

TABLE 2.5.2-205 (Sheet 2 of 2)
SUMMARY OF EPRI SEISMIC SOURCES - RONDOUT ASSOCIATES

WLS COL 2.5-2

Source	Description	Pa[a]	Mmax (m_b) and Weights[b]	Smoothing Options and Weights[c]	Inter-dependencies[d]	Geom.[e]	Mmax[f]	RI[g]
C07	50 (02) + 12	NA	4.8 [0.20] 5.5 [0.60] 5.8 [0.20]	3 [1.00]	none	No	No	No
C09	49+32	NA	4.8 [0.20] 5.5 [0.60] 5.8 [0.20]	3 [1.00]	none	No	No	No
50	Grenville Province	NA	4.8 [0.20] 5.5 [0.60] 5.8 [0.20]	2 [1.00]	none	No	No	No

a) Pa = probability of activity (from EPRI NP-6452-D 1989) (Reference 207)

b) Maximum Magnitude (Mmax) and weights (from EPRI NP-6452-D 1989)

c) Smoothing options are defined as follows (from EPRI NP-6452-D 1989):
1, 6, 7, 8 = a, b values as listed above, with weights shown;
3 = Low smoothing on a, constant b (strong prior of 1.0);
5 = a, b values as listed above, with weights shown.

d) ME = mutually exclusive; PD = perfectly dependent

e) No, unless (1) new geometry proposed in literature or (2) new seismicity pattern

f) No, unless (1) new data suggests Mmax exceeds or differs significantly from the EPRI Mmax distribution or (2) exceeded by historical seismicity.

g) RI = recurrence interval; assumed no change if no new paleoseismic data or rate of seismicity has not significantly changed

h) Replace this source with the Updated Charleston Seismic Source (UCSS) Model - original Charleston sources shown in bold.

TABLE 2.5.2-206 (Sheet 1 of 4)
SUMMARY OF EPRI SEISMIC SOURCES - WESTON GEOPHYSICAL

WLS COL 2.5-2

Source	Description	Pa[a]	Mmax (m_b) and Weights[b]	Smoothing Options and Weights[c]	Inter-dependencies[d]	Geom.[e]	Mmax[f]	RI[g]
Primary sources that contribute to 99% of hazard								
23	Giles County	0.90	6.0 [0.81] 6.6 [0.19]	1b [1.00]	Contained in 103	No	No	No
24	New York-Alabama-Clingman	0.90	5.4 [0.26] 6.0 [0.58] 6.6 [0.16]	1b [1.00]	Contained in 103	No	No	No
25	**Charleston, SC**	0.99	6.6 [0.90] 7.2 [0.10]	1b [1.00]	none	**Yes**[h]	**Yes**[h]	**Yes**[h]
26	S. Carolina	0.86	6.0 [0.67] 6.6 [0.27] 7.2 [0.06]	1b [1.00]	none	No	No	No
103	S. Appalachians	1.00	5.4 [0.26] 6.0 [0.58] 6.6 [0.16]	1a [0.20] 2a [0.80]	Background; P_B=1.00	No	No	No
C17	103-23	NA	5.4 [0.26] 6.0 [0.58] 6.6 [0.16]	1a [0.70] 2a [0.30]	NA	No	No	No
C18	103-24	NA	5.4 [0.26] 6.0 [0.58] 6.6 [0.16]	1a [0.70] 1b [0.30]	NA	No	No	No

TABLE 2.5.2-206 (Sheet 2 of 4)
SUMMARY OF EPRI SEISMIC SOURCES - WESTON GEOPHYSICAL

WLS COL 2.5-2

Source	Description	Pa[a]	Mmax (m_b) and Weights[b]	Smoothing Options and Weights[c]	Inter-dependencies[d]	Geom.[e]	Mmax[f]	RI[g]
C19	103-23-24	NA	5.4 [0.26] 6.0 [0.58] 6.6 [0.16]	1a [1.00]	NA	No	No	No
C33	26-25	NA	6.6 [0.90] 7.2 [0.10]	1b [1.00]	NA	No	No	No
Additional sources that do not contribute to 99% of hazard								
104	S. Coastal Plain	1.00	5.4 [0.24] 6.0 [0.61] 6.6 [0.15]	1a [0.20] 2a [0.80]	Background; P_B=1.00	No	No	No
C01	28A through E	NA	5.4 [0.65] 6.0 [0.25] 6.6 [0.10]	1b [1.00]	NA	No	No	No
C20	104-22	NA	6.0 [0.85] 6.6 [0.15]	1a [0.30] 2a [0.70]	NA	No	No	No
C21	104-25	NA	5.4 [0.24] 6.0 [0.61] 6.6 [0.15]	1a [0.30] 2a [0.70]	NA	No	No	No
C22	104-26	NA	5.4 [0.24] 6.0 [0.61] 6.6 [0.15]	1a [0.30] 1b [0.70]	NA	No	No	No

TABLE 2.5.2-206 (Sheet 3 of 4)
SUMMARY OF EPRI SEISMIC SOURCES - WESTON GEOPHYSICAL

WLS COL 2.5-2

Source	Description	Pa[a]	Mmax (m_b) and Weights[b]	Smoothing Options and Weights[c]	Inter-dependencies[d]	Geom.[e]	Mmax[f]	RI[g]
C23	104-22-26	NA	5.4 [0.80] 6.0 [0.14] 6.6 [0.06]	1a [0.50] 2a [0.50]	NA	No	No	No
C24	104-22-25	NA	5.4 [0.80] 6.0 [0.14] 6.6 [0.06]	1a [0.50] 2a [0.50]	NA	No	No	No
C25	104-28BCDE	NA	5.4 [0.26] 6.0 [0.58] 6.6 [0.16]	1a [0.30] 2a [0.70]	NA	No	No	No
C26	104-28BCDE-22	NA	5.4 [0.24] 6.0 [0.61] 6.6 [0.15]	1a [0.30] 2a [0.70]	NA	No	No	No
C27	104-28BCDE-22-25	NA	5.4 [0.30] 6.0 [0.70]	1a [0.70] 2a [0.30]	NA	No	No	No
C28	104-28BCDE-22-26	NA	5.4 [0.30] 6.0 [0.70]	1a [0.70] 2a [0.30]	NA	No	No	No

TABLE 2.5.2-206 (Sheet 4 of 4)
SUMMARY OF EPRI SEISMIC SOURCES - WESTON GEOPHYSICAL

WLS COL 2.5-2

Source	Description	Pa[a]	Mmax (m_b) and Weights[b]	Smoothing Options and Weights[c]	Inter-dependencies[d]	Geom.[e]	Mmax[f]	RI[g]
C34	104-28BE-26	NA	5.4 [0.24] 6.0 [0.61] 6.6 [0.15]	1a [0.20] 1b [0.80]	NA	No	No	No
C35	104-28BE-25	NA	5.4 [0.24] 6.0 [0.61] 6.6 [0.15]	1a [0.20] 1b [0.80]	NA	No	No	No

a) Pa = probability of activity (from EPRI NP-6452-D 1989) (Reference 207)

b) Maximum Magnitude (Mmax) and weights (from EPRI NP-6452-D 1989)

c) Smoothing options are defined as follows (from EPRI NP-6452-D 1989):
1a = Constant a, constant b (medium prior of 1.0);
1b = Constant a, constant b (medium prior of 0.9);
1c = Constant a, constant b (medium prior of 0.7);
2a = Medium smoothing on a, medium smoothing on b (medium prior of 1.0);
2b = Medium smoothing on a, medium smoothing on b (medium prior of 0.9);
2c = Medium smoothing on a, medium smoothing on b (medium prior of 0.7).

d) ME = mutually exclusive; PD = perfectly dependent

e) No, unless (1) new geometry proposed in literature or (2) new seismicity pattern

f) No, unless (1) new data suggests Mmax exceeds or differs significantly from the EPRI Mmax distribution or (2) exceeded by historical seismicity.

g) RI = recurrence interval; assumed no change if no new paleoseismic data or rate of seismicity has not significantly changed

h) Replace this source with the Updated Charleston Seismic Source (UCSS) Model - original Charleston sources shown in bold.

TABLE 2.5.2-207 (Sheet 1 of 2)
SUMMARY OF EPRI SEISMIC SOURCES - WOODWARD-CLYDE CONSULTANTS

WLS COL 2.5-2

Source	Description	Pa[a]	Mmax (m_b) and Weights[b]	Smoothing Options and Weights[c]	Inter-dependencies[d]	Geom.[e]	Mmax[f]	RI[g]
Primary sources that contribute to 99% of hazard								
29	**S. Carolina Gravity Saddle (Extended)**	0.122	6.7 [0.33] 7.0 [0.34] 7.4 [0.33]	2 [0.25] 3 [0.25] 4 [0.25] 5 [0.25]	ME with 29A, 29B, 30	**Yes**[h]	**Yes**[h]	**Yes**[h]
29A	**SC Gravity Saddle No. 2 (Combo C3)**	0.305	6.7 [0.33] 7.0 [0.34] 7.4 [0.33]	2 [0.25] 3 [0.25] 4 [0.25] 5 [0.25]	ME with 29, 29B, 30	**Yes**[h]	**Yes**[h]	**Yes**[h]
29B	SC Gravity Saddle No. 3 (NW portion)	0.183	5.4 [0.33] 6.0 [0.34] 7.0 [0.33]	2 [0.25] 3 [0.25] 4 [0.25] 5 [0.25]	ME with 29, 29A	No	No	No
30	**Charleston (includes NOTA)**	0.573	6.8 [0.33] 7.3 [0.34] 7.5 [0.33]	2 [0.25] 3 [0.25] 4 [0.25] 5 [0.25]	ME with 29, 29A	**Yes**[h]	**Yes**[h]	**Yes**[h]
31	Blue Ridge Combo.	0.024	5.9 [0.33] 6.3 [0.34] 7.0 [0.33]	2 [0.25] 3 [0.25] 4 [0.25] 5 [0.25]	ME with 31A	No	No	No
31A	Blue Ridge - Alternate Configuration	0.211	5.9 [0.33] 6.3 [0.34] 7.0 [0.33]	2 [0.10] 3 [0.10] 4 [0.10] 5 [0.10] 9 [0.60] (a=-1.005, b=0.852)	ME with 31	No	No	No

TABLE 2.5.2-207 (Sheet 2 of 2)
SUMMARY OF EPRI SEISMIC SOURCES - WOODWARD-CLYDE CONSULTANTS

WLS COL 2.5-2

Source	Description	Pa[a]	Mmax (m_b) and Weights[b]	Smoothing Options and Weights[c]	Inter-dependencies[d]	Geom.[e]	Mmax[f]	RI[g]
BG-CH	Lee Nuclear Station Background	NA	5.8 [0.33] 6.2 [0.34] 6.6 [0.33]	1 [0.25] 6 [0.25] 7 [0.25] 8 [0.25]	NA	No	No	No

Additional sources that do not contribute to 99% of hazard: **None**

a) Pa = probability of activity (from EPRI NP-6452-D 1989) (Reference 207)
b) Maximum Magnitude (Mmax) and weights (from EPRI NP-6452-D 1989)
c) Smoothing options are defined as follows (from EPRI NP-6452-D 1989):
1 = Low smoothing on a, high smoothing on b (no prior);
2 = High smoothing on a, high smoothing on b (no prior);
3 = High smoothing on a, high smoothing on b (moderate prior of 1.0);
4 = High smoothing on a, high smoothing on b (moderate prior of 0.9);
5 = High smoothing on a, high smoothing on b (moderate prior of 0.8);
6 = Low smoothing on a, high smoothing on b (moderate prior of 1.0);.
7 = Low smoothing on a, high smoothing on b (moderate prior of 0.9);
8 = Low smoothing on a, high smoothing on b (moderate prior of 0.8). Weights on magnitude intervals are all 1.0.
9 = a and b values as listed.
d) ME = mutually exclusive; PD = perfectly dependent
e) No, unless (1) new geometry proposed in literature or (2) new seismicity pattern
f) No, unless (1) new data suggests Mmax exceeds or differs significantly from the EPRI Mmax distribution or (2) exceeded by historical seismicity.
g) RI = recurrence interval; assumed no change if no new paleoseismic data or rate of seismicity has not significantly changed
h) Replace this source with the Updated Charleston Seismic Source (UCSS) Model - original Charleston sources shown in bold.

TABLE 2.5.2-208 (Sheet 1 of 2)
CONVERSION BETWEEN BODY-WAVE (m_b) AND MOMENT (**M**) MAGNITUDES[(a)]

WLS COL 2.5-2

Convert: m_b	To: M	Convert: M	To: m_b
4.00	3.77	4.00	4.28
4.10	3.84	4.10	4.41
4.20	3.92	4.20	4.54
4.30	4.00	4.30	4.66
4.40	4.08	4.40	4.78
4.50	4.16	4.50	4.90
4.60	4.24	4.60	5.01
4.70	4.33	4.70	5.12
4.80	4.42	4.80	5.23
4.90	4.50	4.90	5.33
5.00	4.59	5.00	5.43
5.10	4.69	5.10	5.52
5.20	4.78	5.20	5.61
5.30	4.8	5.30	5.70
5.40	4.97	5.40	5.78
5.50	5.08	5.50	5.87
5.60	5.19	5.60	5.95
5.70	5.31	5.70	6.03
5.80	5.42	5.80	6.11
5.90	5.54	5.90	6.18
6.00	5.66	6.00	6.26
6.10	5.79	6.10	6.33
6.20	5.92	6.20	6.40
6.30	6.06	6.30	6.47
6.40	6.20	6.40	6.53
6.50	6.34	6.50	6.60
6.60	6.49	6.60	6.66
6.70	6.65	6.70	6.73
6.80	6.82	6.80	6.79
6.90	6.98	6.90	6.85
7.00	7.16	7.00	6.91
7.10	7.33	7.10	6.97
7.20	7.51	7.20	7.03
7.30	7.69	7.30	7.09
7.40	7.87	7.40	7.15
7.50	8.04	7.50	7.20

TABLE 2.5.2-208 (Sheet 2 of 2)
CONVERSION BETWEEN BODY-WAVE (M_b) AND MOMENT (**M**) MAGNITUDES[(a)]

Convert: m_b	To: M	Convert: M	To: m_b
		7.60	7.26
		7.70	7.32
		7.80	7.37
		7.90	7.43
		8.00	7.49

a) Average of relations given by Atkinson and Boore (1995) (Reference 208), EPRI TR-102293 (1993) (Reference 273), and Frankel et al. (1996) (Reference 209)

TABLE 2.5.2-209
SUMMARY OF USGS SEISMIC SOURCES

WLS COL 2.5-2

Source	Mmax (M) and Wts.	Largest Mmax Value Considered by USGS M	m_b[1]
Sources within 200 mi (320 km)			
Extended Margin Background	7.5 [1.00]	7.5	7.2
Charleston	**6.8 [0.20]** **7.1 [0.20]** **7.3 [0.45]** **7.5 [0.15]**	**7.5**	**7.2**
Eastern Tennessee	7.5 [1.00]	7.5	7.2
Selected Sources Beyond 200 mi (320km)			
New Madrid	7.3 [0.15] 7.5 [0.20] 7.7 [0.50] 8.0 [0.15]	8.0	7.5
Stable Craton Background	7.0 [1.00]	7.0	6.9

Notes:

Data from Frankel et al. (2002) (Reference 210)

1 mb converted from **M** using average of Atkinson and Boore (1995) (Reference 208), EPRI TR-102293 (1993) (Reference 273), and Frankel et al. (1996) (Reference 209)

TABLE 2.5.2-210 (Sheet 1 of 2)
SCDOT SEISMIC SOURCE ZONE PARAMETERS

						Mmax[2]
Charleston Characteristic Sources			Mean Recurrence		m_{blg}	M
		Charleston Area Source	550 years		nr	7.1 [.2] 7.3 [.6] 7.5 [.2]
WLS COL 2.5-2		ZRA Fault Source (Zone of River Anomalies)	550 years		nr	7.1 [.2] 7.3 [.6] 7.5 [.2]
		Ashley River-Woodstock Fault Source (modeled as 3 parallel faults)	550 years		nr	7.1 [.2] 7.3 [.6] 7.5 [.2]
Non-Characteristic Background Sources			a^1	b^1	m_{blg}	M
	1.	Zone1	0.242	0.84	6.84	7.00
	2.	Zone2	-0.270	0.84	6.84	7.00
	3.	Central Virginia	1.184	0.64	6.84	7.00
	4.	Zone4	0.319	0.84	6.84	7.00
	5.	Zone5	0.596	0.84	6.84	7.00
	6.	Piedmont and Coastal Plain	1.537	0.84	6.84	7.00
	6a.	Pied&CP NE	0.604	0.84	6.84	7.00
	6b.	Pied&CP SW	1.312	0.84	6.84	7.00
	7.	South Carolina Piedmont	2.220	0.84	6.84	7.00
	8.	Middleton Place	1.690	0.77	6.84	7.00
	9.	Florida and continental margin	1.371	0.84	6.84	7.00
	10.	Alabama	1.800	0.84	6.84	7.00
	11.	Eastern Tennessee	2.720	0.90	6.84	7.00
	12.	Southern Appalachian	2.420	0.84	6.84	7.00
	12.a.	Southern Appalachian North	2.185	0.84	6.84	7.00

TABLE 2.5.2-210 (Sheet 2 of 2)
SCDOT SEISMIC SOURCE ZONE PARAMETERS

Charleston Characteristic Sources		Mean Recurrence		m_{blg}	Mmax[2] M
13.	Giles County, VA	1.070	0.84	6.84	7.00
14.	Central Appalachians	1.630	0.84	6.84	7.00
15.	Western Tennessee	2.431	1.00	6.84	7.00
16.	Central Tennessee	2.273	1.00	6.84	7.00
17.	Ohio-Kentucky	2.726	1.00	6.84	7.00
18.	West VA-Pennsylvania	2.491	1.00	6.84	7.00
19.	USGS (1996) gridded seismicity rates and b value	nr	0.95	6.84	7.00

Notes:

1 a and b values in terms of m_{blg} magnitude, reported in Chapman and Talwani (2002) (Reference 211).

2 Mmax range for characteristic events was designed to "represent the range of magnitude estimates of the 1886 Charleston shock proposed by Johnston (1996)" (Reference 231) (Chapman and Talwani 2000, p. 12) (Reference 211). Square brackets indicate weights assigned to characteristic magnitudes. For non-characteristic background events, a truncated form of the exponential probability density function was used (Chapman and Talwani 2002, p. 6-7).

nr = not reported

TABLE 2.5.2-211 (Sheet 1 of 2)
COMPARISON OF EPRI CHARACTERIZATIONS OF THE CHARLESTON SEISMIC ZONE

WLS COL 2.5-2

EST	Source	Description	Pa[a]	Mmax (m_b) and Wts.[b]	Mmax (**M**) and Wts.[b]	Upper Bound Mmax m_b	Upper Bound Mmax M[c]	Weighted Mean Mmax m_b	Weighted Mean Mmax M[c]
Bechtel	H	Charleston Area	0.50	6.8 [0.20] 7.1 [0.40] 7.4 [0.40]	6.82 [0.20] 7.33 [0.40] 7.87 [0.40]	7.4	7.9	7.2	7.4
	N3	Charleston Faults	0.53	6.8 [0.20] 7.1 [0.40] 7.4 [0.40]	6.82 [0.20] 7.33 [0.40] 7.87 [0.40]	7.4	7.9	7.2	7.4
	BZ4	Atlantic Coastal Region	1.00	6.6 [0.10] 6.8 [0.40] 7.1 [0.40] 7.4 [0.10]	6.49 [0.10] 6.82 [0.40] 7.33 [0.40] 7.87 [0.10]	7.4	7.9	7.0	7.1
Dames & Moore	54	Charleston Seismic Zone	1.00	6.6 [0.75] 7.2 [0.25]	6.49 [0.75] 7.51 [0.25]	7.2	7.5	6.8	6.7
Law Engineering	35	Charleston Seismic Zone	0.45	6.8 [1.00]	6.82 [1.00]	6.8	6.8	6.8	6.8
Rondout Associates	24	Charleston	1.00	6.6 [0.20] 6.8 [0.60] 7.0 [0.20]	6.49 [0.20] 6.82 [0.60] 7.16 [0.20]	7.0	7.2	6.8	6.8
Weston Geophysical	25	Charleston Seismic Zone	0.99	6.6 [0.90] 7.2 [0.10]	6.49 [0.90] 7.51 [0.10]	7.2	7.5	6.7	6.6

TABLE 2.5.2-211 (Sheet 2 of 2)
COMPARISON OF EPRI CHARACTERIZATIONS OF THE CHARLESTON SEISMIC ZONE

WLS COL 2.5-2

EST	Source	Description	Pa[a]	Mmax (m_b) and Wts.[b]	Mmax (**M**) and Wts.[b]	Upper Bound Mmax m_b	Upper Bound Mmax M[c]	Weighted Mean Mmax m_b	Weighted Mean Mmax M[c]
Woodward-Clyde Consultants	29	S. Carolina Gravity Saddle (Extended)	0.122	6.7 [0.33] 7.0 [0.34] 7.4 [0.33]	6.65 [0.33] 7.16 [0.34] 7.87 [0.33]	7.4	7.9	7.0	7.2
	29A	SC Gravity Saddle No. 2 (Combo C3)	0.305	6.7 [0.33] 7.0 [0.34] 7.4 [0.33]	6.65 [0.33] 7.16 [0.34] 7.87 [0.33]	7.4	7.9	7.0	7.2
	30	Charleston (includes NOTA)	0.573	6.8 [0.33] 7.3 [0.34] 7.5 [0.33]	6.82 [0.33] 7.69 [0.34] 8.04 [0.33]	7.5	8.0	7.2	7.5

Composite Range of Mmax Values for all EPRI ESTs = m_b 6.6 - 7.5 (**M** 6.5 - 8.0)

a) Pa = probability of activity; from EPRI NP-6452-D 1989 (Reference 207)

b) Maximum Magnitude (Mmax) and weights (wts.) from EPRI NP-6452-D 1989 (Reference 207)

c) Moment magnitude (**M**) converted from body wave magnitude (mb) using average of Atkinson and Boore (Reference 208), EPRI TR-102293 (1993) (Reference 273), and Frankel et al. (1996) (Reference 209)

TABLE 2.5.2-212
GEOGRAPHIC COORDINATES (LATITUDE AND LONGITUDE)
OF CORNER POINTS OF UPDATED CHARLESTON SEISMIC
SOURCE (UCSS) GEOMETRIES

	Source Geometry	Longitude (decimal degrees)	Latitude (decimal degrees)
	A	-80.707	32.811
	A	-79.840	33.354
WLS COL 2.5-2	A	-79.527	32.997
	A	-80.392	32.455
	B	-81.216	32.485
	B	-78.965	33.891
	B	-78.3432	33.168
	B	-80.587	31.775
	B'	-78.965	33.891
	B'	-78.654	33.531
	B'	-80.900	32.131
	B'	-81.216	32.485
	C	-80.397	32.687
	C	-79.776	34.425
	C	-79.483	34.351
	C	-80.109	32.614

TABLE 2.5.2-213 (Sheet 1 of 2)
LOCAL CHARLESTON-AREA TECTONIC FEATURES

Name of Feature	Evidence	Key References
Adams Run fault	**subsurface stratigraphy**	**Weems and Lewis (2002)** (Reference 252)
Ashley River fault	microseismicity	Talwani (1982, 2000) (References 253 and 254) Weems and Lewis (2002) (Reference 252)
Appalachian detachment (decollement)	gravity & magnetic data, seismic reflection & refraction	Cook et al. (1979, 1981) (Reference 255 and 256) Behrendt et al. (1981, 1983) (References 257 and 258) Seeber and Armbruster (1981) (Reference 259)
Blake Spur fracture zone	oceanic transform postulated to extend westward to Charleston	Seeber and Armbruster (1981) (Reference 259)
Bowman seismic zone	microseismicity	Smith and Talwani (1985) (Reference 260)
Charleston fault	subsurface stratigraphy	Lennon (1986) (Reference 261) Talwani (2000) (Reference 254) Weems and Lewis (2002) (Reference 252)
Cooke fault	seismic reflection	Behrendt et al. (1981, 1983) (References 257 and 258) Hamilton et al. (1983) (Reference 262) Wentworth and Mergner-Keefer (1983) (Reference 263) Behrendt and Yuan (1987) (Reference 223)
Drayton fault	seismic reflection	Hamilton et al. (1983) (Reference 262) Behrendt et al. (1983) (Reference 258) Behrendt and Yuan (1987) (Reference 223)

WLS COL 2.5-2

TABLE 2.5.2-213 (Sheet 2 of 2)
LOCAL CHARLESTON-AREA TECTONIC FEATURES

Name of Feature	Evidence	Key References
East Coast fault system/ Zone of river anomalies (ZRA)	**geomorphology seismic reflection microseismicity**	**Marple and Talwani (1993)** (Reference 264) **Marple and Talwani (2000, 2004)** (References 226 and 265)
Gants fault	seismic reflection	Hamilton et al. (1983) (Reference 262) Behrendt and Yuan (1987) (Reference 223)
Helena Banks fault zone	seismic reflection	Behrendt et al. (1981, 1983) (References 257 and 258) Behrendt and Yuan (1987) (Reference 223)
Middleton Place-Summerville seismic zone	microseismicity	Tarr et al. (1981) (Reference 215) Madabhushi and Talwani (1993) (Reference 216)
Sawmill Branch fault	**microseismicity**	**Talwani and Katuna (2004)** (Reference 266)
Summerville fault	**microseismicity**	**Weems et al. (1997)** (Reference 267)
Woodstock fault	geomorphology microseismicity	Talwani (1982, 1999) (References 253 and 268) Marple and Talwani (2000) (Reference 226)

Notes:

Those tectonic features identified following publication of the EPRI teams' reports (post-1986) are highlighted by **bold-face** type.

TABLE 2.5.2-214
COMPARISON OF POST-EPRI MAGNITUDE ESTIMATES FOR THE 1886 CHARLESTON EARTHQUAKE

Study	Magnitude Estimation Method	Reported Magnitude Estimate	Assigned Weights	Mean Magnitude (**M**)
Johnston et al. (1994) (Reference 269)	worldwide survey of passive-margin, extended-crust earthquakes	**M**7.56 ± 0.35 (a)	--	7.56
Martin and Clough (1994) (Reference 270)	geotechnical assessment of 1886 liquefaction data	**M**7 - 7.5	--	7.25
WLS COL 2.5-2 Johnston (1996) (Reference 231)	isoseismal area regression, accounting for eastern North America anelastic attenuation	**M**7.3 ± 0.26	--	7.3
Chapman and Talwani (2002) (SCDOT) (Reference 211)	consideration of available magnitude estimates	**M**7.1 **M**7.3 **M**7.5	0.2 0.6 0.2	7.3
Frankel et al. (2002) (USGS) (Reference 210)	consideration of available magnitude estimates	**M**6.8 **M**7.1 **M**7.3 **M**7.5	0.20 0.20 0.45 0.15	7.2
Bakun and Hopper (2004) (Reference 232)	isoseismal area regression, including empirical site corrections	M_I 6.4 - 7.2 (b)	--	6.9 (c)

a) Estimate from Johnston et al. (1994) Chapter 3 (Reference 269).

b) 95% confidence interval estimate; M_I (intensity magnitude) is considered equivalent to **M** (Bakun and Hopper 2004) (Reference 232).

c) Bakun and Hopper's (2004) (Reference 232) *preferred* estimate.

WLS COL 2.5-2

TABLE 2.5.2-215
COMPARISON OF TALWANI AND SCHAEFFER (2001) AND UCSS AGE CONSTRAINTS ON CHARLESTON-AREA PALEOLIQUEFACTION EVENTS

			Talwani and Schaeffer (2001) [a]				
			scenario 1		scenario 2		(this study)
	Liquefaction Event	Event Age (YBP) [b]	Source	M	Source	M	Event Age (YBP) [b], [c]
	1886 A.D.	64	Charleston	7.3	Charleston	7.3	64
	A	546 ± 17	Charleston	7+	Charleston	7+	600 ± 70
	B	1,021 ± 30	Charleston	7+	Charleston	7+	1,025 ± 25
WLS COL 2.5-2	C	1,648 ± 74	*Northern*	6+	--	--	--
	C'	1,683 ± 70	--		Charleston	7+	1,695 ± 175
	D	1,966 ± 212	*Southern*	6+	--	--	--
	E	3,548 ± 66	Charleston	7+	Charleston	7+	3,585 ± 115
	F	5,038 ± 166	*Northern*	6+	Charleston	7+	--
	F'	--	--	--	--	--	5,075 ± 215
	G	5,800 ± 500	Charleston	7+	Charleston	7+	--

a) Modified after Talwani and Schaeffer's (2001) (Reference 222) Table 2.

b) Years before present, relative to 1950 A.D.

c) Event ages based upon our recalibration of radiocarbon to 2-sigma using OxCal 3.8 (References 271 and 272) data presented in Talwani and Schaeffer's (2001) Table 2.

WLS COL 2.5-2

TABLE 2.5.2-216
COMPARISON OF MEAN ANNUAL FREQUENCIES OF EXCEEDANCE CALCULATED USING 1989 EPRI ASSUMPTIONS TO RESULTS AT NEARBY SITES PUBLISHED IN THE 1989 EPRI STUDY

	Mean Annual Frequency of Exceedance for varying PGA amplitudes, cm/sec^2			
Site	50 cm/sec^2	100 cm/sec^2	250 cm/sec^2	500 cm/sec^2
Lee	2.01E-3	5.13E-4	5.96E-5	8.24-6
Catawba	9.70E-4	3.00E-4	4.50E-5	6.50E-6
% difference	107%	71%	32%	27%
McGuire	8.70E-4	2.30E-4	2.80E-5	3.40E-6
% difference	131%	123%	113%	142%
Oconee	1.40E-3	4.40E-4	5.90E-5	8.00E-6
% difference	44%	17%	1%	3%

WLS COL 2.5-2

TABLE 2.5.2-217
UHRS AMPLITUDES FOR 10^{-4}, 10^{-5}, AND 10^{-6}

	URHS results, g		
ground motion frequency	mean 10^{-4}	mean 10^{-5}	mean 10^{-6}
0.5 Hz	0.0218	0.123	0.284
1 Hz	0.0423	0.160	0.343
2.5 Hz	0.0946	0.307	0.705
5 Hz	0.152	0.527	1.35
10 Hz	0.197	0.82	2.23
25 Hz	0.249	1.29	3.91
PGA	0.104	0.471	1.35

WLS COL 2.5-2

TABLE 2.5.2-218
CONTROLLING EARTHQUAKES FROM DEAGGREGATION

	10^{-4}		10^{-5}		10^{-6}	
	1 & 2.5 Hz	5 & 10 Hz	1 & 2.5 Hz	5 & 10 Hz	1 & 2.5 Hz	5 & 10 Hz
mean **M** (overall)	7.0	6.6	6.9	5.8	6.6	5.7
mean R (overall)	300	210	270	52	180	19
mean **M** [for R>62 mi. (100 km)]	7.3	7.2	7.4	7.2	7.5	7.3
mean R [for R>62 mi. (100 km)]	380	330	430	300	470	270

WLS COL 2.5-2

TABLE 2.5.2-219 (Sheet 1 of 2)
HORIZONTAL UHRS AND GMRS AMPLITUDES

Frequency Hz	10^{-4} Horizontal UHRS, g	10^{-5} Horizontal UHRS, g	AR	DF	Horizontal GMRS, g
100	1.04E-01	4.71E-01	4.523	2.007	2.12E-01
90	1.14E-01	5.21E-01	4.583	2.028	2.35E-01
80	1.30E-01	6.05E-01	4.650	2.052	2.72E-01
70	1.55E-01	7.33E-01	4.725	2.078	3.30E-01
60	1.87E-01	8.98E-01	4.810	2.108	4.04E-01
50	2.17E-01	1.07E+00	4.908	2.142	4.80E-01
45	2.30E-01	1.14E+00	4.962	2.161	5.13E-01
40	2.39E-01	1.20E+00	5.020	2.181	5.40E-01
35	2.45E-01	1.25E+00	5.081	2.202	5.60E-01
30	2.48E-01	1.28E+00	5.141	2.223	5.75E-01
25	2.49E-01	1.29E+00	5.193	2.241	5.81E-01
20	2.42E-01	1.21E+00	4.991	2.171	5.43E-01
15	2.27E-01	1.06E+00	4.675	2.060	4.77E-01
12.5	2.14E-01	9.54E-01	4.447	1.980	4.29E-01
10	1.97E-01	8.20E-01	4.152	1.874	3.70E-01
9	1.91E-01	7.73E-01	4.043	1.834	3.51E-01
8	1.84E-01	7.21E-01	3.921	1.790	3.29E-01
7	1.75E-01	6.63E-01	3.785	1.740	3.05E-01
6	1.65E-01	5.99E-01	3.634	1.685	2.77E-01
5	1.52E-01	5.27E-01	3.467	1.622	2.47E-01
4	1.33E-01	4.43E-01	3.332	1.571	2.09E-01
3	1.09E-01	3.45E-01	3.161	1.506	1.64E-01
2.5	9.46E-02	3.07E-01	3.246	1.539	1.46E-01

WLS COL 2.5-2

TABLE 2.5.2-219 (Sheet 2 of 2)
HORIZONTAL UHRS AND GMRS AMPLITUDES

Frequency Hz	10^{-4} Horizontal UHRS, g	10^{-5} Horizontal UHRS, g	AR	DF	Horizontal GMRS, g
2	8.20E-02	2.78E-01	3.387	1.592	1.31E-01
1.5	6.47E-02	2.31E-01	3.561	1.657	1.07E-01
1.25	5.40E-02	1.98E-01	3.666	1.696	9.17E-02
1	4.23E-02	1.60E-01	3.789	1.742	7.36E-02
0.9	3.85E-02	1.58E-01	4.121	1.863	7.16E-02
0.8	3.45E-02	1.54E-01	4.467	1.987	6.93E-02
0.7	3.04E-02	1.47E-01	4.830	2.115	6.60E-02
0.6	2.61E-02	1.36E-01	5.216	2.249	6.13E-02
0.5	2.18E-02	1.23E-01	5.633	2.392	5.53E-02
0.4	1.74E-02	9.82E-02	5.633	2.392	4.42E-02
0.3	1.31E-02	7.37E-02	5.633	2.392	3.32E-02
0.2	8.72E-03	4.91E-02	5.633	2.392	2.21E-02
0.15	6.54E-03	3.68E-02	5.633	2.392	1.66E-02
0.125	5.45E-03	3.07E-02	5.633	2.392	1.38E-02
0.1	3.49E-03	1.96E-02	5.633	2.392	8.84E-03

WLS COL 2.5-2

TABLE 2.5.2-220 (Sheet 1 of 2)
VERTICAL UHRS AND GMRS AMPLITUDES

Frequency (Hz)	10^{-4} Vertical UHRS, g	10^{-5} Vertical UHRS, g	AR	DF	Vertical GMRS, g
100	8.60E-02	3.88E-01	4.51	2.00	1.74E-01
90	9.80E-02	4.53E-01	4.62	2.04	2.04E-01
80	1.13E-01	5.39E-01	4.75	2.09	2.43E-01
70	1.34E-01	6.57E-01	4.91	2.14	2.96E-01
60	1.62E-01	8.25E-01	5.09	2.21	3.71E-01
50	2.03E-01	1.08E+00	5.32	2.28	4.86E-01
45	2.02E-01	1.10E+00	5.42	2.32	4.93E-01
40	2.02E-01	1.11E+00	5.53	2.36	5.01E-01
35	2.01E-01	1.14E+00	5.66	2.40	5.11E-01
30	2.02E-01	1.12E+00	5.52	2.35	5.02E-01
25	2.05E-01	1.08E+00	5.29	2.27	4.87E-01
20	1.92E-01	9.63E-01	5.02	2.18	4.33E-01
15	1.76E-01	8.29E-01	4.70	2.07	3.73E-01
12.5	1.67E-01	7.54E-01	4.51	2.00	3.39E-01
10	1.57E-01	6.71E-01	4.28	1.92	3.02E-01
9	1.50E-01	6.26E-01	4.18	1.88	2.83E-01
8	1.42E-01	5.79E-01	4.07	1.84	2.63E-01
7	1.34E-01	5.31E-01	3.94	1.80	2.42E-01
6	1.26E-01	4.79E-01	3.81	1.75	2.20E-01
5	1.16E-01	4.25E-01	3.65	1.69	1.97E-01
4	9.91E-02	3.56E-01	3.59	1.67	1.65E-01
3	8.07E-02	2.84E-01	3.52	1.64	1.32E-01
2.5	7.08E-02	2.46E-01	3.47	1.62	1.15E-01

WLS COL 2.5-2

TABLE 2.5.2-220 (Sheet 2 of 2)
VERTICAL UHRS AND GMRS AMPLITUDES

Frequency (Hz)	10^{-4} Vertical UHRS, g	10^{-5} Vertical UHRS, g	AR	DF	Vertical GMRS, g
2	5.82E-02	2.08E-01	3.57	1.66	9.68E-02
1.5	4.53E-02	1.68E-01	3.71	1.71	7.76E-02
1.25	3.86E-02	1.47E-01	3.80	1.74	6.74E-02
1	3.18E-02	1.24E-01	3.91	1.78	5.68E-02
0.9	2.87E-02	1.19E-01	4.15	1.87	5.43E-02
0.8	2.57E-02	1.14E-01	4.44	1.98	5.18E-02
0.7	2.26E-02	1.08E-01	4.79	2.10	4.90E-02
0.6	1.95E-02	1.02E-01	5.23	2.25	4.60E-02
0.5	1.64E-02	9.48E-02	5.80	2.45	4.27E-02
0.4	1.32E-02	7.48E-02	5.66	2.40	3.37E-02
0.3	1.01E-02	5.51E-02	5.48	2.34	2.48E-02
0.2	6.83E-03	3.58E-02	5.24	2.26	1.61E-02
0.15	5.20E-03	2.64E-02	5.08	2.20	1.19E-02
0.125	4.37E-03	2.17E-02	4.97	2.17	9.78E-03
0.1	2.95E-03	1.49E-02	5.03	2.19	6.69E-03

WLS COL 2.5-2

TABLE 2.5.2-221
POINT SOURCE PARAMETERS

M 5.1, single-corner

G(g)	Distance, mi. [km]	Depth, mi. [km]
1.50	0 [0]	1.25 [2]
1.25	0 [0]	1.25 [2]
1.00	0 [0]	2.5 [3]
0.75	0 [0]	2.5 [8]
0.50	0 [0]	3 [5]
0.40	0 [0]	4 [6]
0.30	0 [0]	5 [8]
0.20	4 [7]	5 [8]
0.10	10 [16]	5 [8]
0.05	17 [27]	5 [8]
0.01	50 [80]	5 [8]

Notes: Additional parameters used in each model are:

$Q = 670\ f^{0.33}$
$\Delta\sigma$ (1c) = 110 bars
k = 0.006 sec, hard rock

Hard Rock Crustal Model

Thickness, mi. [km]	Vs (km/sec)	Vp (km/sec)	ρ (cgs)
0.6 [1]	2.83	4.90	2.52
7 [1]	3.52	6.10	2.71
17 [28]	3.75	6.50	2.78
[infinite]	4.62	8.00	3.35

WLS COL 2.5-2

TABLE 2.5.2-222
WEIGHTING SCHEME TO DEVELOP V/H RATIOS

	Weighting		Empirical Relation Weights		Site Condition Weights	
Profile	Empirical	Model	A&S (1997)	C&B (2003)	Soft Rock	Soil
A1	0.2	0.8	0.5	0.5	1.0	0.0

Notes:

A&S (1997) = Abrahamson and Silva (1997) (Reference 296)
C&B (2003) = Campbell and Bozorgnia (2003) (Reference 298)

TABLE 2.5.2-223
MOMENT MAGNITUDE, DISTANCE RANGES, AND WEIGHTS
FOR V/H RATIOS

Empirical V/H Ratio Weights

	High-Frequency ≥ 5.0 Hz			Low-Frequency ≤ 2.5 Hz		
	Magnitude (**M**)			Magnitude (**M**)		
APE (yr^{-1})	5.1	7.0	8.0	5.1	7.0	8.0
	weights			weights		
10^{-4}	0.37	0.37	0.26	0.20	0.40	0.40
10^{-5}	1.00	0.	0.	0.25	0.25	0.50
10^{-6}	1.00	0.	0.	0.43	0.14	0.43

Empirical V/H Ratio Distances

Magnitude (**M**)	Distance, mi. (km)
5.1	3 (5)
7.0	35 (57)
8.0	35 (57)

Model V/H Ratio Weights (**M** 5.1)

	High-Frequency ≥ 5.0 Hz			Low-Frequency ≤ 2.5 Hz		
	Distance, mi. (km)			Distance, mi. (km)		
APE (yr^{-1})	17 (28)	4 (7)	0 (0)	17 (28)	4 (7)	0 (0)
	weights			weights		
10^{-4}	0.6	0.2	0.2	0.8	0.1	0.1
10^{-5}	0.3	0.7	0.0	0.8	0.1	0.1
10^{-6}	0.1	0.6	0.3	0.4	0.3	0.3

WLS COL 2.5-2

TABLE 2.5.2-224 (Sheet 1 of 2)
FIRS AND UHRS FOR PROFILE A1

Frequency (Hz)	FIRS Horizontal SA (G)	FIRS Vertical SA (G)	UHRS(10^{-4}) Horizontal SA (G)	UHRS(10^{-4}) Vertical SA (G)	UHRS(10^{-5}) Horizontal SA (G)	UHRS(10^{-5}) Vertical SA (G)	UHRS(10^{-6}) Horizontal SA (G)	UHRS(10^{-6}) Vertical SA (G)
100	0.224	0.168	0.110	0.086	0.497	0.374	1.439	1.192
90	0.256	0.193	0.123	0.097	0.570	0.428	1.664	1.385
80	0.298	0.224	0.141	0.111	0.663	0.497	1.956	1.637
70	0.355	0.265	0.163	0.129	0.788	0.590	2.350	1.978
60	0.433	0.323	0.193	0.154	0.962	0.718	2.905	2.462
50	0.548	0.407	0.236	0.190	1.217	0.905	3.733	3.190
45	0.569	0.424	0.240	0.193	1.264	0.942	3.859	3.274
40	0.593	0.443	0.244	0.195	1.318	0.985	4.005	3.372
35	0.622	0.466	0.248	0.198	1.383	1.036	4.176	3.486
30	0.616	0.467	0.252	0.201	1.369	1.037	4.088	3.423
25	0.598	0.460	0.257	0.205	1.329	1.023	3.912	3.298
20	0.534	0.410	0.241	0.191	1.186	0.909	3.424	2.852
15	0.461	0.353	0.222	0.175	1.024	0.781	2.883	2.365
12.5	0.420	0.321	0.211	0.165	0.933	0.710	2.586	2.100
10	0.375	0.286	0.198	0.154	0.833	0.631	2.263	1.816
9	0.352	0.267	0.190	0.147	0.778	0.588	2.097	1.671
8	0.329	0.248	0.182	0.139	0.721	0.542	1.926	1.523
7	0.304	0.228	0.173	0.131	0.662	0.495	1.748	1.371
6	0.277	0.207	0.163	0.122	0.599	0.446	1.564	1.214
5	0.249	0.184	0.153	0.113	0.533	0.394	1.370	1.052
4	0.211	0.156	0.132	0.097	0.449	0.334	1.113	0.858

WLS COL 2.5-2

TABLE 2.5.2-224 (Sheet 2 of 2)
FIRS AND UHRS FOR PROFILE A1

Frequency (Hz)	FIRS Horizontal SA (G)	FIRS Vertical SA (G)	UHRS(10^{-4}) Horizontal SA (G)	UHRS(10^{-4}) Vertical SA (G)	UHRS(10^{-5}) Horizontal SA (G)	UHRS(10^{-5}) Vertical SA (G)	UHRS(10^{-6}) Horizontal SA (G)	UHRS(10^{-6}) Vertical SA (G)
3	0.170	0.127	0.109	0.080	0.360	0.269	0.852	0.659
2.5	0.148	0.111	0.096	0.071	0.313	0.235	0.719	0.558
2	0.125	0.094	0.079	0.059	0.267	0.201	0.602	0.472
1.5	0.101	0.076	0.061	0.046	0.217	0.164	0.479	0.380
1.25	0.088	0.067	0.052	0.039	0.190	0.144	0.415	0.332
1	0.074	0.057	0.043	0.032	0.162	0.123	0.347	0.281
0.9	0.071	0.054	0.039	0.029	0.155	0.118	0.337	0.269
0.8	0.068	0.051	0.034	0.026	0.148	0.112	0.325	0.257
0.7	0.064	0.048	0.030	0.023	0.141	0.106	0.313	0.244
0.6	0.060	0.045	0.026	0.019	0.133	0.099	0.299	0.230
0.5	0.056	0.041	0.022	0.016	0.124	0.092	0.284	0.215
0.4	0.044	0.033	0.018	0.013	0.098	0.073	0.226	0.171
0.3	0.033	0.024	0.014	0.010	0.073	0.054	0.169	0.128
0.2	0.021	0.016	0.009	0.007	0.048	0.035	0.112	0.085
0.15	0.016	0.012	0.007	0.005	0.035	0.026	0.084	0.064
0.125	0.013	0.010	0.006	0.004	0.029	0.022	0.070	0.053
0.1	0.009	0.007	0.004	0.003	0.021	0.015	0.047	0.036

WLS COL 2.5-4

TABLE 2.5.3-201
SUMMARY OF BEDROCK FAULTS MAPPED WITHIN THE SITE VICINITY

Feature Name	Distance from Site	Mapped Length	Strike Orientation	Reference(s)	Assigned Age	Evidence for Age
Kings Mountain shear zone	~5 mi.	>70 mi.	NE	Garihan et al. (1993) (Reference 231) Hibbard et al. (2006) (Reference 210) Horton (1981a, 1981b) (References 224 and 225) West et al. (1998) (Reference 228)	Paleozoic (possibly Mesozoic)	Syn- to post-kinematic dikes have Rb/Sr isochron age of 325 Ma; Cut by a 326 Ma granite
Tinsley Bridge fault	~6 mi.	~20 mi.	NE	Dennis (1995) (Reference 229) Hibbard et al. (2006) (Reference 210)	Paleozoic	Cut by 383 Ma granite
Brindle Creek thrust fault	~11 mi.	>100 mi.	NE, variable	Hibbard et al. (2006) (Reference 210) Hatcher et al. (2007) (Reference 238) Giorgis et al. (2002) (Reference 240)	Paleozoic	Cuts a 366 Ma granite; Fault-related migmatites have ~350 Ma age
SW extension of Boogertown shear zone	~8 mi.	~12 mi.	NE	Hibbard et al. (2006) (Reference 210) Horton (1981b) (Reference 225) Maybin and Nystrom (1997) (Reference 230)	Paleozoic	Cut by an undated pluton (Pluton mapped as Ordovician to Devonian
Reedy River thrust fault	>10 mi.	>100 mi.	NE	Hibbard et al. (2006) (Reference 210) Horton and Dicken (2001) (Reference 209) Maybin and Nystrom (1997, 2002) (References 230 and 233) Nystrom (2001) (Reference 232)	Paleozoic	
Unnamed fault north of Gaffney	>12 mi.	20 mi.	N	Hibbard et al. (2006) (Reference 210) Goldsmith et al. (1988) (Reference 242)	Paleozoic	

TABLE 2.5.4-201
PETROGRAPHIC TEST RESULTS

	Sample Borehole	Depth of Sample (ft. b.g.s.)	Lee Nuclear Station Rock Type	Mineral Composition (Percent)					Petrographic Rock Name
				Quartz	Plagioclase	Potassium Feldspar	Micaceous Mineral	Other	
WLS COL 2.5-1	B1000	80.2-80.3	Meta-Quartz Diorite	20	40	---	25	15	Meta-Quartz Diorite
	B1000	129.6-129.8	Meta-Diorite	15	45	---	19	21	Meta-Dacite Porphyry
	B1004	23.3-23.4	Meta-Quartz Diorite	26	45	5	19	5	Meta-Quartz Diorite
	B1004	33.2-33.3	Meta-Quartz Diorite	25	38	6	26	5	Meta-Quartz Diorite
	B1004	44.4-44.5	Meta-Quartz Diorite	30	50	0	18	2	Meta-Quartz Diorite
	B1007	22.8-22.9	Meta-Diorite	8	65	---	25	2	Meta-Dacite Porphyry
	B1013	21.6-21.7	Meta-Quartz Diorite	25	50	5	16	4	Meta-Quartz Diorite
	B1014	7.3-7.4	Meta-Diorite	25	---	---	65	10	Mica Schist
	B1014	16.3-16.4	Meta-Quartz Diorite	25	50	2	14	9	Meta-Quartz Diorite
	B1015	29.5-29.6	Meta-Quartz Diorite	25	38	9	22	6	Meta-Quartz Diorite
	B1018	39.8-39.9	Meta-Diorite (Monzodiorite)	10	36	1	12	41	Meta-Basalt
	B1018	46.5-46.6	Meta-Diorite	10	41	---	---	49	Meta-Basalt
	B1025	48.5-49.0	Meta-Granodiorite	53	---	---	43	4	Mica Schist
	B1025	49.8-50.1	Meta-Diorite	68	10	---	15	7	Mica Schist
	B1050	65.2-65.4	Meta-Quartz Diorite	18	55	---	21	6	Meta-Quartz Diorite

b.g.s. = below ground surface

ft. = feet

TABLE 2.5.4-202
SUMMARY OF LEE NUCLEAR STATION GEOTECHNICAL EXPLORATION

WLS COL 2.5-1

Test Type	Number
Soil and Rock Borings/Geotechnical Monitoring Well Borings	124/24
Monitoring Wells/Packer Tests	21/4
Cone Penetrometer Test/SCPT	29/10
Geotechnical Test Pits and Geologic Trenches	14
Goodman Jack	14 (2 borings)
Pressuremeter Testing	24 (2 borings)
P-S Suspension Log	13
Downhole Velocity	4
Televiewer Survey	13
Spectral Analysis of Surface Waves (SASW) Survey	15
Petrographic Analysis	15

TABLE 2.5.4-203 (Sheet 1 of 5)
SUMMARY OF COMPLETED EXPLORATION BORINGS AND FIELD TESTS

Facility or Zone	Boring Number	Coordinates and Elevation			Boring Type					SPT Interval		Depth (ft bgs)		Borehole Geophysical Testing			In-situ Testing	
					Rock Coring		Soil Sampling Method											
		Northing	Easting	Elevation (ft MSL)	HQ	NQ	SPT	UD	CME	From	To	Proposed	Actual	P-S Velocity	Televiewer	Packer Test	Goodman Jack	Pressuremeter
Power Block and Adjacent Structures WLS COL 2.5-1																		
Unit 1	**B-1000**	1166072.097	1846189.261	581.537	X		X			0	60	150	151	X	X			
(Basemat elevation 550.5 ft.)	**B-1000-UD**	1166063.067	1846192.595	581.519				X		--	--	--	23					
	B-1000-UDA	1166062.371	1846181.346	581.615				X		--	--	--	29.2					
	B-1000-UDB	1166107.231	1846117.365	588.931				X		--	--	--	48					
	B-1001	1166067.122	1846370.397	565.473	X					--	--	100	118.1		X			
	B-1001A	1166085.286	1846293.470	568.083		X				--	--	--	270.8 (length)					
	B-1002	1166061.781	1846444.433	565.338	X					--	--	150	170.3	X	X		X	
	B-1003	1165938.073	1846226.728	597.163	X					--	--	100	100					
	B-1004	1165831.988	1846407.915	558.997	X	X				--	--	175	175	X	X	X	X	
	B-1004A	1165831.298	1846430.369	558.997		X				--	--	--	284.7 (length)					
	B-1074	1166069.515	1846246.401	569.244	X	X	X			--	--	--	67.5					X
	B-1074A	1166067.457	1846252.141	569.233	X	X				--	--	--	121.9	X	X			X
	B-1075	1166030.303	1846255.956	569.667			X			--	--	--	23.7					
	B-1075A	1166035.846	1846256.754	569.535	X					--	--	--	150.4	X	X			
Adjacent Structures	**B-1005**	1165715.711	1846277.806	562.189		X				--	--	50	50					
	B-1006	1165456.872	1846165.621	589.158		X				--	--	50	30					
	B-1006A	1165453.953	1846160.471	589.622		X				--	--	--	90					
	B-1007	1165712.405	1846489.105	563.038		X				--	--	50	51.25					
	B-1008	1165623.375	1846335.376	563.175		X				--	--	50	51					
	B-1009	1165530.408	1846393.253	562.965						--	--	50	2.5					
	B-1009A	1165529.086	1846392.312	562.948		X				--	--	--	51					

TABLE 2.5.4-203 (Sheet 2 of 5)
SUMMARY OF COMPLETED EXPLORATION BORINGS AND FIELD TESTS

Facility or Zone	Boring Number	Coordinates and Elevation			Boring Type					SPT Interval		Depth (ft bgs)		Borehole Geophysical Testing			In-situ Testing	
					Rock Coring		Soil Sampling Method											
		Northing	Easting	Elevation (ft MSL)	HQ	NQ	SPT	UD	CME	From	To	Proposed	Actual	P-S Velocity	Televiewer	Packer Test	Goodman Jack	Pressuremeter
	B-1010	1165551.531	1846525.693	563.107		X				--	--	75	51					
	B-1011	1165997.940	1846673.057	537.714	X					--	--	150	220	X	X			
Unit 2	**B-1012**	1166228.569	1847098.384	566.153	X					--	--	150	150.2	X	X		X	
(Basemat elevation 550.5 ft.)	**B-1013**	1166266.998	1847167.699	558.699		X				--	--	50	52					
	B-1014	1166150.213	1847262.006	544.382	X	X				--	--	75	75.5		X		X	
	B-1015	1166134.365	1847192.566	560.052	X					--	--	400	250.3	X	X	X		
	B-1016	1166124.243	1847132.581	559.249		X	X			0	3	100	100					
	B-1017	1166004.443	1847155.562	560.724	X					--	--	175	175.6	X	X		X	
	B-1018	1166028.814	1847265.117	552.733		X				--	--	100	100.3					
Adjacent Structures	**B-1019**	1166204.465	1847001.388	558.168		X	X			0	9	75	75					
	B-1020	1166389.650	1847104.154	589.996		X	X			0	13.5	75	75					
	B-1021	1165897.314	1847301.608	565.519		X	X			0	5	75	75.4					
	B-1022	1165733.403	1847334.894	571.450		X	X			0	40	75	76					
	B-1023	1165696.674	1847233.087	571.173		X	X			0	27	75	75					
	B-1024	1166077.813	1846927.534	539.369	X	X				--	--	150	220.2	X	X			
	B-1037	1166205.496	1847506.541	589.279			X			0	78.75	50	78.75					
	B-1037A	1166215.133	1847504.721	589.279	X					--	--	--	96.6	X	X			
	B-1037-UD	1166209.149	1847500.977	589.246				X		--	--	--	68					
	B-1038	1166165.152	1847350.980	546.544		X				--	--	50	50.2					
Pipelines (Non-Safety Related)																		
Unit 1	**B-1050**	1164915.459	1846053.459	596.956		X	X			--	--	50	73.4					
	B-1051	1164991.018	1846392.558	587.676		X	X			--	--	50	71.5					
	B-1052	1165181.111	1846736.893	587.367		X	X			--	--	50	70.7					

TABLE 2.5.4-203 (Sheet 3 of 5)
SUMMARY OF COMPLETED EXPLORATION BORINGS AND FIELD TESTS

Facility or Zone	Boring Number	Coordinates and Elevation			Boring Type					SPT Interval		Depth (ft bgs)		Borehole Geophysical Testing			In-situ Testing	
					Rock Coring		Soil Sampling Method											
		Northing	Easting	Elevation (ft MSL)	HQ	NQ	SPT	UD	CME	From	To	Proposed	Actual	P-S Velocity	Televiewer	Packer Test	Goodman Jack	Pressuremeter
Unit 2	B-1053	1165781.941	1847797.307	589.279			X			--	--	50	13.5					
	B-1053A	1165778.372	1847798.567	589.279			X			--	--	--	16					
	B-1053B	1165778.077	1847780.641	589.583						--	--	--	13.5					
	B-1053C	1165682.617	1847809.363	589.482		X	X			--	--	--	69.2					
	B-1053-UD	1165682.863	1847817.422	589.327				X		--	--	--	26.3					
	B-1054	1165836.297	1847569.662	590.947		X	X			--	--	50	83.5					
	B-1055	1166463.354	1847463.729	590.486		X	X			--	--	50	66					
Cooling Tower Unit 1	B-1025	1165263.848	1845471.841	609.654		X	X			0	28.5	50	52					
	B-1025-UD	1165268.740	1845470.006	609.654				X		--	--	--	21					
	B-1026	1164883.450	1845089.201	610.168		X				0	99.9	50	99.9					
	B-1026-UD	1164870.682	1845091.797	609.875				X		--	--	--	47					
	B-1027	1165384.243	1845448.133	609.673		X	X			--	--	--	50					
Cooling Tower Unit 2	B-1028	1166140.124	1848027.639	609.765			X			0	103.55	80	103.55					
	B-1028-UD	1166150.119	1848024.643	609.875				X		--	--	--	94.6					
	B-1029	1165581.365	1848117.315	609.811			X			0	99.25	80	99.25					
	B-1030	1165963.148	1848403.477	609.697			X			0	98.8	80	98.8					
	B-1070	1165725.759	1848283.701	610.663			X			--	--	--	106	X				
	B-1070-UD	1165720.845	1848293.604	610.657				X		--	--	--	57.7					
	B-1071	1165707.327	1848320.308	610.545			X			--	--	--	100					
Switchyard (525 and 230 kV)	B-1031	1164731.622	1847445.498	603.991			X			0	38.8	50	38.8					
	B-1031-UD	1164740.021	1847445.261	603.991				X		--	--	--	16					
	B-1031-UDA	1164728.537	1847439.841	603.836				X		--	--	--	37					

TABLE 2.5.4-203 (Sheet 4 of 5)
SUMMARY OF COMPLETED EXPLORATION BORINGS AND FIELD TESTS

Facility or Zone	Boring Number	Coordinates and Elevation			Boring Type					SPT Interval		Depth (ft bgs)		Borehole Geophysical Testing			In-situ Testing	
		Northing	Easting	Elevation (ft MSL)	Rock Coring		Soil Sampling Method			From	To	Proposed	Actual	P-S Velocity	Televiewer	Packer Test	Goodman Jack	Pressuremeter
					HQ	NQ	SPT	UD	CME									
	B-1032	1164553.105	1846696.598	603.938			X			0	40.2	40	40.2					
	B-1033	1164557.162	1847059.050	604.405			X			0	40.5	40	40.5					
	B-1033-UD	1164563.916	1847059.310	604.110				X		--	--	--	28					
	B-1034	1164327.544	1847522.550	603.997			X			0	39.3	40	29					
	B-1035	1164164.327	1847146.518	604.562			X			--	--	--	40.1					
	B-1068	1164807.458	1847481.381	605.704			X			--	--	--	39	X				
	B-1068-UD	1164805.263	1847471.664	605.786				X		--	--	--	32					
	B-1069	1164802.003	1847447.979	604.878			X			--	--	--	40					
Make-Up Pond B Dam																		
	B-1036	1166863.111	1844076.180	591.051			X			0	23.5	160	23.5					
General Site Coverage and Facilities																		
	B-1044	1167711.138	1847455.765	587.987		X	X			0	13.6	--	43.6					
	B-1045	1167756.187	1847636.642	588.394		X	X			--	--	--	54					
	B-1045-UD	1167749.848	1847628.174	588.394				X		--	--	--	16					
	B-1046	1167815.000	1847834.473	588.315		X	X			--	--	--	93.3					
	B-1046-UD	1167822.860	1847835.327	588.046				X		--	--	--	54					
	B-1047	1167543.561	1847907.867	588.079		X	X			--	--	--	93.5					
	B-1047-UD	1167548.776	1847908.725	588.231				X		--	--	--	40					
	B-1048	1167477.305	1847718.329	587.526		X	X			--	--	--	84.5					
	B-1048-UD	1167471.096	1847715.977	587.526				X		--	--	--	26					
	B-1049	1167470.743	1847541.280	587.444		X	X			--	--	--	81					

TABLE 2.5.4-203 (Sheet 5 of 5)
SUMMARY OF COMPLETED EXPLORATION BORINGS AND FIELD TESTS

Facility or Zone	Boring Number	Coordinates and Elevation			Boring Type					SPT Interval		Depth (ft bgs)		Borehole Geophysical Testing			In-situ Testing	
		Northing	Easting	Elevation (ft MSL)	Rock Coring		Soil Sampling Method			From	To	Proposed	Actual	P-S Velocity	Televiewer	Packer Test	Goodman Jack	Pressuremeter
					HQ	NQ	SPT	UD	CME									
Borrow Areas																		
	B-1056	1163896.899	1846786.571	642.830			X			0	58.9	45	58.9					
	B-1057	1163743.790	1846819.978	639.064			X			0	54.8	50	54.8					
	B-1058	1163577.599	1846860.987	638.355			X			0	44.96	45	44.96					
	B-1059	1164621.202	1845733.239	686.991			X			0	55	40	55					
	B-1060	1163796.990	1847079.841	634.499			X			0	54.4	40	54.4					
	B-1061	1164300.248	1845630.540	685.282			X			0	50	40	50					
	B-1062	1164027.320	1847313.772	621.610			X			0	40	30	40					
	B-1063	1165768.794	1845001.137	610.939			X			0	28.8	30	28.8					
	B-1064	1166042.294	1845355.995	609.393			X			0	20	30	20					
	B-1065	1165642.457	1845273.637	610.082			X			0	30	25	30					
	B-1066	1163965.942	1847564.670	632.799			X			0	35	25	35					
	B-1067	1163861.880	1847598.060	629.049			X			0	60	25	60					
	B-1072	1164001.659	1847171.959	630.173			X			--	--	--	45					
	B-1073	1163676.681	1847239.214	626.706		X	X			--	--	--	78.5					

Notes:

1. ft b.g.s. = feet below ground surface
2. ft MSL = feet above mean sea level

TABLE 2.5.4-204 (Sheet 1 of 2)
SUMMARY OF GEOTECHNICAL BORINGS FOR COMPLETED MONITORING WELLS

Facility or Zone	Well Number	Coordinates and Elevation			Depth (ft bgs)		Boring Type					Packer Test Performed
							Rock Coring		Soil Sampling Method			
		Northing (ft)	Easting (ft)	Elevation (ft MSL)	Proposed Max.	Actual	HQ	NQ	SPT	UD	CME	
Power Block and Adjacent Structures												
WLS COL 2.5-1 **Unit 1 - Adjacent Structure**	**MW-1211**	1165196.276	1846389.259	589.318	150	65.5		X			X	
Unit 2 - Adjacent Structure	**MW-1210**	1165324.031	1847451.588	589.438	150	38					X	
	MW-1210A	1165324.523	1847455.093	589.438	--	126.3		X	X			X
Cooling Tower												
Unit 1	**MW-1212**	1165375.527	1845450.152	609.717	150	22.0					X	
	MW-1212A	1165371.506	1845450.693	609.291	--	89.2		X				
Unit 2	**MW-1203**	1166694.460	1847841.558	589.519	150	112.5		X			X	
	MW-1204	1166135.181	1848031.336	609.844	150	98.4					X	
	MW-1204A	1166132.228	1848026.567	609.861	--	135		X				
Switchyard (525 and 230 kV)												
	MW-1213	1164716.565	1847770.708	587.549	150	78.3		X			X	
	MW-1214	1164174.596	1847143.086	604.508	150	15.0					X	
	MW-1214A	1164175.677	1847147.851	604.508	--	96.0		X				
General Site Coverage and Facilities												
	MW-1200	1166347.301	1845577.653	591.514	150	8.5					X	
	MW-1200A	1166348.244	1845580.355	591.771	--	63.5		X				
	MW-1201	1166696.031	1846574.254	589.524	150	150.0		X			X	X
	MW-1202	1167007.315	1847460.055	587.318	150	53.5					X	
	MW-1202A	1167013.537999999	1847466.675	587.550	--	115.6		X	X			
	MW-1205	1165628.988	1848312.858	609.588	150	150		X			X	
	MW-1206	1166650.035	1846689.096	589.559	150	93.0		X			X	

TABLE 2.5.4-204 (Sheet 2 of 2)
SUMMARY OF GEOTECHNICAL BORINGS FOR COMPLETED MONITORING WELLS

Facility or Zone	Well Number	Coordinates and Elevation			Depth (ft bgs)		Boring Type					Packer Test Performed
							Rock Coring		Soil Sampling Method			
		Northing (ft)	Easting (ft)	Elevation (ft MSL)	Proposed Max.	Actual	HQ	NQ	SPT	UD	CME	
	MW-1207	1166840.186	1846668.529	588.785	150	62.0					X	
	MW-1207A	1166836.619	1846666.697	588.785	--	133.5		X				
	MW-1208	1167184.041	1846588.623	587.071	150	139.3		X			X	
	MW-1209	1165080.624	1848078.551	586.612	150	125.5		X			X	
	MW-1215	1166710.545	1846624.819	589.687	--	101.5						

Notes:

1. ft b.g.s. = feet below ground surface

2. ft MSL = feet above mean sea level

TABLE 2.5.4-205 (Sheet 1 of 2)
SUMMARY OF COMPLETED CONE PENETROMETER TEST SOUNDINGS

	Facility or Zone	CPT Number	Coordinates and Elevation			Depth (ft)		Tests Performed	
			Northing (ft)	Easting (ft)	Elevation (ft MSL)	Proposed	Actual	SCPT	Dissipation Test Depth (ft bgs)
WLS COL 2.5-1	Pipelines (Non-Safety Related)								
		CPT-1314	1164932.132	1846220.577	589.951	50	6.1		
		CPT-1315	1165032.071	1846589.827	586.86	50	40		
		CPT-1316	1165442.267	1847364.975	589.604	50	57.6		
		CPT-1317	1165480.571	1847652.112	588.745	50	8.7		
		CPT-1317A	1165481.237	1847632.773	588.636	50	19.5		
		CPT-1317B	1165497.097	1847636.906	588.802	50	20.7		
	Cooling Tower								
	Unit 1	CPT-1300	1165285.875	1845003.070	609.238	30	30		18.5, 30.0
		CPT-1301	1164894.227	1845085.762	609.833	30	30		
	Unit 2	CPT-1302	1166124.625	1848040.223	609.27	80	80.1		34.9, 80.1
		CPT-1303	1165582.495	1848103.243	609.599	80	90.6		65.9, 80.2
		CPT-1304	1165892.587	1848181.888	609.838	80	74		74
		CPT-1323	1165679.210	1848305.418	610.468	100	84.2	X	81.0, 84.2
		CPT-1324	1165733.296	1848334.24	610.241	100	3.1		
		CPT-1324B	1165733.296	1848334.24	610.241	100	77.3	X	77.3
		CPT-1325	1165730.729	1848273.936	610.349	100	40.0	X	
		CPT-1325A	1165728.968	1848272.952	610.057	100	55.1	X	55.1
	Switchyard (525 and 230 kV)								
		CPT-1305	1164732.401	1847452.325	603.729	50	34.3		
		CPT-1306	1164174.233	1847132.668	604.291	50	18.9		
		CPT-1306A	1164172.987	1847128.893	604.336	50	21.2		
		CPT-1320	1164809.635	1847497.262	604.865	40	32.3	X	32.3

TABLE 2.5.4-205 (Sheet 2 of 2)
SUMMARY OF COMPLETED CONE PENETROMETER TEST SOUNDINGS

Facility or Zone	CPT Number	Coordinates and Elevation			Depth (ft)		Tests Performed	
		Northing (ft)	Easting (ft)	Elevation (ft MSL)	Proposed	Actual	SCPT	Dissipation Test Depth (ft bgs)
Make-Up Pond B Dam	CPT-1321	1164802.257	1847460.695	604.865	40	43.3	X	43.3
	CPT-1322	1164794.98	1847472.656	605.226	40	48.1	X	48.1
General Site Coverage and Facilities	CPT-1307	1166393.067	1847138.502	589.841	80	20.2		
	CPT-1308	1166994.841	1844214.370	538	60	8.0		
	CPT-1308A	1167001.502	1844206.906	538	60	41.2	X	41.2
	CPT-1308B	1167008.152	1844199.436	538	60	39.5	X	
	CPT-1309	1166860.560	1844074.210	591.001	160	85.1	X	60.0, 85.1
	CPT-1318	1167614.443	1847587.310	586.374	50	16.2		
	CPT-1319	1167695.014	1847778.705	587.888	50	47.6		

Notes:

1. ft b.g.s. = feet below ground surface
2. ft MSL = feet above mean sea level
3. CPT-1308A; SCPT attempted, no useful data recovered.

TABLE 2.5.4-206 (Sheet 1 of 2)
SUMMARY OF COMPLETED GEOTECHNICAL TEST PIT AND GEOLOGIC TRENCH LOCATIONS

	Facility or Zone		Test Pit Number	Coordinates and Elevation(3) Northing	Easting	Elevation (ft MSL)
WLS COL 2.5-1	Power Block and Adjacent Structures					
		Unit 1	T-1400A	1165454.547	1846181.692	589.426
			T-1400B	1165328.497	1845955.529	590.177
		Unit 2	T-1401	1166317.379	1846815.739	590.44
			T-1402	1166376.698	1846887.698	590.032
			T-1403	1166394.130	1847140.590	589.882
			T-1404	1166250.245	1846714.042	551.273
	Cooling Tower					
		Unit 1	T-1426	1166029.449	1845369.840	609.56
	General Site Coverage and Facilities					
			T-1421	1164323.917	1845632.897	685.464
	Proposed Borrow Area					
	(former Borrow Area '1')		T-1419	1163896.961	1846789.678	642.468
			T-1420	1163582.443	1846854.298	638.047
			T-1422	1163992.360	1847171.647	630.767
			T-1423	1163666.925	1847256.094	625.823

TABLE 2.5.4-206 (Sheet 2 of 2)
SUMMARY OF COMPLETED GEOTECHNICAL TEST PIT AND GEOLOGIC TRENCH LOCATIONS

Facility or Zone	Test Pit Number	Coordinates and Elevation(3)		
		Northing	Easting	Elevation (ft MSL)
	T-1424	1164081.712	1847436.633	628.342
	T-1425	1163869.581	1847595.432	629.604

Notes:

1. ft b.g.s. = feet below ground surface

2. ft MSL = feet above mean sea level

3. Coordinates and elevation given for northernmost corner of test pit or northernmost end of test pit trench

TABLE 2.5.4-207
SUMMARY OF COMPLETED SURFACE GEOPHYSICAL TEST LOCATIONS

WLS COL 2.5-1

Facility or Zone	Seismic Line Number	Point A Coordinates (northern point) Northing	Point A Coordinates (northern point) Easting	Point B Coordinates (southern point) Northing	Point B Coordinates (southern point) Easting	Bearing	Total Length (ft)	Point A Elevation (ft MSL)
Power Block and Adjacent Structures								
Unit 1	S-1505	1166231.515	1846134.432	1165997.350	1845947.172	S38.7°W	299.833	589.148
Unit 2	S-1503A (Profiles 1 and 2)	1166294.705	1847205.937	1166173.432	1847172.201	S13.5°W	126.204	558.857
	S-1503B (Profile 3)	1166277.379	1847189.534	1166174.904	1847147.062	S22.6°W	110.953	560.357
	S-1504	1166219.947	1847229.069	1166202.741	1847218.988	S30.4°W	19.950	558.799
Adjacent Structures	S-1506	1166518.953	1847248.339	1166468.130	1846952.787	S79.9°W	299.938	589.286
	S-1507	1166432.500	1847505.178	1166139.308	1847567.671	S12.1°E	299.782	589.653
Cooling Tower								
Unit 1	S-1500	1165271.782	1845003.690	1164967.172	1845070.314	S12.2°E	311.815	609.216
	S-1501	1165118.678	1845267.690	1165066.423	1845049.417	S76.5°W	224.443	609.789
	S-1502	1165210.841	1845229.408	1164913.862	1845270.135	S7.6°E	299.769	609.564
Unit 2	S-1508	1165995.359	1848380.679	1165805.968	1848147.121	S50.6°W	300.746	610.085
	S-1509	1165824.517	1848410.455	1165685.278	1848233.625	S51.7°W	225.071	610.190
	S-1510	1166132.383	1848050.349	1166025.972	1848247.572	S61.7°E	224.099	609.670
Make-Up Pond B Dam								
	S-1513	1166936.563	1844002.862	1166749.091	1844236.750	S51.3°E	299.749	591.358
General Site Coverage and Facilities								
	S-1511	1167786.501	1847736.262	1167714.948	1847445.373	S76.1°W	299.562	588.490
	S-1512	1167874.136	1847914.115	1167622.486	1847750.398	S33.0°W	300.219	587.774

Notes:

1. ft MSL = feet above mean sea level

TABLE 2.5.4-208
SUMMARY OF GOODMAN JACK TEST RESULTS

WLS COL 2.5-1

Hole	Test Number	Test Interval (ft. b.g.s.)	E_{calc} (psi)	E_{true} (psi)
B1004	CKE-01	13.22 - 13.89	1,038,000	1,100,000
B1004	CKE-02	12.22 - 12.89	1,345,000	1,800,000
B1004	CKE-03	23.22 - 23.89	2,077,000	3,400,000
B1004	CKE-04	22.22 - 22.89	1,554,000	2,100,000
B1004	CKE-05	33.89 - 34.56	2,559,000	5,200,000
B1004	CKE-06	32.89 - 33.56	2,376,000	4,500,000
B1004	CKE-07	44.64 - 45.31	2,024,000	4,300,000
B1004	CKE-08	43.64 - 44.53	1,934,000	3,200,000
B1014	CKE-09	8.29 - 8.96	1,913,000	3,100,000
B1014	CKE-10	6.29 - 6.96	184,000	184,000
B1014	CKE-11	7.29 - 7.96	1,730,000	2,600,000
B1014	CKE-12	16.49 - 17.16	2,176,000	3,700,000
B1014	CKE-13	14.89 - 15.56	2,772,000	6,200,000
B1014	CKE-14	24.89 - 25.56	1,986,000	3,200,000

ft. = feet

b.g.s. = below ground surface

E_{calc} = Calculated maximum Young's Modulus

E_{true} = True Young's Modulus

TABLE 2.5.4-209
SUMMARY OF PRESSUREMETER TEST RESULTS

WLS COL 2.5-1

Borehole	Test Number	Bottom of Instrument (ft. b.g.s.)	Center of Membrane (ft. b.g.s.)	Initial Shear Modulus (G) (psi)	Unload-Reload Shear Modulus (G) (psi)
B1074	Lee2	44.1	42.7	14,000	90,000
B1074	Lee1	45.6	44.4	10,000	65,000
B1074	Lee4	49.5	48.2	12,000	76,000
B1074	Lee3	51.0	49.2	39,000	225,000
B1074	Lee6	54.5	52.8	130,000	450,000
B1074	Lee5	56.0	54.8	310,000	1,000,000
B1074	Lee7	59.5	58.3	52,000	220,000
B1074	Lee9	64.0	62.8	120,000	450,000
B1074	Lee8	65.5	64.3	180,000	560,000
B1074A	Lee12	53.4	51.7	350,000	740,000
B1074A	Lee11	54.9	53.2	220,000	700,000
B1074A	Lee10	56.4	54.7	320,000	1,000,000
B1074A	Lee14	62.0	60.8	No useful data	No useful data
B1074A	Lee13	63.5	62.3	870,000	1,500,000
B1074A	Lee17	66.5	65.3	350,000	1,000,000
B1074A	Lee16	68.0	66.8	440,000	6,000,000
B1074A	Lee15	69.5	68.3	160,000	2,000,000
B1074A	Lee21	73.5	72.3	360,000	5,000,000
B1074A	Lee20	75.0	73.8	250,000	6,000,000
B1074A	Lee19	76.5	75.3	200,000	1,800,000
B1074A	Lee18	77.0	75.8	40,000[a]	220,000[a]
B1074A	Lee22	81.7	80.5	320,000	6,000,000
B1074A	Lee24	82.9	81.7	140,000	6,000,000
B1074A	Lee23	84.4	83.2	160,000	6,000,000

ft. = feet

b.g.s. = below ground surface

psi = pounds per square inch

a) indicates data that is anomalously low, not used in analysis

TABLE 2.5.4-210
LABORATORY TESTING QUANTITIES BY SAMPLE TYPE AND TEST METHOD

WLS COL 2.5-6

		Tests Per Sampling Method			
		Soil			Rock
	Test Standard	Bulk[a]	Jar	Undisturbed	Rock Cores
Moisture Content	ASTM D 2216 – 05	-	113	39	0
Atterberg Limits	ASTM D 4318 – 05	-	7	37	0
Grain Size - Wash #200	ASTM D 6913 – 04	-	53	23	0
Grain Size - Sieve + Hydrometer	ASTM D 422 – 63 (2002)	-	8	14	0
Specific Gravity	ASTM D 854 – 06	-	8	37	0
Chemical Analysis	ASTM G 51 – 95 (2005) ASTM G 57 – 95a (2001) EPA SW – 846 9056/300.0 EPA SW – 846 8056/300.0	-	0	1	0
Consolidated-Undrained Triaxial Shear	ASTM D 4767 – 04	-	0	20	0
Unconfined Compression (UC)	ASTM D 7012 – 04	-	0	0	30
UC with Stress-Strain Analysis	ASTM D 7012 – 04	-	0	0	11
Consolidation	ASTM D 2435 – 04	-	0	24	0

a) The test data on bulk samples are removed because the materials are not used in the vicinity of the nuclear islands or under structures adjacent to the nuclear islands where only granular backfill is used.

TABLE 2.5.4-211 (Sheet 1 of 2)
AVERAGE ENGINEERING PROPERTIES OF SOIL

(Reported Values are Mean ± One Standard Deviation)

		All Fill Samples[a]			Granular Fill			Residual Soil			Saprolite			PWR
WLS COL 2.5-6		$N_{60} \le 10$ ($N \le 8$)[b]	$11 < N_{60} \le 30$ ($8 < N \le 23$)[b]	$31 < N_{60} \le 100$ ($23 < N \le 75$)[b]	GW	GP	SW	$N_{60} \le 10$ ($N \le 8$)[b]	$11 < N_{60} \le 30$ ($8 < N \le 23$)[b]	$31 < N_{60} \le 100$ ($23 < N \le 75$)[b]	$N_{60} \le 10$ ($N \le 8$[b])	$11 < N_{60} \le 30$ ($8 < N \le 23$)[b]	$31 < N_{60} \le 100$ ($23 < N \le 75$)[b]	$N_{60} > 100$ ($N > 75$)[b]
N_{60}-value[c]		21 ± 8 [75]			45[d]	45[d]	29-30[d]	25 ± 26 [14]			28 ± 23 [64]			-
Corrected tip resistance, qc	tsf	46.6 ± 31.4 [1,646]			-	-	-	62.5 ± 41.1 [330]			69.3 ± 61.2 [367]			-
Friction ratio, FR	ft/sec	5.4 ± 1.7 [1,646]			-	-	-	3.5 ± 1.5 [330]			4.0 ± 2.0 [367]			-
Percent gravel[e]	%	0 [1][f]	4 ± 6 [36]	6 ± 8 [6]	40-70[g]	40-70[g]	0-10[g]	0 [1]	0 [4]	0 [1]	3 ± 3 [8]	3 ± 7 [20]	1 ± 1 [11]	9 ± 14 [8]
Percent sand[e]	%	42 [1][f]	34 ± 8 [36]	47 ± 19 [6]	18-60[g]	18-60[g]	86-100[g]	57[f] [1]	46 ± 15 [4]	40[f] [1]	44 ± 11 [8]	52 ± 12 [20]	52 ± 13 [11]	55 ± 19 [8]
Percent fines (<#200 sieve)[e]	%	58[1][f]	62 ± 11 [36]	47 ± 21 [6]	0-12[g]	0-12[g]	0-4[g]	43[f] [1]	54 ± 14 [4]	60[f] [1]	54 ± 13 [8]	46 ± 15 [20]	47 ± 13 [11]	36 ± 22 [8]
Percent silt	%	-	41 ± 9 [13]	42[f] [1]	-	-	-	-	55[f] [1]	56[f] [1]	53[f] [2]	41 ± 10 [3]	34[f] [1]	-
Percent clay (<5μm)	%	-	18 ± 9 [13]	19[f] [1]	-	-	-	-	19[f] [1]	4[f] [1]	6[f] [2]	5 ± 2 [3]	8[f] [1]	-
Plasticity index, PI	%	-	NP [20]	NP [1]	NP	NP	NP	-	NP [2]	-	NP [5]	NP [10]	NP [5]	NP [1]
Liquid limit, LL	%	-	NV [20]	NV [1]	NV	NV	NV	-	NV [2]	-	NV [5]	NV [10]	NV [5]	NV [1]
Water content[e], *w*	%	33[f] [1]	23 ± 6 [59]	21 ± 10 [9]	-	-	-	22[f] [1]	32 ± 6 [9]	28 ± 10 [3]	32 ± 6 [15]	30 ± 12 [27]	20 ± 6 [16]	14 ± 4 [9]
Initial void ratio, e_o		-	0.69 ± .17 [13]	-	0.18	0.29	0.39	-	0.94[f] [2]	-	0.84 ± 0.23 [4]	0.84 ± 0.33 [8]	0.83[f] [2]	-
Specific gravity, G_s		-	2.71 ± .06 [20]	2.68[f] [1]	2.65[g]	2.65[g]	2.65[g]	-	2.72[f] [2]	2.70[f] [1]	2.72 ± 0.04 [6]	2.71 ± .04 [11]	2.69 ± .04 [4]	-
Dry unit weight, γ_{dry}	pcf	-	101 ± 8 [13]	-	140	128	119	-	88[f] [2]	-	93 ± 11 [4]	94 ± 15 [8]	93[f] [2]	-
Wet unit weight, γ_t	pcf	-	122 ± 5 [13]	-	150	142	136	-	113[f] [2]	-	116 ± 11 [4]	117 ± 7 [8]	114[f] [2]	135[h]
Saturated unit weight, γ_{sat}	pcf	-	125 ± 5 [13]	-	150	142	136	-	118[f] [2]	-	121 ± 7 [4]	124 ± 7 [7]	121[f] [2]	140[h]
Overconsolidation ratio[i], OCR		4.9 ± 2.8[j] [11]			-	-	-	-	1.6[f] [1]	-	4.2 ± 2.4 [3]	3.5 ± 2.0 [7]	2.4[f] [2]	-
Preconsolidation pressure[i], σρ'	ksf	8.8 ± 1.6[j] [11]			-	-	-		10.0[f] [1]		10.0 ± 1.5 [3]	9.4 ± 2.0 [7]	8.9[f] [2]	-
Compression index[i], C_c		0.19 ± 0.09[j] [11]			-	-	-	-	0.34[f] [1]	-	0.29 ± 0.03 [3]	0.33 ± 0.22 [7]	0.19[f] [2]	-
Re-compression index[i], C_r		0.024 ± 0.015[j] [11]			-	-	-	-	0.030[f] [1]	-	0.024 ± 0.016 [3]	0.027 ± 0.012 [7]	0.026[f] [2]	-
Consolidation coefficient[i], C_v	ft^2/day	5.6 ± 2.2[j] [11]			-	-	-	-	6[f] [1]	-	6.3 ± 0.6 [3]	5.1 ± 2.3 [7]	7[f] [2]	-
Total cohesion[i], *c*	psf	1,887 ± 178[j] [13]			-	-	-	224 ± 61[k]	-1,243 ± 346[k]	1,406[k]	224 ± 61 [4]	1,243 ± 346 [6]	1,406[f] [2]	1,000[h]
Total friction angle[i], ϕ	deg	20 ± 2[j] [13]			-	-	-	27 ± 5[k]	20 ± 5[k]	19[k]	27 ± 5 [4]	20 ± 5 [6]	19[f] [2]	45[h]
Effective cohesion[i][l], *c'*	psf	276 ± 49[j] [14]			0	0	0	-	130[f] [3]	-	0 [4]	439 ± 94 [6]	230[f] [2]	1,000[h]

TABLE 2.5.4-211 (Sheet 2 of 2)
AVERAGE ENGINEERING PROPERTIES OF SOIL

(Reported Values are Mean ± One Standard Deviation)

		All Fill Samples[a]			Granular Fill			Residual Soil			Saprolite			PWR
WLS COL 2.5-6		$N_{60} \le 10$ ($N \le 8$)[b]	$11 < N_{60} \le 30$ ($8 < N \le 23$)[b]	$31 < N_{60} \le 100$ ($23 < N \le 75$)[b]	GW	GP	SW	$N_{60} \le 10$ ($N \le 8$)[b]	$11 < N_{60} \le 30$ ($8 < N \le 23$)[b]	$31 < N_{60} \le 100$ ($23 < N \le 75$)[b]	$N_{60} \le 10$ ($N \le 8$[b])	$11 < N_{60} \le 30$ ($8 < N \le 23$)[b]	$31 < N_{60} \le 100$ ($23 < N \le 75$)[b]	$N_{60} > 100$ ($N > 75$)[b]
Effective friction angle[i][l], ϕ'	deg	28 ± 4 [j] [14]			≥35	≥35	≥35	-	30[f] [3]	-	31 ± 4 [4]	23 ± 5 [6]	28[f] [2]	45[h]
Hydraulic conductivity[m], k	ft/year	-	-	-	<~5,173 to 51,730	<~5,173 to 77,598	~5,173 to 17,589	-	-	-	-	-	-	-
	cm/sec	-	-	-	<~5.0E-03 to 5.0E-02	<~5.0E-03 to ~7.5E-02	~5.0E-03 to ~1.7E-02	-	-	-	-	-	-	-

a) All Fill includes samples classified as fill on boring logs.

b) Field SPT-N values to correlate to N_{60}-values are computed using the average energy transfer ratio (ETR) of 80.0 percent. $N=N_{60}(60/80.0)$.

c) N_{60}- value is obtained from field values corrected to Energy Transfer Ratios of 60%. The values for granular fill are $(N_1)_{60}$, and are for typical materials (see footnote d).

d) Reported value is for $(N_1)_{60}$. Value obtained using correlations in Reference 230 (Idriss and Boulanger, 2008) for sand (SW) and Reference 232 (Rollins et al., 1998) for gravel (GW and GP) for relative density = 80% corresponding to relative compaction = 96% (ASTM D 1557).

e) Three samples of alluvium were tested for moisture content and two underwent grain size analysis; the results are not shown in this table.

f) Insufficient data to determine standard deviation.

g) Values listed are for typical granular fill materials and will be verified by laboratory testing when the source of and specific materials to be used are known. Unit weight, friction angle, and hydraulic conductivity values reported are obtained from Reference 228 (NAVFAC, 1986). Grain sizes for typical granular fill materials are obtained from Reference 224 (SCDOT, 2007). The specific gravity of granular fill material is assumed as 2.65.

h) These values are from PSAR, Table 2D-3 and Table 2A-1 (Reference 201).

i) The design engineer (i.e., engineer that will use data for design) must give careful consideration to compressibility and strength parameters based on test data, and the values reported in this table are estimates.

j) Samples tested were all in the $11 < N_{60} \le 30$ range. The resulting consolidation and shear parameters may be applied to existing fill regardless of N_{60}.

k) Insufficient data to determine total strength parameters; strength parameters have been assigned same as for saprolite having similar N_{60}. Little residual soil remains.

l) For consolidated-undrained triaxial tests on undisturbed specimens, failure was said to occur at peak pore pressure.

m) 1 ft/year * 9.67×10^{-7} = 1 cm/sec.

Note: The number in brackets is the count, [Number]

TABLE 2.5.4-212
CORROSION TESTING OF SOIL FILL

WLS COL 2.5-6

Sample Type	pH	Resistivity (Ohm-cm)		Chlorides (mg/kg)	Sulfates (mg/kg)
		As Received	Saturated		
Undisturbed	3.9 [1]	2.43 E+05 [1]	2.92 E+05 [1]	2.5 [1]	5.6 [1]

Note: The number in the brackets is the count, [*count*]

TABLE 2.5.4-213
SUMMARY OF LABORATORY TEST RESULTS FOR INTACT ROCK CORES

			Meta Granodiorite	Meta Quartz Diorite	Meta Diorite	All Rock Types
WLS COL 2.5-6	Unit Weight, γ	pcf	168±1 [19]	169±3 [14]	177±2 [8]	170±4 [41]
	Unconfined Compressive Strength	ksi	23±5 [19]	17±7 [14]	22±6 [8]	21±7 [41]
	Young's Modulus, E	$x10^6$ psi	7.8±0.3 [3]	7.1±1.0 [7]	8.1 [1]	7.4±0.9 [11]
	Poisson's Ratio, ν	-	0.29±0.06 [3]	0.27±0.05 [7]	0.23 [1]	0.27±0.05 [11]

1. The number in the brackets is the count, [Number].

TABLE 2.5.4-214 (Sheet 1 of 7)
SUMMARY OF SASW VELOCITY SURVEY

WLS COL 2.5-6

Survey Line Number	Layer No.	Thickness, (ft)	Depth to Top of Layer (ft)	Assumed Poisson's Ratio	S-Wave Velocity (ft/sec)	P-Wave Velocity (ft/sec)
S-1500	1	1.5	0	0.33	480	120
	2	3	1.5	0.33	630	120
	3	5	4.5	0.33	720	120
	4	2	9.5	0.33	550	120
	5	15	11.5	0.33	760	120
	6	40	27	0.33	860	120
	7	7	67	0.47	1100	125
	8[(a)]	43	74	0.47	1100	125
	9[(a)]	11	117	0.44	1600	125
	10[(a)(b)]	Half Space	128	0.44	1600	125
S-1501	1	2	0	0.33	470	120
	2	2.6	1.5	0.33	600	120
	3	5	4.6	0.33	680	120
	4	15	9.6	0.33	730	120
	5	42	24.6	0.33	760	120
	6	28	67	0.47	1200	125
	7[(a)]	27	95	0.47	1200	125
	8[(a)(b)]	Half Space	122	0.47	1200	125

TABLE 2.5.4-214 (Sheet 2 of 7)
SUMMARY OF SASW VELOCITY SURVEY

WLS COL 2.5-6

Survey Line Number	Layer No.	Thickness, (ft)	Depth to Top of Layer (ft)	Assumed Poisson's Ratio	S-Wave Velocity (ft/sec)	P-Wave Velocity (ft/sec)
S-1502	1	1.7	0	0.33	430	120
	2	1	1.7	0.33	500	120
	3	1	2.7	0.33	580	120
	4	2.3	3.7	0.33	690	120
	5	32	6	0.33	820	120
	6	10	38	0.33	900	120
	7	19	48	0.33	2200	130
	8[(b)]	Half Space	67	0.38	2200	130
S-1503A, Profile 1	1	0.27	0	0.25	4300	7448
	2	0.5	0.27	0.25	7800	13510
	3	14.38	0.77	0.25	8500	14722
	4[(b)]	Half Space	15.15	0.25	8500	14722
S-1503A, Profile 2	1	0.3	0	0.25	4900	8487
	2	1.5	0.3	0.25	8500	14722
	3	13.35	1.8	0.25	9000	15589
	4[(b)]	Half Space	15.15	0.25	9000	15589

TABLE 2.5.4-214 (Sheet 3 of 7)
SUMMARY OF SASW VELOCITY SURVEY

WLS COL 2.5-6

Survey Line Number	Layer No.	Thickness, (ft)	Depth to Top of Layer (ft)	Assumed Poisson's Ratio	S-Wave Velocity (ft/sec)	P-Wave Velocity (ft/sec)
S-1503B, Profile 3	1	0.27	0	0.25	4000	6928
	2	0.5	0.27	0.25	6500	11258
	3	14.38	0.77	0.25	7000	12124
	4[(b)]	Half Space	15.15	0.25	7000	12124
S-1504	1	0.2	0	0.25	4500	7794
	2	0.5	0.2	0.25	5500	9526
	3	0.5	0.7	0.25	6500	11258
	4	1.2	1.2	0.25	7500	12990
	5	1.7	2.4	0.25	10500	18187
	6[(b)]	Half Space	4.1	0.25	10500	18187
S-1505	1	2.2	0	0.33	1000	1985
	2	7	2.2	0.33	600	1191
	3	10	9.2	0.33	750	1489
	4	10	19.2	0.33	850	1688
	5	20	29	0.48	1000	5000
	6	23	49	0.33	2500	5000
	7[(b)]	Half Space	72	0.33	2500	5000

TABLE 2.5.4-214 (Sheet 4 of 7)
SUMMARY OF SASW VELOCITY SURVEY

WLS COL 2.5-6

Survey Line Number	Layer No.	Thickness, (ft)	Depth to Top of Layer (ft)	Assumed Poisson's Ratio	S-Wave Velocity (ft/sec)	P-Wave Velocity (ft/sec)
S-1506	1	1	0	0.33	1500	2978
	2	1	1	0.33	600	1191
	3	5.5	2	0.33	500	993
	4	5	7.5	0.33	650	1290
	5	5	12.5	0.33	780	1549
	6	10	17.5	0.33	1000	1985
	7	10	28	0.45	1500	5000
	8	30	38	0.38	2200	5000
	9	23	68	0.30	2850	5332
	10[(b)]	Half Space	91	0.30	2850	5332
S-1507	1	1.8	0	0.33	880	1747
	2	0.9	1.8	0.33	780	1549
	3	5.2	2.7	0.33	680	1350
	4	13	7.9	0.33	590	1171
	5	12	20.9	0.33	700	1390
	6	10	33	0.49	700	5000
	7	15	43	0.48	950	5000
	8	10	58	0.46	1350	5000
	9	5	68	0.33	2500	5000
	10	84	73	0.30	3000	5613
	11[(b)]	Half Space	157	0.30	3000	5613

TABLE 2.5.4-214 (Sheet 5 of 7)
SUMMARY OF SASW VELOCITY SURVEY

WLS COL 2.5-6

Survey Line Number	Layer No.	Thickness, (ft)	Depth to Top of Layer (ft)	Assumed Poisson's Ratio	S-Wave Velocity (ft/sec)	P-Wave Velocity (ft/sec)
S-1508	1	1.1	0	0.33	350	695
	2	2.4	1.1	0.33	580	1151
	3	3	3.5	0.33	670	1330
	4	5	6.5	0.33	700	1390
	5	10	11.5	0.33	760	1509
	6	20	22	0.33	890	1767
	7	30	42	0.48	890	5000
	8	36	72	0.48	1050	5000
	9[(a)]	51	108	0.48	1050	5000
	10[(a)]	28	159	0.48	1050	5000
	11[(a)(b)]	Half Space	187	0.47	1200	5000
S-1509	1	2.5	0	0.33	630	1251
	2	4.5	2.5	0.33	590	1171
	3	17	7	0.33	735	1459
	4	23	24	0.33	860	1707
	5	19	47	0.49	830	5000
	6	23	66	0.48	1000	5000
	7	17	89	0.46	1300	5000
	8[(b)]	Half Space	106	0.46	1300	5000

TABLE 2.5.4-214 (Sheet 6 of 7)
SUMMARY OF SASW VELOCITY SURVEY

WLS COL 2.5-6

Survey Line Number	Layer No.	Thickness, (ft)	Depth to Top of Layer (ft)	Assumed Poisson's Ratio	S-Wave Velocity (ft/sec)	P-Wave Velocity (ft/sec)
S-1510	1	2	0	0.33	500	993
	2	6	2	0.33	600	1191
	3	7	8	0.33	700	1390
	4	20	15	0.33	760	1509
	5	5	35	0.33	900	1787
	6	35	40	0.48	900	5000
	7	29	75	0.48	1080	5000
	8[(a)]	21	104	0.48	1080	5000
	9[(a)]	13	125	0.45	1500	5000
	10[(a)(b)]	Half Space	138	0.45	1500	5000
S-1511	1	1.5	0	0.33	485	963
	2	3.5	1.5	0.33	630	1251
	3	8	5	0.33	900	1787
	4	5	13	0.33	1030	2045
	5	10	18	0.33	1370	2720
	6	8	28	0.30	2150	4022
	7	15	36	0.39	2150	5000
	8	15	51	0.30	3300	6174
	9	74	66	0.30	4500	8419
	10[(b)]	Half Space	140	0.30	4500	8419

TABLE 2.5.4-214 (Sheet 7 of 7)
SUMMARY OF SASW VELOCITY SURVEY

WLS COL 2.5-6

Survey Line Number	Layer No.	Thickness, (ft)	Depth to Top of Layer (ft)	Assumed Poisson's Ratio	S-Wave Velocity (ft/sec)	P-Wave Velocity (ft/sec)
S-1512	1	3.5	0	0.33	780	1549
	2	4	3.5	0.33	600	1191
	3	13	7.5	0.33	735	1459
	4	15	20.5	0.33	800	1588
	5	5	36	0.49	800	5000
	6	10	41	0.48	900	5000
	7	10	51	0.47	1200	5000
	8	26	61	0.35	2400	5000
	9(b)	Half Space	87	0.35	2400	5000
S-1513	1	2.8	0	0.33	700	1390
	2	1.6	2.8	0.33	450	893
	3	6.7	4.4	0.33	700	1390
	4	28	11.1	0.33	800	1588
	5	72	39	0.48	890	5000
	6(b)	14	97	0.48	1050	5000

a) Based on Sparse Data

b) Layer below maximum depth of the V_s Profile

TABLE 2.5.4-215 (Sheet 1 of 7)
SUMMARY OF SEISMIC CPT SHEAR WAVE (VS) VELOCITY RESULTS

	Test Number	Test Depth (ft)	Geophone Depth (ft)	Point Shear Velocity (fps)	Point Depth (ft)
WLS COL 2.5-1	CPT-1308A	No useful data recovered			
WLS COL 2.5-6	CPT-1308B	3.12	2.46	---	---
		6.07	5.41	---	3.93
		9.02	8.36	1533.6	6.89
		12.14	11.48	702.1	9.92
		15.09	14.43	875.1	12.96
		19.03	18.37	927.5	16.40
		21.16	20.50	940.6	19.44
		24.11	23.45	908.1	21.98
		27.23	26.57	886.6	25.01
		30.02	29.36	868.7	27.97
		33.14	32.48	853.7	30.92
		36.91	36.25	922.8	34.36

TABLE 2.5.4-215 (Sheet 2 of 7)
SUMMARY OF SEISMIC CPT SHEAR WAVE (VS) VELOCITY RESULTS

WLS COL 2.5-1

Test Number	Test Depth (ft)	Geophone Depth (ft)	Point Shear Velocity (fps)	Point Depth (ft)
CPT-1309	3.12	2.46	---	---
	6.07	5.41	1356.8	3.93
	9.02	8.36	1007.8	6.89
	12.14	11.48	845.1	9.92
	15.09	14.43	617.1	12.96
	18.04	17.38	1345.3	15.91
	21.16	20.50	718.9	18.94
	24.11	23.45	1184.5	21.98
	27.07	26.41	1086.6	24.93
	30.02	29.36	863.0	27.88
	33.14	32.48	1086.5	30.92
	36.09	35.43	770.4	33.95
	39.04	38.38	868.3	36.91
	42.16	41.50	949.3	39.94
	45.11	44.45	962.6	42.98
	48.06	47.40	919.2	45.93
	51.06	50.36	1261.8	48.88
	54.13	53.47	1040.4	51.92
	57.09	56.43	809.0	54.95
	60.04	59.38	1100.5	57.90
	63.32	62.66	1297.7	61.02
	66.11	65.45	1150.2	64.05
	69.06	68.40	914.2	66.93
	72.34	71.68	956.8	70.04
	75.13	74.47	1152.9	73.08
	78.08	77.42	1028.6	75.95
	81.04	80.38	1011.4	78.90
	84.15	83.49	1147.2	81.93

TABLE 2.5.4-215 (Sheet 3 of 7)
SUMMARY OF SEISMIC CPT SHEAR WAVE (VS) VELOCITY RESULTS

WLS COL 2.5-1

Test Number	Test Depth (ft)	Geophone Depth (ft)	Point Shear Velocity (fps)	Point Depth (ft)
CPT-1320	3.12	2.46	---	---
	6.07	5.41	744.1	3.93
	9.02	8.36	904.4	6.89
	12.14	11.48	661.4	9.92
	15.09	14.43	789.1	12.96
	18.04	17.38	730.3	15.91
	21.16	20.50	1019.6	18.94
	24.11	23.45	707.6	21.98
	27.07	26.41	738.9	24.93
	30.02	29.36	790.0	27.88
	32.32	31.66	879.7	30.51
CPT-1321	3.12	2.46	---	---
	6.07	5.41	1098.4	3.93
	9.02	8.36	766.8	6.89
	12.14	11.48	861.0	9.92
	15.09	14.43	641.8	12.96
	18.04	17.38	866.5	15.91
	21.16	20.50	789.8	18.94
	24.11	23.45	746.4	21.98
	27.73	26.57	780.2	25.01
	30.02	29.36	757.0	27.97
	33.14	32.48	786.3	30.92
	36.09	35.43	791.8	33.95
	39.04	38.38	895.5	36.91
	42.16	41.50	855.7	39.94
	43.31	42.65	1319.9	42.07

TABLE 2.5.4-215 (Sheet 4 of 7)
SUMMARY OF SEISMIC CPT SHEAR WAVE (VS) VELOCITY RESULTS

WLS COL 2.5-1

Test Number	Test Depth (ft)	Geophone Depth (ft)	Point Shear Velocity (fps)	Point Depth (ft)
CPT-1322	3.12	2.46	---	---
	6.07	5.41	699.0	3.93
	9.02	8.36	860.3	6.89
	12.14	11.48	814.9	9.92
	15.09	14.43	752.1	12.96
	18.04	17.38	751.8	15.91
	21.16	20.50	950.5	18.94
	24.11	23.45	801.3	21.98
	27.07	26.41	759.1	24.93
	30.02	29.36	710.0	27.88
	33.14	32.48	776.1	30.92
	36.09	35.43	791.8	33.95
	39.21	38.55	657.6	36.99
	42.32	41.66	750.2	40.10
	45.11	44.45	909.2	43.06
	48.06	47.40	1868.1	45.93

TABLE 2.5.4-215 (Sheet 5 of 7)
SUMMARY OF SEISMIC CPT SHEAR WAVE (VS) VELOCITY RESULTS

WLS COL 2.5-1

Test Number	Test Depth (ft)	Geophone Depth (ft)	Point Shear Velocity (fps)	Point Depth (ft)
CPT-1323	3.12	2.46	---	---
	6.07	5.41	2562.9	3.93
	9.02	8.36	881.8	6.89
	12.14	11.48	773.5	9.92
	15.09	14.43	802.2	12.96
	18.04	17.38	866.5	15.91
	21.16	20.50	616.2	18.94
	24.11	23.45	656.5	21.98
	27.07	26.41	839.6	24.93
	30.02	29.36	919.5	27.88
	33.14	32.48	703.0	30.92
	36.09	35.43	950.1	33.95
	39.04	38.38	764.1	36.91
	42.32	41.66	969.0	40.02
	45.11	44.45	1212.2	43.06
	48.06	47.40	965.2	45.93
	51.02	50.36	983.8	48.88
	54.13	53.47	1023.1	51.92
	57.09	56.43	910.1	54.95
	60.04	59.38	1041.6	57.90
	63.48	62.82	841.2	61.10
	66.11	65.45	1039.3	64.14
	69.06	68.40	928.7	66.93
	72.01	71.35	1027.2	69.88
	75.13	74.47	1237.0	72.91
	78.08	77.42	1085.7	75.95
	81.04	80.38	1197.1	78.90
	84.15	83.49	1376.6	81.93

TABLE 2.5.4-215 (Sheet 6 of 7)
SUMMARY OF SEISMIC CPT SHEAR WAVE (VS) VELOCITY RESULTS

WLS COL 2.5-1

Test Number	Test Depth (ft)	Geophone Depth (ft)	Point Shear Velocity (fps)	Point Depth (ft)
CTP-1324B	3.12	2.46	---	---
	6.07	5.41	1537.7	3.93
	9.02	8.36	783.8	6.89
	12.14	11.48	845.1	9.92
	15.09	14.43	740.5	12.96
	18.04	17.38	1043.3	15.91
	21.16	20.50	737.9	18.94
	24.11	23.45	813.2	21.98
	27.07	26.41	923.6	24.93
	30.02	29.36	876.4	27.88
	33.14	32.48	866.0	30.92
	36.09	35.43	850.9	33.95
	39.37	38.71	1044.2	37.07
	42.16	41.50	1087.4	40.10
	45.11	44.45	946.8	42.98
	48.06	47.40	1034.1	45.93
	51.02	50.36	1018.3	48.88
	54.13	53.47	1006.3	51.92
	57.09	56.43	820.4	54.95
	60.04	59.38	1121.7	57.90
	63.16	62.50	963.1	61.10
	66.11	65.45	942.9	63.97
	69.06	68.40	1194.0	66.93
	72.01	71.35	992.4	69.88
	75.13	74.47	1212.7	72.91
	77.26	76.60	1176.1	75.54

TABLE 2.5.4-215 (Sheet 7 of 7)
SUMMARY OF SEISMIC CPT SHEAR WAVE (VS) VELOCITY RESULTS

WLS COL 2.5-1

Test Number	Test Depth (ft)	Geophone Depth (ft)	Point Shear Velocity (fps)	Point Depth (ft)
CPT-1325	3.12	2.46	---	---
	6.07	5.41	2989.8	3.93
	9.02	8.36	1146.4	6.89
	12.14	11.48	1007.4	9.92
	15.09	14.43	1027.4	12.96
	18.04	17.38	1012.6	15.91
	21.16	20.50	874.6	18.94
	24.11	23.45	892.2	21.98
	27.07	26.41	982.0	24.93
	30.02	29.36	1016.4	27.88
	33.30	32.64	910.0	31.00
	36.09	35.43	913.2	34.03
	40.03	39.37	1484.2	37.40
CPT-1325A	43.14	42.48	---	---
	46.10	45.44	947.7	43.96
	49.05	48.39	1136.4	46.91
	51.34	50.68	806.5	49.54
	54.63	53.97	1133.9	52.33
	55.12	54.46	---	54.21

TABLE 2.5.4-216 (Sheet 1 of 4)
BOREHOLE GEOPHYSICAL TEST LOCATIONS – P-S SUSPENSION, DOWNHOLE, AND TELEVIEWER TESTS

	Borehole	Tool and Run Number	Depth Range (ft.)	Total Depth as Drilled (ft.)	Depth to Bottom of Casing (ft)	Sample Interval (ft)
	B1000	Suspension	6.6 - 142.7	151.0	60.0 PVC	1.6
	B1000	Downhole	3.0 - 150.0	151.0	60.0 PVC	3.0-10.0
WLS COL 2.5-1	B1000	Optical Televiewer	60.0 - 153.2	151.0	60.0 PVC	0.008
WLS COL 2.5-6	B1000	Acoustic Televiewer 1	60.0 - 153.2	151.0	60.0 PVC	0.008
	B1000	Acoustic Televiewer 2	60.0 - 153.0	151.0	60.0 PVC	0.008
	B1001	Acoustic Televiewer	29.3 - 120.6	120.0	29.3 PVC	0.008
	B1002	Suspension	24.6 - 157.5	170.0	24.5 PVC	1.6
	B1002	Acoustic Televiewer	24.8 - 169.9	170.0	24.5 PVC	0.008
	B1004	Suspension	9.8- 162.4	175.0	---	1.6
	B1004	Optical Televiewer	6.2 - 174.0	175.0	---	0.008
	B1004	Acoustic Televiewer	9.8 - 174.6	175.0	---	0.008
	B1011	Suspension 1	8.2 - 211.6	220.5	---	1.6
	B1011	Suspension 2	6.6 - 196.9	220.5	---	1.6
	B1011	Downhole	3.0 - 217.0	220.5	---	20
	B1011	Optical Televiewer	4.5 - 222.0	220.5	---	0.008

TABLE 2.5.4-216 (Sheet 2 of 4)
BOREHOLE GEOPHYSICAL TEST LOCATIONS – P-S SUSPENSION, DOWNHOLE, AND TELEVIEWER TESTS

Borehole	Tool and Run Number	Depth Range (ft.)	Total Depth as Drilled (ft.)	Depth to Bottom of Casing (ft)	Sample Interval (ft)
B1011	Acoustic Televiewer	1.6 - 160.8	220.5	---	0.008
B1012	Suspension	13.1 - 137.8	150.0	---	1.6
B1012	Optical Televiewer	4.5 - 149.8	150.0	---	0.008
B1012	Acoustic Televiewer	12.5 - 149.8	150.0	---	0.008
B1014	Optical Televiewer	6.4 - 67.4	75.0	3.0 PVC	0.008
B1014	Acoustic Televiewer	3.6 - 67.3	75.0	3.0 PVC	0.008
B1015	Suspension	6.6 - 241.1	255.0	5.0 PVC	1.6
B1015	Optical Televiewer	5.0 - 255.0	255.0	5.0 PVC	0.008
B1015	Acoustic Televiewer	5.5 - 254.7	255.0	5.0 PVC	0.008
B1017	Suspension	8.2 - 162.4	175.0	10.0 PVC	1.6
B1017	Optical Televiewer	6.5 - 176.2	175.0	10.0 PVC	0.008
B1017	Acoustic Televiewer	6.7 - 175.9	175.0	10.0 PVC	0.008

TABLE 2.5.4-216 (Sheet 3 of 4)
BOREHOLE GEOPHYSICAL TEST LOCATIONS – P-S SUSPENSION, DOWNHOLE, AND TELEVIEWER TESTS

Borehole	Tool and Run Number	Depth Range (ft.)	Total Depth as Drilled (ft.)	Depth to Bottom of Casing (ft)	Sample Interval (ft)
B1024	Suspension	18.0 - 208.3	220.2	4.0 STEEL	1.6
B1024	Downhole	5.0 - 210.0	Blocked at 210.0	4.0 STEEL	5.0-10.0
B1024	Optical Televiewer	5.4 - 222.0	220.2	4.0 STEEL	0.05
B1024	Acoustic Televiewer	15.5 - 115.0	220.2	4.0 STEEL	0.05
B1037A	Suspension	5.3 - 85.3	97.5	70.6 PVC	1.6
B1037A	Downhole	3.0 - 84.0	97.5	70.6 PVC	3
B1037A	Optical Televiewer	71.8 - 97.8	97.5	70.6 PVC	0.008
B1037A	Acoustic Televiewer	72.0 - 97.5	97.5	70.6 PVC	0.008
B1068	Suspension	1.6 - 25.3	38.0	---	0.82
B1070	Suspension	1.6 - 91.9	105.0	---	1.6
B1074A	Acoustic Televiewer 1	28.0 - 40.2	121.9	29.4 STEEL	0.008
B1074A	Acoustic Televiewer 2	28.0 - 108.2	121.9	29.4 STEEL	0.008
B1074A	Acoustic Televiewer 2	108.2 - 28.0	121.9	29.4 STEEL	0.008
B1074A	Suspension 1	27.9 - 95.1	121.9	29.4 STEEL	1.6
B1075A	Acoustic Televiewer 1	18.0 - 28.0	150.4	18.5 STEEL	0.008

TABLE 2.5.4-216 (Sheet 4 of 4)
BOREHOLE GEOPHYSICAL TEST LOCATIONS – P-S SUSPENSION, DOWNHOLE, AND TELEVIEWER TESTS

Borehole	Tool and Run Number	Depth Range (ft.)	Total Depth as Drilled (ft.)	Depth to Bottom of Casing (ft)	Sample Interval (ft)
B1075A	Acoustic Televiewer 2	27.7 - 18.0	150.4	18.5 STEEL	0.008
B1075A	Acoustic Televiewer 3	18.0 - 149.7	150.4	18.5 STEEL	0.008
B1075A	Acoustic Televiewer 4	149.7 - 23.0	150.4	18.5 STEEL	0.008
B1075A	Suspension 1	26.3 - 136.2	150.4	18.5 STEEL	1.6

TABLE 2.5.4-217 (Sheet 1 of 3)
SUMMARY OF INTERPRETED P-S SUSPENSION VELOCITY LAYER MODELS

WLS COL 2.5-6

Boring Number	Layer No.	Depth to Top (ft.)	Depth to Bottom (ft.)	Layer model V_s (ft./sec.)	Layer model V_p (ft./sec.)
B-1000	1	4.1	23.8	1069.47	--
	2	23.8	36.9	1741.59	5024.47
	3	36.9	46.8	2921.97	6270.22
	4	46.8	63.2	2138.64	6846.60
	5	63.2	97.6	3858.39	9498.04
	6	97.6	107.5	5163.41	12097.82
	7	107.5	120.6	9011.92	18208.60
	8	120.6	138.6	10960.66	21638.16
B-1002	1	27.1	32.0	8248.31	14766.43
	2	32.0	104.2	9998.31	18750.08
	3	104.2	156.7	10240.85	19149.11
B-1004	1	10.7	22.2	6099.08	11869.06
	2	22.2	50.0	8459.07	16006.10
	3	50.0	161.6	9891.54	18465.19
B-1011	1	9.0	210.8	9835.41	17208.75
B-1012	1	15.6	22.2	7424.31	15025.56
	2	22.2	137.0	9588.94	18728.29

TABLE 2.5.4-217 (Sheet 2 of 3)
SUMMARY OF INTERPRETED P-S SUSPENSION VELOCITY LAYER MODELS

Boring Number	Layer No.	Depth to Top (ft.)	Depth to Bottom (ft.)	Layer model V_s (ft./sec.)	Layer model V_p (ft./sec.)
B-1015	1	9.0	71.4	8435.61	17102.59
	2	71.4	174.7	9288.90	18530.31
	3	174.7	240.3	9889.88	18932.41
B-1017	1	10.7	59.9	8474.78	17928.08
	2	59.9	122.2	9582.69	18860.15
	3	122.2	161.6	10197.85	18191.23
B-1024	1	18.9	48.4	9440.02	17871.07
	2	48.4	207.5	10263.27	20293.93
B-1037A[(a)]	1	5.9	13.9	728.00	1228.23
	2	13.9	28.7	763.42	1780.00
	3	28.7	64.8	740.24	4853.70
	4	64.8	84.5	3971.86	9785.20
B-1068	1	2.0	7.7	676.51	1418.23
	2	7.7	24.9	796.06	1779.29

TABLE 2.5.4-217 (Sheet 3 of 3)
SUMMARY OF INTERPRETED P-S SUSPENSION VELOCITY LAYER MODELS

Boring Number	Layer No.	Depth to Top (ft.)	Depth to Bottom (ft.)	Layer model V_s (ft./sec.)	Layer model V_p (ft./sec.)
B-1070	1	2.5	5.7	601.80	1503.77
	2	5.7	36.9	812.54	1852.83
	3	36.9	77.9	1011.06	2321.05
	4	77.9	91.0	1262.00	2621.05
B-1074A	1	28.7	40.2	4600.92	11333.75
	2	40.2	59.9	4424.71	12588.16
	3	59.9	68.1	6209.01	16494.41
	4	68.1	94.3	8086.92	16969.15
B-1075A	1	27.1	32.0	3238.00	7888.55
	2	32.0	43.5	4578.38	10703.25
	3	43.5	61.5	6315.67	14688.74
	4	61.5	135.3	9242.34	17840.32

a) As B-1037A was not used to calculate the smoothed velocity profiles, this data was not used in the evaluations presented herein. The layers presented in this table were developed by GEOVision (Subsection 2.5.4.4).

TABLE 2.5.4-218
SUMMARY OF DOWNHOLE VELOCITY LAYER MODELS

			Layer Data			Layer Velocity	
	Borehole	Layer Number	Top (ft. b.g.s.)	Bottom (ft. b.g.s.)	Thickness (ft.)	Vs (ft/s)	Vp (ft/s)
	B1000	1	0.0	6.0	6.0	525	1295
	B1000	2	6.0	27.0	21.0	995	1774
	B1000	3	27.0	49.5	22.5	2150	4257
WLS COL 2.5-1	B1000	4	49.5	58.5	9.0	1755	6397
WLS COL 2.5-6	B1000	5	58.5	110.0	51.5	4958	12018
	B1000	6	110.0	130.0	20.0	11269	20053
	B1011	1	0.0	217.0	217.0	9230	17456
	B1024	1	0.0	20.0	20.0	6022	14555
	B1024	2	0.0	0.0	0.0	0	0
	B1024	3	30.0	210.0	180.0	9317	18236
	B1037A	1	0.0	12.0	12.0	695	1577
	B1037A	2	12.0	33.0	21.0	792	1544
	B1037A	3	33.0	66.0	33.0	736	4384
	B1037A	4	66.0	93.0	27.0	4634	11246

TABLE 2.5.4-219
QUALITY CONTROL RECOMMENDATIONS FOR NUCLEAR ISLAND FOUNDATION MATERIALS

WLS COL 2.5-6
WLS COL 2.5-7

Material	Test	Minimum Sampling and Testing Frequency
Rock or Existing Concrete	Visual Inspection	Visual inspection of final exposed rock and concrete surface to confirm materials are in general conformance with expected foundation materials based on boring logs. Visual inspection to confirm that cleaning and surface preparation are properly completed prior to placement of fill concrete or foundation materials.
	Geologic Mapping	Geologic mapping of final exposed excavation surface prior to placement of fill concrete or foundation materials. Mapping at a minimum scale of 1 inch equals 10 feet. More detail may be provided as necessary.

TABLE 2.5.4-220
QUALITY CONTROL RECOMMENDATIONS FOR NUCLEAR ISLAND FILL CONCRETE

WLS COL 2.5-6
WLS COL 2.5-7

Material	Test	Minimum Sampling and Testing Frequency
Fill Concrete	Compressive Strength	One set of 4 cylinders for every 500 cubic yards placed. Minimum of one set each day material is placed. (Verify strength complies with mix design[(a)] and minimum strength of 2,500 psi)

a) Note: The compressive strength as determined from the preconstruction mix design and testing program will ensure that the fill concrete will exhibit an average shear wave velocity greater than or equal to 7,500 ft/sec. This may result in compressive strength greater than the minimum of 2,500 psi.

TABLE 2.5.4-221
DELETED

TABLE 2.5.4-222 (Sheet 1 of 3)
QUALITY CONTROL RECOMMENDATIONS FOR GENERIC
ENGINEERED GRANULAR BACKFILL - GW, GP, AND SW

WLS COL 2.5-6
WLS COL 2.5-7

Material	Test	Minimum Sampling and Testing Frequency
Granular Backfill	Field Density	Minimum 1 sample per lift per 10,000 square feet. One test for every 250 square feet per lift when manually operated compactors are used. Use sand cone (ASTM D 1556) or rubber balloon (ASTM D 2167) for at least 33% of field density measurements. Nuclear gauge (ASTM D 6938) may be used for 67% of measurements. The sand cone or rubber balloon test shall be performed at the location of at least two of the nuclear gauge tests (if used) for each day's work.
	Moisture	One test for each sand cone or rubber balloon test. (ASTM D 2216)
	Moisture-Density Relationship (Modified Proctor)	One test for every borrow source and material type and any time material type changes. Additional test for every 40 Field Density tests, or as directed by geotechnical engineer in responsible charge. (ASTM D 1557)
	Gradation	One test for each Moisture-Density test. (ASTM D 422 and D 1140)
	Atterberg Limits	One test for each Moisture-Density test. (ASTM D 4318)
	Material Type	Granular fill must come from an approved borrow source (e.g. a quarry) and be the approved material for the project.

TABLE 2.5.4-222 (Sheet 2 of 3)
QUALITY CONTROL RECOMMENDATIONS FOR GENERIC
ENGINEERED GRANULAR BACKFILL - GW, GP, AND SW

The following laboratory tests will be performed on samples of the proposed granular fill materials before they are approved for use.

Test	Minimum No. of Tests	Criterion for Acceptance Unless Approved by Engineer of Record
All below		An engineering report exists that concludes the granular fill material will produce a backfill having acceptable engineering properties.
Grain Size ASTM D 6913	1 per material type per source as-is, and 1 per material type per source scalped if necessary	Complies with SCDOT Specifications for Material Type (Reference 224) (may differ on some sieve sizes with approval of Engineer of Record).
Specific Gravity ASTM D 854	1 per material type per source	
Modified Proctor ASTM D 1557 and ASTM D 4718	1 per material type per source	Maximum Dry Density $\geq$ 124 lb/ft^3.
Constant Head Permeability ASTM D 2434	1 per material type per source	
pH ASTM G 51	1 per material type per source	
Chloride Content EPA SW-846 9056/300.0	1 per material type per source	
Sulfate Content EPA SW-846 8056/300.0	1 per material type per source	

TABLE 2.5.4-222 (Sheet 3 of 3)
QUALITY CONTROL RECOMMENDATIONS FOR GENERIC
ENGINEERED GRANULAR BACKFILL - GW, GP, AND SW

Test	Minimum No. of Tests	Criterion for Acceptance Unless Approved by Engineer of Record
Resistivity ASTM G 57	1 per material type per source	
Consolidated Drained Triaxial Shear USACE EM-1110-2-1906 Appendix X (30 Nov. 70)	1 per material type per source (scalped) (minimum 2 confining pressures per material type)	$\phi' \geq 35°$
Consolidation ASTM D 2435	1 per material type per source (up to 50 kip/ft^2 effective vertical stress)	
Resonant Column Torsional Shear University of Texas Procedure PBRCTS-1	1 per material type per source (scalped) Test at 4 to 6 isotropic confining stress values	Maximum shear modulus, modulus ratio, and damping ratio consistent with upper range and lower range values used for site response calculation to determine compatibility with site response for Category II structures (Annex Building and Turbine Building Bay 1).
Free-Free Resonant Column Test University of Texas Procedure Fr-Fr-1	1 per material type per source (scalped) Test free-free resonance and direct travel time tests	

TABLE 2.5.4-223
ASSUMED MATERIAL PROPERTIES FOR CONCRETE MATERIALS

	Concrete Source	Unit Weight (pcf)	Compressive Strength (f'c) (psi)	Young's Modulus (E) (psi x 10^6)	Poisson's Ratio (ν)
WLS COL 2.5-6	Pre-Existing Fill Concrete	145	3,000	3.16	0.17
	Pre-Existing Foundation Concrete	145	3,000	3.16	0.17
	Lee Nuclear Station Fill Concrete	145	3,000	3.16	0.17

Note: Unit weight and compressive strength are assumed. E and ν are from ASCE Standard 4-98.

TABLE 2.5.4-224
DELETED

TABLE 2.5.4-224A (Sheet 1 of 4)
BEST ESTIMATE LAYERING, VELOCITIES, MODULI, AND RANGES OF GRANULAR FILL (GW OR MACADAM BASE COURSE)

Layer Name	Depth (ft)	Elevation (ft)	Water Table Elev. (ft)	Unit Weight[a] (pcf)	Best Estimates					G_{max}[b] Lower Range (ksf)	G_{max}[b] Upper Range (ksf)
					V_p[b] (ft/sec)	V_s[b] (ft/sec)	Poisson's Ratio, v	G_{max}[b] (ksf)	E_{max}[b] (ksf)		
Fill	0-5.5	589.5-584	-	150	1306	754	0.25	2649	6621	1766	3973
	5.5-10.5	584-579	584[c]	150	1504 [5000][d]	868	0.25 [0.5][d]	3512	8779 [10536][d]	2341	5267
Fill	10.5-15.5	579-574	-	150	1601 [5000][d]	925	0.25 [0.5][d]	3982	9955 [11946][d]	2655	5973
	15.5-20	574-569.5	-	150	1685 [5000][d]	973	0.25 [0.5][d]	4410	11026 [13230][d]	2940	6616
Fill	20-30	569.5-559.5	-	150	1869 [5000][d]	1079	0.25 [0.5][d]	5426	13565 [16278][d]	3617	8139
Fill	30-40	559.5-549.5	-	150	2082 [5000][d]	1202	0.25 [0.5][d]	6733	16831 [20199][d]	4488	10099
Fill	40-50	549.5-539.5	-	150	2263 [5000][d]	1306	0.25 [0.5][d]	7949	19874 [23847][d]	5300	11924
Fill	50-60	539.5-529.5	-	150	2421 [5000][d]	1398	0.25 [0.5][d]	9100	22749 [27300][d]	6066	13649
Fill	60-70	529.5-519.5	-	150	2563 [5000][d]	1480	0.25 [0.5][d]	10197	25493 [30591][d]	6798	15296

TABLE 2.5.4-224A (Sheet 2 of 4)
BEST ESTIMATE LAYERING, VELOCITIES, MODULI, AND RANGES OF GRANULAR FILL (GW OR MACADAM BASE COURSE)

Layer Name	Depth (ft)	Elevation (ft)	Water Table Elev. (ft)	Unit Weight[(a)] (pcf)	Best Estimates					G_{max}[(b)] Lower Range (ksf)	G_{max}[(b)] Upper Range (ksf)
					V_p[(b)] (ft/sec)	V_s[(b)] (ft/sec)	Poisson's Ratio, v	G_{max}[(b)] (ksf)	E_{max}[(b)] (ksf)		
Fill	70-80	519.5-509.5	-	150	2692 [5000][(d)]	1554	0.25 [0.5][(d)]	11252	28130 [33756][(d)]	7501	16878
Fill	80-90	509.5-499.5	-	150	2811 [5000][(d)]	1623	0.25 [0.5][(d)]	12271	30678 [36813][(d)]	8181	18407
Fill	90-100	499.5-489.5	-	150	2922 [5000][(d)]	1687	0.25 [0.5][(d)]	13259	33147 [39777][(d)]	8839	19888

TABLE 2.5.4-224A (Sheet 3 of 4)
BEST ESTIMATE LAYERING, VELOCITIES, MODULI, AND RANGES OF GRANULAR FILL (GW OR MACADAM BASE COURSE)

Layer Name	Depth (ft)	Elevation (ft)	Water Table Elev. (ft)	Unit Weight[a] (pcf)	Best Estimates					G_{max}[b] Lower Range (ksf)	G_{max}[b] Upper Range (ksf)
					V_p[b] (ft/sec)	V_s[b] (ft/sec)	Poisson's Ratio, v	G_{max}[b] (ksf)	E_{max}[b] (ksf)		
Fill	0-5.5	589.5-584	-	150	1306	754	0.25	2649	6621	1766	3973
	5.5-10.5	584-579	-	150	1563	902	0.25	3793	9483	2529	5690
Fill	10.5-15.5	579-574	-	150	1753	1012	0.25	4772	11930	3181	7158
	15.5-20	574-569.5	574[e]	150	1868 [5000][d]	1079	0.25 [0.5][d]	5419	13547 [16257][d]	3612	8128
Fill	20-30	569.5-559.5	-	150	2025 [5000][d]	1169	0.25 [0.5][d]	6367	15918 [19101][d]	4245	9551
Fill	30-40	559.5-549.5	-	150	2213 [5000][d]	1278	0.25 [0.5][d]	7607	19017 [22821][d]	5071	11410
Fill	40-50	549.5-539.5	-	150	2377 [5000][d]	1372	0.25 [0.5][d]	8775	21937 [26325][d]	5850	13162
Fill	50-60	539.5-529.5	-	150	2523 [5000][d]	1457	0.25 [0.5][d]	9886	24716 [29658][d]	6591	14829
Fill	60-70	529.5-519.5	-	150	2656 [5000][d]	1533	0.25 [0.5][d]	10953	27382 [32859][d]	7302	16429
Fill	70-80	519.5-509.5	-	150	2778 [5000][d]	1604	0.25 [0.5][d]	11981	29953 [35943][d]	7988	17972

TABLE 2.5.4-224A (Sheet 4 of 4)
BEST ESTIMATE LAYERING, VELOCITIES, MODULI, AND RANGES OF GRANULAR FILL (GW OR MACADAM BASE COURSE)

Layer Name	Depth (ft)	Elevation (ft)	Water Table Elev. (ft)	Unit Weight[a] (pcf)	Best Estimates					G_{max}[b] Lower Range (ksf)	G_{max}[b] Upper Range (ksf)
					V_p[b] (ft/sec)	V_s[b] (ft/sec)	Poisson's Ratio, v	G_{max}[b] (ksf)	E_{max}[b] (ksf)		
Fill	80-90	509.5-499.5	-	150	2891 [5000][d]	1669	0.25 [0.5][d]	12978	32444 [38934][d]	8652	19466
Fill	90-100	499.5-489.5	-	150	2997 [5000][d]	1730	0.25 [0.5][d]	13946	34865 [41838][d]	9297	20919

a) Moisture unit weight above water table = saturated unit weight below water table.

b) Free field condition, confining stress of building foundation not considered. G_{max} lower range = $G_{max}/1.5$; G_{max} upper range = $1.5xG_{max}$ (ASCE 4-98) (Reference 220).

c) Upper range of water table.

d) Below the water table, V_p will be 5000 ft/sec, Poisson's ratio of soil-water system will be 0.5, and $E_{max} = 3xG_{max}$, as shown in brackets [ ].

e) Lower range of water table.

TABLE 2.5.4-224B (Sheet 1 of 4)
BEST ESTIMATE LAYERING, VELOCITIES, MODULI, AND RANGES OF GRANULAR FILL (GP OR MACADAM BASE COURSE)

Layer Name	Depth (ft)	Elevation (ft)	Water Table Elev. (ft)	Unit Weight[a] (pcf)	Best Estimates					G_{max}[b] Lower Range (ksf)	G_{max}[b] Upper Range (ksf)
					V_p[b] (ft/sec)	V_s[b] (ft/sec)	Poisson's Ratio, v	G_{max}[b] (ksf)	E_{max}[b] (ksf)		
Fill	0-5.5	589.5-584	-	142	1167	674	0.25	2003	5007	1335	3004
	5.5-10.5	584-579	584[c]	142	1306 [5000][d]	754	0.25 [0.5][d]	2506	6266 [7518][d]	1671	3759
Fill	10.5-15.5	579-574	-	142	1370 [5000][d]	791	0.25 [0.5][d]	2759	6897 [8277][d]	1839	4138
	15.5-20	574-569.5	-	142	1425 [5000][d]	823	0.25 [0.5][d]	2985	7462 [8955][d]	1990	4477
Fill	20-30	569.5-559.5	-	142	1546 [5000][d]	893	0.25 [0.5][d]	3515	8789 [10545][d]	2344	5273
Fill	30-40	559.5-549.5	-	142	1686 [5000][d]	974	0.25 [0.5][d]	4181	10452 [12543][d]	2787	6271
Fill	40-50	549.5-539.5	-	142	1803 [5000][d]	1041	0.25 [0.5][d]	4780	11949 [14340][d]	3186	7169
Fill	50-60	539.5-529.5	-	142	1904 [5000][d]	1099	0.25 [0.5][d]	5330	13326 [15990][d]	3553	7995
Fill	60-70	529.5-519.5	-	142	1994 [5000][d]	1151	0.25 [0.5][d]	5844	14610 [17532][d]	3896	8766

TABLE 2.5.4-224B (Sheet 2 of 4)
BEST ESTIMATE LAYERING, VELOCITIES, MODULI, AND RANGES OF GRANULAR FILL (GP OR MACADAM BASE COURSE)

Layer Name	Depth (ft)	Elevation (ft)	Water Table Elev. (ft)	Unit Weight[(a)] (pcf)	Best Estimates					G_{max}[(b)] Lower Range (ksf)	G_{max}[(b)] Upper Range (ksf)
					V_p[(b)] (ft/sec)	V_s[(b)] (ft/sec)	Poisson's Ratio, v	G_{max}[(b)] (ksf)	E_{max}[(b)] (ksf)		
Fill	70-80	519.5-509.5	-	142	2075 [5000][(d)]	1198	0.25 [0.5][(d)]	6328	15820 [18984][(d)]	4219	9492
Fill	80-90	509.5-499.5	-	142	2149 [5000][(d)]	1241	0.25 [0.5][(d)]	6788	16969 [20364][(d)]	4525	10182
Fill	90-100	499.5-489.5	-	142	2217 [5000][(d)]	1280	0.25 [0.5][(d)]	7227	18067 [21681][(d)]	4818	10840

TABLE 2.5.4-224B (Sheet 3 of 4)
BEST ESTIMATE LAYERING, VELOCITIES, MODULI, AND RANGES OF GRANULAR FILL (GP OR MACADAM BASE COURSE)

Layer Name	Depth (ft)	Elevation (ft)	Water Table Elev. (ft)	Unit Weight[(a)] (pcf)	Best Estimates					G_{max}[(b)] Lower Range (ksf)	G_{max}[(b)] Upper Range (ksf)
					V_p[(b)] (ft/sec)	V_s[(b)] (ft/sec)	Poisson's Ratio, v	G_{max}[(b)] (ksf)	E_{max}[(b)] (ksf)		
Fill	0-5.5	589.5-584	-	142	1167	674	0.25	2003	5007	1335	3004
	5.5-10.5	584-579	-	142	1350	779	0.25	2678	6694	1785	4017
Fill	10.5-15.5	579-574	-	142	1481	855	0.25	3225	8062	2150	4837
	15.5-20	574-569.5	574[(e)]	142	1558 [5000][(d)]	899	0.25 [0.5][(d)]	3568	8920 [10704][(d)]	2379	5352
Fill	20-30	569.5-559.5	-	142	1659 [5000][(d)]	958	0.25 [0.5][(d)]	4044	10109 [12132][(d)]	2696	6065
Fill	30-40	559.5-549.5	-	142	1779 [5000][(d)]	1027	0.25 [0.5][(d)]	4655	11637 [13965][(d)]	3103	6982
Fill	40-50	549.5-539.5	-	142	1883 [5000][(d)]	1087	0.25 [0.5][(d)]	5215	13037 [15645][(d)]	3476	7822
Fill	50-60	539.5-529.5	-	142	1975 [5000][(d)]	1140	0.25 [0.5][(d)]	5736	14339 [17208][(d)]	3824	8603
Fill	60-70	529.5-519.5	-	142	2058 [5000][(d)]	1188	0.25 [0.5][(d)]	6226	15564 [18678][(d)]	4150	9338
Fill	70-80	519.5-509.5	-	142	2133 [5000][(d)]	1232	0.25 [0.5][(d)]	6690	16726 [20070][(d)]	4460	10035

TABLE 2.5.4-224B (Sheet 4 of 4)
BEST ESTIMATE LAYERING, VELOCITIES, MODULI, AND RANGES OF GRANULAR FILL (GP OR MACADAM BASE COURSE)

Layer Name	Depth (ft)	Elevation (ft)	Water Table Elev. (ft)	Unit Weight[a] (pcf)	Best Estimates					G_{max}[b] Lower Range (ksf)	G_{max}[b] Upper Range (ksf)
					V_p[b] (ft/sec)	V_s[b] (ft/sec)	Poisson's Ratio, v	G_{max}[b] (ksf)	E_{max}[b] (ksf)		
Fill	80-90	509.5-499.5	-	142	2203 [5000][d]	1272	0.25 [0.5][d]	7133	17834 [21399][d]	4756	10700
Fill	90-100	499.5-489.5	-	142	2268 [5000][d]	1309	0.25 [0.5][d]	7558	18896 [22674][d]	5039	11337

a) Moisture unit weight above water table = saturated unit weight below water table.

b) Free field condition, confining stress of building foundation not considered. G_{max} lower range = $G_{max}/1.5$; G_{max} upper range = $1.5xG_{max}$ (ASCE 4-98) (Reference 220).

c) Upper range of water table.

d) Below the water table, V_p will be 5000 ft/sec, Poisson's ratio of soil-water system will be 0.5, and $E_{max} = 3xG_{max}$, as shown in brackets [ ].

e) Lower range of water table.

TABLE 2.5.4-224C (Sheet 1 of 4)
BEST ESTIMATE LAYERING, VELOCITIES, MODULI, AND RANGES OF GRANULAR FILL (SW)

Layer Name	Depth (ft)	Elevation (ft)	Water Table Elev. (ft)	Unit Weight[a] (pcf)	Best Estimates					G_{max}[b] Lower Range (ksf)	G_{max}[b] Upper Range (ksf)
					V_p[b] (ft/sec)	V_s[b] (ft/sec)	Poisson's Ratio, v	G_{max}[b] (ksf)	E_{max}[b] (ksf)		
Fill	0-5.5	589.5-584	-	136	964	557	0.25	1309	3272	873	1963
	5.5-10.5	584-579	584[c]	136	1070 [5000][d]	618	0.25 [0.5][d]	1611	4028 [4833][d]	1074	2417
Fill	10.5-15.5	579-574	-	136	1117 [5000][d]	645	0.25 [0.5][d]	1755	4388 [5265][d]	1170	2633
	15.5-20	574-569.5	-	136	1157 [5000][d]	668	0.25 [0.5][d]	1884	4710 [5652][d]	1256	2826
Fill	20-30	569.5-559.5	-	136	1248 [5000][d]	720	0.25 [0.5][d]	2192	5480 [6576][d]	1461	3288
Fill	30-40	559.5-549.5	-	136	1353 [5000][d]	781	0.25 [0.5][d]	2575	6438 [7725][d]	1717	3863
Fill	40-50	549.5-539.5	-	136	1440 [5000][d]	831	0.25 [0.5][d]	2918	7294 [8754][d]	1945	4376
Fill	50-60	539.5-529.5	-	136	1515 [5000][d]	875	0.25 [0.5][d]	3230	8075 [9690][d]	2153	4845
Fill	60-70	529.5-519.5	-	136	1581 [5000][d]	913	0.25 [0.5][d]	3520	8800 [10560][d]	2347	5280

TABLE 2.5.4-224C (Sheet 2 of 4)
BEST ESTIMATE LAYERING, VELOCITIES, MODULI, AND RANGES OF GRANULAR FILL (SW)

Layer Name	Depth (ft)	Elevation (ft)	Water Table Elev. (ft)	Unit Weight[(a)] (pcf)	Best Estimates					G_{max}[(b)] Lower Range (ksf)	G_{max}[(b)] Upper Range (ksf)
					V_p[(b)] (ft/sec)	V_s[(b)] (ft/sec)	Poisson's Ratio, v	G_{max}[(b)] (ksf)	E_{max}[(b)] (ksf)		
Fill	70-80	519.5-509.5	-	136	1641 [5000][(d)]	948	0.25 [0.5][(d)]	3792	9480 [11376][(d)]	2528	5688
Fill	80-90	509.5-499.5	-	136	1696 [5000][(d)]	979	0.25 [0.5][(d)]	4049	10123 [12147][(d)]	2699	6074
Fill	90-100	499.5-489.5	-	136	1746 [5000][(d)]	1008	0.25 [0.5][(d)]	4294	10735 [12882][(d)]	2863	6441

TABLE 2.5.4-224C (Sheet 3 of 4)
BEST ESTIMATE LAYERING, VELOCITIES, MODULI, AND RANGES OF GRANULAR FILL (SW)

Layer Name	Depth (ft)	Elevation (ft)	Water Table Elev. (ft)	Unit Weight[a] (pcf)	Best Estimates					G_{max}[b] Lower Range (ksf)	G_{max}[b] Upper Range (ksf)
					V_p[b] (ft/sec)	V_s[b] (ft/sec)	Poisson's Ratio, v	G_{max}[b] (ksf)	E_{max}[b] (ksf)		
Fill	0-5.5	589.5-584	-	136	964	557	0.25	1309	3272	873	1963
	5.5-10.5	584-579	-	136	1105	638	0.25	1719	4298	1146	2579
Fill	10.5-15.5	579-574	-	136	1206	696	0.25	2047	5119	1365	3071
	15.5-20	574-569.5	574[e]	136	1264 [5000][d]	730	0.25 [0.5][d]	2248	5621 [6744][d]	1499	3373
Fill	20-30	569.5-559.5	-	136	1338 [5000][d]	772	0.25 [0.5][d]	2520	6300 [7560][d]	1680	3780
Fill	30-40	559.5-549.5	-	136	1427 [5000][d]	824	0.25 [0.5][d]	2868	7169 [8604][d]	1912	4301
Fill	40-50	549.5-539.5	-	136	1504 [5000][d]	868	0.25 [0.5][d]	3184	7960 [9552][d]	2123	4776
Fill	50-60	539.5-529.5	-	136	1572 [5000][d]	907	0.25 [0.5][d]	3477	8693 [10431][d]	2318	5216
Fill	60-70	529.5-519.5	-	136	1632 [5000][d]	942	0.25 [0.5][d]	3752	9379 [11256][d]	2501	5628
Fill	70-80	519.5-509.5	-	136	1688 [5000][d]	974	0.25 [0.5][d]	4011	10027 [12033][d]	2674	6016

TABLE 2.5.4-224C (Sheet 4 of 4)
BEST ESTIMATE LAYERING, VELOCITIES, MODULI, AND RANGES OF GRANULAR FILL (SW)

Layer Name	Depth (ft)	Elevation (ft)	Water Table Elev. (ft)	Unit Weight[a] (pcf)	Best Estimates					G_{max}[b] Lower Range (ksf)	G_{max}[b] Upper Range (ksf)
					V_p[b] (ft/sec)	V_s[b] (ft/sec)	Poisson's Ratio, v	G_{max}[b] (ksf)	E_{max}[b] (ksf)		
Fill	80-90	509.5-499.5	-	136	1739 [5000][d]	1004	0.25 [0.5][d]	4257	10643 [12771][d]	2838	6386
Fill	90-100	499.5-489.5	-	136	1786 [5000][d]	1031	0.25 [0.5][d]	4493	11232 [13479][d]	2995	6739

a) Moisture unit weight above water table = saturated unit weight below water table.

b) Free field condition, confining stress of building foundation not considered. G_{max} lower range = $G_{max}/1.5$; G_{max} upper range = $1.5xG_{max}$ (ASCE 4-98) (Reference 220).

c) Upper range of water table.

d) Below the water table, V_p will be 5000 ft/sec, Poisson's ratio of soil-water system will be 0.5, and $E_{max} = 3xG_{max}$, as shown in brackets [ ].

e) Lower range of water table.

TABLE 2.5.4-224D
MODULUS AND DAMPING RATIO OF GRANULAR FILL (GW OR MACADAM BASE COURSE)

	Granular Fill (GW or Macadam Base Course)					
	Depth Range (up to 10.5 ft)[a]		Depth Range (10.5 - 50 ft)[a]		Depth Range (> 50 ft)[a]	
Shear Strain γ(%)	Modulus Ratio, G/G_{max}	Damping Ratio, D_s	Modulus Ratio, G/G_{max}	Damping Ratio, D_s	Modulus Ratio, G/G_{max}	Damping Ratio, D_s
0.00001	1.00	0.54	1.00	0.50	1.00	0.47
0.0001	0.97	0.72	0.98	0.66	0.98	0.61
0.0002	0.95	0.92	0.96	0.83	0.97	0.75
0.0003	0.93	1.12	0.94	1.00	0.95	0.89
0.0005	0.89	1.50	0.91	1.33	0.93	1.17
0.001	0.82	2.36	0.85	2.08	0.88	1.83
0.002	0.72	3.82	0.76	3.39	0.79	2.99
0.003	0.65	4.99	0.69	4.49	0.73	4.00
0.005	0.55	6.79	0.59	6.23	0.63	5.66
0.01	0.41	9.53	0.44	9.07	0.48	8.53
0.02	0.28	12.15	0.30	12.00	0.33	11.72
0.03	0.22	13.49	0.23	13.56	0.26	13.50
0.05	0.15	14.91	0.16	15.25	0.18	15.49
0.1	0.09	16.35	0.10	16.99	0.11	17.58
0.2	0.05	17.22	0.06	18.04	0.06	18.88
0.3	0.04	17.47	0.04	18.36	0.04	19.29
1	0.01	17.32	0.01	18.27	0.01	19.30

a) Depths are below elevation 589.5± ft.

TABLE 2.5.4-224E
MODULUS AND DAMPING RATIO OF GRANULAR FILL (GP OR MACADAM BASE COURSE)

	Granular Fill (GP or Macadam Base Course)					
	Depth Range (up to 10.5 ft)[a]		Depth Range (10.5 - 50 ft)[a]		Depth Range (> 50 ft)[a]	
Shear Strain γ(%)	Modulus Ratio, G/G_{max}	Damping Ratio, D_s	Modulus Ratio, G/G_{max}	Damping Ratio, D_s	Modulus Ratio, G/G_{max}	Damping Ratio, D_s
0.00001	1.00	0.49	1.00	0.46	1.00	0.44
0.0001	0.99	0.54	0.99	0.50	1.00	0.47
0.0002	0.98	0.60	0.99	0.55	0.99	0.50
0.0003	0.97	0.65	0.98	0.59	0.99	0.54
0.0005	0.96	0.76	0.97	0.68	0.98	0.60
0.001	0.93	1.03	0.95	0.89	0.96	0.77
0.002	0.89	1.54	0.91	1.30	0.93	1.10
0.003	0.85	2.02	0.88	1.69	0.91	1.41
0.005	0.78	2.88	0.82	2.41	0.86	2.01
0.01	0.67	4.63	0.72	3.95	0.77	3.32
0.02	0.53	7.05	0.59	6.22	0.64	5.39
0.03	0.45	8.65	0.50	7.84	0.56	6.96
0.05	0.35	10.67	0.39	10.03	0.44	9.21
0.1	0.23	13.12	0.26	12.87	0.30	12.39
0.2	0.15	15.06	0.16	15.24	0.19	15.22
0.3	0.11	15.94	0.12	16.33	0.14	16.58
1	0.04	17.39	0.05	18.22	0.05	19.04

a) Depths are below elevation 589.5± ft.

TABLE 2.5.4-224F
MODULUS AND DAMPING RATIO OF GRANULAR FILL (SW OR MACADAM BASE COURSE)

	Granular Fill (SW or Macadam Base Course)					
	Depth Range (up to 10.5 ft)[a]		Depth Range (10.5 - 50 ft)[a]		Depth Range (> 50 ft)[a]	
Shear Strain γ(%)	Modulus Ratio, G/G_{max}	Damping Ratio, D_s	Modulus Ratio, G/G_{max}	Damping Ratio, D_s	Modulus Ratio, G/G_{max}	Damping Ratio, D_s
0.00001	1.00	0.75	1.00	0.71	1.00	0.67
0.0001	0.99	0.79	0.99	0.74	1.00	0.69
0.0002	0.99	0.83	0.99	0.77	0.99	0.72
0.0003	0.98	0.87	0.99	0.80	0.99	0.74
0.0005	0.97	0.94	0.98	0.86	0.99	0.78
0.001	0.95	1.13	0.96	1.00	0.97	0.89
0.002	0.91	1.48	0.94	1.28	0.95	1.11
0.003	0.88	1.82	0.91	1.54	0.94	1.32
0.005	0.83	2.46	0.87	2.05	0.90	1.72
0.01	0.74	3.83	0.79	3.19	0.83	2.64
0.02	0.61	5.89	0.67	5.02	0.73	4.21
0.03	0.53	7.38	0.59	6.44	0.65	5.50
0.05	0.43	9.41	0.48	8.50	0.54	7.48
0.1	0.29	12.07	0.34	11.45	0.39	10.61
0.2	0.19	14.31	0.22	14.14	0.26	13.72
0.3	0.14	15.37	0.17	15.46	0.19	15.33
1	0.06	17.38	0.07	18.05	0.08	18.65

a) Depths are below elevation 589.5± ft.

TABLE 2.5.4-225
DELETED

TABLE 2.5.4-225A
ACTIVE EARTH PRESSURE FROM GRANULAR BACKFILL

Depth Below 589.5 ft MSL (ft)	Active earth pressure, WLS, for design water (d_w) table at 5.5 ft: GW (psf)	GP (psf)	SW (psf)
0	0	0	0
5.5	224	212	203
10.5	342	319	302
15.5	461	427	402
33.0	876	805	751
39.0	1019	934	871

TABLE 2.5.4-225B
AT-REST EARTH PRESSURE FROM GRANULAR BACKFILL

Depth Below 589.5 ft MSL (ft)	At-rest earth pressure, WLS, for design water (d_w) table at 5.5 ft: GW (psf)	GP (psf)	SW (psf)
0	0	0	0
5.5	352	333	319
10.5	539	503	476
15.5	725	672	633
33.0	1379	1266	1182
39.0	1603	1470	1370

TABLE 2.5.4-225C
PASSIVE EARTH PRESSURE FROM GRANULAR BACKFILL

Depth Below 589.5 ft MSL	Passive earth pressure, WLS, for design water (d_w) table at 5.5 ft:		
(ft)	GW (psf)	GP (psf)	SW (psf)
0	0	0	0
5.5	3044	2882	2760
10.5	4661	4351	4118
15.5	6277	5819	5476
33.0	11,934	10,960	10,229
39.0	13,874	12,722	11,859

TABLE 2.5.4-226 (Sheet 1 of 3)
COMPACTION-INDUCED EARTH PRESSURE FROM
GRANULAR BACKFILL MATERIAL

			Hand-Guided Roller[(a)] Adjacent to NI Wall		Heavy Roller[(b)] 5 ft from NI Wall	
WLS Elevation	Depth	At-Rest Pressure	Residual + At-Rest Pressure	Residual Pressure	Residual + At-Rest Pressure	Residual Pressure
(ft)	(ft)	(lb/ft^2)	(lb/ft^2)	(lb/ft^2)	(lb/ft^2)	(lb/ft^2)
589.5	0.0	0	0	0	0	0
589.0	0.5	32	277	245	36	4
588.5	1.0	64	416	352	105	41
588.0	1.5	96	432	336	169	73
587.5	2.0	128	448	320	225	97
587.0	2.5	160	463	304	274	114
586.5	3.0	192	479	287	316	124
586.0	3.5	224	495	271	352	128
585.5	4.0	256	511	255	383	128
585.0	4.5	288	527	239	412	124
584.5	5.0	320	542	222	438	118
584.0	5.5	352	558	206	463	111
583.5	6.0	384	574	190	487	104
583.0	6.5	416	590	174	512	96
582.5	7.0	448	605	158	536	88
582.0	7.5	480	621	141	560	80
581.5	8.0	512	637	125	585	73
581.0	8.5	544	653	109	610	66
580.5	9.0	576	668	93	636	60
580.0	9.5	608	684	77	662	54

TABLE 2.5.4-226 (Sheet 2 of 3)
COMPACTION-INDUCED EARTH PRESSURE FROM
GRANULAR BACKFILL MATERIAL

			Hand-Guided Roller[a] Adjacent to NI Wall		Heavy Roller[b] 5 ft from NI Wall	
WLS Elevation (ft)	Depth (ft)	At-Rest Pressure (lb/ft^2)	Residual + At-Rest Pressure (lb/ft^2)	Residual Pressure (lb/ft^2)	Residual + At-Rest Pressure (lb/ft^2)	Residual Pressure (lb/ft^2)
579.5	10.0	640	700	60	689	49
579.0	10.5	672	716	44	716	44
578.5	11.0	704	732	28	744	40
578.0	11.5	736	747	12	772	36
577.5	12.0	768	768	0	800	33
577.0	12.5	800	800	0	829	30
576.5	13.0	832	832	0	858	27
576.0	13.5	864	864	0	888	24
575.5	14.0	895	895	0	917	22
575.0	14.5	927	927	0	947	20
574.5	15.0	959	959	0	977	18
574.0	15.5	991	991	0	1008	16
573.5	16.0	1023	1023	0	1038	15
573.0	16.5	1055	1055	0	1069	13
572.5	17.0	1087	1087	0	1100	12
572.0	17.5	1119	1119	0	1131	11
571.5	18.0	1151	1151	0	1162	10
571.0	18.5	1183	1183	0	1193	9
570.5	19.0	1215	1215	0	1224	8
570.0	19.5	1247	1247	0	1255	8

TABLE 2.5.4-226 (Sheet 3 of 3)
COMPACTION-INDUCED EARTH PRESSURE FROM
GRANULAR BACKFILL MATERIAL

			Hand-Guided Roller[a] Adjacent to NI Wall		Heavy Roller[b] 5 ft from NI Wall	
WLS Elevation	Depth	At-Rest Pressure	Residual + At-Rest Pressure	Residual Pressure	Residual + At-Rest Pressure	Residual Pressure
(ft)	(ft)	(lb/ft^2)	(lb/ft^2)	(lb/ft^2)	(lb/ft^2)	(lb/ft^2)
569.5	20.0	1279	1279	0	1286	7

a) Steel drum, p = 190 lb/in, roller width = 21.6 in.

b) Steel drum, p = 800 lb/in, roller width = 84 in.

TABLE 2.5.4-227
DYNAMIC EARTH PRESSURE FROM GRANULAR BACKFILL MATERIAL

Plant Elevation (ft)	Site-Specific WLS Backfill Dynamic Earth Pressure by Typical Backfill Group Symbol[a]		
	GW	GP	SW
	$\gamma = 150$ lb/ft^3	$\gamma = 142$ lb/ft^3	$\gamma = 136$ lb/ft^3
99.5 (=589.5 WLS)	1888	1788	1712
97.55	2124	2010	1925
95.6	2252	2132	2042
91.7	2369	2243	2148
87.8	2397	2269	2174
83.9	2353	2228	2134
80.0	2252	2132	2042
76.1	2095	1984	1900
75.71	2080	1969	1886
72.2	1895	1794	1718
68.3	1637	1550	1485
66.35	1486	1407	1348
64.4	1320	1249	1197
60.5	956	905	867

a) Per Reference 220, ASCE 4-98, Section 3.5.3, Figure 3.5-1, “Variation of Normal Dynamic Soil Pressures for the Elastic Solution.”

Soil Properties:
γ = unit weight as shown
$\nu = 0.5$
Acceleration:
a = 0.30g, applied uniform along the height of the wall.

TABLE 2.5.4-228
ALLOWABLE BEARING PRESSURE BASED ON FACTOR OF SAFETY

Structure	Subsurface	B x L (ft)	Bearing Pressure (k/ft^2) q_{ult}[(a)]	q_{safe}[(b)]	$q_{applied}$ (k/ft^2)	$q_{safe} > q_{applied}$
			SW Sand Granular Fill			
Annex Building	Granular Fill - SW	70 x 289	77.25	25.75	2.06	Yes
Turbine Building	Granular Fill - SW	127 x 312	120.04	40.01	1.70	Yes
Radwaste Building	Granular Fill - SW	69 x 178	72.71	24.24	0.52	Yes
			GP Gravel Granular Fill			
Annex Building	Granular Fill - GP	70 x 289	82.74	27.58	2.06	Yes
Turbine Building	Granular Fill - GP	127 x 312	128.82	42.94	1.70	Yes
Radwaste Building	Granular Fill - GP	69 x 178	77.84	25.95	0.52	Yes
			GW Gravel Granular Fill			
Annex Building	Granular Fill - GW	70 x 289	90.06	30.02	2.06	Yes
Turbine Building	Granular Fill - GW	127 x 312	140.53	46.84	1.70	Yes
Radwaste Building	Granular Fill - GW	69 x 178	84.68	28.23	0.52	Yes

a) Groundwater level is assumed to be at elevation 584 ft, or 5.5 ft below the yard surface.

b) Factor of safety of 3 is used in the analyses.

TABLE 2.5.4-229
ALLOWABLE BEARING PRESSURE BASED ON LIMITING SETTLEMENT

Structure	Subsurface	q_{allow}[(a)] (k/ft^2)	$q_{applied}$ (k/ft^2)	$q_{allow} > q_{applied}$	Anticipated Settlement (inches)
		SW Sand Granular Backfill			
Annex Building	Granular Fill - SW	7.11	2.06	Yes	< 2
Turbine Building	Granular Fill - SW	6.88	1.70	Yes	< 2
Radwaste Building	Granular Fill - SW	7.11	0.52	Yes	< 2
		GP Gravel Granular Backfill			
Annex Building	Granular Fill - GP	10.66	2.06	Yes	< 2
Turbine Building	Granular Fill - GP	10.32	1.70	Yes	< 2
Radwaste Building	Granular Fill - GP	10.67	0.52	Yes	< 2
		GW Gravel Granular Backfill			
Annex Building	Granular Fill - GW	10.66	2.06	Yes	< 2
Turbine Building	Granular Fill - GW	10.32	1.70	Yes	< 2
Radwaste Building	Granular Fill - GW	10.67	0.52	Yes	< 2

a) For limiting settlement to 2 inches.

TABLE 2.5.4-230
STRUCTURE SIZES

Structure	Seismic Category	Elevation of Base of Foundation (ft)	Depth of Foundation D_f (ft)	Width[(a)] B (ft)	Length L (ft)	$q_{applied}$[(b)] (k/ft^2)
Annex Building	II	588	1.5	70	289	2.06
Turbine Building	Non-seismic	586 - 569[(c)]	3.5	127	312	1.70
Radwaste Building	Non-seismic	588	1.5	69	178	0.52

a) Smallest width of building shown; Reference 235.

b) See Reference 236.

c) Higher elevation used.

WLS COL 2.5-14

TABLE 2.5.5-201
PERMANENT SLOPES WITHIN ONE-QUARTER MILE OF UNIT 1 AND 2 NUCLEAR ISLAND STRUCTURES

Slope (Number)	Constructed Condition	Approximate Distance to Toe (feet)	Approximate Distance to Crest (feet)	Approximate Slope Height (feet)	Approximate Slope Inclination (Horizontal to Vertical)
Unit 1 Cooling Tower Pad (1)	Engineered Fill	600	650	20	2.0:1.0
Unit 2 Cooling Tower Pad (2)	Engineered Fill	500	550	20	2.0:1.0
CNS Construction Laydown Area (3)	Engineered Fill	700	750	20	2.0:1.0
Hill Northwest of Unit 1 (4)	Natural Slope – cut	800	950	70	2.0:1.0
Hill Southwest of Unit 1 (5)	Natural Slope – cut	900	1350	100	2.5:1.0
Switchyard (6)	Engineered Fill	1100	1150	15	2.0:1.0
Pond North of Units (7)	Engineered Fill	1250	1100	55	2.0:1.0

APPENDIX 2AA
LEE NUCLEAR STATION FIELD EXPLORATION DATA

WLS COL 2.5-1

This Appendix contains geotechnical boring logs, test pit logs, SPT energy measurements, and Packer Test results that are the basis for discussion in relevant sections of 2.5. The logs and tests represent a record of subsurface conditions at the William States Lee III Nuclear Station site. Attachment 1 contains geotechnical boring logs (124 borings in total) and monitoring well construction logs (24 in total) resulting from the COL investigation as well as a key to symbols and descriptions. Attachment 2 contains the results of SPT energy measurement testing performed on the Lee Nuclear Station site. Attachment 3 contains test pit logs resulting from the COL investigation, 14 logs in total. Attachment 4 contains Packer Test results from four locations on the Lee site. Attachment 5 contains the Cone Penetrometer Test, Seismic Cone Penetrometer Test, and Pore Pressure Dissipation Test results performed on the Lee Nuclear Station site.

APPENDIX 2BB
CHEROKEE NUCLEAR STATION GEOTECHNICAL BORING LOGS

WLS COL 2.5-1 This Appendix contains historic geotechnical boring logs developed as part of the Cherokee Nuclear Station Project investigation, and a list of the included borings (189 in total).

APPENDIX 2CC

WLS COL 2.3-1

EVALUATION OF METEOROLOGICAL DATA

This Appendix provides an evaluation of the second year of Lee Nuclear Station meteorological data and a comparison with the first year of meteorological data. In addition, comparison of the site data with data covering a longer period of record from the nearest local National Weather Service station demonstrates how well the site data represents the long term conditions at the Lee Nuclear Station site. Because the one year and two year data sets are consistent and representative of the long term conditions, there is no need to update the data and values currently provided in Section 2.3.

APPENDIX 2DD
COOLING TOWER PLUME ANALYSES

This Appendix provides an evaluation of the meteorological data used in the cooling tower plume analyses.